

UCLA

UCLA Electronic Theses and Dissertations

Title

Template-Based Synthesis of Peptidomimetic Macrocycles - Discovery of Pin1 Inhibitors by Direct Stabilization of a Consensus Binding Sequence

Permalink

<https://escholarship.org/uc/item/0mx7x1st>

Author

Rose, Tristin E.

Publication Date

2015

Peer reviewed|Thesis/dissertation

UNIVERSITY OF CALIFORNIA
Los Angeles

Template-Based Synthesis of Peptidomimetic Macrocycles - Discovery of Pin1
Inhibitors by Direct Stabilization of a Consensus Binding Sequence

A dissertation submitted in partial satisfaction
of the requirements for the degree Doctor of Philosophy
in Chemistry

by

Tristin Estée Rose

2015

© Copyright by
Tristin Estée Rose
2015

ABSTRACT OF THE DISSERTATION

Template-Based Synthesis of Peptidomimetic Macrocycles –
Discovery of Pin1 Inhibitors by Direct Stabilization of a Consensus Binding Sequence

by

Tristin Estée Rose

Doctor of Philosophy in Chemistry

University of California, Los Angeles, 2015

Professor Patrick G. Harran, Chair

The constitution and ring size of peptide-derived macrocycles directly influence target binding affinity and physicochemical properties. Here, we describe means to recapitulate key features of peptide-protein interaction linear motifs (LM) in diverse, macrocyclic small molecules. Large ring-forming reactions of exceptional substrate scope are achieved using latently reactive templates that engage peptide side chain functional groups. The template is activated to transiently generate either a cinnamyl carbocation or a palladium(π -cinnamyl) complex, which rapidly form carbon-carbon or carbon-heteroatom bonds. Cyclizations occur at room temperature and are typically insensitive to peptide composition or ring size. Multiply reactive templates couple macrocyclization with additional annulation reactions to further restrict conformation, to mask polar groups, and to access complex polycyclic structures of reduced peptidic character in two or three synthetic steps. Divergent Friedel-Crafts macrocyclization reactions are of special utility for exploring multiple ring connectivities within a given peptide sequence. This method

has been coupled to standard solid-phase peptide synthesis to prepare a pilot library of 1000-1700 template-bridged macrocycles, which derive from 384 sequences that mimic the aryl-rich consensus substrate LM of the mitotic regulator Pin1. A new fluorescence polarization assay has been developed to support mixture-based screening of this library in 96-well format. Hit validation, mixture deconvolution, and structure elucidation has led to the identification of two series of non-phosphorylated, macrocyclic ligands which bind the Pin1 prolyl isomerase domain ($K_d = 24$ or 35 nM) with similar avidity to existing phosphorylated inhibitors. We show that binding affinity is directly influenced by core ring size and connectivity, in one example leading to a greater than seven-fold difference in affinity between isomeric macrocycles of identical ring size. These findings suggest that template-based methods should be useful for surveying the pharmacological properties of composite peptide macrocycles and for identifying new bioactive chemotypes by targeting protein surfaces via cognate consensus binding motifs.

The dissertation of Tristin Estée Rose is approved.

Kenneth A. Bradley

Ohyun Kwon

Patrick G. Harran, Committee Chair

University of California, Los Angeles

2015

This dissertation is dedicated to the many great scientists past and present who've inspired me, to friends and family who've supported my journey, and to my parents, Dr. Janine Marin and Dr. Allan Rose.

TABLE OF CONTENTS

Introduction	1
1 Revised synthesis of sesquiterpenoid-based template 1	8
1.1 Prior synthesis of (-)- 1-1	8
1.2 Routes to (+)- 1-1 via stereoselective 1,4-additions	9
1.3 A scalable route to conjugate addition precursors	18
2 Continued evaluation of the reactivity of template 1 towards arene-containing oligopeptides	22
2.1 Introduction	22
2.2 Complex oligomers harboring multiple nucleophilic side chain arenes	27
2.3 Evaluating peptidyl substrates 2-49–2-52 in reactions with template (+)- 2-1 .	34
2.4 Conclusions & remarks regarding the use of template 1 in property-altering, large ring-forming processes.	41
3 A simplified template for examining Pd-catalyzed and acid-promoted large ring-forming cinnamylations	44
3.1 Introduction	44
3.2 Trifunctional templates designed to promote large ring annulations by electrophilic aromatic substitution	47
3.3 A ² H-labeling approach to survey large ring-forming reactions of templates 3-3 , 3-16 and 3-17 : Discovery of a large ring-forming Friedel-Crafts reaction	52
3.4 Reactions of simplified template 3-3 with prototypical peptide Trp-Trp-Tyr	62
3.5 Conclusions & remarks regarding revised templates 3-3 , 3-16 and 3-17 , and the use of ² H labeling to probe large ring-forming reactions	75
4 Pd-Catalyzed allylation accesses template-constrained macrocyclic peptides prepared from native, unprotected precursors	80
4.1 Introduction	80
4.2 Impact of solvent, substrate concentration, and base additives on catalyzed cycloetherification of tyrosyl phenols	83
4.3 Evaluating the Scope of Catalyzed Cycloetherification	85
4.4 Longer Sequences Undergo Efficient Macrocyclization	92
4.5 Template 4-1 stabilizes secondary Structure and Enhances Proteolytic Stability in Vitro	93
4.6 Conclusions	95

5	Large ring-forming alkylations provide facile access to composite macrocycles	98
5.1	Direct, large ring-forming Friedel-Crafts alkylation of substituted benzene rings	98
5.2	Selective macrocyclizations enabled by arene symmetry or substrate geometry	110
5.3	Large ring-forming alkylations using alternative template architectures	117
5.4	Remarks and conclusions regarding template-induced large ring-forming cinnamylations.	128
6	A solid-phase approach to template-induced macrocyclizations: Application to the discovery of Pin1 inhibitors	132
6.1	Introduction	132
6.2	Non-natural amino acids as diversity-generating partners in large ring-forming Friedel-Crafts alkylations.	137
6.3	Surveying large ring-forming reactions of 5-substituted tryptophans	142
6.4	Methods for solid-phase synthesis of template-based composite macrocycles	151
6.5	<i>In vitro</i> kinetics and assays of human Pin1	160
6.6	Construction, screening, and hit deconvolution of a mixture-based Pin1-targeted macrocycle library	169
	Experimental Appendices	187
	Experimental Procedures Supporting Chapter 1	188
	Experimental Procedures Supporting Chapter 2	200
	Acidolysis of macrocyclic cinnamyl ether 2-59 and HPLC separation of product mixture 2-61	216
	Experimental Procedures Supporting Chapter 3	230
	General remarks	230
	NMR methods	230
	Optimized synthesis of simplified template 3-1	230
	Synthesis of fluorinated template 3-16	233
	Synthesis of fluorinated template 3-17	235
	NMR solution structure of pyrroloindoline 3-71h	266
	² H labeling studies and large ring-forming Friedel-Crafts reactions	269
	Experimental Procedures Supporting Chapter 4	278

Experimental Procedures Supporting Chapter 5	279
X-ray Crystal Structure of Macrocycle 5-22a .	279
Procedures for template couplings, Pd ⁰ -catalyzed and acid-promoted macrocyclizations:	279
Amino acids and building blocks therefore – Compounds 5-S1 – 5-S23 :	280
Macrocycles from template 5-1 :	288
Template 5-2 synthesis:	375
Macrocycles from template 5-2 :	375
Template 5-3 synthesis:	379
Macrocycles from template 5-3 :	383
Experimental Procedures Supporting Chapter 6	408
General procedures for template couplings and acid-promoted macrocyclization	408
Non-natural tryptophan and phenylalanine analogs	408
Macrocycles from divergent internal cinnamylations of 5-substituted tryptophans	412
On-resin acidolysis using the Rink amide linker	457
Solid-phase synthesis using the 2-chlorotrityl linker	458
hPin1 Subcloning, expression and purification	461
Synthesis of Pin1 chromogenic substrates	462
Determination of hPin1 kinetic constants	464
Development of a Pin1 fluorescence polarization assay	467
Synthesis of a Pin1-targeted library using synchronous resin release and template-induced macrocyclization	468
Pilot Library A sequences	469
Quality Control HPLC-UV/MS analysis of random sequences	478
Singlicate screening of Pilot Library A	482
HPLC Analysis of hits & re-screening at 1 μM	486
Re-synthesis & assay of hits, des-glycine congeners & acyclic congeners	489
Scale up, isolation & structure determination of Pin1-active macrocycles	497
Focused Library A	518
Focused Library B	524

ACKNOWLEDGEMENTS

“Do important science.”

“It’s not enough to just be good. Always put yourself in a position to be lucky.”

I am indebted to the many individuals who have been aided in this work, both directly and otherwise, and to those who’ve patiently taken time to share their knowledge with me. The opportunity to bridge synthetic chemistry and biology, and to realize scientific breakthroughs together has been an absolute privilege.

A majority of the work described here was carried out jointly with Dr. Ken Lawson. I greatly appreciate your talents, hard work, and friendship. Our efforts have led to the following publications, also drafted jointly, which embody a substantial portion of the work discussed herein:

Lawson, K. V.; Rose, T. E.; Harran, P. G. *Tetrahedron Lett.* **2011**, *52*, 653. (Chapter 1)

Lawson, K. V.; Rose, T. E.; Harran, P. G. *Tetrahedron* **2013**, *69*, 7683. (Chapter 3)

Lawson, K. V.; Rose, T. E.; Harran, P. G. *Proc. Natl. Acad. Sci. U. S. A.* **2013**, *110*, E3753. (Chapter 4)

Rose, T. E.; Lawson, K. V.; Harran, P. G. *Chem. Sci.* **2015**, *6*, 2219. (Chapter 5)

Dr. Albert Chan and Ashay Patel entertained helpful discussions regarding NMR and structure calculations (Ch. 3, 4). Dr. Robert Peterson provided much-needed insight into the practical implementation of two-dimensional NMR experiments which were pivotal throughout this work, and provided the E.COSY spectra utilized in our solution structure of a 38-membered ring (Ch. 4). Dr. Robert Taylor also helped with early NMR endeavors. Dr. Carly Ferguson and Dr. Huilin Li of Dr. Joseph Loo’s laboratory acquired the tandem mass spectrometry data used for metabolite ID (Ch. 4). Dr. Saeed Khan conducted the X-ray crystallographic analysis of our first crystalline macrocycle (Ch. 5). Dr. Steven Ludmerer and Stuart Black of Merck & Company (Kenilworth, NJ) assayed for Hepatitis C viral protease inhibition of the vaniprevir analog (Ch. 5). Dr. Hui Ding helped synthesize pyrrole-containing macrocycles (Ch. 5). Ankur Gholkar of Dr. Jorge Torres’s lab aided in the preparation of recombinant Pin1 (Ch. 6).

Funding was provided by the NSF GRFP (DGE-0707424), NIH CBI (T32GM008496), and an NSF instrumentation grant (CHE-1048804). The Pin1 work was supported by a grant from the University of California Cancer Research Coordinating Committee (2013-2014).

I am grateful for the early influence of outstanding industry and undergraduate mentors. My sincere thanks go to Luis, David, Fred, Kathy, Curt and others at PTRL for revealing the power of radioisotopes, Dr. John Newman for demystifying mass spectrometry, Dr. James Sanborn for good old-fashioned chalkboard discussions, Dr. Sung Hee Hwang for being an exemplary labmate, Dr. Christophe Morisseau for teaching me to embrace both the round bottom flask and 96-well plate, and Dr. Bruce Hammock for introducing me to the world of medicinal chemistry. Above all, I owe two chemistry heroes, my parents, for fostering my childhood scientific curiosity, and for always having the answer.

A special thanks goes to my doctoral advisor, Patrick Harran, for striving to tackle challenging scientific problems with synthetic chemistry and creativity, and for challenging me to do the same.

To my friends in chemistry, CBI, and the MBI, to my enduring labmates – Ken, Andrew, Ryan, Hui, Brice, Jack, and others – to my friends at the Center who’ve kept me afloat, and to Luis, Sheila and Trevor. Thank you.

CURRICULUM VITAE

Education:

B.S. Chemistry University of California, Davis. 2009

Publications & Patents:

Rose, T. E.; Lawson, K. V.; Harran, P. G. *Large ring-forming alkylations provide facile access to composite macrocycles.* *Chem. Sci.* **2015**, 6, 2219.

Xie, L. X.; Williams, K. J.; He, C. H.; Weng, E.; Khong, S.; **Rose, T. E.**; Kwon, O.; Bensinger, S. J.; Marbois, B. N.; Clarke, C. F. *Resveratrol and para-coumarate serve as ring precursors for coenzyme Q biosynthesis.* *J. Lipid Res.* **2015**, 56, 909.

Lawson, K. V.; **Rose, T. E.**; Harran, P. G., *Template-constrained macrocyclic peptides prepared from native, unprotected precursors.* *Proc. Natl. Acad. Sci. USA.*, **2013** 110(40), E3753-E3760.

Lawson, K. V.; **Rose, T. E.**; Harran, P. G., *Template-induced macrocycle diversity through large ring-forming alkylations of tryptophan.* *Tetrahedron*, **2013**, 69(36), 7683-7691.

Liu, J.-Y.; Lin, Y.P.; Qiu, H.; Morisseau, C.; **Rose, T. E.**; Hwang, S. H.; Chiamvimonvat, N.; Hammock, B.D., *Substituted phenyl groups improve the pharmacokinetic profile and anti-inflammatory effect of urea-based soluble epoxide hydrolase inhibitors in murine models.* *Eur. J. Pharm. Sci.*, **2013**, 48(4), 619-627.

Hammock, B. D.; Lee, K. S.; Morisseau, C.; **Rose, T. E.**, inventors; The Regents of the University of California, assignee. *Acyl Piperidine Inhibitors of Soluble Epoxide Hydrolase.* World Patent WO 054093A2, 2012 Apr. 26 English.

Ulu, A.; Appt, S.E.; Morisseau, C.; Hwang, S.H.; Jones, P.D.; **Rose, T. E.**; Lango, J.; Liu, J.; Tsai, H.J.; Miyabe, C.; Fortenbach, C.; Adams, M.R.; Hammock, B.D. *Pharmacokinetics and in vivo potency of soluble epoxide hydrolase inhibitors in cynomolgus monkeys.* *Brit. J. Pharmacol.*, **2011**, 165(5), 1401-1412.

Inceoglu, B.; Wagner, K.; Schebb, N.; Morisseau, C.; Jinks, S.; Ulu, A.; Hegedus, C.; **Rose, T.**; Brosnan, R.; Hammock, B. *Analgesia mediated by soluble epoxide hydrolase inhibitors is dependent on cAMP.* *Proc. Natl. Acad. Sci. U.S.A.*, **2011**, 108(12), 5093-5097.

Lawson, K.V.; **Rose, T. E.**; Harran, P.G. *Scalable Synthesis of a Reagent That Forms Useful Composites with Peptides and Related Polymers.* *Tetrahedron Lett.*, **2011**, 52(6), 653-654.

Schebb, N.H.; Inceoglu, B.; **Rose, T. E.**; Wagner, K.; Hammock, B.D. *Development of an ultra fast online-solid phase extraction (SPE) liquid chromatography electrospray tandem mass spectrometry (LC-ESI-MS/MS) based approach for the determination of drugs in pharmacokinetic studies.* *Anal. Methods*, **2011**, 3, 420-428.

Rose, T. E.; Morisseau, C.; Liu, J.Y.; Jones, P.D.; Sanborn, J.R.; Hammock, B.D. *1-Aryl-3-(1-acylpiperidin-4-yl)urea Inhibitors of Human and Murine Soluble Epoxide Hydrolase: Structure-Activity Relationships and Pharmacokinetic Screening.* *J. Med. Chem.*, **2010**, 53(19), 7067-7075.

Baumann, A.; Lohmann, W.; **Rose, T.**; Ahn, K.C.; Hammock, B.D.; Karst, U.; Schebb, N.H. *Electrochemistry-mass spectrometry unveils the formation of reactive triclocarban (TCC) metabolites.* *Drug Metab. Dispos.*, **2010**, 38(12), 2130-2138.

Awards:

UCLA NIH Chemistry-Biology Interface Training Program (T32GM008496)	2010–2013
National Science Foundation Graduate Research Fellow (DGE-0707424)	2011–2014
UCLA Dissertation Year Fellow	2014–2015

Introduction

Macrocyclic small molecules have potential to expand the repertoire of lead compounds for drug discovery, and have special utility for investigating challenging biological targets.¹ Large ring structures can scaffold extended pharmacophores and typically have improved pharmacological properties relative to linear counterparts.^{2,3} Macrocyclic natural products show exceptionally rich biological activity and have a longstanding history in medicine.^{4,5} However, an increasing number of *de novo* designed macrocycles are being advocated for development,⁶⁻⁸ including thirteen that have recently entered into clinical trials.^{9,10} Exemplary synthetic macrocycles are shown in Figure 1. TMC-647055¹¹ and Vaniprevir¹² are currently in clinical trials for treatment of Hepatitis C infection (Phase III, US), respectively. Glycosylated bicyclic lactam Nepadutant¹³ is in development for gastro-intestinal disorders (Phase II, US). Though ghrelin receptor agonist Ulimorelin recently failed Phase III trials for lack of efficacy, this peptidic macrocycle, which

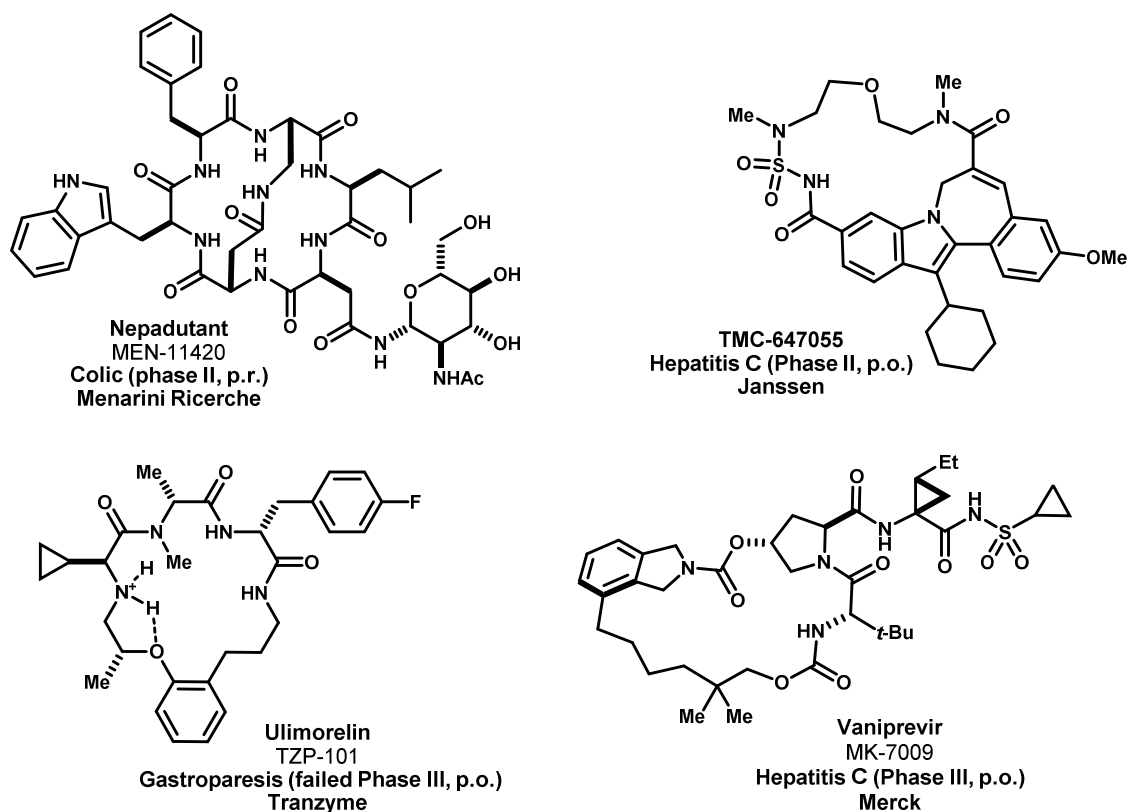


Figure 1 Exemplary *de novo* designed macrocyclic drugs currently under clinical development in the United States.

bears structural resemblance to macrocycles studied herein, showed excellent pharmacokinetic performance in humans.^{14,15} Interest in macrocyclic drugs is expected to accelerate as pharmaceutical research strives to control frontier therapeutic targets, such as protein-protein interactions (PPIs) and certain receptors and enzymes with large, solvent-exposed, or cryptic binding sites.^{10,16} The success of synthetic macrocycles in small molecule discovery and development is critically dependent on efficient, generally useful methods to prepare them. Arguably most needed are discovery-oriented methods to broadly survey the chemical space of macrocycles, and which may advance biological screening beyond the confines of conventional high-throughput screening collections^{17,18} and prevailing notions of drug-like chemotypes.^{19,20}

Peptide-derived macrocycles are especially attractive, because the embedded peptide can mimic localized protein structural motifs and can inherently complement native recognition elements at protein surfaces.^{21,22} Of particular interest to us and others^{23,24} are protein-protein interactions mediated by conserved linear motifs (LMs), wherein binding is affected by a contiguous sequence of amino acids. High-resolution structures, mutagenesis, and computational studies of peptide-protein interaction surfaces have identified features that drive binding, and which may be targeted by small molecules. Despite relatively large contact areas and variable secondary structure elements involved, binding energy is often localized to so-called hot-spots.²⁵⁻²⁷ Aromatic amino acid side chains are prevalent and contribute significantly to binding and recognition at these sites.^{28-30,24} Peptide-protein interfaces are also characterized by tight complementarity of surface shape and charge.^{23,31} In an effort to capture these evolved features in stabilized small molecules, we have sought methods to convert linear peptides into constrained macrocycles based upon their aromatic content.

Recent developments in peptide cyclization methods have improved generality and efficiency over conventional lactamizations. Intramolecular azide-alkyne cycloadditions,^{32,33} olefin metatheses³³⁻³⁵ and cysteine-based ligations^{21,36,37} have been widely studied in this regard, and used successfully to prepare combinatorial libraries and to stabilize α -helices^{35,38,39} and β -strands.⁴⁰ These techniques are valuable, yet often require substrate tailoring and reaction optimization in order to vary the size and constitution of the macrocyclic core. DNA-templated macrocyclizations^{6,41} and genetically encoded biosynthetic methods,⁴² have also been reported. An alternative approach involves late-stage synthetic incorporation of

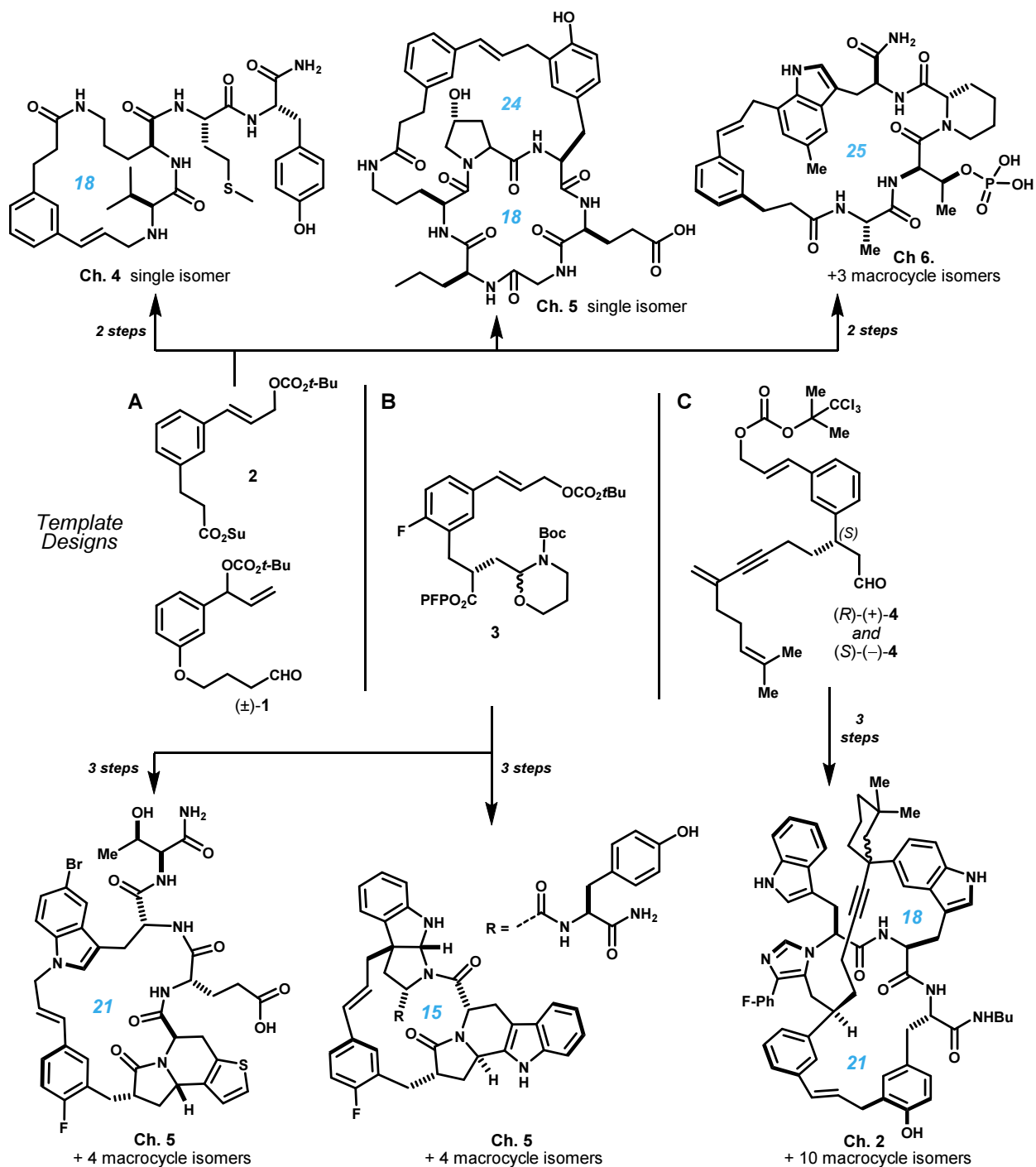


Figure 2. Select template-derived macrocycles discussed herein. Products obtained in two or three steps from linear peptides by reactions with: **A)** Di-functional templates **1** and **2**, **B)** Tri-functional template **3** which also initiates *N*-acyliminium ion cyclizations, and **C)** Tri-functional templates **4**, designed to form annulated macrocycles.

templates that induce cyclization by bridging native functional groups.^{43–45} This allows macrocycle shape, size and physicochemical properties to be influenced by template structure.

Contributions from our laboratory have primarily focused on highly functional group tolerant ring-forming reactions and unique template architectures which can modify the peptide more substantially (see Figure 2). Uniquely, our methods can access multiple macrocycle connectivities within a given peptide sequence by forming stable carbon–carbon or carbon–heteroatom bonds with native peptide side chains. This is achievable through either switchable chemoselectivity in the case of heteroatom nucleophiles or through divergent reactions in the case of arene nucleophiles. Tuning macrocycle constitution in this way provides novel means to hone the properties and target affinity of peptidyl macrocycles, and to rapidly explore isomeric macrocycles that would be otherwise time-consuming to prepare.

This dissertation documents several template-based approaches, in-depth explorations of two new large ring-forming methods, and preliminary efforts to identify macrocyclic inhibitors of the mitotic regulator Pin1. Chapter 1 concerns a revised synthesis of tri-functional template (*R*)-(+)-**4** (Figure 2) in enantiomerically enriched form.⁴⁶ The enantiomer of this material was previously investigated in our laboratory,⁴⁷ and continued efforts to understand its reactivity and propensity to promote large ring annulations are the subject of Chapter 2. Several key discoveries are discussed in Chapter 3: revisions to template **4** designed to increase the abundance of annulated macrocycles; a ²H-labeling strategy to map ring-forming cinnamylation reactions by mass spectrometry; the synthesis of simplified template **2** and subsequent discovery of a direct large ring-forming Friedel-Crafts reaction; and identification of products from reactions of **2** and model peptide Trp-Trp-Tyr.⁴⁸ Chapter 4 concerns the use of **2** in Pd⁰-catalyzed internal cinnamylations of phenols, imidazoles, amines, anilines and carboxylates within unprotected peptides.⁴⁹ Further, these heteroatom-liked macrocycles are shown to resist proteolytic degradation and to stabilize native peptide secondary structure in solution. Chapter 5 further examines kinetic factors governing direct large ring-forming Friedel-Crafts alkylations, and charts methods to control regioselectivity using substituent effects in both selective and divergent reactions.⁵⁰ Additionally, Chapter 5 addresses special applications of template **2** in drug analog synthesis, and the synthesis and implementation of tri-functional template **3**.

Final Chapter 6 brings several of our goals to fruition in an application of divergent macrocyclizations, promoted by template **2**, to identify inhibitors of the mitotic regulatory enzyme Pin1. Foremost, a series of

incremental synthetic developments are detailed: the use of 5-substituted tryptophans as diversity-generating nucleophiles in ring-forming Friedel-Crafts reactions; the integration of solid-supported parallel synthesis with cyclizations mediated by **2**; and the demonstration of an exceptionally broad substrate scope. These efforts culminated in the synthesis of a pilot library targeting the Pin1 peptidyl-prolyl isomerase (PPIase) domain. This library comprised 384 peptide sequences – cyclized by template **2** – which harbor the isosteric substrate consensus motif Xxx-Glu-Pro-Xxx (est. 1000 to 1700 macrocyclic constituents). A new fluorescence polarization (FP) binding assay was developed to support testing of this library in 96-well format. Mixture-based screening, hit deconvolution and structure elucidation by NMR led to the identification of two series of non-phosphorylated macrocyclic ligands that bound Pin1 with avidity comparable to the best phosphorylated inhibitors reported in the literature. Critically, these data confirm that macrocycle connectivity and ring size can affect binding affinity. In one instance, we observed four- and six-fold changes in affinity upon changing ring size by one and two atoms, respectively. In another instance, affinity varied greater than seven-fold between isomeric macrocycles of identical ring size, but of differing connectivity. These findings set an exciting precedent, and suggest that template-based methods such as these should be helpful for surveying the pharmacological properties of complex peptide-derived macrocycles and for identifying new bioactive chemotypes.

References

- (1) Driggers, E. M.; Hale, S. P.; Lee, J.; Terrett, N. K. *Nat. Rev. Drug Discov.* **2008**, *7*, 608.
- (2) Bock, J. E.; Gavenonis, J.; Kritzer, J. A. *ACS Chem. Biol.* **2013**, *8*, 488.
- (3) Marsault, E.; Peterson, M. L. *J. Med. Chem.* **2011**, *54*, 1961.
- (4) Yudin, A. K. *Chem. Sci.* **2015**, *6*, 30.
- (5) Wessjohann, L. A.; Ruijter, E.; Garcia-Rivera, D.; Brandt, W. *Mol. Divers.* **2005**, *9*, 171.
- (6) Maianti, J. P.; McFedries, A.; Foda, Z. H.; Kleiner, R. E.; Du, X. Q.; Leissring, M. a; Tang, W.-J.; Charron, M. J.; Seeliger, M. A.; Saghatelian, A.; Liu, D. R. *Nature* **2014**, *511*, 94.
- (7) White, T. R.; Renzelman, C. M.; Rand, A. C.; Rezai, T.; McEwen, C. M.; Gelev, V. M.; Turner, R. A.; Linington, R. G.; Leung, S. S. F.; Kalgutkar, A. S.; Bauman, J. N.; Zhang, Y.; Liras, S.; Price, D. A.; Mathiowetz, A. M.; Jacobson, M. P.; Lokey, R. S. *Nat. Chem. Biol.* **2011**, *7*, 810.
- (8) Rand, A. C.; Leung, S. S. F.; Eng, H.; Rotter, C. J.; Sharma, R.; Kalgutkar, A. S.; Zhang, Y.; Varma, M. V.; Farley, K. a.; Khunte, B.; Limberakis, C.; Price, D. a.; Liras, S.; Mathiowetz, A. M.; Jacobson, M. P.; Lokey, R. S. *Medchemcomm* **2012**, *3*, 1282.
- (9) Cummings, S. V. and M. D. In *Annual Reports in Medicinal Chemistry*; Desai, M. C., Ed.; Elsevier Ltd: San Diego, CA, 2013; pp 371–386.

- (10) Giordanetto, F.; Kihlberg, J. *J. Med. Chem.* **2014**, *57*, 278.
- (11) Cummings, M. D.; Lin, T. I.; Hu, L.; Tahri, A.; McGowan, D.; Amssoms, K.; Last, S.; Devogelaere, B.; Rouan, M. C.; Vijgen, L.; Berke, J. M.; Dehertogh, P.; Franssen, E.; Cleiren, E.; Van Der Helm, L.; Fanning, G.; Nyanguile, O.; Simmen, K.; Van Remoortere, P.; Raboisson, P.; Vendeville, S. *J. Med. Chem.* **2014**, *57*, 1880.
- (12) McCauley, J. A.; McIntyre, C. J.; Rudd, M. T.; Nguyen, K. T.; Romano, J. J.; Butcher, J. W.; Gilbert, K. F.; Bush, K. J.; Holloway, M. K.; Swestock, J.; Wan, B. L.; Carroll, S. S.; Dimuzio, J. M.; Graham, D. J.; Ludmerer, S. W.; Mao, S. S.; Stahlhut, M. W.; Fandozzi, C. M.; Trainor, N.; Olsen, D. B.; Vacca, J. P.; Liverton, N. J. *J. Med. Chem.* **2010**, *53*, 2443.
- (13) Catalioto, R. M.; Criscuoli, M.; Cucchi, P.; Giachetti, a; Gianotti, D.; Giuliani, S.; Lecci, a; Lippi, a; Patacchini, R.; Quartara, L.; Renzetti, a R.; Tramontana, M.; Arcamone, F.; Maggi, C. a. *Br. J. Pharmacol.* **1998**, *123*, 81.
- (14) Bochicchio, G.; Charlton, P.; Pezzullo, J. C.; Kosutic, G.; Senagore, A. *World J. Surg.* **2012**, *36*, 39.
- (15) Lasseter, K. C.; Shaughnessy, L.; Cummings, D.; Pezzullo, J. C.; Wargin, W.; Gagnon, R.; Oliva, J.; Kosutic, G. *J. Clin. Pharmacol.* **2008**, *48*, 193.
- (16) Arkin, M. R.; Wells, J. A. *Nat. Rev. Drug Discov.* **2004**, *3*, 301.
- (17) Mullard, A. *Nat. Rev. Drug Discov.* **2012**, *11*, 173.
- (18) Wells, J. A.; McClendon, C. L. *Nature* **2007**, *450*, 1001.
- (19) Lipinski, C. A. *Drug Discov. Today Technol.* **2004**, *1*, 337.
- (20) Lipinski, C. A.; Lombardo, F.; Dominy, B. W.; Feeney, P. J. *Adv. Drug Deliv. Rev.* **2001**, *46*, 3.
- (21) Wrighton, N. C.; Farrell, F. X.; Chang, R.; Kashyap, a K.; Barbone, F. P.; Mulcahy, L. S.; Johnson, D. L.; Barrett, R. W.; Jolliffe, L. K.; Dower, W. J. *Science* **1996**, *273*, 458.
- (22) Livnah, O.; Stura, E. A.; Johnson, D. L.; Middleton, S. A.; Mulcahy, L. S.; Wrighton, N. C.; Dower, W. J.; Jolliffe, L. K.; Wilson, I. A. *Science* **1996**, *273*, 464.
- (23) London, N.; Movshovitz-Attias, D.; Schueler-Furman, O. *Structure* **2010**, *18*, 188.
- (24) Davey, N. E.; Van Roey, K.; Weatheritt, R. J.; Toedt, G.; Uyar, B.; Altenberg, B.; Budd, A.; Diella, F.; Dinkel, H.; Gibson, T. J. *Mol. Biosyst.* **2012**, *8*, 268.
- (25) Clackson, T.; Wells, J. *Science (80-.)*. **1995**, *267*, 383.
- (26) Bullock, B. N.; Jochim, A. L.; Arora, P. S. *J. Am. Chem. Soc.* **2011**, *133*, 14220.
- (27) Watkins, A. M.; Arora, P. S. *ACS Chem. Biol.* **2014**, *9*, 1747.
- (28) Kelley, R. F.; Costas, K. E.; O'Connell, M. P.; Lazarus, R. a. *Biochemistry* **1995**, *34*, 10383.
- (29) Bogan, A. A.; Thorn, K. S. *J. Mol. Biol.* **1998**, *280*, 1.
- (30) Pillutla, R. C.; Hsiao, K. C.; Beasley, J. R.; Brandt, J.; Østergaard, S.; Hansen, P. H.; Spetzler, J. C.; Danielsen, G. M.; Andersen, A. S.; Brissette, R. E.; Lennick, M.; Fletcher, P. W.; Blume, A. J.; Schäffer, L.; Goldstein, N. I. *J. Biol. Chem.* **2002**, *277*, 22590.
- (31) Moreira, I. S.; Fernandes, P. A.; Ramos, M. J. *Proteins Struct. Funct. Bioinforma.* **2007**, *68*, 803.
- (32) Beckmann, H. S. G.; Nie, F.; Hagerman, C. E.; Johansson, H.; Tan, Y. S.; Wilcke, D.; Spring, D. R. *Nat. Chem.* **2013**, *5*, 861.
- (33) Isidro-Llobet, A.; Murillo, T.; Bello, P.; Cilibrizzi, A.; Hodgkinson, J. T.; Galloway, W. R. J. D.; Bender, A.; Welch, M.; Spring, D. R. *Proc. Natl. Acad. Sci. U. S. A.* **2011**, *108*, 6793.
- (34) Miller, S. J.; Blackwell, H. E.; Grubbs, R. H. *J. Am. Chem. Soc.* **1996**, *118*, 9606.
- (35) Blackwell, H. E.; Grubbs, R. H. *Angew. Chemie - Int. Ed.* **1998**, *37*, 3281.
- (36) Jackson, D. Y.; King, D. S.; Chmielewski, J.; Singh, S.; Schultz, P. G. *J. Am. Chem. Soc.* **1991**, *113*, 9391.
- (37) Giebel, L. B.; Cass, R. T.; Milligan, D. L.; Young, D. C.; Arze, R.; Johnson, C. R. *Biochemistry* **1995**, *34*, 15430.
- (38) Schafmeister, C. E.; Po, J.; Verdine, G. L. *J. Am. Chem. Soc.* **2000**, *122*, 5891.

- (39) Kim, Y.-W.; Grossmann, T. N.; Verdine, G. L. *Nat. Protoc.* **2011**, *6*, 761.
- (40) Chua, K. C. H.; Pietsch, M.; Zhang, X.; Hautmann, S.; Chan, H. Y.; Bruning, J. B.; Gütschow, M.; Abell, A. D. *Angew. Chemie - Int. Ed.* **2014**, *53*, 7828.
- (41) Gartner, Z. J.; Tse, B. N.; Grubina, R.; Doyon, J. B.; Snyder, T. M.; Liu, D. R. *Science* **2004**, *305*, 1601.
- (42) Scott, C. P.; Abel-Santos, E.; Jones, A. D.; Benkovic, S. J. *Chem. Biol.* **2001**, *8*, 801.
- (43) Jackson, S.; DeGrado, W.; Dwivedi, A.; Parthasarathy, A.; Higley, A.; Krywko, J.; Rockwell, A.; Markwalder, J.; Wells, G.; Wexler, R.; Mousa, S.; Harlow, R. *J. Am. Chem. Soc.* **1994**, *116*, 3220.
- (44) Boger, D. L.; Myers, J. B. *J. Org. Chem.* **1991**, *56*, 5385.
- (45) Hill, R.; Rai, V.; Yudin, A. K. *J. Am. Chem. Soc.* **2010**, *132*, 2889.
- (46) Lawson, K. V.; Rose, T. E.; Harran, P. G. *Tetrahedron Lett.* **2011**, *52*, 653.
- (47) Zhao, H.; Negash, L.; Wei, Q.; LaCour, T. G.; Estill, S. J.; Capota, E.; Pieper, A. A.; Harran, P. G. *J. Am. Chem. Soc.* **2008**, *130*, 13864.
- (48) Lawson, K. V.; Rose, T. E.; Harran, P. G. *Tetrahedron* **2013**, *69*, 7683.
- (49) Lawson, K. V.; Rose, T. E.; Harran, P. G. *Proc. Natl. Acad. Sci. U. S. A.* **2013**, *110*, E3753.
- (50) Rose, T. E.; Lawson, K. V.; Harran, P. G. *Chem. Sci.* **2015**, *6*, 2219.

1 Revised synthesis of sesquiterpenoid-based template 1

1.1 Prior synthesis of 1

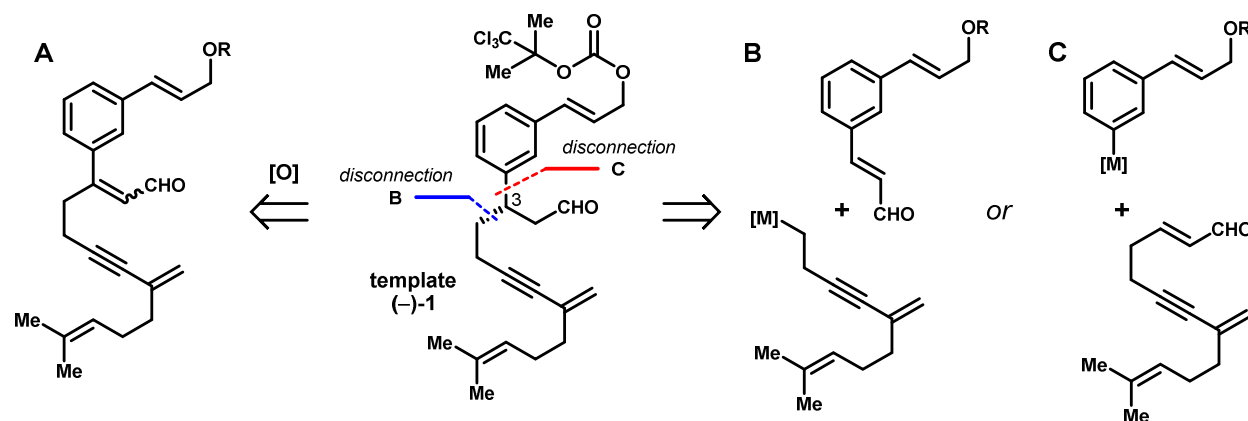
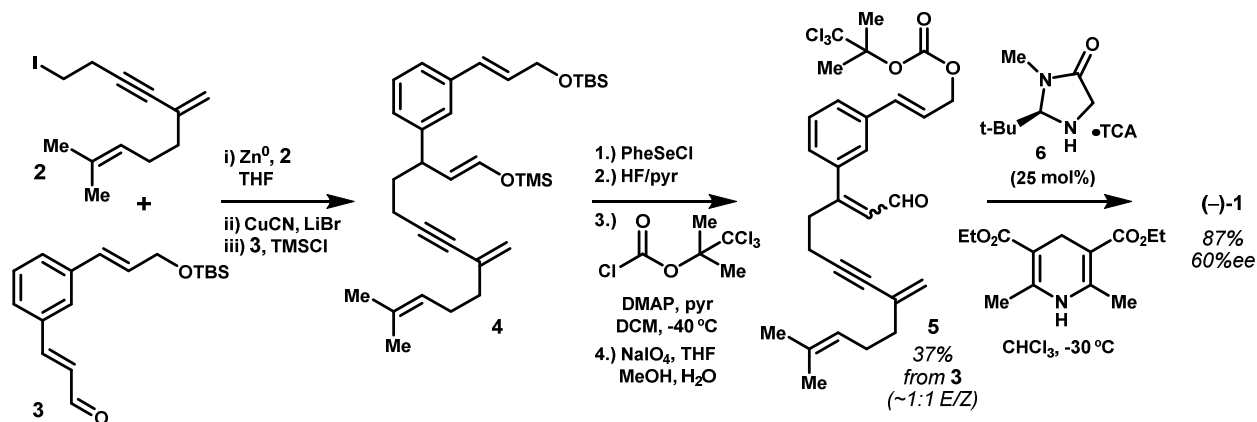


Figure 1.1.1 Potential disconnections for the stereoselective synthesis of sesquiterpenoid template 1. Approach **A** entails asymmetric reduction, whereas **B** and **C** entail 1,4-addition of either a homopropargyl or an aryl nucleophile.

In order to fuel further studies of the reactivity of trifunctional template **1** (Figure 1.1.1) and construction of pilot libraries for biological screening, we sought revised synthesis of **1** with improved scalability. Central to this goal is a robust means to establish the *C3* stereocenter in high optical purity. The route initially employed by Zhao and co-workers¹ to prepare (-)-**1** installed the *C3* stereocenter by enantioselective reduction of an oxidized precursor (**A**, Figure 1). In light of challenges faced in the previous route, we viewed disconnections at *C3*, either of the aryl group (**B**) or of the dienyl appendage (**C**), as potentially viable, given the availability of asymmetric conjugate addition methodologies.^{2,3,4} Stereoisomeric enals **5** in turn were derived in five steps from cinnamaldehyde **3** and iodide **2**, each prepared in four and three steps from isophthalaldehyde and 2-methyl-1-butene-3-yne, respectively. From **2**, the organozinc iodide was prepared by classical oxidative addition of Zn^0 , which then underwent 1,4-addition into cinnamaldehyde **3** promoted by copper(I) cyanide in the presence of chlorotrimethylsilane at $-78\text{ }^{\circ}\text{C}$, yielding trimethylsilyl enol ether **4**. Treatment with phenylselenenyl chloride formed the α -phenylselenenyl aldehyde, which was desilylated, transformed to the mixed carbonate by the action of 2,2,2-trichloro-1,1-dimethylethyl chloroformate in the presence of dimethylaminopyridine (DMAP) and pyridine. Subsequent oxidation with sodium periodate led

Scheme 1.1.1 Previously reported synthesis of sesquiterpenoid-based template **1**.¹ The key transformation involved enantioselective conjugate reduction of enals **5** to establish the stereochemistry at C3.



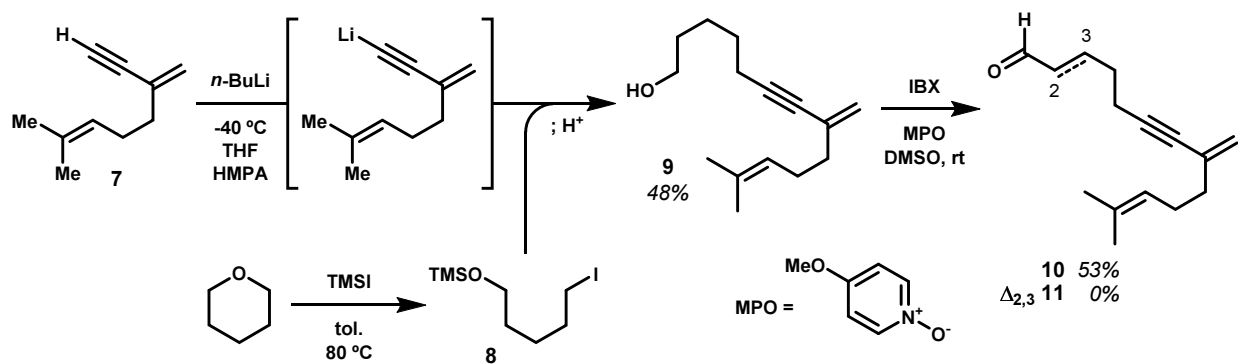
to elimination, giving **5** as an inconsequential mixture of stereoisomers. Lastly, the key conjugate reduction was achieved using by *tert*-butylimidazolodinone catalyst **6** (25 mol%) in the presence of the Hantzsch ester.⁵ High conversion was achieved in this reaction, but (–)-**1** was obtained in moderate 60 %ee. While this route provided material sufficient to fuel studies of the reactivity of this template design, and an impressive pilot drug discovery exercise,¹ the relatively low optical purity of **1** led to undesirable mixtures of diastereomers when coupled to enantiopure peptides. Consequently, we sought to improve upon this synthesis to both improve the enantiopurity of the product, and to improve scalability by reducing step count, minimizing chromatography, and reducing the use of toxic or expensive reagents.

1.2 Routes to **1** via stereoselective 1,4-additions

Initially, we favored benzylic disconnection **B** (Figure 1.1.1) for its convergence and potential to use reported methods for enantioselective conjugate additions of aryl boronic acids – a likely accessible, stable intermediate - using low catalytic loading of chiral rhodium(I) complexes.^{2,6,7,8} Requisite to this route was enal fragment **10** (Scheme 1.1.1). Borrowing from the prior synthesis of **1**, we prepared dienyne fragment **7** by alkylation of the dipotassium salt of 2-methyl-1-buten-3-yne with prenyl bromide, generated by the action of *n*-BuLi in the presences of KO-*t*Bu, according to the methods of Klusener and co-workers.⁹ Attempted alkylation of the residual potassium acetylide resulting from this reaction was unsuccessful, and thus we opted to isolate **7**, form the lithium acetylide, and alkylate with TMS protected 5-iodo-1-pentanol

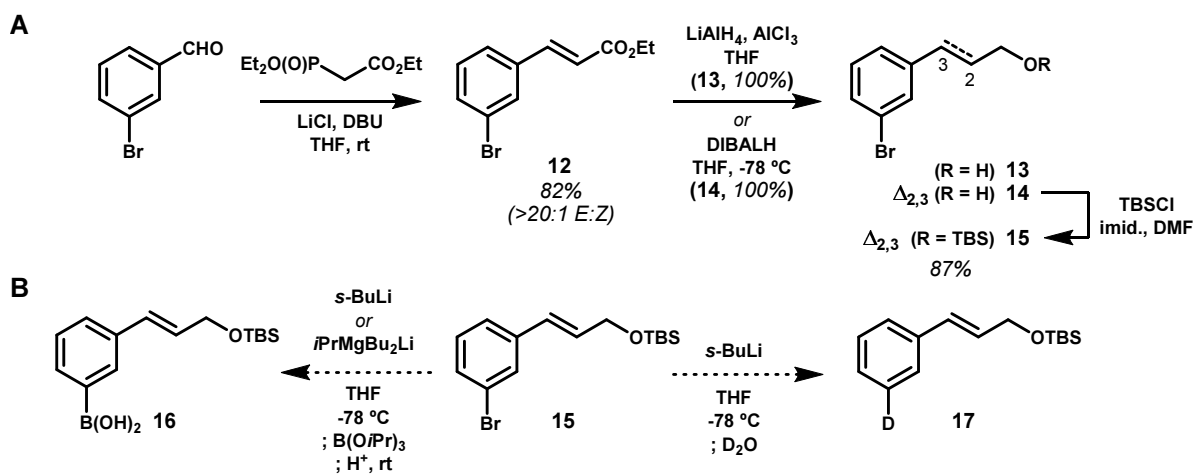
(8). Iodide **8** was prepared from tetrahydropyran by reaction with trimethylsilyl iodide.¹⁰ The addition of hexamethylphosphoramide (HMPA)¹¹ was found necessary in the alkylation of **7**, consistent with its known propensity to enhance the reactivity of metal acetylides.¹² Aqueous acidic workup hydrolyzed the silyl group giving alcohol **9**. Attempts to oxidize this alcohol directly to α,β -unsaturated aldehyde **11** with excess *ortho*-iodoxybenzoic acid (IBX) in DMSO or DMSO:DCM in the presence of excess 4-methoxy-pyridine-*N*-oxide (MPO) at room temperature afforded only saturated aldehyde **10**. MPO has been shown to accelerate dehydrogenations of this type¹³, the success of which seems to be dependent upon the quality of the IBX, which was found to contain other hypervalent iodine species depending on the oxidant used in its preparation,¹⁴ with Oxone[®] yielding higher purity IBX.¹⁵ Concurrent with efforts to prepare **11**, we approached the preparation of a suitable arylboronic acid fragment targeted in disconnection **C** (Figure 1.1.1).

Scheme 1.2.1 Attempted preparation of enal **11** as an electrophilic partner for enantioselective conjugate additions



Arylboronic acids can be typically be prepared from the corresponding aryl halide via the aryl lithium or aryl Grignard intermediate by reaction with trimethyl- or triisopropyl borate and subsequent hydrolysis,¹⁶ and therefore this constituted our initial approach. Ethyl 3-bromocinnamate (**12**, Scheme 1.2.2A) was prepared from 3-bromobenzaldehyde by Horner-Wadsworth-Emmons olefination with triethyl phosphonoacetate under mild conditions according to the Masamune-Roushe protocol.¹⁷ Subsequent 1,2-reduction of the ester was first attempted with AlH₃, generated by the metathesis of AlCl₃ and three equivalents of LiAlH₄ as was done previously in the synthesis of **1**,^{1,18} returned only saturated phenylpropanol **13**. Reduction of **12** with diisobutylaluminum hydride at -78 °C, however, cleanly afforded the cinnamyl alcohol **14**, which was silyl protected to give **15**. This material, as well as alcohol **14**, was

Scheme 1.2.2 Attempted preparation of allylated aryl boronic acid **16** as a nucleophilic partner for enantioselective conjugate additions.



carried into attempted metal halogen exchange reactions to allow subsequent boronation. Low temperature metal-halogen exchange of **14** and **15** with *sec*-butyllithium, and subsequent reaction with triisopropylborate followed by acidic hydrolysis returned only complex product (Scheme 1.2.2B). Quenching the reaction with D₂O following metal-halogen exchange failed to return the deuteration product, giving also a complex mixture by NMR and TLC, suggesting that the metalation was problematic, rather than the boronation. Consequently, we attempted an analogous sequence by initial magnesiation using a magnesium ate complex generated by the reaction of isopropylmagnesium bromide and *n*-butyllithium, which is reported to affect rapid metal-halogen exchange at low temperature.¹⁹ Using **15** in this reaction returned only desilylated **14**, likely resulting from the acidic hydrolysis, suggesting metalation had not occurred. While numerous other methods exist for boronation of aryl halides that might reasonably be able to access boronic acid **16**, such as the mild Pd-catalyzed Miyaura borylation,²⁰ we instead began pursuing alternative routes employing disconnection **B** (Figure 1.1.1) given our previous success with homopropargyl metals as nucleophiles in conjugate addition reactions.¹

Late installation of the complete dienynyl appendage of **1** would maximize convergence, and we expected this could be achieved using a chiral auxiliary approach and an organocopper nucleophile. This approach would utilize an allylated cinnamate analogous to enal intermediate **3** utilized previously, but at the acid oxidation state to allow installation of the chiral auxiliary. We again viewed two possible disconnection **B** at the sp²-sp² single bond to bring in all three carbons of the allyl group. In order to quickly

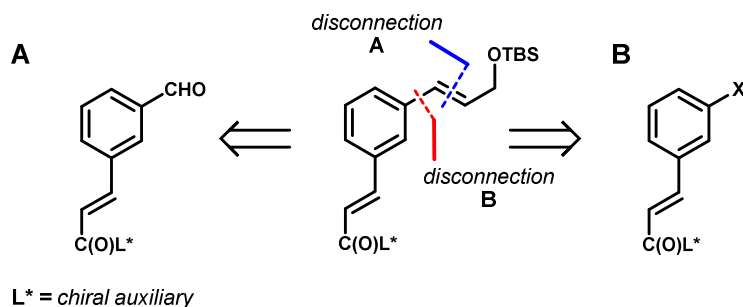
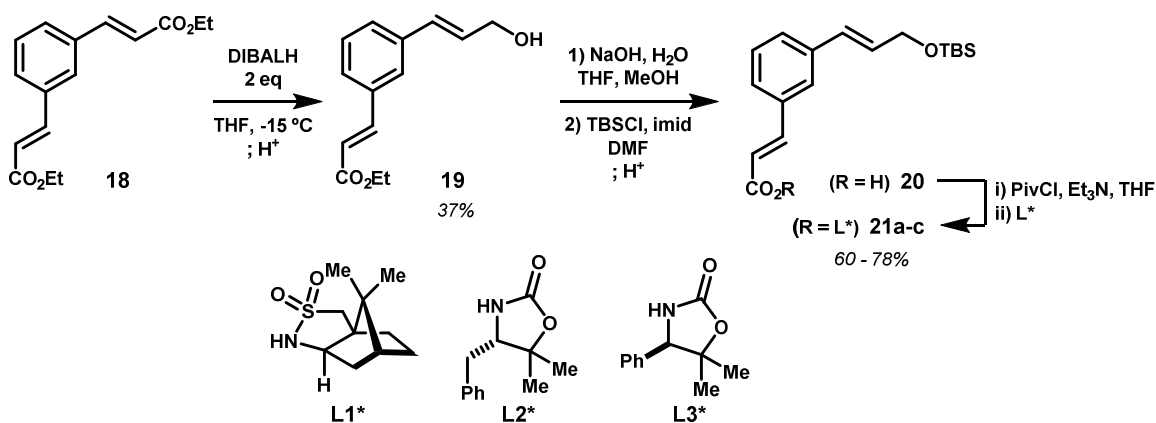


Figure 1.2.1 Disconnections for the assembly of the cinnamyl core of template **1**.

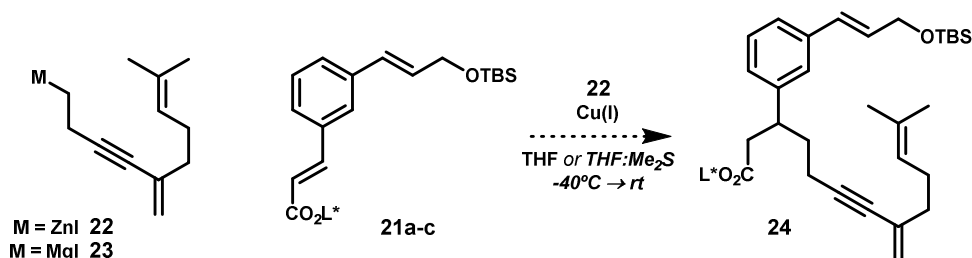
supply the cinnamyl imide precursors to begin examining conjugate addition reactions, we adopted a desymmetrization approach from bis-ester **18** (Scheme 1.2.3), an intermediate on hand from the prior route to **1**. While desymmetrization reactions can be made to favor a given singly reacted product,²¹ such an outcome is often entropically driven. This can be accomplished by differential solubility of intermediates, by transformation of the first functional group in a manner that slows reaction at the second, or by biasing reaction stoichiometry. More often than not, desymmetrization reactions afford statistical mixtures of products. Such was the case in the diisobutylaluminum hydride (DIBALH) reduction of **18**, which afforded a statistical mixture of mono- and bis-cinnamyl alcohols, along with residual starting material. The desired mono-ol **19** was isolated in 37% yield by column chromatography, and sufficed to begin optimizing 1,4-addition reactions. Oppolzer's camphor-derived sultam (**L1***, Scheme 1.2.3),^{22–24} and *L*-phenylalanine- and *D*-phenylglycine-derived 5,5-dimethyloxazolidinones (**L2***, **L3***, respectively),²⁵ colloquially known as Superquat auxiliaries, were *N*-acylated by means of the mixed pivaloyl anhydride of intermediate cinnamic

Scheme 1.2.3 Reductive desymmetrization of bis-ester **18** allowed rapid access to chiral Michael acceptors **21a–c**.



acid **20** giving chiral imides **21a–c**.²⁶ Though a more efficient means would be required to access these intermediates, we first examined diastereoselective conjugate additions of **21a–c**.

Scheme 1.2.4 Attempted installation of intact dienyne appendage via its organozinc or organomagnesium reagent.

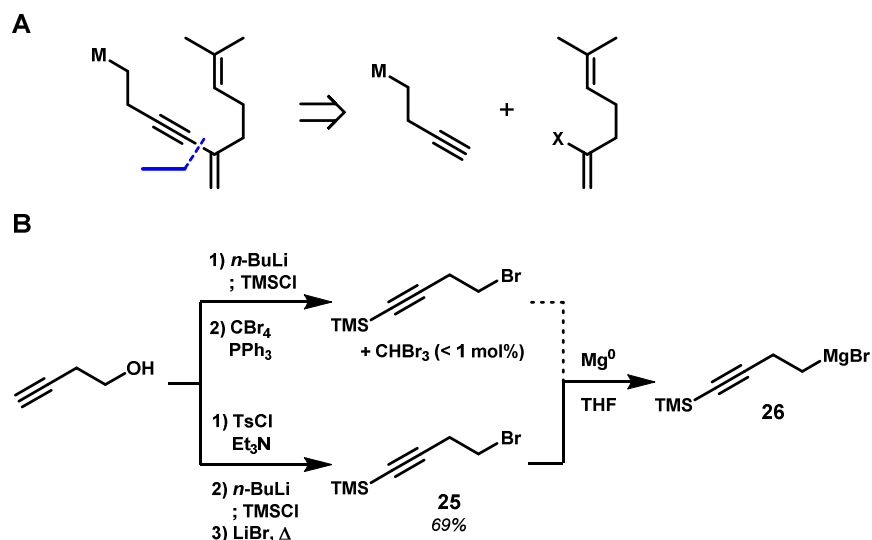


In an effort to install the intact dienyne appendage, we examined unification of chiral enimides **21a–c** with iodide **2**, also on hand from the prior route to **1**. We attempted reactions of the organozinc reagent **22**, derived from **2**, as was utilized in 1,4-addition into enals **3**. Stoichiometric transmetalation using either CuBr or CuCN both with and without dimethylsulfide as a solubilizing additive, and mixing with enimides **21** gave only starting material by TLC. Reactions were also attempted using BF₃·(OEt₂) as an additive, given its reported ability to enhance the reactivity of the alkyl copper species,²⁷ but this too was unsuccessful. In general, monoalkylzinc halides are less reactive than dialkylzinc reagents,²⁸ which in turn are substantially less reactive than their corresponding Grignard or lithium reagent. Curiously, we were unable to prepare the Grignard reagent derived from iodide **2** (i.e. **23**). Addition of **2** to activated magnesium metal in THF or ether led to formation of a heavy white precipitate and a supernatant with no titre of the Grignard reagent, or titre of base upon quenching with water. Given that the use of a dialkylzinc reagent analogous to **22** would likely transfer only one alkyl group, leading to poor atom economy, or would necessitate the use of mixed dialkylzincs,²⁹ we instead opted to further disconnect the dienyne at the acetylenic sp-sp² bond.

Disconnection the dienyne to homopropargyl and dienyl fragments allowed use of known Grignard reagent **26** (Scheme 1.2.5),³⁰ which ultimately proved successful, and also accommodated potential modification of the diene portion of **1** in future iterations of the template. Initially, the requisite TMS protected homopropargyl bromide **25** was uneventfully prepared from homopropargyl alcohol in two steps by lithiation

and C-silylation, and subsequent introduction of the bromide in an Appel reaction with carbon tetrabromide and triphenylphosphine, as reported (Scheme 1.2.5B).³¹ However, this material failed to react with activated

Scheme 1.2.5 A) Targeted sp-sp² disconnection of the dienyne. B) Synthesis of TMS-protected homopropargyl Grignard reagent.

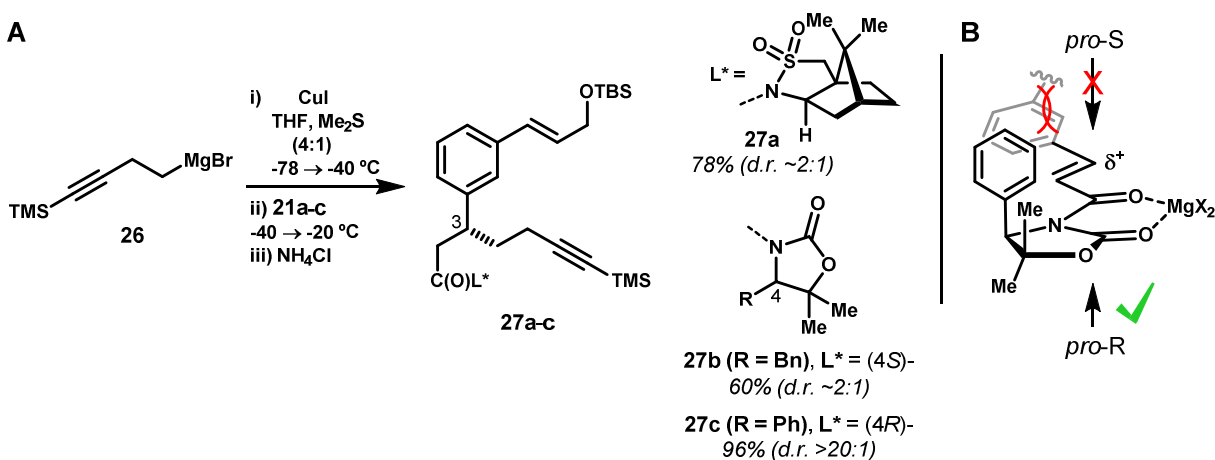


magnesium; a result which was ultimately attributed to trace contamination by bromoform, which exhibited a boiling point similar to that of the product. This contaminant was initially overlooked in the ¹H NMR, but was positively identified by GC-MS. Similar inhibition of Grignard reactions by bromoform has been reported.³² Indeed, bromide **25** free of this contaminant – prepared by *O*-tosylation of homopropargyl alcohol, *C*-silylation, and Finkelstein swap with LiBr in acetone³³ – was reactive towards magnesium metal. Grignard reagent **26** was generated on numerous occasions as moderately concentrated solutions in THF (~0.4–0.6 M), which was quantified by titration against menthol to a red 1,10-phenanthroline endpoint.³⁴ This titration, however, proved rather challenging, as the endpoint was not sharp; a faint pink color typically preceded the true endpoint. Solutions of **26** were alternatively assayed by quenching into water and back titrating against a standardized HCl solution to the phenolphthalein endpoint.³⁵

Homopropargyl Grignard **26** was reactive towards enamide intermediates **21a–c**, and the 1,4-addition was rendered regioselective by stoichiometric transmetalation with copper(I) salts.³⁶ While numerous examples of copper catalyzed 1,4-additions of this type have been reported,^{37,38} we observed substantially cleaner reactions when stoichiometric copper(I) iodide was used. Presumably, transmetalation in this manner using 1:1 Grignard:Cu(I) generates a mono-alkyl copper (RCu) species, rather than the more

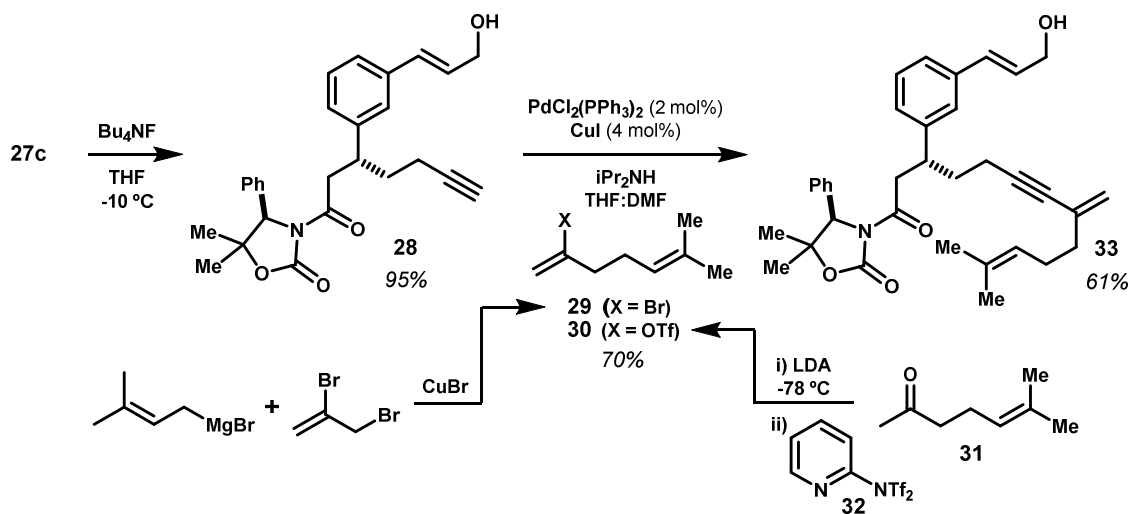
commonly encountered Gilman-type dialkylcuprates (e.g. R_2CuLi or R_2CuMg) or higher-order cuprates (e.g. $R_2Cu(CN)Mg_2X_2$).³⁹ Many organocopper species of these types suffer low solubility in organic solvents, and consequently Me_2S was found to be an essential co-solvent for maintaining a homogeneous, reproducible reaction. We also found the transmetalation step to be somewhat temperature sensitive, with the reaction changing color from dark green to amber. Procedurally, the Grignard reagent was added to a solution of $Cu(I)$ iodide in $Me_2S:THF$ at $-78\text{ }^\circ\text{C}$, then warmed to $-40\text{ }^\circ\text{C}$ and aged for 10 minutes before introduction of the electrophile, with the reaction reliably proceeding to completion at $-20\text{ }^\circ\text{C}$. Of the three chiral auxiliaries examined for diastereoselective 1,4-additions to **21**, phenylglycine-derived 5,5-dimethyloxazolidinone **21c** resulted in the highest diastereoselectivity (Scheme **1.2.6A**). Both Oppolzer's camphor-derived sultam, and the corresponding phenylalanine-derived oxazolidinone yielded **27a** and **27b**, respectively, in an approximately 2:1 ratio of *C3* diastereomers. The improved performance of phenyl versus benzy at this position was consistent with reported conjugate additions using Superquat auxiliaries.³⁶ After optimization of the reaction conditions and workup protocol, intermediate **27c** was obtained in 96% yield as a single diastereomer in high purity without column chromatography. The stereoinduction in this step derives from steric hindrance of the *pro-S* face of the enamide by the phenyl group of the oxazolidinone auxiliary, thereby leading to approach of the cuprate from the *pro-R* face (Scheme **1.2.6B**).

Scheme 1.2.6 A Copper promotes selective 1,4-addition of Grignard reagent **26** into enimides **27**. **B**) Diastereoselectivity results, in the case of substrate **27c**, from steric hindrance by the phenyl group, resulting in addition from the *pro-R* face.



Desilylation of **27c** with tetrabutylammonium fluoride gave alkyne **28**, which was used in the Sonogashira cross coupling reactions to install the 1,5-diene (Scheme 1.2.7).⁴⁰ Vinyl bromide **29**, itself prepared by Gilman addition to 2,3-dibromopropene,⁴¹ while competent in the coupling reaction, was difficult to prepare in high purity, and appeared to be unstable to attempted vacuum distillations. However, the analogous vinyl triflate **30** was readily prepared by reacting the kinetic enolate of 6-methylhept-5-en-2-one (**31**),⁴⁰ an inexpensive commercial flavoring agent, with Comins' 2-pyridyl triflimide.⁴² Triflate **30** was readily purified by distillation *in vacuo*. Unification with alkyne **28** was accomplished using a palladium(II) precatalyst (2 mol%), and copper(I) iodide co-catalyst (4 mol%) at room temperature.⁴⁰ Despite attempts using other amine bases, copper-free conditions,⁴³ and lower temperatures, **33** was obtained in moderate 61% yield after column chromatography.

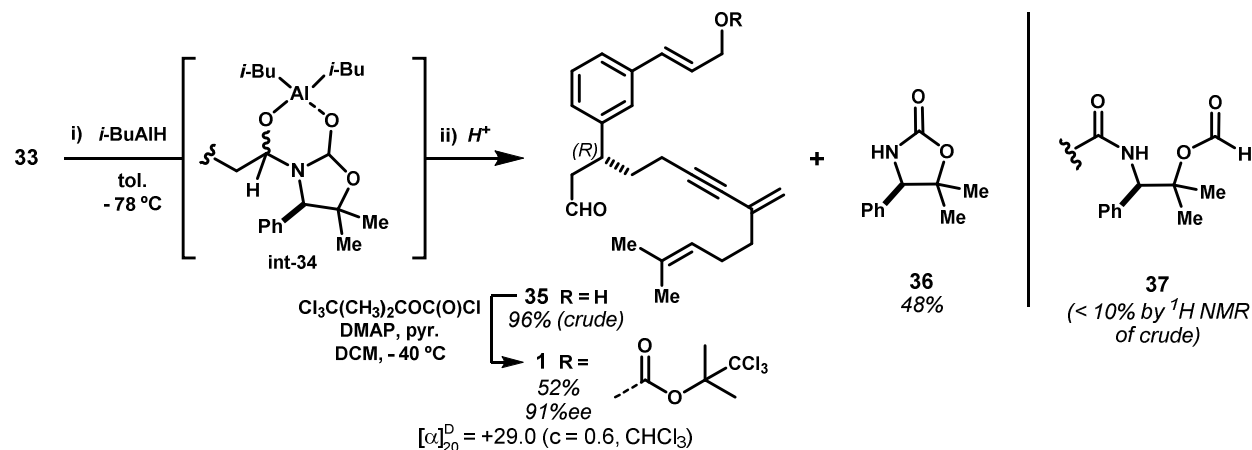
Scheme 1.2.7 Desilylation yielded terminal alkyne **28**, which was used in Sonogashira cross coupling reactions to assemble the diyne moiety.



We next examined reductive removal of the chiral auxiliary to form the aldehyde present in **1**. The dimethyl oxazolidinones had been selected over the more widely used Evans auxiliaries for this purpose; dimethylated variants reportedly slow endocyclic ring opening by strong nucleophiles or reducing agents.³⁶ Semi-reduction of acyloxazolidinone intermediate **33** was achieved using excess diisobutylaluminum hydride in toluene at $-78\text{ }^\circ\text{C}$.⁴⁴ Subsequent aqueous hydrolysis in the presence of Rochelle salt or ammonium chloride liberated desired aldehyde **35** (Scheme 1.2.8). Superstoichiometric reducing agent was required, because 1 equivalent is necessarily consumed by deprotonation of the cinnamyl alcohol.

Nonetheless, we observed only trace over-reduction of the intermediate hemiaminal; likely a result of a stable aluminum chelate (e.g. int-**34**) following 1,2-reduction of the exocyclic carbonyl group. However,

Scheme 1.2.8 Reductive removal of the oxazolidinone chiral auxiliary using DIBALH.

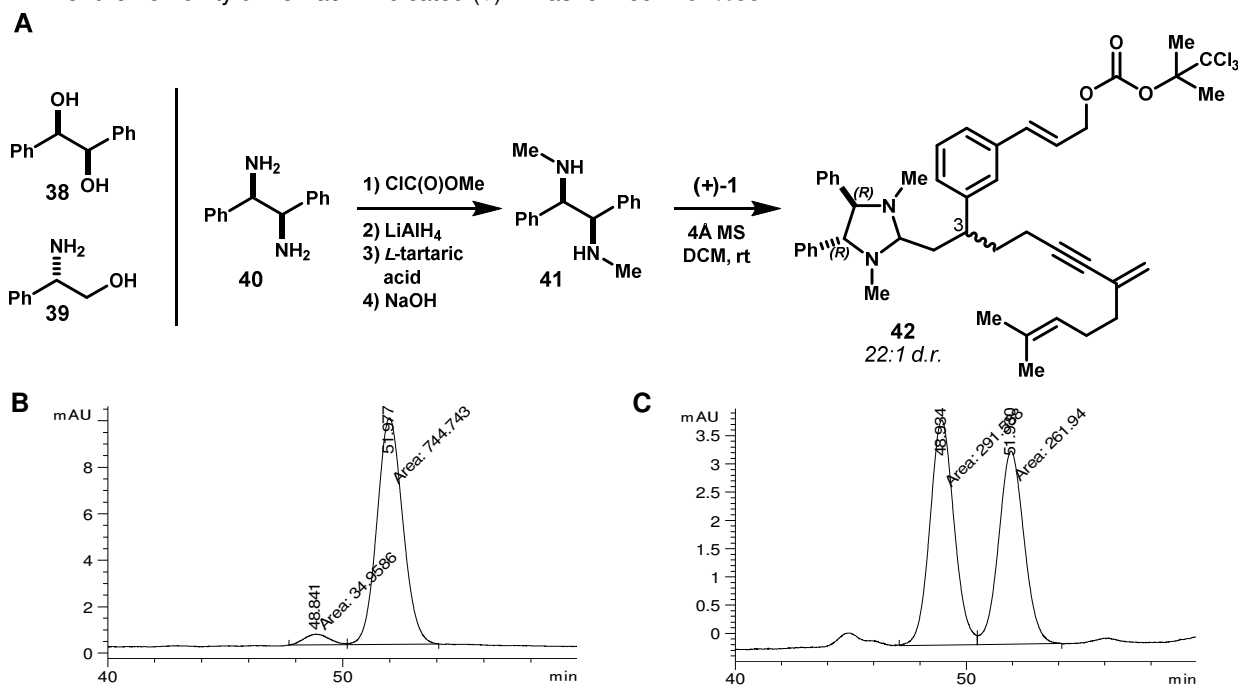


despite judicious choice of oxazolidinone auxiliary, we did observe the endocyclic reduction product **37** as a trace contaminant (<10% by crude ¹H NMR). Additionally, we sought to recover the chiral auxiliary. Despite containing an aryl group, the phenylglycine-derived oxazolidinone was not UV dense at 254 nm, stained poorly with KMnO₄, and stained only moderately with ninhydrin, which complicated chromatographic isolation. Ultimately, auxiliary **36** was recovered from the crude product mixture, albeit in fair yield, by crystallization from Et₂O:pentane solution. This allowed **35** to be carried into the final carbonate formation, as reported previously, without further purification. The optical rotation of **1** was signed opposite that of material produced by the original route, thus confirming the present enantiomer as *R*-(+)-**1**, as expected from the *R*-oxazolidinone.

Whereas chiral HPLC analysis had been utilized previously to determine the enantiopurity of **1**,¹ we instead opted to derivatize the aldehyde to allow assessment as *d.r.* by either NMR or HPLC on achiral stationary phase.⁴⁵ Attempted condensations of *R,R*-hydrobenzoin (**38**, Scheme 1.2.9A), *S*-phenylglycinol (**39**), and *R,R*-1,2-diphenylethanediamine (**40**) were unsuccessful. A more nucleophilic *N,N'*-dimethyl derivative of **40** was therefore prepared.⁴⁶ The bis-methyl carbamate formed from diamine **40** was exhaustively reduced with LiAlH₄, and product **41** was recrystallized as its *L*-tartarate salt to ensure enantiopurity. The diamine underwent condensation with aldehyde **1** at room temperature in the presence of molecular sieves. HPLC analysis indicated 22:1 *d.r.* (Scheme 1.2.9B), and showed no residual **1**, verifying

that we had not incidentally induced kinetic resolution of the *C3* diastereomers. A minor correction was applied based on the non-uniform peak areas (5% anomaly, Scheme 1.2.9C) observed for the *C3* racemate derived by the identical derivatization of *rac*-1, indicating (+)-1 was obtained in 91%*ee*.

Scheme 1.2.9 A) Diastereomeric derivatization of (+)-1. **B)** HPLC analysis indicated 22:1 *d.r.* **C)** Correction for the non-unity *d.r.* of *rac*-1 indicated (+)-1 was formed in 91%*ee*.

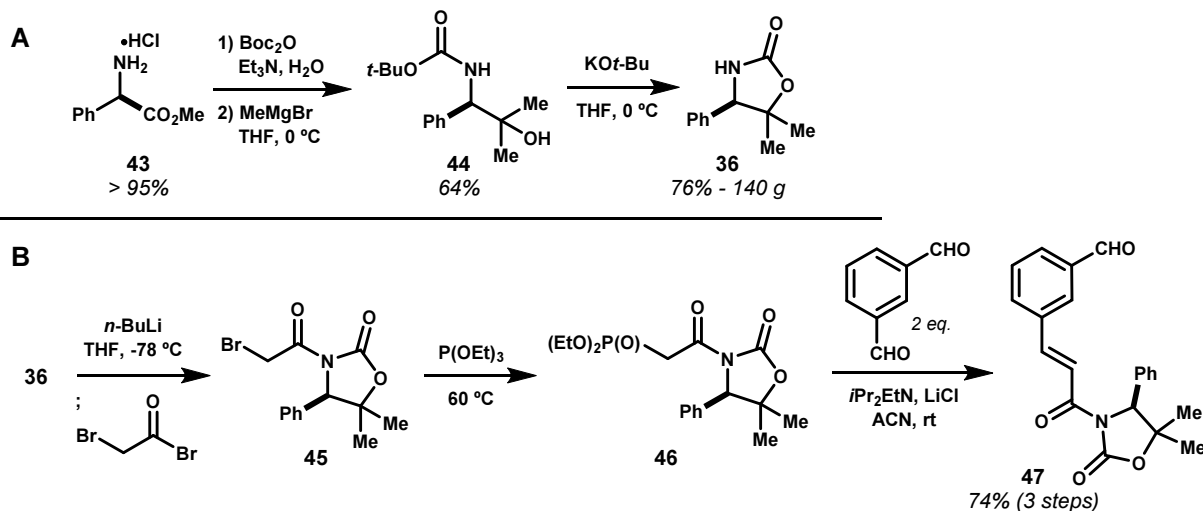


1.3 A scalable route to conjugate addition precursors

Having validated this diastereoselective 1,4-addition approach to set the *C3* stereocenter, we returned to identifying scalable access of intermediate **21c**. The *D*-phenylglycine-derived oxazolidinone **36** was prepared on 140 g scale according to the literature protocol (Scheme 1.3.1A).⁴⁷ In keeping with desymmetrization approaches using isophthalaldehyde as an inexpensive starting material, we envisioned concomitantly installing the chiral auxiliary and the two additional carbons of the cinnamate moiety by Horner-Wadsworth-Emmons olefination using a suitably tailored phosphonacetyl oxazolidinone (**46**, Scheme 1.3.1B). The auxiliary could be deprotonated and *N*-acylated with bromoacetyl bromide, affording **45**, which was subjected to Michaelis-Arbuzov reaction with triethylphosphite. Crude phosphonate **46** of relatively high purity could be produced in this manner, and was taken forward into the olefination reaction. This desymmetrization reaction required the use of excess isophthalaldehyde in order to favor mono-

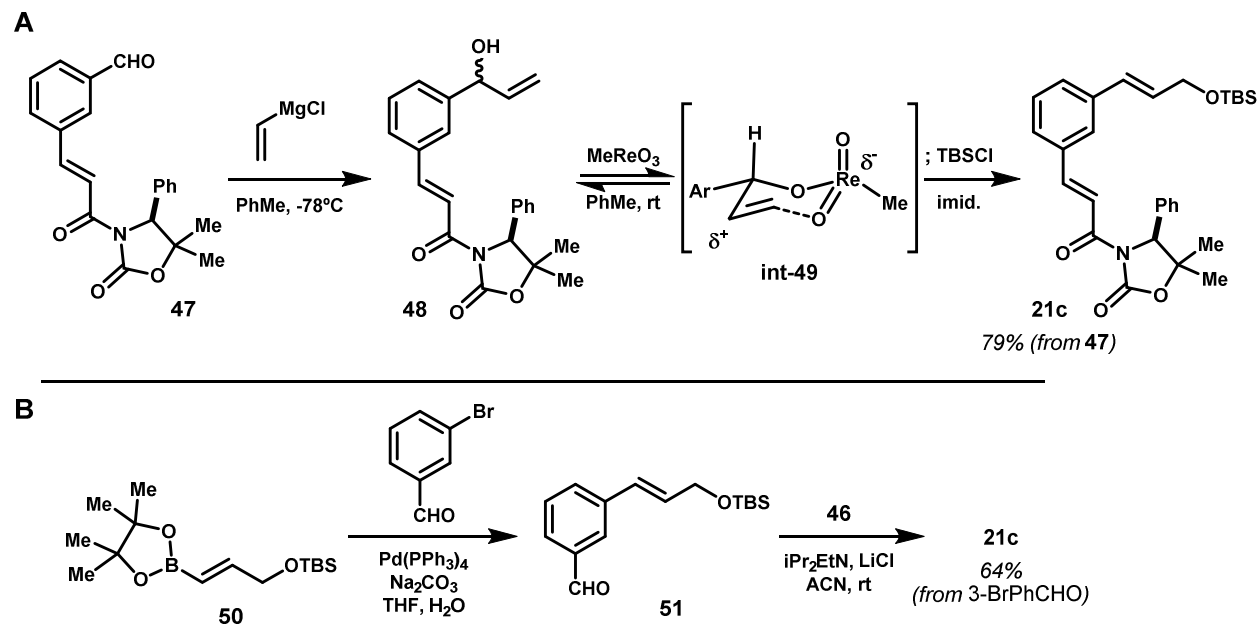
olefination over its C2 symmetric bis-olefin congener. Though some residual isophthalaldehyde could be removed by sublimation, this proved unreliable, and product **47** was ultimately isolated in 74% yield by column chromatography.

Scheme 1.3.1 A) Large-scale synthesis of *D*-phenylglycine-derived chiral auxiliary. **B)** Installation of the chiral oxazolidinone **36** by Horner-Wadsworth-Emmons olefination and desymmetrization of isophthalaldehyde.



We then targeted introduction of the remaining two carbons of the cinnamyl alcohol moiety present in intermediate **21c**. A reported Julia-Kocienski olefination seemed ideal for this transformation,⁴⁸ because it would also install the silyl protecting group. However, preparation of the required sulfonyltetrazole was both step-intensive and poorly scalable. We instead developed a two-step protocol employing 1,2-addition of vinylmagnesium bromide to the aldehyde of **47** to give α -phenylallyl alcohol **48** (Scheme 1.3.2A), and rearrangement to the cinnamyl alcohol with catalytic amounts of MeReO_3 (3 mol%). This rearrangement is driven thermodynamically by the increased conjugation of the product, and is thought to proceed by reversible condensation to form an alkoxy rhenium complex (int-**49**), which undergoes sigmatropic rearrangement and hydrolysis. Upon completion of the rearrangement, observed by HPLC, TBSCl and imidazole were added to give silyl protected product **21c** in good yield following chromatographic purification.

Scheme 1.3.2 A) Assembly of the cinnamyl alcohol by 1,2-addition of vinyl Grignard and Re(IV)-catalyzed rearrangement. **B)** Installation of the cinnamyl alcohol by Suzuki-Miyaura coupling with vinylboronate **50**.



We prepared over 15 g of *R*-(+)-**1** across several batches, each in good optical purity, using the revised synthetic routes discussed here. A revised route to (+)-**1** was communicated in 2011,⁴⁹ and supplied material to reinitiate investigations of its reactions with peptidic substrates, the results of which comprise discussions in Chapters 2 and 3.

References

- (1) Zhao, H.; Negash, L.; Wei, Q.; LaCour, T. G.; Estill, S. J.; Capota, E.; Pieper, A. A.; Harran, P. G. *J. Am. Chem. Soc.* **2008**, *130*, 13864.
- (2) Hayashi, T. *Synlett* **2001**, 879.
- (3) Rossiter, B. E.; Swingle, N. M. *Chem. Rev.* **1992**, *92*, 771.
- (4) Alexakis, A.; Ba, J. E.; Krause, N.; Pa, O.; Die, M. *Chem. Rev.* **2008**, *108*, 2796.
- (5) Ouellet, S. G.; Tuttle, J. B.; MacMillan, D. W. C. *J. Am. Chem. Soc.* **2005**, *127*, 32.
- (6) Sörgel, S.; Tokunaga, N.; Sasaki, K.; Okamoto, K.; Hayashi, T. *Org. Lett.* **2008**, *10*, 589.
- (7) Paquin, J. F.; Stephenson, C. R. J.; Defieber, C.; Carreira, E. M. *Org. Lett.* **2005**, *7*, 3821.
- (8) Sakuma, S.; Sakai, M.; Itooka, R.; Miyaura, N. *J. Org. Chem.* **2000**, *65*, 5951.
- (9) Klusener, P. A. A.; Kulik, W.; Brandsma, L. *J. Org. Chem.* **1987**, *52*, 5261.
- (10) Ohshita, J.; Iwata, A.; Kanetani, F.; Kunai, A.; Yamamoto, Y.; Matui, C. *J. Org. Chem.* **1999**, *64*, 8024.
- (11) Ramana, C. V.; Suryawanshi, S. B.; Gonnade, R. G. *J. Org. Chem.* **2009**, *74*, 2842.
- (12) Normant, H. *Angew. Chemie - Int. Ed.* **1967**, *6*, 1046.
- (13) Nicolaou, K. C.; Montagnon, T.; Baran, P. S. *Angew. Chemie - Int. Ed.* **2002**, *41*, 993.

- (14) Boeckman, R. K. J.; Shao, P.; Mullins, J. J. *Org. Synth.* **2000**, *77*, 141.
- (15) Frigerio, M.; Santagostino, M.; Sputore, S. *J. Org. Chem.* **1999**, *64*, 4537.
- (16) Matteson, D. S. *Tetrahedron* **1989**, *45*, 1859.
- (17) Blanchette, M. A.; Choy, W.; Davis, J. T.; Essenfled, A. P.; Masamune, S.; Roush, W. R.; Sakai, T. *Tetrahedron Lett.* **1984**, *25*, 2183.
- (18) Michels, H.-P.; Nieger, M.; Vögtle, F. *Chem. Ber.* **1994**, *127*, 1167.
- (19) Kitagawa, K.; Inoue, A.; Shinokubo, H.; Oshima, K. *Angew. Chem. Int. Ed. Engl.* **2000**, *39*, 2481.
- (20) Ishiyama, T.; Murata, M.; Miyaura, N. *J Org Chem* **1995**, *60*, 7508.
- (21) Hobbs, D. M.; Schubert, P.; Tung, H. *Ind. Eng. Chem. Res.* **1997**, *36*, 5302.
- (22) Oppolzer, W. *Tetrahedron* **1987**, *43*, 1969.
- (23) Weismiller, M. C.; Towson, J. C.; Davis, F. A. *Org. Synth.* **1990**, *69*, 154.
- (24) Towson, J. C.; Weismiller, M. C.; Lal, S.; Sheppard, A. C.; Kumar, A.; Davis, F. A. *Org. Synth.* **1990**, *69*, 158.
- (25) Bull, S. D.; Davies, S. G.; Nicholson, R. L.; Sanganee, H. J.; Smith, A. D. *Org. Biomol. Chem.* **2003**, *1*, 2886.
- (26) Ho, G.; Mathre, D. J. *J. Org. Chem.* **1995**, *60*, 2271.
- (27) Yamamoto, Y.; Maruyama, K. **1978**, *100*, 3240.
- (28) Knochel, P.; Singer, R. D. *Chem. Rev.* **1993**, *93*, 2117.
- (29) Jones, P.; Kishan Reddy, C.; Knochel, P. *Tetrahedron* **1998**, *54*, 1471.
- (30) Bian, J.; Van Wingerden, M.; Ready, J. M. *J. Am. Chem. Soc.* **2006**, *128*, 7428.
- (31) Dobbs, A. P.; Jones, K.; Veal, K. T. *Tetrahedron* **1998**, *54*, 2149.
- (32) Bartley, D. M.; Coward, J. K. *J. Org. Chem.* **2005**, *70*, 6757.
- (33) Dower, W. V.; Vollhardt, P. C. *Tetrahedron* **1986**, *42*, 1873.
- (34) Lin, H.-S.; Paquette, L. A. *Synth. Commun.* **1994**, *24*, 2503.
- (35) Silverman, G. S.; Rakita, P. E. *Handbook of Grignard Reagents*; CRC Press: New York, NY, 1996.
- (36) Davies, S. G.; Sanganee, H. J.; Szolcsanyi, P. *Tetrahedron* **1999**, *55*, 3337.
- (37) López, F.; Harutyunyan, S. R.; Minnaard, A. J.; Feringa, B. L. *J. Am. Chem. Soc.* **2004**, *126*, 12784.
- (38) Kharash, M. S.; Tawney, P. O. *J. Am. Chem. Soc.* **1941**, *63*, 2308.
- (39) Ley, S. V.; Kouklovsky, C. In *Comprehensive Organic Functional Group Transformations: Synthesis: carbon with one heteroatom attached by a single bond*; Katritzky, A. R., Ley, S. V., Meth-Cohn, O., Rees, C. W., Eds.; Elsevier Ltd: Cambridge, UK, 1995; pp 585–586.
- (40) Miller, M. W.; Johnson, C. R. *J. Org. Chem.* **1997**, *62*, 1582.
- (41) Mushti, C. S.; Kim, J.; Corey, E. J. *J. Am. Chem. Soc.* **2006**, *128*, 14050.
- (42) Comins, D. L.; Dehghani, A.; Foti, C. J.; Joseph, S. P. *Org. Synth.* **1997**, *74*, 77.
- (43) Soheili, A.; Albanese-Walker, J.; Murry, J. A.; Dormer, P. G.; Hughes, D. L. *Org. Lett.* **2003**, *5*, 4191.
- (44) Bach, J.; Bull, S. D.; Davies, S. G.; Nicholson, R. L.; Sanganee, H. J.; Smith, A. D. *Tetrahedron Lett.* **1999**, *40*, 6677.
- (45) Cuvilot, D.; Mangeney, P.; Alexakis, A.; Normant, J. F.; Lellouche, J. P. *J. Org. Chem.* **1989**, *54*, 2420.
- (46) Kuznetsov, V. F.; Jefferson, G. R.; Yap, G. P. A.; Alper, H. *Organometallics* **2002**, *21*, 4241.
- (47) Bull, S. D.; Davies, S. G.; Jones, S.; Polywka, M. E. C.; Shyam Prasad, R.; Sanganee, H. J. *Synlett* **1998**, 519.
- (48) Pospíšil, J.; Markó, I. E. *Org. Lett.* **2006**, *8*, 5983.
- (49) Lawson, K. V.; Rose, T. E.; Harran, P. G. *Tetrahedron Lett.* **2011**, *52*, 653.

2 Continued evaluation of the reactivity of template 1 towards arene-containing oligopeptides

2.1 Introduction

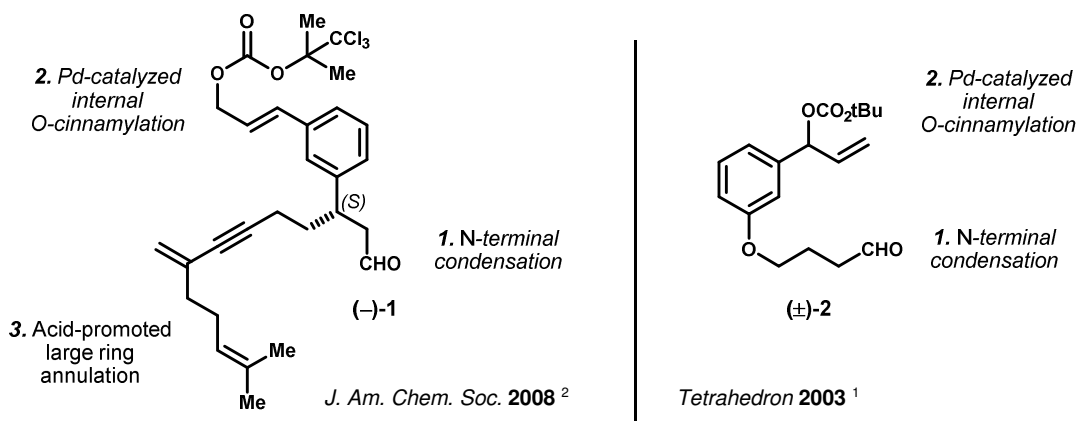
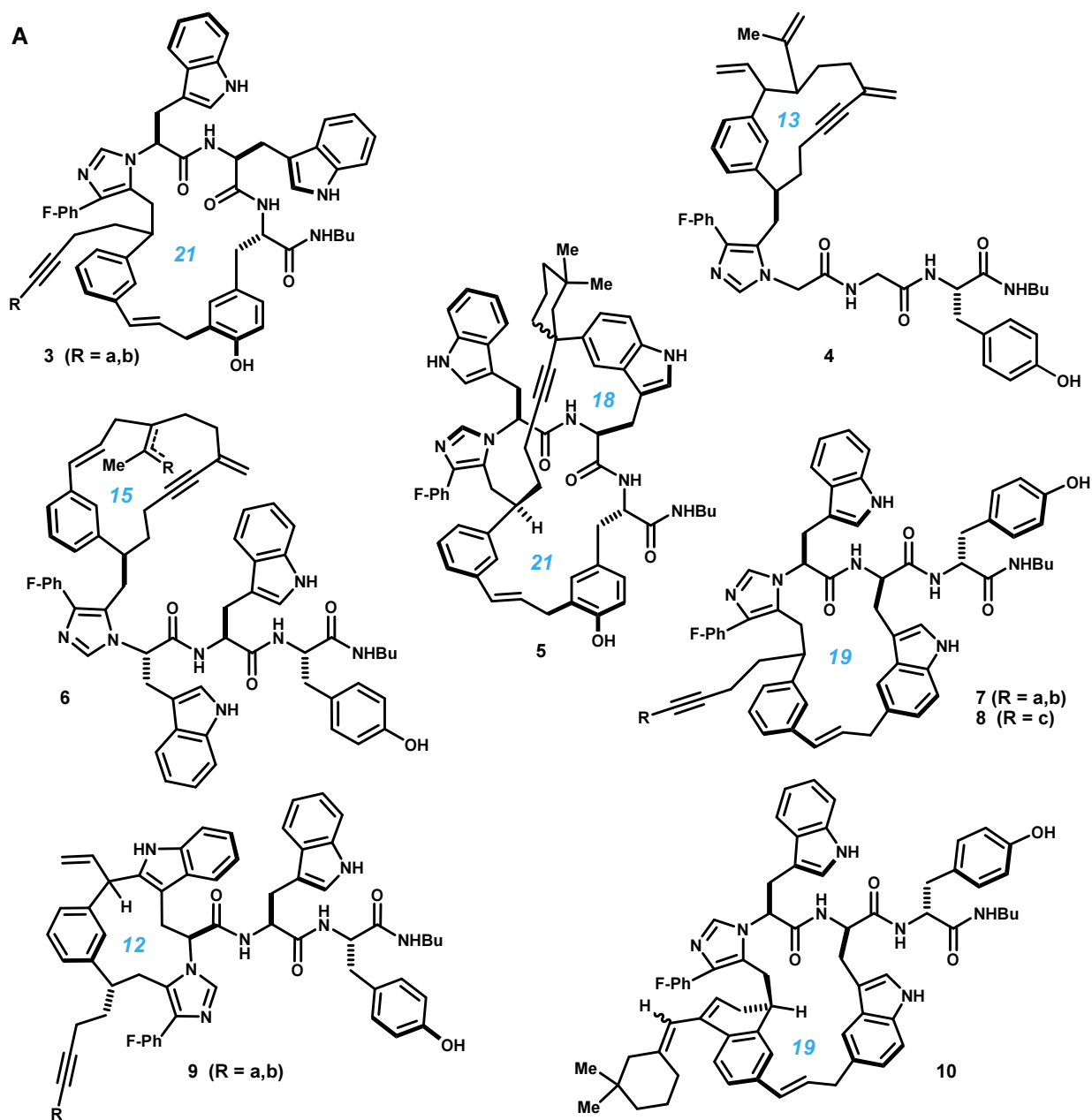


Figure 2.1.1 Prototype templates 1 and 2 initiate structural remodeling of oligopeptides. Both 1 and 2 undergo condensation with a peptidyl amino group and Pd-catalyzed large ring-forming *O*-cinnamylation. The dienyne appendage in 1 is designed to affect large ring annulations by electrophilic substitution of peptide side chain aryl groups.

Building upon a previous bi-functional template design (2, Figure 2.1.1) reported by our laboratory in 2003,¹ congener 1 was designed to function in three steps: 1) condensation between the aldehyde and the N-terminus of the peptide and dipolar cycloaddition of a tosylmethyl isonitrile at the resultant imine; 2) palladium-catalyzed internal *O*-cinnamylation of a tyrosyl phenol, and 3) acid-promoted rearrangement of the dienyne appendage to give a second internal linkage to the peptide by electrophilic substitution at aryl side chains by the dienyne appendage.² Studies reported by our laboratory in 2008 using (-)-1 with model tripeptides Gly-Gly-Tyr, Gly-Trp-Tyr and Trp-Trp-Tyr provided initial insight into the inherent reactivity of this template and a strong validation of the overall drug discovery approach. Through a bioactivity-guided isolation of a single product which induced hippocampal neurogenesis *in vivo* in the mouse.² These impressive initial studies of both the palladium-catalyzed cyclization and acid-promoted rearrangements generated additional questions surrounding each of these steps, which we hoped to address.

Towards the goal of using 1 to process a diverse array of peptide substrates to continue biological screening efforts, we first sought to more broadly examine the generality and efficiency of this template. In particular, we were interested in its performance in the context of highly functionalized peptide substrates



B

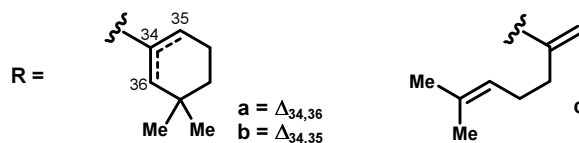
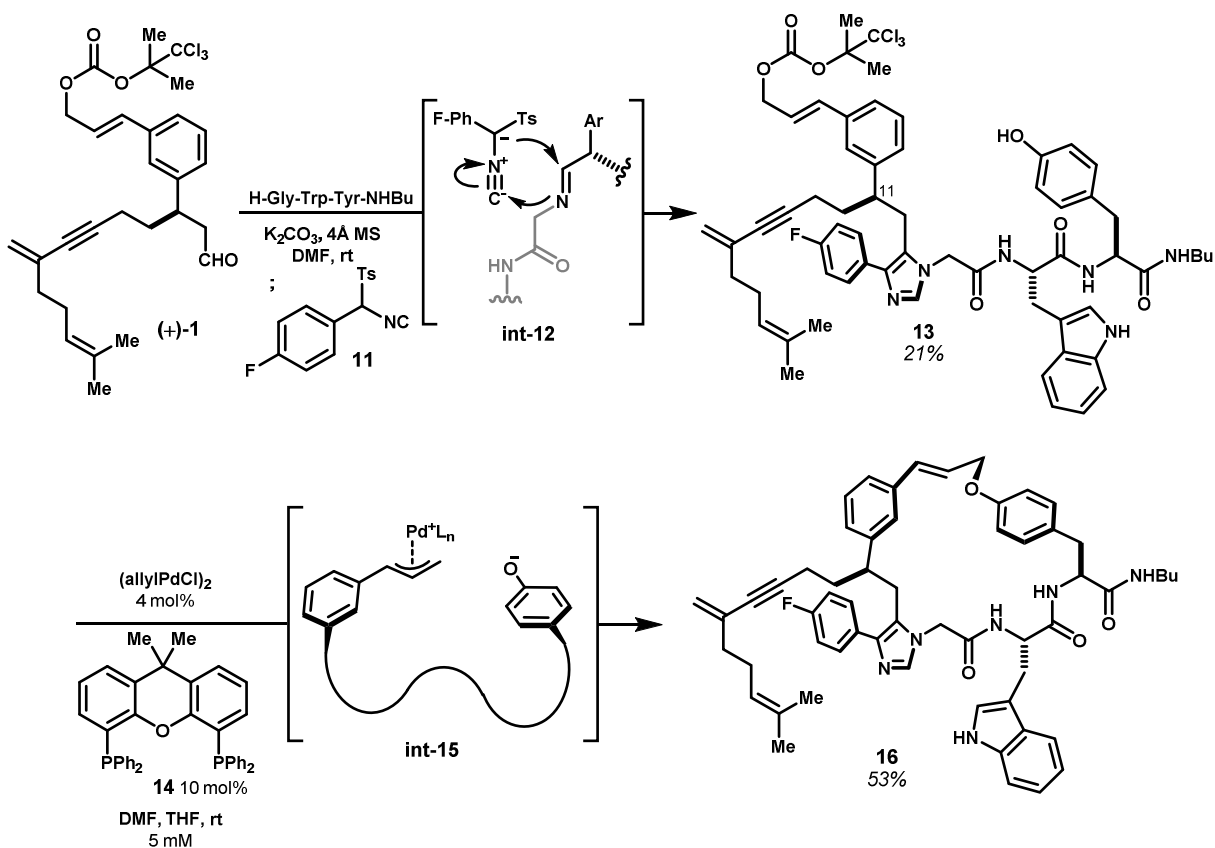


Figure 2.1.2 Previously reported products derived from acidolysis of the cyclic tyrosyl ether derived from ligation of (-)-1 with model tripeptide Trp-Trp-Tyr-NHBu. Unique product **4** derived from Gly-Gly-Tyr-NHBu. **A)** Primary large-ring structures in these products derive mainly from long-range *O*→*C* cinnamyl migration. Products **3**, **4** and **6**–**10** possess constitutionally diverse 12, 13, 15, 19- or 21-membered rings. Uniquely, product **5** possesses a second macrocyclic linkage from transannular electrophilic substitution of the diene appendage, presumably arising via compounds **3a,b** *in situ*. **B)** The 1,5-diene motif (**c**) showed a propensity to rearrange to isomeric cyclohexenes (**a,b**).

containing all natural amino acid side chains – less cysteine, given its unvalued propensity to dimerize by disulfide bonding. It was unclear whether polar side chains, such as those of arginine, serine/threonine, aspartate/glutamate or histidine, might interfere with Pd-catalyzed processes or act as nucleophiles in acid-promoted cationic reactions. Additionally, **1** had been designed to affect transannular carbon-carbon bond formation by electrophilic substitution reactions at the dienyne appendage, but only one such outcome (**5**, Figure 2.1.2A) was observed from peptide substrate Trp-Trp-Tyr. Therefore, we questioned whether this outcome, desired for its rigidification of the product, would occur generally in the context of peptides harboring multiple electron-rich aryl side chains. In addition to the one bi-macrocyclic product, eleven structural isomers were reported, each monocyclic, resulting from long-range *O*→*C* rearrangement from the intermediate cinnamyl tyrosyl ether to the aryl side chains of both tyrosine and tryptophan (e.g. **3–10** Figure 2.1.2). Concomitantly with these very intriguing cinnamyl migrations, the dienyne was found to have rearranged under the strongly acidic reaction conditions, affording primarily cyclohexene products as a result of cyclization of the 1,5-diene motif (Figure 2.1.2B).

Using (+)-**1**, derived by a revised synthetic route (see Chapter 1), we re-visited model peptide Gly-Trp-Tyr-NHBu in order to verify comparable performance between this template and its enantiomer (–)-**1**, studied previously. Template (+)-**1** and this tripeptide were dissolved in DMF and treated with molecular sieves and powdered K_2CO_3 to facilitate condensation between the aldehyde of **1** and the peptide N-terminus (Scheme 2.1.1). Subsequent van Leusen cyclization was initiated by addition of TosMIC reagent 4-fluorophenyltosylmethylisonitrile (**11**)^{3,4} to form imidazole **13**. Mechanistically, this proceeds by deprotonation of the TosMIC reagent, addition of this stabilized anion into the aldimine (int-**12**), 5-*endo* cyclization of the resultant amine onto the isonitrile, and lastly β -elimination of toluenesulfinate to form the aromatic imidazole ring.⁵ While the authors previously reported isolation of C11 *epi*-**13** in 70% yield, we obtained **13** in mere 21% yield after chromatographic purification. We observed consistently low yields in this reaction over several attempts, despite using freshly prepared **2**,^{3,4} and across a range of peptide substrates (*vide infra*). Purified **13** was then dissolved in DMF to a concentration of 5 mM, carefully degassed by sparging with argon, and treated with a pre-catalyst generated from η^3 -allylpalladium chloride dimer (4 mol%) and bisphosphine ligand Xantphos (**14**, 10 mol%), as reported.^{1,2} Over several attempts, we found this reaction to be sensitive to oxygen, the purity of the starting material, the protocol used for

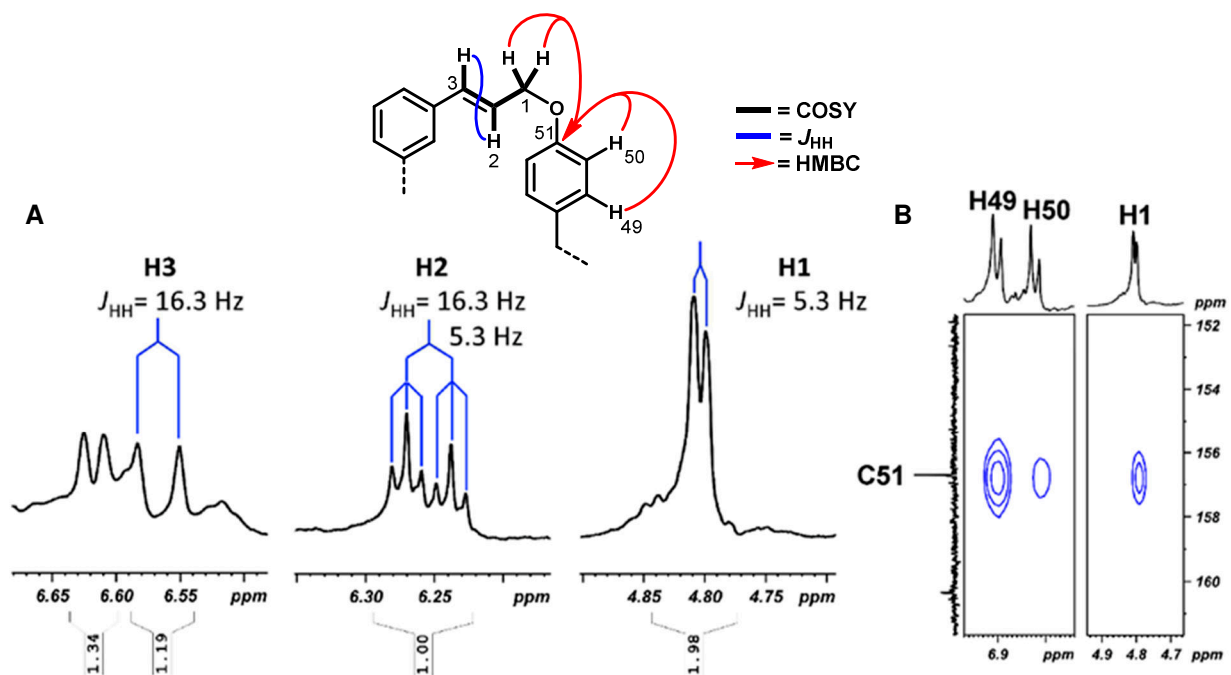
Scheme 2.1.1 A) Template (+)-1 undergoes condensation at the N-terminus of Gly-Trp-Tyr followed by van Leusen cyclization with TosMIC reagent **11**, yielding linear imidazole **13**. Treatment of this material with catalytic Pd⁰ leads to cyclization by *O*-cinnamylation of the tyrosyl phenol, presumably via an intermediate cationic cinnamyl-Pd^{II} complex and phenolate nucleophile.



preparing the precatalyst mixture, and the catalyst loading. Crystallographic characterization and kinetic studies of the complex in related allylation reactions reported by the Hartwig laboratory suggest that the wide bite angle of Xantphos plays an important role in accelerating nucleophilic addition to the intermediate (allyl)Pd complex, as well as catalyst turnover.⁶ Notably, they also observed (Xantphos)PdCl₂ as a catalytically inactive decomposition product. When properly prepared, we observed that stock solutions of catalytically active precatalyst developed a yellow color that was substantially more intense than the starting η³-allylpalladium chloride dimer. Additionally, this color quickly faded upon exposure to air. Ultimately, through careful control of these parameters, we observed rapid conversion of **13** to **16** (< 1 hr) at room temperature.

We posit that the catalyst inserts into the cinnamyl carbonate, and that dissociation, and possibly decomposition, of the resulting *tert*-butyl carbonate provides an equivalent of base which deprotonates the

tyrosyl phenol pronucleophile. This results in an internal ion pair (int-**15**) then undergoes internal nucleophilic substitution of the (cinnamyl)Pd^{II} complex by the phenolate ion,^{7,8} forming the macrocyclic C–O bond. From the cyclization of **13** in this manner, we isolated the anticipated macrocyclic cinnamyl tyrosyl ether **16** in moderate yield (53% vs. 67% reported previously²) and relatively high purity following purification by column chromatography. Though this outcome tracked a large number of successful reactions of this type performed in our laboratory, we nonetheless were careful to fully assign the macrocyclic linkage using 2D NMR correlation spectra.



The ¹H NMR spectrum of **16** displayed prominent signals for the propenyl moiety within the cinnamyl bridge, which allowed straightforward assignment of the tyrosyl ether bond. This propenyl spin system (Figure 2.1.3) was also apparent by ¹H-¹H COSY, and the expected *trans* olefin stereochemistry confirmed by the 16.3 Hz coupling constant. The ether C–O bond was subsequently assigned on the basis of a correlation observed in the ¹H-¹³C HMBC spectrum from H1 to a carbon at 156.7 ppm. The two doublets ($J_{\text{HH}} = 8.5$ Hz, 2H) of the *para*-substituted tyrosine side chain were also clearly visible, and both exhibited correlation to the carbon at 156.7 ppm, thereby confirming this ¹³C resonance as C51 of tyrosine. The

complete structure was thereby assigned based on its mass spectrum and 1D-¹H, 1D-¹³C, homonuclear and heteronuclear correlation NMR spectra.

With macrocyclic tyrosyl ether **16** in hand, we were confident that template (+)-**1** would perform as expected. Compound **16** was not taken forward to the acid-promoted rearrangement reaction. Given that the enantiomer of **1** now being used would afford diastereomeric products relative to those previously isolated and characterized from model sequence Gly-Trp-Tyr, we would not have been able to directly compare our results to the reported structural data. Consequently, we shifted efforts to preparing novel peptidyl substrates to begin examining the acid-promoted rearrangement chemistry.

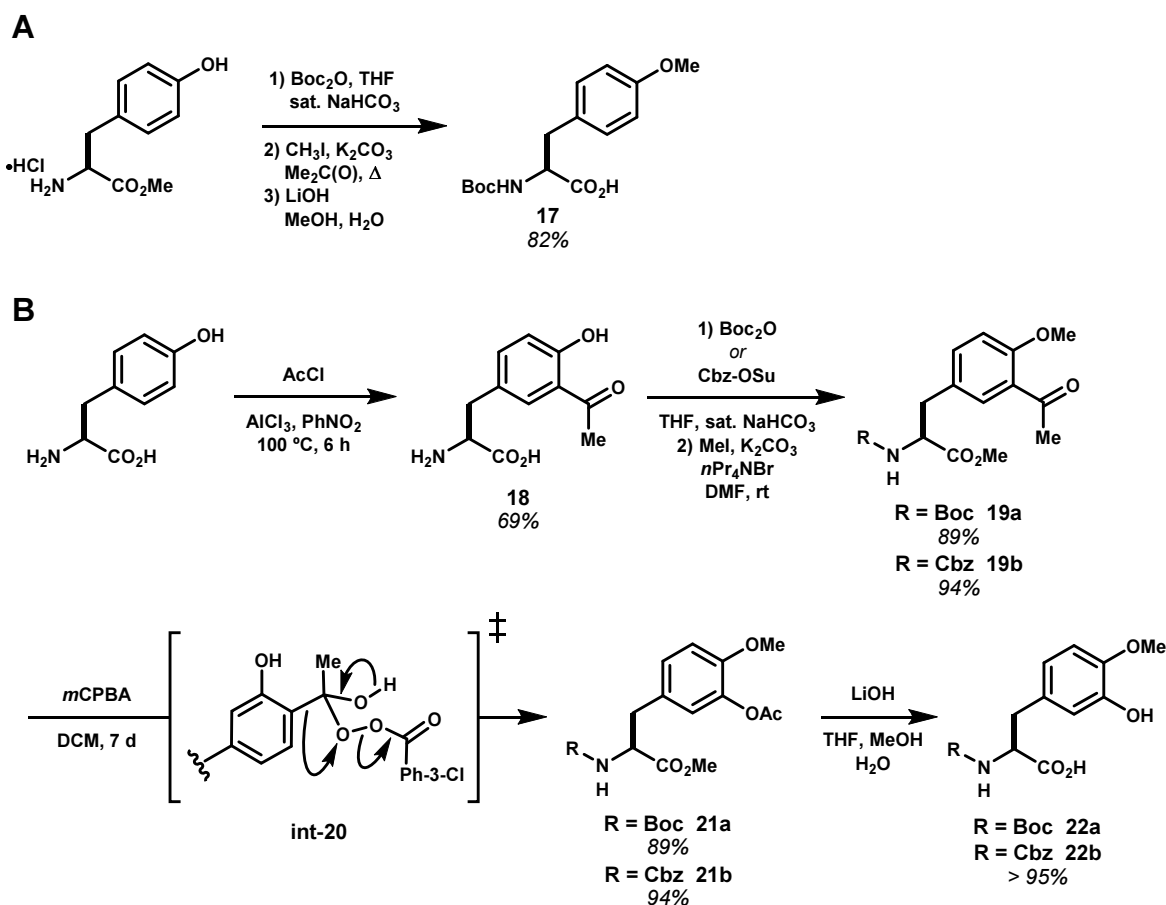
2.2 Complex oligomers harboring multiple nucleophilic side chain arenes

In our continued efforts to explore the reactivity of template **1**, we were cognizant that the structures being generated would ideally need to be distinct from those discovered previously. In this vein, we prepared a small collection of synthetic amino acids bearing aryl side chains that we expected would act as nucleophiles during the acid-promoted rearrangement reaction of macrocyclic cinnamyl ethers. Given that the cinnamyl group was previously found to migrate primarily by ring contraction to the position *ortho* to the tyrosyl phenol, peptidyl substrates were prepared which displayed additional aryl side chains designed to engage the dienyne appendage.

To begin testing for transannular engagement of the dienyne, eleven non-natural amino acids were synthesized which displayed electron rich side chain arenes. For simplicity, we began from naturally-derived *L*-amino acids, rather than approach enantioselective amino acid syntheses at this time (see also Chapter 6). Tyrosine was transformed, via its *N*-Boc methyl ester, to methyl ether **17** by treatment with MeI and K₂CO₃ (Scheme **2.2.1A**). It was hoped that this side chain would be similarly reactive to tyrosine, but allow incorporation into peptides alongside tyrosine without competing in the Pd-catalyzed *O*-cinnamylation. Additionally, a mono-methyl *L*-DOPA derivative, anticipated to be highly reactive in electrophilic reactions, was prepared by the route reported by Boger and co-workers (Scheme **2.2.1A**).⁹ Free tyrosine was first acetylated under Friedel-Crafts conditions to give acetophenone **18**, which was readily recrystallized from 5 N hydrochloric acid, then *N*^α-Boc or -Cbz protected and doubly *O*-methylated to give **19**. Baeyer-Villiger oxidation using *meta*-chloroperbenzoic acid, while sluggish, afforded high conversion to acetate **21** after 7

days. This oxidation proceeds regioselectively, wherein the aryl group migrates to decompose the Criegee intermediate (int-20), rather than the methyl group. This preference is generally thought to result from the larger steric bulk and ability of the migrating group to stabilize positive charge developing in the transition state.¹⁰ The rearrangement of acetophenones to phenolic esters in this manner is well-documented.¹¹ Subsequent saponification of both the aryl acetate and methyl ester provide **22**.

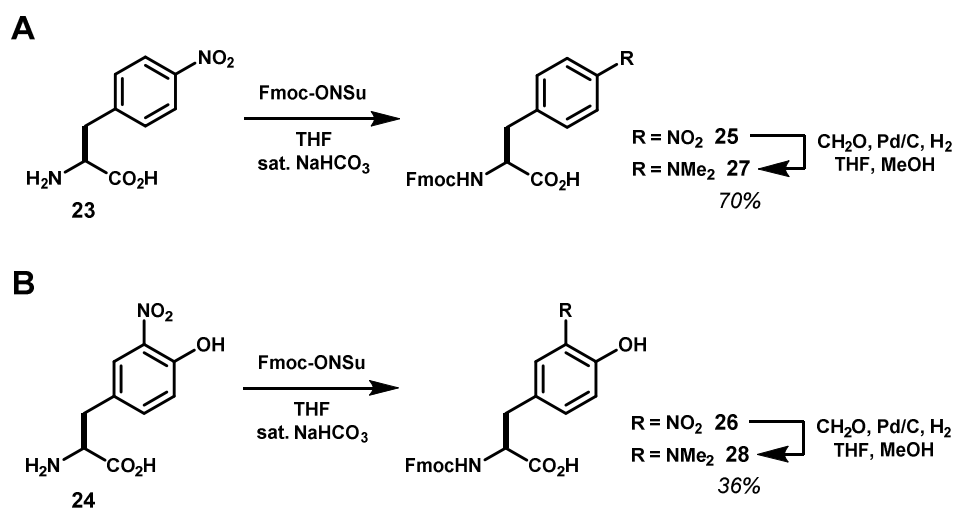
Scheme 2.2.1 A) 4-Methoxyphenylalanine is accessible by *O*-methylation of *L*-tyrosine. B) *L*-DOPA derivatives **22** were prepared from *L*-tyrosine by Friedel-Crafts acetylation, Baeyer-Villiger oxidation and saponification.⁹



N,N-Dimethylamino-substituted phenylalanines were also prepared, given the strong electron-donating ability of this substituent.¹² Unfortunately, it wasn't recognized at the time that, despite being favorably electron rich, anilines would likely be unreactive as nucleophiles in Friedel-Crafts reactions during the acid-promoted rearrangement step.¹³ Under strongly protic- or Lewis-acidic conditions, anilines are readily protonated/coordinated, thereby abrogating the activating power of the amino substituent.

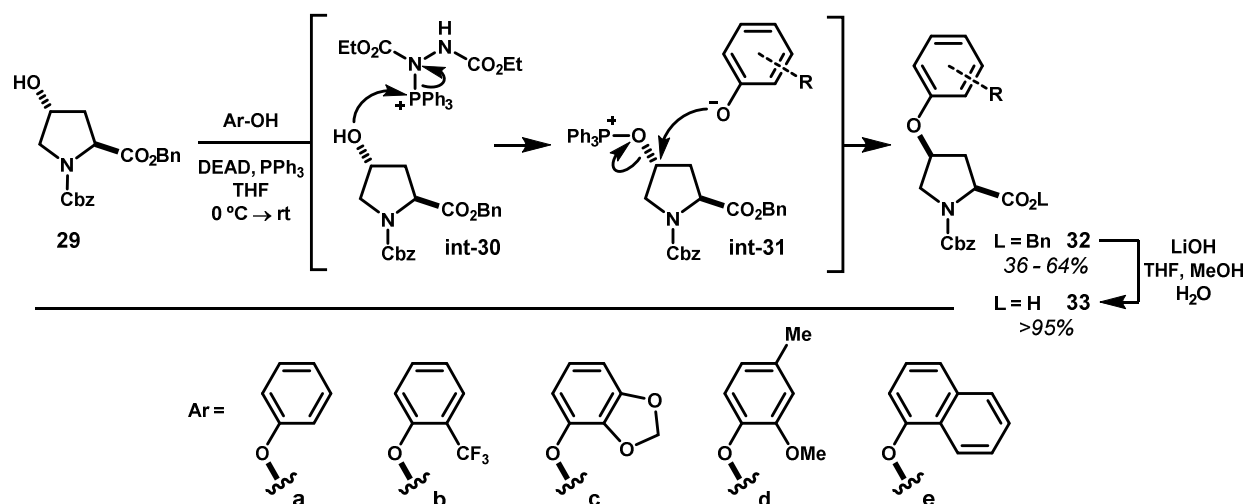
Irrespective of this, these phenylalanine derivatives may be interesting for their biological or chemical properties. *N*^α-Fmoc derivatives **25** and **26** (Scheme 2.2.2) were prepared starting from nitrophenylalanine¹⁴ (**23**) and nitrotyrosine^{15,16} (**24**), respectively. These materials were reduced by the action of palladium on charcoal under an atmosphere of hydrogen, and in the presence of formaldehyde underwent reductive amination of the resulting aniline in situ. Fmoc-(4-Dimethylaminophenyl)alanine (**27**) and 3-dimethylamino-4-hydroxyphenylalanine (**28**) were isolated in moderate yield following column chromatography, but were nonetheless obtained in multi-gram quantities.

Scheme 2.2.2 Synthesis of dimethylamino substituted phenylalanine (**A**) and tyrosine (**B**) by hydrogenation of the respective *N*^α-Fmoc derivatives of nitrated amino acids **23** and **24** followed by *in situ* reductive amination with formaldehyde.



O-Arylated derivatives of 4-hydroxy-*L*-proline were also targeted, because the aryl group, derived from the corresponding phenol, could be readily modified. We postulated that the pyrrolidine ring might force the aryl group to be displayed angularly to an initially formed cinnamyl macrocycle, thereby assisting in large ring-forming annulations of the diene. Additionally, these amino acids were readily accessible following reported protocols.¹⁷ Hydroxyproline was *N*-Cbz protected, and further protected as its benzyl ester to give **29** (Scheme 2.2.3), which served as substrate in Mitsunobu reactions. Five derivatives were prepared using phenols **a–d**. Protected hydroxyproline, the appropriate phenol and triphenylphosphine were dissolved in THF and treated with diethylazodicarboxylate (DEAD). Initial reaction between triphenylp-

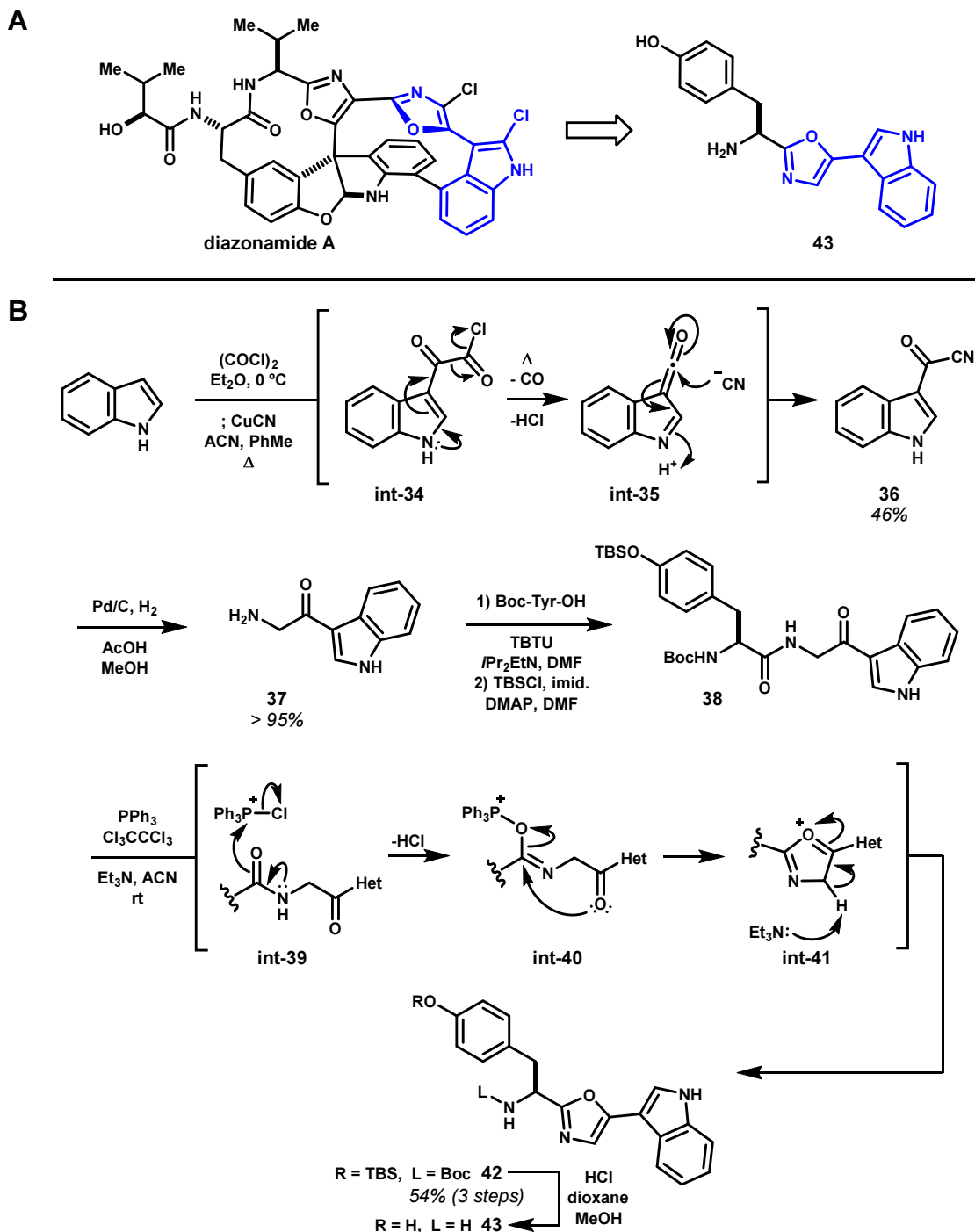
Scheme 2.2.3 Synthesis of *cis*-*O*-aryl hydroxyprolines by Mitsunobu inversion using phenols **a–e**.



phosphine and DEAD generates a phosphonium aza-ylide, which deprotonates the phenol, and then reacts with the prolyl hydroxyl group (int-30). The resulting oxophosponium salt is then susceptible to nucleophilic displacement by the phenolate, which proceeds in a purely S_N2 fashion to give *cis*-4-aryloxyprolines **32**. These products were isolated in low to moderate yield, likely resulting from the isolation, though the reaction also appeared highly sensitive to the quality of the commercial DEAD reagent. Following completion of the reaction, the solvent was removed, and the residue was triturated with diethyl ether to precipitate the triphenylphosphine oxide generated in the reaction. This was found necessary to facilitate effective dry loading of the crude product onto silica gel to allow flash chromatography. Isolated products **32a–d** were then saponified to remove the benzyl ester. This poorly-chosen protecting group, initially selected to allow removal by hydrogenolysis with little risk of epimerization, necessitated purification away from the liberated benzyl alcohol, which was accomplished by partitioning between aqueous K_2CO_3 and diethyl ether, followed by acidification and back-extraction of the product.

In addition to these phenylalanine and aryloxyproline derivatives, we also prepared a diazonamide-inspired fragment containing an indole which we expected would participate in the acid-promoted rearrangement step (Scheme **2.2.4A**). When incorporated into a peptide, we envisioned that the phenol would allow initial Pd-catalyzed cyclization, and that the cinnamyl group might undergo ring-expansion by migrating to the indole in the subsequent acid-promoted rearrangement step. To this point, only ring-contractions had been identified. The targeted biheterocycle was synthesized using a cyclodehydration

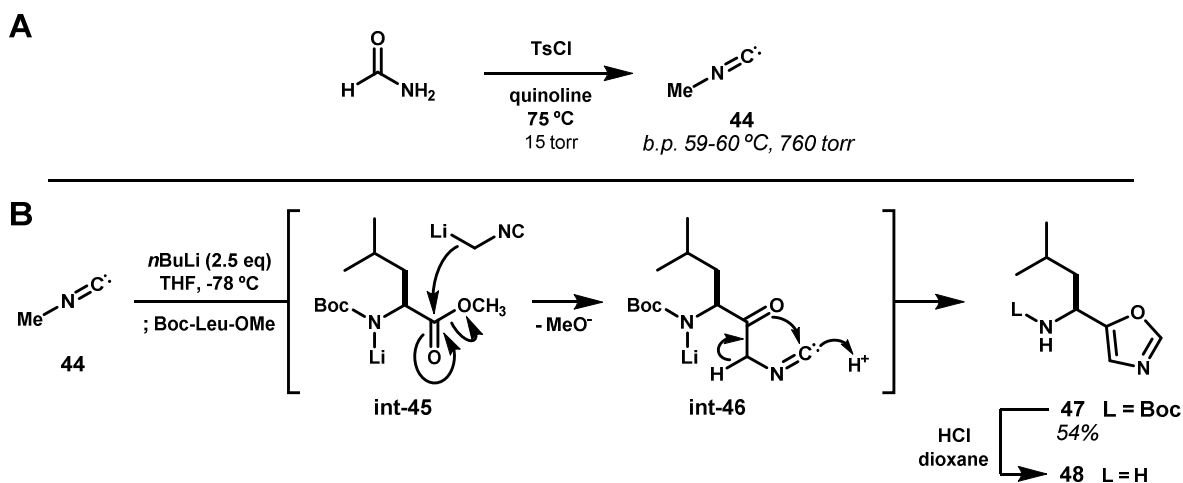
Scheme 2.2.4 A) Diazonamide-inspired indole-oxazole motif (**blue**). **B)** Biheterocycle **43** was synthesized from indolyl aminoketone **37** by cyclodehydration mediated by triphenylphosphine and hexachloroethane.



approach to prepare the central oxazole ring, borrowing from efforts towards diazonamide reported by the Wipf laboratory.^{18,19} Indolyl α -aminoketone **37** was prepared by reduction of the corresponding nitrile. Starting from indole, the 3-glyoxalyl chloride (**int-34**, Scheme 2.2.4B) was formed by treatment with oxalyl

chloride in diethyl ether, and subsequently cupric cyanide was added and the solvent exchanged to toluene/acetonitrile.²⁰ Heating this mixture led to nitrile **36**, presumably by elimination of carbon monoxide and hydrogen chloride and trapping of the resultant cumulene by cyanide ion (**int-35**). Hydrogenation over palladium on charcoal in acetic acid/methanol yielded aminoketone **37**, which was coupled to Boc-tyrosine. Cyclodehydration of this material was unsuccessful, and therefore the phenol was protected as its TBS ether (**38**) to prevent it from interfering under the strongly electrophilic conditions generated in the next step. Treatment of ketoamide **38** with triphenylphosphine and hexachloroethane induced cyclization to the desired oxazole **42**.^{18,19} Mechanistically, this likely proceeds by initial oxidation of triphenylphosphine by hexachloroethane to generate chlorotriphenylphosphonium chloride, with loss of tetrachloroethylene, which then affects dehydration by activation of the amide (**int-39**). 5-*Endo-trig* cyclization and collapse of the tetrahedral intermediate to eject triphenylphosphine oxide (i.e. **int-40**) followed by β -elimination (**int-41**) would then form the oxazole ring. It is also possible that activation may occur by initial activation of the ketone, and then cyclization of the amide in a reverse sense. Lastly, this pseudo-dipeptide was Boc-deprotected using HCl in dioxane with methanol added to ensure concurrent desilylation.

Scheme 2.2.5 A) Dehydration of formamide by the action of tosyl chloride yields gaseous methyl isonitrile (**44**), which is distilled from the reaction in vacuo, and then re-distilled at atmospheric pressure.²³ **B)** *N*-Boc Leucine methyl ester is converted to isoxazole **47** by treatment with the lithium salt of **44**.



The final tailored amino acid monomer was designed in order to test for potential electrophilic substitutions of oxazoles. In general, however, azoles are substantially less reactive than indole- or benzeneoid-type nucleophiles in such reactions.²¹ A straightforward approach was adapted from an

analogous reaction of *N*-Boc alanine methyl ester with the lithium salt of methyl isocyanide, which furnished the oxazole in one step while maintaining stereochemical integrity of the starting amino acid.²² Methyl isocyanide (**44**, Scheme 2.2.5A) was first synthesized according to a published protocol by dehydration of formamide using tosyl chloride.²³ The extremely malodorous, low boiling product was distilled from the reaction under vacuum, and then re-distilled to high purity at atmospheric pressure. Subsequently, methyl isocyanide was lithiated by treatment with *n*-BuLi at -78 °C, and *N*-Boc leucine methyl ester was introduced. This leads, presumably, to deprotonation of the carbamate, followed by addition of methyl isocyanide into the ester and elimination of methoxide (**int-45**, Scheme 2.2.5B). The resulting ketone then undergoes 5-*endo*-type cyclization onto the isocyanide carbon, yielding oxazole **47** upon tautomerization (**int-46**). Deprotection of the Boc group with HCl furnished amine hydrochloride **48**, which was carried forward crude.

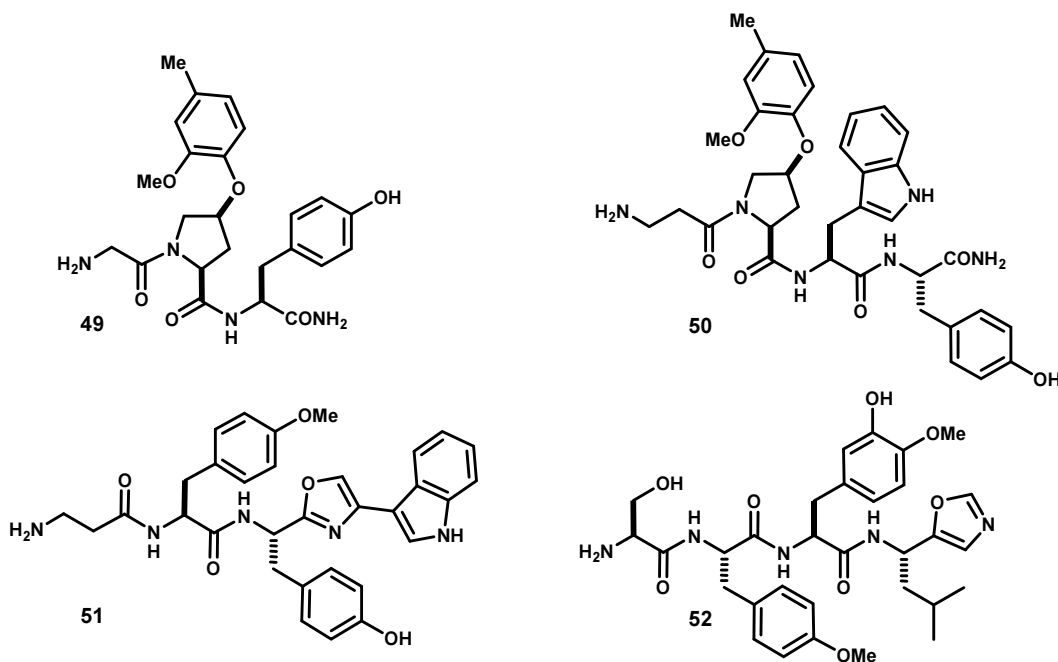


Figure 2.2.1 Peptidyl oligomers synthesized using custom monomers **17**, **22**, **33d**, **43** and **48**. Each substrate possesses an amino group to allow condensation and van Leusen cyclization to ligate template **1**, a phenolic residue to facilitate internal *O*-cinnamylation, and a second aryl side that could participate in large ring annulations with the dienyne motif of **1**.

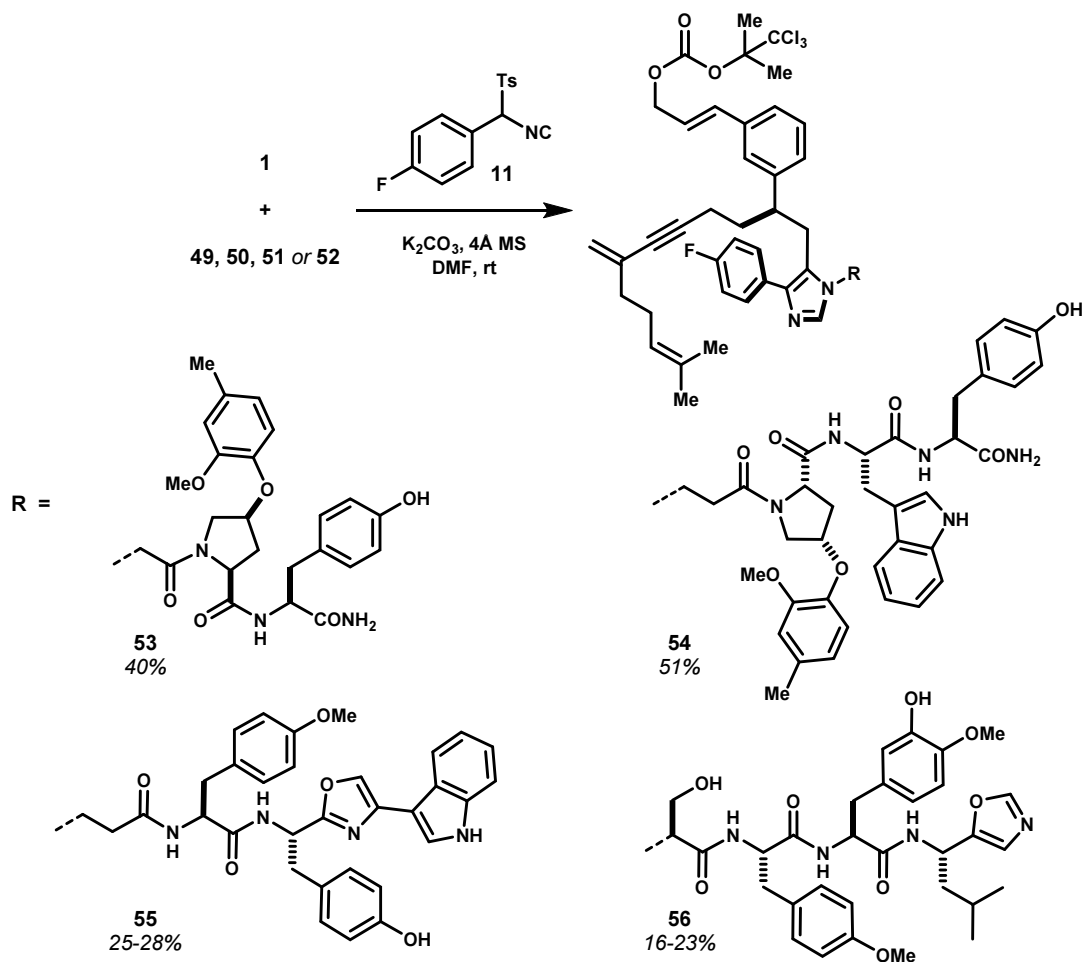
Amino acid monomers **17**, **22**, **33d**, **43**, and **48** were utilized in solution-phase peptide synthesis to construct model peptides **49–52** (Figure 2.2.1). Standard coupling and deprotection methodologies were used, and the assembled oligomers were purified prior to removal of the final *N*-Boc protecting group.

Whereas C-terminal *n*-butyl amides were used previously – which likely results in improved organosolubility of these peptides, but is otherwise unnecessary – substrates **49** and **50** were instead prepared as primary carboxamides. Each was designed to contain an unhindered amino group for initial ligation to **1**, given the generally lower yields observed in the van Leusen reaction of α -branched amino groups. Serine-containing substrate **52** was designed to test the compatibility of branched but small side chains. Each oligomer also possessed a phenolic side chain for initial cyclization by Pd-catalyzed *O*-cinnamylation, as well as a second aryl side chain designed to facilitate large ring annulations (*vide supra*). The reactions of these oligopeptides with template **1** are discussed in the following section.

2.3 Evaluating peptidyl substrates 49–52 in reactions with template (+)-1.

Peptidyl substrates **49–52** were ligated to template (+)-**1** and cyclized under catalysis with Pd⁰ in the same manner as model substrate Gly-Trp-Tyr (Scheme **2.3.1**). As anticipated, ligation of these oligomers to **1** using the van Leusen imidazole synthesis with TosMIC reagent **11** afforded products in moderate yield after purification, and even lower yield with α -branched substrate **52**. However, the presumably less sterically hindered β -Ala did not necessarily improve the yield over glycine in this step (e.g. **55**). Notably, these reactions led also to multiple byproducts, detected by both TLC and HPLC, suggesting that the chemoselectivity of the TosMIC reagent towards reaction at the imine may be poor. While imidazole syntheses of this type can be high yielding, this has typically been observed in less complex settings.⁵ Purified linear intermediates **53–56** appeared to be single compounds by HPLC-UV. However, given the relatively large number of unique nuclei in these molecules, most exhibited consistent but extremely complex 1D NMR spectra, and were positively identified by mass spectrometry. Worryingly, compounds **53** and **54** each appeared to contain a second set of peaks in the ¹H-NMR, prominently visible for key cinnamyl resonances (e.g. **53**, Figure **2.3.1**), but apparent throughout the spectra. At the time, we were concerned over the possibility of this being a result of contamination by a second diastereomer formed during peptide synthesis. More likely is that the mixture observed in the NMR spectra – and homogeneity observed by HPLC-UV – instead arises from *cis-trans* isomerization of the tertiary amide bond at proline. Such rotational isomerism is commonly observed in proline-containing peptides owing to the relatively high barrier to rotation of prolyl amide bonds (~13-19 kcal/mol) – leading to slow interconversion (i.e. non-interconverting)

Scheme 2.3.1 Peptidyl oligomers **49–52** undergo condensation with **1** and van Leusen imidazole synthesis at the free amino group, affording linear intermediates **53–56** in low to moderate yield.



on the timescale of the NMR experiment – and small free energy difference between *cis*- and *trans*-amide rotamers (avg. $\Delta G_{cis-trans} \approx 1.2$ kcal/mol). Both the rotational barrier and free energy difference are dependent upon peptide sequence,²⁴ solvent,²⁵ and pH.²⁶ In this case, NMR of **53** acquired in methanol-*d*₄ at room temperature showed a ~2:1 mixture indicating a $\Delta G_{cis-trans} \approx 0.4$ kcal/mol. Though we attempted to confirm rotational isomerism by increasing the temperature of the sample, little change in the ¹H spectrum was observed within the window below the solvent's boiling point. Consequently, we cautiously carried these materials forward, cognizant that the presence of minor diastereomers had not been ruled out (see also Chapter 5.1).

Palladium-catalyzed cyclization of substrates **53–56** yielded macrocyclic cinnamyl tyrosyl ethers **57–60**, respectively, in low to moderate yield following column chromatography. All materials exhibited the

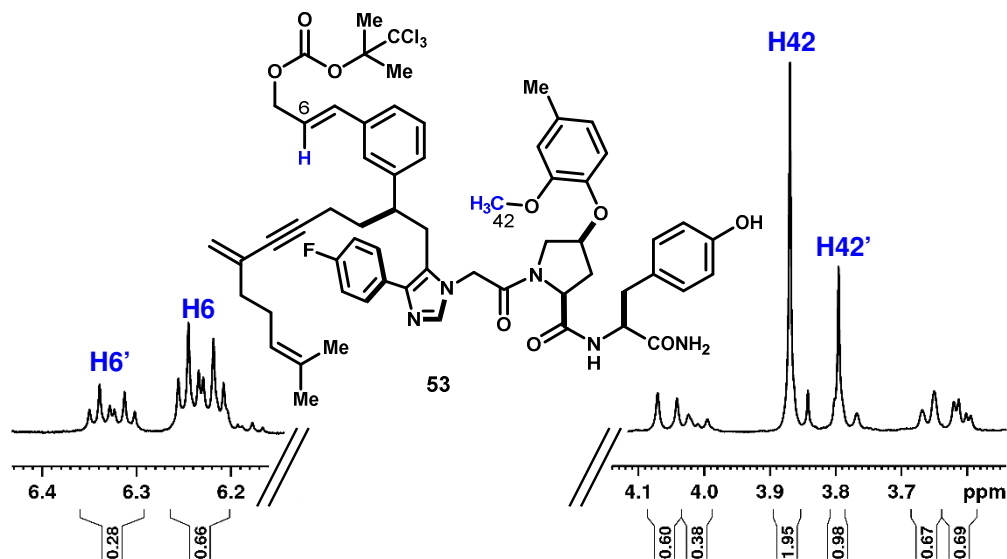


Figure 2.3.1 ^1H NMR of acyclic intermediate **53** illustrating doubled signals for vinyl proton H_6 , and methyl protons H_{42} .

expected molecular mass by ESI-MS, and good purity by HPLC-UV. However, proline-containing products **57** and **58** again exhibited substantially more complex ^1H -NMR spectra, both as a doubling of characteristic peaks and broadening of peaks throughout the spectrum, despite proper shimming of the spectrometer (evidenced by sharp signals arising from residual protiated NMR solvent). Product macrocycles **59** and **60**, however, yielded high quality spectra, and full ^1H and ^{13}C resonance assignments for each were made on the basis of 2D correlation spectra (^1H - ^1H -COSY, ^1H - ^{13}C -HSQC, ^1H - ^{13}C -HMBC, see Chapter 2 Data Appendix). The key macrocyclic ether linkages were confirmed analogously to the Gly-Trp-Tyr model (**16**, Figure **2.1.3A**). Notably, these examples confirmed the performance of (+)-**1** in this step, and also demonstrated the compatibility of this Pd-catalyzed step with oxazoles, which often display appreciable metal-binding ability.

Macrocyclic cinnamyl phenyl ethers **58** and **59** were treated with methanesulfonic (75 mM) acid in nitromethane (10 mM final) at 0 °C for 2 hours, following reported conditions.² The reactions were halted by aqueous workup, and the crude materials were analyzed by HPLC-UV-MS (Figure **2.3.3**). In both reactions, the starting macrocyclic ether had been completely consumed, generating primarily products of unchanged molecular mass. This result was consistent with previous observations. Unexpected, however, was the production of a broad, poorly resolved set of peaks from the reaction of **58**. Though initial analysis

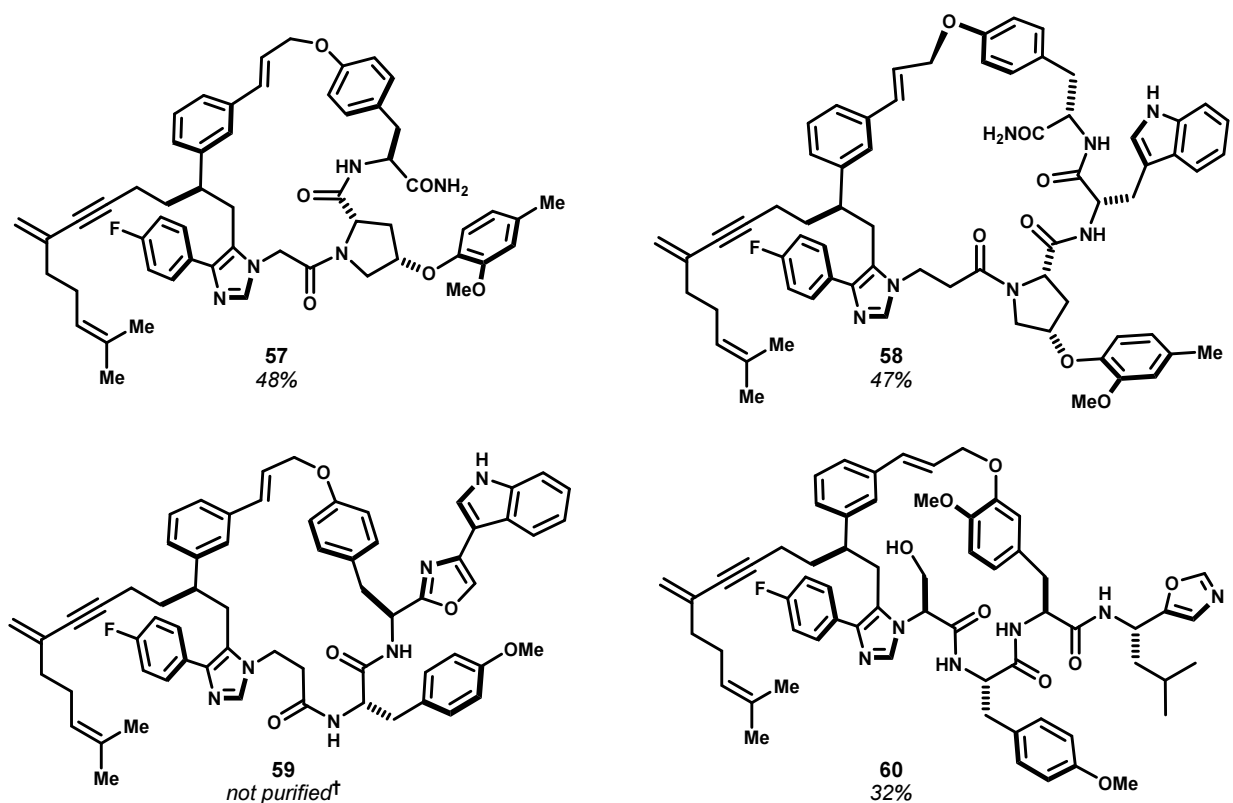


Figure 2.3.2 Acyclic intermediates **53–56** underwent internal phenol *O*-cinnamylation catalyzed by $[\text{Pd}(\text{C}_3\text{H}_5)\text{Cl}]_2/\text{Xantphos}$ to give macrocyclic cinnamyl ethers **57–60** in low to moderate yield. †A portion of product **59** was purified for spectroscopic characterization, and the remainder was carried forward crude.

was performed using a substantially faster HPLC separation than was used to achieve the separation of **3–10** (Figure 2.1.2), this seemed insufficient to explain the observed chromatogram (Figure 2.3.3A). By contrast, the product mixture resulting from the reaction of **59** showed discernible, albeit unresolved, constituent peaks by the same HPLC method (Figure 2.3.2B), and consequently became the focus of isolation and structure elucidation efforts.

For the product mixture derived from **59**, substantially improved peak resolution was achieved through optimization of the HPLC elution gradient, revealing twelve to fifteen peaks which appeared to possess the desired product mass (Figure 2.3.3A). This gradient was subsequently translated to preparative-scale HPLC and used to resolve this mixture into eight initial fractions (Figure 2.3.3B). Each fraction was re-analyzed by RP-HPLC on several stationary phases, and fractions *B–H* were targeted for re-purification. Fraction *C* appeared to contain primarily a single component, and was re-purified by preparative TLC (PTLC) on SiO_2 . Separation was achieved only after developing the plate multiple times,

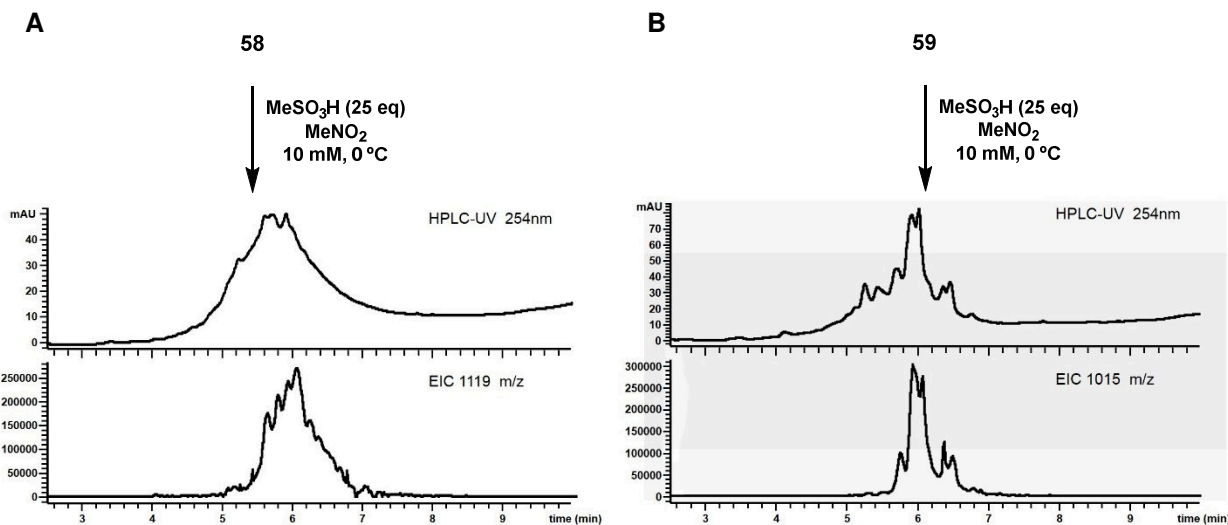


Figure 2.3.3 Crude HPLC-UV (254 nm) and corresponding extracted ion chromatograms (EIC) of acidolysis reactions: **A**) of macrocyclic ether **58**; **B**) of macrocyclic cinnamyl ether **59**. HPLC conditions: 20→100% ACN + 0.1% HCO₂H, 10 min, 1 mL/min, Waters Sunfire C18, 4.6x150mm, 5 μ.

which resolved *C* into a major (12.6 mg) and minor (3.2 mg) component, along with two trace components. Fraction *D* was similarly re-purified by PTLC to isolate the major component. Fractions *B* and *E–G* were re-purified by semi-preparative RP-HPLC. However, ¹H NMR of these isolates still showed considerable contamination. Consequently, the sub-fractions of *E–G* were further re-purified by PTLC, which provided, in most cases, material which was sufficiently pure for further NMR analysis and structure elucidation.

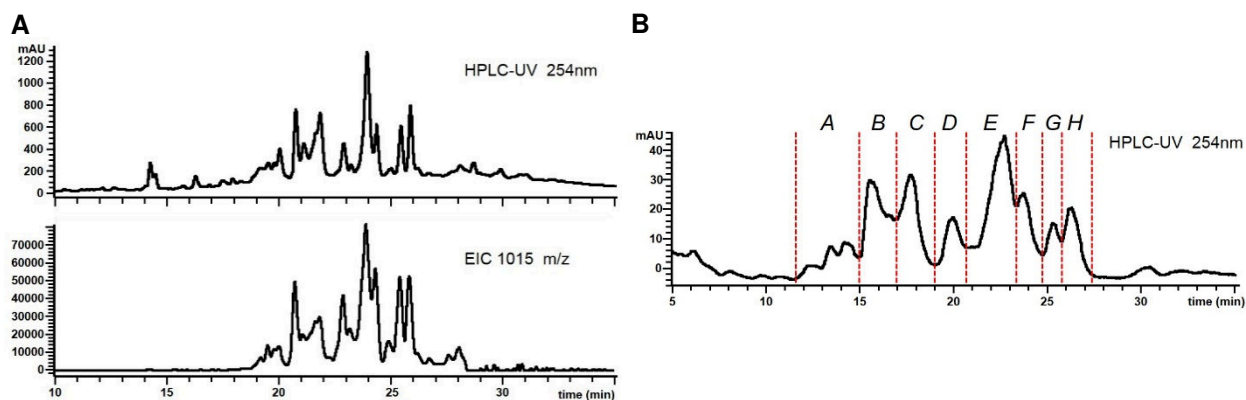
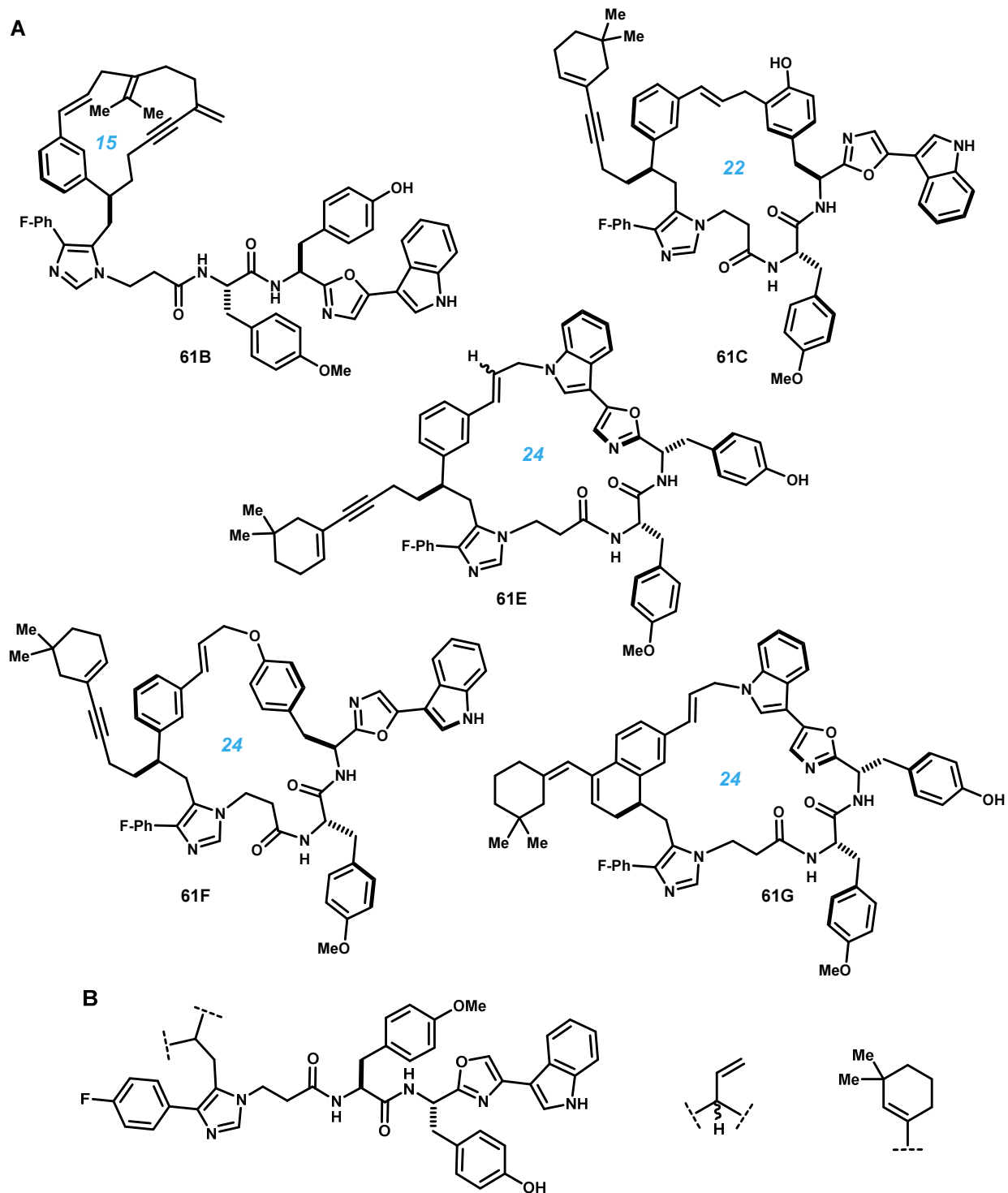


Figure 2.3.4 Optimized conditions for HPLC separation of the crude products resulting from acidolysis of macrocyclic cinnamyl ether **59**. HPLC conditions: **A**) Analytical, 50→100% ACN + 0.1% TFA, 38 min, 1 mL/min, Waters Sunfire C18, 4.6x250mm, 5 μ. **B**) Preparative, 55→70% ACN + 0.1% TFA, 29 min, 30 mL/min Waters Sunfire C18, 30x250mm, 5μ.

The major products from initial fractions *B–G* were obtained in sufficient quantity and purity for detailed NMR analysis. Minimally, 1D ^1H and 2D correlation spectra including ^1H - ^1H -COSY, ^1H - ^1H -TOCSY, ^1H - ^{13}C -HSQC or -HMQC, and ^1H - ^{13}C -HMBC were collected for each compound. Annotation of these spectra proved exceptionally challenging, particularly given our inexperience in optimizing complex multi-pulse NMR experiments, and in interpreting the data. While our laboratory ostensibly had experience in these areas, most of this knowledge had been lost with the departure of prior group members. Ultimately, this initial structure elucidation exercise served a pivotal role in establishing our laboratory's NMR expertise. Conclusive structural assignments were made for fractions *B1*, *C3*, *E1*, *F4* and *G1* (number denotes elution order in secondary purification). These five structures (**61B**, **C**, **E–G**) are shown in Figure 2.3.5A.

The products isolated from the acidolysis of macrocyclic cinnamyl ether **59** comprised isomeric macrocycles, as expected. Macrocycles **61B** and **C** contained carbon-carbon linkages resulting from migration of the cinnamyl *C–O* bond. The macrocyclic connection in compound **61B** is analogous to previously identified *meta*-cyclophane **6** (Figure 2.1.2), resulting from reaction between a transient cinnamyl carbocation and the dienyne. Compound **61C** is analogous to **3**, resulting from intraresidue *O*→*C*_{ortho} isomerization and cyclization of the 1,5-diene motif to its corresponding cyclohexene. The cinnamyl rearrangements leading to compounds **61E–G** were not identified previously. In **61E**, the cinnamyl group had undergone *O*→*N* migration to the nitrogen of the indole ring. Analogous *N*-allylations of indole have been reported, exemplified in the promiscuous enzyme-catalyzed prenylations of tryptophans wherein the *N*-prenyl product was identified along with products of *C*-prenylation at indole *C3*, *C5* and *C7*.²⁷ Surprisingly, we did not identify analogous products of *C*-cinnamylation of indole; indeed, we had designed this oligomer in hopes of observing these outcomes, because they would constitute ring-expansions from cyclic precursor **59**. It seems likely that these products may have been present in the crude product mixture, but in lesser quantities and therefore not identified.

The structural assignment of component *D4*, the major component of initial fraction *D*, remained incomplete. Despite a very dense aryl region in the ^1H NMR, it was readily apparent that the all four aryl rings of the peptide remained unsubstituted, thereby ruling out the possibility of a doubly macrocyclic structure that we had hoped to identify. Partial structures gleaned from the NMR data reasonably suggested a 3,3-disubstituted propenyl moiety – likely the cinnamyl group – as a mixture of diastereomers in a ~1.6:1



ratio (Figure 2.3.5B). However, we were unable to determine the precise substitution at this key linkage. It was clear that the dienyne had undergone the typical cyclization to a cyclohexene, but the alkyne was not apparent in the 1H - ^{13}C -HMBC. It was unclear whether the alkyne had indeed reacted, or whether the typically weak correlations of this moiety were simply not detected. While potentially interesting, assignment of this rearrangement product was abandoned.

Taken together with the previous structures isolated from the reactions of (-)-1, these new structures derived from (+)-1 suggest that the dienyne appendage generally does not undergo transannular electrophilic substitutions as intended. Rather, the 1,5-diene tends to rapidly cyclize to a mixture of regioisomeric cyclohexenes. Indeed, this diene rearrangement looked to proceed at a comparable rate to ionization of the cinnamyl ether, given that the ether linkage remained intact in 61F, whereas the cinnamyl ether had ionized but the 1,5-diene remained intact in *meta*-cyclophanes 6 and 61B. The cyclohexene products are sometimes resolved by HPLC, thereby introducing unvalued complexity in the product mixtures. In other cases, the cyclohexenes were isolated together, and necessitated concurrent assignment within the same NMR spectra – an often difficult task. Though alkynyl cyclohexenes could be re-protonated during the reaction, thereby re-generating a stabilized carbocation that could potentially undergo large ring-forming electrophilic substitution, this generally looked not to occur. Instead, these cyclohexenyl alkyne intermediates generally appear to proceed to dihydronaphthalene products (i.e. 10, 61G) by *6-exo-dig* cyclization of the central template benzene ring onto the alkyne.

2.4 Conclusions & remarks regarding the use of template 1 in property-altering, large ring-forming processes.

These exercises with (+)-1, while focused on a narrow set of peptidyl oligomers, ultimately led to identification of fewer than half of the total number of products arising from acidolysis of macrocyclic ether 59, a number of important questions evolved which we aimed to study further. Though our use of Pd-catalyzed *O*-allylation was unique in the context of peptide macrocyclization, bimolecular substitution reactions of transiently formed π -allyl palladium intermediates (i.e. the Trost-Tsuji reaction) have been demonstrated with a wide array of oxygen-, nitrogen- and carbon-based nucleophiles. Could peptide side chains other than tyrosine be made to participate in large ring-forming Pd-catalyzed cinnamylations? If so,

this might allow unique opportunities to study transannular substitution reactions (e.g. of the dienyne) independent of complex long-range rearrangements of the dienyne. With regard to these cinnamyl migrations, we recognized that we were constructing a macrocyclic C–O linkage, only to break the same bond in the subsequent step. Was this ‘pre-cyclization’ necessary, or beneficial for entropic pre-organization? If the carbon-carbon linked isomers could be obtained directly, a phenol-presenting side chain would no longer be required, broadening the potential substrate scope and obviating the air-sensitive Pd-catalyzed step. However, to this point we had not isolated a ring-expansion product, suggesting that there may be a kinetic barrier to forming larger rings or to forming C–C bonded products directly. These ideas are further explored in Chapters 3 through 6.

Notably, we were unable to rationalize the large number of products formed in the acidolysis reactions of oligopeptides ligated to **1** (e.g. **59**, **60**). Had we simply missed minor, doubly macrocyclic products in the process of purifying major components? Or were most of the products merely olefin isomers resulting from rearrangements of the dienyne? In either case, it was clear that predominantly mono-macrocyclic products were formed. We considered possibly inducing cinnamyl migration, then changing reaction conditions or temperature to force formation of a second macrocyclic linkage. However, it seemed difficult to accomplish this without a more thorough understanding of the cinnamyl ion chemistry. It was also clear that transannular substitutions would almost certainly occur via a prochiral alkynylcyclohexene intermediate, thereby leading to an uncontrolled mixture of diastereomers. Potential revision of the dienyne to either a primary or symmetric (non-prochiral) electrophile might reduce the number of possible products, and maximize the potential to form - and identify - novel ring isomers. Additionally, revisions in either the chain length between the alkyne and the benzene ring of **1**, or by addition of a blocking group (e.g. aryl halide) could prevent formation of unvalued dihydronaphthalene byproducts, and thereby enhance the potential for transannular substitution. Given that nuisance *tert*-butylation and benzylation of tyrosine^{28,29} and tryptophan^{30,29} have are well-known side reactions in peptide synthesis, it seems likely that suitably designed carbocations could be made to form transannular linkages by electrophilic substitution within constrained peptidyl macrocycles. Indeed, we synthesized two variants of template **1** taking these considerations into account (see Chapter 3.2), though only cursory attempts were made to characterize the performance of these new templates in transannular electrophilic substitution reactions.

References

- (1) Wei, Q.; Harran, S.; Harran, P. G. *Tetrahedron* **2003**, *59*, 8947.
- (2) Zhao, H.; Negash, L.; Wei, Q.; LaCour, T. G.; Estill, S. J.; Capota, E.; Pieper, A. A.; Harran, P. G. *J. Am. Chem. Soc.* **2008**, *130*, 13864.
- (3) Sisko, J.; Mellinger, M.; Sheldrake, P. W.; Baine, N. H. *Tetrahedron Lett.* **1996**, *37*, 8113.
- (4) Sisko, J.; Mellinger, M.; Sheldrake, P. W.; Baine, N. H. *Org. Synth.* **2000**, *77*, 198.
- (5) Van Leusen, A. M.; Wildeman, J.; Oldenziel, O. H. *J. Org. Chem.* **1977**, *42*, 1153.
- (6) Johns, A. M.; Utsunomiya, M.; Incarvito, C. D.; Hartwig, J. F. *J. Am. Chem. Soc.* **2006**, *128*, 1828.
- (7) Evans, L. A.; Fey, N.; Harvey, J. N.; Hose, D.; Lloyd-Jones, G. C.; Murray, P.; Orpen, A. G.; Osborne, R.; Owen-Smith, G. J. J.; Purdie, M. *J. Am. Chem. Soc.* **2008**, *130*, 14471.
- (8) Trost, B. M.; Bunt, R. C. *Tetrahedron Lett.* **1993**, *34*, 7513.
- (9) Boger, D. L.; Yohannes, D. *J. Org. Chem.* **1987**, *52*, 5283.
- (10) Waters, W. A. *Mechanisms of Oxidation of Organic Compounds*; Methuen and Company: London, 1964.
- (11) Krow, G. R. In *Organic Reactions*; 2004; pp 266–267.
- (12) Brown, H. C.; Okamoto, Y. *J. Am. Chem. Soc.* **1958**, *80*, 4979.
- (13) Smith, M. B.; March, J. In *March's Advanced Organic Chemistry: Reactions, Mechanisms, and Structure*; John Wiley & Sons, Inc.: Hoboken, NJ, 2007; pp 622–623.
- (14) Bergel, F.; Stock, J. A. *J. Chem. Soc.* **1954**, 2409.
- (15) Johnson, T. B.; Kohmann, E. F. *J. Am. Chem. Soc.* **1915**, *37*, 1863.
- (16) Waser, E. *Helv. Chim. Acta* **1913**, *4*, 657.
- (17) Krapcho, J.; Turk, C.; Cushman, D. W.; Powell, J. R.; DeForrest, J. M.; Spitzmiller, E. R.; Karanewsky, D. S.; Duggan, M.; Rovnyak, G.; Schwartz, J.; Natarajan, S.; Gofrey, J. D.; Ryono, D. E.; Neubeck, R.; Atwal, K. S.; Petrillo, E. W. *J. Med. Chem. Chem.* **1988**, *31*, 1148.
- (18) Wipf, P.; Methot, J. L. *Org. Lett.* **2001**, *3*, 1261.
- (19) Wipf, P.; Yokokawa, F. *Tetrahedron Lett.* **1998**, *39*, 2223.
- (20) Hogan, I. T.; Sainsbury, M. *Tetrahedron* **1984**, *40*, 681.
- (21) Joule, J. A.; Mills, K. In *Heterocyclic Chemistry*; John Wiley & Sons, Inc.: West Sussex, UK, 2010; pp 455–459.
- (22) Ohba, M.; Kubo, H.; Fuji, T.; Ishibashi, H.; Sargent, M. V.; Arbain, D. *Tetrahedron* **1997**, *38*, 6697.
- (23) Schuster, R. E.; Scott, J. E.; Casanova, J. J. *Org. Synth.* **1966**, *46*, 75.
- (24) Reimer, U.; Scherer, G.; Drewello, M.; Kruber, S.; Schutkowski, M.; Fischer, G. *J. Mol. Biol.* **1998**, *279*, 449.
- (25) Steinberg, I. Z.; Harrington, W. F.; Berger, A.; Sela, M.; Katchalski, E. *J. Am. Chem. Soc.* **1960**, *82*, 5263.
- (26) Grathwohl, C.; Wüthrich, K. *Biopolymers* **1976**, *15*, 2025.
- (27) Rudolf, J. D.; Wang, H.; Poulter, C. D. *J. Am. Chem. Soc.* **2013**, *135*, 1895.
- (28) Iselin, von B. *Helv. Chim. Acta* **1962**, *45*, 1510.
- (29) Bodanszky, M.; Martinez, J. *Synthesis (Stuttg.)* **1981**, *5*, 333.
- (30) Wünsch, E.; Jaeger, E.; Kisfaludy, L.; Löw, M. *Angew. Chem. Int. Ed. Engl.* **1977**, *16*, 317.

3 A simplified template for examining Pd-catalyzed and acid-promoted large ring-forming cinnamylations

3.1 Introduction

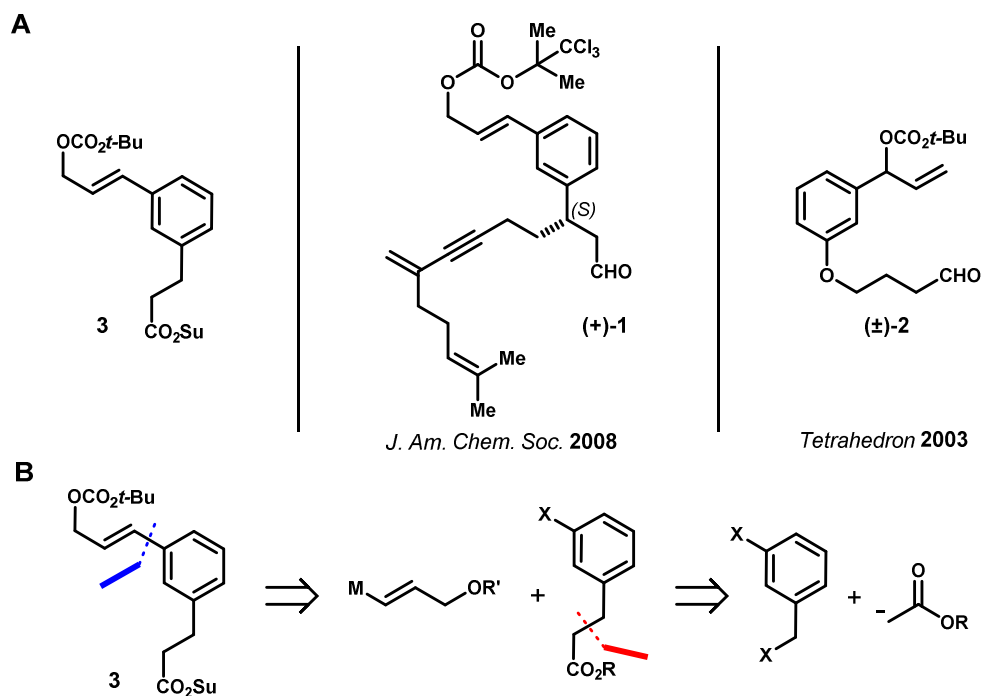
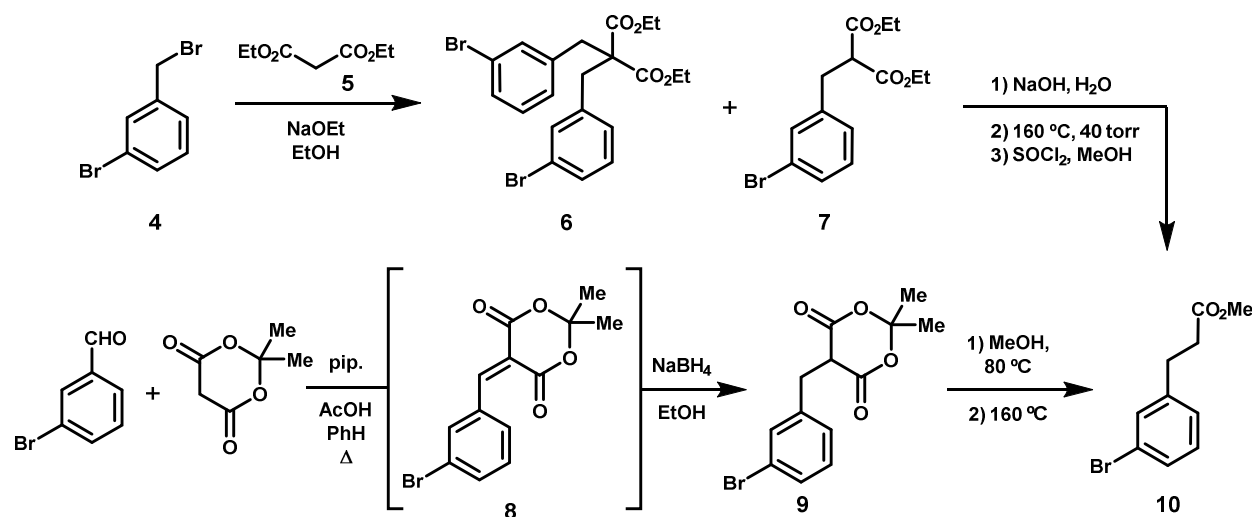


Figure 3.1.1 Macrocyclic tyrosyl ethers **62**, **63** and **65** were prepared by Pd-catalyzed internal *O*-cinnamylation from their respective acyclic mixed cinnamyl carbonates.

The pioneering studies from our laboratory using prototype template **2**¹ and tri-functional derivative (+)-**1**² provided a captivating glimpse of the reactivity of the cinnamyl carbocation, and metal complexes thereof, in the context of large ring-forming processes with oligopeptides. These studies have since also been extended by us using (–)-**1** (see Chapter 2). Here, we describe the design and synthesis of template **3** (Figure 3.1.1A), which allowed us to study the Pd- and acid-initiated steps individually. The diene-yne appendage of **1** was removed, given the complex competing isomerism observed for this motif. Rather than reverting to **2**, template **3** retained an all-carbon framework to allow direct comparison to the reactivity observed with **1**. Additionally **3** was designed to form an initial amide bond to the peptide by *N*-acylation as an alternative to the generally low-yielding ligations between peptides and templates **1** and **2** via van Leusen imidazole synthesis. Though an amide bond might potentially prove disadvantageous in pharmacological settings, we were confident that high yielding amidation could be achieved, and thereby provide larger

quantities of materials for structural studies. Borrowing from our revised syntheses of (–)-**1**, we pursued an analogous sp^2 - sp^2 disconnection to install the key cinnamyl moiety present in **3** (Figure 3.1.1B). The requisite phenylpropionic acid component could then be assembled from the appropriate benzyl halide and an acetate synthon.

Scheme 3.1.1 Two scalable and efficient routes were successfully implemented to prepare 3-bromophenylpropionic acid methyl ester (**10**), utilizing either malonic ester synthesis or Knoevenagel condensation, reduction and decarboxylation to supply a two-carbon acetate equivalent.



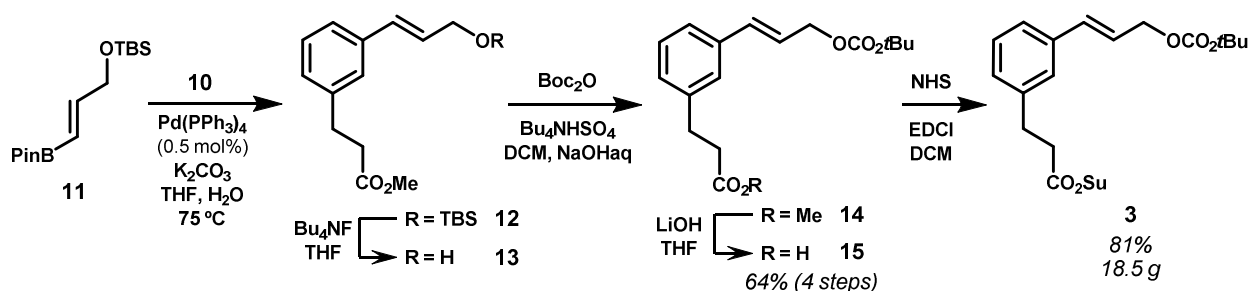
To maintain scalability, we sought a route to simplified template **3** which minimized chromatographic separation, and which utilized inexpensive starting materials. We first required the key intermediate 3-(*m*-bromophenyl)propionic acid. Though several small-scale preparations of this compound have been reported,^{3–5} we found malonic ester synthesis to be reliable and easily scaled. *m*-Bromobenzyl bromide was reacted with diethylmalonate in the presence of sodium ethoxide, which yielded a mixture of desired product **7** along with dibenzylated **6** as a major byproduct (Scheme 3.1.1). Overreaction in this manner is commonly observed in malonate alkylations of this type, and is usually countered by biasing the reaction stoichiometry.⁶ Using a 1:1 ratio of benzyl bromide **4** to diethyl malonate (**5**), we observed by crude ¹H NMR the formation of **6** and **7** in a 5:6 ratio, whereas using instead 3 equivalents of diethyl malonate and 3 equivalents of sodium ethoxide afforded a 1:3 ratio favoring **7**. We found that excess diethyl malonate could be easily recovered and **7** isolated by fractional distillation *in vacuo*. Subsequent saponification of **7**,

thermal decarboxylation, and Fisher esterification provided intermediate **10**, which was also distilled to excellent purity.

Intermediate aryl bromide **10** was also prepared by an alternative route that obviated competing dialkylation pathway by utilizing a Knoevenagel condensation, thereby simplifying purification and reducing the number of steps (Scheme 3.1.1). *m*-Bromobenzaldehyde underwent rapid condensation with Meldrum's acid in the presence of catalytic piperidinium acetate⁷ to give benzylidene Meldrum's acid **8**, which was reduced *in situ* by the action of NaBH₄.^{8,9,10} Notably, Meldrum's acid is preferable to diethyl malonate in this sequence, because the resulting alkylidene Meldrum's acid derivatives are more electrophilic. Alkylidene malonates are unreactive towards sodium borohydride.⁸ Additionally, **9** was readily solvolyzed to the corresponding mono-methyl malonate, which was decarboxylated to give **10** directly, without the need for re-esterification. Though we observed relatively poor yield at the final decarboxylation step, ¹H NMR analysis of the crude material indicated high purity, implicating loss on purification as a result of the small scale on which this alternative route was carried out.

Suzuki cross-coupling of aryl bromide **10** with vinyl boronate **11** (Scheme 3.1.2) was successfully carried out in a similar manner as in our revised route to template **1**. Likely owing to the high purity of starting **10**, we were able to reduce the loading of Pd(PPh₃)₄ by half to 0.5 mol%, though the reaction was sluggish, taking four days to near completion. We also observed good reactivity using a catalyst generated from Pd(OAc)₂ and JohnPhos, reported to be highly active in Suzuki-Miyaura cross-couplings,¹¹ but ultimately retained Pd(PPh₃)₄ to reduce cost on scale. Alternatively, it may be possible to accelerate this reaction by increasing the temperature, though more thermostable supporting ligands such as tri(*o*-tolyl)phosphine may

Scheme 3.1.2 The carbon framework of template **3** was readily assembled by Suzuki cross-coupling between aryl bromide **10** and vinyl boronate **11**.



be required.^{12,13} Intermediate **12** was treated with tetrabutylammonium fluoride to remove the silyl protecting group, and subsequently reacted with di-*tert*-butyl dicarbonate under phase-transfer conditions with tetrabutylammonium hydrogen sulfate¹⁴ to form cinnamyl *tert*-butyl carbonate **14**. Saponification gave **15**, which was obtained in good purity and 64% yield by telescoping material through the preceding steps without purification. Lastly, condensation of **15** with *N*-hydroxysuccinimide by the action of EDCI formed targeted template **3**, which was readily purified by chromatography, and obtained as a solid. Over 18 g of material was produced in a single batch using this route, and was stored at room temperature for a period of several years without appreciable decomposition.

3.2 Trifunctional templates designed to promote large ring annulations by electrophilic aromatic substitution

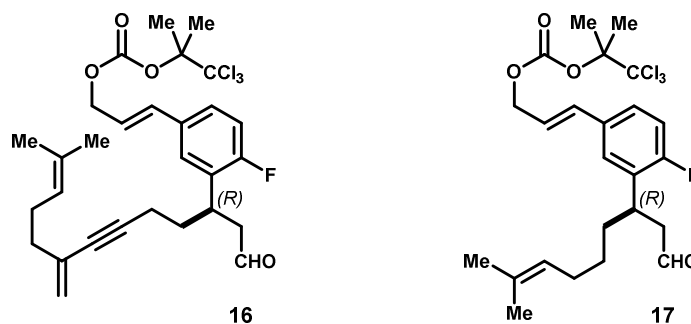
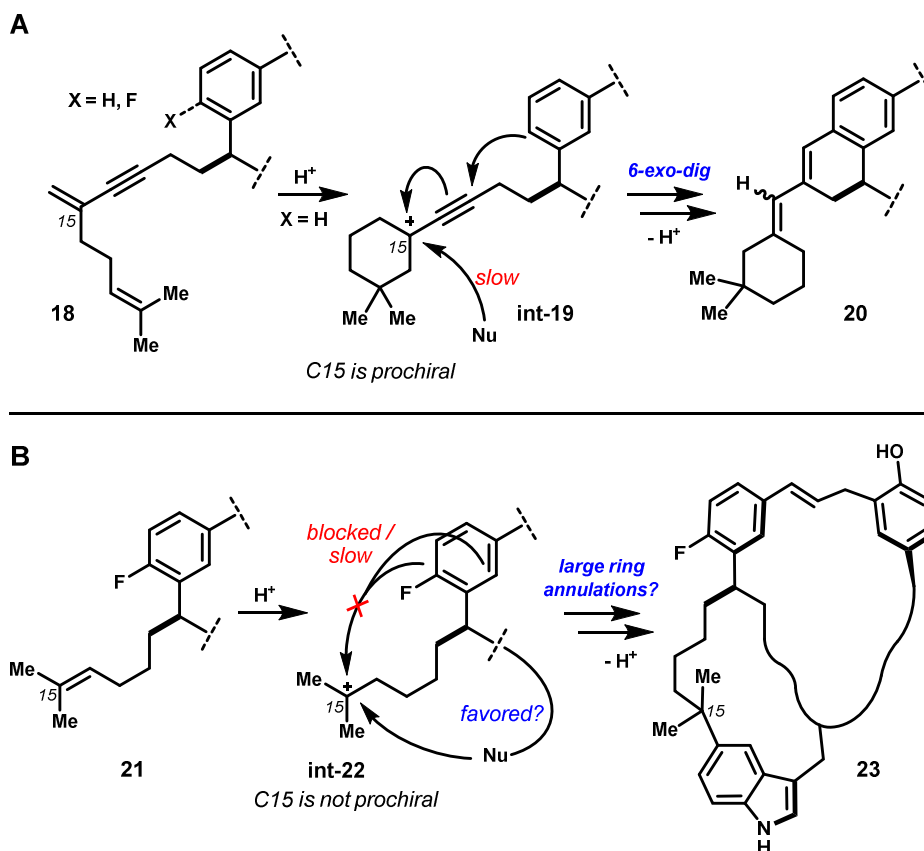


Figure 3.2.1 Templates **16** and **17** – derivatives of template **1** – were designed to engage peptides by 1) peptide condensation and van Leusen imidazole synthesis at the aldehyde group. 2) Pd-catalyzed O-cinnamylation by the cinnamyl carbonate, and 3) acid-promoted large ring annulations of either the diene (**16**) or 2-methylhexenyl (**17**) appendages.

In light of the observed complications of the diene motif in template **1** and the general tendency for this motif to form dihydronaphthalene products, we also synthesized trifunctional templates designed to overcome these limitations. Whereas simplified template **3** was well-suited to investigate specific questions we had concerning the cinnamyl-based chemistry, the two templates discussed here were aimed at continuing exploration of transannular electrophilic aromatic substitution reactions. Revised template **16** (Figure 3.2.1) utilized an appropriately placed aryl fluoride to block the formation of dihydronaphthalene products, but retained the diene motif of template **1**. Template design **17** incorporated many of our ideas formulated in the course of our studies of template **1** (see Chapter 2.4). Specifically, the diene appendage was exchanged for an achiral trisubstituted olefin. We anticipated that **17** would give simpler product mixt-

Scheme 3.2.1 A) Fluorination of the aryl ring in revised templates **16** and **17** was designed to block undesired 6-*exo-dig* cyclization leading to dihydronaphthalene products. **B)** The non-prochiral 2-methylhexenyl group of **17** was designed to promote large ring annulations by minimizing competing isomerization of carbocations produced upon protonation of this olefin.



ures by virtue of being non-prochiral and less prone to non-productive isomerization, and therefore might show greater tendency to form transannular linkages.

Specifically, revised template architectures **16** and **17** were designed to slow the competing 6-*exo-trig* cyclizations of the dienyne onto the aryl nucleus of template (Scheme **3.2.1A**), which lead to the dihydronaphthalene products observed with materials derived from template **1**. Conceptually, we envisioned achieving this by either substituting the aryl group to block electrophilic substitution (i.e. aryl fluoride), or by altering the chain length of between a reactive appendage and the aryl group so as to kinetically disfavor this ring closure. Though fluorination seemed straightforward, it was unclear how this group might in turn affect the electronic structure of the cinnamyl group. The sigma withdrawing character of an electronegative substituent *para* to the allyl group might lead to destabilization of the corresponding cinnamyl cation¹⁵,

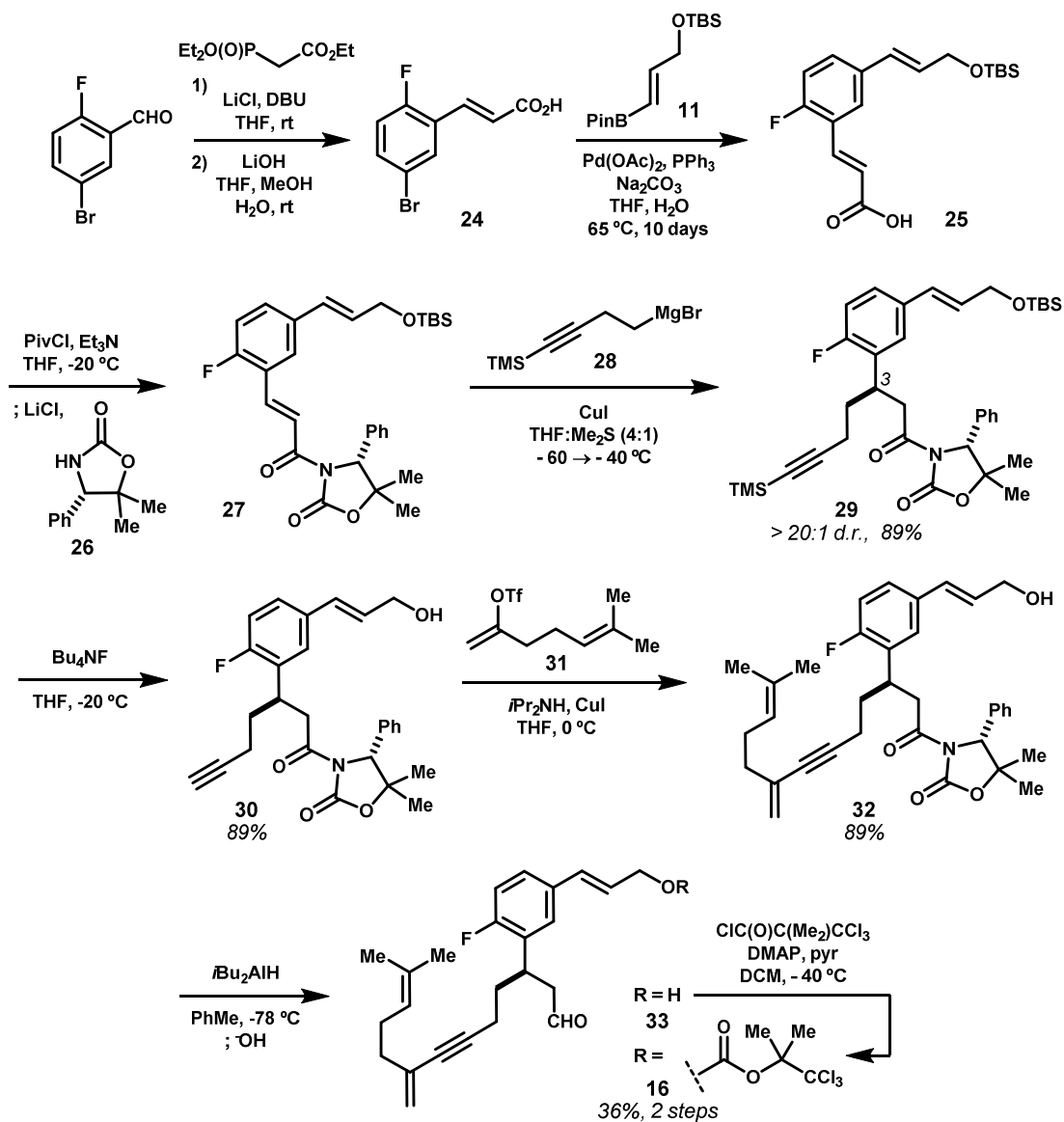
potentially enhancing its reactivity, or potentially leading to aberrant reactivity. Template **16** would allow direct evaluation of this single atom change. The tertiary olefin in **17** departed from the dienyne entirely.

Upon protonation of this olefinic appendage, the resulting non-prochiral tertiary cation might alkylate electron rich amino acid side chains in a manner directly analogous to *tert*-butylation (i.e. **int-22**, Scheme **3.2.1B**); a familiar side reaction in peptide synthesis.^{16,17} Beta-elimination of this carbocation would also revert preferentially to the more stable internal olefin (e.g. **21**), and possible rearrangement pathway seemed unfavorable. Critically, cyclization of this cation onto the aryl nucleus was blocked by the 4-fluoro substituent, and alkylation at the 2-position to form an eight-membered ring would proceed through a kinetically unfavorable, strained transition state (**int-22**).¹⁸ By minimizing alternative pathways, we hoped that **17** would show an improved tendency to form secondary macrocyclic linkages by reaction at this olefin (i.e. **23**), and that, if necessary, stronger reaction conditions or higher temperatures could be employed to achieve this.

The synthesis of **16** and **17** was carried out by direct extension of our revised route to prototype template **1** (see Chapter 1); no attempt was made to optimize yields. Fluorinated Michael acceptor **27** was assembled from commercially available 5-bromo-2-fluorobenzaldehyde by first constructing 5-bromo-2-fluorocinnamic acid (**24**) by Horner-Wadsworth-Emmons olefination and saponification (Scheme **3.2.2**). Subsequent Suzuki-Miyaura cross coupling, while successful, proved exceptionally sluggish, taking 10 days and high loading of a combination of Pd(PPh₃)₄ and Pd(OAc)₂/PPh₃ to reach high conversion. This despite that *p*-fluoro substitution in substrate **24** would be expected to accelerate oxidative addition by weakening the C–Br bond.^{19,20} Sluggish reactions were also observed in other cases when the using bromocinnamic acid substrates, whereas their corresponding esters proved less problematic. This may owe to insolubility or diminished reactivity of bromocinnamate sodium salts generated during the reaction. The mixed anhydride of **25** and pivaloyl chloride was generated, and reacted with *D*-phenylglycine-derived oxazolidinone **26** (**1-36**, Chapter 1) and LiCl *in situ* to give acyloxazolidinone **27**. This intermediate was carried forward to both **16** and **17**.

Towards **16**, copper-promoted conjugated addition of silyl protected homopropargyl Grignard reagent **28** into eneimide **27** afforded intermediate **29** in good yield as a single diastereomer (Scheme **3.2.2**), as indicated by HPLC-UV and NMR analysis. Silyl deprotection and Sonogashira cross coupling

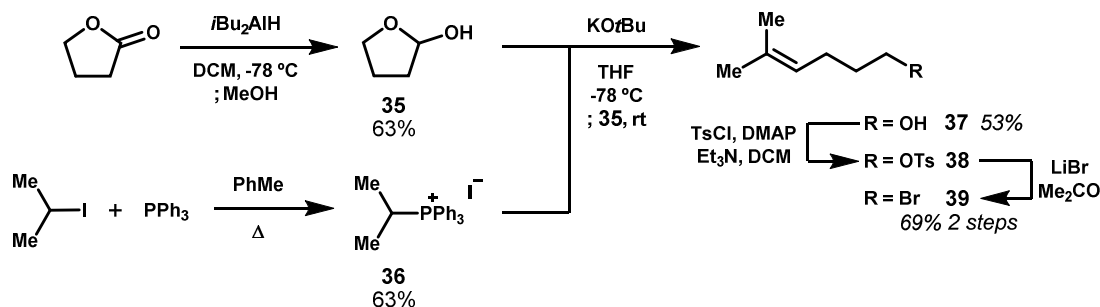
Scheme 3.2.2 Template **16** was assembled analogously to template **1**. The dienyne appendages were installed by diastereoselective conjugate additions to set the stereochemistry at *C3*.



between alkyne **30** and vinyl triflate **31** completed the dienyne appendage without incident. Reductive cleavage of the chiral auxiliary, and carbonate formation was carried out successfully, albeit in low yield, likely as a result of telescoping relatively impure material through earlier steps in this sequence.

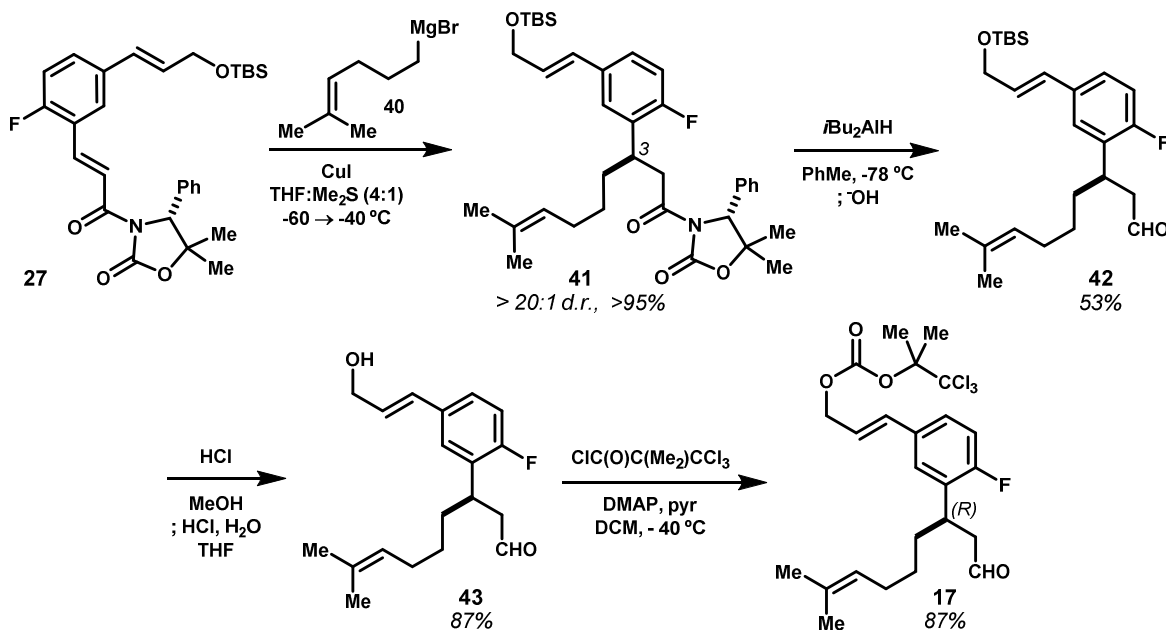
Template **17** was assembled analogously from intermediate **27**, but using an alternative Grignard reagent. The targeted 2-methyl-2-hexene moiety was derived by Wittig olefination of 2-hydroxytetrahydrofuran (**35**)²¹ using isopropyltriphenylphosphonium iodide (**36**),²² giving alcohol **37** in moderate yield (Scheme 3.2.3). Tosylation and Finkelstein swap provided the corresponding bromide **39**,

Scheme 3.2.3 Bromide **39**, required to prepare **17** via the corresponding Grignard reagent of **39**, was prepared by Wittig olefination of hydroxytetrahydrofuran (**35**) and Finkelstein swap to install the bromide.



which was readily distilled to high purity. The corresponding Grignard reagent of **40** was easily formed in THF, and carried into the copper-promoted conjugate addition with enamide **27** without incident (Scheme 3.2.4). Product **41** was obtained in quantitative yield as a single diastereomer, as assessed by HPLC and NMR analysis. With the silyl protecting group still in place, the chiral auxiliary was reductively removed using DIBALH, but this reaction was incidentally taken to partial conversion and **42** was recovered in only moderate yield. Over concern that fluoride-based deprotection of the silyl group might degrade the aldehyde group by aldol reaction, we instead opted to solvolyzed this group using acidic methanol solution, which also formed the dimethyl acetal *in situ*. Despite this reaction turning an alarming black color, aldehyde **43**

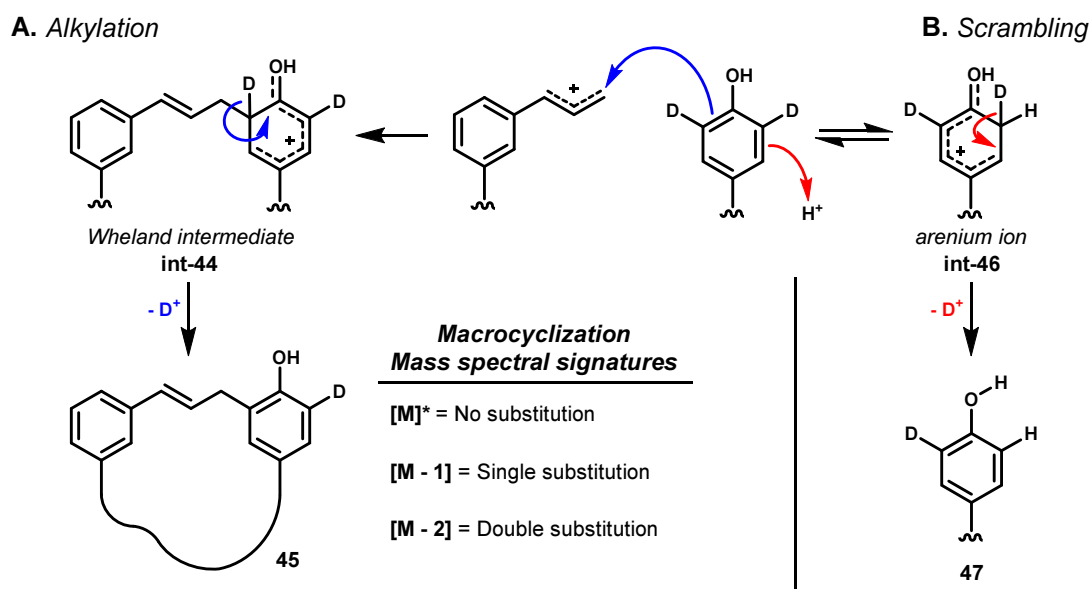
Scheme 3.2.4 Template **17** was also synthesized using a diastereoselective conjugate addition to install the methylhexenyl appendage and set the stereochemistry at *C3*.



was recovered in 87% following hydrolysis of the acetal. Lastly, the carbonate group was installed in an analogous manner to **1** and **16**, affording 3 g of template **17**.

3.3 A ^2H -labeling approach to survey large ring-forming reactions of templates **3**, **16** and **17**: Discovery of a large ring-forming Friedel-Crafts reaction

Scheme 3.3.1 A deuterium labeling/mass spectrometry approach to rapidly assess large ring-forming C-cinnamylations. **A)** Under acidic conditions, a cinnamyl carbocation is generated, which would lead to electrophilic substitution with loss of one deuterium atom upon re-aromatization from the Wheland intermediate. **B)** Scrambling by direct protonation of activated arenes, and loss of deuterium, is a potential competing reaction that would complicate analysis.



Our previous efforts to assess the performance of template **1** in reactions of arene-rich oligopeptides proved time-consuming, though informative (see Chapter 2.3). Consequently, we sought alternative means to more rapidly survey the reactivity and transannular bond-forming capabilities of revised templates **3**, **16** and **17**. The mechanism of the electrophilic aromatic substitutions under question proceeds by net substitution of an aryl C–H bond; an event which should be traceable using deuterium labeled substrates. Indeed, both deuterium and tritium have been extensively utilized in kinetic and mechanistic studies of bimolecular aryl and heteroaryl substitution reactions and in quantification of substituent effects based on isotope exchange kinetics.^{23–25} If successfully employed to investigate our large ring-forming rearrangements, isotope labeling would provide a means to rapidly trace aryl substitutions based on changes in the molecular masses of the products.

Deuterium labeling would indicate whether an aryl $C-D$ bond(s) had been substituted by either the cinnamyl carbocation, or by the olefinic appendages in templates **16** and **17**. This would thereby indicate the number of new rings formed in the product (Scheme **3.3.1**). Addition of an activated arene to a transiently formed carbocation (e.g. the cinnamyl cation) leads to an intermediate arenium ion, known as the Wheland intermediate (**int-44**), which is then rearomatized by loss of the deuterium label. The loss of deuterium would ideally be observable by analytical HPLC-MS, thereby obviating the need to isolate products (i.e. **45**) and determine their structures by NMR. However, in order for this analysis to succeed, alkylation would need to out-compete scrambling of the label by $H-D$ exchange with the acid promoter used in the reaction. In the same manner as alkylation, reversible protonation of the labeled arene (**int-46**) would lead to eventual loss of the isotopic label. To test these hypotheses, we prepared selectively deuterated variants of peptides comprising tyrosine and *cis*-4-(3-methoxyphenoxy)-*L*-proline, a highly electron-rich derivative of the arylated prolines we had employed previously when probing reactions of template **1** (see Chapter 2.2, 2.3).

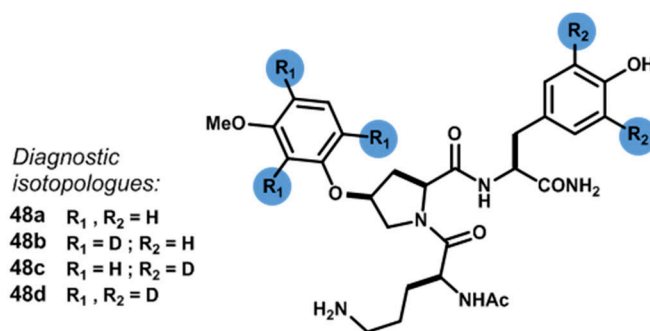


Figure 3.3.1 Selectively deuterated peptides **48a–d** were designed to probe large ring-forming cinnamylations and subsequent annulations in reactions with templates **1**, **3**, **16** and **17**.

Peptide isotopologues **48a–d** were designed to probe large ring-forming cinnamylations and secondary large ring annulations with templates **1**, **3**, **16** and **17**, and to determine which amino acid side chain(s) had reacted (Figure **3.1.1**). Ornithine was chosen, because its unhindered side chain had been found to undergo the van Leusen imidazole syntheses in generally good yield. Tyrosine was included to facilitate initial Pd^0 -catalyzed macrocyclic cinnamyl ether formation, and the aryloxyproline was again used as a modular aryl nucleophile that we hoped would react in transannular electrophilic substitutions. To ensure uniformly high incorporation, we installed the deuterium labels after peptide assembly by reduction

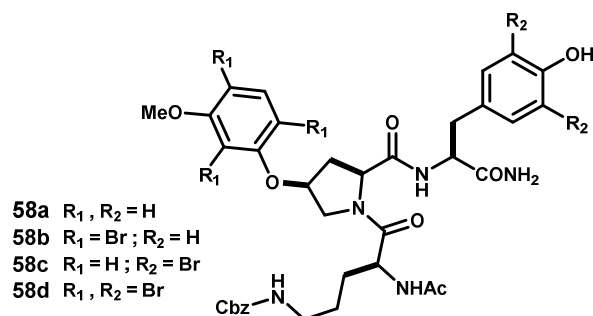
of the corresponding aryl bromides. In this manner, potential scrambling during acid-promoted deprotection steps would be avoided.

Selectively brominated amino acids were prepared by electrophilic bromination, such that upon reductive dehalogenation, deuterium would be placed at the canonically reactive sites of each aryl group (Scheme 3.3.1). Treatment of tyrosine carboxamide hydrochloride with bromine in acetic acid yielded 3,5-dibromo-*L*-tyrosine (**50**), which was used directly in peptide assembly. Aryloxyproline **57** was prepared by first tribromination of 3-methoxyphenol to form **52**, and subsequent Mitsunobu reaction between phenol **52** and protected *trans*-4-hydroxy-*L*-proline **53** to give **55**, the benzyl ester of which was saponified to give **57**. The analogous non-brominated amino acid **56**, required for isotopologues **48a** and **48c**, was prepared in the same manner, except that final deprotection of the benzyl ester was accomplished by hydrogenolysis over Pd/C.

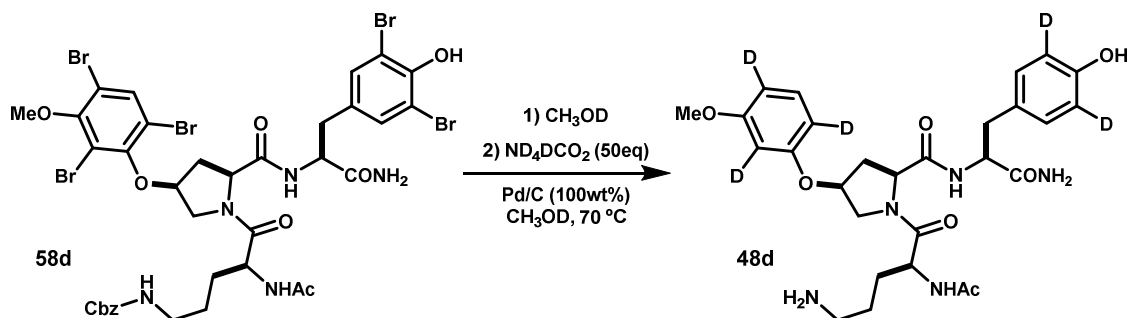
The three selectively brominated tripeptides **58b–c** and natural abundance isotopologue **58a** were assembled by solution-phase peptide synthesis, which reliably accessed relatively large amounts of these

Scheme 3.3.2 A) Selectively brominated precursors were assembled by peptide synthesis using appropriately brominated amino acids. **B)** Deuterium was incorporated by Pd-catalyzed reductive dehalogenation with concurrent deprotection of the ornithine *N*₅-Cbz group.

A



B



materials (Scheme 3.3.2A). Ornithine was introduced using orthogonal N_α -Boc- N_δ -Cbz protection, which allowed installation of the N-terminal acetamide and then deprotection of the side chain N_δ -Cbz concomitantly with reductive deuteration of the aryl bromides. This strategy is illustrated in the reduction of brominated precursor **58c** to pentadeuterated isotopologue **48c** (Scheme 3.3.2B). Peptidyl substrates were first dissolved in methanol- d_1 to exchange labile hydrogens (i.e. $N-H/O-H$) for deuterium to avoid isotopic dilution of either the solvent or reducing agent in the following step. Reductive deuteration was carried out using ammonium formate- d_5 and palladium on charcoal in methanol- d_1 , which promoted clean dehalogenation and N_δ -Cbz hydrogenolysis. Attempts using deuterium gas, both with and without base additives, were inferior, and attempted reductions with nickel^{26,27}, zinc²⁸ or copper²⁶ were unsuccessful or led to only partial reduction. Isotopologue **48d** was particularly important, because it would be able to diagnose double cyclizations (see Scheme 3.3.1), whereas trideuterated isotopologues **48b** and **48c** would indicate which ring(s) had been substituted.

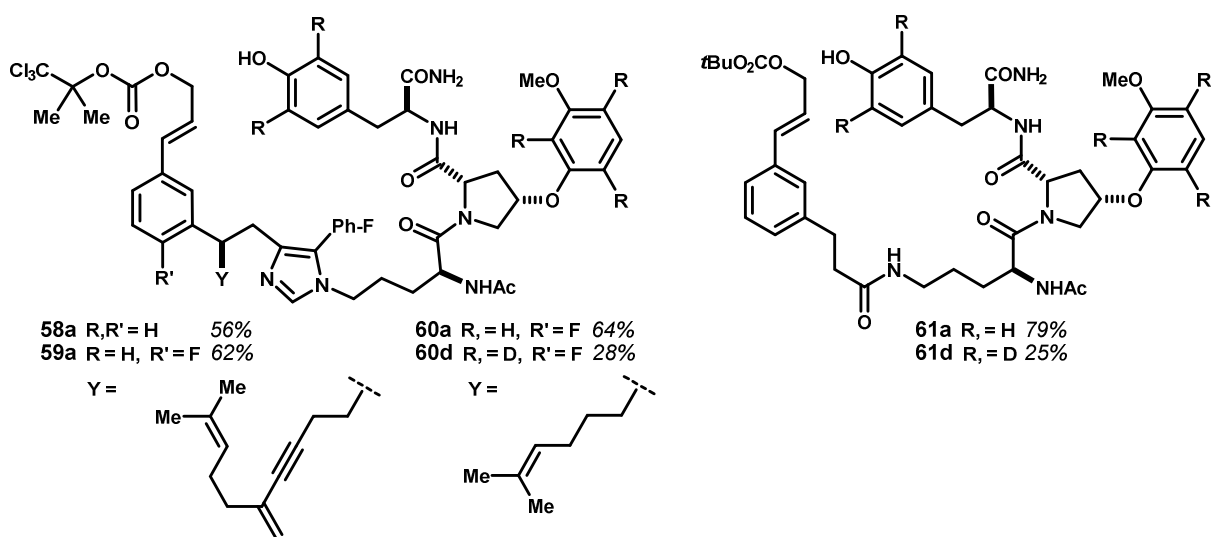
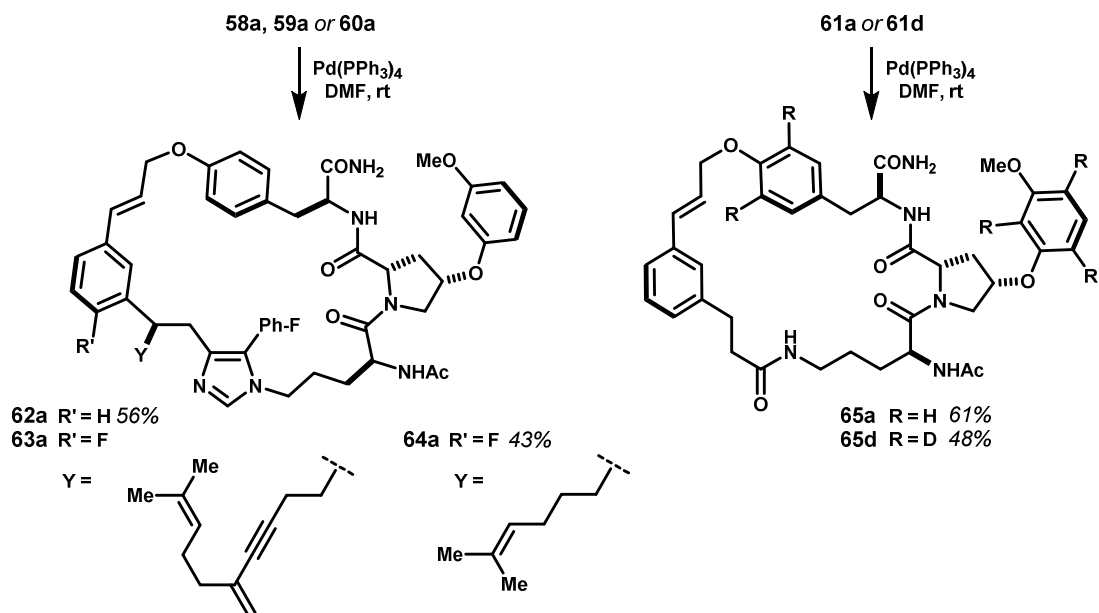


Figure 3.3.2 Acyclic intermediates **58**, **59**, and **60** were prepared by van Leusen imidazole synthesis between the appropriate peptide (**48**) and template **1**, **16** or **17**. Intermediates **61a,d** were prepared by acylation of the corresponding peptide by template **3**.

Natural abundance analog **48a** was first ligated to templates **1**, **16** and **17** by either van Leusen imidazole synthesis using 4-fluorophenyl-TosMIC or to template **3** by spontaneous amidation to give acyclic intermediates **58a–61a** (Figure 3.3.2). Though we had initially sought to investigate the reactions of all possible template/peptide isotopologue combinations, ultimately only a few were completed. Nonetheless,

these examples provided unanticipated new information that quickly garnered the focus of our research. Revised template **17**, the potential performance of which was highly anticipated, was coupled to pentadeuterated peptide isotopologue **48d** to give the corresponding deuterated acyclic intermediate **60d**. Additionally, pentadeuterated congener **61d** was prepared using simplified template **3** in order to assess whether long-range $O_{Tyr} \rightarrow C$ cinnamyl migrations to the aryloxyproline side chain were possible.

Scheme 3.3.3 Macrocyclic tyrosyl ethers **62**, **63** and **65** were prepared by Pd-catalyzed internal O -cinnamylation from their respective acyclic mixed cinnamyl carbonates.



Acyclic intermediates **58a**, **59a**, **60a**, **61a** and **61d** were transformed to their corresponding cyclic cinnamyl tyrosyl ethers by treatment with catalytic $\text{Pd}(\text{PPh}_3)_4$ (Scheme **3.3.3**); the development of this simplified catalyst system is discussed in Chapter 4. Despite repeated attempts, and re-purification of the starting material by PTLC, we were unable to cyclize pentadeuterated intermediate **60d**. Pentadeuterated **61d**, however, was cyclized without incident to give macrocycle **65d**. Mass spectra of acyclic intermediates **60d**, **61d** and macrocycle **65b** showed isotopic distributions consistent with high incorporation of five deuterium atoms. Additionally, these labelled materials co-eluted by HPLC with their corresponding natural abundance analogs, which were characterized by NMR.

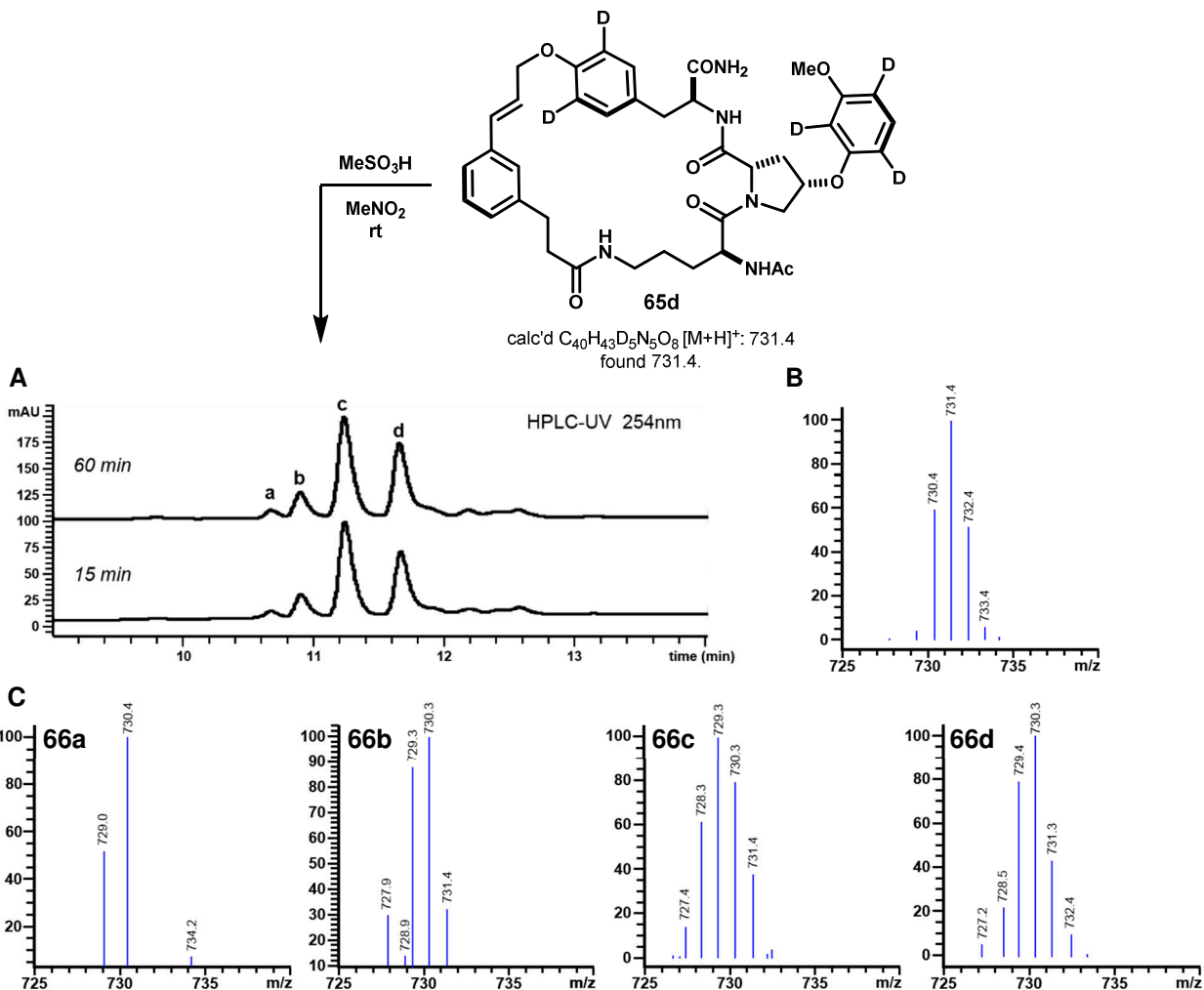


Figure 3.3.3 Acidolysis of pentadeuterated probe **65d** produced four new compounds as observed by HPLC. MS analysis showed that each product had lost one deuterium atom relative to starting **65d**, indicating long-range $O \rightarrow C$ cinnamyl migration to the deuterated positions had taken place.

Deuterium labeled macrocyclic ether **65d** was treated under our standard acidolysis conditions with 75 mM methanesulfonic acid in dry nitromethane (5 mM final), and an aliquot was removed after 15 minutes, quenched with methanolic Hünig's base, and analyzed by HPLC-UV/MS (Figure 3.3.3A). The reaction was sampled at an earlier time point, relative to the standard 2 hour reaction time, in the hope of observing partial conversion to control for scrambling of deuterium in the starting material. After just 15 minutes, **65d** had been completely consumed and cleanly converted to four new products, all of which appeared to have lost one to two Da relative to the mass of starting **65d** (Figure 3.3.3B,C). These anomalously low product masses likely resulted from partial scrambling, and therefore analysis at even shorter reaction times may

be required to confidently infer double internal alkylation by templates such as **16** or **17**. Indeed, while the ratio of products had not changed when the reaction was re-analyzed after 60 minutes (Figure **3.3.3A**), the mass spectral signatures had shifted lower, consistent with scrambling of deuterium. Pleasingly, however, analysis of the reaction at 15 minutes suggested that the aryloxyproline had reacted, as intended. This result was important, because it demonstrated that long-range $O \rightarrow C$ cinnamyl migrations to activated benzene rings were possible, and that this rearrangement was not restricted to the highly electron-rich indole side chain of tryptophan. Fundamentally, this suggested the possibility of a much broader substrate scope, with regard to the arene nucleophile, than had been previously recognized. Additionally, this experiment validated the performance of simplified template **3**, which gave a very tractable product mixture by comparison to the complex mixtures previously observed with acidolysis reactions involving template **1**.

Non-labeled variant **65a** was reacted analogously, yielding an identical product mixture, from which $C-C$ linked macrocycles **67a-d** were isolated in 60% combined yield (Figure **3.3.4**). The structures were

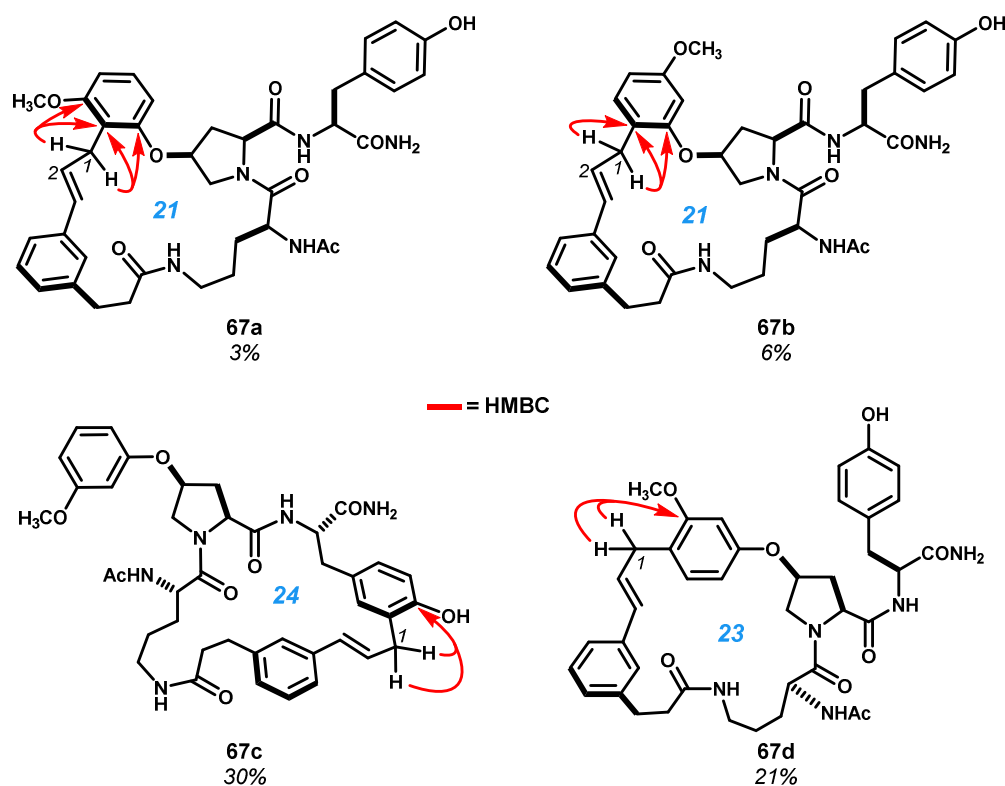


Figure 3.3.4 The structures of acidolysis products **67a-d** were confidently assigned by complete resonance assignment on the basis of 2D NMR correlation spectra. The key $C-C$ bond was assigned by HMBC correlations (indicated by red arrows) from cinnamyl methylene $H1/1'$ and carbons of the connected arene.

confidently assigned on the basis of 2D NMR correlation data, including 1H - 1H -COSY, 1H - 1H -TOCSY, 1H - ^{13}C -HSQC and 1H - ^{13}C -HMBC, and complete resonance assignments are listed in Experimental Appendix for this chapter. Key HMBC correlations from the cinnamyl methylene (i.e. *C1*) to key resonances of the connected arene are denoted by red arrows in Figure 3.3.4. While these correlations are sufficient to assign the structure, reciprocal correlations from the arene back to the cinnamyl unit were, in most cases, also observed. In some cases (e.g. **61a**, **b**) correlations from the central methine (i.e. *C2*) of the propenyl moiety was also correlated by HMBC to key carbon resonances of the connected peptidyl arene. As expected, the major product **67c** derived from alkylation *ortho* to the tyrosyl phenol; we had characterized this frequent outcome in all peptides previously examined with template **1**. The three other products derived from alkylation at each of the three canonically reactive sites within the 3-methoxyphenoxy side chain (**67a**, **b**, **d**), precisely as predicted based on substituent effects and the pattern of electrophilic bromination leading to the deuterated materials.

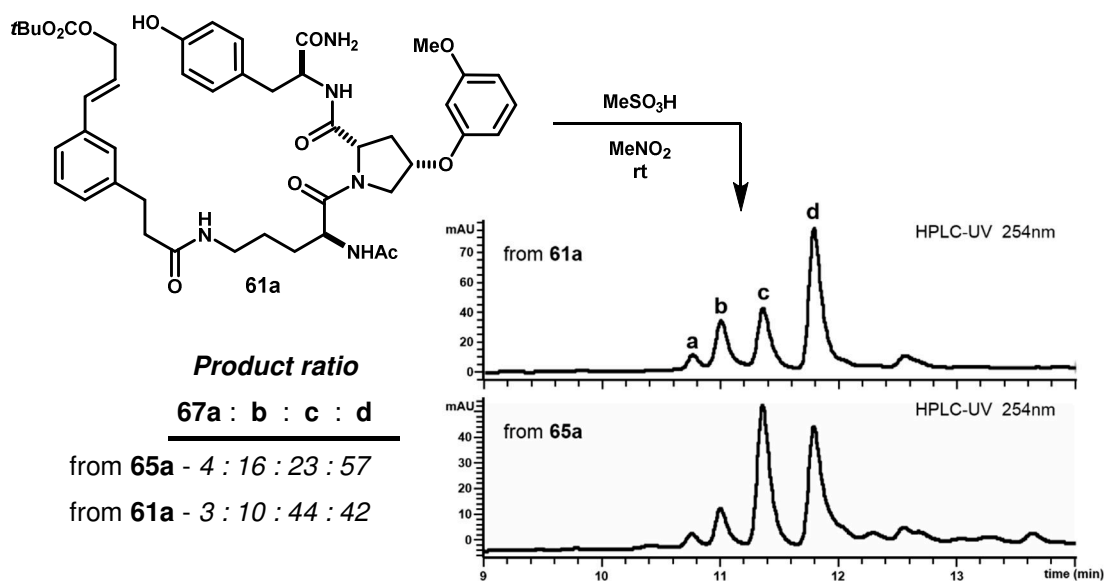


Figure 3.3.5 Acidolysis of acyclic intermediate **61a** directly formed macrocycles **67a–d**, but in different ratios than were produced by acidolysis of macrocyclic ethers **65**.

We next sought to test whether or cyclic cinnamyl ether **65a** was a requisite precursor to *C–C* linked isomers **67a–d**. Acyclic intermediate **61a** was treated with methanesulfonic acid in nitromethane under the same conditions as for the acidolysis of cyclic starting material **65d**, and analyzed by HPLC-UV/MS (Figure 3.3.6). Surprisingly, this reaction afforded the same four products **67a–d**, though in different relative ratios

than obtained from acidolysis of **65a**, with product **67d** becoming the major product. Though the net structural outcomes were identical, this was, to our knowledge, the first instance of direct large ring-forming Friedel-Crafts alkylation in the context of peptides and substrates harboring polar functional groups. In general, direct macrocyclization would carry great practical advantage by obviating the need for a phenolic group, and circumventing the air-free technique and relatively low throughput of the Pd-catalyzed cyclization. Systematic studies of direct ring *C*-cinnamylation by comparison to *O*→*C* cinnamyl migrations are discussed further in Chapter 3.4, and extensively in Chapters 5 and 6.

Critically, the observation of direct cyclizations from **61a** suggested that, despite our inability to cyclize **60d** with Pd⁰, deuterated isotopologue **60d** might still prove valuable in probing large ring-forming cinnamylations and secondary annulations of revised template **17**. The mass spectrum of **60d** also indicated very high isotopic purity, and acidolysis of this material was carried out analogously. Aliquots were removed and quenched at 1, 5, 15, 30 and 60 minutes following the addition of methanesulfonic acid, and analyzed by HPLC-UV/MS (Figure **3.3.6**). In this case, nine products were observed, four of which exhibited target masses corresponding to loss of the cinnamyl carbonate group, as well as one deuterium atom. Notably, the ratios of these products changed significantly in time, whereas the products of analogous acidolysis reactions with simplified template **3** did not. These results are consistent with a more rapid initial cinnamylation leading to products **68a, c, d** and **f**, and slower subsequent reactions, perhaps resulting from the 2-methylhexenyl group. However, no products were observed with masses corresponding to double internal substitution. Curiously, products **68e, g** and **h** exhibited masses consistent with double hydration (+36 Da) relative to the expected macrocycle pseudomolecular ion (961.5 m/z). This may result from initial *C*-cinnamylation at one of the deuterated positions, and subsequent hydration of the trisubstituted olefin and styrenyl double bond. However, the decreased polarity of these products (based on RP-HPLC retention time) and lack of dehydration fragments (-18 Da) in the mass spectra suggest that these products are not alcohols. Additionally, intermediate **68i**, which was slowly consumed during the reaction, exhibited a mass consistent with hydration of the starting material *without* the cinnamyl carbonate having ionized. No starting **60d** was observed after just one minute. Regrettably, we did not venture to isolate and characterize products from this reaction, and therefore the implications of these mass spectrometry data and performance of revised template **17** remain uncertain.

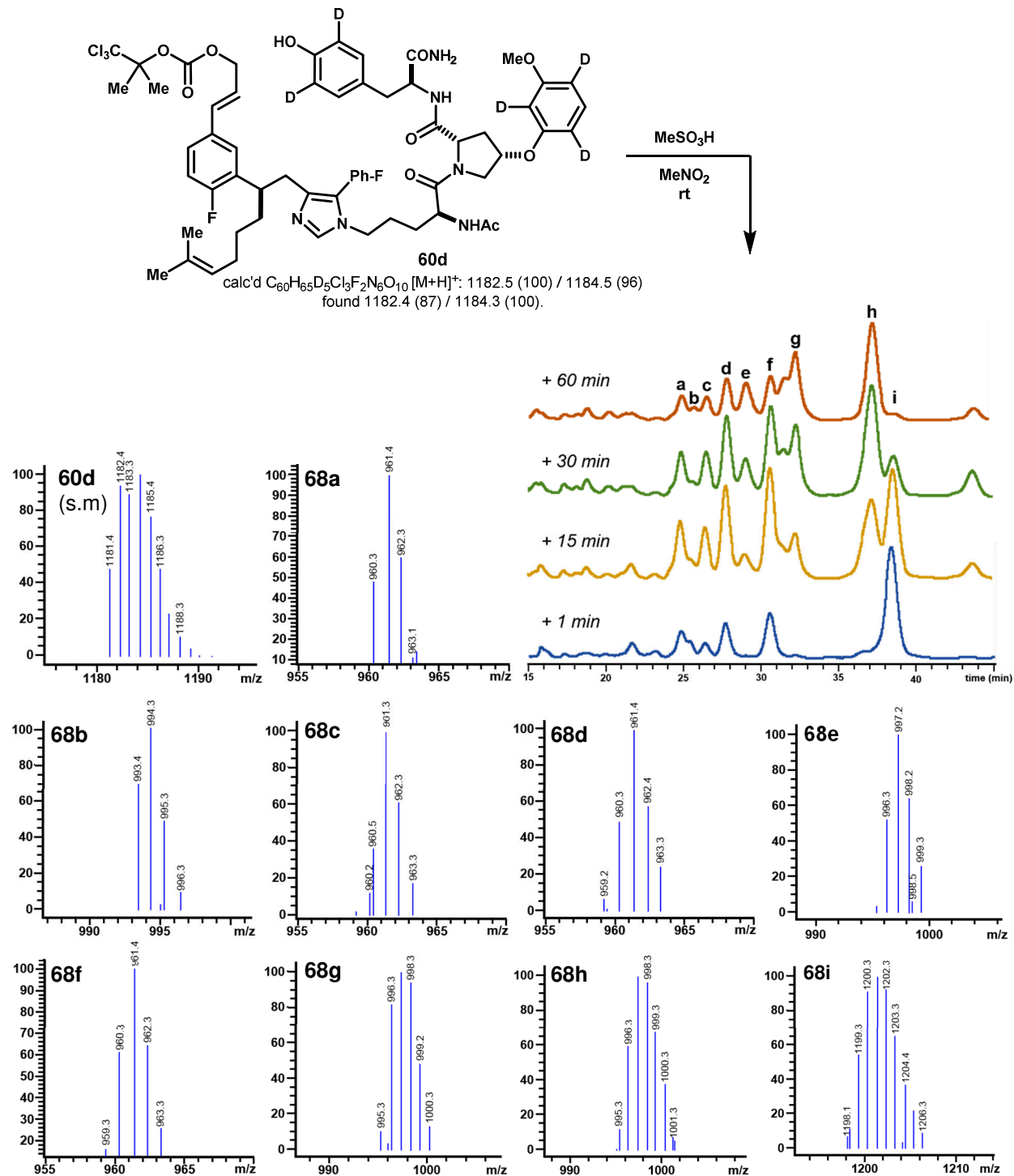
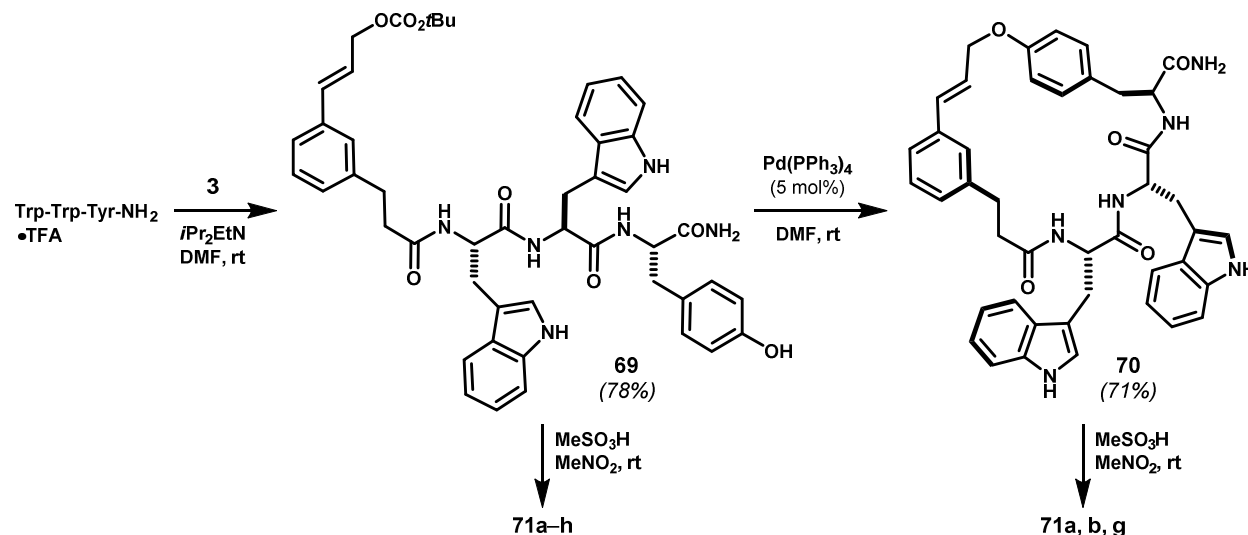


Figure 3.3.6 Acidolysis of deuterium labelled acyclic intermediate **60d**, harboring template **17**, led to a diverse product mixture. MS analysis indicated productive internal electrophilic substitution, in some cases, but did not reveal annulations by the intended reactions of the 2-methylhexenyl group.

Though no doubly alkylated products were detected from the acidolysis of **60d**, the time-course experiment indicated that *H/D* exchange – by the action of methanesulfonic acid – was slow relative to the rate of cinnamylation. At one or five minutes, the product mass spectra showed good agreement with calculated isotopic patterns corresponding to the loss of one deuterium. Later time points, however, showed an erosion of isotopic purity relative to spectra recorded for the same product peaks at earlier time points. The accuracy of detecting double internal aromatic substitutions is therefore critically dependent on controlling for background scrambling of the isotopic labels. Cinnamylation reactions appeared to be exceptionally rapid, and therefore less prone to scrambling interference when probing macrocyclization reactions. However, if more strongly acidic reaction media or elevated temperatures are required to ionize a second, less reactive group, such as the 2-methylhexenyl moiety of template **17**, then this labeling strategy may not be feasible. The use of Lewis acids, rather than Brønsted acids used here, may minimize scrambling in this regard (see Chapter 3.4).

3.4 Reactions of simplified template **3** with prototypical peptide Trp-Trp-Tyr

Scheme 3.4.1 Model peptide Trp-Trp-Tyr was readily acylated by template **3** and cyclized to its macrocyclic tyrosyl ether **70** by the action of catalytic Pd⁰.



The discovery of direct internal cinnamylations using simplified template **3** led us to concurrently revisit prototypical peptide Trp-Trp-Tyr. In doing so, we hoped to verify the direct Friedel-Crafts macrocyclization we had observed with peptidyl substrate Orn-Pro(OAr)-Tyr (Chapter 3.3) and to compare the reactivity of

template **3** to that of template **1** with model peptide Trp-Trp-Tyr, reported previously.² Additionally, we sought to more broadly survey reaction conditions leading to direct internal *C*-cinnamylations, and to further test the utility of deuterium labeling in probing these reactions. The results of these studies were reported by us in 2013, and the following discussion derives primarily from this communication.²⁹

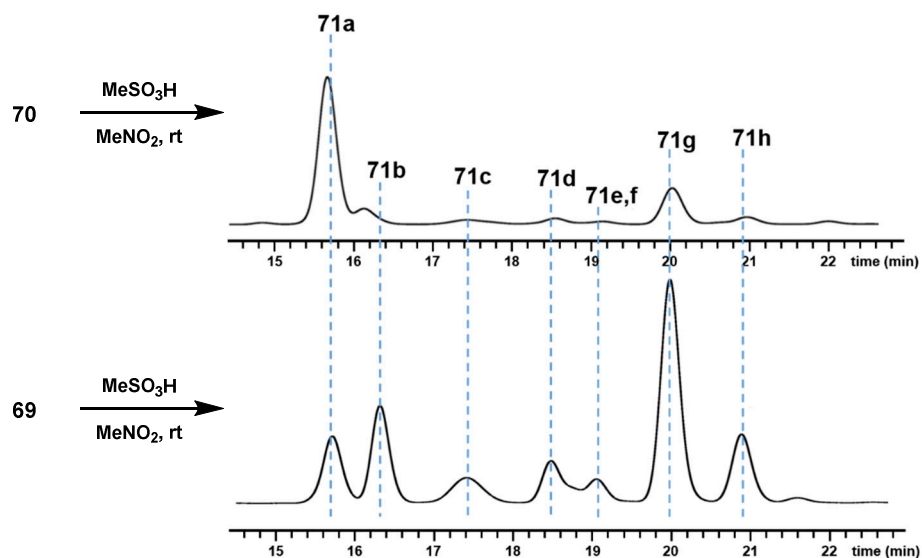


Figure 3.4.1 Acidolysis of cyclic ether **70** led to seven distinct isomeric product peaks by HPLC-UV (254 nm) analysis, each of which displayed a molecular mass identical to starting **70**. The analogous reaction of acyclic intermediate **69** led to the same products, but in a more even distribution.

Template **3** was ligated to Trp-Trp-Tyr-NH₂, providing acyclic intermediate **69** in good yield (Scheme 3.4.1). Exposure of **69** to 5 mol% Pd(PPh₃)₄ catalyzed efficient *O*-cinnamylation of tyrosine to give macrocyclic ether **70**. Treatment of macrocycle **70** under standard acidolysis conditions with methanesulfonic acid yielded a mixture of seven isomeric products (**71a–h**), observed by HPLC-MS (Figure 3.4.1), the three most abundant of which were isolated in sufficient amounts for NMR analysis. These products were characterized as **71a**, **b** and **g**, which derived from competing ring contractions by intra residue cinnamyl *O*→*C*_{ortho} migration (**71a**) and long-range cinnamyl migrations to *C*₅ of the indole side chains of each tryptophan (**71b**, **g**). These outcomes were consistent with the high reactivity of this position of indole in bimolecular reactions.^{30–33} Notably, these linkages comprised three of the four outcomes anticipated from previous reactions of Trp-Trp-Tyr with template **1** (see Chapter 1).² This suggested that

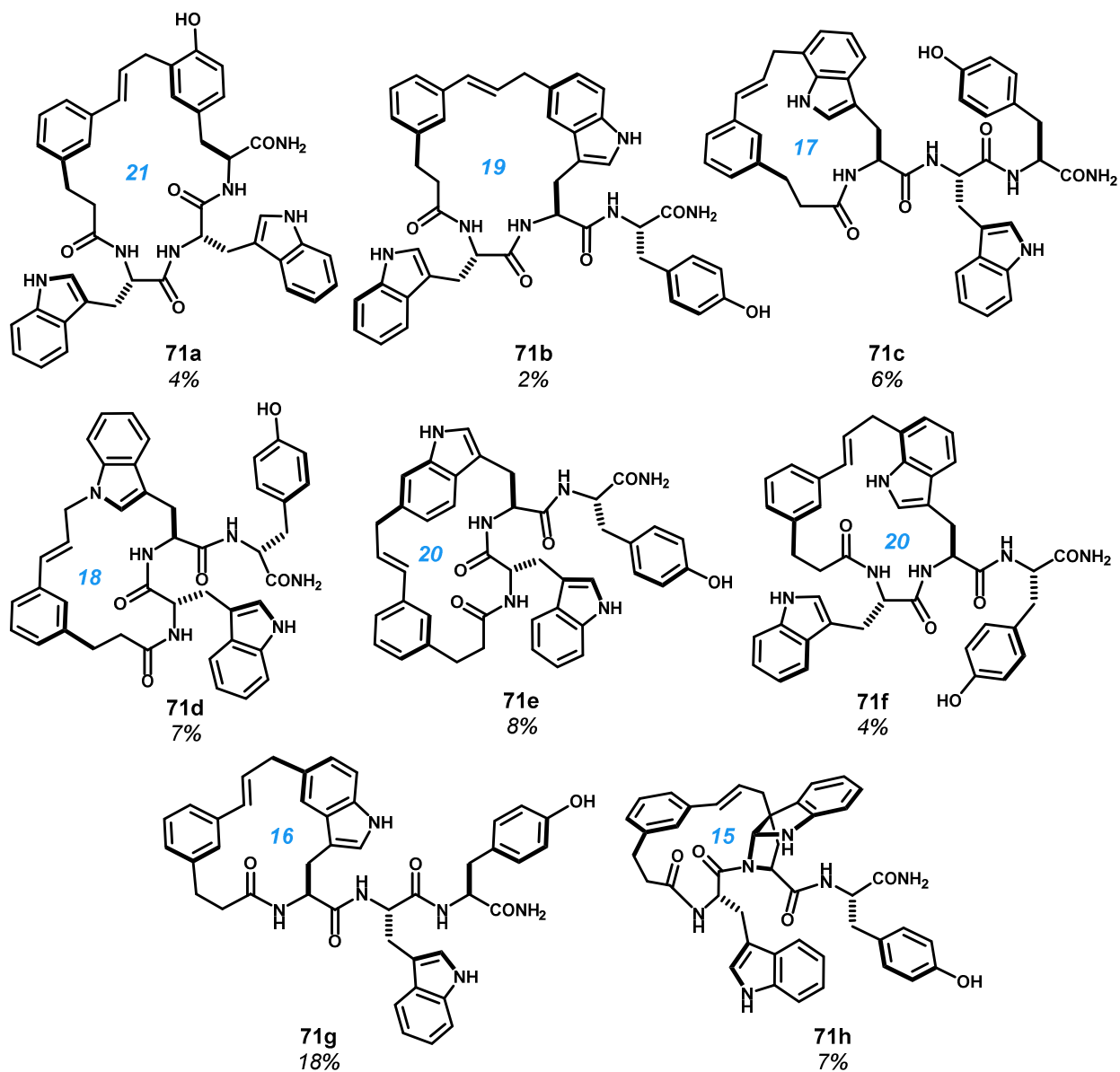


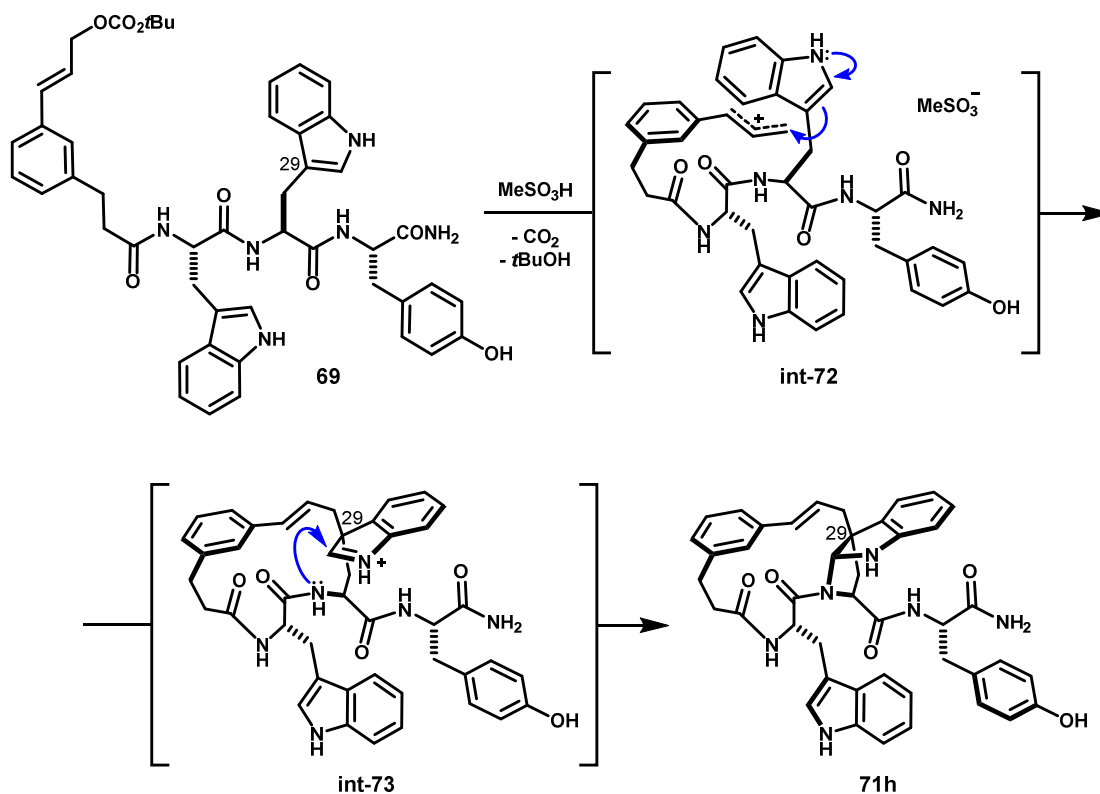
Figure 3.4.2 The macrocyclic structures of acidolysis products **71a-h** were rigorously determined by complete resonance assignment on the basis of 2D NMR correlation spectra. These products comprised both anticipated (**71a, b, g**) and novel (**71c, d, e, f, h**) cinnamyl linkages.

cinnamylations observed with simplified template **3** would likely translate to more complex template architectures, such as **1, 16** or **17**.

We next examined acidolysis reactions of acyclic material **69**, and were pleased to find that this reaction proceeded to a mixture of the same products as from macrocyclic ether **70** (Figure 3.4.1). As with model substrate Orn-Pro(OAr)-Tyr (see Chapter 3.3), the product ratios differed substantially when starting from acyclic **69** versus cyclic substrate **70**. In this case, acidolysis of the acyclic material yielded a more

even mixture, from which were then able to isolate and characterize the remaining products **71c–f, h**. These products comprised five novel macrocycles resulting from alkylation of tryptophan at indole *N1*, *C3*, *C6*, and *C7* (Figure 3.4.2). Tyrosine alkylation product **71a**, the major product from **70**, now comprised only 12% of the product mixture. Lesser products arising from alkylation at *C7* of Trp1 (**71c**) and Trp2 (**71f**), *C6* of Trp2 (**71e**), and *N1* of Trp2 (**71d**) were also obtained. Product **71h**, comprising the final 12% of the mixture, was determined to be a macrocyclic pyrroloindoline arising from indole *C3* alkylation of Trp2 and trapping of the resultant indolium ion (**int-73**) by the proximal amide nitrogen (Scheme 3.4.2).³⁴ Curiously, this product was obtained as a single *C29* diastereomer; the origin of diastereoselectivity was not immediately clear.

Scheme 3.4.2 Macrocyclic pyrroloindoline **71h**, which was obtained as a single diastereomer, results from cinnamylation of indole *C3* of Trp2, and trapping of the resulting indolium ion by the proximal amide nitrogen. Diastereoselectivity may result from inherent facial bias or reversibility of the initial alkylation.



Structural elucidation involved (1) sequential assignment of the peptide backbone, (2) correlation of backbone atoms to their corresponding side chain aromatic ring, and (3) determination of the connectivity of the cinnamyl moiety to an aromatic side chain. Complete ^1H and ^{13}C resonance assignments were made for all eight products (see Chapter 3 Experimental Appendix); in this model substrate, this was necessary

to differentiate between the two tryptophans. Sequential assignment of the amide backbone was made by $H^N-C(O)$ and $H^\alpha-C(O)$ correlations observed by $^1H-^{13}C$ HMBC,^{35,36} or by $H_i^\alpha-H_{i+1}^\alpha$ NOE where ambiguities arose from weak correlations or overlapping carbonyl resonances.^{37,38} Assignment of residue specific $H^N-H^\alpha-H^\beta$ spin systems from $^1H-^1H$ TOCSY spectra was then possible,³⁹ and connectivity of H^β to the aromatic portion of the side chain was established from reciprocal HMBC correlations.

In most cases, the key cinnamyl linkages were assigned based on through-bond $^{2,3,4}J_{CH}$ correlations from the cinnamyl methylene to the connected arene, as observed in $^1H-^{13}C$ HMBC experiments (Figure 3.4.3). In cases where the HMBC was weak or ambiguous, cinnamyl connectivity was inferred from through-space $^1H-^1H$ ROESY or NOESY correlations between the cinnamyl methylene and protons of the connected arene, in conjunction with $^1H-^1H$ TOCSY supporting an aryl spin system having lost one proton from the parent side chain (e.g. indole C7 isomer, **71f**, Figure 3.4.B). For **71f**, the use of ROESY experiments was found necessary, as only weak 2D-NOESY spectra were obtained in DMSO- d_6 . This likely resulted from the high viscosity of this solvent and medium molecular weight of these materials leading to weak signal in the so-called “cross-over region”, wherein $\omega\tau_c \approx 1$ at moderate mixing times (300-500 ms) at 14.1 T (i.e. 600 MHz).⁴⁰ This complication is ameliorated by use of the ROESY experiment, whereby coherence transfer occurs in the transverse plane at much lower field of the transmitter coils, rather than at the higher external field. Other compounds, such as pyrroloindoline **71h**, showed sufficiently strong NOE, but of negative sign.

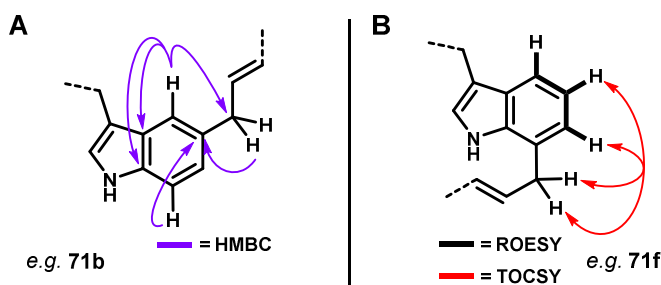


Figure 3.4.3 The precise connectivity of the key macrocyclic C–C bond was assigned either by **A**) HMBC correlation between the cinnamyl methylene and the connected indole, or **B**) by observation of an aryl spin system (TOCSY) having lost one proton from the parent side chain, and ROESY correlation between this aryl group and the cinnamyl methylene.

Products **71e** and **71f** were inseparable by HPLC, and therefore characterized simultaneously by careful deconvolution of the 2D-NMR spectra. Curiously, these products were both found to harbor 20-

membered rings. Though procedurally identical to assigning purified compounds individually (*vide supra*), the processes of elucidating the components of this mixture required careful annotation of a particularly dense aromatic region (Figure 3.4.4) and a large number of coincident signals given the structural similarity between **71e** and **71f**. Additionally, these components were present in a 5:4 ratio, leading to similarly intense correlations in 2D-NMR spectra, which can be more challenging to discern. For this reason, less even mixtures have generally proven easier to assign.

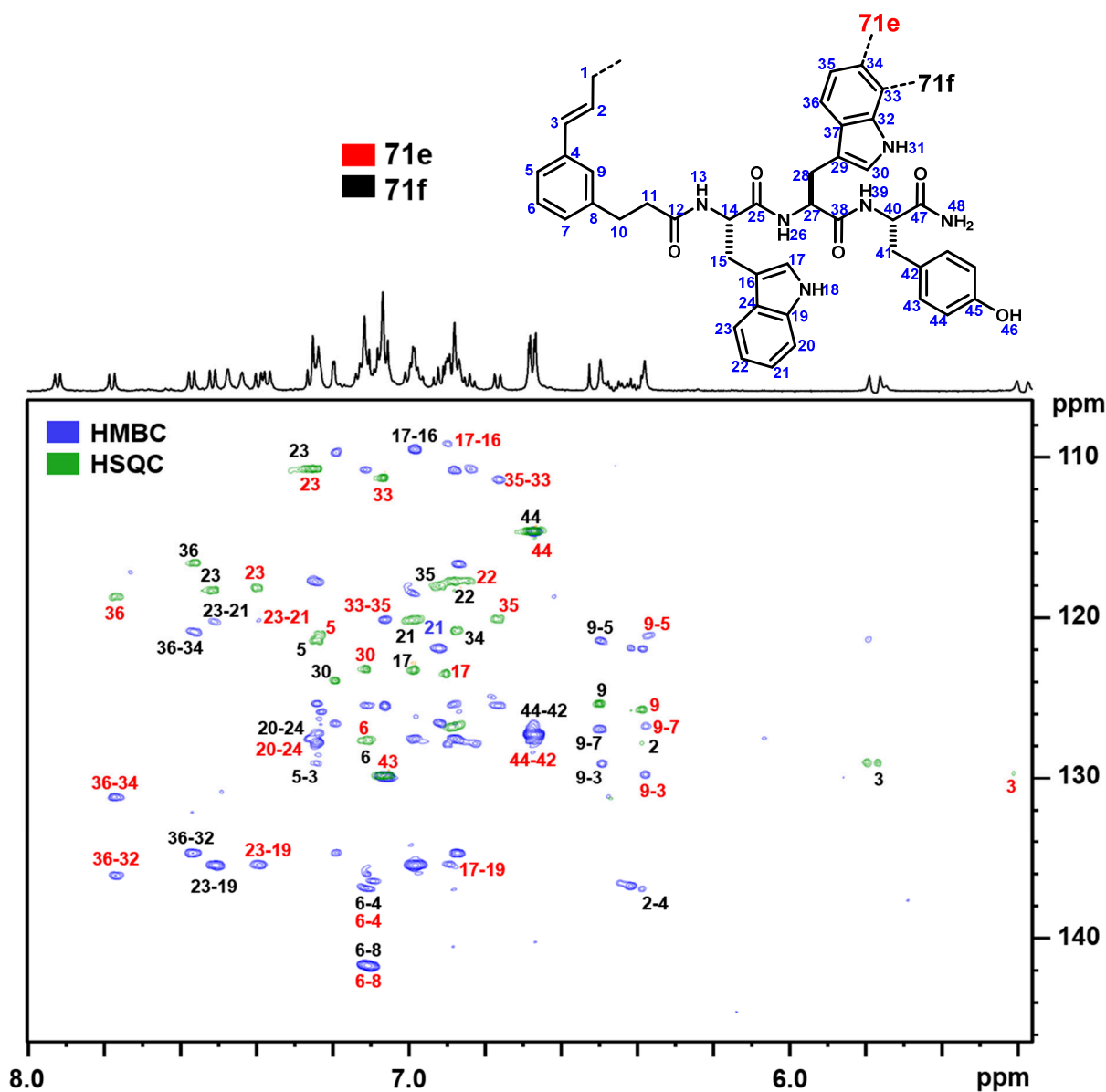


Figure 3.4.4 Compounds **71e** and **71f** were inseparable, and therefore were characterized simultaneously within a 5:4 mixture of the two. This entailed careful annotation of carbon resonances in the 1H - ^{13}C HSQC (green) and 1H - ^{13}C HMBC (blue) spectra, given the particularly dense aromatic region.

Product **71h**, the least polar component of the mixture, harbored a macrocyclic pyrroloindoline, which bears structural resemblance to large families of natural products possessing these motifs.^{41–44} Compound **71h** is a rare example of a macrocyclic pyrroloindoline bridged by an all carbon quaternary center at the core *cis*-5,5 ring juncture, a motif also found in prenylated diketopiperazine (+)-nocardioazine A isolated from a marine actinomycete (Figure 3.4.5).^{45,46} Both naturally- and synthetically-derived pyrroloindolines have been studied spectroscopically and computationally in an effort to characterize the stability and conformational equilibria of this ring system.^{47,48} Intrigued by this heterocyclic motif in the context of macrocycle **71h**, we further examined its structure and three-dimensional conformation using NMR.

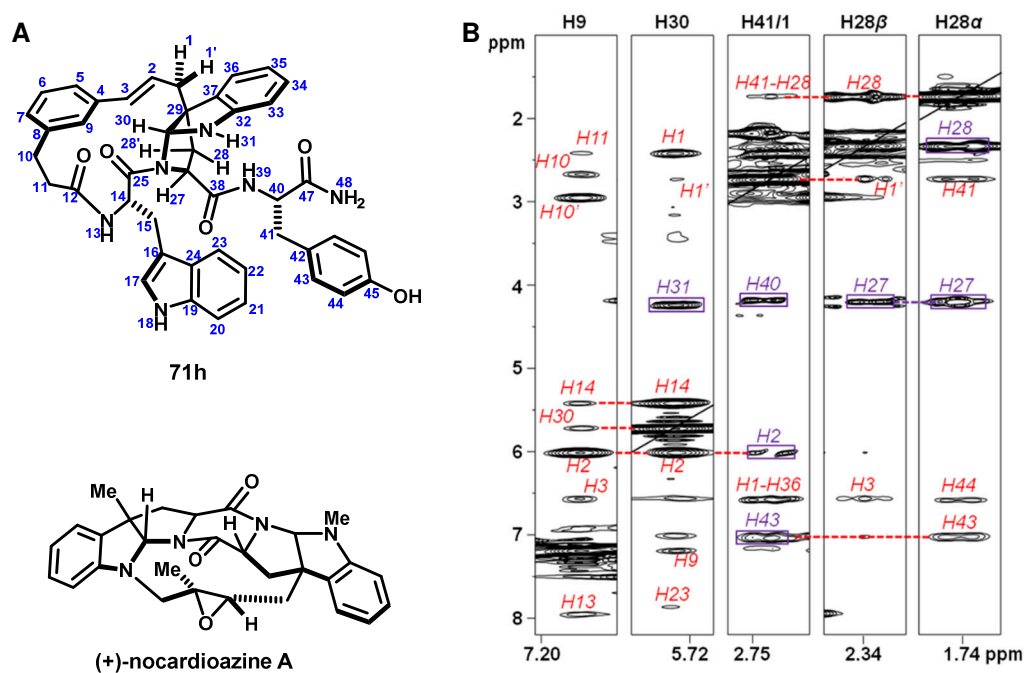


Figure 3.4.5 **A)** Macrocyclic pyrroloindoline product **71h** is a rare example harboring these motifs, which are also found in marine-derived natural product nocardioazine A. **B)** The relative stereochemistry of **71h** was assigned from 1D and 2D NOESY, as well as 2D ROESY spectra. Slices of the 2D NOESY spectrum which support key assignments are shown

The conformation of **71h** in solution appeared to be relatively homogenous based on its ¹H-NMR spectra. The core pyrroloindoline was clearly observed as a methine, weakly split by the adjacent *H*31, with an adjoining carbon with a chemical shift of 81.1 ppm, characteristic of an aminal. Heteronuclear correlations codified connectivity of the cinnamyl moiety at bridging quaternary center *C*29. As anticipated,

the 5,5 ring juncture was formed with the thermodynamically preferred *cis* geometry, which was readily apparent from NOE correlation of methine *H30* to the geminal methylene *H1/1'* (Figure 3.4.5). Spectral overlap in the aliphatic region, and of *H27*, *H31*, and *H41* frustrated the use of correlations to *H1/1'* in assigning the *ansa*-bridge stereochemistry relative to the *27S* stereocenter, preserved from *L*-tryptophan. Stereospecific assignment of the geminal pair *H28/28'* was tenuous, with no significant difference observed by NOE to *H30*. Analysis of $^3J_{27-28}$ and $^3J_{27-28'}$ suggested an *H28'-endo* configuration, which appeared contradictory to their relative chemical shift in comparison to related systems reported in the literature.^{47,48} We viewed a distinct possibility that the macrocyclic motif or tyrosine residue could distort this pyrrolidine ring, leading to atypical *J*-values. A single unambiguous long-range NOE from *H2* to *H27* led to the tentative assignment of the *C38-endo 27S,29R,30R* stereochemistry, as shown (Figure 3.4.5). Careful analysis of selective 1D-NOESY, 2D-NOESY, and 2D-ROESY spectra obtained in DMSO-*d*₆ or DMSO-*d*₆/D₂O supported this configuration, revealing seven prominent long-range correlations. Notably, strong NOEs within the tetrad *H14*, *H30*, *H9*, and *H2* indicated arrangement of these positions along the interior of the macrocycle. An initial model generated from a conformational search incorporating these constraints facilitated assignment of 29 additional long-range NOEs, and calculation of a refined structural ensemble (Figure 3.4.6) showing agreement with experimental NOEs. Complete analysis of the solution conformation is detailed in the Experimental Appendix for this chapter.

The bridged pyrroloindoline motif formed from cyclization of Trp2 onto the backbone effectively acts as a proline mimic. The backbone amide at this position retains the *trans* configuration, and the highly puckered *endo*-pyrroloindoline induces a turn conformation, analogously to proline, yielding a potential hydrogen bond between the Trp1-*C(O)* and Tyr3 carboxamide. The anomalous *J*-values associated with *H28/28'* were rectified on basis of long-range NOEs from *H28* to *H43* and *H44* indicating a *syn* relationship of *H28* to the C-terminal tyrosine residue, though details of the pyrrolidine ring conformer were not revealed from these force field calculations.^{49,50} These data suggest that compound **71h** occupies a relatively ordered conformation in solution that is enforced by both the macrocyclic and pyrroloindoline motifs.

The solution structure revealed several notable features induced by template **3**. Planarity of the cinnamyl unit was retained, as evidenced by strong NOE between *H3* and *H5*, and between *H2* and *H9*, thereby limiting the overall conformational flexibility of the 15-membered ring. The Trp1 side chain appeared

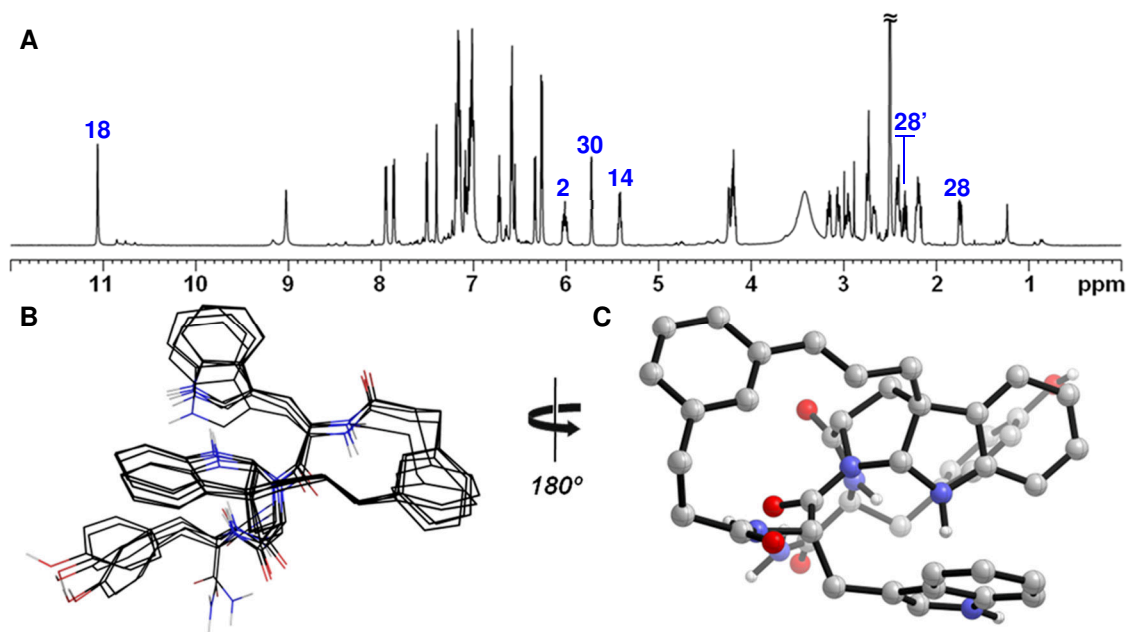


Figure 3.4.6 **A)** ^1H NMR spectrum of compound **12** ($\text{DMSO-}d_6$, 600 MHz). **B)** Overlay of the five lowest energy conformers calculated using NOE distance constrained molecular mechanics simulation and **C)** the lowest energy conformer obtained from this analysis. Spectral annotations correspond to numbering scheme in Figure 3.4.5.

to populate a single rotamer resulting in a close proximity of the indole ring to the benzene ring of the pyrroloindoline, which was supported by NOE observed between H_{20} and H_{33} . While side chain torsions were indirectly restrained by long-range NOEs, the calculated rotamer preferences of Trp1 (+ g) and Tyr3 (- g) agreed loosely with observed coupling constants ($\pm 30^\circ$), suggesting potential motional averaging at these side chains.⁵¹

Given the unique structure of **71h**, we sought reactions conditions that might bias towards its formation. Counterion and solvent effects are known to perturb the reaction rate and product distributions of Friedel–Crafts alkylation and rearrangement reactions.^{52–55} Accordingly, we examined alternative conditions to promote large ring-forming reactions of mixed carbonate **69** and rearrangements of cyclic cinnamyl ether **70**.

The nature of the acidic counterion was examined using a range of Brønsted and Lewis acids in both polar and non-polar solvents, the results of which are summarized in Table 3.4.1. Strong organic acids, including methanesulfonic acid and trifluoroacetic acid (TFA) were superior in promoting clean conversion to products **71a–h** by ring contractions of **70** (entries 1–10) and direct large-ring formations from **69** (entries 11–17). Weaker acids, such as aqueous acetic acid (not shown) and formic acid, returned only the starting

material. Using methanesulfonic acid, but changing the solvent from nitromethane to dichloromethane, led to intractable decomposition of **69** as observed by HPLC-MS. Consistent with previous studies by Olah and others, nitromethane likely stabilizes ion-paired intermediates along the reaction pathway.⁵⁶⁻⁵⁹ In dichloromethane, stoichiometric amounts of TFA reacted only slowly, whereas higher concentrations of TFA rapidly converted both **69** and **70** to well-distributed mixtures, which were comparable to those seen in reactions of **69** with methanesulfonic acid in nitromethane. Superacids showed mixed results. Stoichiometric triflic acid caused decomposition of **69** to non-isomeric products, even in nitromethane solvent. On the other hand, 2 equivalents of bistriflimide caused rapid reaction of **69**, and doubled the relative abundance of pyrroloindoline **71h**. Lewis acids also efficiently promoted these reactions. Relative to Brønsted acids, metal triflates, such as Sc(OTf)₃ enhanced the conversion of acyclic precursor **69** to Trp1 indole C5 alkylation product **71g** (see Figure 3.4.2). The product distribution from reactions of **69** is tunable with choice of acid promoter and solvent.

Table 3.4.1 Effect of substrate, solvent and acid promoter on product distribution in rearrangement reactions of cyclic ether **70** and direct large-ring closure reactions of acyclic mixed carbonate **69**. Reaction conditions: substrate (5 mM) in indicated solvent, 2 hr unless otherwise noted. Bold signifies substantial changes in product distribution.

Entry	Substrate	Promoter	Equiv.	Temp	Solvent	Product (HPLC-UV area %)						
						71a	71b	71c	71d	71e/f	71g	71h
1	70	MeSO ₃ H	5	rt	CH ₃ NO ₂	74	4	3	3	1	12	3
2	70	MeSO ₃ H	15	0 °C	CH ₃ NO ₂	71	6	3	2	2	13	3
3	70	MeSO ₃ H	15	rt	CH ₃ NO ₂	63	7	4	3	2	17	4
4	70	MeSO ₃ H	25	-20 °C	CH ₃ NO ₂	58	10	4	3	2	20	4
5 ^a	70	MeSO ₃ H	5	-20 °C	CH ₃ NO ₂	95	<1	<1	<1	<1	4	<1
6	70	MeSO ₃ H	15	rt	CH ₂ Cl ₂	N/A ^b	-	-	-	-	-	-
7 ^a	70	CF ₃ SO ₃ H	15	rt	CH ₂ Cl ₂	N/A ^b	-	-	-	-	-	-
8	70	TFA	50% v	rt	CH ₂ Cl ₂	3	24	8	15	3	34	13
9	70	TFA	15	rt	CH ₂ Cl ₂	95	<1	<1	<1	<1	4	<1
10	70	Sc(OTf) ₃	1	rt	CH ₃ NO ₂	61	3	6	2	1	22	5
11	69	MeSO₃H	15	rt	CH₃NO₂	12	16	6	9	5	40	12
12	69	TFA	50% v	rt	CH ₂ Cl ₂	32	17	7	7	1	28	8
13 ^a	69	TFA	15	rt	CH ₂ Cl ₂	21	14	6	7	5	36	11
14	69	CF ₃ SO ₃ H	1	rt	CH ₃ NO ₂	N/A ^b	-	-	-	-	-	-
15	69	HCO ₂ H	50% v	rt	H ₂ O	-	-	-	-	-	-	-
16 ^c	69	Tf ₂ NH	2	rt	CH ₃ NO ₂	5	14	5	8	6	38	24
17	69	Sc(OTf) ₃	1	rt	CH ₃ NO ₂	9	1	9	<1	<1	68	13

^a 16 hr reaction time

^b Decomposition to non-isomeric products observed.

^c 30 min reaction

As expected from earlier investigations (see Chapter 3.3), significantly different product distributions were, under certain reaction conditions, observed when starting from cyclic ether **70** relative to **69**. Reaction of **70** with dilute TFA in dichloromethane at room temperature (entry 9, Table 3.4.1), while

sluggish, formed tyrosine alkylation product **71a** selectively. This outcome was a prominent reversal of selectivity relative to reaction of **69** under the same conditions (entry 13). This selectivity was lost at high concentrations of TFA. Similar trends were observed with methanesulfonic acid. Using only 5 equivalents of methanesulfonic acid in nitromethane at -20 °C, cyclic **70** was rearranged to **71a** in a 20:1 ratio relative to all other isomers. These dramatic differences appear to reflect the influence of conformational pre-organization in **70** on the resulting reaction pathways.

One way to rationalize these results is in terms of a qualitative least motion argument.⁶⁰ All else considered equal, the conformationally pre-organized template in **70** rearranges more selectively, with the cinnamyl unit migrating to electron rich positions adjacent to the original attachment site.⁶¹ In contrast, ionization of acyclic carbonate **69** occurs in the context of a complex ensemble of peptide conformations, leading to a solvated cinnamyl ion pair that approaches multiple internal reactive sites, whereby less selectivity is manifest and a more diverse mixture results. These results are consistent with an intermediate phenylallyl carbocation.^{57,62,63} The attenuated selectivity observed from **70** in higher concentrations of acid may reflect accelerated ion pair return or altered solvation thereby permitting relaxation away from the cyclic conformation and leading to products by similar pathways as **69**.^{64,65} The nature of this conformational bias is further explored in experiments discussed Chapter 5.

Having rigorously characterized the product mixture **71a–h**, and identified means to alter the distribution of this mixture, we next examined the use of deuterium labeling/mass spectrometry, as outlined in Chapter 3.3, to predict these outcomes. In this instance, we examined selectively deuterated substrates isotopologues Trp(indole-*d*₅)-Trp-Tyr and Trp-Trp(indole-*d*₅)-Tyr, which would, in principle, be able discern which tryptophan side chain had reacted. However, only alkylation at deuterated sites *C*2, *C*4, *C*5, *C*6 or *C*7 would lead to loss of a deuterium atom and detection by mass spectrometry (Figure **3.4.7B**). The indole ring of tryptophan was perdeuterated by *H/D* exchange by heating with DCl in D₂O in the presence of thioglycolic acid as an antioxidant (Figure **3.4.7A**). This process was repeated once, yielding *L*-tryptophan(indole-*d*₅) (**72**) with >95% deuterium incorporation at each position, which was protected as its *N*_α-Fmoc derivative **73**. These two peptide isotopologues were assembled by solution-phase synthesis to incorporate deuterated monomer **73** in high isotopic purity.⁶⁶ This avoided potential scrambling under conditions required to deprotect standard Cbz or Boc protecting groups used in solution-phase peptide

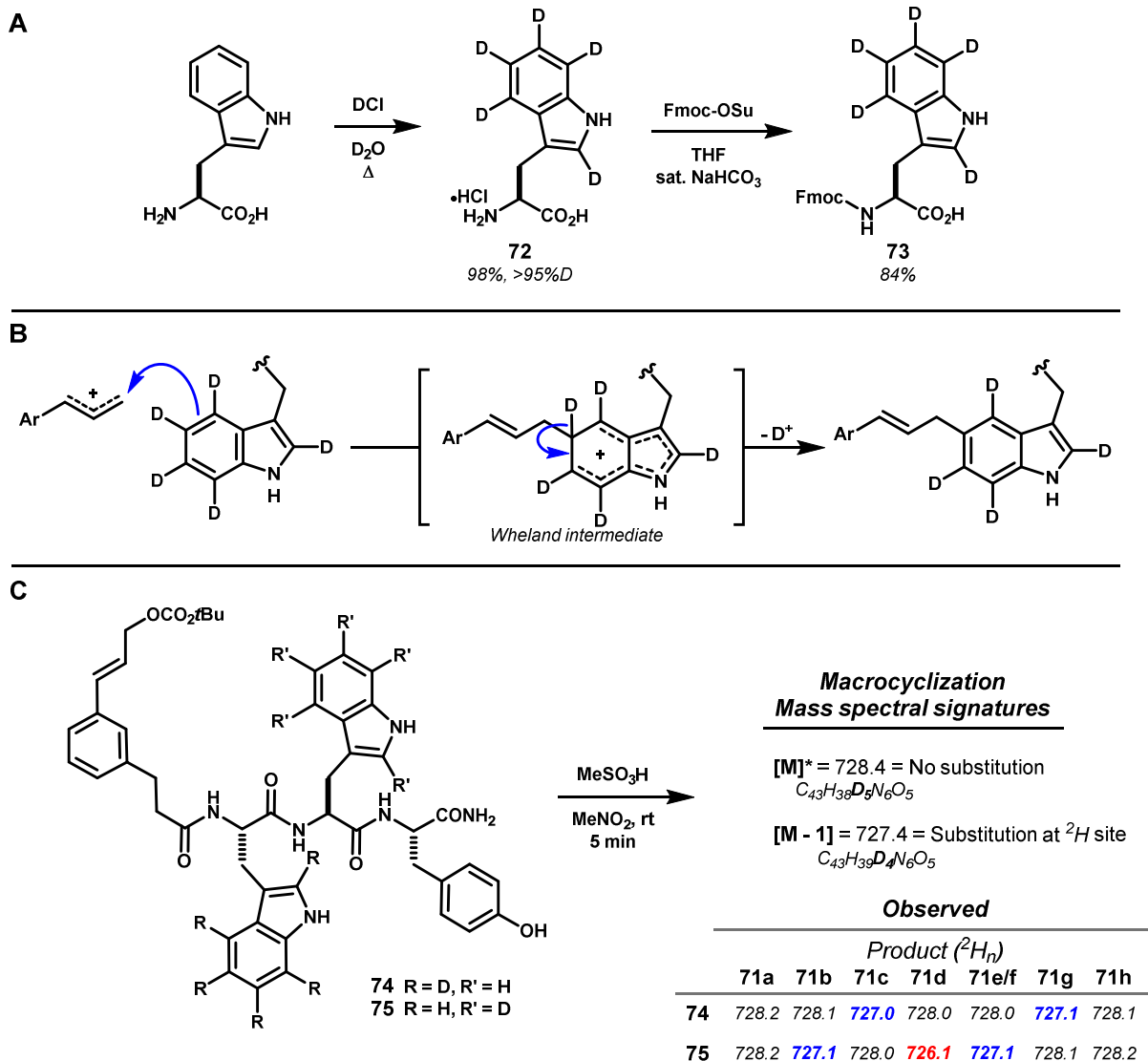


Figure 3.4.7 A) *L*-Tryptophan(indole- d_5) was synthesized by *H/D* exchange, and N_α -Fmoc protected for peptide synthesis. **B)** *C*-Cinnamylation at deuterated positions would lead to loss of one deuterium atom upon rearomatization from the Wheland intermediate. **C)** MS analysis of the acidolysis reactions of diagnostic isotopologues **74** and **75** successfully predicted the position of internal substitutions of tryptophan (**blue**). *N*-Linked product **71d** led to an anomalous loss of two deuterium (**red**), and pyrroloindoline **71h** retained all deuterium labels, because it is not substituted at deuterated positions.

synthesis, or acidic conditions required for cleavage from resins used in solid-phase synthesis. Subsequent acylation of each peptide with template **3** afforded acyclic mixed carbonates **74** and **75** (Figure 3.4.7C). After purification, MS analysis showed >95% average 2H -incorporation at each position.

Acidolysis of **74** and **75** under the standard conditions with methanesulfonic acid in nitromethane proceeded to product mixtures, which were, by HPLC-UV, identical to that observed with unlabeled

substrate **69**. To control for scrambling (see Chapter 3.3), these reactions were analyzed at partial and full conversion, and also under Lewis acidic conditions. The rate of product formation appeared to outcompete scrambling. In control experiments, treatment of tryptophan(indole- d_5) with 75 mM methanesulfonic acid in nitromethane caused considerable $^2H/H$ -exchange at 16 hours. Early time points (< 10 min) did not show appreciable exchange, indicating the rate of internal cinnamylation would outcompete scrambling. When the same control reaction was carried out instead with $Sc(OTf)_3$ in nitromethane, no $^2H/H$ -exchange was observed, even after 16 hours.

As anticipated, alkylation of Trp1(indole- d_5) leading to products **71c** and **71g** was revealed as a loss of 1 Da, as observed by HPLC–MS analysis of the reaction of isotopologue **74** (Figure 3.4.7C). This characteristic mass was also observed for products **71b**, **71e**, and **71f**, arising from alkylation of Trp2(indole- d_5) in the reaction of **75**. While complete retention of deuterium was observed, as expected, for product **71h**, an unexpected loss of two deuterium was found for Trp2 *N*-alkylated product **71d** from the acidolysis of **75**. Whether this loss is mechanism based or due to increased exchange rate in the product is not yet known. *N*-alkylation of indole may accelerate $^2H/H$ -exchange by enhancing the basic character of the resulting aromatic system.^{67,68} Though scrambling was minimal in reactions promoted by $Sc(OTf)_3$, we were unable to rectify the anomalous mass of **71d**, as this product was in only trace quantities under these conditions. Although this non-diagnostic outcome limits the accuracy of deuterium labeling in probing macrocycle connectivity to tryptophan, this result nonetheless remains characteristic of substitution at Trp2 in this model peptide.

These data further demonstrate the utility of deuterium labeling in conjunction with HPLC-MS analysis for rapidly predicting large ring structures arising from aromatic substitution using templates, such as **3**. This analytical approach may be particularly useful when investigating peptide sequences harboring multiple aromatic amino acids, such as Trp-Trp-Tyr investigated here, where spectral overlap can complicate structural assignment.

3.5 Conclusions & remarks regarding revised templates **3**, **16** and **17**, and the use of ^2H labeling to probe large ring-forming reactions

Preliminary investigation of the reactions of revised templates **16** and **17** did not yield clear successes towards our goal of initiating large ring annulations. Given the limited data generated with these templates, and dearth of rigorous structural characterization of products derived therefrom, it's difficult to fairly generalize their performance. Similarly to template **1**, the initial condensation and van Leusen imidazole synthesis to ligate **16** and **17** to model peptides proved problematic. Low yields in this step made it difficult to obtain acyclic template-peptide conjugates in sufficient quantities and purity to carefully study subsequent ring-forming reactions. Though we were able to overcome this by simply scaling up the reactions, this quickly consumed our supply of the templates, which were themselves time-consuming to prepare.

Though fluorination of the central aryl ring in **16** caused clear changes in resulting acidolysis mixtures, it did not appear to substantially decrease the number of products. We neither ventured to isolate products derived from **16**, nor undertook deuterium labeling experiments with this template. Whether **16** achieved transannular ring-forming reactions of the diene-yne is unknown. However, given the improved understanding of large ring-forming cinnamylations from reactions of template **3**, it seems likely that the highly complex mixtures resulting from reactions of **16** likely reflect isomerizations of the diene-yne appendage, productive or otherwise.

Template **17** reflects logical revisions of the template design, and led to substantially less complex product mixtures. In reactions with model peptide Orn-Pro(OAr)-Tyr, template **17** appeared to lead to four isomeric products, consistent with the four possible sites of electrophilic aromatic cinnamylation. However, at least four other products were also formed, all of which exhibited higher masses than the desired product. While several of these products are consistent with double hydration (+36 Da) by mass, it remains unclear what the precise fate of the 2-methylhexenyl motif is in these acidolysis reactions. Had this tertiary olefin formed the desired cation, but reacted bimolecularly? If so, could reaction conditions be tuned to minimize these side reactions? These questions could likely be answered by isolation and NMR elucidation of product structures. During NMR analysis of the macrocyclic ether **65a**, for instance, it became evident that both fluorine resonances very substantially complicate structure elucidation. The splitting of ^1H and ^{13}C resonances up to four bonds away in both 1D and 2D spectra is, at best, complicating, and frequently

renders fully substituted carbon centers undetectable. In this regard, it would behoove the experimenter to first alter reaction conditions to minimize byproduct formation, and then attempt to force the tertiary olefin to cross-link the resulting cinnamyl C–C linked macrocycles.

Simplified template **3**, though reminiscent of template **2**, led to several critical discoveries, and constituted a major breakthrough. The experiments documented in this chapter provide a glimpse of the untapped potential of the cinnamyl carbocation, as well as transiently formed cinnamyl-Pd complexes, to rapidly access unique peptidyl macrocycles of diverse connectivity. The ability to directly engage aromatic amino acid side chains in Friedel-Crafts reactions is unprecedented, and uniquely powerful. Palladium-catalyzed and acid-promoted activation of template **3** are further explored in Chapters 4 and 5, respectively.

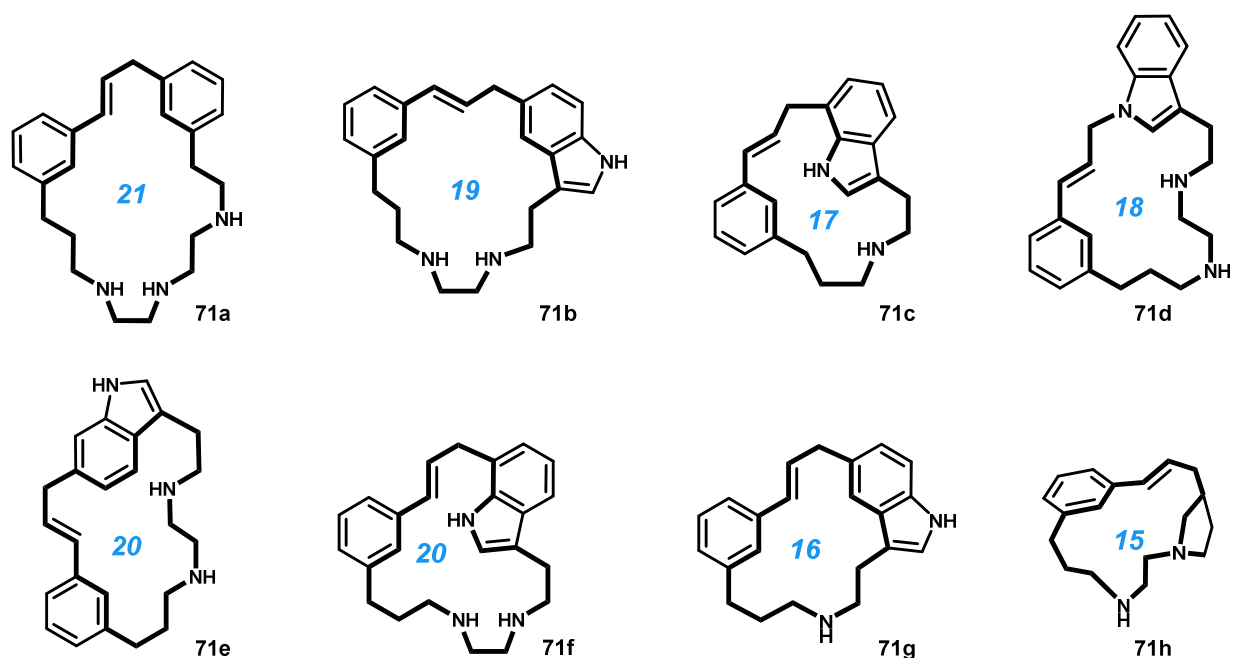


Figure 3.5.1 Reactions of template **3** with Trp-Trp-Tyr lead to a structurally diverse mixture of isomeric products. Macrocycles core structures comprising 15, 16, 17, 18, 19, 20, and 21-membered rings, which have, to our knowledge, not been reported in the literature, are formed in two steps from the starting peptide.

From a single reaction, we isolated eight unique macrocyclic cores comprising 15, 16, 17, 18, 19, 20, and 21-membered rings (Figure 3.5.1). While analogous collections of *ansa*-bridged macrocyclic rings could be accessed in a convergent manner, this would likely be time intensive. Harnessing divergent reactions, however, ultimately requires high performance separations to resolve product mixtures. This

appears to be, in many cases, possible, given the greater polarity difference between products of substantially different ring constitution.

Whereas conformational equilibria and geometric constraints of small rings (e.g. 3- to 8-membered rings) are well understood and widely exploited for their synthetic/pharmacological utility, no analogous understanding exists, at this point, for macrocyclic rings. Divergent ring-forming cinnamylations offer a viable means to explore the effect of large ring constitution on the structure and properties of the products. Furthermore, divergent transformation of a given peptide motif – which could be made to reflect a given native binding sequence – into macrocyclic products of varying ring size and shape would allow rapid access collections of peptidomimetics for biological screening.

While the initial acidolysis conditions using methanesulfonic acid gave a desirable, evenly-distributed product mixture, there are reasons to perturb this outcome. To retain tractability in biological screening exercises, a mixture should optimally contain an equal concentration of products so as to minimize the incidence of false negatives. Conversely, in the event that a single component becomes desirable as a result of either structure or function, it may be possible to enhance its abundance by subtle changes in reaction conditions, rather than undertaking a target-oriented synthesis. We have shown this is possible by biasing the template-induced macrocyclization toward the 15-membered macrocyclic pyrroloindoline **71h**, 16-membered ring **71g**, or 21-membered ring **71a**. Cyclic cinnamyl ether **70** was essential in this regard. While we were successful in biasing the product distribution in favor of initially abundant compounds **71a**, **g** or **h**, it is not yet clear this can be accomplished for minor constituents to the same degree.

References

- (1) Wei, Q.; Harran, S.; Harran, P. G. *Tetrahedron* **2003**, *59*, 8947.
- (2) Zhao, H.; Negash, L.; Wei, Q.; LaCour, T. G.; Estill, S. J.; Capota, E.; Pieper, A. A.; Harran, P. G. *J. Am. Chem. Soc.* **2008**, *130*, 13864.
- (3) Lin, W.; Chen, X.; Wang, Q.; Xiao, Y.; Zheng, J.; He, H.; Chen, S. Method for fast synthesizing 3-substituted aromatic acid. CN 101747171, 2010.
- (4) End, N.; Furet, P.; van Campenhout, N.; Wartmann, M.; Altmann, K.-H. *Chem. Biodivers.* **2004**, *1*, 1771.
- (5) Matveeva, E. D.; Podrugina, T. a.; Morozkina, N. Y.; Zefirova, O. N.; Seregin, I. V.; Bachurin, S. O.; Pellicciari, R.; Zefirov, N. S. *Russ. J. Org. Chem.* **2002**, *38*, 1769.

- (6) Smith, M. B.; March, J. In *March's Advanced Organic Chemistry: Reactions, Mechanisms, and Structure*; John Wiley & Sons, Inc.: Hoboken, NJ, 2007; pp 622–623.
- (7) Dumas, A. M.; Seed, A.; Zorzitto, A. K.; Fillion, E. *Tetrahedron Lett.* **2007**, *48*, 7072.
- (8) Wright, D.; Haslego, M. L.; Smith, X. *Tetrahedron Lett.* **1979**, *20*, 2325.
- (9) Frost, C. G.; Penrose, S. D.; Gleave, R. *Synthesis (Stuttg.)*. **2009**, 627.
- (10) Akué-gédu, R.; El-hafidi, H.; Couturier, D. *J. Heterocycl. Chem.* **2006**, *43*, 365.
- (11) Martin, R.; Buchwald, S. L. *Acc. Chem. Res.* **2008**, *41*, 1461.
- (12) Böhm, V. P. W.; Herrmann, W. A. *Chem. - A Eur. J.* **2001**, *7*, 4191.
- (13) Herrmann, W. A.; Brossmer, C.; Öfele, K.; Reisinger, C.-P.; Priermeier, T.; Beller, M.; Fischer, H. *Angew. Chemie Int. Ed. English* **1995**, *34*, 1844.
- (14) Weix, D. J.; Marković, D.; Ueda, M.; Hartwig, J. F. *Org. Lett.* **2009**, *11*, 2944.
- (15) Hallett-Tapley, G.; Cozens, F. L.; Schepp, N. P. *J. Phys. Org. Chem.* **2009**, *22*, 343.
- (16) Wünsch, E.; Jaeger, E.; Kisfaludy, L.; Löw, M. *Angew. Chem. Int. Ed. Engl.* **1977**, *16*, 317.
- (17) Bodanszky, M.; Martinez, J. *Synthesis (Stuttg.)*. **1981**, *5*, 333.
- (18) Calli, C.; Illuminati, G.; Mandolini, L.; Tamborra, P. *J. Am. Chem. Soc.* **1977**, *99*, 2591.
- (19) Miyaura, N.; Suzuki, A. *J. Chem. Soc., Chem. Commun.* **1979**, 866.
- (20) Stille, J. K.; Lau, K. S. *Acc. Chem. Res.* **1977**, *10*, 434.
- (21) Corey, E. J.; Wang, Z. *Tetrahedron Lett.* **1994**, *35*, 539.
- (22) Lo, C. Y.; Lin, C. C.; Cheng, H. M.; Liu, R. S. *Org. Lett.* **2006**, *8*, 3153.
- (23) Jerina, D. M.; Daly, J. W.; Landis, W. R.; Witkop, B.; Udenfriend, S. *J. Am. Chem. Soc.* **1967**, *89*, 3347.
- (24) Terrier, F. G.; Debleds, F. L.; Verchere, J. F.; Chatrousse, A. P. *J. Am. Chem. Soc.* **1985**, *107*, 307.
- (25) A. Streitwieser Jr., P. J. Scannon, H. M. N. *J. Am. Chem. Soc.* **1972**, *94*, 7936.
- (26) Narisada, M.; Horibe, I.; Watanabe, F.; Takeda, K. *J. Org. Chem.* **1989**, *54*, 5308.
- (27) Colon, I. *J. Org. Chem.* **1982**, *47*, 2622.
- (28) Guijarro, A.; Rosenberg, D. M.; Rieke, R. D. *J. Am. Chem. Soc.* **1999**, *121*, 4155.
- (29) Lawson, K. V.; Rose, T. E.; Harran, P. G. *Tetrahedron* **2013**, *69*, 7683.
- (30) Demopoulos, V. J.; Nicolaou, I. *Synthesis (Stuttg.)*. **1998**, 1998, 1519.
- (31) Murakami, Y.; Tani, M.; Tanaka, K.; Yokoyama, Y. *Heterocycles* **1984**, *22*, 241.
- (32) Pérez Schmit, M. C.; Jubert, A. H.; Vitale, A.; Lobayan, R. M. *J. Mol. Model.* **2011**, *17*, 1227.
- (33) Li, J.; Li, B.; Chen, X.; Zhang, G. *Synlett* **2003**, 1447.
- (34) Taniguchi, M.; Hino, T. *Tetrahedron* **1981**, *37*, 1487.
- (35) Kessler, H.; Griesinger, C.; Zarbock, J.; Loosli, H. *J. Magn. Reson.* **1984**, *57*, 331.
- (36) Bermel, W.; Griesinger, C.; Kessler, H.; Wagner, K. *Magn. Reson. Chem.* **1987**, *25*, 325.
- (37) Chazin, W. J.; Wright, P. E. *Biopolymers* **1987**, *26*, 973.
- (38) Wüthrich, K. *Biopolymers* **1983**, *22*, 131.
- (39) Bax, A.; Davis, D. G. *J. Magn. Reson.* **1985**, *65*, 355.
- (40) Claridge, T. D. W. In *High-Resolution NMR Techniques in Organic Chemistry*; Baldwin, J. E., Willaims, F., Williams, R. M., Eds.; Elsevier Ltd: Oxford, UK, 2008; pp 285–319.
- (41) Driggers, E. M.; Hale, S. P.; Lee, J.; Terrett, N. K. *Nat. Rev. Drug Discov.* **2008**, *7*, 608.
- (42) Kalaitzis, J. A.; A.Neilan, B. In *Drug Discovery from Natural Products*; Genilloud, O., Vicente, F., Eds.; The Royal Society of Chemistry, 2012; pp 159–197.

- (43) Faulkner, D. J. *Nat. Prod. Rep.* **2001**, *18*, 1.
- (44) Ruiz-Sanchis, P.; Savina, S. a.; Albericio, F.; Álvarez, M. *Chem. - A Eur. J.* **2011**, *17*, 1388.
- (45) Wang, H.; Reisman, S. E. *Angew. Chemie - Int. Ed.* **2014**, *53*, 6206.
- (46) Raju, R.; Piggott, A. M.; Huang, X. C.; Capon, R. J. *Org. Lett.* **2011**, *13*, 2770.
- (47) Crich, D.; Chan, C.; Davies, J. W.; Natarajana, P. S.; Vinterb, J. G.; Oaj, W. C. I. H.; Chemistry, C.; Kline, S.; Pharmaceuticals, B.; Frythe, T. *J. Chem. Soc. Perkin Trans. 2* **1992**, 2233.
- (48) Morales-Ríos, M. S.; Santos-Sánchez, N. F.; Suárez-Castillo, O. R.; Joseph-Nathan, P. *Magn. Reson. Chem.* **2002**, *40*, 677.
- (49) Napolitano, J. G.; Gavín, J. A.; García, C.; Norte, M.; Fernández, J. J.; Daranas, A. H. *Chem. - A Eur. J.* **2011**, *17*, 6338.
- (50) Altona, C.; Sundaralingam, M. *J. Am. Chem. Soc.* **1973**, *95*, 2333.
- (51) Hyberts, S. G.; Märki, W.; Wagner, G. *Eur. J. Biochem.* **1987**, *164*, 625.
- (52) Weiss, R.; Koelbl, H.; Schlierf, C. *J. Org. Chem.* **1976**, *41*, 2258.
- (53) Olah, G. A.; Flood, S. H.; Kuhn, S. J.; Moffatt, M. E.; Overchuck, N. A. *J. Am. Chem. Soc.* **1964**, *86*, 1046.
- (54) Brown, H. C.; Jungk, H. *J. Am. Chem. Soc.* **1955**, *77*, 5584.
- (55) Olah, G. A. *Acc. Chem. Res.* **1971**, *4*, 240.
- (56) Gore, P. G. *Friedel-Crafts and Related Reactions, Vol. III*; Olah, G. A., Ed.; Interscience: New York, NY, 1964.
- (57) George A. Olah; Kuhn, S. J.; Flood, S. H. *J. Am. Chem. Soc.* **1962**, *84*, 1688.
- (58) Keumi, T.; Nakamura, M.; Kitamura, M.; Tomioka, N. *J. Chem. Soc. Perkin Trans. 2* **1985**, 909.
- (59) Keumi, T.; Yagi, Y.; Kato, Y. K.; Taniguchi, R.; Temporin, M.; Kitajima, H. *J. Chem. Soc. Perkin Trans. 2* **1984**, 799.
- (60) Rice, F. O.; Teller, E. *J. Chem. Phys.* **1938**, *6*, 489.
- (61) Hine, J. *J. Org. Chem.* **1966**, *31*, 1236.
- (62) Goering, H. L.; Dilgreen, R. E. *J. Am. Chem. Soc.* **1960**, *82*, 5744.
- (63) Goering, H. L.; Linsay, E. C. *J. Am. Chem. Soc.* **1969**, *91*, 7435.
- (64) Winstein, S.; Clippinger, E.; Fainberg, A. H.; Heck, R.; Robinson, G. C. *J. Am. Chem. Soc.* **1956**, *78*, 328.
- (65) Valkanas, G.; Waight, E. S.; Weinstock, M. *J. Chem. Soc.* **1963**, 4248.
- (66) Sheppeck, J. E.; Kar, H.; Hong, H. *Tetrahedron Lett.* **2000**, *41*, 5329.
- (67) Hinman, R. L.; Whipple, E. B. *J. Am. Chem. Soc.* **1962**, *84*, 2534.
- (68) Hinman, R. L.; Lang, J. *J. Am. Chem. Soc.* **1964**, *86*, 3796.

4 Pd-Catalyzed allylation accesses template-constrained macrocyclic peptides prepared from native, unprotected precursors

4.1 Introduction

Early efforts in our laboratory to explore template-based methods to restructure the form and physicochemical properties of oligopeptides leveraged a Pd⁰-catalyzed internal allylation of phenols to generate macrocyclic structures.¹ Ring-forming allylic substitution reactions promoted by Pd⁰, widely known as the Tsuji-Trost reaction, are broadly versatile,^{2,3} have been well-studied, and can efficiently access macrocyclic structures.⁴⁻⁷ However, relatively few reports chart the use of this reaction in highly functionalized substrates. The initial results from our laboratory showed an impressive functional group tolerance in the context of synthetic oligopeptides, and used carefully designed templates **3-1** and **3-2** to achieve this (Figure 4.1.1, see also Chapter 3).

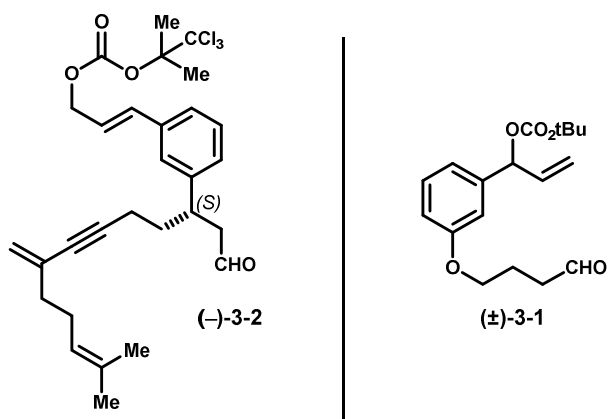


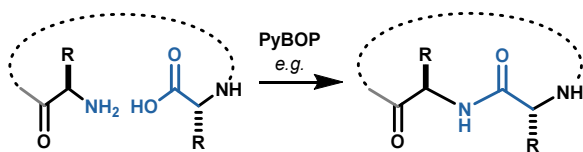
Figure 4.1.1 Previously investigated template architectures harboring a cinnamyl or α -phenylallyl mixed carbonate designed to initiate Pd⁰-catalyzed internal etherification of tyrosine.

These templates were ligated to peptide amino groups via the aldehyde group, and initiated large ring-forming *O*-cinnamylation via the cinnamyl mixed carbonate. Efficient ring closure was demonstrated for an array of tyrosine-containing peptide substrates ligated to these templates, and was initiated by catalytic quantities (10-20 mol%) of a pre-catalyst complex generated from [Pd(η^3 -allyl)Cl]₂ and bidentate phosphine ligand Xantphos.^{1,8,9} Mechanistically, this proceeds by oxidative addition of Pd⁰ into the cinnamyl carbonate to give an electrophilic π -allyl-palladium complex, which is prone to nucleophilic substitution (see Subsection 4.2). Importantly, an appropriately chosen leaving group (e.g. mixed carbonate) can generate

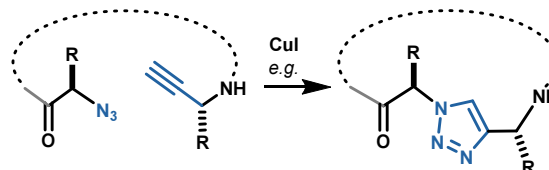
an equivalent of base (e.g. $t\text{-Bu-CO}_2^-$ or $t\text{-BuO}^- + \text{CO}_{2(g)}$) following oxidative addition, and can thereby lead to deprotonation of a pronucleophile. In this case, deprotonation of the acidic tyrosyl phenol occurs within the same molecule, and begets macrocyclization. Activation of a pronucleophile in this manner is uncommon among existing macrocyclizations, and may relate to the high intramolecularity observed here.^{10,11} Catalytic activation of both the electrophilic *and* nucleophilic centers effectively limits the concentration of reactive intermediates to not more than the catalyst loading. Consequently, the bimolecular rate is reduced at least by the square of the catalyst concentration (assuming first-order kinetics in nucleophile and electrophile). Here, we continue investigations of Pd-catalyzed large ring-forming allylations, and also examine role of charge-separated intermediates in this reaction.

A. Established methods for peptide macrocyclization

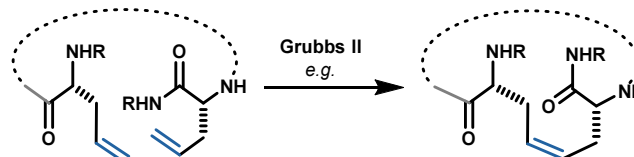
Lactamization



Azide-alkyne cycloaddition

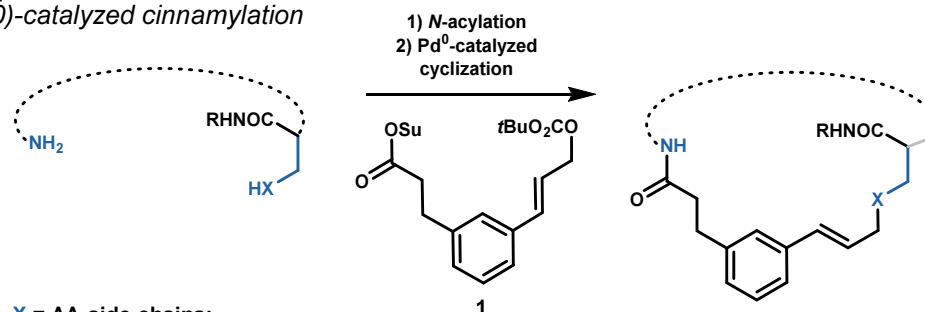


Olefin metathesis

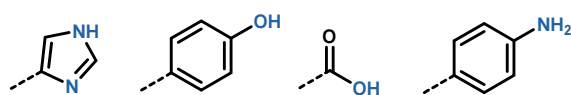


B. This work

Template-based Pd(0)-catalyzed cinnamylation



X = AA side-chains:



- Rapid & efficient macrocyclization
- Diverse ring connectivities
- Utilizes natural AA side chains
- Tunable chemoselectivity

Figure 4.1.2 A) Existing methods for peptide cyclization can be sensitive to substrate conformational preferences and require tailored amino acid residues. B) The template-based macrocyclizations described here engage native peptide side chains in carbon-heteroatom bond-forming allylations.

Relative to their acyclic counterparts, cyclic peptides have more defined conformations and improved pharmacological properties.^{12,13} Head-to-tail lactamization is the most common method to synthesize cyclic peptides.^{14–16} Internal disulfide bonding is also used,^{17,18} as are newer techniques such as ring-closing olefin metathesis¹⁹ and catalyzed azide-alkyne cycloaddition.^{20–22} These procedures rely on judicious use of protecting groups and tailored amino acid residues to achieve cyclization (Figure 4.1.2).^{23,24} Careful attention must be paid to substrate conformational biases to avoid competing oligomerization. Moreover, lactamization of peptides shorter than five residues can be particularly difficult.^{15,25} That said, when we simplified our templates to further study Pd⁰-catalysis in the context of cyclic-peptide synthesis, we discovered a combination of scope and functional group tolerance that was remarkable.

We show that intramolecular palladium-catalyzed cinnamylation of heteroatom nucleophiles can operate within highly functionalized native peptides. The nucleophile in the macrocyclization can be an amine, a carboxylic acid, a phenol, an imidazole, or an aniline. Chemoselectivity is predictable and, in many cases, switchable. With one exception (*vide infra*), the reaction is catalyzed by the commercial Pd⁰ complex Pd(PPh₃)₄. No exotic or costly ligand sphere for the metal is necessary. No protecting groups are used in any substrate. Reactions proceed rapidly and in high yield at room temperature and, thus far, independent of product-ring size and composition.

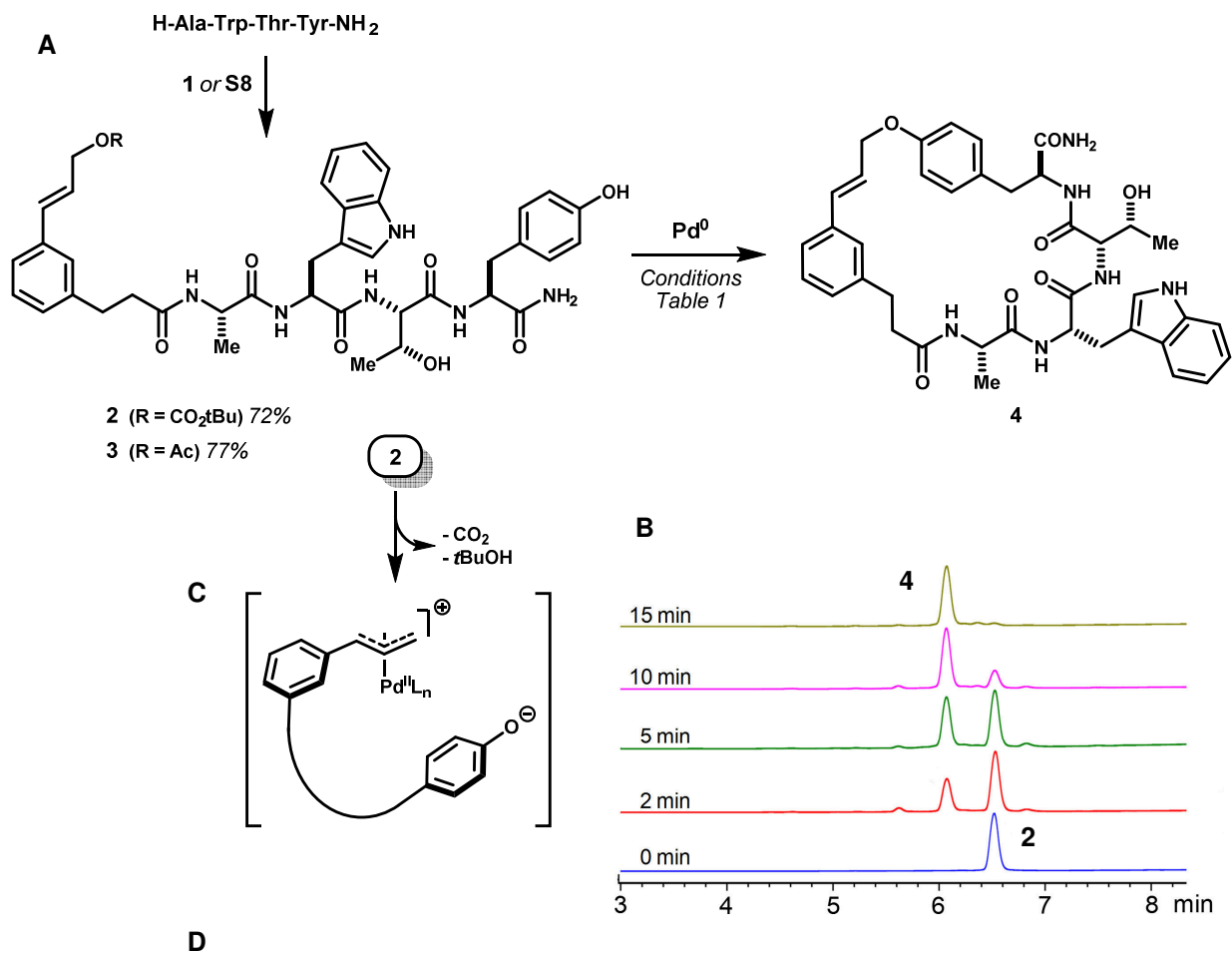
Initial experiments probed the internal *O*-cinnamylation of tyrosine residues (Figure 4.1.2B, XH = PhOH). Attention focused on how ring size, solvent, additives, and substrate concentration affected reaction rate and efficiency. As these experiments progressed, we observed a much broader functional group tolerance than expected. Moreover, residues such as aspartic acid, glutamic acid, and histidine would participate as nucleophiles in the cyclization, as would a free carboxyl or amino terminus under appropriate conditions. Chemoselectivity was both predictable and tunable. In two steps, beginning with **1** and an unprotected peptide, we could achieve any one of several cyclization modes including head-to-tail, side chain-to-tail, and side chain-to-side chain. Peptides up to 11 residues long were readily transformed into template-constrained macrocycles.

4.2 Impact of solvent, substrate concentration, and base additives on catalyzed cycloetherification of tyrosyl phenols

Linear substrate **2** (Scheme 4.2.1A) was chosen to evaluate the effects of solvent and additives on catalyzed internal etherification of its tyrosyl phenol. *N*-acylation of synthetic Ala-Trp-Thr-Tyr with *N*-hydroxysuccinimidyl ester **1** gave acyclic intermediate **2** in 72% yield. Exposure of **2** to 5 mol % Pd(PPh₃)₄ in deoxygenated DMF (5 mM in **2**) at room temperature caused rapid conversion to cyclic ether **4** in 91% HPLC assay yield (78% when isolated by preparative HPLC). Reaction monitoring showed complete conversion to product within 15 min (Scheme 4.2.1B). No dimeric or oligomeric materials were detected in the experiment. As illustrated in Scheme 4.2.1D, the catalysis proceeded efficiently in several polar aprotic solvents. The use of water as cosolvent was tolerated (entry 5), but it slowed the reaction rate ~30-fold and resulted in formation of an unidentified side-product (~15%). In neat DMF, contact ion pairing of transient intermediates within the catalytic cycle may explain the rapid reaction rate and high product yield.^{26,27} Consistent with literature precedent, *tert*-butoxide formed from decomposition of the cinnamyl carbonate following oxidative addition of Pd⁰ to the allylic C–O sigma bond likely deprotonates the proximal phenol, resulting in a new, more product-like (i.e., cyclic, Scheme 4.2.1C) metal ion pair. Reductive elimination or displacement of palladium would follow, leading to product. Electrostatic preorganization of amphoteric peptides has been discussed previously.^{28,29} The inner salts invoked here as intermediates formed at low concentration would likewise be expected to offset entropic costs associated with ring formation.^{29,30} It is also consistent with a general lack of oligomeric products formed in the catalysis, which can limit other peptide cyclization methods.^{25,31,32} High macrocyclization efficiency (calculated Emac index = 7.77)¹¹ was observed at 20-fold higher concentration (0.1 M), wherein the isolated yield was lowered only slightly (Scheme 4.2.1D, entry 2).

When cinnamyl acetate **3** (Scheme 4.2.1A) was subjected to identical cyclization conditions, conversion to **4** was not observed, even upon prolonged heating (Scheme 4.2.1D, entry 6). We speculated that, unlike the situation for **2**, acetate ion liberated by oxidative addition of Pd⁰ to **3** was insufficiently basic to propagate a catalytic cycle involving a tyrosyl phenoxide. Consistent with this hypothesis, addition of Cs₂CO₃ (2 eq., Scheme 4.2.1D, entry 7) rescued the reaction, promoting rapid conversion of **3** to cinnamyl ether **4**. Under buffered aqueous conditions, the cyclization rate was pH dependent. No conversion of **2** to **4**

Scheme 4.2.1 A) Catalyzed cycloetherification of substrates derived from templates **1** or **S8** and Ala-Trp-Thr-Tyr. **B)** HPLC analyses (C18, 40→100% MeCN/H₂O 0.1%TFA, 10 min, monitoring at 254 nm) of samples taken from reaction of **2** with 5 mol% Pd(PPh₃)₄ (Table in D, entry 1) at the indicated time points. **C)** Partial schematic of internally ion-paired π -allyl palladium(II) complex putatively generated from **2** via oxidative addition of Pd(0). **D)** Media and additive effects on the palladium-catalyzed synthesis of macrocyclic ether **4** from precursors **2** and **3**. Reactions were run for 2 h at room temperature in argon sparged media containing 5 mol % Pd(PPh₃)₄. ^aYield determined by HPLC assay. Isolated yield in parentheses. ^bNo conversion at 16 h. ^c16 hr reaction time. PBS, phosphate buffered solution; nr, no reaction.



Entry	Substrate	Solvent/additive	Yield (%) ^a
1	3	DMF (5 mM)	91 (78)
2	3	DMF (100 mM)	84
3	3	THF (5 mM)	77
4	3	DMSO (5 mM)	91
5	3	1:1 DMF/H ₂ O (5 mM)	57
6	4	DMF (5 mM) ^b	nr
7	4	DMF (5 mM), Cs ₂ CO ₃ (2 eq.)	88
8	3	1:1 DMF/100mM PBS (pH 5.5, 5mM) ^b	nr
9	3	1:1 DMF/100mM PBS (pH 7.4, 5mM) ^c	70
10	3	1:1 DMF/100mM PBS (pH 8.5, 5mM) ^d	89

was observed when an equal mixture of DMF and pH 5.5 phosphate buffer was used as solvent (entry 8). Increasing the buffer pH to 7.4 induced sluggish conversion to **4**, and required 16 h. However, at pH 8.5 the reaction was complete within 2 h and **4** was formed in 89% HPLC assay yield. Taken together, data in Scheme **4.3.1D** suggested 5 mM solutions of carbonate substrate in neat DMF (no additives) would be the most convenient to further evaluate the scope of the macrocyclization, because substrate solubility and reaction rate would be generally highest.

4.3 Evaluating the scope of catalyzed cycloetherification

A set of unprotected, *L*-amino acid-derived peptides were prepared to assess the range of macrocycles available through catalyzed *O*-cinnamylation of phenols. Peptides ranged from three to five residues long and each possessed a free amino terminus and a tyrosine residue in the sequence. All functional groups present in natural amino acids were represented in the set, with the exception of thiols (cysteine) to avoid complications from oxidative lability.

Acylation of each peptide with template **1** was achieved by mixing in DMF in the presence of *i*Pr₂NEt. Treatment of the resulting acyclic intermediates with 5 mol % Pd(PPh₃)₄ gave macrocyclic cinnamyl ethers **5–9** and **11–14** (Table **4.3.1**) in high isolated yields (72–85%). No branched α -phenylallyl ethers were detected in these experiments. Polar functional groups including alcohols, amides, and guanidines were well-tolerated. Notably, efficient macroetherification was not restricted to tyrosine. 5-Hydroxyindole, incorporated as commercial 5-hydroxytryptamine, was equally competent as a nucleophile, affording macrocycle **10** in 75% yield. For each product, the macrocyclic ether linkage was assigned by NMR, wherein a diagnostic heteronuclear multiple bond correlation (HMBC) between the cinnamyl methylene protons and the phenolic carbon resonance ($\sim \delta$ 155 ppm) was observed.

When the peptide-template **1** conjugate of Ala-Leu-Glu-Tyr (**15**, Scheme **4.3.1A**) was treated with Pd(PPh₃)₄, ¹H-¹³C HMBC analysis of the resultant product did not reveal the anticipated cinnamyl ether. Rather, it indicated cyclization had formed macrolactone **16** (67% isolated yield) from cinnamylation of glutamic acid. This connectivity was assigned based on HMBC correlation between the cinnamyl methylene protons (*H1*, Scheme **4.3.1C**) and Glu-C20 (δ 171.6 ppm). No other products were observed by HPLC (Scheme **4.3.1B**). We were cognizant that **16** could form from **15**, yet expected this compound to be susce-

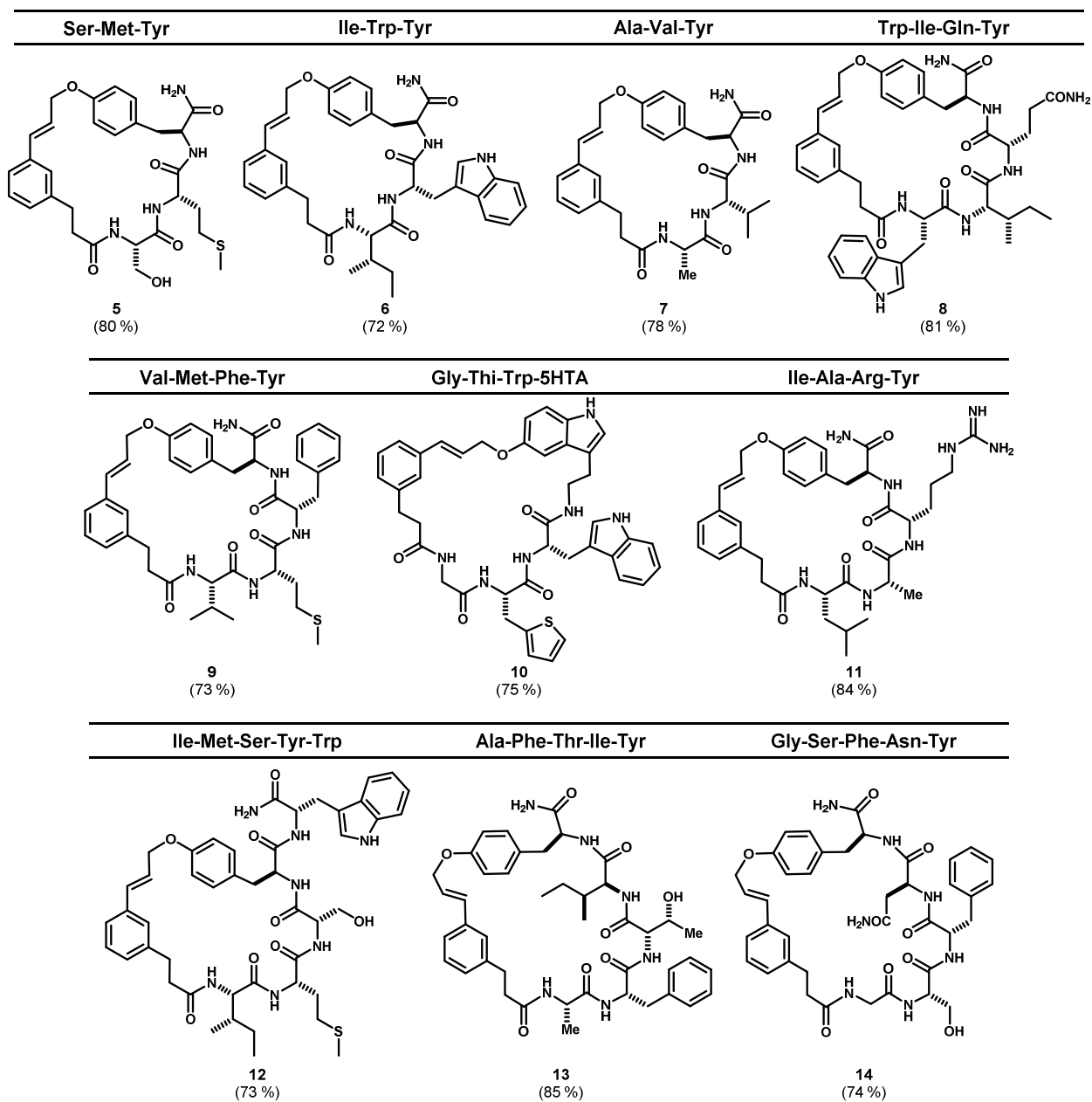
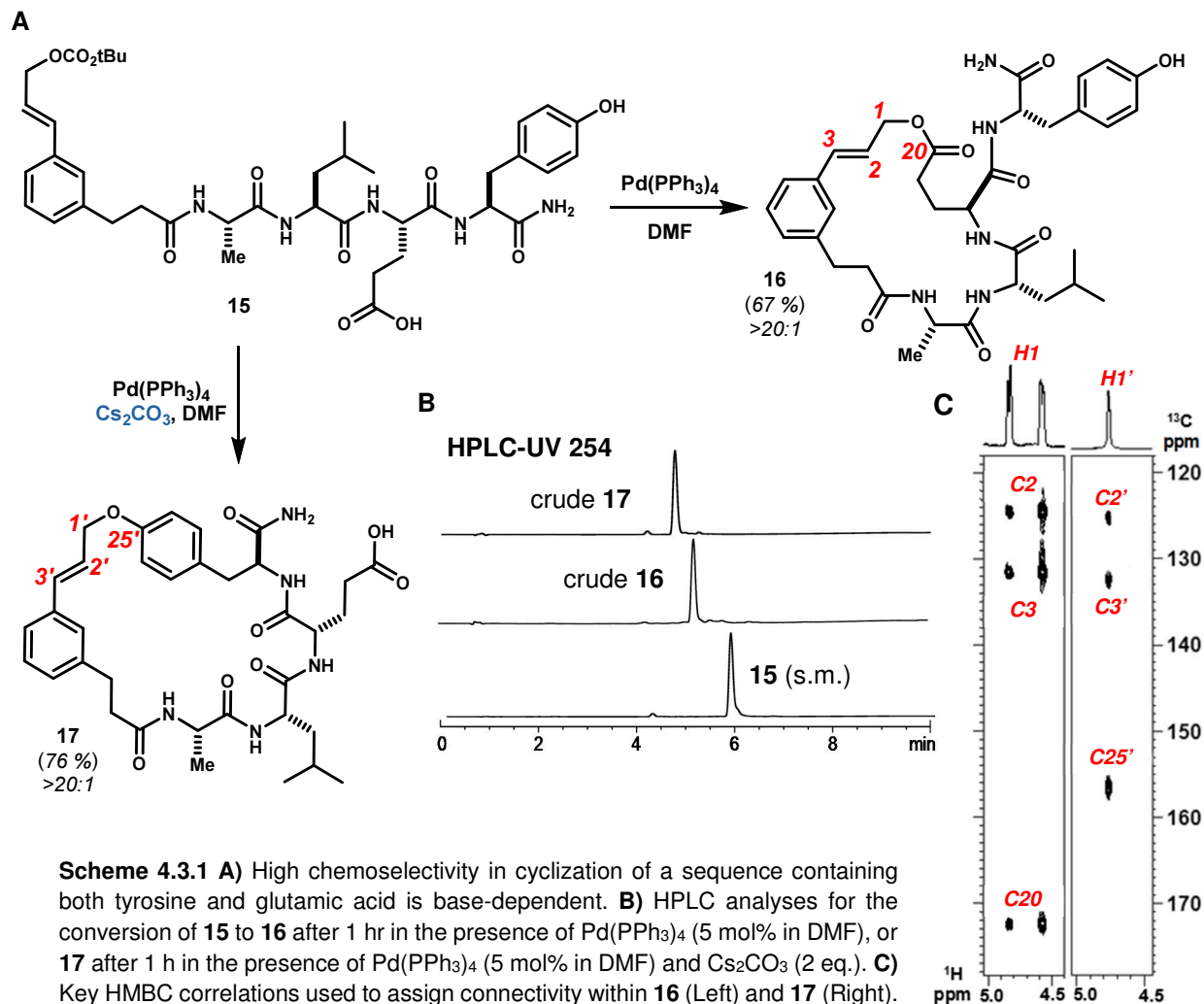


Table 4.3.1 Macrocyclic ethers obtained in two steps from template **1** and the indicated unprotected peptides.

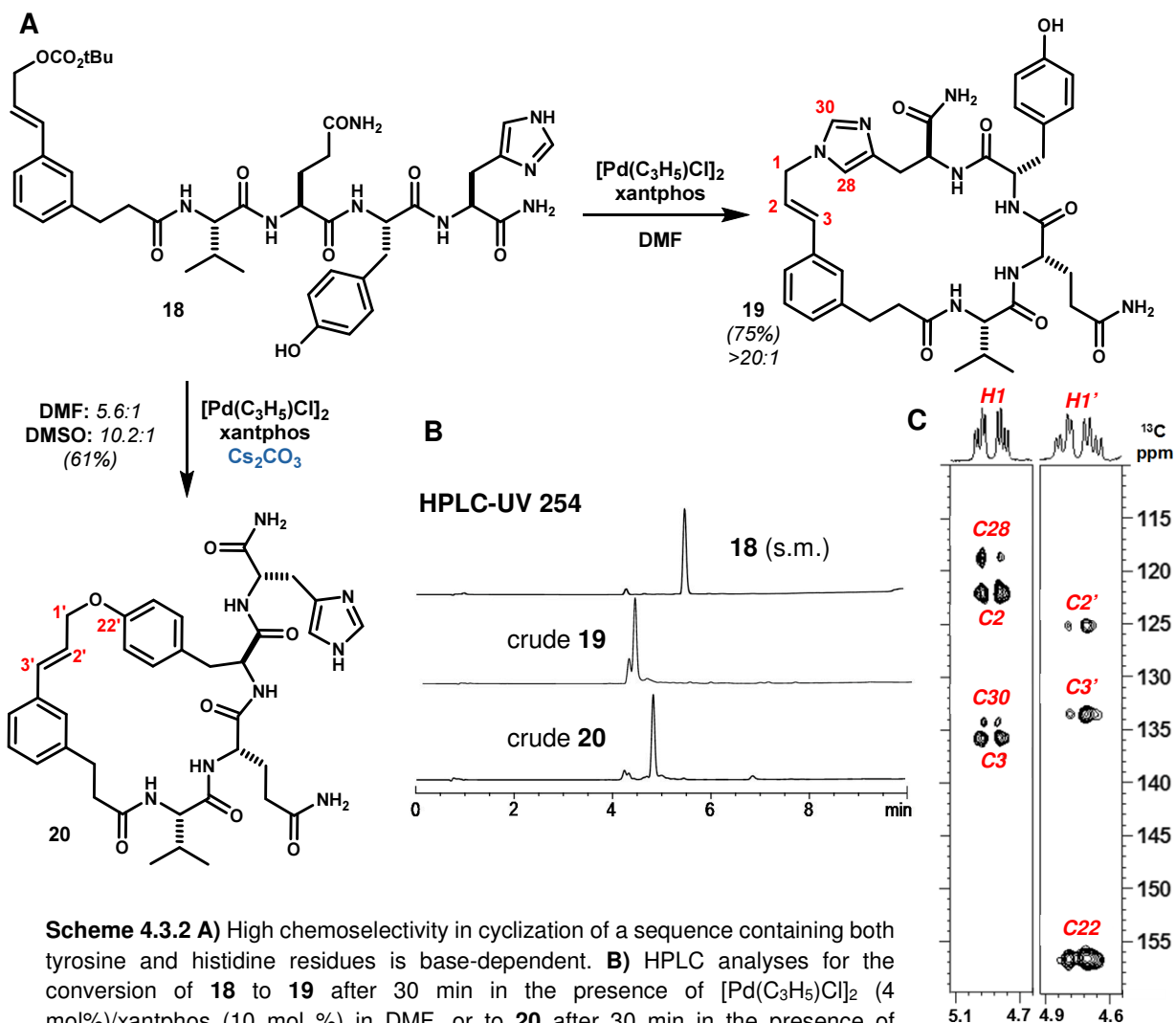
ptible to reionization by palladium(0). However, consistent with the inertness of cinnamyl acetate **3** to Pd(PPh₃)₄ in the absence of base (Scheme 4.2.1D, entry 6), macrolactone **16** proved stable and isolable. Resubjecting **16** to the reaction conditions did not result in isomerization to cyclic ether **17**. In contrast, when **15** was treated with 5 mol% Pd(PPh₃)₄ in the presence of Cs₂CO₃, macrocyclic ether **17** was formed

exclusively and isolated in good yield (Scheme 4.3.2A,B). Lactone **16** was not observable by HPLC during the course of the reaction. The absence or presence of Cs₂CO₃ was a convenient means to select for a 26-membered or 21-membered ring product. Such tunable outcomes bode well for preparing structurally distinct macrocycles from a single peptide sequence.



Catalyzed internal esterification also proved suitable for head-to-tail macrolactonization. Substrates prepared from **1** and peptides harboring a free C-terminus readily cyclized in the absence of exogenous base. For example, *N*-acylation of Gly-Val-Trp-OH and Phe-Ile-Hyp-OH with template **1** followed by cyclization with Pd(PPh₃)₄ efficiently produced macrolactones **21** and **22** (Table 4.3.2), respectively. Branched α -phenylallyl ester **22** was isolated as a 1:1 mixture of diastereomers. No linear cinnamyl linkage

was detected in this instance, an atypical outcome that may result from the added geometric constraints imposed by hydroxyproline.



Scheme 4.3.2 A) High chemoselectivity in cyclization of a sequence containing both tyrosine and histidine residues is base-dependent. **B)** HPLC analyses for the conversion of **18** to **19** after 30 min in the presence of $[\text{Pd}(\text{C}_3\text{H}_5)\text{Cl}]_2$ (4 mol%)/xantphos (10 mol %) in DMF, or to **20** after 30 min in the presence of $[\text{Pd}(\text{C}_3\text{H}_5)\text{Cl}]_2$ (4 mol%)/xantphos (10 mol%) and Cs_2CO_3 (2 eq.) in DMSO. **C)** Key HMBC correlations used to assign connectivity within **19** (Left) and **20** (Right). *Note: 19* is formed as a ~5:1 mixture of regioisomeric *N*-alkyl imidazoles (see HPLC trace. Major isomer drawn).

Histidine-containing substrates were also examined. Compound **18**, derived from **1** and Val-Gln-Tyr-His, was recovered unchanged after exposure to $\text{Pd}(\text{PPh}_3)_4$ for extended reaction times. Stable ligation of palladium by histidine-containing peptides has been reported.^{33–35} To mitigate suspected catalyst poisoning, we turned to a less labile/dynamic ligand sphere for the metal. When a precatalyst generated from $[\text{Pd}(\text{C}_3\text{H}_5\text{Cl})]_2$ (4 mol%) and the chelating bis-phosphine xantphos (10 mol%) was used,³⁶ complete

consumption of **18** was observed within 30 min (Scheme 4.3.2 Error! Reference source not found. B). Two regioisomeric products were obtained in a 5:1 ratio and 75% combined yield. 1H - ^{13}C HMBC correlations from the cinnamyl methylene *H1* to *C28* and *C30* confirmed the major product as histidine *N29*-alkylated macrocycle **20** (Scheme 4.3.2A,C). The minor product was determined to be the analogous *N31*-linked regioisomer. Neutral imidazole is a weak nucleophile in solution. Direct participation of imidazoles in large ring-forming reactions is rare,³⁷ yet alkylation occurred solely at histidine in this reaction. Competition from the tyrosyl phenol was not observed. However, as observed for substrate **15**, chemoselectivity was switch-

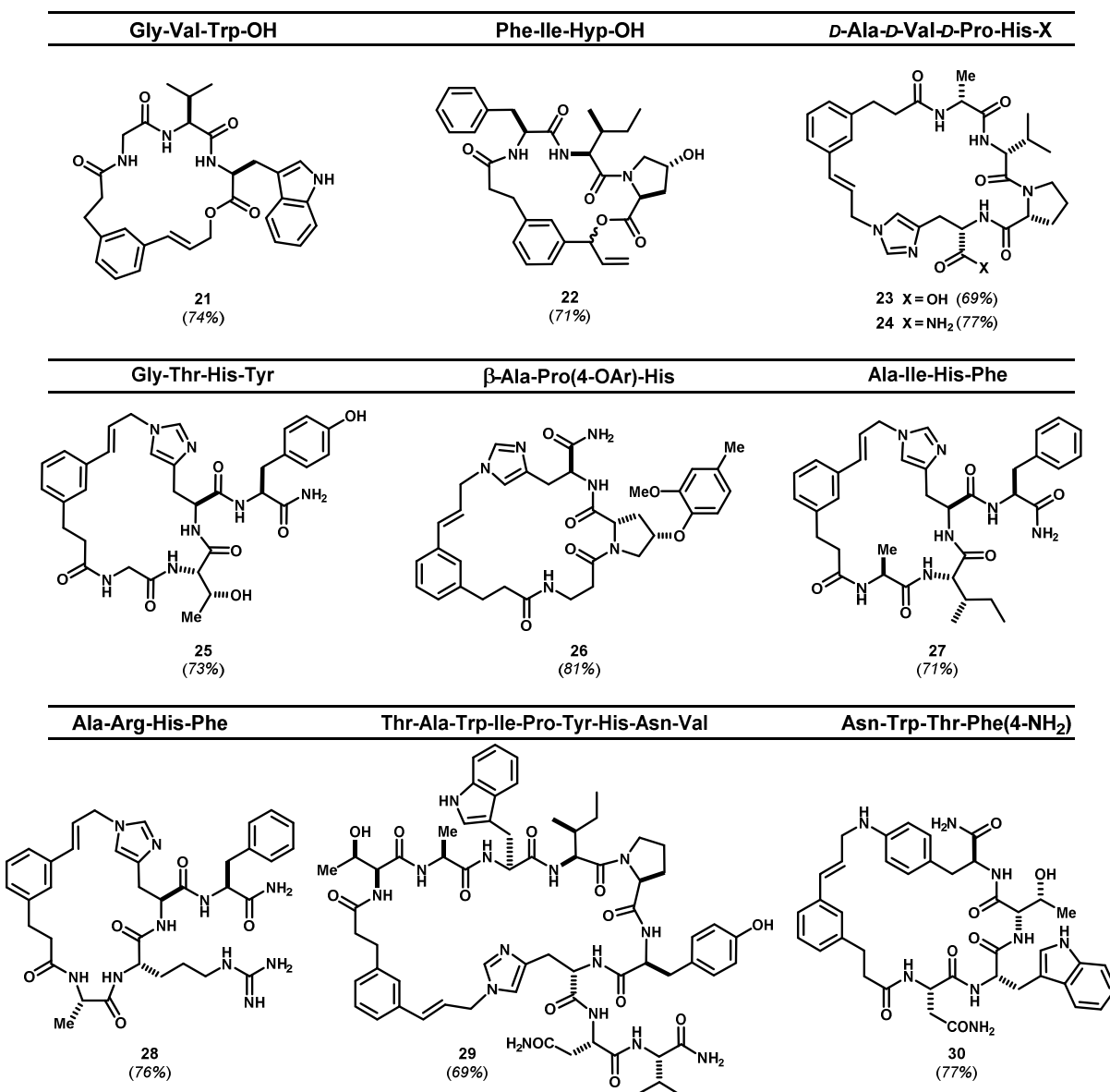


Table 4.3.2 Macrocycles obtained from templated macrocyclization of oligomers containing carboxylic acids, imidazoles, and anilines. Isolated yield of Pd-catalyzed cyclization step indicated in parentheses.

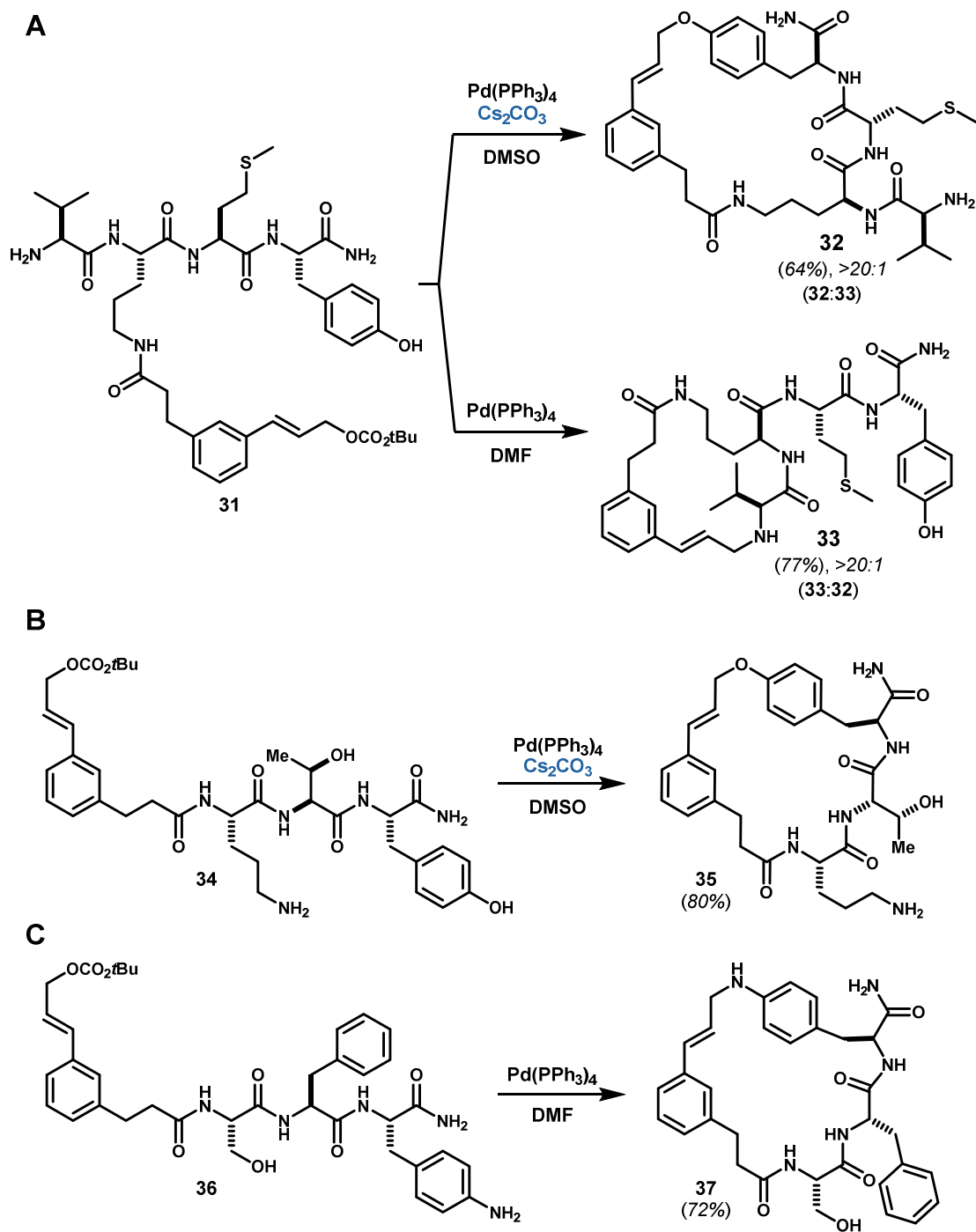
able by the addition of base. Treatment of **18** with $[\text{Pd}(\text{C}_3\text{H}_5\text{Cl})_2/\text{xantphos}]$ and Cs_2CO_3 (2 eq.) in DMF afforded macrocyclic ether **20** in a 5.7:1 ratio relative to regioisomers **19** (Scheme **4.3.2A**). Changing the reaction solvent to DMSO improved the selectivity to 10.2:1, likely due to the increased solubility of Cs_2CO_3 in DMSO.³⁸

A set of peptides was prepared to examine the generality of histidine-based macrocyclization (Table **4.3.2**). In each case, treatment with $[\text{Pd}(\text{C}_3\text{H}_5\text{Cl})_2/\text{xantphos}]$ afforded exclusively histidine-alkylated macrocycles in high yield. Where possible, tyrosine alkylation was not detected regardless of resultant ring size (e.g. **25** versus **29**). Histidine alkylation also occurred in preference to macrolactone formation in the presence of free carboxylic acids (see **23**). Other polar functional groups including amides, alcohols, and guanidines were well tolerated. Sequences containing both histidine and residues displaying primary amines (i.e. Lys or Orn) were unique in that cyclization was unselective and low yielding. Only cyclizations of histidine caused this result with amines, which could likely be managed using orthogonal protecting groups.

In other settings, amines were useful and competent reaction partners in Pd^0 -catalyzed cinnamylation.⁶ Moreover, use of the xantphos ligand was no longer necessary. For example, acylation of Fmoc-Val-Orn-Met-Tyr with template **1** followed by treatment with piperidine gave acyclic intermediate **31** (Scheme **4.3.3A**). Exposure of this material to 5 mol % $\text{Pd}(\text{PPh}_3)_4$ resulted in exclusive cinnamylation of the amino terminus to afford **33** (>95% HPLC peak area purity). Analogous to previous examples, chemoselectivity was sensitive to added base. The addition of Cs_2CO_3 (3 eq.) and use of DMSO as solvent provided cinnamyl ether **32** as the sole cyclization product. Under the same conditions, substrate **34** derived from **1** and Orn-Thr-Tyr gave macrocyclic ether **35** in 80% yield. The primary amine and secondary alcohol were unaffected.

We next examined a third type of nitrogen nucleophile in the cyclization reaction. Sequences were prepared containing the non-proteinogenic amino acid 4-aminophenylalanine, which is readily available and used as a tyrosine isostere.^{39,40} Peptides Ser-Phe-Phe(4-NH₂) and Asn-Trp-Thr-Phe(4-NH₂) were independently reacted with **1**, which selectively acylated the N-termini. Exposure of the resulting acyclic intermediates to 5 mol% $\text{Pd}(\text{PPh}_3)_4$ rapidly formed macrocyclic aryl amines **37** and **30** in high yield (Scheme **4.3.3C** and Table **4.3.2**).

Scheme 4.3.3 A) Cyclization of a sequence containing tyrosine and a free N-terminus is chemoselective and base-dependent. Conditions: For **32**, Pd(PPh₃)₄ (5 mol%), Cs₂CO₃ (3 eq.), DMSO (5 mM in **31**); for **33**, Pd(PPh₃)₄ (5 mol%), DMF (5 mM in **31**). **B)** In the presence of base, primary amines do not interfere with tyrosyl cyclizations. Conditions: Pd(PPh₃)₄ (5 mol%), Cs₂CO₃ (3 eq.), DMSO (5 mM in **34**). **C)** A sequence containing *p*-aminophenylalanine readily cyclizes in the absence of base. Conditions: Pd(PPh₃)₄ (5 mol%), DMF (5 mM in **36**). Yields in parentheses refer to material isolated by preparative HPLC.



4.4 Longer sequences undergo efficient macrocyclization

Nascent secondary structure elements in longer peptides can assist or hinder cyclization attempts, depending upon how they influence access to the transition state for intramolecular reaction. Hindrance is common, and oligomeric by-products often form as a result.^{31,32} High dilution,⁴¹ pseudodilution on solid-support,⁴² and conformationally restrained pseudoproline^{43,44} are used to improve cyclization efficiency. Techniques such as helical peptide stapling, based on ring-closing olefin metathesis, require folding of the helical element for efficient cyclization.⁴⁵ To begin testing the utility of palladium π -allyl chemistry for cyclizing longer sequences, we prepared octa- and dodecapeptides WLQMTGFY and AFSVPGVWISYV. Acylation of these materials with template **1** and treatment of the resulting acyclic intermediates with 5 mol% Pd(PPh₃)₄ gave macrocyclic cinnamyl ethers **39** and **38**, respectively (Figure 4.4.1A). As observed for shorter sequences, these cyclization reactions were efficient at room temperature and complete within 1 hour. The 38- and 47-membered ring products were readily isolated by preparative HPLC and characterized. Competing dimerization or oligomerization was not observed.

These impressive results prompted us to investigate whether we had inadvertently chosen sequences poised to cyclize. Both **38** and **39** harbor potential turn-inducing motifs centered at proline and glycine, respectively, which may accelerate the rate of ring closure. To explore this possibility, we used NMR to probe conformational preferences of macrocycles **38** and **39** relative to their linear precursors **S32** and **S33**.^{46,47} Comparison of ¹³C α shifts, expressed as $\Delta\delta_{\text{cyclic-linear}}$ in (Figure 4.4.1B,C), revealed distinct differences in the backbone conformations of linear and cyclic structures.^{48,49} These data imply that the linear precursors do not tightly occupy a product-like conformation, but perhaps sample an ensemble of states under these conditions. Differences were further evidenced by changes in the temperature dependence of backbone H^N chemical shifts following cyclization.^{50,51} Notably, Val⁷ and Gly⁶ in macrocycles **38** and **39**, respectively, showed a temperature dependence of greater than -3 ppb/K, suggestive of internal hydrogen bonding at these positions.^{46,52} Similar interactions were not observed in the linear precursors, wherein a smaller temperature dependence was measured at the same positions; these comparisons are illustrated in Figure 4.4.1C as $\Delta(\Delta\delta/\Delta T)_{\text{cyclic-linear}}$. It appears that a product-like conformation of the linear precursor need not predominate in order for the palladium-catalyzed cyclization to occur.

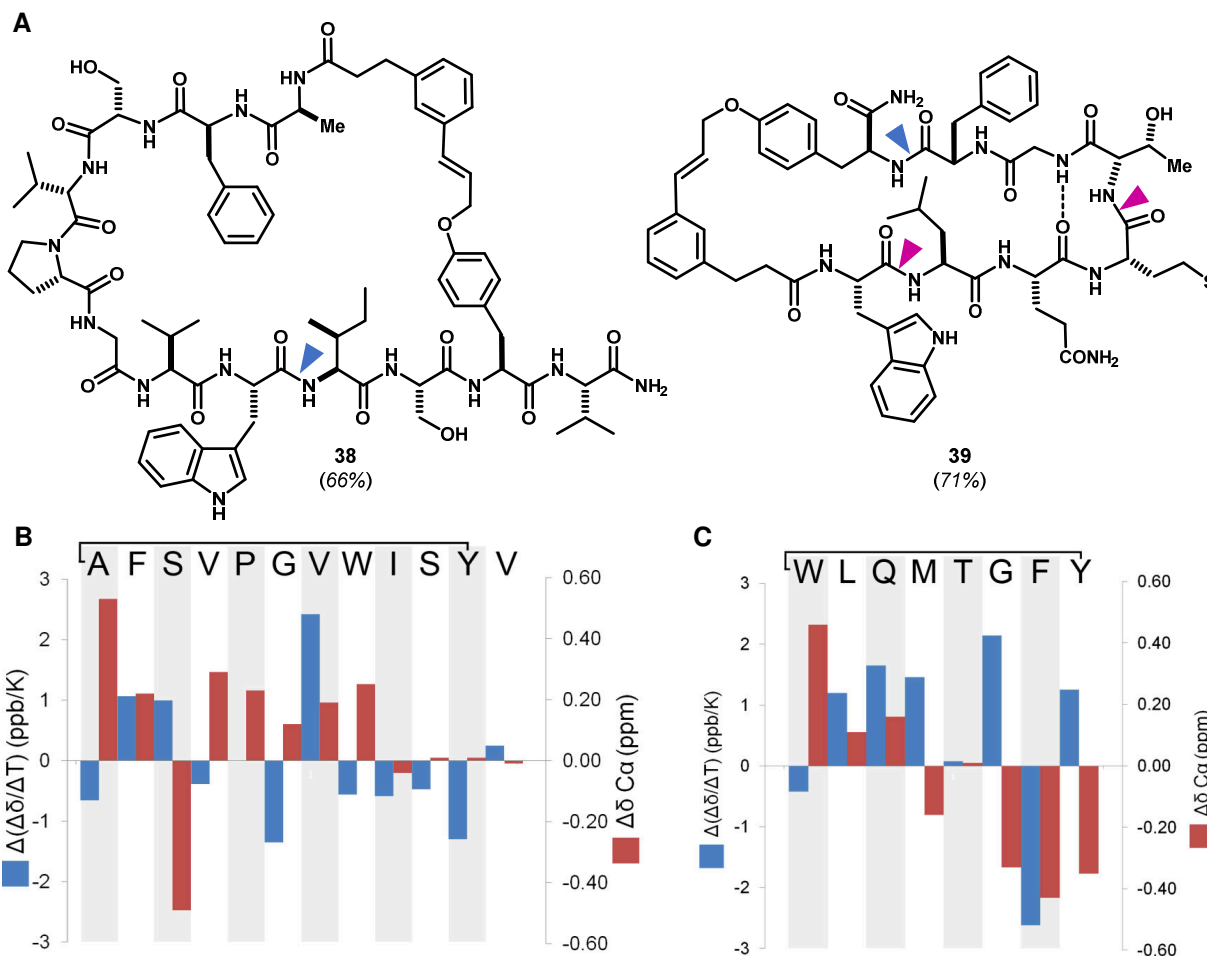


Figure 4.4.1 Conformational analysis and proteolytic stability of **38** and **39**. **A)** Planar structures of macrocycles **38** and **39**. Hydrogen bond H^N -Gly⁶-Gln³ in **39** was inferred from analysis of backbone amide chemical shift temperature dependence. **Blue** triangle denotes primary α -chymotrypsin cleavage site; **magenta** triangles denote secondary cleavage sites (see Figure 4.5.1C,D). **B)** Comparison of NMR metrics for backbone amide solvent exposure (H^N $\Delta(\Delta\delta/\Delta T)_{\text{cyclic-linear}}$) and backbone conformation ($^{13}C\alpha$ $\Delta\delta_{\text{cyclic-linear}}$) between macrocycles **38**, **39**, and their respective linear precursors **S32** and **S33**.

4.5 Template 1 stabilizes secondary structure and enhances proteolytic stability in Vitro

Based on NMR evidence for internal hydrogen bonding, we next examined whether templated macrocycle **39** exhibited a defined conformation in solution. Complete resonance annotations from NMR spectra acquired in 9:1 DMSO- d_6 :H₂O–facilitated assignment of 80 intramolecular NOEs and 13 dihedral angle restraints. Sequential H^N NOEs within the triad Met⁴-Thr-Gly⁶ indicated the presence of a beta turn. Transannular NOEs between Leu² and Phe⁷, and between Gln³ and the C-terminus were indicative of the

ring structure. Distance- and angle-constrained molecular mechanics calculations identified a tight ensemble of low energy conformers. The global energy minimum and an overlay of conformers of similar energy are shown in Figure 4.5.1A and B. The region Gln³-Met-Thr-Gly-Phe⁷ occupies a type I β -turn, consistent with the observed Gly⁶ H^N temperature coefficient (-2.4 ppb/K). These data indicate a well-ordered core macrocycle and stabilization of the peptide domain, despite potential flexibility of the template.

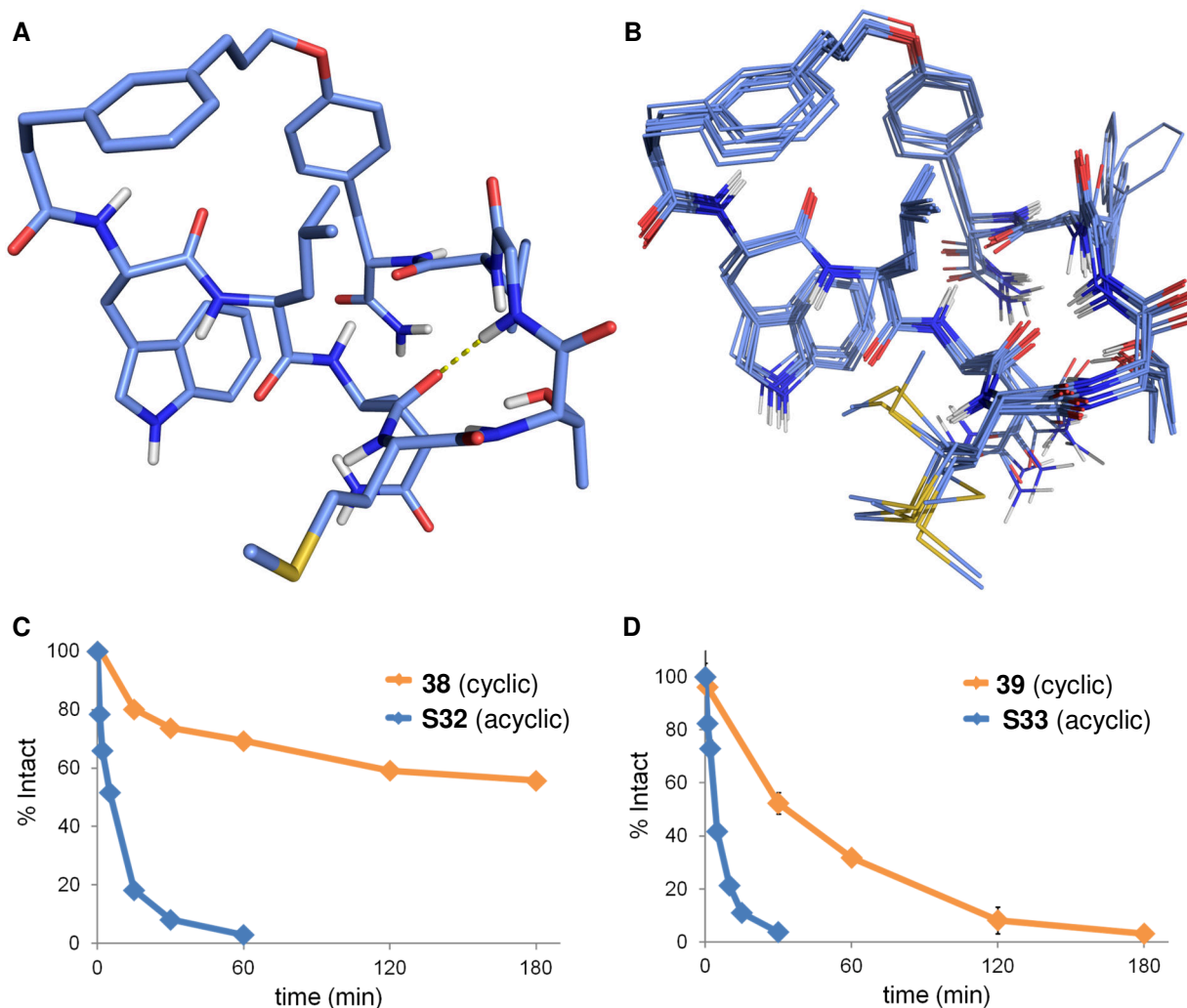


Figure 4.5.1 **A)** Lowest energy conformation of compound **39** determined from NMR analyses in DMSO- d_6 :H₂O (9:1). **B)** Ensemble of top 10 low-energy conformers of **39**. Core macrocycle rmsd = 0.36 Å. **C)** Macrocycle **38** exhibited greater stability against proteolysis by α -chymotrypsin in comparison with **S32**. **D)** Analogous stability was observed for macrocycle **39** over **S33**.

Restricted conformational mobility is one means by which folded polypeptides evade enzymatic degradation.^{12,13,53} Accordingly, we examined the extent to which macrocycles **38** and **39** were protected

against proteolytic degradation by α -chymotrypsin *in vitro*. As expected, linear compound **S33** was degraded rapidly, with primary cleavage occurring between Phe⁷ and Tyr⁸ as judged by MS analysis of the resulting metabolites. Corresponding macrocycle **39** was 8.7-fold more stable in this assay (Figure **4.5.1D**) and was cleaved at the same site. In the case of cyclic materials, proteolysis sites were determined by MS/MS analysis. Macrocycle **38** also exhibited resistance to proteolysis, but apparent product inhibition precluded accurate determination of its half-life and comparison with linear counterpart **S32** (Figure **4.5.1C**). Enzymatic hydrolysis between Trp⁸ and Ile⁹ was invariant between cyclic **38** and the linear material. These preliminary results are encouraging and imply that enhanced proteolytic stability observed for conventional cyclic peptides will be a feature of macrocycles derived from template **1** as well.

4.6 Conclusions

Template **1** enables conversion of unmodified, unprotected linear peptides directly to stable macrocycles by internal *C–O* or *C–N* bond formation. Non-natural amino acids are not required. The Pd⁰-catalyzed ring-forming reaction is uniquely versatile and operates independent of product ring size and composition. Side chain functional groups present in tyrosine, histidine, glutamic acid, and aspartic acid participate in the cyclization, as do a free carboxyl or amino terminus under appropriate conditions. Alcohols, guanidines, carboxamides, and thioethers neither participate nor interfere with the catalysis. The chemistry is well-suited to probe consensus peptide binding sites, to generate peptide-based positive controls for assay development, to stabilize and protect elements of secondary structure (i.e., turns, helices), and to create prototype leads for medicinal chemistry programs targeting protein/protein interactions. Simple procedures, mild reaction conditions, high yields, and tunable chemoselectivity provide for myriad possibilities. The chemistry compares favorably with other methods for peptide cyclization, and is complementary to *C–C* bond-forming macrocyclizations of template **1** (see Chapters 3, 5, 6). Notably, the bioorthogonal nature and room temperature reactivity of this Pd⁰-catalyzed macrocyclization may also allow integration with a myriad of possible biochemical experiments *in vitro* or *in vivo*.

References

- (1) Wei, Q.; Harran, S.; Harran, P. G. *Tetrahedron* **2003**, *59*, 8947.
- (2) Trost, B. M.; Zhang, T.; Sieber, J. D. *Chem. Sci.* **2010**, *1*, 427.
- (3) Trost, B. M. *J. Org. Chem.* **2004**, *69*, 5813.
- (4) Vosburg, D. a.; Vanderwal, C. D.; Sorensen, E. J. *J. Am. Chem. Soc.* **2002**, *124*, 4552.
- (5) Trost, B. M.; Ohmori, M.; Boyd, S. A.; Okawara, H.; Brickner, S. J. *J. Am. Chem. Soc.* **1989**, *111*, 8281.
- (6) Trost, B. M.; Cossy, J. *J. Am. Chem. Soc.* **1982**, *104*, 6881.
- (7) Fürstner, A.; Weintritt, H. *J. Am. Chem. Soc.* **1998**, *120*, 2817.
- (8) Zhao, H.; Negash, L.; Wei, Q.; LaCour, T. G.; Estill, S. J.; Capota, E.; Pieper, A. A.; Harran, P. G. *J. Am. Chem. Soc.* **2008**, *130*, 13864.
- (9) Lawson, K. V.; Rose, T. E.; Harran, P. G. *Tetrahedron* **2013**, *69*, 7683.
- (10) Lawson, K. V.; Rose, T. E.; Harran, P. G. *Proc. Natl. Acad. Sci. U. S. A.* **2013**, *110*, E3753.
- (11) Collins, J. C.; James, K. *Medchemcomm* **2012**, *3*, 1489.
- (12) Bird, G. H.; Madani, N.; Perry, A. F.; Princiotto, A. M.; Supko, J. G.; He, X.; Gavathiotis, E.; Sodroski, J. G.; Walensky, L. D. *Proc. Natl. Acad. Sci. U. S. A.* **2010**, *107*, 14093.
- (13) Gentilucci, L.; De Marco, R.; Cerisoli, L. *Curr. Pharm. Des.* **2010**, *16*, 3185.
- (14) Montalbetti, C. A. G. N.; Falque, V. *Tetrahedron* **2005**, *61*, 10827.
- (15) Davies, J. S. *J. Pept. Sci.* **2003**, *9*, 471.
- (16) Thakkar, A.; Trinh, T. B.; Pei, D. *ACS Comb. Sci.* **2013**, *15*, 120.
- (17) Jackson, D. Y.; King, D. S.; Chmielewski, J.; Singh, S.; Schultz, P. G. *J. Am. Chem. Soc.* **1991**, *113*, 9391.
- (18) Giebel, L. B.; Cass, R. T.; Milligan, D. L.; Young, D. C.; Arze, R.; Johnson, C. R. *Biochemistry* **1995**, *34*, 15430.
- (19) Blackwell, H. E.; Grubbs, R. H. *Angew. Chemie - Int. Ed.* **1998**, *37*, 3281.
- (20) Jacobsen, Ø.; Maekawa, H.; Ge, N. H.; Görbitz, C. H.; Rongved, P.; Ottersen, O. P.; Amiry-Moghaddam, M.; Klaveness, J. *J. Org. Chem.* **2011**, *76*, 1228.
- (21) Pehere, A. D.; Abell, A. D. *Org. Lett.* **2012**, *14*, 1330.
- (22) Chouhan, G.; James, K. *Org. Lett.* **2011**, *13*, 2754.
- (23) Kates, S. A.; Solé, N. A.; Johnson, C. R.; Hudson, D.; Barany, G.; Albericio, F. *Tetrahedron Lett.* **1993**, *34*, 1549.
- (24) Lundquist IV, J. T.; Pelletier, J. C. *Org. Lett.* **2002**, *4*, 3219.
- (25) Schmidt, U.; Langner, J. *J. Pept. Res.* **1997**, *49*, 67.
- (26) Evans, L. A.; Fey, N.; Harvey, J. N.; Hose, D.; Lloyd-Jones, G. C.; Murray, P.; Orpen, A. G.; Osborne, R.; Owen-Smith, G. J. J.; Purdie, M. *J. Am. Chem. Soc.* **2008**, *130*, 14471.
- (27) Trost, B. M.; Bunt, R. C. *Tetrahedron Lett.* **1993**, *34*, 7513.
- (28) Hill, R.; Rai, V.; Yudin, A. K. *J. Am. Chem. Soc.* **2010**, *132*, 2889.
- (29) Rotstein, B. H.; Rai, V.; Hili, R.; Yudin, A. K. *Nat. Protoc.* **2010**, *5*, 1813.
- (30) Londregan, A. T.; Farley, K. a.; Limberakis, C.; Mullins, P. B.; Piotrowski, D. W. *Org. Lett.* **2012**, *14*, 2890.
- (31) Jagasia, R.; Holub, J. M.; Bollinger, M.; Kirshenbaum, K.; Finn, M. G. *J. Org. Chem.* **2009**, *74*, 2964.
- (32) Punna, S.; Kuzelka, J.; Wang, Q.; Finn, M. G. *Angew. Chemie - Int. Ed.* **2005**, *44*, 2215.
- (33) Pitner, T. P.; Wilson, E. W.; Martin, R. B. *Inorg. Chem.* **1972**, *11*, 738.

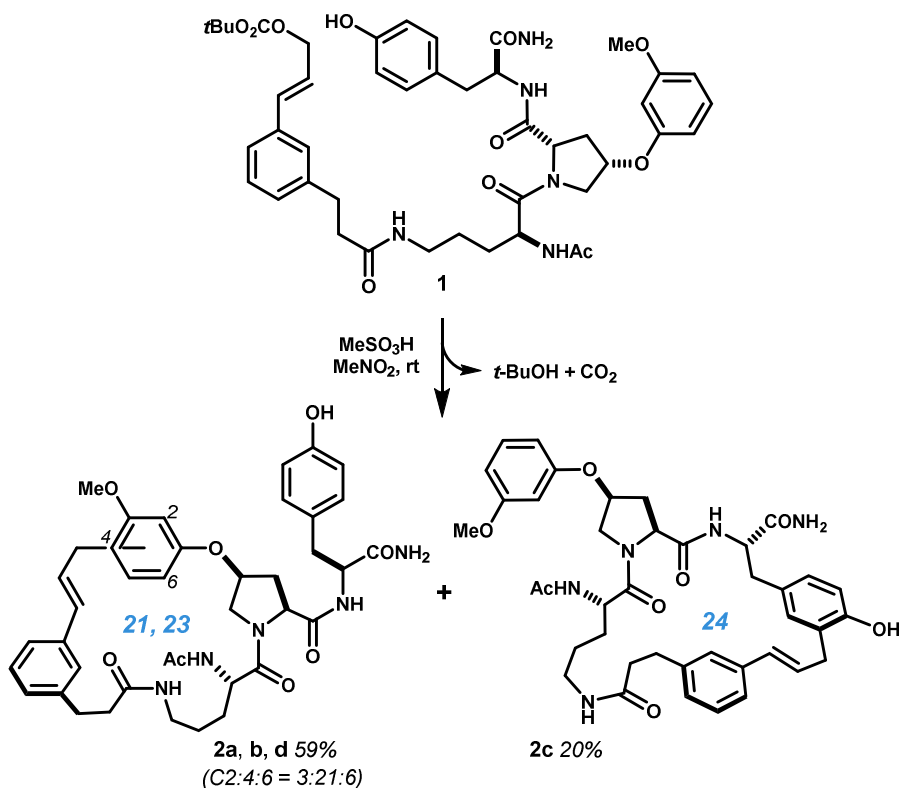
- (34) Best, S. L.; Chattopadhyay, T. K.; Djuran, M. I.; Palmer, R. A.; Sadler, P. J.; Sóvágó, I.; Varnagy, K. *J. Chem. Soc., Dalton Trans.* **1997**, 15, 2587.
- (35) Pneumatikakis, G. *J. Inorg. Biochem.* **1993**, 49, 83.
- (36) Klingensmith, L. M.; Strieter, E. R.; Barder, T. E.; Buchwald, S. L. *Organometallics* **2006**, 25, 82.
- (37) Collins, J. C.; Farley, K. a.; Limberakis, C.; Liras, S.; Price, D.; James, K. *J. Org. Chem.* **2012**, 77, 11079.
- (38) Dijkstra, G.; Kruizinga, W. H.; Kellogg, R. M. *Org. Chem.* **1987**, 52, 4230.
- (39) Geurink, P. P.; Van Der Linden, W. a.; Mirabella, A. C.; Gallastegui, N.; De Bruin, G.; Blom, A. E. M.; Voges, M. J.; Mock, E. D.; Florea, B. I.; Van Der Marel, G. a.; Driessen, C.; Van Der Stelt, M.; Groll, M.; Overkleef, H. S.; Kisselev, A. F. *J. Med. Chem.* **2013**, 56, 1262.
- (40) Mattern, I. E.; Pittard, J. *J. Bacteriol.* **1971**, 107, 8.
- (41) Malesevic, M.; Strijowski, U.; Bächle, D.; Sewald, N. *J. Biotechnol.* **2004**, 112, 73.
- (42) Regen, S. L.; Dulak, L. *J. Am. Chem. Soc.* **1977**, 99, 625.
- (43) Botti, P.; Pallin, T. D.; Tam, J. P. *J. Am. Chem. Soc.* **1996**, 118, 10018.
- (44) Wöhr, T.; Wahl, F.; Nefzi, A.; Rohwedder, B.; Sato, T.; Sun, X.; Mutter, M. *J. Am. Chem. Soc.* **1996**, 118, 9218.
- (45) Kim, Y.-W.; Grossmann, T. N.; Verdine, G. L. *Nat. Protoc.* **2011**, 6, 761.
- (46) Kessler, H. *Angew. Chemie Int. Ed.* **1982**, 21, 512.
- (47) Wuthrich, K. *NMR in biological research: Peptides and proteins*; American Elsevier Pub. Co: New York, NY, 1976.
- (48) Wishart, D. S.; Sykes, B. D.; Richards, F. M. *J. Mol. Biol.* **1991**, 222, 311.
- (49) Saitô, H. *Magn. Reson. Chem.* **1986**, 24, 835.
- (50) Cierpicki, T.; Otlewski, J. *J. Biomol. NMR* **2001**, 21, 249.
- (51) Baxter, N. J.; Williamson, M. P. *J. Biomol. NMR* **1997**, 9, 359.
- (52) Bara, Y. A.; Friedrich, A.; Kessler, H.; Molter, M. *Chem. Ber.* **1978**, 111, 1045.
- (53) Rozek, A.; Powers, J. P. S.; Friedrich, C. L.; Hancock, R. E. W. *Biochemistry* **2003**, 42, 14130.

5 Large ring-forming alkylations provide facile access to composite macrocycles

5.1 Direct, large ring-forming Friedel-Crafts alkylation of substituted benzene rings

Our initial discovery of direct large ring-forming *C*-cinnamylations led us to more closely examine this remarkable reaction (See Chapter 3).¹ Treatment of acyclic intermediate **1** with methanesulfonic acid in nitromethane at room temperature cleanly proceeded to a mixture of isomeric macrocycles **2a–d** (Scheme 5.1.1). Presumably, protonolysis of the cinnamyl mixed carbonate had generated a stabilized cinnamyl carbocation, which then underwent internal electrophilic aromatic substitution at electron-rich positions. Despite being one of the oldest and most studied organic reactions, Friedel–Crafts alkylation has seldom been used in complex settings and rarely to form large rings.² For this reason, we were surprised by the ease and efficiency of this transformation.

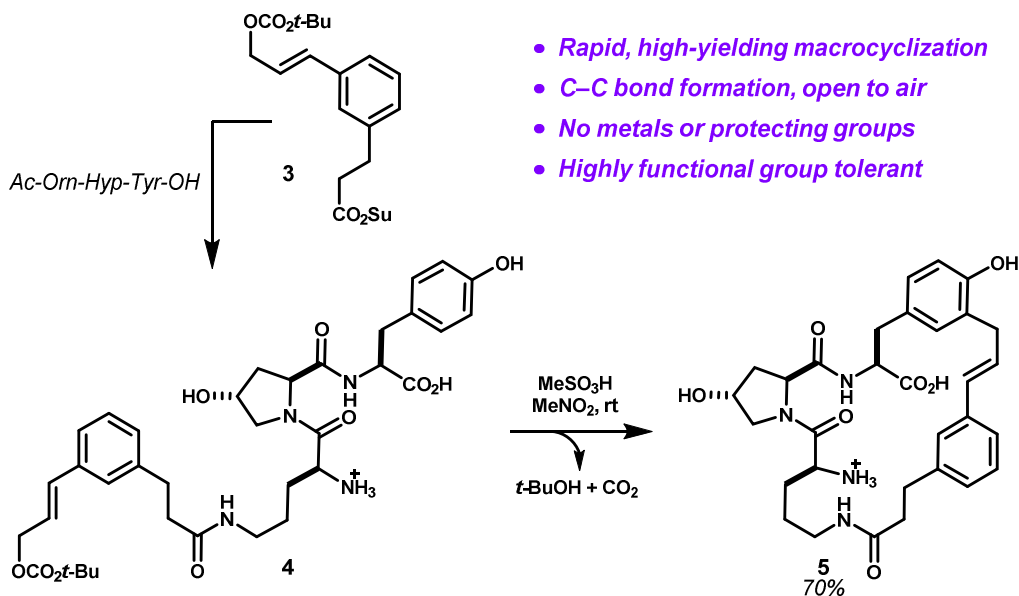
Scheme 5.1.1 Mild protonolysis of a cinnamyl mixed carbonate leads to competing internal Friedel-Crafts alkylations of electron rich positions of aromatic amino acid side chains. Macrocyclization in this manner provides a facile means to explore large ring constitution.



To test the limits of the large ring-forming cinnamylation reaction, we examined the acidolysis reaction of prototype template **3** ligated to highly polar tripeptide H-Orn-Hyp-Tyr-OH (Scheme 5.1.2). Treatment of acyclic intermediate **4** under standard conditions with 75 mM methanesulfonic acid in nitromethane gave composite macrocycle **5** in 70% yield. Internal substitution *ortho* to the tyrosyl phenol had occurred orthogonally in the presence of the primary amine, the carboxylic acid, and the secondary alcohol. Uniquely, whereas other contemporary macrocyclizations require exotic reagents or conditions, this reaction required no metals, ligands, protecting groups or air-free techniques, and led to rapid ring closure at room temperature. The simplicity and utility of the reaction prompted us to; (1) survey reaction efficiency, electronic tunability, and kinetics for a variety of ring constitutions and arene nucleophiles, (2) compare reaction trajectories of direct macrocyclizations to the isomerization of cognate cinnamyl tyrosyl ethers, and (3) evaluate the cinnamyl carbocation as one module in a multi-functional template able to transform linear peptides into polycyclic products.

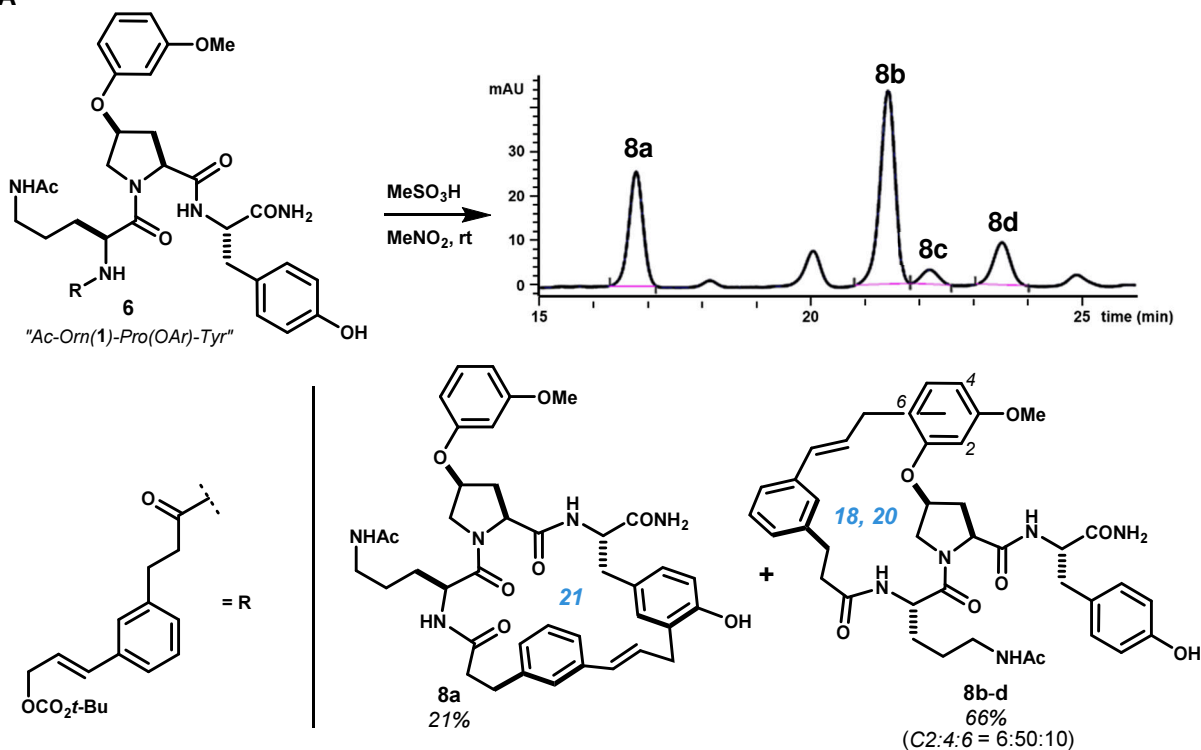
To further probe Friedel–Crafts alkylations within the framework of **1**, related macrocyclizations were examined in two additional isomeric settings. In each of these, the *meta*-methoxyphenoxy group allowed assessment of the relative rates of competing internal alkylations between this side chain and tyrosine. Whereas **2** was connected to template **3** by acylation of the ornithine side chain δ -amino group,

Scheme 5.1.2 Unprotected peptides acylated with cinnamyl carbonate-containing template **3** readily macrocyclize in acidic media. Large ring-forming Friedel–Crafts alkylation is insensitive to polar protic functional groups. Su = *N*-succinimidyl.

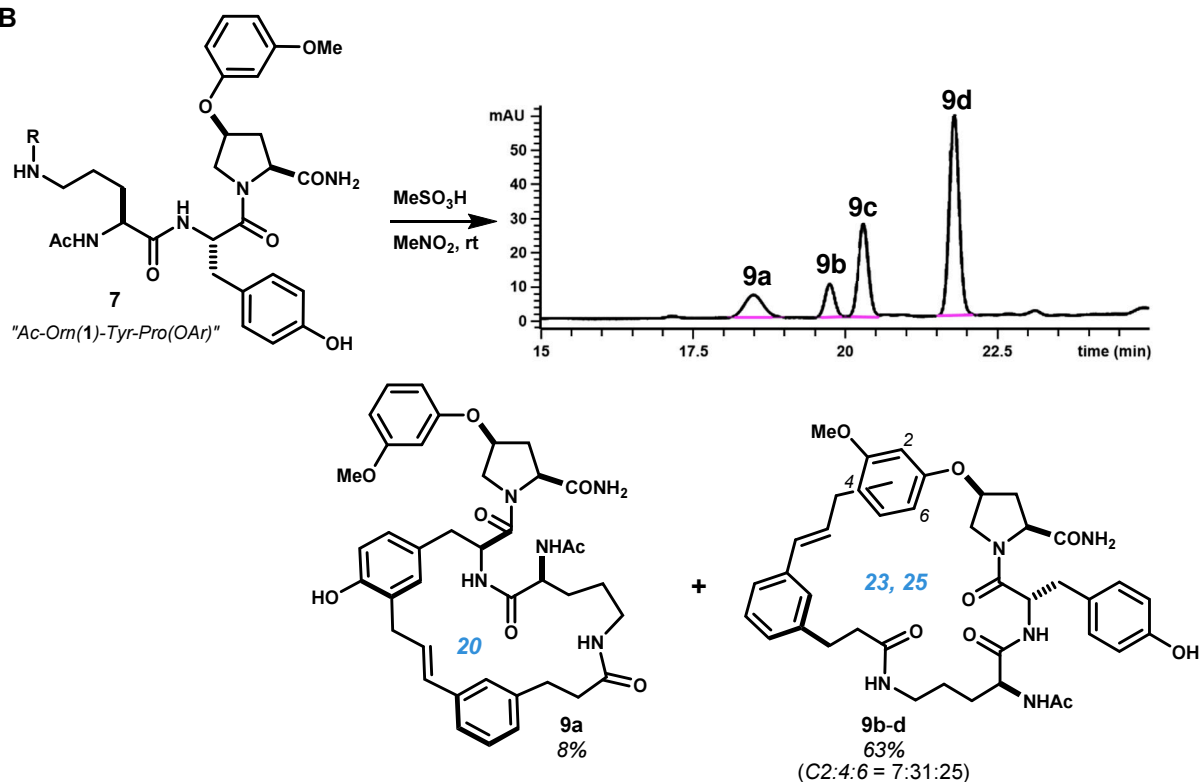


Scheme 5.1.3 Substrates **6** (part **A**) and **7** (part **B**), isomers of substrate **2** (Scheme 5.1.1), also readily cyclize under acidic conditions by electrophilic substitution at the analogous four sites. These data suggest that these systems are not intrinsically predisposed towards cyclization, and that diverse ring sizes are accessible. Crude HPLC-UV traces (254 nm) showing product distributions (**A**: 30→42% **B**: 30→55% ACN + 0.1% TFA, C18).

A



B

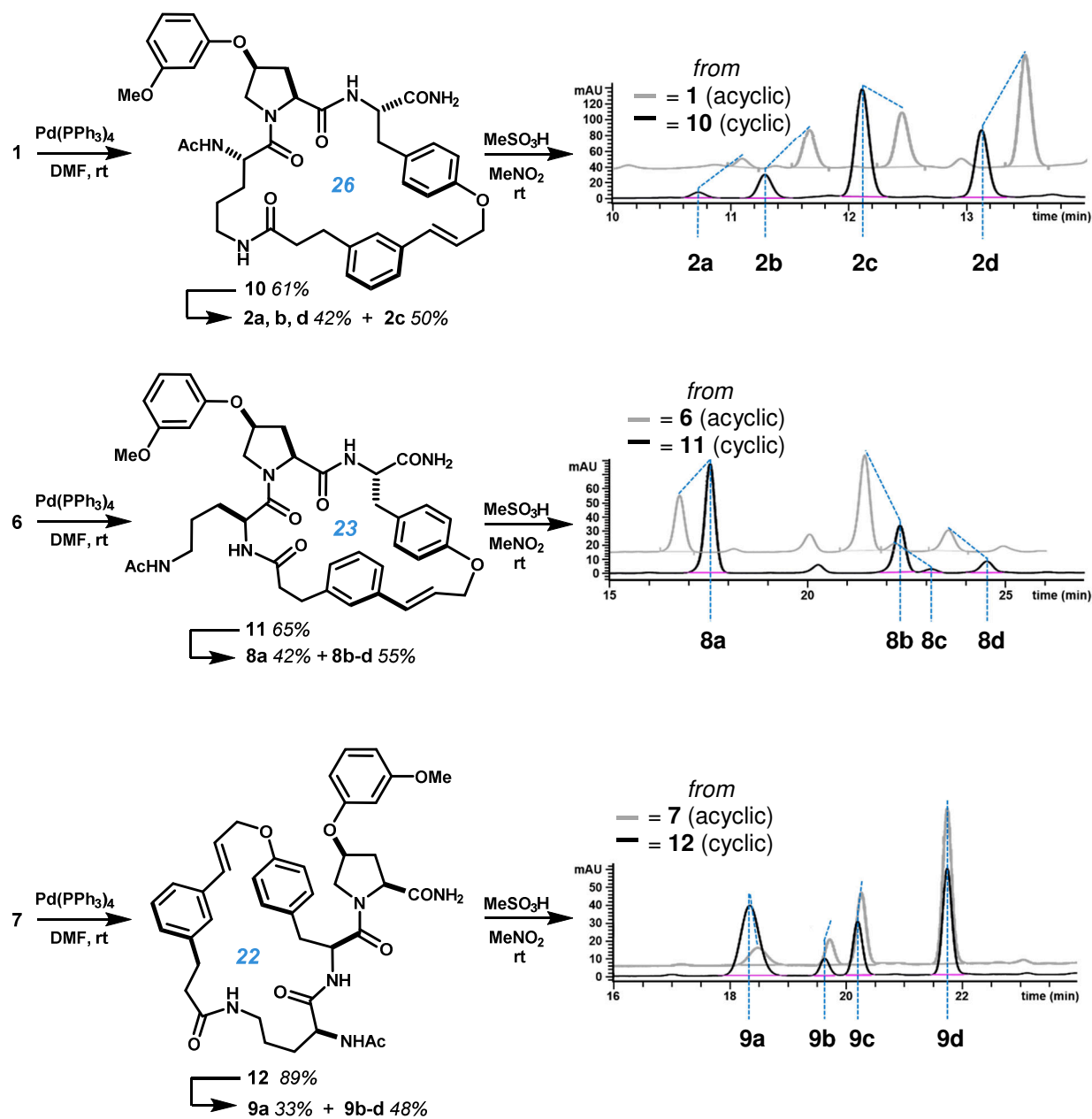


substrate **6** was acylated at the α -amino group. Compound **7** reversed the order of the aryloxyproline and tyrosine residues, relative to **2** (Scheme 5.1.3). Analogously to the reaction of **1**, acidolysis of acyclic intermediates **6** and **7** each led to the formation of four isomeric products, as judged by HPLC-UV/MS. These eight products were isolated and characterized by full resonance assignment, as was done for **2a–d** (see Chapter 3.3), based upon 2D NMR correlation spectra. Acidolyses of isomers **1**, **6** and **7** yielded twelve distinct macrocyclic isomers comprising 18, 20, 21, 22, 23, 24 and 25-membered rings (**2a–d** and **8**, **9a–d**, as shown in Scheme 5.1.1, Scheme 5.1.3). No *meta*-alkylation relative to electron donating groups, formation of branched α -phenylallyl products, or dimerization was observed. Friedel–Crafts reactions can be reversible,³ particularly in cases where the leaving group is tertiary,^{4,5} though simple alkyl groups have also been shown to migrate under relatively mild conditions.^{6–8} However, despite the mesomeric stabilization of the cinnamyl C–C bonds formed here, no equilibration was detected when isolated macrocycles **2**, **8** and **9a–d** were independently re-subjected to the reaction conditions. Further support of these product ratios being kinetic in nature, rather than thermodynamic, was derived from acidolysis reactions of the cognate macrocyclic ethers of **1**, **6** and **7**.

Acyclic substrates **1**, **6** and **7** were converted to macrocyclic cinnamyl tyrosyl ethers **10**, **11** and **12**, respectively, by treatment with catalytic amounts of Pd(PPh₃)₄ (Scheme 5.1.4). In line with our preliminary observations (see Chapter 3), acidolysis of these cyclic ethers afforded the same twelve C–C linked products, also in good yield, but in different ratios than from linear substrates **1**, **6** and **7**. These data further evidenced that products were formed kinetically. Additionally, these differences implied that conformational preorganization as tyrosyl ethers can alter the trajectory of the cinnamyl carbocation intermediate in competing intramolecular alkylation reactions.

The change in kinetic product ratio implies that cyclic tyrosyl ethers conformationally bias the incipient cinnamyl carbocation towards the transition state leading to tyrosine alkylation. Results indicate a path-dependence consistent with kinetic quenching (also known as conformational control^{9–11}), rather than Curtin–Hammett kinetics.¹¹ Indeed, such a scenario less commonly encountered, having been reported typically in reactions of highly reactive intermediates, including strong protic acids,¹² organopotassium compounds,¹³ and carbocations.¹⁴ In the case of internal cinnamylation, a low barrier to C–C bond formation presumably leads to alkylation at a comparable or faster rate than conformational relaxation. Competing

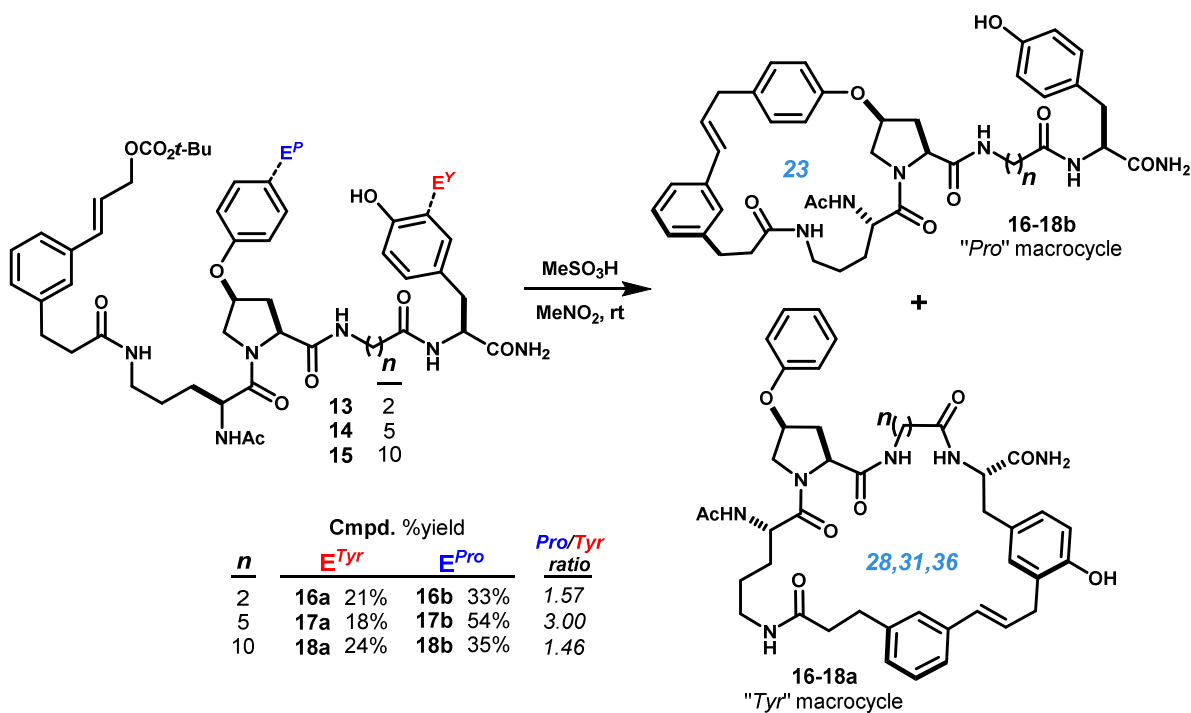
Scheme 5.1.4 Substrates **1**, **6** and **7** underwent internal *O*-cinnamylation of tyrosine when treated with Pd(PPh₃)₄ (5 mol%). Acidolysis of the resulting cinnamyl tyrosyl ethers **10-12** also led to macrocyclic C–C linked products, but in different ratios than from acyclic precursors.



solvolysis or ion pair return would be expected to permit relaxation of the quasi-macrocyclic conformation biased towards tyrosine alkylation. These side reactions appeared minimal under these conditions (*vide infra*).

The widely-disseminated definition of the Curtin-Hammett principle states that, for a given reaction that produces multiple products, "...the product composition is not in direct proportion to the relative concentrations of the conformational isomers in the substrate; it is controlled only by the difference in standard free energies ($\delta\Delta^\ddagger G$) of the respective transition states." Assuming that the acidolysis of macrocyclic tyrosyl ethers and their acyclic counterparts proceed to the same products via chemically identical cinnamyl carbocation intermediate and analogous transition states, this principle does not anticipate the sometimes marked differences between product ratios that we observed. For instance, acidolysis of cyclic ether **12**, by comparison to reaction of its acyclic congener **7**, led to a five-fold increase in the ratio of $O_{Tyr} \rightarrow C_{ortho}$ rearrangement product **9a** relative to the three other isomers. Thus, the substrate conformation affects, at least in part, the distribution of product isomers. While this conformation control is

Scheme 5.1.5 Increasing ring size minimally influences macrocyclization kinetics. Substrates **13**, **14** and **15** cyclize to 28-, 31- and 36-membered rings **16a**, **17a** and **18a**, respectively, in a nearly equal ratio to 23-membered ring products **16–18b**.



noteworthy, and potentially useful for increasing the abundance of particular product isomers, it also occurs simultaneously with other enthalpic and entropic factors.

The ring expansion from tyrosyl ether **12** (22 atoms) to products **9b–d** (23 or 25 atoms) was also possible, whereas **8a–c** and **2a–c** and previously observed migrations (see also Chapter 2) demonstrated ring contractions. These data suggest that ring closure rate, while sensitive to substrate conformation, is governed primarily by arene reactivity, and not by ring size. This was born out in a series of desmethoxy analogs of **1** incorporating an aliphatic spacer between *cis*-4-phenoxy-*L*-proline and tyrosine. Consistent with kinetic studies reported for ring-forming Friedel–Crafts acylations,¹⁵ we observed little change in product distribution as the spacer was lengthened from four to twelve atoms. To ensure accurate measurement of molar ratios, product yields were assayed by HPLC-UV quantification against external calibrants prepared from purified macrocyclic products. The ratio of products (i.e. “Pro/Tyr ratio”) formed from homologous substrates **13–15** allows indirect assessment of the *change* in the rate of tyrosine alkylation, assuming a constant rate leading to 23-membered “proline” macrocycles **16–18a** (Scheme 5.1.5). In this regard, the remarkably similar product ratios observed between acidolysis reactions of **16** and **18** indicate that ring closure rate is unaffected by chain length separating reacting groups. While the ratio observed from the reaction of **14** was two-fold higher, this appeared to be driven by the relatively higher yield observed for the proline macrocycle product **16b**, and only slightly depressed yield of the tyrosine-linked product **16a**. Such small variations in ring closure rate have also been observed in kinetic studies of many-membered cycloalkanes.^{16–18} In conjunction with the reactivity observed for isomeric substrates **1**, **6** and **7**, these data anticipate cyclization of extended peptides of diverse sequence will be possible, and that a turn-inducing proline is not required.

In many peptidyl substrates, the inclusion of proline led to a doubling of NMR resonances, which was most prominent in ¹H NMR spectra. This behavior appeared to be consistent with widely documented proline *cis-trans* isomerization, which results from the relatively high barrier to rotation of the proline tertiary amide bond (~13-19 kcal/mol).¹⁹ The slow interconversion of *cis/trans* isomers on the timescale of the NMR experiment and the small free energy difference between *cis*- and *trans*-amide rotamers (avg. $\Delta G_{cis-trans} \approx 1.2$ kcal/mol) leads to two discrete sets of peaks in the NMR spectra.^{20–22} Similar behavior was previously observed with macrocyclic products containing proline and hydroxyproline derivatives (see Chapter 2.3). In

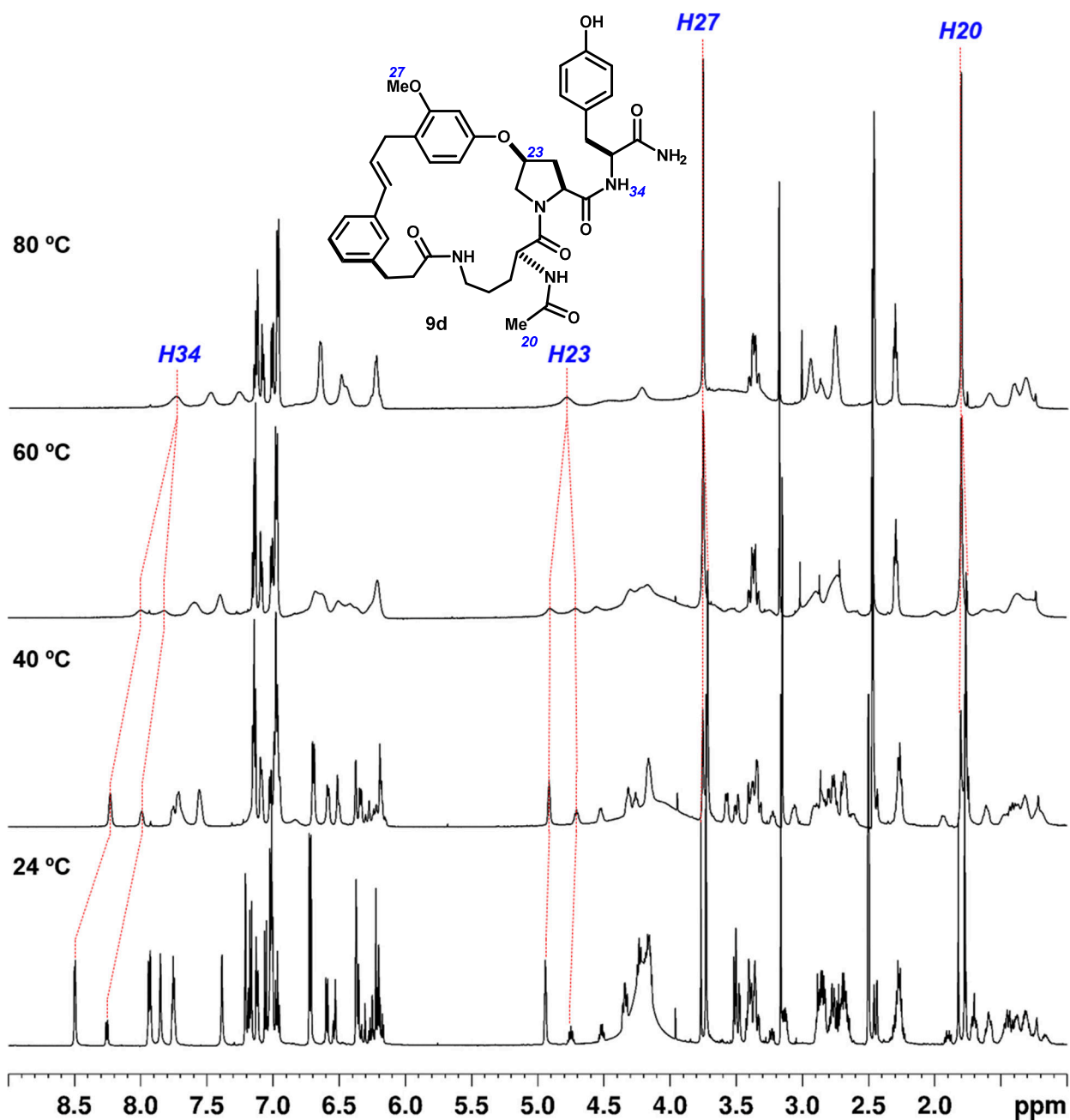


Figure 5.1.1 Variable-temperature ^1H NMR experiments (600 MHz, $\text{DMSO-}d_6$) showing the coalescence of key peaks at higher temperatures, suggesting that the observed doubling of peaks ($\sim 3:1$ ratio) results from restricted rotation, presumably about the prolyl tertiary amide bond. Only intermediate exchanges is reached between 60–80 $^\circ\text{C}$, leading to severe line broadening. Key coalescing resonances are highlighted in blue.

most cases, resonance assignments were made for the major set of peaks. However, we sought to experimentally confirm that these peaks were rotational isomers and not contaminants. Macrocyclic product **9d** was selected as a representative example, and showed two sets of peaks in a 3.5:1 ratio in the ^1H NMR spectrum in $\text{DMSO-}d_6$. Spectra were recorded at several temperatures from room temperature to 80 °C, which caused doubled signals to coalesce to a single set of peaks, consistent with a pair of interconverting isomers. The extreme broadening and near disappearance of some signals across the spectrum at 60 °C and at 80 °C is indicative of intermediate rate of exchange.

Nine additional derivatives of substrate **1** were prepared to survey arene electronic requirements and reaction regioselectivity. The products and results from these reactions are abbreviated in Scheme **5.1.6** and adjoining Table **5.1.1**. In the absence of a competing arene, ring closure occurred selectively at tyrosine (**19**, entry 1). The desmethoxy analog of **1** (entry 2) showed high selectivity for *para*-alkylation of the phenoxy group on proline (site III, Scheme **5.1.6**) and comparable reactivity between this ring and tyrosine (site I). Dichlorination of the tyrosyl phenol also led to selective formation of the site III core yielding **22a**. X-ray crystallographic analysis of this molecule confirmed the structure assigned from NMR correlation spectra (Scheme **5.1.6**). 4-(Phenylthio)proline did not compete with tyrosine for alkylation (entry 3, Table **5.1.1**), but underwent *para*-alkylation in good yield when tyrosine alkylation was blocked by dichlorination (entry 5). Lack of a suitably reactive arene led to an intractable mixture over a several hour period (entry 9). This quinoline, inspired by hepatitis C Virus NS3/4a protease inhibitors containing this motif,²³ appeared not to be a competent nucleophile, despite being relatively electron rich. This observation echoed the broader dearth of electrophilic substitutions of quinolines and isoquinolines reported in the literature.^{24–26} Conversely, benzene rings proved electronically tunable. Substituting tyrosine in substrate **2** with electron rich (4-hydroxy-2-methoxyphenyl)alanine enhanced the rate of reaction at this side chain, as expected, leading to an equal ratio of alkylation between this ring (**27a, f**) and the methoxyphenoxy group (**27b, d, g**). Unanticipated, however, was the production of branched diastereomeric α -phenylallyl products **27c** and **27h**, in this case. These potentially derive from rotamer preferences in the side chain, transient *O*-alkylation and Claisen rearrangement,²⁷ or a combination thereof (Scheme **5.1.7**). Trace branched product **27e** was also observed; an outcome not identified, but potentially present, in other related substrates. Large ring-forming alkylations to give products **16–25** and **27** show that cyclization typically gives unbranched

cinnamylated products, and that regioselectivity can be tuned with substituent effects about the arene nucleophile.²⁸

Scheme 5.1.6 Nucleophile survey within the scaffold Ac-Orn(1)-Pro(X-Ar)-Tyr. Macrocyclization can be tuned for selective or divergent outcome using substituent effects or blocking groups. Alkylation at sites I, II and III accesses 24, 21 and 23-membered rings, respectively (ring size indicated in blue; E^P = aryloxypropyl linkage, E^Y = tyrosyl linkage).

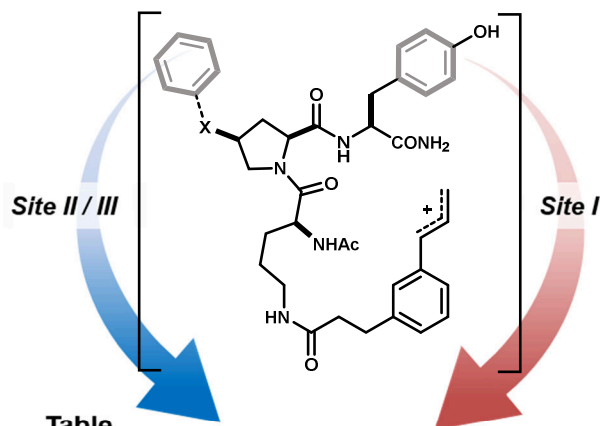
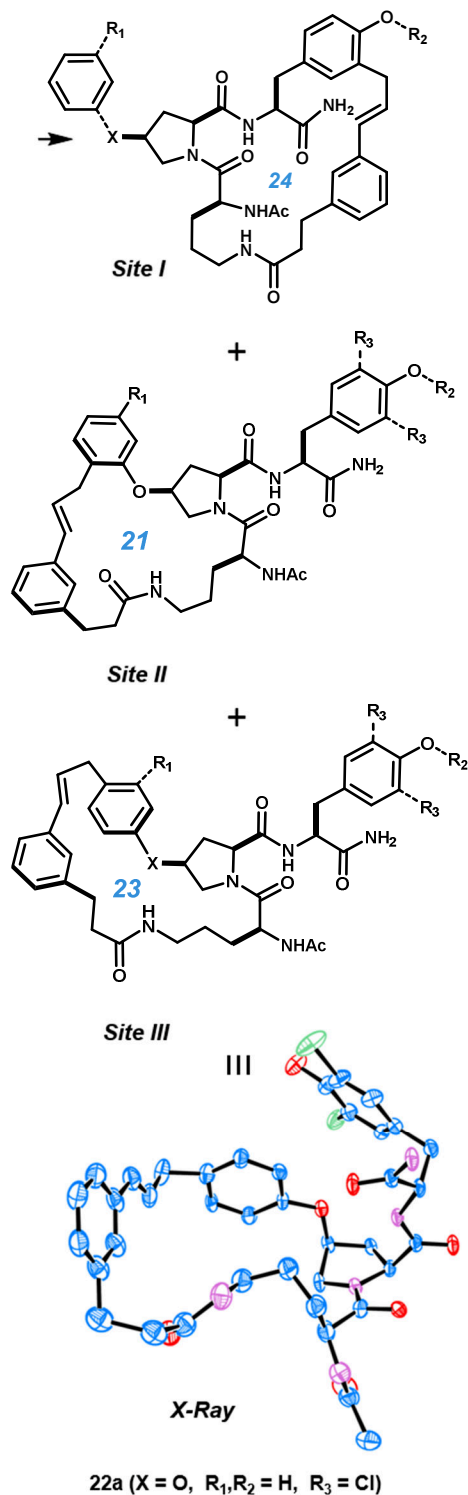
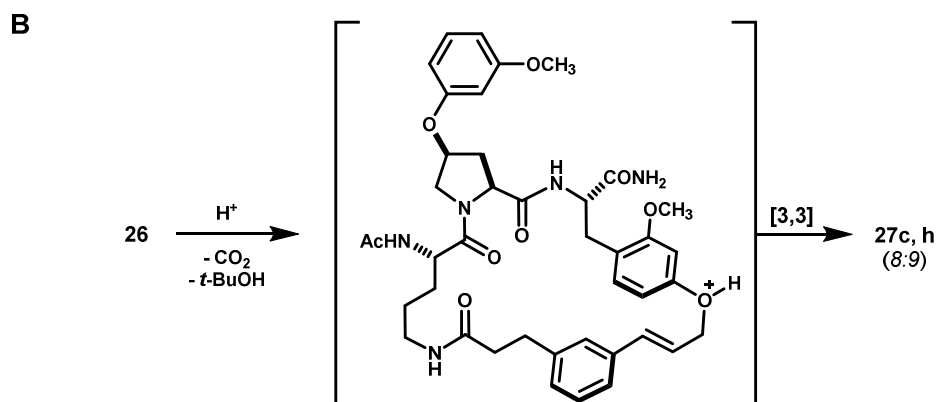
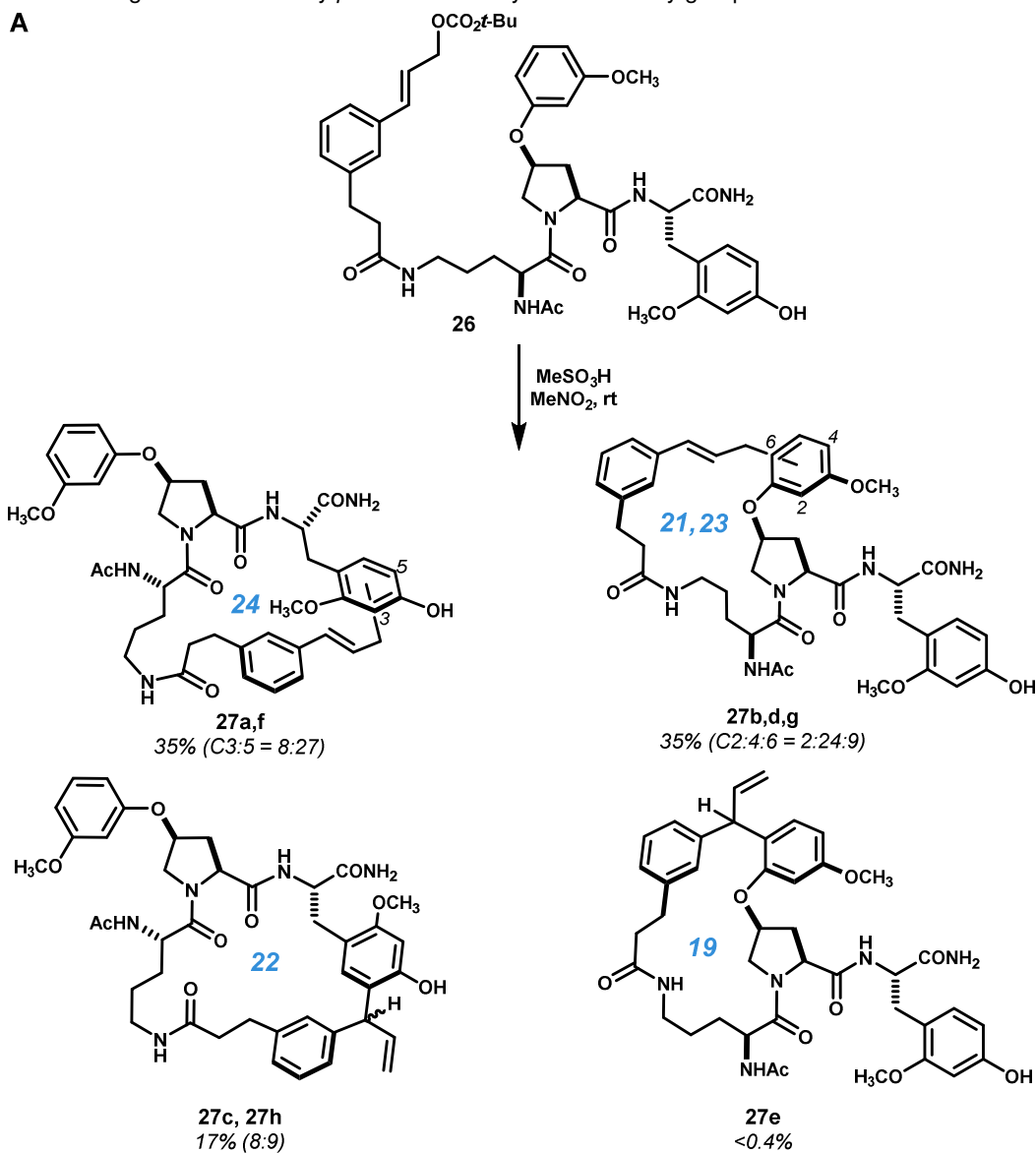


Table 5.1.1. Pro – aryl substituent – Tyr

Entry	Isomeric Macrocycle(s) %yield	
	Site II / III	Site I
1 X = H	n/a	19 68%
2 X = O	20a 54%	20b 42%
3 X = S	21a 0%	21b 64%
4 X = O	22a 86%	22b 0%
5 X = S	23a 59%	23b 0%
6	2a,b,d 59%	2c 20%
7	24a-c 68%	24d 13%
8	25a 0%	25b 65%
9	0%	0%



Scheme 5.1.7 Reaction of 2-(4-hydroxy-2-methoxyphenyl)alanine uniquely yields two branched α -phenylallyl products. **A)** Structural isomers isolated and characterized from the reaction of **26**. **B)** The formation of products **27c** and **27h** may result from initial *O*-alkylation followed by acid-promoted *ortho*-Claisen rearrangement enabled by *para*-activation by the 2-methoxy group.



5.2 Selective macrocyclizations enabled by arene symmetry or substrate geometry

Large ring-forming cinnamylations mediated by template **3** are rendered selective when arene symmetry or substrate geometry dictates a single outcome. In the case of tyrosine alkylation, C2 symmetry of the side chain *para*-disubstituted benzene ring and strong directing effect of the phenol leads to *ortho*-alkylation of the phenol as the only possible product. Compounds **5**, **19** and **20b** were each obtained selectively as a result of this type of symmetry (Figure 5.2.1A); **25b** was also selectively produced (not shown).

Alternatively, C2 symmetry in monosubstituted arenes can, in concert with steric hindrance, lead to selective alkylation. In this case, an *ortho/para*-directing substituent would be anticipated to give a mixture of *ortho* and *para* isomers, favoring *para*-substitution. When the activating substituent is bulky, even greater

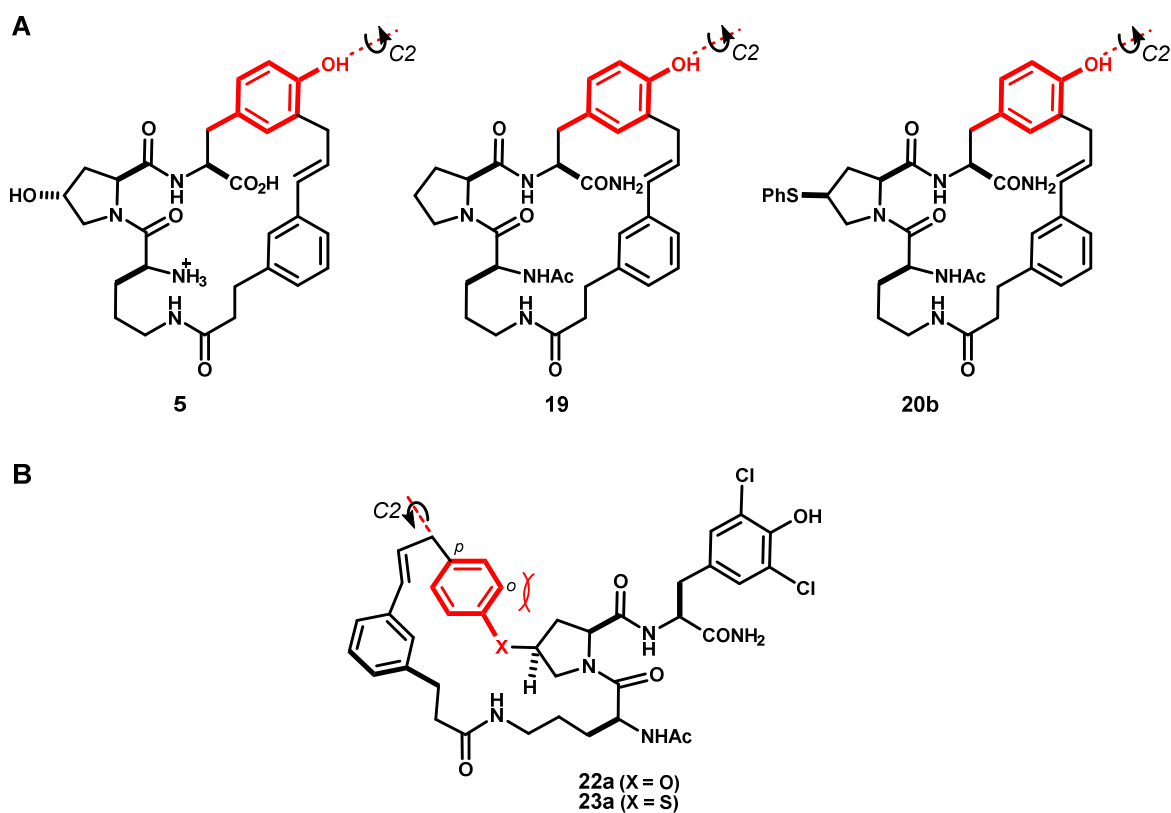
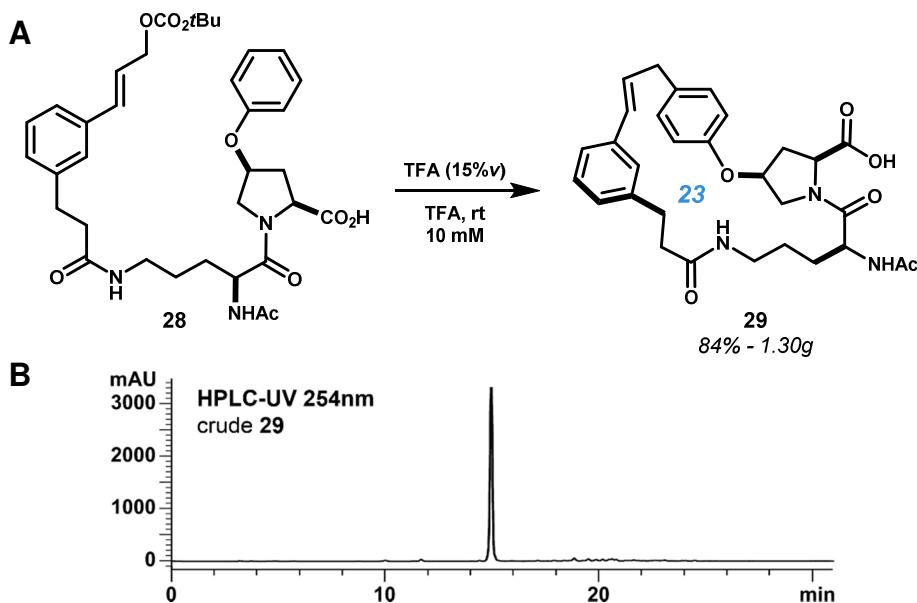


Figure 5.2.1 Examples of (A) polarized *para*-di-substituted and (B) mono-substituted benzene rings as C2 symmetry elements which can lead to selective macrocyclization.

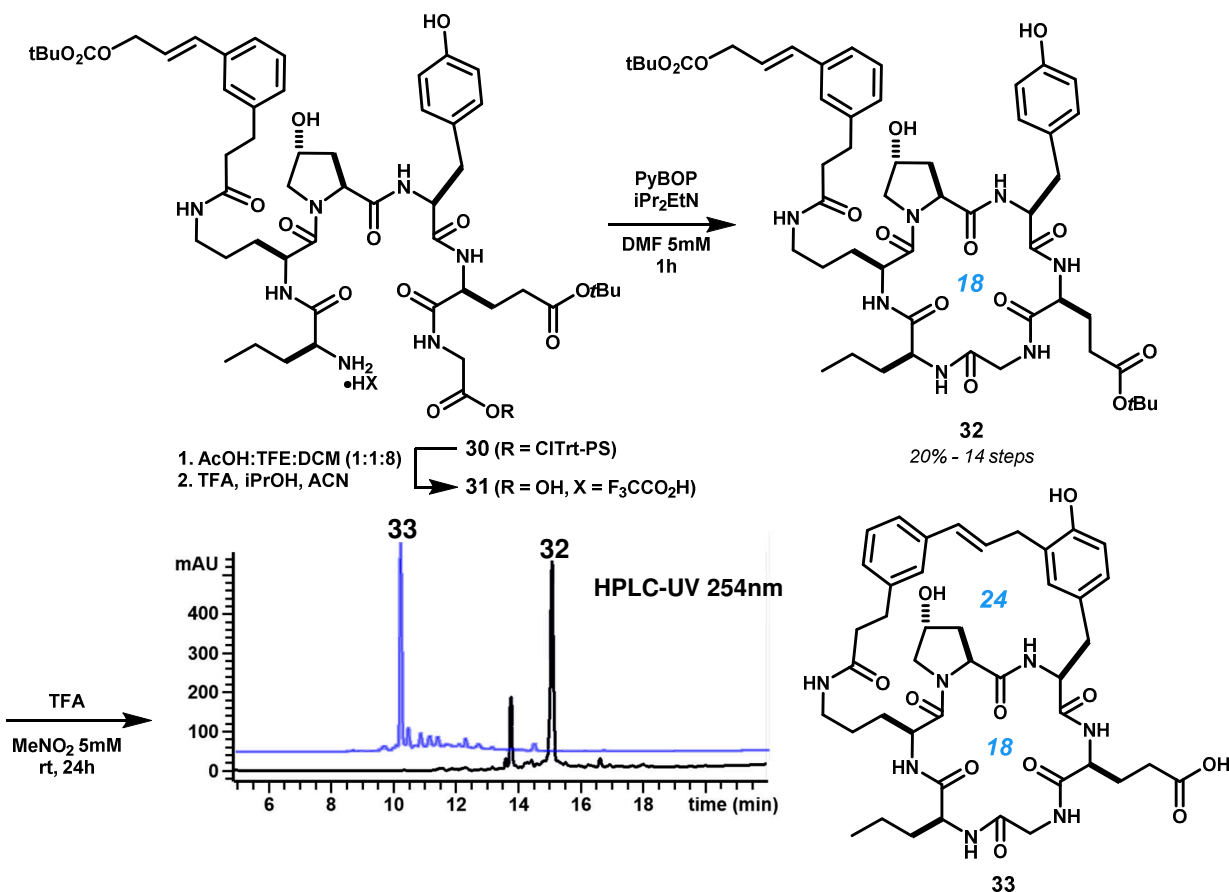
selectivity may be anticipated.^{29,30} Additionally, more stabilized electrophiles tend to proceed via a late transition state resembling a σ -complex, which may further increase the *para/ortho* ratio.^{31,32} Solvent effects have also been shown to influence isomer distribution in bimolecular Friedel-Crafts reactions.^{32–35} This mono-substituted benzene manifold leads, somewhat surprisingly, to the complete selectivity observed in the formation of products **22a** and **23a** because of steric hindrance of the *ortho* position by the pyrrolidine ring (Figure 5.2.1B). This selectivity was also leveraged in the synthesis of compound **29**, the macrocyclic core of **20a** and **22a** (site III). 23-Membered ring **29** was prepared on gram scale in 84% yield from acidolysis truncated dipeptidyl substrate **28** (Scheme 5.2.1). HPLC-UV analysis of the crude reaction showed complete selectivity for product **29**. While monosubstituted arenes bearing *meta*-directing groups could, in principle, lead to selectivity by symmetry alone, substrates of this type would likely be unreactive towards the cinnamyl carbocation. In the case of phenoxy and phenylthioprolines, the observed *para* selectivity may also derive from inherent geometric biases present in the peptidic substrates investigated here, or potentially also strained transition state geometries.

Scheme 5.2.1 A) Selective, gram-scale synthesis of the 23-membered ring **29**, the macrocyclic core of compounds **20a** and **22a**. B) HPLC-UV analysis following concentration of the crude reaction mixture (C18, 4.6 × 250 mm 5 μ , 30 → 60% ACN + 0.1% TFA, 1 mL min⁻¹). TFE = 2,2,2-trifluoroethanol.



To test the capabilities of template **3** in selective large ring-forming reactions, we designed macrolactam substrate **32** wherein internal cinnamylation of tyrosine would occur transannularly. Linear hexapeptide **30** was assembled by solid-phase peptide synthesis on 2-chlorotrityl polystyrene resin. Template **3** was installed during peptide assembly by utilizing Fmoc-ornithine which had been previously acylated (*N*₆) with **3**. Completed acyclic precursor **30** was then cleaved from the solid support under mild conditions with acetic acid in TFE:DCM,³⁶ which left the Glu *tert*-butyl ester and cinnamyl *tert*-butyl carbonate groups intact. Intermediate **31** was sufficiently pure that we carried this material forward crude. The counterion (i.e. HX, Scheme 5.2.2) was exchanged for trifluoroacetate prior to macrolactamization in order to avoid competing bimolecular acetylation. We were cognizant that peptide lactamization reactions often lead to epimerization of the C-terminal amino acid,^{36–38} and therefore engineered the lactam disconnection between glycine and norvaline. Treatment of **31** with PyBOP in DMF under high dilution led

Scheme 5.2.2 Linear precursor **31** was assembled on solid support, and cleaved to retain side chain protecting groups. Lactamization formed intermediate **32**, harboring template **3**, which smoothly underwent transannular *Ortho*-cinnamylation of the tyrosyl phenol under mild acidic conditions yielding bicycle **33**.



to rapid formation of 18-membered ring lactam **32**,³⁹ which was recovered in 20% yield over the preceding 14 steps following preparative HPLC purification. This material was then treated with TFA in nitromethane, which cleanly formed annulated macrocycle **33** (Scheme 5.2.2).

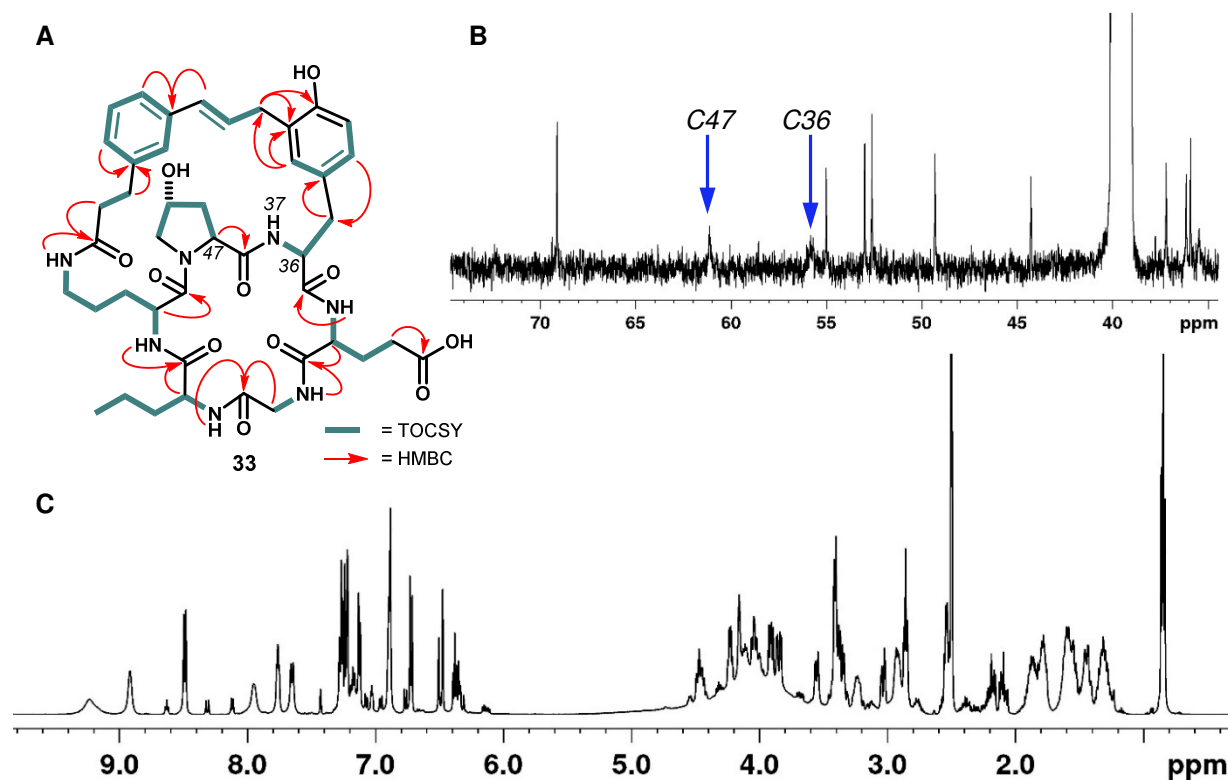


Figure 5.2.2 A) proton spin systems observed by ¹H-¹H TOCSY (grey) and ¹H-¹³C HMBC correlations leading to the assignment of bicyclic compound **33**. B) Broad resonance **36** and **47** in the 1D-¹³C NMR suggested intermediate conformational exchange in this portion of the molecule. C) ¹H-NMR spectrum of **33** showing putative second conformational population in a ~10:1 ratio.

The structure of **33** was confirmed by complete resonance assignment. Key ¹H-¹³C HMBC correlations and ¹H-¹H TOCSY spin systems confirming the ring connectivity are shown as red arrows in Figure 5.2.2. Notably, however, we did not observe HMBC correlations linking the *cis*-hydroxyproline to its neighboring residues, tyrosine and ornithine. The connectivity in this region was therefore inferred based on the synthesis, observed molecular mass, and the chemical shift, integration and multiplicity of the amide proton *H37*. This observation was also reflected in the 1D-¹³C NMR spectrum, which showed unusual broadening of the α -carbon resonance of tyrosine (*H36*) and of hydroxyproline (*H47*, see Figure 5.2.2B). Additionally, despite the molecule appearing homogeneous by HPLC on multiple stationary phases, macrocycle **33** exhibited a second set of peaks in the ¹H NMR in a 10:1 ratio. This behavior is consistent

with slowly exchanging conformers or proline rotamers, as observed in other proline-containing macrocycles (see Chapters 2.3, 5.1), though we did not attempt to confirm this spectroscopically.

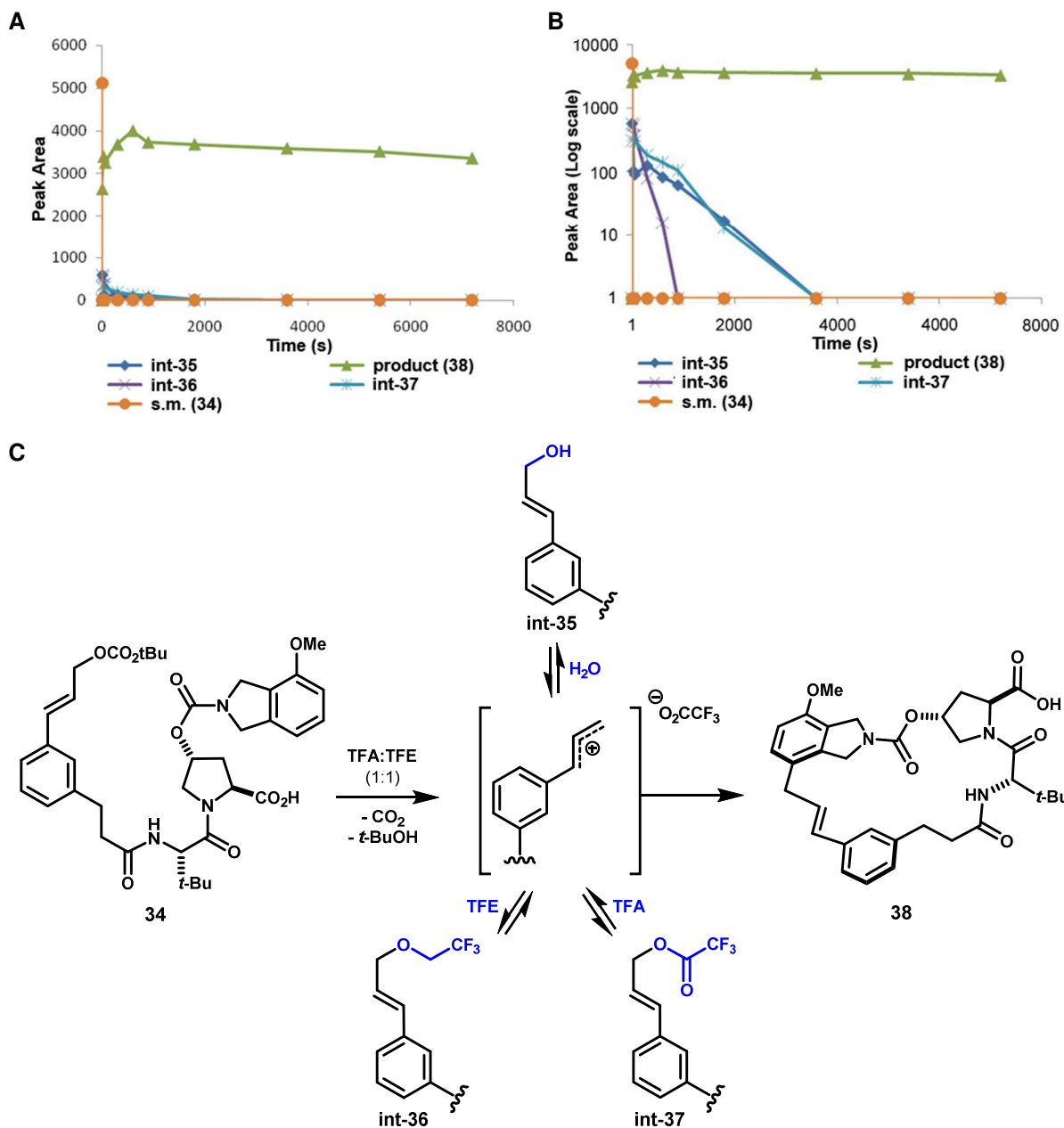
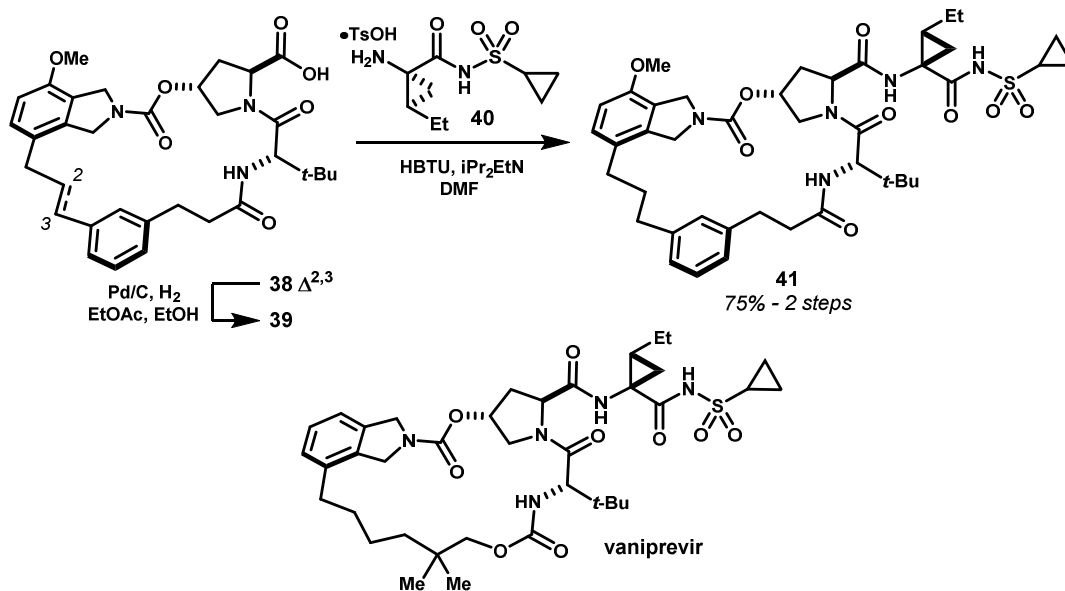


Figure 5.2.3 **A)** Time-course HPLC-UV analysis shows rapid conversion of **34** to product **38**. **B)** Semi-log plot showing the slower conversion of the intermediate cinnamyl alcohol, trifluoroacetate and trifluoroethyl ether to product. **C)** HPLC-MS analysis indicated the reaction of **34** in TFA:TFE (1:1) proceeds directly to macrocycle **38**, and to a lesser extent through the intermediate cinnamyl alcohol, 2,2,2-trifluoroethyl ether, and trifluoroacetate.

Given current interest in macrocyclic hepatitis C virus NS3/4a protease inhibitors, we sought to employ our methodology to selectively prepare a structural analog of the clinical candidate vaniprevir.⁴⁰ Linear precursor **34** (Scheme 5.2.4) containing a 4-methoxyisoindoline was readily prepared, and cyclized to **38** under optimized conditions using TFA:TFE (1:4, v:v) as the reaction medium. As was observed with isomerization of cyclic tyrosyl ethers, ring closure proceeded faster than solvolysis and ion pair return. Time course HPLC-UV analysis indicated greater than 75% conversion to product within 5 seconds, and concomitant formation of trace products corresponding to the cinnamyl alcohol (**int-35**), its 2,2,2-trifluoroethyl ether (**int-36**), and its trifluoroacetate (**int-37**). These reacted further, but at slower rates, yielding the 21-membered ring **38** as the sole product within 1 hour (Figure 5.2.3A,B). We have observed similarly efficient reactions in many other cases when using mixtures of TFA:TFE as solvent. In this medium, reversible equilibria of this sort may play an important role in preventing irreversible side-reactions of the cinnamyl carbocation⁴¹ the precise nature of which we have not ventured to characterize.

Scheme 5.2.3 Vaniprevir analog **41** was completed by hydrogenation of **38** and amide coupling with **40**.

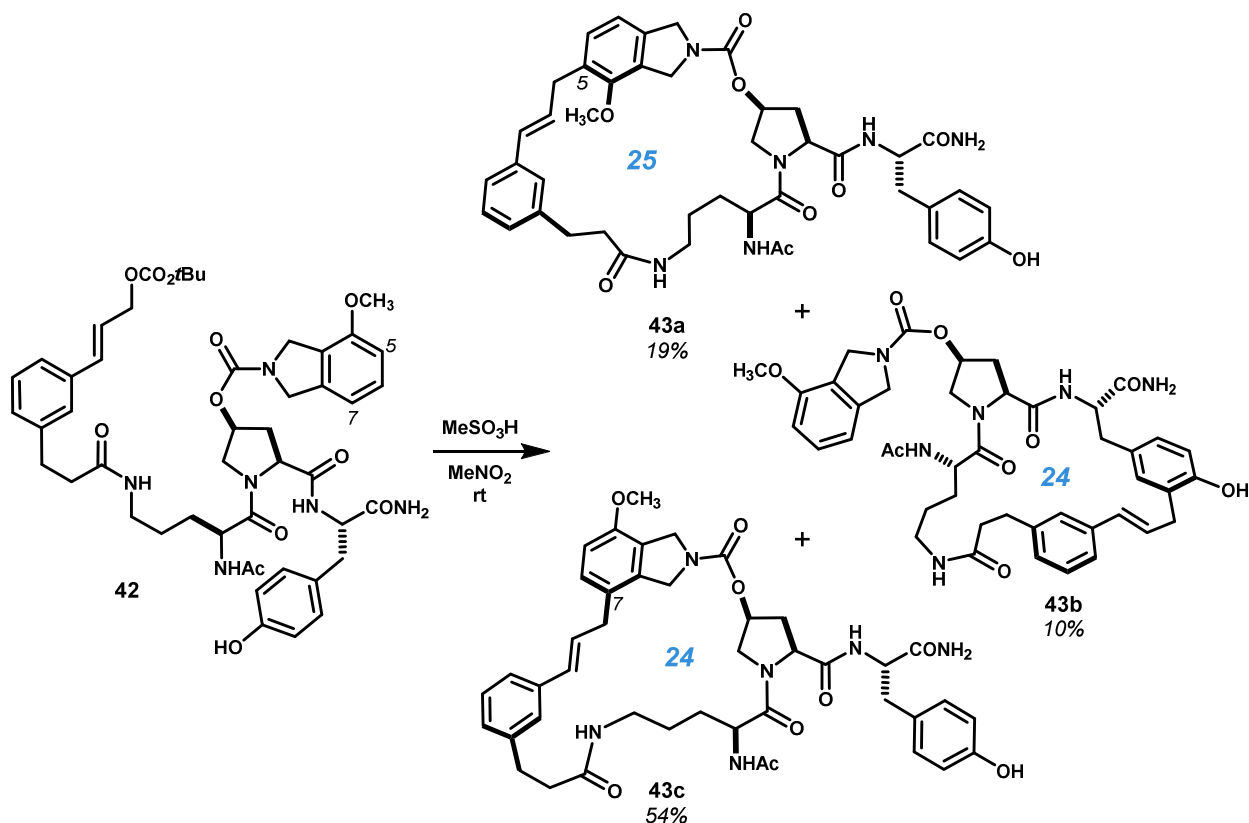


Hydrogenation of isolated macrocyclic intermediate **38** followed by condensation with aminocyclopropane **40** completed the synthesis of **41**. This analog differs from vaniprevir by one ring atom, the constitution of the bridging hydrocarbon, and the methoxy substituent. Compound **41** was active against wild type NS3 in cellular HCV replicon assays of genotypes 1a and 1b with EC₅₀ = 1.2 μM and 1.9 μM,

respectively. Though **41** was, perhaps unsurprisingly, substantially less potent than vaniprevir itself, these data imply that macrocycles of this type can permeate membranes and persist intracellularly. This, despite that **41** possesses a molecular weight (806.0 g mol^{-1}) and hydrogen bonding capability well in excess of widely embraced Lipinski's rules for predicting druglikeness,^{42,43} and despite several potentially metabolically labile sites.

To address whether the regioselectivity observed in acidolysis reactions of **34** was inherent to this heterocyclic nucleophile, we prepared an analogous 4-methoxyisoindoline carbamate within the *cis*-hydroxyproline framework of **1** (Scheme 5.2.4). In this case, products were obtained from alkylation at both the 7- and 5-positions of the isoindoline to give 24- and 25-membered rings **43a** and **43c**, respectively, along with the product of tyrosine alkylation (**43b**). These results highlight the broader difficulty in predicting the influence of strain or steric hindrance on the rate of large ring-forming reactions. Nonetheless, these factors can be exploited with good effect.

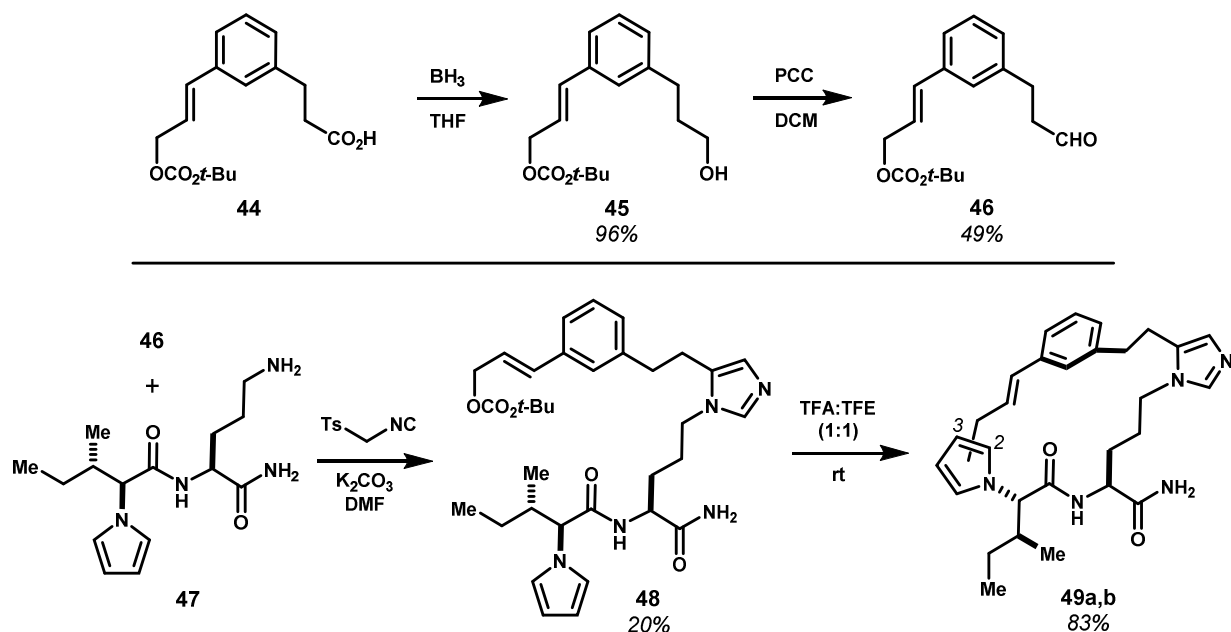
Scheme 5.2.4 4-Methoxyisoindoline shows inherent reactivity at the 7-position (**43c**), but also the 5-position (**43a**). This suggests that the complete selectivity in the cyclization of **34** to **38** may result from conformational bias which impedes alkylation of the 5-position.



5.3 Large ring-forming alkylations using alternative template architectures

Efficient ring-forming reactions initiated by template **3** provide a small glimpse of possibilities for template designs. Even minor modifications of the substance permit valuable variations in product structures. For example, the aldehyde congener of **3** (**46**, Scheme 5.3.1A) was prepared to facilitate initial ligation other than amidation, an alteration which could potentially enhance physicochemical properties and metabolic stability of the products. Aldehyde **46** was prepared by first borane reduction of carboxylic acid **44**, an intermediate in the preparation of **3**, and subsequent oxidation of alcohol **45** with pyridinium chlorochromate. Aldehyde template **46** was ligated to a pyrrolyl Leu-Orn dipeptide derivative using a van Leusen three-component condensation with unsubstituted tosylmethylisocyanide to afford 1,2-dialkyl imidazole **48**.⁴⁴ This substance smoothly underwent macrocyclization via pyrrole alkylations in TFA:TFE (1:1, v:v) to give **49a,b** (Scheme 5.3.1B) in high yield. This was a remarkable result given the notorious lability and reactivity of monosubstituted pyrroles, particularly under acidic conditions.^{45,46}

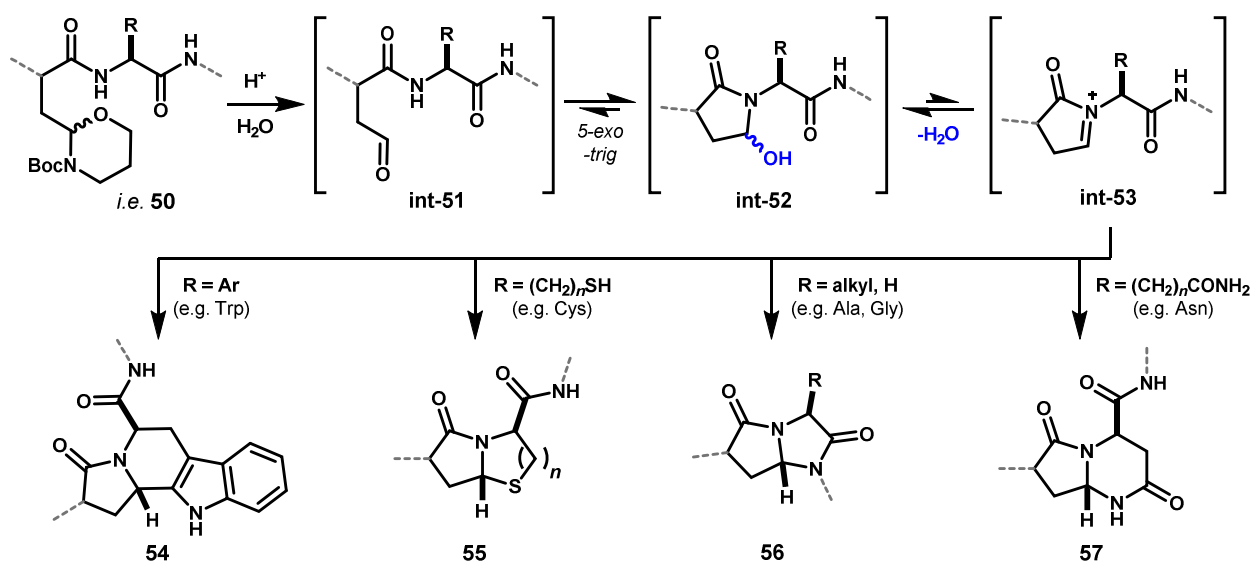
Scheme 5.3.1 A) Conversion of carboxylic acid **44** – the free acid of template **3** – to aldehyde template **46**,
B) Template **46** underwent van Leusen imidazole synthesis with pyrrolyl dipeptide to give acyclic intermediate **48**, which cyclized to **49a** and **b** without degrading the acid-sensitive pyrrole ring.



We next investigated a third variant of **3**, namely **50**, harboring a tetrahydro-1,3-oxazine as a latent aldehyde positioned to initiate *N*-acyliminium ion chemistry.⁴⁷ This template architecture was designed to

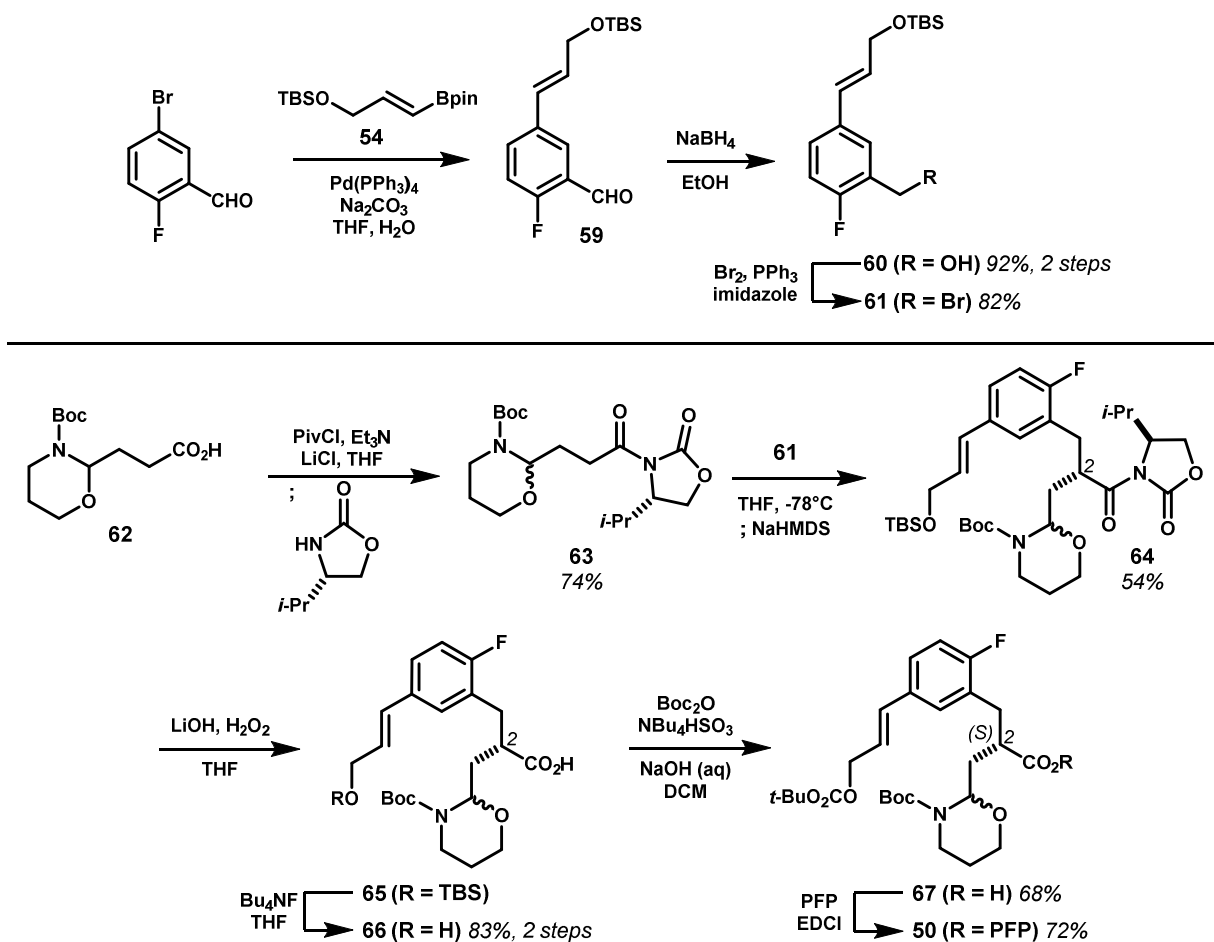
rigidify peptides in a sequence-dependent, diversity-generating manner. Macrocycle constitution would be dictated by the position and nature of an arene side chain(s), and additionally, *N*-acyliminium ion cyclizations would be dictated by the nature of the P1 amino acid side chain. When treated with aqueous acetic acid, the *N*-Boc oxazine degrades to the corresponding aldehyde (**int-51**, Scheme 5.3.2), which spontaneously forms hydroxylactams **int-52** by *5-exo-trig* cyclization onto the proximal amide nitrogen. Loss of water then reversibly generates *N*-acyliminium ion **int-53**. This intermediate is anticipated to engage an array of side chains, including aryl side chains leading to fused piperidines (**54**), thiols to thiazolidines (**55**), backbone amides to imidazolidinones (**56**), and carboxamides to give diazinones (**57**). Whereas Pictet-Spengler type cyclizations to give indolopiperidines (**54**) proceed under mild conditions which are orthogonal to the cinnamyl carbocation chemistry, it is not yet clear whether this can be achieved with less nucleophilic side chains.⁴⁷

Scheme 5.3.2 *N*-Boc-1,3-Oxazine **50** serves as an aldehyde synthon, which, when revealed by mild acid hydrolysis, leads to an *N*-acyliminium ion by condensation onto the proximal amide nitrogen. This electrophilic species has been reported to undergo diastereoselective cyclizations with a variety of aryl and heteroatom nucleophiles to form small and medium-sized rings.



Template **50** was convergently synthesized by unification of benzyl halide fragment **61** and acyloxazolidinone **63** by diastereoselective α -alkylation to set the stereochemistry at *C2*. Benzyl bromide **61** was prepared from commercial 5-bromo-2-fluorobenzaldehyde by Suzuki-Miyaura cross-coupling to install the propenyl moiety, analogously the other template synthesis (see Chapter 2). Subsequent sodium

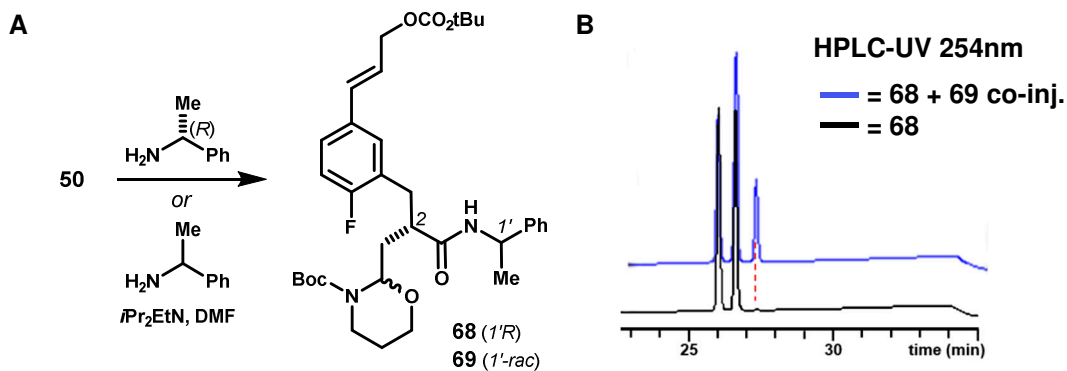
Scheme 5.3.3 Template **50** – and its carboxylic acid congener **67** – was synthesized by diastereoselective α -alkylation of *N*-acyloxazolidinone **63** with functionalized benzyl bromide **61**.



borohydride reduction of the aldehyde and Appel reaction gave bromide **61** in good yield. *N*-Acylloxazolidinone **63** was prepared from reported *N*-Boc-1,3-oxazine **62**⁴⁸ via its mixed pivalic anhydride.⁴⁹ α -Alkylation of **63** was found to be sensitive to the order in which reagents were added to the reaction. When the sodium enolate of **63** was pre-formed by treatment with sodium hexamethyldisilazide at -78 °C, and subsequently treated with benzyl bromide **61**, product **64** was obtained in only 52–61% yield across several attempts. However, when **61** and **63** were pre-mixed, and then treated with strong base at -78 °C, **64** was isolated in 74–79% yield as single *C2* diastereomer (but 1:1 mixture of *N,O*-acetal diastereomers). This material was treated with lithium hydroperoxide, followed by sodium sulfite, to cleave the chiral auxiliary to give acid **65**. Desilylation and carbonate formation under phase transfer conditions formed carbonate **67**,

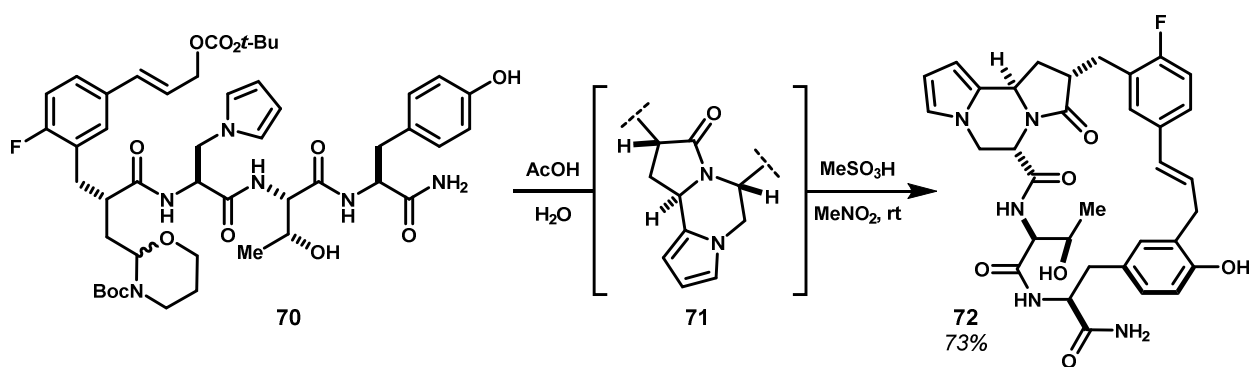
which was transformed to template **50** by carbodiimide-mediated condensation with pentafluorophenol. Formation of the activated ester in this manner is convenient for subsequent amidation of peptides, improves the stability of the template for storage, and also allowed chromatographic resolution of the two *N,O*-acetal diastereomers for characterization purposes. The enantiomeric purity of template **50** was assessed by chiral derivatization with optically pure (*R*)-(+)- α -methylbenzylamine to give (*1'R*)-**68** and HPLC-UV analysis of the resulting amides (Scheme 5.3.4). Rather than prepare racemic or *2R* template **50**, analytical standards were analogously prepared by derivatization still of (*2S*)-**50** but with (\pm)- α -methylbenzylamine to give amides (*1'-rac*)-**69**. In this manner, we prepared a mixture containing the *enantiomer* of the minor *C2* diastereomer, which allowed us to establish the HPLC retention times of all possible diastereomers. Somewhat complicating was the 1:1 mixture *N,O*-acetal center, which led to four possible diastereomers. After extensive gradient optimization, we identified conditions which resolved three peaks within the mixture (*1'-rac*)-**69**. Co-injection of (*1'-rac*)-**69** with (*1'R*)-**68** indicated that the first peak corresponded to the major *C2* diastereomer (presumed to be *2S,1'R* or its mirror image), and that the last peak corresponded to the *enantiomer* (i.e. *2S,1'S*) of the minor *C2* diastereomer (i.e. *2R,1'R*). The central peak then comprised a mixture of the remaining two *N,O*-acetal diastereomers of both the major and minor *C2* epimers. HPLC-UV analysis of (*1'R*)-**68** by the same method showed only trace amounts of the minor *C2* diastereomer (>20:1 *dr*) (Scheme 5.3.4B), indicating **50** was formed in >95%*ee*.

Scheme 5.3.4 The enantiopurity of template **50** was assessed by derivatization with optically pure (*R*)-(+)- α -methylbenzylamine to allow analysis of the resulting diastereomers (i.e. **68**) by HPLC-UV on an achiral stationary phase against a standard containing all four possible diastereomers (**68** + **69**, see text). These analyses indicated **50** was prepared in >95%*ee*.



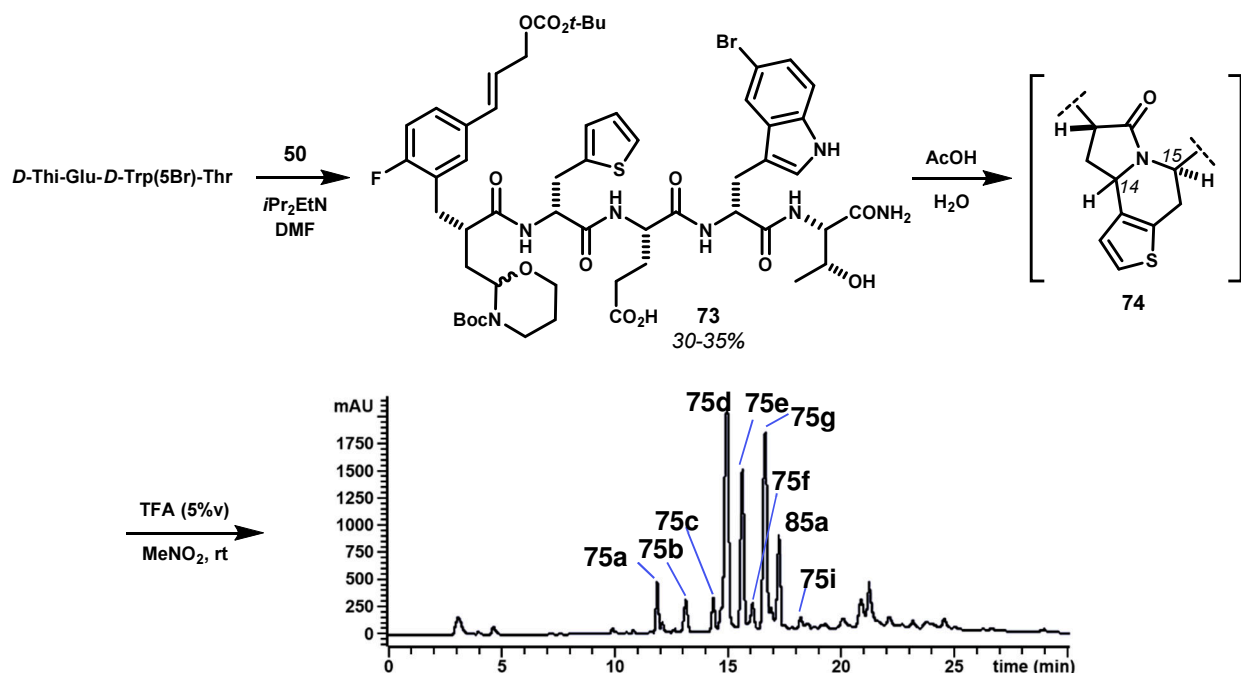
The active ester of template **50** readily and spontaneously acylated peptidyl amino groups, and its carboxylic acid precursor **67** reacted analogously in the presence of uronium-based coupling reagents (e.g. HBTU). Condensation of **67** with a pyrrolic tripeptide gave intermediate **70** (Scheme 5.3.5). When this material was treated with aqueous acetic acid, the *N*-Boc-1,3-oxazine was hydrolyzed (*vide supra*), promoting diastereoselective Pictet–Spengler cyclization with the adjacent pyrrole in situ (i.e. **71**). Exposure of the crude product to methanesulfonic acid initiated internal Friedel–Crafts alkylation of the phenol to afford complex macrocyclic pyrroloperazine **72** as the sole product in good yield.

Scheme 5.3.5 Bi-functional template **50** initiates two-step *P1* *N*-acyliminium ion cyclization (i.e. Pictet–Spengler to **71**) and large ring-forming *C*-cinnamylation (e.g. **72**).



Divergent ring-forming processes of template **50** analogous to those observed with simplified template **3** (see Chapters 3, 5.1, 5.2) were also possible. The activated ester **50** was used to ligate tetrapeptide *D*-Thi-Glu-*D*-Trp(5Br)-Thr, albeit in low yield owing to the small scale and HPLC purification of acyclic intermediate **73** (Scheme 5.3.6). Notably, **50** is essential in this case, because the substrate Glu is incompatible with peptide coupling reagents necessary to incorporate carboxylic acid template **67**. Acyclic intermediate **73** was treated with aqueous acetic acid to initiate Pictet–Spengler cyclization without decomposition of the cinnamyl carbonate. By HPLC-UV/MS analysis at short reaction times, we observed two intermediate hydroxylactams and their conversion to thienopiperazine **74** over a period of twelve hours. The crude product of this reaction (i.e. **74**) was treated with TFA (5% *v*) in nitromethane at room temperature to induce macrocyclization; these mild conditions were identified as an inexpensive alternative to TFA:TFE, and also afforded rapid kinetics at lower concentrations of TFA.

Scheme 5.3.6 Template **50** engages a polar tetrapeptide by large ring-forming *C*-cinnamylations of *D*-5-bromo-tryptophan in concert with *N*-acyliminium ion cyclization of 2-thienylalanine.



Optimized HPLC separation of the crude acidolysis product mixture from cyclization of **74** revealed more products than anticipated based on our understanding of cinnamylation reactions of 5-substituted tryptophans (Scheme **5.3.6**). This mixture was fractionated by semi-preparative HPLC and, where necessary, products were re-purified using a different stationary phase. Though we were only able to solve a subset of these products given the small scale of the reaction (21 μmol), these results were telling (Figure **5.3.1**). The major components of **75d**, **e**, **g–i** were isolated in sufficient quantity (0.9–3.4 mg) and purity for NMR analysis. These products resulted from large ring-forming *C*-cinnamylation and cyclization of the 2-thienylalanine side chain. The planar structures were, in all cases, definitively assigned from 2D NMR correlation spectra. However, it appeared that *N*-acyliminium ion cyclization, in this case, was not diastereoselective (*vide infra*); this result became clear upon characterization of **75g** and **75h** which bear identical macrocycle connectivity. Whether this resulted from poor diastereoselectivity in the initial reaction with acetic acid or from equilibration in the subsequent acidolysis with TFA is unknown. Unfortunately, the scant quantities of product made it challenging to assign relative stereochemistry, and therefore the author has tentatively assigned the 14*R*,15*R* stereochemistry in **75d**, **h** and **i**. Despite appearing straightforward to assign the stereochemistry about the central piperidine ring, no diagnostic NOE correlations were

observed between methine *H*14 and either *H*11 or *H*15 in any of the five products. In the case of **75e** and **75g**, we observed definitive correlations between *H*14 and backbone amide proton *H*22 indicating the 14*S*, 15*R* configuration shown (**B**). This diagnostic correlation is the same as reported by Meldal and co-workers in assigning this ring stereochemistry in analogous non-macrocyclic examples.⁴⁷ Product **75h**, the *C*14 epimer of **75g**, was assigned based upon the lack of NOE correlation *H*14↔*H*22. However, we observed no distinct NOE correlations corroborating this assignment. These data suggest that template **50** functions as designed when the P1 amino acid side chain is an electron rich arene, but that the *N*-acyliminium ion ring closure may, in some cases, require optimization to achieve high diastereoselectivity.

Diastereoselectivity in *N*-acyliminium ion Pictet-Spengler cyclizations of this type is thought to arise

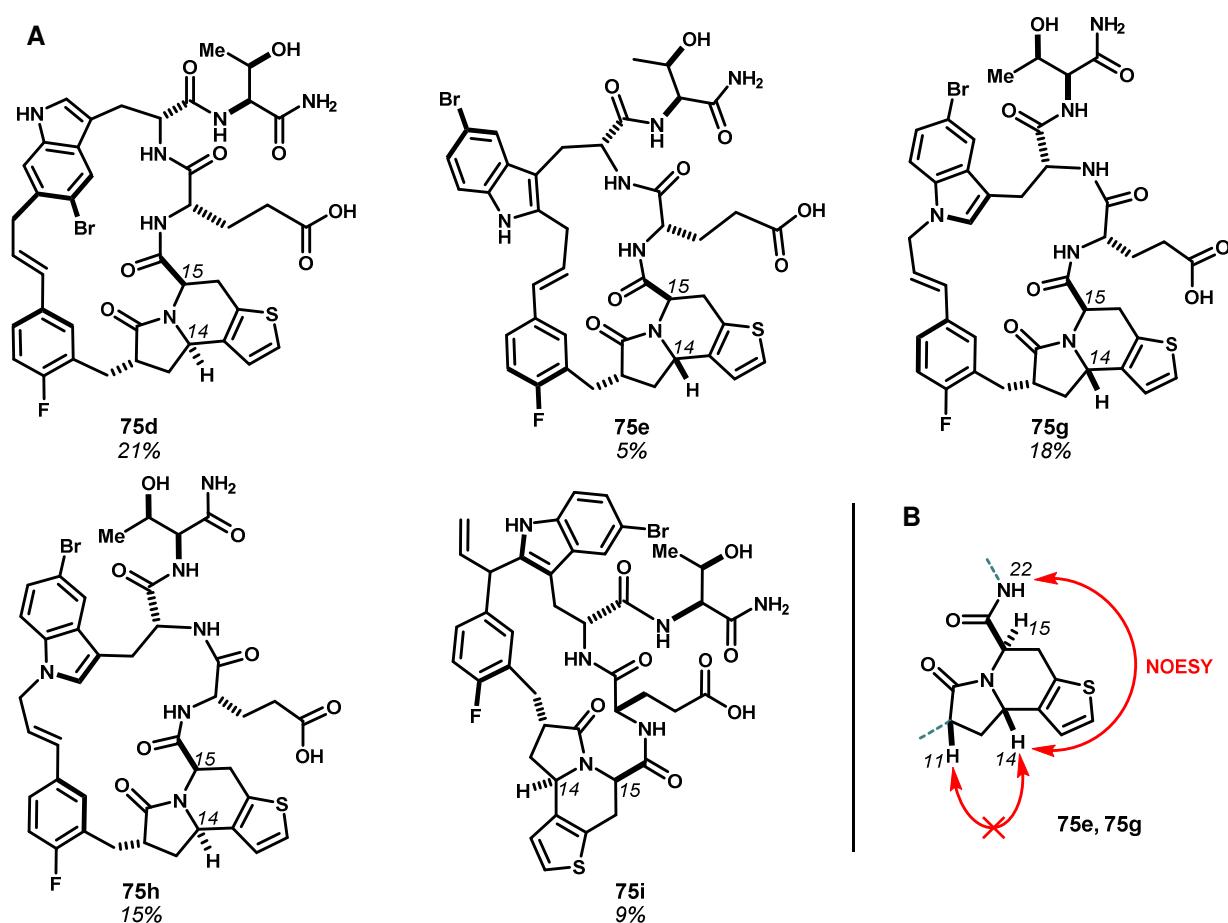
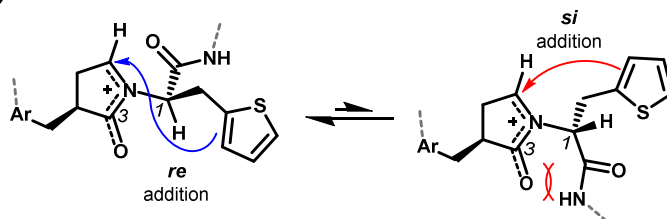


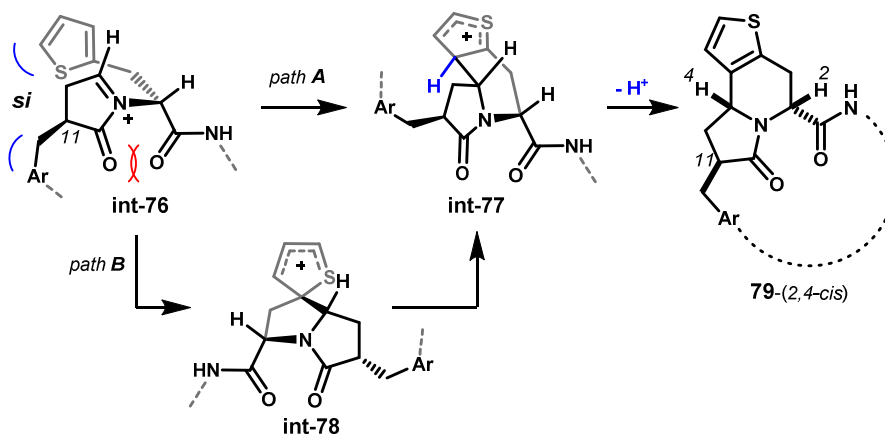
Figure 5.3.1 **A**) Products characterized from the two-step acidolysis reaction of intermediate **73** resulting from *N*-acyliminium ion Pictet-Spengler cyclization of thiophene, and *C*-cinnamylations of 5-bromotryptophan. **B**) Key 2D NOESY correlations leading to assignment of the 14*S*, 15*R* configuration in **75e** and **75g**. The *C*14 stereochemistry is tentatively assigned in **75d**, **h** and **i** for lack of this correlation.

by minimization of steric congestion leading up to the transition state.⁴⁷ Though not explicitly noted as such in the literature, this author believes these results may be simply viewed as minimization of 1,3-allylic strain leading up to the transition state, wherein the carbonyl of the delocalized *N*-acyliminium ion serves as the

A. 1,3-Allylic strain model



B. Disfavored



C. Favored

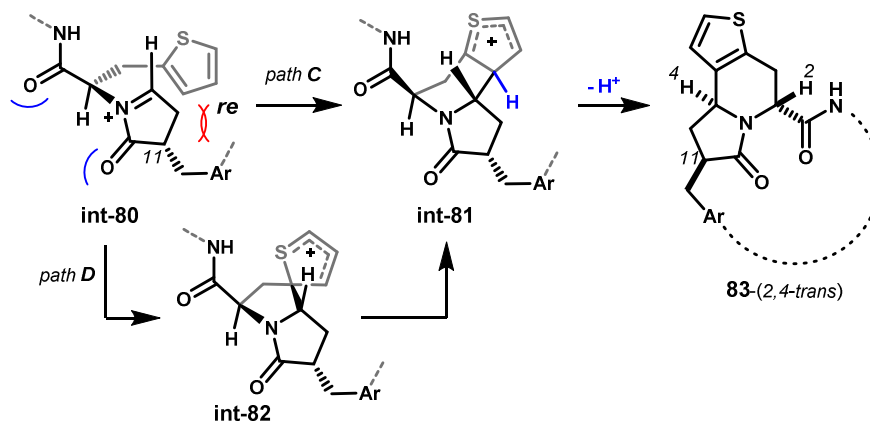
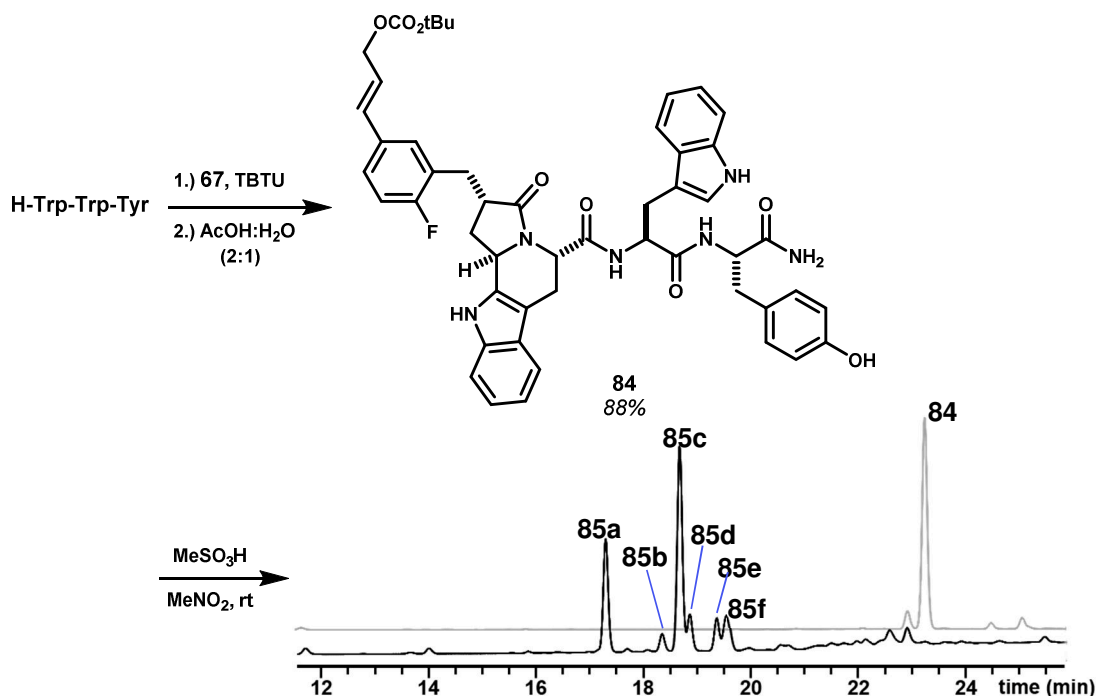


Figure 5.3.2 Models rationalizing the diastereoselectivity of *N*-acyliminium ion Pictet-Spengler cyclization applied explicitly to substrate **73** (abbreviated as *D*-thienylalanine). **A**) Treating the cationic pyrrolinone as a heteroallylic system predicts more favorable approach of the arene from the *re* face by reduction of 1,3-allylic strain. **B**) Adaptation of the reported model suggests that *si* attack is disfavored by steric interaction between the pyrrolinone carbonyl and proximal amide, whereas this interaction is alleviated by *re* approach of the arene nucleophile **C**). Annulation may proceed by either spirocyclization/1,2-migration (path C) or direct attack at C3 of thiophene (path D).

allyl moiety (Figure 5.3.2A). This leads, in the case of *D*-(2-thienyl)alanine investigated here, to more favorable addition of the arene to the *re* face (*pro-R*) of the *N*-acyliminium ion. An alternative steric model, consistent with that put forth by Meldal and co-workers,⁴⁷ is shown in Figure 5.3.2B and C. This model accounts for possible spirocyclization/1,2-rearrangement (paths B, D) mechanism, as well as a direct electrophilic aromatic substitution of thiophene at the 3-position (paths A, C). In a similar manner, steric interactions of the pyrrolinone carbonyl group are minimized in paths C and D (Figure 5.3.2C). However, both models A and B/C suggest potential secondary steric interactions between the *C11* substituent – the remainder of the template (i.e. **50**), abbreviated here as its benzyl portion – and the approaching thiophene nucleophile (i.e. **int-80**). Such interactions are unique to our template, and may explain the poor diastereoselectivity observed in Pictet-Spengler reactions leading to **75d, e** and **g–i**. If true, this would indicate a ‘mismatch’ scenario for *N*-acyliminium ion cyclizations of template (*2S*)-**50** with peptides bearing *D*-configured amino acids at the first position.

Scheme 5.3.7 Ligation of bifunctional template **50** (as **67**) with prototypical tripeptide Trp-Trp-Tyr and *N*-acyliminium ion Pictet-Spengler cyclization of Trp1 formed acyclic intermediate **84** in good yield as a single diastereomer. Acidolysis of this material led to divergent large ring-forming *C*-cinnamylations with complete consumption of starting **84** after 2 hrs.



The performance of bifunctional template **50** was also evaluated using the prototypical tripeptide Trp-Trp-Tyr. In this manner, we hoped to compare results to those obtained from the reactions of this model peptide with simplified template **3** (see Chapter 3), and to assess whether rigidification of the P1 residue by *N*-acyliminium cyclization would impede subsequent macrocyclization. Template **67** was ligated to Trp-Trp-Tyr by the action of TBTU, and treated with aqueous acetic acid (2:1, *v:v*) to give acyclic intermediate **84** (Scheme 5.3.7). This material was treated with 75 mM methanesulfonic acid in nitromethane, which induced complete conversion of **84** into a mixture of six discernible product by HPLC-UV/MS. The structures of products **85a–c**, **e** and **f** were determined by complete resonance assignment (Figure 5.3.3A). Product **85d** proved to contain two components, the structures of which were not determined. The remaining products derived from cinnamylation of Trp2 at indole positions *C1*, *2*, *3*, *4*, and *5*. These outcomes paralleled cinnamylation reactions observed with template **3**. Notably lacking, however, were products of alkylation at Trp1 and Tyr3. We previously identified branched α -phenylallyl products by reaction of Trp1 at indole *C2*. The analogous outcome here is blocked by the tetrahydro- β -carboline ring formed by Pictet-Spengler cyclization of Trp1. The lack of tyrosine alkylation, a major product from reactions of **3**, suggests that acyclic materials derived from template **50** may be geometric restricted by initial *N*-acyliminium ion cyclization, thereby leading to altered product distributions compared to more flexible template **3**. We were, however, able to observe tyrosine *O*→*C*_{ortho} cinnamyl migrations when starting from the cognate cinnamyl tyrosyl ether of **84** derived by Pd-catalyzed internal *O*-cinnamylation (not shown). These data indicate that the cinnamyl mixed carbonate reacts modularly, and can likely be incorporated in to a variety of template architectures to induce Friedel-Crafts macrocyclization.

We were particularly intrigued by product **85e**, because its structure is substantially modified from the parent peptide. The relative stereochemistry of the bridged pyrroloindoline was determined by careful analysis of 2D-NOESY spectra (Figure 5.3.3B). The cinnamyl methylene (*H1/1'*) was showed strong correlations to aminal methine *H38*, confirming the *cis*-5,5 ring juncture. Stereospecific assignment of diastereotopic methylene *H29/29'* was made on the basis of scalar couplings to methine *H28*, which was presumed to retain the (*S*) configuration of *L*-tryptophan. *Pro-S* proton *H29* showed through-space correlation to Tyr3 amide *H40*, whereas *Pro-R* *H29'* was strongly correlated to protons *H1'* and *H3* of the bridging cinnamyl group, indicating an *H1/1'-H29'-syn* relationship and therefore the *30R,38R*

stereochemistry as shown. This was corroborated by NOESY correlations $H_{38} \leftrightarrow H_{28}$ indicating a *syn* relationship between these two protons. The stereochemistry of the pyrroloindole ring juncture was also made on the basis of 2D-NOESY spectra (Figure 5.3.3C). In this case, spectral overlap prevented stereospecific assignments of methylenes H_{10} , H_{13} and H_{16} . Very weak through-space correlations between methine H_{14} and methylene H_{10} and aryl proton H_9 led to assignment of the $14S$ configuration,

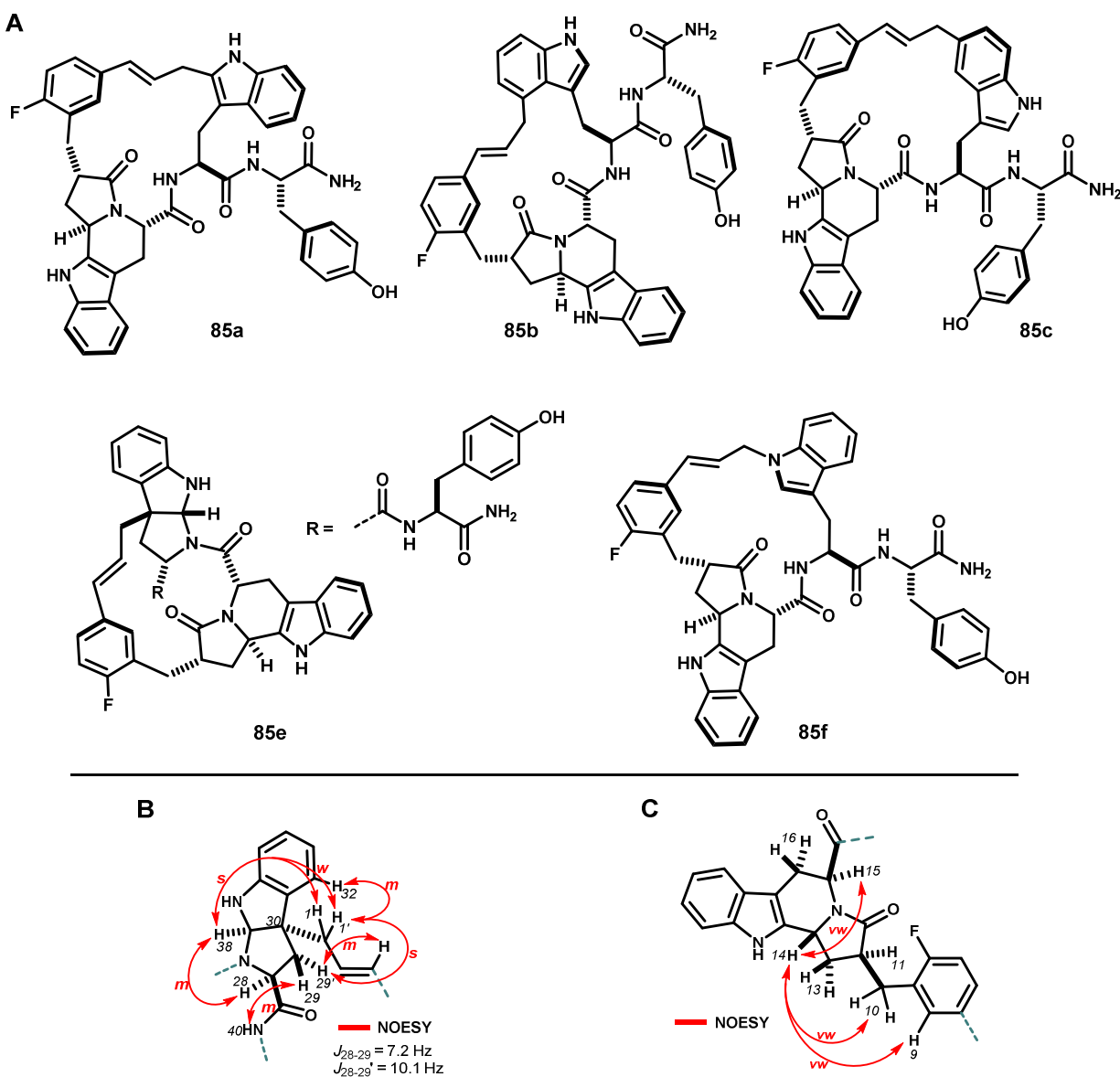


Figure 5.3.3 A) Product structures resulting from the acidolysis reaction of acyclic intermediate **84**. B) Selected 2D-NOESY correlations (500 MHz, DMSO- d_6) leading to the assignment of the $30R,38R$ stereochemistry of the endo-pyrroloindole moiety of **85e**. C) Weak NOESY assignments leading to the assignment of the $14S$ stereochemistry of the pyrrolo tetrahydro- β -carboline moiety of product **85e**.

as shown, in line with the stereochemical predictions (*vide supra*). These NOESY spectra also revealed several intriguing long-range correlation (not shown) which suggest that macrocycle **85e** occupies a highly condensed conformation in solution.

The macrocycle, pyrrolo tetrahydro- β -carboline, and pyrroloindoline motifs of **85e** greatly restrict the conformation of this otherwise large molecule. This product possesses a mere five fully rotatable bonds, whereas Trp-Trp-Tyr itself possesses eleven rotatable bonds. Additionally, **85e** displays less polar surface area (161 Å²) than the starting peptide (181 Å²), despite the template having contributed additional total surface area (1026 Å² v. 770 Å²). Calculated octanol-water partition coefficients (cLogD, pH 7.4) also indicate that the structure modifications induced by template **50** lead to greater lipophilicity for **85e** (cLogD = 5.4) than the parent peptide (cLogD = 2.0). While **85e** has no biological activity, that we know of, structural remodeling and rigidification of this type is a critical modification towards improving the target affinity⁵⁰ and pharmacokinetic properties^{51,52} of native binding peptides.

5.4 Remarks and conclusions regarding template-induced large ring-forming cinnamylations.

The cinnamyl carbocation is uniquely capable as a diversity-generating element in template-based methods to explore macrocyclic peptidomimetics. Internal Friedel-Crafts alkylations are particularly powerful in this regard, and provide a relatively facile means to vary ring constitution within series of isomeric macrocycles harboring a conserved polypeptide motif. By comparison to conventional peptidomimetic drug discovery approaches, divergent macrocycle approaches may be able to overcome the limiting pharmacological properties of peptides by fine-tuning of the conformationally restricted macrocyclic structure, rather than by extensive modification of the parent polypeptide. The macrocyclic structures synthesized here offer a glimpse of the possibilities for template-based approaches to remodeling the shape and properties of peptides.

Despite the high reactivity of the cinnamyl carbocation, this transiently formed intermediate exerts remarkable chemoselectivity for internal electrophilic substitution of activated arenes, even within complex substrates bearing numerous polar functional groups. Though macrocyclization in this manner can be sensitive to substrate conformation, the generality of this reaction exemplified throughout this chapter

suggests a truly broad substrate scope. Additionally, in no cases have we observed clear evidence of dimerization or oligomerization, problems which plague Huisgen cycloadditions,^{53,54} lactamizations,³⁸ ring closing olefin metathesis,^{55,56} and other contemporary macrocyclization approaches.⁵⁷ While our laboratory is particularly interested in divergent ring-forming reactions as a logical entry to peptidomimetic drug discovery, selective reactions are equally powerful. We have rigorously characterized fifty nine examples of large-ring forming *C*-cinnamylation spanning 15- to 36-membered rings. These products include drug analogs, heterocyclic motifs, and bicyclic macrocycles, each of which hold potential utility for applications in drug development and biochemical studies.

Template architectures incorporating the cinnamyl cation-based macrocyclization as one of several reactive modules hold unique promise for rapid and divergent construction of complex molecules. This fundamental idea has borne out in preliminary studies of template **50**, which transforms short peptides into conformationally restricted polycyclic products in three straightforward steps. Though we have charted only a small subset of possible *N*-acyliminium cyclizations of this next-generation template, these results demonstrate means to incrementally increase product structural complexity beyond the macrocyclizations achieved by prototype template **3**. With several such templates in hand, it may become possible to rapidly generate diverse collections of macrocycles, all bearing a peptide sequence of interest, but each varying in shape, physicochemical properties, and ideally biological function. Macrocylic, natural product-like molecules of this sort have excellent potential to identify small molecules against challenging biological targets, such as protein interaction surfaces, where traditional screening collections are often unfruitful.

In the fundamental studies documented here, we have made an effort to isolate and rigorously characterize products in order to survey the reactivity of these template designs. By comparison to target-oriented synthetic exercises, the present template-based methods are operationally trivial to carry out, instead requiring greater care in isolation and structure elucidation phases. In screening exercises, we expect it will be possible to forego these more time-intensive steps until substantive biological activity has been identified. While analogous to natural products screening in this regard, the synthetic mixtures produced here are substantially less complex than natural isolates, are of designed molecular makeup, and are readily replenished. With a fundamental understanding of the template reactivity, it may also be possible predict products, and to then quickly establish structure-activity relationships simply by modifying the

peptide sequence. We have experimentally approached a number of these ideas, the results of which comprise the discussions in Chapter 6.

References

- (1) Rose, T. E.; Lawson, K. V.; Harran, P. G. *Chem. Sci.* **2015**, *6*, 2219.
- (2) Kato, T.; Nagae, K.; Hoshikawa, M. *Tetrahedron Lett.* **1999**, *40*, 1941.
- (3) Smith, M. B.; March, J. In *March's Advanced Organic Chemistry: Reactions, Mechanisms, and Structure*; John Wiley & Sons, Inc.: Hoboken, NJ, 2007; pp 742–745.
- (4) Liu, Y.; Kim, B.; Taylor, S. D. *J. Org. Chem.* **2007**, *72*, 8824.
- (5) Tashiro, M. *Synthesis (Stuttg.)* **1979**, 1979, 921.
- (6) Brown, H. C.; Jungk, H. *J. Am. Chem. Soc.* **1955**, *77*, 5579.
- (7) Allen, R. H.; Yats, L. D. *J. Am. Chem. Soc.* **1959**, *81*, 5289.
- (8) Olah, G. A.; Meyer, M. W.; Overchuk, N. A. *J. Org. Chem.* **1964**, *29*, 2313.
- (9) Zefirov, N. S. *Tetrahedron* **1977**, *33*, 2719.
- (10) Winstein, S.; Holness, N. J. *J. Am. Chem. Soc.* **1951**, *420*, 5562.
- (11) Seeman, J. I. *Chem. Rev.* **1983**, *83*, 83.
- (12) McKenna, J. *Tetrahedron* **1974**, *30*, 1555.
- (13) Schlosser, M.; Hartmann, J. *J. Am. Chem. Soc.* **1976**, *98*, 4674.
- (14) Hartmann, J.; Schlosser, M.; Stahle, M. *Helv. Chim. Acta* **1977**, *60*, 1730.
- (15) Galli, C.; Illuminati, G.; Mandolini, L. *J. Org. Chem.* **1980**, *45*, 311.
- (16) Casadei, M. A.; Galli, C.; Mandolini, L. *J. Am. Chem. Soc.* **1984**, *106*, 1051.
- (17) Illuminati, G.; Mandolini, L.; Masci, B. *J. Am. Chem. Soc.* **1975**, *97*, 4960.
- (18) Bennett, G. M. *Trans. Faraday Soc.* **1941**, *37*, 794.
- (19) Grathwohl, C.; Wüthrich, K. *Biopolymers* **1976**, *15*, 2025.
- (20) Reimer, U.; Scherer, G.; Drewello, M.; Kruber, S.; Schutkowski, M.; Fischer, G. *J. Mol. Biol.* **1998**, *279*, 449.
- (21) Kang, Y. K.; Young Choi, H. *Biophys. Chem.* **2004**, *111*, 135.
- (22) Steinberg, I. Z.; Harrington, W. F.; Berger, A.; Sela, M.; Katchalski, E. *J. Am. Chem. Soc.* **1960**, *82*, 5263.
- (23) Goudreau, N.; Brochu, C.; Cameron, D. R.; Duceppe, J.; Faucher, A.; Ferland, J.; Grand-mai, C.; Poirier, M.; Simoneau, B.; Tsantrizos, Y. S. *J. Org. Chem.* **2004**, *69*, 6185.
- (24) Okada, E.; Sakaemura, T.; Shimomura, N. *Chem. Lett.* **2000**, *29*, 50.
- (25) Dewar, M. J. S.; Maitlis, P. M. *J. Chem. Soc.* **1957**, 2521.
- (26) Joule, J. A. In *Heterocyclic Chemistry*; John Wiley & Sons, Inc.: West Sussex, UK, 2010; pp 177–203.
- (27) Svanholm, U.; Parker, V. D. *J. Chem. Soc. Perkin Trans. 2* **1974**, *2*, 169.
- (28) Brown, H. C.; Okamoto, Y. *J. Am. Chem. Soc.* **1958**, *80*, 4979.
- (29) Nelson, K. L.; Brown, C. *J. Am. Chem. Soc.* **1951**, *73*, 5605.
- (30) Smith, M. B.; March, J. In *March's Advanced Organic Chemistry: Reactions, Mechanisms, and Structure*; John Wiley & Sons, Inc.: Hoboken, NJ, 2007; pp 670–671.
- (31) Olah, G. A.; Kobayashi, S.; Tashiro, M. *J. Am. Chem. Soc.* **1972**, *94*, 7448.

- (32) Olah, G. A. *Acc. Chem. Res.* **1971**, *4*, 240.
- (33) George A. Olah; Kuhn, S. J.; Flood, S. H. *J. Am. Chem. Soc.* **1962**, *84*, 1688.
- (34) Keumi, T.; Nakamura, M.; Kitamura, M.; Tomioka, N. *J. Chem. Soc. Perkin Trans. 2* **1985**, 909.
- (35) Keumi, T.; Yagi, Y.; Kato, Y. K.; Taniguchi, R.; Temporin, M.; Kitajima, H. *J. Chem. Soc. Perkin Trans. 2* **1984**, 799.
- (36) Barlos, K.; Gatos, D.; Kaposos, S.; Poulos, C.; Schäfer, W.; Yao, W. Q. *Int. J. Pept. Protein Res.* **1991**, *38*, 555.
- (37) Humphrey, J. M.; Chamberlin, a. R. *Chem. Rev.* **1997**, *97*, 2243.
- (38) Schmidt, U.; Langner, J. *J. Pept. Res.* **1997**, *49*, 67.
- (39) Thakkar, A.; Trinh, T. B.; Pei, D. *ACS Comb. Sci.* **2013**, *15*, 120.
- (40) McCauley, J. A.; McIntyre, C. J.; Rudd, M. T.; Nguyen, K. T.; Romano, J. J.; Butcher, J. W.; Gilbert, K. F.; Bush, K. J.; Holloway, M. K.; Swestock, J.; Wan, B. L.; Carroll, S. S.; Dimuzio, J. M.; Graham, D. J.; Ludmerer, S. W.; Mao, S. S.; Stahlhut, M. W.; Fandozzi, C. M.; Trainor, N.; Olsen, D. B.; Vacca, J. P.; Liverton, N. *J. Med. Chem.* **2010**, *53*, 2443.
- (41) Olah, G. A.; Asensio, G.; Mayr, H. *J. Am. Chem. Soc.* **1978**, *43*, 1518.
- (42) Lipinski, C. A.; Lombardo, F.; Dominy, B. W.; Feeney, P. J. *Adv. Drug Deliv. Rev.* **2001**, *46*, 3.
- (43) Lipinski, C. A. *Drug Discov. Today Technol.* **2004**, *1*, 337.
- (44) Van Leusen, A. M.; Wildeman, J.; Oldenziel, O. H. *J. Org. Chem* **1977**, *42*, 1153.
- (45) Schmuck, C.; Rupprecht, D. *Synthesis (Stuttg)*. **2007**, 3095.
- (46) Joule, J. A. In *Heterocycles*; Blackwell Scientific Publications: West Sussex, UK, 2010; pp 295–323.
- (47) Nielsen, T. E.; Meldal, M. *J. Org. Chem.* **2004**, *69*, 3765.
- (48) Groth, T.; Meldal, M. *J. Comb. Chem.* **2001**, *3*, 34.
- (49) Ho, G.; Mathre, D. J. *J. Org. Chem.* **1995**, *60*, 2271.
- (50) Andrews, P. R.; Craik, D. J.; Martin, J. L. *J. Med. Chem.* **1984**, *27*, 1648.
- (51) Veber, D. F.; Johnson, S. R.; Cheng, H.-Y.; Smith, B. R.; Ward, K. W.; Kopple, K. D. *J. Med. Chem.* **2002**, *45*, 2615.
- (52) Lu, J. J.; Crimin, K.; Goodwin, J. T.; Crivori, P.; Orrenius, C.; Xing, L.; Tandler, P. J.; Vidmar, T. J.; Amore, B. M.; Wilson, A. G. E.; Stouten, P. F. W.; Burton, P. S. *J. Med. Chem.* **2004**, *47*, 6104.
- (53) Punna, S.; Kuzelka, J.; Wang, Q.; Finn, M. G. *Angew. Chemie - Int. Ed.* **2005**, *44*, 2215.
- (54) Turner, R. A.; Oliver, A. G.; Lokey, R. S. *Org. Lett.* **2007**, *9*, 5011.
- (55) Lee, C. W.; Grubbs, R. H. *J. Org. Chem.* **2001**, *66*, 7155.
- (56) Yamamoto, K.; Biswas, K.; Gaul, C.; Danishefsky, S. J. *Tetrahedron Lett.* **2003**, *44*, 3297.
- (57) White, C. J.; Yudin, A. K. *Nat. Chem.* **2011**, *3*, 509.

6 A solid-phase approach to template-induced macrocyclizations: Application to the discovery of Pin1 inhibitors

6.1 Introduction

Collections of template-stabilized peptidic macrocycles varying in both sequence and shape are highly desirable for screening applications in small molecule discovery for challenging therapeutic targets.¹ Protein-protein interactions are amongst such targets, hallmarked by the broad difficulty in identifying drug development leads by screening conventional small molecule libraries. Many small molecule collections were originally engineered to target receptors and enzymes,²⁻⁴ and are now widely regarded as poorly suited for other biological targets,⁵⁻⁷ including protein-protein interactions (PPIs).⁸ Peptide-derived macrocycles are particularly attractive for overcoming these limitations, because the embedded peptide sequence can, in some cases, logically reflect a consensus binding motif of a native peptide or protein partner.^{9,10} Such is the case when binding is driven by contiguous amino acids, as in small molecule mimetics of the Smac N-terminal motif Ala-Val-Pro-Ile.^{11,12} A growing number of so-called “linear recognition motifs” (LMs) have been identified that bear five to fifteen contiguous amino acids and drive protein-protein interactions involved in a protein trafficking, signal transduction, enzyme-substrate or -inhibitor binding, antigen recognition, and many other cellular events.^{13,14} We believe that methods to prepare conformationally restricted, macrocyclic mimetics of these LMs will provide useful antagonists and probes of protein-protein interactions.

An interesting case of PPIs exists for a superfamily of proteins known as peptidyl-prolyl isomerases (PPIases),^{15,16} including the parvulin,¹⁷ cyclophilin,¹⁸ and FK-506 binding protein (FKBP)^{19,20} families of enzymes. These proteins bind other protein substrates via conserved LMs, and catalyze sequence-specific *cis-trans* isomerization of proline tertiary amide bonds. This isomerization, though spontaneous at room temperature, is frequently the rate-limiting step in protein folding.¹⁵ Though substrate binding likely occurs only transiently in the case of PPIases,²¹ these enzymes are an example of proteins which exert their biological function without forming or breaking covalent bonds; a feature shared by all PPIs, and also by receptors, gated channels, and others. From a pharmacological standpoint, PPIs continue to present a substantial hurdle for drug development, with relatively few reported successes in small molecule

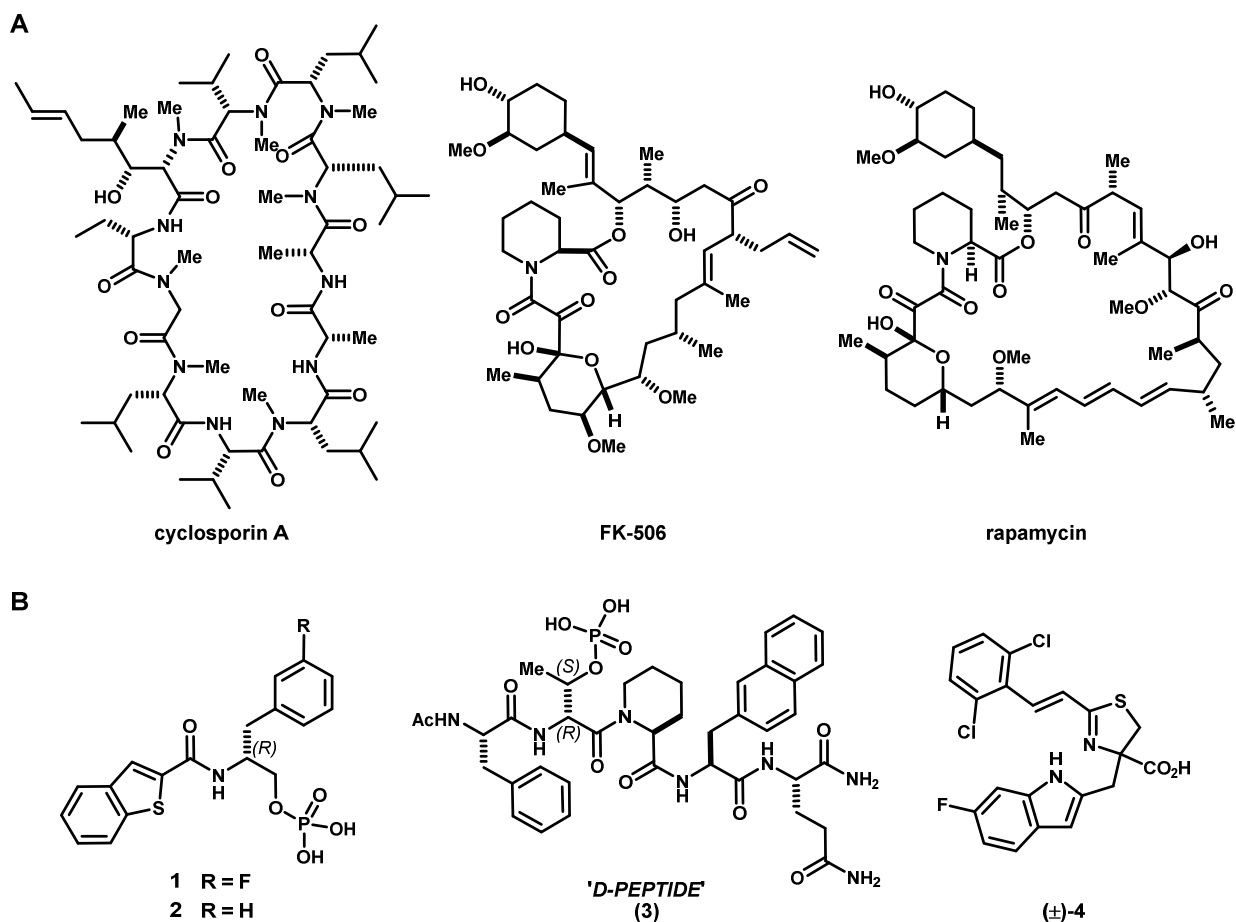


Figure 6.1.1 A) Macrocyclic natural products cyclosporine A, FK-506 and rapamycin played key roles in early discovery of peptidyl-prolyl isomerase enzymes involved in cell proliferation and immune response, and are pioneering examples of therapeutic macrocycles which lie well outside standard metrics of 'drug-likeness'. **B)** Selected examples of investigational Pin1 inhibitors.

development towards these targets.^{8,10,14,22} Interestingly, the macrocyclic natural products cyclosporin A,²³ FK-506 (Tacrolimus),²⁴ and rapamycin (Sirolimus)²⁵ played critical roles in the discovery and functional elucidation of cyclophilins and FKBP's (Figure 6.1.1A). All three of these macrocycles have since come into widespread clinical use as immunosuppressive therapies and are pioneering examples of protein-protein interaction modulators, although their modes of action reach beyond inhibition of PPIase activity.^{26,27}

While related to cyclophilins and FKBP's, the parvulins do not bind cyclosporin A or FK-506, and have not yet seen the same degree of attention as therapeutic targets. This may owe, at least in part, to the limited availability of suitably potent, selective and drug-like small molecule probes.²⁸ Human Pin1 is perhaps the most widely studied of the parvulins, and has garnered substantial attention from both fundamental biochemistry and drug discovery standpoints owing to the involvement of Pin1 in normal cell

proliferation²⁹ and its overexpression in human cancers.³⁰ Pin1 plays myriad roles in cellular signaling downstream of proline-directed serine/threonine kinases such as mitogen-activated protein kinases (MAPKs),^{31,32} cyclin-dependent kinases (CDKs) and glycogen-synthase kinase 3 β (GSK3 β),^{29,33} all of which are also critically involved in cell proliferation. Leading up to mitotic division, these kinases affect broad, site-specific phosphorylation of substrates bearing the -Xxx-Ser/Thr-Pro-Xxx- motif. These kinases likely also recognize specific substrate conformations depending on the geometry of the proline amide bond.^{34,35} Pin1 catalyzes prolyl isomerization at these -pSer/pThr-Pro- motifs, specifically, and preferentially binds

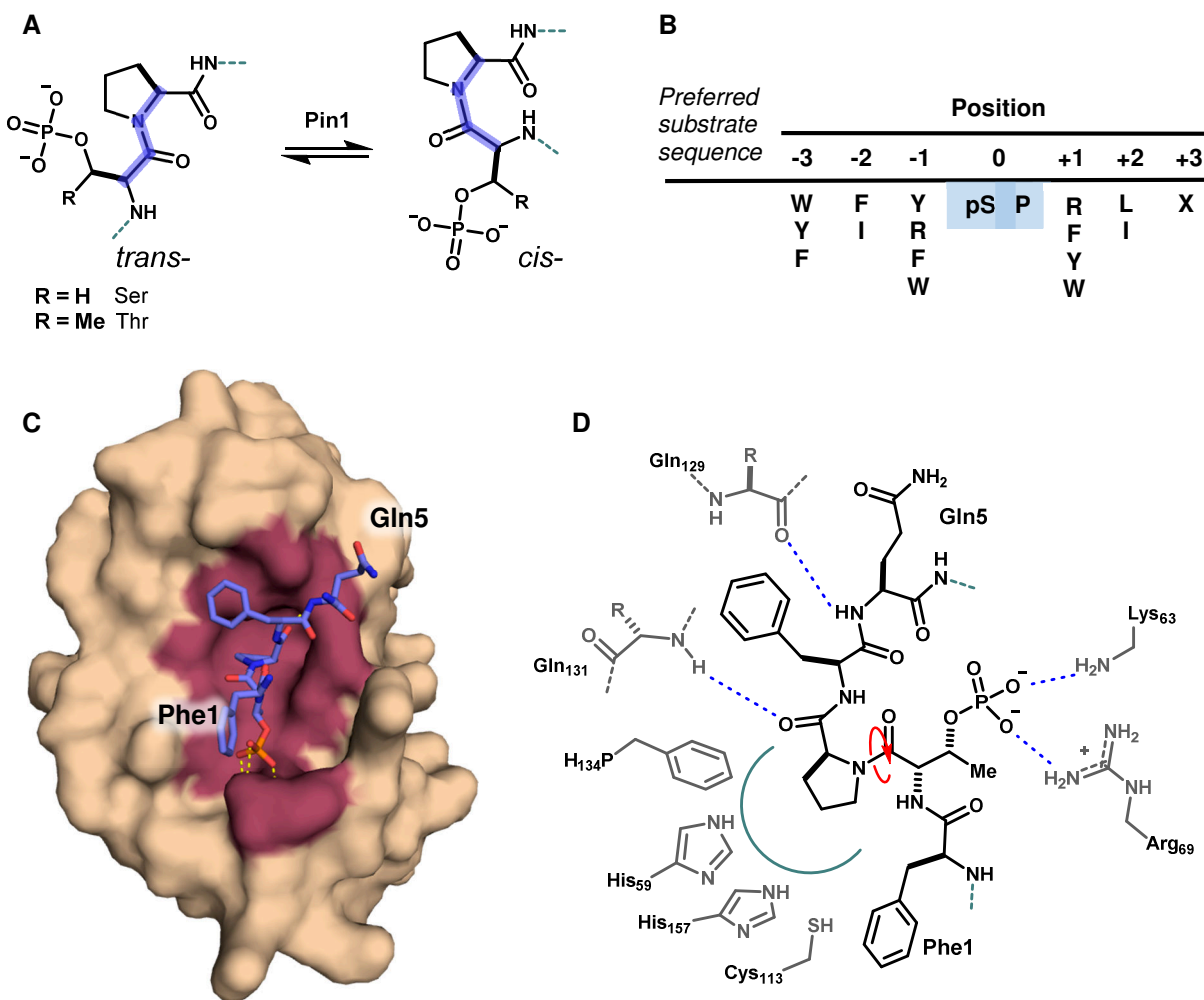


Figure 6.1.2 The peptidyl-prolyl isomerase Pin1 recognizes phosphorylated protein substrates. A) Pin1 catalyzes the cis-trans isomerization of proline amide bond in the motifs pSer/pThr-Pro. **B)** Substrate preference determined by affinity chromatography of combinatorial peptide libraries. **C)** Substrate binding model (-Phe-pThr-Pro-Phe-Gln-) showing protein contact surface (maroon) and select polar contacts (yellow). Model constructed from X-ray structure PDB 2Q5A.³⁶ **D)** Planar schematic detailing key interactions and the isomerizing bond.

this motif when flanked by aromatic side chains (Figure **6.1.2B**).³⁷ It has therefore been hypothesized that Pin1 exerts additional regulatory control by catalyzing substrate conformational change following phosphorylation, and that Pin1 functions to coordinate molecular timing in mitosis in a manner related to but distinct from the cyclins.^{38,39} Several Pin1 inhibitors have been reported (see Figure **6.1.1B**),⁴⁰ but have progressed little beyond *in vitro* studies. Consequently, Pin1 garnered our attention as both an important target and a model PPI with an associated LM amenable to our template-based approach to peptidomimetic macrocycles.

Protein crystallography,⁴¹ combinatorial peptide libraries^{37,42,43} and kinetic studies³⁷ led to the identification of high affinity substrate motifs and ultimately inhibitors of Pin1, which revealed a critical role of the phosphoryl group in binding and turnover. Based on the reported crystallographic structure a Pin1-inhibitor complex,³⁶ we prepared a model depicting key active site-substrate interactions which guided our design of substrate/product-mimetic libraries by a template-based synthetic approach. We hypothesized that it would be possible to synthesize composite macrocycles by directly restructuring the known substrate consensus motif (*vide supra*), and to identify Pin1 inhibitors of improved potency by tuning the macrocycle connectivity and thereby the molecular geometry. These goals were approached incrementally, and are documented in the remainder of this chapter.

Targeting Pin1 using constrained macrocyclic mimetics of the cognate phosphorylated motif -X-pSer/pThr-Pro-X- would require exceptional orthogonality in the large ring-forming step. Based on previous studies by others,^{42,44,45} we expected that phosphorylation might be necessary, at least for initial inhibitor discovery. We therefore sought both tolerant reaction conditions and means to integrate phosphopeptide synthesis with template-based methods for macrocyclization. Additionally, while we had previously observed excellent functional group tolerance in internal Friedel-Crafts alkylations of template **5** (Figure **6.1.3**), we hoped to demonstrate compatibility with all natural amino acids (less cysteine, *vide infra*) to allow broad survey of the embedded peptide sequence. Additionally, we moved to expand the number of nucleophilic arene partners available for large ring-forming reactions beyond tryptophan and tyrosine, and here demonstrate a series of competent arene nucleophiles, and diversity-generating reactions thereof. Investigations of these novel arene partners also led to the identification of mild, practical and inexpensive reaction conditions which maximize orthogonality (Subsection **6.2**). These conditions facilitated developm-

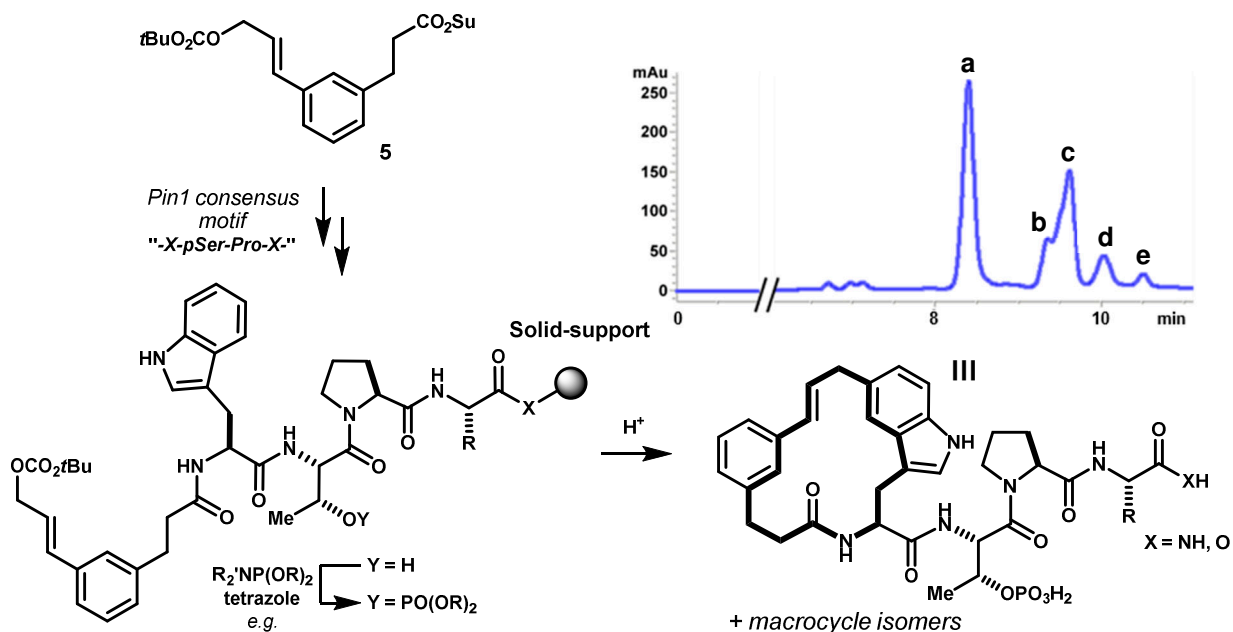


Figure 6.1.3 Proposed divergent, solid-supported access to macrocyclic congeners of the Pin1 consensus motif $''\text{-X-pSer/pThr-Pro-X-}''$ using template **5** and synchronous resin release/internal cinnamylation to give mixtures of regioisomeric macrocycles (hypothetical chromatogram).

ent of solid-supported reactions that enabled a substantial increase synthetic throughput, accessing 96 mixtures of macrocyclic products per day (Subsections **6.4**, **6.6**). This method was in turn used to construct a Pin1-targeted pilot library derived from 384 sequences based on the Pin1 consensus binding sequence, estimated to contain 1000 to 1700 macrocyclic constituents. This library was screened in a mixture-based format using a novel competitive binding assay that was amenable to 96-well plate format. Hit validation, mixture deconvolution, and structure elucidation led to the identification of two series of non-phosphorylated, macrocyclic Pin1 inhibitors (Subsections **6.5**, **6.6**). Iterative optimization of these two structural series was ongoing at the time of writing. Despite that these macrocycles derive from template **5**, the simplest of our template architectures, these efforts outline promising first steps towards general methods to generate potent ligands of protein surfaces by directly stabilizing consensus binding sequences.

6.2 Non-natural amino acids as diversity-generating partners in large ring-forming Friedel-Crafts alkylations.

Large ring-forming *C*-cinnamylations lead to unique ring connectivities depending on the nature of the arene nucleophile. Ring diversity of this type is potentially enabling for small molecule discovery, and underexplored at present, owing at least partly to a lack of methods to explore macrocycles broadly. In our composite macrocycles, the template structure and large ring connectivity are expected to directly influence the shape, properties and biological functions of the products. Consequently, we sought to maximize the number of accessible macrocycle connectivities by building an expanded collection of reactive aromatic amino acids which could be substituted into the native Pin1 binding consensus (see Subsection 6.1 - Introduction).

We previously demonstrated divergent cinnamylation reactions of tryptophan (Chapter 3), phenylalanine analogs and arylated hydroxyprolines derivatives (Chapter 5) that generate tractable mixtures of diverse macrocyclic products (Figure 6.2.1). Tryptophan was particularly special in this regard. In acid-promoted cyclizations of prototype sequence Trp-Trp-Tyr with templates **5**, we observed internal cinnamylation of the indole side chain at *N1*, *C2*, *C3*, *C5*, *C6* and *C7*, each giving a distinct product ring size/shape. By contrast, the side chain benzene rings of phenylalanine-type amino acids are necessarily restricted to three possible connectivities (i.e. *ortho*, *meta*, and *para* relative to the connected alanyl moiety). In practice, only two or one of these can be accessed by any given phenylalanine analog; tyrosine leads

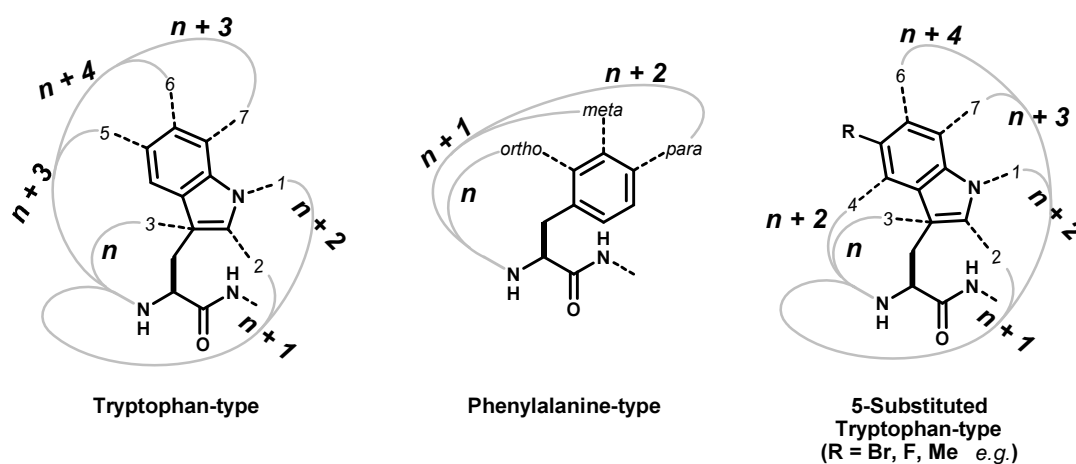


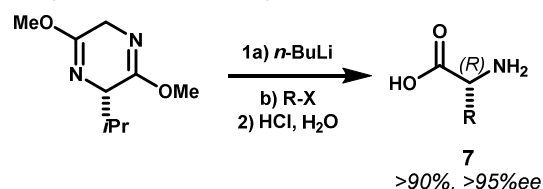
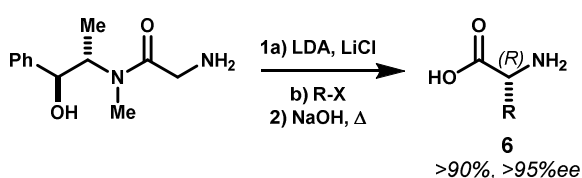
Figure 6.2.1 Potential ring connectivities and ring sizes (n = smallest ring) resulting from large ring-forming cinnamylations of tryptophan-, phenylalanine- and 5-substituted tryptophan-type side chains. No C4 alkylation was observed in reactions of Trp-Trp-Tyr (see Chapter 3). **Grey** = macrocyclic connection.

selectively to alkylation *ortho* to the phenol, whereas 4-hydroxy-2-methoxyphenylalanine leads to two possible ring sizes (see Chapter 5). For these reasons, we focused our efforts on preparing tryptophan analogues which were anticipated to react with the cinnamyl carbocation at multiple positions so as to maximize the diversity of resulting macrocycles.

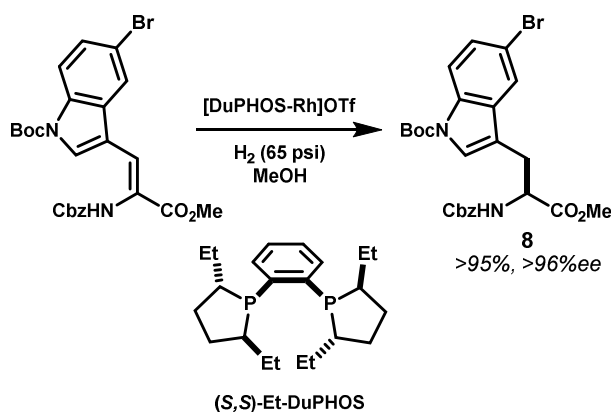
Internal cinnamylations of tryptophan and the peptide P2 position led to alkylation at indole C5 as the major product. Accordingly, we prepared 5-substituted tryptophans that would block this predominant outcome and instead yield other connectivities. Though commercially available, these non-natural amino acids are generally prohibitively expensive. A host of methods have been reported for the asymmetric synthesis of α -amino acids, including enantioselective⁴⁶ and diastereoselective^{47–50} alkylation of glycine

Scheme 6.2.1 Selected methods for the asymmetric synthesis of α -amino acids.

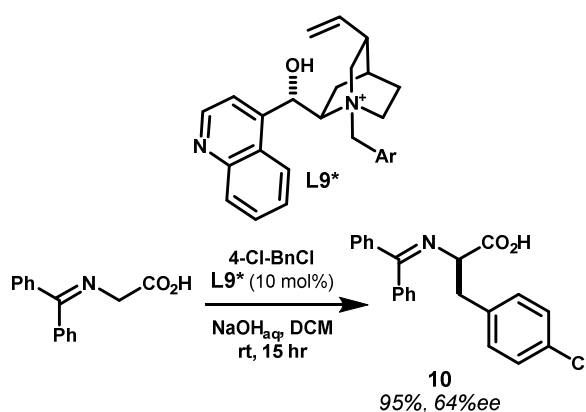
Diastereoselective alkylation of glycine enolates – Myers pseudoephedrine & Schöllkopf auxiliaries.^{50,133,134}



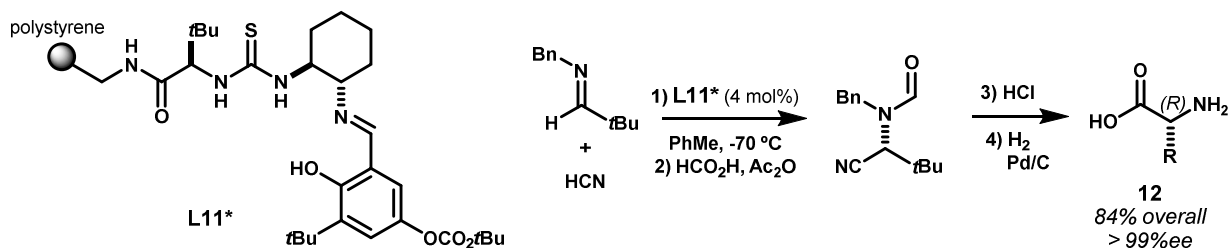
*Enantioselective hydrogenation.*⁶⁷



*Enantioselective alkylation.*¹³⁵



Enantioselective Strecker reaction.^{59,60}

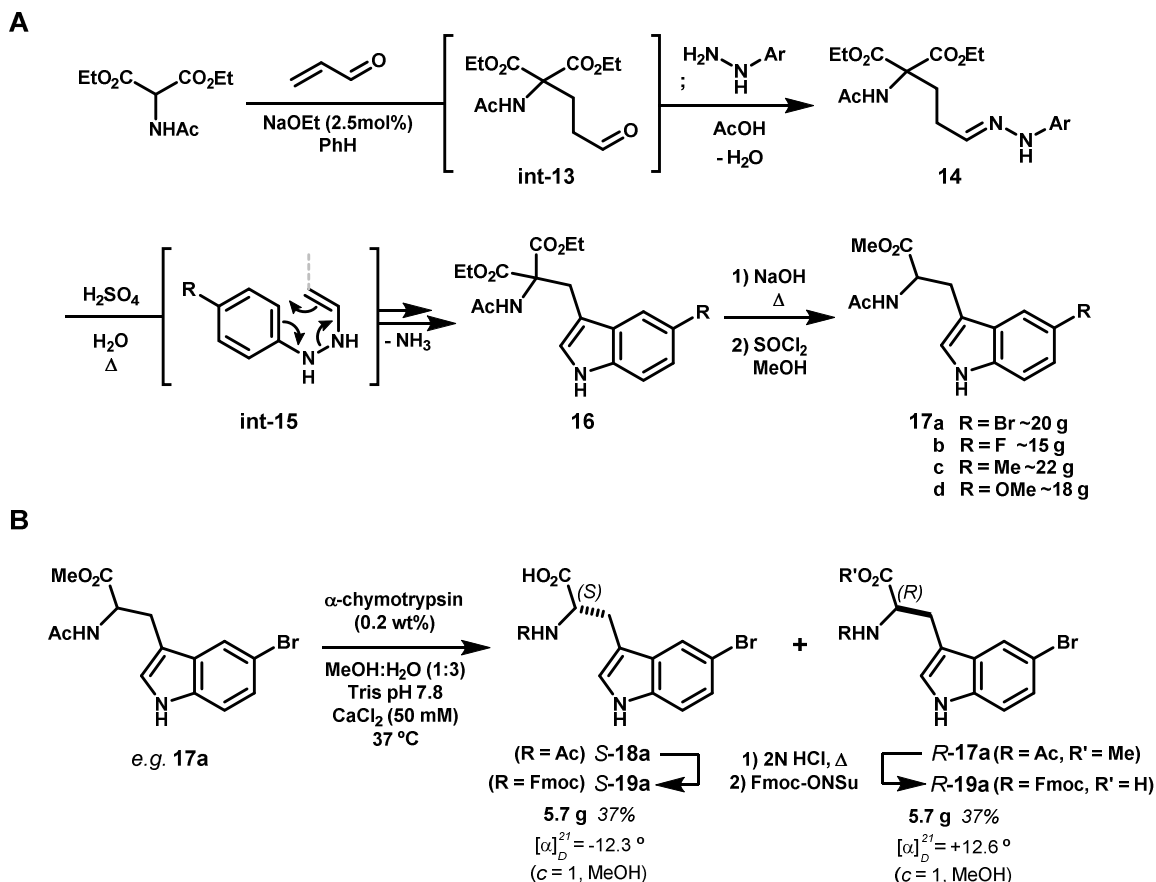


enolates, enantioselective reduction of dehydro α -aminoacids,^{51–58} enantioselective Strecker reactions,^{59–63} and others.⁶⁴ While useful, many of these methods utilize exotic catalysts or stoichiometric chiral auxiliaries, and are therefore not scalable. Hydrogenation of dehydro amino acids is the notable exception, as a number of highly active catalysts are in use for the industrial preparation of pharmaceutical intermediates including *L*-DOPA.^{52–54,65} These catalysts have also been successfully employed in the synthesis of ring-substituted tryptophans.^{66,67} For our purposes, however, these routes were disfavored because of the potential need to optimize reaction conditions to achieve high enantiopurity across different substrates, and the need to re-run the enantioselective reaction in order to access both *D*- and *L*-amino acid enantiomers.

Kinetic enzymatic resolution of racemic amino acids offers a robust and cost-effective means of divergently preparing both enantiomers of 5-substituted tryptophans and phenylalanine analogs.⁶⁸ Commercially available proteases have been utilized for this purpose, including porcine or *Aspergillus sp.* acylase I,^{69,70} bovine α -chymotrypsin,^{71–73} and *Bacillus licheniformis* subtilisin Carlsberg.^{74,75} Acylase I catalyzes enantioselective hydrolysis of *N*-acetyl or *N*-benzoyl amino acids, whereas chymotrypsin and subtilisin affect enantioselective hydrolysis of *N*-acetyl amino acid esters. Following the methods of Porter and co-workers,⁷² we successfully prepared multi-gram quantities of both enantiomers of 5-bromo, fluoro, methyl, and methoxy tryptophans. This was achieved by synthesis of the respective racemic tryptophans starting from diethyl acetamidomalonate as a glycine synthon (Scheme **6.2.2**).^{76,77} Initial ethoxide catalyzed conjugate addition of this malonate into acrolein generated aldehyde int-**13**, which was reacted with the appropriate phenylhydrazine in situ. Hydrazones **14** formed rapidly in the presence of acetic acid by using a Dean Stark apparatus to remove the water formed in the reaction. Crude hydrazones **14** were then heated in aqueous sulfuric acid, which induced [3,3]-sigmatropic rearrangement (int-**15**) and Fisher indolization by loss of ammonia. Subsequent saponification and thermal decarboxylation followed by re-esterification formed racemic *N*-acetyl tryptophan methyl esters **17**. This route proved straightforward and scalable, and did not require chromatographic purification; substantial purity upgrade was realized in acid/base-extractions intervening the transformation of malonates **16** to racemic intermediates **17a–d**.

Kinetic enzymatic resolution of racemic tryptophans was achieved using bovine α -chymotrypsin in

Scheme 6.2.2 A) Synthesis of racemic 5-substituted *N*-acetyl tryptophan methyl esters from diethyl acetamidomalonate by conjugate addition into acrolein, Fisher indole synthesis, thermal decarboxylation, and Fisher esterification. **B)** Kinetic enzymatic resolution and conversion to *N*_α-Fmoc derivatives.



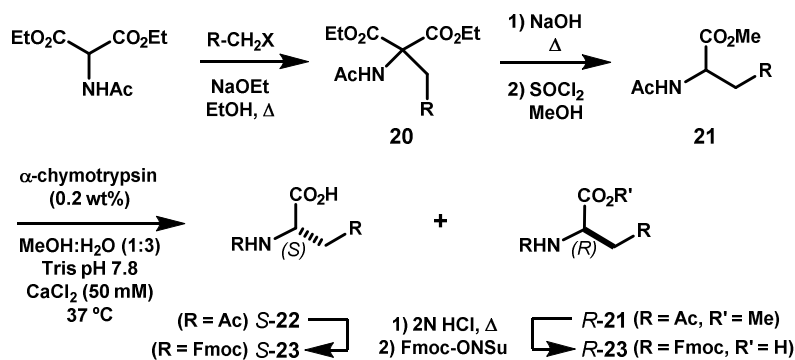
aqueous buffer containing up to 30% *v/v* of an organic co-solvent (Scheme 6.2.2B). Methanol and acetonitrile were effective for maintaining near homogeneity of the reaction, and in the case of recalcitrant substrates (e.g. Trp(5F), **17b**) DMSO was also added. These co-solvents appeared to have a negligible impact on enzymatic activity. Complete resolution was typically achieved by overnight reaction with 0.2 *w/v* α -chymotrypsin at 37 °C, corresponding to >18,000 *TON*. No background hydrolysis of the *D*-amino acid ester was observed, even at prolonged reaction times. The resulting mixtures of *N*-acetyl *L*-amino acid and *N*-acetyl *D*-tryptophan methyl ester were then separated by acid/base-extraction and converted to the *N*_α-Fmoc derivatives for use in solid-phase peptide synthesis.⁷⁸ Enzymatic resolution in this manner accessed relatively large quantities of protected 5-substituted tryptophans of high optical purity.

A series of phenylalanine analogs and heterocyclic side chains were also produced on multi-gram scale by alkylation of diethyl acetamidomalonate in a process otherwise analogous to the synthesis of

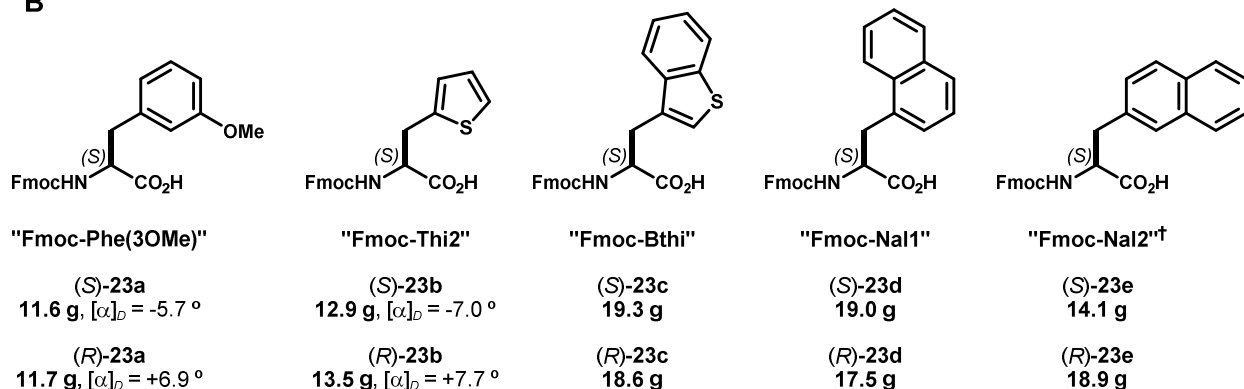
racemic tryptophans (Scheme 6.2.3). These side chains were selected based on their reported propensity to undergo bimolecular electrophilic substitution under mild conditions (e.g. nitration by HNO₃ at room temperature). While similar to phenylalanine analogs prepared previously (see Chapter 2.2), 3-methoxyphenylalanine (**23a**) was designed to access *ortho* and *para* cinnamylation, relative to the connected alanyl moiety. These regioisomers are inherently inaccessible from tyrosine-type 1,4-disubstituted benzene side chains (e.g. **2-17**, **2-22**, **5-S20**, see also Figure 6.2.1).

Scheme 6.2.3 A) Synthesis of racemic phenylalanine analogs and heterocyclic amino acid side chains, and kinetic enzymatic resolution. **B)** Fmoc-derivatives prepared by this route and optical rotation evidencing resolution of enantiomers. †Resolved by the action of *Aspergillus sp.* acylase I on the *N*-acetyl amino acid (i.e. (±)-**22**); not hydrolyzed by α-chymotrypsin. **C)** Activated *L*-phenylalanine analogs prepared previously (see Chapters 2, 5).

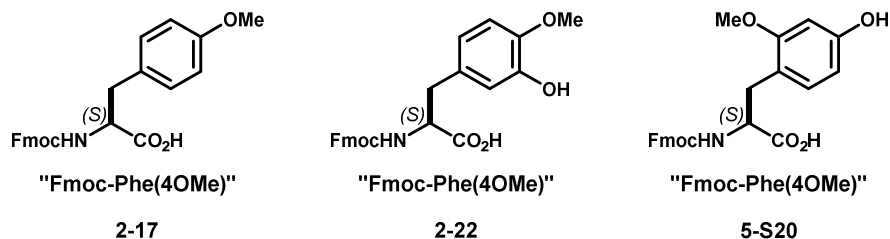
A



B



C



These non-natural amino acids are structurally and electronically perturbed from their natural amino acid counterparts in order to facilitate the formation of diverse macrocycle connectivity. Whether these modifications will be tolerable when applied to a given biological peptide-protein interaction is not yet known. Given the frequent involvement of aromatic side chains at ‘hot spots’ that drive binding and recognition at protein-protein interaction surfaces, we anticipate a diverse collection of aromatic amino acids, including those described here, will prove useful in identifying avid peptidomimetics targeting these surfaces.

6.3 Surveying large ring-forming reactions of 5-substituted tryptophans

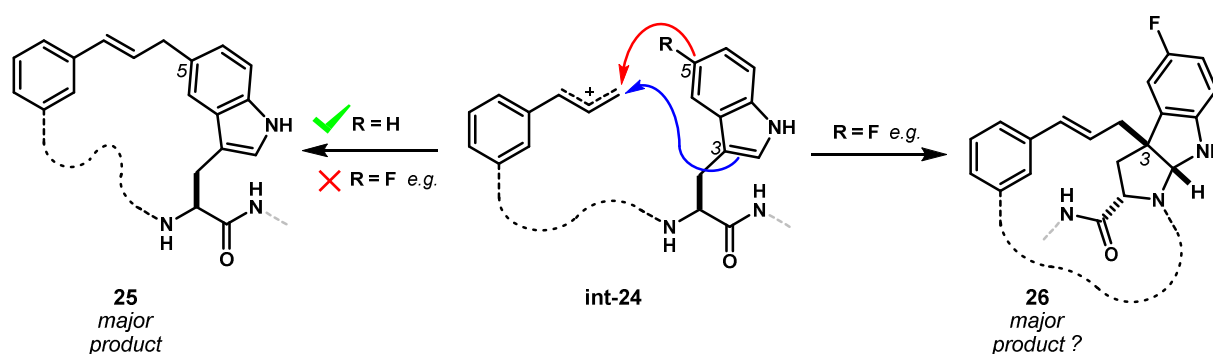


Figure 6.3.1 Internal cinnamylation of tryptophan (e.g. Trp-Trp-Tyr) leads to substitution of indole C5 as the major product. Blocking this position may lead to increased abundance of other isomers, including pyrroloindolines (i.e. **26**) resulting from C3 alkylation and cyclization of the proximal amide nitrogen onto the resulting 3*H*-indolium ion.

Large ring-forming cinnamylation reactions of template **5** (Figure 6.1.3) within the prototype sequence Trp-Trp-Tyr yielded an impressive diversity of macrocyclic products from the divergent reactivity of tryptophan (see Chapter 3).⁷⁹ This led us to prepare 5-substituted tryptophans (see Chapter 6.2) in an effort to block reaction at this site, and to thereby perturb the product distribution in favor of other isomers. We hypothesized that derivatives with electron-withdrawing substituents at indole C5 (e.g. F, Br) might slow reactions involving the benzenoid nucleus of these systems, and lead to an increased abundance of the structurally distinct pyrroloindoline product resulting from initial C3 cinnamylation and cyclization of the proximal amide nitrogen onto the resulting 3*H*-indolium ion (Figure 6.3.1). We questioned whether cyclizations leading to pyrroloindoline products of this type would be consistently *endo*-selective, or whether

we had simply overlooked a minor *exo* diastereomer in our previous studies of Trp-Trp-Tyr. Accordingly, we prepared a series of peptides bearing 5-substituted tryptophans in order to begin testing these hypotheses. Given that polar protic functional groups did not appear to interfere with Friedel-Crafts macrocyclization reactions (see Chapter 5), we also sought to examine peptidyl substrates spanning all natural amino acids – less cysteine, given its unvalued tendency to form dimeric disulfides – and in particular those with polar side chains. We viewed demonstration of broad substrate scope in this manner as a crucial step towards our goal of preparing diverse collections of peptidic macrocycles targeted to protein surfaces.

Seven peptide substrates containing 5-substituted tryptophans within diverse sequences were prepared to test the ability of these non-natural side chains as nucleophilic partners in ring-forming C-cinnamylations. Acyclic precursors were generated by the straightforward *N*-acylation of oligopeptides with template **5**, and reacted under standard acidolysis conditions with MeSO₃H in MeNO₂. The resulting product mixtures were fractionated by preparative HPLC, and individual components re-purified on a second stationary phase where necessary. Rather than exhaustively characterize the products of these reactions, as done previously, we sought to broadly survey the substrate scope, as well as the generality and diastereoselectivity of the pyrroloindoline-forming *C3* alkylation of tryptophan.

Template-induced macrocyclization of the first test sequence, Ala-Gln-His-Trp(5F)-Arg-NH₂, yielded a mixture of five isomeric products, all of which were obtained in sufficient quantity and purity for NMR analysis. The structures of these products are shown in Figure **6.3.2A**. These resulted from C-cinnamylation at *N1* (**26e**), *C2* (**26b**), *C3* (**26a**), *C4* (**26c**), and *C6* (**26d**) of the 5-fluoroindole side chain. These outcomes are an impressive example of Friedel-Crafts macrocyclization in the context of highly polar functional groups, and demonstrate that fluorination of tryptophan is well-tolerated. No side reactions of either arginine or histidine were observed, presumably because these side chains are protonated under the reaction conditions. The most polar component of the product mixture was determined to be bridged *endo*-pyrroloindoline **26a**. The *cis*-5,5 ring juncture and *30R,43R* stereochemistry was assigned by relaying the *33S* configuration retained from *L*-5-fluorotryptophan by sequential NOE correlation between *H33*, *H43* and *H1* (Figure **6.3.2B**). This example corroborates the diastereoselectivity observed in the cyclization of Trp-Trp-Tyr. The remaining four regioisomeric macrocycles indicate that the 5-fluoroindole side chain is both highly competent nucleophile in this reaction, and complementary reactivity to the indole side chain of

Ala-Gln-His-Trp(5F)-Arg

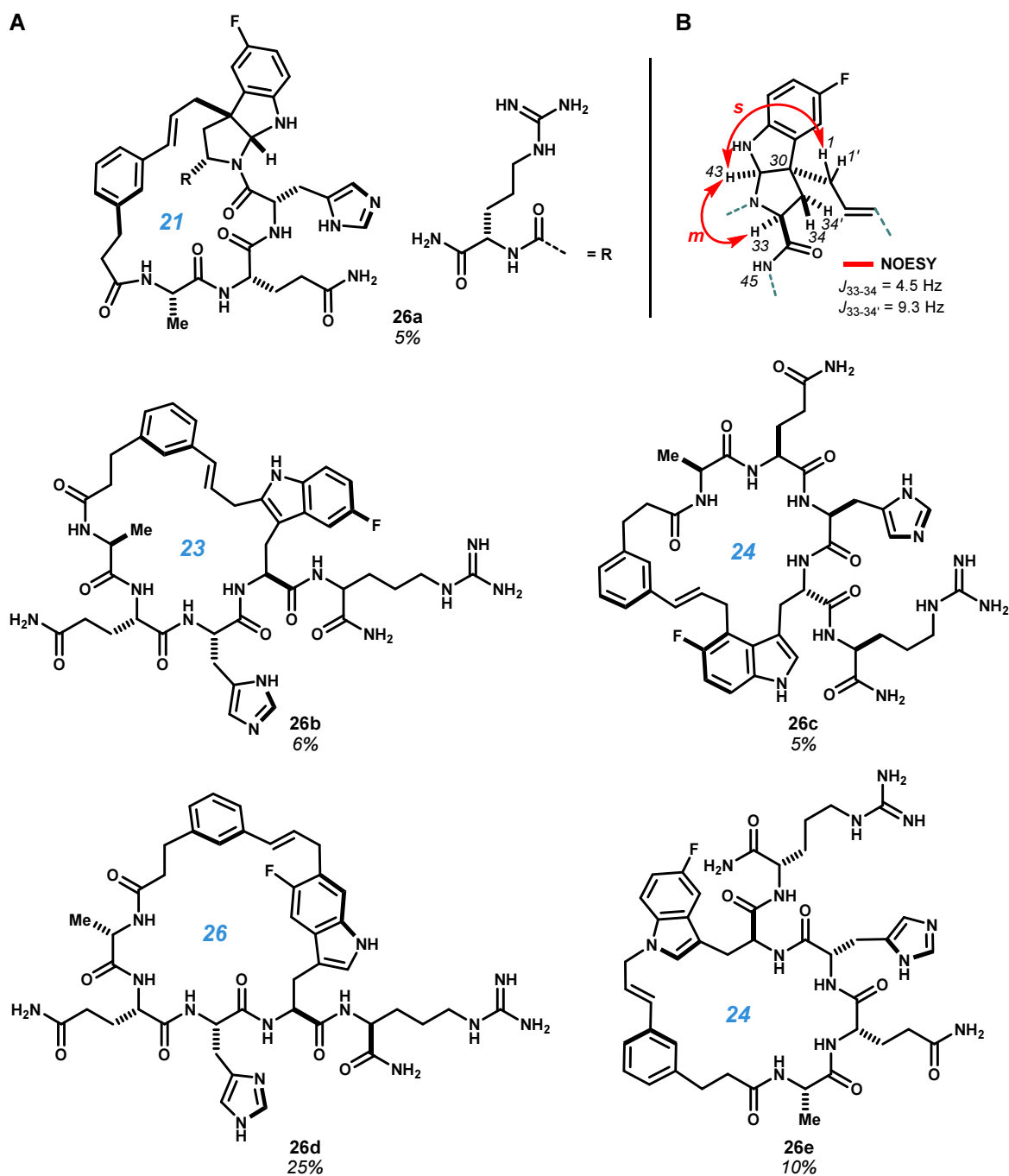


Figure 6.3.2 A) Products resulting from the acidolysis of template **5** ligated to Ala-Gln-His-Trp(5F)-Arg-NH₂. These result from *C*-cinnamylation at *N1* (**26e**), *C2* (**26b**), *C3* (**26a**), *C4* (**26c**), and *C6* (**26d**) of the 5-fluoroindole. Products span 21-, 23-, 24- and 26-membered rings (ring sizes in blue). **B)** Stereochemical assignment of the *endo*-pyrroloindoline moiety of **26a**. Isolated yields following preparative HPLC purification.

tryptophan itself. In particular, fluorination prevented formation of a 5-linked isomer – the major product from reactions of unsubstituted tryptophan – and favored alkylation at C6, which was previously obtained as a relatively minor outcome.

The second test sequence, Ser-Ile-Trp(5Br)-Ala-NH₂, again afforded a mixture of five isomeric products as detected by HPLC-UV/MS analysis, demonstrating the orthogonality of serine in this reaction. Fortunately, these products were again well-resolved, and isolated in sufficient quantities for structure elucidation. The structures of these products are shown in Figure 6.3.3A. Similarly to 5-fluoroindole, the 5-bromoindole side chain led to cinnamylation at N1 (27e), C2 (27a), C3 (27c), C4 (27b), and C6 (27d), and yielded C6 substitution as the major product. Macrocyclic pyrroloindoline 27c was again obtained as the

Ser-Ile-Trp(5Br)-Ala

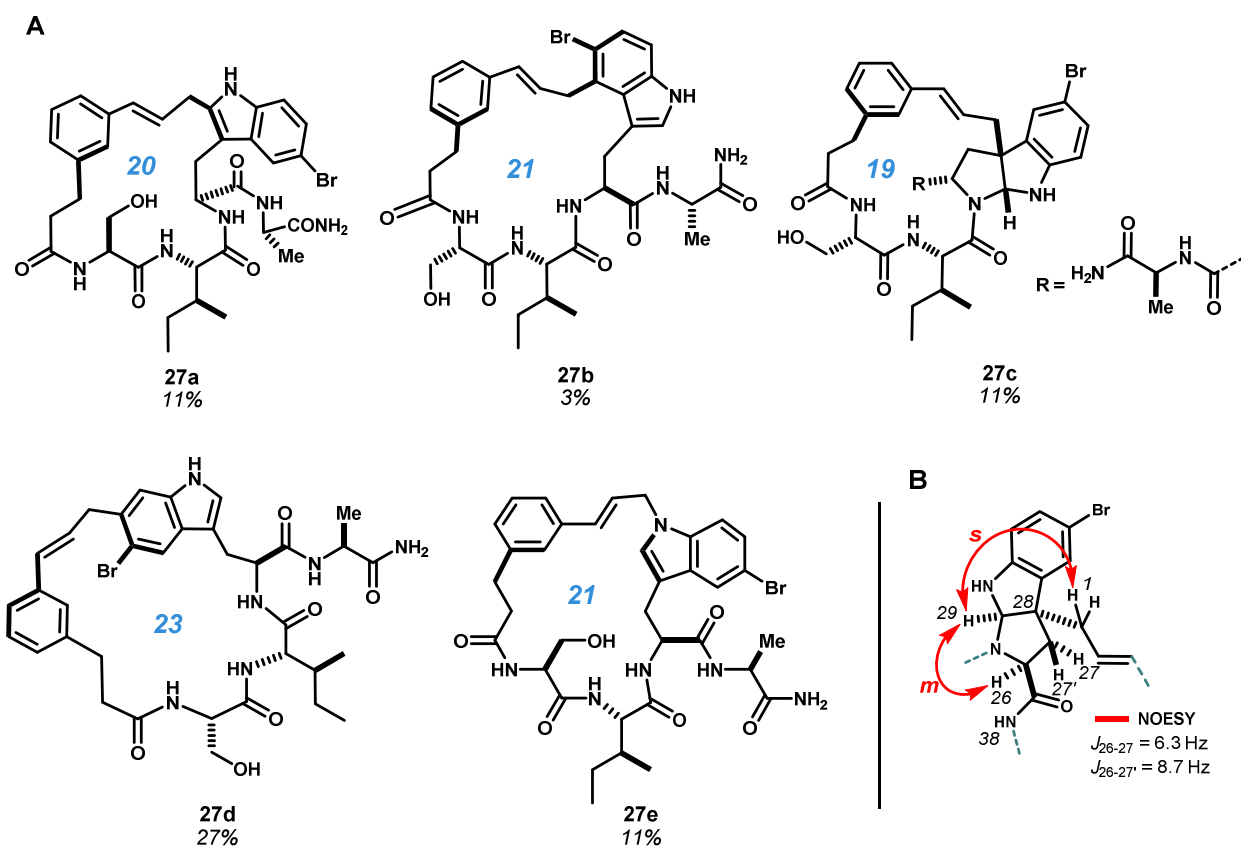


Figure 6.3.3 A) Products obtained from the acidolysis of template 5 ligated to Ser-Ile-Trp(5Br)-Ala-NH₂. These result from C-cinnamylation at N1 (27e), C2 (27a), C3 (27c), C4 (27b), and C6 (27d) of the 5-bromoindole. Products span 19-, 20-, 21- and 23-membered rings (ring sizes in blue). **B).** Stereochemical assignment of the *endo*-pyrroloindoline moiety of 27a based on sequential NOE from H26(S) to H29 and H1. Isolated yields following preparative HPLC purification.

C26-endo diastereomer, the stereochemical configuration of which was determined by NMR in the same manner as for **27a** based on sequential correlations from the *26S* stereocenter (Figure **6.3.3B**). Whether the slight differences in product ratio between this example with 5-bromotryptophan at P3 and the previous sequence bearing 5-fluorotryptophan at P4 resulted from the halogen substituent or from the position of these side chains (i.e. resulting ring size) is uncertain. Nonetheless, this sequence afforded somewhat greater yield of the structurally interesting pyrroloindoline product **27c**.

The third test sequence, Ac-Orn-Ile-Pro-Trp(5F)-NH₂, positioned 5-fluorotryptophan at P4, as in the first test sequence leading to **26a–e**, in order to probe the effect of proline on the product mixture. In this case, we observed only two products after acid-promoted macrocyclization, whereas sequence Ala-Gln-His-Trp(5F)-Arg-NH₂ had yielded five (*vide supra*). These two isomers were characterized as **28a** and **28b** resulting from *N1* and *C6* cinnamylation, respectively (Figure **6.3.4**). This result suggests that the conformational restrictions imparted by the proline tertiary amide bond can substantially influence product distribution. This conformational effect seems to occur irrespectively of the flexibility gained from the ornithine-template linkage.

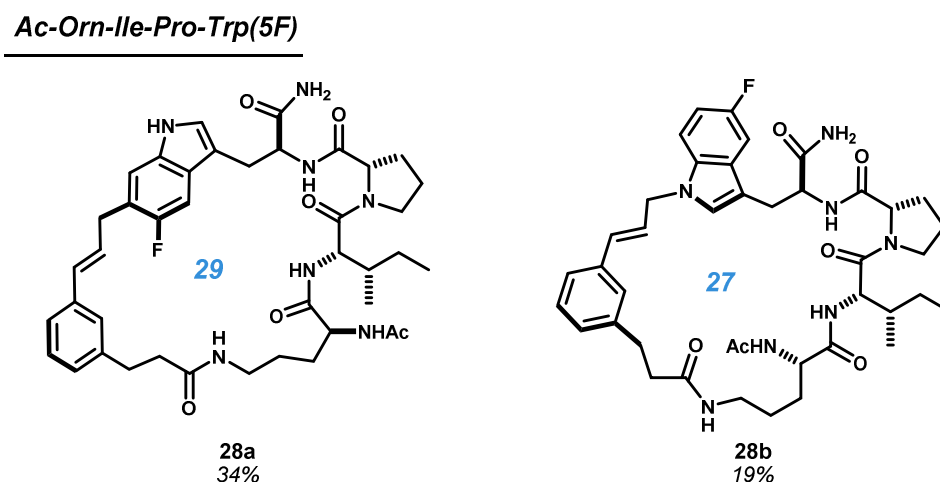


Figure 6.3.4 Products obtained from the acidolysis of template **5** ligated to Ac-Orn-Ile-Pro-Trp(5F)-NH₂ result from *C*-cinnamylation at *N1* (**28b**), and *C6* (**28a**) of the 5-bromoindole to give 27- and 29-membered rings (ring sizes in blue).

The fourth test sequence, Val-Gly-Trp(5Br)-Phe-NH₂, was designed to test the influence of glycine on cyclization efficiency and product distribution. Similarly to proline, glycine often either promotes^{80–84} or impedes⁸⁵ peptide macrolactamization owing to its ability to promote internally hydrogen bonded β -turns

conformations. HPLC analysis showed six products from cyclization of this sequence by template **5**, and we succeeded in characterizing the four major components. These resulted from cinnamylation of 5-bromotryptophan at *N1* (**29f**), *C2* (**29a**), *C4* (**29d**) and *C6* (**29b**) in a 14:6:8:20 ratio. A pyrroloindoline product was not identified in this case. This product distribution reflects that produced from second test sequence Ser-Ile-Trp(5Br)-Ala (11:11:3:27, *N1:C2:C4:C6*) suggesting that glycine minimally impacts template-based cyclizations of this type, and that product distribution is governed primarily by the tryptophan substitution pattern and electronic structure and not by macrocycle ring size.

Val-Gly-Trp(5Br)-Phe

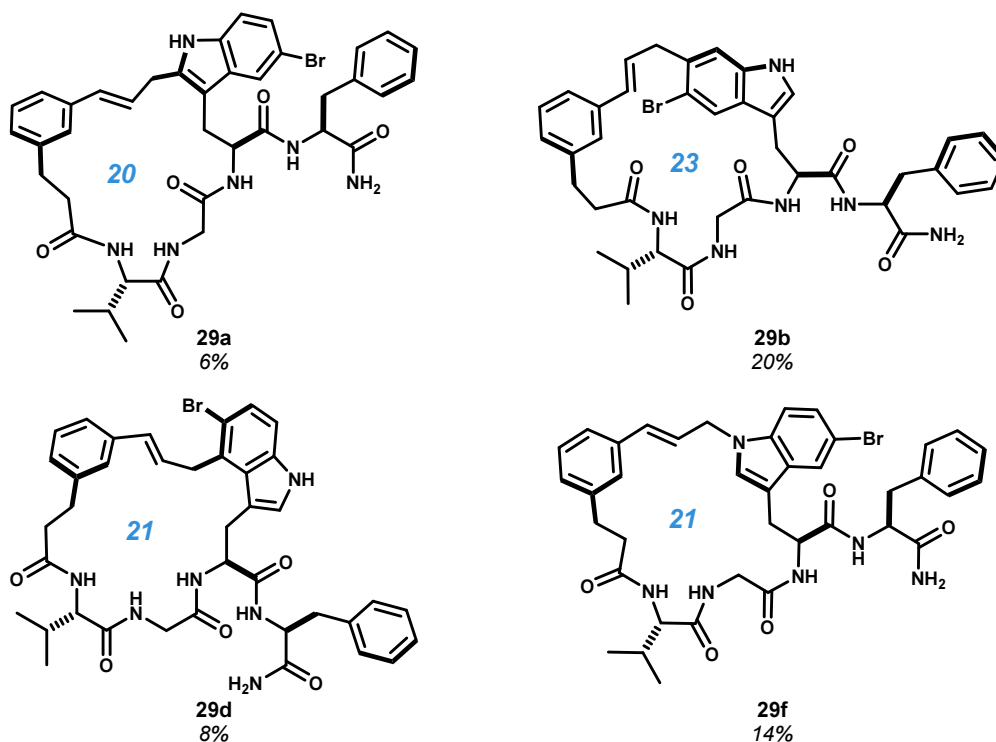
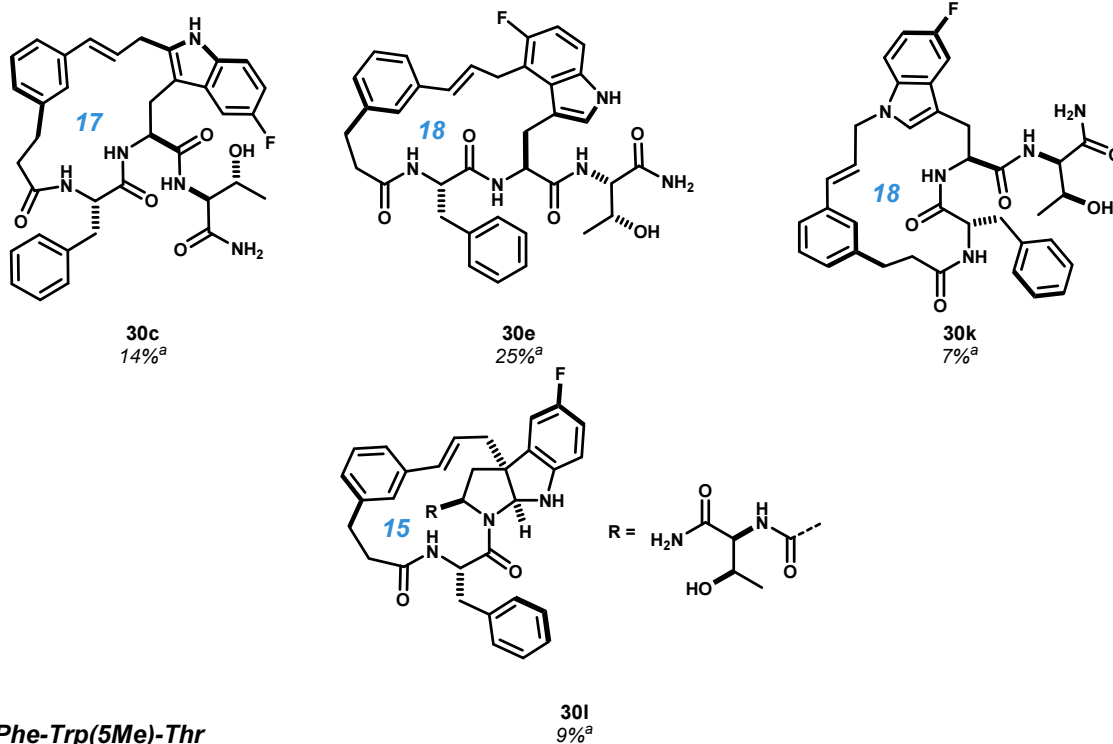


Figure 6.3.5 Products obtained from the acidolysis of template **5** ligated to Val-Gly-Trp(5Br)-Phe-NH₂ result from *C*-cinnamylation at *N1* (**29f**), *C2* (**29a**), *C4* (**29d**) and *C6* (**29b**) of the 5-bromoindole spanning 20-, 21- and 23-membered rings (ring sizes in blue).

The next two sequences, Phe-Trp(5F)-Thr-NH₂ and Phe-Trp(5Me)-Thr-NH₂, were designed to directly compare the effect of the 5-substituent on the electronic structure of the indole nucleophile and in turn on the resulting distribution of macrocyclic products. Unexpectedly, acidolysis of the sequence containing 5-fluorotryptophan gave nine products upon initial HPLC analysis, and an additional two were

resolved during preparative HPLC purification of this mixture. Though an intriguing result, albeit potentially spurious, we were only able to characterize the four major products resulting from internal cinnamylation of *N1* (**30k**), *C2* (**30c**), *C3* (**30l**) and *C4* (**30e**) cinnamylation. By contrast, the sequence containing 5-methyltryptophan gave only five products – in line with the five possible regioisomers identified in other sequences containing 5-bromo and 5-fluorotryptophan (*vide supra*) – from which we identified the three

Phe-Trp(5F)-Thr



Phe-Trp(5Me)-Thr

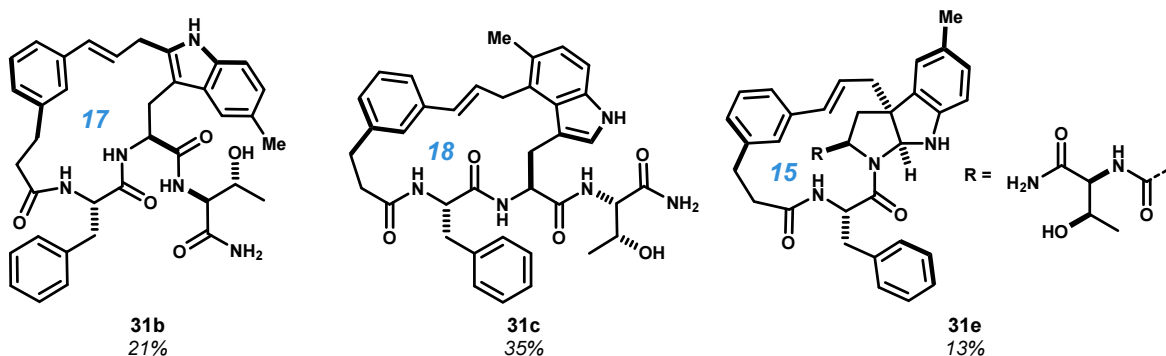


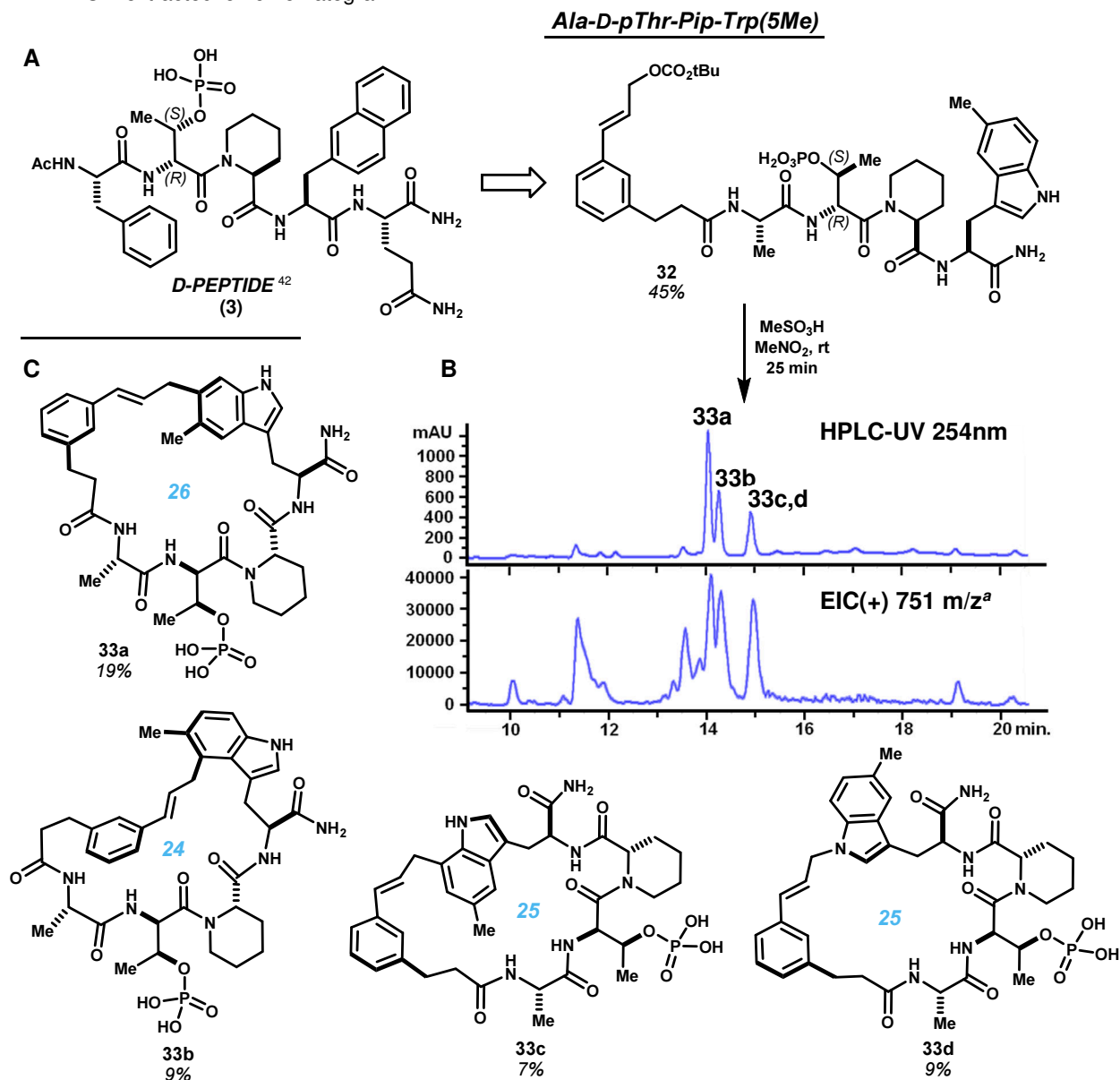
Figure 6.3.6 Products obtained from the acidolysis of template **5** ligated to analogous peptides Phe-Trp(5F)-Thr-NH₂ and Phe-Trp(5Me)-Thr-NH₂. These data suggest comparable reactivity between 5-fluoro and 5-methyltryptophans, despite the difference in 5-substituent electronegativity. ^aPeak ratio from integration of all isomers observed by HPLC-UV (254 nm). Isolated yields not determined.

most abundant isomers. These resulted from *C2* (**31b**), *C3* (**31e**) and *C4* (**31c**) cinnamylation. The *endo*-configurations of pyrroloindolines **30i** and **31e** were inferred from previous examples, but were not explicitly confirmed by 2D-NOESY/ROESY analysis. These data suggest that the distribution of regioisomeric linkages about 5-substituted tryptophan side chains is sensitive to the nature of the 5-substituent, and may offer a straightforward means of perturbing product mixtures in favor of desirable regioisomeric linkages. Whether these differences arise from steric bulk or inductive effects of the 5-substituent is not immediately evident.

The final test sequence placed 5-methyltryptophan, observed to give clean mixture in the previous example, in the context of biologically relevant motif. Borrowing from the reported peptidic Pin1 inhibitor '*D*-PEPTIDE',^{36,42} we prepared analogous sequence Ala-*D*-pThr-Pip-Trp(5Me)-NH₂ and incorporated template **5** to give acyclic precursor **32** (Scheme **6.3.1A**). This phosphorylated substrate provided a unique opportunity to test the orthogonality of our large ring-forming cinnamylations. Acid-promoted cyclization of intermediate **32** proceeded smoothly to a mixture of three isomeric products with no observable loss of the phosphoryl group. Upon semi-preparative HPLC purification and re-analysis, the third peak was further resolved into two components **33c** and **33d**. In this case, cinnamylation of 5-methyltryptophan had occurred at *N1* (**33d**), *C4* (**33b**), *C6* (**33a**) and *C7* (**33c**). This narrower product distribution, relative to the apparent reactivity of 5-methyltryptophan in other sequences (*vide supra*), corroborates the similar behavior observed with 5-bromotryptophan in the sequence Ac-Orn-Ile-Pro-Trp(5F)-NH₂. Together, these data suggest that 5-substituted tryptophans will generally give fewer products when preceded by either a proline or a pipercolic acid residue.

The aforementioned seven peptide substrates and resulting twenty seven macrocyclic products demonstrate facile access to highly functionalized composite macrocycles by divergent, template-induced Friedel-Crafts alkylation. In conjunction with previous examples, these cyclizations show compatibility with 15 of the 20 natural amino acid side chains, and also with the phosphoryl group. The side chains of asparagine, aspartic acid, and lysine, though not explicitly tested, are not anticipated to interfere with this macrocyclization reaction given the orthogonality of free peptide N- and C-termini observed in a previous example (see Chapter 5). Leucine, also not tested, will assuredly not interfere. In some cases, methionine-containing substrates appear to undergo non-selective *S*-alkylation leading to epimeric sulfonium salts (not

Scheme 6.3.1 A) Sequence Ala-*D*-pThr-Pip-Trp(5Me)-NH₂ was designed to mimic the reported Pin1 inhibitor '*D*-PEPTIDE' (**3**). **B)** HPLC-UV/MS analysis of the crude acidolysis reaction of acyclic intermediate **32** (C18, 20→100% ACN + 0.1%v TFA, 18 min). Compounds **33c** and **33d** were resolved subsequently on an alternative stationary phase. The isomeric peak at 11.5 min likely corresponds to the acyclic cinnamyl alcohol. **C)** Product structures arising from cinnamylation at N1 (**33d**), C4 (**33b**), C6 (**33a**) and C7 (**33c**).
^a EIC = extracted ion chromatogram.



shown), but the breadth of this side reaction is not yet known. Internal Friedel-Crafts alkylations involving 5-substituted tryptophans afford a subtle but useful shift in macrocycle connectivity relative to tryptophan itself, which appears to be driven by blockage of the 5-position, rather than by electronic substituent effects. Additionally, 5-substituted tryptophans show a broad propensity to form pyrroloindoline products following C3 cinnamylation, and appear to do so in a diastereoselective manner. These results led us to pursue larger

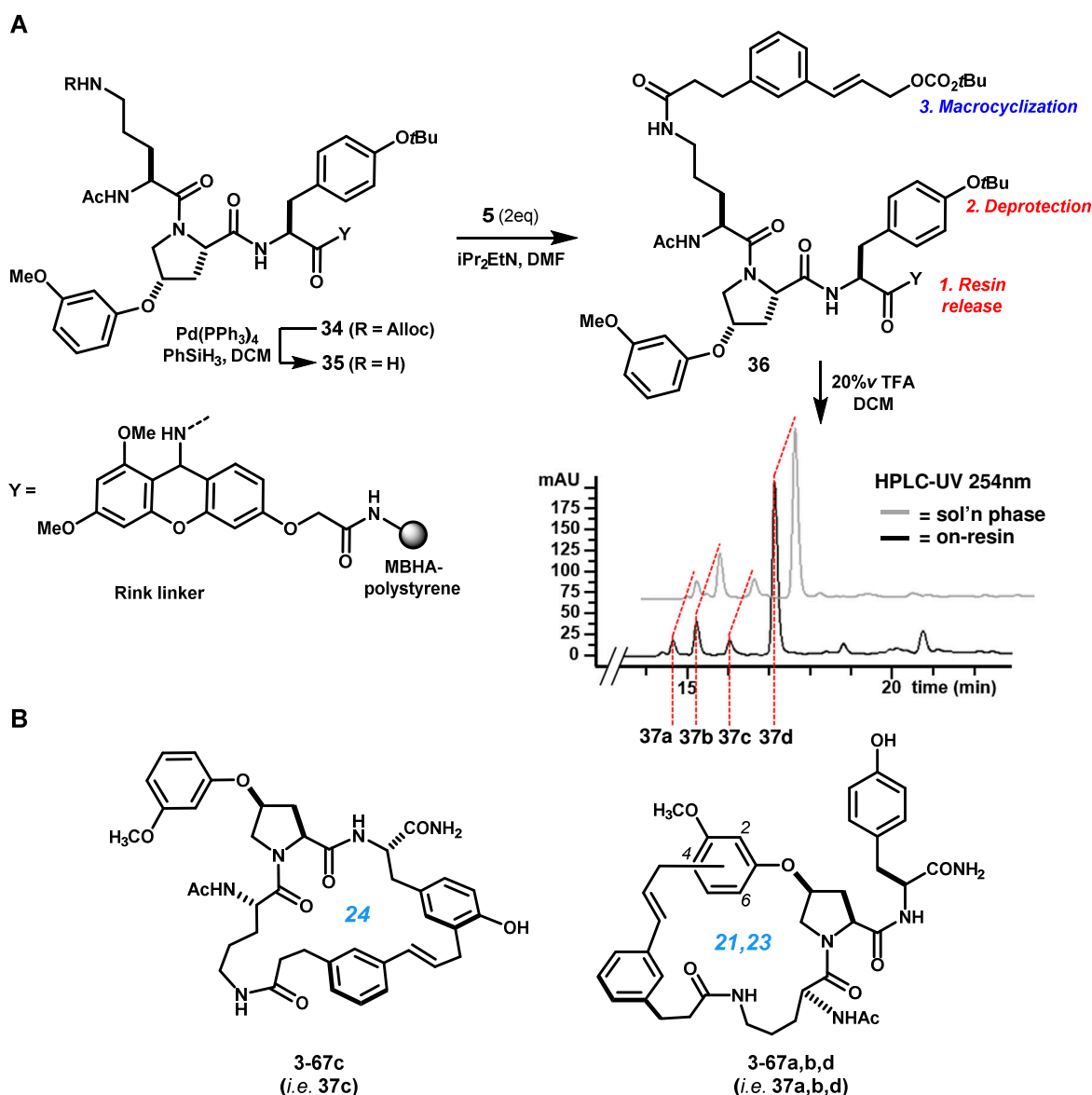
collections of synthetic macrocycles using template **5**, and to apply these libraries towards the discovery of biologically active substances. The results of these efforts are documented in the following subsections. Indeed, we observed potent inhibition of Pin1 by phosphorylated macrocycles **33a–d**. Discernable differences in activity between the four regioisomers provided an important proof of concept for our template-based synthetic methods and for exploring large ring constitution as a structural basis for biological activity (see Subsections 6.5, 6.6).

6.4 Methods for solid-phase synthesis of template-based composite macrocycles

Solid-supported synthesis allows straightforward means to run many reactions in parallel by obviating the need for workup and purification at each step, and has been widely adopted for step-intensive peptide synthesis for this reason.⁸⁶ Immobilizing the nascent molecule, for instance by covalent attachment to a polymer bead, allows reactions to be accelerated by using a large excess of reactant(s) at each step. When the reaction is complete, the excess reactants are filtered away from the bead. This approach has been extensively optimized for peptide synthesis^{87–90} in particular, and has also been applied to combinatorial synthesis of peptide macrolactam libraries⁹¹ ranging from thousands^{92–94} to potentially millions of peptide sequences.^{87,95,96} Peptide synthesis resins commonly consist of a polystyrene support, or more exotic copolymer, and an acid-labile linker from which the polypeptide is iteratively constructed.^{2,97} The Rink amide linker⁹⁸ is perhaps the most commonly used for peptide synthesis, and yields C-terminal carboxamides upon release of the peptide from the linker by treatment with trifluoroacetic acid (TFA). The 2-chlorotrityl linker is also widely employed, and allows peptidyl products to be released from the resin as C-terminal carboxylic acids,^{99–101} and, notably, can yield products with side chain protecting groups intact if mild conditions are used.¹⁰¹ Given that our cinnamyl carbocation-based templates are also activated under strongly acidic conditions, including by TFA which is used to cleave the Rink and chlorotrityl linker, we hypothesized that it might be possible to initiate simultaneous release from the resin and large ring-forming internal C-cinnamylation. If successful, this approach would access valuable template-based composite macrocycles by adding a *single step* to established solid-phase peptide synthesis protocols.

An initial attempt at releasing the product from the Rink amide linker with concurrent macrocyclization yielded macrocyclic products in surprisingly high purity. In this experiment, we investigated tripeptide Ac-Orn(H)-Hyp-Tyr, which we had previously examined in solution-phase acidolysis reactions with several template designs (see Chapter 3). Peptidyl intermediate **35** (Scheme 6.4.1) was assembled

Scheme 6.4.1 A) Solid-phase assembly of template-containing acyclic intermediate **36** and subsequent treatment with TFA led to release from the Rink linker (**Y**), deprotection of the phenolic *tert*-butyl protecting group, and large ring-forming *C*-cinnamylations. Products **37a–d** co-chromatographed (traces offset for clarity) with products from the analogous acyclic precursor in solution (i.e. **3-67a–d**, see Chapter 3). **B)** Macrocyclic structures characterized previously from the analogous solution-phase macrocyclization. MBHA = methylbenzhydrylamine, styrene + 1% divinylbenzene copolymer.



using standard Fmoc-based solid-phase peptide synthesis protocols, and acylated with template **5** to give resin-bound acyclic precursor **36**. Treating this material with 20%*v* TFA in DCM led cleanly to a mixture of four isomeric products by HPLC-UV/MS. These products co-chromatographed with materials derived from solution-phase acidolysis of the same precursor, and exhibited masses consistent with these products. Integration of the respective HPLC-UV traces showed that solid-phase and solution-phase reactions led to products **37a-d** in a ratio of 5:14:7:74 and 6:17:7:70, respectively. The similarity between these ratios suggests that *tert*-butyl deprotection and resin release likely precede cyclization.

Attempts to apply this solid-phase approach more broadly were not initially successful. In a test set of 33 peptide sequences, each containing at least one nucleophilic aryl side chain, we observed both inconsistent mass recovery and product mixtures of non-characteristic molecular masses. The average recovery was 91% ($\pm 51\%$, std. dev.) of theory. In library constructions where crude acidolysis product mixtures would be diluted and assayed directly, this erratic mass recovery would translate to unacceptable variation in the concentration of DMSO stock solutions. Though 27 of 33 reactions (82%) afforded products consistent with macrocycles, in 12 of these examples we observed highly complex mixtures of primarily non-characteristic products. To control for the quality of resin-bound peptides entering this step, a portion of the resin was removed and instead *N*-acetylated. In 32 of 33 controls, HPLC-UV analysis indicated predominantly single product of the anticipated molecular mass. The average mass recover was 45% ($\pm 22\%$). Consequently, we attributed the complex mixtures to the template, and to the acidolysis step, specifically. Attempts to mitigate this behavior by modifying the reaction medium – such as by using 2,2,2-trifluoroethanol (TFE) in TFA, etc. – were not successful.

These problems may result, at least in part, from the highly electron rich Rink linker, which itself may lead to undesired capture of the cinnamyl carbocation intermediate (Figure **6.4.1**). This may occur by internal electrophilic substitution of the linker by the cinnamyl carbocation if the rate of C-cinnamylation exceeds the rate of resin release. Similarly, the linker may capture the cinnamyl ion intermolecularly. Acid-promoted resin release forms a stabilized xanthylium carbocation (Figure **6.4.1B**), which is normally quenched by scavengers, such as phenol, thioanisole or triisopropylsilane, that are added when cleaving polypeptides from the resin. In template-initiated macrocyclizations, these scavengers must be omitted to prevent quenching the intermediate cinnamyl carbocation.

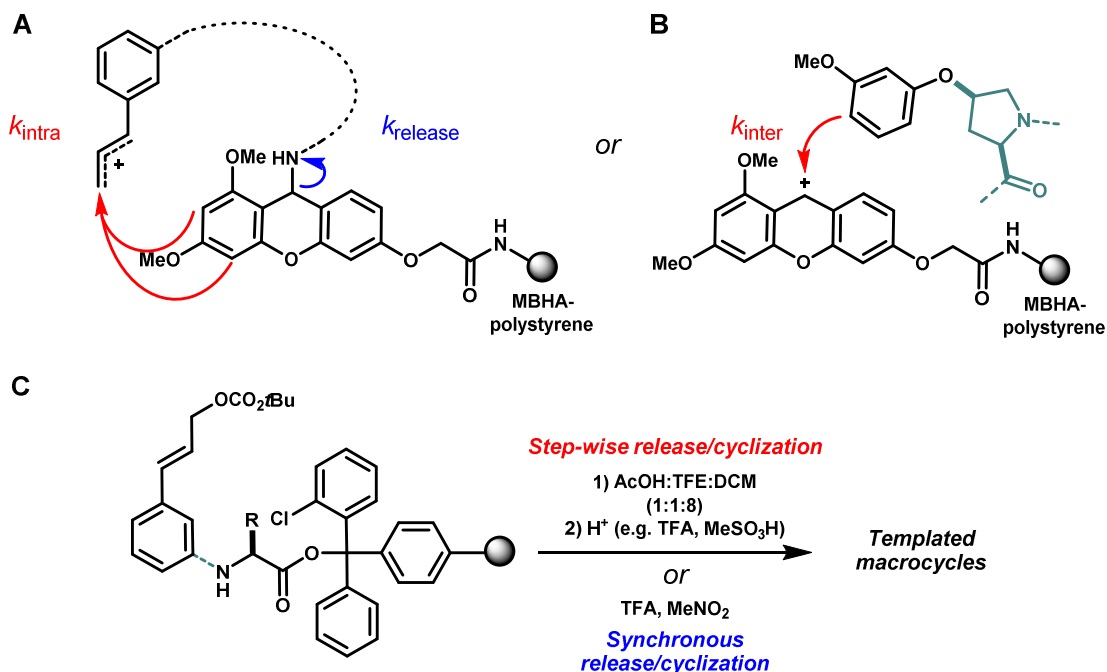
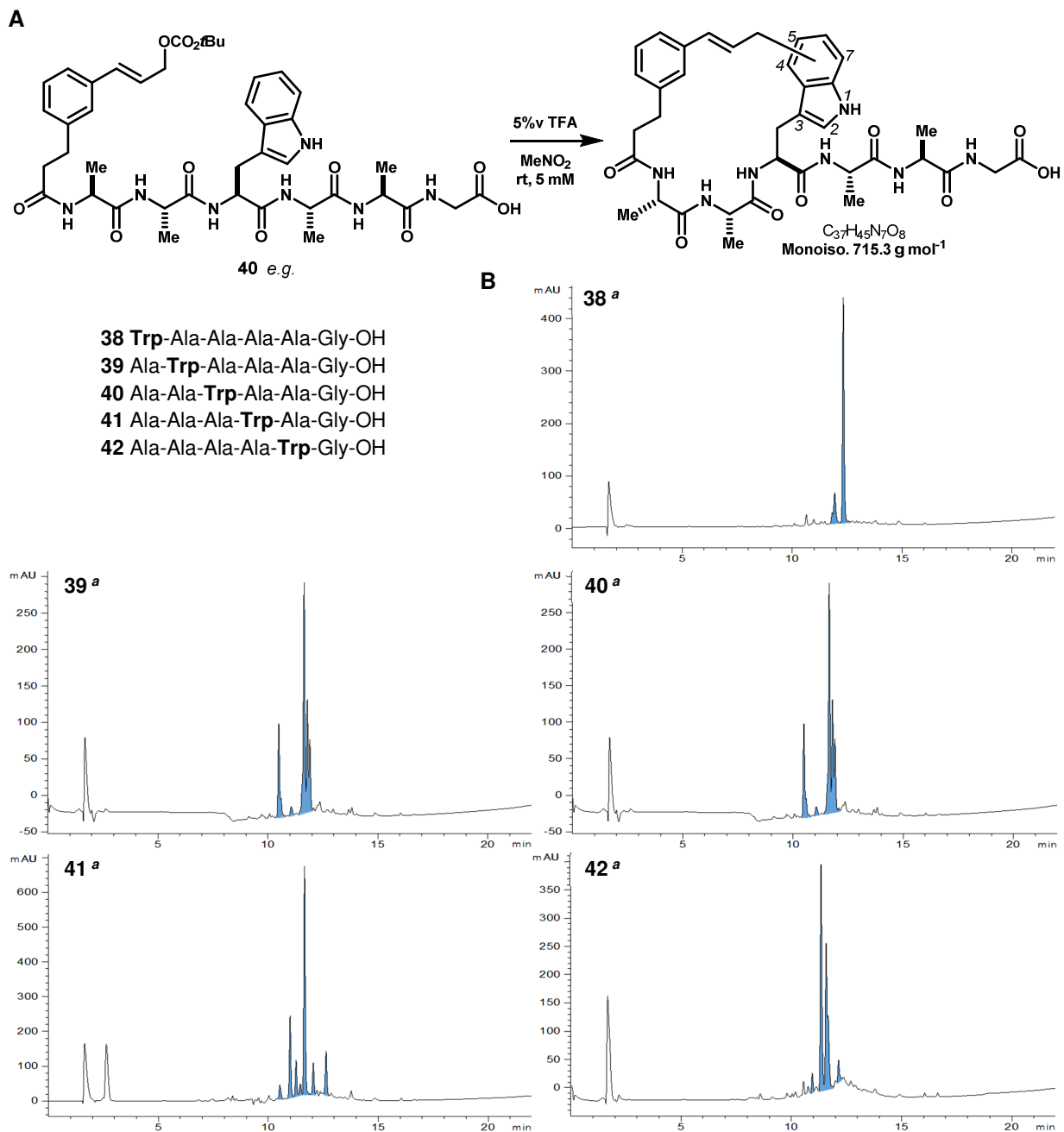


Figure 6.4.1 Erratic mass recovery in acid-promoted resin release and internal cinnamylation reactions may result from side reactions of the Rink linker. **A**) intramolecular electrophilic cinnamylation (i.e. $k_{intra} > k_{release}$) **B**) In the absence of cation scavengers (e.g. iPr_3SiH , $PhOH$) – which would also quench the cinnamyl carbocation – intermolecular reaction (i.e. k_{inter}) of aryl side chains may also lead to re-capture of macrocyclic products by the Rink linker. **C**) Use of the 2-chlorotrityl linker accelerates resin release, and allows orthogonal release and subsequent cyclization.

Similar test reactions were carried out using the 2-chlorotrityl chloride linker in an attempt to avoid the aforementioned problems with the Rink linker. This linker is substantially more labile, and is not anticipated to react with either the cinnamyl carbocation. Consequently, we were able to achieve both orthogonal cleavage of the acyclic precursor using acetic acid¹⁰¹ and simultaneous release and macrocyclization under strongly acidic conditions. After extensive optimization of the reaction parameters, we found mixtures of 5-10% v TFA in $MeNO_2$ to be uniquely effective for direct release/cyclization, despite that these appeared to swell polystyrene resins only poorly. Higher concentrations of TFA (25-50%) in TFE were also effective, but generally resulted in unfavorably slow reactions and inferior product purity. In mixtures containing TFA or TFE, ion pair return and solvolysis equilibria compete with macrocyclization, but may also favorably compete with aberrant reaction pathways (see Chapter 5). These conditions generally result in substantially slower reactions, but are highly effective at mitigating the formation of non-characteristic products.

Figure 6.4.2. Positional scanning of tryptophan-based macrocyclizations using on-resin assembly of acyclic intermediates **38–42** and solution-phase macrocyclization. **B)** HPLC-UV/MS analysis of crude acidolysis reactions of shows clean conversion to mixtures of isomeric macrocycles. Shaded peaks (UV 254nm) exhibited characteristic product masses (i.e. pseudomolecular ion $[M+H]^+ = 716.3\ m/z$ & $[M-H]^- = 714.3\ m/z$.
^a HPLC conditions: C18, ACN + 0.1%v TFA linear 15→100%, 18min; 100% to 20min.

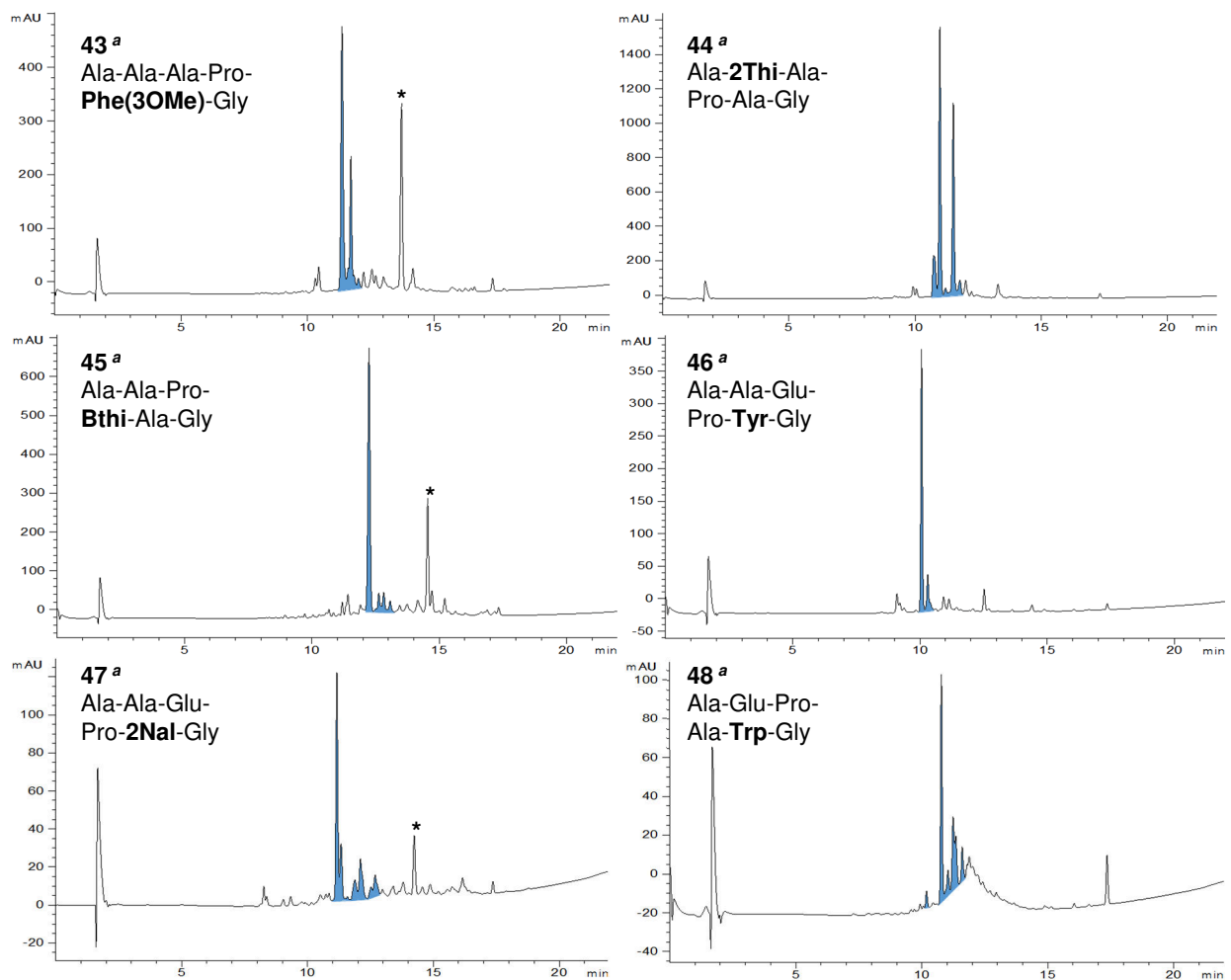
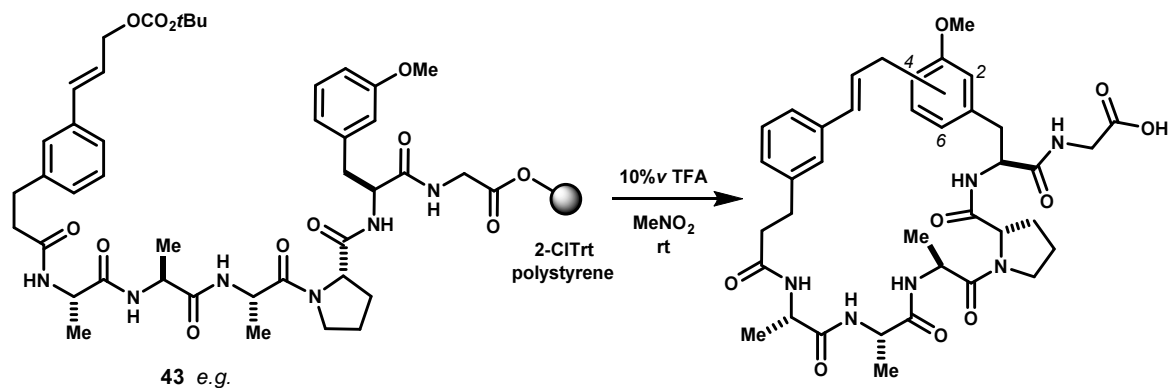


The optional orthogonal release of acyclic precursors allowed us to verify the identity and purity of materials directly prior to acid-promoted macrocyclization, and to compare resin-supported and solution phase cyclizations. In a pilot study, we examined internal cinnamylations of *L*-tryptophan in positions P1–

P5 of a hexapeptide bearing alanine at the remaining positions, and a C-terminal glycine residue (P6). The peptides were synthesized on a 20 μmol scale using 2-chlorotrityl chloride polystyrene resin pre-loaded with glycine (0.64 mmol/g), and the N-termini were acylated with template **5**. Each resin was split, and half was cleaved with AcOH:TFE:DCM (1:1:8) to give the respective acyclic precursors **38–42**, which were >95% crude purity by HPLC-UV analysis (254nm). Portions of these acyclic intermediates (2 μmol) were treated with 5%*v* TFA in MeNO₂ for 1 hour, then evaporated. HPLC-UV/MS analysis of these crude materials showed complete conversion to mixtures of isomeric products in excellent purity (Figure **6.4.2**) – arrived at over 15 steps without purification. The results of these five test sequences showed excellent promise for a purification-free parallel library synthesis approach, and we next sought to combine this approach with the broad substrate scope observed previously.

We examined cyclization reactions of tyrosine, 3-methoxyphenylalanine, 2-thienylalanine, 3-benzothienylalanine and 2-naphthylalanine using similar positional scanning experiments. In these cases, however, we treated resin-bound acyclic materials with TFA in MeNO₂ and obtained macrocyclic products directly. Aryl amino acids were incorporated into progressively more functionalized peptides, incrementally moving toward testing compatibility of these cyclizations with the motif Glu-Pro designed to mimic the native pSer/pThr-Pro Pin1 substrate motif. Key findings are illustrated in Figure **6.4.3**, and complete data for all 48 test sequences examined are listed in the Chapter 6 Experimental Appendix. These data indicate productive reactions in all cases, including the previously undemonstrated 3-methoxyphenylalanine, 2-thienylalanine, 3-benzothienylalanine and 2-naphthylalanine side chains. Examples **43** and **45** yielded major byproducts (*, Figure **6.4.3**), mass spectra of which were consistent with cinnamyl trifluoroacetates resulting from ion pair return from a cinnamyl carbocation intermediate. These reacted further when re-subjected to the reaction, and proceeded to near completion at extended reaction times with no appreciation degradation of product purity. In the case of 2-naphthylalanine (**47**), however, cyclization seemed sluggish, and the intermediate trifluoroacetate persisted even at extended reaction times. Analogous reactions of 1-naphthylalanine, however, showed acceptably rapid cyclization. We viewed cinnamyl trifluoroacetates as relatively innocuous contaminants – where present – as these readily hydrolyzed to linear cinnamyl alcohols when diluted into DMSO as 10 mM stock solutions for bioassay.

Figure 6.4.3. Representative examples of internal cinnamylations of Phe(3-OMe), 2-Thi, 3-Bthi, Tyr, 2-Nal, and Trp via synchronous resin release and macrocyclization. Shaded peaks (UV 254nm) denote products of characteristic masses. Examples **43**, **45** and **47** yielded major byproducts (*) consistent with cinnamyl trifluoroacetates, which proceed to product under extended reaction times (see text). ^a See HPLC conditions Figure 6.4.2.



These pilot reaction surveys provided an impressive glimpse of the practical utility of this solid-supported method. Several critical observations were made in the course of these experiments which deserve attention. On one occasion, we observed a frustrating erosion of product purity when attempting to repeat previously successful reactions – specifically, the tryptophan positional scanning experiments described above. Ultimately, the nitromethane solvent was pinpointed as the source of this problem. When commercial MeNO₂ was used, we observed a broad mound and substantially diminished peak area relative to the flat baseline and sharp product peaks noted previously (Figure 6.4.2). This phenomenon was alleviated somewhat by using lower concentrations of TFA (5% v vs. 10% v). Surprisingly, the reaction purity was fully rescued when the MeNO₂ solvent had been aged over 4Å molecular sieves for one week (Figure 6.4.2D). Additionally, pre-treated MeNO₂ caused a marked change in the color of these reactions, and completely ameliorated the brown color resulting from reactions in commercial nitromethane (Figure 6.4.4).

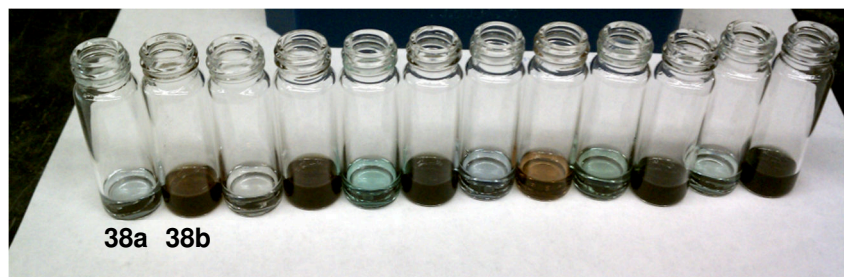
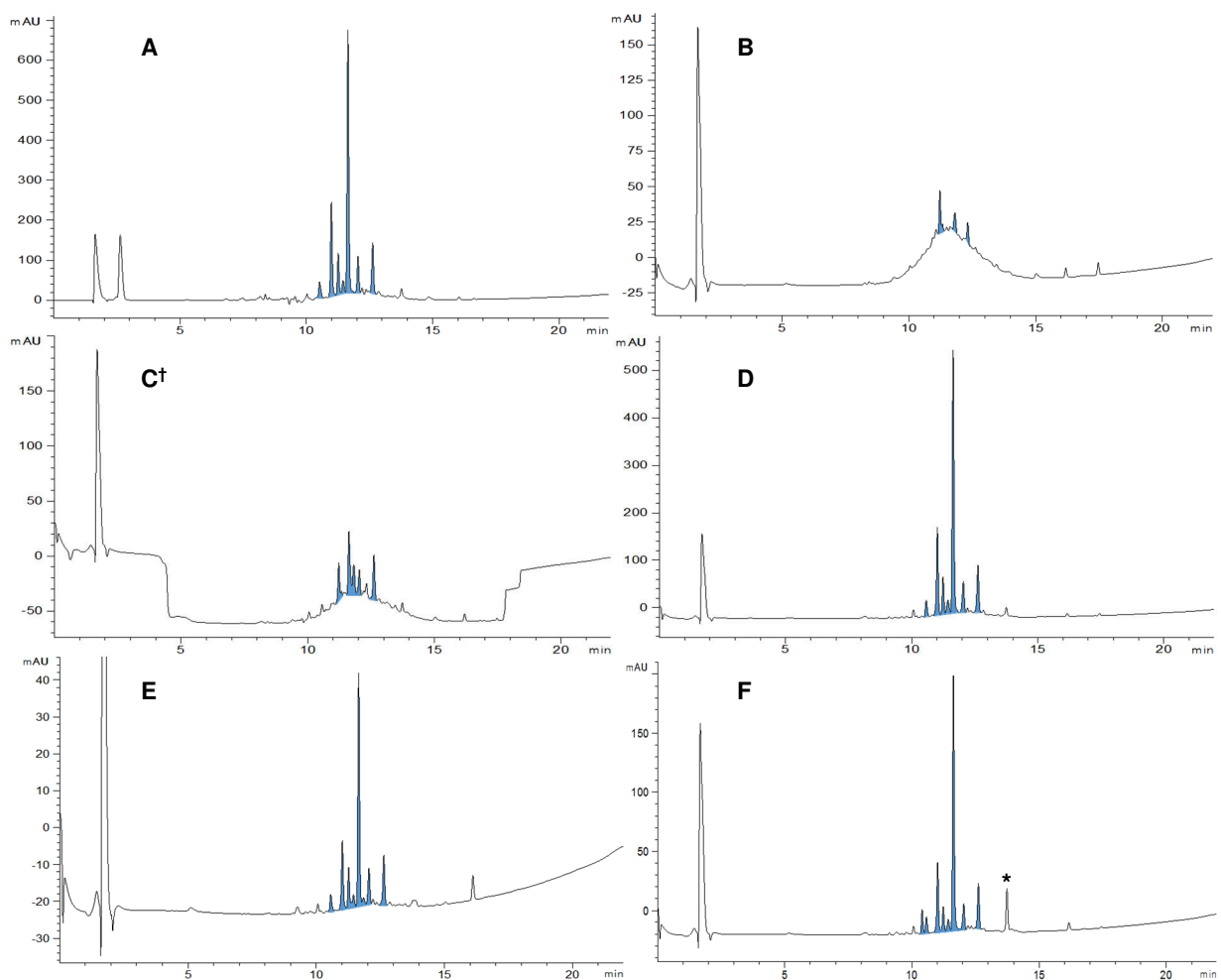
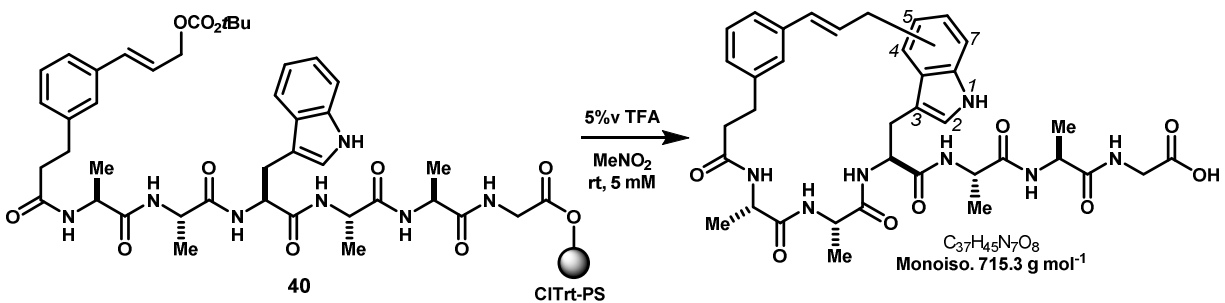


Figure 6.4.4. Acidolysis reactions of tryptophan-containing sequences **38–42** acylated with template **5**. From **38** (left), alternating vials containing reactions with 5% v TFA in MeNO₂ aged over 4Å molecular sieves (e.g. **38a**) or in untreated commercial MeNO₂ (e.g. **38b**), which caused a brown color to develop.

Karl Fisher titration indicated that the commercial solvent contained 203 ppm water, whereas molecular sieves reduced this to a mere 30 ppm. Curiously, when 100-1000 ppm water was added back to reactions using dried MeNO₂, we observed no erosion in product purity. This indicated that trace water does not substantially affect the reaction, and suggests that the molecular sieves function by also removing impurities other than water. We also attempted to use activated neutral alumina to dry nitromethane,^{102,103} which proved relatively ineffective after aging overnight (147 ppm H₂O). Nonetheless, this alumina-treated nitromethane was equally effective at rescuing product purity (Figure 6.4.2E). Purification of nitromethane by distillation was not attempted, despite this being common practice,^{104,105} due to the risk of explosion.¹⁰⁶ Notably, treating nitromethane with neutral alumina (Brockmann type I) led to an intense yellow color, which was entirely adsorbed to the alumina and did not dissipate upon acidification. While we observed no

Figure 6.4.5. Solvent purity substantially affects product purity, but water content does not. Acidolyses of resin-bound sequence Ala-Ala-Ala-Trp-Ala-Gly-[CITrt-PS] (**40**, 5 μmol) acylated with template **5** using different sources of MeNO_2 . Shaded peaks (UV 254nm) denote products of characteristic mass. **A**) Previous solution-phase reaction (see also Figure 6.4.2). Repeated reactions with: **B**) commercial MeNO_2 (Alfa Aesar) + 10%v TFA; **C**)† commercial MeNO_2 (Alfa Aesar) + 5%v TFA; **D**) MeNO_2 aged over 4Å molecular sieves + 5%v TFA; **E**) Conditions D + 1000 ppm H_2O ; **F**) Conditions D + 1%v *N,N*-DMF. †Baseline anomalies due to failing UV detector lamp. *Byproduct consistent with cinnamyl trifluoroacetate.



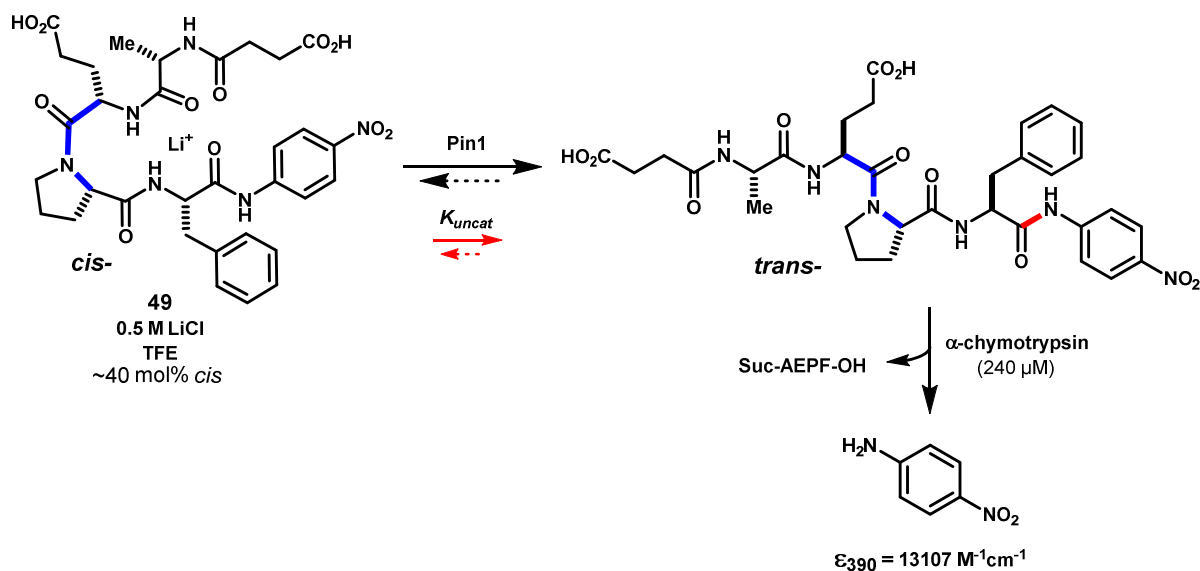
impurities by NMR analysis of highly concentrated samples of commercial MeNO₂, these empirical results may implicate aldehydes or nitriles, known contaminants of MeNO₂,^{105,106} as the causative impurities. Similarly, control experiments adding *N,N*-DMF (1%v) – a possible contaminant introduced from solid-phase synthesis – to the reaction led to diminished purity and substantially slower reactions, as evidenced by residual cinnamyl trifluoroacetate intermediates (Figure 6.4.2F). Fortunately, the aforementioned variables are easily controlled.

The solid-supported synthesis of acyclic template-containing intermediates provides rapid, purification-free access to collections of macrocyclic products. By judicious choice of resin and linker, here optimized using inexpensive 2-chlorotrityl polystyrene resin, it is possible to release products from the resin and induce internal Friedel-Crafts alkylation in a single step. This integrated approach yields macrocyclic template-peptide composites in comparable purity to solution-phase reactions. Furthermore, this approach expands the scope of possible peptide substrates by introducing the template onto fully protected, resin-bound intermediates. For instance, template 5 can selectively acylate the peptide *N*-terminus in the presence of side chain amino groups (e.g. Lys, Orn) which remain protected. The experiments in this subsection revealed few limitations of this method, and laid groundwork for library construction for biological screening and efforts to discover small molecule Pin1 inhibitors.

6.5 In vitro kinetics and assays of human Pin1

Peptidyl prolyl isomerases (PPIases) catalyze the *cis-trans* isomerization of proline tertiary amide bonds, and require special techniques to observe this fleeting process. Unlike many other enzymatic processes, isomerization involves neither forming/breaking bonds nor turnover of cosubstrates, such as NADPH, CoA or FAD. Furthermore, in the case of proline *cis-trans* isomerization, the reaction is both spontaneous at room temperature and reversible as a result of the moderate rotational barrier ($\Delta G^\ddagger \approx 13\text{-}19$ kcal/mol) and similar free energy between the two isomers ($\Delta \bar{G}^0_{cis-trans} \approx 1.2$ kcal/mol).^{107–109} Elegant analytical methods have been developed to overcome these challenges, and generally detect prolyl isomerase activity by linking this reaction to an auxiliary protease that acts specifically on the product isomer to provide a readout for quantification.^{110–113}

Scheme 6.5.1. Assay of Pin1 prolyl *cis-trans* isomerase activity by a chymotrypsin-linked continuous spectrophotometric readout.

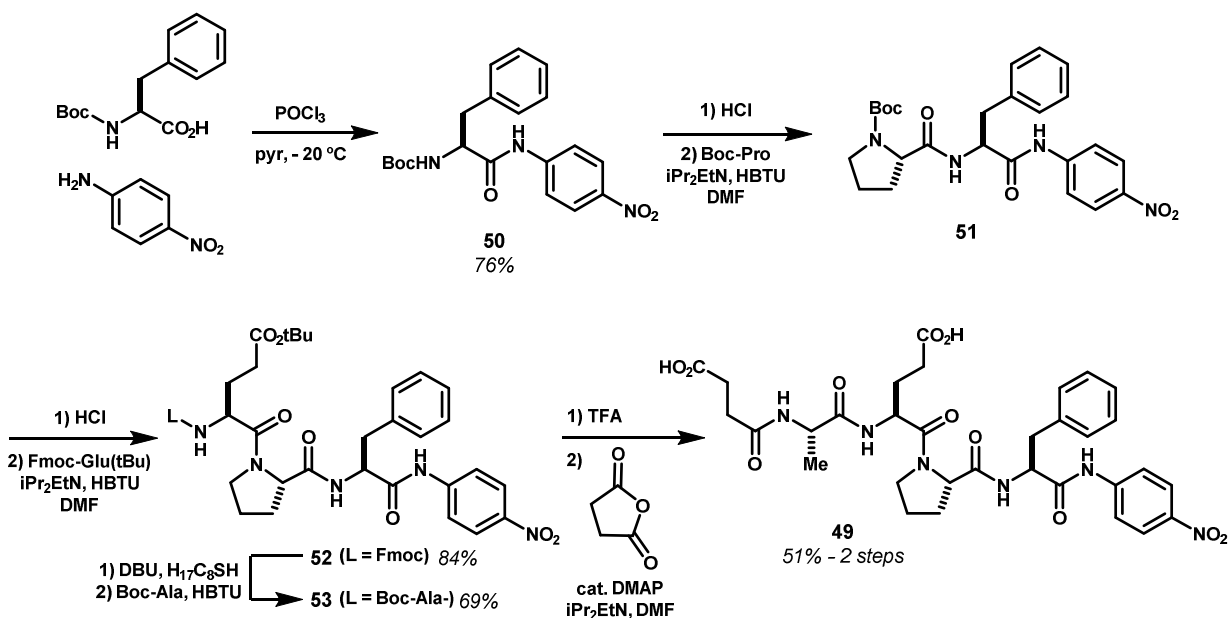


In the case of Pin1, the most widely used kinetic assay employs surrogate substrate Suc-Ala-Glu-Pro-Phe-*p*NA (**49**, Scheme 6.5.1), α -chymotrypsin as the auxiliary protease, and continuous spectrophotometric readout of the released *p*-nitroaniline.^{37,41,111,114,115} In this assay, α -chymotrypsin selectively hydrolyzes the phenylalanine amide bond of the *trans*-proline isomer, and minimally degrades Pin1 over the duration of the assay. By using high concentrations of α -chymotrypsin, the *trans* isomer is promptly degraded, and it becomes possible to observe pseudo-first order kinetics for the *cis* to *trans* isomerization. To increase the concentration of the higher energy *cis* isomer (~10 mol% in aqueous media), the substrate is first dissolved in a solution of anhydrous TFE containing 0.5 M LiCl. Presumably, chelation of the lithium ion stabilizes this isomer. In our hands, this led to an approximately 4-fold increase in the proportion of *cis* isomer.¹¹⁰ This perturbed equilibrium is kinetically retained through the solvent jump upon dilution into the aqueous assay buffer. Additionally, interference from the background reaction (i.e. k_{uncat}) can be reduced by cooling the reaction to 0 °C.¹¹⁰ This assay format has been used to survey the substrate preferences of Pin1 by using a series of phosphorylated substrates.³⁷ We established this assay in our laboratory in order to validate these reports, and to ultimately test macrocyclic Pin1 inhibitors.

Human *PIN1* was subcloned into a pGEX-6P-1 bacterial vector using the Gateway® recombinase system. Full-length hPin1 was expressed in *E. coli* (DH5 α) as an N-terminal GST fusion bearing a linker and PreScission protease site, though the intact fusion protein was used directly after affinity purification

on glutathione-sepharose. Over 30 mg of protein was produced from a single 6 L culture, and showed stable solubility (~6mg/mL) and PPLase activity.

Scheme 6.5.2. Synthesis of Pin1 surrogate substrate Suc-AEPF-pNA.

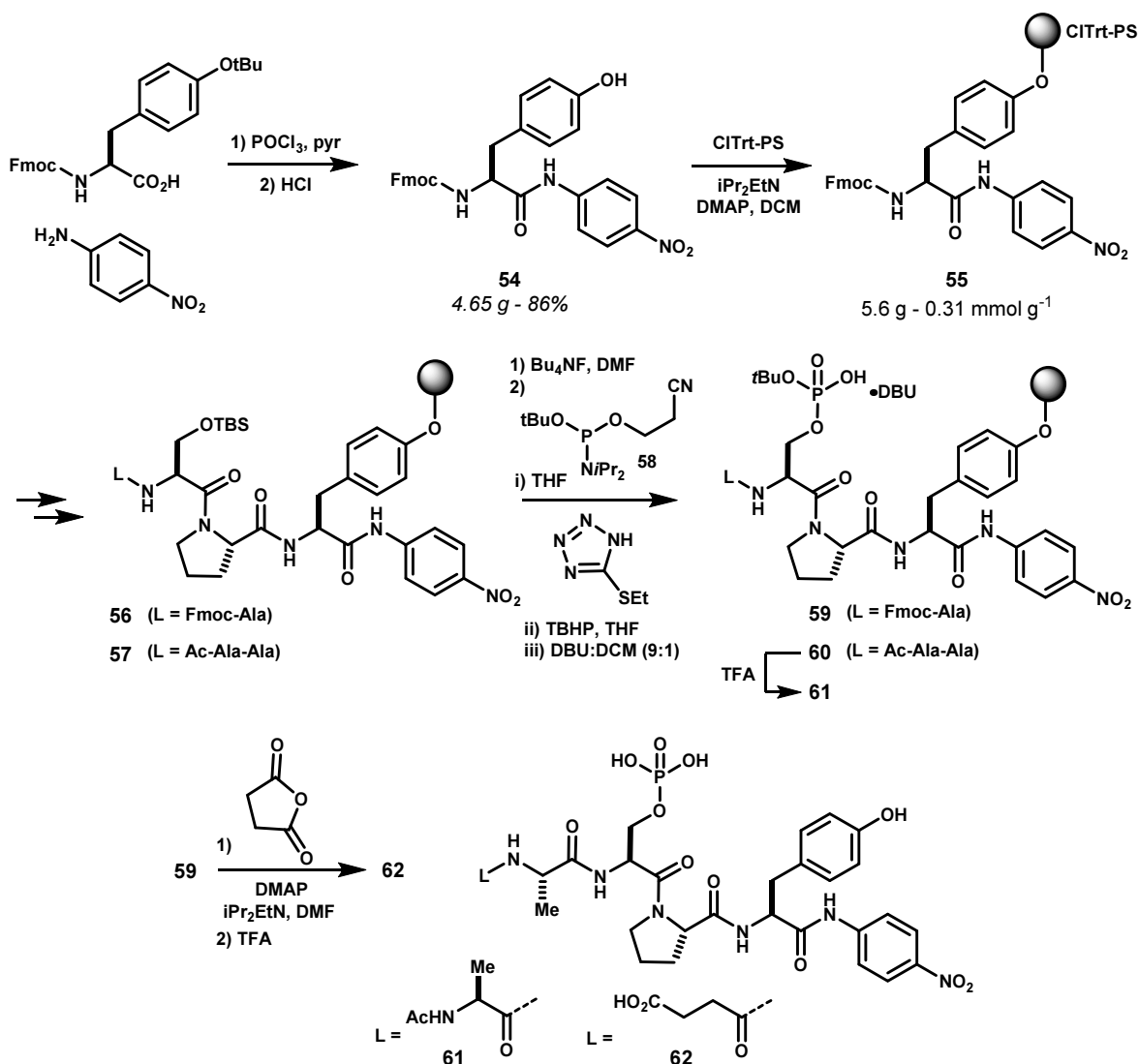


The reported peptidyl substrate Suc-AEPFpNA (**49**) was synthesized by solution-phase peptide synthesis starting from Boc-*L*-phenylalanine, which was transformed to the key *p*-nitroanilide by the action of POCl_3 in pyridine (Scheme 6.5.2).¹¹⁶ Chain extension was achieved in the usual way, except that orthogonally protected Fmoc-Glu($t\text{Bu}$)-OH was used in order to maintain the side chain protecting group. The Fmoc group was deprotected by the action of DBU in the presence of octyl mercaptan, alanine was coupled and deprotected, and the N-terminus was acylated with succinic anhydride to give **49**. This route sufficed to produce over 400 mg of this substrate.

We also prepared novel phosphorylated substrates Ac-AApSPYpNA (**61**) and Suc-ApSPYpNA (**62**) in order to verify the reported substrate preferences of Pin1, and to ensure that substrate 49 was a suitable surrogate for more precious phosphorylated substrates (Scheme 6.5.3). Protected tyrosine *p*-nitroanilide **54** was produced analogously to that of phenylalanine, and the side chain phenol was immobilized by attachment to 2-chlorotrityl chloride polystyrene resin. Chain extension using standard Fmoc solid phase techniques provided intermediates **56** and **57**. The serine side chain was then desilylated with Bu_4NF . On-resin phosphorylation of serine was achieved using unsymmetrically protected *O*- β -cyanoethyl-*O*'-tert-butyl

N,N-diisopropyl phosphoramidite (**58**) in the presence of 2-ethylthiotetrazole, followed by oxidation of the intermediate trialkyl phosphite by *tert*-butylhydroperoxide (TBHP) and β -elimination of the cyanoethyl group with DBU to generate the phosphate mono-*tert*-butyl ester (**59**, **60**) *in situ*.

Scheme 6.5.3. Synthesis of phosphorylated Pin1 substrates Ac-AApSPYpNA (**61**) & Suc-ApSPYpNA (**62**).



The individual kinetic constants (K_{cat} , K_m , K_{cat}/K_m) for Pin1-catalyzed isomerization of substrates **49**, **59** and **69** were determined using the α -chymotrypsin-linked continuous assay by construction of the complete Michaelis-Menten curves. For each kinetic run, a masked semi-micro cuvette containing the assay buffer was incubated in the spectrophotometer at 10 °C for two minutes. Though reported protocols conduct this reaction at 0–4 °C, we observed condensation and unacceptable baseline drift below 10 °C. For each

substrate, the proportion of the *cis* isomer was quantified by solvent jump experiments by running the reaction to completion and quantifying the proportion of *p*-nitroaniline released under biphasic kinetics of α -chymotrypsin cleavage (see details Experimental Appendix 6). A typical progress curve for this reaction is shown in Figure **6.5.1A**, wherein the addition of Pin1 (70 nM) causes a clear rate acceleration, as expected. In kinetic runs, the reaction was instead initiated by the addition of both chymotrypsin and substrate, and only the portion of this progress curve corresponding to Pin1-catalyzed turnover of the *cis* isomer was considered for kinetic analysis. Control experiments omitting either Pin1, α -chymotrypsin, or both made clear that the background thermal *cis-trans* isomerization remained a major competing pathway, and needed to be accounted for in kinetic analyses (Figure **6.5.1B**). Accordingly, we determined *catalyzed* initial rates over varying substrate concentrations (corrected also for %*cis* composition), and fit these data to the Michaelis-Menten equation to extract kinetic parameters K_{cat} , K_m , and K_{cat}/K_m (see Figure **6.5.1C**). These parameters are tabulated in Figure **6.5.1D**, and compared to reported substrates and K_{cat}/K_m values.³⁷ Our data confirmed that the phosphorylated substrates are indeed turned over at a faster rate, and exhibit higher affinity (K_m) towards the Pin1 active site by comparison to standard substrate Suc-AEPF-*p*NA. Additionally, our data for Ac-ApSPY-*p*NA (**62**) compared favorably with that reported by Yaffe and co-workers,³⁷ who obtained a similar value for K_{cat}/K_m for this substrate (K_{cat} , K_m not determined). However, in the case of substrate Suc-AEPF-*p*NA (**49**), we observed a K_{cat}/K_m that was approximate 10-fold lower than the reported value, but similar to values reported by Etzkorn¹¹⁷ and Ranganathan.⁴¹ Together, these data suggest that, despite showing relatively low affinity for Pin1, surrogate substrate **49** is an adequate model of native phosphorylated substrates, and that the non-peptidic succinyl moiety does not artificially enhance binding of this substrate. As noted by others,¹¹⁷ substrate **49** was accessible in larger quantities, and was therefore used subsequently in competition assays.

Using this kinetic assay, we next examined the competitive inhibition of Pin1 catalysis by reported inhibitor *D*-PEPTIDE (**3**, see Figure **6.1.1**) and template-constrained macrocyclic mimetics **33a–d** (see Scheme **6.3.1**). Given the relative difficulty, and low throughput of this assay, these compounds were qualitatively compared at 10 μ M in the reaction. The resulting progress curves are shown in Figure **6.1.1A**.

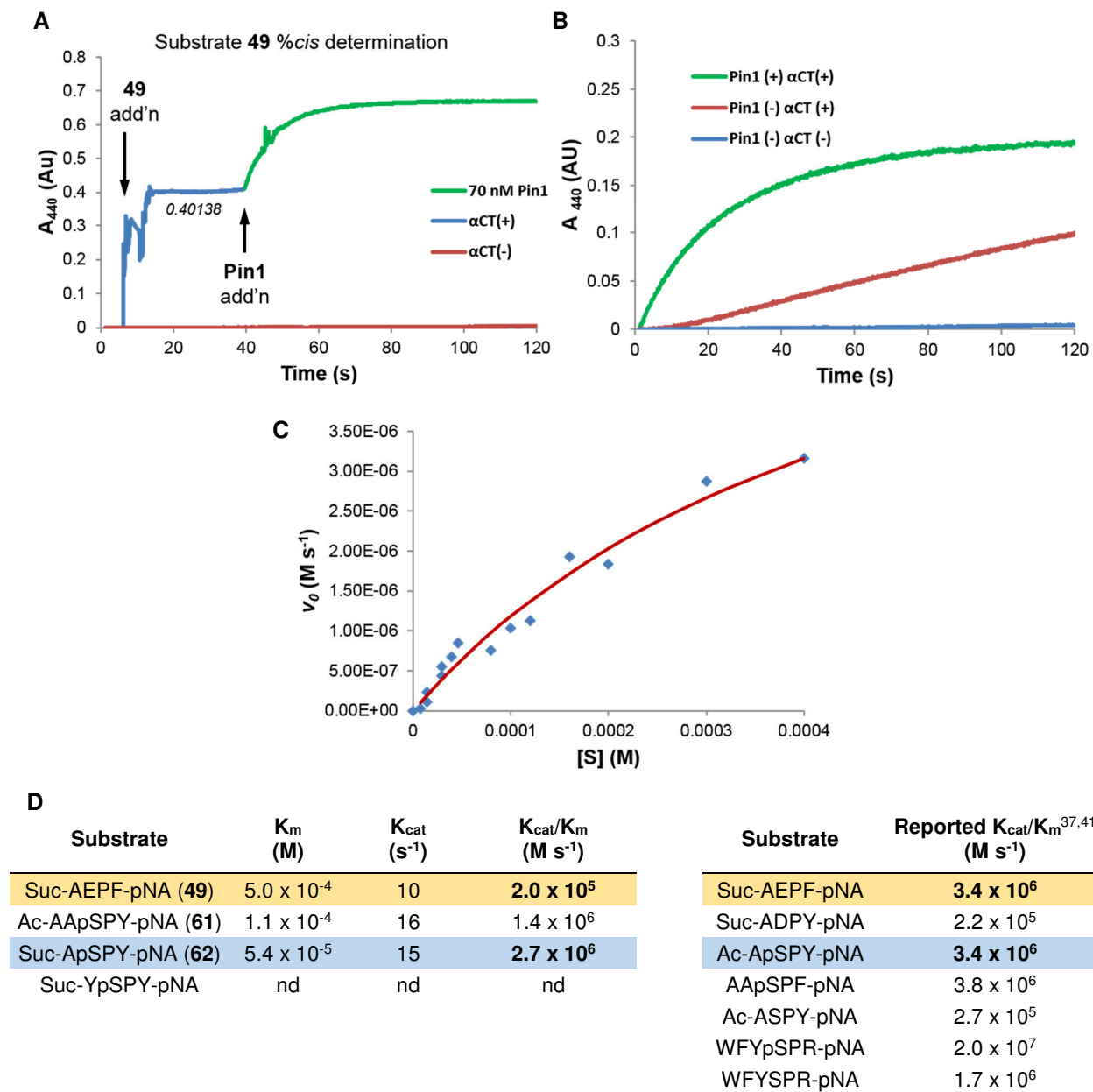


Figure 6.5.1. **A)** Complete progress curve for biphasic α -chymotrypsin hydrolysis of substrate **49** following solvent jump from TFE+0.5M LiCl showing rapid consumption of the *trans* prolyl isomer. Addition of Pin1 accelerates isomerization of the residual *cis* isomer, and allows calculation of the substrate *cis/trans* isomeric composition. **B)** Control experiments showing Pin1-catalyzed (**green**), thermal (**red**), and null (**blue**) turnover of the *cis* isomer of **49**. **C)** Initial rate data from substrate **49**, and fitting to the Michaelis-Menten equation allowed kinetic parameters to be extracted. **D)** Comparison of experimental K_m , K_{cat} and K_{cat}/K_m with reported values.

Control compound **3** showed good potency, as expected, and completely halted Pin1 catalysis at this concentration, resulting in substrate turnover at a rate identical to the background thermal isomerization. Interestingly, we observed substantially different activity between the macrocycle isomers **33a–d**. Though all four were less potent than **3**, compound **33b** clearly outperformed the remaining three isomers. Preliminary titration of this compound indicated an $IC_{50} = 162$ nM for **33b** (Figure 6.5.2B). Assuming competitive inhibition, this IC_{50} corresponds to $K_i \approx 270$ nM, which is approximately 10-fold higher than that reported for **3** (20.4 ± 4.3 nM).³⁶ Critically, these data bolstered our hypothesis that large ring constitution, and therefore shape, can significantly influence the biological activity of an embedded peptide motif. However, the aforementioned experiments highlighted major limitations in the throughput and precision of

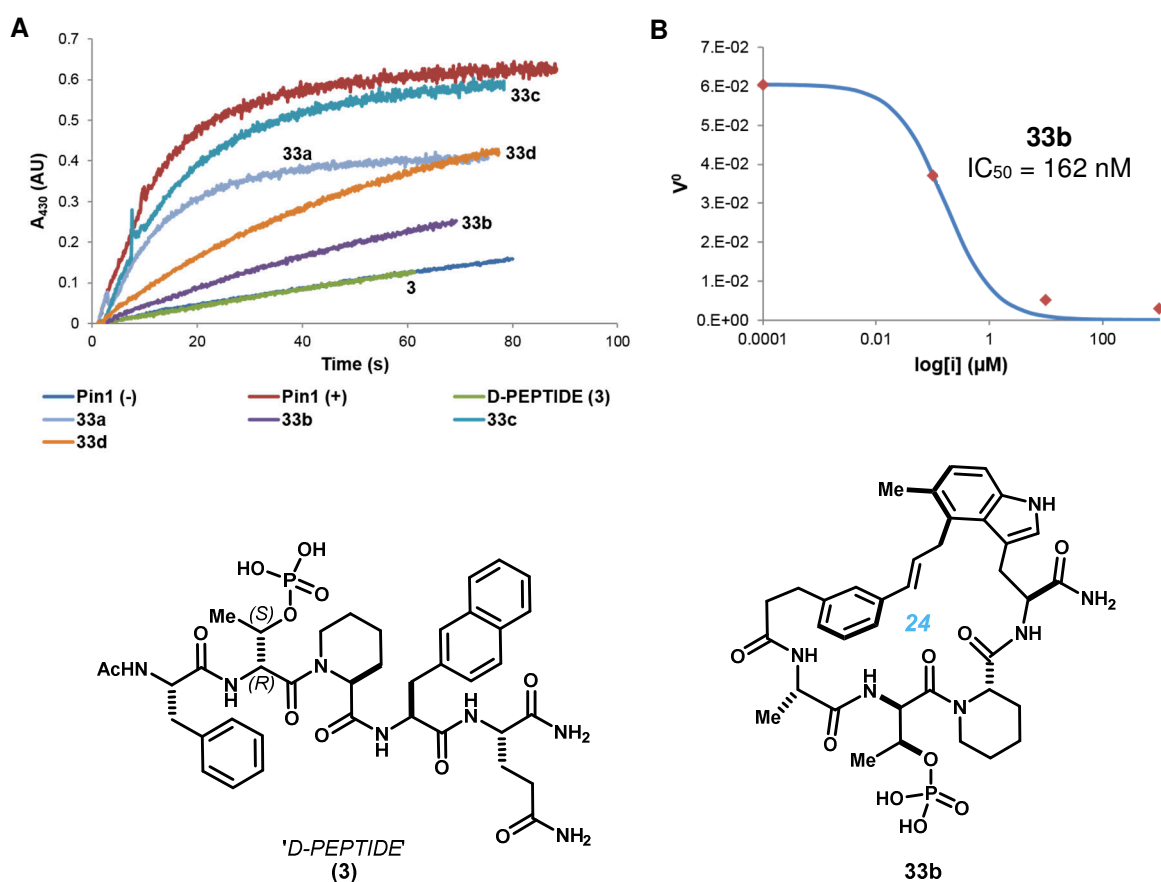


Figure 6.5.2. A) Comparison of reported inhibitor *D-PEPTIDE* (**3**, $K_i = 18\text{--}20$ nM)^{36,42} to template-constrained macrocycles **33a–d** at 10 μM . Macrocycle **33b** showed substantially higher potency than the remaining three isomers. **B)** Titration series for compound **33b**. Half-maximal inhibitory concentration was determined by non-linear least squares curve fitting to $v = v_{\text{max}} / (1 + [I]/IC_{50})$.

this kinetic assay, and suggested that an alternative assay was necessary in order to screen a larger collection of macrocycles.

Based on a reported Pin1 high-throughput screen reported by Pfizer⁴⁴ and high-affinity Pin1 WW domain-binding peptide sequences examined by a fluorescence-polarization (FP) assay,¹¹⁸ we aimed to develop a novel binding FP against the Pin1 PPlase domain. Interestingly, the sequence WFYpSPFLE was shown to bind both the Pin1 WW and PPlase domains in a phosphorylation-dependent manner.¹¹⁸ A fluorescently labeled variant of this peptide substrate was used to probe the Pin1 catalytic domain in a high-throughput screen conducted by Pfizer (the details of which are sparse).⁴⁴ For our purposes, we sought to adapt validated inhibitor *D*-PEPTIDE (**3**) to an analogous binding assay. Inhibitor **3** is reported to be completely selective for the PPlase domain over the WW domain.⁴² Fluorescently labeled *FITC-D*-PEPTIDE (**L63***, Figure 6.5.3) was synthesized by on-resin phosphorylation, analogously to phosphopeptides **61** and **62**, and solution-phase reaction with fluorescein 5-isothiocyanate. Ligand **L63*** was well-behaved in a series

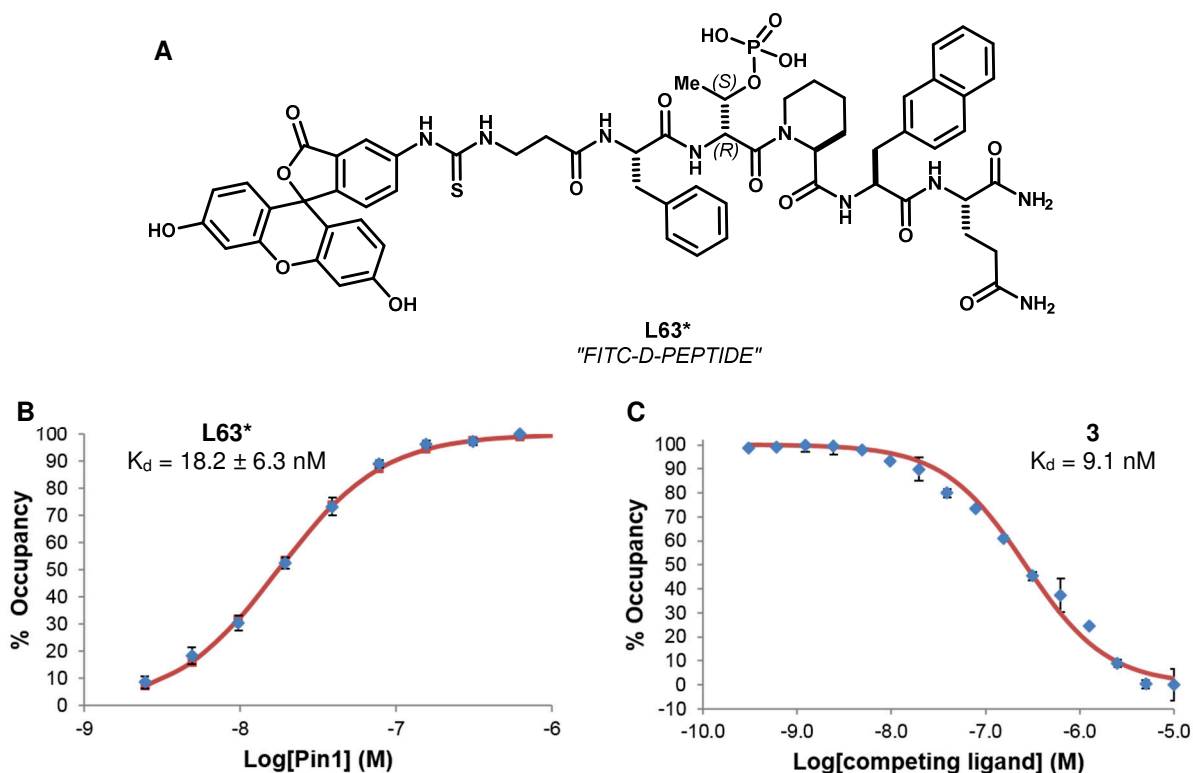


Figure 6.5.3. **A**) Fluorescein labeled *FITC-D*-PEPTIDE (**L63***) was synthesized for use in fluorescence polarization (FP) Pin1 binding assays. **B**) The dissociation constant of **L63*** was determined by equilibrium saturation binding by direct FP detection ($h = 1.3$). **C**) The dissociation constant of unlabeled *D*-PEPTIDE (**3**) and Pin1 (100 nM) was determined by competition binding with **L63*** (0.5 nM).

of control experiments conducted by us (see Chapter 6 Experimental Appendix),¹¹⁹ and showed strong fluorescence that was not quenched by Pin1. The dissociation constant was determined by equilibrium saturation binding (**L63*** = 5 nM) from titration of Pin1 (5 μ M \rightarrow 2.4 nM). These data were fitted to the Hill equation, which yielded $K_d = 18.2 \pm 6.3$ nM. This value was in exceptional agreement with the reported values $K_i = 20.4 \pm 4.3$ nM³⁶ and $K_i = 18.3 \pm 1.3$ nM⁴² determined by kinetic assays, and indicated that introduction of the FITC- β -alanine fragment neither disrupts nor enhances binding. In competition binding experiments with **L63*** (0.5 nM), unlabeled *D*-PEPTIDE (**3**) exhibited $K_d = 9.1$ nM, also consistent with reported values for this inhibitor.

Having verified the performance of **L63*** in competition binding with *D*-PEPTIDE, we next assayed additional control inhibitors **1** and **2** and isomeric macrocycles **33a–d** (Figure 6.5.4). Phosphorylated *D*-phenylalaninol derivatives **1** and **2** reported by Guo, Hou, and co-workers at Pfizer are among the most potent known Pin1 inhibitors, but are devoid of cellular activity.⁴⁴ Our novel FP assay confirmed that **1** was indeed potent ($K_d = 17$ nM), rivaling the affinity observed for peptidyl inhibitor **3**. Non-fluorinated analog **2** ($K_d = 44$ nM) was only 2.5-fold less potent than **1**; this result belied the reported 30-fold gain in potency in going from **2** to its fluorinated congener **1**.⁴⁴ Nonetheless, these inhibitors further substantiated the perform-

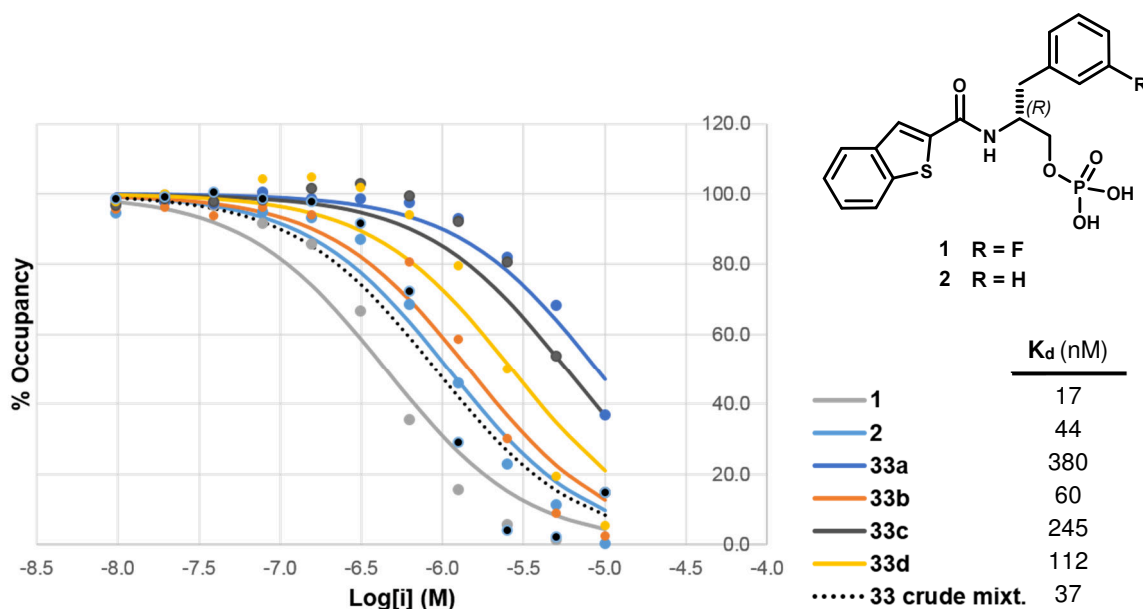


Figure 6.5.4. Binding isotherms showing that isomers **33a–d** exhibit different affinity towards the Pin1 PPIase domain depending on the connectivity of the macrocycle, with **33b** being most potent. The crude acidolysis mixture containing **33a–d** was also active. Control inhibitor **1** showed potent activity consistent with its reported value ($K_i = 6$ nM), whereas compound **2** did not ($K_i = 179$ nM).⁴⁴

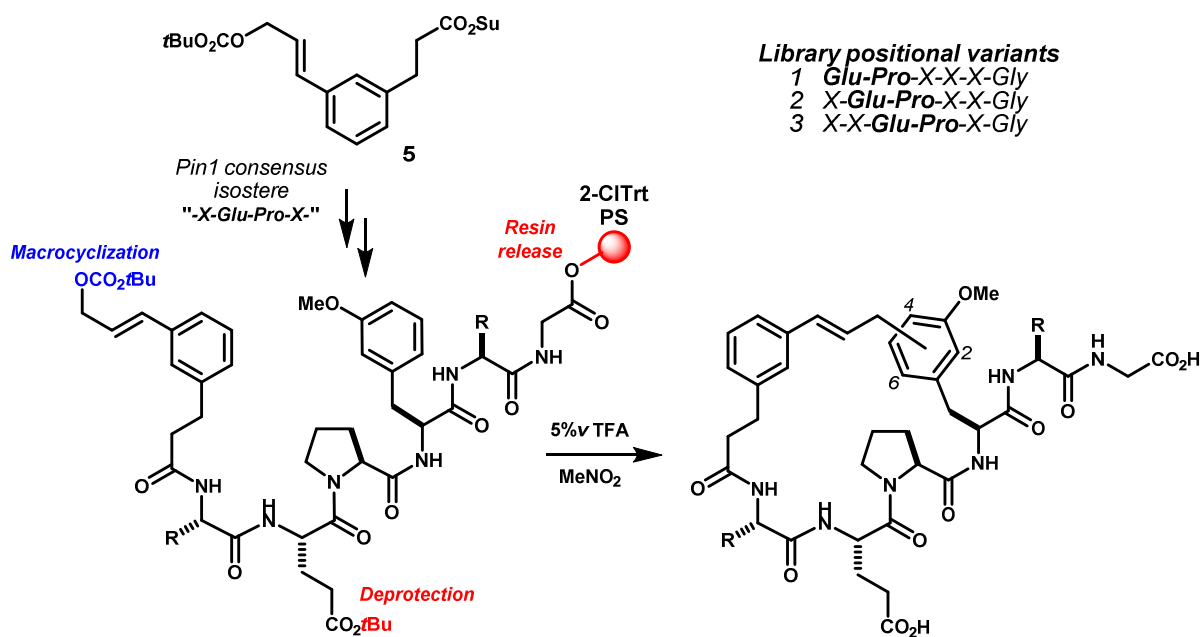
ance of our assay. As was observed using the kinetic assay (*vide supra*), isomers **33a–d** exhibited different potencies depending on the macrocycle connectivity. Indole *C4*-linked isomer **33b** was again most potent ($K_d = 60$ nM), followed by **33d** ($K_d = 112$ nM). Isomer **33c** ($K_d = 245$ nM) was more potent than **33a** ($K_d = 380$ nM). Notably, the crude acidolysis product mixture (**33 crude mixt.**) was also active. The apparent potency of the mixture exceeded that of any individual constituent, but this likely owed to inaccuracy of the sample concentration. The 6-fold difference in binding affinity between *C4*-linked isomer **33b** and *C7*-linked isomer **33c** was remarkable given the subtle difference between these molecules. This unprecedented outcome was a powerful demonstration of the utility of divergent macrocyclization reactions for small molecule lead discovery and optimization, which was in this case enabled by the designed reactivity of template **5**.

6.6 Construction, screening, and hit deconvolution of a mixture-based Pin1-targeted macrocycle library

Having established a suitably high-throughput fluorescence polarization (FP) Pin1 binding assay, we next moved to construct a pilot library of macrocyclic mimetics of the Pin1 substrate linear motif (LM) -Xxx-pSer-Pro-Xxx-. Our investigations of Pin1 kinetics confirmed that phosphorylation plays a critical role in substrate recognition (see Subsection 6.5). Accordingly, we initially aimed to integrate an on-resin phosphorylation step with our methods for synchronous resin release and template-induced macrocyclization. Though we made substantial progress towards this goal by use of tailored unsymmetrical phosphoramidites, we viewed the phosphoryl group as a substantial liability from a drug development standpoint. Indeed, reported phosphorylated inhibitors **1**, **2** and *D*-PEPTIDE (**3**) are inactive in cellular assays, presumably because the phosphoryl group – doubly anionic at physiological pH ($pK_{a2} \approx 5-6$)¹²⁰ – is unable to penetrate similarly charged lipid membranes. Furthermore, these and related inhibitors suffer a near complete loss of potency upon removal of the phosphoryl group.^{42,44} Mutation of the phosphate to a carboxylic acid or tetrazole is similarly detrimental,⁴⁵ though several non-phosphorylated inhibitors have been reported.^{121,122} Given these challenges, we cautiously opted to construct a collection of non-phosphorylated macrocycles by using Glu-Pro in place of the native pSer-Pro motif analogously to non-phosphorylated Pin1 surrogate substrate **49**. Though the glutamic acid side chain bears a negatively charged group at roughly the same distance from

the peptide backbone, the carboxylate is a decidedly poor isostere of the phosphoryl group given the drastic differences in charge delocalization, pKa (Glu \approx 4.1, pSer pKa₁ \approx -1, pKa₂ \approx 5-6), geometry, and hydration potential.^{123,124} Nonetheless, we remained optimistic that a diverse collection of peptidic macrocycles might overcome this energetically unfavorable, but pharmacologically favorable, isosteric replacement by optimization of the surrounding peptide side chains. While a conceptually related attempt to identify Pin1 inhibitors has been reported using phage display,¹²¹ the present methods differ substantially and explore entirely different chemotypes. Critically, we designed a pilot library which included non-proteinogenic amino acids, and a collection of phenylalanine and tryptophan analogues which had been shown to react in large ring-forming cinnamylation reactions (see Subsection 6.2). In this manner, we aimed to identify non-phosphorylated composite macrocycles bearing ring connectivities pre-organized to bind the Pin1 active site, as had been observed for isomeric phosphorylated macrocycles **33a–d** (see Subsection 6.5).

Scheme 6.6.1 Schematic overview of the resin-supported synthesis of acyclic template-containing intermediates and synchronous resin release/macrocyclization strategy. Library sequences comprised positional variants 1–3.



Pin1-targeted peptide sequences were designed within the three positional variants Glu-Pro-X-X-X-Gly, X-Glu-Pro-X-X-Gly, X-X-Glu-Pro-X-Gly, where positions X constituted randomly selected *L*-amino acids. Sequences contained at least one nucleophilic aromatic side chain. For practical reasons, histidine, arginine, cysteine and *D*-configured amino acids were excluded from this exercise. A complete list of

sequences prepared is given in the Experimental Appendix for this section. The C-terminal glycine was necessary for the synchronous resin release/macrocyclization strategy, and also ensured uniform resin loading across the entire library. Peptides were synthesized on 5 μ mol scale in parallel using two 48-well Bohdan MiniBlock™ reactors, and the N-termini were acylated with template **5**. Synchronous resin release and large ring-forming cinnamylation was achieved under optimized conditions with 5% v TFA in MeNO₂. Using this protocol, we were able to complete the assembly of hexapeptides and acylation with **5** in one work day, and then allow macrocyclization to proceed overnight, thereby freeing the reactors to begin a subsequent set of materials the following day. Pilot Library A, comprising product mixtures from 384 peptide sequences targeting the Pin1 PPlase domain, was completed in four days. Crude acidolysis product mixtures were individually diluted in DMSO as ~10 mM stock solutions for screening.

Forty randomly chosen samples (10% of the library) were analyzed by HPLC-UV/MS as a quality control check, which revealed a 90% synthetic success rate. Only four samples showed no products of characteristic mass. Though purity (UV area%) varied between sequences, those reactions which were successful contained primarily products of the expected molecular mass (see complete HPLC-UV data in Experimental Appendix). Major identifiable byproducts included cinnamyl trifluoroacetate esters, as expected (see Subsection 6.4), and tritylated materials in sequences bearing asparagine. The latter derived from the use of Fmoc-Asn(Trt), which was found to be requisite for successful peptide synthesis, but is evidently poorly deprotected under the present acidolysis conditions. Additionally, these analyses indicated an average of 2.9 ± 1.4 apparent products per sequence, or an estimated library size of >1002 members; broad analysis conducted for Focused Library A indicated 4.4 ± 1.4 products per sequence, or an estimated >1690 members. These relatively small number of products per sequence reflect the narrowing of product distributions observed in cinnamylation reactions of 5-substituted tryptophans in proline-containing sequences (see Subsection 6.3). In some cases, reactions appeared to give only one product, consistent with the expected selectivity of side chains such as tyrosine and 4-methoxyphenylalanine.

Pilot Library A, comprising 384 *mixtures*, was screened for Pin1 binding using our FP assay for competitive displacement of tight-binding ligand **L63***. In order to assess the role the substrate-mimetic -Glu-Pro- motif, we assayed both targeted sequences (Mol. ID **A0193–A0576**) and a collection of non-

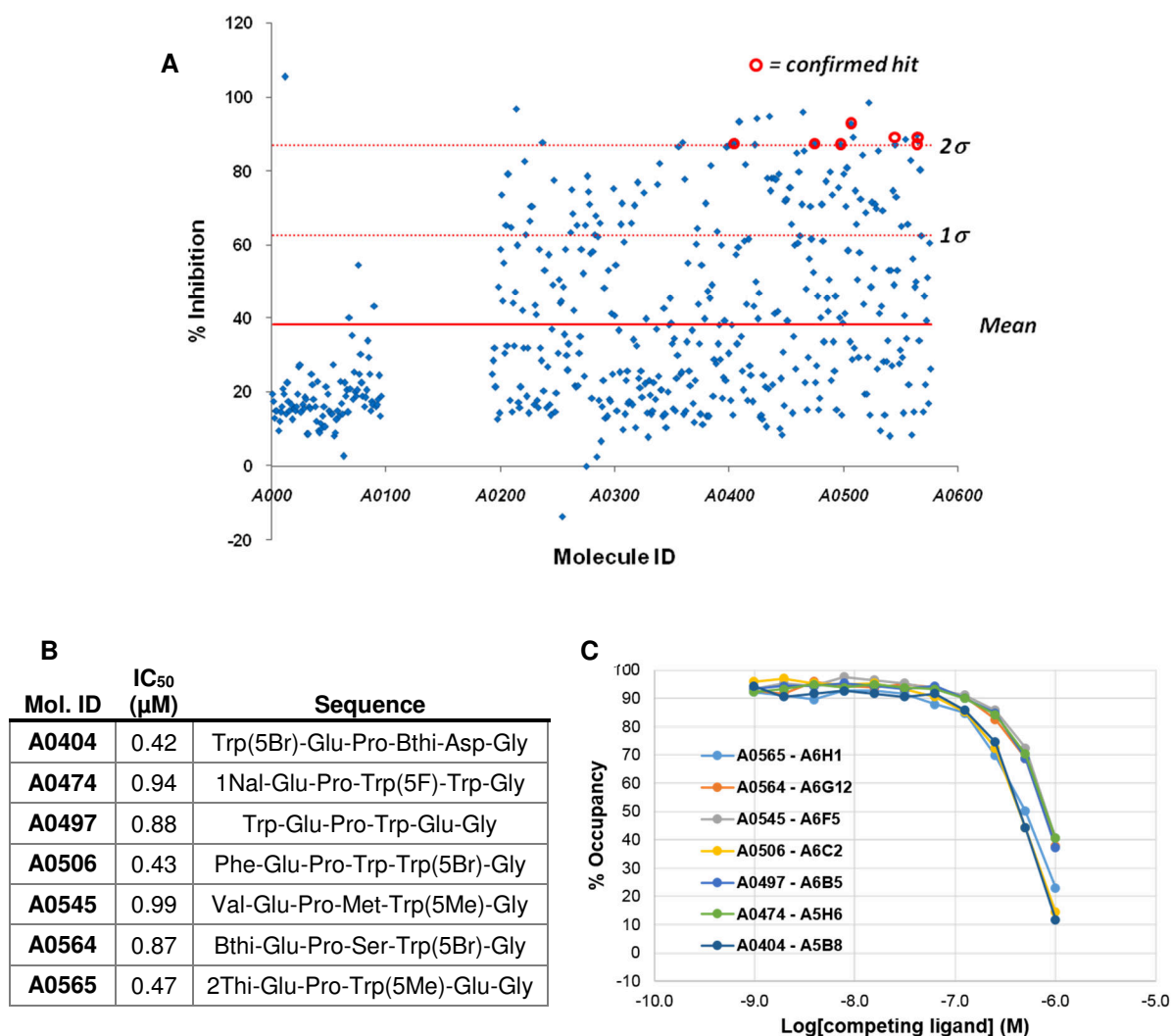


Figure 6.6.1 **A**) Data from the mixture-based singlicate screening at 10 μM of macrocycle sets **A0001–A0096**^a (non-targeted) and **A0193–A0576**^a (Pin1-targeted)^a showed greater activity across peptides bearing the substrate-mimicking -Glu-Pro- motif. Confirmed hit (red circles) showed initial activity >2σ above the mean at 10 μM and retained activity at 1 μM. **B**) Hit sequences and associated IC₅₀ values. **C**) Half-maximal inhibitory concentrations (IC₅₀) were estimated by non-linear least squares fitting to partial binding curves (see Experimental Appendix 6). ^aMol IDs **A0097–A0192** were unfilled library wells.

targeted sequences that had been accumulated in the course of synthetic methods development (Mol. ID **A0001–A0096**, Figure 6.6.1A). From a primary screen at 10 μM, we identified 21 hits which lied above a relatively stringent cutoff of +2σ from the mean (i.e. > 87% inhibition at 10 μM). Markedly lower activity was observed within the non-targeted set, which suggested that the designed isosteric substrate -Glu-Pro- motif was important for binding. However, this may also be due to the limited sequence diversity and smaller size of this non-targeted collection. Hits were re-screened at 1 μM, and the seven mixtures which retained

activity were titrated to estimate IC_{50} (Figure 6.6.1B,C), and were analyzed by HPLC-UV/MS to assess the tractability and identity of the mixture (see full data in Experimental Appendix). Interestingly, all seven hit sequences shared the positional sequence X-Glu-Pro-X-X-Gly. Additional sequence similarity was observed between hits **A0404**, **A0474**, **A0497**, **A0506** and **A0565**, which harbored aromatic side chains at P1 and P4, and specifically tryptophan-type side chains at P4. Additional similarity was noted within sequences **A0404**, **A0497** and **A0565**, which all possessed an acidic side chain (Glu or Asp) at P5. These preliminary trends lent credence to the observed activity, as did the apparent preference for aromatic side chains also seen in inhibitor *D-PEPTIDE* (**3**)⁴² and reported high-affinity substrate sequences (see Figure 6.1.2).³⁷

The seven hits were re-synthesized on 25 μ mol scale in order to deconvolute and validate the activity of these mixture. Seven analogous des-glycine analogs bearing C-terminal carboxamides (e.g. **A0404 Δ Gly**) were also synthesized. In both series, acyclic materials bearing template **5** were purified prior to acid-promoted macrocyclization in order to maximize purity of the resulting mixtures. Acidolyses were carried out in the same manner as previously, and the resulting product mixtures were fractionated by preparative HPLC and diluted as 10 mM DMSO stock solutions. These acidolysis reactions gave product mixtures which were consistent with their library counterparts (see details Experimental Appendix). However, these semi-purified fractions showed unexpectedly lower activity than predicted from the primary mixture-based screen (Figure 6.6.2A,B). Constituents of hit **A0404** retained low micromolar IC_{50} , as did **A0474**, **A0564** and **A0565**. Surprisingly, however, removal of the C-terminal glycine from **A0564** and **A0565** led to a significant loss of potency, whereas activity remained comparable in the case of des-glycine analogs **A0404 Δ Gly** and **A0474 Δ Gly**. Surprisingly, a single component from des-glycine sequence **A0506 Δ Gly** – the parent sequence of which was relatively less active upon re-synthesis – was highly active.

Sequences **A0404** and **A0506 Δ Gly** contained constituents of highest apparent affinity for Pin1, and were therefore pursued further. Closer inspection of the binding curves for individual components of these mixtures revealed several salient features (Figure 6.6.2C). In the case of **A0404**, the three resolved fractions showed nearly equal potency. This observation ran counter to our expectation that isomeric macrocycles would display differential activity. Indeed, in the case of **A0506 Δ Gly**, fraction **A** exhibited markedly greater activity ($\geq 25\times$) than any of the four remaining isomeric fractions (Figure 6.6.2C). Fraction

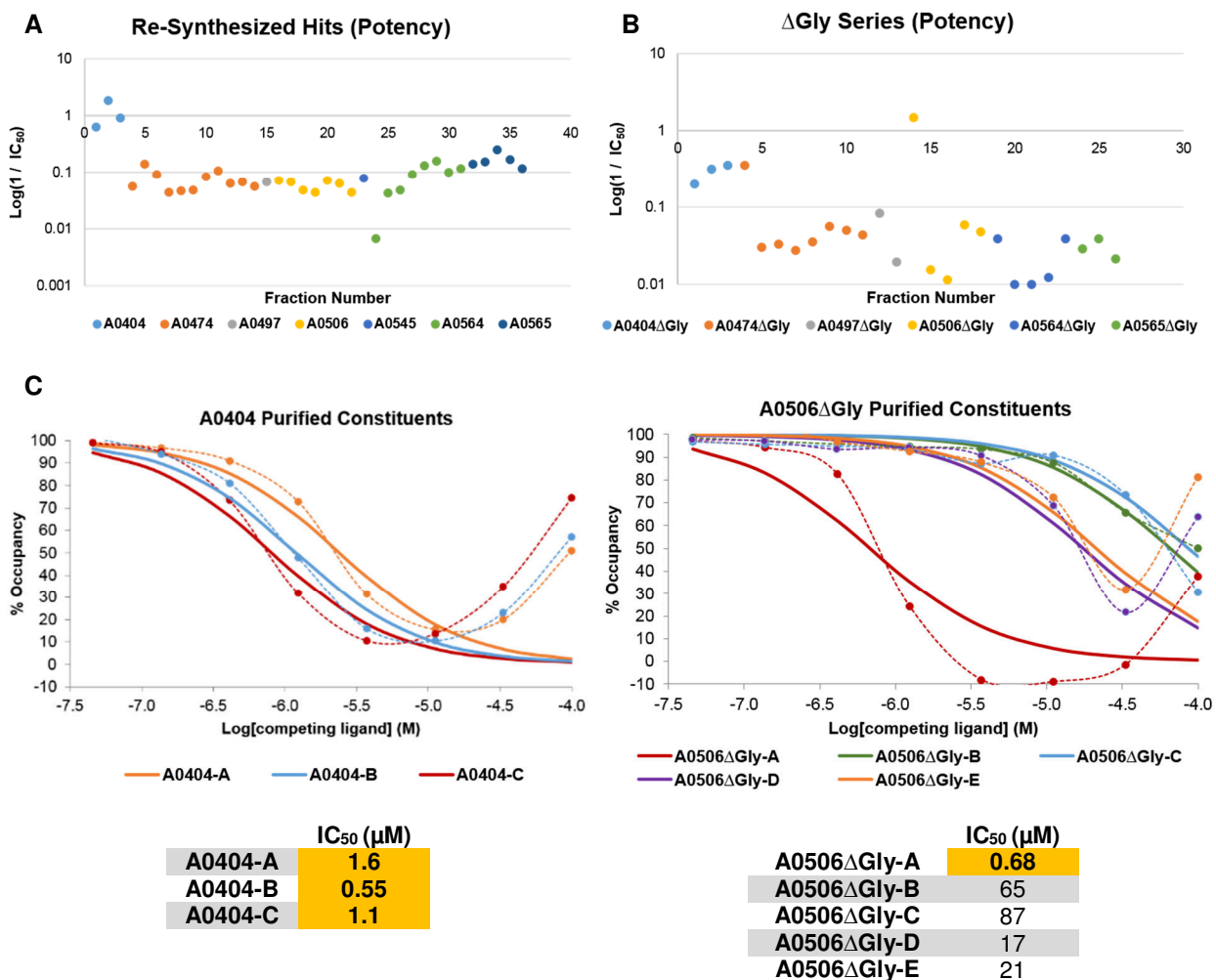


Figure 6.6.2 Pin1 FP assay of partially purified constituents of hits. Potency visualized as $\log(1/IC_{50})$. **A)** Re-synthesized hits showed generally lower activity than predicted from the primary screen. **B)** Removal of the N-terminal glycine generally led to a decrease in potency. **C)** Binding isotherms (dashed = experimental, solid = best-fit) and calculated half-maximal inhibitor concentrations (IC_{50}) for isolated components of sequences **A0404** and **A0506 Δ Gly**. Anomalous signal at concentrations $> 10 \mu$ M was excluded from least squares analysis.

A0506 Δ Gly-A appeared to exhibit a positive Hill coefficient, which may suggest positive cooperativity. Notably, in this FP assay format, we frequently observed anomalous polarization data at concentrations $> 10 \mu$ M, which limited the accuracy of IC_{50} measurements. This behavior was restricted to macrocyclic materials, appeared to be exacerbated by higher purity samples, and was *not* observed with control inhibitors **1**, **2** or **3**. This behavior appeared to be consistent with inhibitor aggregation,^{125–127} and may warrant future optimization and more rigorous statistical validation of this assay. Highest activity components **A0404-B** and **A0506 Δ Gly-A** exhibited $K_i = 65 \mu$ M and 7.7μ M, respectively, in preliminary tests

using the chymotrypsin-linked kinetic assay (data not shown). The relatively poor performance of these two components in this secondary assay, while not rigorously confirmed at the time of writing, prompted us to determine the structures of these materials and to construct focused libraries in an effort to optimize inhibitor potency.

Sequences Trp(5Br)-Glu-Pro-Bthi-Asp-Gly and Phe-Glu-Pro-Trp-Trp(5Br)-Gly, corresponding to **A0404** and **A0506 Δ Gly**, were again re-synthesized on larger scale (0.2 mmol) to facilitate isolation and

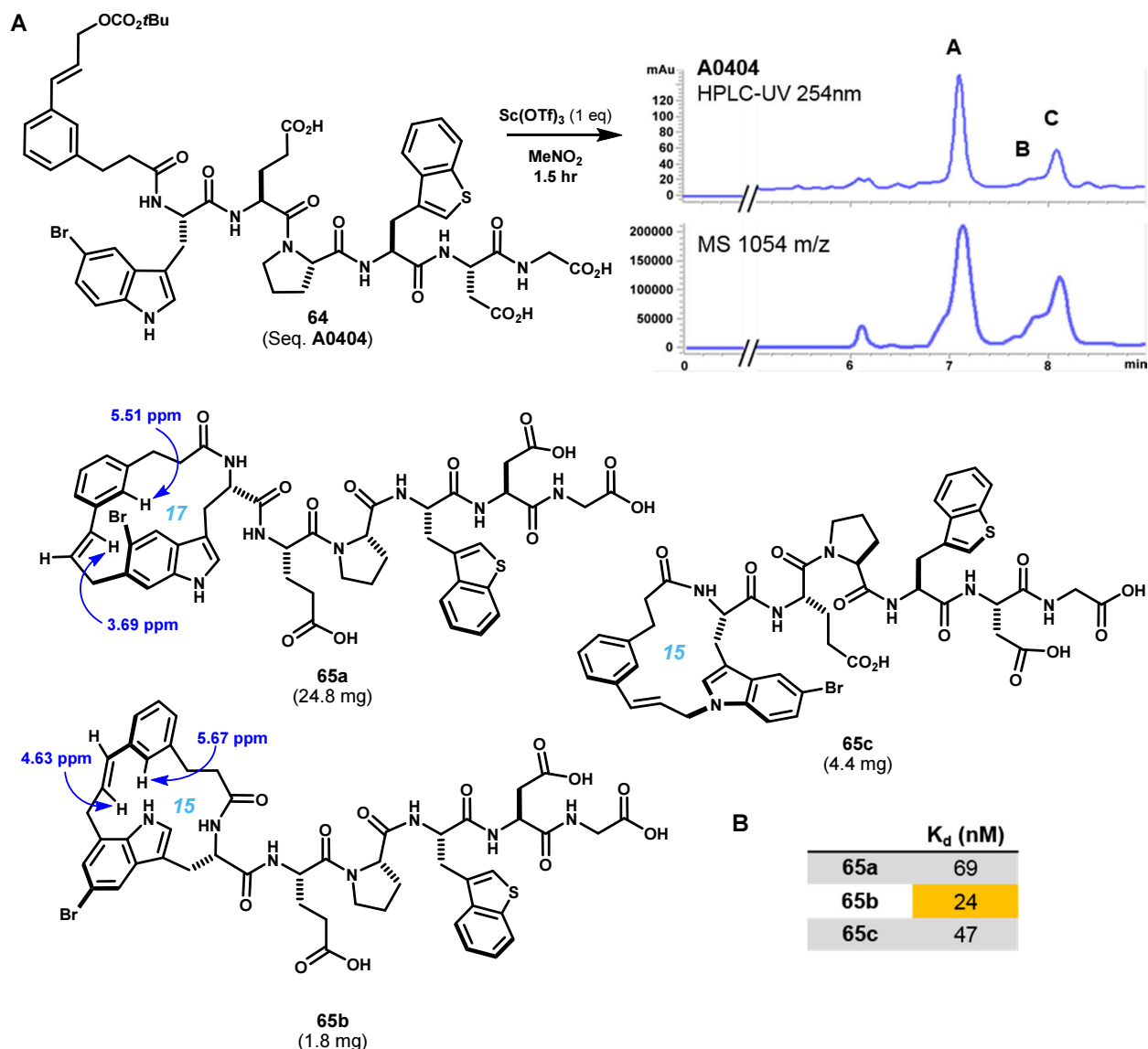


Figure 6.6.3 A) Scale up of hit **A0404**. Acidolysis of acyclic intermediate **64** allowed isolation and structure elucidation of the isomeric macrocycles **65a**, **65b** and **65c** bearing 15- or 17-member rings. Unusual ^1H chemical shifts were observed for **65a** and **65b**, consistent with compact *ansa*-bridged structures.

B) Dissociation constants of ligands **65a–c** determined by competitive FP assay with **L63***.

structure determination of acidolysis products. The abundance of exceptionally scarce component **A0404-B** was enhanced somewhat by the use of $\text{Sc}(\text{OTf})_3$ (1 eq) in MeNO_2 in the macrocyclization step, whereas the standard conditions with 5% v TFA in MeNO_2 were optimal for **A0506 Δ Gly**. Products were isolated by preparative HPLC and structures were unequivocally assigned on the basis of 2D ^1H - ^1H and ^1H - ^{13}C NMR correlation spectra in the same manner as previously (see details Subsection 6.4, Experimental Appendix).

Three products were isolated from the acidolysis reaction of acyclic intermediate **64** (hit sequence **A0404**, Figure 6.6.3A). These resulted from cinnamylation of the 5-bromotryptophan side chain at indole *N1* (**65c**), *C6* (**65a**) and *C7* (**65b**). These outcomes represented the first instances of cyclizations on a P1 side chain other than that of tryptophan itself. The relatively small 15- and 17-membered rings of **65a** and **65b** exhibited atypical ^1H chemical shifts within the bridging cinnamyl group as a result of shielding by the proximal indole aromatic ring current (Figure 6.6.3). Surprisingly, alkylation of 5-bromotryptophan had entirely outcompeted alkylation of benzothienylalanine in this case. The similarity between structures **65a**–**65c** explained their relatively uniform affinity for Pin1. Presumably, the distal macrocyclic motifs bear little influence on the substrate mimicking Glu-Pro sequence.

Six products were obtained from acidolysis of acyclic intermediate **66** (hit sequence **A0506 Δ Gly**, Figure 6.6.4). These resulted from cinnamylation of the P4 tryptophan side chain at indole *C2* (**67b1**), *C3* (**67e1**) and *C5* (**67c3**) and also of the P5 5-bromotryptophan side chain at indole *C2* (**67a3**) and *C6* (**67c1**). Pyrroloindoline product **67e1** was obtained as the *endo* diastereomer, consistent with all previously identified structures of this type. The activity of this mixture was attributed solely to compound **67a3** ($K_d = 35$ nM). Due to the aforementioned limitations of our FP assay, we were unable to accurately determine the affinity of the other isomers. The greater than 7-fold increase in potency between 26-membered ring **67a3** and all other isomers was remarkable. Product **67b1**, also a 26-membered ring, was inactive, suggesting that connectivity of the macrocycle at the P5 side chain was critical. However, product **67c1**, connected at the P5 5-bromotryptophan (doubly *ansa*-bridged), was also inactive, despite differing from **67a3** (singly *ansa*-bridged) by only three ring atoms. Presumably, these six *ansa*-bridged macrocycles occupy meaningfully different conformations, certain of which are predisposed to bind Pin1. Whether this observed dependence of binding affinity on macrocycle connectivity represents a general approach to ligand optimization by substrate mimicry or an isolated instance of an avid small molecule remains to be

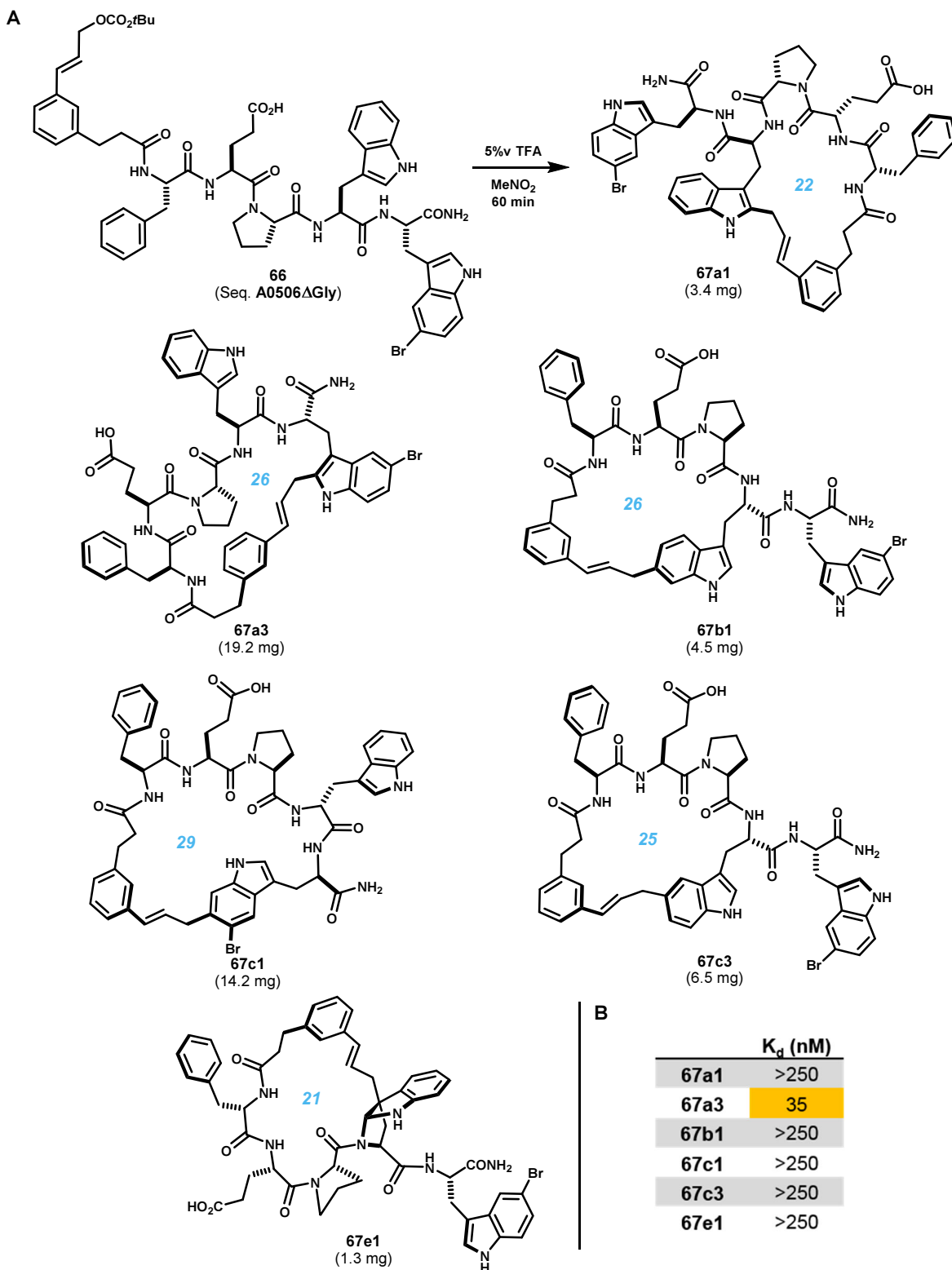


Figure 6.6.4 A) Macrocyclic products isolated and characterized from acidolysis of acyclic intermediate **66** (hit sequence **A0506ΔGly**). **B)** Dissociation constants of ligands **67a1**, **a3**, **b1**, **c1**, **c3** and **e1** determined by competitive FP assay with **L63***.

seen. Regardless, these non-phosphorylated ligands (**65b** and **67a3**, specifically) exhibited binding affinities which rivaled high-affinity phosphorylated inhibitors including **1**, **3**.

We next synthesized two focused libraries starting from the hit sequences of **A0404** and **A0506 Δ Gly** in order to assess structure-activity relationships (SAR) within these two series (Table **6.6.1**). Only single mutations were made in order to maintain pairwise comparisons. Mutations were designed to test the contribution of side chains at each position to the observed Pin1 binding affinity. In the case of **A0506 Δ Gly**, three alternative side P5 side chains were examined, each of which were expected to yield at least one product connected analogously to macrocycle **67a3**. Acyclic peptide-template **5** conjugates were synthesized in parallel, purified, and treated with 5%v TFA in MeNO₂ to induce cyclization and side chain deprotection. The resulting mixtures were then fractionated by HPLC giving 181 total fractions, which were diluted as 10 mM DMSO stocks for testing. Only Focused Library A had been parsed at the time of writing.

Table 6.6.1 Focused libraries (single mutations only) synthesized based on hit sequences **A0404** and **A0506 Δ Gly**. ^a Synthesized by on-resin phosphorylation. ^b Pip = *L*-pipecolic acid. ^c Mor = (*S*)-morpholine-2-carboxylic acid.

Focused Library A

Parent	Trp5Br	Glu	Pro	Bthi	Asp	Gly
A0404						
68	Trp5Br	Glu	Pro	Trp	Asp	Gly
69	Trp5Br	Glu	Pro	Thi	Asp	Gly
70	Trp5Br	Asp	Pro	BThi	Asp	Gly
71	Trp5Br	D-Glu	Pro	BThi	Asp	Gly
72	Trp5Br	Ser	Pro	BThi	Asp	Gly
73	Trp5Br	pSer^a	Pro	BThi	Asp	Gly
74	Trp5Br	Glu	Pip^b	Bthi	Asp	Gly
75	Trp5Br	Glu	Mor^c	Bthi	Asp	Gly
76	Ala	Glu	Pro	Bthi	Asp	Gly
77	Tyr	Glu	Pro	Bthi	Asp	Gly
78	Trp5F	Glu	Pro	Bthi	Asp	Gly
79	Trp5Me	Glu	Pro	Bthi	Glu	Gly
80	Trp5Br	Glu	Pro	Bthi	Glu	Gly
81	Trp5Br	Glu	Pro	Bthi	Ala	Gly

Focused Library B

Parent	Trp	Glu	Pro	Trp	Trp(5Br)
A05060					
Δ Gly					
82	Ala	Glu	Pro	Trp	Trp(5Br)
83	Tyr	Glu	Pro	Trp	Trp(5Br)
84	1Nal	Glu	Pro	Trp	Trp(5Br)
85	2Nal	Glu	Pro	Trp	Trp(5Br)
86	Phe	Ala	Pro	Trp	Trp(5Br)
87	Phe	D-Glu	Pro	Trp	Trp(5Br)
88	Phe	Ser	Pro	Trp	Trp(5Br)
89	Phe	D-Ser	Pro	Trp	Trp(5Br)
90	Phe	Glu	Pip^b	Trp	Trp(5Br)
91	Phe	Glu	Mor^a	Trp	Trp(5Br)
92	Phe	Glu	Pro	Ala	Trp(5Br)
93	Phe	Glu	Pro	Phe	Trp(5Br)
94	Phe	Glu	Pro	1Nal	Trp(5Br)
95	Phe	Glu	Pro	2Nal	Trp(5Br)
96	Phe	Glu	Pro	Trp	Trp(5F)
97	Phe	Glu	Pro	Trp	Trp(5Me)
98	Phe	Glu	Pro	Trp	Phe(3OMe)

Focused Library A was screened at 1 μ M in duplicate using the Pin1 FP assay and analyzed for structure-activity correlations. As expected, substantial activity was observed across analogs in this library, and therefore hits were stringently defined as lying above one standard deviation of the mean (i.e. >89%

inhibition, Figure 6.6.5). Sequences which contained at least one hit were then titrated to determine IC_{50} of *all* isomeric constituents. These experiments revealed several unexpected features which appear to drive binding. Critically, the central Glu-Pro motif was relatively insensitive to the changes made. Expanding the pyrrolidine ring of proline to either a piperidine ring (74) or morpholine ring (75) had little effect on binding.

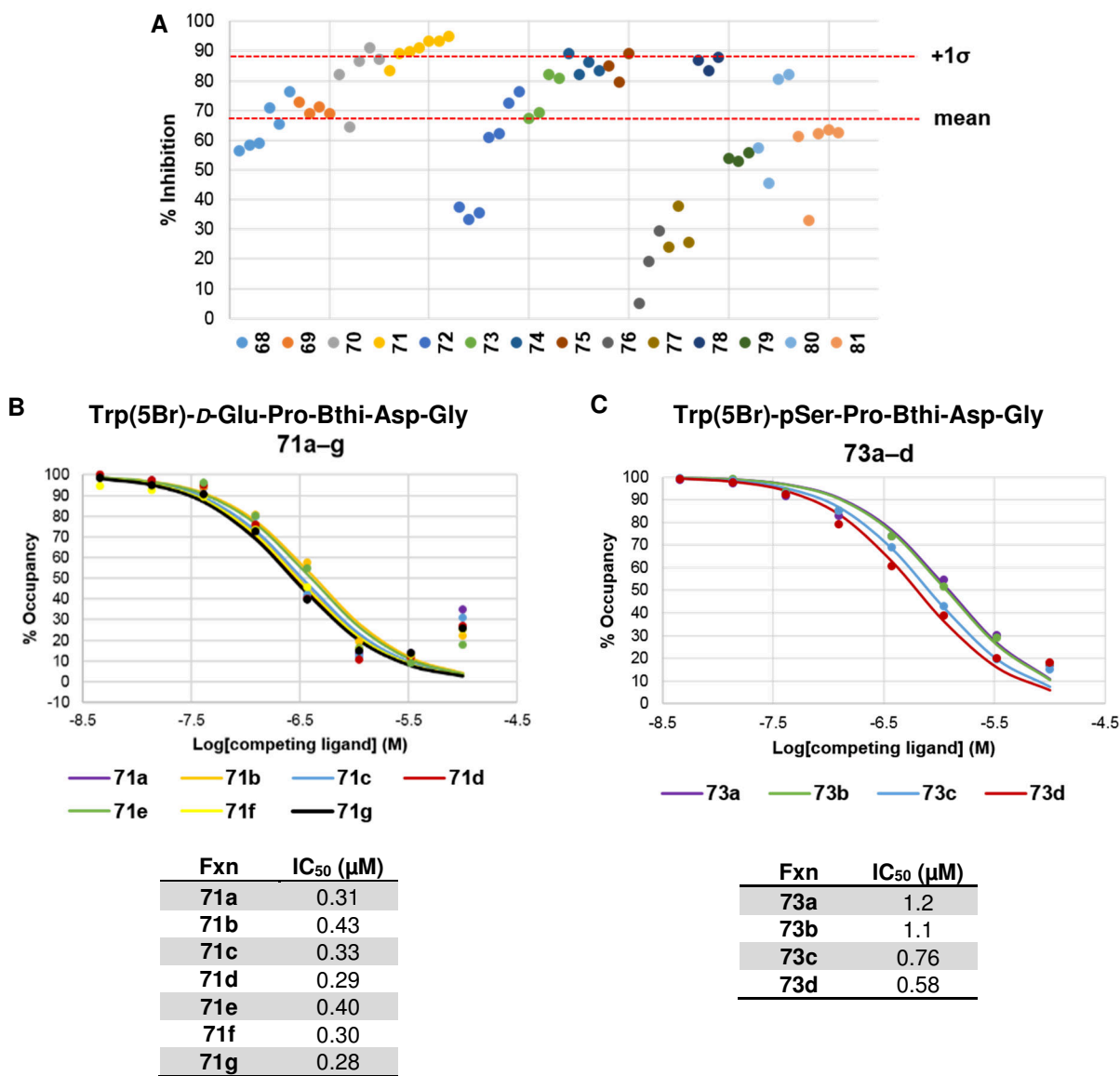


Figure 6.6.5 A) Duplicate screening of Focused Library A at 1 μM by competitive FP binding assay. All components of mixtures containing at least one component $>1\sigma$ of mean (i.e. $\geq 89\%$ inhibition) were titrated to determine IC_{50} . **B,C)** Selected binding isotherms of refined sequences. Components of non-phosphorylated *D*-Glu-containing sequence **71** showed greater affinity than the analogous pSer sequence **73**.

Changing the glutamic acid side chain to aspartate (**70**) resulted in a moderate *gain* in potency. Additionally, substituting glutamate for phosphoserine (**73**), presumed to more closely mimic the native substrate motif, was detrimental. Surprisingly, two components derived from the corresponding non-phosphorylated sequence (**72**) were only moderately less potent. These correlations run contrary to the changes in $\text{Pin1 } K_{\text{cat}}/K_{\text{M}}$ observed for the analogous *substrate* pS Δ S, pS Δ D or pS Δ E mutations observed by others,³⁷ and changes in K_{M} upon mutation pS Δ E observed by us (see Subsection 6.5). Strikingly, however, changing the stereochemical configuration of Glu2 from *L*- to *D*- (**71**) led to an *increase* in binding affinity. Curiously, cyclization of this sequence also appeared to yield more products than parent sequence **A0404**. This beneficial inversion of configuration at glutamic acid, while highly unusual, reflects an analogous finding which led to reported inhibitor *D*-PEPTIDE (**3**) bearing *D*-pThr.⁴² To our knowledge, no inhibitors based on *D*-Glu have been reported.

Beyond the substrate-mimicking Glu-Pro motif, a particularly strong dependence was observed for the P1 side chain. Changing only the halogen from 5-bromo- to 5-fluorotryptophan (**78**) yielded comparably avid materials, whereas substitution for 5-methyltryptophan (**79**) resulted in a significantly lower affinity. P1 Mutation of P1 to tyrosine (**77**) or alanine (**76**) led to a complete loss of activity. Similarly, mutations of the P4 benzothienylalanine to either thienylalanine (**68**) or tryptophan (**69**) were detrimental. These reactive arenes likely compete in the large ring-forming step, and the resulting P4 macrocycles may incidentally destabilize binding. Homologation of the P5 aspartic acid side chain to glutamic acid (**80**) was tolerated, whereas mutation to charge-neutral side chain alanine (**81**) led to a drop in binding affinity. This apparent preference for anionic moieties near the C-terminus has not, to our knowledge, been noted previously. Whether these differences result from a novel binding mode, or from true mimicry of the substrate linear motif is not yet known. Efforts to elucidate the structures of these ligands (e.g. **71**), to further refine activity of series **A0404**, and to assess the performance of Focused Library B were ongoing at the time of writing.

Though these apparent improvements to parent sequence **A0404** have not yet been validated in a secondary assay or attributed to discrete structures, this focused library illustrates the straightforward and rapid process of examining key binding interactions within the peptide domain of composite macrocycles. Iterative sequence optimization in this manner is often effective, and is possible for all peptide-based ligand discovery approaches, including conventional peptide macrolactams¹²⁸ and internally disulfide-bridged

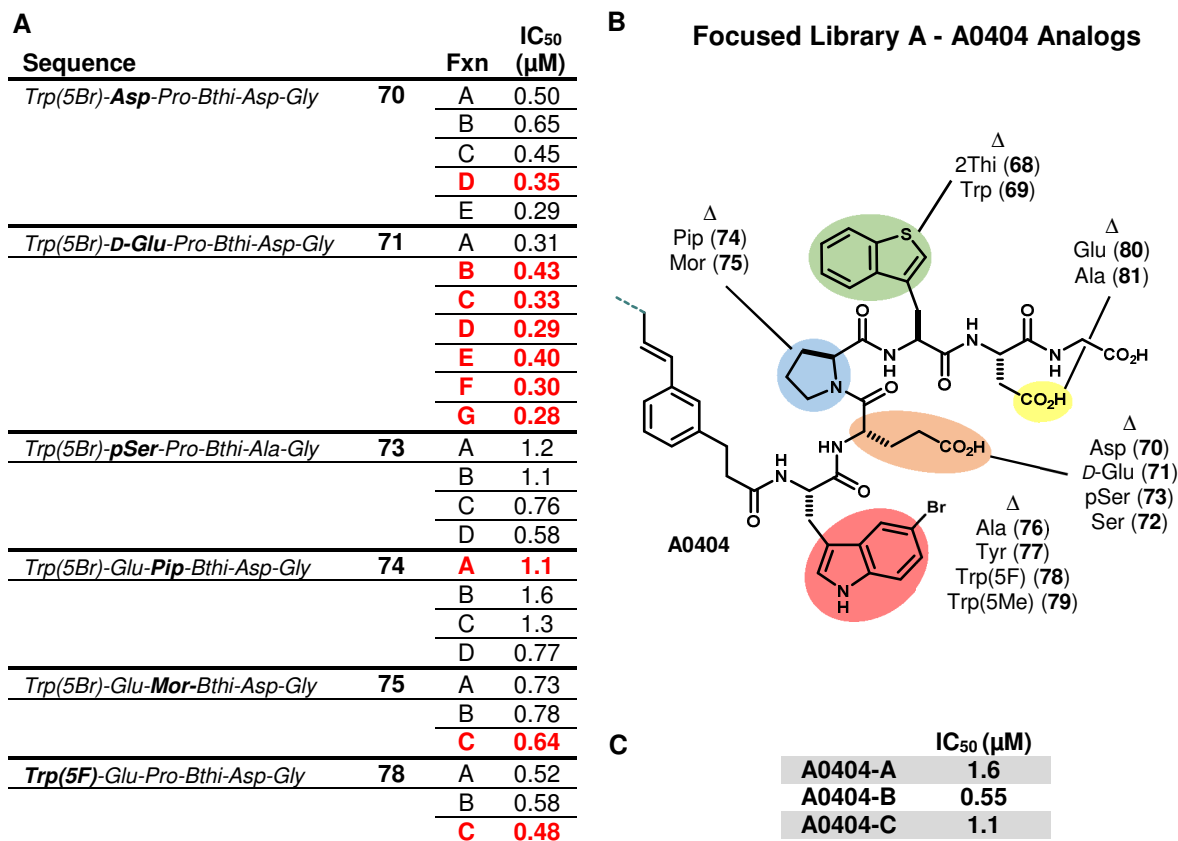


Figure 6.6.6 Best performing ligands. A) Half-maximal inhibitory concentrations (IC₅₀) of individual components from mixtures containing at least one hit (red) identified in single-point screen at 1 μM. Phosphoserine analog **73**, while not a hit, was included for comparison. **B)** Schematic of single mutations examined in Focused Library A. **C)** Previously determined activity for parent sequence **A0404**.

peptides.¹²⁹ Conventional modifications such as backbone *N*-methylation are also possible.¹³⁰ Uniquely, our template-based approach offers several additional points for potential optimization. This synthetic platform and orthogonal large ring-forming Friedel-Crafts reaction place few restrictions on sequence diversity. No tailored amino acids are necessary. Template-induced macrocyclization of di- and tripeptides, the latter of which typically fail to undergo lactamization,^{131,132} would also be possible. Critically, the structure and reactivity of the template offers vast possibilities for structural diversification. Several alternative template architectures have been explored by us see (Chapters 2, 3, 5), but have yet to be explored for honing the activity of the Pin1-targeted macrocycles identified here. Even minor modifications to the template structure would provide useful perturbations of product structure and properties. Enhancing the reaction capabilities of the template and improving synthetic protocols carries great potential to enable small molecule discovery for challenging targets involving solvent-exposed protein surfaces.

References

- (1) Rose, T. E.; Lawson, K. V.; Harran, P. G. *Chem. Sci.* **2015**, *6*, 2219.
- (2) Thompson, L. A.; Ellman, J. A. *Chem. Rev.* **1996**, *96*, 555.
- (3) Ellman, J. A. *Acc. Chem. Res.* **1996**, *29*, 132.
- (4) Bleicher, K. H.; Böhm, H.-J.; Müller, K.; Alanine, A. I. *Nat. Rev. Drug Discov.* **2003**, *2*, 369.
- (5) Tan, D. S. *Nat. Chem. Biol.* **2005**, *1*, 74.
- (6) Bauer, R. A.; Wurst, J. M.; Tan, D. S. *Curr. Opin. Chem. Biol.* **2010**, *14*, 308.
- (7) Drewry, D. H.; Macarron, R. *Curr. Opin. Chem. Biol.* **2010**, *14*, 289.
- (8) Wells, J. A.; McClendon, C. L. *Nature* **2007**, *450*, 1001.
- (9) Souroujon, M. C.; Mochly-Rosen, D. *Nat. Biotechnol.* **1998**, *16*, 919.
- (10) Arkin, M. R.; Wells, J. A. *Nat. Rev. Drug Discov.* **2004**, *3*, 301.
- (11) Li, L.; Thomas, R. M.; Suzuki, H.; De Brabander, J. K.; Wang, X.; Harran, P. G. *Science (80-)*. **2004**, *305*, 1471.
- (12) Receptors, M. *ACS Chem. Biol.* **2006**, *1*, 525.
- (13) Diella, F.; Haslam, N.; Chica, C.; Budd, A.; Michael, S.; Brown, N. P.; Trave, G.; Gibson, T. J. *Front. Biosci.* **2008**, *13*, 6580.
- (14) Neduva, V.; Russell, R. B. *Curr. Opin. Biotechnol.* **2006**, *17*, 465.
- (15) Gothel, S. F.; Marahiel, M. A. *Cell Mol Life Sci* **1999**, *55*, 423.
- (16) Lang, K.; Schmid, F. X.; Fischer, G. *Nature* **1987**, *329*, 268.
- (17) Scholz, C.; Rahfeld, J.; Fischer, G.; Schmid, F. X. *J. Mol. Biol.* **1997**, *273*, 752.
- (18) Fischer, G.; Wittmann-Liebold, B.; Lang, K.; Kiefhaber, T.; Schmid, F. X. *Nature* **1989**, *337*, 476.
- (19) Dolinski, K.; Muir, S.; Cardenas, M.; Heitman, J. *Proc. Natl. Acad. Sci. U. S. A.* **1997**, *94*, 13093.
- (20) Siekierka, J. J.; Hung, S. H.; Poe, M.; Lin, C. S.; Sigal, N. H. *Nature* **1989**, *341*, 755.
- (21) Ingelfinger, D.; Göthel, S. F.; Marahiel, M. a.; Reidt, U.; Ficner, R.; Lührmann, R.; Achsel, T. *Nucleic Acids Res.* **2003**, *31*, 4791.
- (22) Mullard, A. *Nat. Rev. Drug Discov.* **2012**, *11*, 173.
- (23) Handschumacher, R. E.; Harding, M. W.; Rice, J.; Drugge, R. J.; Speicher, D. W. *Science (80-)*. **1984**, *226*, 544.
- (24) Choi, J.; Chen, J.; Schreiber, S. L.; Clardy, J. *Science* **1996**, *273*, 239.
- (25) Chiu, M. I.; Katz, H.; Berlin, V. *Proc. Natl. Acad. Sci. U. S. A.* **1994**, *91*, 12574.
- (26) Bierer, B. E.; Mattila, P. S.; Standaert, R. F.; Herzenberg, L. a.; Burakoff, S. J.; Crabtree, G.; Schreiber, S. L. *Proc. Natl. Acad. Sci. U. S. A.* **1990**, *87*, 9231.
- (27) Dumont, F. J.; Melino, M. R.; Staruch, M. J.; Koprak, S. L.; Fischer, P. a.; Sigal, N. H. *J. Immunol.* **1990**, *144*, 1418.
- (28) Wang, X. J.; Etkorn, F. a. *Biopolym. - Pept. Sci. Sect.* **2006**, *84*, 125.
- (29) Lu, Z.; Hunter, T. *Cell Res.* **2014**, *24*, 1.
- (30) Bao, L.; Kimzey, A.; Sauter, G.; Sowadski, J. M.; Lu, K. P.; Wang, D.-G. *Am. J. Pathol.* **2004**, *164*, 1727.
- (31) Lim, J. H.; Liu, Y.; Reineke, E.; Kao, H. Y. *J. Biol. Chem.* **2011**, *286*, 44403.
- (32) Hsu, T.; McRackan, D.; Vincent, T. S.; Gert de Couet, H. *Nat. Cell Biol.* **2001**, *3*, 538.
- (33) Lu, K. P.; Zhou, X. Z. *Nat. Rev. Mol. Cell Biol.* **2007**, *8*, 904.
- (34) Brown, N. R.; Noble, M. E.; Endicott, J. a.; Johnson, L. N. *Nat. Cell Biol.* **1999**, *1*, 438.
- (35) Weiwad, M.; Küllertz, G.; Schutkowski, M.; Fischer, G. *FEBS Lett.* **2000**, *478*, 39.
- (36) Zhang, Y.; Daum, S.; Wildermann, D.; Zhou, X. Z.; Verdecia, M. a.; Bowman, M. E.; Lücke, C.; Hunter, T.; Lu, K. P.; Fischer, G.; Noel, J. P. *ACS Chem. Biol.* **2007**, *2*, 320.
- (37) Yaffe, M. B.; Schutkowski, M.; Shen, M.; Zhou, X. Z.; Stukenberg, P. T.; Rahfeld, J. U.; Xu, J.; Kuang, J.; Kirschner, M. W.; Fischer, G.; Cantley, L. C.; Lu, K. P. *Science (80-)*. **1997**, *278*, 1957.
- (38) Liou, Y.-C.; Ryo, A.; Huang, H.-K.; Lu, P.-J.; Bronson, R.; Fujimori, F.; Uchida, T.; Hunter, T.; Lu, K. P. *Proc. Natl. Acad. Sci. U. S. A.* **2002**, *99*, 1335.

- (39) Lu, K. P.; Lu, K. P.; Finn, G.; Finn, G.; Lee, T. H.; Lee, T. H.; Nicholson, L. K.; Nicholson, L. K. *Nat. Chem. Biol.* **2007**, *3*, 1.
- (40) Moore, J. D.; Potter, A. *Bioorganic Med. Chem. Lett.* **2013**, *23*, 4283.
- (41) Ranganathan, R.; Lu, K. P.; Hunter, T.; Noel, J. P. *Cell* **1997**, *89*, 875.
- (42) Wildemann, D.; Erdmann, F.; Alvarez, B. H.; Stoller, G.; Zhou, X. Z.; Fanghänel, J.; Schutkowski, M.; Lu, K. P.; Fischer, G. *J. Med. Chem.* **2006**, *49*, 2147.
- (43) Songyang, Z.; Shoelson, S. E.; Chaudhuri, M.; Gish, G.; Pawson, T.; Haser, W. G.; King, F.; Boberts, T.; Ratnofsky, S.; Lechleider, R. J.; Neel, B. G.; Birge, R. B.; Fajardo, J. E.; Chou, O. M. M.; Schaffhausen, O. B.; Cantley, L. C. *Cell* **1993**, *72*, 767.
- (44) Guo, C.; Hou, X.; Dong, L.; Dagostino, E.; Greasley, S.; Ferre, R.; Marakovits, J.; Johnson, M. C.; Matthews, D.; Mroczkowski, B.; Parge, H.; Vanarsdale, T.; Popoff, I.; Piraino, J.; Margosiak, S.; Thomson, J.; Los, G.; Murray, B. W. *Bioorg. Med. Chem. Lett.* **2009**, *19*, 5613.
- (45) Dong, L.; Marakovits, J.; Hou, X.; Guo, C.; Greasley, S.; Dagostino, E.; Ferre, R.; Johnson, M. C.; Kraynov, E.; Thomson, J.; Pathak, V.; Murray, B. W. *Bioorganic Med. Chem. Lett.* **2010**, *20*, 2210.
- (46) O'Donnell, M. J. *Aldrichimica Acta* **2001**, *34*, 3.
- (47) Williams, R. M.; Im, M.-N. *Tetrahedron Lett.* **1988**, *29*, 6075.
- (48) Schollkopf, B. U.; Neubauer, H.; Hauptreif, M. *Angew. Chemie - Int. Ed.* **1985**, *24*, 1066.
- (49) Xu, P. F.; Chen, Y. S.; Lin, S. I.; Lu, T. J. *J. Org. Chem.* **2002**, *67*, 2309.
- (50) Myers, A. G.; Gleason, J. L.; Yoon, T. *J. Am. Chem. Soc.* **1995**, *117*, 8488.
- (51) Vineyard, B. D.; Knowles, W. S.; Sabacky, M. J.; Bachman, G. L.; Weinkauff, D. J. *J. Am. Chem. Soc.* **1977**, *1841*, 5946.
- (52) Noyori, R. *Angew. Chemie - Int. Ed.* **2002**, *41*, 2008.
- (53) Burk, M. J. *Acc. Chem. Res.* **2000**, *33*, 363.
- (54) Burk, M. J.; Gross, M. F.; Harper, T. G. P.; Kalberg, C. S.; Lee, J. R.; Martinez, J. P. *Pure Appl. Chem.* **1996**, *68*, 37.
- (55) Burk, M. J.; Feaster, J. E.; Nugent, W. a; Harlow, R. L. *J. Am. Chem. Soc.* **1993**, *115*, 10125.
- (56) Tang, W.; Zhang, X. *Chem. Rev.* **2003**, *103*, 3029.
- (57) Nagel, U.; Kinzel, E.; Andrade, J.; Prescher, G. *Chem. Ber.* **1986**, *119*, 3326.
- (58) Tang, W.; Zhang, X. *Angew. Chemie - Int. Ed.* **2002**, *41*, 1612.
- (59) Vachal, P.; Jacobsen, E. N. *Org. Lett.* **2000**, *2*, 867.
- (60) Sigman, M. S.; Jacobsen, E. N. *J. Am. Chem. Soc.* **1998**, *120*, 4901.
- (61) Sigman, M. S.; Vachal, P.; Jacobsen, E. N. *Angew. Chemie - Int. Ed.* **2000**, *39*, 1336.
- (62) Su, J. T.; Vachal, P.; Jacobsen, E. N. *Adv. Synth. Catal.* **2001**, *343*, 197.
- (63) Ishitani, H.; Komiyama, S.; Kobayashi, S. *Angew. Chemie - Int. Ed.* **1998**, *37*, 3186.
- (64) Corey, E. J.; Link, J. O. *J. Am. Chem. Soc.* **1992**, *114*, 1906.
- (65) Burk, M. J.; Feaster, J. E.; Nugent, W. a; Harlow, R. L. *J. Am. Chem. Soc.* **1993**, *115*, 10125.
- (66) Wang, W.; Xiong, C.; Yang, J.; Hruby, V. J. *Tetrahedron* **2001**, *42*, 7717.
- (67) Wang, W.; Xiong, C.; Zhang, J.; Hruby, V. J. *Tetrahedron* **2002**, *58*, 3101.
- (68) Miyazawa, T. *Amino Acids* **1999**, *16*, 191.
- (69) Chibata, I.; Tosa, T.; Sato, T.; Mori, T. *Methods Enzymol.* **1976**, *44*, 746.
- (70) Chenault, H. K.; Dahmer, J.; Whitesides, G. M. *J. Am. Chem. Soc.* **1989**, *111*, 6354.
- (71) Tong, J. H.; Petitclerc, C.; D'Iorio, a; Benoiton, N. I. *Can. J. Biochem.* **1971**, *49*, 877.
- (72) Porter, J.; Dykert, J.; Rivier, J. *Int. J. Pept. Protein Res.* **1987**, *30*, 13.
- (73) Gerig, J. T.; Klinkenborg, J. C. *J. Am. Chem. Soc.* **1980**, *102*, 4267.
- (74) Morihara, K. *Adv. Enzymol. Relat. Areas Mol. Biol.* **1974**, *41*, 179.
- (75) Chen, S.-T.; Wang, K.-T.; Wong, C.-H. *J. Chem. Soc. Chem. Commun.* **1986**, 1514.
- (76) Snyder, H. R.; Shekleton, J. F.; Lewis, C. D. *J. Am. Chem. Soc.* **1945**, *67*, 310.
- (77) Albertson, N. F. *J. Am. Chem. Soc.* **1946**, *68*, 450.

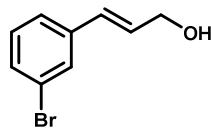
- (78) Paquet, A. *Can. J. Chem.* **1982**, *60*, 976.
- (79) Lawson, K. V.; Rose, T. E.; Harran, P. G. *Tetrahedron* **2013**, *69*, 7683.
- (80) Ahmed, M. I.; Harper, J. B.; Hunter, L. *Org. Biomol. Chem.* **2014**, *9*.
- (81) Klose, J.; Ehrlich, A.; Bienert, M. *Lett. Pept. Sci.* **1998**, *5*, 129.
- (82) Besser, D.; Olender, R.; Rosenfeld, R.; Arad, O.; Reissmann, S. *J. Pept. Res.* **2000**, *56*, 337.
- (83) Haddadi, M. E. L.; Cavelier, F.; Vives, E.; Azmani, a; Verducci, J.; Martinez, J. *J. Pept. Sci.* **2000**, *570*, 560.
- (84) Schmidt, U.; Langner, J. *J. Pept. Res.* **1997**, *49*, 67.
- (85) Titlestad, K. *Acta Chem. Scand. B* **1977**, *31*, 641.
- (86) Fields, G. B.; Noble, R. L. *Int. J. Pept. Protein Res.* **1990**, *35*, 161.
- (87) Lam, K. S.; Salmon, S. E.; Hersh, E. M.; Hruby, V. J.; Kazmierski, W. M.; Knapp, R. J. *Nature* **1991**, *354*, 82.
- (88) Houghten, R. a; Pinilla, C.; Blondelle, S. E.; Appel, J. R.; Dooley, C. T.; Cuervo, J. H. *Nature* **1991**, *354*, 84.
- (89) Merrifield, R. B. *J. Am. Chem. Soc.* **1963**, *85*, 2149.
- (90) Houghten, R. A. *Proc. Natl. Acad. Sci. U. S. A.* **1985**, *82*, 5131.
- (91) Lambert, J. N.; Mitchell, J. P.; Roberts, K. D. *J. Chem. Soc. Perkin Trans. 1* **2001**, 471.
- (92) Fluxa, V. S.; Reymond, J. L. *Bioorganic Med. Chem.* **2009**, *17*, 1018.
- (93) Li, Y.; Dooley, C. T.; Mislser, J. a.; Debevec, G.; Giulianotti, M. a.; Cazares, M. E.; Maida, L.; Houghten, R. a. *ACS Comb. Sci.* **2012**, *14*, 673.
- (94) Xiao, Q.; Xiao, Q.; Pei, D.; Pei, D. *J. Med. Chem* **2007**, *4*, 3132.
- (95) Liu, T.; Joo, S. H.; Voorhees, J. L.; Brooks, C. L.; Pei, D. *Bioorg. Med. Chem.* **2009**, *17*, 1026.
- (96) Thakkar, A.; Trinh, T. B.; Pei, D. *ACS Comb. Sci.* **2013**, *15*, 120.
- (97) Chang, C. D.; Meienhofer, J. *Int. J. Pept. Protein Res.* **1978**, *11*, 246.
- (98) Rink, H. *Tetrahedron Lett.* **1987**, *28*, 3787.
- (99) Orosz, G.; Kiss, L. P. *Tetrahedron Lett.* **1998**, *39*, 3241.
- (100) Barlos, K.; Gatos, D.; Kallitsis, J.; Papaphotiu, G.; Sotiriou, P.; Wenqing, Y.; Schäfer, W. *Tetrahedron Lett.* **1989**, *30*, 3943.
- (101) Barlos, K.; Chatzi, O.; Gatos, D.; Stavropoulos, G. *Int. J. Pept. Protein Res.* **1991**, *37*, 513.
- (102) Lee, K.; Burfield, D. R.; Smithers, R. H. *J. Org. Chem* **1977**, *42*, 3060.
- (103) Pangborn, A. B.; Giardello, M. a.; Grubbs, R. H.; Rosen, R. K.; Timmers, F. J. *Organometallics* **1996**, *15*, 1518.
- (104) Torssell, K. B. G.; Gothelf, K. V.; Linsay, V. N. G. *Encycl. Reagents Org. Synth.* **2012**, *1*.
- (105) Armarego, W. L. F.; Chai, C. L. L. In *Purification of laboratory chemicals*; Butterworth-Heinemann: Waltham, MA, 2013; p 190.
- (106) Coetze, J. F.; Chang, T.-H. *Int. Union Pure Applied Chem.* **1986**, *58*, 1541.
- (107) Reimer, U.; Scherer, G.; Drewello, M.; Kruber, S.; Schutkowski, M.; Fischer, G. *J. Mol. Biol.* **1998**, *279*, 449.
- (108) Steinberg, I. Z.; Harrington, W. F.; Berger, A.; Sela, M.; Katchalski, E. *J. Am. Chem. Soc.* **1960**, *82*, 5263.
- (109) Grathwohl, C.; Wüthrich, K. *Biopolymers* **1976**, *15*, 2025.
- (110) Kofron, J. L.; Kuzmic, P.; Kishore, V.; Colón-Bonilla, E.; Rich, D. H. *Biochemistry* **1991**, *30*, 6127.
- (111) Fischer, G.; Bang, H.; Berger, E.; Schellenberger, A. *Biochim. Biophys. Acta* **1984**, *791*, 87.
- (112) Harrison, R. K.; Stein, R. L. *Biochemistry* **1990**, *29*, 3813.
- (113) Liu, J.; Albers, M. W.; Chen, C. M.; Schreiber, S. L.; Walsh, C. T. *Proc. Natl. Acad. Sci. U. S. A.* **1990**, *87*, 2304.
- (114) Janowski, B.; Wöllner, S.; Schutkowski, M.; Fischer, G. *Anal. Biochem.* **1997**, *252*, 299.
- (115) Wang, X. J.; Xu, B.; Mullins, A. B.; Neiler, F. K.; Etkorn, F. a. *J. Am. Chem. Soc.* **2004**, *126*, 15533.
- (116) Rijkers, D. T. S.; Adams, H. P. H. M.; Hemker, H. C.; Tesser, G. I. *Tetrahedron* **1995**, *51*, 11235.
- (117) Zhao, S.; Etkorn, F. a. *Bioorganic Med. Chem. Lett.* **2007**, *17*, 6615.
- (118) Lu, P. J.; Zhou, X. Z.; Shen, M.; Lu, K. P. *Science* **1999**, *283*, 1325.

- (119) Rossi, A. M.; Taylor, C. W. *Nat. Protoc.* **2011**, *6*, 365.
- (120) Andrew, C. D.; Warwicker, J.; Jones, G. R.; Doig, A. J. *Biochemistry* **2002**, *41*, 1897.
- (121) Duncan, K. E.; Dempsey, B. R.; Killip, L. E.; Adams, J.; Bailey, M. L.; Lajoie, G. a.; Litchfield, D. W.; Brandl, C. J.; Shaw, G. S.; Shilton, B. H. *J. Med. Chem.* **2011**, *54*, 3854.
- (122) Guo, C.; Hou, X.; Dong, L.; Marakovits, J.; Greasley, S.; Dagostino, E.; Ferre, R.; Catherine Johnson, M.; Humphries, P. S.; Li, H.; Paderes, G. D.; Piraino, J.; Kraynov, E.; Murray, B. W. *Bioorganic Med. Chem. Lett.* **2014**, *24*, 4187.
- (123) Elliott, T. S.; Slowey, A.; Ye, Y.; Conway, S. J. *Medchemcomm* **2012**, *3*, 735.
- (124) Hunter, T. *Philos. Trans. R. Soc. B Biol. Sci.* **2012**, *367*, 2513.
- (125) Gribbon, P.; Sewing, A. *Drug Discov. Today* **2003**, *8*, 1035.
- (126) Thorne, N.; Auld, D. S.; Inglese, J. *Curr. Opin. Chem. Biol.* **2010**, *14*, 315.
- (127) Xinyi Huang, A. A. In *Methods in Molecular Biology - High Throughput Screening*; Janzen, W. P., Bernasconi, P., Eds.; Humana Press: Totowa, NJ, 2009; pp 127–143.
- (128) Kohli, R. M.; Walsh, C. T.; Burkart, M. D. *Nature* **2002**, *418*, 658.
- (129) Baeriswyl, V.; Rapley, H.; Pollaro, L.; Stace, C.; Teufel, D.; Walker, E.; Chen, S.; Winter, G.; Tite, J.; Heinis, C. *ChemMedChem* **2012**, *7*, 1173.
- (130) Dechantsreiter, M. A.; Planker, E.; Matha, B.; Lohof, E.; Jonczyk, A.; Goodman, S. L.; Kessler, H. *J. Med. Chem.* **1999**, *42*, 3033.
- (131) Rothe, M.; Steffen, K.-D.; Rothe, I. *Angew. Chem. Int. Ed.* **1965**, *4*, 356.
- (132) Rückle, T.; De Lavallaz, P.; Keller, M.; Dumy, P.; Mutter, M. *Tetrahedron* **1999**, *55*, 11281.
- (133) Schroder, R.; Schollkopf, U.; Hoppe, E. B. I.; Chem, L. A.; Schroder, R.; Schollkopf, U.; Blume, E. *Justus Liebigs Ann. Chem.* **1975**, 533.
- (134) Schöllkopf, U.; Hartwig, W.; Groth, U. *Angew. Chemie Int. Ed. English* **1979**, *18*, 863.
- (135) O'Donnell, M.; Bennett, W.; Wu, S. *J. Am. Chem. Soc.* **1989**, *111*, 2353.

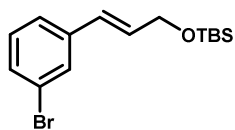
Experimental Appendices

Note: Spectroscopic data are available via the electronic form of this dissertation.

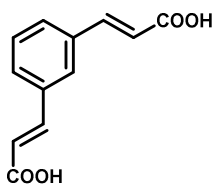
3-Bromocinnamyl alcohol (14). Ethyl 3-bromocinnamate (**12**) (3.83 g, 15 mmol) was dissolved in dry THF (100 mL) and cooled to -78°C. DIBALH (30 mL, 1M in hexanes) was slowly over 10 min. After 2 hrs, the reaction appeared incomplete by TLC, and additional DIBALH (7.5 mL) was added and the reaction was allowed to warm to -30°C. The mixture was stirred for 30 min, quenched by the addition of EtOAc followed by sat. NH₄Cl, diluted with 1N HCl, and extracted with EtOAc (x2). The organic phase was washed with 1N HCl, 1M NaOH, and brine, dried over MgSO₄ and concentrated to give **14** (3.36 g, quant) as a colorless oil, which was used without purification. ¹H NMR (CDCl₃, 300 MHz): δ 2.20 (br s, 1H), 4.30 (dd, *J* = 5.3, 1.4 Hz, 2H), 6.33 (dd, *J* = 15.8, 5.3 Hz, 1H), 6.52 (br d, *J* = 15.8 Hz, 1H), 7.15 (dd, *J* = 7.8, 7.8 Hz, 1H), 7.26 (br d, *J* = 7.8 Hz, 1H), 7.35 (br d, *J* = 7.8 Hz, 1H), 7.50 (dd, *J* = 1.5, 1.5 Hz, 1H). ¹³C NMR (CDCl₃, 75 MHz): δ 138.9, 130.6, 130.2, 130.2, 129.4, 129.3, 125.1, 122.8, 63.3.



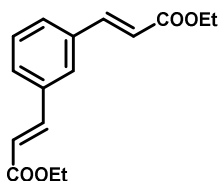
(E)-((3-(3-bromophenyl)allyl)oxy)(tert-butyl)dimethylsilane (15). 3-Bromocinnamyl alcohol **14** (2.13 g, 10 mmol) was dissolved in DMF (5 mL) and treated with imidazole (1.70 g, 25 mmol) followed by TBSCl (1.81 g, 12 mmol). The reaction was stirred overnight, diluted with EtOAc and washed with H₂O (x4), brine, dried over MgSO₄ and evaporated. Flash chromatography on SiO₂ eluted with 10% DCM in hexanes afforded **15** (2.83 g, 87%) as a colorless oil. ¹H NMR (CDCl₃, 300 MHz): δ 0.12 (s, 6H), 0.95 (s, 9H), 4.35 (dd, *J* = 4.7, 1.7 Hz, 1H), 6.29 (dt, *J* = 15.8, 4.7 Hz, 1H), 6.53 (dt, *J* = 15.8, 1.6 Hz, 1H). ¹³C NMR (CDCl₃, 75 MHz): δ 139.5, 131.0, 130.2, 130.1, 129.4, 127.9, 125.1, 122.8, 63.6, 26.1, 18.6.



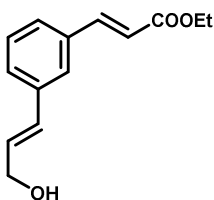
(2E,2'E)-3,3'-(1,3-phenylene)diacrylic acid (S1).^{6,7} Isophthalaldehyde (75.8 g, 565 mmol) was dissolved in pyridine (208 ml) and malonic acid (176.3 g, 1695 mmol) was added. The mixture was heated to 50 °C and stirred for 2 h, then warmed to 100 °C overnight. The reaction was cooled to rt and poured into aqueous H₂SO₄ (70 ml in 1300 ml H₂O). The precipitate was filtered and dried to give **S1** (109 g, 88%) as a white solid, the NMR of which matched that reported previously.⁷



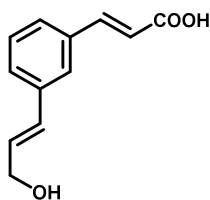
Diethyl 3,3'-(1,3-phenylene)(2E,2'E)-diacrylate (18).⁷ Bis-carboxylic acid **S1** (109 g, 499 mmol) was dissolved in EtOH (450 ml), and conc. H₂SO₄ (25 ml) was added. The solution was refluxed overnight, cooled to rt and concentrated to approximately 1/3 its original volume. The alcoholic solution was carefully poured into saturated aqueous Na₂CO₃, and this solution was extracted with EtOAc (3x). The combined organic phase was washed with saturated aqueous NaHCO₃, brine, dried over MgSO₄ and concentrated to give **18** (131.3 g, 96%) as an off white solid, the NMR of which matched that reported previously.⁷



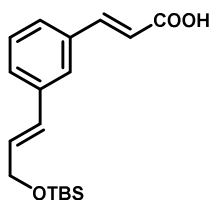
(E)-Ethyl 3-(3-((E)-2-hydroxyvinyl)phenyl)acrylate (19). Bis-ethyl ester **18** (20.02 g, 73 mmol) was dissolved in THF (200 ml) and cooled to -15 °C. Diisobutylaluminum hydride (161 ml, 1.0 M in hexanes, 161 mmol) was added over 10 min. The solution was stirred cold for 15 min then warmed to rt and stirred for 2 h. The reaction was re-cooled to -15 °C and quenched by cannulating into a stirred solution of aqueous Rochelle's salt (100 ml). The organic phase was decanted, and the aqueous remained was stirred with Celite and filtered through a pad of the same. The filtrate was extracted with EtOAc (2x), and the combined organic phase was washed with 1N HCl, H₂O, brine, dried over MgSO₄ and concentrated. Flash chromatography eluted with 2:1 → 1:1 hexane:EtOAc afforded mono-ester **19** (6.27 g, 37%) as a colorless oil. ¹H NMR (CDCl₃, 300 MHz): δ 1.33 (t, *J* = 7.1 Hz, 3H), 4.26 (q, *J* = 7.1 Hz, 2H), 7.34 (d, *J* = 5.3 Hz, 2H), 6.39 (dt, *J* = 15.9, 5.3 Hz, 1H), 6.43 (d, *J* = 16.0 Hz, 1H), 6.62 (br d, *J* = 15.9 Hz, 1H), 7.31 (d, *J* = 8.9 Hz, 1H), 7.32 (dd, *J* = 8.9, 6.1 Hz, 1H), 7.36-7.42 (m, 2H), 7.48-7.51 (m, 1H), 7.66 (d, *J* = 16.0 Hz, 1H). ¹³C NMR (CDCl₃, 75 MHz): δ 167.0, 144.4, 137.4, 134.8, 130.1, 129.7, 129.1, 128.1, 127.1, 126.2, 118.6, 63.5, 60.6, 14.3.



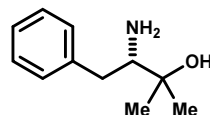
(E)-3-(3-((E)-3-hydroxyprop-1-en-1-yl)phenyl)acrylic acid (S2). Ester **19** (6.27 g, 27 mmol) was dissolved in THF (30 ml) and MeOH (30 ml), and NaOH (10.3 ml, 5.26 M, 54 mmol) was added. The reaction was stirred overnight, poured into 1N HCl (100ml) and extracted with EtOAc (3x). The combined organic extract was dried over MgSO₄ and concentrated to give **S2** (5.07 g, 92%) as a colorless oil which was used without further purification.



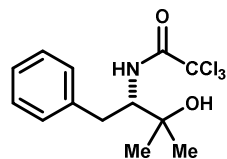
(E)-3-(3-((E)-3-((tert-Butyldimethylsilyl)oxy)prop-1-en-1-yl)phenyl)acrylic acid (20). Carboxylic acid **S2** (5.07 g, 24.8 mmol) was dissolved in DMF (12.5 ml) and treated with imidazole (5.07 g, 75 mmol) and TBSCl (7.48 g, 49.6 mmol). The reaction was stirred overnight and poured into cold 10% citric acid (100 ml), and partitioned into EtOAc. The combined organic phase was washed with H₂O (5x), brine, dried over MgSO₄ and concentrated. Flash chromatography eluted with 7:3 → 6:4 hexane:EtOAc gave **20** (8.92 g, >100%) as a colorless oil which was used without further purification. ¹H NMR (DMSO-*d*₆, 300 MHz): δ 0.09 (s, 6H), 0.91 (s, 9H), 4.32 (br d, *J* = 4.6 Hz, 2H), 6.47 (dt, *J* = 16.0, 4.6 Hz, 1H), 6.58 (br d, *J* = 16.0 Hz, 2H), 7.36 (dd, *J* = 7.8, 7.8 Hz, 1H), 7.46 (br d, *J* = 7.8 Hz, 1H), 7.54 (br d, *J* = 7.8 Hz, 1H), 7.58 (d, *J* = 16.1 Hz, 1H), 7.75-7.78 (m, 1H), 12.38 (s, 1H). ¹³C NMR (DMSO-*d*₆, 75 MHz): δ 167.6, 143.8, 137.3, 134.6, 130.4, 129.1, 128.1, 128.0, 127.1, 125.9, 119.5, 63.2, 25.8, 25.8, 18.0, -3.2.



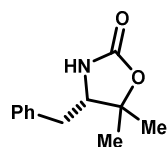
(S)-3-Amino-2-methyl-4-phenylbutan-2-ol (S3).⁸ Methylmagnesium bromide (37 mL, 3.0 M in THF) was added to dry Et₂O (100 mL), to which was then added L-phenylalanine methyl ester hydrochloride (4.0 g, 18.5 mmol) at rt via a solid addition funnel. A thick precipitate formed which resisted stirring, and the mixture was allowed to stand for 16 hrs. The reaction was quenched with H₂O followed by 1N HCl until solubilized. The organic phase was removed, and the aqueous remainder was washed with Et₂O (x1), cooled in an ice bath, basified to pH >10 with solid NaOH, and extracted with EtOAc (x3). The organic phase was washed with brine, dried over Na₂SO₄ and concentrated to give **S3** (2.99 g, 90%) as an oil, which was used without further purification. ¹H NMR (CDCl₃, 300 MHz): δ 1.20 (s, 3H), 1.29 (s, 3H), 2.62 (dd, *J* = 13.5, 11.2 Hz, 1H), 2.80 (dd, *J* = 11.2, 2.5 Hz, 1H), 3.02 (dd, *J* = 13.5, 2.5 Hz, 1H), 7.15-7.35 (m, 5H). ¹³C NMR (CDCl₃, 75 MHz): δ 140.0, 129.2, 128.7, 126.4, 71.5, 61.6, 39.2, 27.3, 24.0.



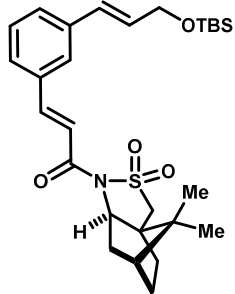
N-Trichloroacetyl-(S)-3-amino-2-methyl-4-phenylbutan-2-ol (S4).⁸ Amine **S3** (3.03 g, 16.9 mmol) was dissolved in DCM (30 mL), cooled to -78°C, and treated with Et₃N (3.06 mL, 22 mmol) followed by slow addition of trichloroacetyl chloride (2.3 mL, 20 mmol). The reaction was stirred for 15 min, then allowed to warm to rt and stirred for an additional 30 min. The light orange mixture was diluted with DCM (50 mL) and washed with H₂O, 1N HCl (x2), brine, dried over Na₂SO₄ and concentrated. Flash chromatography on SiO₂ eluted with 20→30% EtOAc in hexanes afforded **S4** (3.21 g, 59%) as a dark red oil of moderate purity by NMR. ¹H NMR (CDCl₃, 300 MHz): δ 1.31 (s, 3H), 1.40 (s, 3H), 2.76 (dd, *J* = 14.2, 10.8 Hz, 1H), 3.20 (dd, *J* = 14.2, 4.1 Hz, 1H), 4.05-4.12 (m, 1H), 6.78 (br d, *J* = 9.6 Hz, 1H), 7.15-7.31 (m, 5H).



(R)-5,5-Dimethyl-4-benzyloxazolidin-2-one (S5).⁸ Trichloroacetamide **S4** (2.5 g, 7.7 mmol) was dissolved in EtOH (20 mL), treated with K₂CO₃ (1.2 g, 8.5 mmol), and heated to reflux for 2.5 hr. The solvent was exchanged to DCM and washed with brine, dried over Na₂SO₄ and concentrated. Flash chromatography on SiO₂ eluted with 30%EtOAc in hexanes afforded a light brown solid, which was recrystallized from Et₂O/petroleum ether to give **S5** (970 mg, 61%) as large, cubic, faintly brown crystals. ¹H NMR (CDCl₃, 300 MHz): δ 1.44 (s, 6H), 2.69 (dd, *J* = 13.4, 10.3 Hz, 1H), 2.82 (dd, *J* = 13.4, 4.2 Hz, 1H), 3.69 (dd, *J* = 10.3, 4.2 Hz, 1H), 5.29 (br s, 1H), 7.14-7.21 (m, 2H), 7.21-7.29 (m, 1H), 7.29-7.37 (m, 2H). ¹³C NMR (CDCl₃, 75 MHz): δ 158.1, 137.0, 129.1, 128.9, 127.2, 83.2, 63.1, 37.1, 27.6, 22.0. [α]_D²⁰ = -86.8 (c = 0.5, CHCl₃).

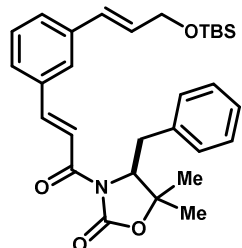


(E)-3-(3-((E)-3-((tert-Butyldimethylsilyl)oxy)prop-1-en-1-yl)phenyl)-1-((3aR,6R,7aR)-8,8-dimethyl-2,2-dioxidohexahydro-1H-3a,6-methanobenzo[c]isothiazol-1-yl)prop-2-en-1-one (**21a**).⁹



Acyl sultam **21a** (3.064g, 78%) was prepared analogously to compound **21b**. ¹H NMR (CDCl₃, 300 MHz): δ 0.12 (s, 6H), 0.95 (s, 9H), 1.00 (s, 3H), 1.21 (s, 3H), 1.85-2.00 (m, 2H), 2.20-2.23 (m, 2H), 3.48 (d, *J* = 13.8 Hz, 1H), 3.55 (d, *J* = 13.7 Hz, 1H), 4.00 (dd, *J* = 7.4, 5.3 Hz, 1H), 4.36 (dd, *J* = 4.9, 1.7 Hz, 1H), 6.32 (dt, *J* = 15.8, 4.9 Hz, 1H), 6.60 (dt, *J* = 15.8, 1.7 Hz, 1H), 7.17 (d, *J* = 15.4 Hz, 1H), 7.32 (dd, *J* = 7.7, 7.5 Hz, 1H), 7.41 (br d, *J* = 7.7 Hz, 1H), 7.45 (br d, *J* = 7.5 Hz, 1H), 7.51-7.54 (m, 1H), 7.78 (d, *J* = 15.4 Hz, 1H). ¹³C NMR (CDCl₃, 75 MHz): δ 165.6, 152.9, 146.2, 138.0, 137.2, 135.0, 130.5, 129.2, 129.1, 128.8, 128.6, 128.6, 127.5, 126.9, 126.8, 117.7, 82.4, 64.0, 63.8, 35.4, 28.7, 27.1, 26.1, 22.5, 18.6.

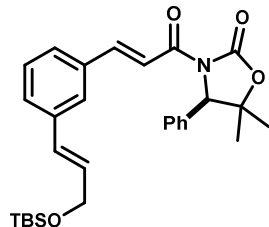
(S)-4-Benzyl-3-((E)-3-(3-((E)-3-((tert-butyl dimethylsilyl)oxy)prop-1-en-1-yl)phenyl)acryloyl)-5,5-dimethyloxazolidin-2-one (**21b**).⁹



Carboxylic acid **20** (3.20 g, 10.0 mmol) was dissolved in THF (60 ml) and cooled to -20 °C. Triethylamine (3.5 ml) was added followed by pivaloyl chloride (1.30 ml, 10.5 mmol). The reaction was stirred cold for 2 h, and added to a flask containing calcinated LiCl (424 mg, 10.0 mmol) and (S)-4-benzyl-5,5-dimethyloxazolidin-2-one (2.05 g, 10.0 mmol) at -20 °C. The reaction was stirred overnight, allowing the cooling bath to warm to rt. The solvent was removed and the residue was partitioned between EtOAc/H₂O. The combined organic phase was washed with H₂O (3x 40 ml), brine, dried over MgSO₄ and concentrated. Flash chromatography eluted with 8→10% EtOAc in hexanes gave

21b (3.03 g, 60%) as a light yellow oil. ¹H NMR (CDCl₃, 300 MHz): δ 0.13 (s, 6H), 0.96 (s, 9H), 1.39 (s, 3H), 1.41 (s, 3H), 2.93 (dd, *J* = 14.3, 9.6 Hz, 1H), 3.28 (dd, *J* = 14.3, 3.5 Hz, 1H), 4.37 (dd, *J* = 4.8, 1.6 Hz, 2H), 4.63 (dd, *J* = 9.6, 3.6 Hz, 1H), 6.34 (dt, *J* = 15.8, 4.8 Hz, 1H), 6.62 (dt, *J* = 15.8, 1.6 Hz, 1H), 7.20-7.28 (m, 1H), 7.30-7.39 (m, 5H), 7.42 (br d, *J* = 7.7 Hz, 1H), 7.49 (br d, *J* = 7.6 Hz, 1H), 7.82 (d, *J* = 15.8 Hz, 1H), 7.93 (d, *J* = 15.8 Hz, 1H). ¹³C NMR (CDCl₃, 75 MHz): δ 165.6, 152.9, 146.2, 138.0, 137.2, 135.0, 130.5, 129.2, 129.1, 128.8, 128.6, 128.6, 127.5, 126.9, 126.8, 117.7, 82.4, 64.0, 63.8, 35.4, 28.7, 27.1, 26.1, 22.5, 18.6.

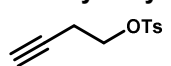
(R)-3-((E)-3-(3-((E)-3-((tert-Butyldimethylsilyl)oxy)prop-1-en-1-yl)phenyl)acryloyl)-5,5-dimethyl-4-phenyloxazolidin-2-one (**21c**) – by rearrangement of **48** and silylation.



Methyltrioxorhenium (107 mg, 0.430 mmol) was added in one portion to a solution of 1-phenylallyl alcohol **48** (5.40 g, 14.32 mmol) in toluene (115 mL). After complete consumption of starting material (typically 12 h), as monitored by HPLC, imidazole (2.92 g, 43.0 mmol) was added followed by TBSCl (2.59 g, 17.2 mmol). After 1h the mixture was diluted with EtOAc (200 mL) and washed sequentially with sat. NH₄Cl, NaHCO₃, and brine, dried over Na₂SO₄ and concentrated. Cinnamyl silyl ether **21c** (5.56 g, 79 % from **36**) was obtained as an off-white foam.

– by Horner-Wadsworth-Emmons olefination of aldehyde **51**. LiCl (17.2 g, 406 mmol) was placed in a 1 L flask and dried by heating in vacuo. Once cooled, phosphonate **46** (53.2 g, 122 mmol) and dry ACN (200 mL) were added, followed by iPr₂EtN (21.2 mL). Aldehyde **51** (28.5 g, 103 mmol) as a solution in ACN (300 mL), and the mixture was stirred overnight at rt. The solvent was exchanged to EtOAc, and washed with sat. NH₄Cl (x3), brine, dried over Na₂SO₄ and concentrated. Flash chromatography on SiO₂ eluted with 20% EtOAc in hexanes afforded **21c** (32.05 g, 64%). ¹H NMR (CDCl₃, 400 MHz): δ 8.01 (d, *J* = 15.7 Hz, 1H), 7.76 (d, *J* = 15.7 Hz, 1H), 7.58 (s, 1H), 7.30-7.50 (m, 6H), 7.20 (d, *J* = 6.8 Hz, 2H), 6.61 (dt, *J* = 15.8, 1.6 Hz, 1H), 6.33 (dt, *J* = 15.8, 4.9 Hz, 1H), 5.21 (s, 1H), 4.37 (dd, 4.9, 1.6 Hz, 2H), 1.65 (s, 3H), 1.03 (s, 3H), 0.95 (s, 9H), 0.12 (s, 6H). ¹³C NMR (CDCl₃, 100 MHz): δ 165.1, 153.3, 146.5, 137.9, 136.3, 134.8, 130.4, 129.1, 129.0, 128.9, 128.6, 128.5, 127.4, 126.7, 117.3, 82.5, 67.3, 63.7, 29.0, 26.0, 23.8, 18.5. HRMS (ESI) Calculated for C₂₉H₃₇NO₄Si [M+Na]⁺: 514.2384, found 514.2394.

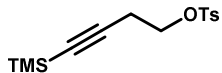
But-3-yn-1-yl toluenesulfonate (S6).¹⁰



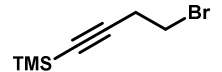
Homopropargyl alcohol (30.0 g, 428 mmol) was dissolved in DCM (500 mL) and triethylamine (119 mL, 856 mmol) was added. The mixture was cooled to 0 °C and a solution of tosyl chloride (85.7 g, 449 mmol) in DCM (400 mL) was added via addition funnel over 30 min. The reaction was warmed to rt, stirred for 2.5 h, and poured into chipped ice. The organic phase was removed and the aqueous remained was extracted with DCM (2x

200mL). The combined organic phase was washed with saturated $\text{NH}_4\text{Cl}:\text{H}_2\text{O}$ (1:1), saturated NaHCO_3 , brine, dried over MgSO_4 and concentrated to give **S6** (109g, >100%) as a red oil, which was used without purification. ^1H NMR (CDCl_3 , 400 MHz): δ 1.97 (t, $J = 2.7$ Hz, 1H), 2.45 (s, 3H), 2.55 (td, $J = 7.0, 2.6$ Hz, 2H), 4.10 (t, $J = 7.0$ Hz, 2H), 7.35 (d, $J = 8.2$ Hz, 2H), 7.80 (d, $J = 8.2$ Hz, 2H). ^{13}C NMR (CDCl_3 , 100 MHz): δ 145.1, 132.9, 130.0, 128.1, 78.5, 70.9, 67.5, 21.8, 19.5.

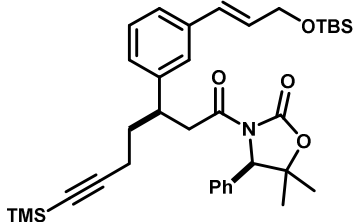
4-(Trimethylsilyl)but-3-yn-1-yl toluenesulfonate (S7).¹⁰ Alkyne **S6** (109g, 428mmol) was dissolved in THF (550 mL), cooled to -78 °C and stirred for 15 min. $n\text{BuLi}$ (188 mL, 2.5 M, 471 mmol) was added via a dropping funnel over 20 min, and stirring was maintained for 1 h before adding TMS chloride (71 mL, 556 mmol) as a solution in THF (55 mL) over 20 min (**Caution!** The reaction must not be allowed to warm up before addition of TMSCl . An explosion was observed in one incidence when this was accidentally allowed to occur). The cooling bath was allowed to warm to rt over 2 h, and the reaction was poured into chipped ice (200 mL). The organic phase was removed and the aqueous remainder was extracted with EtOAc (2x 150 mL). The combined organic phase was washed with saturated NH_4Cl (2x 200 mL), brine, dried over MgSO_4 , filtered and concentrated to give **S7** (118g, 93%) as a red oil.



(4-Bromobut-1-yn-1-yl)trimethylsilane (25).¹⁰ Tosylate **S7** (118 g, 399 mmol) was dissolved in acetone (1200 mL), and dry lithium bromide (69.3 g, 797 mmol) was added. The mixture was heated to reflux overnight, cooled and filtered. The filtrate was concentrated to approximately half its original volume and poured into ether (1000 mL) and water (500 mL). Brine (200 mL) was added, and the aqueous layer was removed and extracted with ether (300 mL). The combined organic phase was washed with brine (300 mL), dried over MgSO_4 and concentrated to give a dark red oil which was distilled in vacuo to give **25** (61.0 g, 74%, bp $63\text{--}65$ °C, 8.75 torr) as a colorless oil. ^1H NMR (CDCl_3 , 400 MHz): δ 0.15 (s, 9H), 2.77 (t, $J = 7.5$ Hz, 2H), 3.42 (t, $J = 7.5$ Hz, 2H). ^{13}C NMR (CDCl_3 , 100 MHz): δ 103.3, 87.1, 29.3, 24.4, 0.1.

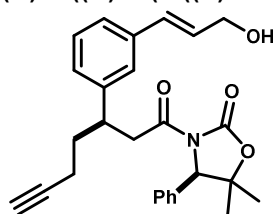


(R)-3-((R)-3-((E)-3-((tert-butyl)dimethylsilyloxy)prop-1-en-1-yl)phenyl)-7-(trimethylsilyl)hept-6-ynoyl)-5,5-dimethyl-4-phenyloxazolidin-2-one (27c). Grignard reagent **26** was prepared by addition of



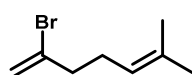
4-bromo-1-trimethylsilyl-1-butyne (16.4 g, 80 mmol) in THF (80 mL) to magnesium filings (2.92 g, 120 mmol); initial addition of 8 mL followed by dropwise addition of the remainder via syringe pump over 1 h. The solution was warmed to reflux for 15 min, cooled to room temperature, diluted with 80 mL THF and titrated against a standard solution of menthol in THF ($c = 0.50$ M) containing 1,10-phenanthroline as an indicator. Copper(I) iodide (10.11 g, 53.1 mmol) was dissolved in THF (90 mL) and dimethylsulfide (22 mL), cooled to -78 °C and stirred for 15 min. The Grignard reagent (101 mL) was added via cannula over 10 minutes, and the mixture was stirred for 10 minutes at -78 °C, then 10 minutes at -40 °C. A pre-cooled solution of **9** (22.53g, 45.8 mmol) in THF (60 mL) was added over 10 minutes, and stirring continued at -40 °C for 30 min and then at -20 °C for 4h. The reaction was quenched with saturated NH_4Cl (25 mL) and diluted with H_2O (150 mL). The aqueous phase was extracted with EtOAc , and the combined organic phase was washed with H_2O , brine, dried over MgSO_4 , and concentrated. The residue was freed from copper salts by repeated trituration with 1:1 hexane: EtOAc and filtration through short plugs of silica gel. Compound **27c** (27.30 g, 96%, single diastereomer by ^1H NMR) was used without purification. $R_f = 0.39$, 10% EtOAc /hexanes (x2). ^1H NMR (CDCl_3 , 400 MHz): δ 7.28–7.38 (m, 3H), 7.18–7.24 (m, 3H), 7.05–7.10 (m, 3H), 6.55 (dt, $J = 15.8, 1.7$ Hz, 1H), 6.27 (dt, $J = 15.8, 5.0$ Hz, 1H), 4.87 (s, 1H), 4.35 (dd, $J = 5.0, 1.7$ Hz, 2H), 3.67 (dd, $J = 16.2, 9.6$ Hz, 1H), 3.27 (dddd, $J = 10.0, 9.6, 5.4, 4.9$ Hz, 1H), 3.09 (dd, $J = 16.2, 5.4$ Hz, 1H), 1.75–2.12 (m, 4H), 1.34 (s, 3H), 0.95 (s, 9H), 0.90 (s, 3H), 0.12 (brs, 15H). ^{13}C NMR (CDCl_3 , 100 MHz): δ 171.5, 153.4, 143.1, 137.4, 136.4, 129.5, 129.4, 129.0, 128.8, 128.7, 126.9, 126.1, 124.9, 106.7, 85.1, 82.5, 67.1, 64.0, 41.5, 41.2, 35.4, 28.7, 26.1, 25.8, 23.7, 18.6, 18.1, 0.3, -5.0. HRMS (ESI) Calculated for $\text{C}_{36}\text{H}_{51}\text{NO}_4\text{Si}_2$ $[\text{M}+\text{Na}]^+$: 640.3249, found 640.3243.

(R)-3-((R)-3-(3-((E)-3-Hydroxyprop-1-en-1-yl)phenyl)hept-6-ynoyl)-5,5-dimethyl-4-phenyloxazolidin-2-one (28).

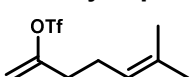


To a solution of **27c** (24.40 g, 39.48 mmol) in THF (400 mL) at -10 °C was added tetrabutylammonium fluoride (1.0M/THF, 98.70 mL, 98.71 mmol) over 15 min. The resulting orange solution was stirred for 1h at this temperature then diluted with EtOAc (500 mL) and washed with sat. NH₄Cl, and brine, dried over Na₂SO₄ and concentrated by rotary evaporation. The crude oil was taken up in chloroform (100 mL) and filtered through a plug of silica with 1:1 ethyl acetate:hexanes (1.0 L). The filtrate was concentrated to give **28** (16.25 g, 95 %) as an orange foam. ¹H NMR (CDCl₃, 400 MHz): δ 7.24-7.34 (m, 3H), 7.14-7.24 (m, 3H), 7.02-7.1 (m, 3H), 6.54 (dt, *J* = 15.9, 1.4 Hz, 1H), 6.31 (dt, *J* = 15.9, 5.6 Hz, 1H), 4.86 (s, 1H), 4.24 (dd, *J* = 5.6, 1.4 Hz, 2H), 3.63 (dd, *J* = 16.2, 9.3 Hz, 1H), 3.24-3.34 (m, 1H), 3.08 (dd, *J* = 16.2, 5.7 Hz, 1H), 2.65 (brs, 1H), 1.70-2.05 (m, 5H), 1.30 (s, 3H), 0.88 (s, 3H). ¹³C NMR (CDCl₃, 100 MHz): δ 171.3, 153.3, 143.0, 137.1, 136.2, 130.5, 129.1, 128.9, 128.8, 128.7, 128.6, 127.0, 126.0, 124.9, 83.7, 82.5, 69.1, 66.9, 63.3, 41.5, 40.8, 35.0, 28.5, 23.5, 16.5. HRMS (ESI) Calculated for C₂₇H₂₉NO₄ [M+Na]⁺: 454.1989, found 454.1992.

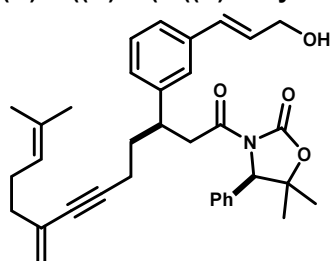
2-bromo-6-methylhepta-1,5-diene (29).¹¹ To a suspension of Mg⁰ powder (4.84 g, 201 mmol) in Et₂O (225 mL) at -10°C was added prenyl bromide (7.75 mL, 67 mmol) dropwise over 1.5 hr. The mixture was stirred for 30 min, then allowed to warm to rt and stirred for an additional 30min. Excess Mg⁰ was allowed to settle, and the supernatant was added dropwise to a suspension of CuCN (0.60 g, 6.7 mmol) in THF (20 mL) at -78 °C. Stirred for 30 min, then added 2,3-dibromo-1-propene (5.25 mL, 54 mmol) dropwise as a solution in THF (15 mL), and continued stirring at -78 °C for 4h before warming to rt. The reaction was quenched by the addition of sat. NH₄Cl (50 mL), diluted with EtOAc, and washed with sat. NH₄Cl, 1% EDTA, brine, dried over Na₂SO₄ and concentrated. Flash chromatography on SiO₂ eluted with hexanes afforded **29** as a colorless liquid of moderate purity. ¹H NMR (CDCl₃, 400 MHz): δ 1.64 (s, 3H), 1.70 (s, 3H), 2.25 (ddd, *J* = 7.3, 7.3, 7.3 Hz, 2H), 2.44 (t, *J* = 7.5 Hz, 2H), 5.05-5.15 (m, 1H), 5.38-5.42 (m, 1H), 5.55-5.58 (m, 1H). ¹³C NMR (CDCl₃, 100 MHz): δ 134.5, 133.1, 131.6, 124.6, 122.4, 116.6, 41.7, 26.8, 25.8, 17.9.



6-Methylhepta-1,5-dien-2-yl trifluoromethanesulfonate (30).¹² A solution of diisopropylamine (10.2 ml, 72 mmol) in THF (90 ml) was cooled to 0 °C and *n*-BuLi (30 ml, 2.5M in hexanes, 72 mmol) was added slowly. The solution was stirred for 30 min, and cooled to -78 °C. A cold solution of 6-methylhept-5-en-2-one (7.57 g, 60 mmol) in THF (35 ml) was added and the solution was stirred for 30 min before adding 2-pyridyltriflimide¹³ (22.6 g, 63 mmol) as a solution in THF (35 ml). After stirring for 30 min, the reaction was warmed to -20 °C and stirred for 1.5 h. The red suspension was diluted with diethyl ether (100 ml) and quenched with saturated NaHCO₃ (50 ml). The aqueous phase was removed and extracted with ether (2x 50ml). The combined organic phase was washed with water (2x 100ml), brine, dried over magnesium sulfate and concentrated. The residue was distilled in vacuo to give vinyl triflate **30** (10.8g, 70%, bp 70-74 °C, 5 torr) as a colorless oil. ¹H NMR (CDCl₃, 400 MHz): δ 1.61 (br s, 3H), 1.68-1.70 (m, 3H), 2.22 (ddd, *J* = 7.2, 7.2, 7.2 Hz, 2H), 2.35 (dd, *J* = 7.8, 7.2 Hz, 2H), 4.92 (dt, *J* = 3.5, 1.0 Hz, 1H), 5.03-5.08 (m, 1H), 5.08 (d, *J* = 3.5 Hz, 1H).

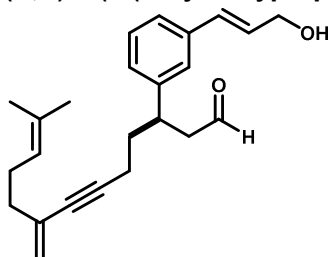


(R)-3-((R)-3-(3-((E)-3-Hydroxyprop-1-en-1-yl)phenyl)-12-methyl-8-methylenetric-11-en-6-ynoyl)-5,5-dimethyl-4-phenyloxazolidin-2-one (33).¹² A mixture of PdCl₂(PPh₃)₂ (641mg, 0.913 mmol), CuI (349 mg, 1.83 mmol), diisopropylamine (12.8 mL, 91.3 mmol) and vinyl triflate **30** (11.31 g, 43.8 mmol) in argon-sparged THF (40 mL) and DMF (10 mL) was cooled to 0 °C, and a solution of alkyne **28** (15.75 g, 36.5 mmol) in THF (50 mL) was added over 10 min. The reaction was allowed to warm to room temperature and stir an additional 1h. The reaction mixture was diluted with EtOAc, washed with H₂O, brine, dried over MgSO₄ and concentrated. Purification by flash chromatography (SiO₂, gradient 0 → 50% EtOAc/hexanes) gave diene-yne **33** (12.04 g, 61%) as a light brown oil. ¹H NMR (CDCl₃, 300 MHz): δ 7.28-7.38 (m, 3H), 7.20-7.24 (m, 3H), 7.04-7.14 (m, 3H), 6.57 (brd, *J* = 15.9 Hz, 1H), 6.34 (td, *J* = 15.9, 5.6 Hz, 1H), 5.19 (d, *J* = 1.3 Hz, 1H), 5.11 (d, *J* = 1.3 Hz, 1H), 5.05-5.10 (m, 1H), 4.87 (s, 1H), 4.29 (d, *J* = 5.6 Hz, 2H), 3.66 (dd, *J* = 16.1, 9.4 Hz, 1H), 3.23-3.36 (m, 1H), 3.10 (dd, *J* = 16.1, 5.4 Hz, 1H), 1.76-2.23 (m, 9H), 1.67 (s, 3H), 1.59 (s, 3H), 1.33 (s, 3H), 0.91 (s, 3H). ¹³C



NMR (CDCl₃, 75 MHz): δ 171.4, 153.3, 143.2, 137.0, 136.3, 132.1, 131.8, 131.1, 129.0, 128.9, 128.8, 128.7, 127.3, 126.6, 126.1, 124.9, 123.6, 119.9, 89.2, 82.5, 81.6, 67.0, 63.7, 41.6, 41.1, 37.7, 35.5, 28.6, 26.9, 25.8, 23.6, 17.8, 17.5. HRMS (ESI) Calculated for C₃₅H₄₁NO₄ [M+Na]⁺: 562.2933, found 562.2912.

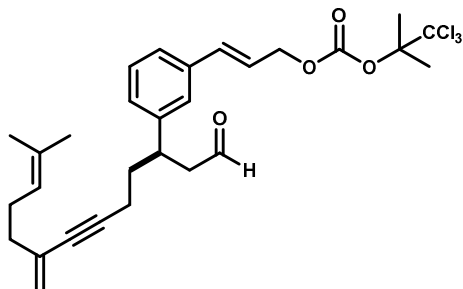
(*R,E*)-3-(3-(3-Hydroxyprop-1-en-1-yl)phenyl)-12-methyl-8-methylenetric-11-en-6-ynal (35**).**¹⁴



A solution of 1-acyl-oxazolidin-2-one **33** (8.84 g, 16.4 mmol) in toluene (160 mL) was cooled to -78 °C and diisobutylaluminum hydride (49 mL, 1.0 M/hexanes) was added. After stirring 20 min at this temperature, 10 % (w/v) aqueous Rochelle's salt (100 mL) was added and the reaction was warmed to rt, stirred for 15 min, and filtered through Celite. The aqueous filtrate was extracted with EtOAc and the combined organic phase was washed with brine, dried over Na₂SO₄ and concentrated. The partially solidified residue was reconstituted in Et₂O and treated with pentane to induce crystallization.

After chilling, the mixture was filtered and the cake washed with cold 2:1 pentane:Et₂O to recover the chiral auxiliary (1.503 g, 48%) as colorless needles. The filtrate was concentrated to give **35** (5.49 g) as a light brown oil, which was used without purification. An aliquot was purified for characterization (preparative TLC eluent 1:1:1 hexane:DCM:EtOAc). ¹H NMR (CDCl₃, 400 MHz): δ 9.66 (t, *J* = 1.8 Hz, 1H), 7.30-7.24 (m, 3H), 7.23-7.20 (m, 1H), 6.60 (brd, *J* = 15.9 Hz, 1H), 6.36 (dt, *J* = 15.9, 5.6 Hz, 1H), 5.23 (d, *J* = 1.1 Hz, 1H), 5.16 (d, *J* = 1.1 Hz, 1H), 5.14-5.08 (m, 1H), 4.32 (dd, *J* = 5.6, 1.0 Hz, 2H), 3.40-3.30 (m, 1H), 2.75 (dt, *J* = 7.1, 1.8 Hz, 2H), 2.26-2.06 (m, 7H), 1.97-1.76 (m, 2H), 1.69 (s, 3H), 1.62 (s, 3H). ¹³C NMR (CDCl₃, 75 MHz): δ 201.5, 143.1, 137.3, 132.2, 131.8, 131.0, 129.2, 129.0, 127.0, 125.9, 125.1, 123.5, 120.1, 89.0, 81.9, 63.7, 50.1, 39.0, 37.8, 35.4, 26.9, 25.8, 17.9, 17.4.

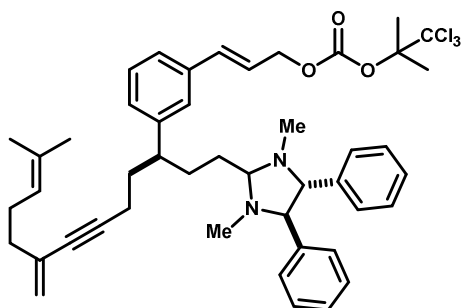
(*R,E*)-3-(3-(12-Methyl-8-methylene-1-oxotridec-11-en-6-yn-3-yl)phenyl)allyl (1,1,1-trichloro-2-methylpropan-2-yl) carbonate (1**).**¹⁵



A solution of alcohol **35** (9.74 g, 27.8 mmol) in DCM (280 mL) was cooled to -40 °C. A solution of pyridine (3.6 mL, 44.5 mmol) and DMAP (408 mg, 3.3 mmol) in DCM (90 mL) was added, followed by dropwise addition of 1,1-dimethyl-2,2,2-trichloroethyl chloroformate (9.33 g, 38.9 mmol) in DCM (90 mL). The reaction was stirred for 2 h, diluted with EtOAc (700 mL), washed with cold sat. NaHCO₃, H₂O, brine, dried over MgSO₄ and concentrated. Purification by flash chromatography (SiO₂, 15% EtOAc/hexanes) afforded (+)-**1** as a colorless oil (8.06 g, 52% from **33**, 91% ee). (Note: This material

was stable for upwards of 2 years as a 0.3 M solution degassed DMF, and stored at -20 °C). [α]_D²⁰ = +30.5° (c 0.56, CHCl₃). ¹H NMR (CDCl₃, 500 MHz): δ 9.66 (t, *J* = 1.9 Hz, 1H), 7.10-7.32 (m, 4H), 6.67 (brd, *J* = 15.8 Hz, 1H), 6.30 (dt, *J* = 15.8, 6.6 Hz, 1H), 5.23 (s, 1H), 5.15 (s, 1H), 5.08-5.14 (m, 1H), 4.78 (d, *J* = 6.7 Hz, 2H), 3.33-3.42 (m, 1H), 2.75 (dt, *J* = 7.5, 1.9 Hz, 2H), 2.07-2.29 (m, 6H), 1.96 (s, 6H), 1.75-1.95 (m, 2H), 1.69 (s, 3H), 1.62 (s, 3H). ¹³C NMR (CDCl₃, 125 MHz): δ 201.3, 152.4, 143.2, 136.6, 135.1, 132.2, 131.8, 129.2, 127.6, 126.1, 125.4, 123.5, 122.7, 120.2, 105.6, 90.1, 88.9, 81.9, 68.6, 50.1, 39.0, 37.8, 35.4, 26.9, 25.8, 21.3 (2), 17.9, 17.4.

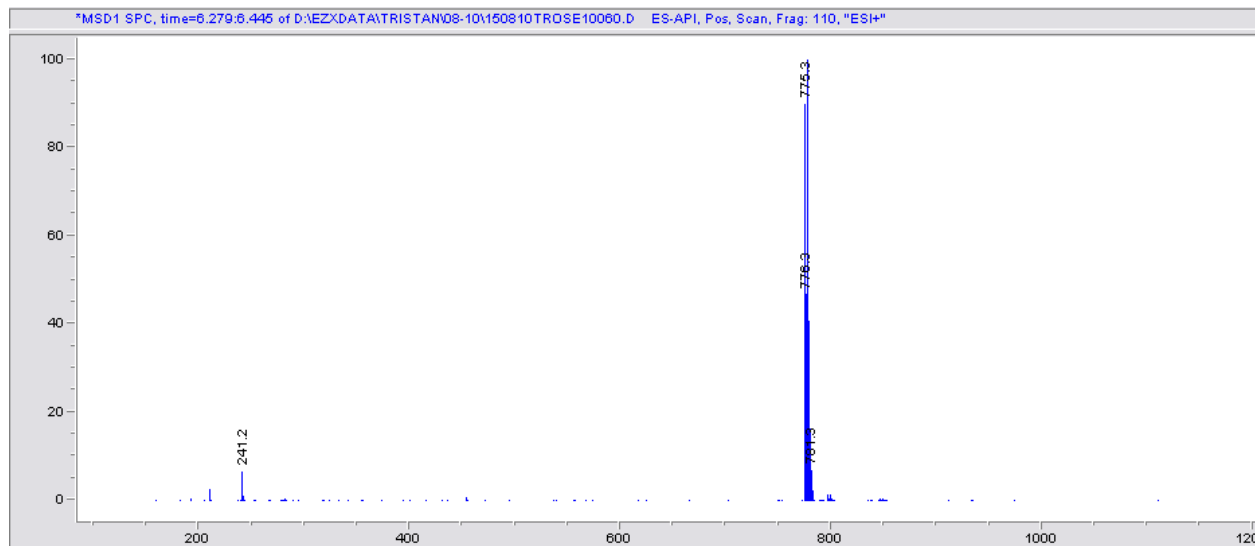
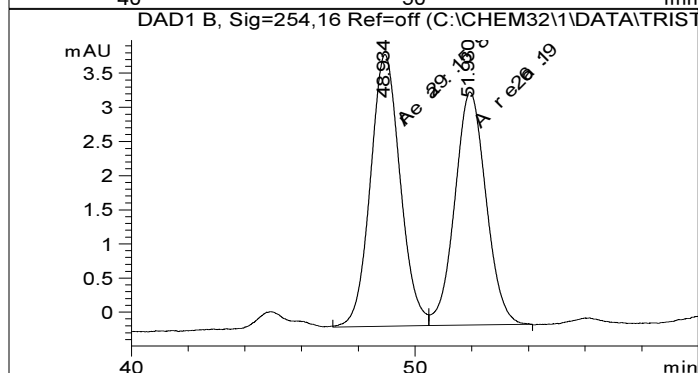
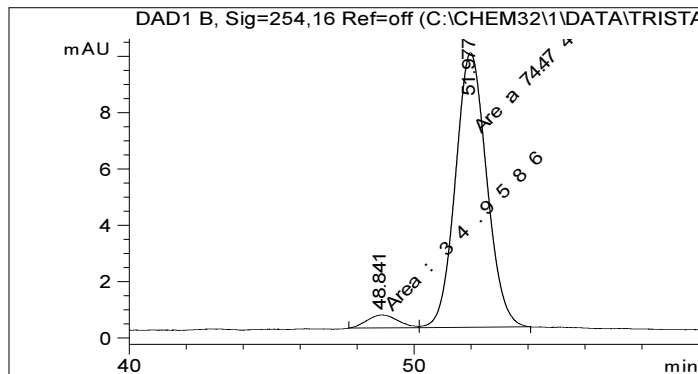
Derivatization of **1 for %ee Determination.**^{16,17}



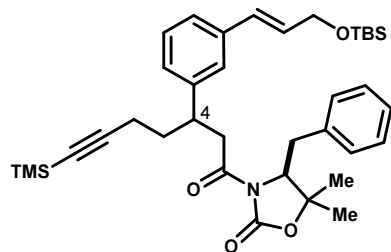
Aldehyde (+)-**1** (20 mg, 36 μ mol), (*R,R*)-*N,N'*-dimethyl-1,2-diphenylethylene diamine **41** (8.7 mg, 36 μ mol) and activated 4Å molecular sieves were stirred in DCM (2 ml) overnight. The reaction mixture was filtered and analyzed directly by HPLC-UV. The diastereomeric mixture was prepared from (\pm)-**1** and diamine **41** in the same manner. ESI-(+) [M+H]⁺ calc: 776.3 m/z found: 776.3 m/z

HPLC: Agilent 1200
Column: Waters Sunfire 4.6x250mm, 5 μ C18
Flow: 1 mL/min
Temp: ambient
Solv. A: H₂O + 0.1% HCO₂H
Solv. B: ACN + 0.1% HCO₂H
UV: 254nm, 220nm

time (min)	%A	%B
0	40	60
60	40	60



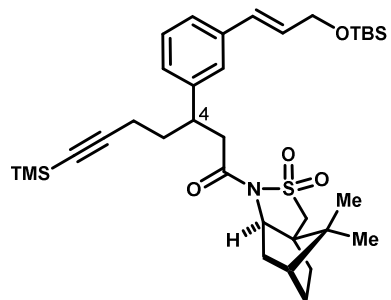
(4S)-4-Benzyl-3-(3-(3-((E)-3-((tert-butyl)dimethylsilyloxy)prop-1-en-1-yl)phenyl)-7-



(trimethylsilyl)hept-6-ynoyl)-5,5-dimethyloxazolidin-2-one (27b).

Trimethylsilyl alkyne **27b** (1.813 g, 83%, ~2:1 mixture of C4 diastereomers) was prepared analogously to compound **27c**. ¹H NMR (CDCl₃, 300 MHz, mixture of C4 diastereomers): δ 0.10 (s, 3H), 0.11 (s, 6H), 0.15 (s, 13.5H), 0.94 (s, 4.5H), 0.94 (s, 9H), 1.05 (s, 3H), 1.25 (s, 1.5H), 1.29 (s, 3H), 1.30 (s, 1.5H), 1.72-1.99 (m, 4H), 1.99-2.17 (m, 3.5H), 2.58 (dd, *J* = 14.3, 9.8 Hz, 0.5H), 2.77 (dd, *J* = 14.4, 9.5 Hz, 1H), 2.88 (dd, *J* = 14.4, 3.4 Hz, 1H), 3.03 (dd, *J* = 14.3, 4.2 Hz, 0.5H), 3.05 (dd, *J* = 15.8, 6.1 Hz, 1H), 3.13 (dd, *J* = 15.6, 6.4 Hz, 0.5H), 4.23-4.38 (m, 1.5H), 3.47 (dd, *J* = 15.6, 8.3 Hz, 0.5H), 3.56 (dd, *J* = 15.8, 9.1 Hz, 1H), 4.29-4.39 (m, 4.5H), 4.42 (dd, *J* = 9.8, 3.6 Hz, 0.5H), 6.26 (dt, *J* = 15.8, 5.0 Hz, 1H), 6.55 (dd, *J* = 15.9, 1.7 Hz, 1H), 7.04-7.12 (m, 1.5H), 7.12-7.32 (m, 13.5H). ¹³C NMR (CDCl₃, 75 MHz, mixture of diastereomers): δ 171.9, 171.7, 152.6, 152.6, 142.9, 137.4, 137.3, 136.93, 136.92, 129.4, 129.3, 129.0, 128.9, 128.8, 128.7, 128.64, 128.61, 126.8, 126.7, 126.03, 126.01, 124.9, 124.8, 106.7, 85.03, 85.00, 82.1, 82.0, 63.8, 63.41, 63.35, 41.7, 41.30, 41.27, 41.1, 35.3, 35.2, 35.1, 34.8, 28.5, 28.0, 26.0, 22.3, 22.2, 18.5, 18.0, 0.2, -5.1.

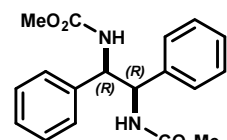
3-(3-((E)-3-((tert-Butyl)dimethylsilyloxy)prop-1-en-1-yl)phenyl)-1-((3aR,6R,7aR)-8,8-dimethyl-2,2-dioxidohexahydro-1H-3a,6-methanobenzo[c]isothiazol-1-yl)-7-



(trimethylsilyl)hept-6-yn-1-one (27a).

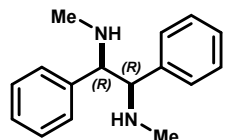
Trimethylsilyl alkyne **27a** (103 mg, 32%, ~2:1 mixture of C4 diastereomers) was prepared analogously to compound **27c**. ¹H NMR (CDCl₃, 300 MHz, mixture of diastereomers): δ 0.10 (s, 3H), 0.11 (s, 6H), 0.130 (s, 4.5H), 0.133 (s, 9H), 0.72 (s, 3H), 0.96 (s, 3H), 0.92-0.95 (m, 13.5H), 1.19-1.38 (m, 3.5H), 1.51-1.60 (m, 1H), 1.64-1.70 (m, 1H), 1.72-1.95 (m, 7.5H), 1.95-2.15 (m, 3.5H), 2.81 (dd, *J* = 15.0, 5.5 Hz, 1H), 3.02-3.07 (m, 0.5H), 3.20 (d, *J* = 15.0 Hz, 0.5H), 3.22 (d, *J* = 15.0 Hz, 1H), 3.29-3.41 (m, 4H), 3.45 (dd, *J* = 14.0, 14.0 Hz, 1H), 3.72-3.80 (m, 1.5H), 4.32 (dd, *J* = 5.0, 1.5 Hz, 3H), 6.21-6.30 (m, 1.5H), 6.52 (dd, *J* = 16.0, 1.5 Hz, 1H), 6.54 (dd, *J* = 15.6, 1.5 Hz, 0.5H), 7.03-7.09 (m, 1.5H), 7.14-7.22 (m, 4.5H).

Dimethyl ((1R,2R)-1,2-diphenylethane-1,2-diyl)dicarbamate (S8).¹⁸



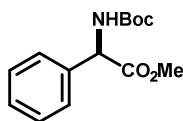
1R,2R-1,2-diamino-1,2-diphenylethane (1.0 g, 4.7 mmol) was dissolved in THF (40 mL), and H₂O (5 mL) and K₂CO₃ (1.6 g, 11.6 mmol) were added. The mixture was cooled in an ice bath, and methyl chloroformate (1.7 mL, 22 mmol) was added. The reaction was allowed to warm to rt and stirred for 3.5 hrs. The organic phase was collected, exchanged for DCM (100 mL), and then dried over MgSO₄ and concentrated to give **S8** (1.53 g, >100%) as a white solid, which was used without further purification. MS *m/z* 329.1, (calc'd: C₁₈H₂₁N₂O₄, [M+H]⁺, 329.1 *m/z*).

(1R,2R)-N,N'-Dimethyl-1,2-diphenylethane-1,2-diamine (41).¹⁸

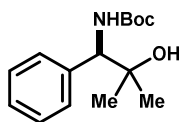


Lithium aluminum hydride (770 mg, 20.2 mmol) was suspended in dry THF (35 mL), and cooled in an ice bath. *Bis*-carbamate **S8** (2.03 g, 6.2 mmol) was added in several portions as a solid, and the reaction was allowed to warm to rt and stirred for 1 hr, and was then heated to reflux overnight. The reaction was cooled, quenched by adding EtOAc and then 1 M NaOH, and extracted into Et₂O (x3). The organic phase was dried over K₂CO₃ and concentrated to give 1.04 g of an oil, which was dissolved in EtOH (26 mL), and treated with *L*-tartaric acid (651 mg, 4.3 mmol). The resulting precipitate was collected by filtration, and the salt was broken with 5M NaOH and extracted into EtOAc (x3). The organic phase was dried over K₂CO₃ and concentrated to give **41** as a white solid (598 mg, 40%). ¹H NMR (CDCl₃, 300 MHz): δ 1.92 (br s, 2H), 2.25 (s, 6H), 3.53 (s, 2H), 7.01-7.05 (m, 4H), 7.09-7.18 (m, 6H).s

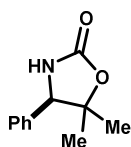
N-Boc-(R)-Phenylglycine methyl ester (S9).¹⁹ *N*-Boc-(R)-(-)-phenylglycine methyl ester hydrochloride (300 g, 1.49 mol) was dissolved in water (1.5L) and treated with triethylamine (217 mL, 1.56 mol) followed by Boc₂O (340 g, 1.56 mol) which caused a mild exotherm. The mixture was stirred for 40 min, and the resulting precipitate was filtered and dried under vacuum to give **S9** as a white solid (397 g, ~100%). ¹H NMR (CDCl₃, 400 MHz): δ 1.43 (s, 9H), 3.72 (s, 3H), 5.32 (d, *J* = 7.2 Hz, 1H), 5.55 (br d, *J* = 7.2 Hz, 1H), 7.29-7.39 (m, 5H).



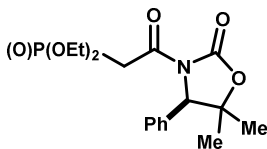
N-Boc-(R)-1-amino-2-methyl-1-phenylpropan-2-ol (44).¹⁹ Ester **S9** (397 g, 1.49 mol) was dissolved in dry THF (6 L) and stirred for 30 min to give a milky white suspension, which was cooled to 0 °C and stirred for an additional 30 min. Methylmagnesium bromide (1995 mL, 3 M in Et₂O, 6.0 mol) was added (**Caution!** gas evolution) over 75 min. The reaction was stirred cold for 30 min, then allowed to warm to rt and stir overnight. The reaction was re-cooled, and quenched by dropwise addition of methanol (350 mL) (**Caution!** gas evolution) followed by water (340 mL). Rochelle's salt (500 g) was added and the mixture stirred for 1 h. The supernatant was removed and the residual solids rinsed with several portions of ether. The combined organic phase was filtered through Celite and concentrated by rotary evaporation. The amber residue was reconstituted in EtOAc (2.5 L) and washed with water (3x 500 mL), brine (2x 500 mL), dried over magnesium sulfate and concentrated to give **44** as a white solid (254 g, 64%). ¹H NMR (CDCl₃, 400 MHz): δ 1.060 (s, 3H), 1.33 (s, 3H), 1.41 (s, 9H), 4.46-4.57 (m, 1H), 5.43-5.58 (m, 1H), 7.25-7.38 (m, 5H).



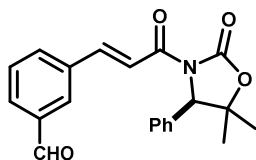
(R)-5,5-Dimethyl-4-phenyloxazolidin-2-one (36).¹⁹ Alcohol **44** (254 g, 958 mmol) was dissolved in THF (3.5 L), cooled to 0 °C and stirred for 30 min. Potassium *tert*-butoxide (129 g, 1.15 mol) in one portion, which caused an exotherm of 11 °C. The reaction mixture was stirred for 40 min, and quenched with brine (300 mL) followed by 1N HCl (800 mL). The organic phase was removed, and the aqueous remainder extracted with EtOAc (2x 200 mL). The combined organic phase was washed with brine, dried over MgSO₄ and concentrated. The resulting solid was recrystallized from THF/EtOAc/hexanes under stirring to give **36** (140 g, 76%) as a white crystalline solid. [α]_D²⁰ = -78.3 (*c* = 0.5, CHCl₃). ¹H NMR (CDCl₃, 300 MHz): δ 0.95 (s, 3H), 1.62 (s, 3H), 4.66 (s, 1H), 5.51 (br s, 1H), 7.27-7.31 (m, 2H), 7.33-7.42 (m, 3H).



Diethyl {2-[(4R)-4-Phenyl-2-oxo-1,3-oxazolidin-3-yl]-2-oxoethyl}-phosphonate (46). To a solution of oxazolidinone **36** (62.09 g, 324.7 mmol) in THF (1.3 L) at -78 °C was added *n*-BuLi (2.5 M in hexane, 132.5 mL, 331.2 mmol) dropwise over 30 minutes. The resulting solution was stirred 30 min at this temperature prior to the addition of bromoacetyl bromide (65.5 g, 325 mmol) over 3 minutes via syringe. After stirring an addition 45 minutes the solution was allowed to slowly warm to 0 °C and sat. NH₄Cl (300 mL) is added. The organic layer is separated and washed with sat. NH₄Cl and brine, dried over Na₂SO₄ and concentrated. This material was taken up in triethylphosphite (670 mL) and heated to 60 °C for 2h then concentrated under reduced pressure. The resulting dark viscous oil was taken up in ethyl acetate (2.0 L) and washed sequentially with water and brine, dried over Na₂SO₄ and concentrated to give an amber oil. This material is used without further purification. ¹H NMR (CDCl₃, 400 MHz): δ 7.28-7.39 (m, 3H), 7.16-7.22 (m, 2H), 5.07 (s, 1H), 4.09-4.17 (m, 4H), 3.98 (dd, *J*_{HP} = 22.5 Hz, *J*_{HH} = 13.7 Hz, 1H), 3.66 (dd, *J*_{HP} = 22.5 Hz, *J*_{HH} = 13.7 Hz, 1H), 1.62 (s, 3H), 1.30 (t, *J* = 7.1 Hz, 1H), 1.27 (t, *J* = 7.1 Hz, 1H), 0.99 (t, *J* = 7.1 Hz, 1H). ¹³C NMR (CDCl₃, 100 MHz): δ 164.6 (d, *J*_{CP} = 6.8 Hz), 153.2, 135.8, 128.8, 128.6, 126.5, 82.7, 67.3, 62.8 (d, *J*_{CP} = 6.0 Hz), 34.6 (d, *J*_{CP} = 129 Hz), 28.8, 23.6, 16.32 (d, *J*_{CP} = 1.7 Hz), 16.26 (d, *J*_{CP} = 1.7Hz).

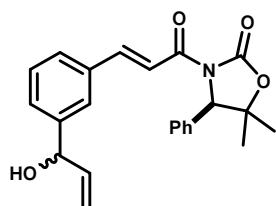


(R,E)-3-(3-(5,5-Dimethyl-2-oxo-4-phenyloxazolidin-3-yl)-3-oxoprop-1-en-1-yl)benzaldehyde (47). Diisopropylethylamine (62.2 mL, 357 mmol) was added to a solution of phosphonoacetate **46** (119 g, 324 mmol) and LiCl (15.1 g, 357.2 mmol) in ACN (2 L) at rt. This mixture was stirred for 5 minutes prior to the addition of isophthalaldehyde (87.1 g, 649.4 mmol) in one portion. After stirring overnight, water (500 mL) was added and the mixture was extracted with EtOAc (1.0 L). The organic phase was washed with sat. NH₄Cl, sat. NaHCO₃, and brine, dried over Na₂SO₄ and concentrated in vacuo. Purification by flash chromatography (SiO₂, gradient 70:15:10 →



45:15:40 hexanes:CHCl₃:Et₂O) gave aldehyde **47** (83.5 g, 74 % over 3 steps) as a white solid. ¹H NMR (CDCl₃, 400 MHz): δ 10.05 (s, 1H), 8.10 (d, *J* = 15.7 Hz, 1H), 8.05 (d, *J* = 0.6, 1H), 7.92 (dd, *J* = 7.6, 1.3 Hz, 1H), 7.86 (d, *J* = 7.8 Hz, 1H), 7.80 (d, *J* = 15.7 Hz, 1H), 7.57 (app t, *J* = 7.7 Hz, 1H), 7.30-7.45 (m, 3H), 7.15-7.25 (m, 2H), 5.21 (s, 1H), 1.66 (s, 3H), 1.04 (s, 3H). ¹³C NMR (CDCl₃, 100 MHz): δ 191.7, 164.6, 153.3, 144.5, 136.9, 136.2, 135.5, 133.9, 131.0, 129.9, 129.7, 128.9, 128.7, 126.4, 119.0, 82.7, 67.3, 29.0, 23.8. HRMS (ESI) Calculated for C₂₁H₁₉NO₄ [M+Na]⁺: 372.1206, found 372.1207.

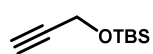
(4R)-3-((E)-3-(3-(1-Hydroxyallyl)phenyl)acryloyl)-5,5-dimethyl-4-phenyloxazolidin-2-one (48). To a



solution of aldehyde **47** (5.0 g, 14.3 mmol) in toluene (190 mL) at -78 °C was added dropwise vinylmagnesium chloride (1.6 M in THF, 10.3 mL, 16.47 mmol) over 45 minutes maintaining an internal temperature < -65 °C. The mixture was stirred an additional 4h at this temperature and quenched with saturated NH₄Cl (50 mL). The organic layer was separated, diluted with ethyl acetate (100 mL) and washed sequentially with sat. NH₄Cl, water, and brine. The solution was dried over Na₂SO₄, filtered and concentrated to give a crude yellow foam which was used in the next step without further purification. An analytically pure sample of

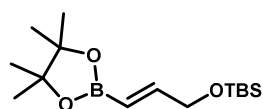
48 was obtained by flash chromatography (SiO₂, gradient 15 → 40% EtOAc/hexanes). ¹H NMR (CDCl₃, 400 MHz): δ 8.00 (d, *J* = 15.7 Hz, 1H), 7.76 (d, *J* = 15.7 Hz, 1H), 7.58 (s, 1H), 7.53 (dd, *J* = 7.2, 1.6 Hz, 1H), 7.30-7.45 (m, 5H), 7.25-7.05 (m, 2H), 6.03 (ddd, *J* = 16.8, 10.3, 5.9 Hz, 1H), 5.36 (ddd, *J* = 16.8, 1.2, 1.2 Hz, 1H), 5.15-5.25 (m, 3H), 2.09 (s, 1H), 1.64 (s, 3H), 1.03 (s, 3H). ¹³C NMR (CDCl₃, 100 MHz): δ 165.1, 153.3, 146.4, 143.4, 140.0, 136.3, 134.8, 129.1, 128.9, 128.7, 128.6, 127.9, 126.6, 117.4, 115.6, 82.5, 75.0, 74.9, 67.3, 29.0, 23.8. HRMS (ESI) Calculated for C₂₃H₂₃NO₄ [M+Na]⁺: 400.1519, found 400.1521.

O-tert-Butyldimethylsilyl propargyl alcohol (S10).²⁰ Propargyl alcohol (17.7 mL, 0.3 mol) and imidazole



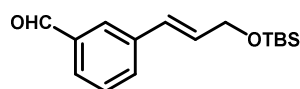
(40.8 g, 0.6 mol) were dissolved in dry DCM (300 mL), and cooled in an ice bath. TBSCl (47.5 g, 0.32 mol) was added in several portions, and the mixture was allowed to warm to rt and stirred overnight. The mixture was filtered, and the filtrate was washed with H₂O (x3), dried over MgSO₄, concentrated and distilled in vacuo (65-75 °C, 110-120 mbar) to give **S10** as a colorless liquid (46.4 g, 91%). ¹H NMR (CDCl₃, 300 MHz): δ 0.12 (s, 6H), 0.91 (s, 9H), 2.38 (t, *J* = 2.4 Hz, 1H), 4.31 (d, *J* = 2.4 Hz, 1H). ¹³C NMR (CDCl₃, 125 MHz): δ 82.6, 73.0, 51.6, 25.9, 18.4, -5.1.

((E)-3-tert-Butyldimethylsilyloxyprop-1-en-1-yl)boronic acid pinacol ester (50).²¹ To alkyne **S10** (13.6



g, 80 mmol) was added Schwartz's reagent (206 mg, 0.8 mmol), triethylamine (112 μL, 0.8 mmol) and pinacolborane (12.7 mL, 88 mmol). The mixture was warmed to 60 °C and stirred overnight. The reaction was cooled, diluted with hexanes, and filtered through a pad of SiO₂, rinsing with 5% EtOAc in hexanes. The filtrate was concentrated to give **50** (21.4 g, 90%) as a colorless oil, which solidifies upon prolonged storage at -20 °C. ¹H NMR (CDCl₃, 500 MHz): δ 0.10 (s, 6H), 0.95 (s, 9H), 1.31 (s, 12H), 4.29 (dd, *J* = 3.3, 2.1 Hz, 1H), 5.79 (dd, *J* = 18.0, 1.9 Hz, 1H), 6.72 (dt, *J* = 18.0, 3.5 Hz, 1H). ¹³C NMR (CDCl₃, 125 MHz): δ 152.3, 83.3, 64.6, 26.1, 24.9, 18.5. (one carbon missing, consistent with previous reports^{22,23})

O-tert-Butyldimethylsilyl-(E)-3-(3-hydroxyprop-1-en-1-yl)benzaldehyde (51). A flask was charged with



3-bromobenzaldehyde (7.55 g, 41 mmol), vinyl boronate **50** (14.6 g, 49 mmol), Na₂CO₃ (13.0 g, 123 mmol), and 5:1 THF:H₂O (200 mL). The mixture was sparged with argon for 20 min, Pd(PPh₃)₄ (948 mg, 0.82 mmol) was added, and the mixture was heated to 65 °C. After 65 hrs, the reaction was cooled, and partitioned between EtOAc and H₂O. The organic phase was washed with sat. NaHCO₃ (x2) and brine, dried over MgSO₄ and concentrated. The residue was reconstituted in 5% EtOAc in hexanes and filtered through a pad of SiO₂, rinsing with the same. The filtrate was concentrated to give **51** (11.7 g, ~100%) in moderate purity, contaminated primarily with pinacol, as a light yellow oil. ¹H NMR (CDCl₃, 500 MHz): δ 0.16 (s, 6H), 0.99 (s, 9H), 4.42 (dd, *J* = 4.6, 1.7 Hz, 2H), 6.43 (dt, *J* = 15.8, 4.7 Hz, 1H), 6.70 (br d, *J* = 15.8 Hz, 1H), 7.51 (dd, *J* = 7.8, 7.6 Hz, 1H), 7.66 (br d, *J* = 7.8 Hz, 1H), 7.76 (br d, *J* = 7.6 Hz, 1H), 7.91 (br s, 1H), 10.05 (s, 1H). ¹³C NMR (CDCl₃, 125 MHz): δ 192.5, 138.3, 136.8, 132.3, 131.3, 129.3, 128.7, 127.9, 127.4, 63.6, 26.1, 18.6, -5.1.

References

- (1) Ramana, C. V.; Suryawanshi, S. B.; Gonnade, R. G. *J. Org. Chem.* **2009**, *74*, 2842.
- (2) Klusener, P. A. A.; Kulik, W.; Brandsma, L. *J. Org. Chem.* **1987**, *52*, 5261.
- (3) Ohshita, J.; Iwata, A.; Kanetani, F.; Kunai, A.; Yamamoto, Y.; Matui, C. *J. Org. Chem.* **1999**, *64*, 8024.
- (4) Nicolaou, K. C.; Montagnon, T.; Baran, P. S. *Angew. Chemie - Int. Ed.* **2002**, *41*, 993.
- (5) Blanchette, M. A.; Choy, W.; Davis, J. T.; Essenfled, A. P.; Masamune, S.; Roush, W. R.; Sakai, T. *Tetrahedron Lett.* **1984**, *25*, 2183.
- (6) Ried, W.; Königstein, F.-J. *Chem. Ber.* **1959**, *92*, 2532.
- (7) Michels, H.-P.; Nieger, M.; Vögtle, F. *Chem. Ber.* **1994**, *127*, 1167.
- (8) Davies, S. G.; Sanganee, H. J.; Szolcsanyi, P. *Tetrahedron* **1999**, *55*, 3337.
- (9) Ho, G.; Mathre, D. J. *J. Org. Chem.* **1995**, *60*, 2271.
- (10) Dower, W. V.; Vollhardt, P. C. *Tetrahedron* **1986**, *42*, 1873.
- (11) Mushti, C. S.; Kim, J.; Corey, E. J. *J. Am. Chem. Soc.* **2006**, *128*, 14050.
- (12) Miller, M. W.; Johnson, C. R. *J. Org. Chem.* **1997**, *62*, 1582.
- (13) Comins, D. L.; Dehghani, A.; Foti, C. J.; Joseph, S. P. *Org. Synth.* **1997**, *74*, 77.
- (14) Bull, S. D.; Davies, S. G.; Nicholson, R. L.; Sanganee, H. J.; Smith, A. D. *Org. Biomol. Chem.* **2003**, *1*, 2886.
- (15) Zhao, H.; Negash, L.; Wei, Q.; LaCour, T. G.; Estill, S. J.; Capota, E.; Pieper, A. A.; Harran, P. G. *J. Am. Chem. Soc.* **2008**, *130*, 13864.
- (16) Mangeney, P.; Alexakis, A.; Normant, A. *Tetrahedron Lett.* **1988**, *29*, 2677.
- (17) Cuvilot, D.; Mangeney, P.; Alexakis, A.; Normant, J. F.; Lellouche, J. P. *J. Org. Chem.* **1989**, *54*, 2420.
- (18) Kuznetsov, V. F.; Jefferson, G. R.; Yap, G. P. A.; Alper, H. *Organometallics* **2002**, *21*, 4241.
- (19) Bull, S. D.; Davies, S. G.; Jones, S.; Polywka, M. E. C.; Shyam Prasad, R.; Sanganee, H. J. *Synlett* **1998**, 519.
- (20) Wender, P. a.; Sieburth, S. M.; Petratis, J. J.; Singh, S. K. *Tetrahedron* **1981**, *37*, 3967.
- (21) Wang, Y. D.; Kimball, G.; Prashad, A. S.; Wang, Y. *Tetrahedron Lett.* **2005**, *46*, 8777.
- (22) Fürstner, A.; Ackerstaff, J. *Chem. Commun. (Camb)*. **2008**, 2870.
- (23) Lee, H. M.; Nieto-Oberhuber, C.; Shair, M. D. *J. Am. Chem. Soc.* **2008**, *130*, 16864.

Chapter 2 Experimental Appendix

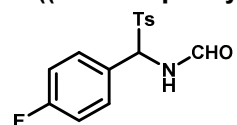
General remarks

See general remarks Chapter 3 Experimental Appendix.

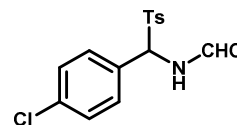
NMR methods:

See NMR methods Chapter 3 Experimental Appendix.

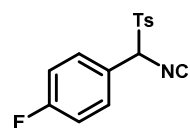
***N*-((4-Fluorophenyl)(tosyl)methyl)formamide (S1).**^{1,2} 4-Fluorobenzaldehyde (2.9 ml, 27 mmol) was dissolved in ACN (14 ml) and toluene (14 ml), and treated with formamide (2.6 ml, 67.5 mmol) and TMSCl (3.7 ml, 30 mmol). The reaction was heated to 50 °C for 4 h, and toluenesulfinic acid (6.2 g, 41 mmol) was added. The temperature was maintained at 50 °C for 4 h then cooled to rt. The reaction was treated with MTBE (15 ml), stirred for 5 min, and quenched with H₂O (70 ml). After cooling at 0 °C for 1 h, a precipitate formed which was filtered and dried to give **S1** (3.99 g, 48%) as a white solid. ¹H NMR (DMSO-*d*₆, 500 MHz, major rotamer): δ 2.40 (s, 3H), 6.46 (d, *J* = 10.6 Hz, 1H), 7.27 (dd, *J* = 8.9, 8.9 Hz, 2H), 7.43 (d, *J* = 8.3 Hz, 2H), 7.59-7.66 (m, 2H), 7.72 (d, *J* = 8.3 Hz, 2H), 7.97 (br s, 1H), 9.77 (d, *J* = 10.6 Hz, 1H). ¹³C NMR (DMSO-*d*₆, 125 MHz): δ 160.2, 144.9, 133.3, 131.7, 131.6, 129.64, 129.61, 129.2, 126.7, 69.4, 21.1.



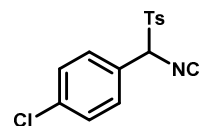
***N*-((4-Chlorophenyl)(tosyl)methyl)formamide (S2).**^{1,2} Compound **S2** (10.97 g, 64%) was prepared analogously to compound **S1**. ¹H NMR (DMSO-*d*₆, 500 MHz, major rotamer): δ 2.40 (s, 3H), 6.48 (d, *J* = 10.5 Hz, 1H), 7.43 (d, *J* = 8.4 Hz, 2H), 7.52 (d, *J* = 8.5 Hz, 2H), 7.60 (d, *J* = 8.6 Hz, 2H), 7.73 (d, *J* = 8.3 Hz, 2H), 7.97 (br s, 1H), 9.79 (d, *J* = 10.5 Hz, 1H). ¹³C NMR (DMSO-*d*₆, 125 MHz): δ 160.7, 145.4, 134.9, 133.7, 131.7, 130.1, 129.8, 129.6, 128.8, 69.9, 21.6.

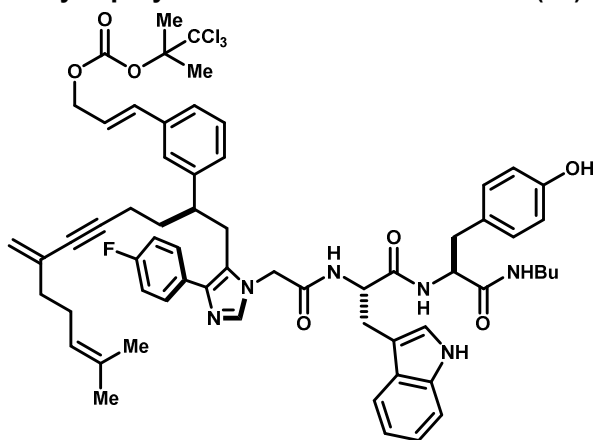


1-Fluoro-4-(isocyano(tosyl)methyl)benzene (11).^{1,2} Formamide **S1** (3.99 g, 13.0 mmol) was dissolved in THF (27 ml) and phosphorus oxychloride (2.4 ml, 26.0 mmol) was added at once. The reaction was stirred at rt for 5 min, then cooled to 0 °C and triethylamine (10.9 ml, 78 mmol) was added over 30 min. The reaction was allowed to warm to 10-15 °C and stir for 45 min, and was then diluted with EtOAc (20 ml) and washed with water (2x 20 ml), saturated NaHCO₃ (1x 20 ml), brine and concentrated. The residue was reconstituted in a small amount of MeOH and chilled overnight. The resulting precipitate was removed and dried to give isonitrile **11** (910 mg, 24%) as a light brown solid. ¹H NMR (CDCl₃, 400 MHz): δ 2.47 (s, 3H), 5.60 (s, 1H), 7.09 (dd, *J*_{HH} = 8.5 Hz, *J*_{HF} = 8.5 Hz, 2H), 7.31-7.38 (m, 4H), 7.62 (d, *J* = 8.3 Hz, 2H). ¹³C NMR (CDCl₃, 125 MHz): δ 22.0, 75.8, 116.1 (d, *J*_{CF} = 22 Hz), 122.6 (d, *J*_{CF} = 3.3 Hz), 130.01, 130.02, 130.61 (d, *J*_{CF} = 8.9 Hz), 130.63, 147.0, 164.2 (d, *J*_{CF} = 252 Hz), 166.5.



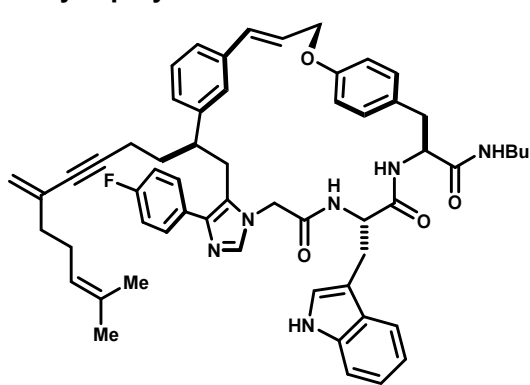
1-Chloro-4-(isocyano(tosyl)methyl)benzene (S3).^{1,2} Isonitrile **S3** (1.30 g, 28%) was prepared analogously to compound **11**. ¹H NMR (CDCl₃, 500 MHz): δ 2.47 (s, 3H), 5.59 (s, 1H), 7.28 (d, *J* = 8.6 Hz, 2H), 7.35 (d, *J* = 8.2 Hz, 2H), 7.38 (d, *J* = 8.6 Hz, 2H), 7.63 (d, *J* = 8.2 Hz, 2H). ¹³C NMR (CDCl₃, 101 MHz): δ 166.7, 147.0, 137.3, 130.6, 130.04, 129.98, 129.8, 129.2, 125.2, 75.9, 22.0.



H-Gly-Trp-Tyr-NH-*n*-Bu Derived Imidazole (13).^{3,4}

Aldehyde **1** (332 mg, 600 μmol), tripeptide H-Gly-Trp-Tyr-NH-*n*-Bu (316 mg, 660 μmol), powdered K_2CO_3 (207 mg, 1.5 mmol) and 4Å molecular sieves (330 mg) were stirred DMF (6 ml) for 4 h. Fluorophenyl tosylmethyl isonitrile **11** (208 mg, 720 μmol) was added, the mixture was stirred at rt overnight, then diluted with EtOAc, filtered through Celite and concentrated. Purification by column chromatography on SiO_2 eluted with 0→10% MeOH in DCM gave acyclic intermediate **13** (148 mg, 21%) as a light yellow solid. ^1H NMR (CD_3OD , 500 MHz, mixture of conformers): δ 0.80 (t, $J = 7.3$ Hz, 3H), 1.08-1.19 (m, 2H), 1.22-1.30 (m, 2H), 1.52 (s, 3H), 1.62 (s, 3H), 1.97-2.04 (m, 3H), 1.97-2.12 (m, 2H), 2.61-2.80 (m, 4H), 2.86 (dd, $J = 13.1, 7.9$ Hz, 1H), 2.93-3.01 (m, 1H),

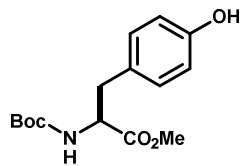
3.03-3.13 (m, 3H), 3.21-3.28 (m, 1H), 4.21 (br d, $J = 17.0$ Hz, 1H), 4.29 (br d, $J = 17.0$ Hz, 1H), 4.52 (apt t, $J = 7.2$ Hz, 1H), 4.65-4.72 (m, 2H), 4.98 (dd, $J = 8.5, 5.4$ Hz, 1H), 5.00-5.05 (m, 1H), 5.06 (br s, 1H), 6.12 (dt, $J = 15.8, 6.5$ Hz, 1H), 6.45 (d, $J = 15.8$ Hz, 1H), 6.64 (d, $J = 8.3$ Hz, 2H), 6.70 (br d, $J = 7.0$ Hz, 1H), 6.77 (br s, 1H), 6.85 (d, $J = 8.3$ Hz, 2H), 6.95-7.08 (m, 6H), 7.08-7.15 (m, 5H), 7.23-7.27 (m, 2H), 7.34 (d, $J = 8.1$ Hz, 1H), 7.56 (d, $J = 7.9$ Hz, 1H) (*tyrosyl OH not observed). ^{13}C NMR (CD_3OD , 125 MHz, major conformer): δ 173.1, 172.7, 168.6, 163.0 (d, $J_{\text{CF}} = 246$ Hz), 157.2, 153.5, 144.1, 138.6, 137.9, 137.4, 135.7, 133.1, 132.8, 132.2, 131.5, 130.3, 130.3, 129.7, 128.8, 128.6, 128.4, 127.7, 127.3, 126.0, 124.5, 123.6, 122.6, 120.3, 120.1, 119.5, 116.2, 116.1, 116.0, 112.5, 110.8, 106.7, 90.8, 90.1, 82.5, 69.5, 61.5, 56.3, 55.4, 47.9, 45.4, 40.1, 38.7, 35.0, 32.2, 31.5, 29.4, 27.8, 26.0, 21.6, 20.9, 18.0, 14.5, 14.1. MS (ESI) m/z calc'd for $\text{C}_{63}\text{H}_{71}\text{Cl}_3\text{FN}_6\text{O}_7$ [$\text{M}+\text{H}$] $^+$: 1147.4, found 1147.4.

H-Gly-Trp-Tyr-NH-*n*-Bu Derived Imidazole (16).^{3,4}

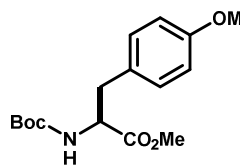
Solvents were sparged with dry argon for 1.5 hr before use. THF was freshly distilled from sodium benzophenone ketyl. Peptide imidazole **16** (47 mg, 41 μmol) was dissolved in DMF (9 mL) and sparged for 15 min. Stock solutions of (η^3 -allylPdCl) $_2$ (0.59 mg/ml) and Xantphos (2.4 mg/ml) in DMF:THF (1:1, v:v) were prepared, and combined (1:1, v:v) to give the pre-catalyst as a bright yellow solution. This solution (2 mL, 4.1 μmol Xantphos, 1.6 μmol (η^3 -allylPdCl) $_2$) was added to the solution of **16**. Consumption of **13** was observed after 75 min by HPLC-MS. The reaction was concentrated and purified by flash chromatography eluted with 0→8% MeOH in DCM to give macrocyclic tyrosyl ether **16** (20 mg, 53%) as a white solid. ^1H NMR (CD_3CN , 500

MHz, mixture of conformers): δ 8.90 (t, $J = 7.3$ Hz, 3H), 1.25-1.37 (m, 4H), 1.37-1.45 (m, 2H), 1.56 (s, 3H), 1.66 (s, 3H), 1.75-1.86 (s, 1H), 1.86-1.93 (m, 1H), 1.94-2.21 (m, 7H), 2.74 (dd, $J = 15.1, 9.0$ Hz, 1H), 2.83 (d, $J = 6.8$ Hz, 1H), 2.83-2.92 (m, 2H), 2.96 (dd, $J = 15.1, 4.8$ Hz, 1H), 3.08-3.18 (m, 2H), 3.18 (dd, $J = 14.7, 5.7$ Hz, 1H), 3.45 (d, $J = 16.6$ Hz, 1H), 3.81 (d, $J = 16.7$ Hz, 1H), 4.51-4.56 (m, 1H), 4.81 (br d, $J = 4.9$ Hz, 1H), 5.03-5.07 (m, 1H), 5.09 (d, $J = 18.8$ Hz, 1H), dt, $J = 16.4, 5.3$ Hz, 1H), 6.57 (d, $J = 16.4$ Hz, 1H), 6.62 (d, $J = 7.8$ Hz, 1H), 6.68-6.75 (m, 1H), 6.82 (d, $J = 8.5$ Hz, 2H), 6.90 (d, $J = 8.5$ Hz, 2H), 6.90 (br s, 1H), 7.00-7.18 (m, 7H), 7.21 (br d, $J = 7.7$ Hz, 1H), 7.35 (d, $J = 8.1$ Hz, 1H), 7.53 (d, $J = 7.9$ Hz, 1H), 7.67 (dd, $J = 8.4, 5.6$ Hz, 2H), 9.17 (br s, 1H). ^{13}C NMR (CDCl_3 , 125 MHz, major conformer): δ 170.4, 170.2, 170.1, 161.3 (d, $J_{\text{CF}} = 243$ Hz), 156.7, 143.2, 136.9, 136.8, 136.6, 136.3, 132.0, 131.8, 131.7, 130.0, 128.8, 128.5, 128.4, 128.3, 128.1, 127.4, 125.5, 124.8, 124.4, 123.8, 123.2, 121.4, 119.3, 118.9, 118.4, 115.0, 114.90, 114.86, 111.3, 109.4, 89.1, 81.2, 67.2, 53.8, 53.4, 53.3, 46.3, 44.5, 38.8, 38.6, 37.1, 32.8, 31.1, 27.4, 26.3, 24.7, 19.7, 16.8, 16.7, 13.0. MS (ESI) m/z calc'd for $\text{C}_{58}\text{H}_{64}\text{FN}_6\text{O}_4$ [$\text{M}+\text{H}$] $^+$: 927.5, found 927.5.

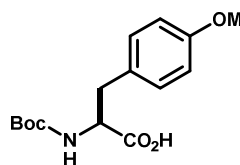
N-Boc-Tyrosine methyl ester (S4). Tyrosine methyl ester hydrochloride (10 g, 43 mmol) was dissolved in THF (40 mL) and H₂O (40 mL) containing NaHCO₃ (7.2 g, 86 mmol), and Boc₂O (10.3 g, 47 mmol) was added. The mixture was stirred overnight, and the organic phase was collected. The aqueous was extracted with EtOAc (x2), and the combined organic phase was washed with sat. NaHCO₃ (x3), 1N HCl (x3), brine, dried over MgSO₄ and concentrated to give **S4** (14.2 g, >100%), which was used without purification. ¹H NMR (DMSO-*d*₆, 400 MHz): δ 1.29 (s, 9H), 2.69 (dd, J = 13.5, 9.8 Hz, 1H), 2.81 (dd, J = 13.5, 5.2 Hz, 1H), 3.29 (s, 3H), 3.55 (s, 3H), 3.99-4.08 (m, 1H), 6.61 (d, J = 8.2 Hz, 2H), 6.96 (d, J = 8.2 Hz, 2H), 7.17 (d, J = 7.8 Hz, 1H), 9.16 (s, 1H). MS (ESI) *m/z* calc'd for C₁₅H₂₀NO₅ [M+H]⁺: 294.1, found 294.1.



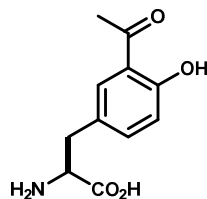
N-Boc-2-(4-Methoxyphenyl)alanine methyl ester (S5).⁵ Compound **S4** (8.5 g crude, ~29 mmol) was dissolved in acetone and treated with K₂CO₃ (15.9 g, 115 mmol) and iodomethane (7.2 mL, 115 mmol), and heated to reflux for 4 hr. The mixture was cooled, filtered, and concentrated. The residue was partitioned between EtOAc and H₂O, and the organic phase was washed with 1M NaOH (x3), brine, dried over Na₂SO₄ and concentrated to give **S5** (9.6 g, >100%) as a viscous oil, which was used without purification. ¹H NMR (CDCl₃, 300 MHz): δ 1.41 (s, 9H), 3.70 (s, 3H), 2.78 (s, 3H), 4.46-4.60 (m, 1H), 4.90-5.04 (m, 1H), 6.82 (d, J = 8.5 Hz, 2H), 7.03 (d, J = 8.5 Hz, 2H). ¹³C NMR (CDCl₃, 75 MHz): δ 172.5, 158.7, 155.1, 130.3, 130.2, 127.9, 121.3, 114.0, 79.9, 55.2, 52.2, 28.3. MS (ESI) *m/z* calc'd for C₁₆H₂₃NNaO₅ [M+Na]⁺: 332.2, found 332.2.



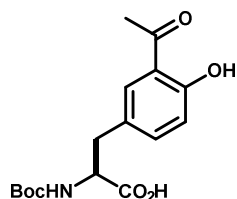
N-Boc-2-(4-Methoxyphenyl)alanine (17). Methyl ester **S5** (9.6 g crude, ~29 mmol) was dissolved in MeOH (150 mL) and H₂O (50 mL) and treated with LiOH·H₂O (1.95 g, 47 mmol). The mixture was stirred at rt overnight, then concentrated, and partitioned between 10% K₂CO₃ and Et₂O. The aqueous phase was washed with Et₂O (x2). EtOAc was added, the mixture was cooled in an ice bath, and 3N HCl was added to pH < 2, and the mixture was extracted with EtOAc (x3). The organic phase was washed with brine, dried over Na₂SO₄ and concentrated to give **17** (7.05 g, 82% 2 steps) as a glassy solid. ¹H NMR (CDCl₃, 300 MHz): δ 1.38 (s, 9H), 2.84 (dd, J = 13.9, 8.7 Hz, 1H), 3.08 (dd, J = 13.9, 5.1 Hz, 1H), 3.75 (s, 3H), 4.29 (dd, J = 8.7, 5.1 Hz, 1H), 6.83 (d, J = 8.6 Hz, 2H), 7.13 (d, J = 8.6 Hz, 2H). ¹³C NMR (CDCl₃, 75 MHz): δ 175.4, 159.9, 157.6, 131.2, 130.3, 116.1, 114.8, 80.5, 55.6, 37.8, 28.7. MS (ESI) *m/z* calc'd for C₁₅H₂₀NO₅ [M-H]⁻: 294.1, found 294.1.



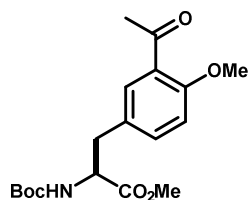
3-Acetyl-L-tyrosine (18).⁶ L-Tyrosine (14.5 g, 80 mmol) was suspended in nitrobenzene (350 mL) and treated with AlCl₃ (42.4 g, 315 mmol), which caused a mild exotherm. Acetyl chloride (6.8 mL, 95 mmol) was added in one portion, and the mixture was warmed to 100 °C and stirred for 6 hrs. The mixture was cooled, poured into chipped ice (~500 g) containing conc. HCl (80 mL). The mixture was transferred to a separatory funnel, and the heterogeneous lower layer was removed. The aqueous phase was washed with EtOAc (x2), and concentrated to ~250 mL, which induced precipitation. This mixture was allowed to cool to rt, then to 0 °C overnight. The solids were collected by filtration and recrystallized from 5N HCl (~200 mL) to give **18** (14.3 g, 69%) as tan needles. ¹H NMR (D₂O, 600 MHz): δ 2.62 (s, 3H), 3.27 (dd, J = 14.8, 5.8 Hz, 1H), 3.27 (dd, J = 14.8, 5.8 Hz, 1H), 4.26 (dd, J = 7.3, 5.9 Hz, 1H), 6.94 (d, J = 8.6 Hz, 1H), 7.44 (dd, J = 8.6, 2.0 Hz, 1H), 7.77 (d, J = 2.0 Hz, 1H). MS (ESI) *m/z* calc'd for C₁₁H₁₄NO₄ [M+H]⁺: 224.1, found 224.0.



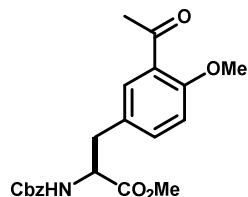
***N*-Boc-3-Acetyl-*L*-tyrosine (S6a).**⁶ Amino acid **18** (14.3 g, 55 mmol) was dissolved in a mixture of THF (165 mL) and sat. NaHCO₃ (165 mL), and treated with Boc₂O (12.0 g, 55 mmol). The mixture was stirred at rt overnight, and the volatiles removed at the rotovap. The aqueous remainder was basified with NaOH to pH 10, washed with Et₂O (x2), then cooled in an ice bath, acidified to pH < 2 with 3N HCl, and extracted with EtOAc (x3). The organic phase was washed with brine, dried over Na₂SO₄ and concentrated to give **S6a** (18.1 g, ~100%) of moderate purity as a foam, which was used without purification. MS (ESI) *m/z* calc'd for C₁₆H₂₀NO₆ [M-H]⁻: 322.1, found 322.0.



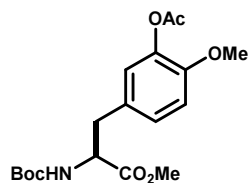
***N*-Boc-(*S*)-2-(3-Acetyl-4-methoxyphenyl)alanine methyl ester (19a).**⁶ Compound **S6a** (18.1 g crude, 55 mmol) was dissolved in DMF (250 mL) and treated with K₂CO₃ (34 g, 246 mmol), iodomethane (7.7 mL, 123 mmol) and tetrapropylammonium bromide (1.5 g, 5.6 mmol). The mixture was stirred at rt for 4 hr, then filtered and concentrated. The residue was reconstituted in EtOAc, washed with H₂O (x2), 1M NaOH (x2), 1N HCl (x2), brine, dried over MgSO₄ and concentrated to give **19a** (17.4 g, 89%) as an orange oil of moderate purity, which was used without purification. ¹H NMR (CDCl₃, 300 MHz): δ 1.39 (s, 9H), 2.57 (s, 3H), 2.93-3.10 (m, 2H), 3.71 (s, 3H), 3.87 (s, 3H), 4.44-4.63 (m, 1H), 5.95-5.06 (m, 1H), 6.89 (d, J = 8.6 Hz, 1H), 7.22 (dd, J = 8.6, 2.7 Hz, 1H), 7.47 (br d, J = 2.7 Hz, 1H). ¹³C NMR (CDCl₃, 75 MHz): δ 199.5, 172.3, 158.2, 134.5, 131.3, 128.2, 111.9, 60.5, 55.6, 54.5, 52.4, 37.4, 31.9, 29.7, 28.3, 27.8. MS (ESI) *m/z* calc'd for C₁₈H₂₅NNaO₆ [M+H]⁺: 374.2, found 374.0.



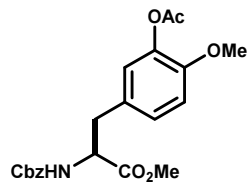
***N*-Cbz-(*S*)-2-(3-Acetyl-4-methoxyphenyl)alanine methyl ester (19b).**⁶ Compound **19b** (13.0 g, 94%) was prepared analogously to *N*-Boc derivative **19a**, and was used without purification. ¹H NMR (CD₃OD, 400 MHz): δ 2.55 (s, 3H), 2.90 (dd, J = 13.9, 9.2 Hz, 1H), 3.11 (dd, J = 13.9, 5.3 Hz, 1H), 3.70 (s, 3H), 3.90 (s, 3H), 4.41 (dd, J = 9.2, 5.3 Hz, 1H), 5.00 (d, J = 12.5 Hz, 1H), 5.05 (d, J = 12.5 Hz, 1H), 7.03 (d, J = 8.5 Hz, 1H), 7.24-7.34 (m, 5H), 7.36 (dd, J = 8.5, 2.3 Hz, 1H), 7.52 (d, J = 2.3 Hz, 1H). MS (ESI) *m/z* calc'd for C₂₁H₂₄NO₆ [M+H]⁺: 386.2, found 386.0.



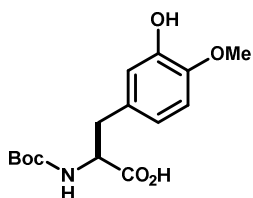
***N*-Boc-(*S*)-2-(3-Acetoxy-4-methoxyphenyl)alanine methyl ester (21a).**⁶ Compound **19a** (17 g crude, ~48 mmol) was dissolved in DCM (400 mL), shielded from light, and treated with *m*-CPBA (24 g, 96 mmol). The mixture was stirred at rt for 7 days, and the organic phase was washed with half saturated NaHCO₃ (x4), brine, dried over Na₂SO₄ and concentrated. Purification by chromatography on SiO₂ eluted with 1:1 hexanes:EtOAc afforded **21a** (5.71 g, 32%). ¹H NMR (CDCl₃, 300 MHz): δ 1.42 (s, 9H), 2.29 (s, 3H), 2.95-3.08 (m, 2H), 3.69 (s, 3H), 3.80 (s, 3H), 4.47-4.59 (m, 1H), 4.94-5.04 (m, 1H), 6.80 (br s, 1H), 6.88 (d, J = 8.4 Hz, 1H), 6.96 (dd, J = 8.3, 1.3 Hz, 1H).



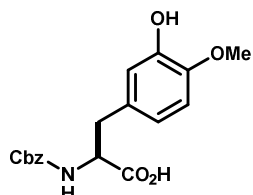
***N*-Cbz-(*S*)-2-(3-Acetoxy-4-methoxyphenyl)alanine methyl ester (21b).**⁶ Compound **19b** (13 g crude, ~34 mmol) was dissolved in DCM (340 mL), shielded from light, and treated with *m*-CPBA (16.6 g, 67.5 mmol). The mixture was stirred at rt for 7 days, and the organic phase was washed with half saturated NaHCO₃ (x4), brine, dried over Na₂SO₄ and concentrated to give **21b** (15.2 g, >100%) as a viscous oil that solidified upon standing, which was used without purification. ¹H NMR (CDCl₃, 300 MHz): δ 2.24 (s, 3), 2.89 (dd, J = 14.0, 9.0 Hz, 1H), 3.07 (dd, J = 14.0, 5.5 Hz, 1H), 3.69 (s, 3H), 3.78 (s, 3H), 4.36-4.47 (m, 1H), 5.02 (d, J = 12.7 Hz, 1H), 5.06 (d, J = 12.7 Hz, 1H), 6.88 (d, J = 2.0 Hz, 1H), 6.97 (d, J = 8.4 Hz, 1H), 7.05 (dd, J = 8.4, 2.0 Hz, 1H), 7.25-7.38 (m, 5H). MS (ESI) *m/z* calc'd for C₂₁H₂₄NO₇ [M+H]⁺: 402.2, found 402.0.



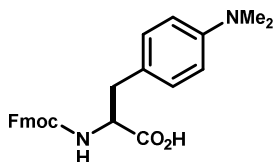
N-Boc-(S)-2-(3-Hydroxy-4-methoxyphenyl)alanine (22a).⁶ Compound **21a** (5.71 g, 15.5 mmol) was dissolved in THF:MeOH:H₂O (3:1:1, 50 mL) and treated with LiOH·H₂O (2.6 g, 62 mmol). The mixture was stirred at rt for 2.5 hr, then partitioned between 10% citric acid and EtOAc. The aqueous phase was extracted with EtOAc (x2), and the combined organic phase was washed with brine, dried over MgSO₄ and concentrated to give **22a** (4.9 g, 100%) as a tan solid. MS (ESI) *m/z* calc'd for C₁₅H₂₀NO₆ [M-H]⁻: 310.1, found 310.0.



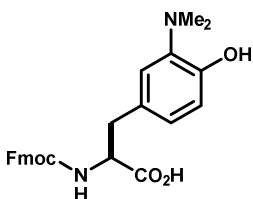
N-Boc-(S)-2-(3-Hydroxy-4-methoxyphenyl)alanine (22b). Compound **22b** was prepared analogously to Boc- derivative **22a**. MS (ESI) *m/z* calc'd for C₁₅H₂₀NO₆ [M-H]⁻: 310.1, found 310.0.



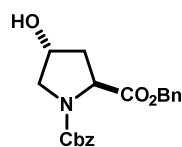
N $^{\alpha}$ -Fmoc-(S)-2-(4-Dimethylaminophenyl)alanine. (27). 4-Nitrophenylalanine⁷ (36.9 g, 176 mmol) was dissolved in a mixture of THF (400 mL) and sat. NaHCO₃ (400 mL), and treated with Fmoc-ONSu (59.2 g, 176 mmol). The mixture was stirred at rt overnight, and the volatiles removed at the rotovap. The aqueous remainder was basified with NaOH to pH 10, washed with Et₂O (x2), then cooled in an ice bath, acidified to pH < 2 with 3N HCl, and extracted with EtOAc (x3). The organic phase was washed with brine, dried over Na₂SO₄ and concentrated. A portion of this material (20 g, ~46 mmol) and dissolved in THF (250 mL) and MeOH (250 mL). Formaldehyde (37% aq., 22 mL, 276 mmol) was added, followed by Pd/c (10wt%, 1 g). The mixture was stirred under an atmosphere of hydrogen at rt for 48 hrs, then filtered through Celite, concentrated, and purified by chromatography on SiO₂ eluted with 6% MeOH in DCM to give **27** (13.9 g, 70%) as a faintly yellow solid. ¹H NMR (CD₃OD, 300 MHz): δ 2.80 (s, 6H), 3.10 (dd, J = 13.9, 4.7 Hz, 1H), 4.06-4.18 (m, 2H), 4.29 (dd, J = 10.1, 6.8 Hz, 1H), 4.36 (dd, J = 9.4, 4.7 Hz, 1H), 6.68 (d, J = 8.6 Hz, 2H), 7.07 (d, J = 8.6 Hz, 2H), 7.22-7.30 (m, 2H), 7.36 (br dd, J = 7.6, 7.4 Hz, 2H), 7.57 (br d, J = 7.4 Hz, 2H), 7.76 (d, J = 7.6 Hz, 2H). MS (ESI) *m/z* calc'd for C₂₆H₂₆N₂O₄ [M+H]⁺: 430.2, found 431.0.



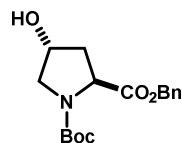
N $^{\alpha}$ -Fmoc-(S)-2-(3-Dimethylamino-4-hydroxyphenyl)alanine. (28). 3-Nitrotyrosine^{8,9} (30.4 g, 134 mmol) was dissolved in a mixture of THF (300 mL) and sat. NaHCO₃ (300 mL), and treated with Fmoc-ONSu (45.2 g, 134 mmol). The mixture was stirred at rt overnight, and the volatiles removed at the rotovap. The aqueous remainder was basified with NaOH to pH 10, washed with Et₂O (x2), then cooled in an ice bath, acidified to pH < 2 with 3N HCl, and extracted with EtOAc (x3). The organic phase was washed with brine, dried over Na₂SO₄ and concentrated to give Fmoc-nitrotyrosine (57.5 g, 96%) as a yellow solid. This material (25.0 g, 56 mmol) was dissolved in THF:MeOH (1:1, 560 mL), formaldehyde (37% aq, 27 mL, 335 mmol) and Pd/C (10wt%, 1.25 g) were added, and the mixture was stirred under an atmosphere of hydrogen for 3 days. The mixture was filtered through Celite and concentrated to give a brown foam, which was adsorbed onto SiO₂ and chromatographed on SiO₂ eluted with 10→25% MeOH in EtOAc to give **28** (8.9 g, 36%) as an off-white foam. ¹H NMR (CD₃OD, 400 MHz): δ 2.83 (s, 6H), 2.87 (dd, J = 13.8, 8.6 Hz, 1H), 3.12 (dd, J = 13.8, 4.8 Hz, 1H), 4.14 (apt t, J = 6.8 HZ, 1H), 4.22 (dd, J = 10.4, 6.8 Hz, 1H), 4.28 (dd, J = 10.4, 7.4 Hz, 1H), 4.32 (dd, J = 8.4, 4.8 Hz, 1H), 6.76 (d, J = 8.1 Hz, 1H), 6.90 (dd, J = 8.1, 1.7 Hz, 1H), 7.10 (d, J = 1.7 Hz, 1H), 7.22-7.30 (m, 2H), 7.32-7.39 (m, 2H), 7.54-7.60 (m, 2H), 7.76 (d, J = 7.5 Hz, 2H). MS (ESI) *m/z* calc'd for C₂₆H₂₇N₂O₅ [M+H]⁺: 447.2, found 446.9.



***N*-Cbz-*trans*-4-Hydroxy-L-proline benzyl ester (29):** Compound **29** was prepared from *trans*-4-hydroxy-L-proline as described.^{10,11}



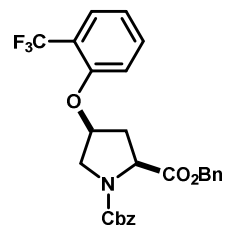
***N*-Cbz-*trans*-4-Hydroxy-L-proline benzyl ester (S6):** Compound **S6** was prepared from *trans*-4-hydroxy-L-proline as described.^{10,11}



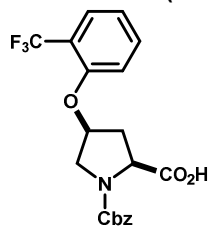
***N*-Cbz-*cis*-4-phenoxy-L-proline benzyl ester (32a).**¹² Cbz hydroxyproline benzyl ester (**29**) (3.01 g, 8.5 mmol), phenol (1.20 g, 12.7 mmol) and PPh₃ (3.33 g, 12.7 mmol) were dissolved in THF (25 mL) and cooled to 0 °C. Diethylazodicarboxylate was introduced via syringe over ~1hr, and the mixture was allowed to warm to rt and stirred overnight. The solvent was exchanged to Et₂O, the mixture was filtered, and the filtrate was adsorbed onto SiO₂. Purification by column chromatography on SiO₂ eluted with 0→100% Et₂O afforded prolyl phenyl ether **32a** (2.62 g, 48%) as a white solid, which remained contaminated by *bis*-methoxycarbonyl hydrazine, and was carried forward without further purification. ¹H NMR (CDCl₃, 500 MHz, mixture of rotamers): δ 2.31-2.44 (m, 1H), 2.47-2.54 (m, 1H), 3.71-3.79 (m, 2H), 4.51 (dd, J = 9.1, 2.1 Hz, 0.5H), 4.60 (dd, J = 9.2, 1.8 Hz, 0.5H), 4.82-4.87 (m, 1H), 4.97-5.09 (m, 3H), 5.14 (dd, J = 12.4, 2.6 Hz, 1H), 6.65 (d, J = 8.0 Hz, 1H), 6.88 (t, J = 7.4 Hz, 1H), 7.12-7.32 (m, 13H). MS (ESI) *m/z* calc'd for C₂₆H₂₆NO₅ [M+H]⁺: 432.2, found 432.2.

***N*-Cbz-*cis*-4-phenoxy-L-proline (33a).**¹² Benzyl ester **32a** (2.62 g, 6.1 mmol) was dissolved in MeOH (25 mL), THF (10 mL) and H₂O (5 mL), treated with LiOH·H₂O (764 mg, 18.3 mmol), and stirred for 8.5 hr. The volatiles were removed in vacuo, and the mixture was diluted with 10% K₂CO₃ and washed with Et₂O (x1). The aqueous was acidified to pH < 2 with HCl, and extracted into EtOAc (x4). The combined extract was dried over MgSO₄ and concentrated to give **33a** (2.08 g, > 95%) as a foam. ¹H NMR (DMSO-*d*₆, 500 MHz, mixture of rotamers): δ 2.22 (br d, J = 13.8 Hz, 0.5H), 2.27 (br d, J = 13.6 Hz, 0.5H), 2.50-2.63 (m, 1H), 3.49 (br d, J = 11.6 Hz, 1H), 3.77 (dd, J = 12.1, 5.1 Hz, 0.5H), 3.83 (dd, J = 11.8, 5.0 Hz, 0.5H), 4.38 (dd, J = 9.6, 1.7 Hz, 0.5H), 4.44 (dd, J = 9.5, 1.5 Hz, 0.5H), 5.04 (d, J = 7.1 Hz, 1H), 5.07 (d, J = 7.1 Hz, 1H), 5.11 (d, apt t, J = 13.0 Hz, 1H). ¹³C NMR (DMSO-*d*₆, 125 MHz, mixture of rotamers): δ 172.9, 172.6, 156.6, 156.5, 156.5, 153.95, 153.89, 136.9, 136.8, 129.6, 128.4, 128.3, 127.9, 127.7, 127.6, 127.1, 121.0, 115.65, 115.61, 75.2, 74.2, 66.1, 66.0, 57.7, 57.3, 52.2, 51.7, 35.7, 34.7. MS (ESI) *m/z* calc'd for C₁₉H₁₈NO₅ [M-H]⁻: 340.1, found 340.0.

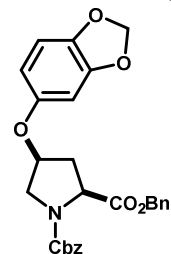
***N*-Cbz-*cis*-4-(2-trifluoromethylphenoxy)-L-proline benzyl ester (32b).**¹² Compound **32b** (2.71 g, 64%) was prepared analogously to compound **32a**. (**Caution!** 2-Trifluoromethylphenol is extremely malodorous and should be handled accordingly.) ¹H NMR (CDCl₃, 500 MHz, mixture of rotamers): δ 2.41-2.60 (m, 2H), 3.71 (dd, J = 12.1, 1.6 Hz, 0.5H), 3.77 (dd, J = 12.3, 1.2 Hz, 0.5H), 3.89 (dd, J = 12.3, 5.8 Hz, 0.5H), 3.94 (dd, J = 12.4, 5.7 Hz, 0.5H), 4.52 (dd, J = 9.0, 2.6 Hz, 0.5 H), 4.62 (dd, J = 9.0, 2.6 Hz, 1H), 4.81-4.86 (m, 1H), 4.90 (d, J = 12.4 Hz, 0.51H), 4.97-5.17 (m, 3.5H), 6.73 (d, J = 8.4 Hz, 0.5H), 6.77 (d, J = 8.3 Hz, 0.5H), 6.95 (apt dt, J = 7.6, 2.4 Hz, 1H), 7.13-7.30 (m, 10H), 7.33-7.41 (m, 1H), 7.49 (br d, H = 7.7 Hz, 1H). ¹³C NMR (CDCl₃, 125 MHz, mixture of rotamers): δ 170.6, 170.4, 154.9, 154.6, 154.4, 136.4, 136.3, 135.7, 135.6, 133.2, 128.51, 128.48, 128.47, 128.4, 128.25, 128.21, 128.15, 128.13, 128.0, 127.9, 127.5-127.7 (m), 120.8, 113.2, 113.1, 76.7, 75.7, 67.4, 67.3, 67.2, 67.1, 58.2, 57.9, 52.5, 52.0, 36.6, 35.6. MS (ESI) *m/z* calc'd for C₂₇H₂₅F₃NO₅ [M+H]⁺: 500.2, found 500.1.



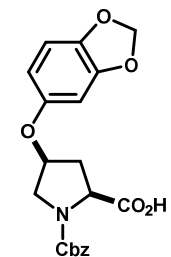
***N*-Cbz-*cis*-4-(2-trifluoromethylphenoxy)-*L*-proline (33b).**¹² Compound **33b** was prepared analogously to compound **33a**. ¹H NMR (DMSO-*d*₆, 500 MHz, mixture of rotamers): δ 2.23 (br d, *J* = 13.9 Hz, 0.5H), 2.28 (br d, *J* = 14.0 Hz, 0.5H), 2.66-2.78 (m, 1H), 3.46 (d, *J* = 1.2 Hz, 0.5H), 3.48 (d, *J* = 1.1 Hz, 0.5H), 3.97 (dd, *J* = 12.1, 5.8 Hz, 0.5H), 3.99-4.04 (m, 0.5H), 4.41 (dd, *J* = 9.6, 2.4 Hz, 0.5H), 4.48 (dd, *J* = 9.7, 2.1 Hz, 0.5H), 5.03-5.10 (m, 1.5H), 5.10-5.17 (m, 1.5H), 7.10 (ddd, *J* = 7.4, 7.4, 4.1 Hz, 1H), 7.22 (dd, *J* = 8.4, 5.9 Hz, 1H), 7.27-7.41 (m, 5H), 7.57-7.64 (m, 2H), 12.57 (br s, 1H). ¹³C NMR (DMSO-*d*₆, 125 MHz, mixture of rotamers): δ 172.3, 172.1, 172.0, 170.4, 154.7, 154.7, 153.9, 153.8, 136.8, 136.8, 134.1, 128.4, 128.3, 127.9, 127.7, 127.1, 127.0 (q, *J*_{CF} = 5.0 Hz), 123.5 (q, *J*_{CF} = 273 Hz), 120.6, 117.63 (q, *J*_{CF} = 30.2 Hz), , 114.0, 76.4, 75.4, 66.2, 66.1, 57.8, 57.4, 52.4, 51.8, 35.8, 34.9, 21.1, 20.8. MS (ESI) *m/z* calc'd for C₂₀H₁₇F₃NO₅ [M-H]⁻: 408.1, found 408.0.



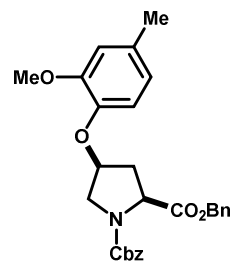
***N*-Cbz-*cis*-4-(3,4-Methylenedioxyphenoxy)-*L*-proline benzyl ester (32c).** Compound **32c** (1.74 g, 37%) was prepared analogously to compound **32a**. ¹H NMR (CDCl₃, 500 MHz, mixture of rotamers): δ 2.38-2.51 (m, 1H), 2.57-2.65 (m, 1H), 3.76-3.91 (m, 2H), 4.61 (br d, *J* = 9.1 Hz, 0.5H), 4.70 (br d, *J* = 9.1 Hz, 0.5H), 4.84 (br s, 1H), 5.09-5.33 (m, 4 H), 5.95 (s, 2H), 6.17-6.24 (m, 1H), 6.33 (br s, 1H), 6.67-6.72 (m, 1H), 7.28-7.45 (m, 10H).



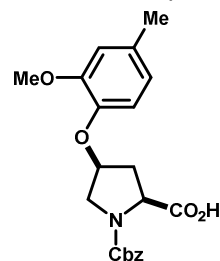
***N*-Cbz-*cis*-4-(3,4-Methylenedioxyphenoxy)-*L*-proline (33c).** Compound **33c** (1.44 g, >95%) was prepared analogously to compound **33a**. ¹H NMR (DMSO-*d*₆, 500 MHz, mixture of rotamers): δ 2.18 (d, *J* = 14.0 Hz, 0.5H), 2.23 (d, *J* = 14.0 Hz, 0.5H), 2.41-2.54 (m, 1H), 3.46 (br d, *J* = 11.7 Hz, 1H), 3.68 (dd, *J* = 11.7, 3.7 Hz, 0.5H), 3.73 (dd, *J* = 11.2, 3.5 Hz, 0.5H), 4.33 (d, *J* = 8.9 Hz, 0.5H), 4.40 (d, *J* = 8.9 Hz, 0.5H), 4.91 (br s, 1H), 4.98-5.14 (m, 1H), 5.93 (br s, 1H), 6.26-6.34 (m, 1H), 6.53 (br s, 1H), 6.74-6.82 (m, 1H), 7.24-7.40 (m, 5H), 12.65 (br s, 1H). ¹³C NMR (DMSO-*d*₆, 125 MHz, mixture of rotamers): δ 172.9, 172.7, 153.9, 153.9, 151.6, 148.0, 141.6, 136.94, 136.86, 128.4, 128.3, 127.9, 127.7, 127.6, 127.1, 108.1, 107.8, 107.7, 101.1, 99.2, 99.1, 79.2, 76.3, 75.3, 66.1, 66.0, 57.7, 57.3, 52.0, 51.5, 35.6, 34.6. MS (ESI) *m/z* calc'd for C₂₀H₂₀NO₇ [M+H]⁺: 386.1, found 386.1.



***N*-Cbz-*cis*-4-(4-Methy-2-methoxyphenoxy)-*L*-proline benzyl ester (32d).** Cbz-Hydroxyproline benzyl ester (**29**) (4.22 g, 11.9 mmol), triphenylphosphine (4.67 g, 17.8 mmol), and 2-methoxy-4-methylphenol (2.46 g, 17.8 mmol) were dissolved in THF (36 mL) and cooled to 0 °C. Diethylazodicarboxylate (2.8 mL, 17.8 mL) was added dropwise over 1 h, and the mixture was allowed to warm to rt and stirred overnight. Workup and purification analogous to that carried out for compound **32a** afforded **32d** (2.03 g, 36%) as a viscous, colorless oil. ¹H NMR (CDCl₃, 500 MHz, mixture of rotamers): δ 2.34 (s, 3H), 2.40-2.52 (m, 1H), 2.58-2.67 (m, 1H), 3.77 (dd, *J* = 12.2, 5.2 Hz, 0.5H), 3.80 (s, 1.5H), 3.81 (s, 1.5H), 3.82-3.90 (m, 1.5H), 4.61 (dd, *J* = 9.2, 2.6 Hz, 0.5H), 4.69 (dd, *J* = 9.2, 2.4 Hz, 0.5H), 4.92-4.98 (m, 1H), 5.09 (d, *J* = 12.4 Hz, 0.5H), 5.14-5.26 (m, 3H), 5.30 (d, *J* = 12.4 Hz, 0.5H), 6.64-6.69 (m, 1H), 6.70-6.76 (m, 2H), 7.29-7.45 (m, 10H).

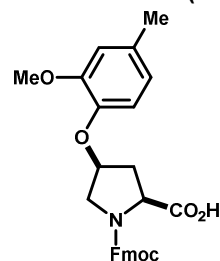


***N*-Cbz-*cis*-4-(4-Methy-2-methoxyphenoxy)-*L*-proline (33d).** Compound **33d** (1.55 g, >95%) was prepared analogously to compound **33a**. ¹H NMR (DMSO-*d*₆, 500 MHz, mixture of rotamers): δ 2.20 (br d, *J* = 14.0 Hz, 0.5H), 2.22-2.27 (m, 0.5H), 2.23 (s, 1.5H), 2.24 (s, 1.5H), 2.45-2.58 (m, 1H), 3.47 (br d, *J* = 3.6 Hz, 0.5H), 3.49 (br d, *J* = 3.6 Hz, 0.5H), 3.68-3.73 (m, 0.5H), 3.72 (s, 1.5H), 3.73 (s, 1.5H), 3.75 (dd, *J* = 11.6, 5.3 Hz, 0.5H), 4.35 (dd, *J* = 9.5, 2.0 Hz, 0.5H), 4.42 (dd, *J* = 9.5, 1.7 Hz, 0.5H), 4.85-4.91 (m, 1H), 5.05 (d, *J* = 13.1 Hz, 1H), 5.07-5.13 (m, 1H), 5.09 (d, *J* = 13.1 Hz, 1H), 6.65 (ddd, *J* = 7.7, 5.4, 1.1 Hz, 1H), 6.78 (dd, *J* = 7.7, 1.8 Hz, 1H), 6.81 (br d, *J* = 5.3 Hz, 1H), 7.27-7.39 (m, 5H), 12.64 (br s, 1H). ¹³C NMR (DMSO-*d*₆, 125 MHz, mixture of rotamers): δ

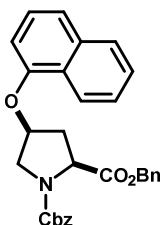


172.9, 172.6, 154.0, 153.9, 150.23, 150.21, 143.5, 136.9, 136.9, 132.0, 128.4, 128.3, 127.9, 127.7, 127.5, 127.1, 120.8, 118.0, 117.9, 113.9, 76.9, 76.0, 66.0, 57.7, 57.3, 55.7, 52.1, 51.6, 35.8, 34.8, 20.7. MS (ESI) m/z calc'd for $C_{21}H_{24}NO_6$ $[M+H]^+$: 386.2, found 386.1.

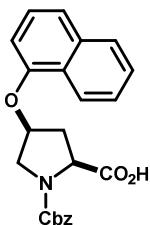
N-Fmoc-cis-4-(4-Methoxy-2-methoxyphenoxy)-L-proline (S7). Compound **32d** (2.03 g, 4.3 mmol) was treated with Pd/C in MeOH under an atmosphere of hydrogen overnight. The mixture was filtered through Celite, concentrated. This material (617 mg) was redissolved in THF (40 mL) and sat. $NaHCO_3$ (40 mL), treated with Fmoc-ONSu (828 mg, 2.5 mmol), and stirred at rt overnight. The volatiles removed at the rotovap. The aqueous remainder was basified with NaOH to pH 10, washed with Et_2O (x2), then cooled in an ice bath, acidified to pH < 2 with 3N HCl, and extracted with EtOAc (x3). The organic phase was washed with brine, dried over Na_2SO_4 and concentrated to give **S7** (1.4 g, 69% 2 steps). 1H NMR (DMSO- d_6 , 500 MHz, mixture of rotamers): δ 2.19 (br d, J = 13.6 Hz, 0.5H), 2.24 (s, 1.5H), 2.26 (s, 1.5H), 2.29 (br d, J = 14.1 Hz, 0.5H), 2.46-2.60 (m, 1H), 3.48 (br d, J = 9.9 Hz, 0.5H), 3.50 (br d, J = 9.9 Hz, 0.5H), 3.66-3.74 (m, 1H), 3.737 (s, 1.5H), 3.743 (s, 1.5H), 4.17-4.36 (m, 3.5H), 4.47 (dd, J = 9.5, 1.8 Hz, 0.5H), 4.88-4.93 (m, 1H), 6.65-6.71 (m, 1H), 6.80 (d, J = 8.1 Hz, 1H), 6.83 (dd, J = 7.7, 1.2 Hz, 1H), 7.30-7.35 (m, 2H), 7.42 (dd, J = 7.4, 7.4 Hz, 2H), 7.63-7.68 (m, 2H), 7.89 (d, J = 7.7 Hz, 2H), 12.65 (br s, 1H). ^{13}C NMR (DMSO- d_6 , 125 MHz, mixture of rotamers): δ 173.0, 172.6, 154.0, 153.9, 150.3, 150.3, 143.9, 143.8, 143.45, 143.40, 140.78, 140.75, 140.70, 140.68, 132.2, 132.0, 127.7, 127.20, 127.17, 125.3, 125.24, 125.19, 120.9, 120.2, 120.1, 118.3, 118.1, 113.9, 77.0, 76.0, 67.0, 66.7, 57.6, 57.4, 55.69, 55.68, 52.1, 51.4, 46.7, 46.6, 35.9, 34.8, 20.7. MS (ESI) m/z calc'd for $C_{28}H_{28}NO_6$ $[M+H]^+$: 472.2, found 474.2.



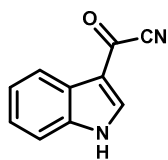
N-Cbz-cis-4-(1-Naphthyloxy)-L-proline benzyl ester (32e). Compound **32e** (2.55 g, 62%) was prepared analogously to compound **32a**. MS (ESI) m/z calc'd for $C_{30}H_{28}NO_5$ $[M+H]^+$: 482.2, found 482.2.



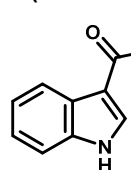
N-Cbz-cis-4-(1-Naphthyloxy)-L-proline (33e). 1H NMR (DMSO- d_6 , 500 MHz, mixture of rotamers): δ 2.44 (br d, J = 14.0 Hz, 0.5H), 2.49 (br d, J = 14.1 Hz, 1H), 2.63-2.75 (m, 1H), 5.05 (d, J = 12.5 Hz, 0.5H), 5.06 (d, J = 12.9 Hz, 0.5H), 5.12 (d, J = 12.9 Hz, 0.5H), 5.14 (d, J = 12.5 Hz, 0.5H), 5.25 (dd, J = 9.0, 4.5 Hz, 1H), 6.94 (dd, J = 8.3, 8.2 Hz, 1H), 7.24-7.54 (m, 9H), 7.85 (br d, J = 8.2 Hz, 1H), 8.07 (d, J = 8.3 Hz, 1H), 12.76 (br s, 1H). ^{13}C NMR (DMSO- d_6 , 125 MHz, mixture of rotamers): δ 173.0, 172.7, 153.95, 153.93, 152.01, 151.99, 136.9, 136.8, 134.2, 128.4, 128.3, 127.9, 127.7, 127.3, 127.1, 126.5, 126.0, 125.32, 125.25, 122.1, 120.2, 105.90, 105.89, 75.5, 74.4, 66.1, 66.0, 58.0, 57.6, 52.4, 51.8, 36.1, 35.2. MS (ESI) m/z calc'd for $C_{23}H_{22}NO_5$ $[M+H]^+$: 392.2, found 392.1.



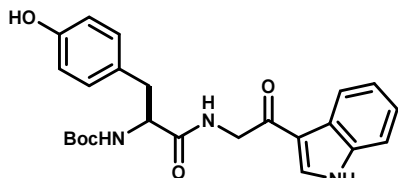
Indole-3-carbonyl cyanide (36).¹³ Indole (5.0 g, 43 mmol) was dissolved in Et₂O (100 mL) and cooled in an ice bath. Oxalyl chloride (4.4 mL, 51 mmol) was added dropwise, and stirred for 1 hr. To the bright yellow suspension was added CuCN (7.3 g, 81 mmol), ACN (4 mL), toluene (75 mL) and the mixture was heated to 110 °C allowing the Et₂O to escape. After 6 hr, the reaction was filtered through Celite, washing the cake with ACN. The filtrate was then boiled with activated charcoal for 30 min, then dissolved in DCM:MeOH:AcOH and adsorbed into SiO₂. Chromatography on SiO₂ eluted with DCM afforded nitrile **36** (3.3 g, 46%) as a red solid. ¹H NMR (DMSO-*d*₆, 500 MHz): δ 7.33 (ddd, *J* = 7.8, 7.1, 0.8 Hz, 1H), 7.36 (ddd, *J* = 7.8, 7.1, 0.9 Hz, 1H), 7.58 (d, *J* = 7.9 Hz, 1H), 8.04 (d, *J* = 7.9 Hz, 1H), 8.31 (br d, *J* = 3.2 Hz, 1H), 12.91 (br s, 1H). ¹³C NMR (DMSO-*d*₆, 125 MHz): δ 158.6, 141.4, 137.6, 124.9, 124.2, 123.8, 121.0, 116.2, 114.4, 113.3. MS (ESI) *m/z* calc'd for C₁₀H₇N₂O [M+H]⁺: 171.1, found 171.0.



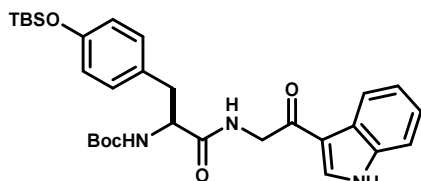
3-(2-Aminoacetyl)indole (37). Nitrile **36** (3.3 g, 19 mmol) was dissolved in MeOH (10 mL) and AcOH (50 mL) and treated with Pd/C (10%wt, 500 mg) under an atmosphere of hydrogen. The mixture was stirred for 12 hr, then filtered through Celite and concentrated. The residue was partitioned between Et₂O and 1N HCl, and the aqueous was collected, basified to pH > 10 with NaOH, and extracted with DCM (x3). The organic phase was washed with brine, dried over K₂CO₃ and concentrated to give **37** (3.43 g, >95%) as a red oil. ¹H NMR (CD₃OD, 500 MHz): δ 4.02 (s, 2H), 7.19-7.28 (m, 2H), 7.45 (dd, *J* = 7.0, 1.8 Hz, 1H), 8.15 (s, 1H), 8.23 (dd, *J* = 6.7, 1.8 Hz, 1H). MS (ESI) *m/z* calc'd for C₁₀H₁₁N₂O [M+H]⁺: 175.1, found 175.0.



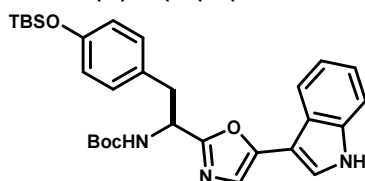
N2-Boc-(S)-N-(2-(Indol-3-yl)-2-oxoethyl)-2-amino-3-(4-hydroxyphenyl)propanamide (S8). Amino ketone **37** (900 mg, 5.2 mmol), Boc-Tyr-OH (1.46 g, 5.2 mmol) and iPr₂EtN (900 μL, 5.2 mmol) were dissolved in DMF, and treated with TBTU (1.67 g, 5.2 mmol). The reaction was stirred for 2 hr, then partitioned between EtOAc and sat. NaHCO₃. The organic phase was washed with sat. NaHCO₃ (x2), sat. NH₄Cl (x3), brine, dried over Na₂SO₄ and concentrated to give **S8**, which was used without purification. ¹H NMR (DMSO-*d*₆, 500 MHz): δ 1.32 (s, 9H), 2.61-2.69 (m, 1H), 2.96 (dd, *J* = 13.9, 3.5 Hz, 1H), 4.14-4.21 (m, 1H), 4.45 (dd, *J* = 17.7, 5.3 Hz, 1H), 4.55 (dd, *J* = 17.7, 5.5 Hz, 1H), 6.65 (br d, *J* = 8.2 Hz, 2H), 6.90 (d, *J* = 8.7 Hz, 1H), 7.08 (br d, *J* = 8.2 Hz, 2H), 7.17-7.26 (m, 2H), 7.48 (d, *J* = 7.3 Hz, 1H), 8.15-8.20 (m, 2H), 8.45 (d, *J* = 2.8 Hz, 1H), 9.14 (s, 1H), 12.02 (br s, 1H). MS (ESI) *m/z* calc'd for C₂₄H₂₈N₃O₅ [M+H]⁺: 438.2, found 438.0.



N2-Boc-O-tert-Butyldimethylsilyl-(S)-N-(2-(indol-3-yl)-2-oxoethyl)-2-amino-3-(4-hydroxyphenyl)propanamide (38). Phenol **S8** (2.0 g, 4.6 mmol) was dissolved in DMF (10 mL) and treated with imidazole (953 mg, 14 mmol), DMAP (56 mg, 0.46 mmol) and TBSCl (830 mg, 5.5 mmol). The mixture was stirred for 1 hr, diluted with EtOAc and washed with H₂O (x5), dried over MgSO₄, and concentrated to give crude **38**, which was used without purification. ¹H NMR (DMSO-*d*₆, 500 MHz): δ 0.18 (s, 6H), 0.96 (s, 9H), 1.32 (s, 9H), 2.71 (dd, *J* = 13.7, 11.4 Hz, 1H), 3.03 (dd, *J* = 13.7, 3.2 Hz, 1H), 4.21-4.29 (m, 1H), 4.48 (dd, *J* = 17.6, 5.3 Hz, 1H), 4.57 (dd, *J* = 17.6, 5.5 Hz, 1H), 6.76 (br d, *J* = 8.3 Hz, 2H), 6.98 (d, *J* = 8.8 Hz, 1H), 7.19 (d, *J* = 8.4 Hz, 1H), 7.20-7.27 (m, 2H), 7.50 (br d, *J* = 7.3 Hz, 1H), 8.17-8.23 (m, 2H), 8.47 (d, *J* = 2.7 Hz, 1H), 12.05 (br s, 1H). MS (ESI) *m/z* calc'd for C₃₀H₄₀N₃O₅Si [M-H]⁻: 552.3, found 550.0.

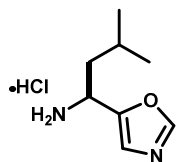


N-Boc-(S)-4-(2-(5-(1H-Indol-3-yl)oxazol-2-yl)-2-aminoethyl)phenol (42). Ketoamide **38** (1.38 g, 2.5 mmol), PPh₃ (1.31 g, 5.0 mmol) and Et₃N (1.7 mL, 12.5 mmol) were dissolved in ACN (80 mL), and hexachloroethane (1.32 g, 5.0 mmol) was added in portions over 30 min. The mixture was stirred overnight, diluted with EtOAc and washed with H₂O (x2), brine, dried over MgSO₄ and concentrated. The residue was dry loaded on SiO₂, and purified by

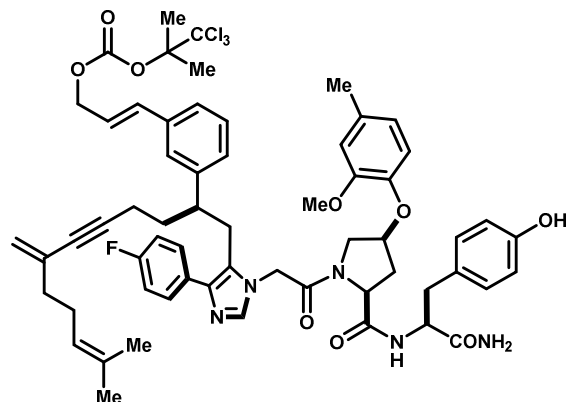


chromatography on SiO₂ eluted with 10→50% EtOAc in hexanes to give **42** (725 mg, 54%) as an orange solid. ¹H NMR (CDCl₃, 500 MHz): δ 0.14 (s, 6H), 0.95 (s, 9H), 1.44 (br s, 9H), 3.21 (br s, 1H), 5.21 (br s, 1H), 6.71 (d, J = 8.1 Hz, 1H), 6.95 (d, J = 7.8 Hz, 1H), 7.15 (s, 1H), 7.22-7.26 (m, 1H), 7.27-7.30 (m, 1H), 7.43 (d, J = 8.0 Hz, 1H), 7.47 (d, J = 2.5 Hz, 1H), 7.77 (d, J = 7.8 Hz, 1H), 8.40 (br s, 1H). MS (ESI) *m/z* calc'd for C₃₀H₄₀N₃O₄Si [M+H]⁺: 534.3, found 534.0.

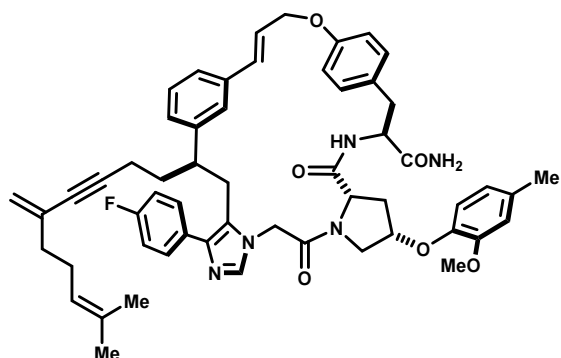
(S)-3-Methyl-1-(oxazol-5-yl)butan-1-amine hydrochloride (48).^{14,15} Methyl isonitrile¹⁶ (2.8 mL, 54 mmol) was dissolved in THF (110 mL) and cooled to -78 °C. (**Caution!** Methyl isonitrile has an extremely foul odor, and must be handled carefully within a fume hood) *n*-BuLi (24 mL, 59 mmol) was added via syringe, and the resulting mixture was stirred for 20 min before adding Boc-leucine methyl ester (5.32 g, 22 mmol) as a solution in THF (15 mL). The mixture was stirred for 40 min, then warmed to 0 °C and quenched by the addition of AcOH. The reaction was concentrated, and the residue was partitioned between Et₂O and H₂O. The organic phase was washed with H₂O (x1), brine, dried over MgSO₄ and concentrated. Purification by flash chromatography on SiO₂ eluted with 30% EtOAc in hexanes afforded the intermediate Boc-**48** (2.94 g, 53%) as a light yellow oil. This material was deprotected with 4N HCl in dioxane and used without further purification.



Linear intermediate 53. Compound **53** (171 mg, 40%) was prepared from aldehyde **1**, Tosmic reagent **11** and peptide H-Gly-Pro(4-OAr)-Tyr-NH₂ (itself synthesized from aryloxyproline **33d**) analogously to compound **13**. ¹H NMR (CD₃OD, 600 MHz, mixture of rotamers): δ 1.54 (s, 3H), 1.64 (s, 3H), 1.85-1.99 (m, 9H), 1.99-2.05 (m, 3H), 2.06-2.14 (m, 2.5H), 2.20-2.24 (m, 0.5H), 2.24-2.28 (m, 1H), 2.29 (s, 0.75H), 2.35 (s, 2.25H), 2.45 (ddd, J = 14.0, 10.2, 4.9 Hz, 0.75 H), 2.47 (br d, J = 13.8 Hz, 0.5H), 2.62 (ddd, J = 14.1, 9.6, 4.4 Hz, 0.25H), 2.77-2.94 (m, 2.5H), 2.95-3.01 (m, 0.75H), 3.04 (dd, J = 14.0, 5.9 Hz, 0.75H), 3.09 (d, J = 5.1 Hz, 0.25H), 3.12 (br d, J = 5.0 Hz, 0.25H), 3.15 (dd, J = 15.3, 3.7 Hz, 0.75H), 3.51 (dd, J = 13.3, 3.9 Hz, 0.4H), 3.61 (dd, J = 11.1, 4.3 Hz, 0.6H), 3.66 (br d, J = 11.1 Hz, 0.6H), 3.80 (d, 1H), 3.87 (s, 2H), 3.99-4.03 (m, 0.4H), 4.06 (d, J = 17.6 Hz, 0.6H), 4.33 (br d, J = 8.8 Hz, 0.25H), 4.36 (d, J = 17.6 Hz, 0.75H), 4.41 (dd, J = 9.9, 6.7 Hz, 1H), 4.56 (dd, J = 7.6, 6.1 Hz, 1H), 4.63 (ddd, J = 12.7, 6.9, 0.9 Hz, 1H), 4.69 (ddd, J = 12.6, 6.2, 1.0 Hz, 1H), 4.72-4.77 (m, 1H), 4.78-4.81 (m, 0.25H), 4.93-4.98 (m, 0.75H), 5.01-5.08 (m, 2H), 6.23 (dt, J = 15.8, 6.5 Hz, 0.7H), 6.33 (dt, J = 15.9, 6.5 Hz, 0.3H), 6.54 (br s, 0.4H), 6.55-6.57 (m, 1H), 6.58 (d, J = 8.5 Hz, 1.4H), 6.64 (d, J = 15.8 Hz, 0.3H), 6.68 (br d, J = 7.9 Hz, 0.3H), 6.79 (br d, J = 8.0 Hz, 0.7H), 6.82 (d, J = 8.0 Hz, 1.3H), 6.90-6.94 (m, 2H), 6.97 (d, J = 8.5 Hz, 1.4H), 7.00 (d, J = 8.5 Hz, 0.7H), 7.05-7.13 (m, 4H), 7.16-7.20 (m, 1H), 7.23 (br d, J = 7.7 Hz, 0.75H), 7.26 (br d, J = 7.8 Hz, 0.25H), 7.38 (s, 0.75H), 7.40-7.44 (m, 0.5H), 7.46-7.50 (m, 0.75H), 7.49-7.54 (m, 1.5H). MS (ESI) *m/z* calc'd for C₆₁H₆₈Cl₃FN₅O₉ [M+H]⁺: 1138.4, found 1137.7.

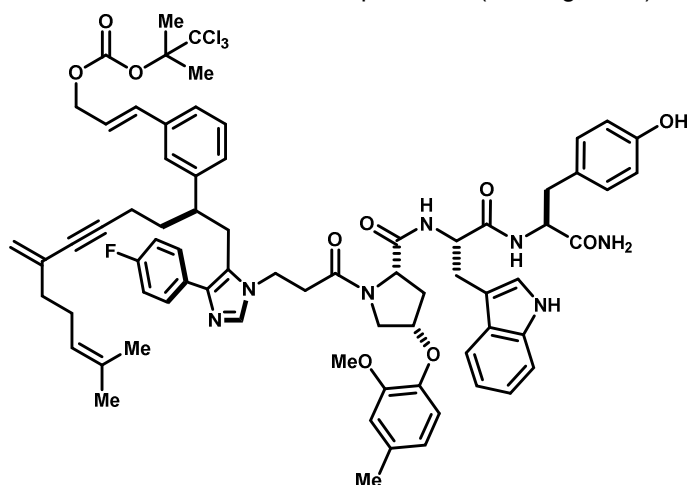


Macrocyclic tyrosyl ether 57. Compound **57** (66 mg, 48%) was obtained by cyclization of linear



intermediate **49** (171 mg, 0.15 mmol) analogously to compound **16**. $^1\text{H NMR}$ (CD_3CN , 300 MHz, major conformer): δ 1.54 (s, 3H), 1.63 (s, 3H), 1.67-1.83 (m, 1H), 1.82-2.19 (m, 8H), 2.31 (s, 3H), 2.36-2.53 (m, 2H), 2.80-3.04 (m, 3H), 3.05-3.26 (m, 2H), 3.33-3.44 (m, 1H), 3.55-3.57 (m, 1H), 3.69-3.78 (m, 1H), 3.80 (s, 3H), 4.39-4.52 (m, 2H), 4.68-4.81 (m, 2H), 4.85-4.95 (m, 1H), 4.96-5.12 (m, 3H), 5.85 (apt dt, $J = 16.2, 5.4\text{ Hz}$, 1H), 6.39-6.54 (m, 1H), 6.54-6.67 (m, 2H), 6.67-6.83 (m, 4H), 6.83-6.98 (m, 4H), 6.98-7.19 (m, 5H), 7.19-7.26 (m, 2H), 7.42-7.54 (m, 2H). MS (ESI) m/z calc'd for $\text{C}_{56}\text{H}_{61}\text{FN}_5\text{O}_6$ $[\text{M}+\text{H}]^+$: 918.5, found 918.0.

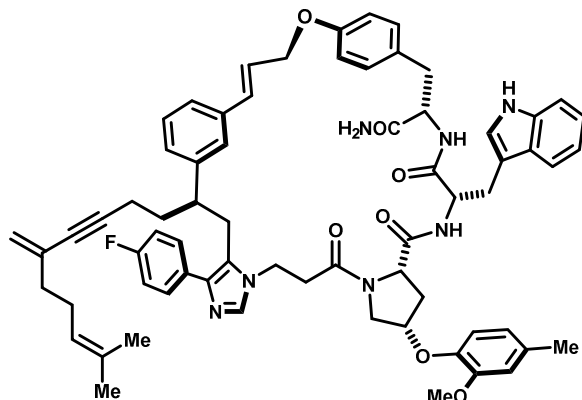
Linear intermediate 54. Compound **54** (342 mg, 51%) was prepared from aldehyde **1**, Tosmic reagent **11**



and peptide H- β -Ala-Pro(4-OAr)-Trp-Tyr-NH₂ (itself synthesized from aryloxyproline **33d**) analogously to compound **13**. $^1\text{H NMR}$ (CD_3OD , 600 MHz, mixture of rotamers): δ 1.54 (s, 1.4H), 1.56 (s, 1.6H), 1.65 (s, 1.4H), 1.66 (s, 1.6H), 1.76-1.82 (m, 1H), 1.82-1.89 (m, 1H), 1.927 (s, 1.5H), 1.930 (s, 1.5H), 1.94 (s, 3H), 1.95-1.99 (m, 1H), 2.00-2.06 (m, 3H), 2.06-2.14 (m, 3H), 2.13-2.19 (m, 1H), 2.24 (s, 1.7H), 2.30 (s, 1.3H), 2.44-2.56 (m, 1H), 2.63-2.74 (m, 2H), 2.86-2.92 (m, 2H), 2.95 (dd, $J = 14.9, 8.9\text{ Hz}$, 1H), 2.98-3.17 (m, 5H), 3.17-3.23 (m, 1H), 3.23-3.29 (m, 1H), 3.59 (s, 1.3H), 3.66 (s, 1.7H), 3.79-3.89 (s, 1H), 4.04-4.13 (m, 1.6H), 4.34 (dd, $J = 10.6, 2.4\text{ Hz}$,

0.4H), 4.57-4.63 (m, 0.5H), 4.67-4.70 (m, 0.5H), 4.70-4.75 (m, 1.7H), 4.78 (dd, $J = 8.5, 5.8\text{ Hz}$, 1H), 5.02-5.08 (m, 2H), 5.08-5.11 (m, 1H), 6.19 (dt, $J = 15.8, 6.3\text{ Hz}$, 0.3H), 6.23 (dt, $J = 15.8, 6.5\text{ Hz}$, 0.7H), 6.49-6.54 (m, 1.8H), 6.55-6.60 (m, 1.2H), 6.67 (d, $J = 8.0\text{ Hz}$, 1.2H), 6.69-6.67 (m, 1.8H), 6.78 (br d, $J = 7.6\text{ Hz}$, 0.5H), 6.82-6.86 (m, 1.2H), 6.88-6.92 (m, 1.8H), 6.94-7.00 (m, 1.5H), 7.00-7.14 (m, 4H), 7.14-7.18 (m, 0.8H), 7.21-7.25 (m, 1.2H), 7.30-7.34 (m, 1.2H), 7.40-7.43 (m, 0.8H), 7.44-7.48 (m, 1H), 7.68 (s, 1H). MS (ESI) m/z calc'd for $\text{C}_{73}\text{H}_{80}\text{Cl}_3\text{FN}_7\text{O}_{10}$ $[\text{M}+\text{H}]^+$: 1338.5, found 1338.8.

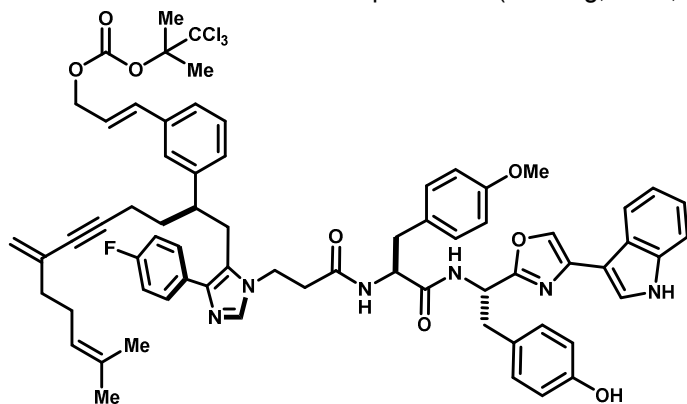
Macrocyclic tyrosyl ether 58. Compound **58** (139 mg, 47%) was obtained by cyclization of linear



intermediate **50** (350 mg, 0.26 mmol) analogously to compound **16**. $^1\text{H NMR}$ (CD_3OD , 600 MHz, mixture of rotamers): δ 1.50 (s, 3H), 1.60 (s, 3H), 1.77-1.91 (m, 2H), 1.90-2.10 (m, 8H), 2.11-2.31 (m, 5H), 2.66-2.95 (m, 2H), 2.95-3.15 (m, 4H), 3.15-3.28 (m, 2H), 3.38-3.53 (m, 2H), 3.61 (s, 2H), 3.65 (s, 1H), 3.83-3.96 (m, 0.5H), 4.00-4.15 (m, 2H), 4.16-4.26 (m, 0.5H), 4.43-4.48 (m, 3H), 4.94-5.11 (m, 3H), 6.15-6.34 (m, 1H), 6.44-6.56 (m, 1.7H), 6.56-6.63 (m, 1.3H), 6.63-6.76 (m, 2.7H), 6.79-6.87 (m, 0.6H), 6.87-6.98 (m, 3.3H), 6.98-7.16 (m, 7.3H), 7.17-7.24 (m, 1H), 7.25-7.31 (m, 1H), 7.32-7.42 (m, 2H), 7.42-7.55 (m, 1H), 7.56-7.67 (m, 1H). MS (ESI) m/z calc'd for $\text{C}_{68}\text{H}_{73}\text{FN}_7\text{O}_7$ $[\text{M}+\text{H}]^+$:

1118.6, found 1118.0.

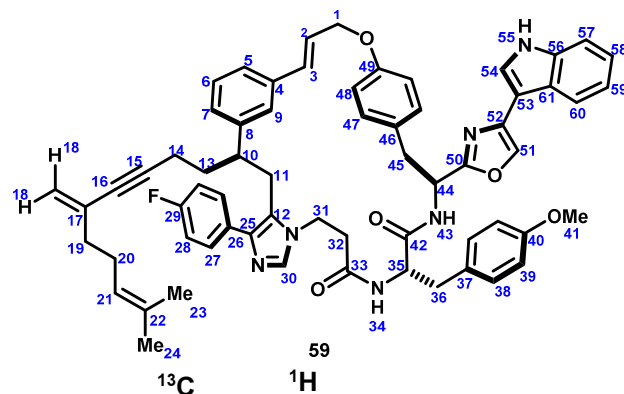
Linear intermediate 55. Compound **55** (162 mg, 25%; 468 mg, 28%) was prepared from aldehyde **1**, Tosmic reagent **11** and peptide H- β -Ala-Phe(4-OMe)-Tyr-oxazole-indole (itself synthesized from oxazole **43**) analogously to compound **13**.



$^1\text{H NMR}$ ($\text{CD}_3\text{CN}:\text{CD}_3\text{OD}$ (5:1), 500 MHz): δ 1.51 (s, 3H), 1.61 (d, $J = 0.9$ Hz, 3H), 1.79 (dd, $J = 13.9, 7.3$ Hz, 2H), 1.88 (s, 6H), 1.94-2.02 (m, 3H), 2.02-2.14 (m, 3H), 2.47 (t, $J = 6.5$ Hz, 2H), 2.71 (dd, $J = 13.9, 7.1$ Hz, 1H), 2.88 (dd, $J = 13.9, 6.3$ Hz, 1H), 2.89-3.00 (m, 2H), 3.03 (dd, $J = 14.0, 7.7$ Hz, 1H), 3.03 (dd, $J = 14.9, 5.5$ Hz, 1H), 3.17 (dd, $J = 13.9, 7.0$ Hz, 1H), 3.43 (s, 3H), 3.93 (br t, $J = 6.5$ Hz, 2H), 4.52 (t, $J = 6.7$ Hz, 1H), 4.69 (dd,

$J = 6.5, 1.1$ Hz, 1H), 4.98-6.03 (m, 1H), 5.04 (d, $J = 1.9$ Hz, 1H), 5.07-5.08 (m, 1H), 5.25 (t, $J = 7.5$ Hz, 1H), 6.18 (dt, $J = 16.0, 6.5$ Hz, 1H), 6.50 (d, $J = 16.0$ Hz, 1H), 6.53 (d, $J = 8.7$ Hz, 2H), 6.60 (d, $J = 8.6$ Hz, 2H), 6.80 (br d, $J = 7.6$ Hz, 1H), 6.86 (d, $J = 8.7$ Hz, 2H), 6.93-6.94 (m, 1H), 6.95 (d, $J = 8.6$ Hz, 2H), 7.00 (dd, $J_{\text{HH}} = 8.9$ Hz, $J_{\text{CF}} = 8.9$ Hz, 2H), 7.01-7.07 (m, 3H), 7.14 (dd, $J = 7.0, 1.0$ Hz, 1H), 7.15 (s, 1H), 7.20 (ddd, $J = 8.3, 7.0, 1.1$ Hz, 1H), 7.32-7.42 (m, 4H), 7.39 (s, 1H), 7.45 (ddd, $J = 8.3, 0.8, 0.8$ Hz, 1H), 7.57 (s, 1H), 7.69 (s, 0.5H), 7.77 (ddd, $J = 8.0, 1.0, 1.0$ Hz, 1H). $^{13}\text{C NMR}$ (CDCl_3 , 125 MHz, mixture of rotamers): δ 170.3, 169.5, 161.9 (d, $J_{\text{CF}} = 246$ Hz), 160.3, 158.2, 155.8, 151.9, 148.3, 143.1, 136.9, 136.4, 136.3, 136.1, 135.3, 134.3, 131.8, 131.7, 131.5 (d, $J_{\text{CF}} = 3.5$ Hz), 130.2 (2), 130.1, 129.5 (d, $J_{\text{CF}} = 8.1$ Hz), 128.9, 128.8, 128.5, 128.4, 127.5, 127.4, 125.8, 124.9, 123.8, 123.2 (2), 122.8, 122.4, 122.4, 120.3, 119.4, 119.3, 118.9, 115.2 (d, $J_{\text{CF}} = 22$ Hz), 115.0, 114.9, 114.7, 113.3, 111.8, 105.4, 104.1, 89.5, 89.0, 81.2, 68.2, 54.3, 54.2, 54.1, 48.8, 44.1, 40.3, 37.9, 37.1, 36.9, 36.1, 33.5, 30.3, 26.3, 24.7, 20.4, 16.7, 16.6. MS (ESI) m/z calc'd for $\text{C}_{69}\text{H}_{71}\text{Cl}_3\text{FN}_6\text{O}_8$ $[\text{M}+\text{H}]^+$: 1235.4, found 1234.7.

Macrocyclic tyrosyl ether 59. Compound **59** (660 mg, >100%) was obtained by cyclization of linear intermediate **51** (468 mg, 0.378 mmol) analogously to compound **16**. A portion was purified by preparative TLC on SiO_2 developed with 7% MeOH in CHCl_3 (x2) for characterization, and the remainder was carried forward crude. MS (ESI) m/z calc'd for $\text{C}_{64}\text{H}_{64}\text{FN}_6\text{O}_5$ $[\text{M}+\text{H}]^+$: 1015.5, found 1015.9.

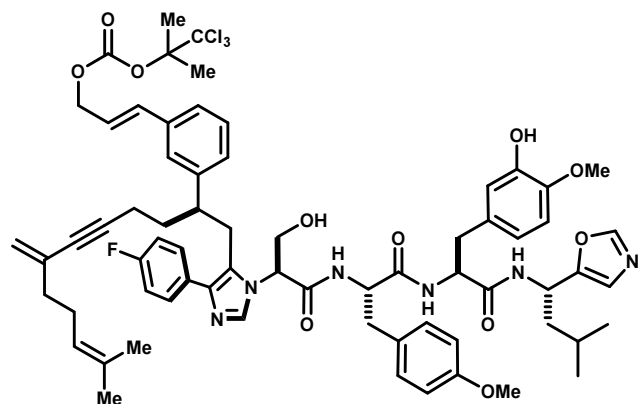


	^{13}C	^1H	key correlation
1	68.8	4.81 (dd, $J = 5.4, 1.1$ Hz, 2H)	HMBC 1→49
2	126.8	3.40 (dt, $J = 16.1, 5.4$ Hz, 1H)	COSY 2→1,3 HMBC 2→4
3	133.1	6.62 (d, $J = 16.1$ Hz, 1H) overlap	HMBC 3→4
4	137.8	-	
5	126.3	7.13-7.17 (m, 1H) overlap	HMBC 5→7
6	129.6	7.04 (dd, $J = 7.6, 7.6$ Hz, 1H)	HMBC 6→4,8
7	129.2	6.57-6.61 (m, 1H) overlap	HMBC 7→5
8	144.4	-	
9	125.1	7.31 (br s, 1H)	HMBC 9→3,5,7

10	44.9	2.87-2.92 (m, 1H) overlap	
11	31.7	2.85-2.91 (m, 1H) overlap, 3.07-3.13 (m, 1H)	HMBC 11→8,10,12,13,25
12	126.9	-	
13	34.1	1.72-1.88 (m, 2H) overlap	
14	17.7	1.86-1.95 (m, 1H) overlap, 2.09-2.16 (m, 1H)	
15	90.0	-	
16	82.2	-	
17	132.8	-	
18	120.5	5.01-5.02 (m, 1H) overlap, 5.07-5.09 (m, 1H)	HMBC 18→16,17
19	38.2	1.97-2.00 (m, 2H) overlap	HMBC 19→17,18,20,21
20	27.4	1.98-2.06 (m, 2H) overlap	HMBC 20→19,21,22
21	124.3	4.97-5.03 (m, 1H) overlap	HMBC 21→22
22	132.8	-	
23	17.7	1.53 (d, $J = 0.5$ Hz, 3H)	HMBC 23→21,22
24	25.7	1.63 (d, $J = 0.8$ Hz, 3H)	HMBC 24→21,22
25	137.5	-	
26	132.8	-	
27	129.6	7.58-7.63 (m, 2H) overlap	HMBC 27→25
28	116.1	7.08-7.14 (m, 2H)	HMBC 28→26
29	162.5 (d, $J_{CF} \approx 240$ Hz)	-	
30	136.9	7.20 (s, 1H) overlap	
31	40.8	3.54-3.61 (m, 1H) overlap, 3.73-3.81 (m, 1H)	HMBC 31→30,32
32	37.3	1.86-1.92 (m, 1H) overlap, 2.56 (ddd, $J = 15.5, 6.7$ Hz, 1H)	HMBC 32→31,33
33	170.5	-	
34	-	not obs.	
35	55.0	4.44-4.50 (m, 1H)	HMBC 35→33,42
36	37.7	2.67 (dd, $J = 14.0, 7.9$ Hz, 1H), 2.89-2.96 (m, 1H) overlap	
37	125.1	-	
38	131.0	6.95 (d, $J = 8.6$ Hz, 2H)	HMBC 38→40
39	114.4	6.61 (d, $J = 8.6$ Hz, 2H)	HMBC 39→37,40
40	159.2	-	
41	55.5	3.49 (s, 3H)	
42	171.7	-	
43	-	not obs.	
44	49.3	5.35 (dd, $J = 11.1, 3.1$ Hz, 1H)	HMBC 44→42,50
45	38.3	3.06 (dd, $J = 14.2, 11.1$ Hz, 1H), 3.30 (dd, $J = 14.2, 3.1$ Hz, 1H)	
46	124.9	-	
47	131.3	7.17 (d, $J = 8.6$ Hz, 2H) overlap	HMBC 47→49 COSY 47→48
48	116.0	6.89 (d, $J = 8.6$ Hz, 2H)	HMBC 48→46,49

49	158.0	-	
50	161.9	-	
51	120.1	7.22 (s, 1H)	
52	149.4	-	
53	105.1	-	
54	123.8	7.61 (s, 1H) overlap	
55	-	not obs.	
56	137.3	-	
57	112.9	7.49 (ddd, $J = 7.9, 0.9, 0.9$ Hz, 1H)	HMBC 57→59,61
58	123.5	7.20-7.24 (m, 1H) overlap	
59	121.4	7.14-7.18 (m, 1H) overlap	
60	120.5	7.87 (ddd, $J = 7.9, 0.9, 0.9$ Hz, 1H)	HMBC 60→56,58
61	124.9	-	

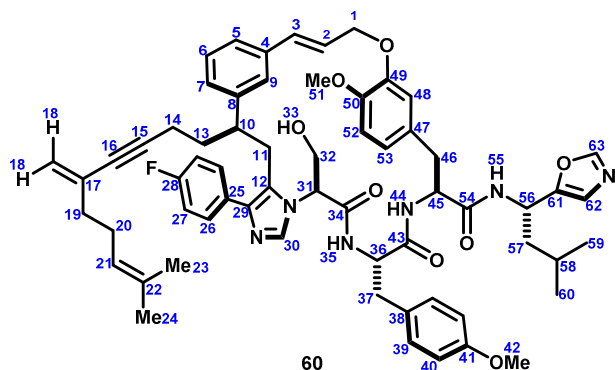
Linear intermediate 56. Compound **56** (147 mg, 23%; 241 mg, 16%) was prepared from aldehyde **1**,



Tosmic reagent **11** and peptide H-Ser-Phe(4-OMe)-Phe(4-OMe-3-OH)-Leu-oxazole (itself synthesized from leucine-derived oxazole **48**) analogously to compound **16**. ^1H NMR (CD_3OD , 600 MHz, mixture of rotamers): δ 0.90 (t, $J = 6.0$ Hz, 6H), 1.53 (s, 3H), 1.62 (s, 3H), 1.55-1.88 (m, 9H), 1.90 (s, 6H), 1.93-2.14 (m, 5H), 2.63-2.96 (m, 7H), 3.10 (dd, $J = 14.1, 4.2$ Hz, 1H), 3.58 (s, 3H), 3.62-3.76 (m, 2H), 3.76 (s, 3H), 4.12 (br d, $J = 6.0$ Hz, 1H), 4.53 (dd, $J = 7.5, 7.5$ Hz, 1H), 4.69-4.75 (m, 1H), 4.70 (br d, $J = 6.2$ Hz, 2H), 4.77-4.84 (m, 1H), 4.98-5.17 (m, 4H), 6.14 (dt, $J = 15.6, 6.2$ Hz, 1H), 6.47 (d, $J = 15.6$ Hz, 1H), 6.48-6.55 (m, 1H),

6.61-6.77 (m, 6H), 6.84 (br s, 1H), 6.90-7.16 (m, 6H), 7.80 (s, 1H), 8.01 (s, 1H). ^{13}C NMR (CDCl_3 , 75 MHz): δ 172.7, 172.5, 169.8, 163.0 (d, $J_{\text{CF}} = 254$ Hz) 159.8, 153.9, 153.6, 152.7, 147.8, 147.3, 143.8, 138.4, 137.4, 137.0, 135.8, 133.1, 132.8, 132.2, 131.1, 130.9, 130.8, 130.4, 129.7, 129.6, 128.8, 127.1, 127.0, 126.1, 124.6, 123.5, 122.9, 121.5, 120.3, 117.4, 116.1, 115.8, 115.0, 112.5, 106.8, 90.8, 90.1, 82.5, 69.5, 63.2, 56.4, 56.3, 55.9, 55.6, 54.8, 44.5, 42.7, 38.7, 37.9, 35.2, 31.4, 27.8, 26.0, 25.7, 23.2, 22.3, 21.6, 18.01, 17.96. MS (ESI) m/z calc'd for $\text{C}_{68}\text{H}_{79}\text{Cl}_3\text{FN}_6\text{O}_{11}$ $[\text{M}+\text{H}]^+$: 1279.5, found 1280.8.

Macrocyclic tyrosyl ether 60. Compound **60** was obtained by cyclization of linear intermediate **52** (147 mg, 0.12 mmol) analogously to compound **16**. The crude product was adsorbed onto Celite and purified by chromatography on SiO₂ eluted with 0→10% MeOH in CHCl₃ to give **60** (39 mg, 32%) as a light yellow film. MS (ESI) *m/z* calc'd for C₆₃H₇₂FN₆O₈ [M+H]⁺: 1059.5, found 1059.0.



600 MHz, CD₃OD (no amide NH/OH observed)

	¹³ C	¹ H	key correlations
1	68.8	4.77 (dd, <i>J</i> = 14.4, 6.7 Hz, 1H), 4.91 (ddd, <i>J</i> = 14.4, 4.8, 1.1 Hz, 1H)	HMBC 1→49
2	124.7	6.48 (ddd, <i>J</i> = 15.8, 6.7, 4.8 Hz, 1H)	COSY 2→1,3
3	132.8	6.66 (br d, <i>J</i> = 15.8 Hz, 1H)	HMBC 3→4
4	136.8	-	
5	126.1	7.18 (br d, <i>J</i> = 7.5 Hz, 1H) overlap	HMBC 5→3,7
6	128.8	7.14 (dd, <i>J</i> = 7.5, 7.5 Hz, 1H)	HMBC 6→4,8
7	125.7	6.87 (br d, <i>J</i> = 7.4 Hz, 1H)	HMBC 7→5
8	143.7	-	
9	125.9	7.33 (br s, 1H)	HMBC 9→3,5,7
10	44.8	2.75-2.81 (m, 1H) overlap	
11	30.0	2.87 (br d, <i>J</i> = 15.3 Hz, 1H) overlap, 3.10 (dd, <i>J</i> = 15.3, 8.4 Hz, 1H)	HMBC 11→8,12
12	126.4	-	
13	34.0	1.45-1.60 (m, 2H) overlap	
14	16.4	1.70-1.76 (m, 1H), 1.78-1.85 (m, 1H)	
15	88.9	-	
16	80.7	-	
17	131.9	-	
18	118.5	5.02-5.03 (m, 1H)m 5.04-5.06 (m, 1H) overlap	HMBC 18→17
19	37.4	1.98-2.02 (m, 2H)	HMBC 19→17,18,20,21
20	26.5	2.04-2.10 (m, 2H)	HMBC 20→17,19,20,21
21	123.1	5.03-5.07 (m, 1H) overlap	HMBC 21→22,23,24
22	131.4	-	
23	16.6	1.66 (d, <i>J</i> = 0.8 Hz, 3H)	HMBC 23→21,22
24	24.6	1.55 (s, 3H)	HMBC 24→21,22
25	131.1	-	
26	129.5	7.62 (dd, <i>J</i> _{HH} = 8.6 Hz, <i>J</i> _{HF} = 5.4 Hz, 2H)	COSY 26→27 HMBC 26→28,29
27	115.1	7.16 (dd, <i>J</i> _{HH} = 8.6 Hz, <i>J</i> _{HF} = 8.5 Hz, 2H)	HMBC 27→25,28

28	162.0 (d, $J_{CF} \approx 238\text{Hz}$)	-	
29	137.2	-	
30	135.5	7.78 (s, 1H)	HMBC 30→12,29
31	59.9	4.34 (dd, $J = 5.9, 5.9\text{ Hz}, 1\text{H}$)	HMBC 31→34
32	62	3.68-3.76 (m, 1H), 3.91 (dd, $J = 11.0, 5.9\text{ Hz}, 1\text{H}$)	HMBC 32→34
33	-	not observed	
34	167.7	-	
35	-	not observed	
36	53.7	4.46 (dd, $J = 6.7, 5.6\text{ Hz}, 1\text{H}$)	HMBC 36→34,37,38,43
37	35.6	2.86 (dd, $J = 13.9, 7.3\text{ Hz}, 1\text{H}$) overlap, 3.07 (dd, $J = 13.9, 5.1\text{ Hz}, 1\text{H}$)	HMBC 37→43
38	127.4	-	
39	129.9	6.90 (d, $J = 8.6\text{ Hz}, 2\text{H}$)	HMBC 39→41
40	113.7	6.71 (d, $J = 8.6\text{ Hz}, 2\text{H}$)	HMBC 40→41
41	158.6	-	
42	54.3	3.66 (s, 3H)	HMBC 42→41
43	170.7	-	
44	-	not observed	
45	54.4	4.79 (dd, $J = 10.3, 4.5\text{ Hz}, 1\text{H}$) overlap	HMBC 45→43,47,54
46	37.4	2.75 (dd, $J = 14.0, 10.4\text{ Hz}, 1\text{H}$), 3.04 (dd, $J = 14.0, 4.3\text{ Hz}, 1\text{H}$)	HMBC 46→45,47,54
47	129.3	-	
48	114.9	7.01 (d, $J = 1.6\text{ Hz}, 1\text{H}$)	HMBC 48→49,50,53
49	147.2	-	
50	148.3	-	
51	55.1	3.81 (s, 3H)	HMBC 51→50
52	112.0	6.82 (d, $J = 8.3\text{ Hz}, 1\text{H}$)	HMBC 52→47,49,50,53
53	121.6	6.69-6.72 (m, 1H) overlap	
54	171.8	-	
55	-	not observed	
56	43.3	5.20 (dd, $J = 9.4, 5.8\text{ Hz}, 1\text{H}$)	HMBC 56→57,61
57	41.6	1.67-1.77 (m, 2H)	HMBC 57→56
58	24.6	1.62-1.66 (m, 1H) overlap	
59	21.9	0.95 (d, $J = 6.2\text{ Hz}, 3\text{H}$)	
60	20.9	0.96 (d, $J = 6.3\text{ Hz}, 3\text{H}$)	
61	152.8	-	
62	121.7	6.97 (s, 1H)	HMBC 62→61,63
63	151.6	8.14 (s, 1H)	HMBC 63→61,62

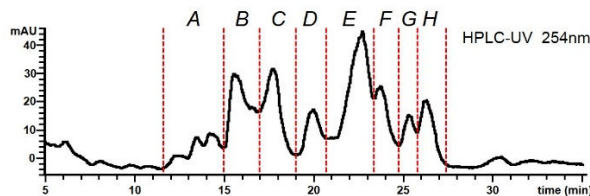
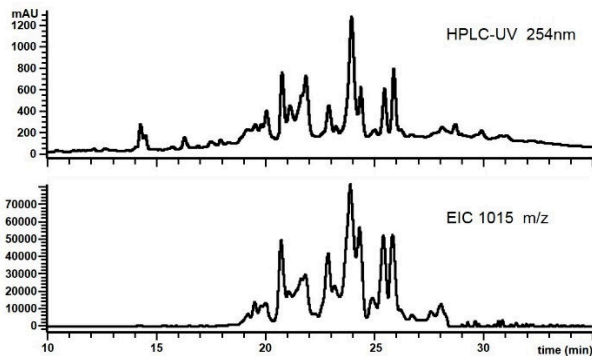
Acidolysis of macrocyclic cinnamyl ether 59 and HPLC separation of product mixture 61. To macrocyclic cinnamyl ether 59 (crude, ~0.38 mmol) was added MeNO₂ (38 mL), and the mixture was cooled in an ice bath. MeSO₃H (614 μL, 9.5 mmol) was added, and the mixture was stirred for 2 hr, then partitioned between EtOAc and sat. NaHCO₃. The organic phase was washed with brine, dried over MgSO₄, concentrated, and re-dissolved in DMF for preparative HPLC purification. Purified over multiple injections of ~75 mg per injection using the following method. Fractions were pooled, freed of ACN at the rotovap, and lyophilized.

Analytical HPLC method:
Waters Sunfire C18
4.6x250mm, 5μ, 1 mL/min
A: H₂O + 0.1% TFA
B: ACN + 0.1% TFA

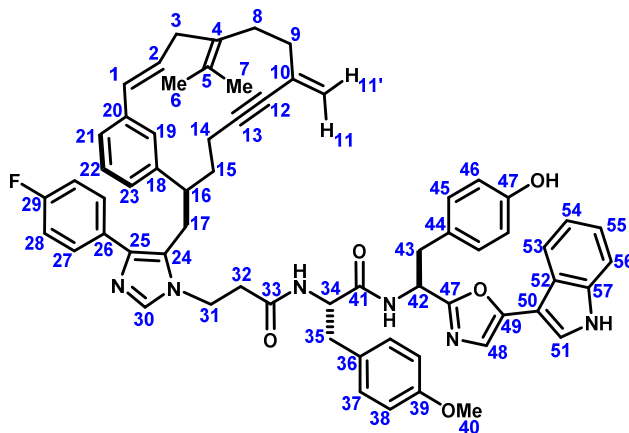
Time	%C	%D
0	50	50
2	50	50
40	0	100
45	0	100
50	50	50
57	50	50

Preparative HPLC method:
Waters Sunfire C18
30x150mm, 5μ, 30 mL/min
A: H₂O + 0.1% TFA
B: ACN + 0.1% TFA

Time	%C	%D
0	50	50
2	50	50
40	0	100
45	0	100
50	50	50
57	50	50



Macrocyclic acidolysis product 61B. Initial fraction *B* was re-purified by semi-preparative HPLC, after which NMR showed still complex mixture. Secondary Fraction B1 was again re-purified by PTLC on SiO₂ (20x20 cm, 500 μm) developed with 6% MeOH in CH₂Cl₂ (x3), yielding three bands R_f = 0.44 (trace); 0.37 (major); 0.34 (minor). The band R_f = 0.37 was collected to recover **61B** (4.6 mg) as a colorless film.



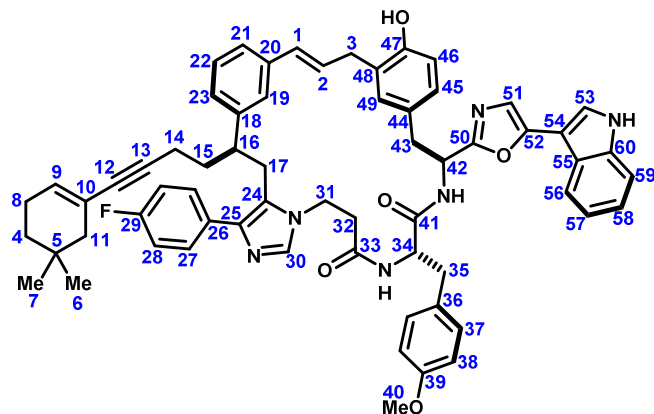
61b

(600 MHz, CD₃OD, 295K)

¹³ C	¹ H	key correlations
1	6.39 (d, <i>J</i> = 15.7 Hz, 1H)	HMBC 1→20
2	6.25 (ddd, <i>J</i> = 15.7, 8.3, 7.1 Hz, 1H)	HMBC 2→20
3	2.89 - 2.95 (m, 1H, obscured), 3.14 - 3.18 (m, 1H, obscured)	TOCSY 3→7 HMBC 3→4,5
4	-	
5	-	
6	1.70 (s, 3H)	HMBC 6→4,5
7	1.72 (s, 3H)	HMBC 7→4,5
8	2.11 - 2.17 (m, 1H, obscured), 2.22 (dd, <i>J</i> = 12.7, 5.7 Hz, 1H)	HMBC 8→4,5
9	2.04 - 2.10 (m, 1H), 2.11 - 2.15 (m, 1H, obscured)	TOCSY 9→11' HMBC 9→10
10	-	
11	5.12 (apt. t, <i>J</i> = 2.1 Hz, 1H), 5.16 (br s, 1H)	HMBC 11→10,12,13
12	-	
13	-	
14	1.80 - 1.86 (m, 1H, obscured), 1.98 - 2.04 (m, 1H, obscured)	TOCSY 14→15,16,17
15	1.57 - 1.63 (m, 1H), 1.82 - 1.89 (m, 1H)	
16	3.13 - 3.22 (m, 1H, obscured)	HMBC 16→18,19,22,24
17	2.89 - 2.94 (m, 1H, obscured), 3.14 - 3.19 (m, 1H, obscured)	
18	not detected	-
19	7.36 (dd, <i>J</i> = 1.8, 1.8 Hz, 1H)	TOCSY 19→21,22,23
20	-	
21	6.78 (ddd, <i>J</i> = 7.6, 1.3, 1.3, 1H)	COSY 21→22
22	7.05 - 7.11 (m, 1H, obscured)	
23	6.95 (d, <i>J</i> = 7.7 Hz, 1H, obscured)	COSY 23→22
24	-	
25	141.3	-

26	136.5	-	
27	128.8	7.40 - 7.44 (dd, $J_{HH} = 8.4$, $J_{HF} = 5.4$, 2H)	HMBC 27→25,26,29
28	114.2	7.05 - 7.10 (m, 2H, obscured)	HMBC 28→25,26
29	161.9 (d, $J_{CF} = 249$ Hz)	-	
30	135.9	7.61 (br s, 1H)	
31	40.4	4.10 - 4.23 (m, 2H)	HMBC 31→33,30,24
32	36.0	2.61-2.66 (m, 2H)	COSY 32→31, HMBC 32→33
33	170.3	-	
34	54.3	4.57 (dd, $J = 7.3$, 7.3, 1H)	HMBC 34→36
35	36.6	2.74 (dd, $J = 13.7$, 7.3 Hz 1H), 2.93 (dd, $J = 13.7$, 7.3 Hz, 1H)	HMBC 35→C36
36	128.1	-	
37	124.5	6.93 - 6.96 (m, 2H, obscured)	COSY 37→38 HMBC 37→36,39
38	112.8	6.56 (d, $J = 8.7$ Hz, 2H)	
39	158.3	-	
40	53.4	3.37 (s, 3H)	HMBC 40→39
41	171.2	-	
42	48.6	5.29 (dd, $J = 7.6$, 7.6 Hz, 1H)	HMBC 42→41,47, COSY 42→43
43	37.6	3.06 (dd, $J = 13.5$, 7.5 Hz, 1H), 3.19 (m, obscured)	HMBC 43→44,45
44	127.3	-	
45	129.4	6.95 - 6.98 (m, 2H, obscured)	COSY 45→46
46	156.0	-	HMBC 46→47
47	160.3	-	
48	117.5	7.16 (s, 1H)	HMBC 48→47,59
49	149.0	-	
50	103.9	-	
51	122.3	7.60 (s, 1H)	HMBC 51→50,52,57
52	123.8	-	
53	118.7	7.78 (ddd, $J = 8.0$, 1.0, 1.0 Hz, 1H)	HMBC 53→54,55,56
54	119.5	7.16 (ddd, $J = 8.0$, 7.1, 1.0 Hz, 1H)	
55	121.3	7.21 (ddd, $J = 8.1$, 7.1, 1.0 Hz, 1H)	
56	110.9	7.44 (ddd, $J = 8.1$, 1.0, 1.0 Hz, 1H)	
57	136.7	-	

Macrocyclic acidolysis product 61C. Initial fraction C appeared to contain primarily one component upon HPLC analysis on multiple stationary phases, and was therefore re-purified by PTLC on SiO₂ (20x20 cm, 500 μm) developed with 6% MeOH in CH₂Cl₂ (x3), yielding three bands $R_f = 0.50$ (trace); 0.46 (trace); 0.42 (major); 0.34 (minor). The band $R_f = 0.42$ was collected to recover **61C** (12.6 mg) as a colorless film.



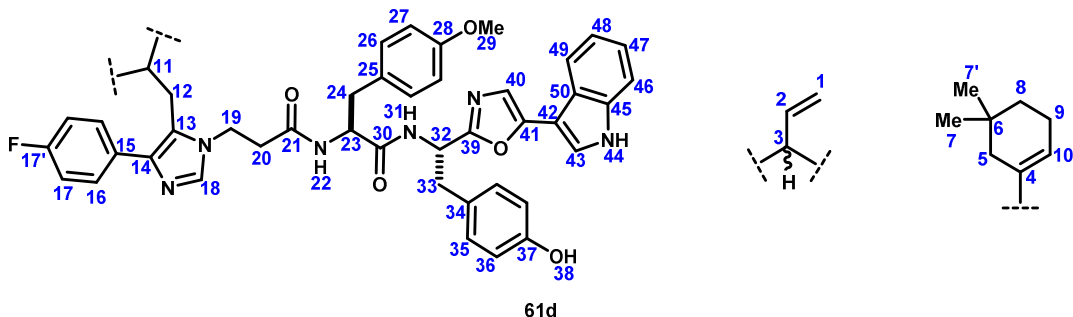
61c

(500 MHz, CD₃OD, 294K)

	¹³ C	¹ H	key correlation
1	129.4	6.35 (d, <i>J</i> = 15.8 Hz, 1H)	TOCSY 1→2,3, HMBC 1→19, 20
2	129.0	6.50 (ddd, <i>J</i> = 15.8, 6.6, 6.6 Hz, 1H)	HMBC 2→20,48
3	32.6	3.39 (dd, <i>J</i> = 15.3, 6.6 Hz, 1H), 3.50-3.55 (m, 1H) overlap	HMBC 3→47,49
4	33.2	1.27 - 1.30 (m, 2H) overlap	HMBC 4→5
5	27.4	-	
6	26.3	0.874 (s, 3H)	HMBC 6→11
7	26.3	0.871 (s, 3H)	
8	22.2	2.04 - 2.09 (m, 2H) overlap	HMBC 8→5
9	130.6	5.73 - 5.75 (m, 1H)	TOCSY 9→4,8,11
10	119.0	-	
11	42.2	1.69-1.71 (m, 2H) overlap	HMBC 11→5,12
12	84.7	-	
13	82.4	-	
14	15.8	1.92 - 1.97 (m, 1H) overlap, 1.89 - 1.98 (m, 1H) overlap	HMBC 14→12,13
15	33.2	1.81 - 1.87 (m, 1H) overlap, 1.89 - 1.98 (m, 1H) overlap	
16	43.1	2.92 - 3.00 (m, 1H) overlap	HMBC 16→18,19,23 TOCSY 16→14,15,17
17	30.0	2.87 - 2.95 (dd, <i>J</i> = 14.7, 10.4 Hz, 1H), 3.17 - 3.22 (d, <i>J</i> = 14.7, 4.1 Hz, 1H)	HMBC 17→24,25,18
18	142.7	-	
19	123.3	7.35 (br s, 1H)	TOCSY 19→21,22,23
20	138.2	-	
21	123.9	7.17 (d, <i>J</i> = 7.9 Hz, 1H)	
22	127.6	6.99 (dd, <i>J</i> = 7.5, 7.5 Hz, 1H)	HMBC 22→18,20
23	126.8	7.14 (d, <i>J</i> = 7.1 Hz, 1H)	
24	126.0	-	
25	136.2	-	

26	131.0	-	
27	128.3	7.60 (dd, $J_{CH} = 8.3\text{Hz}$, $J_{CF} = 5.5\text{ Hz}$, 2H)	COSY 27→28
28	114.4	7.12 - 7.16 (m, 2H) overlap	
29	161.5 (d, $J_{CF} = 241\text{ Hz}$)	-	
30	135.4	7.42 (s, 1H)	
31	39.2	3.69 - 3.75 (m, 1H), 3.82 - 3.88 (m, 1H)	HMBC 31→30,25
32	35.6	2.04 - 2.09 (m, 1H) overlap, 2.10 - 2.16 (m, 1H) overlap	
33	169.9	-	
34	54.1	4.51 (dd, $J = 7.8, 6.5\text{ Hz}$, 1H)	COSY 34→35 HMBC 34→33,41
35	36.4	2.69 (dd, $J = 13.8, 7.8\text{ Hz}$, 1H), 2.95 (dd, $J = 13.8, 6.4\text{ Hz}$, 1H)	
36	128.2	-	
37	129.4	6.98 (d, $J = 8.7\text{ Hz}$, 2H)	COSY 37→38 HMBC 37→39
38	112.8	6.60 (d, $J = 8.7\text{ Hz}$, 2H)	HMBC 38→36,39
39	158.3	-	
40	53.3	3.45 (s, 3H)	HMBC 40→39
41	171.3	-	
42	47.8	5.45 (dd, $J = 9.8, 4.2\text{ Hz}$, 1H)	COSY 42→43,43' HMBC 1→41,44,50
43	37.0	3.11 (dd, $J = 14.3, 9.8\text{ Hz}$, 1H), 3.28 (dd, $J = 14.3, 4.2\text{ Hz}$, 1H)	HMBC 43→44
44	127.3	-	
45	127.6	6.87 (dd, $J = 8.1, 2.1\text{ Hz}$, 1H)	TOCSY 45→46,49 HMBC 45→47,49
46	114.1	6.68 (d, $J = 8.1\text{ Hz}$, 1H)	HMBC 46→48
47	153.7	-	
48	126.3	-	
49	130.2	7.06 (d, $J = 1.9\text{ Hz}$, 1H)	
50	160.5	-	
51	117.6	7.19 (s, 1H)	
52	148.8	-	
53	122.3	7.63 (s, 1H)	
54	103.7	-	
55	123.7	-	
56	118.6	7.80 (ddd, $H = 8.0, 1.1, 0.9\text{ Hz}$, 1H)	
57	119.5	7.16 (ddd, $J = 8.0, 7.0, 1.0\text{ Hz}$, 1H)	
58	121.7	7.21 (ddd, $J = 8.1, 7.0, 1.1\text{ Hz}$, 1H)	
59	110.7	7.45 (ddd, $J = 8.1, 1.0, 0.9\text{ Hz}$, 1H)	
60	136.5	-	

Partial structures of acidolysis product 61D. Initial fraction *D* appeared to contain primarily one component upon HPLC analysis on multiple stationary phases, and was therefore re-purified by PTLC on SiO₂ (20x20 cm, 500 μm, pre-developed with MeOH and oven dried) developed with 7% MeOH in CHCl₃ (x2), yielding three bands R_f = 0.63 (trace); 0.51 (trace); 0.45 (minor); 0.35 (major); 0.18 (minor). The band R_f = 0.45 was collected to recover **61D** as a colorless film.

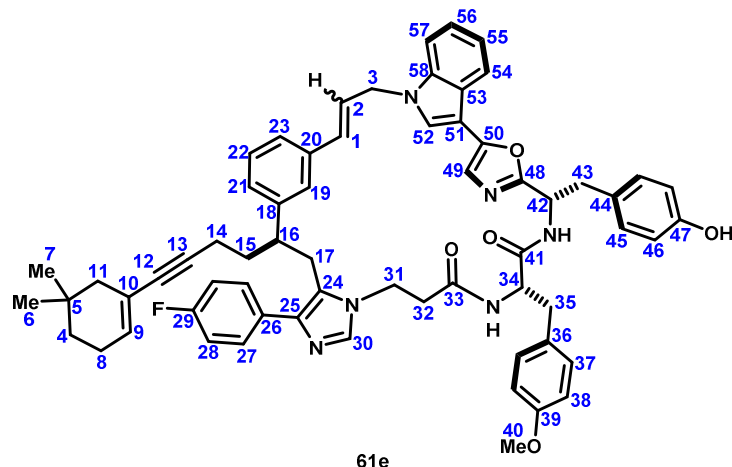


(500 MHz, CD₃OD 300K) *mixture of C3 diastereomers, data is of major

	¹³ C	¹ H	key correlations
1	116.7	5.16 (ddd, <i>J</i> = 10.0, 2.0, 0.6 Hz, 1H), 5.29 (ddd, <i>J</i> = 17.1, 2.0, 0.9 Hz, 1H)	COSY 1→2 TOCSY 1→1',2,3
2	138.6	5.39-5.45 (m, 1H) overlap	
3	56.2	4.12-4.16 (m, 1H)	
4	not detected	-	
5	43.2	1.82-1.88 (m, 1H), 2.20-2.25 (m, 1H)	TOCSY 5→10
6	29.9	-	
7	27.9	0.92 (s, 3H)	HMBC 7→5,6,8
7'	29.0	0.96 (s, 3H)	HMBC 7→7'
8	35.6	1.36 (apt t, 6.4 Hz, 1H), 1.43 (apt t, <i>J</i> = 6.4 Hz, 1H)	COSY 8→9 HMBC 8→9
9	24.3	2.18-2.25 (m, 2H) overlap	COSY 9→10
10	127.5	5.65-5.67 (m, 1H)	
11	37.0	3.12-3.21 (m, 1H)	
12	28.3	3.01-3.11 (m, 2H)	HMBC 12→11, 14
13	not detected	-	
14	130.6	-	
15	130.0	-	
16	130.5	7.07-7.13 (m, 2H) overlap	HMBC 16→14,17'
17	116.1	6.99-7.03 (m, 2H) overlap	HMBC 17→15
17'	164.3 (d, <i>J</i> _{CF} ≈ 240 Hz)	-	
18	134.7	8.74 (s, 1H)	HMBC 18→13,14
19	43.3	4.36-4.48 (m, 2H)	HMBC 19→18
20	35.0	2.74-2.83 (m, 1H) overlap, 2.85-2.92 (m, 1H) overlap	
21	170.1	-	

22	-	not observed	
23	55.5	4.53-4.58 (m, 1H)	COSY 23→24
24	37.1	2.73-2.82 (m, 1H) overlap, 2.85-2.92 (m, 1H) overlap	HMBC 24→25
25	128.5	-	
26	130.0	7.01 (d, $J = 8.5$ Hz, 2H) overlap	HMBC 26→28
27	113.5	6.59 (d, $J = 8.5$ Hz, 2H)	HMBC 27→25 COSY 27→26
28	158.7	-	
29	54.2	3.40 (s, 3H)	HMBC 29→28
30	171.8	-	
31	-	not observed	
32	49.6	5.20-5.55 (m, 1H)	HMBC 32→39 COSY 32→33
33	38.4	3.01-3.08 (m, 1H) overlap, 3.15-3.21 (m, 1H) overlap	HMBC 33→34
34	127.4	-	
35	130.7	7.07-7.13 (m, 2H) overlap	
36	116.0	6.59-6.63 (m, 2H)	
37	156.1	-	
38	-	not observed	
39	160.7	-	
40	118.3	7.14 (s, 1H)	HMBC 40→41
41	149.9	-	
42	104.2	-	
43	123.1	7.59 (s, 1H)	HMBC 43→42,42,50
44	-	11.04 (br s, 1H)	
45	137.2	-	
46	111.7	7.44 (ddd, $J = 8.1, 0.9, 0.8$ Hz, 1H)	HMBC 46→48,50
47	122.5	7.21 (ddd, $J = 8.1, 7.1, 0.9$ Hz, 1H)	HMBC 47→45
48	120.2	7.13-7.17 (m, 1H) obscured	HMBC 48→50
49	119.6	7.75 (ddd, $J = 7.9, 0.9, 0.9$ Hz, 1H)	HMBC 49→45 TOCSY 49→48,47,46
50	124.2	-	

Macrocyclic acidolysis product 61E. Initial fraction *E* was re-purified by semi-preparative HPLC.

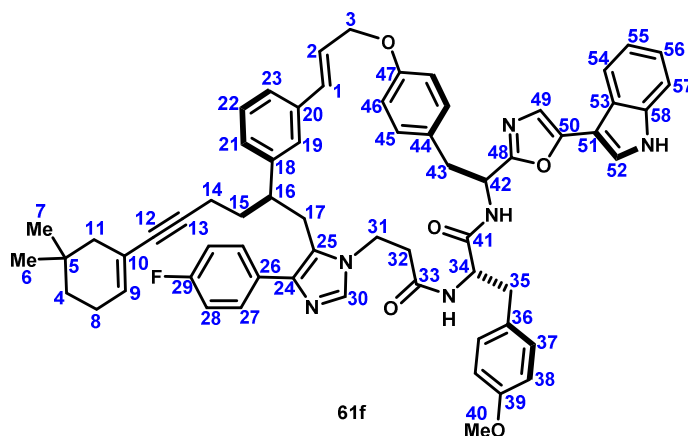


(600 MHz, CD₃OD, 294K)

	¹³ C	¹ H	key correlations
1	126.2	6.51-6.54 (m, 1H) overlap	HMBC 1→2,20
2	133.8	6.51-6.54 (m, 1H) overlap	HMBC 2→1,20
3	48.0	4.89-4.93 (m, 1H, obscured), 5.06 (dd, <i>J</i> = 15.8, 3.9Hz, 1H)	TOCSY 3 → 1,2 HMBC 3 → 58
4	35.1	1.25-1.28 (m, 1H)	HMBC 51 → 55
5	29.4	-	
6	28.0	0.87 (s, 3H)	HMBC 6 → 4,5,11
7	28.0	0.86 (s, 3H)	HMBC 6 → 4,5,11
8	24.0		
9	132.3	5.71 - 5.74 (m, 1H)	TOCSY 9 → 4,8,11
10	133.3	-	
11	44.0	1.67 - 1.70 (m, 1H)	HMBC 11→10
12	83.9	-	
13	86.0	-	
14	17.4	1.87 - 1.93 (m, 1H), 2.08 - 2.16 (m, 1H)	HMBC 14 → 13,12
15	34.6	1.71 - 1.79 (m, 1H), 1.80 - 1.88 (m, 1H)	COSY 15 → 14 HMBC 15 → 18
16	44.9	2.79 - 2.86 (m, 1H)	COSY 16 → 17
17	30.4	2.94 - 3.00 (m, 1H, obscured), 3.10 - 3.14 (m, 1H, obscured)	TOCSY 17 → 14,15,16, HMBC 17 → 18
18	143.4	-	
19	126.2	7.26 (br s, 1H) overlap	
20	138.4	-	
21	128.7	7.25 (br d, <i>J</i> = 7.7 Hz, 1H) overlap	COSY 21 → 22 HMBC 21 → 16
22	129.9	7.06 (dd, <i>J</i> = 7.7, 7.7Hz, 1H, obscured)	HMBC 22→18, 20
23	126.1	6.56 (br d, <i>J</i> = 7.7 Hz, 1H)	HMBC 23→19, 1
24	138.1	-	
25	149.6	-	
26	not detected	-	

27	131.1	7.51 (dd $J_{HH} = 8.5\text{Hz}$, $J_{HF} = 5.1\text{Hz}$, 2H)	COSY 27 → 28 HMBC 27 → 29,25
28	117.2	7.27 - 7.32 (m, 2H, obscured)	HMBC 27 → 29
29	164.7 (d, JCF = 245Hz)	-	
30	134.9	8.44 (brs, 1H)	HMBC 30 → 25,24
31	43.3	3.68 - 3.73 (m, 1H, obscured), 3.95 - 4.00 (m, 1H)	HMBC 31 → 30
32	36.5	2.50 (ddd, $J = 15.5, 7.1, 7.1\text{ Hz}$, 1H) 2.56 - 2.62 (m, 1H, obscured)	COSY 32 → 31 HMBC 32 → 33
33	171.4	-	
34	56.4	4.55 (dd, $J = 10.7, 4.2\text{Hz}$, 1H)	COSY 34 → 35 HMBC 34 → 33, 41
35	37.4	2.62 (dd, $J = 14.2, 10.7\text{ Hz}$, 1H), 2.98 - 3.02 (m, 1H, obscured)	HMBC 35 → 36,41
36	130.7	-	
37	130.9	7.07 (d, $J = 8.4\text{Hz}$, 2H)	HMBC 37 → 39
38	114.8	6.78 (d, $J = 8.4\text{Hz}$, 2H)	COSY 38 → 37 HMBC 38 → 36
39	159.8	-	
40	53.8	3.70 (s, 3H)	HMBC 40 → 39
41	171.4	-	
42	50.9	5.20 (dd, $J = 9.4, 5.4\text{ Hz}$, 1H)	COSY 42 → 43 HMBC 42 → 41, 48
43	37.8	3.44 (dd, $J = 14.0, 5.4\text{ Hz}$, 1H), 3.26 (dd, $J = 14.0, 9.4\text{Hz}$, 1H)	HMBC 43 → 44
44	128.9	-	
45	131.0	7.08 (d, $J = 8.4\text{ Hz}$, 2H)	HMBC 45 → 47
46	116.0	6.73 (d, $J = 8.4\text{ Hz}$, 2H)	COSY 46 → 45 HMBC 46 → 44
47	157.3	-	
48	162.0	-	
49	119.6	7.26 (s, 1H, obscured)	
50	149.4	-	
51	105.4	-	
52	126.3	7.74 (s, 1H)	HMBC 52 → 3, 50, 51
53	125.3	-	
54	120.5	7.78 (ddd, $J = 8.0, 0.9, 0.7\text{Hz}$, 1H)	COSY 54 → 55 TOCSY 54 → 55, 56, 57, 58 HMBC 54 → 51
55	121.5	7.22 (ddd, $J = 8.0, 7.1, 0.7\text{Hz}$, 1H)	
56	123.5	7.25 - 7.30 (m, 1H, obscured)	
57	110.8	7.56 (ddd, $J = 8.3, 7.1, 0.9\text{ Hz}$, 1H)	
58	138.0	-	

Macrocyclic acidolysis product 61F. Initial fraction *F* was re-purified by semi-preparative HPLC.

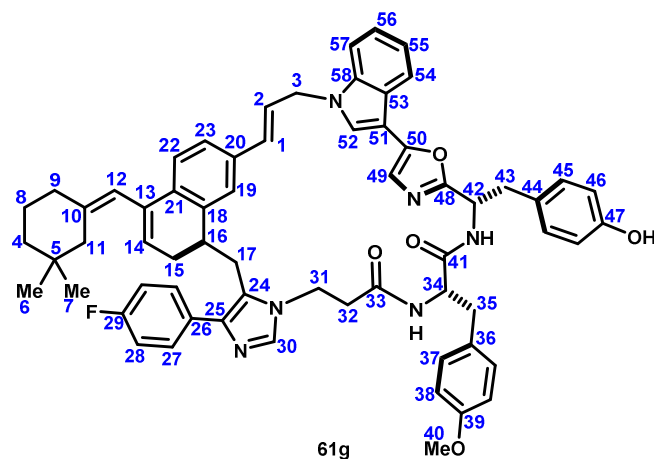


~3:1 mixture $\Delta_{9,10} : \Delta_{10,11}$, data is of major
(600 MHz, CD₃OD, 295K)

	¹³ C	¹ H	key correlation
1	133.0	6.66 (d, <i>J</i> = 16.1Hz, 1H)	TOCSY 1 → 2,3 HMBC 1 → 19, 23
2	127.2	6.38 (ddd, <i>J</i> = 16.1, 5.4, 5.4 Hz, 1H)	
3	68.7	4.83 (dd, <i>J</i> = 9.1, 5.4 Hz, 1H)	HMBC 3 → 47
4	35.1	1.29 - 1.34 (m, 2H) overlap	HMBC 4 → 11, 7, 6
5	29.4	-	
6	28.1	0.89 (s, 3H)	HMBC 6 → 11, 4
7	28.1	0.90 (s, 1H)	HMBC 7 → 11, 4
8	24.1	2.07 - 2.12 (m, 2H)	COSY 8 → 4
9	132.4	5.76 - 5.78 (m, 1H)	HMBC 9 → 8, 11
10	121.0	-	
11	44.0	1.71 - 1.73 (m, 1H)	HMBC 11 → 6, 7
12	84.1	-	
13	86.2	-	
14	17.5	1.97 - 2.04 (m, 1H) overlap, 2.17 - 2.25 (m, 1H) overlap	COSY 14 → 15
15	34.5	1.80 - 1.89 (m, 1H) 1.93 - 1.99 (m, 1H) overlap	HMBC 15 → 18
16	45.3	2.87 - 2.93 (m, 1H)	TOCSY 16 → 14, 15 17, HMBC 16 → 24
17	30.7	2.94 - 3.01 (m, 1H) overlap, 3.24 (dd, <i>J</i> = 15.6, 3.9 Hz, 1H)	HMBC 17 → 18
18	143.2	-	
19	125.8	7.12 (s, 1H)	HMBC 19 → 21, 23, 16, 1
20	138.6	-	
21	128.2	6.75 (d, <i>J</i> = 7.4 Hz, 1H)	TOCSY 21 → 22, 23, 19 HMBC 21 → 19, 23
22	130.1	7.16 → 7.19 (m, 1H) overlap	
23	126.9	7.26 - 7.30 (m, 1H) overlap	

24	130.7	-	
25	not detected	-	
26	124.9	-	
27	131.4	7.61 - 7.66 (m, 1H) overlap	
28	117.6	7.30 - 7.36 (m, 2H) overlap	HMBC 28 → 26
29	164.8 (d, $J_{CF} \approx 245\text{Hz}$)	-	
30	134.9	8.02 (s, 1H)	
31	43.1	3.65 - 3.71 (m, 2H)	COSY 31 → 32
32	36.3	2.17 - 2.24 (m, 1H) overlap, 2.40 - 2.47 (m, 1H)	
33	170.7	-	
34	56.0	4.49 - 4.55 (m, 1H)	
35	37.8	2.72 (dd, $J = 13.8, 8.5\text{Hz}$, 1H), 2.97 (dd, $J = 13.8, 6.9\text{Hz}$, 1H)	HMBC 35 → 36
36	129.7	-	
37	130.8	6.92 (d, $J = 8.8\text{Hz}$, 2H)	HMBC 37 → 39
38	114.6	6.60 (d, $J = 8.8\text{Hz}$, 2H)	HMBC 38 → 36, 39
39	159.8	-	
40	55.2	3.43 (s, 3H)	HMBC 40 → 39
41	173.3	-	
42	49.7	5.43 - 5.49 (m, 1H)	COSY 42 → 43
43	38.5	3.13 (dd, $J = 14.0, 11.7\text{Hz}$, 1H), 3.27 - 3.33 (m, 1H) overlap	HMBC 43 → 44
44	130.6	-	
45	131.1	7.28 (d, $J = 8.5\text{Hz}$, 2H)	HMBC 45 → 47
46	115.8	6.93 (d, $J = 8.5\text{Hz}$, 2H)	HMBC 46 → 44
47	158.7	-	
48	not detected	-	
49	119.7	7.24 - 7.27 (m, 1H) overlap	
50	150.4	-	
51	105.0	-	
52	124.1	7.63 (s, 1H)	
53	125.2	-	
54	120.4	7.85 (d, $J = 8.0\text{Hz}$, 1H)	COSY 54 → 55, TOCSY 54 → 55, 56, 57, HMBC 54 → 58
55	121.4		HMBC 55 → 53
56	123.5		HMBC 56 → 58
57	112.6	7.45 (d, $J = 7.4\text{Hz}$, 1H)	HMBC 57 → 53
58	138.04	-	

Macrocyclic acidolysis product 61G. Initial fraction G was re-purified by semi-preparative HPLC.



	¹³ C	¹ H	key correlations
1	134.5	6.54 (d, <i>J</i> = 15.7Hz, 1H)	HMBC 1 → 2, 3, 19
2	126.8	6.43 (ddd, <i>J</i> = 15.7, 6.4, 6.3 Hz, 1H)	COSY 2 → 3, HMBC 2 → 3, 20
3	48.1	4.87 - 4.92 (m, 1H, obscured), 5.00 (dd, <i>J</i> = 15.4, 6.3 Hz, 1H)	HMBC 3 → 1, 2, 52, 58
4	40.7	1.40 (apt t, <i>J</i> = 5.9 Hz, 2H)	COSY 4 → 8, HMBC 4 → 5, 6, 7
5	33.2	-	
6	28.5	0.799 (s, 3H)	
7	29.6	0.803 (s, 3H)	
8	24.8	1.62 - 1.68 (m, 2H)	COSY 8 → 9
9	37.4	2.18 - 2.24 (m, 2H)	TOCSY 9 → 4, 8, 12, HMBC 9 → 12
10	143.1	-	
11	43.6	1.91 (d, <i>J</i> = 13.3 Hz, 1H), 1.99 (d, <i>J</i> = 13.3 Hz, 1H)	HMBC 11→4,5,6,9,10,12 TOCSY 11→12
12	122.3	5.81 (br s, 1H)	
13	134.4	-	
14	124.9	5.26-5.28 (m, 1H)	
15	28.2	2.08 (dd, <i>J</i> = 17.0, 6.4 Hz, 1H), 2.37-2.44 (m, 1H)	
16	38.9	2.81 (apt q, <i>J</i> = 7.4 Hz, 1H)	HMBC 16→18
17	28.3	2.91 (dd, <i>J</i> = 15.0, 7.6 Hz, 1H), 2.97 (dd, <i>J</i> = 15.0, 8.3 Hz, 1H)	HMBC 17→18,25
18	139.0	-	
19	126.3	7.85 (br s, 1H)	COSY 19→23 HMBC 19→16,21,23
20	136.3	-	
21	135.1	-	
22	125.7	7.06 (d, <i>J</i> = 7.9 Hz, 1H)	HMBC 22→18,20
23	126.6	7.16 (dd, <i>J</i> = 7.9, 1.7 Hz, 1H)	COSY 23→24 HMBC 23→21

24	not detected	-	
25	127.0	-	
26	132.2	-	
27	not detected	7.33-7.38 (m, 2H)	HMBC 27→25
28	115.7	7.00-7.04 (m, 2H) obscured	HMBC 28→26,29
29	163.0 (d, J_{CF} = 245 Hz)	-	
30	not detected	8.54 (s, 1H)	
31	41.4	3.82-3.87 (m, 2H)	COSY 31→32
32	38.3	2.48 (ddd, J = 15.0, 6.2, 6.2 Hz, 1H), 2.54 (ddd, J = 15.0, 7.1, 5.9 Hz, 1H)	
33	172.6	-	
34	56.5	4.48 (dd, J = 10.1, 4.8 Hz, 1H)	COSY 34→35
35	36.9	2.60 (dd, J = 14.4, 10.1 Hz, 1H), 2.99 (dd, J = 14.4, 4.8 Hz, 1H)	
36	130.0	-	
37	130.5	6.98 (d, J = 8.7 Hz, 2H)	COSY 37→38 HMBC 37→39
38	114.7	6.70 (d, J = 8.7 Hz, 2H)	HMBC 38→36
39	159.6	-	
40	55.3	3.60 (s, 3H)	HMBC 40→39
41	173.3	-	
42	50.7	5.23 (dd, J = 9.2, 6.1 Hz, 1H)	COSY 42→43 HMBC 42→48
43	37.8	3.25 (dd, J = 14.1, 9.2 Hz, 1H), 3.40 (dd, J = 14.1, 6.1 Hz, 1H)	
44	128.7	-	
45	131.0	7.02 (d, J = 8.5 Hz, 2H)	COSY 45→46 HMBC 45→47
46	116.0	6.69 (d, J = 8.5 Hz, 2H)	HMBC 46→44
47	157.1	-	
48	161.5	-	
49	119.4	7.28 (s, 1H)	HMBC 49→48,50
50	149.7	-	
51	105.2	-	
52	126.2	7.85 (s, 1H)	HMBC 52→50,53,58
53	125.4	-	
54	120.3	7.66 (d, J = 7.9 Hz, 1H)	COSY 54→55 TOCSY 54→55,56,57 HMBC 54→58
55	121.5	7.21 (apt t, J = 7.4 Hz, 1H)	HMBC 55→53
56	123.4	7.29 (ddd, J = 8.1, 7.4, 0.8 Hz, 1H) obscured	HMBC 56→58
57	110.8	7.55 (d, J = 8.1 Hz, 1H)	HMBC 57→53
58	138.0	-	

References

- (1) Sisko, J.; Mellinger, M.; Sheldrake, P. W.; Baine, N. H. *Tetrahedron Lett.* **1996**, *37*, 8113.
- (2) Sisko, J.; Mellinger, M.; Sheldrake, P. W.; Baine, N. H. *Org. Synth.* **2000**, *77*, 198.
- (3) Zhao, H.; Negash, L.; Wei, Q.; LaCour, T. G.; Estill, S. J.; Capota, E.; Pieper, A. A.; Harran, P. G. *J. Am. Chem. Soc.* **2008**, *130*, 13864.
- (4) Wei, Q.; Harran, S.; Harran, P. G. *Tetrahedron* **2003**, *59*, 8947.
- (5) Dourtoglou, V.; Gross, B.; Lambropoulou, V.; Zioudrou, C. *Synthesis (Stuttg.)*. **1984**, *1984*, 572.
- (6) Boger, D. L.; Yohannes, D. *J. Org. Chem.* **1987**, *52*, 5283.
- (7) Bergel, F.; Stock, J. A. *J. Chem. Soc.* **1954**, 2409.
- (8) Waser, E. *Helv. Chim. Acta* **1913**, *4*, 657.
- (9) Johnson, T. B.; Kohmann, E. F. *J. Am. Chem. Soc.* **1915**, *37*, 1863.
- (10) Qiu, X. L.; Qing, F. L. *J. Org. Chem.* **2002**, *67*, 7162.
- (11) Thottathil, J. K.; Moniot, J. *Tetrahedron Lett.* **1986**, *27*, 151.
- (12) Krapcho, J.; Turk, C.; Cushman, D. W.; Powell, J. R.; DeForrest, J. M.; Spitzmiller, E. R.; Karanewsky, D. S.; Duggan, M.; Rovnyak, G.; Schwartz, J.; Natarajan, S.; Gofrey, J. D.; Ryono, D. E.; Neubeck, R.; Atwal, K. S.; Petrillo, E. W. *J. Med. Chem. Chem.* **1988**, *31*, 1148.
- (13) Hogan, I. T.; Sainsbury, M. *Tetrahedron* **1984**, *40*, 681.
- (14) Schroder, R.; Schollkopf, U.; Hoppe, E. B. I.; Chem, L. A.; Schroder, R.; Schollkopf, U.; Blume, E. *Justus Liebigs Ann. Chem.* **1975**, 533.
- (15) Ohba, M.; Kubo, H.; Fuji, T.; Ishibashi, H.; Sargent, M. V.; Arbain, D. *Tetrahedron* **1997**, *38*, 6697.
- (16) Schuster, R. E.; Scott, J. E.; Casanova, J. J. *Org. Synth.* **1966**, *46*, 75.

Chapter 3 Experimental Appendix

General remarks

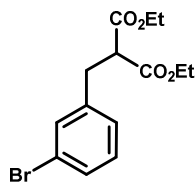
Reactions were performed in air unless otherwise noted. Dichloromethane was dried by passing through an activated alumina solvent drying system. Anhydrous *N,N*-dimethylformamide (EMD DriSolv®) was used without further purification. Nitromethane was dried over 4 Å molecular sieves for at least 24 h before use. Methanesulfonic acid (≥99.5%, Sigma Aldrich) was used without further purification. Column chromatography was performed on silica gel 60 (SiliCycle, 240–400 mesh). Thin layer chromatography (TLC) utilized pre-coated plates (Sorbent Technologies, silica gel 60 PF254, 0.25 mm) visualized with UV 245 nm, iodine, or basic potassium permanganate stain.

Purification of acidolysis products employed an Agilent 1100/1200 HPLC system equipped with G1361A preparative pumps, a G1314A autosampler, a G1314A VWD, and a G1364B automated fraction collector. Analytical HPLC was performed using the same system, but with a G1312A binary pump. Mass spectra were recorded using an Agilent 6130 LC/MS system equipped with an ESI source. High-resolution mass spectra were recorded on a Waters LCT Premier equipped with an Acquity HPLC and autosampler.

NMR methods:

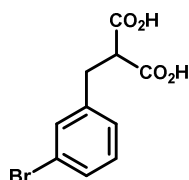
NMR spectra were recorded on Bruker Avance (500 or 600 MHz) spectrometers. Data for ¹H NMR spectra are reported as follows: chemical shift (δ parts per million) (multiplicity, coupling constant (Hertz), integration), and are referenced to a residual protonated solvent peak.¹ ¹³C resonances are reported in terms of chemical shift (δ ppm) as referenced to DMSO-*d*₆. For mass-limited samples, solvent magnetic susceptibility matched Shigemi tubes were used with a sample volume of ~300 μ L. Optimization of on-axis shims was accomplished using the TopShim automated tool within Bruker Topspin™ 2.1. Optimization of off-axis shims was performed manually.² ¹H 90° transmitter pulse lengths were calibrated by back calculation from the 360° or 180° null.^{3,4} The pulse width or power level for soft pulses and shaped pulses were calculated using the Shape Tool within TopSpin™ 2.1. ¹H–¹H COSY spectra were recorded using a phase sensitive, gradient enhanced double-quantum-filtered experiment, using States-TPPI acquisition.^{5–7} TOCSY spectra were recorded using a sensitivity improved, phase sensitive experiment using a 60 ms DIPSI-2 pulse train for homonuclear Hartman–Hahn transfer.⁸ NOESY spectra were recorded using a phase sensitive experiment with selection gradients during the mixing time.⁹ ROESY spectra were recorded using a phase sensitive experiment with selection gradients and water suppression with excitation sculpting.^{10,11} Carbon chemical shifts were measured from 2D plots of either HSQC spectra for protonated carbons or HMBC spectra for non-protonated carbons. ¹H–¹³C HSQC spectra were recorded using a sensitivity improved phase sensitive experiment using an adiabatic shape pulse for ¹³C inversion, and ¹³C decoupling during acquisition.^{12–14} Experimental parameters were optimized for ¹J_{CH}=145 Hz. ¹H–¹³C HMBC spectra were recorded using a gradient selected experiment with a two-fold J-filter optimized for ¹J_{CH}=125–165 Hz. Experimental parameters were optimized for long-range ⁿJ_{CH}=8 Hz.

Diethyl 2-(3-bromobenzyl)malonate (7). To absolute EtOH (200 mL) was added sodium (13.8 g, 600 mmol) in portions. The resulting solution was cooled to rt in a water bath and fitted with a mechanical stirrer, and diethyl malonate (96 g, 600 mmol) was added, which caused a heavy precipitate to form. A solution of 3-bromobenzyl bromide (50 g, 200 mmol) in THF was then added dropwise over 30 min, which caused a mild exotherm. The mechanical stirrer was exchanged for a stir bar, and the mixture was heated under reflux for 90 min. The mixture was cooled, concentrated, quenched with sat. NH₄Cl and extracted with Et₂O (x3). The combined organic phase was washed with brine, dried over Na₂SO₄, concentrated and distilled *in vacuo* to recover diethyl malonate (63 g, 98%, b.p. 64–65 °C, 5 torr) followed by **7** (43.2 g, 66%, b.p. 165–170°C, 5 torr) as a colorless oil. ¹H NMR (CDCl₃, 400 MHz): δ 1.21 (t, *J* = 7.1 Hz, 6H), 3.17 (d, *J* = 7.8 Hz, 2H), 3.60 (t, *J* = 7.8 Hz, 1H), 4.16 (qd, *J* = 7.1, 1.4 Hz, 4H),

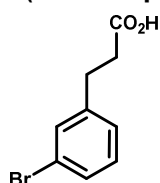


7.11-7.16 (m, 2H), 7.32-7.38 (m, 2H). ^{13}C NMR (CDCl_3 , 100 MHz): δ 140.4, 132.1, 130.2, 130.0, 127.7, 122.6, 61.7, 53.7, 34.3, 14.1.

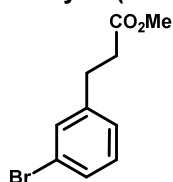
2-(3-Bromobenzyl)malonic acid (S1).¹⁵ NaOH (21 g, 524 mmol) was dissolved in H_2O (45 mL) and diester **7** (43.2 g, 131 mmol) was added slowly to the still hot solution (*Caution! exotherm*), which caused a heavy white precipitate to form. The mixture was heated to reflux for 4 hr, then chilled in an ice bath. Et_2O was added, and the mixture was carefully acidified to $\text{pH} < 2$ with conc. HCl such that the temperature did not rise. The organic phase was collected, and the aqueous extracted with Et_2O (x3). The combined organic extract was washed with brine, dried over Na_2SO_4 and concentrated to give malonic acid **S1** (37.8 g, >100%), which was used without purification. ^1H NMR (CDCl_3 , 400 MHz, major rotamer): δ 3.02 (d, $J = 7.9$ Hz, 2H), 3.62 (t, $J = 7.9$ Hz, 1H), 7.21-7.26 (m, 2H), 7.37-7.41 (m, 1H), 7.44-7.46 (m, 1H), 12.79 (br s, 1H). ^{13}C NMR (CDCl_3 , 100 MHz): δ 170.1, 141.4, 131.6, 130.4, 129.3, 128.0, 121.6, 53.1, 33.7.



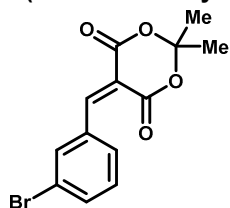
3-(3-Bromophenyl)propionic acid (S2). Malonic acid **S1** (37.8 g crude, ~131 mmol) under vacuum (40 torr) was placed in a pre-heated oil bath at 160 $^\circ\text{C}$. The reaction was heated until gas evolution ceased (~45 min), and cooled to give **S2** (29.1g, 97% two steps) as a solid. ^1H NMR ($\text{DMSO}-d_6$, 500 MHz, major rotamer): δ 2.68 (d, $J = 7.7$ Hz, 2H), 2.93 (t, $J = 7.7$ Hz, 2H), 7.11-7.20 (m, 2H), 7.32-7.40 (m, 2H), 11.70 (br s, 1H). ^{13}C NMR (CDCl_3 , 100 MHz): δ 179.2, 142.5, 131.5, 130.2, 129.7, 127.1, 122.7, 35.4, 30.2. MS (ESI) Calculated for $\text{C}_9\text{H}_8\text{BrO}_2$ [M-H] $^-$: 227.0, found 227.0/229.0.



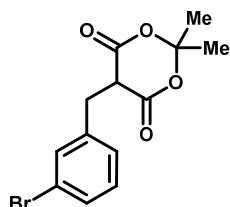
Methyl 3-(3-bromophenyl)propionate (10). By Fisher esterification of **S2**: Carboxylic acid **S2** (29.1 g, 128 mmol) was dissolved in MeOH (300 mL) and cooled in an ice bath. SOCl_2 (11.2 mL, 154 mmol) was added dropwise, and the mixture was allowed to warm to rt and stirred overnight. The mixture was concentrated and distilled in vacuo (b.p. 110-115 $^\circ\text{C}$, 3.9 torr) to give **10** (30.13 g, 97%) as a colorless oil. By decarboxylation of **S3**: Mono-methyl ester **S3** (2.9 g crude, ~9.6 mmol) was placed in an oil bath pre-heated to 160 $^\circ\text{C}$ under an atmosphere of argon until gas evolution ceased (45 min). Distillation in vacuo (b.p. 138-140 $^\circ\text{C}$, 6 torr) afforded **10** (1.2 g, 52%) as a colorless oil. ^1H NMR (CDCl_3 , 500 MHz): δ 7.29-7.35 (m, 2H), 7.08-7.15 (m, 2H), 3.67 (s, 3H), 2.90 (t, $J = 7.7$ Hz, 2H), 2.62 (t, $J = 7.7$ Hz, 2H). ^{13}C NMR (CDCl_3 , 125 MHz): δ 172.9, 142.9, 131.4, 130.1, 129.4, 127.0, 122.5, 51.7, 35.3, 30.5. MS (ESI) Calculated for $\text{C}_{11}\text{H}_{11}\text{BrO}_2$ [M+H] $^+$: 243.0, found 242.6.



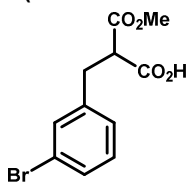
5-(3-bromobenzylidene)-2,2-dimethyl-1,3-dioxane-4,6-dione (8). Benzylidene Meldrum's acid **8** was characterized as an intermediate in the synthesis of reduced congener **9**. ^1H NMR (C_6D_6 , 500 MHz): δ 1.16 (s, 1H), 6.63 (dd, $J = 8.1, 7.8$ Hz, 1H), 7.13 (br d, $J = 8.1$ Hz, 1H), 7.57 (br d, $J = 7.8$ Hz, 1H), 7.83 (br s, 1H), 8.03 (s, 1H).



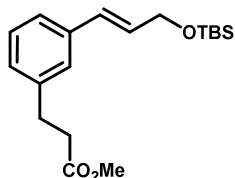
5-(3-Bromobenzyl)-2,2-dimethyl-1,3-dioxane-4,6-dione (9). 3-Bromobenzaldehyde (1.85 g, 10 mmol) and Meldrum's acid (1.44 g, 10 mmol) were dissolved in benzene (20 mL) and treated with piperidine (79 μL , 0.8 mmol) and AcOH (173 μL , 3 mmol). The resulting mixture was heated to reflux using a Dean-Stark apparatus for 30 min, then cooled in an ice bath. EtOH (10 mL) was added, followed by NaBH_4 (756 mg, 20 mmol) in several portions (*Caution!* gas evolution). The mixture was stirred for 1 hr, then diluted with EtOAc and washed with 1N HCl, brine dried over Na_2SO_4 and concentrated to give **9** (3.00 g, 96%) as a white solid. ^1H NMR (CDCl_3 , 500 MHz): δ 1.61 (s, 3H), 1.76 (s, 3H), 3.42-3.45 (m, 2H), 3.75 (t, $J = 4.0$ Hz, 1H), 7.16 (dd, $J = 7.8, 8.0$ Hz, 1H), 7.27 (br d, $J = 8.0$ Hz, 1H), 7.37 (br d, $J = 7.8$ Hz, 1H), 7.49 (br s, 1H). ^{13}C NMR (CDCl_3 , 125 MHz): δ 165.0, 139.7, 132.8, 130.4, 130.2, 128.6, 122.6, 105.4, 48.1, 31.5, 28.6, 27.1.



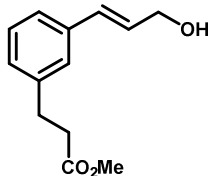
2-(3-Bromobenzyl)malonic acid mono-methyl ester (S3).¹⁶ Benzylated Meldrum's acid **9** (3.00 g, 9.6 mmol) was dissolved in MeOH (75 mL) and heated to 80 °C in a sealed bottle overnight (*Caution! Heating above this temperature may induce decarboxylation, and should be avoided to prevent over-pressuring the reaction vessel. Crude NMR indicated no decarboxylation had taken place after overnight reaction at 80°C*). The mixture was cooled, then transferred to a round bottom flask and concentrated to give mono ester **S3** (2.9 g, > 100%) as an oil, which was used without purification. ¹H NMR (CDCl₃, 400 MHz): δ 3.17 (dd, *J* = 14.2, 7.6 Hz, 1H), 3.22 (dd, *J* = 14.2, 7.8 Hz, 1H), 3.69 (dd, *J* = 7.6, 7.8 Hz, 1H), 3.72 (s, 3H), 7.12-7.18 (m, 2H), 7.33-7.38 (m, 2H), 9.83 (br s, 1H).



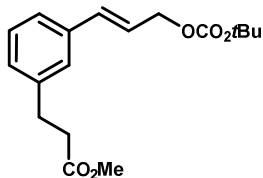
Methyl (E)-3-(3-(3-((tert-butyldimethylsilyloxy)prop-1-en-1-yl)phenyl)propanoate (12). A three-neck flask fitted with a reflux condenser was charged with aryl bromide **10** (21.8 g, 89.7 mmol), vinyl boronate **11** (**1-50**) (32.1 g, 108 mmol) and K₂CO₃. THF:H₂O (5:1, 180 mL) was added, and the mixture was vigorously sparged with argon for 30 min, then heated to 75 °C for 4 days after which HPLC-UV (220 nm) analysis showed > 95% conversion. The mixture was cooled, and the aqueous phase was collected and extracted with EtOAc (x2). The combined organic phase was washed with H₂O (x1), brine, dried over Na₂SO₄, reconstituted in 9:1 hexanes:EtOAc, and filtered through a pad of SiO₂, rising with the same. The filtrate was concentrated to give **12** (37 g, > 100%) as an orange oil, contaminated by boronate **11**, which was used without purification. ¹H NMR (CDCl₃, 500 MHz): δ 7.19-7.25 (m, 3H), 7.04-7.08 (m, 1H), 6.56 (dt, *J* = 15.9, 1.7 Hz, 1H), 6.27 (dt, *J* = 15.9, 5.0 Hz, 1H), 4.34 (dd, *J* = 5.0, 1.7 Hz, 2H), 3.67 (s, 3H), 2.94 (t, *J* = 7.9 Hz, 2H), 2.63 (t, *J* = 7.9 Hz, 2H), 0.94 (s, 9H), 0.11 (s, 6H). ¹³C NMR (CDCl₃, 125 MHz): δ 173.4, 140.7, 137.3, 129.32, 129.27, 128.7, 127.3, 126.4, 124.4, 63.9, 51.7, 35.7, 30.9, 26.0, 18.5, -5.1. MS (ESI) Calculated for C₁₉H₃₀O₃Si [M+Na]⁺: 357.2, found 357.4.



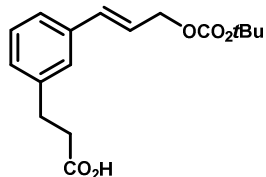
Methyl (E)-3-(3-(3-hydroxyprop-1-en-1-yl)phenyl)propanoate (13). Silyl ether **12** (37 g crude, ~ 89.7 mmol) was dissolved in THF (60 mL), and Bu₄NF (1M in THF, 127 mL) was added over 5 min via a dropping funnel. The mixture was stirred for 30 min, then diluted with EtOAc (*Note: The use of Et₂O is favorable to EtOAc in this partition, as it leads to more effective exclusion of tetrabutylammonium salts*) and washed with sat. NH₄Cl, brine, dried over Na₂SO₄ and concentrated to give a red oil. This material was reconstituted in 1:1 hexanes:EtOAc and passed through a pad of SiO₂ rinsing with the same. The filtrate was concentrated and purified by chromatography on SiO₂ eluted with 30→50% EtOAc in hexanes to give **13** (15.5 g, 79%) in moderate purity as a yellow oil. ¹H NMR (CDCl₃, 400 MHz): δ 7.16-7.25 (m, 3H), 7.02-7.1 (m, 1H), 6.57 (dt, *J* = 16.0, 1.3 Hz, 1H), 6.33 (dt, 16.0, 5.7 Hz, 1H), 4.29 (dd, *J* = 3.7, 3.7 Hz, 2H), 3.65 (s, 3H), 2.92 (t, *J* = 7.9 Hz, 2H), 2.61 (t, *J* = 7.9 Hz, 2H), 2.29 (br. s, 1H). ¹³C NMR (CDCl₃, 100 MHz): δ 173.4, 140.8, 137.0, 130.8, 128.8, 127.6, 126.5, 124.4, 63.5, 51.7, 35.6, 30.8. MS (ESI) Calculated for C₁₃H₁₆O₃ [M+Na]⁺: 243.1, found 243.0.



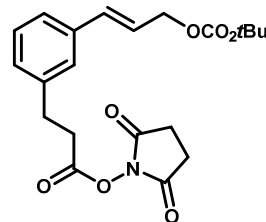
Methyl (E)-3-(3-(3-((tert-butoxycarbonyloxy)prop-1-en-1-yl)phenyl)propanoate (14).¹⁷ Cinnamyl alcohol **13** (15.5 g, ~70.4 mmol) was dissolved in DCM (140 mL) and treated with NaOH (70 mL, 15 wt%), tetrabutylammonium hydrogen sulfate (717 mg, 2.1 mmol) and di-*tert*-butyl dicarbonate (23.0 g, 106 mmol). The mixture was stirred at rt overnight. The solvent was exchanged for EtOAc, and the aqueous phase was extracted with EtOAc (x1). The combined extract was washed with H₂O (x2), brine and concentrated, re-dissolved in EtOH, and treated with a large excess of imidazole. When gas evolution ceased, the solvent was exchanged for DCM, and the mixture was filtered through a pad of SiO₂, rinsing with the same. Intermediate **14** (22.6 g, ~100%) was obtained as a heavy oil, contaminated by residual Boc-imidazole, which was used without further purification. ¹H NMR (CDCl₃, 500 MHz): δ 7.20-7.25 (m, 3H), 7.06-7.12 (m, 1H), 6.63 (br. d, *J* = 15.9 Hz, 1H), 6.27 (dt, *J* = 15.9, 6.4 Hz, 1H), 4.70 (dd, *J* = 6.4, 1.2 Hz, 2H), 3.66 (s, 3H), 2.93 (t, *J* = 7.9 Hz, 2H), 2.62 (t, *J* = 7.9 Hz, 2H), 1.49 (s, 9H). ¹³C NMR (CDCl₃, 125 MHz): δ 173.3, 153.4, 140.9, 136.4, 134.3, 128.8, 128.1, 126.7, 124.7, 123.0, 82.2, 67.5, 51.7, 35.6, 30.8, 27.8. MS (ESI) Calculated for C₁₈H₂₄O₅ [M+Na]⁺: 343.2, found 343.2.



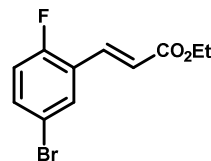
(E)-3-(3-(3-((tert-Butoxycarbonyl)oxy)prop-1-en-1-yl)phenyl)propionic acid (15). Methyl ester **14** (22.5 g, ~70.4 mmol) was dissolved in THF (230 mL) and H₂O (75 mL), and treated with LiOH·H₂O (5.91 g, 141 mmol). The mixture was stirred at rt overnight, concentrated to remove the THF, and partitioned between 1N HCl and EtOAc. The aqueous phase was extracted with EtOAc (x1), and the combined extract was washed with H₂O (x1), brine, dried over Na₂SO₄ and concentrated to give **15** (17.5 g, 81%) as a heavy oil, which was used without purification. ¹H NMR (CDCl₃, 500 MHz): δ 7.21-7.27 (m, 3H), 7.08-7.13 (m, 1H), 6.64 (d, *J* = 15.9 Hz, 1H), 6.29 (dt, *J* = 15.8, 6.4 Hz, 1H), 4.71 (br. d, *J* = 6.3 Hz, 2H), 2.95 (t, *J* = 7.9 Hz, 2H), 2.7 (t, *J* = 7.8 Hz, 1H), 1.5 (s, 9H). ¹³C NMR (CDCl₃, 125 MHz): δ 178.0, 153.4, 140.5, 136.5, 134.3, 128.9, 128.1, 126.7, 124.8, 123.1, 82.3, 67.4, 35.3, 30.5, 27.8. MS (ESI) Calculated for C₁₇H₂₂O₅ [M-H]⁻: 305.1, found 305.2.



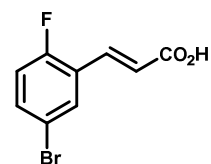
(E)-3-(3-(3-((tert-Butoxycarbonyl)oxy)prop-1-en-1-yl)phenyl)propionic acid N-hydroxysuccinimidyl ester (3). Carboxylic acid **3** (17.5 g crude, ~57 mmol) was dissolved in DCM (115 mL), cooled in an ice bath, and treated with *N*-hydroxysuccinimide (7.89 g, 69 mmol) and EDCI·HCl (12.1 g, 63 mmol). The mixture was allowed to warm to rt and stirred for 3.5 hr. Additional *N*-hydroxysuccinimide (2.6 g, 23 mmol) and EDCI·HCl (4.4 g, 23 mmol) were added, and the mixture was stirred overnight. The solvent was exchanged for EtOAc, and washed with H₂O (x3), brine, dried over Na₂SO₄ and concentrated. Chromatography on SiO₂ eluted with 35→50% EtOAc in hexanes (*Note: CHCl₃ was added to solubilize material for loading*) afforded **3** (18.5 g, 81%) as a white solid. Analytically pure crystals may be obtained by slow evaporation from THF/hexanes (2:1). ¹H NMR (CDCl₃, 500 MHz): δ 7.24-7.28 (m, 3H), 7.11-7.15 (m, 1H), 6.65 (br. d, *J* = 15.9 Hz, 1H), 6.3 (dt, *J* = 15.9, 6.4 Hz, 1H), 4.72 (dd, *J* = 6.4, 1.3 Hz, 2H), 3.05 (t, *J* = 7.8 Hz, 2H), 2.92 (t, *J* = 7.8 Hz, 2H), 2.84 (br. s, 4H), 1.5 (s, 9H). ¹³C NMR (CDCl₃, 125 MHz): δ 169.0, 167.8, 153.4, 139.4, 136.7, 134.1, 129.0, 128.0, 126.7, 125.1, 123.3, 82.2, 67.4, 32.6, 30.4, 27.8, 25.6. IR (ATR) ν = 2947, 1820, 1781, 1732, 1370, 1269, 1252, 1211, 1160, 1068, 972, 930, 793 cm⁻¹. MS (ESI) Calculated for C₂₁H₂₅NO₇ [M+Na]⁺: 426.2, found 426.2.



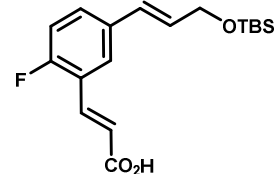
Methyl 5-bromo-2-fluorocinnamate (S4). To a stirred suspension of freshly dried LiCl (1.94 g, 50 mmol) in THF (250 mL) was added DBU (7.1 mL, 50 mmol), triethyl phosphonoacetate (11.9 mL, 60 mmol) and 5-bromo-2-fluorobenzaldehyde (10.6 g, 50 mmol). The reaction was stirred for at rt until complete by HPLC-UV (220 nm), filtered, and the solvent exchanged to EtOAc. The organic phase was washed with H₂O, 1M NaOH, 1N HCl, brine, dried over MgSO₄ and concentrated to give **S4** (11.47 g, 88%). ¹H NMR (CDCl₃, 400 MHz): δ 1.34 (t, *J* = 7.1 Hz, 3H), 4.28 (q, *J* = 7.1 Hz, 2H), 6.52 (d, *J* = 16.2 Hz, 1H), 7.00 (dd, *J*_{HF} = 10.0 Hz, *J*_{HH} = 8.8 Hz, 1H), 7.45 (ddd, *J*_{HH} = 8.8, 2.5 Hz, *J*_{HF} = 4.5 Hz, 1H), 7.66 (dd, *J*_{HF} = 6.4 Hz, *J*_{HH} = 2.5 Hz, 1H), 7.71 (d, *J* = 16.2 Hz, 1H). MS (ESI) Calculated for C₁₁H₁₁BrFO₂ [M+H]⁺: 273.0, found 272.9/274.8.



5-Bromo-2-fluorocinnamic acid (24). Ethyl ester **S4** (9.83 g, 36 mmol) was dissolved in THF:MeOH:H₂O (3:1:1, 145 mL) and treated with LiOH (871 mg, 36.4 mmol). The mixture was stirred at rt overnight, then concentrated to remove the organic solvent. EtOAc was added, and the mixture was acidified with 3N HCl with external cooling. ¹H NMR (CDCl₃, 400 MHz): δ 6.54 (d, *J* = 16.5 Hz, 1H), 7.02 (dd, *J*_{HF} = 9.9 Hz, *J*_{HH} = 8.8 Hz, 1H), 7.49 (ddd, *J*_{HH} = 8.8, 2.4 Hz, *J*_{HF} = 4.5 Hz, 1H), 7.68 (dd, *J*_{HF} = 6.4 Hz, *J*_{HH} = 2.4 Hz, 1H), 7.82 (d, *J* = 16.2 Hz, 1H). MS (ESI) Calculated for C₉H₇BrFO₂ [M+H]⁺: 245.0, found 244.8/246.8.



(E)-3-(5-((E)-3-((tert-Butyldimethylsilyl)oxy)prop-1-en-1-yl)-2-fluorophenyl)acrylic acid (25). (*Note: the use of the substrate free acid leads to extremely sluggish reaction, whereas in similar cases corresponding esters appeared less problematic*) A three-neck round bottom flask fitted with a condenser and two septa was charged with aryl bromide **24** (10.9 g, 44.3 mmol), vinyl boronate **11 (1-50)** (15.9 g, 53 mmol), and Na₂CO₃ (9.43 g, 89 mmol). THF:H₂O (3:1, 200 mL) was added, and the mixture was vigorously sparged with argon for 20 min. A septum was briefly removed to introduce Pd(PPh₃)₄ (500 mg, 0.44 mmol), and sparging was continued for 20 min. The mixture was heated



to 65 °C for 3 days, at which point Pd(OAc)₂ (0.2 g, 0.8 mmol) and PPh₃ (0.4 g, 1.7 mmol) were added, the mixture again sparged and reflux continued for an additional 7 days. The mixture was cooled, and diluted with 10% citric acid and extracted with EtOAc (x3). The combined extract was washed with brine, dried over MgSO₄ and concentrated to give **25** (14.9 g, ~100%) in moderate purity, contaminated by both starting materials as judged by ¹H NMR, which was used without purification. ¹H NMR (CDCl₃, 400 MHz): δ 0.95 (s, 6H), 1.24 (s, 9H), 4.35 (dd, *J* = 4.8, 1.7 Hz, 2H), 6.24 (dd, *J* = 15.8, 4.8 Hz, 1H), 6.56 (apt d, *J* = 16.1 Hz, 2H), 7.05 (dd, *J*_{HF} = 10.1 Hz, *J*_{HH} = 8.6 Hz, 1H), 7.38 (ddd, *J*_{HH} = 8.5, 2.3 Hz, *J*_{HF} = 5.1 Hz, 1H), 7.52 (dd, *J*_{HH} = 2.3 Hz, *J*_{HF} = 6.9 Hz, 1H), 7.88 (d, *J* = 16.1 Hz, 1H).

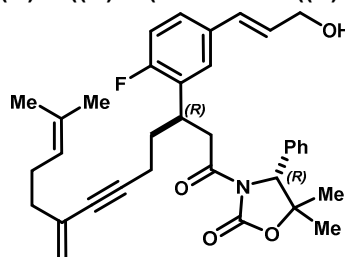
O-tert-Butyldimethylsilyl (S)-3-((E)-3-(2-fluoro-5-((E)-3-hydroxyprop-1-en-1-yl)phenyl)acryloyl)-5,5-dimethyl-4-phenyloxazolidin-2-one (27). Cinnamic acid **25** (14.9 g, 44.3 mmol) was dissolved in dry THF (200 mL), cooled to -20 °C and treated with Et₃N (15.4 mL, 111 mmol) and pivaloyl chloride (5.4 mL, 44.3 mmol). The mixture was stirred for 2 hrs, then D-phenylglycine-derived oxazolidinone **1.36** (8.47 g, 44.3 mmol) and dry LiCl (1.87 g, 44.3 mmol) were added. The mixture was stirred for 36 hr, then diluted with EtOAc and washed with sat. NaHCO₃ (x3), brine, dried over MgSO₄ and concentrated. Purification by column chromatography on SiO₂ eluted with 20% EtOAc in hexanes afforded **27** (a yield was not recorded). ¹H NMR (CDCl₃, 400 MHz): δ 0.12 (s, 6H), 0.95 (s, 9H), 1.04 (s, 3H), 1.65 (s, 3H), 4.35 (dd, *J* = 4.8, 1.7 Hz, 2H), 5.20 (s, 1H), 6.25 (dt, *J* = 15.8, 4.8 Hz, 1H), 6.57 (dt, *J* = 15.8, 1.7 Hz, 1H), 7.03 (dd, *J*_{HF} = 10.0 Hz, *J*_{HH} = 8.6 Hz, 1H), 7.18-7.22 (m, 2H), 7.32-7.41 (m, 4H), 7.60 (dd, *J*_{HF} = 6.9 Hz, *J*_{HH} = 2.1 Hz, 1H), 7.91 (d, *J* = 15.9 Hz, 1H), 8.07 (d, *J* = 15.9 Hz, 1H). ¹³C NMR (CDCl₃, 100 MHz): δ 165.0, 153.4, 138.9 (d, *J*_{CF} = 3.4 Hz), 136.4, 133.9 (d, *J*_{CF} = 3.8 Hz), 130.2 (d, *J*_{CF} = 2.1 Hz), 129.9 (d, *J*_{CF} = 8.9 Hz), 129.1, 128.8, 127.6, 127.0 (d, *J*_{CF} = 2.1 Hz), 122.7 (d, *J*_{CF} = 12.1 Hz), 119.5 (d, *J*_{CF} = 5.8 Hz), 116.4 (d, *J*_{CF} = 22.6 Hz), 82.7, 67.5, 63.8, 29.8, 29.2, 26.1, 23.9, 18.6, -5.0. (CF not detected). MS (ESI) Calculated for C₂₉H₃₇FNO₄Si [M+H]⁺: 510.3, found 510.1.

(R)-3-((R)-3-(2-fluoro-5-((E)-3-hydroxyprop-1-en-1-yl)phenyl)-7-(trimethylsilyl)hept-6-ynoyl)-5,5-dimethyl-4-phenyloxazolidin-2-one (29). The conjugate addition of homopropargyl Grignard to acyl oxazolidinone **27** (5.6 g, 11.0 mmol) was carried out analogously to the preparation of non-fluorinated variant **1-27c**. Compound **29** (6.20 g, 89%) was obtained as a colorless oil in moderate purity following workup and passing through a plug of SiO₂. ¹H NMR (CDCl₃, 400 MHz): δ 0.11 (s, 9H), 0.12 (s, 6H), 0.94 (br s, 3H), 0.95 (s, 9H), 1.44 (br s, 3H), 1.85-1.93 (m, 2H), 2.03-2.10 (m, 2H), 3.21-3.28 (m, 1H), 3.51-3.66 (m, 2H), 4.32 (dd, *J* = 5.0, 1.7 Hz, 2H), 4.93 (s, 1H), 6.17 (dt, *J* = 15.9, 5.0 Hz, 1H), 6.50 (dt, *J* = 15.0, 1.6 Hz, 1H), 6.92 (dd, *J*_{CF} = 10.1 Hz, *J*_{HH} = 8.3 Hz, 1H), 7.06-7.11 (m, 2H), 7.13-7.21 (m, 2H), 7.28-7.39 (m, 3H).

(R)-3-((R)-3-(2-Fluoro-5-((E)-3-hydroxyprop-1-en-1-yl)phenyl)hept-6-ynoyl)-5,5-dimethyl-4-phenyloxazolidin-2-one (30). Compound **29** (6.20g, 9.75 mmol) was dissolved in THF (100 mL) and cooled to -20 °C. Bu₄NF (24.5 mL, 1.0 M in THF) was added dropwise, and the resulting mixture was stirred for 1 hr. The mixture was diluted with EtOAc and washed with sat. NH₄Cl (x3), brine, dried over MgSO₄ and concentrated (*Note: The use of Et₂O is favorable to EtOAc in this partition, as it leads to more effective exclusion of tetrabutylammonium salts*). The resulting residue was redissolved in 1:1 hexanes:EtOAc and filtered through a pad of SiO₂ rinsing with the same. The filtrate was concentrated to give **30** (3.88 g, 89%) of moderate purity. ¹H NMR (CDCl₃, 400 MHz): δ 1.38 (s, 3H), 1.45 (s, 3H), 1.87-1.94 (m, 3H), 1.96-2.10 (m, 2H), 3.20-3.30 (m, 1H), 3.54-3.65 (m, 2H), 4.30 (br d, *J* = 5.2 Hz, 2H), 4.94 (s, 1H),

6.26 (dt, $J = 15.9, 5.7$ Hz, 1H), 6.53 (dt, $J = 15.9, 1.4$ Hz, 1H), 6.94 (dd, $J_{HF} = 10.2$ Hz, $J_{HH} = 8.4$ Hz, 1H), 7.07-7.11 (m, 2H), 7.18-7.25 (m, 2H), 7.30-7.39 (m, 3H).

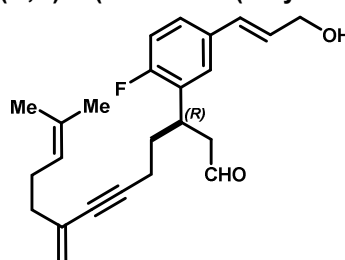
(R)-3-((R)-3-(2-Fluoro-5-((E)-3-hydroxyprop-1-en-1-yl)phenyl)-12-methyl-8-methylenetridec-11-en-6-ynoyl)-5,5-dimethyl-4-phenyloxazolidin-2-one (32). Sonogashira



coupling between alkyne **30** (3.88 g, 8.6 mmol) and vinyl triflate **1-30** were coupled analogously to the reaction to form **1-33**. Purification by column chromatography on SiO₂ eluted with 40% EtOAc in hexanes afforded **32** (2.76 g, 55%) in moderate purity. ¹H NMR (CDCl₃, 400 MHz): δ 0.94 (s, 3H), 1.45 (s, 3H), 1.58 (s, 3H), 1.67 (s, 3H), 1.87-1.95 (m, 2H), 2.06-2.19 (6H), 3.20-3.30 (m, 1H), 3.52-3.67 (m, 2H), 4.30 (dd, $J = 5.7, 1.3$ Hz, 2H), 4.94 (s, 1H), 5.05-5.10 (m, 1H), 5.10-5.12 (m, 1H), 5.17-5.19 (m, 1H), 6.26

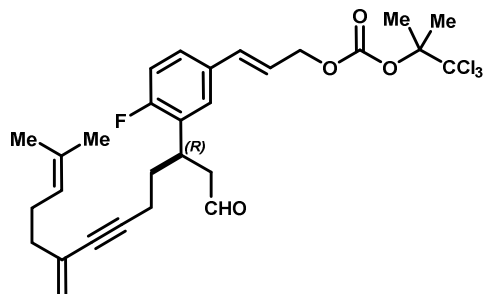
(dt, $J = 15.9, 5.7$ Hz, 1H), 6.53 (dt, $J = 15.9, 1.3$ Hz, 1H), 6.94 (dd, $J_{HF} = 10.0$, $J_{HH} = 8.2$ Hz, 1H), 7.06-7.11 (m, 2H), 7.17-7.25 (m, 2H), 7.30-7.38 (m, 3H).

(R,E)-3-(2-fluoro-5-(3-hydroxyprop-1-en-1-yl)phenyl)-12-methyl-8-methylenetridec-11-en-6-ynal (33). Acyl oxazolidinone **32** (2.76 g, 4.9 mmol) was reductively cleaved by



the action of DIBALH analogously to the procedure used for compound **1-35**. 2.39 g of an oil (>100%) was obtained, following crystallization to recover the auxiliary, and was used without purification.

(R,E)-3-(4-Fluoro-3-(12-methyl-8-methylene-1-oxotridec-11-en-6-yn-3-yl)phenyl)allyl (1,1,1-trichloro-2-methylpropan-2-yl) carbonate (16). Carbonate **16** was formed analogously to the procedure used for



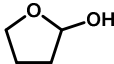
1-1. Purification by column chromatography on SiO₂ eluted with 15% EtOAc in hexanes afforded **16** (1.82 g, 65%) as a light yellow oil, which was stored at -20 °C as a 0.3 M solution in degassed DMF. ¹H NMR (CDCl₃, 400 MHz): δ 1.61 (s, 3H), 1.68-1.69 (m, 3H), 1.90-1.97 (m, 2H), 1.96 (s, 6H), 2.10-2.29 (m, 6H), 2.82 (dd, $J = 7.3, 1.7$ Hz, 2H), 3.57-3.68 (m, 1H), 4.76 (dd, $J = 6.6, 1.1$ Hz, 2H), 5.07-5.13 (m, 1H), 5.03-5.17 (m, 1H), 5.21-5.24 (m, 1H), 6.22 (dt, $J = 15.8, 6.6$ Hz, 1H), 6.63 (dt, $J = 15.8, 1.1$ Hz, 1H), 6.99 (dd, $J_{HF} = 10.2$ Hz, $J_{HH} = 8.5$ Hz, 1H),

7.20-7.28 (m, 2H), 9.69 (t, $J = 1.7$ Hz, 1H). ¹³C NMR (CDCl₃, 125 MHz): δ 200.9, 161.0 (d, $J_{CF} = 248$ Hz), 152.4, 134.1, 132.6 (d, $J_{CF} = 3.3$ Hz), 132.2, 131.8, 129.7 (d, $J_{CF} = 14.6$ Hz), 128.0 (d, $J_{CF} = 5.3$ Hz), 126.8 (d, $J_{CF} = 8.6$ Hz), 123.6, 122.5 (d, $J_{CF} = 2.3$ Hz), 120.3, 116.4 (d, $J_{CF} = 23.4$ Hz), 105.6, 90.1, 88.6, 82.0, 68.5, 48.9, 37.8, 33.9 (d, $J_{CF} = 1.5$ Hz), 33.5, 26.9, 25.8, 21.3, 17.9, 17.5.

Isopropyltriphenylphosphonium iodide (36).¹⁸ Triphenylphosphine (26.2 g, 100 mmol) and isopropyl

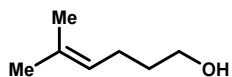
iodide (10 mL, 100 mmol) were dissolved in toluene (20 mL) and heated to reflux under argon for 20 hrs. The mixture was cooled to rt, and the resulting solids were collected by filtration and washed with hexanes to give **36** (29.8 g, 69%) as a white solid. ¹H NMR (DMSO-*d*₆, 500 MHz): δ 1.22 (d, $J = 6.9$ Hz, 3H), 1.27 (d, $J = 6.9$ Hz, 3H), 4.41 (dq, $J_{HP} = 18.3$ Hz, $J_{HH} = 6.9$ Hz, 1H), 7.72-7.82 (m, 2H), 7.86-7.95 (m, 2H). ³¹P NMR (DMSO-*d*₆, 162 MHz): δ 30.7.

2-Hydroxytetrahydrofuran (35).¹⁹ γ-Butyrolactone (7.6 mL, 100 mmol) was dissolved in DCM (40 mL) and cooled to -78 °C. DIBALH (120 mL, 1.0 M in hexanes) was added slowly via an addition funnel, and the resulting mixture was stirred for 1hr, then quenched with MeOH (10 mL) and then sat. Rochelle's salt (10 mL), and allowed to warm to rt. After stirring for 2 hr at rt, a thick white

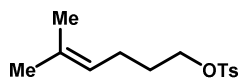


precipitate had formed, and the mixture was filtered through Celite, rinsing with a large amount of DCM. The aqueous was discarded, and the organic phase was dried over MgSO₄ and concentrated to give **35** (5.55 g, 63%) as a colorless oil. ¹H NMR (CDCl₃, 400 MHz): δ 1.78-1.97 (m, 3H), 1.98-2.11 (m, 2H), 3.76-3.86 (m, 2H), 4.01 (br dd, *J* = 8.0, 5.3 Hz, 1H), 4.03 (dd, *J* = 8.0, 5.5 Hz, 1H), 5.49-5.53 (m, 1H). ¹³C NMR (CDCl₃, 100 MHz): δ 98.4, 67.4, 33.2, 23.5.

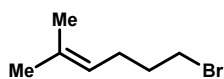
5-Methylhex-4-en-1-ol (37).²⁰ Isopropyltriphenylphosphonium iodide (**36**, 28.5 g, 66 mmol) was suspended in dry THF (65 mL), cooled to -78 °C and treated with KO^tBu (8.13 g, 72 mmol), which resulted in a dark red solution. The mixture was warmed to 0 °C and stirred for 30 min before introducing 2-hydroxytetrahydrofuran (**35**, 5.55 g, 63 mmol) dropwise as a solution in THF (50 mL), which caused the red color to dissipate quickly. The mixture was stirred at rt overnight, then quenched with H₂O (50 mL), and extracted with Et₂O (x3). The combined organic extract was washed with brine, dried over MgSO₄ and concentrated. Purification by column chromatography on SiO₂ eluted with 30% Et₂O in hexanes afforded **37** (3.8 g, 53%) as a colorless oil, the NMR of which matched that reported.²⁰



5-methylhex-4-en-1-yl tosylate (38). Alcohol **37** (3.8 g, 33 mmol) was dissolved in DCM (65 mL) and cooled to 0 °C. Et₃N (9.2 mL, 66 mmol) was added, followed by tosyl chloride (6.7 g, 35 mmol) in several portions. The mixture was warmed to rt, stirred for 3 hr. DMAP (50 mg) was added, and the reaction continued for 2 hr, after which TLC indicated complete consumption of starting **37** (*R_f* = 0.31, 8:2 hex:EtOAc) and formation of a single new spot (*R_f* = 0.62). The mixture was poured into chipped ice, and extracted with DCM (x3). The combined organic extract was washed with sat. NaHCO₃ (x3), brine, dried over MgSO₄ and concentrated to give **38** (9.2 g, >100%) as a light yellow oil, which was used without purification.

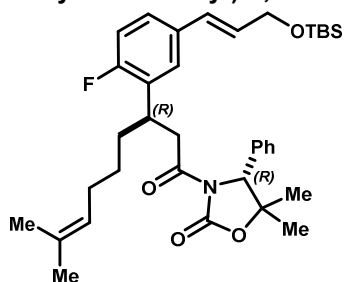


6-bromo-2-methylhex-2-ene (39). Crude Tosylate **38** (9.2 g, ~33 mmol) was dissolved in acetone (110 mL), treated with LiBr (5.73 g, 66 mmol) and heated to reflux for 2 hr, at which point TLC showed complete consumption of starting **38** (*R_f* = 0.32, 9:1 hex:EtOAc) and formation of a new spot (*R_f* = 0.80). The mixture was cooled, concentrated, and partitioned between hexanes and H₂O. The aqueous phase was extracted with hexanes (x1), and the combined extract was washed with H₂O (x2), brine, dried over MgSO₄, concentrated and distilled (b.p. 70-75 °C, 35-40 mbar) to give **39** (4.03 g, 69% over 2 steps) as a colorless oil. ¹H NMR (CDCl₃, 400 MHz): δ 1.63 (br s, 3H), 1.68-1.70 (m, 3H), 1.88 (tt, *J* = 7.1, 6.8 Hz, 2H), 2.13 (br q, *J* = 7.1 Hz, 2H), 3.40 (t, *J* = 6.8 Hz, 2H), 5.04-5.10 (m, 1H). ¹³C NMR (CDCl₃, 100 MHz): δ 133.1, 122.5, 33.5, 32.9, 26.5, 25.7, 17.8.



O-*tert*-Butyldimethylsilyl

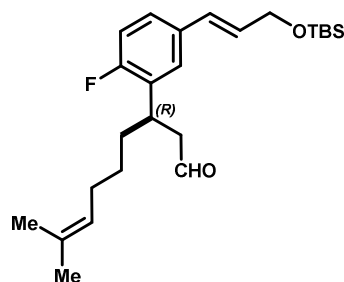
(*R*)-3-((*R*)-3-(2-Fluoro-5-((*E*)-3-hydroxyprop-1-en-1-yl)phenyl)-8-methylnon-7-enoyl)-5,5-dimethyl-4-phenyloxazolidin-2-one (41). *Grignard formation:* A 3-neck round



bottom flask fitted with a reflux condenser and two septa was charged with magnesium filings (803 mg, 33 mmol) and dried by gently heating in vacuo. The apparatus was cooled under argon, and a solution of bromide **39** (3.90 g, 22 mmol) in THF (22 mL) was added – 2.5 mL at once, then the remainder dropwise over 1 hr via syringe pump. After the addition, the mixture was refluxed for 15 min, cooled, and diluted with additional THF (22 mL). Titration by quenching into H₂O and back-titrating with standardized HCl solution to the phenolphthalein endpoint indicated the Grignard solution was 0.47 M. *Conjugate addition:* CuI (4.13 g, 21.7 mmol) was dissolved in THF:Me₂S (4:1, 34 mL) and cooled to -78 °C. The Grignard solution (43 mL, 20 mmol) was added over 10 min, resulting in an orange suspension, which was stirred for 10 min, then warmed to -40 °C for 10 min, and re-cooled to -60 °C. Acyl oxazolidinone **27** (7.88 g, 15.5 mmol) was added dropwise as a solution in THF (15 mL) by cannulating down the cold wall of the reaction flask. The now deep red solution was allowed to warm to -40 °C and stirred for 2 hr, after which HPLC-UV analysis (220 nm) indicated complete conversion to product. The reaction was quenched with sat. NH₄Cl and allowed to warm to rt. The aqueous phase was removed and extracted with EtOAc (x2). The combined organic extract was

washed with NH₄Cl (x2), brine, dried over MgSO₄, concentrated, reconstituted in 1:1 hexanes:EtOAc and filtered through a pad of SiO₂, rinsing with the same. The filtrate was concentrated to give **41** (9.49 g, >20:1 d.r., 100%) as a light yellow oil in high purity. An analytically pure sample was obtained by PTLC. ¹H NMR (CDCl₃, 400 MHz): δ 0.12 (s, 6H), 0.94 (s, 3H), 0.95 (s, 9H), 1.09-1.28 (m, 2H), 1.43 (s, 3H), 1.53 (s, 3H), 1.60-1.68 (m, 2H), 1.63 (s, 3H), 1.80-1.98 (m, 2H), 3.23 (dd, *J* = 16.4, 5.0 Hz, 1H), 3.43-3.53 (m, 1H), 3.57 (dd, *J* = 16.4, 9.1 Hz, 1H), 4.33 (dd, *J* = 5.0, 1.6 Hz, 2H), 4.94 (s, 1H), 4.96-5.02 (m, 1H), 6.18 (dt, *J* = 15.8, 5.1 Hz, 1H), 6.51 (dt, *J* = 15.8, 1.6 Hz, 1H), 6.92 (dd, *J*_{HF} = 10.0 Hz, *J*_{HH} = 8.4 Hz, 1H), 7.06-7.11 (m, 2H), 7.13-7.21 (m, 2H), 7.29-7.37 (m, 4H). ¹³C NMR (CDCl₃, 100 MHz): δ 178.5, 171.5, 160.4 (d, *J*_{CF} = 246 Hz), 153.3, 136.3, 133.2 (d, *J*_{CF} = 3.5 Hz), 131.5, 130.8 (d, *J*_{CF} = 14.8 Hz), 128.9, 128.84, 128.79 (d, *J*_{CF} = 2.5 Hz), 128.54, 128.46, 127.0 (d, *J*_{CF} = 5.1 Hz), 125.6 (d, *J*_{CF} = 8.3 Hz), 124.3, 115.7, 82.4, 81.8, 69.1, 66.9, 63.8, 41.7, 40.7, 35.3, 35.1, 28.7, 27.8, 27.5, 26.3, 26.0, 25.7, 23.6, 18.5, 17.6, -5.2. MS (ESI) Calculated for C₃₆H₅₀FNaO₄Si [M+Na]⁺: 630.4, found 630.2.

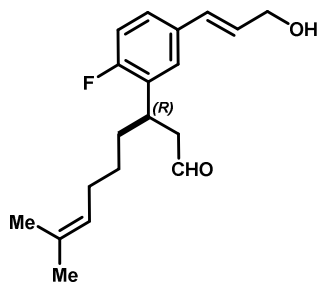
O-tert-Butyldimethylsilyl (R,E)-3-(2-fluoro-5-(3-hydroxyprop-1-en-1-yl)phenyl)-8-methylnon-7-enal (42).



(42). Acyl oxazolidinone **41** (8.92 g, 14.7 mmol) was dissolved in toluene (150 mL) and cooled to -78 °C. DIBALH (1.0 M in hexanes, 29 mL) was added dropwise, and the mixture was stirred for 30 min, then quenched by the addition of sat. Rochelle's salt (15 mL) and 1M NaOH (15 mL). The mixture was warmed to rt, and allowed to stir for 4 hr. The aqueous phase was collected and extracted with EtOAc (x2). The combined organic extract was washed with H₂O (x1), brine, dried over MgSO₄ and concentrated to ~3mL, at which point a precipitate formed. Hexanes was added, and the suspension was filtered to recover auxiliary **1-36** (1.66 g, 60%). The filtrate was filtered through a pad of SiO₂, rinsing with 9:1 hexanes:EtOAc, and the

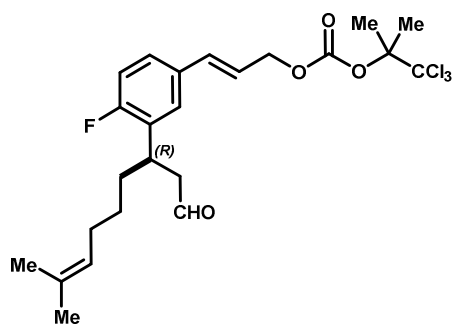
resulting filtrate was concentrated. Purification by column chromatography on SiO₂ eluted with 5→15% EtOAc in hexanes afforded **42** (3.28 g, 53%), as well as recovered starting **41** (720 mg). ¹H NMR (CDCl₃, 400 MHz): δ 0.11 (s, 6H), 0.94 (s, 9H), 1.13-1.33 (m, 2H), 1.56 (s, 3H), 1.62-1.72 (m, 2H), 1.66 (s, 3H), 1.86-2.03 (m, 2H), 3.41-3.52 (m, 1H), 4.33 (dd, *J* = 5.0, 1.7 Hz, 2H), 4.99-5.07 (m, 1H), 6.18 (dt, *J* = 15.8, 5.0 Hz, 1H), dt (*J* = 15.8, 1.7 Hz, 1H), 6.95 (dd, *J*_{HF} = 10.2 Hz, *J*_{HH} = 8.4 Hz, 1H), 7.15 (dd, *J*_{HF} = 7.0 Hz, *J*_{HH} = 2.2 Hz, 1H), 7.20 (ddd, *J*_{HH} = 8.4, 2.2 Hz, *J*_{HF} = 5.0 Hz, 1H), 9.68 (t, *J* = 1.9 Hz, 1H). ¹³C NMR (CDCl₃, 100 MHz): δ 201.7, 160.4 (d, *J*_{CF} = 246 Hz), 133.6 (d, *J*_{CF} = 3.4 Hz), 131.9, 130.5 (d, *J*_{CF} = 15.2 Hz), 129.2 (d, *J*_{CF} = 2.4 Hz), 128.5, 127.1 (d, *J*_{CF} = 5.1 Hz), 126.0 (d, *J*_{CF} = 8.5 Hz), 124.3, 115.9 (d, *J*_{CF} = 23 Hz), 63.9, 49.5, 34.9, 33.8, 27.9, 27.7, 26.1, 25.8, 18.6, 17.8, -5.0.

(R,E)-3-(2-Fluoro-5-(3-hydroxyprop-1-en-1-yl)phenyl)-8-methylnon-7-enal (43).



(43). Silyl ether **42** (3.28 g, 7.8 mmol) was dissolved in MeOH (40 mL), cooled to 0 °C, and treated with 3N HCl in MeOH (3.6 mL). Generated by the solvolysis of AcCl in MeOH). The mixture was warmed to rt and stirred for 15 min, then concentrated, and the black residue was re-dissolved in THF (50 mL) and treated with 0.1 N HCl_{aq} (25 mL) and heated to 50 °C overnight. The mixture was cooled and extracted into EtOAc (x3). The combined extract was washed with brine, dried over MgSO₄ and concentrated. Purification by column chromatography on SiO₂ eluted with 30→50% EtOAc in hexanes to give **43** (2.07 g, 87%) as a colorless oil. ¹H NMR (CDCl₃, 400 MHz): δ 1.13-1.29 (m, 2H), 1.55 (s, 3H), 1.62-1.69 (m, 2H), 1.65 (s, 3H), 1.86-1.99 (m, 3H), 2.75 (dd, *J* = 7.2, 1.7 Hz, 2H), 3.43-3.49 (m, 1H), 4.30 (dd, *J* = 5.6, 1.3 Hz, 2H), 4.99-5.04 (m, 1H), 6.26 (dt, *J* = 15.9, 5.6 Hz, 1H), 6.54 (dt, *J* = 15.9, 1.3 Hz, 1H), 6.96 (dd, *J*_{HF} = 10.0 Hz, *J*_{HH} = 8.5 Hz, 1H), 7.16 (dd, *J*_{HF} = 7.0 Hz, *J*_{HH} = 2.1 Hz, 1H), 7.20 (ddd, *J*_{HH} = 8.5, 2.1 Hz, *J*_{HF} = 5.1 Hz, 1H). ¹³C NMR (CDCl₃, 100 MHz): δ 201.7, 160.6 (d, *J*_{CF} = 246 Hz), 133.2 (d, *J*_{CF} = 3.4 Hz), 131.9, 130.6 (d, *J*_{CF} = 14.9 Hz), 130.1, 128.5 (d, *J*_{CF} = 1.7 Hz), 127.2 (d, *J*_{CF} = 5.7 Hz), 126.0 (d, *J*_{CF} = 8.4 Hz), 124.2, 116.0 (d, *J*_{CF} = 23.5 Hz), 63.6, 49.4 (d, *J*_{CF} = 1.2 Hz), 34.8 (d, *J*_{CF} = 1.1 Hz), 33.7, 27.8, 27.6, 25.8, 17.8.

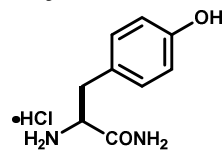
(*R,E*)-3-(4-Fluoro-3-(8-methyl-1-oxonon-7-en-3-yl)phenyl)allyl (1,1,1-trichloro-2-methylpropan-2-yl) carbonate (17).



Cinnamyl alcohol **43** (2.07 g, 6.8 mmol) was dissolved in dry DCM (70 mL) and cooled to $-40\text{ }^{\circ}\text{C}$. DMAP (100 mg, 0.82 mmol) and pyridine (880 μL , 10.9 mmol) were added as a solution in DCM (15 mL), followed by 2,2,2-trichloro-1,1-dimethylethyl chloroformate (2.28 g, 9.5 mmol) dropwise as a solution in DCM (15 mL). The mixture was stirred at $-40\text{ }^{\circ}\text{C}$ for 3 hr, then diluted with DCM and washed with sat. NaHCO_3 (x2, H_2O (x2), brine, dried over MgSO_4 and concentrated (*Note: a recalcitrant emulsion results during this workup, and may be obviated by use of a large amount of EtOAc instead of DCM*). Purification by column chromatography on SiO_2 eluted with

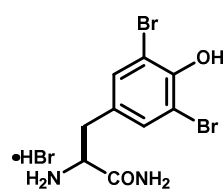
5 \rightarrow 15% EtOAc in hexanes afforded **17** (3.0 g, 87%) as a colorless oil, which was stored at $-20\text{ }^{\circ}\text{C}$ as a 0.3 M solution in degassed DMF. $[\alpha]_D^{24} = +17.7^{\circ}$ ($c = 0.8$, CHCl_3). $^1\text{H NMR}$ (CDCl_3 , 500 MHz): δ 1.11-1.32 (m, 2H), 1.56 (br s, 3H), 1.63-1.70 (m, 1H), 1.66 (brs, 3H), 1.86-2.00 (m, 3H), 1.96 (s, 6H), 2.76 (dd, $J = 7.2$, 1.8 Hz, 2H), 3.43-3.51 (m, 1H), 4.77 (dd, $J = 6.6$, 1.1 Hz, 2H), 4.99-5.06 (m, 1H), 6.22 (dt, $J = 15.8$, 6.6 Hz, 1H), 6.63 (dt, $J = 15.8$, 1.1 Hz, 1H), 6.98 (dd, $J_{\text{HF}} = 10.1$ Hz, $J_{\text{HH}} = 8.4$ Hz, 1H), 7.19 (dd, $J_{\text{HF}} = 7.0$ Hz, $J_{\text{HH}} = 2.2$ Hz, 1H), 7.23 (ddd, $J_{\text{HH}} = 8.4$, 2.2 Hz, $J_{\text{HF}} = 5.0$ Hz, 1H), 9.68 (t, $J = 1.8$ Hz, 1H). $^{13}\text{C NMR}$ (CDCl_3 , 125 MHz): δ 201.2, 160.7 (d, $J_{\text{CF}} = 247$ Hz), 152.1, 134.0, 132.2 (d, $J_{\text{CF}} = 3.4$ Hz), 131.7, 130.6 (d, $J_{\text{CF}} = 15.0$ Hz), 127.3 (d, $J_{\text{CF}} = 5.5$ Hz), 126.2 (d, $J_{\text{CF}} = 8.6$ Hz), 124.0, 122.0 (d, $J_{\text{CF}} = 2.0$ Hz), 115.9 (d, $J_{\text{CF}} = 23.4$ Hz), 105.4, 89.9, 68.4, 49.2, 34.6, 33.5, 27.6, 27.4, 25.6, 24.7, 21.1, 17.6.

***L*-Tyrosine carboxamide hydrochloride (49).**²¹ Tyrosine methyl ester hydrochloride was dissolved in



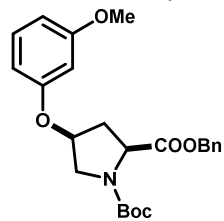
MeOH (500 mL) in a pressure bottle, cooled in an ice bath, and sparged with ammonia until saturated. The reaction vessel was sealed and stirred at rt for 6 days, after which HPLC-UC indicated complete conversion. The mixture was concentrated to dryness, triturated with a small volume of cold 1 N HCl, filtered and dried under vacuum to give **49** (40.7 g, 88%) as a white solid. $[\alpha]_D^{20} = +17.0^{\circ}$ ($c = 1$, 1N HCl). m.p. $\sim 220\text{ }^{\circ}\text{C}$ with decomposition. $^1\text{H NMR}$ (CDCl_3 , 400 MHz): δ 2.71 (dd, $J = 13.8$, 7.7 Hz, 1H), 2.90 (dd, $J = 13.8$, 5.7 Hz, 1H), 3.60 (dd, $J = 7.7$, 5.7 Hz, 1H), 6.19 (br s, 2.4H), 6.69 (8.3 Hz, 2H), 7.03 (d, $J = 8.3$ Hz, 2H), 7.25 (br s, 1H), 7.64 (br s, 1H), 9.30 (br s, 0.7H). MS (ESI) Calculated for $\text{C}_9\text{H}_{13}\text{N}_2\text{O}_2$ $[\text{M}+\text{H}]^+$: 181.1, found 181.2.

3,5-Dibromo-*L*-tyrosine carboxamides hydrobromide (50). Tyrosine carboxamide hydrochloride (4.33



g, 20 mmol) was suspended in AcOH (40 mL) and Br_2 (2.3 mL, 44 mmol) was added dropwise as a solution in AcOH. After addition, the mixture was warmed to $50\text{ }^{\circ}\text{C}$ for 1 hr, then H_2O (15 mL) and additional AcOH (20 mL) were added, which caused the reaction fading to an orange color with formation of a white precipitate. The heating bath was removed, the mixture was cooled in an ice bath, and additional H_2O (20 mL) was added. The precipitate was collected and dried in vacuo to give **50** (3.3 g, 40%) as a white solid, presumed to be the hydrobromide salt. $^1\text{H NMR}$ (CDCl_3 , 400 MHz): δ 2.90 (dd, $J = 14.2$, 8.1 Hz, 1H), 3.07 (dd, $J = 14.2$, 5.1 Hz, 1H), 3.94-3.99 (m, 1H), 7.48 (s, 2H), 7.61 (br s, 1H), 8.04 (br s, 1H), 8.15 (br s, 2.5H), 9.83 (br s, 0.8 H). $^{13}\text{C NMR}$ (CDCl_3 , 125 MHz): δ 169.6, 149.8, 133.3, 129.5, 111.9, 53.4, 35.0.

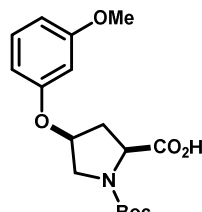
***N*-Boc-*cis*-4-(3-Methoxyphenoxy)-*L*-proline benzyl ester (54).** Boc-Hyp-OBn (**53**, **1-S6**) (10.2 g, 31.7



mmol), 3-methoxyphenol (5.91 g, 47.6 mmol) and PPh_3 (12.5 g, 47.6 mmol) were dissolved in dry THF (65 mL). The mixture was cooled in an ice bath, and diethylazodicarboxylate (20.7 mL, 40 wt% in PhMe, 47.6 mmol) was added dropwise over ~ 1 hr. The mixture was allowed to warm to rt and stirred overnight, then concentrated, reconstituted in Et_2O and filtered. The filtrate was adsorbed onto SiO_2 and purified by column chromatography on SiO_2 eluted with 0 \rightarrow 100% Et_2O in hexanes to give **54** (11.22 g, 83%) as a colorless oil. $^1\text{H NMR}$ (CD_3OD , 400 MHz, $\sim 2:3$ mixture of rotamers): δ 1.35 (s, 5H), 1.45 (s, 4H), 2.38-2.57 (m, 2H), 3.56-3.76 (m, 2H), 3.69 (s, 3H), 4.47 (dd, $J =$

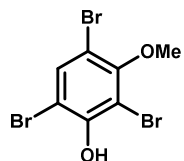
9.0, 2.1 Hz, 0.6H), 4.51 (dd, $J = 5.5, 5.5$ Hz, 0.4H), 4.91-4.99 (m, 1H), 5.03 (d, $J = 12.4$ Hz, 0.4H), 5.10 (d, $J = 12.2$ Hz, 0.6H), 5.17 (d, $J = 12.2$ Hz, 0.6H), 5.19 (d, $J = 12.4$ Hz, 0.4H), 6.32-6.41 (m, 2H), 6.52 (br dd, $J = 8.2, 2.3$ Hz, 1H), 7.13 (dd, $J = 8.2, 8.2$ Hz, 1H), 7.21-7.30 (m, 5H). ^{13}C NMR (CD_3OD , 125 MHz, mixture of rotamers): δ 173.2, 173.1, 162.4, 159.2, 159.1, 156.0, 155.8, 137.2, 137.1, 131.1, 129.5, 129.3, 129.1, 129.0, 108.6, 107.93, 107.88, 103.3, 103.2, 81.6, 76.8, 76.7, 75.9, 75.8, 67.9, 67.8, 59.4, 59.3, 59.1, 59.0, 55.71, 55.68, 53.5, 53.1, 36.9, 36.1, 28.7, 28.5.

***N*-Boc-*cis*-4-(3-Methoxyphenoxy)-*L*-proline benzyl ester (**56**).** Benzyl ester **54** (11.2 g, 26 mmol) was



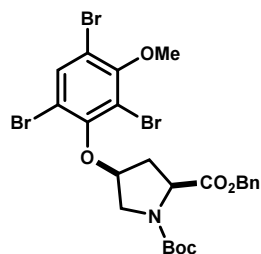
dissolved in MeOH and treated with Pd/C under an atmosphere of H_2 . Upon completion, as observed by HPLC, the mixture was carefully filtered through Celite, rinsing with MeOH. The filtrate was concentrated and dried in vacuo to give **56** (7.52 g, 85%) as a white solid. m.p. 146-147 °C. ^1H NMR ($\text{DMSO-}d_6$, 400 MHz, ~2:3 mixture of Boc rotamers): δ 1.36 (s, 5H), 1.40 (s, 4H), 2.16 (br d, $J = 14.0$ Hz, 1H), 2.57 (ddd, $J = 14.1, 9.4, 4.9$ Hz, 1H), 3.38 (br dd, $J = 11.9, 9.6$ Hz, 1H), 3.68 (dd, $J = 11.9, 5.4$ Hz, 1H), 4.24 (dd, $J = 9.5, 2.5$ Hz, 0.6H), 4.27 (dd, $J = 9.6, 1.9$ Hz, 0.4H), 4.94-5.04 (m, 1H), 6.36-6.41 (m, 1H), 6.42-6.48 (m, 1H), 6.53 (dd, $J = 8.2, 2.2$ Hz, 1H), 7.17 (dd, $J = 8.2, 8.2$ Hz, 1H), 12.51 (br s, 1H). ^{13}C NMR (CD_3OD , 125 MHz, major rotamer): δ 173.1, 160.5, 157.8, 153.2, 130.0, 107.6, 106.7, 101.9, 78.8, 74.2, 57.4, 55.1, 51.5, 35.5, 27.9.

2,4,6-Tribromo-3-methoxyphenol (52**).** 3-Methoxyphenol (1.86 g, 15 mmol) was dissolved in AcOH, and



Br_2 (2.7 mL, 53 mmol) was added dropwise as a solution in AcOH (5 mL) resulting in a mild exotherm. The mixture was stirred for 1 hr, then poured into chipped ice and extracted with DCM (x3). The organic phase was washed with $\text{Na}_2\text{S}_2\text{O}_3$ (x2), brine, dried over MgSO_4 , concentrated, and recrystallized from MeOH:H $_2\text{O}$ to give **52** (2.95 g, 55%) in three crops of faintly brown crystals. ^1H NMR (CDCl_3 , 400 MHz): δ 3.87 (s, 3H), 5.90 (br s, 1H), 7.67 (s, 1H). ^{13}C NMR (CDCl_3 , 100 MHz): δ 154.5, 150.1, 134.3, 108.3, 106.9, 105.1, 60.8.

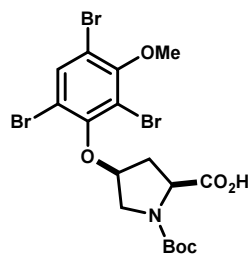
***N*-Boc-*cis*-4-(2,4,6-Tribromo-3-methoxyphenoxy)-*L*-proline benzyl ester (**55**).** Tribromophenol **52** (3.68



g, 10.2 mmol) and Boc-Hyp-OBn (**1-S6**) (2.19 g, 6.8 mmol) were reacted in the same manner as for non-brominated analog **54** to give **55** (3.98 g, 88%) as a viscous, colorless oil. ^1H NMR (CDCl_3 , 400 MHz): δ 1.34 (s, 5H), 1.46 (s, 4H), 2.52-2.61 (m, 0.4H), 2.61-2.71 (m, 1.6H), 3.78 (dd, $J = 11.9, 5.8$ Hz, 0.4H), 3.89-4.00 (m, 1.6H), 4.38 (dd, $J = 8.3, 5.9$ Hz, 0.6H), 4.52 (dd, $J = 9.2, 4.2$ Hz, 0.4H), 5.12 (d, $J = 12.5$ Hz, 0.4H), 5.19 (d, $J = 12.3$ Hz, 0.6H), 5.23 (d, $J = 12.3$ Hz, 0.6H), 5.32 (d, $J = 12.5$ Hz, 0.4H), 7.27-7.40 (m, 5H), 7.72 (s, 1H). ^{13}C NMR (CDCl_3 , 100 MHz): δ 171.8, 171.5, 155.0, 154.2, 153.7, 153.6, 135.8, 135.6, 135.33, 135.29, 128.6,

128.5, 128.4, 128.2, 115.42, 115.37, 113.5, 113.4, 113.22, 113.18, 83.1, 82.1, 80.5, 80.4, 67.0, 60.7, 57.9, 57.6, 52.6, 52.1, 37.3, 36.4, 28.5, 28.3.

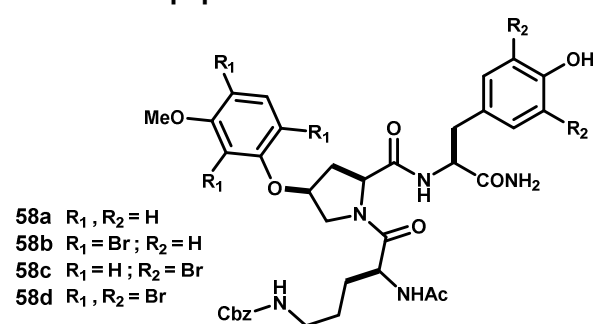
***N*-Boc-*cis*-4-(2,4,6-Tribromo-3-methoxyphenoxy)-*L*-proline (**57**).** Benzyl ester **55** (3.82 g, 5.7 mmol) was



dissolved in THF:MeOH:H $_2\text{O}$ (3:1:1, 25 mL), treated with LiOH (206 mg, 8.6 mmol), and stirred at rt for 3 hr. The volatiles were removed in vacuo, and the aqueous remainder was diluted with 0.1 M NaOH and washed with Et $_2\text{O}$ (x3). The aqueous phase was acidified to pH ~ 3 with citric acid, and extracted with EtOAc (x3). The combined organic extract was washed with brine, dried over Na_2SO_4 and concentrated to give **57** (2.69 g, 82%) in moderate purity, still contaminated by BnOH, as a colorless glass. ^1H NMR (CDCl_3 , 400 MHz, mixture of rotamers): δ 1.44 (s, 6 H), 1.48 (s, 3H), 2.54-2.77 (m, 2H), 3.84 (s, 3H), 3.85-3.94 (m, 2H), 4.32 (dd, $J = 8.9, 5.4$ Hz, 0.6H), 4.39 (dd, $J = 7.5, 6.9$ Hz, 1H), 4.74-4.87 (m, 1H), 7.82 (s,

1H). ^{13}C NMR (CDCl_3 , 75 MHz, major rotamer): δ 175.3, 156.3, 155.1, 136.4, 129.3, 128.2, 127.9, 116.2, 114.0, 81.8, 65.2, 61.2, 53.3, 38.0, 28.5.

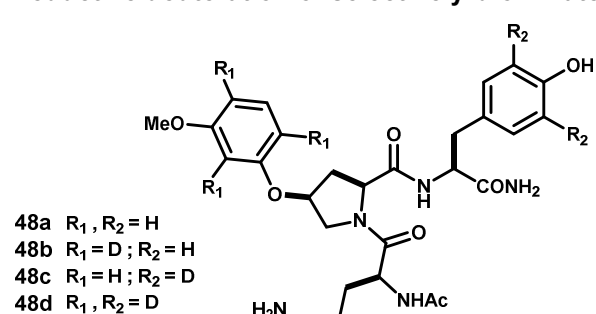
Brominated peptides 58b–d and natural abundance compound 58a. Solution-phase assembly was



carried out using N_α -Boc-protected aryloxyprolines **56** or **57**, and either tyrosine carboxamide (**49**) or corresponding dibromide **50**. Couplings were carried out using each amino acid (1 eq) in DMF (~0.2M) using iPr_2EtN (≥ 2 eq, or to pH > 9) and TBTU or HBTU (1 eq). The mixture was stirred until complete as observed by HPLC-UV/MS analysis (~1 - 4 hrs), then partitioned between EtOAc and sat. $NaHCO_3$. The organic phase was washed with sat. $NaHCO_3$ (x2), sat. NH_4Cl (x3), brine, dried over $MgSO_4$ and concentrated.

Boc deprotection was carried out using 4 N HCl in dioxane for 30min, and then concentrated and dried under vacuum. N_α -Boc- N_δ -Cbz-Ornithine was introduced in the same manner, taken to the N-terminal acetamide, and each resulting crude peptide was purified by column chromatography on SiO_2 eluted with 0→12% MeOH in $CHCl_3$. **58a**: 5.12 g, MS (ESI) Calculated for $C_{36}H_{44}N_5O_9$ $[M+H]^+$: 690.3, found 690.0. **58b**: 765 mg, MS (ESI) Calculated for $C_{36}H_{41}Br_3N_5O_9$ $[M+H]^+$: 924.0, found 925.8. **58c**: A yield was not recorded, MS (ESI) Calculated for $C_{36}H_{42}Br_2N_5O_9$ $[M+H]^+$: 846.1, found 847.6. **58d**: 832 mg, MS (ESI) Calculated for $C_{36}H_{39}Br_5N_5O_9$ $[M+H]^+$: 1079.9, found 1083.6/1085.6.

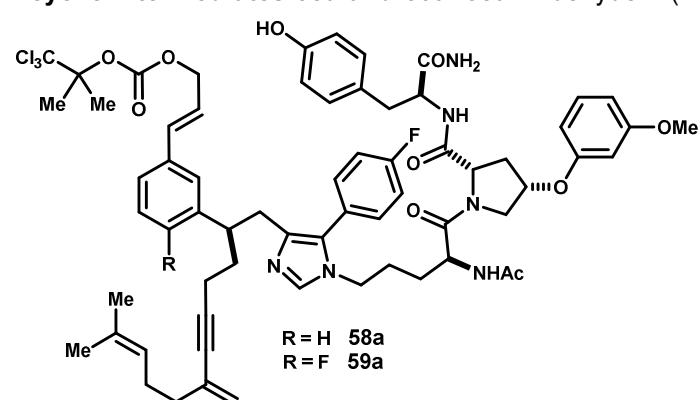
Reductive deuteration of selectively brominated peptides (48a–d). Natural abundance compound **48a**



was prepared by reductive hydrogenolysis over Pd/C in MeOH under an atmosphere of H_2 . Upon completion, the mixture was filtered through Celite, rinsing with MeOH, and concentrated. To prepare deuterium isotopologues **48b** and **48d** (**48c** was not prepared), brominated precursors **58b** and **58c**, respectively, were dissolved in CH_3OD and stirred at rt for 30 min, then concentrated. The residue was re-dissolved in CH_3OD (0.025 M, 99%D atoms) and treated with Pd/C (100 wt% of 10wt% Pd) and

ND_4DCO_2 (50 eq, 98%D atoms, Armar Chemicals). The headspace was flushed with argon, and each mixture was lowered into a pre-heated oil bath at 70 °C. Heating was continued for 3.5 hrs, and the mixture was then cooled, filtered through Celite, concentrated and dried in vacuo. (Note: Crude heavy isotope-labeled peptides produced in this manner are contaminated by NH_4Br , the ammonium ion of which may interfere in subsequent steps if not exchanged) **48a**: A yield was not recorded. MS (ESI) Calculated for $C_{28}H_{38}N_5O_7$ $[M+H]^+$: 556.3, found 556.0. **48b**: 76 mg, > 100%. MS (ESI) Calculated for $C_{28}H_{35}D_3N_5O_7$ $[M+H]^+$: 559.3, found 560.3. **48c**: Not prepared. **48d**: 411 mg, > 100%.

Acyclic intermediates 58a and 59a. **58a**: Aldehyde **1** (1100 μL of 0.3 M soln, 330 μmol), tripeptide **48a**

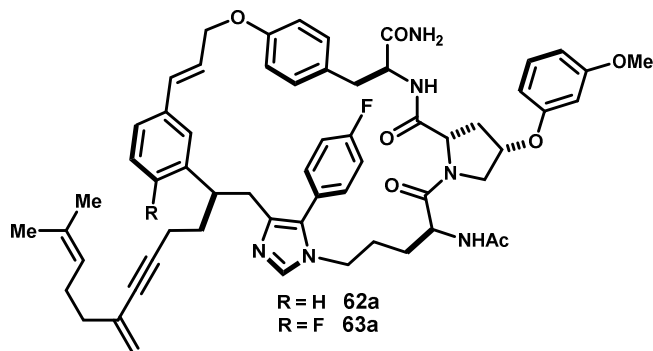


(278 mg, 500 μmol), powdered K_2CO_3 (160 mg, 1.2 mmol) and 4Å molecular sieves (460 mg) were stirred for 3.5 hr. Fluorophenyl tosylmethyl isonitrile (**2-11**) (115 mg, 400 μmol) was added. The mixture was stirred at rt overnight, then diluted with MeOH, filtered through Celite and concentrated. Purification by column chromatography on SiO_2 eluted with 0→11% MeOH in $CHCl_3$ gave acyclic intermediate **58a** (228 mg, 56%) as a light yellow solid. 1H NMR (CD_3OD , 500 MHz): δ 1.55 (s, 3H), 1.64 (s, 3H), 1.76-1.86 (m, 2H), 1.88-1.93 (m, 2H), 1.93 (s, 6H), 1.96 (s, 3H),

1.96-2.00 (m, 1H), 2.00-2.14 (m, 5H), 2.22 (ddd, $J = 16.8, 6.3, 6.3$ Hz, 1H), 2.34 (ddd, $J = 13.8, 2.7, 2.7$ Hz,

1H), 2.52 (ddd, $J = 13.8, 9.8, 5.1$ Hz, 1H), 2.99 (d, $J = 6.4$ Hz, 2H), 3.13-3.20 (m, 2H), 3.72 (s, 3H), 3.78 (br d, $J = 10.7$ Hz, 1H), 3.80-3.94 (m, 2H), 4.17 (dd, $J = 11.2, 4.9$ Hz, 1H), 4.49-4.57 (m, 3H), 4.68-4.74 (m, 2H), 5.02-5.09 (m, 2H), 5.09-5.12 (m, 2H), 6.11 (dt, $J = 15.6, 6.4$ Hz, 1H), 6.46 (d, $J = 15.6$ Hz, 1H), 6.50-6.54 (m, 2H), 6.54-6.58 (m, 1H), 6.66 (d, $J = 8.6$ Hz, 2H), 6.78 (dd, $J = 9.8, 8.9$ Hz, 1H), 6.93-7.01 (m, 4H), 7.03 (d, $J = 8.6$ Hz, 2H), 7.11-7.21 (m, 2H), 7.25-7.33 (m, 2H), 7.65 (s, 1H). ^{13}C NMR (CDCl_3 , 125 MHz): δ 175.3, 173.5, 173.2, 172.5, 163.3, 162.3 (d, $J_{\text{CF}} = 246$ Hz), 159.4, 157.4, 153.6, 139.1, 138.0, 134.7, 133.8, 133.1, 132.9, 132.4, 131.7, 131.5, 131.3, 130.6, 130.54, 130.52, 130.4, 128.8, 128.6, 127.7 (d, $J_{\text{CF}} = 8.7$ Hz), 126.8, 124.6, 123.4, 120.4, 116.2, 116.1 (d, $J_{\text{CF}} = 21.8$ Hz), 108.9, 108.4, 106.8, 103.5, 90.9, 89.8, 82.8, 77.2, 69.4, 61.1, 55.8, 55.5, 54.0, 52.1, 45.6, 38.7, 38.2, 35.2, 34.2, 30.3, 29.6, 27.9, 27.7, 26.0, 22.3, 21.6, 18.1, 17.9. MS (ESI) Calculated for $\text{C}_{65}\text{H}_{75}\text{Cl}_3\text{FN}_6\text{O}_{10}$ $[\text{M}+\text{H}]^+$: 1223.5, found 1223.2. **59a**: Acyclic intermediate **59a** (222 mg, 62%) was prepared from template **16** (970 μL of 0.3 M DMF soln, 290 μmol) and peptide **48a** (243 mg, 440 μmol) analogously to **58a**, except that chromatography was carried out by elution with 2 \rightarrow 12% MeOH in CHCl_3 . ^1H NMR (CD_3OD , 500 MHz): δ 1.55 (s, 3H), 1.56-1.63 (m, 2H), 1.65 (s, 3H), 1.86-1.95 (m, 5H), 1.94 (s, 6H), 1.96 (s, 3H), 1.99-2.06 (m, 3H), 2.06-2.14 (m, 2H), 2.20 (ddd, $J = 16.9, 5.9, 5.9$ Hz, 1H), 2.36 (ddd, $J = 14.0, 2.9, 2.9$ Hz, 1H), 2.53 (ddd, $J = 14.0, 9.9, 5.2$ Hz, 1H), 2.95-3.05 (m, 1H), 2.99 (d, $J = 6.3$ Hz, 1H), 3.17-3.23 (m, 1H), 3.58-3.72 (m, 2H), 3.72-3.77 (m, 1H), 3.74 (s, 3H), 4.16 (dd, $J = 11.3, 4.9$ Hz, 1H), 4.43 (dd, $J = 7.5, 6.2$ Hz, 1H), 4.50-4.56 (m, 2H), 4.70-4.75 (m, 2H), 5.03-5.11 (m, 4H), 6.21 (dt, $J = 15.9, 6.3$ Hz, 1H), 6.51-6.60 (m, 3H), 6.65 (d, $J = 8.5$ Hz, 2H), 6.84 (br d, $J = 7.7$ Hz, 1H), 6.94 (br s, 1H), 7.01-7.12 (m, 2H), 7.03 (d, $J = 8.5$ Hz, 2H), 7.15-7.22 (m, 2H), 7.38-7.45 (m, 2H), 7.58 (s, 1H). ^{13}C NMR (CDCl_3 , 125 MHz): δ 175.3, 173.6, 173.2, 172.5, 163.2 (d, $J_{\text{CF}} = 245$ Hz), 162.5, 159.4, 157.4, 153.6, 144.5, 138.7 (d, $J_{\text{CF}} = 3.3$ Hz), 137.8, 137.6, 135.7, 133.2, 132.9, 132.7, 131.7, 131.3, 130.5, 130.4, 129.8, 128.7, 128.6, 127.4, 126.3, 124.6, 123.8, 120.3, 116.25, 116.20 (d, $J_{\text{CF}} = 21.9$ Hz), 109.0, 108.4, 106.8, 103.6, 90.9, 90.0, 77.3, 69.5, 61.1, 55.8, 55.5, 54.1, 52.1, 45.7, 45.5, 42.7, 38.8, 38.2, 35.2 (d, $J_{\text{CF}} = 5.8$ Hz), 31.9, 29.5, 27.9, 27.5, 25.9, 22.3, 21.6, 18.4, 18.0, 17.9. (Aryl CF not detected). MS (ESI) Calculated for $\text{C}_{65}\text{H}_{74}\text{Cl}_3\text{F}_2\text{N}_6\text{O}_{10}$ $[\text{M}+\text{H}]^+$: 1241.5, found 1243.1.

Macrocyclic cinnamyl ethers 62a and 63a. **62a**: Substrate **58a** (228 mg, 186 μmol) was dissolved in DMF

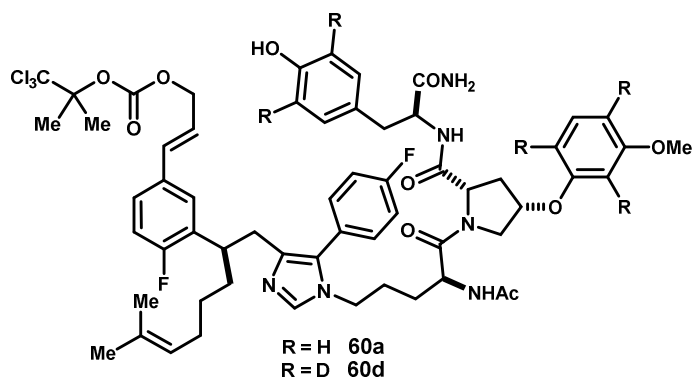


and sparged with argon for 45 min. The reaction vessel was opened briefly, solid $\text{P}(\text{PPh}_3)_4$ (5 mg, 4.7 μmol) was added, and the reaction was again sealed and sparged for an additional 15 min. After 2 hrs, no reaction was observed by HPLC-UV/MS, and additional $\text{Pd}(\text{PPh}_3)_4$ (5 mg, 4.7 μmol) was introduced in the same fashion. The mixture was stirred for 1.5 hr, at which point HPLC analysis indicated complete conversion to product. The reaction vessel was opened, and the mixture was sparged with argon for several

minutes, then concentrated in vacuo. Purification by column chromatography on SiO_2 eluted with 0 \rightarrow 12% MeOH in CHCl_3 afforded **62a** (104 mg, 56%) as a pale yellow residue. ^1H NMR (CD_3OD , 500 MHz): δ 1.55 (s, 3H), 1.65 (s, 3H), 1.77-1.85 (m, 1H), 1.85-1.99 (m, 5H), 1.97 (s, 3H), 2.06-2.12 (m, 3H), 2.18 (ddd, $J = 16.8, 5.8, 5.8$ Hz, 1H), 2.45 (ddd, $J = 14.0, 3.1, 3.1$ Hz, 1H), 2.58 (ddd, $J = 14.0, 9.6, 5.6$ Hz, 1H), 2.90-3.01 (m, 3H), 3.14 (dd, $J = 14.4, 3.3$ Hz, 1H), 3.19 (dd, $J = 14.4, 4.4$ Hz, 1H), 3.24 (dd, $J = 14.7, 8.3$ Hz, 1H), 3.71 (s, 3H), 4.30 (dd, $J = 11.4, 5.5$ Hz, 1H), 4.62 (dd, $J = 3.4, 7.3$ Hz, 1H), 4.70 (dd, $J = 9.6, 3.5$ Hz, 1H), 4.71-4.83 (m, 2H), 5.02-5.10 (m, 4H), 6.26 (ddd, $J = 16.0, 5.5, 5.5$ Hz, 1H), 6.48-6.55 (m, 3H), 6.57 (d, $J = 16.0$ Hz, 1H), 6.75 (br d, $J = 7.3$ Hz, 1H), 6.83 (d, $J = 8.8$ Hz, 2H), 7.07 (s, 1H), 7.10-7.15 (m, 3H), 7.15-7.20 (m, 3H), 7.22 (d, $J = 8.8$ Hz, 2H), 7.44 (s, 1H), 7.56-7.61 (m, 2H). ^{13}C NMR (CDCl_3 , 125 MHz): δ 175.1, 173.1, 172.9, 172.6, 162.4, 159.6, 158.5, 144.5, 138.3, 138.2, 137.5, 133.6, 133.1, 132.8, 131.6, 131.2, 130.4, 130.3, 130.3, 129.8, 128.8, 127.5, 126.9, 126.4, 126.0, 124.6 (2), 120.3, 116.3 (d, $J_{\text{CF}} = 22$ Hz), 116.2, 109.0, 108.4, 103.5, 89.9, 82.6, 77.3, 68.8, 60.6, 55.7, 55.3, 54.0, 51.8, 45.9, 45.4, 38.7, 38.2, 35.4, 34.6, 31.9, 29.7, 27.9, 27.2, 25.9, 22.3, 17.9. (Aryl CF not detected). MS (ESI) Calculated for $\text{C}_{60}\text{H}_{68}\text{FN}_6\text{O}_7$ $[\text{M}+\text{H}]^+$: 1003.5, found 1003.4. **63a**: Compound **63a** was prepared from acyclic precursor **59a** (222 mg, 179

μmol) analogously to compound **58a**. A yield was not recorded. ^1H NMR (CD_3OD , 500 MHz): δ 1.28-1.34 (m, 1H), 1.44-1.51 (m, 1H), 1.55 (s, 1H), 1.59-1.69 (m, 4H), 1.65 (s, 1H), 1.73-1.81 (m, 1H), 1.85-1.96 (m, 2H), 1.97 (s, 3H), 1.98-2.04 (m, 2H), 2.04-2.12 (m, 2H), 2.16 (ddd, $J = 16.5, 6.1, 6.1$ Hz, 1H), 2.49 (ddd, $J = 13.9, 2.7, 2.7$ Hz, 1H), 2.58 (ddd, $J = 13.9, 9.8, 5.4$ Hz, 1H), 2.97 (dd, $J = 14.3, 6.8$ Hz, 1H), 3.08 (dd, $J = 14.9, 8.3$ Hz, 1H), 3.14 (dd, $J = 14.3, 3.2$ Hz, 1H), 3.21 (dd, $J = 15.4, 6.1$ Hz, 1H), 3.33-3.40 (m, 1H), 3.40-3.48 (m, 1H), 3.54-3.62 (m, 1H), 3.70 (s, 3H), 4.31 (dd, $J = 11.4, 5.3$ Hz, 1H), 4.47-4.53 (m, 1H), 4.60 (dd, $J = 6.6, 3.5$ Hz, 1H), 4.69-4.77 (m, 2H), 4.77-4.83 (m, 1H), 5.02-5.09 (m, 4H), 6.23 (ddd, $J = 15.9, 5.3, 5.3$ Hz, 1H), 6.47-6.59 (m, 4H), 6.81 (d, $J = 8.4$ Hz, 2H), 6.88 (apt t, $J = 9.1$ Hz, 1H), 7.11-7.19 (m, 5H), 7.20 (d, $J = 8.4$ Hz, 2H), 7.53-7.58 (m, 2H), 7.70 (s, 1H). ^{13}C NMR (CDCl_3 , 125 MHz): δ 174.9, 173.4, 173.1, 172.6, 163.2 (d, $J_{\text{CF}} = 245$ Hz), 162.5, 160.5 (d, $J_{\text{CF}} = 245$ Hz), 158.5, 138.8, 137.6, 134.6, 133.2, 132.8, 132.8, 132.4, 131.7, 131.2, 130.5 (d, $J_{\text{CF}} = 7.7$ Hz), 130.3, 126.9, 126.7, 124.64, 124.61 (d, $J_{\text{CF}} = 3.6$ Hz), 120.2, 116.18 (d, $J_{\text{CF}} = 21.5$ Hz), 116.16, 109.1, 108.4, 103.6, 89.6, 82.6, 77.5, 68.7, 60.8, 55.8, 55.7, 55.2, 54.1, 51.9, 45.5, 38.7, 38.1, 35.4, 34.0, 30.3, 29.7, 27.9, 27.8, 27.8, 27.6, 25.9, 22.3, 18.0, 17.9. MS (ESI) Calculated for $\text{C}_{60}\text{H}_{67}\text{F}_2\text{N}_6\text{O}_7$ $[\text{M}+\text{H}]^+$: 1020.5, found 1021.2.

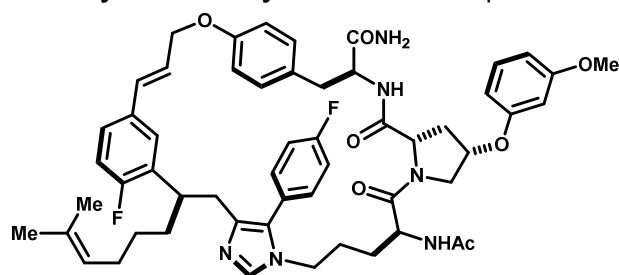
Acyclic intermediate 60a and d5-isotopologue 60d. **60a**: Acyclic intermediate **60a** (364 mg, 64%) was prepared from template **17** (1600 μL of 0.3 M DMF soln, 480 μmol) and peptide **48a** (404 mg, 730 μmol) analogously to **59a**.



^1H NMR (CD_3OD , 600 MHz): δ 1.02-1.17 (m, 2H), 1.47 (s, 3H), 1.51-1.60 (m, 1H), 1.61 (s, 3H), 1.61-1.71 (m, 3H), 1.75-1.88 (m, 4H), 1.94 (s, 6H), 1.96 (s, 3H), 2.36 (ddd, $J = 13.8, 2.8, 2.8$ Hz, 1H), 2.52 (ddd, $J = 14.0, 9.6, 5.1$ Hz, 1H), 2.95-3.02 (m, 2H), 3.05-3.18 (m, 3H), 3.73 (s, 3H), 3.76-3.92 (m, 3H), 4.17 (dd, $J = 11.3, 4.8$ Hz, 1H), 4.50-4.58 (m, 3H), 4.70-4.74 (m, 2H), 4.92-4.97 (m, 1H), 5.04-5.08 (m, 1H),

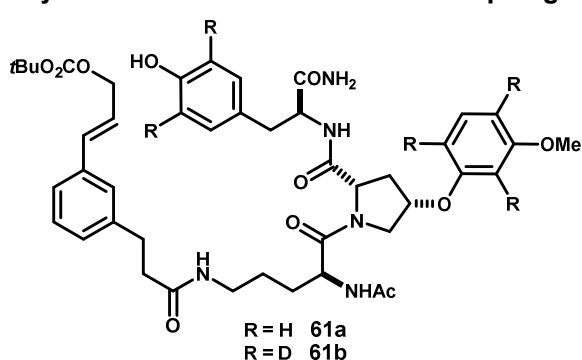
6.12 (ddd, $J = 15.8, 6.5, 6.5$ Hz, 1H), 6.48 (d, $J = 15.8$ Hz, 1H), 6.51-6.58 (m, 3H), 6.66 (d, $J = 8.5$ Hz, 2H), 6.78 (dd, $J = 9.8, 8.8$ Hz, 1H), 6.98-7.02 (m, 3H), 7.03 (d, $J = 8.5$ Hz, 2H), 7.13-7.20 (m, 2H), 7.27-7.32 (m, 2H), 7.64 (s, 1H). ^{13}C NMR (CDCl_3 , 150 MHz): δ 175.4, 173.5, 173.2, 172.5, 163.1 (d, $J_{\text{CF}} = 245$ Hz), 162.5, 162.2 (d, $J_{\text{CF}} = 245$ Hz), 159.4, 157.4, 153.6, 139.0, 137.9, 134.8, 133.8, 132.6, 132.5, 131.7, 131.5 (d, $J_{\text{CF}} = 13.8$ Hz), 131.3, 130.69 (d, $J_{\text{CF}} = 7.8$ Hz), 130.66, 128.5, 128.5, 127.3 (d, $J_{\text{CF}} = 8.6$ Hz), 127.1, 125.3, 123.3, 116.4 (d, $J_{\text{CF}} = 23.5$ Hz), 116.3, 116.0 (d, $J_{\text{CF}} = 21.8$ Hz), 108.9, 108.4, 106.8, 103.5, 90.9, 77.3, 69.5, 61.1, 55.8, 55.5, 54.1, 52.1, 45.6, 39.6, 38.2, 35.2, 35.0, 30.8, 29.6, 28.7, 28.5, 27.8, 25.9, 22.3, 21.6, 17.8. MS (ESI) Calculated for $\text{C}_{60}\text{H}_{70}\text{Cl}_3\text{F}_2\text{N}_6\text{O}_{10}$ $[\text{M}+\text{H}]^+$: 1177.4, found 1177.2. **60d**: Crude peptide **48d** (~ 95 μmol) was dissolved in MeOH, treated with $i\text{Pr}_2\text{EtN}$ (830 μL , 4.8 mmol), and concentrated to give 359 mg of an odorless residue. This material was treated with template **17** (320 μL of 0.3 M DMF soln, 95 μmol), powdered K_2CO_3 (46 mg, 330 μmol) and 4Å molecular sieves (133 mg), and stirred for 3 hr. 4-Fluorophenyl tosylmethyl isonitrile (**2-11**) (33 mg, 110 μmol) was added, and the mixture was stirred overnight, then diluted with MeOH, filtered through Celite and concentrated. Purification by column chromatography on SiO_2 eluted with 2→12% MeOH in CHCl_3 afforded **60d** (31 mg, 28%) as a colorless residue. MS (ESI) Calculated for $\text{C}_{60}\text{H}_{65}\text{D}_5\text{Cl}_3\text{F}_2\text{N}_6\text{O}_{10}$ $[\text{M}+\text{H}]^+$: 1182.5, found 1182.4.

Macrocyclic cinnamyl ether 64a. Compound **64a** (126 mg, 43%) was prepared analogously to **62a**. ¹H NMR (CD₃OD, 600 MHz): δ 1.45 (s, 3H), 1.46-1.54 (m, 2H), 1.55-1.68 (m, 5H), 1.60 (s, 3H), 1.68-1.80 (m, 3H), 1.96 (s, 3H), 2.48 (ddd, *J* = 13.8, 2.9 Hz, 1H), 2.56 (ddd, *J* = 14.0, 9.5, 5.4 Hz, 1H), 2.95-3.04 (m, 2H), 3.07-3.19 (m, 3H), 3.33-3.40 (m, 1H), 3.51-3.57 (m, 1H), 3.67-3.71 (m, 1H), 3.69 (s, 3H), 4.29 (dd, *J* = 11.5, 5.5 Hz, 1H), 4.49 (dd, *J* = 6.7, 6.7 Hz, 1H), 4.61 (dd, *J* = 6.7, 3.6 Hz, 1H), 4.68-4.73 (m, 2H), 4.75-4.80 (m, 1H), 4.87-4.92 (m, 1H), 5.01-5.05



(m, 1H), 6.20 (ddd, *J* = 16.1, 5.5, 5.5 Hz, 1H), 6.49-6.56 (m, 4H), 6.81 (d, *J* = 8.6 Hz, 2H), 6.86 (dd, *J* = 9.7, 8.4 Hz, 1H), 7.09-7.17 (m, 5H), 7.19 (d, *J* = 8.6 Hz, 2H), 7.46 (s, 1H), 7.53-7.57 (m, 2H). ¹³C NMR (CDCl₃, 150 MHz): δ 174.9, 173.4, 173.0, 172.6, 163.3 (d, *J*_{CF} = 244 Hz), 162.5, 161.9 (d, *J*_{CF} = 245 Hz), 159.7, 158.5, 138.8, 137.5, 134.4, 133.0, 132.5, 132.4, 132.2 (d, *J*_{CF} = 15.1 Hz), 131.7, 131.2, 131.1, 130.6 (d, *J*_{CF} = 7.5 Hz), 130.3, 127.53 (d, *J*_{CF} = 8.0 Hz), 127.49 (d, *J*_{CF} = 8.0 Hz), 127.2, 126.5, 125.2, 125.2, 116.5 (d, *J*_{CF} = 24.0 Hz), 116.2, 116.1 (d, *J*_{CF} = 21.8 Hz), 109.1, 108.4, 103.7, 77.6, 68.7, 60.9, 55.8, 55.7, 55.2, 54.1, 51.9, 45.5, 38.1, 35.4, 34.6, 30.5, 29.7, 28.5, 28.3, 27.7, 25.8, 22.3, 17.7. MS (ESI) Calculated for C₅₅H₆₃F₂N₆O₇ [M+H]⁺: 957.5, found 957.2.

Acyclic intermediate 61a and d3-isotopologue 61d. **61a:** Peptide **48a** (56 mg, 140 μmol) and template

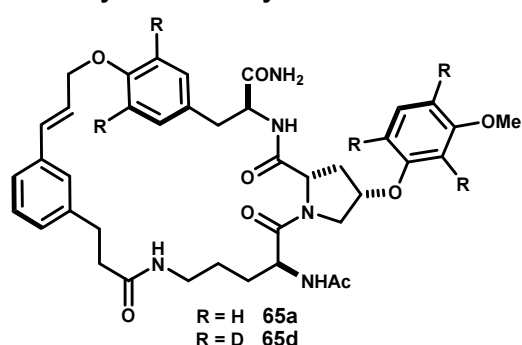


3 (116 mg, 210 μmol) were dissolved in DMF (1 mL), and the mixture was stirred for 4 hrs, then partitioned between EtOAc and sat. NaHCO₃. The organic phase was washed with sat. NaHCO₃ (x2), brine, dried over Na₂SO₄ and concentrated. Purification by column chromatography on SiO₂ eluted with 2→12% MeOH in CHCl₃ afforded **61a** (93 mg, 79%) as a colorless film.

¹H NMR (CD₃OD, 600 MHz): δ 1.40-1.54 (m, 2H), 1.46 (s, 9H), 1.54-1.67 (m, 2H), 1.95 (s, 3H), 2.32 (br d, *J* = 14.0 Hz, 1H), 2.42-2.51 (m, 2H), 2.88 (t, *J* = 7.5 Hz, 2H), 2.95 (d, *J* = 6.4 Hz, 2H), 3.04-3.12 (m, 1H), 3.12-

3.21 (m, 1H), 3.69 (s, 3H), 3.80 (br d, *J* = 11.0 Hz, 1H), 4.17 (dd, *J* = 11.1, 4.7 Hz, 1H), 4.43-4.49 (m, 1H), 4.49-4.55 (m, 2H), 4.63-4.68 (m, 2H), 5.02-5.07 (m, 1H), 6.28 (dt, *J* = 15.9, 6.4 Hz, 1H), 6.48-6.55 (m, 3H), 6.61 (d, *J* = 15.9 Hz, 1H), 6.64 (d, *J* = 8.4 Hz, 2H), 6.99 (d, *J* = 8.4 Hz, 2H), 7.02-7.12 (m, 1H), 7.14-7.26 (m, 4H), 7.88 (s, 0.4H). ¹³C NMR (CDCl₃, 150 MHz): δ 175.4, 175.1, 174.1, 173.2, 172.7, 162.4, 159.3, 157.3, 154.9, 142.6, 137.7, 135.0, 131.6, 131.2, 129.8, 129.2, 128.5, 127.8, 125.6, 124.2, 116.2, 108.7, 108.4, 103.4, 82.9, 77.3, 68.4, 68.1, 61.2, 55.7, 54.2, 52.4, 39.7, 38.9, 38.3, 35.1, 32.8, 29.4, 28.0, 26.2, 22.2. MS (ESI) Calculated for C₄₅H₅₈N₅O₁₁ [M+H]⁺: 844.4, found 845.4. **61b:** Compound **61b** (12 mg, 25%) was prepared analogously from template **3** and peptide **48d**. MS (ESI) Calculated for C₄₅H₅₃D₅N₅O₁₁ [M+H]⁺: 849.4, found 849.4.

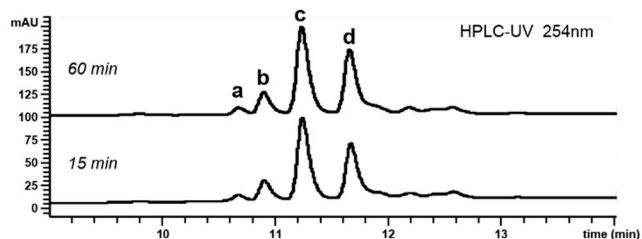
Macrocyclic cinnamyl ether 65a and d3-isotopologue 65d. **65a:** Compound **65a** (128 mg, 61%) was prepared analogously to **62a**. ¹H NMR (600 MHz, CD₃OD): δ 1.30-1.44 (m, 3H), 1.47-1.54 (m, 1H), 1.95 (s, 3H), 2.37-



2.42 (m, 2H), 2.52-2.55 (m, 2H), 2.84-2.96 (m, 2H), 2.98 (dd, *J* = 14.1, 6.7 Hz, 2H), 3.05-3.12 (m, 2H), 3.71 (s, 3H), 3.74 (d, *J* = 10.8 Hz, 1H), 4.27 (dd, *J* = 11.5, 4.9 Hz, 1H), 4.43 (apt t, *J* = 6.6 Hz, 1H), 4.45 (dd, *J* = 6.6, 4.1 Hz, 1H), 4.67 (d, *J* = 6.3 Hz, 1H), 4.78 (d, *J* = 5.9 Hz, 2H), 5.06-5.10 (m, 1H), 6.27 (ddd, *J* = 16.1, 5.9, 5.9 Hz, 1H), 6.49-6.57 (m, 3H), 6.64 (d, *J* = 16.1 Hz, 1H), 6.80 (d, *J* = 8.5 Hz, 2H), 7.06 (br d, *J* = 7.6 Hz, 1H), 7.13-7.19 (m, 4H), 7.21 (dd, *J* = 7.6, 7.6 Hz, 1H),

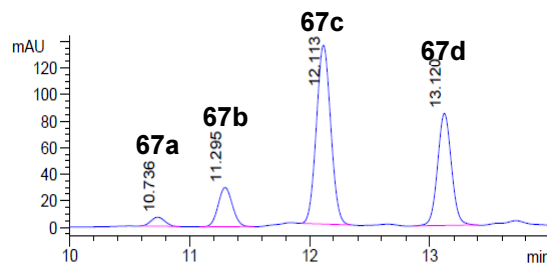
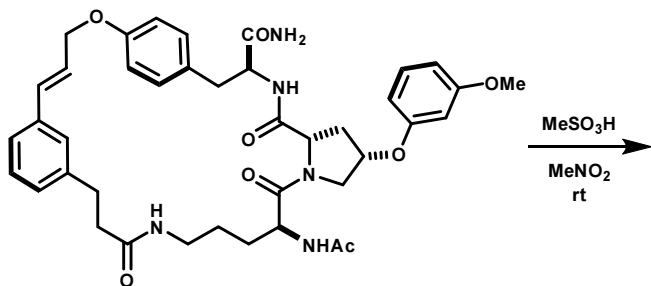
7.26 (br s, 1H). ^{13}C NMR (151 MHz, CD_3OD): δ 175.4, 175.2, 174.2, 173.2, 172.9, 162.5, 159.5, 158.7, 142.5, 138.1, 134.0, 131.7, 131.2, 130.0, 129.8, 129.3, 126.9, 126.5, 126.2, 116.4, 108.9, 108.3, 103.6, 77.6, 71.4, 61.1, 55.7, 55.4, 54.3, 52.2, 39.9, 38.9, 37.9, 35.1, 32.6, 29.5, 26.1, 22.1. MS (ESI) Calculated for $\text{C}_{40}\text{H}_{48}\text{N}_5\text{O}_8$ $[\text{M}+\text{H}]^+$: 726.4, found 726.4. **65d**: Compound **65d** (4.9 mg, 48%) was prepared from acyclic intermediate **61d** analogously to **65a**. MS (ESI) Calculated for $\text{C}_{40}\text{H}_{43}\text{D}_5\text{N}_5\text{O}_8$ $[\text{M}+\text{H}]^+$: 731.4, found 731.4.

Analytical scale acidolysis of *d*3-isotopologue **65d**.



Macrocyclic ether **65d** (1.3 mg, 1.8 μmol) was suspended in MeNO_2 (360 μL) and treated with MeSO_3H (1.7 μL). The mixture was stirred at rt for 15 min, then an aliquot (50 μL) was removed, quenched into *i* Pr_2EtN in MeOH (1M, 200 μL), and taken to dryness. The residue was reconstituted in MeOH and subjected to HPLC-UV/MS analysis (20 \rightarrow 80% ACN + 0.1% HCO_2H over 15 min, 1 mL/min, Waters Sunfire C18 4.6x150mm, 5 μ).

Acidolysis of 65a and purification of products. Macrocyclic ether **65a** (128 mg, 180 μmol) was suspended in MeNO_2 (36 mL) and treated with MeSO_3H (172 μL). The mixture was stirred at rt for 1 hr, then partitioned between sat. NaHCO_3 and EtOAc . The organic phase was washed with brine, dried over Na_2SO_4 and concentrated to give 123 mg of a beige solid, which was dissolved in $\text{DMF}:\text{MeOH}$ (5:1) and purified by semi-preparative HPLC (see method below) to give compounds **67a** (3.8 mg, 3%), **67b** (8.3 mg, 6%), **67c** (38.5 mg, 30%) and **67d** (27.6 mg, 21%).



Analytical HPLC method:

Column: Waters Sunfire™ C₁₈, 4.6x250mm, 5 μm .

Solvent A: H_2O + 0.1%v TFA

Solvent B: ACN + 0.1%v TFA

Flow rate: 1.00 ml/min

Time	%B
0	35
2	35
22	70
30	100
40	100
45	35
47	35

Semi-preparative HPLC method:

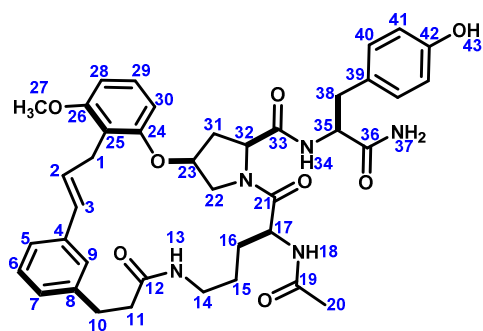
Column: Waters Sunfire™ C₁₈, 10x250mm, 5 μm .

Solvent A: H_2O + 0.1%v TFA

Solvent B: ACN + 0.1%v TFA

Flow rate: 7.50 ml/min

Time	%B
0	30
2	30
22	65
23	30
25	30



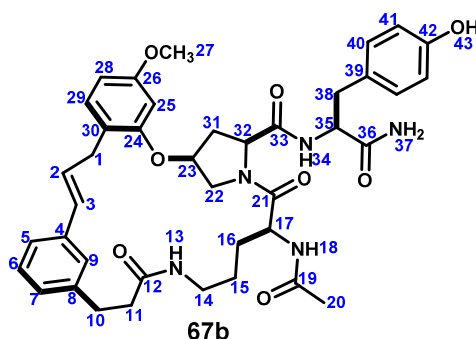
67a

(600MHz, DMSO-*d*₆, 298K)

	¹³ C	¹ H	key correlations
1	25.9	3.43-3.49 (m, 2H) overlap	HMBC 1→24,25,26
2	128.0	6.32(ddd, J=15.8, 6.1, 6.1Hz, 1H)	HMBC 2→1,4,25 COSY 2→1,3
3	129.2	6.27(d, J=15.8Hz, 1H)	HMBC 3→1,4
4	136.9	-	
5	123.7	7.05 (br d, J=7.6Hz, 1H)	
6	128.0	7.11 (dd, J=7.6Hz, 1H)	HMBC 6→4,8
7	127.0	6.96-6.99(m,1H) obscured	
8	141.1	-	
9	124.9	7.26 (br s, 1H)	TOCSY 9→5,6,7
10	30.5	2.80 (apt t, J=6.8Hz, 2H)	COSY 10→11
11	36.3	2.40(ddd, J=14.1, 7.2, 6.0Hz, 1H), 2.33 (ddd, J=14.1, 7.2, 6.0Hz, 1H)	HMBC 11→12
12	171.6	-	
13	-	7.71 (t, J=5.4Hz, 1H)	HMBC 13→12
14	37.8	2.93-2.98 (m, 1H), 2.87-2.92 (m, 1H) overlap	
15	24.6	1.28-1.36 (m, 2H) overlap	HMBC 15→21
16	28.3	1.57-1.63 (m, 1H) 1.28-1.36 (m, 1H) overlap	HMBC 16→21
17	49.2	4.37-4.41 (m, 1H) overlap	
18	-	7.75 (d, J=8.1Hz, 1H)	
19	169.2	-	
20	21.9	1.81 (s, 3H)	
21	171.4	-	
22	51.8	4.37-4.41 (m, 1H) overlap, 3.43-3.49 (m, 1H) overlap	
23	74.1	5.05 (apt p, J=6.5Hz, 1H)	HMBC 23→24,32 COSY 23→22,31
24	155.9	-	
25	116.0	-	
26	157.8	-	
27	55.6	3.78 (s, 3H)	HMBC 27→26
28	104.3	6.67 (d, J=8.3Hz, 1H)	HMBC 28→25,26
29	127.3	7.18 (t, J=8.3Hz, 1H)	HMBC 29→26

30	105.4	6.75 (d, J=8.3Hz, 1H)	HMBC 30→24,25
31	34.1	2.57 (ddd, J=13.0, 8.5, 6.5Hz, 1H), 2.03 (ddd, J=13.0, 6.5, 6.5Hz, 1H)	COSY 31→32
32	58.1	4.35-4.39 (m, 1H) obscured	HMBC 32→33
33	170.2	-	
34	-	7.75 (d, J = 8.1Hz, 1H)	
35	53.9	4.28 (ddd, J=8.1, 8.1, 5.6Hz, 1H)	TOCSY 35→34,38 HMBC 35→33,36
36	172.5	-	
37	-	7.26 (br s, 1H), 7.11 (br s, 1H)	HMBC 37→36
38	36.1	2.86 (dd, J=13.7, 5.6Hz, 1H), 2.76 (dd, J=13.7, 8.1Hz, 1H)	HMBC 38→39, 40
39	127.7	-	
40	130.0	6.98 (d, J=8.5Hz, 2H)	
41	114.6	6.58(d, J=8.5Hz, 2H)	
42	155.7	-	
43	-	9.13 (br s, 1H)	

MS m/z 726.4 (calc'd: C₄₀H₄₈N₅O₈, [M+H]⁺, 726.3).

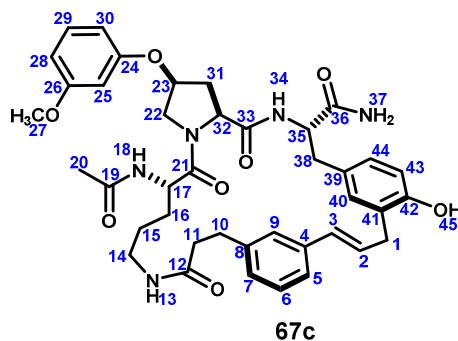


(600MHz, DMSO-*d*₆, 298K)

	¹³ C	¹ H	key correlations
1	33.5	3.63 (dd, J=14.5,6.1Hz, 1H), 3.13 (dd, J=14.5, 7.2Hz, 1H)	HMBC 1→24,30
2	129.0	6.42 (ddd, J=15.8, 7.2, 6.1Hz, 1H)	COSY 2→1 HMBC 2→4,30
3	129.0	6.30 (br d, J=15.8Hz, 1H)	HMBC 3→4
4	137.0	-	
5	124.0	7.03 (br d, J=7.7Hz, 1H)	TOCSY 5→6,7,9
6	128.0	7.12 (dd, J=7.6, 7.6Hz, 1H)	HMBC 6→4,8
7	127.0	6.98 (br d, J=7.7Hz, 1H)	
8	141.2	-	
9	124.6	7.33 (br s, 1H)	
10	30.5	2.74-2.82 (m, 1H) overlap	HMBC 10→7,8
11	36.4	2.41 (ddd, J=14.1, 7.6, 5.6Hz, 1H), 2.34 (ddd, J=14.1, 8.4, 5.5Hz, 1H)	HMBC 11→8,12 COSY 11→10
12	171.1	-	
13	-	7.74 (apt t, J=5.2Hz, 1H) obscured	HMBC 13→12
14	37.7	2.89-2.96 (m, 2H) obscured	COSY 14→13
15	24.5	1.27-1.38 (m, 2H) overlap	COSY 15→14

16	28.1	1.58-1.65 (m, 2H) overlap	COSY 16→15
17	49.3	4.43 (apt dd, J = 13.8, 7.0Hz, 1H)	HMBC 17→19,21 COSY 17→16,18
18	-	8.12 (d, J=7.6Hz, 1H)	HMBC 18→19
19	169.2	-	
20	21.9	1.81 (s, 3H)	HMBC 20→19
21	171.6	-	
22	51.5	4.49 (dd, J=10.2, 6.4Hz, 1H) 3.47 (dd, J=10.2, 6.2Hz, 1H)	
23	73.6	5.08 (apt q, J=6.4Hz, 1H)	HMBC 23→24 COSY 23→22
24	155.8	-	
25	99.5	6.69 (d, J=2.3Hz, 1H)	HMBC 25→24,26
26	159.3	-	
27	54.9	3.76 (s, 3H)	HMBC 27→26
28	105.4	6.49 (dd, J=8.3, 2.3Hz, 1H)	HMBC 28→30
29	130.5	7.10 (d, J=8.3Hz, 1H) overlap	
30	120.6	-	
31	34.1	2.59 (ddd, J=13.0, 8.3, 6.7Hz, 1H), 2.01 (ddd, J=13.0, 7.0, 7.0Hz, 1H)	HMBC 31→33
32	58.1	4.35 (apt t, J=8.0Hz, 1H)	HMBC 32→33
33	170.3	-	
34	-	7.74 (d, J=8.3Hz, 1H) overlap	HMBC 34→33
35	53.8	4.30 (ddd, J=8.3, 8.1, 2.7Hz, 1H)	HMBC 35→36
36	172.6	-	
37	-	7.09 (s, 1H) obscured, 7.02 (s, 1H) obscured	HMBC 37→36
38	36.1	2.88 (dd, J=13.6, 5.3Hz, 1H), 2.74-2.82 (m, 1H) overlap	HMBC 38→36,39
39	127.8	-	
40	130.1	7.01 (d, J=8.4Hz, 2H)	
41	114.5	6.59 (d, J=8.4Hz, 2H)	HMBC 41→39 COSY 41→40
42	155.7	-	
43	-	9.13 (br s, 1H)	

MS m/z 726.4 (calc'd: $C_{40}H_{48}N_5O_8$, $[M+H]^+$, 726.3).

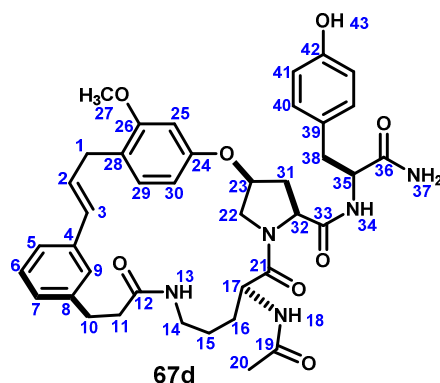


(600MHz, DMSO-*d*₆, 298K)

	¹³ C	¹ H	key correlations
1	31.6	3.46 (dd, J=16.4, 6.3Hz, 1H), 3.28 (dd, J=16.4, 7.7Hz, 1H)	HMC 1→42
2	128.8	6.34 (ddd, J=15.7, 7.7, 6.3Hz, 1H)	COSY 2→1,3 HMBC 2→4
3	130.8	6.46 (br d, J=15.7Hz, 1H)	HMBC 3→4
4	137.2	-	
5	124.4	7.10 (br d, J = 7.7Hz, 1H)	TOCSY 5→6,7,9
6	128.3	7.18 (dd, J=7.7, 7.7Hz, 1H)	HMBC 6→8,4
7	127.2	7.03 (br d, J=7.7Hz, 1H)	
8	141.4	-	
9	124.3	7.43 (br s, 1H)	HMBC 9→10
10	30.8	2.81 (apt t, J=7.5Hz, 2H)	HMBC 10→8
11	37.1	2.43 (apt t, J=7.5Hz, 2H)	HMBC 11→8
12	171.2	-	
13	-	7.58 (t, J=5.5Hz, 1H)	HMBC 13→12
14	37.8	3.00-3.06 (m, 1H), 2.91-2.97 (m, 1H)	COSY 14→13
15	24.6	1.30-1.43 (m, 2H) overlap	
16	28.6	1.55-1.63 (m, 1H), 1.30-1.43 (m, 1H) overlap	HMBC 16→21
17	50.0	4.40-4.45 (m, 1H) obscured	TOCSY 17→14,15,16 COSY 17→16 HMBC17→21
18	-	8.10 (d, J=7.4Hz, 1H)	HMBC 18→19
19	169.2	-	
20	22.2	1.82 (s, 3H)	HMBC 20→19
21	171.8	-	
22	52.2	4.28 (s, J=11.3, 5.6Hz, 1H), 3.69 (d, J=11.3, 3.3Hz, 1H)	
23	75.1	5.04-5.08 (m, 1H)	COSY 23→22
24	158.0	-	
25	101.5	6.48 (br s, 1H)	HMBC 25→24
26	160.5	-	
27	54.7	3.58 (s, 3H)	
28	107.1	6.47-6.52 (m, 1H) obscured	
29	130.1	7.12 (dd, J=8.5, 8.5Hz, 1H)	
30	107.1	6.47-6.52 (m, 1H) obscured	HMBC 30→24
31	33.8	2.45-2.49(m, 1H) obscured, 2.09(ddd, J=13.5, 3.9, 3.9Hz, 1H)	

32	58.8	4.40-4.45 (m, 1H) obscured	
33	170.1	-	
34	-	7.29-7.32 (m, 1H) obscured	TOCSY 34→35,38
35	54.0	4.30 (dd, J=15.1, 7.4Hz, 1H)	HMBC 35→39
36	172.6	-	
37	-	7.31 (br s, 1H) overlap, 7.14 (br s, 1H)	TOCSY 37→37' HMBC 37→36
38	37.4	2.43 (dd, J=7.4, 7.4Hz, 2H)	HMBC 38→35,36,39
39	127.3	-	
40	130.0	6.89 (br s, 1H) overlap	
41	125.8	-	
42	153.3	-	
43	114.4	6.70 (d, J=7.9Hz, 1H)	HMBC 43→39,41 TOCSY 43→40, 44
44	127.4	6.85-6.90 (m, 1H) obscured	
45	-	9.17 (br s, 1H)	

MS m/z 726.4 (calc'd: C₄₀H₄₈N₅O₈, [M+H]⁺, 726.3).



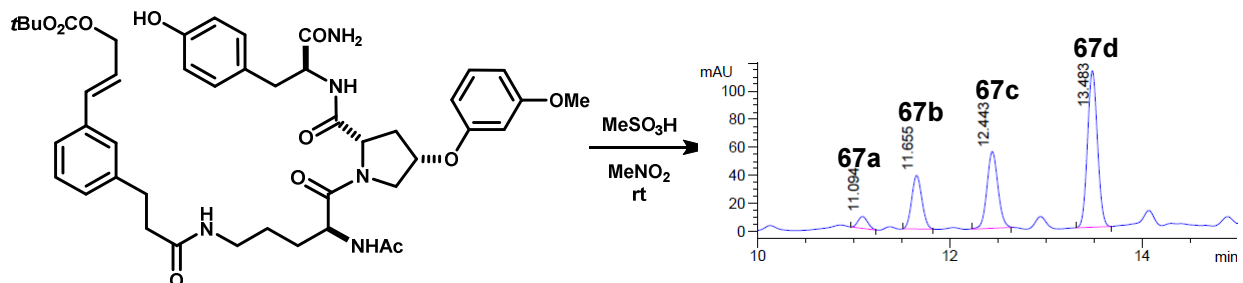
(600MHz, DMSO-*d*₆, 298K)

	¹³ C	¹ H	key correlations
1	32.1	3.48 (dd, J=14.8, 5.5Hz, 1H), 3.27 (dd, J=14.8, 6.5Hz, 1H)	HMBC 1→26
2	129.3	6.17 (ddd, J=15.6, 6.5, 6.5Hz, 1H)	HMBC 2→4
3	128.8	6.26 (d, J=15.6Hz, 1H)	TOCSY 3→1, 2 HMBC 3→5,9
4	137.1	-	
5	124.4	7.07 (d, J=7.9Hz, 1H) overlap	TOCSY 5→6,7,9
6	128.1	7.16 (dd, J=7.5, 7.5Hz, 1H) obscured	HMBC 6→4,8
7	127.1	6.97 (br d, J = 7.4Hz, 1H)	
8	141.7	-	
9	123.3	7.10 (br s, 1H)	
10	35.9	2.23-2.28 (m, 2H)	
11	29.7	2.82-2.29 (m, 1H), 2.69-2.75 (m, 1H) obscured	HMBC 11→8, 12
12	171.4	-	
13	-	7.72 (dd, J=5.2, 5.2Hz, 1H)	TOCSY 13→14,15,16,17,18 HMBC 13→12
14	37.9	2.63-2.75 (m, 2H) obscured	

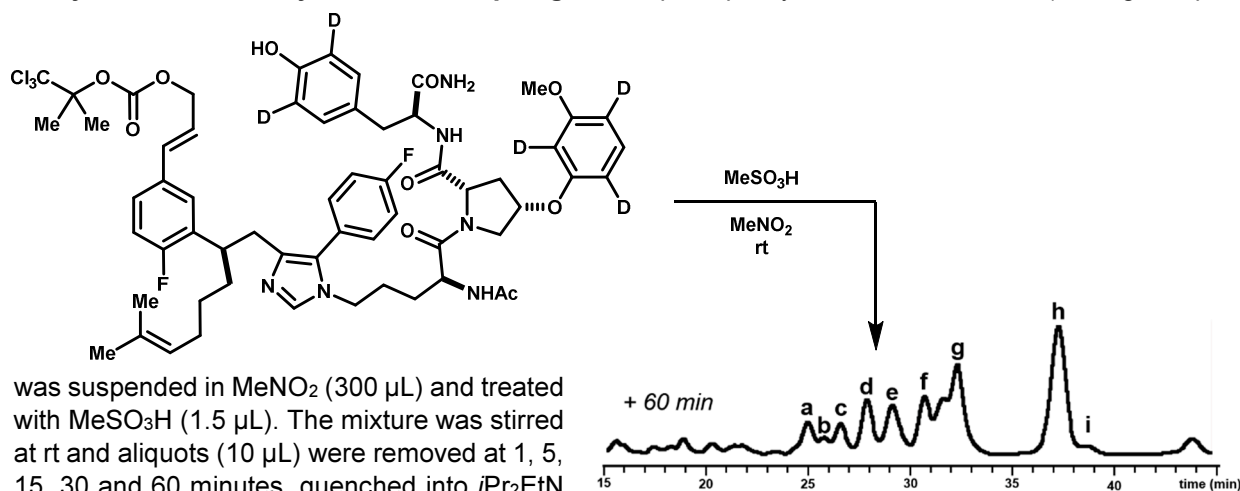
15	24.9	1.19-1.33 (m, 2H)	
16	28.3	1.33-1.47 (m, 2H)	
17	49.6	4.21-4.26 (m, 1H)	COSY 17→18
18	-	8.09 (d, J=8.1Hz, 1H)	HMBC 18→19
19	169.3	-	
20	22.0	1.77 (s, 3H)	HMBC 20→19
21	171.9	-	
22	51.0	3.76 (dd, J=11.4, 3.2Hz, 1H), 3.61 (br d, J=11.4Hz, 1H)	TOCSY 22→22',23,31,32
23	75.9	5.21 (apt dd, J=3.9, 3.9 Hz, 1H)	
24	155.9	-	
25	101.6	6.60 (s, 1H) obscured	
26	157.9	-	
27	55.3	3.72 (s, 3H)	HMBC 27→26
28	121.3	-	
29	130.2	7.06 (d, J=7.9Hz, 1H) overlap	
30	107.3	6.57-6.62 (m, 1H) obscured	
31	34.2	2.53-2.59 (m, 1H), 2.23-2.28 (m, 1H)	HMBC 31→33
32	59.5	4.30 (br d, J=10.8Hz, 1H)	HMBC 32→33
33	169.8	-	
34	-	7.24 (d, J=7.7Hz, 1H)	
35	53.5	4.39 (apt dd, J=13.4, 6.6Hz, 1H)	COSY 35→34,38 HMBC 35→33,36
36	172.5	-	
37	-	7.32 (br s, 1H)	HMBC 37→36
38	37.2	2.96 (dd, J=13.8, 5.9Hz, 1H), 2.83 (dd, J=13.8, 6.6Hz, 1H)	HMBC 38→39
39	127.4	-	
40	130.2	7.00 (d, J=8.3Hz, 2H)	
41	114.5	6.59 (d, J=8.3Hz, 2H)	HMBC 41→39
42	155.9	-	
43	-	9.03 (br s, 1H)	

MS m/z 726.4 (calc'd: $C_{40}H_{48}N_5O_8$, $[M+H]^+$, 726.3).

Acidolysis of acyclic precursor 61a. Acidolysis of acyclic intermediate **61a** (9.3 mg, 11 μ mol) was carried out in the same manner as for substrate **65a**. An aliquot was removed after 60 minutes, and subjected to the quench and analysis protocols used for substrate **65a**.



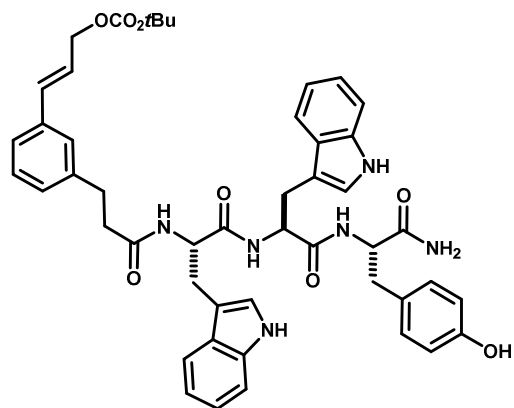
Analytical scale acidolysis of *d*5-isotopologue 60d (68a-i). Acyclic intermediate **60d** (1.8 mg, 1.5 μmol)



was suspended in MeNO₂ (300 μL) and treated with MeSO₃H (1.5 μL). The mixture was stirred at rt and aliquots (10 μL) were removed at 1, 5, 15, 30 and 60 minutes, quenched into *i*Pr₂EtN

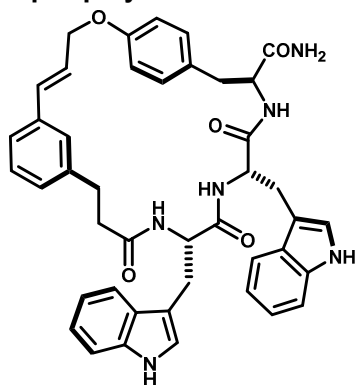
in MeOH (1M, 200 μL), and taken to dryness. The residue was reconstituted in MeOH (500 μL) and subjected to HPLC-UV/MS analysis (isocratic 37.5% ACN + 0.1% TFA, 50 min, 1 mL/min, Waters XSelect C18 4.6x150mm, 5 μ). MS (ESI) Calculated for C₅₅H₅₉D₄F₂N₆O₇ [M+H]⁺: 961.5. observed: **68a**: 961.4 *m/z*. **68a**: 994.3 *m/z*. **68c**: 961.3 *m/z*. **68d**: 961.3 *m/z*. **68e**: 997.2 *m/z*. **68f**: 961.4 *m/z*. **68g**: 997.2 *m/z*. **68h**: 997.3 *m/z*. **68i**: 1201.3 *m/z*.

Trp-Trp-Tyr Derived acyclic intermediate (69). An oven-dried, screw-capped scintillation vial was



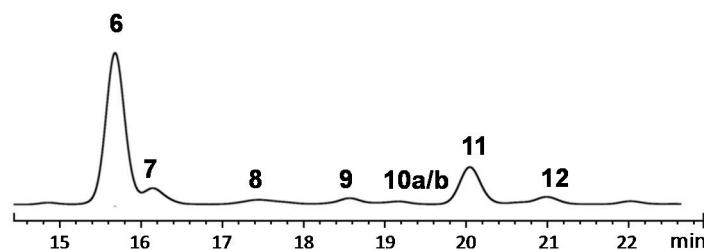
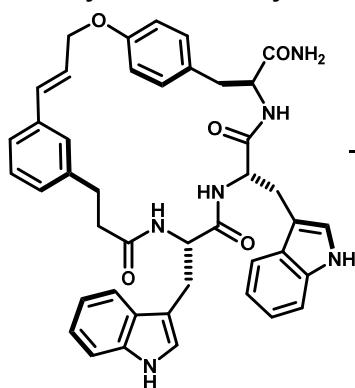
charged with Trp-Trp-Tyr·TFA (343 mg, 0.515 mmol) and template **3** (208 mg, 0.515 mmol) followed by addition of anhydrous DMF (10 ml) and *i*Pr₂NEt (359 μl, 2.06 mmol). The reaction was allowed to stir at room temperature for 3 hours. The DMF was removed by rotary evaporation and the residue was dissolved in MeCN/CHCl₃ (1:3) and purified by column chromatography (SiO₂, gradient 0→10% MeOH/CHCl₃) to give **69** as a white solid (337 mg, 0.402 mmol, 78%). ¹H NMR (DMSO-*d*₆, 600 MHz): δ 10.79 (br. s, 1H), 10.7 (br s, 1H), 9.13 (br s, 1H), 8.07 (d, *J* = 6.8 Hz, 1H), 8.01 (d, *J* = 7.4 Hz, 1H), 7.82 (d, *J* = 8.7 Hz, 1H), 7.56 (d, *J* = 7.6 Hz, 1H), 7.49 (d, *J* = 7.6 Hz, 1H), 7.26-7.31 (m, 2H), 7.11-7.25 (m, 4H), 6.99-7.08 (m, 5H), 6.90-6.99 (m, 5H), 6.62 (d, *J* = 8.1 Hz, 2H), 6.56 (d, *J* = 15.7 Hz, 1H), 6.28 (dt, *J* = 15.4, 7.4 Hz, 1H), 4.60-4.64

(m, 2H), 4.42-4.53 (m, 2H), 4.31-4.37 (m, 1H), 3.01-3.07 (m, 2H), 2.93 (dd, *J* = 12.1, 11.3 Hz, 1H), 2.79-7.86 (m, 2H), 2.71 (dd, *J* = 10.2, 10.2 Hz, 1H), 2.56-2.62 (m, 2H), 1.4 (s, 9H). ¹³C NMR (DMSO-*d*₆, 150 MHz): δ 173.0, 172.6, 172.1, 171.5, 170.4, 157.2, 153.3, 142.1, 136.5, 136.3, 133.9, 130.7, 129.1, 128.4, 127.8, 126.9, 124.7, 124.1, 123.8, 121.3, 119.0, 118.6, 118.3, 115.9, 111.7, 110.6, 82.0, 67.4, 67.0, 58.5, 54.5, 54.0, 52.7, 40.9, 40.6. MS (ESI) Calculated for C₄₈H₅₂N₆O₈ [M+H]⁺: 841.4, found 841.1.

Trp-Trp-Tyr Derived macrocyclic ether (70).

A solution of acyclic carbonate **69** (109 mg, 0.130 mmol) in DMF (26 mL, 5mM) was sparged with Argon for 15 minutes. The septa was removed briefly to allow the addition of Pd(PPh₃)₄ (8 mg, 6.5 μmol, 5 mol%). The mixture was stirred for 1 hr, after which analysis by HPLC-UV showed complete conversion to **70**. Silica-bound thiol (Si-Thiol, Silicycle, 1.29 mmol/gram, ~25 mg) was added to the reaction mixture, mixed for 5 min, and the mixture was filtered and concentrated. Purification by column chromatography (loaded in CHCl₃/MeCN) on SiO₂ eluted with 0→10% MeOH/CHCl₃ afforded **70** as a white solid (67 mg, 0.092 mmol, 71%). ¹H NMR (DMSO-*d*₆, 500 MHz): δ 10.7 (d, *J* = 2.0 Hz, 1H), 10.64 (d, *J* = 2.0 Hz, 1H), 7.99 (d, *J* = 8.1 Hz, 1H), 7.83 (d, *J* = 7.9 Hz, 1H), 7.51 (d, *J* = 8.0 Hz, 1H), 7.48 (d, *J* = 7.8 Hz, 1H), 7.46 (d, *J* = 8.0 Hz, 1H), 7.28 (br d, *J* = 3.7 Hz, 1H), 7.26 (br d, *J* = 3.9 Hz, 1H), 7.10-7.13 (m, 3H), 6.99-7.10 (m, 6H), 6.90-6.96 (m, 3H), 6.74 (d, *J* = 8.9 Hz, 2H), 6.6 (d, *J* = 2.5 Hz, 1H),

6.47 (br d, *J* = 16.1 Hz, 1H), 6.21 (dt, *J* = 15.9, 5.9 Hz, 1H), 4.68 (dd, *J* = 15.3, 6.3 Hz, 1H), 4.6 (dd, *J* = 14.3, 5.6 Hz, 1H), 4.51 (ddd, *J* = 7.6, 7.6, 5.9 Hz, 1H), 4.34 (ddd, *J* = 10.9, 8.1, 2.8 Hz, 1H), 4.22 (app q, *J* = 7.5 Hz, 1H), 3.02 (dd, *J* = 14.8, 5.5 Hz, 1H), 2.92 (dd, *J* = 13.8, 2.6 Hz, 1H), 2.84 (dd, *J* = 14.7, 6.0 Hz, 1H), 2.70-2.77 (m, 4H), 2.59 (dd, *J* = 14.8, 7.8 Hz, 1H), 2.42-2.47 (m, 1H). ¹³C NMR (DMSO-*d*₆, 125 MHz): δ 173.8, 171.9, 171.4, 171.2, 157.0, 141.6, 136.4, 136.3, 133.4, 130.6, 130.3, 128.8, 127.9, 127.8, 126.1, 125.4, 124.8, 124.1, 124.0, 121.3, 121.2, 118.9, 118.8, 118.6, 115.1, 111.69, 111.65, 110.5, 110.3, 68.2, 54.8, 54.1, 53.5, 36.8, 36.3, 35.8, 31.2, 30.6. MS (ESI) Calculated for C₄₃H₄₂N₆O₅ [M+H]⁺: 723.3, found 723.0.

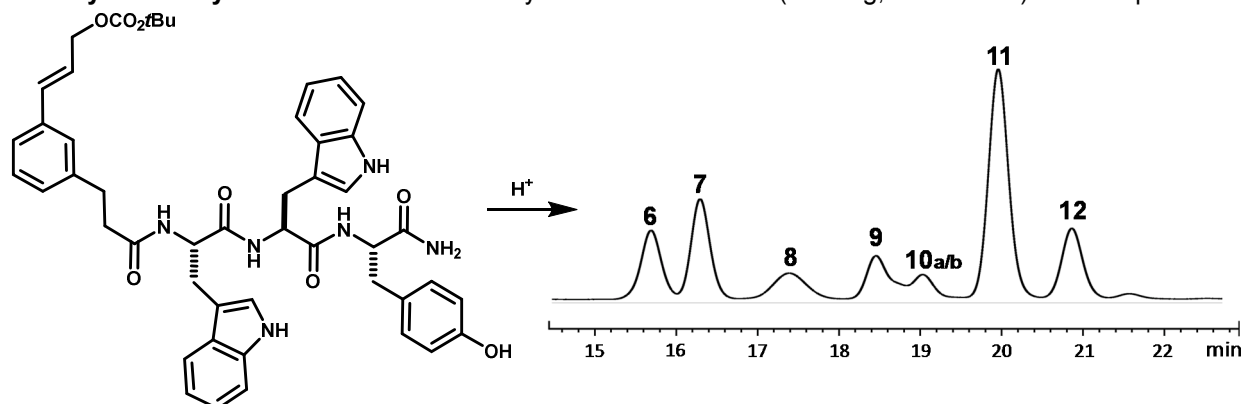
Acidolysis of macrocyclic ether 70.

Analytical HPLC: Waters Sunfire C18, 4.6x250 mm, 5.0 μ. 1 mL/min. A: H₂O + 0.1% TFA, B: ACN + 0.1% TFA

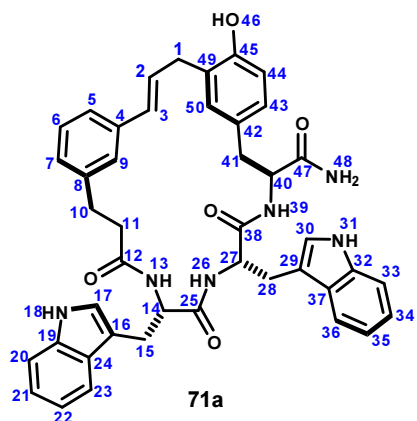
Time (min)	% A	% B
0	55	45
2	55	45
30	45	55

Tyrosyl ether **70** (80 mg, 0.11 mmol) was suspended in dry MeNO₂ (22 ml, 5 mM) under an argon atmosphere, and treated with MeSO₃H (108 μl, 1.66 mmol, 15 eq.) at rt, which caused complete dissolution. After stirring for 2 hrs, the mixture was partitioned between EtOAc and sat. NaHCO₃. The organic phase was washed with sat. NaHCO₃ (x2), brine, dried over Na₂SO₄ and concentrated. The product mixture was reconstituted in *N,N*-DMF and purified by semi-preparative RP-HPLC (Sunfire C18, 10x250 mm, 5 μ, 41→48% ACN + 0.1% TFA, 21 minutes). Fractions were pooled and concentrated under reduced pressure.

Acidolysis of acyclic intermediate 69. Acyclic intermediate **69** (330 mg, 0.39 mmol) was suspended in



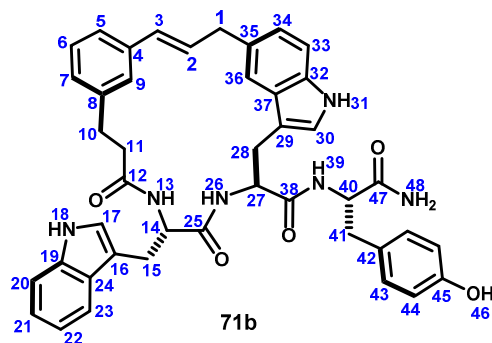
dry MeNO₂ (78 mL) under an argon atmosphere, and treated with MeSO₃H (382 μL, 5.9 mmol) at rt, which caused complete dissolution. After stirring for 2 hrs, the mixture was worked up and purified in the same manner as for the acidolysis of **70** to give **71a** (10.6 mg, 4%), **71b** (6.4 mg, 2%), **71c** (17.3 mg, 6%), **71d** (18.8 mg, 8%), **71e** (22 mg, 8%), **71f** (12.2 mg, 4%), **71g** (10.5 mg, 4%), and **71h** (51 mg, 18%).



(500MHz, DMSO-*d*₆, 298K)

	¹³ C	¹ H	key correlations
1	31.9	3.31-3.42 (m, 2H)	TOCSY→2,3 HMBC→45, 2, 3, 49
2	128.7	6.34 (dt, J = 15.7, 6.6 Hz, 1H)	TOCSY→1, 3 HMBC→3, 4
3	130.8	6.22 (br. d, J = 15.9 Hz, 1H)	TOCSY→1, 2 HMBC→2, 5
4	137.2	-	-
5	123.0	7.02 (m, 1H) overlap	HMBC→7
6	128.1	7.04 (m, 1H) overlap	HMBC→4,8
7	128.0	7.03 (m, 1H) overlap	HMBC→5
8	141.2	-	-
9	126.0	7.08 (m, 1H) overlap	HMBC→7, 5
10	30.4	2.57 (ddd, J = 11.6, 8.3, 2.7 Hz, 1H), 2.84 (m, 1H) overlap	TOCSY→10', 11, 11' HMBC→12, 8, 7
11	36.0	2.23 (ddd, J = 12.3, 8.3, 3.2 Hz, 1H), 2.38 (ddd, J = 12.4, 9.3, 3.1 Hz, 1H)	TOCSY→11', 10, 10, HMBC→12, 8
12	171.6	-	-
13	-	7.91 (d, J = 8.4 Hz, 1H)	HMBC→12

14	53.2	4.37 (m, 1H) overlap	TOCSY→13, 15, 15' HMBC→16, 25, 15
15	26.9	2.92-3.02 (m, 1H), 2.69-2.72 (m, 1H) overlap	TOCSY→15', 13 HMBC→16, 17, 24, 14
16	110.4	-	-
17	123.5	6.94 (m, 1H), overlap	HMBC→16
18	-	10.68 (d, J = 1.8 Hz, 1H)	HMBC→16, 19, 24, 20
19	136.0	-	-
20	111.3	7.29 (br. d, J = 6.3 Hz, 1H)	COSY→21 HMBC→22, 24
21	120.8	7.02 (m, 1H) overlap	COSY→20, 22 HMBC→19, 23
22	118.1	6.91 (m, 1H) overlap	COSY→22, 21 HMBC→20, 24
23	118.0	7.48 (br. d, J = 8.0 Hz, 1H)	COSY→22 HMBC→16, 24, 19
24	127.5	-	-
25	171.3	-	-
26	-	7.46 (d, J = 7.5 Hz, 1H)	TOCSY→27, 28, 28' HMBC→25
27	53.6	4.34 (m, 1H) overlap	TOCSY→26 HMBC→38, 29, 28
28	27.3	2.96 (m, 1H) overlap, 2.72 (m, 1H) overlap	COSY→27 HMBC→27, 29, 38, 37, 30
29	109.6	-	-
30	123.2	6.71 (s, 1H) overlap	HMBC→29
31	-	10.69 (d, J = 1.8 Hz, 1H)	HMBC→32, 29, 37
32	136.0	-	-
33	111.3	7.28 (br. d, J = 6.4 Hz, 1H)	COSY→34 HMBC→35
34	120.7	7.03 (m, 1H) overlap	COSY→33 HMBC→36, 32
35	118.0	6.89 (m, 1H) overlap	COSY→36 HMBC→33, 37
36	118.1	7.43 (br. d, J = 8.1 Hz, 1H)	COSY→35 HMBC→29, 34, 32, 38
37	127.4	-	-
38	120.7	-	-
39	-	7.98 (d, J = 8.2 Hz, 1H)	TOCSY→40 HMBC→38
40	53.2	4.39 (m, 1H)	TOCSY→41, 41', 39 HMBC→47, 41
41	36.3	2.73 (m, 1H) overlap, 2.84 (m, 1H) overlap	HMBC→50, 42, 43, 40
42	127.7	-	
43	127.5	6.9 (m, 1H) overlap	HMBC→45, 50
44	114.7	6.7 (d, J = 6.3 Hz, 1H)	HMBC→45 (weak), 43
45	153.4	-	-
46	-	9.13	
47	173.4	-	-
48	-	7.04, 7.30	HMBC→47
49	125.6	-	
50	131.1	7.07 (br. s, 1H) overlap	TOCSY→44 HMBC→45, 43

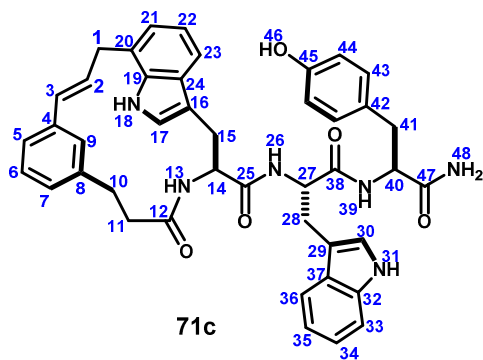


(600MHz, DMSO-*d*₆, 298K)

	¹³ C	¹ H	key correlations
1	37.7	3.57 (d, J = 6.4 Hz, 2H)	HMBC 1→3,34,35,36
2	129.4	6.47 (dt, J = 15.6, 6.4 Hz, 1H)	COSY 2→1 HMBC 2→4
3	130.6	6.27 (d, J = 15.6 Hz, 1H)	HMBC 3→4,5,9
4	136.9	-	
5	123.1	7.13 - 7.17 (m, 1H) overlap	HMBC 5→3,7,9
6	127.8	7.13 - 7.17 (m, 1H) overlap	HMBC 6→4,8
7	127.0	6.97 - 7.00 (m, 1H) overlap	HMBC 7→5,8,9
8	141.2	-	
9	124.7	7.13 - 7.17 (m, 1H) overlap	HMBC 9→7
10	29.3	2.64 (dd, J = 13.4, 8.0 Hz, 1H), 2.93 - 2.99 (m, 1H) overlap	HMBC 10→8,12
11	35.0	2.22 (dd, J = 13.6, 7.7 Hz, 1H), 2.45-2.52 (m,1 H) obscured	HMBC 11→8,12
12	170.3	-	
13	-	7.92 (d, J = 8.1 Hz, 1H)	HMBC 13→12,14 TOCSY 13→14,15
14	52.5	4.56 - 4.62 (m, 1H) overlap	
15	28.2	2.70 - 2.76 (m, 1H) overlap, 2.86 - 2.94 (m, 1H) overlap	HMBC 15→16
16	109.9	-	
17	123.2	6.81 (br s, 1H)	HMBC 17→19,24
18	-	10.72 (s, 1H) or 10.63 (s, 1H)*	
19	135.6	-	
20	110.6	7.27 (d, J = 8.4 Hz, 1H) overlap	HMBC 20→22,24
21	120.4	6.99-7.03 (m, 1H) overlap	HMBC 21→19,23
22	117.6	6.89 (dd, J = 7.4, 7.4 Hz, 1H)	HMBC 22→20,24
23	118.3	7.56 (d, J = 7.9 Hz, 1H)	HMBC 23→16,21 COSY 23→22
24	127.1	-	
25	171.1	-	
26	-	8.30 (d, J = 7.4 Hz, 1H)	TOCSY 26→27,28
27	53.8	4.56 - 4.62 (m, 1H) overlap	HMBC 27→38
28	28.0	2.89 - 2.94 (m, 1H) overlap, 3.08 (dd, J = 14.2, 7.2 Hz,1H)	HMBC 28→29
29	109.2	-	
30	123.8	6.96 - 6.99 (m, 1H) overlap	HMBC 30→29,32

31	-	10.72 (s, 1H) or 10.63 (s, 1H)*	-
32	135.6	-	-
33	110.6	7.27 (d, J = 8.4 Hz, 1H) overlap	HMBC 33→35,37
34	120.4	6.99-7.03 (m, 1H) overlap	HMBC 34→32,36
35	117.6	6.89 (dd, J = 7.4, 7.4 Hz, 1H)	HMBC 35→33,37
36	118.3	7.56 (d, J = 7.9 Hz, 1H)	HMBC 36→29,36 COSY 36→35
37	127.1	-	-
38	170.7	-	-
39	-	7.71 (d, J = 7.6 Hz, 1H)	HMBC 39→38,40,41
40	53.7	4.37 (dd, J = 13.8, 7.6 Hz, 1H)	HMBC 40→38,47
41	36.5	2.70-2.76 (m, 1H) overlap, 2.87-2.93 (m, 1H) overlap	HMBC 41→42,43,47 TOCSY 41→42
42	127.5	-	-
43	129.8	6.97 - 7.00 (m, 2H) overlap	HMBC 43→41,42,45
44	114.5	6.63 (d, J = 8.0 Hz, 2H)	COSY 44→43 HMBC 44→42
45	155.5	-	-
46	-	9.17 (br s, 1H)	HMBC 46→44,45
47	172.4	-	-
48	-	7.05 (s, 1H), 7.26 (s, 1H) overlap	HMBC 48→47

*indole NHs not assigned

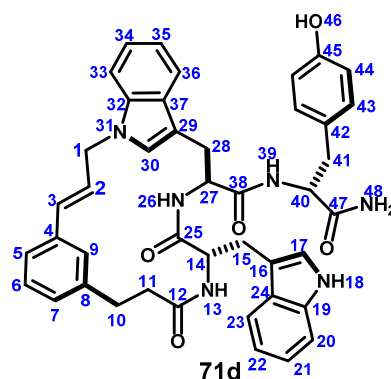


(600MHz, DMSO-*d*₆, 298K)

	¹³ C	¹ H	key correlations
1	34.0	3.47 (br d, J = 17.4 Hz, 1H), 3.92 (dd, J = 17.4, 5.5 Hz, 1H)	HMBC 1→2,3,19,20,21
2	126.8	6.13 (ddd, J = 16.4, 5.5, 2.8 Hz, 1H)	-
3	132.0	4.61 (br d, J = 16.4 Hz, 1H)	HMBC 3→5,9
4	137.3	-	-
5	120.1	7.18 (d, J = 7.7 Hz, 1H) overlap	HMBC 5→3,9
6	127.6	7.06 (dd, J = 7.7, 7.7 Hz, 1H) overlap	HMBC 6→8,4
7	126.2	6.83 (d, J = 7.7 Hz, 1H) overlap	HMBC 7→10
8	142.2	-	-

9	127.3	5.62 (s, 1H)	HMBC 9→5,3,10,7
10	26.9	2.32 (dd, H = 14.9, 7.3 Hz, 1H), 3.05 (dd, J = 14.9, 11.9 Hz, 1H)	HMBC 10→8,12
11	34.3	2.07 (dd, J = 15.5, 11.9 Hz, 1H), 2.24 (dd, J = 15.5, 7.3 Hz, 1H)	HMBC 11→8,12
12	171.9	-	-
13	-	8.05 (d, J = 7.8 Hz, 1H)	HMBC 13→12
14	53.6	4.36 (ddd, J = 12.8, 7.8, 3.1 Hz, 1H)	-
15	26.7	2.75 (dd, J = 13.9, 12.8 Hz, 1H), 3.23 (dd, J = 13.9, 3.1 Hz, 1H)	HMBC 15→16,17
16	109.6	-	-
17	124.7	7.19 (d, J = 2.4 Hz, 1H) overlap	-
18	-	10.28 (br s, 1H)	HMBC 18→17,19
19	135.7	-	-
20	123.5	-	-
21	121.5	6.93 (d, J = 6.8 Hz, 1H)	HMBC 21→1
22	118.3	6.97-7.01 (m, 1H) overlap	HMBC 22→20,24
23	117.1	7.68 (d, J = 7.8 Hz, 1H)	TOCSY 23→22,21
24	126.1	-	-
25	172.3	-	-
26	-	8.18 (d, J = 7.4 Hz, 1H)	TOCSY 26→27,28 HMBC 26→25
27	53.5	4.52 (ddd, J = 8.5, 7.4, 5.0 Hz, 1H)	HMBC 27→29,37
28	27.0	3.05 (dd, J = 14.9, 8.5 Hz, 1H), 3.15 (dd, J = 14.9, 5.0 Hz, 1H)	HMBC 28→29,30
29	109.7	-	-
30	123.2	7.14 (d, J = 2.0 Hz, 1H)	HMBC 30→29,32,37
31	-	10.84 (br d, J = 2.0 Hz, 1H)	HMBC 31→30
32	135.8	-	-
33	111.0	7.32 (d, J = 7.4 Hz, 1H) overlap	-
34	120.6	7.06 (dd, J = 7.4, 7.4 Hz, 1H) overlap	HMBC 34→32,36
35	118.2	6.97-7.01 (m, 1H) overlap	HMBC 35→33,37
36	118.1	7.56 (d, J = 7.8 Hz, 1H)	TOCSY 36→33,34,35
37	127.1	-	-
38	170.8	-	-
39	-	7.84 (d, J = 8.0 Hz, 1H)	TOCSY 39→40,41 HMBC 39→38
40	53.6	4.40 (ddd, J = 8.0, 7.9, 5.7 Hz, 1H)	HMBC 40→38,47
41	36.6	2.77 (dd, 13.8, 7.9 Hz, 1H), 2.89 (dd, J = 13.8, 5.7 Hz, 1H)	HMBC 41→47
42	127.4	-	-
43	129.9	7.02 (d, J = 8.5 Hz, 2H)	HMBC 43→41,45
44	114.6	6.66 (d, J = 8.5 Hz, 2H)	HMBC 44→42,45 COSY 44→43
45	155.6	-	-
46	-	9.15 (br s, 1H)	-
47	172.5	-	-

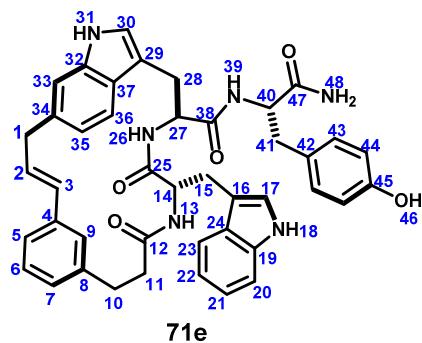
48	-	7.09 (br s, 1H), 7.31 (br s, 1H) overlap	HMBC 48→47
----	---	--	------------



(600MHz, DMSO-*d*₆, 298K)

	¹³ C	¹ H	key correlations
1	46.5	4.93 (br. dd, J = 16.7, 3.9 Hz, 1H), 4.78 (dd, J = 16.3, 6.9 Hz, 1H)	TOCSY→2, 3 HMBC→2, 3, 4
2	125.3	6.11 (ddd, J = 15.8, 6.8, 4.8 Hz, 1H)	TOCSY→3, 1 HMBC→3, 1, 4
3	131.2	6.22 (br. d, J = 16.9 Hz, 1H)	TOCSY→2, 1 HMBC→2, 1, 4
4	136.1	-	-
5	125.2	7.12 (m, 1H) overlap	HMBC→7, 9
6	125.1	7.15 (m, 1H) overlap	COSY→7 HMBC→8, 4
7	127.8	6.94 (m, 1H) overlap	COSY→6 HMBC→9, 5
8	142.0	-	-
9	124.2	7.09 (m, 1H) overlap	HMBC→7
10	28.6	2.46 (m, 1H), 2.96 (dd, J = 13.2, 13.2 Hz, 1H)	COSY→10', 11, 11' HMBC→8, 12, 7, 9
11	35.0	2.06 (m, 1H), 2.38 (m, 1H)	COSY→11', 10, 10' HMBC→12, 10, 8
12	170.5	-	-
13	-	7.67 (d, J = 8.5 Hz, 1H)	TOCSY→15, 15' COSY→14, HMBC→12
14	52.3	4.69 (ddd, J = 7.9, 7.9, 4.6 Hz, 1H)	COSY→15', 13 HMBC→15, 16, 25
15	28.7	3.11 (dd, J = 14.3, 4.3 Hz, 1H), 2.83 (ddd, J = 14.7, 7.7 Hz, 1H)	TOCSY→13 COSY→14, 15', HMBC→14, 16, 17, 24
16	109.8	-	-
17	123.6	6.96 (m, 1H) overlap	COSY→18 HMBC→16, 19, 24 COSY→17 HMBC→16, 17, 24, 19
18	-	10.65 (d, J = 1.9 Hz, 1H)	-
19	135.9	-	-
20	110.6	7.23 (d, J = 8.2 Hz, 1H)	COSY→21 HMBC→22, 24
21	120.4	6.95 (m, 1H)	COSY→22, 20 HMBC→23, 19
22	117.6	6.85 (dd, J = 7.1, 7.1 Hz, 1H)	COSY→23, 21 HMBC→20, 24
23	118.4	7.52 (d, J = Hz, 1H)	COSY→22 HMBC→16, 19, 21
24	127.7	-	-

25	171.3	-	-
26	-	8.49 (d, J = 8.5 Hz, 1H)	TOCSY→27, 28, 28' HMBC→25
27	53.1	4.63 (ddd, J = 11.4, 8.5, 2.1 Hz, 1H)	TOCSY→28, 28', 26 HMBC→28, 29
28	27.8	2.88 (m, 1H), 3.03 (br. d, J = 14.0 Hz, 1H)	HMBC→29, 37, 30
29	111.3	-	-
30	125.2	7.16 (s, 1H) overlap	HMBC→1
31	-	-	-
32	136.4	-	-
33	109.6	7.42 (d, J = 8.1 Hz, 1H) overlap	COSY→34 HMBC→37, 35
34	121.3	7.08 (m, 1H) overlap	COSY→33 HMBC→36, 32
35	118.5	7.01 (m, 1H) overlap	COSY→35, 34 HMBC→37, 33
36	118.7	7.60 (d, J = 7.9 Hz, 1H)	COSY→35 HMBC→29, 34, 32
37	127.8	-	-
38	171.9	-	-
39	-	7.94 (d, J = 7.9 Hz, 1H)	TOCSY→41, 41' COSY→40 HMBC→38
40	54.0	4.44 (ddd, J = 7.8, 7.8, 6.0 Hz, 1H)	COSY→41, 41', 39 HMBC→42, 41, 47
41	37.2	2.78 (dd, J = 13.9, 7.8 Hz, 1H), 2.91 (m, 1H) overlap	TOCSY→39 COSY→40 HMBC→40, 47, 42, 43
42	128.1	-	-
43	130.6	7.03 (m, 2H) overlap	COSY→44 HMBC→45, 44
44	115.1	6.64 (d, J = 8.5 Hz, 2H)	COSY→43 HMBC→45, 42
45	156.1	-	-
46	-	9.16 (s, 1H)	HMBC→44, 45
47	172.7	-	-
48	-	7.08 (m, 1H) overlap, 7.42 (br. s)	HMBC→47



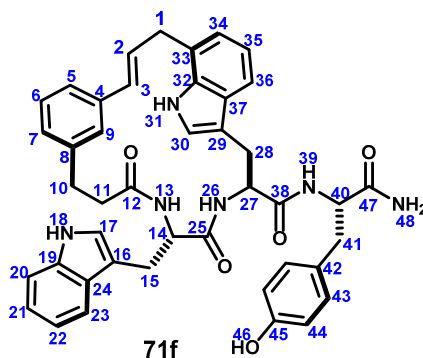
(600MHz, DMSO-*d*₆, 298K)

*Note, this compound was characterized within a 5:4 mixture of **71e**:**71f**.

	¹³ C	¹ H	key correlations
1	34.1	3.53-3.59 (m, 1H), 3.76-3.81 (m, 1H)	-
2	127.9	6.40 (ddd, J = 16.1, 5.5, 5.5 Hz, 1H)	COSY 2→1,3 HMBC 2→4,33 ROESY 2→5

3	129.1	5.78 (d, J = 16.1 Hz, 1H)	HMBC 3→5 ROESY 3→9
4	137.0	-	-
5	121.5	7.23-7.26 (m, 1H)	COSY 5→6 HMBC 5→3
6	127.7	7.10-7.13 (m, 1H)	HMBC 6→4,8 COSY 6→7
7	126.7	6.88-6.91 (m, 1H)	-
8	141.9	-	-
9	125.4	6.50 (br s, 1H)	HMBC 9→3,5 TOCSY 9→5,6,7 ROESY 9→2,3,11
10	27.4	2.37-2.45 (m, 1H), 3.02-3.11 (m, 1H)	HMBC 10→8
11	33.9	2.08-2.17 (m, 1H), 2.30-2.38 (m, 1H)	TOCSY 11→10 HMBC 11→12
12	170.0	-	-
13	-	7.37 (d, J = 8.1 Hz, 1H)	ROESY 13→11,14 HMBC 13→12
14	52.2	4.52-4.57 (m, 1H)	TOCSY 14→13,15 ROESY 14→26
15	28.4	2.87-2.92 (m, 1H), 3.10-3.15 (m, 1H)	HMBC 15→16
16	109.4	-	-
17	123.3	6.98-7.01 (m, 1H)	HMBC 17→16,19
18	-	10.66-10.69 (m, 1H)	HMBC 18→19,24 TOCSY 18→17 ROESY 18→20
19	135.4	-	-
20	110.7	7.25-7.28 (m, 1H)	-
21	120.2	6.98-7.02 (m, 1H)	HMBC 21→19
22	117.7	6.86-6.91 (m, 1H), 6.98-7.02 (m, 1H)	HMBC 22→24
23	118.3	7.52 (d, J = 7.7 Hz, 1H)	HMBC 23→19,21
24	127.6	-	-
25	-	-	-
26	-	8.31 (d, J = 8.6 Hz, 1H)	HMBC 26→25
27	52.8	4.61 (ddd, J = 12.3, 8.6, 2.9 Hz, 1H)	TOCSY 27→26,28 ROESY 27→39
28	27.7	2.80-2.86 (m, 1H), 3.14-3.18 (m, 1H)	ROESY 28→36
29	109.7	-	-
30	124.0	7.20 (d, J = 1.7 Hz, 1H)	HMBC 30→29,32,37 ROESY 30→27,28
31	-	10.54 (br s, 1H)	ROESY 31→1,2,3 COSY 31→30
32	134.9	-	-
33	122.0	-	-
34	120.9	6.86-6.89 (m, 1H)	ROESY 34→1 HMBC 34→1
35	118.1	6.90-6.95 (m, 1H)	-
36	116.6	7.57 (d, J = 8.0 Hz, 1H)	HMBC 36→32,34
37	126.7	-	-
38	-	-	-
39	-	7.92 (d, J = 7.7 Hz, 1H)	TOCSY 39→40,41
40	53.6	4.49-4.54 (m, 1H)	HMBC 40→42,47 ROESY 40→48

41	36.8	2.81-2.87 (m, 1H), 2.94-2.99 (m, 1H)	HMBC 41→47
42	127.4	-	-
43	129.9	7.05-7.09 (m, 2H)	HMBC 43→45,41
44	114.6	6.66-6.69 (m, 2H)	HMBC 44→42,45
45	155.7	-	-
46	-	9.17-9.19 (m, 1H)	HMBC 46→45
47	172.6	-	-
48	-	7.11 (br s, 1H), 7.48 (br s, 1H)	TOCSY 48→48'

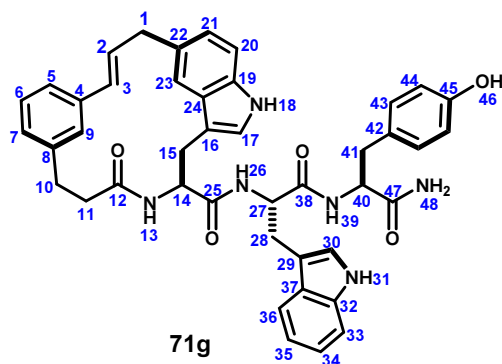


(600MHz, DMSO-*d*₆, 298K)

*Note, this compound was characterized within a 5:4 mixture of 71e:71f.

	¹³ C	¹ H	key correlations
1	37.7	3.41-3.47 (m, 1H), 3.51-3.57 (m, 1H)	HMBC 1→33,34,35 ROESY 1→34,35
2	131.4	6.46 (ddd, J = 15.8, 4.9, 4.9 Hz, 1H)	COSY 2→1,3
3	129.8	5.39 (d, J = 15.8 Hz, 1H)	ROESY 3→9
4	137.0	-	-
5	121.0	7.23-7.26 (m, 1H)	-
6	127.7	7.09-7.13 (m, 1H)	HMBC 6→4,8
7	126.8	6.86-6.89 (m, 1H)	-
8	141.9	-	-
9	125.8	6.38 (br s, 1H)	TOCSY 9→5,6,7 ROESY 9→10,11
10	27.7	2.38-2.45 (m, 1H), 2.95-3.02 (m, 1H)	-
11	34.0	2.09-2.17 (m, 1H), 2.31-2.40 (m, 1H)	-
12	169.8	-	-
13	-	7.12-7.15 (m, 1H)	ROESY 13→11
14	52.7	4.42-4.46 (m, 1H)	TOCSY 14→13,15 ROESY 15→26,27
15	27.8	2.94-3.00 (m, 1H), 3.27-3.34 (m, 1H)	-
16	109.1	-	-
17	123.6	6.91 (br s, 1H)	HMBC 17→16,19,24
18	-	10.62 (br s, 1H)	COSY 18→17 ROESY 18→20 HMBC 18→16,19,24
19	135.5	-	-

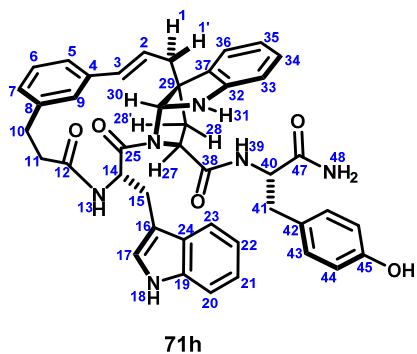
20	110.7	7.23-7.26 (m, 1H)	HMBC 20→24 COSY 20→21
21	120.2	6.96-7.00 (m, 1H)	-
22	117.7	6.84 (dd, J = 8.0, 7.0 Hz, 1H)	-
23	118.2	7.40 (d, J = 8.0 Hz, 1H)	ROESY 23→15 TOCSY 23→20,21,22
24	127.9	-	-
25	-	-	-
26	-	8.28 (d, J = 8.9 Hz, 1H)	-
27	54.5	4.71-4.76 (m, 1H)	TOCSY 27→26,28 ROESY 27→39
28	28.4	2.88-2.94 (m, 1H), 3.12-3.17 (m, 1H)	HMBC 28→29
29	109.6	-	-
30	123.3	7.12 (br s, 1H)	ROESY 30→28 HMBC 30→37
31	-	10.68 (br s, 1H)	TOCSY 31→30 ROESY 31→33
32	136.2	-	-
33	111.3	7.07 (s, 1H)	HMBC 33→1,35,37 ROESY 33→1
34	131.1	-	-
35	120.1	6.77 (d, J = 8.1 Hz, 1H)	HMBC 35→1,33,37 ROESY 35→1
36	118.7	7.78 (d, J = 8.1 Hz, 1H)	HMBC 36→32,34 ROESY 36→27,28
37	125.6	-	-
38	171.7	-	-
39	-	8.14 (d, J = 7.7 Hz, 1H)	HMBC 39→38 TOCSY 39→40,41
40	53.8	4.52-4.56 (m, 1H)	HMBC 40→47
41	36.8	2.81-2.87 (m, 1H), 2.94-2.99 (m, 1H)	HMBC 41→42,43,47
42	127.4	-	-
43	129.9	7.05-7.09 (m, 2H)	HMBC 43→41,45
44	114.6	6.66-6.69 (m, 2H)	HMBC 44→42,45
45	155.7	-	-
46	-	9.17-9.19 (m, 1H)	HMBC 46→45
47	172.5	-	-
48	-	7.07 (br s, 1H), 7.44 (br s, 1H)	TOCSY 48→48'



(600MHz, DMSO-*d*₆, 298K)

	¹³ C	¹ H	key correlations
1	37.7	3.41-3.47 (m, 1H), 3.51-3.57 (m, 1H)	HMBC 1→33,34,35 ROESY 1→34,35
2	131.4	6.46 (ddd, J = 15.8, 4.9, 4.9 Hz, 1H)	COSY 2→1,3
3	129.8	5.39 (d, J = 15.8 Hz, 1H)	ROESY 3→9
4	137.0	-	-
5	121.0	7.23-7.26 (m, 1H)	-
6	127.7	7.09-7.13 (m, 1H)	HMBC 6→4,8
7	126.8	6.86-6.89 (m, 1H)	-
8	141.9	-	-
9	125.8	6.38 (br s, 1H)	TOCSY 9→5,6,7 ROESY 9→10,11
10	27.7	2.38-2.45 (m, 1H), 2.95-3.02 (m, 1H)	-
11	34.0	2.09-2.17 (m, 1H), 2.31-2.40 (m, 1H)	-
12	169.8	-	-
13	-	7.12-7.15 (m, 1H)	ROESY 13→11
14	52.7	4.42-4.46 (m, 1H)	TOCSY 14→13,15 ROESY 15→26,27
15	27.8	2.94-3.00 (m, 1H), 3.27-3.34 (m, 1H)	-
16	109.1	-	-
17	123.6	6.91 (br s, 1H)	HMBC 17→16,19,24
18	-	10.62 (br s, 1H)	COSY 18→17 ROESY 18→20 HMBC 18→16,19,24
19	135.5	-	-
20	110.7	7.23-7.26 (m, 1H)	HMBC 20→24 COSY 20→21
21	120.2	6.96-7.00 (m, 1H)	-
22	117.7	6.84 (dd, J = 8.0, 7.0 Hz, 1H)	-
23	118.2	7.40 (d, J = 8.0 Hz, 1H)	ROESY 23→15 TOCSY 23→20,21,22
24	127.9	-	-
25	-	-	-
26	-	8.28 (d, J = 8.9 Hz, 1H)	-
27	54.5	4.71-4.76 (m, 1H)	TOCSY 27→26,28 ROESY 27→39
28	28.4	2.88-2.94 (m, 1H), 3.12-3.17 (m, 1H)	HMBC 28→29

29	109.6	-	-
30	123.3	7.12 (br s, 1H)	ROESY 30→28 HMBC 30→37
31	-	10.68 (br s, 1H)	TOCSY 31→30 ROESY 31→33
32	136.2	-	-
33	111.3	7.07 (s, 1H)	HMBC 33→1,35,37 ROESY 33→1
34	131.1	-	-
35	120.1	6.77 (d, J = 8.1 Hz, 1H)	HMBC 35→1,33,37 ROESY 35→1
36	118.7	7.78 (d, J = 8.1 Hz, 1H)	HMBC 36→32,34 ROESY 36→27,28
37	125.6	-	-
38	171.7	-	-
39	-	8.14 (d, J = 7.7 Hz, 1H)	HMBC 39→38 TOCSY 39→40,41
40	53.8	4.52-4.56 (m, 1H)	HMBC 40→47
41	36.8	2.81-2.87 (m, 1H), 2.94-2.99 (m, 1H)	HMBC 41→42,43,47
42	127.4	-	-
43	129.9	7.05-7.09 (m, 2H)	HMBC 43→41,45
44	114.6	6.66-6.69 (m, 2H)	HMBC 44→42,45
45	155.7	-	-
46	-	9.17-9.19 (m, 1H)	HMBC 46→45
47	172.5	-	-
48	-	7.07 (br s, 1H), 7.44 (br s, 1H)	TOCSY 48→48'



(600MHz, DMSO-*d*₆, 298K)

	¹³ C	¹ H	key correlations
1 (pro-R)	39.0	2.42 (dd, J = 13.5, 6.4 Hz, 1H)	HMBC 1→28,29,30,37
1' (pro-S)		2.73 (dd, J = 13.5, 9.5 Hz, 1H)	
2	125.3	6.02 (ddd, J = 15.6, 9.0, 6.8 Hz, 1H)	TOCSY 2→1,3 HMBC 2→4
3	132.1	6.57 (d, J = 15.6 Hz, 1H) overlap	HMBC 3→1,4
4	136.8	-	
5	124.1	7.01-7.04 (m, 1H) overlap	

6	128.2	7.13-7.18 (m, 1H) overlap	HMBC 6→4,8
7	127.0	6.99-7.02 (m, 1H) overlap	
8	140.5	-	
9	124.6	7.19 (s, 1H) overlap	HMBC 9→5,3,7
10	30.6	2.64-2.70 (m, 1H), 2.92-2.99 (m, 1H)	HMBC 10→8,11,12
11	37.5	2.15-2.23 (m, 1H) overlap, 2.38-2.45 (m, 1H)	HMBC 11→8,12
12	171.2	-	
13	-	7.96 (d, J = 8.4 Hz, 1H)	
14	49.8	5.39-5.45 (m, 1H)	HMBC 14→25
15	29.9	3.06 (dd, J = 14.2, 5.7 Hz, 1H), 3.16 (dd, J = 14.2, 7.8 Hz, 1H)	HMBC 15→16
16	109.4	-	
17	124.0	7.40 (br s, 1H)	HMBC 17→19,24
18	-	11.07 (br s, 1H)	
19	135.9	-	
20	111.5	7.51 (d, J = 8.1 Hz, 1H)	HMBC 20→24
21	121.3	7.14-7.18 (m, 1H) overlap	
22	118.8	7.09 (dd, J = 7.8, 7.2 Hz, 1H)	TOCSY 22→20,21,23 HMBC 22→24
23	118.4	7.86 (d, J = 7.8 Hz, 1H)	COSY 23→22 HMBC 23→16,19,20,21,24
24	126.9	-	
25	171.3	-	
26	-	-	
27	62.4	4.22 (dd J = 10.3, 6.1 Hz, 1H) overlap	HMBC 27→29,38
28 (pro-S)	40.0	1.74 (dd, J = 13.2, 6.1 Hz, 1H)	HMBC 28→38,29 NOESY 28→41,43,44
28' (pro-R)		2.34 (dd, J = 13.2, 10.3 Hz, 1H)	NOESY 28'→2,3
30	81.1	5.73 (s, 1H)	HMBC 30→27,29
31	-	4.25 (br s, 1H)	NOESY 31→33
32	146.6	-	
33	109.3	6.34 (d, J = 7.7 Hz, 1H)	HMBC 33→37
34	127.9	7.00-7.04 (m, 1H) overlap	
35	119.0	6.72 (dd, J = 7.8, 7.2 Hz, 1H)	HMBC 35→37
36	121.7	7.02-7.06 (m, 1H) overlap	HMBC 36→32
37	134.8	-	
38	169.7	-	
39	-	6.99-7.02 (m, 1H) overlap	HMBC 39→38
40	53.4	4.16-4.20 (m, 1H) overlap	HMBC 40→47 TOCSY 40→39
41	37.3	2.18 (dd, J = 13.6, 9.2 Hz, 1H) overlap, 2.74 (dd, J = 13.6, 5.0 Hz, 1H) overlap	HMBC 41→42,43,47
42	127.2	-	
43	129.8	6.59 (d, J = 8.3 Hz, 2H)	
44	114.4	6.26 (d, J = 8.3 Hz, 2H)	HMBC 44→42

45	155.3	-	
46	-	9.04 (br s, 1H)	HMBC 46→44
47	172.4	-	

NMR solution structure of **71h**:

The solution conformation of pyrroloindoline **71h** was determined from NMR spectra of **7** acquired in DMSO- d_6 to permit the observation of exchangeable protons. ROESY was also acquired in DMSO- d_6 :D₂O (9:1) to resolve potential signal overlap arising from exchangeable protons. The relative stereochemistry of the pyrroloindoline ring juncture was determined by careful analysis of long range inter-residue correlations observed by NOESY and ROESY (see text). Distance restraints were obtained from pairs of NOE correlations from a ¹H-¹H NOESY experiment using a 100 ms mixing time and 4 s interscan delay. The fixed reference distance *H18-H20* (2.8Å)²² was corroborated by distance *H30-H31*²³ and all geminal pairs, suggesting sufficiently linear NOE buildup for stratification of the larger dataset. Volume integrals were grouped into bins, and classified as strong (<2.5Å), medium (<3.5 Å) and weak (<4.5 Å), based on the relationship of r^{-6} . An initial model was generated by a Mixed Monte-Carlo low-mode conformational search incorporating seven key long-distance NOE distance restraints. From this model, an additional 29 NOEs were defined, and prochiral methylenes *H1* (pro-*R*), *H1'* (pro-*S*) and *H28* (pro-*S*), *H28'* (pro-*R*) were defined. Equivalent NOE correlations arising from unassigned prochiral methylenes at *C10*, *C11*, *C15* and *C41*, where present, were assigned the weaker of the two restraint bins. No torsional constraints were utilized. Structure calculations were carried out using Macromodel 9.8 (Schrödinger, Inc., San Diego, CA) using the OPLS-2005 force field with implicit GB/SA solvation and a constant dielectric ($\epsilon = 1.0$). A 5,000 step restrained mixed Monte-Carlo/low-mode conformational search was used. Amide bonds rotations were not restrained. Redundant conformers were filtered within a heavy atom RMSD cutoff of 1.0 Å, which converged to five structures within 11 kcal/mol of the global minimum. The global minimum was located 150 times.

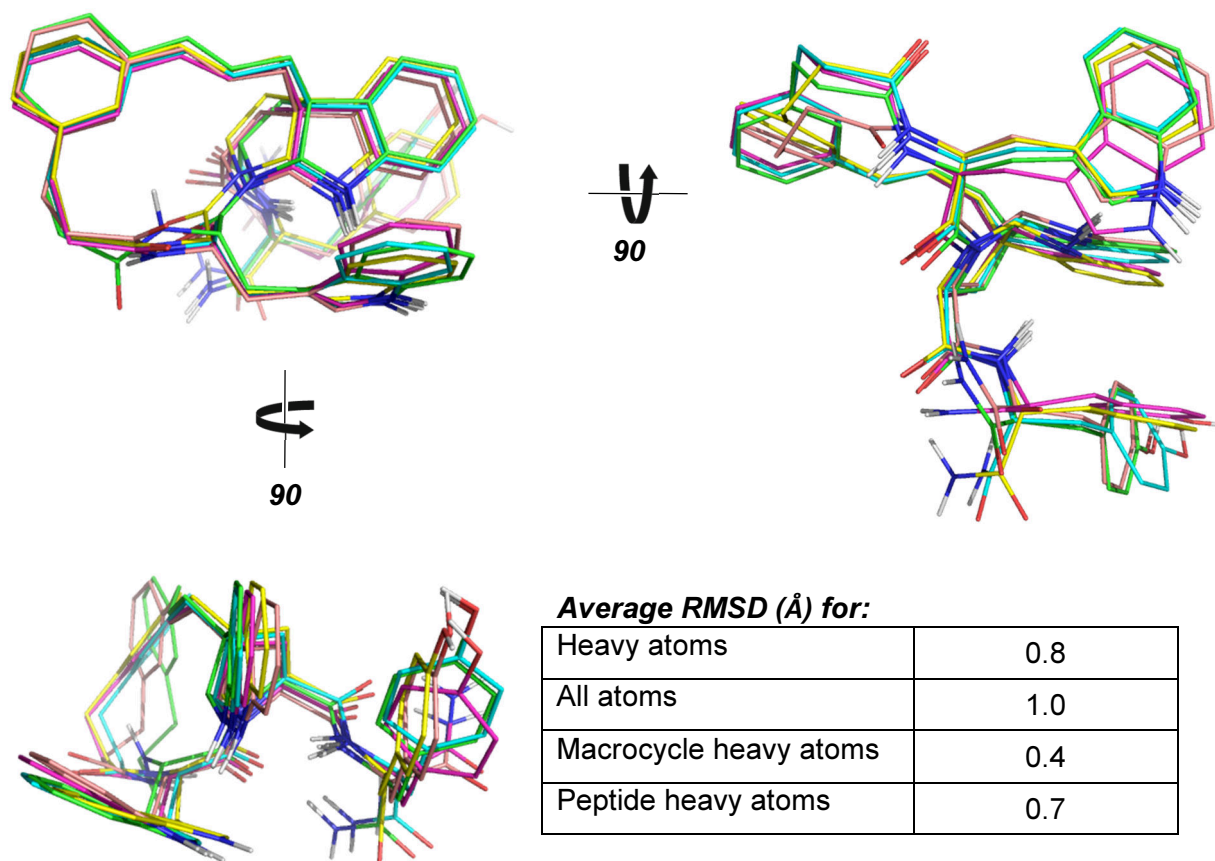
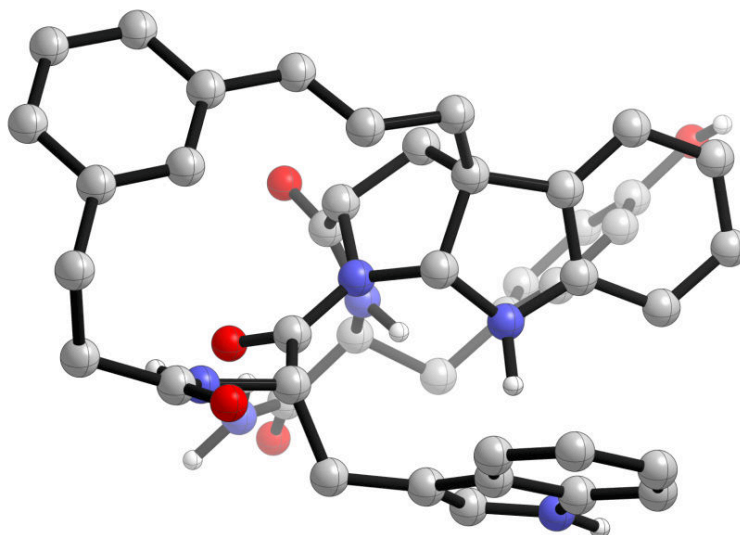


Figure S1. Conformational ensemble and average RMSDs of pyrroloindoline **12** derived from constrained simulations using 36 distances measured by NOE. Rendered with PyMol.



<i>Residue</i>	ϕ	ψ	ω	X_1
Trp1	-149°	137°	-149°	-160°
Pyrlnd2	-71°	-27°	178°	-17°
Tyr3	-96°	111°	n/a	-71°

Figure S2. Lowest energy conformational and peptide torsional angles of pyrroloindoline **12**. Rendered with CYLview.

Table S1. Internuclear distances determined from NOESY, and distances found in solution conformation.

	Long range ¹	prelim. calc. ²	final calc. ³	NOE correlation ⁴	avg. Integration	<i>r</i> exp. (Å) ⁵	bin ⁶	<i>r</i> calc. (Å) ⁷
8	n			18↔20	0.8	2.8	m	2.9
2	n			1↔1'	15.7	1.7	s	1.7
3	y			1↔3	0.9	2.8	m	3.6
4	y			1'↔3	1.5	2.6	s	2.5

¹ Correlation which is greater than three bonds, and which is not geometrically fixed due to small rings, etc.

² Distance restraints used in generating a preliminary model (see text).

³ Long range correlations used in final calculation of solution conformation.

⁴ See numbering scheme, above.

⁵ Internuclear distance calculated from experiment NOE

⁶ Bins were defined as strong (s, <2.5Å), medium (m, <3.5 Å) and weak (w, <4.5 Å)

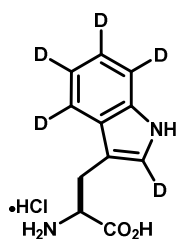
⁷ Internuclear distance measured from lowest energy conformer.

⁸ Reference distance (2.82Å). Bye, E.; Mostad, A.; Romming, C., *Acta. Chem. Scand.*, **1973**, 27, 471-484.

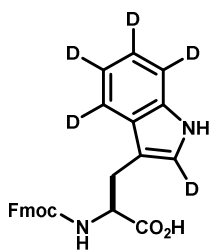
5	y		y	1↔30	1.2	2.7	m	2.8
6	y		y	1'↔30	0.3	3.4	m	3.8
7	y		y	1'↔36	1.8	2.5	s	2.7
8	y		y	1↔36	0.8	2.9	m	3.0
9	n			2↔3	28.2	1.6	s	3.1
10	y	y	y	2↔14	0.8	2.9	m	2.5
11	y		y	2↔27	0.4	3.2	m	3.6
12	y	y	y	2↔30	3.7	2.2	s	2.2
13	y	y	y	2↔9	5.2	2.1	s	2.0
14	y	y	y	3↔5	2.2	2.4	s	2.4
15	y		y	3↔27	0.2	3.5	m	3.2
16	y		y	3↔28'	0.9	2.8	m	3.0
17	y		y	10↔7	0.2	3.6	w	3.6
18	y		y	10'↔7	0.6	2.9	m	2.4
19	y		y	10↔9	0.6	3.0	m	3.7
20	y		y	10'↔9	1.8	2.5	s	2.6
21	n			10↔10'	20.4	1.7	s	1.7
22	n			10↔11	2.9	2.3	s	2.4
23	n			10↔11'	4.3	2.2	s	2.6
24	n			10'↔11	1.6	2.5	m	2.6
25	n			10'↔11'	1.7	2.5	m	3.1
26	y			11↔9	0.2	3.5	m	4.1
27	y			11'↔9	0.4	3.2	m	3.6
28	n			11↔11'	25.6	1.6	s	1.8
29	y			13↔9	0.6	3.0	m	3.5
30	y			13↔10	0.5	3.1	m	4.3 ²⁴
31	y			13↔10'	0.2	3.8	w	4.5
32	y		y	13↔11	1.0	2.7	m	3.3
33	y		y	13↔11'	4.6	2.1	s	2.2
34	y		y	13↔15	0.8	2.8	m	3.2
35	y		y	13↔15'	0.5	3.1	m	3.4
36	y		y	13↔27	0.1	3.9	w	4.2
37	y	y	y	14↔9	0.5	3.0	m	2.8
38	y		y	14↔17	0.4	3.2	m	4.1
39	y		y	14↔23	1.2	2.7	m	2.9
40	y		y	14↔31	0.6	3.0	m	3.5
41	y		y	17↔15	0.3	3.3	m	3.6
42	y		y	17↔15'	0.6	3.0	m	2.4
43	y		y	17↔41	0.3	3.4	m	3.6
44	n			17↔18	2.5	2.4	s	2.6
45	y		y	20↔33	0.2	3.7	w	3.5

46	y			23↔15	0.5	3.1	m	2.8
47	y			23↔15'	0.2	3.6	w	4.3
48	y			23↔31	0.2	3.7	w	4.4
49	n			28↔28'	15.1	1.7	s	1.7
50	y			28↔36	0.7	2.9	m	3.5
51	y			28'↔36	0.2	3.5	m	3.5
52	y		y	28↔39	0.6	3.0	m	3.0
53	y		y	28↔43	0.6	3.0	m	2.9
54	y		y	28↔44	0.2	3.5	m	3.5
55	y			28↔41'	0.9	2.8	m	4.7
56	y	y	y	30↔9	0.6	3.0	m	3.8
57	y		y	30↔13	0.1	3.8	w	4.4
58	y	y	y	30↔14	9.2	1.9	s	1.9
59	y		y	30↔15	0.2	3.6	m	3.9
60	y		y	30↔15'	0.2	3.7	w	4.0
61	y		y	30↔17	0.1	3.9	w	4.1
62	y		y	30↔23	0.2	3.5	m	3.5
63	y			30↔28	0.2	3.6	w	4.0
64	y			30↔28'	0.2	3.7	m	4.2
65	n			30↔31	2.4	2.4	s	2.4
66	y			30↔33	0.2	3.7	w	4.5
67	n			31↔33	1.0	2.7	m	2.6
68	n			41↔41'	14.7	1.8	s	1.7
69	y			41↔43	1.3	2.6	m	2.5
70	y			41'↔43	1.3	2.6	m	2.5

***L*-Tryptophan(indole-*d*₅) hydrochloride (72).**^{24,25} To a degassed solution of *L*-tryptophan (3.0 g, 14.7 mmol) in D₂O (20.0 ml) was added mercaptoacetic acid (0.4 ml, 5.9 mmol) followed by 4M DCl (30 wt% in D₂O). The solution was heated to reflux for 5 hrs, then cooled to rt and extracted with EtOAc. The aqueous layer was lyophilized to give a white powder, which was re-subjected to the conditions above. The DCl/D₂O solution of Trp(*d*₅) was diluted with H₂O (250 mL) and lyophilized to give a white powder (3.01 g, 14.4 mmol, 98%). Analysis by MS (ESI+) showed >95 % average incorporation at each position (~ 75% *d*₅). The percent deuterium at each position was determined by ¹H NMR.²⁵ The residual Ar-H signals were integrated relative to C_α-H to give C2-²H (98%), C4-²H (90%), C5-²H (97%), C6-²H (98%), C7-²H (96%). ¹H NMR (DMSO-*d*₆, 500 MHz): δ 7.58 (s, 0.10H), 7.34 (s, 0.04H), 7.25 (s, 0.02H), 7.06 (s, 0.03H), 6.98 (s, 0.02H), 4.09 (t, *J* = 6.0 Hz, 1H), 3.29 (d, *J* = 6.3 Hz, 2H). MS (ESI) Calculated for C₁₁H₇D₅N₂O₂ [M+H]⁺: 210.1, found 210.1.



Fmoc-L-Tryptophan(indole-*d*₅) (73). To a suspension of **72** (1.79 g, 8.53 mmol) in sat. NaHCO₃ (25 mL) and THF (25 mL) was added Fmoc-OSu (3.45 g, 10.2 mmol) in one portion. The reaction was stirred for 2 hrs at rt. The volatiles were removed by rotary evaporation to give a white aqueous suspension, which was diluted with sat. NaHCO₃ (25 mL) and extracted with Et₂O (x2). The aqueous layer was acidified with 1 N HCl to pH < 3 and extracted with EtOAc (x2) to give **73** as a tan solid (3.09 g, 7.2 mmol, 84%). MS analysis showed no loss of isotopic purity. ¹H NMR (DMSO-*d*₆, 600 MHz): mixture of rotamers. δ 12.67 (s, 1H), 10.82 (s, 1H), 7.84 (br. d, *J* = 7.6 Hz, 2H), 7.68 (d, *J* = 8.1 Hz, 1H), 7.64 (d, *J* = 7.6 Hz, 1H), 7.61 (d, *J* = 7.6 Hz, 1H), 7.32-7.40 (m, 2H), 7.28 (ddd, *J* = 7.6, 7.6, 0.7 Hz, 1H), 7.24 (ddd, *J* = 7.6, 7.6, 0.7 Hz, 1H), 4.12-4.23 (m, 4H), 3.17 (dd, *J* = 14.6, 4.5 Hz, 1H), 3.00 (dd, *J* = 14.6, 9.9 Hz, 1H). MS (ESI) Calculated for C₂₆H₁₇D₅N₂O₄ [M+H]⁺: 432.2, found 432.1.



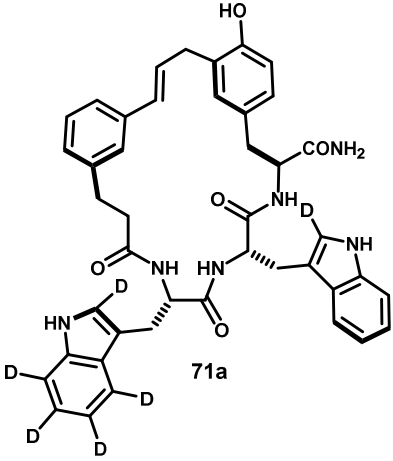
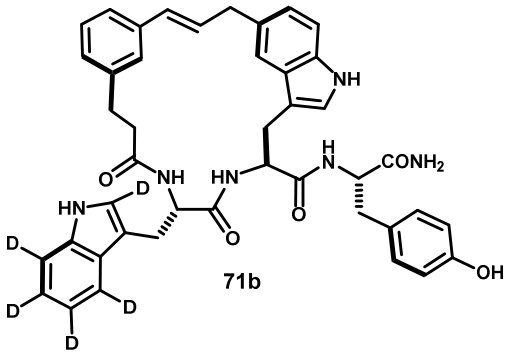
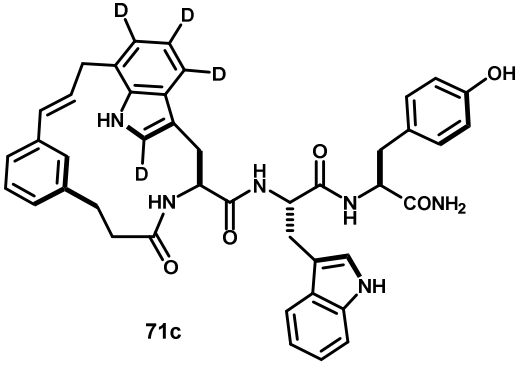
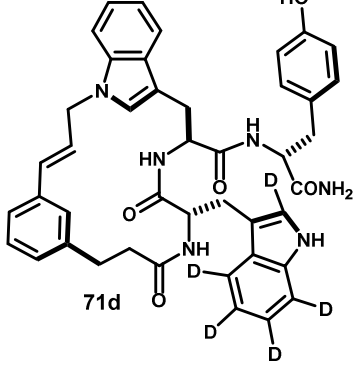
Synthesis of tryptophan-(indole-*d*₅) labeled peptides. Peptides were prepared using solution phase techniques with the Fmoc- protection strategy. Couplings were performed with *O*-(benzotriazol-1-yl)-*N,N,N',N'*-tetramethyluronium tetrafluoroborate (TBTU) (1.2 eq.), Fmoc-AA-OH (1.2 eq.), *i*Pr₂NEt (5 eq.) in DMF (0.1M). Coupling were complete within 2 hrs and diluted with EtOAc and washed sequentially with 1 N HCl, sat. NaHCO₃, H₂O and brine. Fmoc deprotection was achieved with DBU (1 eq.) in THF (0.2 M) in the presence of octyl mercaptan (5 eq.).²⁶ The product was precipitated with Et₂O and pelleted by centrifugation. This process was repeated twice. After final deprotection the peptide was purified by reverse-phase HPLC (C18, ACN/H₂O, 0.1%TFA). Fractions were pooled and lyophilized. No significant loss of isotopic purity was observed under these synthesis and purification conditions.

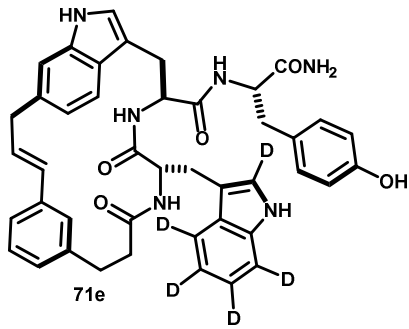
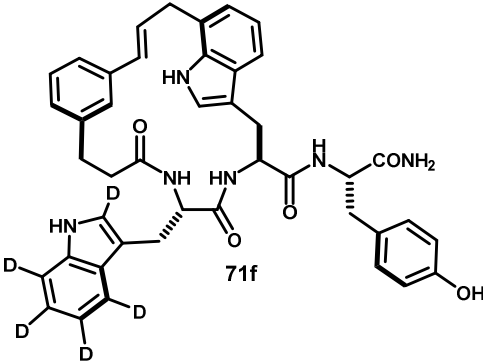
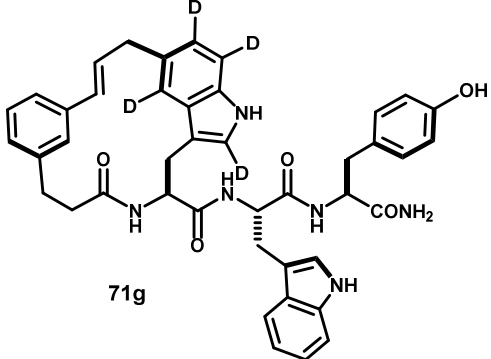
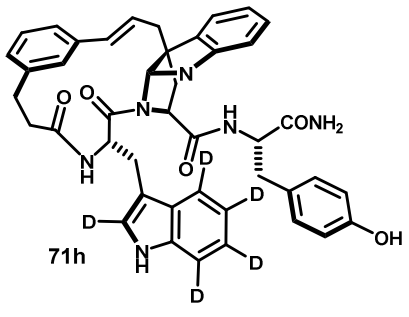
Acidolysis conditions screen.

The tyrosine macroether **70** or acyclic cinnamyl carbonate **69** (~5 mg) in a 1 dr vial was dissolved or suspended in indicated solvent (5 mM) under ambient atmosphere, and treated with acid. All reactions were stopped at 2 hrs, unless otherwise noted. MeSO₃H or CF₃CO₂H was transferred to the reaction vial via a micropipet using polypropylene tips. Bistriflimide was weighed under an argon atmosphere and a 10 mM solution in anhydrous MeNO₂ was prepared and transferred to the reaction vessel via syringe. Volumetric solutions of 50% *v/v* TFA, HCO₂H or AcOH in their respective solvents were prepared and transferred to a reaction vessel containing acidolysis substrate. Metal triflates were weighed under ambient atmosphere and transferred to a suspension of acidolysis substrate. Sc(OTf)₃ uniquely promoted complete dissolution of substrate/acid in the reaction media. Other metal triflates were heterogeneous throughout the reaction which resulted in increased reaction time (16 hrs). Reactions performed below ambient temperatures were performed in a cool aluminum block and the temperature was equilibrated for 30 mins prior to addition of acid. Aliquots for HPLC-MS analysis were removed and quenched with a methanolic solution of Et₃N, concentrated under high vacuum, and reconstituted in DMSO prior to injection. Relative yields were determined by integration at UV 254 nm and were not standardized.

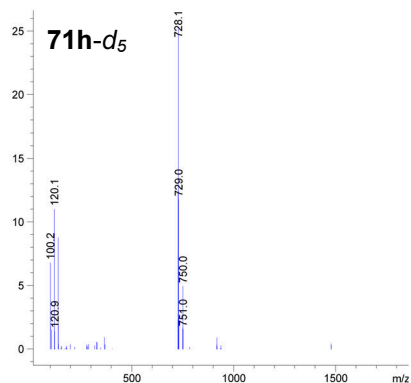
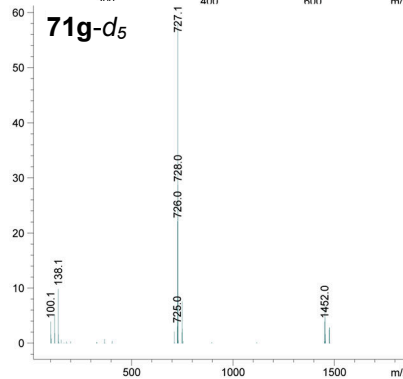
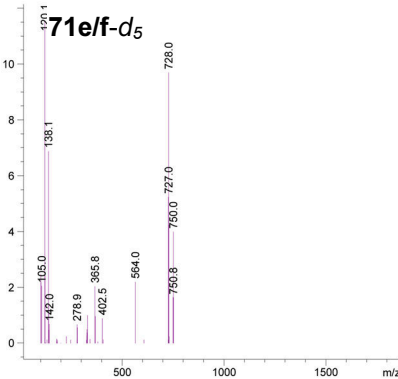
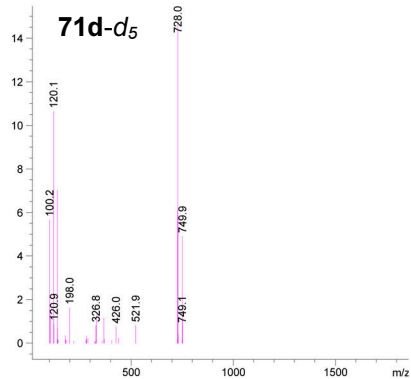
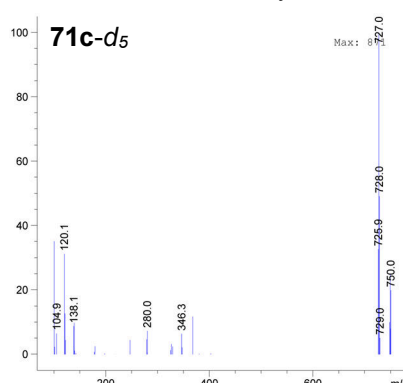
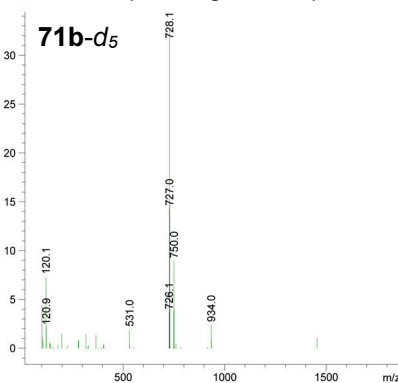
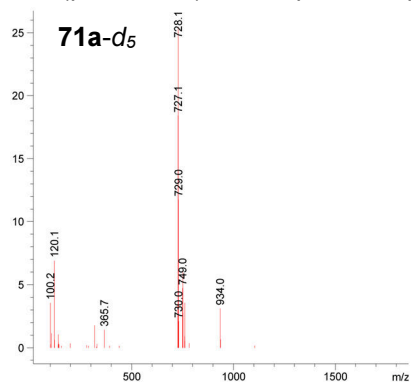
Acidolysis of Trp(indole-*d*₅)-Trp-Tyr (74).

Table S2. MS analysis of acidolysis products derived from 74.

Structure	 <p>71a</p>	 <p>71b</p>
Formula	C ₄₃ H ₃₇ D ₅ N ₆ O ₅	C ₄₃ H ₃₇ D ₅ N ₆ O ₅
Calculated mass [M+H] ⁺	728.4	728.4
Observed mass	728.1	728.1
Structure	 <p>71c</p>	 <p>71d</p>
Formula	C ₄₃ H ₃₈ D ₄ N ₆ O ₅	C ₄₃ H ₃₇ D ₅ N ₆ O ₅
Calculated mass [M+H] ⁺	727.4	728.4
Observed mass	727.0	728.0

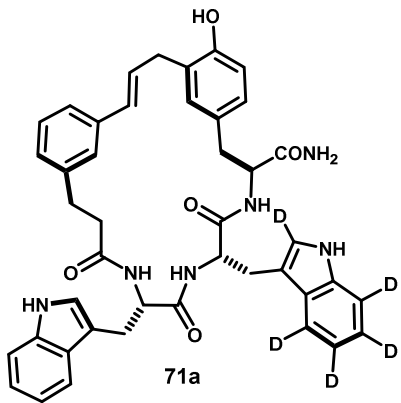
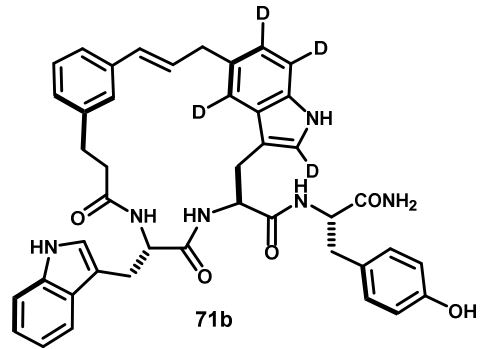
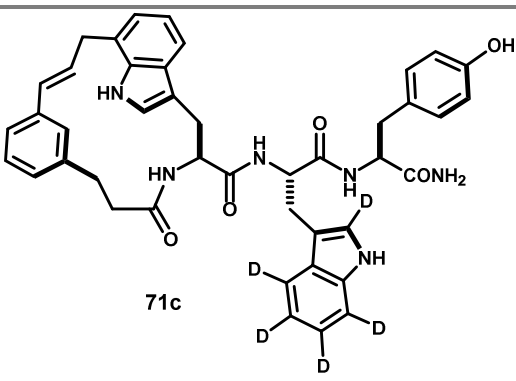
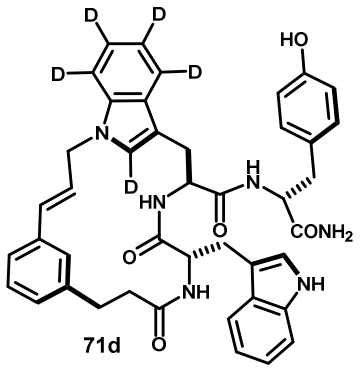
Structure	 <p>71e</p>	 <p>71f</p>
Formula	C ₄₃ H ₃₇ D ₅ N ₆ O ₅	C ₄₃ H ₃₇ D ₅ N ₆ O ₅
Calculated mass [M+H] ⁺	728.4	728.4
Observed mass	728.0	728.0
Structure	 <p>71g</p>	 <p>71h</p>
Formula	C ₄₃ H ₃₈ D ₄ N ₆ O ₅	C ₄₃ H ₃₇ D ₅ N ₆ O ₅
Calculated mass [M+H] ⁺	727.4	728.4
Observed mass	727.1	728.1

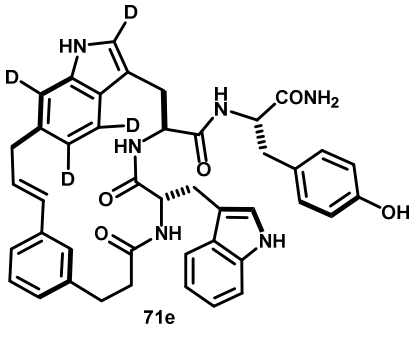
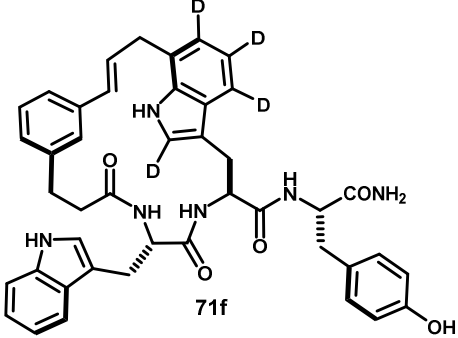
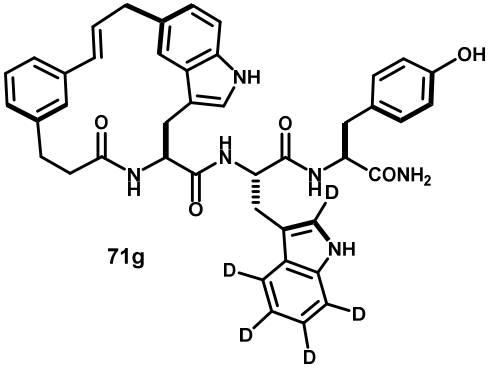
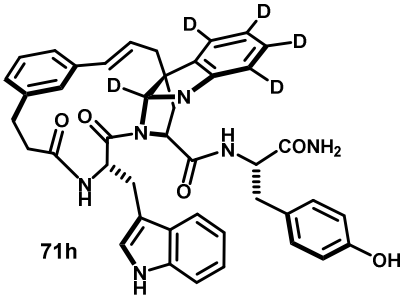
ESI (pos. mode) mass spectra of peaks corresponding to compounds **6-12** derived from acidolysis of **14**.



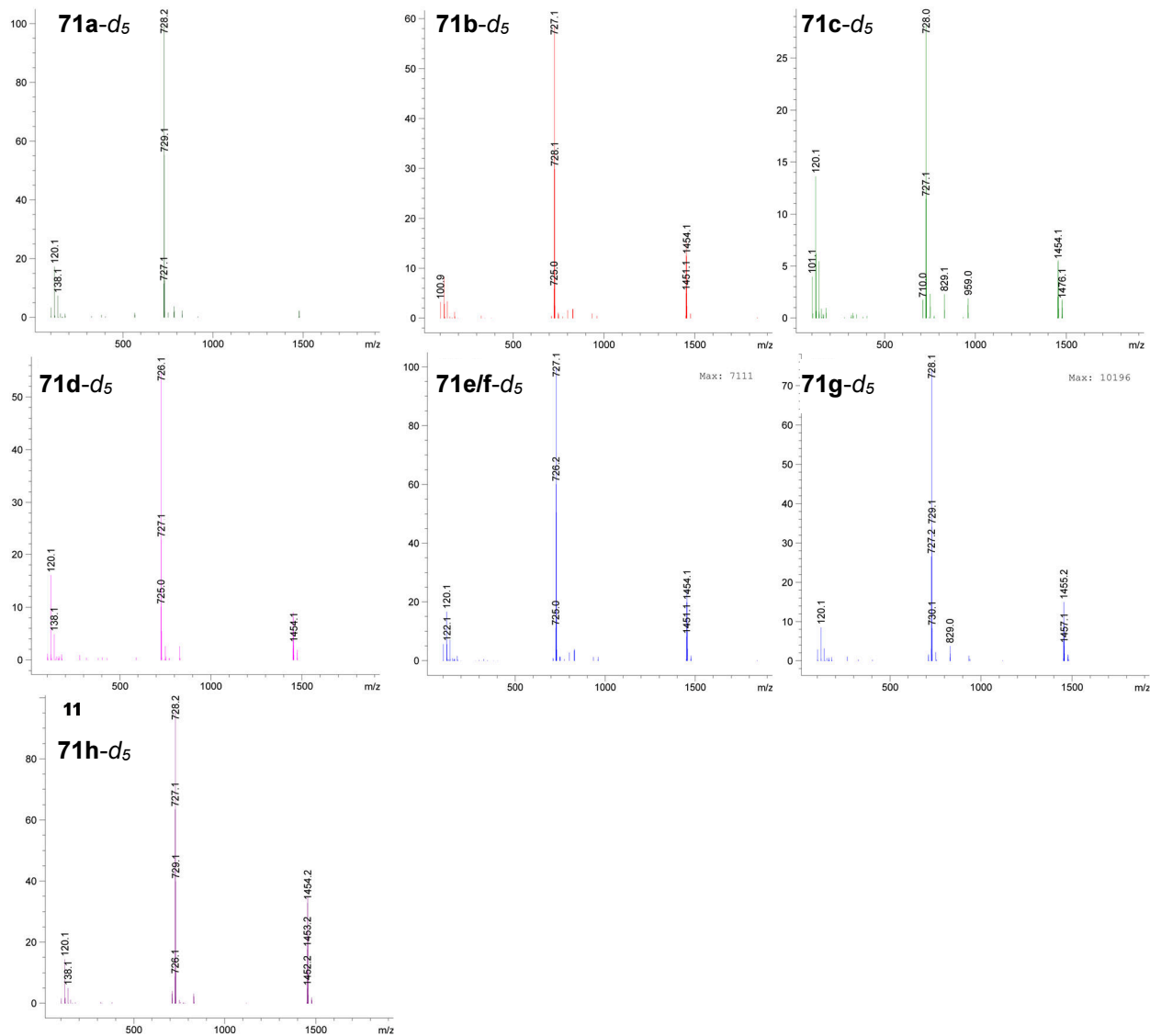
Acidolysis of Trp(indole-*d*₅)-Trp-Tyr (75).

Table S3. MS analysis of acidolysis products derived from 75.

Structure	 <p>71a</p>	 <p>71b</p>
Formula	C ₄₃ H ₃₇ D ₅ N ₆ O ₅	C ₄₃ H ₃₈ D ₄ N ₆ O ₅
Calculated mass [M+H] ⁺	728.4	727.4
Observed mass	728.2	727.1
Structure	 <p>71c</p>	 <p>71d</p>
Formula	C ₄₃ H ₃₇ D ₅ N ₆ O ₅	C ₄₃ H ₃₇ D ₅ N ₆ O ₅
Calculated mass [M+H] ⁺	728.4	728.4
Observed mass	728.0	726.1

Structure	 <p>71e</p>	 <p>71f</p>
Formula	C ₄₃ H ₃₈ D ₄ N ₆ O ₅	C ₄₃ H ₃₈ D ₄ N ₆ O ₅
Calculated mass [M+H] ⁺	727.4	727.4
Observed mass	727.1	727.1
Structure	 <p>71g</p>	 <p>71h</p>
Formula	C ₄₃ H ₃₇ D ₅ N ₆ O ₅	C ₄₃ H ₃₇ D ₅ N ₆ O ₅
Calculated mass [M+H] ⁺	728.4	728.4
Observed mass	728.1	728.2

ESI(+) mass spectra of deuterium-labeled product, derived from acidolysis of **75**, peaks corresponding to compounds **71a–71h**.



References

- (1) Gottlieb, H. E.; Kotlyar, V.; Nudelman, A. *J. Org. Chem.* **1997**, *62*, 7512.
- (2) Berger, S.; Braun, S. *200 and More NMR Experiments*; Wiley-VCH: Weinheim, Germany, 2004.
- (3) Claridge, T. D. W. *High-Resolution NMR Techniques in Organic Chemistry*; Pergamon: Oxford, UK, 1999.
- (4) Berger, S.; Braun, S. *200 and More NMR Experiments*; Wiley-VCH: Weinheim, Germany, 2004.
- (5) Hurd, R. E. *J. Magn. Reson.* **2011**, *213*, 467.
- (6) Brereton, I. M.; Crozier, S.; Field, J.; Doddrell, D. M. *J. Magn. Reson.* **1991**, *93*, 54.
- (7) Shaw, A. a.; Salaun, C.; Dauphin, J.-F.; Ancian, B. *J. Magn. Reson. Ser. A* **1996**, *120*, 110.

- (8) Cavanagh, J.; Rance, M. *J. Magn. Reson.* **1990**, *88*, 72.
- (9) Wagner, R.; Berger, S. *J. Magn. Reson. Ser. A* **1996**, *123*, 119.
- (10) Bax, A.; Davis, D. G. *J. Magn. Reson.* **1985**, *63*, 207.
- (11) Hwang, T. L.; Shaka, A. J. *J. Magn. Reson. Ser. A* **1995**, *112*, 275.
- (12) Palmer, A. G.; Cavanagh, J.; Byrd, R. A.; Rance, M. *J. Magn. Reson.* **1992**, *96*, 416.
- (13) Kay, L. E.; Keifer, P.; Saarinen, T. *J Am Chem Soc* **1992**, 10663.
- (14) Schleucher, J.; Schwendinger, M.; Sattler, M.; Schmidt, P.; Schedletzky, O.; Glaser, S. J.; Sørensen, O. W.; Schwendinger, C. G. *J. Biomol. NMR* **1994**, *4*, 301.
- (15) Marvel, C. S. *Org. Synth.* **1941**, *21*, 99.
- (16) Lawson, K. V.; Rose, T. E.; Harran, P. G. *Proc. Natl. Acad. Sci. U. S. A.* **2013**, *110*, E3753.
- (17) Weix, D. J.; Marković, D.; Ueda, M.; Hartwig, J. F. *Org. Lett.* **2009**, *11*, 2944.
- (18) Lo, C. Y.; Lin, C. C.; Cheng, H. M.; Liu, R. S. *Org. Lett.* **2006**, *8*, 3153.
- (19) Corey, E. J.; Cheng, H.; Baker, C. H.; Matsuda, S. P. T.; Li, D.; Song, X. *J. Am. Chem. Soc.* **1997**, *119*, 1277.
- (20) Corey, E. J.; Wang, Z. *Tetrahedron Lett.* **1994**, *35*, 539.
- (21) Koenigs, E.; Mylo, B. *Berichte der Dtsch. Chem. Gesellschaft* **1908**, *41*, 4427.
- (22) Bye, E.; Mostad, A.; Rømming, C. *Acta Chem. Scand.* **1973**, *27*, 471.
- (23) Flippen, J. L. *Acta Crystallogr. Sect. B* **1978**, *B34*, 995.
- (24) Oba, Y.; Kato, S. I.; Ojika, M.; Inouye, S. *Tetrahedron Lett.* **2002**, *43*, 2389.
- (25) Lamonp, H. M. *Tetrahedron* **1993**, *49*, 10663.
- (26) Shepbeck, J. E.; Kar, H.; Hong, H. *Tetrahedron Lett.* **2000**, *41*, 5329.

Chapter 4 Experimental Appendix

Experimental protocols for this section have been omitted out of space considerations, and are freely accessible via our communication on this material:

Lawson, K. V; Rose, T. E.; Harran, P. G. *Template-constrained macrocyclic peptides prepared from native, unprotected precursors. Proc. Natl. Acad. Sci. U. S. A.* **2013**, *110*, E3753.

doi: 10.1073/pnas.1311706110

Chapter 5 Experimental Appendix

General remarks:

See remarks Chapter 3 Experimental Appendix.

NMR methods:

Special NMR considerations are described in Chapter 3 Experimental Appendix.

X-ray Crystal Structure of Macrocycle 22a.

Macrocycle **22a** was crystallized by slow evaporation from methanol. Data for this product have been deposited in the Cambridge Crystallographic Data Centre under accession number CCDC 1023942. Disorder was apparent within the macrocycle. For clarity, only the predominant conformation is depicted and lattice solvent has been omitted.

Peptide synthesis:

Peptides were prepared using standard solution phase techniques and the Boc protection strategy, or standard solid phase synthesis using the Fmoc protection strategy. Couplings were performed with either *O*-(benzotriazol-1-yl)-*N,N,N',N'*-tetramethyluronium hexafluorophosphate (HBTU) or *O*-(benzotriazol-1-yl)-*N,N,N',N'*-tetramethyluronium tetrafluoroborate (TBTU). Orthogonal protection was accomplished with *N*^α-Boc-*N*^δ-Cbz-ornithine, *N*^α-Cbz-*N*^δ-Boc-ornithine or *N*^α-Fmoc-*N*^δ-Boc-ornithine. Orthogonal protection in compounds containing dichlorotyrosine was accomplished with *N*^α-Fmoc-*N*^δ-Boc-ornithine. Boc deprotection was performed using 4 M HCl in dioxane.¹ Cbz deprotection was performed with palladium on carbon in methanol under an atmosphere of hydrogen. Fmoc deprotection was performed as described using DBU in the presence of octyl mercaptan.² *N*-Acetylation was performed under coupling conditions with acetic acid. Prior to removal of the final protecting group, peptides were purified by column chromatography on SiO₂ eluted with 2→12% MeOH in CHCl₃. Peptide identities were verified by HPLC-ESI-MS.

Procedures for template couplings, Pd⁰-catalyzed and acid-promoted macrocyclizations:

General Procedure A - Acylation of peptides with template 3:

The peptide (1.5eq) was dissolved in *N,N*-DMF (0.2M), neutralized with Hünig's base (1.5eq) to free the ammonium salt, where necessary, and treated with template **3**. The reaction was stirred at room temperature until complete by TLC or HPLC, and was worked up by partitioning between EtOAc and saturated NaHCO₃. The organic phase was washed with saturated NaHCO₃ (x2) and brine, then dried over MgSO₄ and concentrated. Purification was accomplished by flash chromatography on SiO₂ eluted with 0→12% MeOH in CHCl₃.

General Procedure B - Palladium catalyzed macrocyclization:

The acyclic cinnamyl carbonate was dissolved in dry *N,N*-DMF (5 mM) and sparged with argon for approximately 15 min. The reaction vessel was briefly opened to introduce Pd(PPh₃)₄ (5 mol%) as a solid or stock solution in *N,N*-DMF, and sparging was continued for approximately 5 min. All reactions proceeded to completion within 60 min at rt, and were halted by passing air through the reaction for several minutes,

¹Han, G.; Tamaki, M.; Hruby, V. J. *J. Pept. Res.*, **58**, 338 (2001).

²Shepck, J. E.; Kar, H.; Hong, H. *Tetrahedron Lett.*, **41**, 5329 (2000).

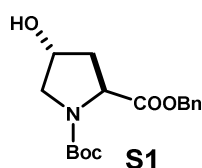
causing the yellow color of the catalyst to fade. The reaction mixture was then concentrated to dryness and promptly purified by flash chromatography on SiO₂ eluted with 0→12% MeOH in CHCl₃.

General Procedure C - Acid promoted macrocyclization / isomerization:

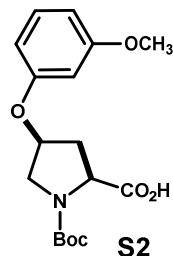
(Note: Commercial nitromethane should be aged over activated 3 Å molecular sieves for approximately one week. Alternatively, nitromethane may be treated with oven dried Brockmann type 1 neutral alumina overnight. These procedures appear to remove an as of yet unidentified contaminant, which without removal results in darkly colored reactions and diminished product purity. Acidolyses appeared to be insensitive to trace water content ~40-200ppm.) The cyclic cinnamyl tyrosyl ether or acyclic tert-butyl carbonate was dissolved or suspended in dry nitromethane (5 mM) under ambient atmosphere, and treated with methanesulfonic acid (15 eq.) at room temperature. After 2 hrs, three aliquots (25 µL ea.) were removed, quenched with methanolic Hünig's base (100 µL, 0.5M), concentrated to dryness and reconstituted in the internal standard solution (600 µL, 10.0 mM mesitylene in MeOH) for yield analysis. The remainder of the reaction was worked up by partitioning between EtOAc and saturated NaHCO₃. The organic phase was washed with saturated NaHCO₃ (x2) and brine, then dried over MgSO₄ and concentrated. Alternatively, reactions were quenched with Hünig's base (15 eq.) and concentrated. The product mixture was reconstituted in *N,N*-DMF and purified by semi-preparative RP-HPLC (see individual examples, below). HPLC assay yield was determined by external calibration normalized against the internal standard. Standard solutions of purified products were prepared in internal standard solution at approximately the same concentration as found in the crude reaction mixture samples (~10 µM to ~200 µM). Samples and calibrants were analyzed by RP-HPLC-UV with detection at 254nm (see individual methods, chromatograms, below).

Amino acids and building blocks therefore – Compounds S1 – S23:

***N*-Boc-*trans*-4-Hydroxy-*L*-proline benzyl ester (S1).** Compound S1 was prepared from *trans*-4-hydroxy-*L*-proline as described.^{3,4}



***N*-Boc-*cis*-4-(3-Methoxyphenoxy)-*L*-proline (S2).** Compound S2 was prepared from S1 by the Mitsunobu reaction with 3-methoxyphenol as described.^{5,6}

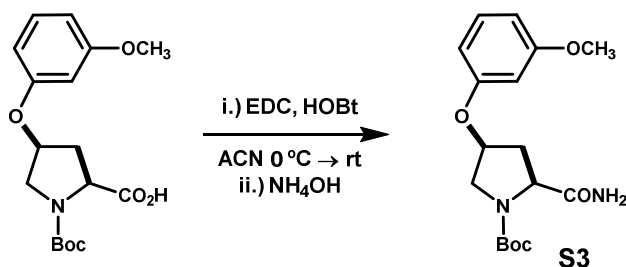


³ J. K. Thottathi, J. L. Moniot, *Tetrahedron Lett.* **27**, 151-154 (1986).

⁴ Q. Xiao-long, Q. Feng-ling, *J. Org. Chem.* **67**, 7162-7164 (2002).

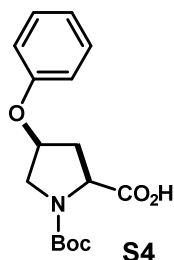
⁵ J. Krapcho, *et al.*, *J. Med. Chem.* **31**, 1148-1160 (1988).

⁶ A. D. Palkowitz, *et al.*, *J. Med. Chem.* **37**, 4508-4521 (1994).

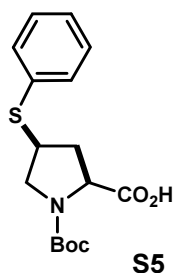


N-Boc-cis-4-(3-Methoxyphenoxy)-L-proline carboxamide (S3). Compound **S2** (503 mg, 1.5 mmol) and hydroxybenzotriazole monohydrate (274 mg, 1.8 mmol) were dissolved in anhydrous ACN (5 mL), cooled in an ice bath, and treated with EDC (343 mg, 1.8 mmol).⁷ The reaction was allowed to warm to room temperature, and stirred for 3.5 hr. The mixture was then re-cooled, treated with concentrated ammonium hydroxide (1.5 mL) and stirred cold for 30min, then at room temperature for 30min. The mixture was diluted with water and extracted into EtOAc (x3). The organic phase was dried over MgSO₄ and exchanged for 95:5 CHCl₃:MeOH, filtered through a plug of SiO₂ and again concentrated to give carboxamide **S3** (504mg, 100%). mp 130-132°C. $[\alpha]_D^{20} = +1.8^\circ$ (c = 0.5, MeOH). ¹H NMR (500 MHz, DMSO-*d*₆, major rotamer): δ 1.36 (s, 9H), 1.99-2.11 (m, 1H), 2.43-2.60 (m, 1H), 3.36-3.45 (m, 1H), 3.72 (s, 3H), 3.70-3.79 (m, 1H), 4.07-4.14 (m, 1H), 4.92-5.00 (m, 1H), 6.40-6.46 (m, 1H), 6.46-6.51 (m, 1H), 6.52 (d, *J* = 8.2 Hz, 1H), 6.95-7.00 (m, 1H), 7.17 (dd, *J* = 8.2, 8.2 Hz, 1H), 7.23 (br s, 1H). ¹³C NMR (126 MHz, DMSO-*d*₆, major rotamer): δ 173.7, 160.5, 158.1, 153.4, 130.0, 107.6, 106.7, 101.9, 78.9, 74.0, 58.7, 55.1, 51.5, 35.9, 28.0. MS *m/z* 237.2 (calc'd: C₁₇H₂₄N₂O₅, [M-CO₂tBu+2H]⁺, 237.2).

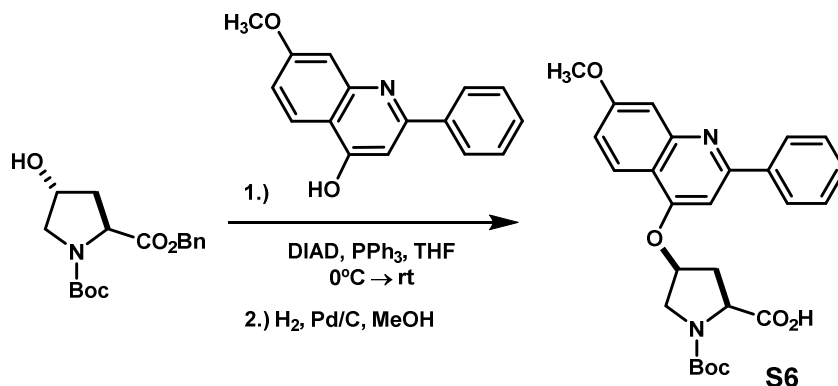
N-Boc-cis-4-Phenoxy-L-proline (S4). Compound **S4** was prepared analogously to **S2**, as described.¹



N-Boc-cis-4-Phenylthio-L-proline (S5). Compound **S5** was prepared as described.^{1,3}

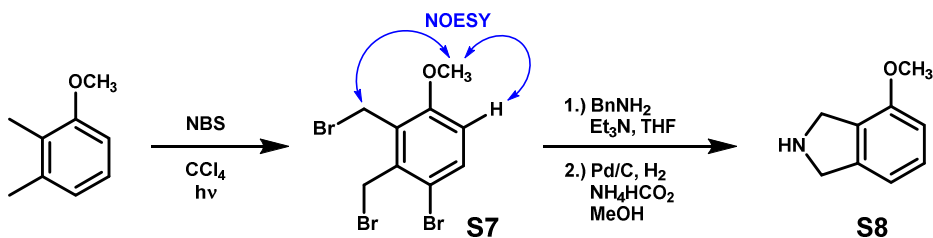


⁷ H. Fukushima, *et al.*, *Bioorg. Med. Chem.* **12**, 23, 6053-6061 (2004).



N-Boc-cis-4-((7-Methoxy-2-phenylquinolin-4-yl)oxy)-L-proline (S6). Compound **S1** (1.55 g, 4.8 mmol), 4-hydroxy-7-methoxy-2-phenylquinoline⁸ (1.21 g, 4.8 mmol) and triphenylphosphine (2.52 g, 9.6 mmol) were suspended in dry THF (20ml) and cooled in an ice bath. Diisopropyl azodicarboxylate was added dropwise over approximately 1 hr to afford a light yellow solution, which was warmed to room temperature and stirred overnight. The reaction mixture was concentrated, diluted with Et₂O, washed with H₂O (x1) and filtered to remove the resulting precipitate. The filtrate was washed with brine, dried over MgSO₄ and directly adsorbed onto silica gel. Flash chromatography on SiO₂ eluted with 0→100% Et₂O in hexanes afforded the intermediate benzyl ester as a light yellow foam. Deprotection with palladium on carbon in methanol under an atmosphere of hydrogen afforded compound **S6** as a light yellow foam (2.04 g, 91% two steps). m.p. softens 91°C melts 116-119°C. [α]_D²⁰ = -16.3° (c = 1, MeOH). ¹H NMR (500 MHz, DMSO-*d*₆, major rotamer): δ 1.37 (s, 9H), 2.40-2.45 (m, 1H), 2.72-2.79 (m, 1H), 3.61 (d, *J* = 12.5 Hz, 1H), 3.84-3.90 (m, 1H), 3.93 (s, 3H), 4.39 (dd, *J* = 9.6, 1.1 Hz, 1H), 5.55 (apt t, *J* = 4.4 Hz, 1H), 7.11 (dd, *J* = 9.2, 2.5 Hz, 1H), 7.37 (d, *J* = 2.5 Hz, 1H), 7.42 (s, 1H), 7.47-7.58 (m, 3H), 7.91 (d, *J* = 9.2 Hz, 1H), 8.26-8.30 (m, 2H), 12.55 (br s, 1H). ¹³C NMR (126 MHz, DMSO-*d*₆, mixture of rotamer): δ 173.2, 173.0, 160.8, 160.0, 159.9, 157.8, 156.2, 153.4, 153.3, 150.7, 139.2, 129.5, 128.6, 127.4, 123.3, 117.7, 114.8, 107.3, 97.7, 97.6, 79.1, 78.9, 76.3, 75.2, 57.7, 57.5, 55.4, 52.0, 51.8, 35.9, 35.1, 28.1, 28.0. MS *m/z* 465.2 (calc'd: C₂₆H₂₉N₂O₆, [M+H]⁺, 465.2).

4-Methoxyisindoline (S8):



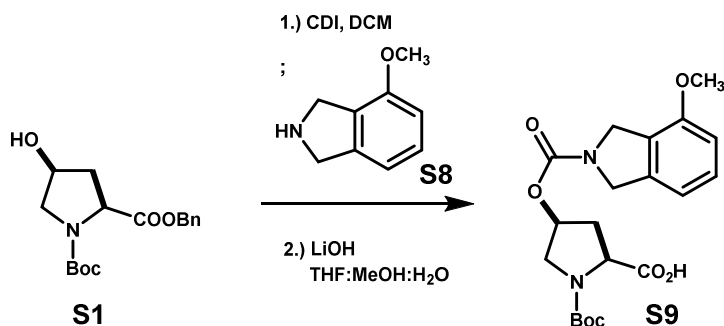
4-Bromo-2,3-bis(bromomethyl)anisole (S7). 2,3-Dimethylanisole⁹ (18.6 g, 137 mmol) was dissolved in benzene (170 mL), *N*-bromosuccinimide (85.1 g, 478 mmol) and dibenzoyl peroxide (332 mg, 1.37 mmol) were added, and the mixture was heated to reflux under an atmosphere of argon and irradiated with a tungsten lamp for 3.5 h. The reaction was diluted with an equal volume of hexanes, and filtered through a pad of SiO₂ rinsing with DCM. The filtrate was concentrated to give an oil, which solidified upon standing to give **S7**¹⁰ (39.7 g, 78%) as an off-white solid which was used without further purification. ¹H NMR (300 MHz, DMSO-*d*₆): δ 7.65 (d, *J* = 8.9 Hz, 1H), 7.05 (d, *J* = 8.9 Hz, 1H), 4.80 (s, 2H), 4.76 (s, 2H) 3.88 (s, 3H).

⁸ N. Goudreau, *et al*, *J. Org. Chem.* **69**, 6185-6201 (2004).

⁹ N. Goudreau, *et al*, *J. Org. Chem.* **69**, 6185-6201 (2004).
00 (2000).

¹⁰ Y. Goldberg, C. Bensimon, H. Alper, *J. Org. Chem.* **57**, 6374-6376 (1992).

4-Methoxyisindoline (S8). Compound **S7** (3.25 g, 8.7 mmol) was dissolved in THF (90 mL), and Et₃N (2.7 mL, 19.2 mmol) and benzylamine (951 μ L, 8.7 mmol) were added. The mixture was refluxed overnight, cooled and adsorbed onto SiO₂. Flash chromatography on SiO₂ eluted with 5→10% EtOAc in hexanes afforded moderately pure *N*-benzyl-4-bromo-7-methoxyisindoline as a viscous oil (1.19 g). Treatment with Pd/C in MeOH (10 mL) and ammonium formate (2.2 g) under an atmosphere of hydrogen at reflux effected debromination and debenzylation. The mixture was concentrated, reconstituted in 1N HCl, and washed with Et₂O (x2). The aqueous phase was basified to pH >10 with 1M NaOH and extracted with DCM (x3). The combined extract was washed with brine, dried over K₂CO₃ and concentrated to give **S8** (363 mg) as a brown oil, the NMR spectra of which matched reported values.^{11,12} MS *m/z* 150.2 (calc'd: C₉H₁₂NO, [M+H]⁺, 150.1).

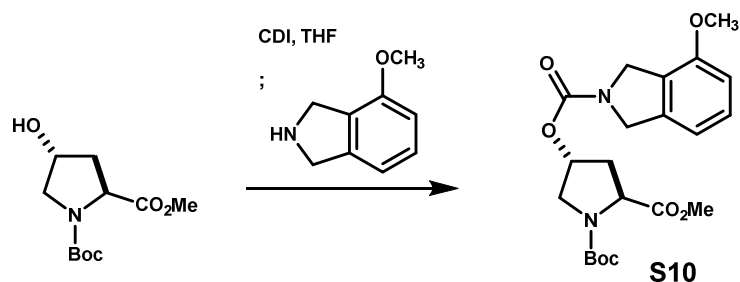


***N*-Boc-*cis*-4-((4-Methoxyisindoline-2-carbonyl)oxy)-*L*-proline (S9).** *N*-Boc-*cis*-4-Hydroxy-*L*-proline benzyl ester¹³ (**S1**) (631 mg, 2.6 mmol) was dissolved in anhydrous DCM (10 mL) and 1,1'-carbonyldiimidazole (459 mg, 2.8 mmol) was added as a solution in DCM (5 mL). The mixture was stirred overnight. 4-methoxyisindoline (**S8**) (383 mg, 2.6 mmol) was added, and the mixture was stirred for 24 hrs. The reaction was diluted with EtOAc, and washed with 1N HCl (x3), H₂O (x1), brine, dried over MgSO₄ and concentrated to give a red oil which was purified by flash chromatography on SiO₂ eluted with 30→50% EtOAc in hexanes to give the incipient methyl ester as a pink foam. The acid was freed by treatment with LiOH (3 eq) in THF:MeOH:H₂O (3:1:1) at room temperature for 3 hrs. The reaction mixture was diluted with 1M NaOH and washed with Et₂O (x1). The aqueous portion was cooled in an ice bath, DCM was added, and the mixture acidified to pH < 2 with 4N HCl. The organic phase was collected, and the aqueous extracted twice more with DCM. The combined extract was dried over MgSO₄ and concentrated to give compound **S9** as a white foam (421 mg, 40% two steps). [α]_D²⁰ = -10.5° (c = 0.5, MeOH). ¹H NMR (500 MHz, CD₃OD, major rotamer): δ 1.45 (s, 9H), 1.85-1.89 (m, 1H), 2.39-2.45 (m, 1H), 2.47-2.61 (m, 1H), 3.58-3.68 (m, 1H), 3.68-3.75 (m, 1H), 3.84 (s, 3H), 4.42-4.46 (m, 1H), 4.53-4.58 (m, 2H), 4.58-4.66 (m, 2H), 5.21-5.26 (m, 1H), 6.82 (d, *J* = 7.8 Hz, 1H), 6.84 (d, *J* = 7.8 Hz, 1H), 7.26 (dd, *J* = 7.8, 7.8 Hz, 1H). ¹³C NMR (126 MHz, CD₃OD, mixture of rotamers): δ 175.4, 175.3, 175.20, 175.17, 156.3, 156.2, 156.1, 156.0, 155.84, 155.78, 139.7, 139.0, 130.6, 130.5, 125.8, 125.2, 115.7, 115.6, 109.92, 109.85, 81.63, 81.62, 76.0, 75.9, 75.0, 74.9, 68.9, 59.2, 58.9, 55.8, 55.7, 54.1, 53.7, 53.63, 53.62, 53.3, 51.2, 51.0, 37.5, 37.4, 36.7, 36.6, 28.7, 28.6. MS *m/z* 406.2 (calc'd: C₂₀H₂₅N₂O₇, [M-H]⁻, 406.2).

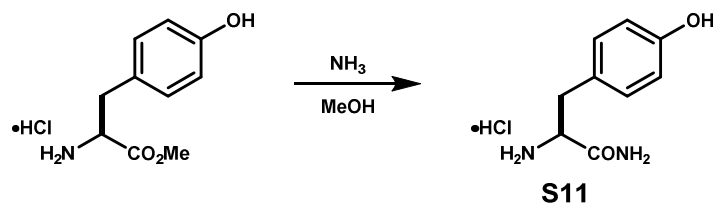
¹¹ J. R. Henry, *et al.*, (Eli Lilly and Co.), June 9, 2005. U.S. Patent Appl. No. 10/577,828.

¹² M. K. Holloway, *et al.*, (Merck and Co., Inc.), June 12, 2006. U.S. Patent Appl. No. 11/484,925.

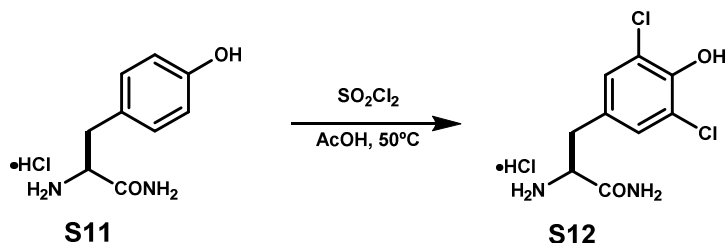
¹³ J. A. Gómez-Vidal, R. B. Silverman, *Org. Lett.* **3**, 2481-2484 (2001).



***N*-Boc-*trans*-4-((4-Methoxyisoindolin-2-carbonyl)oxy)-*L*-proline (S10).** *N*-Boc-*trans*-4-Hydroxy-*L*-proline methyl ester (809 mg, 3.3 mmol) was dissolved in THF (3.3 mL) and treated with 1,1'-carbonyldiimidazole (511 mg, 3.15 mmol). The mixture was stirred for 3 hr at rt, after which HPLC showed complete conversion to the acylimidazole. 4-Methoxyisoindoline (**S8**) (448 mg, 3 mmol) was added as a solution in ACN (15 mL) and the mixture was warmed to reflux for 4 hr. The reaction was cooled, diluted with EtOAc and washed with 1N HCl (x3), H₂O, brine, dried over Na₂SO₄, filtered through a pad of SiO₂ and concentrated to give **S10** as a light brown foam (1.10 g, 87%). An analytical sample was obtained by chromatography on SiO₂ eluted with 30→45% EtOAc in hexanes. $[\alpha]_D^{20} = -43.2^\circ$ (c = 0.5, MeOH). ¹H NMR (400 MHz, CD₃OD, major rotamer): δ 1.43 (s, 9H), 2.17-2.27 (m, 1H), 2.39-2.52 (m, 1H), 2.59-2.66 (m, 1H), 3.74 (s, 3H), 3.83 (s, 3H), 4.34-4.42 (m, 1H), 4.43-4.50 (m, 1H), 4.60 (br s, 2H), 4.72 (br s, 2H), 5.28-5.34 (m, 1H), 6.75 (d, *J* = 8.2 Hz, 1H), 6.86 (d, *J* = 7.6 Hz, 1H), 7.22-7.28 (m, 1H). ¹³C NMR (126 MHz, CD₃OD, mixture of rotamers): δ 172.2, 171.6, 171.5, 170.0, 153.7, 153.1, 141.6, 141.2, 136.8, 128.9, 128.73, 128.68, 128.3, 126.4, 126.0, 124.3, 109.4, 74.1, 60.3, 57.3, 55.4, 54.5, 51.5, 51.0, 39.3, 36.7, 36.0, 35.9, 35.3, 35.2, 31.55, 31.46, 30.5, 29.8, 26.9, 23.8, 19.7, 13.8, 6.5, 6.0. MS *m/z* 321.0 (calc'd: C₁₆H₂₁N₂O₅, [M-Boc+2H]⁺, 321.1).



Tyrosine carboxamide hydrochloride (S11). Compound **S11** was prepared by ammoniolysis of tyrosine methyl ester hydrochloride using saturated ammoniacal methanol as described.¹⁴



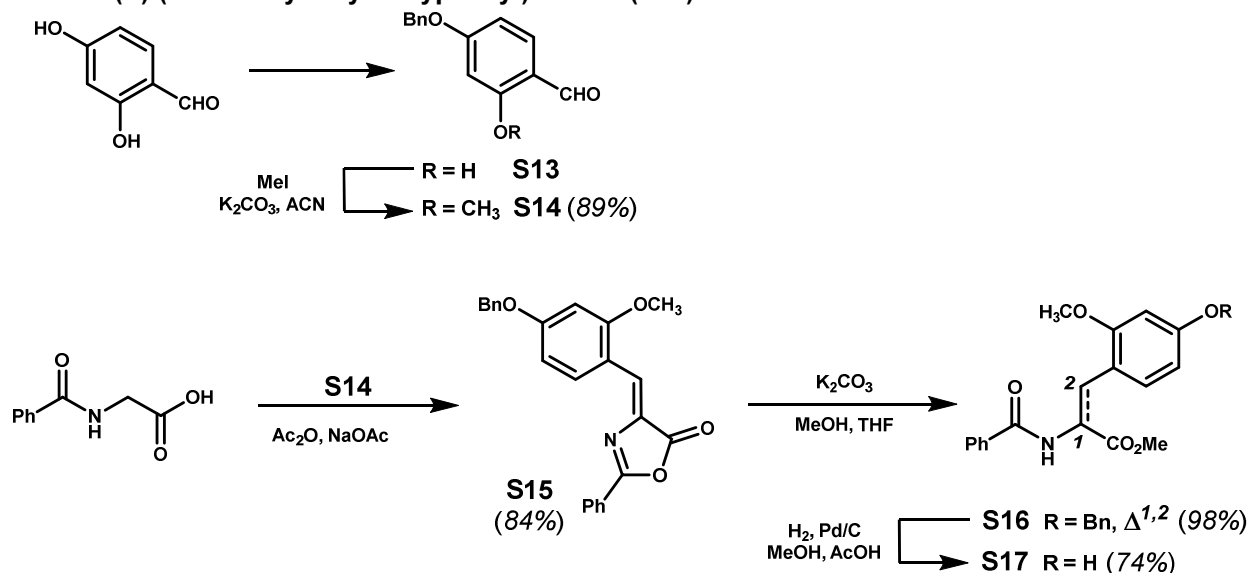
Dichlorotyrosine carboxamide hydrochloride (S12). Compound **S12** was prepared analogously to dichlorotyrosine.¹⁵ Compound **S11** (3.0 g, 13.8 mmol) was suspended in glacial acetic acid (60 mL) and treated with sulfuryl chloride (28 mL, 346 mmol). The reaction was warmed to 50°C for 30 min, concentrated to approximately 1/3 the initial volume, cooled in an ice bath and carefully quenched with MeOH. Once gas evolution ceased, the mixture was cooled in a -78 °C bath and diluted with Et₂O to induce precipitation. The precipitate was collected by centrifugation and dried to give compound **S12** as a white solid (2.4g, 91%). m.p. ~190 °C decomposes. $[\alpha]_D^{20} = +14.2^\circ$ (c = 1, MeOH). ¹H NMR (400 MHz, DMSO-*d*₆): δ 2.88 (dd, *J* = 14.1, 8.1 Hz, 1H), 3.04 (dd, *J* = 14.1, 5.4 Hz, 1H), 3.89-3.98 (m, 1H), 7.27 (s, 2H), 7.61 (s, 1H), 7.92 (s,

¹⁴ E. Koenigs, B. Mylo, *Ber. Dtsch. Chem. Ges.* **41**, 4427-4443 (1908).

¹⁵ T. Golakoti, *et al*, *J. Am. Chem. Soc.* **117**, 12030-12049 (1995).

1H), 8.10 (br s, 3H), 10.08 (br s, 1H). ¹³C NMR (126 MHz, DMSO-*d*₆): δ 169.6, 148.2, 129.7, 128.0, 122.0, 53.3, 35.2. MS *m/z* 249.1 (calc'd: C₉H₁₁Cl₂N₂O₂, [M+H]⁺, 249.0).

***N*-Fmoc-(*S*)-(2-Methoxy-4-hydroxyphenyl)alanine (**S17**):**



4-Benzyloxy-2-methoxybenzaldehyde (S14**).** 4-Benzyloxy-2-Hydroxybenzaldehyde (**S13**) was prepared as described,¹⁶ and obtained as a light red solid (25.4 g, 89%) of moderate purity following recrystallization from methanol. This material (25 g, 111 mmol) was dissolved in acetonitrile, treated with potassium carbonate (23 g, 167 mmol) and methyl iodide (10.4 mL, 167 mmol), and heated under reflux for 2.5 hrs. The reaction mixture was cooled, filtered and concentrated, and the residue was reconstituted in EtOAc and washed with 1M NaOH (x3), water, brine, dried over Na₂SO₄ and again concentrated. The yellow solid obtained was recrystallized twice from EtOH to give 4-benzyloxy-2-methoxybenzaldehyde (**S14**) in ~93% purity (23.9 g, 89%). An analytical sample was obtained by purification of the mother liquor by flash chromatography on SiO₂ eluted with 5→20% EtOAc in hexanes (1.5 g; combined 25.4 g, 94%). ¹H NMR (400 MHz, CDCl₃): δ 3.88 (s, 3H), 5.13 (s, 2H), 6.54 (d, *J* = 2.2 Hz, 1H), 6.62 (ddd, *J* = 8.6, 2.2, 0.4 Hz, 1H), 7.33-7.46 (m, 5H), 7.81 (d, *J* = 8.7 Hz, 1H), 10.29 (d, *J* = 0.4 Hz, 1H). ¹³C NMR (101 MHz, CDCl₃): δ 188.3, 165.3, 163.5, 135.9, 130.7, 128.7, 128.4, 127.5, 119.2, 106.4, 98.9, 70.4, 55.6. MS *m/z* 243.0 (calc'd: C₁₅H₁₅O₃, [M+H]⁺, 243.1).

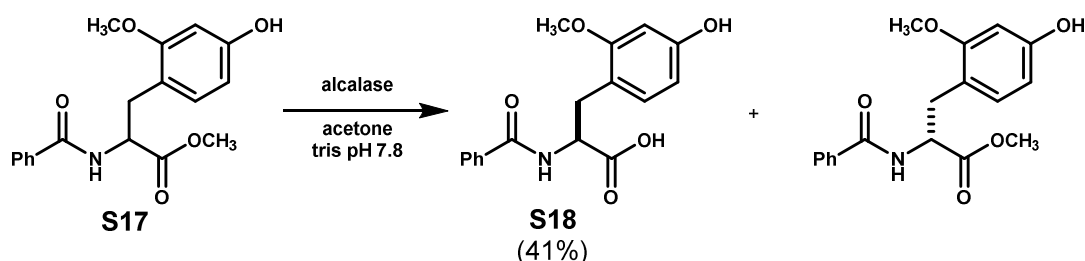
Benzylidene oxazolone (S15**).** Hippuric acid (5.30 g, 29.6 mmol) and aldehyde **S14** (7.17 g, 29.6 mmol) were treated with acetic anhydride (8.4 mL, 89 mmol) and freshly fused NaOAc (2.43 g, 29.6 mmol). The mixture was heated rapidly with a heat gun, which caused near dissolution and then rapid precipitation. This mixture was placed in a pre-heated oil bath at 85°C for 3 hrs, ethanol (~3 mL) was added dropwise, and the mixture was allowed to cool. The resulting solids were collected, rinsed with ethanol and dried *in vacuo* to give benzylidene oxazolone **S15** as a green fluorescent, bright yellow solid (9.59 g, 84%). m.p. 196-199 °C, ¹H NMR (400 MHz, DMSO-*d*₆): δ 3.92 (s, 3H), 5.24 (s, 2H), 6.78 (d, *J* = 2.3 Hz, 1H), 6.83 (dd, *J* = 8.9, 2.3 Hz, 1H), 7.34-7.39 (m, 1H), 7.40-7.45 (m, 2H), 7.47-7.52 (m, 3H), 7.58-7.64 (m, 2H), 7.69 (dddd, *J* = 8.3, 6.4, 1.2, 1.2 Hz, 1H), 8.06-8.10 (m, 2H), 8.77 (d, *J* = 8.8 Hz, 1H). ¹³C NMR (101 MHz, DMSO-*d*₆): δ 167.2, 163.2, 161.5, 160.8, 136.4, 133.6, 133.2, 129.7, 129.3, 128.5, 128.1, 128.0, 127.6, 125.3, 124.2, 115.0, 108.0, 98.8, 69.8, 56.1. MS *m/z* 386.0 (calc'd: C₂₄H₂₀NO₄, [M+H]⁺, 386.1).

Dehydro amino acid methyl ester (S16**).** Compound **S15** was treated with K₂CO₃ (10.4 g, 75 mmol) in THF:MeOH (3:1, 125 mL), and the suspension was stirred for 3 hr, filtered and concentrated. The residual solids were triturated with EtOAc, and the solids collected by filtration and dried *in vacuo* to give the **S16**

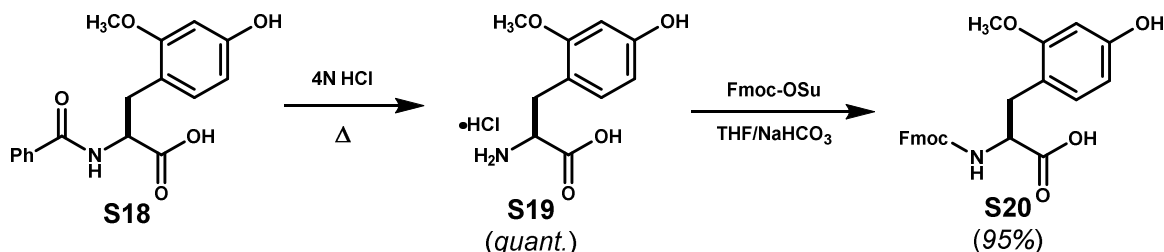
¹⁶ W. L. Mendelson, M. Holmes, J. Dougherty, *Synth. Commun.* **26**, 3, 593-601 (1996).

(10.2 g, 98%). m.p. 157 °C (decomposes). ¹H NMR (400 MHz, DMSO-*d*₆): δ 3.53 (s, 3H), 3.77 (s, 3H), 5.08 (s, 2H), 6.17 (s, 1H), 6.52 (dd, *J* = 8.4, 2.6 Hz, 1H), 6.54 (d, *J* = 2.6 Hz, 1H), 7.25-7.35 (m, 5H), 7.36-7.41 (m, 2H), 7.43-7.47 (m, 2H), 8.04-8.10 (m, 1H), 8.91 (d, *J* = 8.4 Hz, 1H). ¹³C NMR (101 MHz, DMSO-*d*₆): δ 171.6, 166.6, 156.7, 156.6, 143.7, 142.3, 137.4, 130.7, 128.4, 128.2, 127.7, 127.6, 126.8, 120.9, 105.0, 98.3, 69.2, 55.3, 50.5. MS *m/z* 418.0 (calc'd: C₂₅H₂₄NO₅, [M+H]⁺, 418.2).

Racemic amino acid methyl ester (S17). Compound **S16** was treated with Pd/C (5 wt%, 250 mg) in MeOH (75 mL) and acetic acid (10 mL) under 500 psi hydrogen at room temperature. Upon completion, the mixture was filtered through Celite, rinsing with MeOH, and concentrated to ~15 mL, which induced crystallization. Filtered and washed with a small amount of cold EtOAc to give compound **S17** as a white crystalline solid (5.95 g, 74%). m.p. 164-166 °C. ¹H NMR (400 MHz, DMSO-*d*₆): δ 2.87 (dd, *J* = 13.6, 9.6 Hz, 1H), 3.10 (dd, *J* = 13.6, 5.5 Hz, 1H), 3.60 (s, 3H), 3.74 (s, 3H), 4.60 (ddd, *J* = 9.6, 7.7, 5.5 Hz, 1H), 6.23 (dd, *J* = 8.2, 2.3 Hz, 1H), 6.37 (d, *J* = 2.3 Hz, 1H), 6.97 (d, *J* = 8.2 Hz, 1H), 7.43-7.48 (m, 2H), 7.50-7.56 (m, 1H), 7.77-7.81 (m, 2H), 8.65 (d, *J* = 7.7 Hz, 1H), 9.27 (s, 1H). ¹³C NMR (101 MHz, DMSO-*d*₆): δ 172.5, 166.3, 158.1, 157.6, 133.7, 131.4, 131.1, 128.3, 127.3, 115.3, 106.5, 98.9, 55.2, 52.9, 51.7, 30.9. MS *m/z* 330.0 (calc'd: C₁₈H₂₀NO₅, [M+H]⁺, 330.1).



***N*-Benzoyl-(*S*)-2-methoxy-4-hydroxyphenylalanine (S18).** Racemic amino acid methyl ester **S17** (4.5 g, 14 mmol) was dissolved in DMSO (10 mL) and diluted with acetone (120 mL) followed by Tris buffer (80 mM) pH 7.8. The heterogeneous mixture was warmed to 37 °C and Alcalase 2.4 L from *Bacillus licheniformis* (3 mL, >2.4 U/mL, Sigma) was added. The reaction was periodically adjusted to pH 7.8 by the addition of 1M NaOH until conversion ceased by HPLC (2 days). The volatiles were removed in vacuo, solids were removed by filtration, and the aqueous was extracted with EtOAc (x3). This organic extract was back extracted with aqueous NaHCO₃ (x1). The combined aqueous phases were acidified with conc. HCl to pH < 2 and extracted with EtOAc (x3). This organic extract was washed with brine, dried over Na₂SO₄ and concentrated. The resulting solid was recrystallized by dissolving in boiling MeOH diluting with EtOAc (~1:1), and allowing to cool to room temperature, and then chilling to -20 °C. Filtered to give compound (*S*)-acid **S18** as white needles (1.91 g, 41%). m.p. 216 – 217 °C, [α]_D²⁰ = -97° (c = 0.5, DMF). ¹H NMR (400 MHz, DMSO-*d*₆): δ 2.83 (dd, *J* = 13.6, 10.3 Hz, 1H), 3.14 (dd, *J* = 13.6, 4.6 Hz, 1H), 3.74 (s, 3H), 4.56 (ddd, *J* = 10.3, 8.1, 4.6 Hz, 1H), 6.22 (dd, *J* = 8.1, 2.2 Hz, 1H), 6.36 (d, *J* = 2.2 Hz, 1H), 7.00 (d, *J* = 8.1 Hz, 1H), 7.42-7.47 (m, 2H), 7.49-7.54 (m, 1H), 7.75-7.80 (m, 2H), 8.48 (d, *J* = 8.1 Hz, 1H), 9.23 (br s, 1H), 12.54 (br s, 1H). ¹³C NMR (101 MHz, DMSO-*d*₆): δ 173.5, 166.2, 158.1, 157.4, 134.0, 131.3, 131.1, 128.2, 127.3, 115.9, 106.4, 98.9, 55.2, 52.8, 30.9. MS *m/z* 316.1 (calc'd: C₁₇H₁₈NO₅, [M+H]⁺, 316.1).

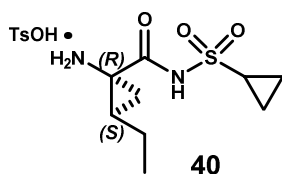


(*S*)-(2-Methoxy-4-hydroxyphenyl)alanine hydrochloride (S19). Compound **S18** (1.21 g, 3.8 mmol) was treated with 4N HCl and refluxed for 6 hrs, after which HPLC showed complete consumption of the starting material. The mixture was cooled, washed with Et₂O (x3) and concentrated to give crude **S19** as a faintly brown solid (964 mg, quant.). [α]_D²⁰ = -15° (c = 0.5, 1N HCl). ¹H NMR (400 MHz, DMSO-*d*₆): δ 2.93 (dd, *J* = 13.9, 6.7 Hz, 1H), 3.00 (dd, *J* = 13.6, 6.8 Hz, 1H), 2.69 (s, 3H), 3.84-3.93 (m, 1H), 6.31 (dd, *J* = 8.1, 2.2 Hz, 1H), 6.42 (d, *J* = 2.2 Hz, 1H), 6.92 (d, *J* = 8.1 Hz, 1H), 8.36 (d, *J* = 4.0 Hz, 3H). ¹³C NMR (101 MHz, DMSO-

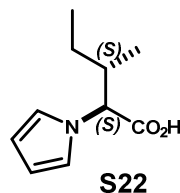
d_6): δ 170.5, 158.5, 158.4, 131.5, 112.7, 106.9, 99.1, 55.1, 52.4, 30.7. MS m/z 212.0 (calc'd: $C_{10}H_{13}NO_4$, $[M+H]^+$, 212.1).

Fmoc-(S)-(2-Methoxy-4-hydroxyphenyl)alanine (S20). Compound **S19** (964 mg, 3.8 mmol) was dissolved in THF (20 mL) and sat. $NaHCO_3$ (20 mL), Fmoc-OSu (1.28 g, 3.8 mmol) was added, and the mixture was allowed to stir overnight. The volatiles were removed, and the aqueous remainder was diluted with 5% K_2CO_3 , washed with MTBE (x2). The ethereal wash was back extracted with 5% K_2CO_3 (x1), and the combined aqueous was acidified with 6N HCl to pH < 2 and extracted with EtOAc (x3). The organic extract was washed with water (x1), brine, dried over Na_2SO_4 and concentrated. The resulting brown oil was triturated with hexanes, and the solids collected by filtration to give **S20** as a light brown solid (1.57 g, 95%). m.p. 102 – 106 °C. $[\alpha]_D^{20} = -11.5^\circ$ (c = 0.5, MeOH) 1H NMR (300 MHz, $DMSO-d_6$): δ 2.65 (dd, $J = 13.5, 10.4$ Hz, 1H), 3.04 (dd, $J = 13.5, 4.6$ Hz, 1H), 3.73 (s, 3H), 4.09–4.17 (m, 1H), 4.16–4.21 (m, 3H), 6.25 (dd, $J = 8.1, 1.9$ Hz, 1H), 6.38 (d, $J = 1.9$ Hz, 1H), 6.96 (d, $J = 8.1$ Hz, 1H), 7.29 (d, $J = 7.6$ Hz, 1H), 7.34 (d, $J = 7.6$ Hz, 1H), 7.42 (br dd, $J = 8.4, 7.6$ Hz, 2H), 7.54 (d, $J = 8.4$ Hz, 1H), 7.66 (dd, $J = 8.4, 7.4$ Hz, 2H), 7.88 (d, $J = 7.4$ Hz, 2H), 9.27 (br s, 1H), 12.54 (br s, 1H). ^{13}C NMR (75 MHz, $DMSO-d_6$): δ 173.8, 158.1, 157.5, 155.9, 143.8, 140.7, 131.3, 127.6, 127.1, 125.32, 125.26, 120.1, 115.7, 106.4, 98.8, 65.6, 55.2, 54.0, 46.6, 31.1. MS m/z 434.0 (calc'd: $C_{25}H_{24}NO_6$, $[M+H]^+$, 434.2).

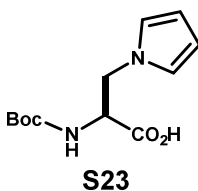
1R,2S-1-Amino-N-(cyclopropylsulfonyl)-2-ethylcyclopropane-1-carboxamide (40). Tosylate salt **40** was prepared from (1R,2S)-1-amino-2-vinylcyclopropanecarboxylic acid¹⁷ and cyclopropanesulfonamide¹⁸ as described.^{19,20}



α -(1-Pyrrolyl)-L-isoleucine (S22). Compound S22²¹ was prepared as reported.²² (3.0 g, 83%) $[\alpha]_D^{20} = +1.8^\circ$ (c = 0.5, $CHCl_3$). 1H NMR (500 MHz, $CDCl_3$): δ 0.87 (t, $J = 7.5$ Hz, 3H), 0.97–1.04 (m, 1H), 1.05 (d, $J = 6.7$ Hz, 3H), 1.20–1.29 (m, 1H), 2.19–2.28 (m, 1H), 4.27 (d, $J = 10.1$ Hz, 1H), 6.20 (t, $J = 2.0$ Hz, 1H), 6.79 (t, $J = 2.0$ Hz, 2H), 11.48 (br s, 1H). ^{13}C NMR (126 MHz, $CDCl_3$): δ 176.9, 120.6, 108.7, 67.5, 37.7, 24.9, 15.7, 10.7. MS m/z 180.2 (calc'd: $C_{10}H_{14}NO_2$, $[M-H]^-$, 180.1).



N-Boc- β -(1-Pyrrolyl)-L-alanine (S23). Compound **S23** was prepared analogously to the reported Paal-Knorr reaction of ornithine.²³ $[\alpha]_D^{20} = +50.3^\circ$ (c = 0.3, $CHCl_3$). 1H NMR (500 MHz, $DMSO-d_6$): δ 1.34 (s, 9H), 4.45 (dd, $J = 13.7, 9.5$ Hz, 1H), 4.18 (ddd, $J = 9.5, 8.2, 4.5$ Hz, 1H), 4.25 (dd, $J = 13.7, 4.5$ Hz, 1H), 5.95 (dd, $J = 1.9, 1.9$ Hz, 2H), 6.72 (dd, $J = 1.9, 1.9$ Hz, 2H), 7.16 (d, $J = 8.2$ Hz, 1H), 12.90 (br s, 1H). ^{13}C NMR (126 MHz, $DMSO-d_6$, major rotamer): δ 171.8, 155.4, 121.2, 107.7, 78.3, 55.4, 48.8, 28.2. MS m/z 253.2 (calc'd: $C_{12}H_{17}N_2O_4$, $[M-H]^-$, 253.1).



¹⁷ P. L. Beaulieu, *et al.*, *J. Org. Chem.* **70**, 15, 5869–5879 (2005).

¹⁸ S. Ny, *et al.*, (Bristol-Myers Squibb Co.) US2006183694 (A1), August 17, 2006.

¹⁹ Z. J. Song, *et al.*, *J. Org. Chem.* **76**, 19, 7804–7815 (2011).

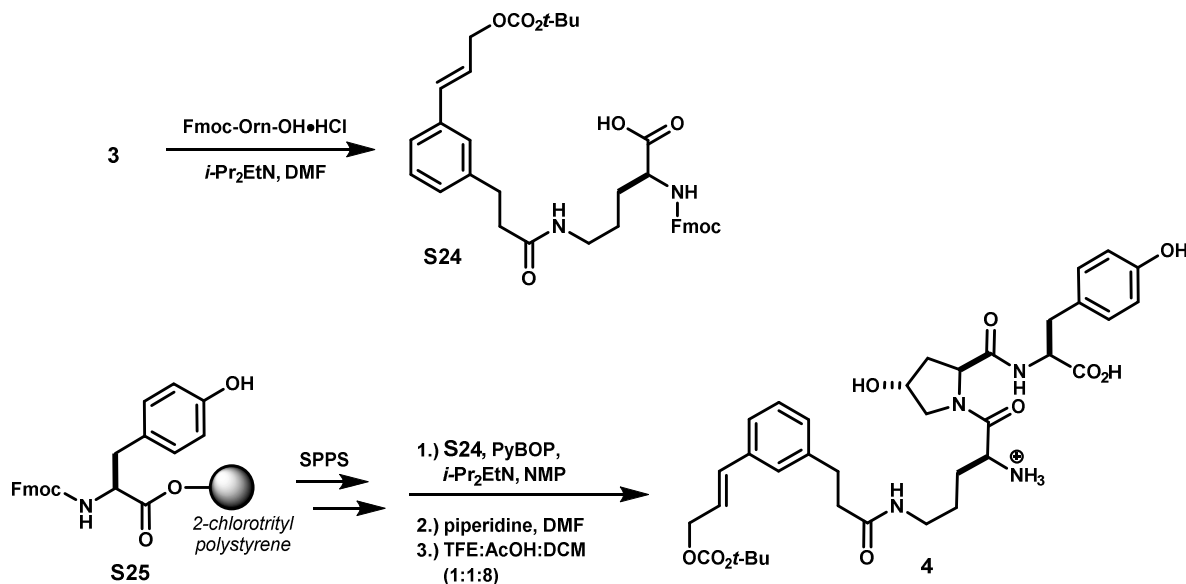
²⁰ N. J. Liverton, *et al.*, (Merck & Co. Inc., USA). WO2008057209 (A1), May 15, 2008.

²¹ J. Gloede, *et al.*, *Collect. Czech. Chem. Commun.* **33**, 1307–1314 (1968).

²² C. W. Jefford, F. de Villedon de Naide, K. Sienkiewicz, *Tetrahedron: Asymmetry* **7**, 4, 1069–1076 (1996).

²³ A. M. Doherty, *et al.*, *J. Med. Chem.* **34**, 1258–1271 (1991).

Macrocycle 5:



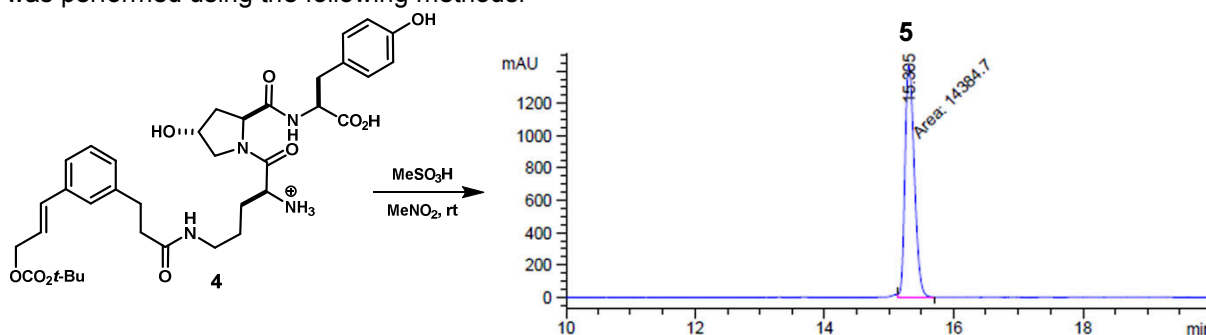
Fmoc-Ornithine-(δ -3)-OH (S24). Fmoc-Ornithine hydrochloride (686 mg, 1.75 mmol) was treated with template **3** (708 mg, 1.75 mmol) and *i*Pr₂EtN (915 μ L, 5.25 mmol) in DMF (5 mL) for 8 hrs. The mixture was partitioned between EtOAc and water, and the organic phase was washed with water, brine, dried over Na₂SO₄ and concentrated. This material was purified by flash chromatography on SiO₂ eluted with 0→15% MeOH in DCM to give **S24** as a vitreous oil (651 mg, 58%). [α]_D²⁰ = +14.2° (c = 0.5, CHCl₃). ¹H NMR (500 MHz, DMSO-*d*₆): δ 1.35-1.50 (m, 2H), 1.42 (s, 9H), 1.50-1.60 (m, 1H), 1.65-1.74 (m, 1H), 2.36 (t, *J* = 7.8 Hz, 2H), 2.80 (t, *J* = 7.8 Hz, 2H), 3.03 (dd, *J* = 12.8, 6.7 Hz, 2H), 3.92 (9.2, 8.1, 4.8 Hz, 1H), 4.22 (t, *J* = 7.0 Hz, 1H), 4.28 (d, *J* = 7.0 Hz, 2H), 4.67 (dd, *J* = 6.2, 1.0 Hz, 2H), 6.33 (dt, *J* = 15.9, 6.2 Hz, 1H), 6.63 (d, *J* = 15.9 Hz, 1H), 7.10 (br d, *J* = 7.3 Hz, 1H), 7.26 (br d, *J* = 7.5 Hz, 1H), 7.29 (br s, 1H), 7.33 (dd, *J* = 7.5, 0.8 Hz, 2H), 7.41 (dd, *J* = 7.5, 7.5 Hz, 2H), 7.63 (d, *J* = 8.1 Hz, 1H), 7.73 (d, *J* = 7.5 Hz, 2H), 7.82 (apt t, *J* = 5.4, Hz, 1H), 7.89 (d, *J* = 7.5 Hz, 2H), 12.56 (br s, 1H). ¹³C NMR (126 MHz, DMSO-*d*₆): δ 173.9, 171.1, 156.1, 152.8, 143.9, 143.8, 141.8, 140.7, 135.8, 133.5, 128.6, 128.0, 127.6, 127.1, 126.4, 125.3, 124.2, 123.3, 120.1, 81.5, 66.9, 65.6, 53.7, 46.7, 38.1, 37.0, 31.0, 28.3, 27.4, 26.0. MS *m/z* 641.1 (calc'd: C₃₇H₄₁N₂O₈, [M-H]⁻, 641.3).

Fmoc-Tyrosine 2-chlorotritylpolystyrene ester (S25). 2-Chlorotrityl chloride polystyrene resin (595 mg, 0.5 mmol) was swollen in anhydrous DCM and reacted with Fmoc-Tyr-OH (605 mg, 1.5 mmol) and *i*Pr₂EtN (523 μ L, 3 mmol) for 2 hr. Methanol was added, and the resin shaken for 15 min, filtered and rinsed thoroughly with DMF, DCM and MeOH, and dried *in vacuo* (862 mg). The loading (0.52 mmol/g) was determined by spectrophotometric quantification of the dibenzofulvene released by treatment of an aliquot with DBU in triplicate.³

Acyclic carbonate 4: Resin-bound **S25** was deprotected, coupled to Fmoc-*cis*-Hyp-OH using PyBOP, and again deprotected. This material (0.2 mmol) was treated with *i*Pr₂EtN (130 μ L, 0.76 mmol), **S24** (241 mg, 0.38 mmol), and PyBOP (198 mg, 0.38 mmol) for 1h, then deprotected with 20% piperidine in DMF for 1 min, and repeated for 30 min. Resin cleavage was achieved by treating with TFE:AcOH:DCM (1:1:8) for 2hr, and the crude residue was purified by preparative HPLC (Waters Sunfire C18, 35→100% ACN + 0.1%TFA) to give **4** (47 mg, ~34% from **S25**). ¹H NMR (500 MHz, DMSO-*d*₆, major rotamer): δ 1.43 (s, 9H), 1.47-1.57 (m, 2H), 1.58-1.66 (m, 1H), 1.66-1.74 (m, 1H), 1.82 (ddd, *J* = 13.0, 8.4, 4.5 Hz, 1H), 2.09 (dd, *J* = 13.0, 8.5 Hz, 1H), 2.37 (dd, *J* = 8.4, 7.4 Hz, 2H), 2.76-2.81 (m, 2H), 2.81 (dd, *J* = 7.8, 3.7 Hz, 1H), 2.87

(dd, $J = 13.9, 5.4$ Hz, 1H), 2.98-3.11 (m, 2H), 3.47 (dd, $J = 10.7, 3.9$ Hz, 1H), 3.56 (br d, $J = 10.7$ Hz, 1H), 4.10-4.16 (m, 1H), 4.29 (ddd, $J = 7.6, 7.6, 5.7$ Hz, 1H), 4.32-4.36 (m, 1H), 4.53 (t, $J = 8.2$ Hz, 1H), 4.67 (dd, $J = 6.2, 1.0$ Hz, 1H), 6.33 (dt, $J = 15.9, 6.2$ Hz, 1H), 6.64 (d, $J = 15.9$ Hz, 1H), 6.65 (d, $J = 8.5$ Hz, 2H), 7.06 (d, $J = 8.5$ Hz, 2H), 7.11 (br d, $J = 7.2$ Hz, 1H), 7.25 (apt t, $J = 7.4$ Hz, 1H), 7.26-7.31 (m, 2H), 7.86 (dd, $J = 5.6, 5.6$ Hz, 1H), 8.09 (br d, $J = 3.8$ Hz, 3H), 8.27 (d, $J = 7.6$ Hz, 1H), 9.25 (br s, 1H), 12.65 (br s, 1H). ^{13}C NMR (126 MHz, DMSO- d_6 , major rotamer): δ 172.8, 171.4, 171.0, 167.2, 156.0, 152.8, 141.8, 135.9, 133.5, 130.2, 128.7, 128.0, 127.4, 126.4, 124.3, 123.3, 115.0, 81.6, 68.9, 66.9, 58.4, 54.1, 50.8, 37.83, 37.79, 37.0, 36.0, 31.0, 27.4, 24.0. MS m/z 697.3 (calc'd: $\text{C}_{36}\text{H}_{49}\text{N}_4\text{O}_{10}$, $[\text{M}+\text{H}]^+$, 697.3).

Macrocycle 5: General procedure B gave **5** as a colorless film (14.4 mg). HPLC analysis and purification was performed using the following methods.



Analytical HPLC method:

Column: Waters Sunfire™ C₁₈, 4.6x250mm, 5 μm .

Solvent A: H₂O + 0.1%v TFA

Solvent B: ACN + 0.1%v TFA

Flow rate: 1.00 ml/min

Time	%B
0	20
2	20
25	45
28	100
35	100
38	20
41	20

Semi-preparative HPLC method:

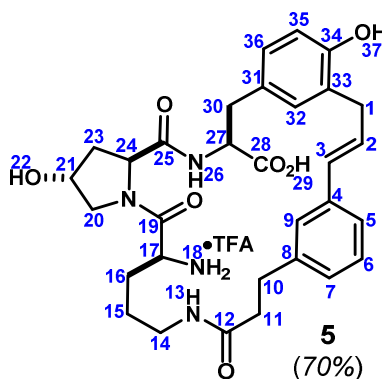
Column: Waters Sunfire™ C₁₈, 10x250mm, 5 μm .

Solvent A: H₂O + 0.1%v TFA

Solvent B: ACN + 0.1%v TFA

Flow rate: 6.00 ml/min

Time	%B
0	23
1	23
20	35
22	23
24	23



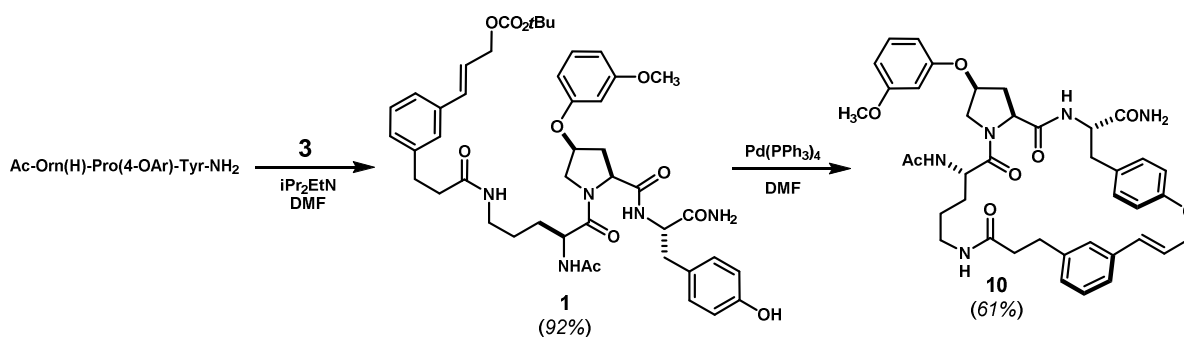
(600MHz, DMSO- d_6 , 298K)

	^{13}C	^1H	key correlations
1	32.0	3.36 (dd, $J = 15.6, 6.9$ Hz, 1H), 3.49 (dd, $J = 15.6, 7.2$ Hz, 1H)	HMBC 1→33,34

2	128.5	6.31 (ddd, $J = 15.7, 7.2, 6.9$ Hz, 1H)	COSY 2→1 HMBC 2→33
3	130.4	6.47 (d, $J = 15.7$ Hz, 1H)	HMBC 3→4
4	136.9	-	
5	124.0	7.16 (br d, $J = 7.6$ Hz, 1H) overlap	HMBC 5→3
6	128.2	7.19 (dd, $J = 7.6, 6.9$ Hz, 1H) overlap	HMBC 6→4,8
7	127.4	7.03 (br d, $J = 6.9$ Hz, 1H)	
8	141.4	-	
9	124.7	7.29 (br s, 1H)	HMBC 9→5,7
10	30.5	2.75-2.85 (m, 2H) overlap	HMBC 10→8,9,12
11	36.4	2.36-2.48 (m, 2H)	HMBC 11→8,12
12	171.1	-	
13	-	7.70 (dd, $J = 5.5, 5.5$ Hz, 1H)	HMBC 13→12 COSY 13→14
14	37.5	2.88-2.97 (m, 1H) overlap, 3.00-3.09 (m, 1H)	COSY 14→15
15	23.1	1.29-1.46 (m, 2H)	COSY 15→16
16	26.5	1.57-1.73 (m, 2H)	TOCSY 16→17,18
17	50.3	4.11-4.19 (m, 1H)	HMBC 17→19
18	-	8.08 (m, 3H) overlap	HMBC 18→17
19	167.2	-	
20	54.7	3.49-3.56 (m, 2H) overlap	
21	68.7	4.30-4.34 (m, 1H)	COSY 21→20,23,23' TOCSY 21→22
22	-	8.14 (br s, 1H)	
23	37.5	1.80 (ddd, $J = 12.9, 8.5, 4.5$ Hz, 1H), 2.04 (br dd, $J = 12.9, 7.7$ Hz, 1H)	
24	58.4	4.47 (dd, $J = 8.5, 7.7$ Hz, 1H)	HMBC 24→19
25	171.0	-	
26	-	8.30 (d, $J = 7.9$ Hz, 1H)	
27	54.4	4.23-4.31 (m, 1H)	HMBC 27→31
28	172.7	-	
29	-	12.66 (br s, 1H)	
30	36.2	2.77 (dd, $J = 13.9, 7.3$ Hz, 1H) overlap, 2.89 (dd, $J = 13.9, 6.7$ Hz, 1H)	HMBC 30→31,32,36
31	127.6	-	
32	129.5	6.95 (d, $J = 1.8$ Hz, 1H)	
33	125.9	-	
34	153.2	-	
35	114.3	6.69 (d, $J = 8.1$ Hz, 1H)	HMBC 35→33
36	127.7	6.87 (dd, $J = 8.1, 1.8$ Hz, 1H)	
37	-	9.33 (br s, 1H)	

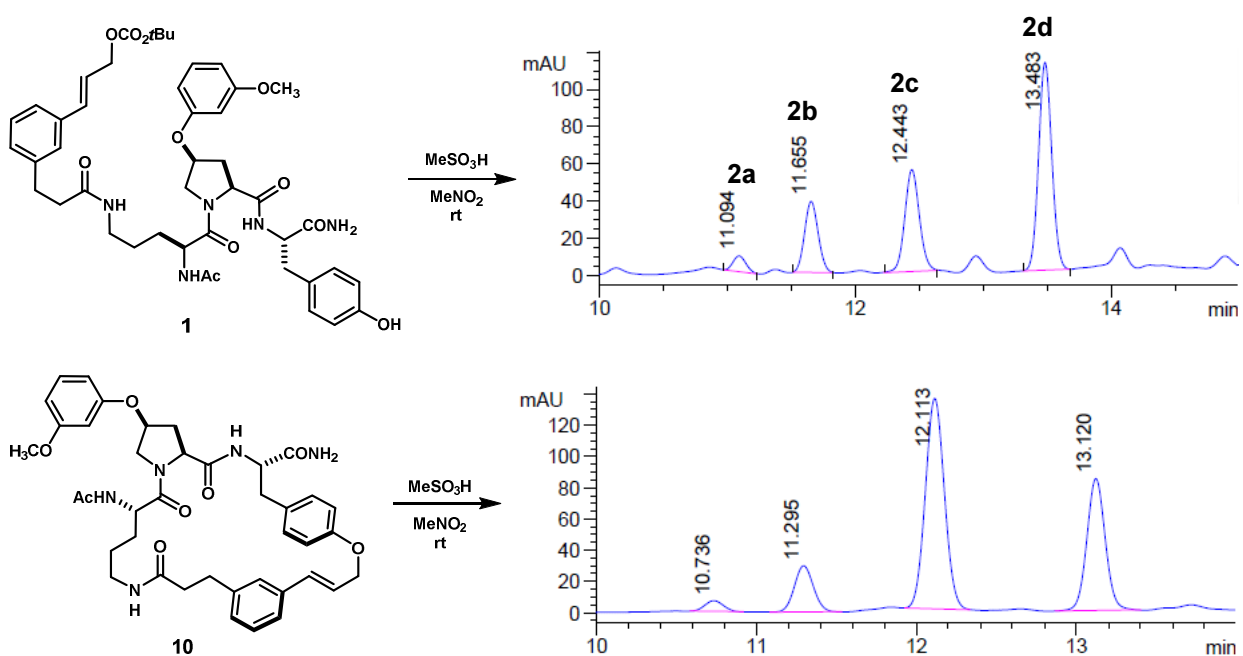
MS m/z 579.3 (calc'd: $C_{31}H_{39}N_4O_7$, $[M+H]^+$, 579.3).

Macrocycles 2a-d and 10:



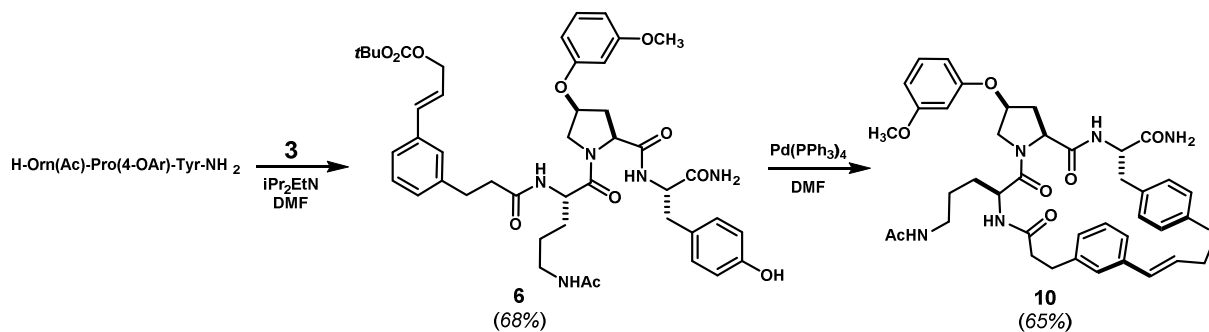
Acyclic carbonate **1**: See compound **3-61a** (Chapter 3).

Tyrosyl ether **10**: See compound **3-65a**.



Acidolysis products **2a-d**: See compounds **3-67a-d**.

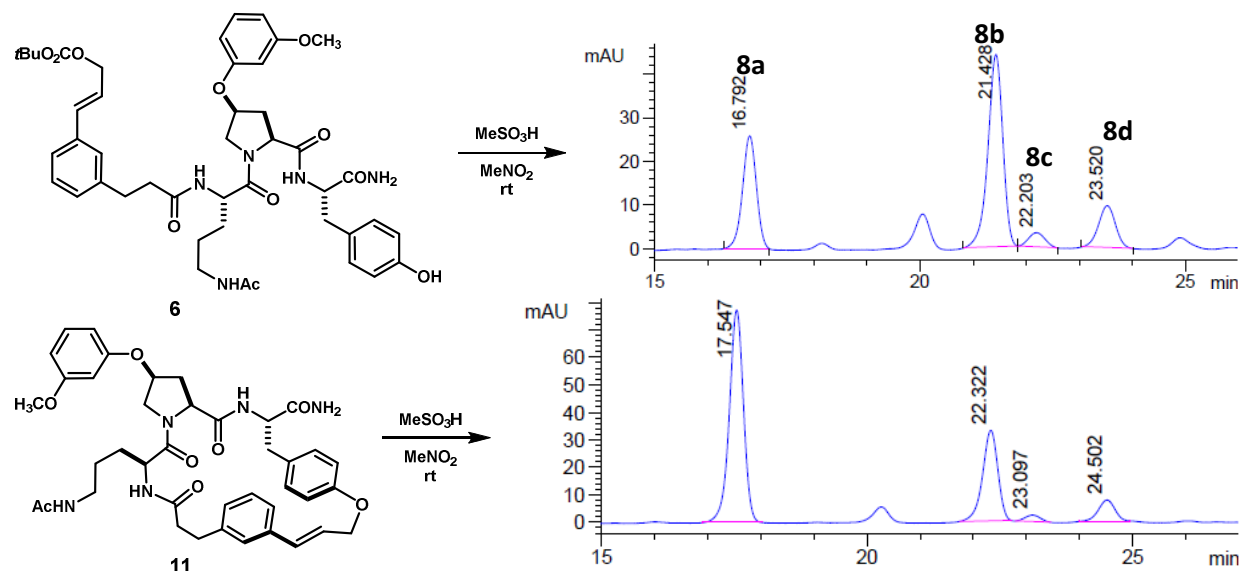
Macrocycles 8a-d, 11:



Acyclic carbonate **6**: General procedure A afforded compound **6** as a colorless foam (242 mg, 68%). ¹H NMR (600 MHz, CD₃OD, major rotamer): δ 1.36-1.53 (m, 3H), 1.45 (s, 9H), 1.54-1.64 (m, 1H), 1.91 (s, 3H),

2.32 (br d, $J = 13.6$ Hz, 1H), 2.39-2.46 (m, 1H), 2.50-2.59 (m, 2H), 2.89 (apt t, $J = 7.1$ Hz, 2H), 2.97 (d, $J = 5.9$ Hz, 2H), 3.04-3.11 (m, 2H), 3.71 (s, 3H), 3.78 (d, $J = 11.3$ Hz, 1H), 3.97 (dd, $J = 11.1, 4.2$ Hz, 1H), 4.45-4.51 (m, 1H), 4.54 (apt t, $J = 6.1$ Hz, 1H), 4.65 (d, $J = 5.7$ Hz, 2H), 4.92-4.97 (m, 1H), 6.30 (dt, $J = 16.0, 6.1$ Hz, 1H), 6.47-6.51 (m, 2H), 6.53-6.57 (m, 1H), 6.62 (d, $J = 16.0$ Hz, 1H), 6.65 (d, $J = 8.2$ Hz, 2H), 7.00 (d, $J = 8.2$ Hz, 2H), 7.10 (d, $J = 6.6$ Hz, 1H), 7.16-7.24 (m, 3H), 7.25 (br s, 1H). ^{13}C NMR (151 MHz, CD_3OD , major rotamer): δ 175.3, 174.8, 173.8, 173.2, 172.6, 162.4, 159.2, 157.3, 154.9, 142.4, 137.7, 134.9, 131.6, 131.2, 129.8, 129.2, 128.4, 127.8, 125.6, 124.3, 116.2, 108.7, 108.3, 103.4, 82.9, 77.3, 68.4, 61.2, 55.8, 55.4, 54.0, 52.2, 39.9, 38.1, 37.9, 35.1, 32.4, 29.5, 28.0, 26.2, 22.8. MS m/z 844.4 (calc'd: $\text{C}_{45}\text{H}_{58}\text{N}_5\text{O}_{11}$, $[\text{M}+\text{H}]^+$, 844.4).

Tyrosyl ether 11: General procedure B afforded compound **11** as a light yellow film (18 mg, 65%). ^1H NMR (600 MHz, CD_3OD): δ 1.07-1.21 (m, 2H), 1.22-1.31 (m, 1H), 1.46-1.54 (m, 1H), 1.89 (s, 3H), 2.53-2.63 (m, 1H), 2.64-2.73 (m, 1H), 2.88-3.04 (m, 5H), 3.10 (dd, $J = 14.6, 3.9$ Hz, 1H), 3.40-2.54 (m, 1H), 3.76 (s, 3H), 3.94-4.02 (m, 1H), 4.31-4.41 (m, 1H), 4.46-4.55 (m, 1H), 4.56 (dd, $J = 9.0, 3.9$ Hz, 1H), 4.77-4.87 (m, 3H), 6.39 (dt, $J = 15.8, 5.2$ Hz, 1H), 6.42-6.44 (m, 1H), 6.47 (dd, $J = 8.1, 2.0$ Hz, 1H), 6.55 (dd, $J = 8.3, 2.0$ Hz, 1H), 6.69 (br d, $J = 15.8$ Hz, 1H), 6.89 (d, $J = 8.7$ Hz, 2H), 7.06 (d, $J = 7.2$ Hz, 1H), 7.13 (d, $J = 8.7$ Hz, 2H), 7.15-7.20 (m, 3H), 7.63 (br s, 1H). ^{13}C NMR (151 MHz, CD_3OD): δ 176.3, 174.6, 173.2, 173.0, 172.6, 162.5, 159.5, 158.8, 141.7, 138.1, 134.3, 131.3 (2), 131.2, 129.8, 129.6, 126.7, 125.7, 116.5 (2), 108.9, 108.1, 103.5, 77.0, 69.4, 59.9, 55.8, 55.2, 53.5, 52.2, 40.0, 37.5 (2), 35.2, 31.6, 30.3, 25.5, 22.7. MS m/z 726.3 (calc'd: $\text{C}_{40}\text{H}_{48}\text{N}_5\text{O}_8$, $[\text{M}+\text{H}]^+$, 726.3).



Compounds **6** and **11** were each subjected to general procedure C. HPLC analysis and purification was performed using the following methods.

Analytical HPLC method:Column: Waters Xbridge™ C₁₈, 4.6x250mm, 5μm.Solvent A: H₂O + 0.1%v TFA

Solvent B: ACN + 0.1%v TFA

Flow rate: 1.00 ml/min

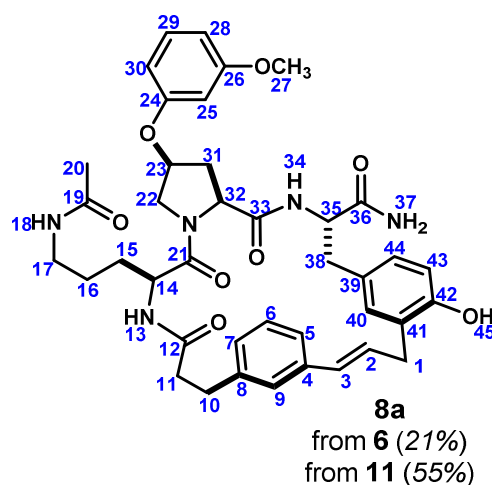
Time	%B
0	30
2	30
42	42
55	100
65	100
70	30
72	30

Semi-preparative HPLC method A:Column: Waters Xbridge™ C₁₈, 10x250mm, 5μm.Solvent A: H₂O + 0.1%v TFA

Solvent B: ACN + 0.1%v TFA

Flow rate: 7.50 ml/min

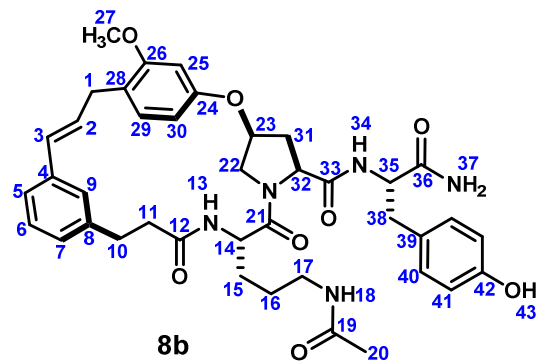
Time	%B
0	25
2	25
42	35.5
44	25
45	25

(600MHz, DMSO-*d*₆, 298K)

	¹³ C	¹ H	key correlations
1	32.8	3.35-.345 (m, 2H)	HMBC 1→2,3,40,41
2	128.5	6.45-6.54 (m, 1H) overlap	HMBC 2→4
3	130.8	6.43-6.54 (m, 1H) overlap	HMBC 3→9
4	137.7	-	
5	122.7	7.24 (br d, <i>J</i> = 7.0Hz, 1H)	HMBC 5→3,9
6	127.6	7.12-7.17 (m, 1H) overlap	HMBC 6→4,8
7	127.2	6.94 (d, <i>J</i> = 7.2Hz, 1H)	HMBC 7→9,10
8	140.9	-	
9	126.0	7.16 (s, 1H) overlap	HMBC 9→10
10	29.7	2.92-3.00 (m, 1H) overlap, 2.72-2.84 (m, 1H) overlap	HMBC 10→8
11	34.3	2.51-2.58 (m, 1H) overlap, 2.34-2.41 (m, 1H) overlap	
12	171.4	-	
13	-	7.72 (t, <i>J</i> = 5.1Hz, 1H)	HMBC 13→12
14	49.8	4.29-4.34 (m, 1H)	HMBC 14→12, 21
15	27.9	1.54-1.61 (m, 1H), 1.38-1.46 (m, 1H) overlap	HMBC 15→21

16	24.9	1.37-1.46 (m, 2H) overlap	
17	37.9	2.92-3.01 (m, 2H) overlap	COSY 17→16
18	-	7.98 (s, $J = 7.2\text{Hz}$, 1H)	COSY 18→19
19	169.0	-	
20	22.3	1.75 (s, 3H)	HMBC 20→19
21	169.8	-	
22	51.0	4.16-4.23 (m, 1H), 3.31 (dd, $J = 9.5, 5.4\text{Hz}$, 1H)	
23	74.3	4.75-4.81 (m, 1H)	
24	158.3	-	
25	101.5	6.45-6.48 (m, 1H) overlap	
26	160.6	-	
27	54.9	3.74 (s, 3H)	HMBC 27→26
28	106.8	6.53 (d, $J = 8.2\text{Hz}$, 1H)	HMBC 28→26
29	129.9	7.16-7.21 (m, 1H) overlap	
30	107.5	6.50 (d, $J = 8.2\text{Hz}$, 1H)	
31	34.1	2.56-2.63 (m, 1H) overlap, 1.83 (ddd, $J = 12.9, 6.5, 6.5\text{Hz}$, 1H)	HMBC 31→33
32	57.2	4.27 (dd, $J = 8.3, 6.5\text{Hz}$, 1H)	HMBC 32→33
33	169.9	-	
34	-	7.52-7.59 (m, 1H)	
35	53.0	4.33-4.38 (m, 1H)	HMBC 35→38,39
36	172.9	-	
37	-	7.19 (br s, 1H) overlap, 7.04 (br s, 1H)	
38	36.0	2.73-2.84 (m, 2H) overlap	
39	127.5	-	
40	131.0	7.13 (br s, 1H) overlap	
41	125.8	-	
42	153.4	-	
43	114.4	6.68 (d, $J = 7.9\text{Hz}$, 1H)	COSY 43→44, HMBC 43→39
44	127.6	6.81 (br d, $J = 7.9\text{Hz}$, 1H)	HMBC 44→40
45	-	9.13 (br s, 1H)	

MS m/z 726.3 (calc'd: $\text{C}_{40}\text{H}_{48}\text{N}_5\text{O}_8$, $[\text{M}+\text{H}]^+$, 726.3).



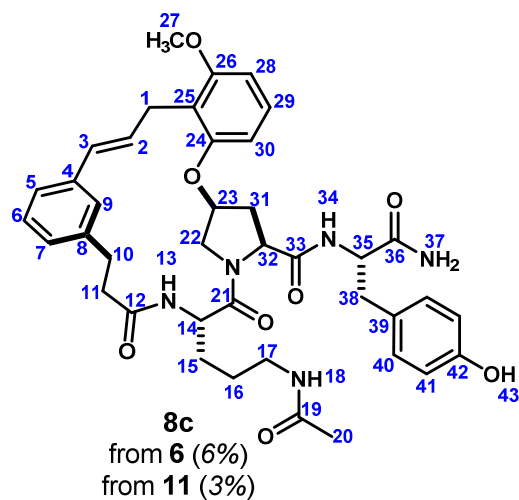
8b
from **6** (50%)
from **11** (32%)

(600MHz, DMSO-*d*₆, 298K)

	¹³ C	¹ H	key correlations
1	30.9	3.43 (dd, <i>J</i> = 16.0, 3.2Hz, 1H), 3.43 (br d, <i>J</i> = 16.0Hz, 1H)	HMBC 1→26,28,29
2	129.1	6.39 (ddd, <i>J</i> = 16.0, 4.6, 4.7Hz, 1H)	COSY 2→1, HMBC 2→4
3	129.7	5.32 (br d, <i>J</i> = 16.0Hz, 1H)	HMBC 3→4
4	136.5	-	
5	121.0	7.26 (d, <i>J</i> = 7.6Hz, 1H) overlap	HMBC 5→2
6	127.8	7.12 (dd, <i>J</i> = 7.6, 7.6Hz, 1H)	HMBC 6→4,8
7	126.8	6.91 (d, <i>J</i> = 7.6Hz, 1H)	
8	141.8	-	
9	128.8	6.76 (br s, 1H)	HMBC 9→3
10	29.2	2.66-2.71 (m, 2H)	HMBC 10→8
11	34.8	2.34 (ddd, <i>J</i> = 7.5, 7.5, 5.2Hz, 1H), 2.23-2.29 (m, 1H)	HMBC 11→8
12	172.1	-	
13	-	7.96 (d, <i>J</i> = 5.2Hz, 1H)	
14	51.2	3.83-3.87 (m, 1H)	HMBC 14→21
15	28.8	1.47-1.54 (m, 1H), 1.36-1.44 (m, 1H)	HMBC 15→21
16	24.9	1.14-1.30 (m, 2H)	
17	38.0	2.89-2.94 (m, 1H) overlap, 2.84-2.89 (m, 1H)	
18	-	7.67 (t, <i>J</i> = 5.8Hz, 1H)	HMBC 18→19
19	169.2	-	
20	22.4	1.77 (s, 3H)	HMBC 20→19
21	171.4	-	
22	51.3	3.73-3.78 (m, 1H) obscured, 3.55 (dd, <i>J</i> = 9.8, 7.5Hz, 1H)	HMBC 23→24 (24 coincides w/ 26)
23	79.2	4.78 (dddd, <i>J</i> = 7.8, 6.8, 6.8, 6.7Hz, 1H)	
24	158.3	-	
25	104.7	6.90 (d, <i>J</i> = 2.0Hz, 1H)	HMBC 25→28
26	158.1	-	
27	55.4	3.75 (s, 3H)	HMBC 27→26
28	123.4	-	

29	131.2	7.10 (d, $J = 8.0\text{Hz}$, 1H)	
30	112.6	6.78 (dd, $J = 8.0, 2.0\text{Hz}$, 1H)	HMBC 30→28, COSY 30→29
31	34.2	2.60 (ddd, $J = 12.5, 6.8, 6.8\text{Hz}$, 1H), 1.93 (ddd, $J = 12.5, 8.9, 8.9\text{Hz}$, 1H)	
32	57.9	4.20 (dd, $J = 8.5, 8.5\text{Hz}$, 1H)	HMBC 32→33
33	170.2	-	
34	-	7.77 (d, $J = 7.9\text{Hz}$, 1H)	
35	53.8	4.31 (ddd, $J = 7.9, 7.9, 5.6\text{Hz}$, 1H)	HMBC 35→33,36,39
36	172.8	-	
37	-	7.26 (br s, 1H), 7.06 (br s, 1H)	HMBC 37→36
38	36.2	2.93 (dd, $J = 13.8, 5.4\text{Hz}$, 1H) overlap, 2.81 (dd, $J = 13.8, 8.3\text{Hz}$, 1H)	HMBC 38→39
39	127.9	-	
40	130.0	7.04 (d, $J = 8.5\text{Hz}$, 2H)	HMBC 40→42
41	114.5	6.64 (d, $J = 8.5\text{Hz}$, 2H)	HMBC 41→39
42	155.8	-	
43	-	9.15 (br s, 1H)	

MS m/z 726.3 (calc'd: $\text{C}_{40}\text{H}_{48}\text{N}_5\text{O}_8$, $[\text{M}+\text{H}]^+$, 726.3).

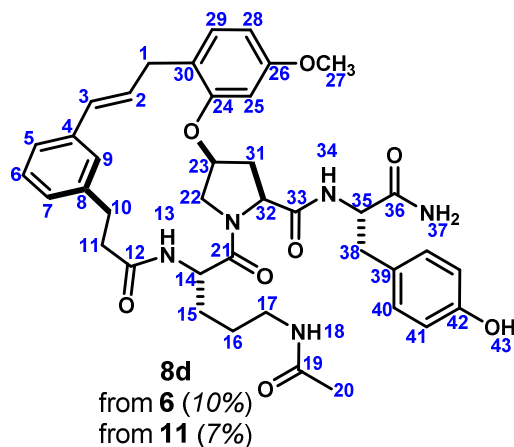


(600MHz, $\text{DMSO-}d_6$, 298K)

	^{13}C	^1H	key correlations
1	25.5	3.59 (dd, $J = 15.4, 4.2\text{Hz}$, 1H), 3.33 (dd, $J = 15.4, 5.9\text{Hz}$, 1H)	HMBC 1→24,25,26
2	128.5	6.30 (ddd, $J = 15.8, 5.9, 4.2\text{Hz}$, 1H)	COSY 2→1 HMBC 2→4, 25
3	129.2	6.08 (d, $J = 15.8\text{Hz}$, 1H)	HMBC 3→4
4	137.1	-	
5	122.7	7.14 (d, $J = 7.4\text{Hz}$, 1H)	HMBC 5→7,9
6	128.6	7.10 (dd, $J = 8.1, 8.1\text{Hz}$, 1H) overlap	HMBC 6→4,8
7	127.1	6.96 (d, $J = 7.4\text{Hz}$, 1H)	HMBC 7→5,9
8	141.8	-	

9	124.3	7.05 (br s, 1H)	HMBC 9→5,7
10	27.8	3.12-3.19 (m, 1H), 2.58-2.64 (m, 1H) overlap	HMBC 10→8,12 COSY 10→10', 11
11	34.1	2.49-2.52 (m, 2H) obscured	HMBC 11→8,12
12	172.8	-	
13	-	8.29 (d, $J = 5.8\text{Hz}$, 1H)	HMBC 13→12,21
14	53.3	4.29-4.35 (m, 1H)	HMBC 14→12,21
15	28.3	1.62-1.69 (m, 1H) overlap, 1.54-1.62 (m, 1H)	HMBC 15→17
16	25.4	1.31-1.47 (m, 2H)	HMBC 16→17
17	38.1	3.00-3.06 (m, 2H) overlap	HMBC 17→19
18	-	7.83 (t, $J = 5.4\text{Hz}$, 1H)	HMBC 18→19
19	169.1	-	
20	22.4	1.80 (s, 3H)	HMBC 20→19
21	170.5	-	
22	50.0	3.97 (dd, $J = 9.1, 7.3\text{Hz}$, 1H), 3.49 (dd, $J = 9.1, 9.1\text{Hz}$, 1H)	HMBC 22→32
23	75.5	4.62 - 4.68 (m, 1H)	
24	156.7	-	
25	117.4	-	
26	157.7	-	
27	55.6	3.80 (s, 3H)	HMBC 27→26
28	105.4	6.76 (d, $J = 8.3\text{Hz}$, 1H)	HMBC 28→25
29	127.6	7.21 (dd, $J = 8.3, 8.3\text{Hz}$, 1H)	HMBC 29→24,26 COSY 29→28,30
30	108.6	6.78 (d, $J=8.3\text{Hz}$, 1H)	HMBC 30→25
31	34.5	2.57-2.64 (m, 1H) overlap, 1.62-1.69 (m, 1H)	HMBC 31→32,33
32	58.9	4.16-4.21 (m, 1H) overlap	HMBC 32→33
33	169.9	-	
34	-	7.66 (d, $J = 8.5\text{Hz}$, 1H)	HMBC 34→33
35	54.1	4.16-4.21 (m, 1H) overlap	
36	172.8	-	
37	-	7.11 (br s, 1H) overlap, 6.98 (br s, 1H)	HMBC 37→36, TOCSY 37→37'
38	35.8	2.97 (dd, $J = 13.9, 4.0\text{Hz}$, 1H), 2.55 (dd, $J = 13.9, 10.3\text{Hz}$, 1H)	HMBC 38→35,39,40
39	128.3	-	
40	129.8	6.77 (d, $J = 8.2\text{Hz}$, 2H)	HMBC 40→42
41	114.6	6.50 (d, $J = 8.2\text{Hz}$, 2H)	HMBC 41→39, 42
42	155.6	-	
43	-	9.11 (br s, 1H)	

MS m/z 726.3 (calc'd: $\text{C}_{40}\text{H}_{48}\text{N}_5\text{O}_8$, $[\text{M}+\text{H}]^+$, 726.3).



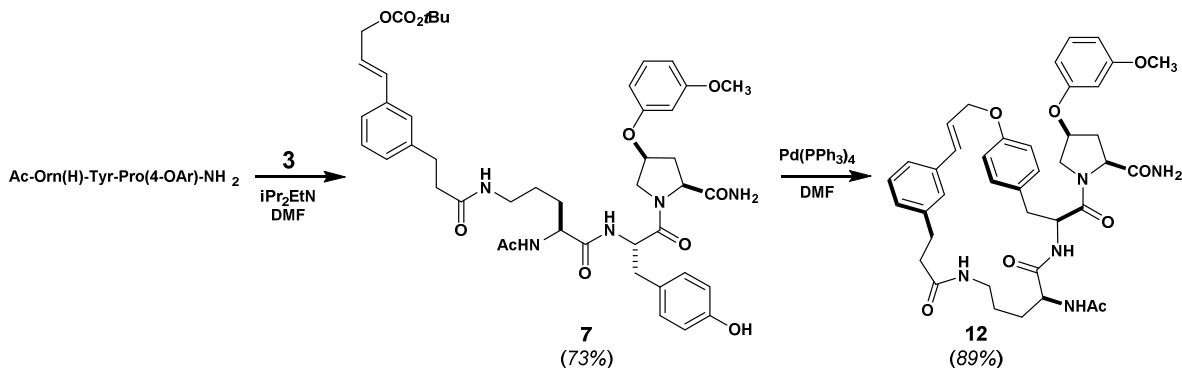
(600MHz, DMSO-*d*₆, 298K)

	¹³ C	¹ H	key correlations
1	33.4	3.56 (dd, <i>J</i> = 16.0, 6.0Hz, 1H), 3.21 (dd, <i>J</i> = 16.0, 4.6Hz, 1H)	HMBC 1→24,29,30
2	129.4	6.37 (ddd, <i>J</i> = 15.8, 6.0, 4.6Hz, 1H)	HMBC 1→24,29,30
3	129.2	4.09 (br d, <i>J</i> = 15.8Hz, 1H)	HMBC 3→4
4	137.0	-	
5	122.7	7.11-7.15 (m, 1H) overlap	
6	128.3	7.10 (dd, <i>J</i> = 7.6, 7.5Hz, 1H)	HMBC 6→4, 8
7	127.1	6.96 (d, <i>J</i> = 7.5Hz, 1H)	HMBC 7→5,9
8	141.5	-	
9	123.9	7.07 (br s, 1H)	
10	27.6	3.15-3.18 (m, 1H) obscured, 2.61-2.66 (m, 1H)	HMBC 10→12
11	33.7	2.53-2.57 (m, 2H) overlap	HMBC 11→8,12
12	172.9	-	
13	-	8.37 (d, <i>J</i> = 5.9Hz, 1H)	HMBC 13→12, 21
14	53.8	4.29 (ddd, <i>J</i> = 7.3, 7.2, 5.9Hz, 1H)	HMBC 14→12
15	28.0	1.58-1.65 (m, 2H) overlap	
16	25.5	1.38-1.50 (m, 2H)	
17	38.1	3.02-3.07 (m, 2H)	
18	-	7.83 (t, <i>J</i> = 5.5Hz, 1H)	HMBC 18→19 TOCSY 18→13,14,15,16,17
19	168.9	-	
20	22.3	1.80 (s, 3H)	HMBC 20→19
21	170.5	-	
22	50.0	4.03 (dd, <i>J</i> = 10.0, 7.0Hz, 1H), 3.44 (dd, <i>J</i> = 10.0, 8.4Hz, 1H)	
23	74.8	4.73-4.79 (m, 1H)	HMBC 23→24
24	156.4	-	
25	102.1	6.72 (d, <i>J</i> = 2.2Hz, 1H)	HMBC 25→30
26	159.1	-	
27	54.9	3.75 (s, 3H)	HMBC 27→26

28	106.7	6.58 (dd, $J = 8.2, 2.2$ Hz, 1H)	HMBC 28→30
29	131.0	7.14 (d, $J = 8.2$ Hz, 1H)	
30	121.1	-	
31	34.2	2.58 (dd, $J = 11.9, 5.9$ Hz, 1H) overlap, 1.58-1.65 (m, 1H) overlap	HMBC 31→32,33
32	59.0	4.18 (dd, $J = 9.4, 7.9$ Hz, 1H)	HMBC 32→33
33	169.6	-	
34	-	7.59 (d, $J = 8.9$ Hz, 1H)	
35	54.1	4.15 (dd, $J = 9.5, 4.1$ Hz, 1H)	
36	172.6	-	
37	-	7.12 (br s, 1H) obscured, 6.94 (br s, 1H) obscured	HMBC 37→36, TOCSY 37→37'
38	35.8	2.98 (dd, $J = 13.8, 4.1$ Hz, 1H)	HMBC 38→39, 40
39	128.3	-	
40	129.5	6.70 (d, $J = 8.4$ Hz, 2H)	
41	114.5	6.48 (d, $J = 8.4$ Hz, 2H)	
42	155.3	-	
43	-	9.09 (br s, 1H)	

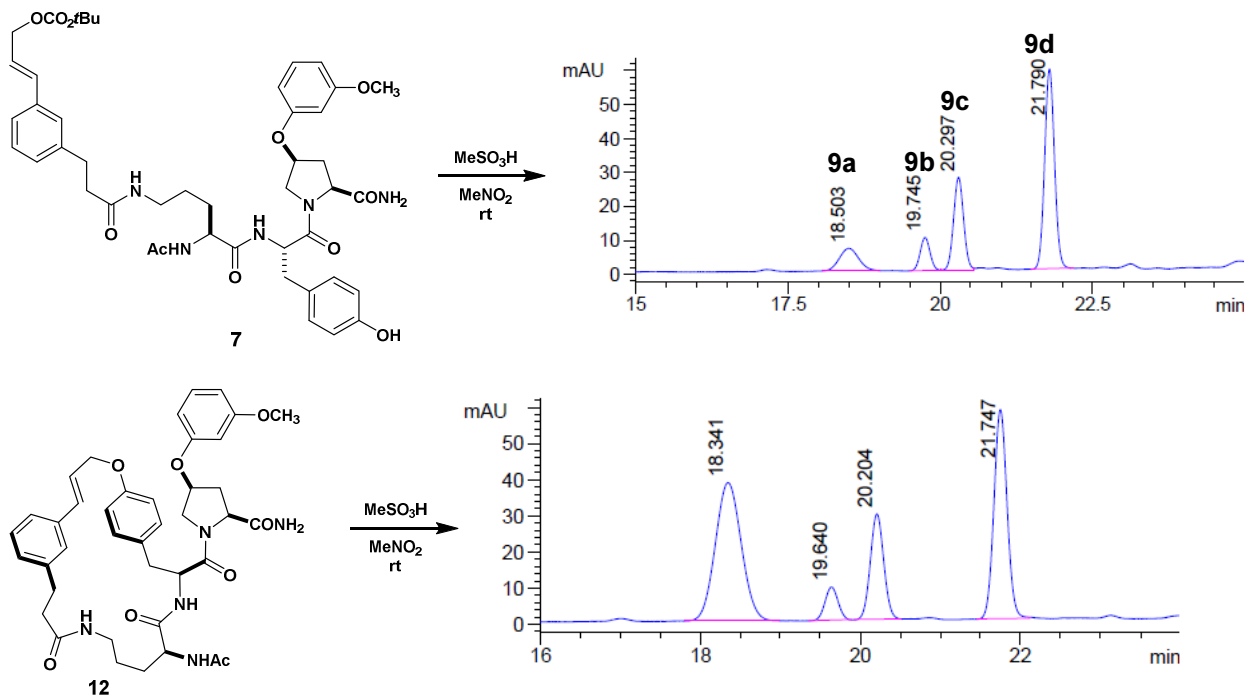
MS m/z 726.3 (calc'd: $C_{40}H_{48}N_5O_8$, $[M+H]^+$, 726.3).

Macrocycles 9a-d, 12:



Acyclic carbonate 7: General procedure A afforded compound 7 as a colorless foam (235 mg, 73%). ¹H NMR (600 MHz, CD₃OD, major rotamer): δ 1.40-1.68 (m, 4H), 1.47 (s, 9H), 1.97 (s, 3H), 2.30 (d, $J = 14.0$ Hz, 1H), 2.40 (d, $J = 14.0$ Hz, 1H), 2.46-2.50 (m, 2H), 2.91 (dd, $J = 14.9, 7.2$ Hz, 2H), 2.97 (d, $J = 7.7$ Hz, 1H), 3.06-3.23 (m, 2H), 3.62 (d, $J = 9.8$ Hz, 1H), 3.63 (d, $J = 11.0$ Hz, 1H), 3.76 (s, 3H), 4.12 (dd, $J = 11.3, 4.5$ Hz, 1H), 4.31 (dd, $J = 7.8, 6.1$ Hz, 1H), 4.44 (br d, $J = 9.8$ Hz, 1H), 4.66-4.69 (m, 2H), 4.75 (dd, $J = 7.8, 7.8$ Hz, 1H), 4.94-4.97 (m, 1H), 6.28-6.34 (m, 1H), 6.36-6.41 (m, 2H), 6.53 (dd, $J = 8.3, 0.9$ Hz, 1H), 6.66 (d, $J = 8.1$ Hz, 2H), 6.76 (d, $J = 8.5$ Hz, 1H), 7.07 (d, $J = 8.1$ Hz, 2H), 7.09-7.13 (m, 1H), 7.15 (dd, $J = 8.1, 8.1$ Hz, 1H), 7.21-7.25 (m, 2H), 7.27-7.29 (m, 1H). ¹³C NMR (151 MHz, CD₃OD, mixture of rotamers): δ 176.1, 175.6, 175.2, 175.2, 174.9, 174.1, 173.6, 173.3, 173.2, 172.9, 162.5, 162.4, 159.0, 158.1, 157.7, 155.0, 142.6, 137.84, 137.82, 135.14, 135.11, 131.6, 131.5, 131.04, 130.96, 129.8, 129.2, 128.1, 127.74, 127.70, 125.7, 125.6, 124.3, 124.2, 116.7, 116.6, 108.6, 108.4, 108.3, 108.0, 103.3, 103.1, 83.0, 76.8, 74.9, 68.5, 60.9, 60.7, 55.74, 55.67, 55.2, 54.4, 54.1, 54.0, 53.8, 53.7, 39.75, 39.68, 38.99, 38.95, 38.91, 37.8, 37.2, 35.4, 32.8, 30.4, 30.2, 28.0, 26.7, 26.4, 22.5, 22.4. MS m/z 844.4 (calc'd: $C_{45}H_{58}N_5O_{11}$, $[M+H]^+$, 844.4).

Tyrosyl ether 14: General procedure B afforded compound **12** as a colorless film (174mg, 89%). ¹H NMR (600 MHz, CD₃OD): δ 0.85-0.89 (m, 2H), 0.95-1.13 (m, 2H), 1.95 (s, 3H), 2.32-2.39 (m, 2H), 2.39-2.45 (m, 1H), 2.47-2.53 (m, 1H), 2.79-2.86 (m, 1H), 2.89-2.93 (m, 3H), 2.95-3.02 (m, 1H), 2.89-2.93 (m, 3H), 2.95-3.02 (m, 1H), 3.12 (dd, *J* = 14.3, 3.9 Hz, 1H), 3.64 (apt s, 1H), 3.76 (s, 3H), 3.87-3.93 (m, 2H), 4.17 (dd, *J* = 11.6, 5.0 Hz, 1H), 4.54 (dd, *J* = 9.7, 2.7 Hz, 2H), 4.82 (dd, *J* = 5.8, 0.8 Hz, 2H), 5.06-5.09 (m, 1H), 6.31 (dt, *J* = 16.0, 5.8 Hz, 1H), 6.50-6.51 (m, 1H), 6.52-6.55 (m, 2H), 6.66 (d, *J* = 16.0 Hz, 1H), 6.86 (d, *J* = 8.7 Hz, 2H), 7.08 (br d, *J* = 7.4 Hz, 1H), 7.11 (d, *J* = 8.7 Hz, 2H), 7.14-7.18 (m, 2H), 7.22 (t, *J* = 7.8 Hz, 1H), 7.24 (br s, 1H). ¹³C NMR (151 MHz, CD₃OD): δ 176.4, 175.0, 173.8, 173.6, 172.3, 162.5, 159.4, 158.5, 142.0, 137.6, 134.1, 131.8 (2), 131.1, 130.0, 129.8, 129.5, 126.7, 126.5, 115.9, 108.8, 108.1, 103.4, 77.0, 68.9, 60.7, 55.7, 54.5, 53.8, 53.0, 38.8, 38.6, 36.8, 35.8, 32.8, 29.6, 26.1, 22.5. MS *m/z* 726.2 (calc'd: C₄₀H₄₈N₅O₈, [M+H]⁺, 726.3).



Compounds **7** and **12** were individually subjected to general procedure C. HPLC analysis and purification was performed using the following methods. The product mixture was first resolved using semi-preparative HPLC method A. Compound **9a** (earliest peak, method A) was re-purified using method B.

Analytical HPLC method:

Column: Waters Sunfire™ C₁₈, 4.6x250mm, 5μm.

Solvent A: H₂O + 0.1%v TFA

Solvent B: ACN + 0.1%v TFA

Flow rate: 1.00 ml/min

Time	%B
0	30
2	30
30	55
35	100
45	100
50	30
55	30

Semi-preparative HPLC method A:

Column: Waters Sunfire™ C₁₈, 10x250mm, 5μm.

Solvent A: H₂O + 0.1%v TFA

Solvent B: ACN + 0.1%v TFA

Flow rate: 7.50 ml/min

Time	%B
0	30
1	30
14	47
15	70
16	70
17	30
20	30

Semi-preparative HPLC method B:

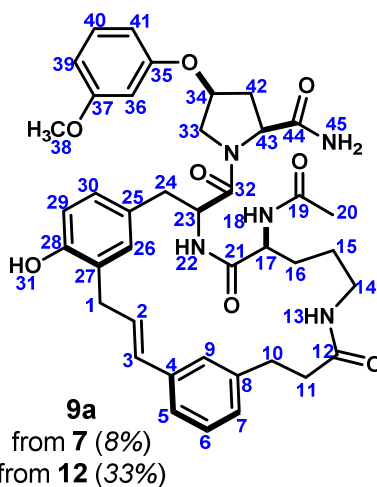
Column: Waters Xbridge™ C₁₈, 10x250mm, 5μm.

Solvent A: H₂O + 0.1%v TFA

Solvent B: ACN + 0.1%v TFA

Flow rate: 7.50 ml/min

Time	%B
0	30
2	30
15	46.7
17	30
20	30



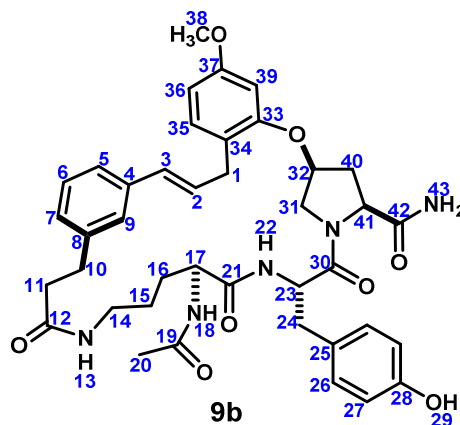
(600MHz, DMSO-*d*₆, 298K, ~2:1 mixture of conformers – data is of major)

	¹³ C	¹ H	key correlations
1	33.0	3.47 (dd, <i>J</i> = 14.9, 4.6Hz, 1H), 3.27 (dd, <i>J</i> = 14.9, 6.3Hz, 1H)	HMBC 1→27
2	128.6	6.31-6.38 (m, 1H) obscured	HMBC 2→4
3	130.1	6.31-6.38 (m, 1H) obscured	HMBC 3→4,5,9
4	137.2	-	

5	123.9	7.13-7.16 (m, 1H) overlap	
6	128.2	7.182 (dd, $J = 7.8, 7.8\text{Hz}$, 1H)	HMBC 6→4,8
7	127.1	7.01 (ddd, $J = 7.8, 1.2, 1.2\text{Hz}$, 1H)	HMBC 7→5,6
8	141.4	-	
9	124.9	7.13-7.14 (m, 1H) overlap	
10	30.7	2.79-2.85 (m, 2H) overlap	HMBC 10→8
11	36.7	2.34 (dd, $J = 7.6, 6.5\text{Hz}$, 1H), 2.24 (dd, $J = 13.9, 6.5\text{Hz}$, 1H)	HMBC 11→8,12
12	171.4	-	
13	-	7.72 (t, $J = 5.6\text{Hz}$, 1H)	HMBC 13→12
14	36.5	2.86-2.94 (m, 1H) overlap, 2.79-2.84 (m, 1H) overlap	
15	24.3	1.09-1.16 (m, 1H) overlap, 0.92-1.00 (m, 1H)	
16	27.9	1.25-1.33 (m, 1H), 1.03-1.12 (m, 1H) overlap	
17	52.1	3.95 (dd, $J = 15.3, 7.7\text{Hz}$, 1H)	COSY 17→16
18	-	7.75 (d, $J = 7.7\text{Hz}$, 1H)	
19	169.2	-	
20	22.3	1.82 (s, 3H)	
21	171.3	-	
22	-	7.47 (d, $J = 8.3\text{Hz}$, 1H)	HMBC 22→21
23	51.2	4.70 (ddd, $J = 8.6, 8.3, 4.6\text{Hz}$, 1H)	HMBC 23→24, COSY 23→22,24
24	35.5	2.91-3.00 (m, 1H) overlap, 2.72 (dd, $J = 14.2, 8.7\text{Hz}$, 1H)	HMBC 24→25,26
25	127.1	-	
26	131.1	6.88 (d, $J = 1.8\text{Hz}$, 1H)	COSY 26→30
27	125.3	-	
28	153.6	-	
29	114.4	6.67 (d, $J = 8.1\text{Hz}$, 1H)	HMBC 29→25,27,28
30	127.9	6.94 (dd, $J = 8.1, 1.8\text{Hz}$, 1H)	COSY 30→29, HMBC 30→28
31	-	9.19 (br s, 1H)	
32	170.1	-	
33	51.7	4.20 (dd, $J = 11.2, 5.7\text{Hz}$, 1H), 3.69 (dd, $J = 11.2, 2.7\text{Hz}$, 1H)	
34	75.0	5.03 (ddd, $J = 8.8, 5.4, 3.4\text{Hz}$, 1H)	
35	158.0	-	
36	101.7	6.48 (dd, $J = 2.1, 2.1\text{Hz}$, 1H)	
37	160.6	-	
38	54.9	3.73 (s, 3H)	HMBC 38→37
39	106.6	6.54 (dd, $J = 8.1, 2.1\text{Hz}$, 1H)	
40	129.8	7.184 (dd, $J = 8.4\text{Hz}$, 1H)	HMBC 40→37
41	107.5	6.52 (dd, $J = 8.1, 2.1\text{Hz}$, 1H)	
42	34.1	2.41-2.48 (m, 1H) overlap, 2.08 (ddd, $J = 13.4, 3.8, 3.5\text{Hz}$, 1H)	HMBC 42→44

43	58.3	4.34 (dd, $J = 9.5, 3.8\text{Hz}$, 1H)	COSY 43→42, HMBC 43→44
44	172.8	-	
45	-	7.09 (s, 1H), 7.03 (s, 1H)	HMBC 45→44, 45'→43

MS m/z 726.3 (calc'd: $\text{C}_{40}\text{H}_{48}\text{N}_5\text{O}_8$, $[\text{M}+\text{H}]^+$, 726.3).



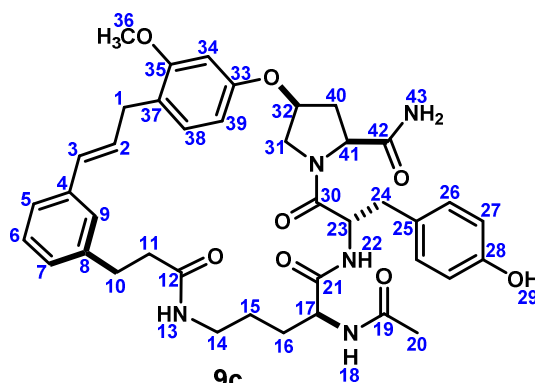
9b
from **7** (25%)
from **12** (19%)

(600MHz, $\text{DMSO}-d_6$, 298K, ~4:1 mixture of conformers – data is of major)

	^{13}C	^1H	key correlations
1	33.2	3.41 (dd, $J = 13.8, 7.5\text{Hz}$, 1H), 3.07 (dd, $J = 13.8, 7.3\text{Hz}$, 1H)	HMBC 1→33,34
2	129.4	6.22 (ddd, $J = 15.8, 7.3, 7.5\text{Hz}$, 1H)	HMBC 2→4, 5
3	129.5	6.35 (d, $J = 15.8\text{Hz}$, 1H)	
4	137.1	-	
5	123.8	7.06 (br d, $J = 7.8\text{Hz}$, 1H)	TOCSY 5→6,7,9
6	128.0	7.14 (dd, $J = 7.8, 7.8\text{Hz}$, 1H)	HMBC 6→4, 8
7	126.5	6.97-7.00 (m, 1H) obscured	
8	141.4	-	
9	125.1	7.22 (br s, 1H)	
10	31.1	2.77 (t, $J = 7.6\text{Hz}$, 2H)	
11	36.9	2.28-2.41 (m, 2H) overlap	HMBC 11→10
12	171.4	-	
13	-	7.64 (t, $J = 5.6\text{Hz}$, 1H)	
14	37.6	2.98-3.04 (m, 2H)	
15	24.8	1.31-1.44 (m, 2H) overlap	HMBC 15→17
16	28.9	1.50-1.57 (m, 1H), 1.37-1.44 (m, 1H) overlap	
17	51.3	4.36-4.42 (m, 1H) overlap	
18	-	7.94 (d, $J = 8.1\text{Hz}$, 1H)	HMBC 18→19
19	168.9	-	
20	22.3	1.84 (s, 3H)	HMBC 20→19
21	171.7	-	
22	-	8.10 (d, $J = 6.1\text{Hz}$, 1H)	

23	53.0	4.36-4.42 (m, 1H) overlap	
24	37.6	2.87 (dd, $J = 12.9, 5.5\text{Hz}$, 1H), 2.73 (dd, $J = 12.9, 9.1\text{Hz}$, 1H)	
25	126.5	-	
26	130.0	6.99 (d, $J = 6.1\text{Hz}$, 2H)	HMBC 26→28
27	115.0	6.70 (d, $J = 8.5\text{Hz}$, 2H)	HMBC 27→25, 28
28	156.1	-	
29	-	9.23 (br s, 1H)	
30	170.1	-	
31	51.9	3.81 (dd, $J = 13.3, 5.4\text{Hz}$, 1H), 3.44 (d, $J = 13.3\text{Hz}$, 1H)	
32	73.2	4.78-4.82 (m, 1H)	HMBC 32→33
33	155.1	-	
34	120.9	-	
35	130.4	7.04 (d, $J = 8.3\text{Hz}$, 1H)	
36	104.8	6.43 (dd, $J = 8.3, 2.3\text{Hz}$, 1H)	HMBC 36→35
37	158.8	-	
38	55.0	3.71 (s, 3H)	HMBC 38→37
39	99.4	6.41 (d, $J = 2.3\text{Hz}$, 1H)	
40	36.0	2.28 (d, $J = 13.6\text{Hz}$, 1H), 1.89 (ddd, $J = 13.6, 9.0, 5.0\text{Hz}$, 1H)	
41	58.6	3.76 (d, $J = 8.5\text{Hz}$, 1H) overlap	HMBC 41→42
42	171.9	-	
43	-	7.27 (s, 1H), 7.18 (s, 1H)	

MS m/z 726.3 (calc'd: $\text{C}_{40}\text{H}_{48}\text{N}_5\text{O}_8$, $[\text{M}+\text{H}]^+$, 726.3).



from **7** (31%)
from **12** (24%)

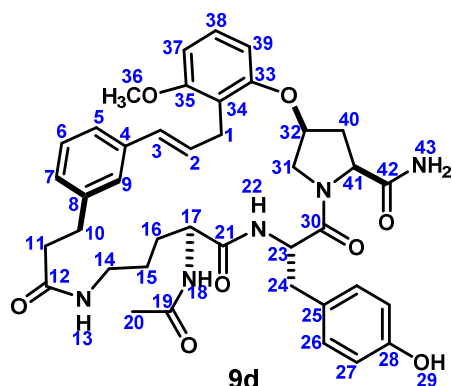
(600MHz, $\text{DMSO}-d_6$, 298K, ~3:1 mixture of conformers – data is of major)

	^{13}C	^1H	key correlations
1	31.6	3.34-3.43 (m, 2H) overlap	HMBC 1→35,37,38
2	130.1	6.19-6.28 (m, 1H) obscured	
3	128.7	6.19-6.23 (m, 1H) obscured	
4	137.3	-	

5	124.0	7.12 (br d, $J = 7.9\text{Hz}$, 1H)	HMBC 5→7,3
6	128.3	7.17 (apt t, $J = 7.5\text{Hz}$, 1H)	
7	126.9	7.00 (d, $J = 7.5\text{Hz}$, 1H) obscured	
8	141.8	-	
9	125.0	7.21 (br s, 1H)	HMBC 9→3
10	31.2	2.70 (dd, $J = 9.1, 7.1\text{Hz}$, 1H), 2.68 dd, $J = 9.1, 7.1\text{Hz}$, 1H)	HMBC 10→8
11	38.1	2.24-2.30 (m, 2H)	COSY 11→10, HMBC 11→8
12	171.1	-	
13	-	7.73 (dd, $J = 5.5, 5.5\text{Hz}$, 1H)	HMBC 13→12
14	37.8	2.81-2.92 (m, 2H)	
15	25.2	1.28-1.41 (m, 2H)	
16	29.2	1.56-1.64 (m, 1H), 1.40-1.50 (m, 1H)	COSY 16→15
17	51.4	4.34 (ddd, $J = 9.8, 8.7, 3.4\text{Hz}$, 1H)	TOCSY 17→13,14,15,16,18 HMBC 17→21
18	-	7.92 (d, $J = 8.5\text{Hz}$, 1H)	
19	169.0	-	
20	22.3	1.77 (s, 3H)	HMBC 20→19
21	172.8	-	
22	-	8.48 (d, $J = 4.6\text{Hz}$, 1H)	HMBC 22→21
23	53.9	4.13-4.19 (m, 1H) overlap	
24	36.0	2.81-2.88 (m, 1H) overlap, 2.37-2.80 (m, 1H) overlap	HMBC 24→25,29
25	126.3	-	
26	130.0	7.02 (d, $J = 8.3\text{Hz}$, 2H)	HMBC 26→28
27	115.1	6.72 (d, $J = 8.3\text{Hz}$, 2H)	HMBC 27→25
28	156.3	-	
29	-	9.39 (br s, 1H)	
30	170.3	-	
31	51.0	3.49 (dd, $J = 14.0, 3.4\text{Hz}$, 1H), 3.38-3.43 (m, 1H)	HMBC 31→30
32	72.5	4.94 (dd, $J = 3.8, 3.8\text{Hz}$, 1H)	COSY 32→31,40, TOCSY 32→31,40,41
33	155.7	-	
34	99.8	6.37-6.38 (m, 1H) overlap	HMBC 34→33,35,37
35	157.7	-	
36	55.3	3.73 (s, 3H)	HMBC 36→35
37	120.2	-	
38	130.5	7.06 (d, $J = 8.2\text{Hz}$, 1H)	HMBC 38→33 COSY 38→39
39	106.9	6.35-6.38 (m, 1H) overlap	
40	36.4	2.45 (d, $J = 13.4\text{Hz}$, 1H), 1.71 (ddd, $J = 13.1, 9.2, 3.8\text{Hz}$, 1H)	HMBC 40→31,42
41	58.5	3.52 (d, $J = 8.9\text{Hz}$, 1H) obscured	
42	172.3	-	

43	-	7.84 (s, 1H), 7.38 (s, 1H)	HMBC 43→42
-----------	---	----------------------------	------------

MS m/z 726.3 (calc'd: C₄₀H₄₈N₅O₈, [M+H]⁺, 726.3).



9d

from **7** (7%)
from **12** (5%)

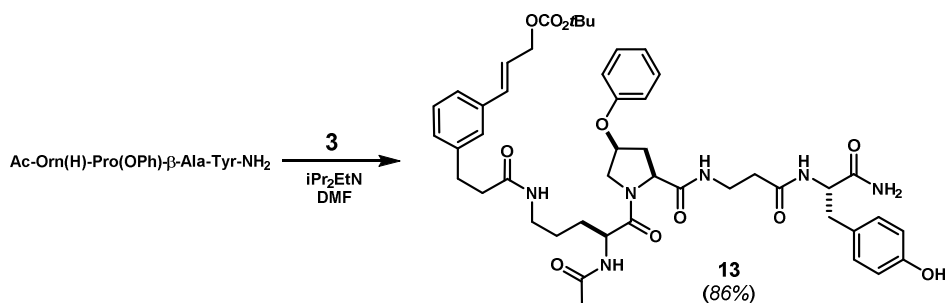
(600MHz, DMSO-*d*₆, 298K, ~4:1 mixture of conformers – data is of major)

	¹³ C	¹ H	key correlations
1	26.0	3.29-3.38 (m, 2H), obscured	HMBC 1→33,34
2	127.8	6.14 (ddd, <i>J</i> = 15.8, 7.3, 7.3Hz, 1H)	COSY 2→1,4
3	130.0	6.34 (d, <i>J</i> = 15.8Hz, 1H)	HMBC 3→4,5,9
4	137.1	-	
5	123.9	7.08 (br d, <i>J</i> = 7.7Hz, 1H)	
6	128.0	7.12 (dd, <i>J</i> = 7.7, 7.7Hz, 1H)	
7	126.3	6.97 (br d, <i>J</i> = 7.7, 7.7Hz, 1H)	HMBC 7→10
8	141.2	-	
9	125.3	7.18 (br s, 1H)	HMBC 9→10
10	31.2	2.76 (t, <i>J</i> = 7.8Hz, 1H)	HMBC 10→12
11	36.9	2.36 (dd, <i>J</i> = 14.4, 7.8Hz, 1H), 2.32 (dd, <i>J</i> = 14.4, 7.8 Hz 1H)	HMBC 11→12
12	171.2	-	
13	-	7.61 (t, <i>J</i> = 5.8Hz, 1H)	COSY 13→14, HMBC 13→12
14	37.5	2.95-3.07 (m, 2H)	COSY 14→15
15	24.7	1.32-1.42 (m, 2H) overlap	HMBC 15→17
16	28.7	1.49-1.56 (m, 1H), 1.36-1.42 (m, 1H) overlap	
17	51.2	4.35-4.40 (m, 1H) overlap	
18	-	7.89 (d, <i>J</i> = 8.1Hz, 1H)	
19	168.9	-	
20	22.2	1.84 (s, 3H)	HMBC 20→19
21	171.6	-	
22	-	8.04 (d, <i>J</i> = 6.2Hz, 1H)	
23	52.8	4.35-4.42 (m, 1H)	

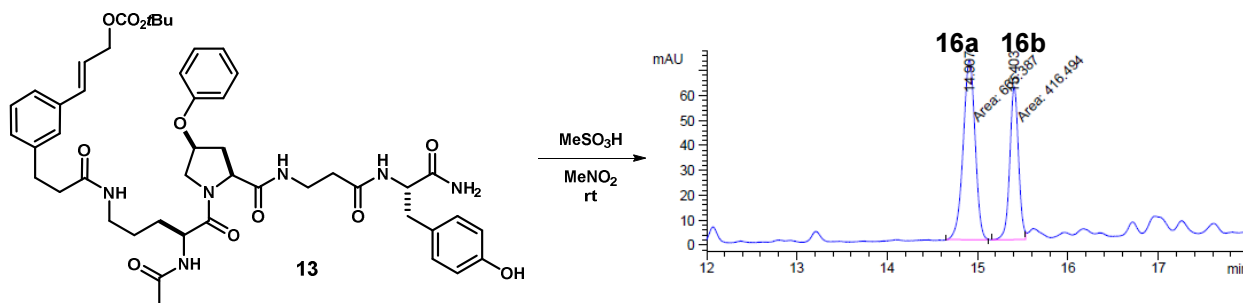
24	37.5	2.87 (dd, $J = 12.9, 5.3\text{Hz}$, 1H), 2.73 (dd, $J = 12.9, 8.8\text{Hz}$, 1H)	HMBC 24→23,29
25	126.3	-	
26	130.0	6.99 (d, $J = 8.5\text{Hz}$, 1H)	HMBC 26→28
27	114.9	6.70 (d, $J = 8.5\text{Hz}$, 1H)	HMBC 27→25, 28
28	156.0	-	
29	-	9.33 (br s, 1H)	
30	169.9	-	
31	52.0	3.78 (dd, $J = 9.4, 1.7\text{Hz}$, 1H), 3.40-3.33 (m, 1H) obscured	
32	73.3	4.72-4.76 (m, 1H)	COSY 32→31
33	155.1	-	
34	115.9	-	
35	157.6	-	
36	55.5	3.76 (s, 3H)	HMBC 36→35
37	103.9	6.61 (d, $J = 8.3\text{Hz}$, 1H)	HMBC 37→35
38	126.9	7.11 (dd, $J = 8.5, 8.3\text{Hz}$, 1H)	
39	104.8	6.51 (d, $J = 8.5\text{Hz}$, 1H)	
40	36.0	2.27 (br d, $J = 13.5\text{Hz}$, 1H), 1.92 (ddd, $J = 13.5, 8.8, 5.1\text{Hz}$, 1H)	
41	58.4	3.78 (dd, $J = 9.3, 1.7\text{Hz}$, 1H)	
42	171.9	-	
43	-	7.71 (br s, 1H), 7.11 (br s, 1H) overlap	

MS m/z 726.3 (calc'd: $\text{C}_{40}\text{H}_{48}\text{N}_5\text{O}_8$, $[\text{M}+\text{H}]^+$, 726.3).

Macrocycles 16a,b:



Acyclic carbonate (13): General procedure A afforded compound **13** as a colorless film (191 mg, 86%). ^1H NMR (500 MHz, CD_3OD , major rotamer): δ 1.48 (s, 9H), 1.52-1.64 (m, 3H), 1.76-1.86 (m, 1H), 1.96 (s, 3H), 2.22-2.33 (m, 2H), 2.37-2.56 (m, 4H), 2.81 (dd, $J = 14.0, 9.3$ Hz, 1H), 2.89 (t, $J = 76$ Hz, 2H), 3.04 (dd, $J = 14.0, 5.4$ Hz, 1H), 3.09-3.18 (m, 1H), 3.22 (dd, $J = 14.8, 7.4$ Hz, 1H), 3.39-3.49 (m, 1H), 3.77 (dd, $J = 11.0, 3.2$ Hz, 1H), 4.27 (dd, $J = 11.0, 5.5$ Hz, 1H), 4.47-4.56 (m, 3H), 4.67 (dd, $J = 6.3, 1.1$ Hz, 1H), 5.03-5.09 (m, 1H), 6.29 (dd, $J = 15.9, 6.3$ Hz, 1H), 6.91 (d, $J = 7.9$ Hz, 2H), 6.95 (dd, $J = 7.3, 7.3$ Hz, 1H), 7.07 (d, $J = 8.3$ Hz, 1H), 7.09 (d, $J = 8.5$ Hz, 2H), 7.21 (dd, $J = 7.4, 7.4$ Hz, 1H), 7.22 (br s, 1H), 7.24-7.29 (m, 3H), 7.92 (t, $J = 6.0$ Hz, 1H), 7.93 (t, $J = 5.3$ Hz, 1H), 8.04 (d, $J = 7.9$ Hz, 1H), 8.25 (d, $J = 7.0$ Hz, 1H). ^{13}C NMR (125 MHz, CD_3OD , major rotamer): δ 176.6, 175.2, 173.9, 173.5, 173.40, 173.39, 158.3, 157.2, 155.0, 142.6, 137.8, 135.1, 131.3, 130.7, 129.8, 129.3, 129.2, 127.8, 125.6, 124.2, 122.6, 116.8, 116.2, 82.9, 76.6, 68.4, 60.7, 56.5, 53.7, 52.7, 40.0, 39.0, 38.2, 37.1, 36.4, 35.5, 32.8, 29.4, 28.0, 26.4, 22.3. MS m/z 885.0 (calc'd: $\text{C}_{47}\text{H}_{61}\text{N}_6\text{O}_{11}$, $[\text{M}+\text{H}]^+$, 885.4).



Compound **13** was subjected to general procedure C. HPLC analysis and purification was performed using the following methods.

Analytical HPLC method:

Column: Waters XBridge™ Phenyl, 4.6x250mm, 5µm.

Solvent A: H₂O + 0.1%v TFA

Solvent B: ACN + 0.1%v TFA

Flow rate: 1.00 ml/min

Time	%B
0	30
2	30
20	70
25	100
35	100
38	30
41	30

Semi-preparative HPLC method A:

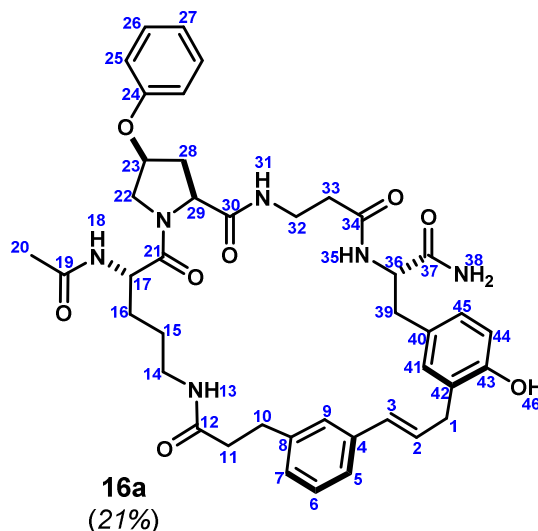
Column: Waters XBridge™ Phenyl, 10x250mm, 5µm.

Solvent A: H₂O + 0.1%v TFA

Solvent B: ACN + 0.1%v TFA

Flow rate: 6.00 ml/min

Time	%B
0	30
2	30
20	65
22	30
25	30



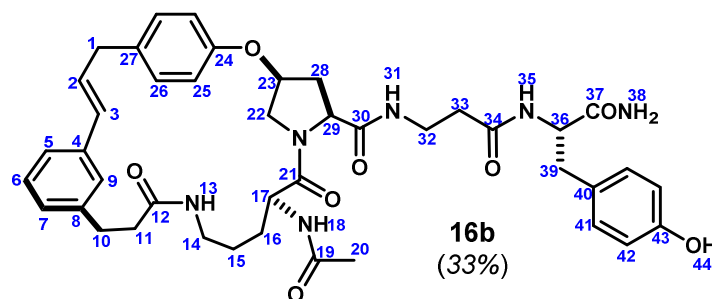
(600MHz, DMSO-*d*₆, 298K, ~6:1 mixture of rotamers, data is of major)

	¹³ C	¹ H	key correlations
1	32.5	3.34-3.45 (m, 2H)	HMBC 1→43,42
2	128.9	6.32-6.35 (m, 1H) overlap	
3	130.0	6.32-6.35 (m, 1H) overlap	HMBC 3→4,5

4	137.2	-	
5	124.1	7.15 (br d, $J = 7.4$ Hz, 1H)	
6	128.4	7.19 (dd, $J = 7.4, 7.4$ Hz, 1H)	HMBC 6→4,8
7	127.1	7.02 (br d, $J = 7.4$ Hz, 1H)	
8	141.6	-	
9	125.3	7.22 (br s, 1H)	HMBC 9→5,7
10	31.1	2.78 (t, $J = 7.6$ Hz, 2H)	HMBC 10→8,12
11	37.3	2.31-2.38 (m, 2H)	HMBC 11→8,12
12	171.4	-	
13	-	7.68 (dd, $J = 5.8, 5.8$ Hz, 1H)	HMBC 13→12
14	37.9	2.94-3.00 (m, 1H), 3.00-3.07 (m, 1H)	
15	24.7	1.35-1.41 (m, 2H)	
16	28.2	1.42-1.50 (m, 1H), 1.64-1.72 (m, 1H)	
17	50.0	4.46 (ddd, $J = 7.9, 7.1, 6.1$ Hz, 1H)	HMBC 17→19,21
18	-	8.07 (d, $J = 7.9$ Hz, 1H)	HMBC 18→19
19	169.2	-	
20	22.1	1.82 (s, 3H)	HMBC 20→19
21	171.0	-	
22	51.9	4.19 (dd, $J = 11.1, 5.7$ Hz, 1H), 3.66 (dd, $J = 11.1, 3.1$ Hz, 1H)	HMBC 22→21,29
23	74.8	5.00-5.05 (m, 1H)	HMBC 23→24
24	156.8	-	
25	115.4	6.87 (d, $J = 8.3$ Hz, 2H) overlap	
26	129.6	7.26 (dd, $J = 8.3, 7.4$ Hz, 2H)	
27	121.0	6.93 (dd, $J = 7.4, 7.4$ Hz, 1H)	
28	34.1	2.04 (ddd, $J = 13.5, 3.8, 3.8$ Hz, 1H), 2.43 (ddd, $J = 13.5, 9.1, 5.4$ Hz, 1H)	HMBC 28→30
29	58.5	4.34-4.39 (m, 1H) overlap	
30	170.7	-	
31	-	7.67 (t, $J = 5.8$ Hz, 1H)	COSY 31→32
32	35.4	3.12-3.17 (m, 2H)	COSY 32→33
33	35.4	2.06-2.12 (m, 1H), 2.21-2.27 (m, 1H)	HMBC 33→34
34	170.4	-	
35	-	7.97 (d, $J = 8.5$ Hz, 1H)	
36	53.9	4.34-4.39 (m, 1H) overlap	HMBC 36→37,40
37	173.6	-	
38	-	7.03 (br s, 1H), 7.39 (br s, 1H)	HMBC 38→37 TOCSY 38→38'
39	36.7	2.62 (dd, $J = 14.0, 10.6$ Hz, 1H), 2.91 (dd, $J = 14.0, 3.5$ Hz, 1H)	HMBC 39→40
40	128.3	-	
41	130.3	6.98 (d, $J = 1.8$ Hz, 1H)	HMBC 41→45
42	125.5	-	

43	153.3	-	
44	114.5	6.69 (d, $J = 8.1$ Hz, 1H)	HMBC 44→40,42
45	127.6	6.89 (dd, $J = 8.1, 1.8$ Hz, 1H) overlap	HMBC 45→41
46	-	9.16 (br s, 1H)	

MS m/z 767.0 (calc'd: $C_{42}H_{51}N_6O_8$, $[M+H]^+$, 767.4).



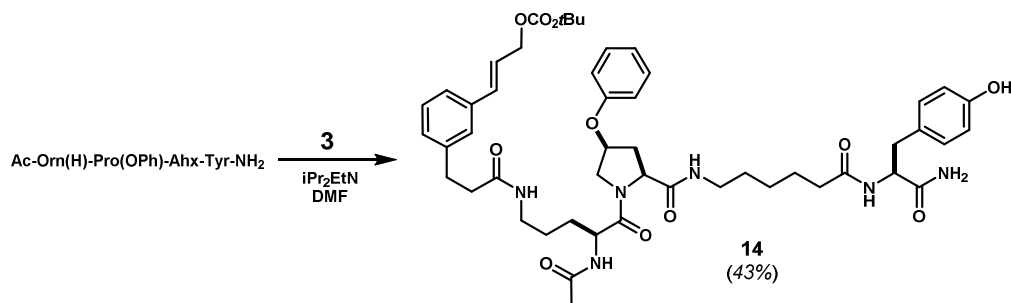
(600MHz, DMSO- d_6 , 298K)

	^{13}C	1H	key correlations
1	37.4	3.40 (dd, $J = 15.9, 6.2$ Hz, 1H), 3.43 (dd, $J = 15.9, 6.6$ Hz, 1H)	HMBC 1→27
2	130.30	6.22 (ddd, $J = 15.8, 6.6, 6.2$ Hz, 1H)	COSY 2→1 HMBC 2→27,4
3	129.10	6.29 (d, $J = 15.8$ Hz, 1H)	HMBC 3→4,5,9
4	136.7	-	
5	124.5	7.10 (br d, $J = 7.7$ Hz, 1H) overlap	TOCSY 5→4,6,7,9
6	128.2	7.18 (dd, $J = 7.7, 7.7$ Hz, 1H)	HMBC 6→4,8 COSY 6→7
7	127.4	6.99 (br d, $J = 7.7$ Hz, 1H)	HMBC 7→10
8	141.5	-	
9	123.7	7.11 (br s, 1H) overlap	HMBC 9→10
10	29.8	2.70-2.76 (m, 1H) overlap, 2.86-2.91 (m, 1H) overlap	HMBC 10→11,12
11	36.0	2.26-2.30 (m, 2H) overlap	HMBC 11→10,12
12	171.1	-	
13	-	7.76 (t, $J = 5.2$ Hz, 1H)	COSY 13→14
14	37.8	2.70-2.76 (m, 2H) overlap	
15	24.8	1.20-1.29 (m, 1H), 1.33-1.40 (m, 1H)	HMBC 15→14
16	28.4	1.40-1.52 (m, 2H)	
17	49.4	4.25 (ddd, $J = 9.1, 7.6, 5.0$ Hz, 1H)	HMBC 17→19
18	-	7.62 (d, $J = 7.6$ Hz, 1H)	
19	169.0	-	
20	21.8	1.78 (s, 3H)	HMBC 20→19
21	171.2	-	
22	50.7	3.49 (d, $J = 11.4$ Hz, 1H), 3.85 (dd, $J = 11.4, 4.1$ Hz, 1H)	HMBC 22→28
23	75.7	5.10-5.14 (m, 1H)	COSY 23→22,22'
24	154.4	-	
25	116.8	6.91 (d, $J = 8.5$ Hz, 2H)	HMBC 25→27

26	129.6	7.16 (d, $J = 8.5$ Hz, 2H)	
27	132.8	-	
28	34.8	2.21-2.25 (m, 1H) overlap, 2.46 (ddd, $J = 13.8, 9.9, 5.1$ Hz, 1H)	
29	58.6	4.40 (dd, $J = 9.9, 1.5$ Hz, 1H)	HMBC 29→30
30	169.9	-	
31	-	7.51 (t, $J = 5.8$ Hz, 1H)	HMBC 31→30
32	35.2	3.17-3.26 (m, 2H)	HMBC 32→30,33,34
33	34.6	2.18-2.23 (m, 1H) overlap, 2.29-2.34 (m, 1H) overlap	
34	170.2	-	
35	-	8.00 (d, $J = 8.5$ Hz, 1H)	HMBC 35→34
36	53.9	4.37 (ddd, $J = 9.5, 8.5, 4.9$ Hz, 1H)	
37	173.3	-	
38	-	7.42 (br s, 1H), 7.02 (br s, 1H) overlap	HMBC 38→37
39	36.7	2.65 (dd, $J = 13.8, 9.5$ Hz, 1H), 2.88 (dd, $J = 13.8, 4.8$ Hz, 1H)	
40	128.0	-	
41	129.8	7.02 (d, $J = 8.4$ Hz, 2H) overlap	
42	114.6	6.63 (d, $J = 8.4$ Hz, 2H)	HMBC 42→40
43	155.5	-	
44	-	9.15 (br s, 1H)	

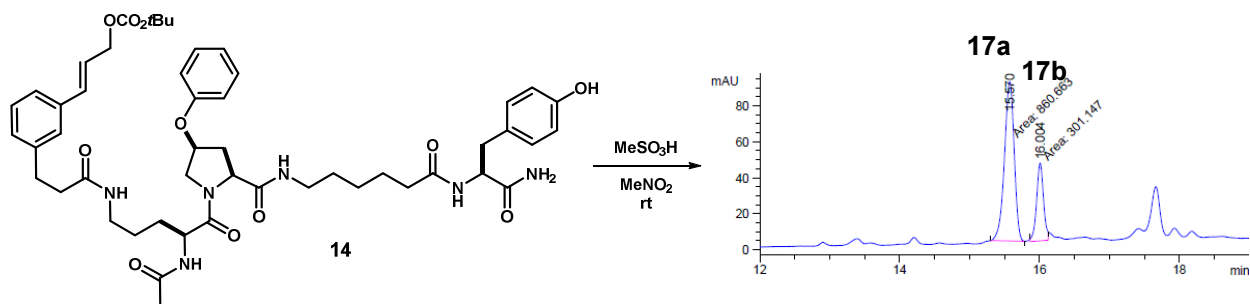
MS m/z 767.0 (calc'd: $C_{42}H_{51}N_6O_8$, $[M+H]^+$, 767.4).

Macrocycles 17a,b:



Acyclic carbonate (14): General procedure A afforded compound **S2** as a white foam (150 mg, 43%). 1H NMR (500 MHz, CD_3OD , major rotamer): δ 1.09-1.17 (m, 2H), 1.35-1.46 (m, 4H), 1.47 (s, 9H), 1.51-1.65 (m, 3H), 1.74-1.82 (m, 1H), 1.96 (s, 3H), 2.11 (t, $J = 7.3$ Hz, 2H), 2.25 (ddd, $J = 13.6, 3.9, 3.9$ Hz, 1H), 2.45 (t, $J = 7.6$ Hz, 2H), 2.54 (ddd, $J = 13.6, 9.3, 5.4$ Hz, 1H), 2.76 (dd, $J = 14.0, 9.5$ Hz, 1H), 2.88 (t, $J = 7.6$ Hz, 2H), 3.05 (dd, $J = 14.0, 5.4$ Hz, 1H), 3.08-3.12 (m, 1H), 3.13 (t, $J = 7.3$ Hz, 2H), 3.20 (dd, $J = 13.6, 6.9$ Hz, 1H), 3.77 (dd, $J = 11.0, 3.2$ Hz, 1H), 4.27 (dd, $J = 11.2, 5.6$ Hz, 1H), 4.52 (dd, $J = 7.8, 7.8$ Hz, 1H), 4.55 (dd, $J = 9.1, 3.9$ Hz, 1H), 4.57 (dd, $J = 9.5, 5.4$ Hz, 1H), 4.66 (dd, $J = 6.3, 1.1$ Hz, 2H), 5.03-5.07 (m, 1H), 6.28 (dt, $J = 15.9, 6.3$ Hz, 1H), 6.61 (br d, $J = 15.9$ Hz, 1H), 6.71 (d, $J = 8.5$ Hz, 2H), 6.90 (d, $J = 7.9$ Hz, 1H), 6.94 (apt t, $J = 7.4$ Hz, 1H), 7.06 (d, $J = 8.5$ Hz, 2H), 7.07-7.10 (m, 1H), 7.20 (apt t, $J = 7.5$ Hz, 1H), 7.21 (br s, 1H), 7.23-7.28 (m, 3H), 7.89 (s, 1H). ^{13}C NMR (125 MHz, CD_3OD , major rotamer): δ 176.5, 175.8, 175.1, 173.30, 173.27, 173.1, 158.3, 157.2, 155.0, 142.6, 137.8, 135.1, 131.3, 130.7, 129.8, 129.24, 129.23, 127.7, 125.6, 124.2, 122.5, 116.7, 116.2, 82.9, 76.6, 68.4, 60.5, 55.8, 53.8, 52.6, 40.4, 39.8, 38.9,

38.3, 36.7, 35.8, 32.8, 30.0, 29.3, 28.0, 27.2, 26.4, 26.3, 22.2. MS m/z 927.0 (calc'd: $C_{50}H_{67}N_6O_{11}$, $[M+H]^+$, 927.5).



Compound **14** was subjected to general procedure C. HPLC analysis and purification was performed using the following methods.

Analytical HPLC method:

Column: Waters X-Bridge™ C₁₈, 4.6x250mm, 5μm.

Solvent A: H₂O + 0.1%v TFA

Solvent B: ACN + 0.1%v TFA

Flow rate: 1.00 ml/min

Time	%B
0	30
2	30
30	100
40	10
50	30
1	30

Preparative HPLC method A:

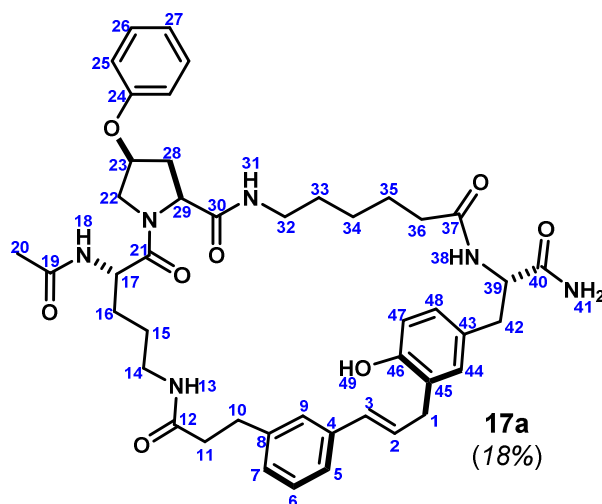
Column: Waters Sunfire™ C₁₈, 19x250mm, 5μm.

Solvent A: H₂O + 0.1%v TFA

Solvent B: ACN + 0.1%v TFA

Flow rate: 18.0 ml/min

Time	%B
0	35
2	35
20	75



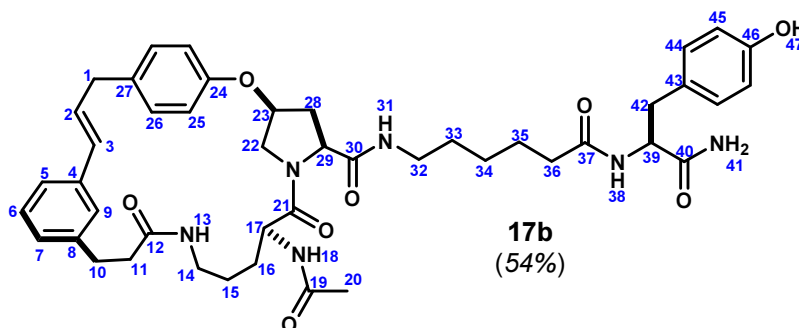
(600MHz, DMSO-*d*₆, 298K, ~8:1 mixture of rotamers, data is of major)

	¹³ C	¹ H	key correlations
1	32.8	3.36 (dd, $J = 15.6, 6.2$ Hz, 1H), 3.40 (dd, $J = 15.6, 6.2$ Hz, 1H)	HMBC 1→2,3,44,45,46
2	128.90	6.37 (ddd, $J = 15.7, 6.2, 6.2$ Hz, 1H)	HMBC 2→4

3	130.00	6.32 (d, $J = 15.7$ Hz, 1H)	HMBC 3→4
4	137.3	-	
5	123.7	7.17-7.21 (m, 1H) overlap	TOCSY 5→6,7,8,9
6	128.5	7.18-7.21 (m, 1H) overlap	HMBC 6→4,9
7	126.8	7.01-7.04 (m, 1H)	
8	141.6	-	
9	125.5	7.18 (br s, 1H) overlap	
10	31.2	2.78 (t, $J = 7.8$ Hz, 2H)	HMBC 10→8,12
11	37.2	2.32-2.37 (m, 2H)	HMBC 11→8,12
12	171.5	-	
13	-	7.78 (dd, $J = 5.7, 5.7$ Hz, 1H)	HMBC 13→12 COSY 13→14
14	37.9	2.96-3.03 (m, 1H) overlap, 3.03-3.10 (m, 1H)	
15	24.9	1.39-1.46 (m, 2H)	
16	28.4	1.46-1.53 (m, 1H), 1.67-1.74 (m, 1H)	
17	49.9	4.52 (apt dd, $J = 14.0, 7.0$ Hz, 1H)	HMBC 17→19,21
18	-	8.13 (d, $J = 7.9$ Hz, 1H)	HMBC 18→19
19	169.2	-	
20	22.1	1.84 (s, 3H)	HMBC 20→19
21	171.0	-	
22	51.9	3.74 (dd, $J = 11.1, 2.7$ Hz, 1H), 4.21 (dd, $J = 11.1, 5.6$ Hz, 1H)	
23	75.1	5.02-5.07 (m, 1H)	
24	156.8	-	
25	115.4	6.87 (d, $J = 8.4$ Hz, 2H) overlap	TOCSY 25→26,27
26	129.5	7.26 (dd, $J = 8.4$ Hz, 2H)	HMBC 26→24
27	120.9	6.92 (t, $J = 7.3$ Hz, 1H)	
28	34.3	2.06 (ddd, $J = 13.6, 3.6, 3.1$ Hz, 1H), 2.45 (ddd, $J = 13.6, 9.4, 5.8$ Hz, 1H)	HMBC 28→30
29	58.5	4.39 (dd, $J = 9.4, 3.6$ Hz, 1H)	
30	170.5	-	
31	-	7.44 (t, $J = 5.9$ Hz, 1H)	HMBC 31→30 COSY 31→32
32	38.6	2.87-2.93 (m, 1H) overlap, 2.95-3.01 (m, 1H) overlap	COSY 32→33, HMBC 32→33,34
33	28.9	1.20-1.27 (m, 2H) overlap	
34	25.7	0.92-1.01 (m, 2H)	
35	24.8	1.22-1.30 (m, 2H)	
36	35.1	1.86-1.98 (m, 2H)	HMBC 36→34,35
37	171.9	-	
38	-	7.76 (d, $J = 8.7$ Hz, 1H)	
39	53.8	4.34 (ddd, $J = 10.0, 8.7, 4.0$ Hz, 1H)	HMBC 39→37,40,43
40	173.6	-	
41	-	7.00 (br s, 1H), 7.35 (br s, 1H)	HMBC 41→40

42	36.9	2.61 (dd, $J = 13.7, 10.0$ Hz, 1H), 2.87 (dd, $J = 13.7, 4.0$ Hz, 1H)	HMBC 42→43,44,48
43	128.5	-	
44	130.6	6.96 (d, $J = 1.5$ Hz, 1H)	
45	125.4	-	
46	153.2	-	
47	114.6	6.69 (d, $J = 8.1$ Hz, 1H)	HMBC 47→45
48	127.8	6.87 (br d, $J = 8.1$ Hz, 1H) overlap	
49	-	9.14 (br s, 1H)	

MS m/z 809.0 (calc'd: $C_{45}H_{57}N_6O_8$, $[M+H]^+$, 809.4).



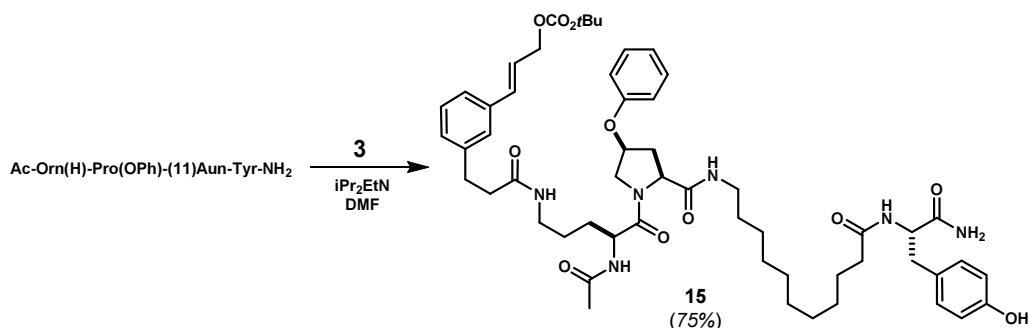
(600MHz, DMSO- d_6 , 298K)

	^{13}C	1H	key correlations
1	37.3	3.40 (dd, $J = 15.5, 6.4$ Hz, 1H), 3.43 (dd, $J = 15.5, 6.4$ Hz, 1H)	HMBC 1→27
2	130.40	6.21 (ddd, $J = 15.7, 6.4, 6.4$ Hz, 1H)	COSY 2→1 HMBC 2→4
3	128.90	6.27 (d, $J = 15.7$ Hz, 1H)	HMBC 3→4
4	136.8	-	
5	124.6	7.10 (d, $J = 7.6$ Hz, 1H) overlap	HMBC 5→7
6	128.3	7.18 (dd, $J = 7.6, 7.6$ Hz, 1H) overlap	HMBC 6→4,8
7	127.5	6.98 (d, $J = 7.6$ Hz, 1H) overlap	HMBC 7→5
8	141.7	-	
9	123.9	7.10 (br s, 1H) overlap	HMBC 9→7,5
10	29.8	2.69-2.75 (m, 1H) overlap, 2.85-2.91 (m, 1H)	HMBC 10→8,12
11	35.9	2.25-2.29 (m, 2H)	HMBC 1→8,12
12	171.2	-	
13	-	7.75 (t, $J = 5.3$ Hz, 1H)	HMBC 13→12 COSY 13→14
14	37.8	2.65-2.78 (m, 2H)	HMBC 14→15
15	25.0	1.22-1.29 (m, 1H), 1.33-1.39 (m, 1H) overlap	HMBC 15→16
16	28.4	1.39-1.45 (m, 1H) overlap, 1.45-1.51 (m, 1H)	TOCSY 16→13,14,15,17,18 HMBC 16→21
17	49.4	4.26 (ddd, $J = 9.0, 7.7, 4.9$ Hz, 1H)	
18	-	8.07 (d, $J = 7.7$ Hz, 1H)	HMBC 18→19
19	169.2	-	
20	22.1	1.79 (s, 3H)	HMBC 20→19

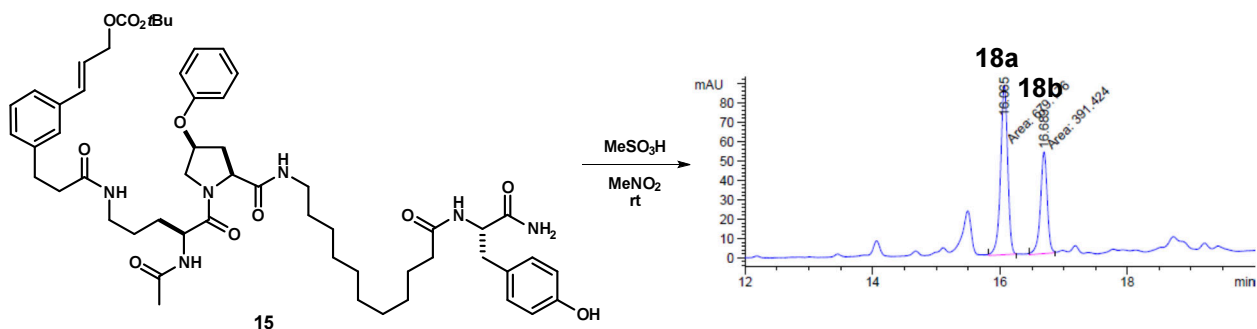
21	171.8	-	
22	50.8	3.50 (d, $J = 11.3$ Hz, 1H), 3.89 (dd, $J = 11.3, 4.4$ Hz, 1H)	
23	75.6	5.12-5.15 (m, 1H)	
24	155.7	-	
25	116.7	6.88 (d, $J = 8.5$ Hz, 2H)	HMBC 25→24
26	129.8	7.16 (d, $J = 8.5$ Hz, 2H)	HMBC 26→1,24 COSY 26→25
27	132.8	-	
28	35.1	2.24 (br d, $J = 14.0$ Hz, 1H), 2.45-2.51 (m, 1H)	
29	58.6	4.42 (dd, $J = 9.7, 1.6$ Hz, 1H)	HMBC 29→30
30	170.0	-	
31	-	7.41 (dd, $J = 5.6, 5.6$ Hz, 1H)	
32	38.5	2.96-3.03 (m, 1H), 3.06-3.13 (m, 1H)	TOCSY 32→31,33,34,35,36
33	28.9	1.34-1.41 (m, 2H) overlap	HMBC 33→32,34
34	25.8	1.13-1.20 (m, 2H)	HMBC 34→35,36
35	24.9	1.37-1.43 (m, 2H) overlap	HMBC 35→36
36	35.1	2.00-2.06 (m, 2H)	HMBC 36→35,37
37	171.9	-	
38	-	7.82 (d, $J = 8.5$ Hz, 1H)	
39	53.9	4.34 (ddd, $J = 9.6, 8.5, 4.7$ Hz, 1H)	HMBC 39→37, 40
40	173.5	-	
41	-	6.97 (br s, 1H), 7.34 (br s, 1H)	HMBC 41→40
42	36.7	2.61 (dd, $J = 13.8, 9.6$ Hz, 1H), 2.85 (dd, $J = 13.8, 4.7$ Hz, 1H)	
43	128.3	-	
44	130.1	7.00 (d, $J = 8.4$ Hz, 2H)	HMBC 44→46
45	114.7	6.62 (d, $J = 8.4$ Hz, 2H)	HMBC 45→46
46	155.7	-	
47	-	9.14 (s, 1H)	

MS m/z 809.0 (calc'd: $C_{45}H_{57}N_6O_8$, $[M+H]^+$, 809.4).

Macrocycles 18a,b:



Acyclic carbonate (15): General procedure A afforded compound **S3** as a colorless film (396 mg, 75%). ¹H NMR (600 MHz, CD₃OD, major rotamer): δ 1.11-1.19 (m, 3H), 1.81-1.31 (m, 12H), 1.42-1.49 (m, 5H), 1.47 (s, 9H), 1.50-1.65 (m, 4H), 1.75-1.81 (m, 1H), 1.96 (s, 3H), 2.14 (t, *J* = 7.6 Hz, 2H), 2.27 (ddd, *J* = 13.9, 3.5, 3.5 Hz, 1H), 2.43-2.49 (m, 2H), 2.54 (ddd, *J* = 13.5, 9.3, 5.4 Hz, 1H), 2.77 (dd, *J* = 13.9, 9.3 Hz, 1H), 2.87-2.93 (m, 2H), 3.05 (dd, *J* = 13.9, 5.3 Hz, 1H), 3.08-3.15 (m, 2H), 3.15-3.24 (m, 1H), 3.78 (dd, *J* = 11.0, 2.7 Hz, 1H), 4.27 (dd, *J* = 11.1, 5.5 Hz, 1H), 4.50-4.59 (m, 3H), 4.66 (br d, *J* = 6.2 Hz, 2H), 5.04-5.08 (m, 1H), 6.29 (dt, *J* = 15.8, 6.2 Hz, 1H), 6.62 (br d, *J* = 15.8 Hz, 1H), 6.69 (d, *J* = 8.3 Hz, 2H), 6.90 (d, *J* = 8.1 Hz, 2H), 6.94 (apt t, *J* = 7.6 Hz, 1H), 7.06 (d, *J* = 8.3 Hz, 2H), 7.10 (d, *J* = 7.4 Hz, 1H), 7.21 (apt t, *J* = 7.6 Hz, 1H), 7.22 (br s, 1H), 7.23-7.29 (m, 5H), 7.74 (t, *J* = 5.7 Hz, 1H), 7.92 (d, *J* = 8.1 Hz, 1H), 7.95 (t, *J* = 5.4 Hz, 1H). ¹³C NMR (151 MHz, CD₃OD, major rotamer): δ 176.6, 176.0, 175.1, 173.4, 173.3, 173.2, 158.3, 157.3, 155.0, 142.6, 137.8, 135.1, 131.2, 130.7, 129.8, 129.2, 129.2, 127.8, 125.6, 124.3, 122.5, 116.8, 116.2, 82.9, 76.8, 68.4, 60.6, 55.8, 53.8, 52.6, 40.7, 39.8, 38.9, 38.3, 36.9, 35.8, 32.9, 30.6, 30.5, 30.44, 30.39, 30.4, 30.1, 29.3, 28.1, 27.9, 26.8, 26.3, 22.2. MS *m/z* 997.1 (calc'd: C₅₅H₇₇N₆O₁₁, [M+H]⁺, 997.6).



Compound **15** was subjected to general procedure C. HPLC analysis and purification was performed using the following methods.

Analytical HPLC method:

Column: Waters X-Bridge™ C₁₈, 4.6x250mm, 5μm.

Solvent A: H₂O + 0.1%v TFA

Solvent B: ACN + 0.1%v TFA

Flow rate: 1.00 ml/min

Time	%B
0	30
2	30
30	100
35	100
38	30
41	30

Preparative HPLC method A:

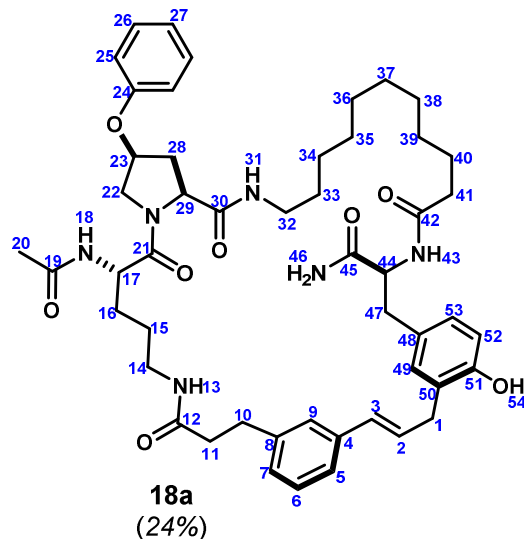
Column: Waters Sunfire™ C₁₈, 19x250mm, 5μm.

Solvent A: H₂O + 0.1%v TFA

Solvent B: ACN + 0.1%v TFA

Flow rate: 18.0 ml/min

Time	%B
0	35
2	35
14	60
17	35

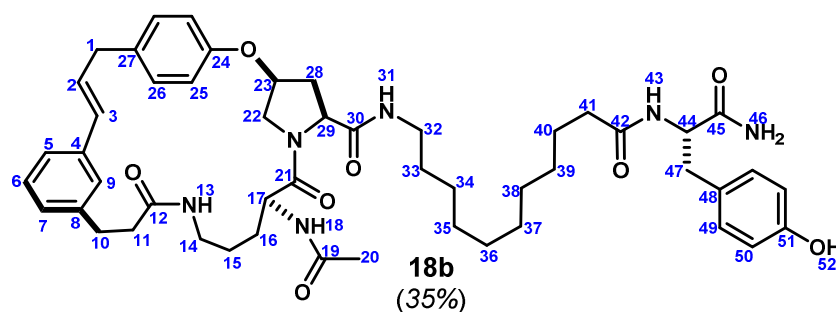


(600MHz, DMSO-*d*₆, 298K, ~9:1 mixture of rotamers, data is of major)

	¹³ C	¹ H	key correlations
1	32.7	3.34-3.44 (m, 1H)	HMBC 1→49,50,51
2	128.8	6.38 (dt, J = 15.9, 6.3 Hz, 1H)	COSY 2→1 HMBC 2→4,50
3	129.8	6.31 (d, J = 15.9 Hz, 1H)	HMBC 3→4,5,9
4	137.2	-	
5	125.7	7.15-7.21 (m, 1H)	
6	128.2	7.15-7.20 (m, 1H) overlap	HMBC 6→4,8
7	126.5	6.99-7.03 (m, 1H)	
8	141.4	-	
9	123.4	7.19 (br s, 1H) overlap	
10	31.0	2.77 (t, J = 7.7 Hz, 2H)	
11	37.0	2.34 (br t, J = 7.7 Hz, 2H)	
12	171.2	-	
13	-	7.79 (t, J = 4.8 Hz, 1H)	HMBC 13→12,14
14	38.0	2.95-3.31 (m, 2H) overlap	
15	24.9	1.39-1.46 (m, 2H)	HMBC 15→14,16
16	28.3	1.46-1.54 (m, 1H), 1.68-1.75 (m, 1H)	HMBC 16→14
17	49.8	4.53 (ddd, J = 7.9, 6.4, 6.4 Hz, 1H)	HMBC 17→16,15
18	-	8.14 (d, J = 7.9 Hz, 1H)	
19	169.1	-	
20	22.0	1.84 (s, 3H)	HMBC 20→19
21	171.0	-	
22	51.9	3.77 (br d, J = 11.1 Hz, 1H), 4.19 (dd, J = 11.1, 5.2 Hz, 1H)	
23	75.0	5.02-5.08 (m, 1H)	
24	156.7	-	
25	115.4	6.87 (d, J = 8.1 Hz, 2H)	
26	129.4	7.26 (dd, J = 8.1, 7.2 Hz, 1H)	HMBC 26→24

27	120.8	6.93 (t, J = 7.2 Hz, 1H)	
28	34.1	2.09 (br d, J = 13.3 Hz, 1H), 2.44 (ddd, J = 13.3, 9.4, 5.5 Hz, 1H)	HMBC 28→29,30
29	58.6	4.37-4.42 (m, 1H) overlap	HMBC 29→30
30	170.4	-	
31	-	7.40 (dd, J = 5.6, 5.6 Hz, 1H)	HMBC 31→30
32	38.5	2.92-3.01 (m, 1H) overlap, 3.06-3.15 (m, 1H) overlap	
33	28.9	1.30-1.37 (m, 2H)	HMBC 33→32
34	26.0	1.13-1.20 (m, 2H) overlap	HMBC 34→35
35	28.7	1.13-1.20 (m, 2H) overlap	HMBC 35→36
36	28.6	1.06-1.14 (m, 2H) overlap	
37	28.6	1.01-1.08 (m, 2H) overlap	
38	28.6	1.01-1.08 (m, 2H) overlap	
39	28.4	0.90-1.01 (m, 2H)	HMBC 39→38
40	25.0	1.23-1.30 (m, 2H)	HMBC 40→39
41	35.2	1.93→1.99 (m, 2H)	HMBC 41→40
42	171.9	-	
43	-	7.75 (d, J = 8.3 Hz, 1H)	COSY 43→44
44	53.7	4.34-4.40 (m, 1H) overlap	
45	173.5	-	
46	-	7.00 (br s, 1H) overlap, 7.36 (br s, 1H)	HMBC 46→45
47	36.8	2.62 (dd, J = 13.2, 10.7 Hz, 1H), 2.89 (dd, J = 13.2, 2.7 Hz, 1H)	HMBC 47→44,48,49,53
48	128.3	-	
49	130.6	6.97 (br s, 1H)	HMBC 49→1
50	125.2	-	
51	153.2	-	
52	114.4	6.69 (d, J = 8.1 Hz, 1H)	HMBC 52→48,50,51
53	127.6	6.88 (d, J = 8.1 Hz, 1H) overlap	
54	-	9.12 (br s, 1H)	

MS m/z 879.0 (calc'd: $C_{50}H_{67}N_6O_8$, $[M+H]^+$, 879.5).



(600MHz, DMSO- d_6 , 298K)

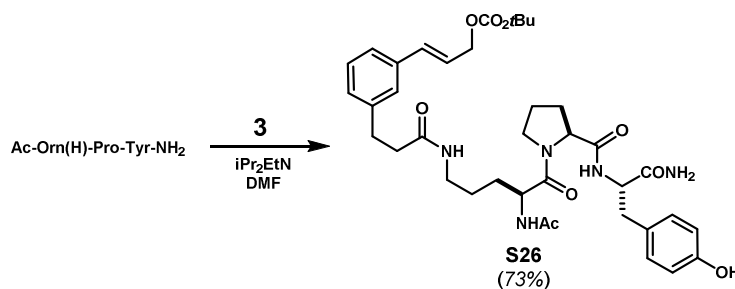
	^{13}C	1H	key correlation
1	37.5	3.39 (dd, J = 15.0, 5.7 Hz, 1H), 3.43 (dd, J = 15.0, 6.6 Hz, 1H)	HMBC 1→27

2	130.50	6.21 (ddd, $J = 15.8, 6.6, 5.7$ Hz, 1H)	COS 2→1 HMBC 2→27
3	129.40	6.27 (d, $J = 15.8$ Hz, 1H)	HMBC 3→5,9
4	136.9	-	
5	124.7	7.09-7.11 (m, 1H) overlap	
6	128.4	7.18 (dd, $J = 7.8, 7.8$ Hz, 1H)	TOCSY 6→5,7,9 HMBC 6→4,8
7	127.6	6.99 (d, $J = 7.8$ Hz, 1H)	
8	141.7	-	
9	124.0	7.10 (br s, 1H) overlap	
10	29.8	2.70-2.75 (m, 1H) overlap, 2.85-2.91 (m, 1H) overlap	HMBC 10→8,12
11	36.1	2.25-2.29 (m, 2H)	
12	171.3	-	
13	-	7.75 (t, $J = 5.2$ Hz, 1H)	COSY 13→14
14	37.9	2.66-2.76 (m, 2H) overlap	
15	25.0	1.23-1.30 (m, 1H) overlap, 1.32-1.39 (m, 1H) overlap	
16	28.7	1.41-1.52 (m, 2H) overlap	
17	49.4	4.27 (ddd, $J = 8.9, 7.7, 5.2$ Hz, 1H)	HMBC 17→19,21
18	-	8.08 (d, $J = 7.7$ Hz, 1H)	HMBC 18→19
19	169.3	-	
20	22.2	1.79 (s, 3H)	HMBC 20→19
21	171.2	-	
22	50.9	3.51 (d, $J = 11.4$ Hz, 1H), 3.89 (dd, $J = 11.4, 4.3$ Hz, 1H)	
23	75.7	5.11-5.15 (m, 1H)	TOCSY 23→22,28,29
24	154.6	-	
25	116.9	6.88 (d, $J = 8.5$ Hz, 2H)	HMBC 25→24,27
26	129.9	7.15 (d, $J = 8.5$ Hz, 2H)	HMBC 26→24
27	132.9	-	
28	35.3	2.23-2.28 (m, 1H) overlap, 2.45-2.51 (m, 1H)	
29	58.6	4.43 (dd, $J = 9.8, 1.4$ Hz, 1H)	HMBC 29→30
30	170.0	-	
31	-	7.38 (dd, $J = 5.6, 5.6$ Hz, 1H)	HMBC 31→30 COSY 31→32
32	38.5	2.98-3.05 (m, 1H), 3.13-3.19 (m, 1H)	HMBC 32→33,34
33	29.2	1.38-1.45 (m, 2H) overlap	
34	26.3	1.23-1.30 (m, 2H) overlap	
35	28.8	1.20-1.27 (m, 2H) overlap	
36	28.8	1.13-1.22 (m, 2H) overlap	
37	28.8	1.13-1.22 (m, 2H) overlap	
38	28.9	1.13-1.22 (m, 2H) overlap	
39	28.5	1.05-1.12 (m, 2H)	
40	25.2	1.32-1.39 (m, 2H)	HMBC 40→42
41	35.3	2.01 (t, $J = 7.4$ Hz, 2H)	HMBC 41→39,40,42

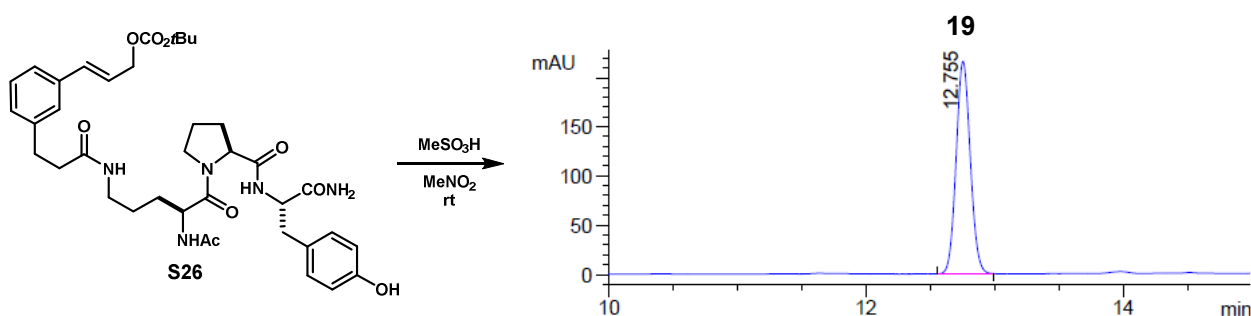
42	172.0	-	
43	-	7.81 (d, $J = 8.5$ Hz, 1H)	
44	53.9	4.35 (ddd, $J = 9.7, 8.5, 4.8$ Hz, 1H)	HMBC 44→42,45
45	173.6	-	
46	-	6.97 (br s, 1H), 7.34 (br s, 1H)	
47	36.9	2.62 (dd, $J = 13.7, 9.7$ Hz, 1H), 2.86 (dd, $J = 13.7, 4.8$ Hz, 1H) overlap	HMBC 47→48,49
48	128.4	-	
49	130.0	7.00 (d, $J = 8.5$ Hz, 2H)	
50	114.7	6.62 (d, $J = 8.5$ Hz, 2H)	COSY 50→49 HMBC 50→48
51	155.8	-	
52	-	9.12 (br s, 1H)	

MS m/z 879.0 (calc'd: $C_{50}H_{67}N_6O_8$, $[M+H]^+$, 879.5).

Macrocycle 19:



Acyclic carbonate (S26): General procedure A afforded compound **S26** as a colorless film (38 mg, 85%). 1H NMR (600 MHz, CD_3OD , major rotamer): δ 1.47 (s, 9H), 1.47-1.57 (m, 3H), 1.64-1.72 (m, 1H), 1.81-1.88 (m, 1H), 1.90-1.95 (m, 1H), 1.97 (s, 3H), 2.06-2.14 (m, 1H), 2.48 (t, $J = 7.6$ Hz, 2H), 2.91 (t, $J = 7.6$ Hz, 2H), 2.89-2.95 (m, 1H), 3.05 (dd, $J = 13.9, 5.8$ Hz, 1H), 3.09-3.15 (m, 1H), 3.15-3.22 (m, 1H), 3.52-3.57 (m, 1H), 3.78 (dd, $J = 16.1, 7.5$ Hz, 1H), 4.34-4.38 (m, 1H), 4.43-4.47 (m, 1H), 4.48-4.52 (m, 1H), 4.67 (br d, $J = 6.0$ Hz, 1H), 6.31 (dt, $J = 15.8, 6.2$ Hz, 1H), 6.64 (d, $J = 15.8$ Hz, 1H), 6.70 (d, $J = 7.9$ Hz, 2H), 7.05 (d, $J = 7.9$ Hz, 2H), 7.11 (d, $J = 6.2$ Hz, 1H), 7.21-7.26 (m, 2H), 7.28 (br s, 1H). ^{13}C NMR (151 MHz, CD_3OD , major rotamer): δ 175.9, 175.1, 173.9, 173.2, 173.1, 157.3, 155.0, 142.6, 137.8, 135.1, 131.4, 129.8, 129.3, 129.0, 127.7, 125.7, 124.3, 116.2, 82.9, 68.4, 61.9, 56.0, 52.5, 39.9, 38.9, 37.6, 32.8, 30.2, 29.4, 28.0, 26.3, 25.9, 22.3. MS m/z 722.4 (calc'd: $C_{38}H_{52}N_5O_9$, $[M+H]^+$, 722.4).



Compound **S26** was subjected to general procedure C. HPLC analysis and purification was performed using the following methods.

Analytical HPLC method:Column: Waters Sunfire™ C₁₈, 4.6x250mm, 5μm.Solvent A: H₂O + 0.1%v TFA

Solvent B: ACN + 0.1%v TFA

Flow rate: 1.00 ml/min

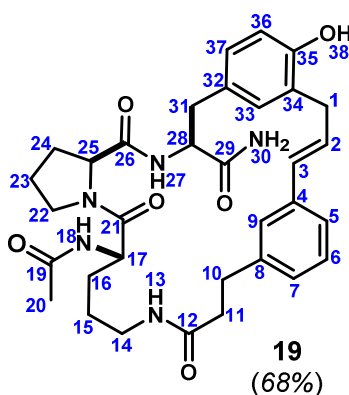
Time	%B
0	25
2	25
27	60
32	100
42	100
44	25
25	30

Semi-preparative HPLC method A:Column: Waters Sunfire™ C₁₈, 10x250mm, 5μm.Solvent A: H₂O + 0.1%v TFA

Solvent B: ACN + 0.1%v TFA

Flow rate: 7.50 ml/min

Time	%B
0	20
20	50
22	20
25	20

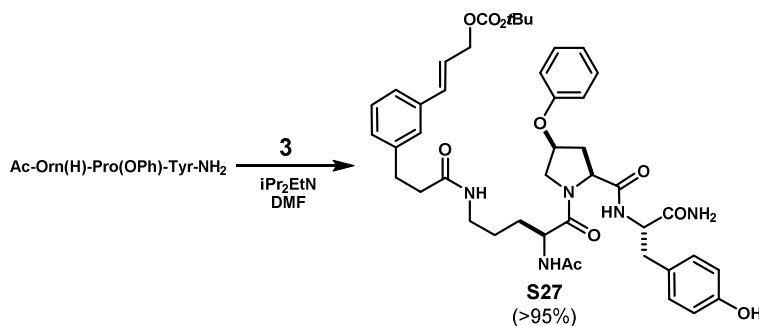
(600MHz, DMSO-*d*₆, 298K)

	¹³ C	¹ H	key correlations
1	31.9	3.44-3.50 (m, 1H) overlap, 3.37 (dd, <i>J</i> = 15.9, 7.1Hz, 1H)	HMBC 1→33, 34, 35
2	128.4	6.33 (ddd, <i>J</i> = 15.7, 7.1, 7.1Hz, 1H)	HMBC 2→4
3	130.6	6.47 (d, <i>J</i> = 15.7Hz, 1H)	
4	137.1	-	
5	124.1	7.13 (ddd, <i>J</i> = 7.5, 1.5, 1.5Hz, 1H)	HMBC 5→3
6	128.2	7.18 (dd, <i>J</i> = 7.5, 7.5Hz, 1H)	HMBC 6→4, 8
7	127.2	7.03 (ddd, <i>J</i> = 7.5, 1.5, 1.5Hz, 1H)	
8	141.4	-	
9	124.5	7.31 (dd, <i>J</i> = 1.5, 1.5Hz, 1H)	
10	30.6	2.76-2.86 (m, 2H)	HMBC 10→8
11	36.5	2.37-2.44 (m, 2H)	
12	171.3	-	
13	-	7.64 (t, <i>J</i> = 5.3Hz, 1H)	
14	37.6	2.99-3.04 (m, 1H), 2.93-2.98 (m, 1H)	
15	24.4	1.31-1.37 (m, 2H) overlap	
16	28.1	1.56-1.62 (m, 1H), 1.31-1.37 (m, 1H) overlap	
17	49.6	4.38-4.43 (m, 1H) obscured	HMBC 17→19, 21

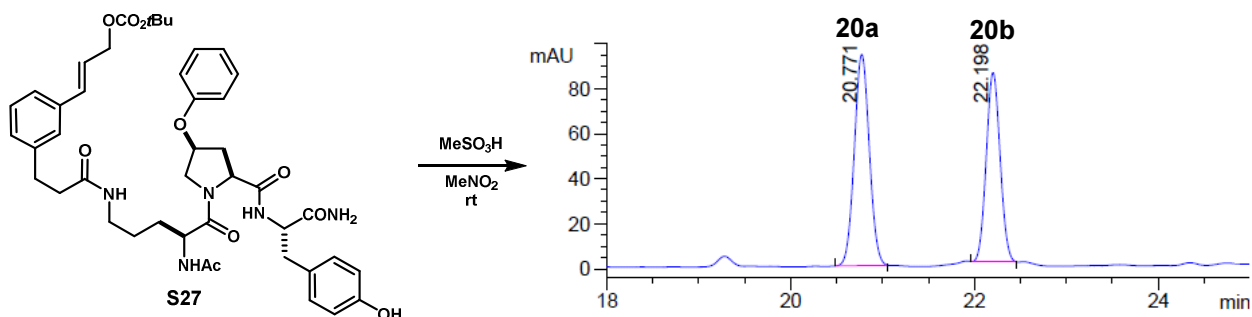
18	-	7.99 (d, $J = 7.6\text{Hz}$, 1H)	
19	169.1	-	
20	22.0	1.81 (s, 3H)	HMBC 20→19
21	170.8	-	
22	46.5	3.58-3.63 (m, 1H), 3.44-3.50 (m, 1H) overlap	COSY 22→23
23	24.0	1.77-1.83 (m, 1H), 1.70-1.76 (m, 1H) overlap	
24	28.6	1.88-1.94 (m, 1H), 1.70-1.76 (m, 1H) overlap	
25	59.4	4.25-4.30 (m, 1H)	
26	171.1	-	
27	-	7.52 (d, $J = 7.9\text{Hz}$, 1H)	HMBC 27→26
28	53.9	4.25-4.30 (m, 1H) overlap	HMBC 28→26,29,32
29	172.9	-	
30	-	7.28 (br s, 1H), 7.02 (br s, 1H)	HMBC 30→29
31	36.7	2.88 (dd, $J = 13.8, 6.0\text{Hz}$, 1H), 2.69 (ss, $J = 13.8, 8.0\text{Hz}$, 1H)	HMBC 31→28, 32
32	127.9	-	
33	129.8	6.92 (d, $J = 2.0\text{Hz}$, 1H)	
34	125.9	-	
35	153.3	-	
36	114.4	6.69 (d, $J = 8.2\text{Hz}$, 1H)	HMBC 36→34
37	127.4	6.85 (dd, $J = 8.2, 2.1\text{Hz}$, 1H)	
38	-	9.20 (br s, 1H)	

MS m/z 604.3 (calc'd: $\text{C}_{33}\text{H}_{42}\text{N}_5\text{O}_6$, $[\text{M}+\text{H}]^+$, 604.3).

Macrocycles 20a,b:



Acyclic carbonate (S27): General procedure A afforded compound **S27** as a colorless film (155 mg, quant.). ^1H NMR (500 MHz, CD_3OD , major rotamer): δ 1.40-1.65 (m, 4H), 1.46 (s, 9H), 1.95 (s, 3H), 2.29-2.34 (m, 1H), 2.42-2.54 (m, 3H), 2.85-2.94 (m, 1H), 2.89 (t, $J = 7.3$ Hz, 2H), 2.95 (d, $J = 7.3$ Hz, 2H), 3.02-3.21 (m, 2H), 3.80 (d, $J = 11.1$ Hz, 1H), 4.20 (dd, $J = 11.3, 4.9$ Hz, 1H), 4.43-4.49 (m, 1H), 4.49-4.56 (m, 2H), 4.66 (dd, $J = 6.3, 0.9$ Hz, 2H), 5.03-5.08 (m, 1H), 6.29 (dt, $J = 15.9, 6.3$ Hz, 1H), 6.61 (d, $J = 15.9$ Hz, 1H), 6.63 (d, $J = 8.4$ Hz, 2H), 6.91 (d, $J = 7.8$ Hz, 2H), 6.95 (t, $J = 7.4$ Hz, 1H), 7.00 (d, $J = 8.4$ Hz, 2H), 7.08-7.11 (m, 1H), 7.18-7.29 (m, 5H). ^{13}C NMR (126 MHz, CD_3OD , major rotamer): δ 175.5, 175.2, 174.1, 173.4, 172.8, 158.1, 157.3, 154.9, 142.6, 137.7, 135.0, 131.6, 130.8, 129.8, 129.3, 128.5, 127.8, 125.6, 124.2, 122.7, 116.8, 116.2, 82.9, 77.2, 68.4, 61.2, 55.7, 54.1, 52.6, 39.8, 39.0, 38.2, 35.1, 32.8, 29.4, 28.0, 26.3, 22.2. MS m/z 814.4 (calc'd: $\text{C}_{39}\text{H}_{46}\text{N}_5\text{O}_7$, $[\text{M}+\text{H}]^+$, 814.4).



Compound **S27** was subjected to general procedure C. HPLC analysis and purification was performed using the following methods.

Analytical HPLC method:

Column: Waters Sunfire™ C₁₈, 4.6x250mm, 5μm.

Solvent A: H₂O + 0.1%v TFA

Solvent B: ACN + 0.1%v TFA

Flow rate: 1.00 ml/min

Time	%B
0	30
2	30
30	50
38	100
45	100
49	30
50	30

Semi-preparative HPLC method:

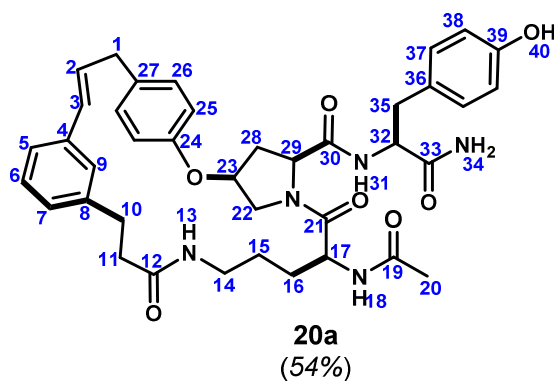
Column: Waters Sunfire™ C₁₈, 10x250mm, 5μm.

Solvent A: H₂O + 0.1%v TFA

Solvent B: ACN + 0.1%v TFA

Flow rate: 7.50 ml/min

Time	%B
0	30
2	30
25	48
27	30
28	30

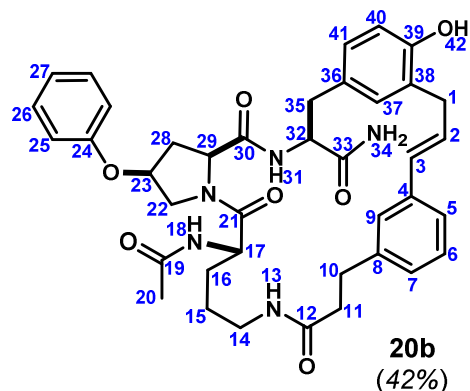


(600MHz, DMSO-*d*₆, 298K)

	¹³ C	¹ H	key correlations
1	37.5	3.42 (br d, <i>J</i> = 6.6Hz, 2H)	HMBC 1→27
2	130.3	6.21 (dt, <i>J</i> = 15.8, 6.6Hz, 1H)	COSY 2→1, HMBC 2→4, 27
3	129.3	6.32 (dd, <i>J</i> = 15.8, 1.3Hz, 1H)	HMBC 3→4
4	136.7	-	
5	124.5	7.09 (ddd, <i>J</i> = 7.7, 1.2, 1.2Hz, 1H)	HMBC 5→3
6	128.3	7.18 (dd, <i>J</i> = 7.7, 7.7Hz, 1H)	HMBC 6→4

7	127.3	6.99 (ddd, $J = 7.7, 1.2, 1.2\text{Hz}$, 1H)	
8	141.4	-	
9	123.3	7.15 (br s, 1H) overlap	
10	29.6	2.86 - 2.91 (m, 1H), 2.71 - 2.76 (m, 1H)	HMBC 10→8,12
11	35.7	2.26 - 2.30 (m, 2H)	HMBC 11→8,10,12
12	171.1	-	
13	-	7.78 (t, $J = 5.2\text{Hz}$, 1H)	COSY 13→14, HMBC 13→12, TOCSY 13→14,15,16,17,18
14	37.9	2.63 - 2.69 (m, 2H)	
15	24.9	1.27 - 1.34 (m, 1H) overlap, 1.19 - 1.26 (m, 1H)	
16	28.4	1.36 - 1.44 (m, 1H), 1.27 - 1.34 (m, 1H) overlap	HMBC 16→21
17	49.6	4.23 (ddd, $J = 9.8, 7.6, 4.1\text{Hz}$, 1H)	HMBC 17→21
18	-	8.10 (d, $J = 7.6\text{Hz}$, 1H)	
19	169.1	-	
20	22.0	1.77 (s, 3H)	HMBC 20→18
21	171.5	-	
22	50.8	3.79 (d, $J = 11.5, 3.7\text{Hz}$, 1H), 3.56 (d, $J = 11.5\text{Hz}$, 1H)	
23	75.7	5.16 (apt t, $J = 4.0\text{Hz}$, 1H)	COSY 23→22,28
24	154.2	-	
25	116.7	6.91 (d, $J = 8.5\text{Hz}$, 1H)	HMBC 25→24,27
26	129.7	7.14 (d, $J = 8.5\text{Hz}$, 1H)	HMBC 26→1, 24
27	132.9	-	
28	34.3	2.53 (ddd, $J = 14.2, 10.5, 5.0\text{Hz}$, 1H), 2.22 (br d, $J = 14.2\text{Hz}$, 1H)	
29	59.1	4.35 (dd, $J = 10.5, 2.1\text{Hz}$, 1H)	
30	169.6	-	
31	-	7.31 (d, $J = 7.8\text{Hz}$, 1H)	
32	53.5	4.34 - 4.38 (m, 1H) overlap	HMBC 32→33,36
33	172.4	-	
34	-	7.24 (br s, 1H), 7.13 (br s, 1H) overlap	TOCSY 34→34', HMBC 34→33
35	36.9	2.93 (dd, $J = 14.0, 5.8\text{Hz}$, 1H), 2.80 (dd, $J = 14.0, 7.1\text{Hz}$, 1H)	HMBC 35→32,36,37
36	127.3	-	
37	130.1	7.01 (d, $J = 8.5\text{Hz}$, 2H)	HMBC 37→39, COSY 37→38
38	114.7	6.60 (d, $J = 8.5\text{Hz}$, 2H)	HMBC 38→36,39
39	155.7	-	
40	-	9.15 (br s, 1H)	

MS m/z 696.3 (calc'd: $\text{C}_{39}\text{H}_{46}\text{N}_5\text{O}_7$, $[\text{M}+\text{H}]^+$, 696.3).



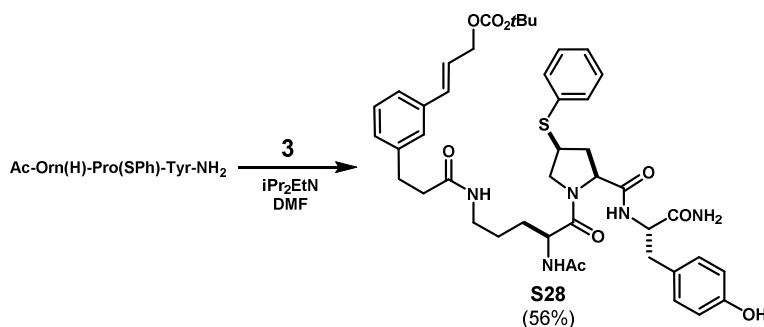
(600MHz, DMSO-*d*₆, 298K)

	¹³ C	¹ H	key correlations
1	31.5	3.45 (dd, <i>J</i> = 16.3, 6.2Hz, 1H), 3.28 (dd, <i>J</i> = 16.3, 7.5Hz, 1H)	HMBC 1→38,39
2	128.5	6.30-6.37 (m, 1H)	HMBC 2→4
3	130.5	6.46 (br d, <i>J</i> = 15.9Hz, 1H)	HMBC 3→4
4	137.1	-	
5	123.4	7.10 (br d, <i>J</i> = 7.6Hz, 1H)	HMBC 5→3, TOCSY 5→6,7,9
6	128.1	7.18 (dd, <i>J</i> = 7.6, 7.7Hz, 1H)	HMBC 6→4,8
7	127.1	7.03 (br d, <i>J</i> = 7.7Hz, 1H)	
8	141.2	-	
9	124.3	7.42 (br s, 1H)	
10	30.6	2.80 (t, <i>J</i> = 7.4Hz, 2H)	HMBC 10→8,12
11	36.8	2.42 (t, <i>J</i> = 7.4Hz, 2H)	HMBC 11→8,12
12	171.1	-	
13	-	7.37 (apt t, <i>J</i> = 6.9Hz, 1H)	HMBC 13→12
14	37.6	2.97-3.04 (m, 1H), 2.90-2.97(m, 1H)	
15	24.6	1.30-1.39 (m, 2H) overlap	HMBC 15→17
16	28.2	1.56-1.63 (m, 1H), 1.34-1.40 (m, 1H)overlap	
17	49.8	4.40-4.45 (m, 1H)overlap	HMBC 17→21
18	-	8.11 (br d, <i>J</i> = 7.4Hz, 1H)	HMBC 18→19
19	169.0	-	
20	21.9	1.82 (s, 3H)	HMBC 20→19
21	171.5	-	
22	51.9	4.27-4.32 (m, 1H) overlap, 3.66-3.70 (m, 1H)	
23	74.9	5.03-5.07 (m, 1H)	
24	156.6	-	
25	115.2	6.90 (d, <i>J</i> = 8.2Hz, 2H) overlap	HMBC 25→24
26	129.2	7.22 (dd, <i>J</i> = 8.2, 7.6Hz, 2H)	HMBC 26→24
27	120.8	6.91 (t, <i>J</i> = 7.6Hz, 1H) overlap	
28	33.6	2.44-2.51 (m, 1H) overlap, 2.08 (ddd, <i>J</i> = 13.4, 4.0, 4.0Hz, 1H)	

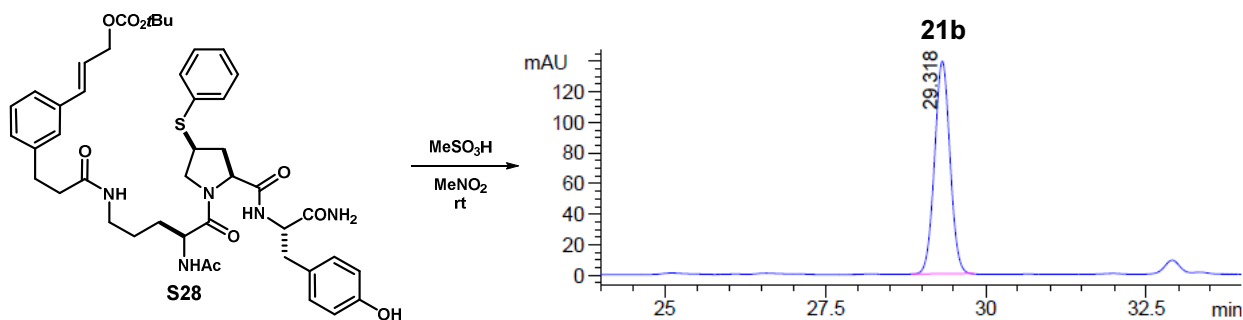
29	58.5	4.41-4.45 (m, 1H) overlap	
30	169.9	-	
31	-	7.35-7.40 (m, 1H)	HMBC 31→30
32	53.9	4.27-4.32 (m, 1H) overlap	HMBC 32→36
33	172.3	-	
34	-	7.30 (br s, 1H), 7.13 (br s, 1H)	HMBC 34→33
35	37.0	2.74 - 2.79 (m, 2H)	HMBC 35→36
36	127.1	-	
37	129.8	6.89-6.91 (m, 1H) overlap	HMBC 37→1
38	125.7	-	
39	153.2	-	
40	114.3	6.69 (d, $J = 8.1\text{Hz}$, 1H)	HMBC 40→39,38
41	127.3	6.86 (dd, $J = 8.1, 1.3\text{Hz}$, 1H)	HMBC 41→39
42	-	9.23 (br s, 1H)	

MS m/z 696.3 (calc'd: $\text{C}_{39}\text{H}_{46}\text{N}_5\text{O}_7$, $[\text{M}+\text{H}]^+$, 696.3).

Macrocycle 21b:



Acyclic carbonate (S28): General procedure A afforded compound **S28** as a colorless film (168 mg, 56%). ¹H NMR (600 MHz, CD₃OD): δ 1.41-1.56 (m, 3H), 1.46 (s, 9H), 1.61-1.69 (m, 1H), 1.80 (ddd, *J* = 12.4, 9.6, 9.5 Hz, 1H), 1.95 (s, 3H), 2.47 (t, *J* = 7.6 Hz, 2H), 2.52-2.58 (m, 1H), 2.90 (t, *J* = 7.6 Hz, 2H), 2.97 (dd, *J* = 14.0, 7.7 Hz, 1H), 3.04 (dd, *J* = 14.0, 6.1 Hz, 1H), 3.07-3.13 (m, 1H), 3.14-3.20 (m, 1H), 3.42 (dd, *J* = 9.6, 9.6 Hz, 1H), 3.73-3.79 (m, 1H), 4.34 (dd, *J* = 10.0, 7.2 Hz, 1H), 4.39 (dd, *J* = 8.2, 8.2 Hz, 1H), 4.42-4.45 (m, 1H), 4.47 (dd, *J* = 7.3, 6.7 Hz, 1H), 4.65 (dd, *J* = 6.2, 0.9 Hz, 2H), 6.28 (dt, *J* = 15.9, 6.3 Hz, 1H), 6.61 (br d, *J* = 15.9 Hz, 1H), 6.71 (d, *J* = 8.4 Hz, 2H), 7.06 (d, *J* = 8.4 Hz, 2H), 7.09-7.13 (m, 1H), 7.19-7.23 (m, 2H), 7.24-7.27 (m, 2H), 7.32 (dd, *J* = 7.9, 7.9 Hz, 2H), 7.42 (dd, *J* = 7.9, 1.0 Hz, 2H). ¹³C NMR (151 MHz, CD₃OD): δ 175.7, 175.0, 173.2, 173.1, 172.9, 157.2, 154.9, 142.5, 137.7, 135.1, 135.0, 132.5, 131.4, 130.3, 129.8, 129.2, 128.9, 128.5, 127.7, 125.6, 124.2, 116.3, 82.9, 68.4, 61.7, 56.0, 54.8, 52.7, 45.0, 39.8, 38.9, 37.5, 36.8, 32.8, 29.3, 28.1, 26.1, 22.3. MS *m/z* 830.2 (calc'd: C₄₄H₅₆N₅O₉S, [M+H]⁺, 830.4).



Compound **S28** was subjected to general procedure C. HPLC analysis and purification was performed using the following methods.

Analytical HPLC method:

Column: Waters Sunfire™ C₁₈, 4.6x250mm, 5μm.

Solvent A: H₂O + 0.1%v TFA

Solvent B: ACN + 0.1%v TFA

Flow rate: 1.00 ml/min

Time	%B
0	30
2	30
37	43
42	100
52	100
54	30
57	30

Semi-preparative HPLC method:

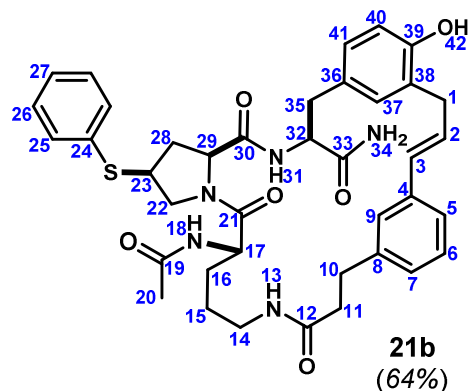
Column: Waters Sunfire™ C₁₈, 10x250mm, 5μm.

Solvent A: H₂O + 0.1%v TFA

Solvent B: ACN + 0.1%v TFA

Flow rate: 7.00 ml/min

Time	%B
0	30
2	30
25	48
27	30
28	30



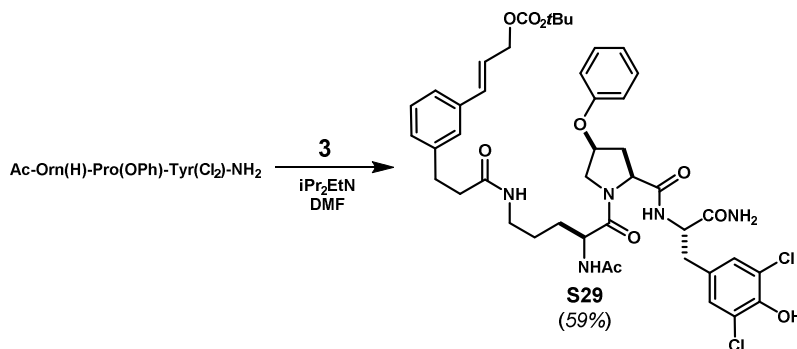
(600MHz, DMSO-*d*₆, 298K)

	¹³ C	¹ H	key correlations
1	31.6	3.47 (dd, <i>J</i> = 16.0, 6.7Hz, 1H), 3.35 (dd, <i>J</i> = 16.0, 7.3Hz, 1H)	HMBC 1→38
2	128.3	6.37 (ddd, <i>J</i> = 15.7, 7.3, 6.7Hz, 1H)	COSY 2→1 HMBC 2→4
3	130.6	6.45 (d, <i>J</i> = 15.7Hz, 1H)	HMBC 3→5
4	137.0	-	
5	124.1	7.11 (br d, <i>J</i> = 7.6Hz, 1H)	HMBC 5→3
6	128.1	7.18 (dd, <i>J</i> = 7.6, 7.6Hz, 1H)	TOCSY 6→5,7,9 HMBC 6→4,8
7	127.2	7.03 (br d, <i>J</i> = 7.6Hz, 1H)	
8	141.3	-	
9	124.5	7.38 (br s, 1H)	
10	30.5	2.82 (t, <i>J</i> = 7.1Hz, 2H)	HMBC 10→8,12
11	36.6	2.42 (t, <i>J</i> = 7.1Hz, 2H)	HMBC 11→8,12
12	171.2	-	
13	-	7.64 (t, <i>J</i> = 5.4Hz, 1H)	TOCSY 13→14,15,16,17,18 HMBC 13→12
14	37.6	3.00-3.07 (m, 1H), 2.91-2.97 (m, 1H)	
15	28.0	1.55-1.62 (m, 1H), 1.33-1.41 (m, 1H)	
16	24.4	1.28-1.41 (m, 2H) overlap	HMBC 16→17,21
17	49.6	4.40 (ddd, <i>J</i> = 7.6, 7.2, 7.1Hz, 1H)	HMBC 17→19,21
18	-	8.06 (d, <i>J</i> = 7.6Hz, 1H)	
19	169.1	-	
20	21.9	1.81 (s, 3H)	
21	170.5	-	
22	52.8	4.41 (apt t, <i>J</i> = 8.2Hz, 1H), 3.33 (apt t, <i>J</i> = 9.8Hz, 1H)	
23	42.3	3.80-3.86 (m, 1H)	COSY 23→22 HMBC 23→24
24	134.3	-	
25	129.7	7.41 (dd, <i>J</i> = 8.1, 1.0Hz, 2H)	
26	128.9	7.34 (dd, <i>J</i> = 8.1, 7.4Hz, 2H)	HMBC 26→24
27	126.4	7.26 (dd, <i>J</i> = 7.4, 1.0Hz, 1H)	

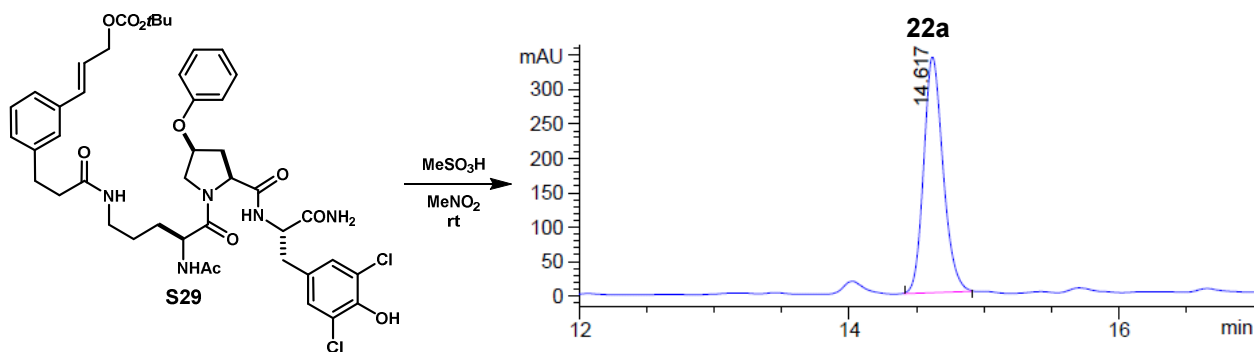
28	35.3	2.52 (ddd, $J = 12.5, 7.6, 7.1\text{Hz}$, 1H), 1.68 (ddd, $J = 12.5, 10.1, 8.7\text{Hz}$, 1H)	COSY 28→23
29	59.0	4.34 (dd, $J = 8.7, 7.6\text{Hz}$, 1H)	COSY 29→28
30	170.1	-	
31	-	7.72 (d, $J = 7.7\text{Hz}$, 1H)	TOCSY 31→32,35
32	54.1	4.26 (ddd, $J = 7.7, 7.7, 6.6\text{Hz}$, 1H)	HMBC 32→30,33,36
33	172.6	-	
34	-	7.29 (br s, 1H), 7.05 (br s, 1H)	HMBC 34→33
35	36.5	2.88 (dd, $J = 13.7, 6.6\text{Hz}$, 1H), 2.73 (dd, $J = 13.7, 7.7\text{Hz}$, 1H)	HMBC 35→36
36	127.6	-	
37	129.6	6.93 (d, $J = 1.8\text{Hz}$, 1H)	
38	125.8	-	
39	153.3	-	
40	114.2	6.70 (d, $J = 8.1\text{Hz}$, 1H)	HMBC 40→36,38
41	127.2	6.85 (dd, $J = 8.1, 1.8\text{Hz}$, 1H)	HMBC 41→39
42	-	9.23 (br s, 1H)	

MS m/z 712.3 (calc'd: $\text{C}_{39}\text{H}_{46}\text{N}_5\text{O}_6\text{S}$, $[\text{M}+\text{H}]^+$, 712.3).

Macrocycle 22a:



Acyclic carbonate (S29): General procedure A afforded compound **S29** as a colorless film (110 mg, 59%). ^1H NMR (500 MHz, CD_3OD , major rotamer): δ 1.44-1.70 (m, 4H), 1.46 (s, 9H), 1.96 (s, 3H), 2.36 (br d, $J = 13.9$ Hz, 1H), 2.47 (br t, $J = 7.1$ Hz, 2H), 2.46-2.55 (m, 1H), 2.82-2.93 (m, 3H), 2.99 (dd, $J = 14.1, 5.7$ Hz, 1H), 3.05-3.19 (m, 2H), 3.86 (br d, $J = 10.8$ Hz, 1H), 4.19 (dd, $J = 11.3, 4.7$ Hz, 1H), 4.47 (dd, $J = 7.0, 6.7$ Hz, 1H), 4.50-4.55 (m, 2H), 4.66 (d, $J = 6.3$ Hz, 2H), 5.06-5.11 (m, 1H), 6.29 (dt, $J = 15.9, 6.4$ Hz, 1H), 6.62 (d, $J = 15.9$ Hz, 1H), 6.89 (d, $J = 8.4$ Hz, 2H), 6.95 (dd, $J = 7.4, 7.4$ Hz, 1H), 7.08 (s, 2H), 7.18-7.31 (m, 6H). ^{13}C NMR (126 MHz, CD_3OD , major rotamer): δ 175.1, 174.7, 174.1, 173.3, 172.9, 158.1, 155.0, 149.4, 142.6, 137.8, 135.1, 130.8, 130.5, 129.8, 129.3, 127.8, 125.6, 124.2, 123.0, 122.7, 116.8, 82.9, 77.3, 68.4, 61.3, 55.2, 54.2, 52.7, 49.8, 39.7, 39.0, 37.9, 34.9, 32.8, 29.4, 28.0, 26.3, 22.2. MS m/z 764.2 (calc'd: $\text{C}_{39}\text{H}_{44}\text{Cl}_2\text{N}_5\text{O}_7$, $[\text{M-OCO}_2\text{tBu}]^+$, 764.3).



Compound **S29** was subjected to general procedure C. HPLC analysis and purification was performed using the following methods.

Analytical HPLC method:

Column: Waters Sunfire™ C₁₈, 4.6x250mm, 5µm.

Solvent A: H₂O + 0.1%v TFA

Solvent B: ACN + 0.1%v TFA

Flow rate: 1.00 ml/min

Time	%B
0	35
2	35
20	65
23	100
25	100
28	35
30	35

Semi-preparative HPLC method:

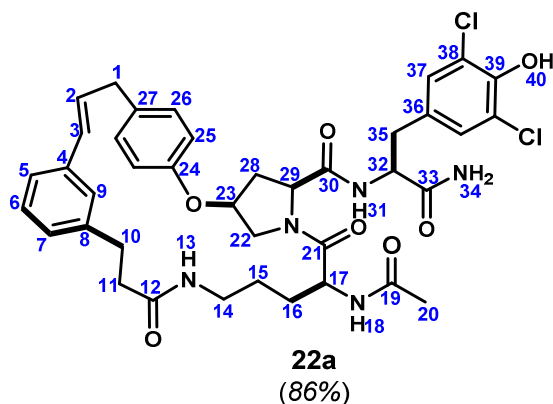
Column: Waters Sunfire™ C₁₈, 10x250mm, 5µm.

Solvent A: H₂O + 0.1%v TFA

Solvent B: ACN + 0.1%v TFA

Flow rate: 7.50 ml/min

Time	%B
0	35
2	35
20	57
22	35
23	35



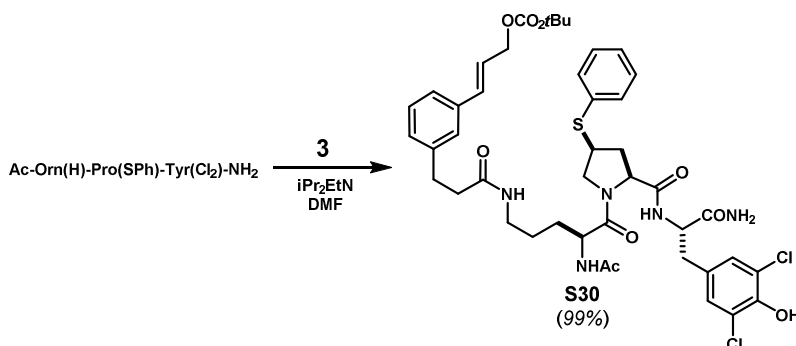
(600MHz, DMSO-*d*₆, 298K)

	¹³ C	¹ H	key correlations
1	37.4	3.42 (br d, <i>J</i> = 6.6Hz, 2H)	HMBC 1→27
2	130.1	6.21 (dt, <i>J</i> = 15.6, 6.6Hz, 1H)	HMBC 2→4, 27
3	129.1	6.32 (br d, <i>J</i> = 15.6Hz, 1H)	HMBC 3→4
4	136.6	-	
5	124.5	7.09 (br d, <i>J</i> = 7.7Hz, 1H)	HMBC 5→3 TOCSY 5→6, 7, 9
6	128.1	7.18 (dd, <i>J</i> = 7.7, 7.7Hz, 1H)	HMBC 6→4, 8

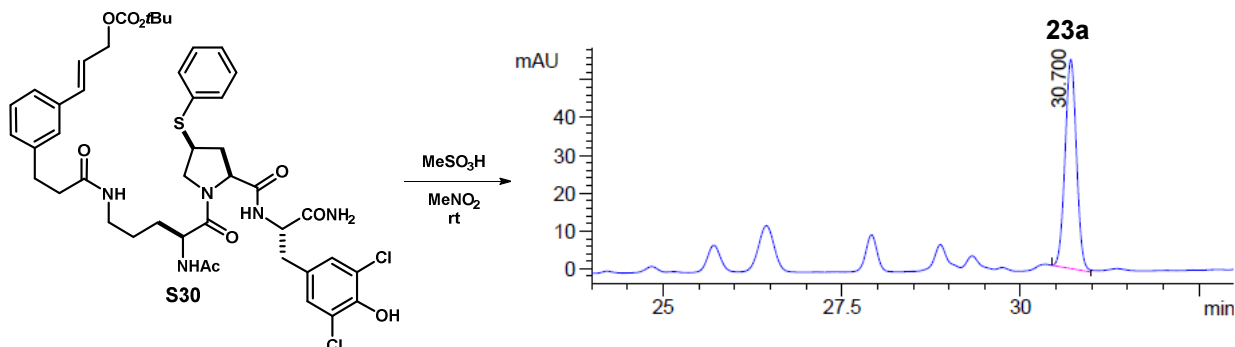
7	127.3	6.99 (br d, $J = 7.7\text{Hz}$, 1H)	
8	141.3	-	
9	123.2	7.14 (br s, 1H)	
10	29.6	2.86 - 2.92 (m, 1H), 2.70 - 2.76 (m, 1H)	HMBC 10→8, 12
11	35.6	2.26 - 2.30 (m, 2H)	HMBC 11→8, 12
12	171.0	-	
13	-	7.76 (t, $J = 5.2\text{Hz}$, 1H)	
14	37.9	2.60 - 2.72 (m, 2H) overlap	COSY 13→14 HMBC 13→12
15	25.0	1.26 - 1.35 (m, 1H) overlap, 1.18 - 1.26 (m, 1H)	
16	28.3	1.37 - 1.45 (m, 1H), 1.26 - 1.35 (m, 1H) overlap	HMBC 16→21
17	49.6	4.23 (ddd, $J = 10.0, 7.7, 4.1\text{Hz}$, 1H)	HMBC 17→21
18	-	8.10 (d, $J = 7.7\text{Hz}$, 1H)	HMBC 18→19
19	169.0	-	
20	21.9	1.77 (s, 3H)	HMBC 20→19
21	171.5	-	
22	50.8	3.77 (dd, $J = 11.5, 3.7\text{Hz}$, 1H), 3.59 (br d, $J = 11.5\text{Hz}$, 1H)	
23	75.6	5.17 (apt t, $J = 4.0\text{Hz}$, 1H)	
24	154.2	-	
25	116.5	6.89 (d, $J = 8.6\text{Hz}$, 2H)	HMBC 25→24
26	129.5	7.13 (d, $J = 8.6\text{Hz}$, 2H)	HMBC 26→1, 24
27	132.8	-	
28	34.1	2.56 (ddd, $J = 14.1, 10.6, 4.8\text{Hz}$, 1H), 2.19 (br d, $J = 14.1\text{Hz}$, 1H)	
29	59.3	4.31 (dd, $J = 10.6, 2.0\text{Hz}$, 1H)	HMBC 29→30
30	169.7	-	
31	-	7.31 (d, $J = 7.8\text{Hz}$, 1H)	HMBC 31→30
32	52.8	4.41 (ddd, $J = 7.8, 7.5, 5.3\text{Hz}$, 1H)	HMBC 32→36
33	171.9	-	
34	-	7.41 (br s, 1H), 7.28 (br s, 1H)	TOCSY 34→34'
35	36.5	2.99 (dd, $J = 13.9, 5.3\text{Hz}$, 1H), 2.78 (dd, $J = 13.9, 7.5\text{Hz}$, 1H)	HMBC 35→36
36	130.1	-	
37	129.1	7.18 (s, 2H)	
38	121.5	-	
39	147.2	-	
40	-	9.84 (br s, 1H)	

MS m/z 764.2 (calc'd: $\text{C}_{39}\text{H}_{44}\text{Cl}_2\text{N}_5\text{O}_7$, $[\text{M}+\text{H}]^+$, 764.3).

Macrocycle 23a:



Acyclic carbonate (S30): General procedure A afforded compound **S30** as a colorless foam (250 mg, 99%). ¹H NMR (500 MHz, CD₃OD, major rotamer): δ 1.42-1.57 (m, 3H), 1.46 (s, 9H), 1.64-1.72 (m, 1H), 1.83 (ddd, *J* = 12.5, 9.5, 9.5 Hz, 1H), 1.96 (s, 3H), 2.48 (t, *J* = 7.6 Hz, 2H), 2.56 (ddd, *J* = 13.0, 7.1, 6.9 Hz, 1H), 2.91 (t, *J* = 7.6 Hz, 2H), 2.94 (dd, *J* = 14.0, 5.5 Hz, 1H), 3.07 (dd, *J* = 14.0, 5.9 Hz, 1H), 3.08-3.13 (m, 1H), 3.14-3.22 (m, 1H), 3.44 (dd, *J* = 9.9, 9.9 Hz, 1H), 3.79 (ddd, *J* = 16.6, 9.3, 6.8 Hz, 1H), 4.34 (dd, *J* = 10.3, 7.1 Hz, 1H), 4.37 (dd, *J* = 8.5, 8.5 Hz, 1H), 4.40-4.45 (m, 2H), 4.65 (dd, *J* = 6.3, 0.9 Hz, 2H), 6.29 (dd, *J* = 16.0, 6.3 Hz, 1H), 6.62 (br d, *J* = 16.0 Hz, 1H), 7.09-7.13 (m, 1H), 7.18 (s, 2H), 7.20-7.24 (m, 2H), 7.25-7.28 (m, 2H), 7.32 (dd, *J* = 7.6, 7.6 Hz, 2H), 7.40-7.43 (m, 2H). ¹³C NMR (126 MHz, CD₃OD, major rotamer): δ 175.21, 175.16, 173.25, 173.22, 173.0, 154.9, 149.4, 142.6, 137.8, 135.2, 135.1, 132.6, 131.3, 130.4, 130.3, 129.8, 129.3, 128.5, 127.8, 125.6, 124.2, 123.1, 82.9, 68.4, 61.8, 55.9, 54.8, 52.9, 45.1, 39.8, 39.0, 36.9, 36.8, 32.9, 29.2, 28.0, 26.1, 22.3. MS *m/z* 780.2 (calc'd: C₃₉H₄₄Cl₂N₅O₆S, [M-OCO₂tBu]⁺, 780.2).



Compound **S30** was subjected to general procedure C. HPLC analysis and purification was performed using the following methods.

Analytical HPLC method:Column: Waters XSelect™ C₁₈, 4.6x250mm, 5µm.Solvent A: H₂O + 0.1%v TFA

Solvent B: ACN + 0.1%v TFA

Flow rate: 1.00 ml/min

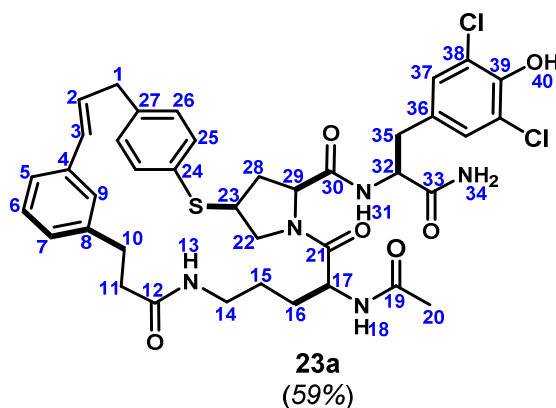
Time	%B
0	30
2	30
30	50
37	100
45	100
48	30
50	30

Semi-preparative HPLC method A:Column: Waters Sunfire™ C₁₈, 10x250mm, 5µm.Solvent A: H₂O + 0.1%v TFA

Solvent B: ACN + 0.1%v TFA

Flow rate: 7.50 ml/min

Time	%B
0	35
2	35
25	52
27	35
28	35

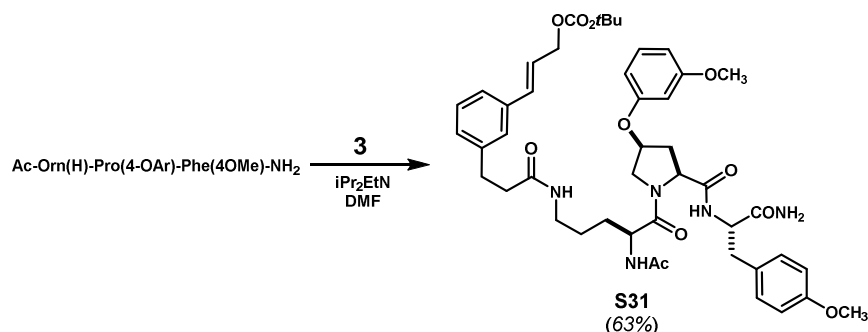
(600MHz, DMSO-*d*₆, 298K, ~6:1 mixture of rotamers, data is of major)

	¹³ C	¹ H	key correlations
1	37.5	3.50 (br d, <i>J</i> = 7.0Hz, 2H)	HMBC 1→27
2	128.9	6.27 (dt, <i>J</i> = 15.9, 6.9Hz, 1H)	HMBC 2→27, 4
3	130.4	6.38 (br d, <i>J</i> = 15.9Hz, 1H)	
4	136.4	-	
5	124.5	7.11 (br d, <i>J</i> = 7.6Hz, 1H)	HMBC 5→3, TOCSY 5→6,7,9
6	128.1	7.17-7.21 (m, 1H) overlap	HMBC 6→4,8
7	127.4	7.02 (br d, <i>J</i> = 7.7Hz, 1H)	
8	141.4	-	
9	123.7	7.20 (br s, 1H)	
10	29.8	2.83-2.89 (m, 1H) overlap, 2.75-2.80 (m, 1H) overlap	HMBC 10→8,12
11	35.7	2.30-2.35 (m, 2H)	HMBC 11→8,12
12	170.9	-	
13	-	7.79 (t, <i>J</i> = 5.7Hz, 1H)	HMBC 13→12,14
14	37.6	2.82-2.88 (m, 1H) overlap, 2.69-2.76 (m, 1H) overlap	
15	25.0	1.29-1.35 (m, 1H), 1.20-1.27 (m, 1H)	

16	27.7	1.37-1.43 (m, 2H)	HMBC 16→21
17	49.6	4.18 (ddd, $J = 8.2, 8.0, 6.8\text{Hz}$, 1H)	HMBC 17→19, 21
18	-	8.12 (d, $J = 8.0\text{Hz}$, 1H)	HMBC 18→19
19	169.3	-	
20	21.9	1.79 (s, 3H)	HMBC 20→19
21	171.2	-	
22	52.6	3.95 (dd, $J = 10.6, 6.3\text{Hz}$, 1H), 3.21 (dd, $J = 10.6, 6.8\text{Hz}$, 1H)	TOCSY 22→23, 28, 29
23	41.8	4.00 (ddd, $J = 14.0, 6.9, 6.9\text{Hz}$, 1H)	HMBC 23→24
24	130.4	-	
25	131.4	7.38 (d, $J = 8.3\text{Hz}$, 2H)	HMBC 25→27
26	129.2	7.24 (d, $J = 8.3\text{Hz}$, 2H)	HMBC 26→1
27	139.3	-	
28	33.1	2.49 - 2.55 (m, 1H) overlap, 1.77-1.85 (m, 1H) overlap	HMBC 28→30
29	59.6	4.32 - 4.36 (m, 1H) overlap	HMBC 29→30
30	170.0	-	
31	-	7.71 (d, $J = 8.3\text{Hz}$, 1H)	TOCSY 31→32,35
32	53.1	4.31-4.36 (m, 1H) overlap	HMBC 32→36
33	171.9	-	
34	-	7.29 (br s, 1H), 7.17 (br s, 1H)	TOCSY 34→34', HMBC 34→33
35	35.4	2.92 (dd, $J = 14.2, 5.4\text{Hz}$, 1H), 2.81 (dd, $J = 14.2, 8.6\text{Hz}$, 1H)	HMBC 35→36,37
36	130.4	-	
37	128.9	7.19 (s, 2H)	HMBC 37→38,39
38	121.6	-	
39	147.3	-	
40	-	9.92 (br s, 1H)	

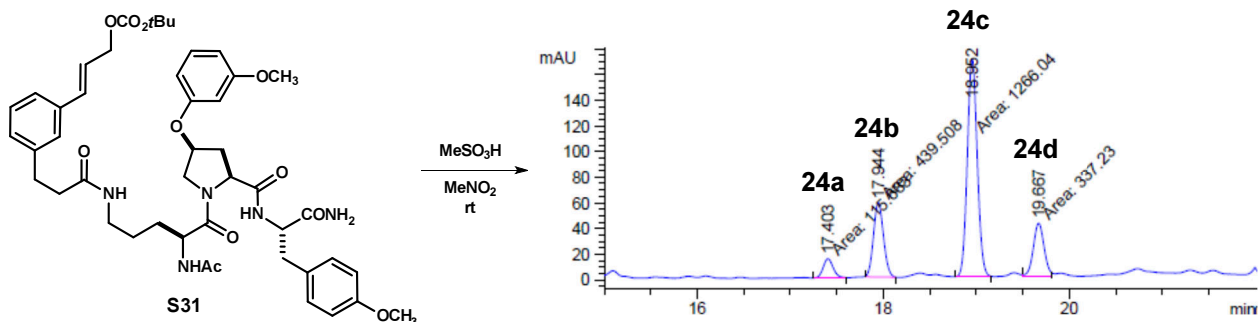
MS m/z 780.2 (calc'd: $\text{C}_{39}\text{H}_{44}\text{Cl}_2\text{N}_5\text{O}_6\text{S}$, $[\text{M}+\text{H}]^+$, 780.2).

Macrocycles 24a-d:



Acyclic carbonate (S31): General procedure A afforded compound **S31** as a colorless glass (113 mg, 63%). ^1H NMR (500 MHz, CD_3OD , major rotamer): δ 1.46 (s, 9H), 1.46-1.61 (m, 3H), 1.61-1.70 (m, 1H), 1.95 (s, 3H), 2.30 (dt, $J = 13.9, 3.1\text{ Hz}$, 1H), 2.46 (t, $J = 7.6\text{ Hz}$, 2H), 2.50 (ddd, $J = 13.9, 9.9, 5.1\text{ Hz}$, 1H), 2.88 (t, $J = 7.6\text{ Hz}$, 2H), 2.94 (dd, $J = 13.8, 7.0\text{ Hz}$, 1H), 3.02 (dd, $J = 13.8, 5.9\text{ Hz}$, 1H), 3.04-3.11 (m, 1H),

3.11-3.21 (m, 1H), 3.66 (s, 3H), 3.69 (s, 3H), 3.81 (br d, $J = 11.4$ Hz, 1H), 4.18 (dd, $J = 11.4, 5.0$ Hz, 1H), 4.47 (dd, $J = 7.5, 6.1$ Hz, 1H), 4.50-4.54 (m, 2H), 4.65 (dd, $J = 6.2, 1.1$ Hz, 2H), 5.02-5.07 (m, 1H), 6.28 (dt, $J = 15.9, 6.2$ Hz, 1H), 6.48-6.55 (m, 3H), 6.61 (br d, $J = 15.9$ Hz, 1H), 6.70 (d, $J = 8.6$ Hz, 2H), 7.06 (d, $J = 8.6$ Hz, 2H), 7.08-7.11 (m, 1H), 7.14-7.24 (m, 2H), 7.25 (br s, 1H). ^{13}C NMR (126 MHz, CD_3OD , major rotamer): δ 175.3, 175.0, 174.0, 173.2, 172.8, 162.5, 159.9, 159.3, 154.9, 142.6, 137.8, 135.1, 131.5, 131.2, 129.85, 129.80, 129.3, 127.8, 125.6, 124.2, 114.8, 108.7, 108.4, 103.5, 82.9, 77.3, 68.4, 61.2, 55.7, 55.61, 55.59, 54.2, 52.5, 39.7, 38.9, 38.3, 35.1, 32.8, 29.5, 28.0, 26.3, 22.2. MS m/z 858.0 (calc'd: $\text{C}_{46}\text{H}_{60}\text{N}_5\text{O}_{11}$, $[\text{M}+\text{H}]^+$, 858.4).



Compound **S31** was subjected to general procedure C. HPLC analysis and purification was performed using the following methods.

Analytical HPLC method:

Column: Waters Sunfire™ C₁₈, 4.6x250mm, 5 μm .

Solvent A: $\text{H}_2\text{O} + 0.1\% \text{v TFA}$

Solvent B: $\text{ACN} + 0.1\% \text{v TFA}$

Flow rate: 1.00 ml/min

Time	%B
0	35
2	35
22	70
30	100
40	100
45	35
47	35

Semi-preparative HPLC method:

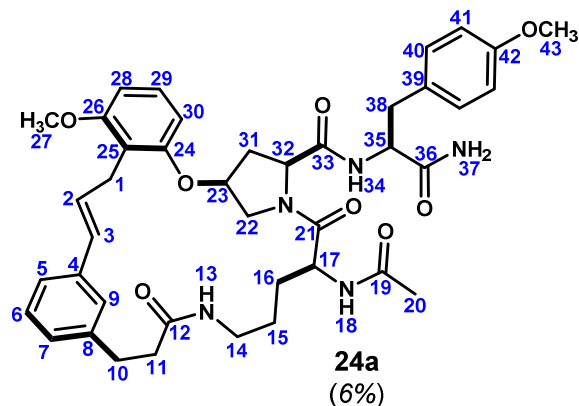
Column: Waters Sunfire™ C₁₈, 10x250mm, 5 μm .

Solvent A: $\text{H}_2\text{O} + 0.1\% \text{v TFA}$

Solvent B: $\text{ACN} + 0.1\% \text{v TFA}$

Flow rate: 6.50 ml/min

Time	%B
0	40
2	40
16	49.1
17	75
18	75
19	40
20	40

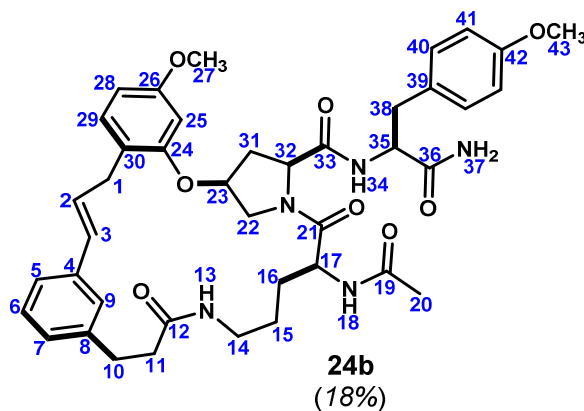


(600MHz, DMSO-*d*₆, 298K)

	¹³ C	¹ H	key correlations
1	25.9	3.41-3.46 (m, 2H)	HMBC 1→24,25,26
2	127.9	6.32 (ddd, <i>J</i> = 15.8, 6.0, 6.0 Hz, 1H)	HMBC 2→4
3	129.1	6.27 (d, <i>J</i> = 15.8 Hz, 1H)	TOCSY 3→2,1 HMBC 3→4,5,9
4	136.7	-	
5	123.6	6.97 (d, <i>J</i> = 7.6 Hz, 1H)	
6	128.0	7.11 (dd, <i>J</i> = 7.6, 7.6 Hz, 1H)	HMBC 6→4,9
7	127.0	7.05 (d, <i>J</i> = 7.6 Hz, 1H) overlap	HMBC 7→10
8	140.9	-	
9	124.8	7.25 (br s, 1H)	HMBC 9→10
10	30.6	2.77-2.83 (m, 2H) overlap	HMBC 10→12
11	36.3	2.30-2.42 (m, 2H)	HMBC 11→12
12	171.3	-	
13	-	7.71 (apt t, <i>J</i> = 5.5 Hz, 1H)	HMBC 13→12
14	37.8	2.86-3.00 (m, 2H) overlap	
15	24.5	1.27-1.37 (m, 2H) overlap	TOCSY 15→13,14,16,17,18
16	28.3	1.30-1.36 (m, 1H) overlap, 1.57-1.63 (m, 1H)	HMBC 16→17,21
17	49.4	4.37-4.41 (m, 1H) overlap	
18	-	8.11 (d, <i>J</i> = 8.1 Hz, 1H)	HMBC 18→19
19	168.9	-	
20	21.9	1.81 (s, 3H)	HMBC 20→19
21	171.3	-	
22	52.0	3.47-3.52 (m, 1H), 4.35-4.40 (m, 1H) overlap	
23	74.2	5.03-5.09 (m, 1H)	HMBC 23→24 COSY 23→22,31
24	155.6	-	
25	115.9	-	
26	157.6	-	
27	55.6	3.78 (s, 3H)	HMBC 27→26
28	105.4	6.74 (d, <i>J</i> = 8.3 Hz, 1H)	HMBC 28→25,26

29	127.3	7.18 (ddd, $J = 8.3, 8.3$ Hz, 1H)	
30	104.3	6.67 (d, $J = 8.3$ Hz, 1H)	HMBC 30→24,25
31	34.1	1.97-2.03 (m, 1H), 2.53-2.60 (m, 1H)	HMBC 31→33 COSY 31→32
32	58.1	4.35-4.40 (m, 1H) overlap	HMBC 32→33
33	170.1	-	
34	-	7.77 (d, $J = 8.1$ Hz, 1H)	
35	53.8	4.30 (ddd, $J = 8.1, 8.0, 5.7$ Hz, 1H)	COSY 35→38
36	172.2	-	
37	-	7.05 (br s, 1H) overlap, 7.16 (br s, 1H)	HMBC 37→36
38	36.1	2.78-2.82 (m, 1H) overlap, 2.89-2.94 (m, 1H) overlap	HMBC 38→39, 40
39	129.3	-	
40	130.0	7.08 (d, $J = 7.8$ Hz, 2H)	HMBC 40→42
41	113.0	6.70 (d, $J = 8.6$ Hz, 2H)	HMBC 41→42,39
42	157.5	-	
43	54.6	3.65 (s, 3H)	HMBC 43→42

MS m/z 740.0 (calc'd: $C_{41}H_{50}N_5O_8$, $[M+H]^+$, 740.4).

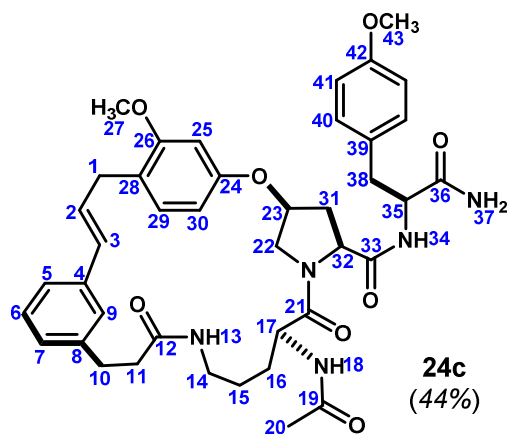


(600MHz, DMSO- d_6 , 298K)

	^{13}C	1H	key correlations
1	33.5	3.14 (dd, $J = 14.5, 7.3$ Hz, 1H), 3.61 (dd, $J = 14.5, 5.7$ Hz, 1H)	HMBC 1→24,29,30
2	129.02	6.41 (ddd, $J = 15.7, 7.3, 5.7$ Hz, 1H)	COSY 2→1 HMBC 2→4
3	128.95	6.30 (d, $J = 15.7$ Hz, 1H)	
4	137.0	-	
5	124.0	7.04 (d, $J = 7.6$ Hz, 1H)	
6	128.0	7.12 (dd, $J = 7.6, 7.6$ Hz, 1H) overlap	HMBC 6→4,8
7	127.3	6.98 (d, $J = 7.6$ Hz, 1H)	HMBC 7→10
8	141.2	-	
9	125.0	7.33 (br s, 1H)	HMBC 9→10
10	30.7	2.78-2.83 (m, 2H) overlap	
11	36.4	2.32-2.43 (m, 2H)	HMBC 11→12
12	171.7	-	

13	-	7.74 (t, $J = 5.3$ Hz, 1H)	HMBC 13→12
14	37.7	2.91-2.95 (m, 2H)	
15	24.5	1.28-1.35 (m, 2H) overlap	
16	28.1	1.32-1.37 (m, 1H) overlap, 1.58-1.65 (m, 1H)	
17	49.3	4.43 (ddd, $J = 7.3, 7.0, 6.8$ Hz, 1H)	HMBC 17→21
18	-	8.12 (d, $J = 7.3$ Hz, 1H)	HMBC 18→19
19	169.2	-	
20	21.9	1.82 (s, 3H)	HMBC 20→19
21	171.6	-	
22	51.6	4.47 (dd, $J = 10.3, 6.5$ Hz, 1H), 3.50 (dd, $J = 10.3, 5.9$ Hz, 1H)	
23	73.7	5.05-5.11 (m, 1H)	HMBC 23→24
24	153.9	-	
25	99.6	6.68 (d, $J = 1.9$ Hz, 1H)	HMBC 25→24,26
26	159.2	-	
27	54.9	3.75 (s, 3H)	HMBC 27→26
28	105.4	6.49 (dd, $J = 8.3, 1.9$ Hz, 1H)	
29	130.6	7.10 (d, $J = 8.3$ Hz, 1H) overlap	
30	120.8	-	
31	34.0	1.95-2.01 (m, 1H), 2.55-2.61 (m, 1H)	
32	58.1	4.35 (dd, $J = 8.1, 8.1$ Hz, 1H)	
33	170.3	-	
34	-	7.77 (d, $J = 8.1$ Hz, 1H)	HMBC 34→33
35	53.9	4.32 (ddd, $J = 8.1, 7.9, 5.6$ Hz, 1H)	HMBC 35→36
36	172.5	-	
37	-	7.05 (br s, 1H), 7.14 (br s, 1H)	TOCSY 37→37'
38	36.0	2.92 (dd, $J = 12.9, 5.6$ Hz, 1H) overlap, 2.81 (dd, $J = 12.9, 7.9$ Hz, 1H) overlap	HMBC 38→39
39	130.4	-	
40	129.2	7.11 (d, $J = 8.4$ Hz, 2H)	HMBC 40→42
41	113.0	6.72 (d, $J = 8.4$ Hz, 2H)	HMBC 41→42
42	157.8	-	
43	54.5	3.65 (s, 3H)	HMBC 43→42

MS m/z 740.0 (calc'd: $C_{41}H_{50}N_5O_8$, $[M+H]^+$, 740.4).

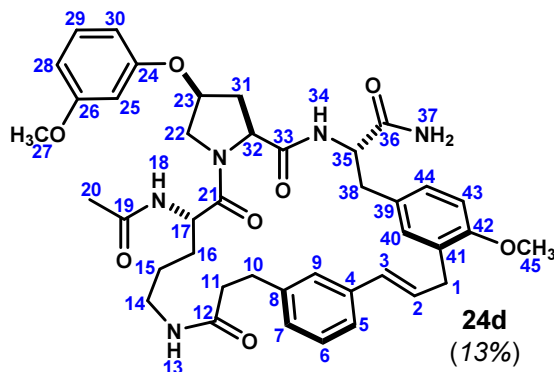


(600MHz, DMSO-*d*₆, 298K)

	¹³ C	¹ H	key correlations
1	32.3	3.28 (dd, <i>J</i> = 14.9, 6.9 Hz, 1H), 3.47 (dd, <i>J</i> = 14.9, 5.3 Hz, 1H)	HMBC 1→26,28,29
2	129.10	6.17 (ddd, <i>J</i> = 15.9, 6.9, 5.3 Hz, 1H)	
3	129.50	6.27 (d, <i>J</i> = 15.9 Hz, 1H)	HMBC 3→4
4	137.0	-	
5	124.6	7.07 (d, <i>J</i> = 7.6 Hz, 1H)	HMBC 5→3,9
6	128.4	7.16 (dd, <i>J</i> = 7.6, 7.6 Hz, 1H)	HMBC 6→4,8
7	127.4	6.97 (d, <i>J</i> = 7.6 Hz, 1H)	HMBC 7→9
8	141.6	-	
9	123.6	7.10 (br s, 1H)	
10	30.0	2.85-2.92 (m, 1H) overlap, 2.69-2.76 (m, 1H) overlap	HMBC 10→12
11	36.1	2.23-2.28 (m, 2H) overlap	HMBC 11→12
12	171.2	-	
13	-	7.70 (t, <i>J</i> = 4.9 Hz, 1H)	HMBC 13→12
14	38.2	2.63-2.73 (m, 2H) overlap	
15	25.2	1.20-1.33 (m, 2H)	
16	28.5	1.33-1.49 (m, 2H)	
17	49.9	4.21-4.27 (m, 1H)	
18	-	8.09 (d, <i>J</i> = 7.6 Hz, 1H)	HMBC 18→19
19	162.2	-	
20	22.2	1.78 (s, 3H)	HMBC 20→19
21	171.8	-	
22	51.2	3.75 (dd, <i>J</i> = 11.4, 2.9 Hz, 1H), 3.57-3.61 (m, 1H) overlap	
23	76.3	5.19-5.23 (m, 1H)	
24	155.8	-	
25	102.0	6.55 (d, <i>J</i> = 1.6 Hz, 1H)	
26	157.7	-	
27	55.5	3.69 (s, 3H)	HBC 27→26
28	121.3	-	

29	130.3	7.06 (d, $J = 8.1$ Hz, 1H)	COSY 29→30
30	107.7	6.57 (dd, $J = 8.1, 1.6$ Hz, 1H)	HMBC 30→25
31	34.3	2.56 (ddd, $J = 14.4, 10.5, 4.3$ Hz, 1H), 2.24 (br d, $J = 14.4$ Hz, 1H) overlap	
32	59.7	4.31 (dd, $J = 10.5, 1.0$ Hz, 1H)	HMBC 32→33
33	169.8	-	
34	-	7.25 (d, $J = 7.6$ Hz, 1H)	HMBC 34→36
35	53.5	4.40-4.46 (m, 1H)	COSY 35→34,38
36	172.2	-	
37	-	7.40 (br s, 1H), 7.21 (br s, 1H)	HMBC 37→36
38	37.3	3.02 (dd, $J = 13.7, 5.6$ Hz, 1H), 2.88 (dd, $J = 13.7, 6.0$ Hz, 1H) overlap	
39	129.1	-	
40	130.4	7.12 (d, $J = 8.5$ Hz, 2H)	HMBC 40→39,42
41	113.4	6.71 (d, $J = 8.5$ Hz, 2H)	HMBC 41→39,42
42	157.8	-	
43	54.8	3.58 (s, 3H)	HMBC 43→42

MS m/z 740.0 (calc'd: $C_{41}H_{50}N_5O_8$, $[M+H]^+$, 740.4).



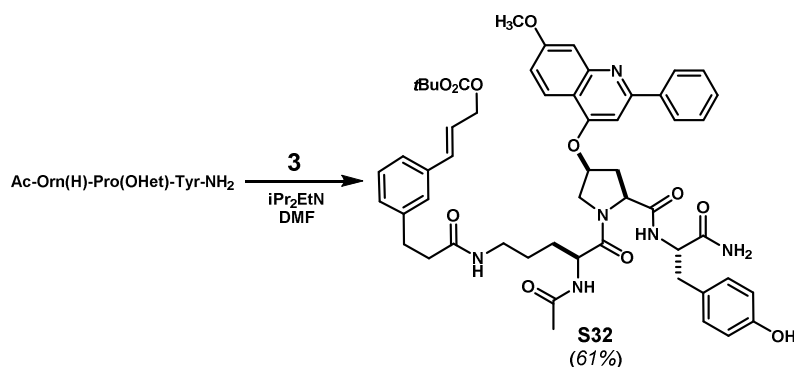
(600MHz, DMSO- d_6 , 298K)

	^{13}C	1H	key correlations
1	31.4	3.47 (dd, $J = 16.6, 6.3$ Hz, 1H), 3.30 (dd, $J = 16.6, 7.7$ Hz, 1H)	HMBC 1→40,42
2	128.10	6.33 (ddd, $J = 15.8, 7.7, 6.3$ Hz, 1H)	HMBC 2→4,41
3	130.70	6.46 (d, $J = 15.8$ Hz, 1H)	HMBC 3→4
4	136.9	-	
5	127.1	7.03 (br d, $J = 7.5$ Hz, 1H)	HMBC 5→4
6	128.1	7.18 (dd, $J = 7.5, 7.5$ Hz, 1H)	HMBC 6→4,8
7	124.5	7.10 (br d, $J = 7.5$ Hz, 1H)	HMBC 7→8
8	141.2	-	
9	124.4	7.44 (br s, 1H)	
10	30.7	2.79-2.83 (m, 2H) overlap	HMBC 10→8,12
11	36.9	2.42 (t, $J = 7.4$ Hz, 2H)	HMBC 11→8,12

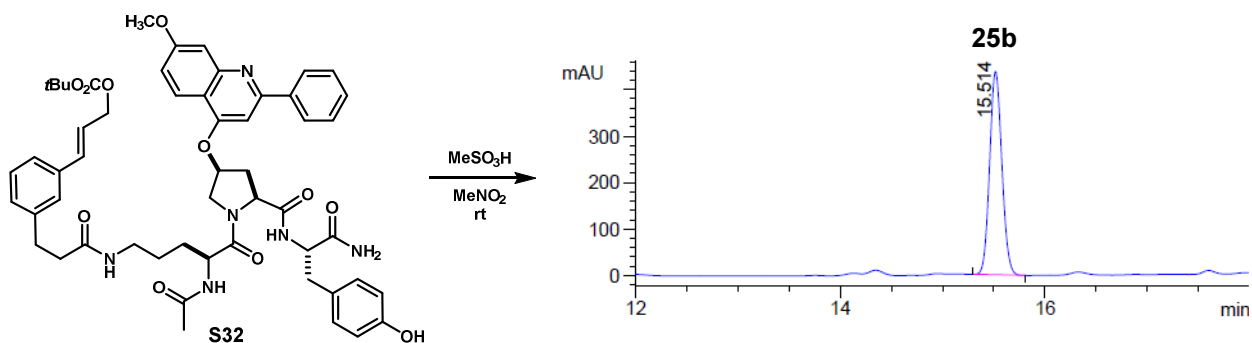
12	171.0	-	
13	-	7.59 (apt t, $J = 5.5$ Hz, 1H)	HMBC 13→12
14	37.6	2.89-2.96 (m, 1H), 2.98-3.04 (m, 1H)	
15	24.5	1.30-1.37 (m, 2H) overlap	HMBC 15→17
16	28.3	1.34-1.42 (m, 1H) overlap, 1.57-1.63 (m, 1H)	HMBC 16→17,21
17	49.7	4.41-4.45 (m, 1H) overlap	HMBC 17→21
18	-	8.11 (d, $J = 7.4$ Hz, 1H)	HMBC 18→19
19	169.0	-	
20	21.9	1.82 (s, 3H)	HMBC 20→19
21	171.5	-	
22	52.0	4.29 (dd, $J = 11.3, 5.5$ Hz, 1H), 3.69-3.73 (m, 1H)	
23	74.9	5.03-5.08 (m, 1H)	COSY 23→22 HMBC 23→24
24	157.7	-	
25	101.3	6.46 (dd, $J = 2.3, 2.3$ Hz, 1H)	
26	160.2	-	
27	54.6	3.57 (s, 3H)	HMBC 27→26
28	106.9	6.47-6.51 (m, 1H) overlap	HMBC 28→25,26,30
29	129.8	7.12 (dd, $J = 8.2, 8.2$ Hz, 1H)	
30	106.9	6.47-6.51 (m, 1H) overlap	HMBC 30→24,25
31	33.6	2.45-2.48 (m, 1H), 2.08 (ddd, $J = 13.4, 4.0, 4.0$ Hz, 1H)	COSY 31→32
32	58.5	4.40-4.44 (m, 1H) overlap	
33	169.9	-	
34	-	7.37 (d, $J = 7.9$ Hz, 1H)	HMBC 34→33
35	53.8	4.30-4.35 (m, 1H)	HMBC 35→38,39
36	172.3	-	
37	-	7.35 (br s, 1H), 7.17 (br s, 1H)	HMBC 37→36
38	36.9	2.79-2.84 (m, 2H)	HMBC 38→39
39	128.6	-	
40	129.6	6.97 (br d, $J = 1.7$ Hz, 1H)	HMBC 40→44
41	127.3	-	
42	155.1	-	
43	110.0	6.85 (d, $J = 8.1$ Hz, 1H)	HMBC 43→41,39
44	127.7	7.04 (dd, $J = 8.1, 1.7$ Hz, 1H)	
45	55.0	3.75 (s, 3H)	HMBC 45→42

MS m/z 740.0 (calc'd: $C_{41}H_{50}N_5O_8$, $[M+H]^+$, 740.4).

Macrocycle 25b:



Acyclic carbonate (S32): General procedure A afforded compound **S32** as a colorless film (89 mg, 61%). ¹H NMR (500 MHz, DMSO-*d*₆, major rotamer): δ 1.61-1.31 (m, 2H), 1.42 (s, 9H), 1.42-1.69 (m, 2H), 1.96 (s, 3H), 2.30-2.37 (m, 1H), 2.61-2.68 (m, 1H), 2.72-2.80 (m, 2H), 2.82-2.96 (m, 2H), 2.98-3.05 (m, 1H), 3.07-3.17 (m, 1H), 3.88 (s, 3H), 3.89-3.96 (m, 1H), 4.37-4.43 (m, 1H), 4.44-4.51 (m, 2H), 4.56-4.61 (m, 2H), 4.56-4.61 (m, 2H), 4.61-4.66 (m, 2H), 4.66-4.72 (m, 1H), 5.43-5.48 (m, 1H), 6.15-6.23 (m, 1H), 6.48-6.56 (m, 3H), 6.83-6.88 (m, 2H), 6.92-6.96 (m, 1H), 7.05-7.14 (m, 3H), 7.16-7.22 (m, 2H), 7.43-7.57 (m, 2H), 7.87 (br s, 1H), 8.01-8.06 (m, 2H). ¹³C NMR (126 MHz, DMSO-*d*₆, mixture of rotamers): δ 173.2, 172.9, 171.4, 171.3, 171.2, 171.1, 170.8, 170.03, 169.98, 169.4, 158.5, 158.2, 158.0, 157.7, 155.8, 155.1, 152.8, 141.8, 141.7, 135.9, 135.8, 133.5, 133.4, 130.0, 129.9, 129.13, 129.06, 128.8, 128.7, 128.5, 128.2, 128.1, 127.9, 127.7, 126.4, 126.3, 124.3, 124.1, 123.4, 123.3, 123.2, 117.6, 115.2, 114.84, 114.78, 114.4, 114.2, 81.6, 66.9, 61.5, 59.4, 58.5, 56.5, 56.1, 56.0, 55.1, 54.2, 52.3, 51.7, 51.6, 49.9, 48.6, 38.1, 37.8, 37.0, 36.91, 36.85, 35.4, 35.2, 34.1, 31.1, 31.0, 28.4, 27.7, 27.4, 25.6, 25.1, 22.3, 22.2. MS *m/z* 971.4 (calc'd: C₅₄H₆₂N₆O₁₁, [M+H]⁺, 971.4).



Compound **S32** was subjected to general procedure C. HPLC analysis and purification was performed using the following methods.

Analytical HPLC method:Column: Waters Sunfire™ C₁₈, 4.6x250mm, 5μm.Solvent A: H₂O + 0.1%v TFA

Solvent B: ACN + 0.1%v TFA

Flow rate: 1.00 ml/min

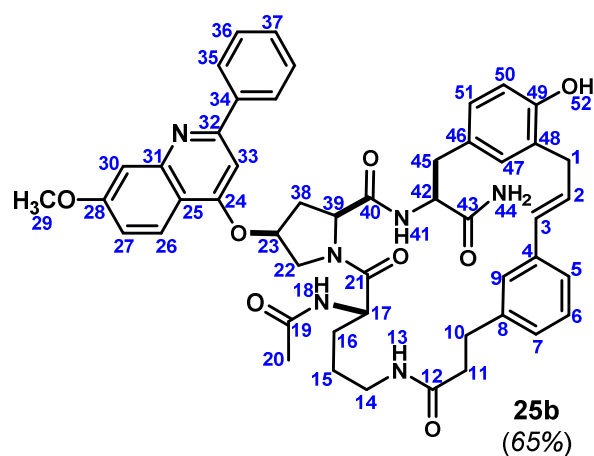
Time	%B
0	25
2	25
30	50
38	100
45	100
49	25
50	25

Semi-preparative HPLC method:Column: Waters Sunfire™ C₁₈, 10x250mm, 5μm.Solvent A: H₂O + 0.1%v TFA

Solvent B: ACN + 0.1%v TFA

Flow rate: 7.50 ml/min

Time	%B
0	20
2	20
22	50
24	20
25	20

(600MHz, DMSO-*d*₆, 298K)

	¹³ C	¹ H	key correlations
1	31.7	3.44 (dd, <i>J</i> = 15.8, 6.1Hz, 1H), 3.25 (dd, <i>J</i> = 15.8, 7.5Hz, 1H)	HMBC 1→48, 49
2	128.4	6.31 (ddd, <i>J</i> = 15.7, 7.5, 6.1Hz, 1H)	HMBC 2→4
3	130.5	6.42 (br d, <i>J</i> = 15.7Hz, 1H)	
4	137.0	-	
5	124.0	7.08 (br d, <i>J</i> = 7.7Hz, 1H)	HMBC 5→3
6	128.0	7.14 (dd, <i>J</i> = 7.7, 7.6Hz, 1H)	HMBC 6→4,8 COSY 6→5,7 TOCSY 6→5,7,9
7	127.0	6.97 (br d, <i>J</i> = 7.6Hz, 1H)	
8	141.1	-	
9	129.3	7.33 (br s, 1H)	
10	30.6	2.60-2.69 (m, 2H) overlap	HMBC 10→8, 12
11	36.7	2.29-2.35 (m, 1H), 2.22-2.27 (m, 1H)	HMBC 11→8, 12
12	171.2	-	
13	-	7.54 (t, <i>J</i> = 5.7Hz, 1H)	HMBC 13→12
14	37.4	2.98-3.05 (m, 1H), 2.81-2.87 (m, 1H)	

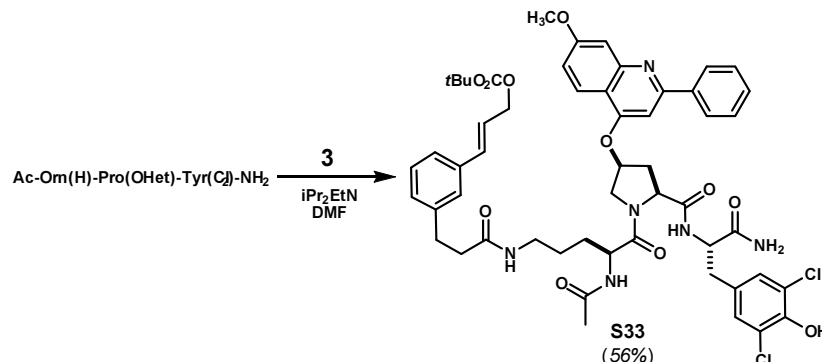
15	24.5	1.23-1.35 (m, 2H)	HMBC 15→17
16	28.1	1.57-1.64 (m, 1H), 1.37-1.42 (m, 1H)	
17	49.4	4.48-4.53 (m, 1H) overlap	HMBC 17→19,21
18	-	8.12 (d, $J = 7.7\text{Hz}$, 1H)	HMBC 18→19
19	169.1	-	
20	21.9	1.84 (s, 3H)	HMBC 20→19
21	171.1	-	
22	51.9	4.48-4.53 (m, 1H) overlap, 4.02 (br d, $J = 11.7\text{Hz}$, 1H)	COSY 22→22'
23	78.1	5.77 (br s, 1H)	COSY 23→22 TOCSY 23→38, 39
24	not observed†	-	
25	114.1	-	
26	124.4	8.07 (d, $J = 9.1\text{Hz}$, 1H)	HMBC 26→28 TOCSY 26→27,30
27	118.8	7.20 (br d, $J = 9.1\text{Hz}$, 1H)	HMBC 27→25
28	162.8	-	
29	55.5	3.93 (s, 2H)	HMBC 29→28
30	not observed†	7.52 (br s, 1H)	HMBC 30→25
31	not observed†	-	
32	not observed†	-	
33	99.8	7.64 (br s, 1H)	HMBC 33→25
34	131.6	-	
35	128.7	7.66-7.71 (m, 2H) overlap	
36	128.2	8.18-8.21 (m, 2H)	HMBC 36→34
37	131.2	7.66-7.71 (m, 1H) overlap	
38	34.0	2.59-2.66 (m, 1H), 2.46-2.51 (m, 1H)	HMBC 38→40
39	58.0	4.69 (dd, $J=9.2, 2.5\text{Hz}$, 1H)	HMBC 39→40
40	170.0	-	
41	-	7.81 (br d, $J=7.6\text{Hz}$, 1H)	COSY 41→42
42	53.7	4.40 (ddd, $J = 8.1, 8.1, 6.8\text{Hz}$, 1H)	HMBC 42→43
43	173.0	-	
44	-	7.39 (br s, 1H), 7.02 (br s, 1H)	TOCSY 44→44' HMBC 44→43
45	37.1	2.75 (dd, $J = 14.0, 6.7\text{Hz}$, 1H), 2.67 (dd, $J = 14.0, 8.4\text{Hz}$, 1H) overlap	HMBC 45→43
46	129.2	-	
47	129.3	6.94-6.95 (m, 1H)	HMBC 47→49
48	125.9	-	
49	153.1	-	
50	114.0	6.64 (d, $J = 8.1\text{Hz}$, 1H)	HMBC 50→49
51	127.3	6.81 (dd, $J = 8.1, 2.0\text{Hz}$, 1H)	HMBC 51→46,47,49

52	-	9.19 (br s, 1H)	
----	---	-----------------	--

†Not observed in HMBC optimized for $^3J_{\text{CH}} = 8.0\text{Hz}$

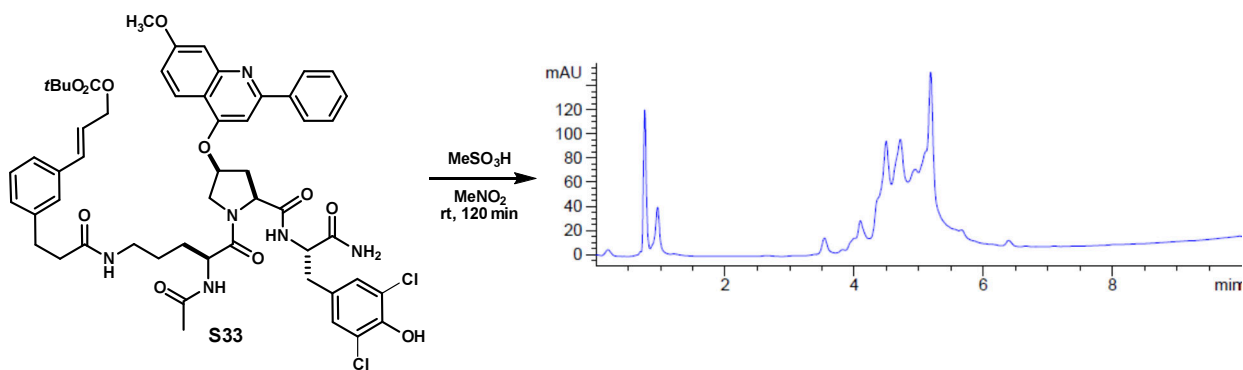
MS m/z 853.3 (calc'd: $\text{C}_{49}\text{H}_{53}\text{N}_6\text{O}_8$, $[\text{M}+\text{H}]^+$, 853.4).

Acidolysis of substrate **S33** (entry 9, Table 5.1.1):



Acyclic carbonate (S33): General procedure A afforded compound **S33** as a colorless film (88 mg, 56%).

^1H NMR (500 MHz, CD_3OD , major rotamer): δ 1.45 (s, 9H), 1.47-1.59 (m, 2H), 1.59-1.71 (m, 2H), 1.98 (s, 3H), 2.35-2.40 (m, 2H), 2.61 (br d, $J = 14.1$ Hz, 1H), 2.71 (dd, $J = 14.1, 7.5$ Hz, 1H), 2.79 (t, $J = 7.7$ Hz, 2H), 2.89-2.93 (m, 1H), 3.00-3.07 (m, 1H), 3.07-3.20 (m, 2H), 3.89 (s, 3H), 4.00 (br d, $J = 11.7$ Hz, 1H), 4.43 (dd, $J = 11.7, 5.0$ Hz, 1H), 4.49-4.54 (m, 1H), 4.61 (br d, $J = 6.4$ Hz, 2H), 4.65 (dd, $J = 6.3, 0.9$ Hz, 1H), 4.71 (dd, $J = 9.4, 3.3$ Hz, 1H), 5.47-5.51 (m, 1H), 6.22 (dt, $J = 15.9, 6.4$ Hz, 1H), 6.53 (br d, $J = 15.9$ Hz, 1H), 6.86 (s, 2H), 6.96-6.99 (m, 1H), 7.03 (s, 1H), 7.09-7.16 (m, 3H), 7.19-7.24 (m, 2H), 7.46-7.56 (m, 4H), 7.96-7.99 (m, 1H), 8.03-8.07 (m, 2H). ^{13}C NMR (126 MHz, CD_3OD , major rotamer): δ 175.1, 174.8, 174.1, 173.3, 172.6, 163.1, 162.0, 161.3, 154.9, 152.1, 149.3, 142.5, 141.3, 137.7, 135.1, 130.6, 130.2, 129.8, 129.7, 129.2, 129.1, 127.7, 125.5, 124.8, 124.1, 122.9, 122.4, 119.4, 116.2, 107.4, 100.1, 82.9, 78.1, 68.4, 61.0, 56.0, 55.2, 54.0, 52.4, 39.6, 38.9, 37.8, 35.1, 32.7, 29.4, 28.0, 26.2, 22.2. MS m/z 1039.3 (calc'd: $\text{C}_{54}\text{H}_{61}\text{Cl}_2\text{N}_6\text{O}_{11}$, $[\text{M}+\text{H}]^+$, 1039.4).



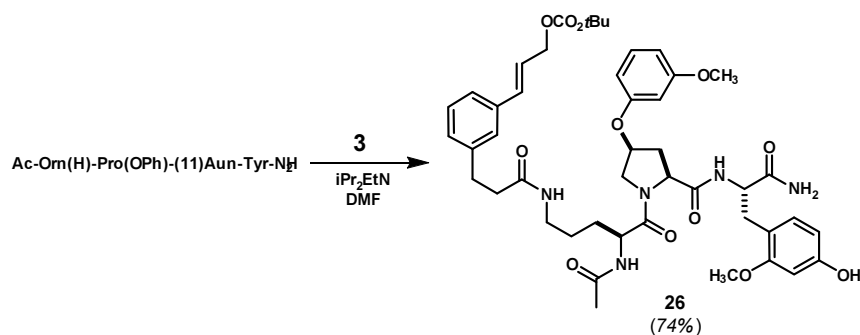
Compound **S33** was subjected to general procedure C. HPLC analysis was performed using the following method. Complete decomposition of starting **S33** was observed, but no putatively cyclic products were detected by MS.

Analytical HPLC method:Column: Phenomenex Gemini C18, 3x100mm, 5 μ m.Solvent A: H₂O + 0.1%v TFA

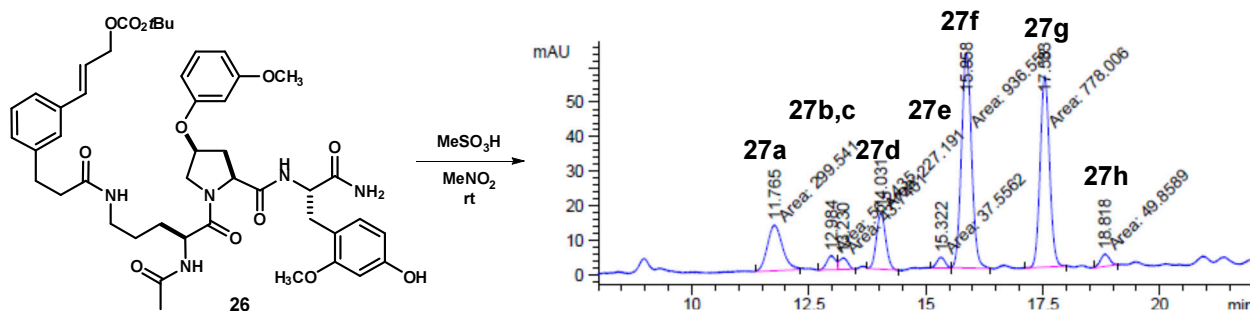
Solvent B: ACN + 0.1%v TFA

Flow rate: 1.00 ml/min

Time	%B
0	20
0.5	20
8	100
10	100

Macrocycles 27a–h:

Acyclic carbonate (26): General procedure A afforded compound **26** as a white foam (323 mg, 74%). ¹H NMR (500 MHz, DMSO-*d*₆, 323K, major rotamer): δ 1.39-1.54 (m, 3H), 1.44 (s, 9H), 1.55-1.66 (m, 1H), 1.84 (s, 3H), 1.97 (ddd, *J* = 13.4, 4.8, 4.8 Hz, 1H), 2.37 (t, *J* = 7.8 Hz, 2H), 2.48-2.54 (m, 1H), 2.74 (dd, *J* = 14.0, 8.2 Hz, 1H), 2.80 (t, *J* = 7.8 Hz, 2H), 2.93 (dd, *J* = 14.0, 6.0 Hz, 1H), 2.99-3.10 (m, 2H), 3.61 (dd, *J* = 10.9, 3.9 Hz, 1H), 3.71 (s, 6H), 4.21 (dd, *J* = 11.0, 5.6 Hz, 1H), 4.30 (ddd, *J* = 8.2, 7.9, 6.0 Hz, 1H), 4.34 (dd, *J* = 9.5, 5.1 Hz, 1H), 4.45 (ddd, *J* = 7.7, 7.7, 5.8 Hz, 1H), 4.67 (d, *J* = 6.3 Hz, 2H), 4.99-5.05 (m, 1H), 6.20 (dd, *J* = 8.2, 2.2 Hz, 1H), 6.31 (dt, *J* = 16.0, 6.3 Hz, 1H), 6.35 (d, *J* = 2.2 Hz, 1H), 6.46-6.49 (m, 1H), 6.49 (d, *J* = 1.0 Hz, 1H), 6.51-6.55 (m, 1H), 6.63 (d, *J* = 16.0 Hz, 1H), 6.84 (d, *J* = 8.2 Hz, 1H), 6.87 (br s, 2H), 7.08-7.11 (m, 1H), 7.16 (apt t, *J* = 8.4 Hz, 1H), 7.23 (dd, *J* = 7.5, 7.5 Hz, 1H), 7.24-7.30 (m, 2H), 7.28 (d, *J* = 7.9 Hz, 1H), 7.67 (dd, *J* = 5.2, 5.2 Hz, 1H), 8.08 (d, *J* = 7.5 Hz, 1H), 9.08 (s, 1H). ¹³C NMR (126 MHz, DMSO-*d*₆, 323K, major rotamer): δ 172.9, 171.4, 171.0, 169.9, 169.1, 160.4, 158.0, 157.9, 157.1, 152.6, 141.7, 135.7, 133.3, 130.5, 129.8, 128.4, 127.8, 126.2, 124.0, 123.2, 115.8, 107.6, 106.9, 106.5, 101.7, 98.9, 81.3, 74.9, 66.7, 58.9, 55.1, 54.9, 52.9, 51.7, 50.4, 38.0, 36.8, 33.7, 31.0, 30.8, 28.2, 27.3, 25.2, 22.0. MS *m/z* 874.0 (calc'd: C₄₆H₆₀N₅O₁₂, [M+H]⁺, 874.4).



Compound **26** was subjected to general procedure C. HPLC analysis and purification was performed using the following methods.

Analytical HPLC method:Column: Waters Sunfire™ C₁₈, 4.6x250mm, 5μm.Solvent A: H₂O + 0.1%v TFA

Solvent B: ACN + 0.1%v TFA

Flow rate: 1.00 ml/min

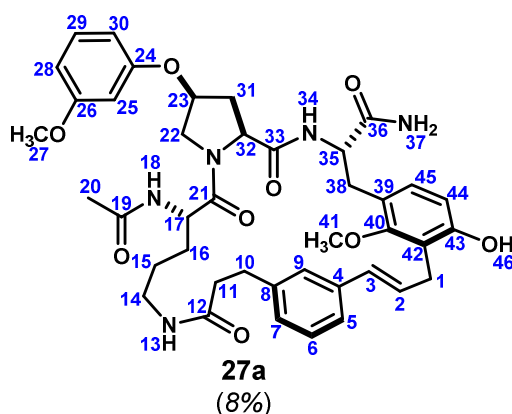
Time	%B
0	45
2	45
25	56.4
30	100
35	100
38	45
41	45

Semi-preparative HPLC method A:Column: Waters Sunfire™ C₁₈, 10x250mm, 5μm.Solvent A: H₂O + 0.1%v TFA

Solvent B: ACN + 0.1%v TFA

Flow rate: 6.00 ml/min

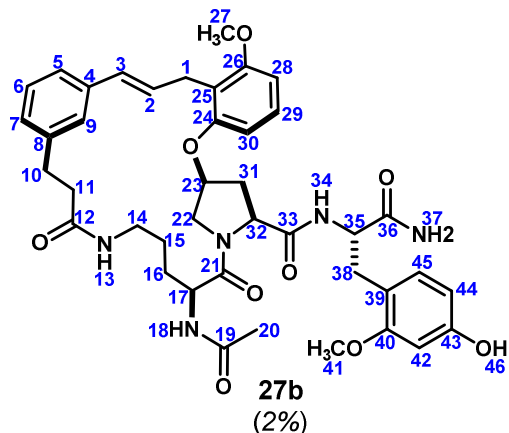
Time	%B
0	37
1	37
16.2	39
17	37
20	37

(600MHz, DMSO-*d*₆, 298K)

	¹³ C	¹ H	key correlation
1	27.0	3.44 (br d, <i>J</i> = 6.5 Hz, 2H)	HMBC 1→40,42,43
2	128.6	6.24 (dt, <i>J</i> = 15.8 Hz, 1H)	COSY 2→1 HMBC 2→4
3	129.3	6.41 (d, <i>J</i> = 15.8 Hz, 1H)	HMBC 3→4
4	137.0	-	
5	123.6	7.11 (br d, <i>J</i> = 7.7 Hz, 1H) overlap	HMBC 5→3
6	128.2	7.15 (dd, <i>J</i> = 7.7, 7.7 Hz, 1H) overlap	HMBC 6→4,8
7	127.0	6.98 (br d, <i>J</i> = 7.7 Hz, 1H)	
8	141.2	-	
9	124.7	7.14 (br s, 1H) overlap	HMBC 9→3
10	30.5	2.76 (dd, <i>J</i> = 7.2, 7.2 Hz, 2H)	HMBC 10→8,12
11	36.6	2.23-2.34 (m, 2H)	HMBC 11→8,12
12	171.1	-	
13	-	7.63 (dd, <i>J</i> = 5.5, 5.5 Hz, 1H)	
14	37.8	2.81-2.93 (m, 2H)	
15	24.8	1.24-1.37 (m, 2H) overlap	
16	28.3	1.30-1.37 (m, 1H) overlap, 1.45-1.53 (m, 1H)	COSY 16→17
17	49.7	4.48 (ddd, <i>J</i> = 8.1, 8.0, 5.3 Hz, 1H)	HMBC 17→19,21

18	-	8.14 (d, $J = 8.0$ Hz, 1H)	HMBC 18→19
19	169.0	-	
20	22.0	1.84 (s, 3H)	HMBC 20→19
21	171.4	-	
22	51.9	3.54 (dd, $J = 11.1, 2.9$ Hz, 1H), 4.20 (dd, $J = 11.1, 5.9$ Hz, 1H)	
23	74.8	5.01-5.05 (m, 1H)	
24	157.8	-	
25	101.3	6.36 (dd, $J = 2.1, 2.1$ Hz, 1H)	HMBC 25→24,26
26	160.3	-	
27	54.8	3.68 (s, 3H)	HMBC 27→26
28	106.5	6.50 (dd, $J = 8.2, 2.1$ Hz, 1H)	HMBC 28→26
29	129.7	7.12-7.15 (m, 1H) overlap	HMBC 29→24,26
30	107.1	6.38 (dd, $J = 8.3, 2.1$ Hz, 1H)	
31	32.9	2.21 (ddd, $J = 13.5, 3.7, 3.0$ Hz, 1H), 2.41 (ddd, $J = 13.5, 9.3, 5.6$ Hz, 1H)	
32	58.3	4.52 (dd, $J = 9.3, 3.7$ Hz, 1H)	HMBC 32→33
33	170.1	-	
34	-	7.65 (d, $J = 7.7$ Hz, 1H)	HMBC 34→33
35	53.4	4.28 (ddd, $J = 7.9, 7.7, 5.7$ Hz, 1H)	HMBC 35→33,36
36	172.9	-	
37	-	7.06 (br s, 1H), 7.19 (br s, 1H)	HMBC 37→36
38	31.0	2.76-2.80 (m, 1H) overlap, 2.90-2.95 (m, 1H) overlap	HMBC 38→39,40,45
39	120.5	-	
40	157.5	-	
41	60.9	3.63 (s, 3H)	HMBC 41→40
42	119.1	-	
43	154.8	-	
44	110.6	6.55 (d, $J = 8.3$ Hz, 1H)	HMBC 44→43
45	127.9	6.94 (d, $J = 8.3$ Hz, 1H)	HMBC 45→40,43
46	-	9.33 (br s, 1H)	

MS m/z 756.0 (calc'd: $C_{41}H_{50}N_5O_9$, $[M+H]^+$, 756.4).

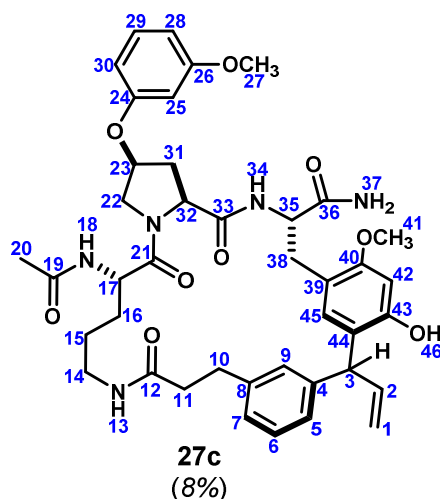


(600MHz, DMSO-*d*₆, 298K) Note: This compound was characterized within a 1:2 mixture of **27b**:**27c**.

¹³ C	¹ H	key correlation	
1	25.8	3.41-3.51 (m, 2H) obscured	HMBC 1→2,3,24,25,26
2	128.1	6.26 (d, <i>J</i> = 16.0 Hz, 1H) overlap	HMBC 2→4
3	129.2	6.30-6.36 (m, 1H) overlap	HMBC 3→4
4	136.7	-	
5	123.7	7.05 (br d, <i>J</i> = 7.7 Hz, 1H)	HMBC 5→3,7,9
6	128.0	7.11 (dd, <i>J</i> = 7.7, 7.7 Hz, 1H) overlap	
7	127.1	6.95-6.98 (m, 1H) overlap	HMBC 7→5,9
8	140.9	-	
9	125.0	7.25 (br s, 1H)	HMBC 9→5,7
10	30.5	2.76-2.83 (m, 2H) overlap	
11	36.3	2.31-2.42 (m, 2H) overlap	
12	171.3	-	
13	-	7.72-7.76 (m, 1H) overlap	HMBC 13→12
14	37.8	2.84-2.95 (m, 2H) overlap	
15	24.6	1.23-1.36 (m, 2H) overlap	
16	28.2	1.28-1.35 (m, 1H) overlap, 1.54-1.61 (m, 1H)	
17	49.3	4.33-4.37 (m, 1H) overlap	HMBC 17→19,21
18	-	8.12 (d, <i>J</i> = 7.3 Hz, 1H)	HMBC 18→19
19	169.1	-	
20	21.9	1.81 (s, 3H)	HMBC 20→19
21	172.6	-	
22	51.7	3.41-3.46 (m, 1H), 4.43 (dd, <i>J</i> = 10.3, 6.9 Hz, 1H)	
23	74.0	5.02-5.06 (m, 1H) overlap	HMBC 23→24 TOCSY 23→22,31,32
24	155.7	-	
25	115.9	-	
26	157.5	-	
27	55.6	3.78 (s, 3H)	HMBC 27→26
28	104.3	6.67 (d, <i>J</i> = 8.4 Hz, 1H)	HMBC 28→25,26

29	127.4	7.18 (dd, $J = 8.4, 8.4$ Hz, 1H) overlap	HMBC 29→24,26
30	105.5	6.75 (d, $J = 8.4$ Hz, 1H)	HMBC 30→24,25
31	34.1	1.94-2.02 (m, 1H), 2.52-2.60 (m, 1H) overlap	
32	58.2	4.28 (dd, $J = 7.9, 7.9$ Hz, 1H) overlap	
33	170.0	-	
34	-	7.72-7.75 (m, 1H) overlap	HMBC 34→33
35	52.5	4.23 (ddd, $J = 9.0, 8.3, 5.4$ Hz, 1H)	HMBC 35→33,36
36	172.8	-	
37	-	6.89 (br s, 1H) overlap, 6.96 (br s, 1H) overlap	TOCSY 37→37'
38	30.5	2.70 (dd, $J = 13.8, 9.0$ Hz, 1H), 2.94 (dd, $J = 13.8, 5.4$ Hz, 1H)	HMBC 38→39
39	115.8	-	
40	157.9	-	
41	54.8	3.69 (s, 3H)	HMBC 41→40
42	98.5	6.32 (br s, 1H) overlap	HMBC 42→40,43
43	156.9	-	
44	106.0	6.13-6.16 (m, 1H) overlap	TOCSY 44→42,45 HMBC 44→42
45	130.7	6.85-6.88 (m, 1H) overlap	HMBC 45→40,43
46	-	9.22 (br s, 1H)	

MS m/z 756.0 (calc'd: $C_{41}H_{50}N_5O_9$, $[M+H]^+$, 756.4).

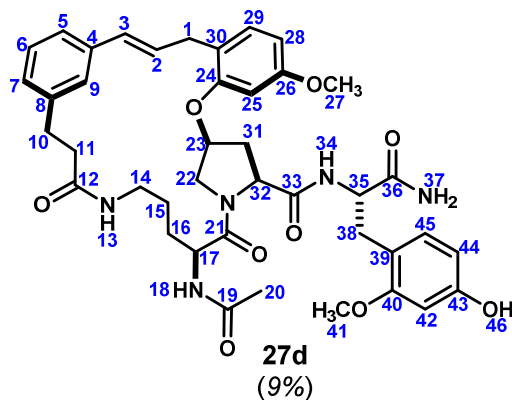


(600MHz, DMSO- d_6 , 298K) Note: This compound was characterized within a 1:2 mixture of **27b**:**27c**.

	^{13}C	1H	key correlation
1	114.4	4.79 (d, $J = 17.0$ Hz, 1H), 5.02 (d, $J = 10.2$ Hz, 1H)	HMBC 1→2
2	140.8	6.12 (ddd, $J = 17.0, 10.2, 6.8$ Hz, 1H)	HMBC 2→4,44
3	46.1	4.90 (d, $J = 6.8$ Hz, 1H)	HMBC 3→2,4,44,45
4	142.7	-	
5	126.7	6.99 (br d, $J = 7.6$ Hz, 1H)	HMBC 5→3,7,9
6	128.0	7.15 (dd, $J = 7.6, 7.6$ Hz, 1H)	HMBC 6→4,8
7	125.9	7.00 (br d, $J = 7.6$ Hz, 1H)	HMBC 7→5,9

8	141.0	-	
9	128.2	7.12 (br s, 1H)	HMBC 9→3,5,7
10	31.8	2.73-2.78 (m, 2H) overlap	HMBC 10→8,12
11	38.4	2.30-2.43 (m, 2H)	HMBC 11→8,12
12	171.2	-	
13	-	7.56 (dd, $J = 5.5, 5.5$ Hz, 1H)	HMBC 13→12 COSY 13→14
14	37.7	2.85-2.91 (m, 1H), 3.14-3.20 (m, 1H)	COSY 14→15
15	24.7	1.35-1.42 (m, 2H) overlap	COSY 15→16
16	29.0	1.36-1.41 (m, 1H) overlap, 1.66-1.73 (m, 1H)	
17	50.1	4.37-4.42 (m, 1H) overlap	HMBC 17→19,21
18	-	8.17 (d, $J = 7.0$ Hz, 1H)	
19	169.2	-	
20	21.9	1.81 (s, 3H)	HMBC 20→19
21	172.3	-	
22	52.5	3.76 (br d, $J = 11.6$ Hz, 1H), 4.13 (dd, $J = 11.6, 4.7$ Hz, 1H)	HMBC 22→21
23	75.4	5.07-5.10 (m, 1H)	
24	157.4	-	
25	100.9	6.40-6.41 (m, 1H) overlap	HMBC 25→24,26
26	160.2	-	
27	54.7	3.53 (s, 3H)	HMBC 27→26
28	106.5	6.40-6.43 (m, 1H) overlap	HMBC 28→26
29	129.9	6.84 (dd, $J = 8.1, 8.1$ Hz, 1H)	HMBC 29→24,26
30	107.7	6.25 (dd, $J = 8.1, 1.6$ Hz, 1H)	HMBC 30→24
31	33.4	2.22 (br d, $J = 13.6$ Hz, 1H), 2.47 (ddd, $J = 13.6, 10.1, 4.9$ Hz, 1H)	HMBC 31→33
32	59.2	4.37-4.41 (m, 1H) overlap	HMBC 32→33
33	169.3	-	
34	-	6.88 (d, $J = 7.9$ Hz, 1H)	
35	52.6	4.36 (ddd, $J = 7.9, 7.9$ Hz, 5.1 Hz, 1H) overlap	HMBC 35→33,36
36	172.7	-	
37	-	7.31 (br s, 1H), 7.51 (br s, 1H)	HMBC 37→36
38	31.8	2.62 (dd, $J = 13.2, 8.2$ Hz, 1H), 2.83 (dd, $J = 13.2, 4.7$ Hz, 1H)	HMBC 38→39,40
39	113.8	-	
40	156.1	-	
41	55.0	3.63 (s, 3H)	HMBC 41→40
42	98.3	6.33 (s, 1H)	HMBC 42→39,40,43,44
43	153.9	-	
44	119.7	-	
45	130.8	6.63 (s, 1H)	HMBC 45→40,43
46	-	9.20 (br s, 1H)	

MS m/z 756.0 (calc'd: $C_{41}H_{50}N_5O_9$, $[M+H]^+$, 756.4).

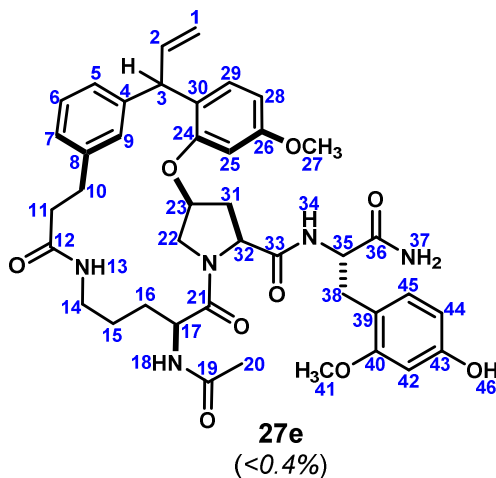


(600MHz, DMSO- d_6 , 298K)

	^{13}C	1H	key correlation
1	33.5	3.14 (dd, $J = 14.5, 7.0$ Hz, 1H), 3.63 (dd, $J = 14.5, 6.0$ Hz, 1H)	HMBC 1→24,29,30
2	129.0	6.42 (ddd, $J = 15.8, 7.0, 6.0$ Hz, 1H)	HMBC 2→4,30
3	128.9	6.30 (br d, $J = 15.8$ Hz, 1H)	HMBC 3→4
4	136.8	-	
5	123.9	7.03 (br d, $J = 7.7$ Hz, 1H)	HMBC 5→3
6	128.0	7.12 (dd, $J = 7.7, 7.7$ Hz, 1H)	HMBC 6→4,8
7	127.1	6.98 (br d, $J = 7.7$ Hz, 1H)	
8	141.0	-	
9	124.7	7.32 (br s, 1H)	HMBC 9→3,5,7 TOCSY 9→5,6,7
10	30.4	2.74-2.85 (m, 2H)	
11	36.3	2.32-2.43 (m, 2H)	
12	171.4	-	
13	-	7.78 (dd, $J = 5.3, 5.3$ Hz, 1H)	HMBC 13→14
14	37.7	2.85-2.96 (m, 2H)	
15	24.5	1.23-1.33 (m, 2H) overlap	
16	28.1	1.28-1.37 (m, 1H) overlap, 1.57-1.64 (m, 1H)	
17	49.2	4.41 (dd, $J = 13.9, 7.1$ Hz, 1H)	
18	-	8.13 (d, $J = 7.1$ Hz, 1H)	HMBC 18→19
19	169.0	-	
20	21.8	1.81 (s, 3H)	HMBC 20→19
21	171.5	-	
22	51.3	3.44 (dd, $J = 10.0, 6.7$ Hz, 1H), 4.52 (dd, $J = 10.0, 6.6$ Hz, 1H)	
23	73.5	5.04-5.09 (m, 1H)	HMBC 23→24
24	155.6	-	
25	99.5	6.69 (d, $J = 2.2$ Hz, 1H)	HMBC 25→24,26,30
26	159.1	-	
27	54.9	3.76 (s, 3H)	HMBC 27→26

28	105.6	6.49 (dd, $J = 8.3, 2.2$ Hz, 1H)	HMBC 28→30
29	130.6	7.10 (d, $J = 8.3$ Hz, 1H) overlap	HMBC 29→1
30	120.5	-	
31	34.1	2.57 (ddd, $J = 12.7, 7.6, 6.7$ Hz, 1H), 1.98 (ddd, $J = 12.7, 7.8, 7.6$ Hz, 1H)	HMBC 31→32,33
32	58.3	4.25-4.39 (m, 1H) overlap	HMBC 32→33
33	170.1	-	
34	-	7.73 (d, $J = 8.1$ Hz, 1H)	
35	52.3	4.26-4.31 (m, 1H) overlap	HMBC 35→33,36,39
36	172.8	-	
37	-	6.86 (br s, 1H), 6.96 (br s, 1H)	
38	30.4	2.70 (dd, $J = 13.8, 9.3$ Hz, 1H), 2.97 (dd, $J = 13.8, 5.5$ Hz, 1H)	HMBC 38→39
39	115.8	-	
40	157.9	-	
41	54.8	3.70 (s, 3H)	HMBC 41→40
42	98.5	6.33 (d, $J = 1.8$ Hz, 1H)	HMBC 42→40,43
43	157.0	-	
44	106.0	6.17 (dd, $J = 8.1, 1.8$ Hz, 1H)	
45	130.7	6.93 (d, $J = 8.1$ Hz, 1H)	HMBC 45→40,43
46	-	9.21 (br s, 1H)	

MS m/z 756.0 (calc'd: $C_{41}H_{50}N_5O_9$, $[M+H]^+$, 756.4).



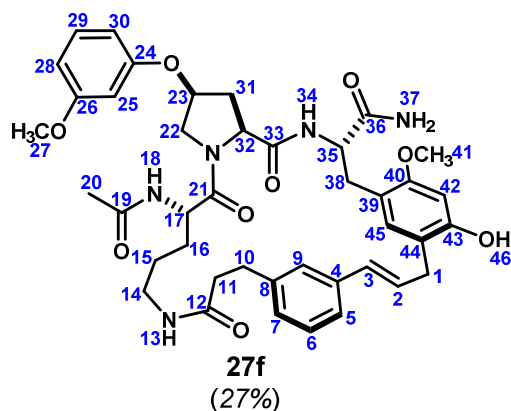
(600MHz, $DMSO-d_6$, 298K)

	^{13}C	1H	key correlation
1	115.5	5.03 (d, $J = 17.1$ Hz, 1H), 5.13 (d, $J = 10.0$ Hz, 1H)	TOCSY 1→1',2,3
2	139.8	6.44 (dd, $J = 17.1, 10.0, 8.3$ Hz, 1H)	
3	51.0	4.62 (d, $J = 8.3$ Hz, 1H)	HMBC 3→4,24,30
4	143.0	-	
5	124.5	6.74 (br d, $J = 7.8$ Hz, 1H)	HMBC 5→3,7
6	127.4	7.06 (dd, $J = 7.8, 7.8$ Hz, 1H) overlap	

7	125.3	6.94 (br d, $J = 7.8$ Hz, 1H)	HMBC 7→5
8	140.8	-	
9	128.1	7.16 (br s, 1H) overlap	HMBC 9→3,5,7
10	30.8	2.68-2.79 (m, 1H) overlap, 2.80-2.91 (m, 1H) overlap	HMBC 10→11,12
11	36.8	2.33-2.44 (m, 2H) overlap	HMBC 11→10,12
12	171.6	-	
13	-	7.76-7.79 (m, 1H)	TOCSY 13→14,15
14	37.4	2.80-2.89 (m, 1H) overlap, 3.15-3.22 (m, 1H)	
15	23.2	1.37-1.49 (m, 2H) overlap	
16	26.7	1.36-1.44 (m, 1H) overlap, 1.61-1.69 (m, 1H)	
17	49.7	4.48-4.53 (m, 1H)	HMBC 17→21 TOCSY 17→15,16,18
18	-	7.98 (d, $J = 7.5$ Hz, 1H)	
19	168.8	-	
20	22.0	1.82 (s, 3H)	HMBC 20→19
21	170.4	-	
22	50.5	2.96-3.01 (m, 1H), 4.05-4.09 (m, 1H)	COSY 22→23 TOCSY 22→23,31,32 NOESY 22→17
23	72.8	4.93-4.99 (m, 1H)	NOESY 23→25
24	155.1	-	
25	100.2	6.62 (d, $J = 2.3$ Hz, 1H)	HMBC 25→24,26,28,30
26	159.1	-	
27	55.0	3.74 (s, 3H)	HMBC 27→26 NOESY 27→25
28	105.0	6.53 (dd, $J = 8.3, 2.3$ Hz, 1H)	HMBC 28→30
29	127.4	7.23 (d, $J = 8.3$ Hz, 1H)	NOESY 29→3 HMBC 29→3,24,26
30	123.9	-	
31	33.5	1.35-1.44 (m, 1H) overlap, 2.51-2.58 (m, 1H) overlap	
32	57.9	4.22 (dd, $J = 9.5, 7.8$ Hz, 1H)	
33	170.3	-	
34	-	7.95 (d, $J = 7.5$ Hz, 1H)	TOCSY 34→35,38
35	53.0	4.14-4.19 (m, 1H)	HMBC 35→26 NOESY 35→37,37'
36	172.7	-	
37	-	6.91 (br s, 1H) overlap, 6.97 (br s, 1H) overlap	
38	29.7	2.69-2.76 (m, 1H) overlap, 2.83-2.90 (m, 1H) overlap	HMBC 38→35,39
39	115.7	-	
40	157.8	-	
41	54.8	2.68 (s, 3H)	HMBC 41→40
42	98.4	6.32 (d, $J = 2.3$ Hz, 1H)	
43	156.9	-	
44	106.2	6.12 (dd, $J = 8.1, 2.3$ Hz, 1H)	HMBC 44→42

45	130.6	6.77 (d, $J = 8.1$ Hz, 1H)	TOCSY 45→42,44
46	-	9.17 (br s, 1H) overlap	

MS m/z 756.0 (calc'd: $C_{41}H_{50}N_5O_9$, $[M+H]^+$, 756.4).

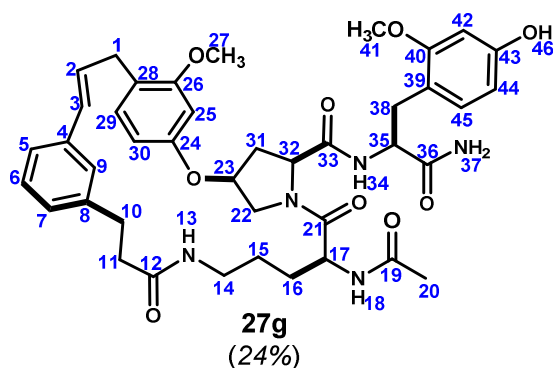


(600MHz, DMSO- d_6 , 298K)

	^{13}C	1H	key correlation
1	30.8	3.21 (dd, $J = 16.5, 7.4$ Hz, 1H), 3.28 (dd, $J = 16.5, 6.4$ Hz, 1H)	HMBC 1→2,3,43,44,45
2	128.9	6.33 (ddd, $J = 15.6, 7.4, 6.4$ Hz, 1H)	COSY 2→1,3 HMBC 2→4
3	130.8	6.45 (d, $J = 15.6$ Hz, 1H) overlap	
4	137.3	-	
5	124.7	7.09 (br d, $J = 7.6$ Hz, 1H) overlap	HMBC 5→3
6	128.1	7.18 (dd, $J = 7.6$ Hz, 1H)	HMBC 6→4,8 TOCSY 6→5,7,9
7	127.4	7.03 (br d, $J = 7.6$ Hz, 1H)	
8	141.5	-	
9	124.8	7.47 (br s, 1H)	HMBC 9→3,5,7
10	30.9	2.79-2.84 (m, 2H) overlap	HMBC 10→8,12
11	37.2	2.44 (br t, $J = 7.5$ Hz, 2H)	HMBC 11→8,12
12	171.4	-	
13	-	7.63 (dd, $J = 5.4, 5.4$ Hz, 1H)	HMBC 13→12 COSY 13→14
14	37.7	2.90-2.97 (m, 1H), 3.09-3.15 (m, 1H)	
15	24.8	1.34-1.44 (m, 2H) overlap	
16	28.3	1.37-1.44 (m, 1H) overlap, 1.61-1.68 (m, 1H)	
17	49.9	4.43-4.49 (m, 1H)	HMBC 17→21
18	-	8.11 (d, $J = 7.4$ Hz, 1H)	
19	169.3	-	
20	22.2	1.83 (s, 3H)	HMBC 20→19
21	171.9	-	
22	52.1	3.69-3.73 (m, 1H) overlap, 4.26 (dd, $J = 11.0, 5.4$ Hz, 1H)	HMBC 22→21
23	74.9	5.03-5.07 (m, 1H)	
24	158.0	-	

25	101.5	6.46 (s, 1H) overlap	HMBC 25→28,30
26	160.5	-	
27	54.9	3.57 (s, 3H)	HMBC 27→26
28	107.2	6.50 (dd, $J = 8.3, 1.9$ Hz, 1H)	HMBC 28→26
29	130.1	7.11 (dd, $J = 8.3, 8.3$ Hz, 1H)	HMBC 29→24,26
30	107.2	6.48 (dd, $J = 8.3, 1.9$ Hz, 1H)	
31	34.1	1.96-2.01 (m, 1H), 2.44-2.49 (m, 1H) overlap	
32	59.1	4.30 (dd, $J = 9.0, 5.4$ Hz, 1H)	HMBC 32→33
33	170.1	-	
34	-	7.31 (br s, 1H)	TOCSY 34→35,38
35	52.6	4.30-4.35 (m, 1H) overlap	HMBC 35→36
36	173.2	-	
37	-	7.07 (br s, 1H) overlap	HMBC 37→36
38	31.9	2.73 (dd, $J = 13.1, 7.2$ Hz, 1H), 2.80-2.85 (m, 1H) overlap	HMBC 38→39
39	130.5	-	
40	156.2	-	
41	55.3	3.71 (s, 3H)	HMBC 41→40
42	98.7	6.43 (s, 1H)	HMBC 42→40,43
43	154.2	-	
44	117.3	-	
45	130.6	6.73 (s, 1H)	HMBC 45→1,38,40,43
46	-	9.25 (br s, 1H)	

MS m/z 756.0 (calc'd: $C_{41}H_{50}N_5O_9$, $[M+H]^+$, 756.4).



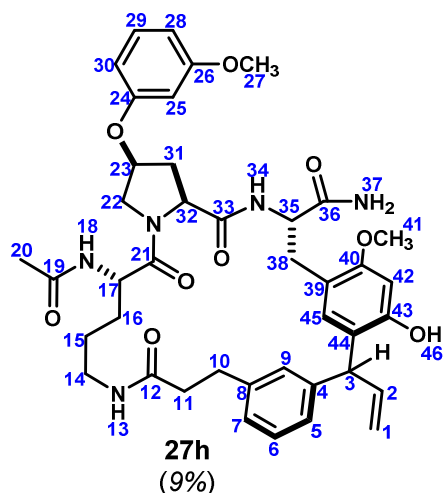
(600MHz, DMSO- d_6 , 298K)

	^{13}C	1H	key correlation
1	31.9	3.28 (dd, $J = 14.9, 6.7$ Hz, 1H), 3.48 (dd, $J = 14.9, 5.2$ Hz, 1H)	HMBC 1→26,28
2	129.4	6.18 (ddd, $J = 15.8, 6.7, 5.2$ Hz, 1H)	HMBC 2→4,28
3	128.7	6.25 (d, $J = 15.8$ Hz, 1H)	HMBC 3→4 TOCSY 3→2,1
4	136.8	-	
5	127.1	6.97 (br d, $J = 7.7$ Hz, 1H)	HMBC 5→4,3,9,7

6	128.1	7.16 (dd, $J = 7.7, 7.7$ Hz, 1H)	HMBC 6→4,8 TOCSY 6→5,7,9
7	124.3	7.07 (br d, $J = 7.7$ Hz, 1H) overlap	
8	141.5	-	
9	123.5	7.08 (br s, 1H) overlap	
10	29.7	2.69-2.75 (m, 1H) overlap, 2.86-2.92 (m, 1H)	HMBC 10→8,12
11	35.9	2.23-2.29 (m, 2H)	HMBC 11→8,12
12	171.1	-	
13	-	7.74 (t, 5.0 Hz, 1H)	HMBC 13→12
14	37.8	2.67-2.76 (m, 2H) overlap	
15	24.8	1.22-1.35 (m, 2H)	
16	28.2	1.36-1.50 (m, 2H)	
17	49.5	4.24 (ddd, $J = 8.9, 7.6, 5.9$ Hz, 1H)	HMBC 17→19,21
18	-	8.11 (d, $J = 7.6$ Hz, 1H)	
19	169.0	-	
20	21.9	1.78 (s, 3H)	HMBC 20→19
21	171.6	-	
22	50.9	3.59 (d, $J = 11.4$ Hz, 1H), 3.79 (dd, $J = 11.4, 3.2$ Hz, 1H) overlap	
23	75.8	5.18-5.22 (m, 1H)	
24	155.7	-	
25	101.4	6.68 (d, $J = 1.8$ Hz, 1H)	HMBC 25→24,26,28,30
26	157.6	-	
27	55.3	3.77 (s, 3H)	HMBC 27→26
28	121.0	-	
29	130.4	7.07 (d, $J = 8.2$ Hz, 1H) overlap	HMBC 29→24,26
30	107.4	6.59 (dd, $J = 8.2, 1.8$ Hz, 1H)	HMBC 30→28
31	34.2	2.19 (br d, $J = 14.0$ Hz, 1H)	
32	59.2	2.48-2.54 (m, 1H) overlap	HMBC 32→33
33	169.5	-	
34	-	7.27 (d, $J = 8.0$ Hz, 1H)	HMBC 34→33
35	52.3	4.40 (ddd, $J = 8.0, 7.4, 6.4$ Hz, 1H)	HMBC 35→33,36
36	172.8	-	
37	-	7.08 (br s, 2H) overlap	HMBC 37→36
38	31.6	2.77 (dd, $J = 13.8, 7.4$ Hz, 1H), 2.95 (dd, $J = 13.8, 6.4$ Hz, 1H)	HMBC 38→39
39	115.4	-	
40	158.0	-	
41	54.8	3.68 (s, 3H)	HMBC 41→40
42	98.5	6.33 (d, $J = 2.0$ Hz, 1H)	HMBC 42→39,40,43
43	157.0	-	
44	106.2	6.21 (dd, $J = 8.1, 2.0$ Hz, 1H)	HMBC 44→39
45	130.6	6.91 (d, $J = 8.1$ Hz, 1H)	

46	-	9.20 (br s, 1H)	
----	---	-----------------	--

MS m/z 756.0 (calc'd: C₄₁H₅₀N₅O₉, [M+H]⁺, 756.4).



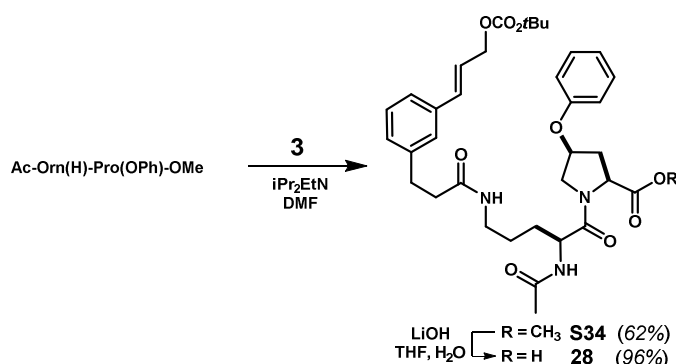
(600MHz, DMSO-*d*₆, 298K)

	¹³ C	¹ H	key correlation
1	114.2	4.73 (br d, <i>J</i> = 17.0 Hz, 1H), 4.98 (br d, <i>J</i> = 10.1 Hz, 1H)	TOCSY 1→1',2,3 HMBC 2→44
2	141.4	6.10 (ddd, <i>J</i> = 17.0, 10.1, 6.6 Hz, 1H)	HMBC 2→4
3	45.5	4.92 (br d, <i>J</i> = 6.6 Hz, 1H)	HMBC 3→43,44,45
4	142.6	-	
5	126.5	7.05 (br d, <i>J</i> = 7.5 Hz, 1H) overlap	HMBC 5→3
6	127.6	7.15 (dd, <i>J</i> = 7.5, 7.5 Hz, 1H) overlap	HMBC 6→8,12
7	125.7	6.99 (br d, <i>J</i> = 7.5 Hz, 1H)	HMBC 7→5,10
8	141.1	-	
9	127.0	7.04 (br s, 1H) overlap	HMBC 9→3
10	31.3	2.71 (ddd, <i>J</i> = 13.3, 11.1, 5.9 Hz, 1H), 2.81 (ddd, <i>J</i> = 13.3, 11.4, 5.3 Hz, 1H)	HMBC 10→8,12
11	37.8	2.32 (ddd, <i>J</i> = 13.8, 11.4, 5.9 Hz, 1H), 2.43 (ddd, <i>J</i> = 13.8, 11.1, 5.3 Hz, 1H)	HMBC 11→8,12
12	171.4	-	
13	-	7.75-7.78 (m, 1H)	COSY 13→14
14	38.2	2.85-2.91 (m, 1H), 3.21-3.29 (m, 1H)	COSY 14→15
15	24.4	1.38-1.47 (m, 2H) overlap	
16	28.9	1.41-1.49 (m, 1H) overlap, 1.71-1.78 (m, 1H)	
17	50.0	4.42-4.47 (m, 1H)	HMBC 17→19,21
18	-	8.19 (d, <i>J</i> = 7.0 Hz, 1H)	
19	169.1	-	
20	21.8	1.82 (s, 3H)	HMBC 20→19
21	171.9	-	
22	52.5	3.88 (br d, <i>J</i> = 11.5 Hz, 1H), 4.21 (dd, <i>J</i> = 11.5, 4.8 Hz, 1H)	HMBC 22→21
23	75.5	5.12-5.16 (m, 1H)	COSY 23→22,31
24	157.6	-	

25	101.4	6.53 (s, 1H) overlap	HMBC 25→24,26
26	160.3	-	
27	54.7	3.63 (s, 3H)	HMBC 27→26
28	106.9	6.51-6.54 (m, 1H) overlap	HMBC 28→26
29	129.9	7.12-7.16 (m, 1H) overlap	HMBC 29→24,26
30	107.1	6.53-6.56 (m, 1H) overlap	
31	33.8	2.18 (br d, $J = 13.7$ Hz, 1H), 2.46-2.52 (m, 1H)	
32	59.1	4.41 (dd, $J = 9.9, 2.9$ Hz, 1H)	HMBC 32→33
33	169.6	-	
34	-	6.99 (br d, $J = 7.4$ Hz, 1H) overlap	
35	51.7	4.53-4.59 (m, 1H)	HMBC 35→33 TOCSY 35→34,38
36	172.5	-	
37	-	6.73 (br s, 1H), 7.27 (br s, 1H)	HMBC 37→36
38	34.1	2.50-2.56 (m, 1H), 3.01 (dd, $J = 13.0, 6.8$ Hz, 1H)	HMBC 38→39
39	114.6	-	
40	156.2	-	
41	54.9	3.71 (s, 3H)	HMBC 41→40
42	98.3	6.39 (s, 1H)	HMBC 42→3,39,40,43,44
43	153.9	-	
44	119.5	-	
45	131.2	6.81 (s, 1H)	HMBC 45→3,40,43
46	-	9.27 (br s, 1H)	

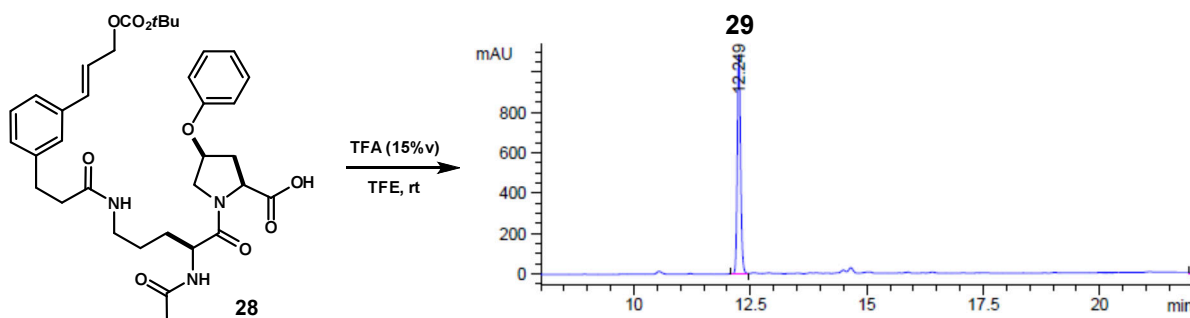
MS m/z 756.0 (calc'd: $C_{41}H_{50}N_5O_9$, $[M+H]^+$, 756.4).

Macrocycle S8:

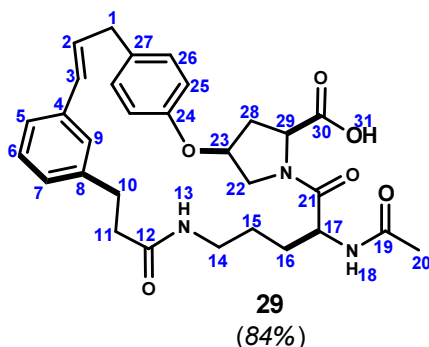


Acyclic carbonate (28): Methyl ester **S34** (1.71 g, 62%) was prepared analogously to compound **S27** and purified by chromatography on SiO_2 eluted with 2→9% MeOH in CHCl_3 . Saponification analogously to compound **34** afforded free acid **28** as a white foam (1.34 g, 96%). (**S34**) $^1\text{H NMR}$ (500 MHz, $\text{DMSO-}d_6$, major rotamer): δ 1.25-1.51 (m, 2H), 1.43 (s, 9H), 1.54-1.66 (m, 1H), 1.83 (s, 3H), 2.16 (br d, $J = 13.7$ Hz, 1H), 2.34 (t, $J = 7.7$ Hz, 2H), 2.48 (ddd, $J = 13.7, 9.4, 4.8$ Hz, 1H), 2.78 (t, $J = 7.7$ Hz, 2H), 2.97-3.04 (m, 1H), 3.58 (s, 3H), 3.66 (br d, $J = 11.4$ Hz, 1H), 4.18 (dd, $J = 11.5, 5.3$ Hz, 1H), 4.40-4.46 (m, 1H), 4.61 (dd, $J = 9.2, 2.4$ Hz, 1H), 4.67 (br d, $J = 6.2$ Hz, 2H), 5.13-5.17 (m, 1H) 6.32 (dt, $J = 15.9, 6.2$ Hz, 2H), 6.62 (br d, $J = 15.9$ Hz, 1H), 6.87 (d, $J = 7.9$ Hz, 2H), 6.94 (dd, $J = 7.3, 7.3$ Hz, 1H), 7.09 (d, $J = 7.3$ Hz, 1H), 7.21-

7.31 (m, 5H), 7.80 (t, $J = 5.4$ Hz, 1H), 8.17 (d, $J = 7.8$ Hz, 1H). ^{13}C NMR (126 MHz, $\text{DMSO-}d_6$, major rotamer): δ 171.2, 171.1, 170.7, 169.1, 156.3, 152.8, 141.8, 135.8, 133.5, 129.6, 128.6, 128.0, 126.4, 124.2, 123.3, 121.2, 115.7, 81.5, 75.4, 66.9, 56.8, 51.9, 51.8, 49.8, 38.1, 37.0, 33.9, 31.1, 28.6, 27.4, 25.2, 22.2. MS m/z 666.1 (calc'd: $\text{C}_{36}\text{H}_{47}\text{N}_3\text{O}_9$, $[\text{M}+\text{H}]^+$, 665.3). (**28**) ^1H NMR (500 MHz, $\text{DMSO-}d_6$, major rotamer): δ 1.28-1.51 (m, 3H), 1.43 (s, 9H), 1.54-1.56 (m, 1H), 1.83 (s, 3H), 2.13 (dt, $J = 13.7, 2.5$ Hz, 1H), 2.33 (t, $J = 8.0$ Hz, 2H), 2.45-2.53 (m, 1H), 2.78 (t, $J = 8.0$ Hz, 2H), 2.96-3.03 (m, 2H), 3.63 (dd, $J = 11.3, 1.8$ Hz, 1H), 4.19 (dd, $J = 11.4, 5.5$ Hz, 1H), 4.41-4.46 (m, 1H), 4.48 (dd, $J = 9.5, 3.1$ Hz, 1H), 4.66 (dd, $J = 6.2, 1.0$ Hz, 2H), 5.09-5.13 (m, 1H), 6.32 (dd, $J = 15.9, 6.3$ Hz, 1H), 6.62 (br d, $J = 15.9$ Hz, 1H), 6.90 (d, $J = 7.9$ Hz, 2H), 6.94 (t, $J = 7.3$ Hz, 1H), 7.09 (d, $J = 7.3$ Hz, 1H), 7.21-7.31 (m, 5H), 7.78 (t, $J = 5.6$ Hz, 1H), 8.15 (d, $J = 8.1$ Hz, 1H), 12.52 (br s, 1H). ^{13}C NMR (126 MHz, $\text{DMSO-}d_6$, major rotamer): δ 172.2, 171.1, 170.5, 169.1, 156.6, 152.8, 141.8, 135.8, 133.5, 129.6, 128.6, 128.0, 126.4, 124.2, 123.3, 121.1, 115.7, 81.5, 75.5, 66.9, 56.9, 51.8, 49.8, 38.0, 37.0, 33.9, 31.1, 28.5, 27.4, 25.2, 22.3. MS m/z 652.0 (calc'd: $\text{C}_{35}\text{H}_{46}\text{N}_3\text{O}_9$, $[\text{M}+\text{H}]^+$, 652.3).



Macrocycle (29): To a stirred solution of **28** (1.89 g, 2.90 mmol) in TFE (247 mL) was added TFA (43.5 mL) in a single portion. The reaction was allowed to stir at rt for 16 hrs, after which the reaction was concentrated under reduced pressure at rt. The crude residue was purified by column chromatography on SiO_2 eluted with 0→10% MeOH in CHCl_3 to afford **29** as an off-white solid (1.30 g, 84%).



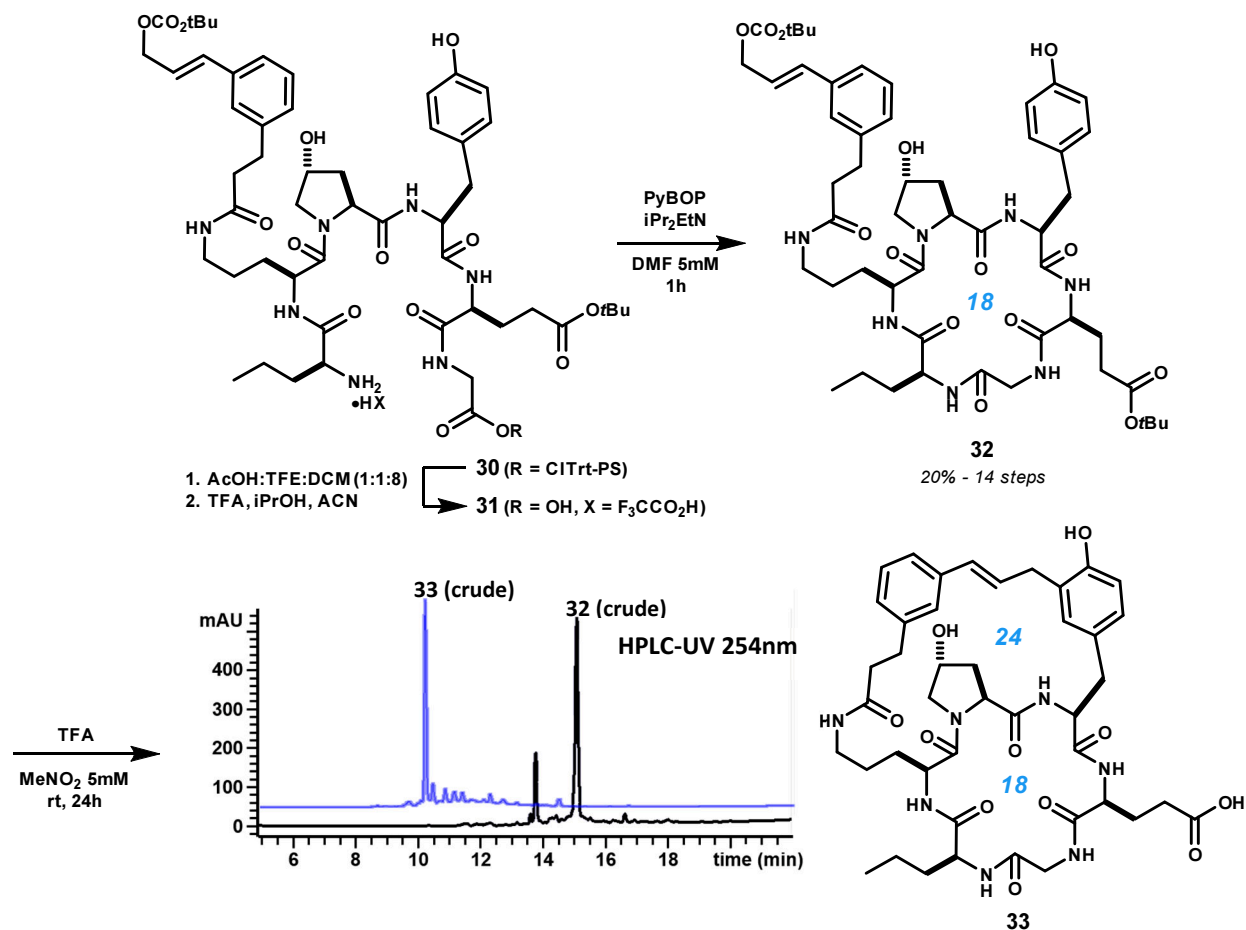
(600MHz, $\text{DMSO-}d_6$, 298K)

	^{13}C	^1H	key correlation
1	37.9	3.42 (br d, $J = 6.6$ Hz, 2H)	HMBC 1→3,27
2	130.5	6.18 (dd, $J = 15.6, 6.6$ Hz, 1H)	TOCSY 2→1,3
3	129.4	6.33 (br d, $J = 15.6$ Hz, 1H)	HMBC 3→5
4	136.9	-	
5	125.1	7.07 (br d, $J = 7.6$ Hz, 1H)	
6	128.5	7.18 (dd, $J = 7.6, 7.5$ Hz, 1H)	HMBC 6→4,8
7	127.6	6.99 (br d, $J = 7.5$ Hz, 1H)	
8	141.6	-	
9	123.4	7.14 (br s, 1H)	

10	30.0	2.70-2.77 (m, 1H), 2.84-2.91 (m, 1H)	HMBC 10→8,12
11	36.0	2.24-2.29 (m, 2H)	HMBC 11→8,12
12	171.3	-	
13	-	7.76 (t, $J = 4.9$ Hz, 1H)	TOCSY 13→14,15,16,17,18
14	38.0	2.58-2.66 (m, 2H)	
15	24.7	1.24-1.33 (m, 2H)	
16	28.6	1.31-1.47 (m, 2H)	HMBC 16→21
17	49.6	4.22 (ddd, $J = 8.4, 7.6, 6.2$ Hz, 1H)	HMBC 17→21
18	-	8.13 (d, $J = 7.6$ Hz, 1H)	HMBC 18→19
19	169.1	-	
20	22.3	1.78 (s, 3H)	HMBC 20→19
21	170.7	-	
22	50.4	3.52 (d, $J = 11.6$ Hz, 1H), 3.80 (dd, $J = 11.6, 3.3$ Hz, 1H)	
23	76.2	5.18 (apt t, $J = 3.5$ Hz, 1H)	TOCSY 23→22,28,29
24	154.3	-	
25	117.4	6.87 (d, $J = 8.4$ Hz, 2H)	HMBC 25→24,27
26	129.9	7.16 (d, $J = 8.4$ Hz, 2H)	HMBC 26→1,24
27	133.3	-	
28	34.7	2.44-2.52 (m, 1H), 2.34 (br d, $J = 13.9$ Hz, 1H)	
29	57.1	4.53 (d, $J = 9.7$ Hz, 1H)	
30	172.0	-	
31	-	not observed.	

MS m/z 534.0 (calc'd: $C_{30}H_{36}N_3O_6$, $[M+H]^+$, 534.3).

Bicyclic macrocycle 33:



Acyclic intermediate 31. 2-Chlorotrityl chloride polystyrene resin pre-loaded with glycine (0.7 mmol/g) analogously to compound **S25**. Peptide synthesis was carried out in the same manner as for compound **4** using PyBOP as the coupling reagent and Fmoc-Ornithine-(δ -3)-OH (**S24**) to incorporate template **3**. Resin-bound intermediate **30** was cleaved by treatment with AcOH:TFE:DCM (1:1:8) for 2 hrs, and the resulting solution was concentrated. This material was taken up in *i*PrOH:ACN + 0.1% TFA and re-concentrated several times, after which ¹H and ¹³C NMR showed very little residual AcOH. Compound **31** (300 mg, ~52% from 2-chlorotrityl chloride polystyrene resin) was carried forward without purification. MS m/z 1038.5 (calc'd: C₅₂H₇₆N₇O₁₅, [M+H]⁺, 1038.5) and 1036.4 (calc'd: C₅₂H₇₄N₇O₁₅, [M-H]⁻, 1036.4). See also crude ¹H-NMR in data appendix.

Macrolactam intermediate 32. Crude 31 (300 mg, ~0.26 mmol) was dissolved in DMF (52 mL) and treated with *i*Pr₂EtN (136 μ L, 0.78 mmol) and PyBOP (163 mg, 0.31 mmol). The mixture was stirred for 1 hr at rt, after which HPLC-UV/MS analysis showed complete conversion. The mixture was stirred an additional 1.5 hrs, then concentrated in vacuo and partitioned between EtOAc and sat. NH₄Cl. The organic phase was washed with sat. NH₄Cl (x1), sat. NaHCO₃ (x2), brine, dried over MgSO₄ and concentrated. Purification by column chromatography on SiO₂ eluted with 2 \rightarrow 12% MeOH in CHCl₃ afforded **32** (101 mg, 38%) as a white film. ¹H NMR (500 MHz, DMSO-*d*₆, major conformer): δ 0.85 (t, *J* = 7.3 Hz, 3H), 1.21-1.36 (m, 2H), 1.38 (s, 9H), 1.43 (s, 9H), 1.52-1.59 (m, 2H), 1.70-1.82 (m, 4H), 1.82-1.96 (m, 2H), 2.07-2.15 (m, 1H), 2.15-2.27 (m, 2H), 2.33-2.42 (m, 3H), 2.75-2.84 (m, 3H), 2.97-3.15 (m, 3H), 3.27-3.32 (m, 1H), 3.46-3.50 (m, 1H), 3.61 (dd, *J* = 11.0, 2.9 Hz, 1H), 3.82 (ddd, *J* = 10.6, 7.3, 4.8 Hz, 1H), 3.91 (dd, *J* = 13.6, 4.6 Hz, 1H), 3.99-4.08 (m, 1H), 4.22-4.30 (m, 2H), 4.34-4.39 (m, 1H), 4.40-4.47 (m, 1H), 4.65-4.69 (m, 2H), 5.14 (d, *J* = 3.1 Hz, 1H), 6.34 (dt, *J* = 16.0, 6.3 Hz, 1H), 6.60-6.65 (m, 1H), 6.64 (d, *J* = 8.4 Hz, 2H), 6.90 (d, *J* = 8.4 Hz, 2H), 7.12 (br d, *J* = 7.2 Hz, 1H), 7.22-7.32 (m, 3H), 7.52 (br d, *J* = 6.7 Hz, 1H), 7.63 (br d, *J* = 9.2 Hz, 1H), 7.84 (apt t, *J* = 5.4 Hz, 1H), 8.17 (br d, *J* = 7.2 Hz, 1H), 8.51 (d, *J* = 8.4 Hz, 1H), 8.81 (apt t, *J* = 5.2 Hz, 1H),

9.14-9.19 (m, 1H), 9.17 (s, 1H). ^{13}C NMR (126 MHz, $\text{DMSO-}d_6$): δ 172.3, 172.14, 172.06, 171.6, 171.5, 171.2, 171.1, 169.4, 156.2, 153.3, 142.3, 136.3, 133.9, 130.3, 129.2, 129.1, 128.9, 128.5, 126.9, 124.7, 123.8, 115.3, 82.0, 80.4, 80.1, 69.7, 67.4, 61.9, 61.1, 57.2, 55.5, 53.8, 52.8, 50.5, 44.8, 38.3, 37.4, 34.8, 33.1, 31.5, 31.3, 28.2, 27.8, 27.7, 27.4, 26.2, 19.4, 14.0. MS m/z 1020.5 (calc'd: $\text{C}_{52}\text{H}_{74}\text{N}_7\text{O}_{14}$, $[\text{M}+\text{H}]^+$, 1020.5).

Macrocycle 33: Intermediate **32** (46 mg, 45 μmol) was suspended in MeNO_2 (8.1 mL) and treated with TFA (900 μL). After 2 hr, HPLC-UV/MS analysis indicated a 3:1 mixture of **33** to the corresponding cinnamyl trifluoroacetate of **32**, and a 4:1 ratio after an additional 5 hrs. The mixture was allowed to stir for an additional 17 hrs, after which complete conversion was observed, and the mixture was concentrated and purified by semi-preparative HPLC. A yield was not recorded.

Analytical HPLC method:

Column: Waters Sunfire™ C_{18} , 4.6x250mm, 5 μm .

Solvent A: H_2O + 0.1%v TFA

Solvent B: ACN + 0.1%v TFA

Flow rate: 1.00 ml/min

Time	%B
0	25
25	45
25	50
30	25
35	25

Semi-preparative HPLC method A:

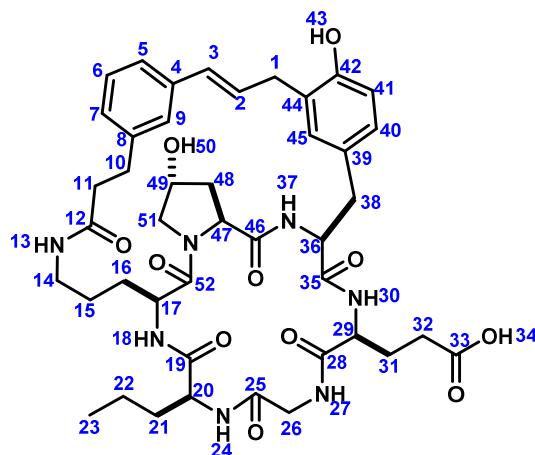
Column: Waters Sunfire™ C_{18} , 10x250mm, 5 μm .

Solvent A: H_2O + 0.1%v TFA

Solvent B: ACN + 0.1%v TFA

Flow rate: 6.00 ml/min

Time	%B
0	10
2	10
6	27
20	35.8
22	10
25	10



33

(500MHz, $\text{DMSO-}d_6$, 298K)

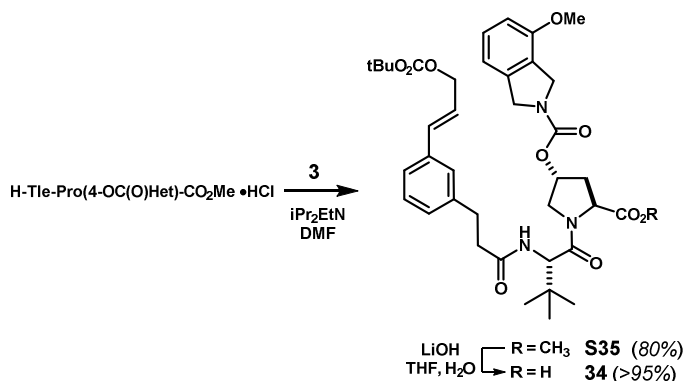
	^{13}C	^1H	key correlation
1	31.7	3.41 (d, $J = 7.0$ Hz, 2H)	HMBC 1 \rightarrow 2,3,42,44,45
2	127.9	6.36 (dt, $J = 15.9, 7.0$ Hz, 1H)	HMBC 2 \rightarrow 3,4,44
3	131.4	6.49 (d, $J = 15.9$ Hz, 1H)	HMBC 3 \rightarrow 2,4,5
4	137.2	-	
5	123.8	7.27 (br d, $J = 7.7$ Hz, 1H)	
6	128.6	7.24 (dd, $J = 7.7, 7.4$ Hz, 1H)	HMBC 6 \rightarrow 4,8 TOCSY 6 \rightarrow 5,7,9
7	127.4	7.13 (br d, $J = 7.4$ Hz, 1H)	

8	141.9	-	
9	125.5	7.22 (br s, 1H)	HMBC 9→5,7
10	30.4	2.86 (t, $J = 7.1$ Hz, 2H)	HMBC 10→8,12
11	35.9	2.51-2.57 (m, 2H)	HMBC 11→8,12
12	171.5	-	
13	-	7.76 (dd, $J = 5.8, 4.6$ Hz, 1H)	HMBC 13→12
14	36.2	2.89-2.96 (m, 1H), 3.20-3.28 (m, 1H)	COSY 14→15 HMBC 14→15,16
15	24.3	1.43-1.51 (m, 1H), 1.54-1.62 (m, 1H)	
16	25.5	1.59-1.66 (m, 1H), 1.76-1.84 (m, 1H)	
17	49.3	4.47 (br dd, $J = 10.9, 9.5$ Hz, 1H)	HMBC 17→52
18	-	7.65 (d, $J = 9.5$ Hz, 1H)	HMBC 18→19
19	171.6	-	
20	53.0	4.04 (ddd, $J = 10.0, 8.4, 3.6$ Hz, 1H)	HMBC 20→25
21	32.5	1.50-1.60 (m, 1H), 1.75-1.85 (m, 1H)	
22	18.8	1.24-1.38 (m, 2H)	
23	13.5	0.85 (t, $J = 7.4$ Hz, 2H)	TOCSY 23→24,22,21,20
24	-	8.49 (d, $J = 8.4$ Hz, 1H)	HMBC 24→25
25	169.0	-	
26	44.3	3.36 (dd, $J = 13.8, 6.4$ Hz, 1H), 3.85 (dd, $J = 13.8, 4.0$ Hz, 1H)	TOCSY 26→27, HMBC 26→25,28
27	-	8.92 (br s, 1H)	
28	171.08	-	
29	52.6	4.23 (apt dd, $J = 12.7, 6.2$ Hz, 1H)	HMBC 29→28
30	-	7.13-7.21 (m, 1H)	
31	27.8	1.82-1.94 (m, 2H)	HMBC 31→33
32	29.8	2.09 (ddd, $J = 16.4, 10.5, 6.0$ Hz, 1H), 2.19 (ddd, $J = 16.3, 10.5, 5.6$ Hz, 1H)	HMBC 32→33
33	173.8	-	
34	-	12.11 (br s, 1H)	
35	171.12	-	
36	55.8	4.08-4.15 (m, 1H)	
37	-	7.95 (br s, 1H)	
38	35.5	2.88-2.97 (m, 1H), 3.04 (dd, $J = 13.3, 3.5$ Hz, 1H)	TOCSY 38'→36,37,38 HMBC 38→35,36,39
39	128.60	-	
40	126.7	6.87-6.91 (m, 1H)	HMBC 40→38,42,45
41	114.8	6.72 (d, $J = 8.4$ Hz, 1H)	HMBC 41→1,39,44
42	153.0	-	
43	-	9.24 (br s, 1H)	
44	125.1	-	
45	129.9	6.88-6.90 (m, 1H)	HMBC 45→1,40,42
46	171.3	-	

47	61.1	3.91 (dd, $J = 11.3, 6.5$ Hz, 1H)	HMBC 47→46
48	37.3	1.39-1.49 (m, 1H), 1.57-1.66 (m, 1H)	
49	69.1	4.16 (br s, 1H)	HMBC 49→47
50	-	not observed	
51	55.0	3.37-3.43 (m, 1H), 3.55 (br d, $J = 10.8$ Hz, 1H)	
52	170.9	-	

MS m/z 846.3 (calc'd: $C_{43}H_{56}N_7O_{11}$, $[M+H]^+$, 846.4).

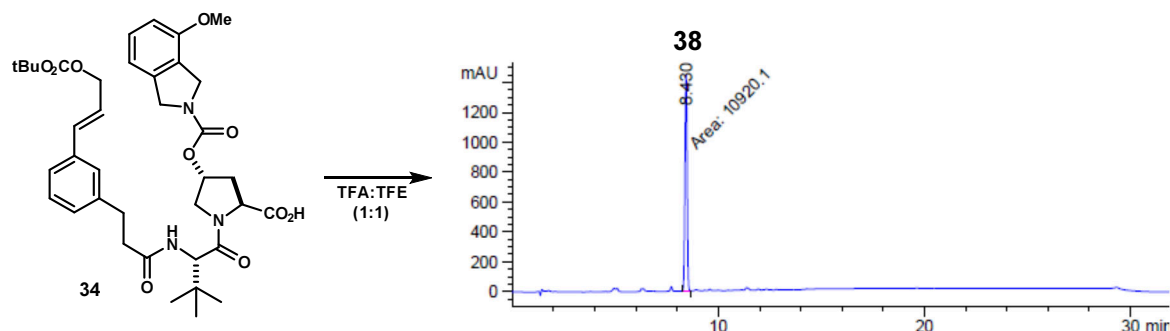
Macrocycle 38:



Methyl ester (S35): General procedure A and purification by flash chromatography on SiO_2 eluted with 0→10% acetone in DCM afforded compound **S35** as a light brown foam (1.50 g, 80%). $^1\text{H NMR}$ (500 MHz, $\text{DMSO-}d_6$, mixture of rotamers): δ 0.99 (s, 9H), 1.46 (s, 9H), 2.16 (ddd, $J = 13.6, 9.7, 3.9$ Hz, 1H), 2.30-2.39 (m, 1H), 2.41-2.45 (m, 2H), 2.58-2.68 (m, 2H), 3.61 (s, 1.5H), 3.72 (s, 3H), 3.76 (s, 1.5H), 3.78-3.85 (m, 1H), 4.32 (d, $J = 11.6$ Hz, 1H), 4.37 (d, $J = 14.7$ Hz, 0.5H), 4.46 (d, $J = 14.7$ Hz, 1H), 4.47-4.54 (m, 2H), 4.54-4.63 (m, 2H), 4.63-4.68 (m, 2H), 4.70 (d, $J = 14.7$ Hz, 1H), 5.28-5.34 (m, 1H), 6.23 (ddd, $J = 16.0, 5.7, 5.7$ Hz, 0.5H), 6.24 (ddd, $J = 16.1, 5.5, 5.5$ Hz, 0.5H), 6.55 (d, $J = 16.0$ Hz, 0.5H), 6.57 (d, $J = 16.1$ Hz, 0.5H), 6.68 (d, $J = 7.4$ Hz, 0.5H), 6.69 (d, $J = 7.4$ Hz, 0.5H), 6.74 (d, $J = 8.2$ Hz, 0.5H), 6.83 (d, $J = 7.5$ Hz, 0.5H), 6.93 (br d, $J = 6.7$ Hz, 1H), 7.06 (br s, 1H), 7.09-7.17 (m, 2H), 7.17-7.22 (m, 1H), 7.80 (d, $J = 8.3$ Hz, 0.5H), 7.85 (d, $J = 8.5$ Hz, 0.5H). $^{13}\text{C NMR}$ (126 MHz, $\text{DMSO-}d_6$, mixture of rotamers): δ 174.77, 174.76, 173.4, 172.7, 156.1, 155.9, 155.54, 155.46, 154.9, 142.6, 142.5, 139.6, 139.1, 137.6, 135.1, 135.0, 130.48, 130.46, 129.6, 129.1, 127.64, 127.60, 125.7, 125.45, 125.43, 125.3, 124.1, 115.7, 115.6, 109.8, 82.8, 75.4, 75.3, 68.37, 68.35, 59.34, 59.27, 59.21, 59.15, 55.8, 55.6, 55.41, 55.38, 53.7, 53.5, 52.7, 51.4, 51.1, 37.9, 37.7, 35.9, 35.69, 35.66, 32.5, 32.3, 28.1, 26.9. MS m/z 744.0 (calc'd: $C_{39}H_{51}N_3O_{10}\text{Na}$, $[M+\text{Na}]^+$, 744.4).

Acyclic precursor carboxylic acid (34): Methyl ester **S35** (244 mg, 0.34 mmol) was dissolved in $\text{THF:H}_2\text{O}$ (1:1, 3 mL), treated with $\text{LiOH}\cdot\text{H}_2\text{O}$ (42 mg, 1.0 mmol), and stirred for 2.5 hr. The mixture was acidified with 1N HCl and extracted with EtOAc (x3). The combined organic phase was washed with H_2O (x1), brine, dried over Na_2SO_4 and concentrated to give **34** as a white foam (242 mg, quant.). $^1\text{H NMR}$ (500 MHz, $\text{DMSO-}d_6$, mixture of rotamers): δ 0.92 (s, 9H), 1.43 (s, 9H), 2.08-2.15 (m, 1H), 2.15-2.22 (m, 1H), 2.36-2.59 (m, 4H), 3.65 (s, 1.5H), 3.71-3.78 (m, 1H), 3.76 (s, 1.5H), 4.15 (apt t, $J = 10.0$ Hz, 1H), 4.37 (apt t, $J = 8.4$ Hz, 1H), 4.39 (apt t, $J = 8.7$ Hz, 1H), 4.45 (br s, 1.2H), 4.48 (br d, $J = 15.0$ Hz, 0.8H), 4.54 (br s, 0.8H), 4.56 (d, $J = 15.0$ Hz, 0.8H), 4.60 (br s, 0.4H), 4.66 (d, $J = 6.2$ Hz, 2H), 5.21-5.28 (m, 1H), 6.29 (dt, $J = 16.0, 6.2$ Hz, 1H), 6.58 (d, $J = 16.0$ Hz, 0.5H), 6.59 (d, $J = 16.0, 0.5$ Hz), 6.78 (d, $J = 7.7$ Hz, 0.5H), 6.80 (d, $J = 7.7$ Hz, 0.5H), 6.83 (d, $J = 8.3$ Hz, 0.5H), 6.90 (d, $J = 7.4$ Hz, 1H), 6.92 (d, $J = 7.4$ Hz, 0.5H), 7.08 (br s, 0.5H), 7.10 (br s, 0.5H), 7.13-7.18 (m, 1H), 7.19-7.25 (m, 2H), 7.89 (d, $J = 8.9$ Hz, 0.5H), 7.92 (d, $J = 8.8$ Hz, 0.5H), 12.59 (br s, 1H). $^{13}\text{C NMR}$ (151 MHz, $\text{DMSO-}d_6$, mixture of rotamers): δ 172.9, 171.7, 170.23, 170.16,

154.4, 154.2, 153.45, 153.39, 152.8, 141.61, 141.6, 138.5, 138.0, 135.73, 135.71, 133.48, 133.46, 129.3, 129.2, 128.4, 127.9, 126.2, 124.3, 124.1, 123.9, 123.2, 114.8, 114.7, 109.1, 109.0, 81.5, 73.53, 73.51, 66.9, 57.4, 57.0, 56.9, 55.2, 55.0, 53.8, 53.7, 52.5, 52.1, 50.1, 49.7, 35.9, 35.7, 34.4, 34.3, 34.2, 30.7, 30.6, 27.4, 27.3, 26.3. MS m/z 706.0 (calc'd: $C_{38}H_{48}N_3O_{10}$, $[M-H]^-$, 706.3).



Macrocycle 38: Compound **34** (246 mg, 0.35 mmol) was dissolved in TFE (3.0 mL) and added dropwise over ~5 min to a stirred solution of TFA (17.4 mL) in TFE (14.4 mL). The reaction was stirred at room temperature for 25 min, concentrated by rotary evaporation (bath 35 °C), dried in vacuo, and purified by flash chromatography on SiO_2 eluted with 0→6% MeOH in DCM to give **38** as a white foam (149 mg, 73%). HPLC analysis was performed using the following method.

Analytical HPLC method:

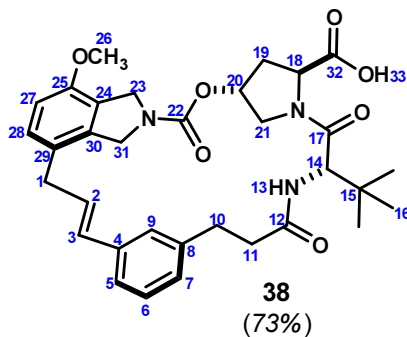
Column: Waters Sunfire™ C₁₈, 4.6x250mm, 5μm.

Solvent A: H₂O + 0.1%v TFA

Solvent B: ACN + 0.1%v TFA

Flow rate: 1.00 ml/min

Time	%B
0	50
1	50
10	100
25	100
27	50
32	50



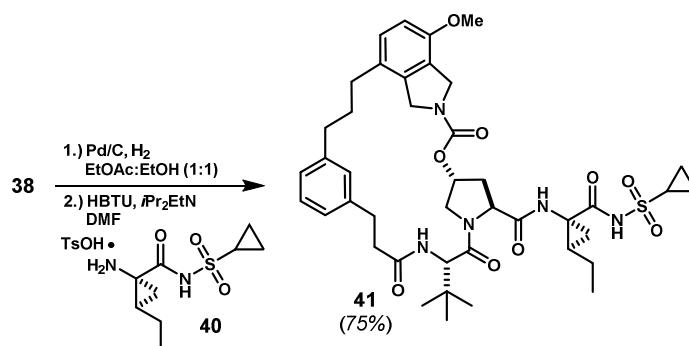
(600MHz, DMSO-*d*₆, 298K)

	¹³ C	¹ H	key correlations
1	36.3	3.44 (d, $J = 3.8$ Hz, 2H)	COSY 1→2,3 HMBC 1→2,3,29,30
2	127.20	6.17-6.21 (m, 1H) overlap	

3	130.40	6.17-6.21 (m, 1H) overlap	
4	136.1	-	
5	121.8	7.23 (br d, $J = 7.8$ Hz, 1H)	HMBC 5→3
6	129.7	7.15 (dd, $J = 7.8, 7.6$ Hz, 1H)	HMBC 6→4,8
7	127.2	7.03 (br d, $J = 7.6$ Hz, 1H)	HMBC 7→10
8	141.7	-	
9	126.8	6.97 (br s, 1H)	HMBC 9→3,10
10	28.8	2.97 (ddd, $J = 14.7, 11.8, 2.3$ Hz, 1H), 2.64 (ddd, $J = 14.7, 6.6, 1.8$ Hz, 1H)	
11	33.9	2.75 (ddd, $J = 16.2, 11.8, 1.8$ Hz, 1H), 2.47 (ddd, $J = 16.2, 6.6, 2.3$ Hz, 1H)	
12	170.9	-	
13	-	7.83 (d, $J = 9.4$ Hz, 1H)	HMBC 13→12
14	55.9	4.52 (d, $J = 9.4$ Hz, 1H)	HMBC 14→12,15,16,17
15	35.8	-	
16	26.3	0.94 (s, 9H)	
17	169.4	-	
18	57.7	4.35 (t, $J = 7.7$ Hz, 1H)	HMBC 18→32
19	34.9	2.14-2.20 (m, 2H)	
20	73.0	5.32-5.36 (m, 1H)	
21	53.1	3.93 (dd, $J = 11.4, 5.5$ Hz, 1H), 3.51 (br d, $J = 11.4$ Hz, 1H)	
22	153.3	-	
23	50.0	4.49-4.51 (m, 2H)	HMBC 23→24,25,30
24	124.0	-	
25	153.1	-	
26	55.1	3.79 (s, 3H)	HMBC 26→25
27	109.6	6.87 (d, $J = 8.3$ Hz, 1H)	HMBC 27→23,24,25,29
28	127.9	7.16 (d, $J = 8.3$ Hz, 1H)	HMBC 28→25,30
29	126.0	-	
30	137.5	-	
31	50.8	4.58 (br d, $J = 14.6$ Hz, 1H), 4.47 (br d, $J = 14.6$ Hz, 1H)	NOESY 31→1 HMBC 31→24,30
32	173.3	-	
33	-	not observed	

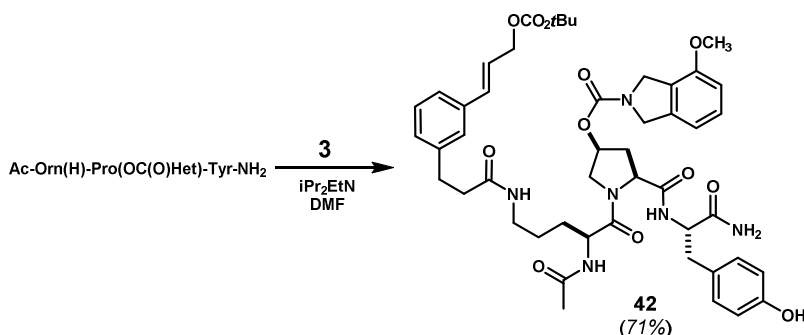
MS m/z 588.0 (calc'd: $C_{33}H_{38}N_3O_7$, $[M-H]^-$, 588.3), $[\alpha]_D^{20} = -37.2^\circ$ (c = 0.5, $CHCl_3$).

Vaniprevir analog 41:



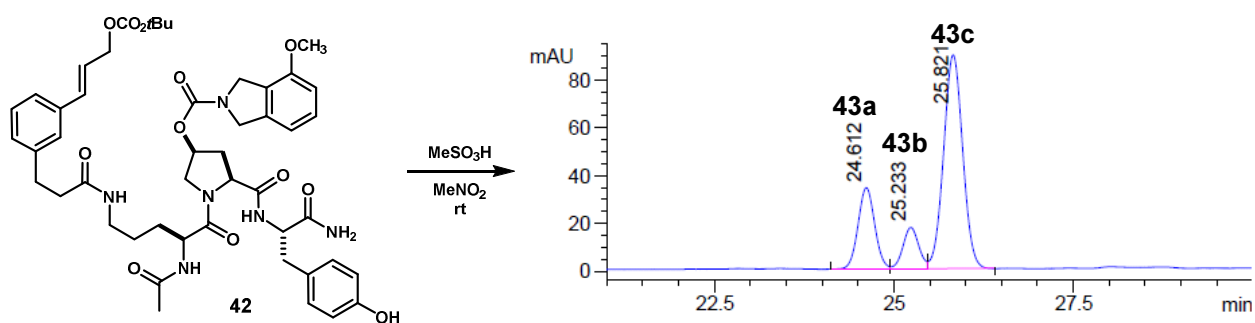
Vaniprevir analog (41): Compound **38** (149 mg, 0.25 mmol) was dissolved in EtOAc:EtOH (1:1, 3 mL), Pd/C (10wt%, 10 mg) was added and the mixture was stirred under 500 psi H₂ for 1 hr after which ¹H NMR indicated complete reduction of the olefin. The mixture was filtered through Celite and concentrated to give a tan foam (143 mg), which was dissolved in DMF (1.5 mL) and used directly in the next reaction. Tosylate salt **40** (98 mg, 0.24mmol) and *i*Pr₂EtN (93 μL, 0.53mmol), were added and the mixture was cooled in an ice bath before adding HBTU (101 mg, 0.27 μmol). The reaction was allowed to warm to room temperature and stirred for 3 h. The mixture was diluted with EtOAc and washed with sat. NH₄Cl (x2), brine, dried over MgSO₄, and concentrated. Purification by flash chromatography on SiO₂ eluted with 0→4% MeOH in DCM afforded **41** as a colorless film (145 mg, 75% over 2 steps). ¹H NMR (500 MHz, CDCl₃): δ 0.96 (t, *J* = 7.3 Hz, 3H), 1.02-1.10 (m, 2H), 1.05 (s, 9H), 1.31-1.36 (m, 2H), 1.38-1.47 (m, 2 H), 1.56-1.73 (m, 2H), 1.69 (ddd, *J* = 7.8, 7.8, 6.0 Hz, 1H), 1.83-2.00 (m, 2H), 2.25 (ddd, *J* = 13.7, 10.8, 4.0 Hz, 1H), 2.43 (dd, *J* = 11.4, 7.2 Hz, 1H), 2.45 (t, *J* = 7.7 Hz, 2H), 2.62-2.67 (m, 2H), 2.67-2.73 (m, 1H), 2.74-2.81 (m, 1H), 2.93 (dddd, *J* = 8.4, 8.4, 4.9, 4.4 Hz, 1H), 3.14 (ddd, *J* = 14.0, 10.5, 2.4 Hz, 1H), 3.83 (s, 3H), 3.89 (dd, *J* = 12.0, 4.2 Hz, 1H), 4.06 (d, *J* = 12.0 Hz, 1H), 4.25 (dd, *J* = 10.8, 6.6 Hz, 1H), 4.61 (d, *J* = 9.5 Hz, 1H), 4.61 (d, *J* = 15.1 Hz, 1H), 4.69 (d, *J* = 15.1 Hz, 1H), 5.42 (apt dd, *J* = 3.6, 3.6 Hz, 1H), 6.38 (d, *J* = 9.5 Hz, 1H), 6.74 (d, *J* = 8.3 Hz, 1H), 6.94 (d, *J* = 7.5 Hz, 1H), 7.08 (d, *J* = 7.5 Hz, 1H), 7.10 (d, *J* = 8.3 Hz, 1H), 7.18 (dd, *J* = 7.5, 7.5 Hz, 1H), 7.27 (s, 1H), 10.34 (s, 1H). ¹³C NMR (151 MHz, CDCl₃): δ 172.2, 171.6, 171.5, 170.0, 153.7, 153.1, 141.6, 141.2, 136.8, 128.9, 128.73, 128.68, 128.3, 126.4, 126.0, 124.3, 109.4, 74.1, 60.3, 57.3, 55.4, 54.5, 51.5, 51.0, 39.3, 36.7, 36.0, 35.9, 35.3, 35.2, 31.55, 31.46, 30.5, 29.8, 26.9, 23.8, 19.7, 13.8, 6.5, 6.0. MS *m/z* 806.0 (calc'd: C₄₂H₅₆N₅O₉S, [M+H]⁺, 806.4).

Macrocycles 43a-c:



Acyclic carbonate (42): General procedure A afforded compound **42** as a colorless film (221 mg, 71%). ¹H NMR (600 MHz, DMSO-*d*₆, major rotamer): δ 1.37-1.48 (m, 2H), 1.42 (s, 9H), 1.48-1.65 (m, 2H), 1.84 (s, 3H), 2.07-2.14 (m, 1H), 2.30-2.44 (m, 2H), 2.71-2.83 (m, 2H), 2.93-3.08 (m, 3H), 3.57-3.66 (m, 1H), 3.69 (s, 1.5H), 3.79 (s, 1.5H), 3.99-4.17 (m, 2H), 4.26-4.32 (m, 1H), 4.38-4.54 (m, 5H), 4.59 (br s, 1H), 4.62-4.70 (m, 3H), 5.13-5.19 (m, 1H), 6.27-6.38 (m, 1H), 6.57-6.63 (m, 2H), 6.80-6.92 (m, 2H), 6.93-7.03 (m, 3H), 7.04-7.08 (m, 1H), 7.09-7.15 (m, 1H), 7.16-7.33 (m, 6H), 7.76-7.80 (m, 1H), 8.15-8.20 (m, 1H), 9.12 (br s, 1H). ¹³C NMR (151 MHz, DMSO-*d*₆, mixture of rotamers): δ 173.6, 173.3, 173.1, 171.8, 171.70, 171.67,

171.64, 171.57, 171.4, 171.03, 170.98, 170.5, 170.4, 169.72, 169.69, 158.8, 158.6, 156.23, 156.21, 156.1, 156.0, 154.9, 154.82, 154.78, 154.7, 153.9, 153.8, 153.6, 153.3, 142.3, 142.2, 139.0, 138.4, 138.3, 136.33, 136.27, 133.9, 130.54, 130.50, 130.4, 129.73, 129.67, 129.1, 129.03, 128.96, 128.9, 128.5, 128.4, 128.2, 128.1, 126.9, 126.4, 125.1, 124.8, 124.7, 124.6, 124.3, 124.2, 123.8, 123.7, 115.3, 115.2, 115.0, 109.5, 109.4, 82.0, 73.54, 73.52, 72.4, 72.2, 69.4, 67.4, 62.0, 59.54, 59.45, 58.9, 58.8, 56.9, 56.7, 55.74, 55.69, 55.55, 55.53, 54.7, 54.6, 52.92, 52.85, 52.8, 52.64, 52.56, 52.4, 51.9, 51.70, 51.67, 50.58, 50.55, 50.4, 50.2, 50.1, 49.8, 49.1, 38.6, 38.5, 37.45, 37.43, 37.2, 37.0, 36.1, 34.6, 34.5, 31.54, 31.49, 28.99, 28.96, 28.9, 28.5, 28.4, 27.8, 26.02, 25.97, 25.75, 25.72, 22.69, 22.67. MS m/z 913.2 (calc'd: C₄₈H₆₁N₆O₁₂, [M+H]⁺, 913.4).



Compound **42** was subjected to general procedure C. HPLC analysis and purification was performed using the following methods. The product mixture was first purified by semi-preparative HPLC method A to isolate minor product **43b**, which was re-purified by the same method. Subsequently, co-eluting products **43a** and **43c** were resolved using method B.

Analytical HPLC method:

Column: Waters Sunfire™ C₁₈, 4.6x250mm, 5μm.

Solvent A: H₂O + 0.1%v TFA

Solvent B: ACN + 0.1%v TFA

Flow rate: 1.00 ml/min

Time	%B
0	30
2	30
37	43
42	100
52	100
54	30
57	30

Semi-preparative HPLC method A:

Column: Waters XBridge™ C₁₈, 10x250mm, 5μm.

Solvent A: H₂O + 0.1%v TFA

Solvent B: ACN + 0.1%v TFA

Flow rate: 7.50 ml/min

Time	%B
0	27
2	27
36.5	37
39	27
42	27

Semi-preparative HPLC method B:

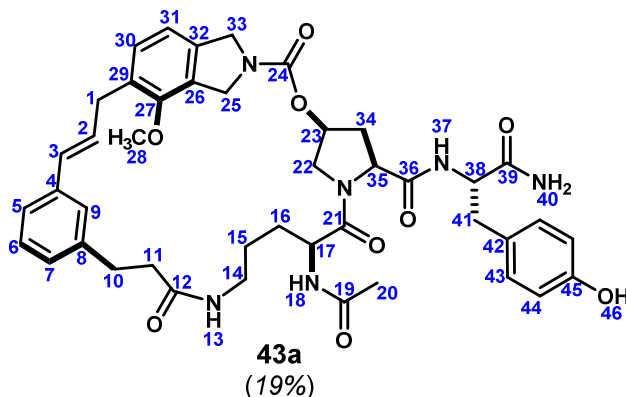
Column: Waters XBridge™ phenyl, 10x250mm, 5μm.

Solvent A: H₂O + 0.1%v TFA

Solvent B: ACN + 0.1%v TFA

Flow rate: 7.50 ml/min

Time	%B
0	30
2	30
18	40.3
20	30
23	30

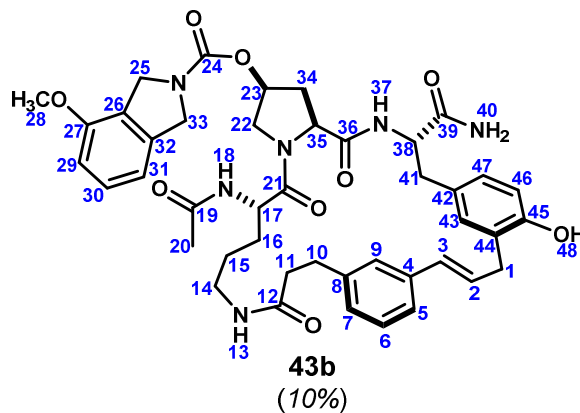


(600MHz, DMSO-*d*₆, 298K, ~3:1 mixture of conformers, data is of major)

¹³ C	¹ H	key correlations
1	33.6 3.70 (dd, <i>J</i> = 14.4, 5.1Hz, 1H) overlap, 3.19 (dd, <i>J</i> = 14.4, 6.2Hz, 1H)	HMBC 1→27,29
2	129.2 6.23 (ddd, <i>J</i> = 15.9, 6.2, 5.1Hz, 1H)	HMBC 2→4
3	129.0 6.18 (br d, <i>J</i> = 15.9Hz, 1H)	HMBC 3→5,9
4	136.9 -	
5	123.5 7.11 (d, <i>J</i> = 7.5Hz, 1H) overlap	HMBC 5→3,7
6	128.1 7.15 (dd, <i>J</i> = 7.5, 7.5Hz, 1H)	HMBC 6→4,8
7	127.0 6.97 (d, <i>J</i> = 7.5Hz, 1H)	
8	141.7 -	
9	124.4 7.02 (br s, 1H) overlap	HMBC 9→3,7
10	29.9 2.71 (ddd, <i>J</i> = 13.9, 6.8, 6.8Hz, 1H), 2.70 - 2.82 (m, 1H) overlap	HMBC 10→8,12
11	36.3 2.23 - 2.29 (m, 2H) overlap	HMBC 11→8 COSY 11→10
12	171.1 -	
13	- 7.68 - 7.71 (m, 1H) overlap	HMBC 13→12 COSY 13→14
14	38.3 2.99 - 3.06 (m, 1H), 2.82 - 2.89 (m, 1H) overlap	HMBC 14→12
15	24.4 1.49 - 1.57 (m, 1H), 1.37 - 1.47 (m, 1H) overlap	
16	29.2 1.60 - 1.68 (m, 1H), 1.41 - 1.49 (m, 1H) overlap	
17	50.0 4.36 (ddd, <i>J</i> = 14.1, 7.6, 6.2Hz, 1H)	HMBC 17→19,21
18	- 8.09 (d, <i>J</i> = 7.6Hz, 1H)	
19	168.9 -	
20	21.9 1.79 (s, 3H)	HMBC 20→19
21	170.5 -	
22	53.8 3.85 (dd, <i>J</i> = 12.0, 4.3Hz, 1H), 3.67 (br d, <i>J</i> = 12.0Hz, 1H) overlap	
23	72.8 5.36 (apt dd, <i>J</i> = 4.2, 4.2Hz, 1H)	COSY 23→22 TOCSY 23→22,34,35
24	153.3 -	
25	50.2 4.97 (dd, <i>J</i> = 15.5, 1.3Hz, 1H), 4.52 (br d, <i>J</i> = 15.5Hz, 1H)	HMBC 25→26,32
26	127.0 -	

27	152.9	-	
28	59.1	3.83 (s, 3H)	HMBC 28→27
29	130.0	-	
30	129.8	7.12 (d, $J = 7.7\text{Hz}$, 1H) overlap	HMBC 30→27,32 COSY 30→31
31	116.9	6.95 (d, $J = 7.7\text{Hz}$, 1H)	HMBC 31→26,29
32	137.3	-	
33	51.0	4.68 (dd, $J = 15.4, 1.3\text{Hz}$, 1H), 4.48 (br d, $J = 15.4\text{Hz}$, 1H)	HMBC 33→32,26
34	34.5	2.46 (ddd, $J = 14.4, 10.3, 5.0\text{Hz}$, 1H), 2.18 (br d, $J = 14.4\text{Hz}$, 1H)	
35	58.1	4.43 (dd, $J = 10.3, 1.7\text{Hz}$, 1H)	HMBC 35→36
36	169.7	-	
37	-	7.69 (d, $J = 7.6\text{Hz}$, 1H) overlap	
38	54.3	4.25 (ddd, $J = 7.7, 7.6, 5.6\text{Hz}$, 1H)	HMBC 38→36,39,42
39	172.8	-	
40	-	7.21 (br s, 1H), 7.03 (br s, 1H) overlap	TOCSY 40→40' HMBC 40→39
41	36.4	2.89 (dd, $J = 13.9, 5.6\text{Hz}$, 1H), 2.77 (dd, $J = 13.9, 7.7\text{Hz}$, 1H)	HMBC 41→42
42	127.7	-	
43	130.0	7.02 (d, $J = 8.3\text{Hz}$, 2H)	HMBC 43→45
44	114.5	6.62 (d, $J = 8.3\text{Hz}$, 2H)	HMBC 44→42
45	155.6	-	
46	-	9.15 (br s, 1H)	

MS m/z 795.3 (calc'd: $\text{C}_{43}\text{H}_{51}\text{N}_6\text{O}_9$, $[\text{M}+\text{H}]^+$, 795.4).



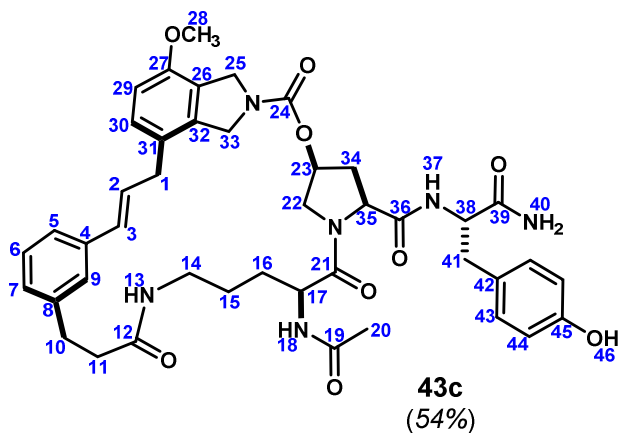
(600MHz, $\text{DMSO}-d_6$, 298K, ~3:1:1 mixture of conformers, data is of major)

	^{13}C	^1H	key correlations
1	31.6	3.45 - 3.51 (m, 1H) overlap, 3.31 (dd, $J = 15.8, 6.7\text{Hz}$, 1H)	HMBC 1→44,45
2	128.3	6.32 (ddd, $J = 15.5, 12.7, 6.8\text{Hz}$, 1H)	COSY 2→1,3 HMBC 2→4,44
3	130.5	6.44 (br d, $J = 15.5\text{Hz}$, 1H)	
4	137.0	-	

5	124.1	7.11 (d, $J = 7.6\text{Hz}$, 1H) overlap	HMBC 5→3
6	128.0	7.16 (dd, $J = 7.6, 7.6\text{Hz}$, 1H)	HMBC 6→4,8
7	127.0	7.00 (d, $J = 7.6\text{Hz}$, 1H) overlap	HMBC 7→10
8	141.2	-	
9	124.5	7.34 (br s, 1H)	TOCSY 9→5,6,7 HMBC 9→10
10	30.7	2.76 - 2.82 (m, 2H) overlap	HMBC 10→8,12
11	36.6	2.34 - 2.41 (m, 1H) overlap	HMBC 11→8,12
12	171.0	-	
13	-	7.61 - 7.65 (m, 1H) overlap	HMBC 13→12 TOCSY 13→14,15,16,17,18
14	37.8	2.90 - 3.07 (m, 2H)	
15	24.5	1.33 - 1.41 (m, 2H) overlap	COSY 14→15
16	28.3	1.58 - 1.65 (m, 1H), 1.35 - 1.43 (m, 1H)	
17	49.6	4.41 - 4.46 (m, 1H) overlap	HMBC 17→19,21
18	-	8.08 (d, $J = 7.6\text{Hz}$, 1H) overlap	HMBC 18→19 COSY 18→17
19	169.0	-	
20	21.9	1.82 (s, 3H)	HMBC 20→19
21	170.9	-	
22	52.3	4.15 (ddd, $J = 11.3, 11.2, 5.7\text{Hz}$, 1H), 3.66 (br d, $J = 11.3\text{Hz}$, 1H)	
23	72.9	5.13 - 5.18 (m, 1H)	COSY 23→22,34
24	?	-	
25	49.6	4.47 (s, 2H) overlap	HMBC 25→27,32
26	123.5	-	
27	154.1	-	
28	55.0	3.78 (s, 3H)	HMBC 28→27
29	108.8	6.79 (d, $J = 8.1\text{Hz}$, 1H)	HMBC 29→26
30	128.8	7.23 (dd, $J = 8.1, 7.6\text{Hz}$, 1H)	HMBC 30→32 COSY 30→31,29
31	114.5	6.87 (d, $J = 7.6\text{Hz}$, 1H)	HMBC 31→26
32	137.5	-	
33	49.4	4.48 (s, 2H) overlap	HMBC 33→26
34	33.9	2.37 - 2.43 (m, 1H) overlap, 2.16 (dddd, $J = 13.4, 13.4, 3.2, 3.2\text{Hz}$, 1H)	HMBC 34→35,36
35	58.0	4.46 - 4.50 (m, 1H) overlap	
36	170.0	-	
37	-	7.67 (d, $J = 8.5\text{Hz}$, 1H)	HMBC 37→36
38	54.1	4.30 - 4.35 (m, 1H)	HMBC 38→36,39,42
39	172.9	-	
40	-	7.34 (br s, 1H) overlap, 7.04 (br s, 1H)	TOCSY 40→40' HMBC 40→39,38
41	37.0	2.72 - 2.83 (m, 2H) overlap	HMBC 41→39,42
42	127.4	-	

43	129.6	6.91 (d, $J = 1.5\text{Hz}$, 1H)	HMBC 43→1,41,45
44	125.9	-	
45	153.1	-	
46	114.2	6.68 (d, $J = 8.1\text{Hz}$, 1H)	HMBC 46→44,45
47	127.2	6.82 - 6.85 (m, 1H) overlap	HMBC 47→45
48	-	9.21 (br s, 1H)	

MS m/z 795.3 (calc'd: $\text{C}_{43}\text{H}_{51}\text{N}_6\text{O}_9$, $[\text{M}+\text{H}]^+$, 795.4).



(600MHz, $\text{DMSO}-d_6$, 298K, ~10:7 mixture of conformers, data is of major)

^{13}C	^1H	key correlations
1	35.6 3.44 (d, $J = 6.4\text{Hz}$, 1H), 3.42 (d, $J = 6.7\text{Hz}$, 1H)	HMBC 1→31,32
2	128.0 6.26 (ddd, $J = 15.8, 6.6, 6.4\text{Hz}$, 1H)	HMBC 2→4,31
3	129.8 6.32 (d, $J = 15.8\text{Hz}$, 1H)	HMBC 3→5,9
4	136.6 -	
5	124.0 7.06 (d, $J = 8.1\text{Hz}$, 1H) overlap	
6	128.1 7.15 (dd, $J = 8.1, 8.1\text{Hz}$, 1H) overlap	HMBC 6→4,8
7	127.1 7.01 (d, $J = 8.1\text{Hz}$, 1H) overlap	
8	141.3 -	
9	124.5 7.27 (br s, 1H)	HMBC 9→7
10	30.7 2.74-2.82 (m, 2H) overlap	HMBC 10→8,11,12
11	36.6 2.30-2.39 (m, 2H)	HMBC 11→8,10,12
12	171.5 -	
13	- 7.69-7.72 (m, 1H) overlap	TOCSY 13→14,15,16,17,18
14	37.8 2.99-3.06 (m, 2H)	
15	24.4 1.37-1.50 (m, 2H) overlap	HMBC 15→17
16	28.2 1.62-1.71 (m, 1H), 1.43-1.49 (m, 1H) overlap	HMBC 16→21
17	49.6 4.41-4.45 (m, 1H)	HMBC 17→21
18	- 8.12 (d, $J = 7.4\text{Hz}$, 1H) overlap	HMBC 18→19
19	169.1 -	
20	21.9 1.81 (s, 3H)	HMBC 20→19

21	170.8	-	
22	51.8	4.10 (dd, $J = 10.8, 6.0\text{Hz}$, 1H), 3.55-3.60 (m, 1H) overlap	
23	71.9	5.25 (ddd, $J = 11.0, 5.6, 5.3\text{Hz}$, 1H)	HMBC 23→24 COSY 23→22,34
24	153.2	-	
25	50.0	4.67 (s, 2H)	HMBC 25→27
26	123.8	-	
27	152.8	-	
28	55.0	3.78 (s, 3H)	HMBC 28→27
29	109.5	6.87 (d, $J = 7.7\text{Hz}$, 1H) overlap	HMBC 29→26,27,31
30	123.8	7.15 (d, $J = 7.7\text{Hz}$, 1H) overlap	HMBC 30→38,32
31	126.4	-	
32	136.8	-	
33	50.7	4.55 (d, $J = 14.8\text{Hz}$, 1H), 4.51 (d, $J = 14.8\text{Hz}$, 1H)	
34	34.0	2.45-2.51 (m, 1H) overlap, 1.96-2.02 (m, 1H)	HMBC 34→35
35	58.0	4.34 (ddd, $J = 7.6, 7.5, 6.2\text{Hz}$, 1H)	
36	170.1	-	
37	-	7.78-7.72 (m, 1H) overlap	HMBC 37→36
38	53.9	4.28 (ddd, $J = 7.6, 7.5\text{Hz}, 6.2\text{Hz}$, 1H)	COSY 38→41 HMBC 38→41,36,42
39	172.5	-	
40	-	7.22 (br s, 1H), 7.01 (br s, 1H)	TOCSY 40→40' HMBC 40→39
41	36.4	2.79-2.85 (m, 1H) overlap, 2.71-2.76 (m, 1H) overlap	HMBC 41→40,42
42	127.5	-	
43	129.9	6.94 (d, $J = 8.3\text{Hz}$, 2H)	HMBC 43→45
44	114.5	6.59 (d, $J = 8.3\text{Hz}$, 2H)	HMBC 44→42
45	155.6	-	
46	-	9.15 (br s, 1H)	

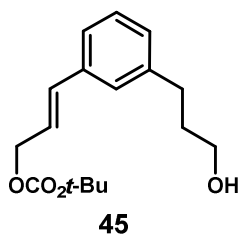
MS m/z 795.3 (calc'd: $\text{C}_{43}\text{H}_{51}\text{N}_6\text{O}_9$, $[\text{M}+\text{H}]^+$, 795.4).

Template 2:

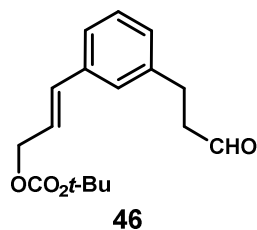
Phenylpropionic acid 44. See compound **3-15** (Chapter 3).⁶⁰

⁶⁰ Lawson, K. V; Rose, T. E.; Harran, P. G. *Proc. Natl. Acad. Sci. U. S. A.* **2013**, *110*, E3753.

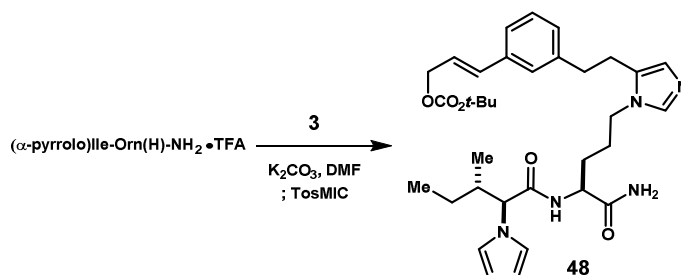
Phenylpropanol 45. Phenylpropionic acid derivative **44** (700 mg, 2.28 mmol) was dissolved in THF (3.0 mL) and cooled in an ice bath. To this mixture was added $\text{BH}_3 \cdot \text{THF}$ (2.8 mL, 1.0M), and the reaction continued cold for 10 min, then allowed to warm to rt and stirred for 15 hr. The reaction was quenched with H_2O , concentrated and partitioned between EtOAc:H₂O. The organic phase was washed with sat. NH_4Cl , dried over MgSO_4 and concentrated to give **45** as a colorless oil (640 mg, 96%). ¹H NMR (CDCl_3 , 500 MHz): δ 1.47 (s, 9H), 1.84 (tt, $J = 7.7, 6.5$ Hz, 2H), 2.64 (t, $J = 7.7$ Hz, 2H), 3.61 (t, $J = 6.5$ Hz, 2H), 3.68 (br s, 1H), 4.67 (br d, $J = 6.5$ Hz, 2H), 6.24 (dt, $J = 15.9, 6.5$ Hz, 1H), 6.60 (br d, $J = 15.9$ Hz, 1H), 7.04-7.08 (m, 1H), 7.16-7.21 (m, 3H). ¹³C NMR (CDCl_3 , 101 MHz): δ 153.3, 142.1, 136.1, 134.3, 128.5, 128.1, 126.7, 124.1, 122.6, 82.0, 67.4, 61.7, 33.9, 31.8, 27.6. MS m/z 315.1 (calc'd: $\text{C}_{17}\text{H}_{24}\text{NaO}_4$, $[\text{M}+\text{Na}]^+$, 315.2).



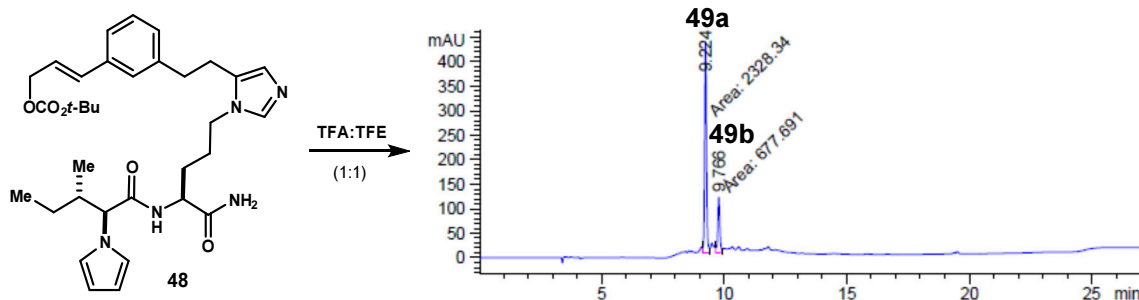
Template 46. Alcohol **45** (85 mg, 0.29 mmol) was dissolved in DCM (2.0 mL), and 4Å molecular sieves (180 mg) were added followed by PCC (108 mg, 0.5 mmol). The mixture was stirred at rt for 2hr, filtered through a pad of Celite and concentrated. Purification by flash chromatography on SiO_2 eluted with 7:1 hexanes:EtOAc afforded template **46** as a colorless oil (41 mg, 49%). ¹H NMR (CDCl_3 , 400 MHz): δ 1.48 (s, 9H), 2.73 (tt, $J = 7.6, 1.1$ Hz, 2H), 2.91 (t, $J = 7.6$ Hz, 2H), 4.69 (dd, $J = 6.4, 1.2$ Hz, 2H), 6.26 (dt, $J = 15.9, 6.4$ Hz, 1H), 6.61 (dt, $J = 15.9, 1.2$ Hz, 1H), 7.04-7.09 (m, 1H), 7.17-7.23 (m, 3H), 9.77 (t, $J = 1.1$ Hz, 1H). ¹³C NMR (CDCl_3 , 101 MHz): δ 201.2, 153.3, 140.7, 136.5, 134.1, 128.8, 128.0, 126.6, 124.6, 123.1, 82.1, 67.3, 45.1, 27.9, 27.8. MS m/z 173.1 (calc'd: $\text{C}_{12}\text{H}_{13}\text{O}$, $[\text{M}-\text{OCO}_2\text{t-Bu}]^+$, 173.1).



Macrocycles 49a,b:



Acyclic carbonate 48. The peptide (56 mg, 0.14 mmol) was dissolved in dry DMF (1.2 mL), template **2** (41 mg, 0.14 mmol) and anhydrous K_2CO_3 (55 mg, 0.40 mmol) were added, and the mixture was stirred for 2 hr. Tosylmethylisocyanide (27 mg, 0.14 mmol) was added, and stirring was continued for 17 hr. The mixture was diluted with H_2O and purified by preparative HPLC (35→100% ACN + 0.1% TFA, 17min, Waters Sunfire C18 19x250mm) to give **48** (17 mg, 20%). ¹H NMR (600 MHz, $\text{DMSO}-d_6$): δ 0.73 (t, $J = 7.3$ Hz, 3H), 0.78-0.83 (m, 1H), 0.84 (d, $J = 6.6$ Hz, 3H), 0.94-1.02 (m, 1H), 1.43 (s, 9H), 1.43-1.64 (m, 4H), 2.07-2.17 (m, 1H), 2.84-2.89 (m, 2H), 2.90-2.95 (m, 2H), 3.97-4.08 (m, 2H), 4.29 (ddd, $J = 8.3, 8.0, 5.5$ Hz, 1H), 4.36 (d, $J = 11.0$ Hz, 1H), 4.68 (dd, $J = 6.2, 0.8$ Hz, 2H), 5.87 (dd, $J = 2.0, 2.0$ Hz, 1H), 6.38 (dt, $J = 15.9, 6.2$ Hz, 1H), 6.66 (br d, $J = 15.9$ Hz, 1H), 6.71 (dd, $J = 2.0, 2.0$ Hz, 2H), 7.13 (br s, 1H), 7.20 (br d, $J = 7.4$ Hz, 1H), 7.29 (dd, $J = 7.6, 7.4$ Hz, 1H), 7.33 (br d, $J = 7.6$ Hz, 1H), 7.41 (br s, 1H), 7.47 (s, 1H), 7.49 (br s, 1H), 8.42 (s, 1H). ¹³C NMR (126 MHz, $\text{DMSO}-d_6$): δ 173.2, 170.0, 153.3, 141.0, 136.5, 135.2, 134.2, 133.7, 129.2, 128.7, 127.1, 125.2, 124.0, 120.2, 117.2, 107.8, 82.0, 67.3, 66.4, 51.6, 45.8, 36.5, 33.0, 29.5, 27.8, 25.9, 24.6, 24.5, 15.7, 10.6. MS m/z 606.3 (calc'd: $\text{C}_{34}\text{H}_{48}\text{N}_5\text{O}_5$, $[\text{M}+\text{H}]^+$, 606.4).



Compounds 49a,b. Compound **48** (11.5 mg, 16 μ mol) was dissolved in TFE (1.6 mL) and treated with TFA (1.6 mL). The reaction was stirred at room temperature for 50 min then concentrated to dryness. HPLC analysis and purification was performed using the following methods.

Analytical HPLC method:

Column: Waters XBridge™ PFP, 4.6x250mm, 5 μ m.

Solvent A: H₂O + 0.1%v TFA

Solvent B: ACN + 0.1%v TFA

Flow rate: 1.00 ml/min

Time	%B
0	10
0.5	10
2	40
17	80
18	100
21	100
22	10
27	10

Preparative HPLC method A:

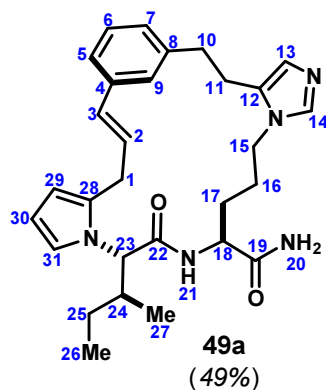
Column: Waters XBridge™ PFP, 19x250mm, 5 μ m.

Solvent A: H₂O + 0.1%v TFA

Solvent B: ACN + 0.1%v TFA

Flow rate: 6.00 ml/min

Time	%B
0	10
0.5	10
2	40
7	42
7.5	100
8.5	100
9	10

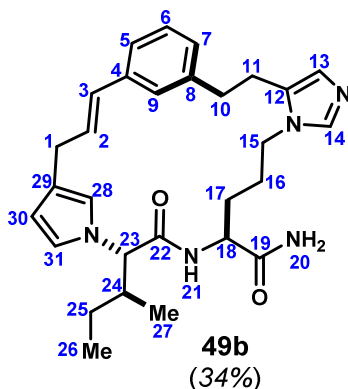


(500MHz, CD₃OD, 298K)

	¹³ C	¹ H	key correlations
1	30.2	3.46 (br dd, <i>J</i> = 17.7, 5.9 Hz, 1H), 3.54 (ddd, <i>J</i> = 17.7, 4.9, 1.8 Hz, 1H)	HMBC 1→2,28,29
2	131.0	6.25 (ddd, <i>J</i> = 15.9, 5.9, 4.9 Hz, 1H)	COSY 2→1,3 HMBC 2→4,29
3	131.2	6.02 (br d, <i>J</i> = 15.9 Hz, 1H)	HMBC 3→4
4	139.4	-	

5	126.8	7.20 (br d, $J = 7.8$ Hz, 1H)	HMBC 5→7,9
6	130.4	7.24 (dd, $J = 7.8, 7.2$ Hz, 1H)	COSY 6→5,7 HMBC 6→4,8
7	129.0	7.05 (br d, $J = 7.2$ Hz, 1H)	HMBC 7→5,9
8	141.6	-	
9	126.5	6.92 (br s, 1H)	
10	26.0	2.96-3.03 (m, 1H) overlap, 3.10-3.16 (m, 1H)	HMBC 10→8,12
11	37.1	2.90-2.95 (m, 1H), 2.99-3.05 (m, 1H) overlap	HMBC 11→8,12
12	136.5	-	
13	118.7	7.42 (d, $J = 1.0$ Hz, 1H)	HMBC 13→14
14	134.9	8.62 (d, $J = 1.0$ Hz, 1H)	HMBC 14→12
15	47.0	3.37 (ddd, $J = 14.0, 8.5, 6.0$ Hz, 1H), 3.66 (ddd, $J = 14.0, 7.9, 6.4$ Hz, 1H)	HMBC 15→12,14
16	26.1	1.19-1.30 (m, 1H), 1.36-1.45 (m, 1H)	
17	30.4	0.93-1.02 (m, 1H), 1.36-1.45 (m, 1H)	
18	53.4	4.17 (ddd, $J = 7.7, 7.7, 6.8$ Hz, 1H)	HMBC 18→19,22
19	175.2	-	
20	-	not observed	
21	-	7.92 (d, $J = 7.7$ Hz, 1H)	HMBC 21→22
22	172.7	-	
23	64.5	4.25 (d, $J = 10.7$ Hz, 1H)	COSY 23→24
24	40.4	2.11-2.19 (m, 1H)	COSY 24→25,27
25	26.0	0.89-0.96 (m, 1H) overlap, 0.97-1.06 (m, 1H) overlap	COSY 25→26
26	11.2	0.81 (dd, $J = 7.4, 7.4$ Hz, 3H)	HMBC 26→24
27	16.0	0.98 (d, $J = 6.7$ Hz, 3H)	HMBC 27→24
28	131.70	-	
29	108.4	5.90 (dd, $J = 3.3, 1.7$ Hz, 1H)	HMBC 29→28,31 COSY 29→30
30	108.5	6.07 (dd, $J = 3.3, 2.8$ Hz, 1H)	HMBC 30→31 COSY 30→31
31	120.5	7.01 (dd, $J = 2.8, 1.7$ Hz, 1H)	HMBC 31→28,29,30

MS m/z 488.2 (calc'd: $C_{29}H_{38}N_5O_2$, $[M+H]^+$, 488.3).



(500MHz, CD₃OD, 298K)

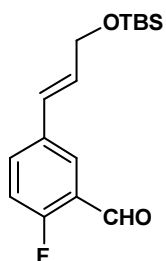
	¹³ C	¹ H	key correlations
1	31.0	3.25 (d, <i>J</i> = 6.6 Hz, 2H)	HMBC 1→2,3,28,29,30
2	133.6	6.11 (dt, <i>J</i> = 16.0, 6.6 Hz, 1H)	COSY 2→1 HMBC 2→1,4,29
3	128.9	6.25(d, <i>J</i> = 16.0 Hz, 1H)	HMBC 3→4
4	139.6	-	
5	125.8	7.10 (br s, 1H)	
6	129.7	7.18 (dd, <i>J</i> = 7.6, 7.3 Hz, 1H)	HMBC 6→4,8
7	128.0	6.96 (br d, <i>J</i> = 7.3 Hz, 1H)	
8	140.9	-	
9	125.7	7.01 (br s, 1H)	
10	25.3	3.03-3.08 (m, 2H)	HMBC 10→8,12
11	34.9	2.91-3.02 (m, 2H)	HMBC 11→8,12
12	135.8	-	
13	118.2	7.20 (s, 1H)	HMBC 13→14
14	135.2	8.57 (s, 1H)	HMBC 14→13,12
15	46.7	3.72-3.79 (m, 1H), 3.84-3.91 (m, 1H)	HMBC 15→14,16 COSY 15→16
16	26.6	1.58-1.72 (m, 2H) overlap	
17	30.4	1.47-1.56 (m, 1H), 1.68-1.77 (m, 1H)	HMBC 17→16 COSY 17→18
18	52.8	4.41-4.45 (m, 1H)	HMBC 18→17,19,22
19	175.1	-	
20	-	not observed	
21	-	8.38 (d, <i>J</i> = 8.1 Hz, 1H)	
22	172.2	-	
23	68.5	4.23 (d, <i>J</i> = 10.9 Hz, 1H)	HMBC 23→22,28 COSY 23→24
24	36.4	2.25-2.35 (m, 1H)	COSY 24→25,27
25	25.5	1.01-1.06 (m 1H) overlap, 1.27-1.33 (m, 1H)	COSY 25→26
26	15.6	0.86 (dd, <i>J</i> = 7.4, 7.4 Hz, 3H)	
27	10.7	0.96 (d, <i>J</i> = 6.5 Hz, 3H)	
28	119.1	6.57-6.59 (m, 1H)	HMBC 28→29,30,31

29	123.2	-	
30	109.8	5.95-5.97 (m, 1H)	HMBC 30→29,31
31	120.2	6.74-6.76 (m, 1H)	HMBC 31→28,29,30

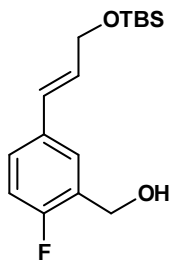
MS m/z 488.2 (calc'd: $C_{29}H_{38}N_5O_2$, $[M+H]^+$, 488.3).

Template 3:

TBS cinnamyl ether 59. A round bottom flask fitted with a reflux condenser was charged with 5-bromo-2-fluorobenzaldehyde (5.2 g, 26 mmol), vinylboronate **1-50**⁶¹ (9.2 g, 31 mmol), Na_2CO_3 (8.1 g, 77 mmol), THF (43 mL) and H_2O (9 mL) and sparged with argon for 20 minutes. The vessel was opened briefly to introduce $Pd(PPh_3)_4$ (296 mg, 0.26 mmol), sparged for an additional 5 minutes, and heated to reflux for two days. The reaction was cooled, diluted with H_2O and partitioned against EtOAc. The aqueous phase was extracted with EtOAc (x2), and the combined organic phase was washed with 10% citric acid (x1), H_2O (x1), brine, dried over Na_2SO_4 and concentrated. The residual oil was reconstituted in 8:2 hexanes:EtOAc and passed through a pad of SiO_2 , washing with the same. The filtrate was concentrated to give a yellow oil (9.1 g), which NMR indicated to be a 5:1 mixture of **59** (NMR assay 24.6 mmol, 96%) and starting boronate **1-50**. An analytical sample was obtained by flash chromatography on SiO_2 eluted with 0→10% EtOAc in hexanes. 1H NMR ($CDCl_3$, 600 MHz): δ 0.11 (s, 6H), 0.94 (s, 9H), 4.35 (dd, $J = 4.7, 1.8$ Hz, 2H), 6.30 (dt, $J = 15.8, 4.7$ Hz, 1H), 6.59 (dt, $J = 15.8, 1.8$ Hz, 1H), 7.12 (dd, $J = 9.8, 8.8$ Hz, 1H), 7.60 (ddd, $J = 8.7, 5.1, 2.4$ Hz, 1H), 7.84 (dd, $J = 6.6, 2.4$ Hz, 1H), 10.36 (s, 1H). ^{13}C NMR ($CDCl_3$, 101 MHz): δ 187.0 (d, $^3J_{CF} = 6.5$ Hz), 163.8 (d, $^1J_{CF} = 258.8$ Hz), 134.2 (d, $^4J_{CF} = 3.8$ Hz), 133.8 (d, $^3J_{CF} = 8.9$ Hz), 131.0 (d, $^5J_{CF} = 1.6$ Hz), 126.8, 63.4, 26.0, 18.4, -5.2. MS m/z 295.1 (calc'd: $C_{16}H_{24}FO_2Si$, $[M+H]^+$, 295.2).



Benzyl alcohol 60. Crude aldehyde **59** (9.1 g, assay 24.6 mmol) was dissolved in EtOH, cooled in an ice bath, and $NaBH_4$ (540 mg, 14.3 mmol) was added in several portions. The mixture was stirred for 30 min, quenched and diluted with water, and extracted with EtOAc (x2). The organic phase was washed with H_2O (x1), brine, dried over Na_2SO_4 and concentrated. The residue was taken up in 5% EtOAc in hexanes and loaded on a SiO_2 flash chromatography column, eluting with the same to collect the vinyl boronate **1-50**. The eluent was changed to 25% EtOAc in hexanes, and **60** was recovered as a light yellow oil (7.1 g, 92% 2 steps). 1H NMR ($CDCl_3$, 300 MHz): δ 0.11 (s, 6H), 0.94 (s, 9H), 4.34 (dd, $J = 4.9, 1.5$ Hz, 2H), 4.75 (s, 2H), 6.22 (dt, $J = 15.8, 4.9$ Hz, 1H), 6.56 (dt, $J = 15.8, 1.5$ Hz, 1H), 6.99 (dd, $J = 9.5, 8.7$ Hz, 1H), 7.27 (ddd, $J = 8.7, 4.9, 2.2$ Hz, 1H), 7.43 (dd, $J = 7.1, 2.1$ Hz, 1H). ^{13}C NMR ($CDCl_3$, 101 MHz): δ 159.9 (d, $^1J_{CF} = 246.7$ Hz), 133.5 (d, $^4J_{CF} = 3.4$ Hz), 129.1 (d, $^3J_{CF} = 1.9$ Hz), 128.4, 127.9 (d, $^2J_{CF} = 15.3$ Hz), 127.12, 127.05 (d, $^3J_{CF} = 4.7$ Hz), 115.3 (d, $^2J_{CF} = 21.8$ Hz), 63.9, 59.1 (d, $^3J_{CF} = 4.0$ Hz), 26.0, 18.5, -5.1. MS m/z 165.0 (calc'd: $C_{10}H_{10}FO$, $[M-OTBS]^+$, 165.1).

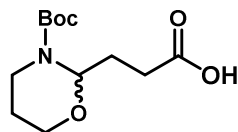


Benzyl bromide 61. To a solution of triphenylphosphine (4.51 g, 17.2 mmol), imidazole (1.17 g, 17.2 mmol) and benzyl alcohol **60** (3.40 g, 11.5 mmol) in dichloromethane (100 mL) at 0 °C was added a solution of bromine (881 μ L, 17.2 mmol) in dichloromethane (25 mL) dropwise via syringe. After two hours the reaction was diluted with dichloromethane (100 mL) and washed sequentially with $Na_2S_2O_3$, 1N HCl, water and brine. The organic layer was dried over Na_2SO_4 , concentrated and purified by column chromatography (SiO_2 , 10→40% EtOAc in hexanes) to provide **61** as a faintly yellow oil (3.40 g, 82%). 1H NMR ($CDCl_3$, 500 MHz): δ 7.37 (dd, $J = 7.2, 2.3$ Hz, 1H), 7.29 (ddd, $J = 8.0, 5.0, 2.3$ Hz, 1H), 7.00 (t, $J = 9.3$ Hz, 1H), 6.53 (br. d, $J = 15.7$ Hz, 1H), 6.21 (dt, $J = 15.7, 5.0$ Hz, 1H), 4.56 (s, 2H), 4.33 (dd, $J = 4.8, 1.6$ Hz, 1H), 0.94 (s, 9H), 0.11 (s, 6H). 160.9, 158.9, 133.84, 133.81, 129.8, 128.3, 127.6, 125.2, 125.1, 116.0, 115.8, 63.6. ^{13}C NMR ($CDCl_3$, 125 MHz): δ 159.8 (d, $J = 250.4$ Hz), 133.8 (d, $J = 3.7$ Hz), 129.8 (d, $J = 2$ Hz), 129 (d, $J = 3.3$ Hz), 128.3 (d, $J = 8.4$ Hz), 127.6, 125.1 (d, $J = 15$

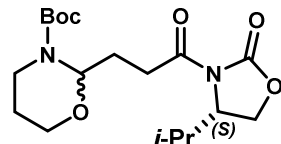
⁶¹ Y. D. Wang, et al., *Tetrahedron Lett.* **2005**, 46, 8777.

H_z), 115.9 (d, *J* = 22 Hz), 63.6, 26.0, 25.7, 18.5, 5.2. MS *m/z* 381.1 (calc'd: C₁₆H₂₄BrFOSiNa, [M+Na]⁺, 381.1).

***N*-Boc-1,3-oxazine 62.** Compound 62 was prepared by the Rosenmund reduction of ethyl succinoyl chloride according to the literature protocol.⁶²

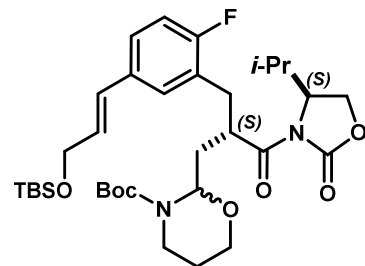


***N*-Acyloxazolidinone 63.** A solution of carboxylic acid **62** (8.66 g, 33.4 mmol) in anhydrous THF (167 mL, 0.2M) was cooled to -10 °C and Et₃N (11.64 ml, 83.5 mmol) was added, followed by dropwise addition of pivaloyl chloride (4.32 ml, 35.1 mmol) via syringe. The reaction mixture was allowed to stir for 1h at -10 °C, then dry LiCl (1.49 g, 35.1 mmol) was added in one portion followed by addition of *L*-valine derived oxazolidinone (4.53 g, 35.1 mmol). This mixture was stirred at 0 °C for one hour then allowed to warm to room temperature and stir overnight. The reaction



mixture was then diluted with EtOAc (200 ml) and transferred to separatory funnel. The organic layer was washed with 1N HCl, brine, and dried over Na₂SO₄. The solvent was removed by rotary evaporation. Purification by column chromatography on SiO₂ eluted with 35% EtOAc in hexanes provided **63** as a viscous oil (9.13 g, 74%). [α]_D²⁰ = +41.3° (c = 1.8, CHCl₃). ¹H NMR (CDCl₃, 400 MHz, 1:1 mixture of diastereomers): δ 5.54 (ddd, *J* = 7.0, 7.0, 4.3 Hz, 1H), 4.39-4.45 (m, 1H), 4.26 (ddd, *J* = 9.0, 8.1, 2.0 Hz, 1H), 4.20 (ddd, *J* = 9.0, 3.1, 0.5 Hz, 1H), 4.02 (br dd, *J* = 13.7, 4.7 Hz, 1H), 3.90 (dddd, *J* = 11.5, 11.5, 3.9, 3.9 Hz, 1H), 3.65-3.72 (m, 1H), 3.13 (ddd, *J* = 13.0, 13.0, 3.4 Hz, 1H), 3.08 (ddd, *J* = 8.5, 8.5, 2.5 Hz, 0.5H), 2.93 (dd, *J* = 8.5, 6.2 Hz, 0.5H), 2.91 (dd, *J* = 8.6, 6.4 Hz, 0.5H), 2.86 (dd, *J* = 8.6, 6.5 Hz, 0.5H), 2.32-2.42 (m, 1H), 2.21-2.33 (m, 1H), 2.07-2.20 (m, 1H), 1.86 (dddd, *J* = 18.3, 12.7, 11.3, 5.5 Hz, 1H), 1.48-1.55 (m, 1H), 1.46 (s, 9H), 0.91 (d, *J* = 7.1 Hz, 3H), 0.88 (d, *J* = 7.0 Hz, 1.5H), 0.87 (d, *J* = 7.0 Hz, 1.5H). ¹³C NMR (CDCl₃, 101 MHz, 1:1 mixture of diastereomers): δ 172.43, 172.39, 154.1, 153.82, 153.78, 81.5, 81.4, 80.2, 63.5, 63.4, 59.83, 59.79, 58.5, 36.8, 31.3, 31.2, 28.5, 28.4, 28.3, 25.2, 23.9, 18.0, 14.8, 14.6. MS *m/z* 393.5 (calc'd: C₁₈H₃₀N₂O₆Na, [M+Na]⁺, 393.2).

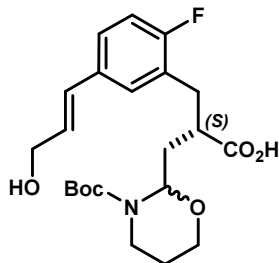
***N*-Acyl oxazolidinone 64.** *N*-Acyloxazolidinone **63** (3.83 g, 10.3 mmol) was co-evaporated once from dry toluene, dried *in vacuo*, and dissolved in dry THF (52 mL). Benzyl bromide **61** (4.83 g, 13.4 mmol) was added, and the mixture cooled to -78°C. A solution of NaHMDS (1.0M/THF, 13.4 mL, 13.4 mmol) was added in one portion. The resulting yellow solution was stirred for 2 hr at the same temperature, then warmed to -40°C and stirred an addition 2 hr. A saturated solution of NH₄Cl (25 mL) was then added to the cold solution. The mixture was diluted with EtOAc, transferred to a separatory funnel, and washed with water and brine. The organic layer was dried over Na₂SO₄ and evaporated. Purification by column chromatography on SiO₂ eluted with 5→30% EtOAc in hexane gave **64** (5.29 g, 79%). ¹H NMR



(CDCl₃, 500 MHz, 1:1 mixture of isomers): δ 7.30 (dd, *J* = 7.1, 2.2 Hz, 1H), 7.23-7.27 (m, 1H), 7.13-7.21 (m, 1H), 6.93 (ddd, *J* = 9.6, 9.6, 2.4 Hz, 1H), 6.49 (app. dd, *J* = 15.6, 2.1 Hz, 1H), 6.16 (dq, *J* = 15.9, 5.1 Hz, 1H), 5.44-5.54 (m, 1H), 4.26-4.41 (m, 4H), 4.18 (ddd, *J* = 9.0, 5.6, 5.6 Hz, 1H), 4.08 (ddd, *J* = 8.2, 4.2, 2.4 Hz, 1H), 3.88-3.96 (m, 1H), 3.72-3.82 (m, 1H), 3.61-3.69 (m, 1H), 3.51-3.59 (m, 1H), 2.87-3.09 (m, 3H), 2.43-2.57 (m, 1H), 2.04-2.22 (m, 2H), 1.91 (ddd, *J* = 10.9, 7.7, 4.1 Hz, 1H), 1.71-1.85 (m, 2H), 1.46 (s, 3H), 1.4 (s, 3H), 0.93 (s, 9H), 0.81 (app. t, *J* = 7.0 Hz, 3H), 0.58 (d, *J* = 6.8 Hz, 1.5H), 0.54 (d, *J* = 6.9 Hz, 1.5H). ¹³C NMR (CDCl₃, 500 MHz, 1:1 mixture of isomers): δ 175.3, 174.5, 174.3, 160.67 (d, *J* = 243.2 Hz), 154.3, 153.9, 153.8, 153.5, 133.3 (d, *J* = 3.5 Hz), 133.3 (d, *J* = 3.5 Hz), 129.2 (d, *J* = 4.7 Hz), 128.9, 128.9, 128.2, 128.2, 6.32 (d, *J* = 8.0 Hz), 126.28 (d, *J* = 8.0 Hz), 125.4, 125.3, 115.4 (d, *J* = 22.6 Hz), 80.2, 77.3, 77.0, 76.8, 63.8, 63.0, 63.0, 60.0, 59.9, 58.7, 58.6, 39.5, 32.1, 31.7, 30.4, 28.7, 28.5, 28.4, 28.3, 28.2, 26.0, 25.2, 25.0, 18.5, 18.0, 18.0, 17.9, 14.3, 14.2, 14.1, -5.2. MS *m/z* 517.4 (calc'd: C₂₈H₃₈FN₂O₆, [M-OTBS]⁺, 517.3).

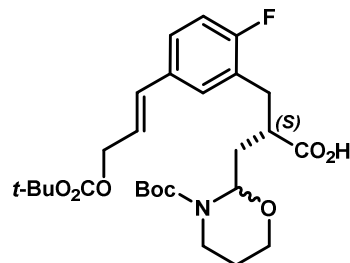
⁶²T. Groth, M. Meldal, *J. Comb. Sci.* **2001**, *3*, 34.

Cinnamyl alcohol 66. To a solution of **64** (1.41 g, 2.17 mmol) in THF (15 ml) was added 50 w/w% H₂O₂ (876 μ L, 15.19 mmol) followed by LiOH (1.0M/H₂O, 4.34 ml, 4.34 mmol). The reaction was allowed to stir overnight at room temperature. A solution of sodium sulfite (1.91 g, 15.19 mmol) in H₂O (15 mL) and the solution was stirred for 15 minutes, then diluted with EtOAc and transferred to a separation funnel containing 75 ml 1M HCl. The organic layer was separated and washed with water and brine, dried over Na₂SO₄ and evaporated to give crude product which was reconstituted in THF (11 mL) and treated with TBAF (1.0M/THF, 4.10 mL, 4.10 mmol) at room temperature. After 6 hrs the reaction was diluted with EtOAc and washed with 1.0N HCl, water and brine. The organic layer was dried over



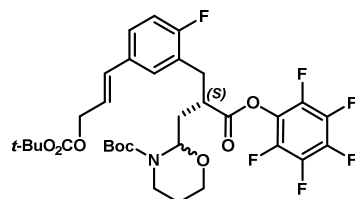
Na₂SO₄, concentrated and purified by column chromatography on SiO₂ eluted with 0→10% MeOH in CHCl₃ to give **66** as a colorless oil (766 mg, 83%). $[\alpha]_{20}^D = +6.3^\circ$ (c = 0.75, CHCl₃). ¹H NMR (CDCl₃, 500 MHz, 4:3 mixture of isomers): δ 1.40 (s, 6.8 H), 1.42 (s, 9H), 1.77 (ddd, *J* = 12.4, 11.3, 5.0 Hz, 0.75H), 1.81 (ddd, *J* = 12.9, 11.4, 5.7 Hz, 0.75H), 1.86 (ddd, *J* = 14.1, 5.8, 4.9 Hz, 1.2H), 1.99 (ddd, *J* = 14.0, 7.5, 4.0 Hz, 1H), 2.25 (ddd, *J* = 14.2, 9.3, 6.9 Hz, 1H), 2.34 (ddd, *J* = 14.3, 8.1, 8.1 Hz, 0.75H), 2.70-2.84 (m, 1.75H), 2.84-2.99 (m, 4.25H), 3.03 (td, *J* = 13.1, 2.9 Hz, 0.75H), 3.60-3.67 (m, 1.75H), 3.70 (td, *J* = 11.4, 3.1 Hz, 1H), 3.82 (td, *J* = 11.5, 3.3 Hz, 0.75H), 3.89-3.97 (m, 1.75H), 4.25 (d, *J* = 5.5 Hz, 3.5H), 5.54 (t, *J* = 6.9 Hz, 0.75H), 5.57 (t, *J* = 7.2 Hz, 1H), 6.226 (dt, *J* = 15.8, 5.7 Hz, 0.75H), 6.230 (dt, *J* = 15.8, 5.7 Hz, 1H), 6.50 (d, *J* = 15.8 Hz, 1.75H), 6.92-6.97 (m, 1.75H), 7.16-7.21 (m, 3.5H). ¹³C NMR (CDCl₃, 126 MHz, mixture of isomers): δ 25.1, 25.2, 28.3 (2), 28.4 (2), 30.8, 31.0, 31.6, 31.9, 36.8, 37.0, 41.9, 42.4, 59.9 (2), 63.5 (2), 80.5 (2), 80.9 (2), 115.6 (d, ²*J*_{CF} = 22.7 Hz), 125.7 (d, ²*J*_{CF} = 16.2 Hz), 125.8 (d, ²*J*_{CF} = 16.2 Hz), 126.5 (d, ³*J*_{CF} = 8.1 Hz) (2), 128.5 (2), 129.3 (d, ³*J*_{CF} = 4.5 Hz), 129.4 (d, ³*J*_{CF} = 4.7 Hz), 129.9 (2), 133.05 (d, ⁴*J*_{CF} = 3.1 Hz), 133.07 (d, ⁴*J*_{CF} = 3.0 Hz), 154.1 (2), 160.84 (d, ¹*J*_{CF} = 247 Hz), 160.86 (d, ¹*J*_{CF} = 247 Hz), 178.5, 178.8. MS *m/z* 446.4 (calc'd: C₂₂H₃₀FNO₆Na, [M+Na]⁺, 446.2).

Template 67. To a solution of **66** (1.0 g, 2.46 mmol) in CH₂Cl₂ (24 mL) at rt was added NaOH (15 wt% aqueous, 2.36 mL) followed by tetrabutylammonium bisulfate (24 mg, 0.071 mmol). Di-*tert*-butyl dicarbonate (773 mg, 3.54 mmol) was subsequently added in one portion and the mixture was allowed to stir overnight at rt. The reaction mixture was diluted with CH₂Cl₂ (75 mL) and washed with water and brine. The colorless crude oil obtained was purified by column chromatography on SiO₂ eluted with 0→10% MeOH in CHCl₃ to afford **67** (876 g, 1.67 mmol, 68%) as a colorless oil. $[\alpha]_{20}^D = +8.9^\circ$ (c = 0.5, CHCl₃). ¹H NMR (CDCl₃, 500 MHz, 4:3 mixture of isomers): δ 1.40 (s, 9H), 1.43 (s, 12H), 1.49 (s, 21H), 1.74-1.88 (m, 3.2H), 1.98 (ddd, *J* = 13.9, 7.6,



3.5 Hz, 1H), 2.23 (ddd, *J* = 14.1, 8.7, 6.8 Hz, 1.2H), 2.34 (ddd, *J* = 14.1, 8.7, 7.9 Hz, 1.2H), 2.71-2.78 (m, 1H), 2.79-2.94 (m, 4.4H), 2.97-3.06 (m, 3.4H), 3.60-3.70 (m, 3.4H), 3.82 (td, *J* = 11.4, 3.5 Hz, 1H), 3.90-3.97 (m, 2.2H), 4.68 (dd, *J* = 6.5, 0.9 Hz, 4.4H), 5.52 (t, *J* = 6.8 Hz, 1H), 5.56 (t, *J* = 7.1 Hz, 1.2H), 6.186 (dt, *J* = 15.7, 6.5 Hz, 1H), 6.191 (dt, *J* = 15.7, 6.5 Hz, 1.2H), 6.58 (brd, *J* = 15.7 Hz, 2.2H), 6.968 (dd, *J* = 9.3, 8.7 Hz, 1H), 6.97 (dd, *J* = 9.4, 8.6 Hz, 1.2H), 7.19-7.26 (m, 4.4H). ¹³C NMR (CDCl₃, 126 MHz, mixture of isomers): δ 25.1, 25.2, 27.9 (2), 28.36, 28.41, 30.6, 30.9, 31.6, 31.8, 36.8, 36.9, 41.7, 42.3, 60.0 (2), 67.4 (2), 80.5, 80.72, 80.76, 80.9, 82.4 (2), 115.8 (d, ²*J*_{CF} = 22.9 Hz) (2), 123.0 (2), 125.8 (d, ²*J*_{CF} = 16.1 Hz), 125.9 (d, ²*J*_{CF} = 16.2 Hz), 126.73 (d, ³*J*_{CF} = 8.4 Hz), 126.75 (d, ³*J*_{CF} = 8.2 Hz), 129.8 (d, ³*J*_{CF} = 4.7 Hz) (2), 132.56 (d, ⁴*J*_{CF} = 2.4 Hz), 132.59 (d, ⁴*J*_{CF} = 2.5 Hz), 133.22, 133.25, 153.5 (2), 154.0 (2), 161.16 (d, ¹*J*_{CF} = 248 Hz), 161.18 (d, ¹*J*_{CF} = 248 Hz), 179.0, 179.1. MS *m/z* 546.5 (calc'd: C₂₇H₃₈FNO₈Na, [M+Na]⁺, 546.3).

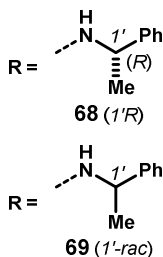
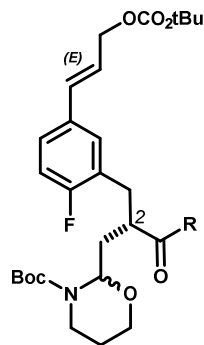
Template 50. Compound **67** (591 mg, 1.13 mmol) and pentafluorophenol (249 mg, 1.39 mmol) were dissolved in DCM (5 mL) and treated with EDCI (238 mg, 1.24 mmol) at rt. The mixture was stirred overnight, then partitioned between Et₂O and sat. NaHCO₃. The organic phase was washed with sat. NaHCO₃ (x1), brine (x1), dried over MgSO₄ and concentrated. Purification by column chromatography on SiO₂ eluted with 15% EtOAc in hexanes afforded **50** (557 mg, 72%) as a colorless oil. The inconsequential ~1:1 mixture of *N,O*-acetal diastereomers was resolved for characterization purposes by flash



chromatography on SiO₂ eluted with 5→15% EtOAc in hexanes: **50a** (*R_f* = 0.59, 7:3 hex:EtOAc + 2%v AcOH), ¹H NMR (CDCl₃, 500 MHz): δ 1.40 (s, 9H), 1.50 (s, 9H), 1.51-1.59 (m, 1H), 1.78-1.90 (m, 2H), 2.61 (dt, *J* = 14.2, 8.9 Hz, 1H), 2.97-3.06 (m, 2H), 3.06-3.13 (m, 1H), 3.13-3.21 (m, 1H), 3.64 (br dt, *J* = 11.1, 4.3 Hz, 1H), 3.81 (ddd, *J* = 11.5, 10.8, 3.9 Hz, 1H), 3.96 (br dd, *J* = 13.6, 4.4 Hz, 1H), 4.69 (d, *J* = 6.4, 0.9 Hz, 2H), 5.51 (br dd, *J* = 9.0, 4.2 Hz, 1H), 6.19 (dt, *J* = 15.9, 6.4 Hz, 1H), 6.59 (br d, *J* = 15.9 Hz, 1H), 7.01 (dd, *J_{HF}* = 9.7 Hz, *J_{HH}* = 8.4 Hz, 1H), 7.22 (dd, *J_{HF}* = 7.2 Hz, *J_{HH}* = 2.2 Hz, 1H), 1.27 (ddd, *J_{HH}* = 8.4, 2.2 Hz, *J_{HF}* = 4.8 Hz, 1H). ¹³C NMR (CDCl₃, 126 MHz): δ 171.2, 161.1 (d, *J_{CF}* = 248 Hz), 153.7, 153.5, 141.2 (br d, *J_{CF}* = 254 Hz), 137.9 (br d, *J_{CF}* = 251 Hz), 133.1, 132.8 (d, *J_{CF}* = 3.6 Hz), 129.7 (d, *J_{CF}* = 4.5 Hz), 127.2 (d, *J_{CF}* = 8.3 Hz), 124.9 (d, *J_{CF}* = 16.1 Hz), 123.2 (d, *J_{CF}* = 1.8 Hz), 115.9 (d, *J_{CF}* = 22.6 Hz), 67.4, 60.3, 42.7, 37.3, 32.2, 32.2, 31.8, 28.4, 27.9, 25.0. ¹⁹F{¹H} NMR (CDCl₃, 376 MHz, unreferenceed): δ -117.9, -152.2 (d, *J_{FF}* = 19.3 Hz), -158.0 (apt br t, *J_{FF}* = 20.9 Hz), -162.4 (apt br t, *J* = 20.5 Hz). **50b** (*R_f* = 0.56, 7:3 hex:EtOAc + 2%v AcOH), ¹H NMR (CDCl₃, 500 MHz): δ 1.43 (s, 9H), 1.50 (s, 9H), 1.51-1.61 (m, 1H), 1.80-1.92 (m, 1H), 2.18-2.36 (m, 2H), 2.99-3.17 (m, 3H), 3.18-3.25 (m, 1H), 3.65-3.77 (m, 2H), 3.99 (br d, *J* = 13.5, 5.0 Hz, 1H), 4.70 (dd, *J* = 6.4, 0.7 Hz, 2H), 5.54 (dd, *J* = 7.4, 6.4 Hz, 1H), 6.20 (dt, *J* = 15.9, 6.4 Hz, 1H), 6.60 (br d, *J* = 15.9 Hz, 1H), 7.02 (dd, *J_{HF}* = 9.6 Hz, *J_{HH}* = 8.4 Hz, 1H), 7.23 (br dd, *J_{HF}* = 7.2 Hz, *J_{HH}* = 2.0 Hz, 1H), 7.26-7.30 (m, 1H), ¹³C NMR (CDCl₃, 126 MHz): δ 171.0, 161.1 (d, *J_{CF}* = 248 Hz), 154.0, 153.5, 133.1, 132.8 (d, *J_{CF}* = 3.6 Hz), 129.7 (d, *J_{CF}* = 4.6 Hz), 127.2 (d, *J_{CF}* = 8.8 Hz), 124.9 (d, *J_{CF}* = 16.1 Hz), 123.2 (d, *J_{CF}* = 1.7 Hz), 116.0 (d, *J_{CF}* = 22.6 Hz), 82.5, 80.8, 80.7, 67.4, 60.5, 41.7, 37.0, 32.2, 31.6, 28.4, 27.9, 25.1 (carbons of PFP not observed). ¹⁹F{¹H} NMR (CDCl₃, 376 MHz, unreferenceed): δ -117.9, -152.1 (d, *J_{FF}* = 18.7 Hz), -157.8 (dt, *J_{FF}* = 5.3, 21.6, 21.6 Hz), -162.3 (dd, *J_{FF}* = 21.6, 21.6 Hz).

Derivatization of template 50 for enantiopurity determination. 68: Template **50** (1 mg, 1.6 μmol) was dissolved in DMF (500 μL) and treated with *R*-(+)-α-methylbenzylamine (1.2 μL, 9.4 μmol) and *i*Pr₂EtN (500 nL, 4 μmol). The mixture was stirred for 14 hrs, after which HPLC-UV analysis showed no **50** remaining and complete conversion to **68**. **68a:** MS *m/z* 626.9 (calc'd: C₃₅H₄₈FN₂O₇, [M+H]⁺, 627.3) **69:** Template **50** was reacted with (±)-α-methylbenzylamine in the same manner. MS *m/z* 626.9 (calc'd: C₃₅H₄₈FN₂O₇, [M+H]⁺, 627.3). **HPLC analysis:** Crude **68** was diluted with MeOH and analyzed alongside a co-injection of a ~1:1 mixture of **68** and **69**.

Analytical HPLC method:



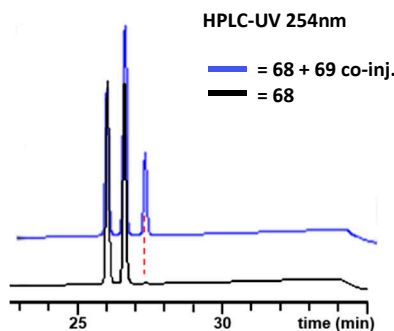
Column: Phenomenex Kinetex C18, 4.6x100mm, 2.6 μ.

Solvent A: H₂O + 0.1%v TFA

Solvent B: ACN + 0.1%v

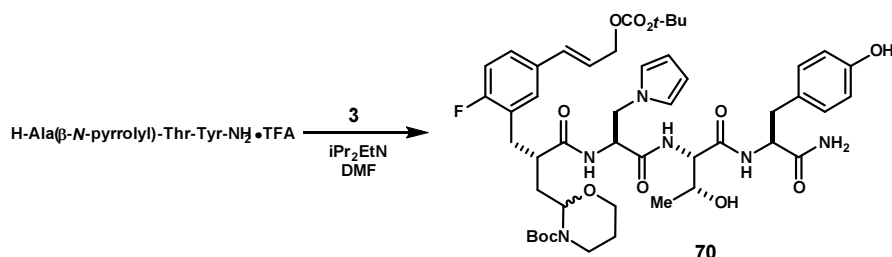
TFA

Flow rate: 1.00 mL/min

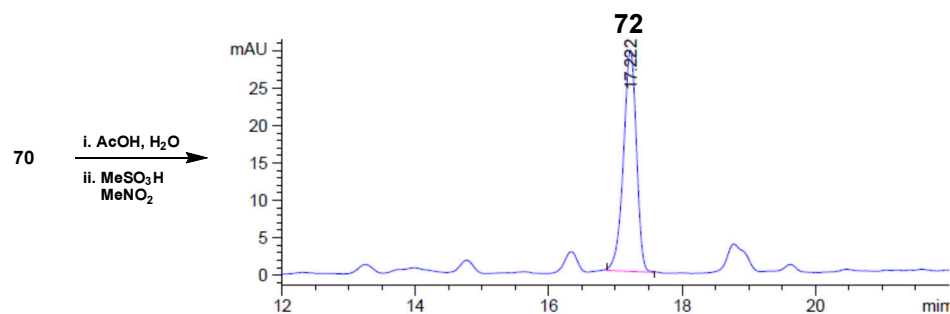


Time	%B
0	35
2	35
32	75
34	35
36	35

Macrocycle 72:



Acyclic cinnamyl carbonate 70. The Boc-Ala(β -*N*-pyrrolyl)-Thr-Tyr-NH₂ (25 mg, 48 μ mol) was deprotected by treatment with 4N HCl in dioxane for 15 min, then concentrated to dryness. The residue dissolved in DMF (1 mL) and treated with *i*Pr₂EtN (28 μ L, 160 μ mol) to pH >9. Template **67** (16.9 mg, 32 μ mol) was added, followed by HBTU (13 mg, 35 μ mol), and the mixture was stirred at rt for 2hr after which HPLC-UV/MS analysis showed complete consumption of the template and formation of **70**. The mixture was concentrated and purified by HPLC (Waters Sunfire C18 19x250mm, 50 \rightarrow 100% ACN + 0.1%v HCO₂H, 15min) to give **70** (16.7 mg, 56%) as a white film. MS ESI(-) *m/z* 1035.3 (calc'd: C₄₉H₆₃F₄N₆O₁₄, [M+TFA-H]⁻, 1035.4), ESI(+) *m/z* 923.3 (calc'd: C₄₇H₆₄F₄N₆O₁₂ 923.5).



Macrocycle 72. To a flask charged with **70** (5.8 mg, 6.3 μ mol) was added 2:1 AcOH/H₂O (1.0 mL). The reaction was allowed to stir overnight and then concentrated. The resulting residue was reconstituted in nitromethane (1.25 mL) and methanesulfonic acid (6.1 μ L, 95 μ mol, 15 equiv.) was added. After one hour *i*Pr₂NEt (6.1 μ L, 18 equiv) was added and reaction was concentrated, reconstituted in DMF and purified by reverse phase preparative HPLC (35 \rightarrow 50% ACN+0.1% TFA, 17min, Waters Sunfire C18 19x250mm) to afford macrocycle **72** as a white film (2.9 mg, 73%).

Analytical HPLC method:

Column: Waters XBridge™ C18, 4.6x250mm, 5 μ m.

Solvent A: H₂O + 0.1%v TFA

Solvent B: ACN + 0.1%v TFA

Flow rate: 1.00 ml/min

Time	%B
0	30
2	30
30	60
35	60
36	30
40	30

Preparative HPLC method A:

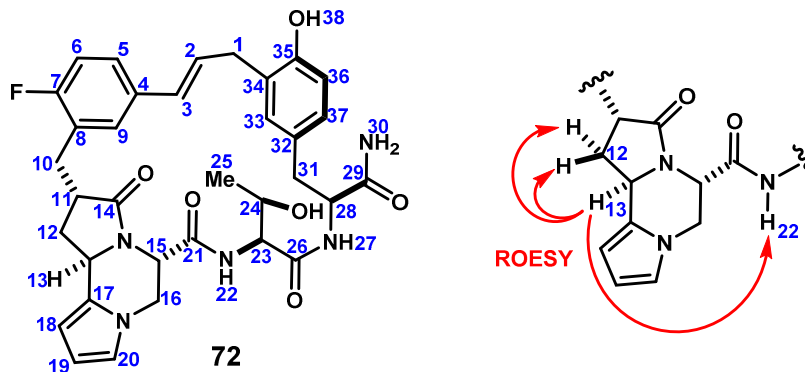
Column: Waters Sunfire™ C18, 19x250mm, 5 μ m.

Solvent A: H₂O + 0.1%v TFA

Solvent B: ACN + 0.1%v TFA

Flow rate: 6.00 ml/min

Time	%B
0	35
1	35
18	50



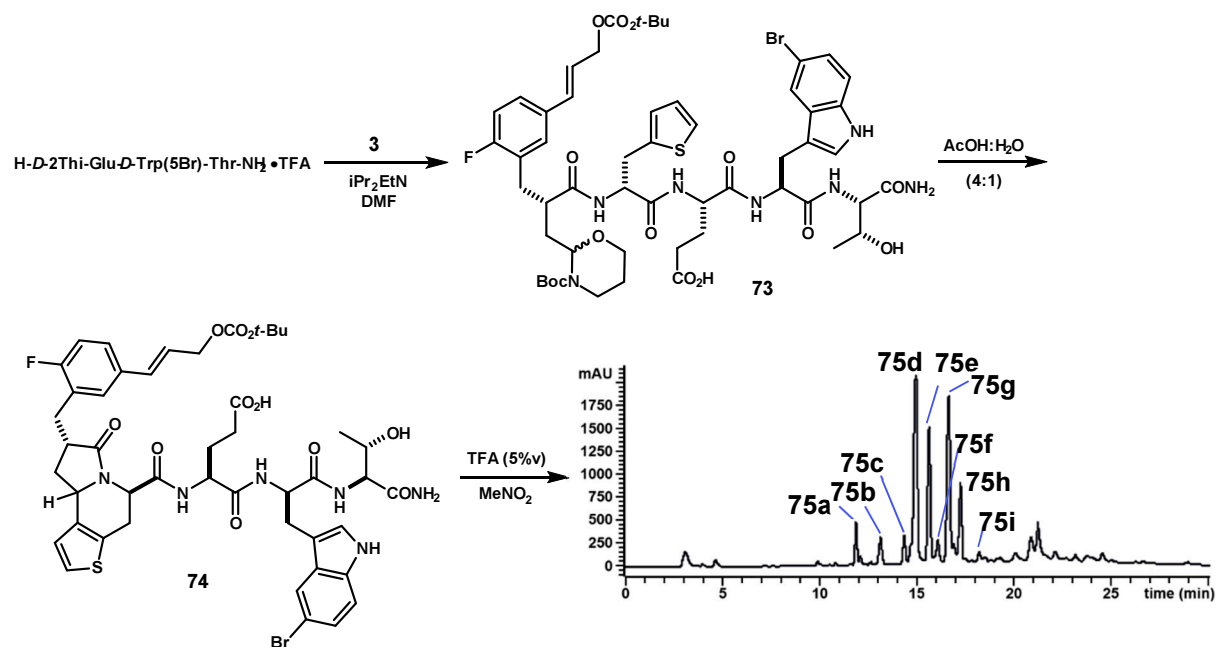
(500MHz, DMSO-*d*₆, 298K)

	¹³ C	¹ H	key correlations
1	30.7	3.45 (br dd, <i>J</i> = 16.9, 6.8 Hz, 1H), 3.32 (br dd, <i>J</i> = 16.9, 5.0 Hz, 1H)	HMBC 1→2,3,33,34,35
2	128.5	6.34 (ddd, <i>J</i> = 16.0, 6.8, 5.0 Hz, 1H)	HMBC 2→4,5
3	129.1	6.05 (br d, <i>J</i> = 16.0 Hz, 1H)	HMBC 3→5,9
4	133.0	-	
5	125.0	7.29 (ddd, <i>J</i> = 8.2, 5.1, 2.4 Hz, 1H)	HMBC 5→3,7 TOCSY 5→6,9
6	114.5	7.06 (d, <i>J</i> = 8.2 Hz, 1H) overlap	COSY 6→5 HMBC 6→7,8
7	159.8	-	
8	125.0	-	
9	130.4	7.34-7.37 (m, 1H)	HMBC 9→7,3
10	31.7	3.17 (br d, <i>J</i> = 9.3 Hz, 1H), 2.72 (dd, <i>J</i> = 12.0, 9.3 Hz, 1H)	HMBC 10→8,9,11,14
11	41.0	2.71-2.76 (m, 1H)	
12	33.7	2.45 (apt dd, <i>J</i> = 12.5, 6.9 Hz, 1H), 2.18-2.25 (m, 1H)	COSY 12→11 HMBC 12→10,11,14
13	49.1	5.00 (dd, <i>J</i> = 8.2, 6.9 Hz, 1H)	HMBC 13→17 ROESY 13→12,12',22
14	174.0	-	
15	50.1	4.79 (dd, <i>J</i> = 5.6, 3.4 Hz, 1H)	HMBC 15→14,21
16	43.3	4.36 (dd, <i>J</i> = 12.6, 3.4 Hz, 1H), 3.94 (dd, <i>J</i> = 12.6, 5.6 Hz, 1H)	HMBC 16→21
17	127.6	-	
18	102.2	5.84-5.86 (m, 1H)	HMBC 18→17 TOCSY 18→19,20
19	107.5	5.98 (dd, <i>J</i> = 3.5, 2.6 Hz, 1H)	HMBC 19→17
20	119.4	6.67 (dd, <i>J</i> = 2.6, 1.7 Hz, 1H)	
21	166.8	-	
22	-	7.08 (d, <i>J</i> = 6.4 Hz, 1H) overlap	HMBC 22→21
23	58.2	3.99 (dd, <i>J</i> = 6.4, 5.2 Hz, 1H)	TOCSY 23→21,22,24,25
24	66.5	3.78-3.83 (m, 1H)	
25	18.7	0.75 (d, <i>J</i> = 6.4 Hz, 3H)	COSY 25→24
26	168.2	-	
27	-	8.14 (d, <i>J</i> = 9.2 Hz, 1H)	HMBC 27→26

28	54.1	4.47 (ddd, $J = 11.4, 9.2, 2.9$ Hz, 1H)	HMBC 28→29
29	172.9	-	
30	-	7.34 (br s, 1H), 7.16 (br s, 1H)	HMBC 30→29 TOCSY 29→29'
31	36.5	3.01 (dd, $J = 13.7, 2.9$ Hz, 1H), 2.55 (dd, $J = 13.7, 11.4$ Hz, 1H)	HMBC 31→32
32	128.1	-	
33	130.7	7.01 (d, $J = 2.1$ Hz, 1H)	TOCSY 33→36,37
34	124.8	-	
35	152.8	-	
36	114.5	6.64 (d, $J = 8.1$ Hz, 1H)	HMBC 36→32,34
37	127.5	6.83 (dd, $J = 8.1, 2.1$ Hz, 1H)	
38	-	9.08 (br s, 1H)	

MS m/z 630.0 (calc'd: $C_{34}H_{37}FN_5O_6$, $[M+H]^+$, 630.3).

Macrocycles 75a–i:



Acyclic cinnamyl carbonate 73. Compound **73** (29.1 mg, 35%) was prepared analogously to compound **70**. MS m/z 1170.3 (calc'd: $C_{54}H_{70}BrFN_7O_{14}S$, $[M+H]^+$, 1170.4). ^1H NMR (CDCl_3 , 500 MHz): δ 0.43 (d, $J = 6.3$ Hz, 3H), 0.48 (d, $J = 6.3$ Hz, 3H), 1.36 (s, 9H), 1.44 (s, 9H), 1.47 (s, 18H), 1.55–1.74 (m, 6H), 1.74–1.97 (m, 6H), 1.97–2.09 (m, 2H), 2.15–2.24 (m, 1H), 2.32 (dt, $J = 13.8, 8.8$ Hz, 1H), 2.64–2.71 (m, 1H), 2.71–2.85 (m, 3H), 2.88–2.95 (m, 2H), 2.95–3.06 (m, 3H), 3.11–3.30 (m, 7H), 3.48–3.58 (m, 2H), 3.58–3.65 (m, 1H), 3.79–3.89 (m, 3H), 3.97 (br d, $J = 15.1$ Hz, 2H), 4.11–4.19 (m, 2H), 4.32–4.45 (m, 6H), 4.66 (d, $J = 6.0$ Hz, 4H), 6.25 (dt, $J = 15.8, 6.3$ Hz, 1H), 6.28 (dt, $J = 15.8, 6.2$ Hz, 1H), 6.59 (d, $J = 15.8$ Hz, 1H), 6.60 (dt, $J = 15.9$ Hz, 1H), 6.90–7.02 (m, 6H), 7.08 (s, 1H), 7.10 (s, 1H), 7.20–7.27 (m, 6H), 7.29–7.35 (m, 2H), 7.64 (s, 1H), 7.67 (s, 1H). ^{13}C NMR (CDCl_3 , 126 MHz): δ 175.5, 175.4, 175.31, 175.28, 175.0, 174.9, 174.2, 174.1, 173.9, 173.8, 172.7, 172.61, 172.55, 172.52, 172.45, 172.42, 161.9, 159.9, 154.3, 154.1, 153.6, 137.9, 137.8, 135.2, 132.75, 132.72, 132.70, 132.68, 132.3, 132.2, 130.3, 130.1, 130.0, 129.14, 129.12, 126.8, 126.6, 126.5, 126.4, 125.7, 125.6, 125.5, 124.8, 124.37, 124.36, 123.8, 122.98, 122.97, 120.70, 120.68, 115.2, 115.1, 115.0, 114.9, 112.6, 111.68, 111.66, 109.2, 109.1, 81.6, 81.3, 80.5, 80.33, 80.30, 67.13, 67.09, 65.9, 65.8, 59.6, 59.5, 58.81, 58.79, 57.2, 57.14, 57.10, 57.0, 56.0, 55.9, 52.3, 52.2, 42.81, 42.76,

42.0, 41.9, 37.1, 37.0, 31.5, 31.4, 30.83, 30.78, 30.7, 29.7, 29.6, 29.54, 29.46, 27.3, 27.2, 26.69, 26.65, 26.4, 26.3, 26.1, 25.0, 24.8, 18.2, 18.1.

Macrocycles 75. Acyclic intermediate **73** (25 mg, 21 μ mol) was treated with AcOH:H₂O (1:1, 1 mL) and stirred at rt for 4 hrs, after which HPLC-UV/MS analysis showed complete conversion. The apparent product peak showed a slight shoulder, but was not purified. The mixture was concentrated to give 52.2 mg of a colorless residue. (**74**): MS *m/z* 879.2 (calc'd: C₄₁H₄₃BrFN₆O₈S, [M-OCO₂tBu]⁺, 877.2). This material was taken up in nitromethane (4.0 mL) and treated with TFA (200 μ L). The resulting mixture was stirred for 2 hrs, then concentrated to dryness and reconstituted in DMSO (500 μ L). Initial fractionation was accomplished using semi-preparative HPLC method A, giving the following fractions: A = 1.6 mg; B = 2.3 mg; C = 1.6 mg; D = 9.9 mg; E = 4.7 mg; F = 2.0; G = 7.1 mg; H (**75h**) = 2.7; I (**75i**) = 1.6. Fraction D was re-purified using semi-preparative method B to recover D1 (**75d**) = 3.8 mg. Fractions E and G were re-purified using semi-preparative method C to recover E1 = 0.7 mg, E2 (**75e**) = 0.9 mg and G1 = 0.4 mg, G2 (**75g**) = 3.4 mg. The remaining fractions A–C and F were not pursued either for lack of material or complex constituency upon reanalysis.

Analytical HPLC method:

Column: Waters XBridge™ Phenyl, 4.6x250mm, 5 μ m.

Solvent A: H₂O + 0.1%v TFA

Solvent B: ACN + 0.1%v TFA

Flow rate: 1.00 ml/min

Time	%B
0	20
1	20
3	45
25	70
27	20
30	20

Semi-preparative HPLC method B:

Column: Waters XBridge™ Phenyl, 10x250mm, 5 μ m.

Solvent A: H₂O + 0.1%v TFA

Solvent B: ACN + 0.1%v TFA

Flow rate: 6.00 ml/min

Time	%B
0	30
1	30
3	47
14	49.5
15	30
17	30

Semi-preparative HPLC method A:

Column: Waters XBridge™ Phenyl, 10x250mm, 5 μ m.

Solvent A: H₂O + 0.1%v TFA

Solvent B: ACN + 0.1%v TFA

Flow rate: 6.00 ml/min

Time	%B
0	20
1	20
4	47
25	52
27	20
30	20

Semi-preparative HPLC method C:

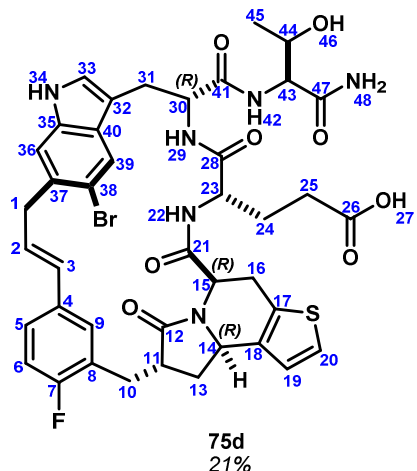
Column: Waters XBridge™ Phenyl, 10x250mm, 5 μ m.

Solvent A: H₂O + 0.1%v TFA

Solvent B: ACN + 0.1%v TFA

Flow rate: 6.00 ml/min

Time	%B
0	40
1	40
3	48
20	58
22	40
25	40



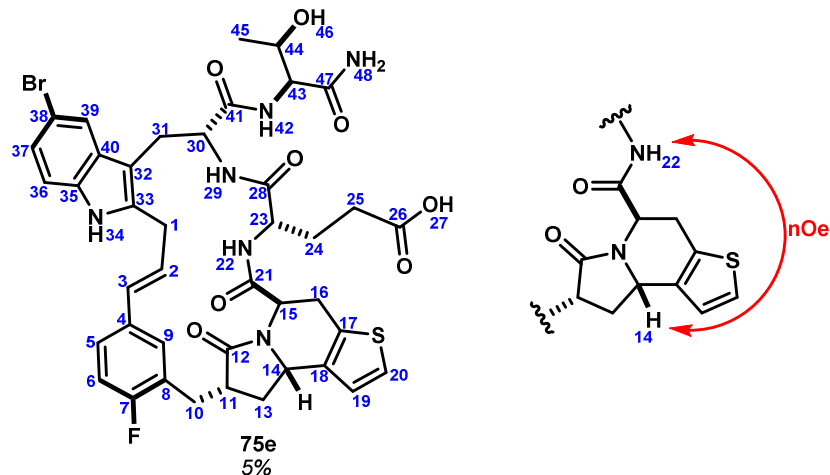
*Intermediate exchange at rt.

**No NOE 14↔22. No diagnostic NOEs from 11,13,15,16. Tentatively assigned 14R.
(500MHz, DMSO-*d*₆, 338K)

	¹³ C	¹ H	key correlation
1	38.1	3.66 (dd, <i>J</i> = 14.7, 6.7 Hz, 1H), 3.73 (dd, <i>J</i> = 14.7, 3.9 Hz, 1H)	HMBC 1→2,3,36,37,38
2	129.0	6.13-6.19 (m, 1H)	HMBC 2→3,4,37
3	128.1	6.22 (d, <i>J</i> = 15.8 Hz, 1H)	TOCSY 3→1,2 HMBC 3→1,2
4	132.5	-	
5	124.9	7.05-7.10 (m, 1H)	HMBC 5→3
6	113.6	6.84-6.88 (m, 1H) overlap	HMBC 6→4,7,8 COSY 6→5
7	159.0 (d, <i>J</i> _{CF} ≈ 230 Hz)	-	
8	124.5	-	
9	126.5	7.24-7.31 (m, 1H)	HMBC 9→3
10	25.5	2.81 (dd, <i>J</i> = 14.8, 3.1 Hz, 1H), 2.87 (dd, <i>J</i> = 12.2, 7.6, 7.6 Hz, 1H)	HMBC 10→7,8,9,11,12,13
11	41.1	2.96-3.03 (m, 1H)	HMBC 11→10
12	173.2	-	
13	30.9	1.21-1.29 (m, 1H), 2.66 (ddd, <i>J</i> = 12.2, 7.6, 7.6 Hz, 1H)	HMBC 13'→11,12 COSY 13→14
14	50.7	4.39-4.45 (m, 1H)	HMBC 14→15 NOESY 14→11,13'
15	48.8	4.33 (d, <i>J</i> = 5.7 Hz, 1H)	HMBC 15→21
16	23.6	2.38-2.45 (m, 1H), 2.83-2.96 (m, 1H) overlap	
17	129.7	-	
18	134.1	-	
19	122.7	6.69 (d, <i>J</i> = 4.9 Hz, 1H)	HMBC 19→17,20 NOESY 19→14
20	123.3	7.20 (d, <i>J</i> = 4.9 Hz, 1H)	HMBC 20→19
21	167.0	-	
22	-	6.92 (d, <i>J</i> = 7.3 Hz, 1H)	

23	52.5	4.04-4.10 (m, 1H)	
24	26.5	1.56-1.64 (m, 1H), 1.88-1.95 (m, 1H)	HMBC 24→26
25	28.8	1.70-1.79 (m, 1H), 1.80-1.87 (m, 1H)	HMBC 26→23
26	172.5	-	
27	-	not observed	
28	not detected	-	
29	-	7.62 (d, <i>J</i> = 6.3 Hz, 1H)	
30	53.6	4.70-4.76 (m, 1H)	
31	27.0	2.91-2.98 (m, 1H), 3.16-3.23 (m, 1H)	HMBC 31→30,32
32	109.1	-	
33	124.4	7.17-7.18 (m, 1H)	HMBC 33→32,35,36
34	-	10.66-10.71 (m, 1H)	COSY 34→33 HMBC 34→32,40 NOESY 34→33,36
35	135.3	-	
36	112.6	7.41 (s, 1H)	HMBC 36→35,38,40 TOCSY 36→39
37	130.0	-	
38	113.4	-	
39	121.5	7.95 (s, 1H)	HMBC 39→38,40
40	130.1	-	
41	170.8	-	
42	-	7.74 (d, <i>J</i> = 8.0 Hz, 1H)	HMBC 42→41
43	57.5	4.21 (dd, <i>J</i> = 8.0, 3.3 Hz, 1H)	HMBC 43→47
44	65.6	4.09-4.14 (m, 1H)	HMBC 44→47
45	19.1	1.13 (d, <i>J</i> = 6.4 Hz, 3H)	COSY 45→44 TOCSY 45→42,43,44
46	-	not observed	
47	171.4	-	
48	-	6.81-6.87 (m, 2H) overlap	

MS *m/z* 877.2/879.2 (calc'd: C₄₁H₄₃BrFN₆O₈S, [M+H]⁺, 877.2/879.2).

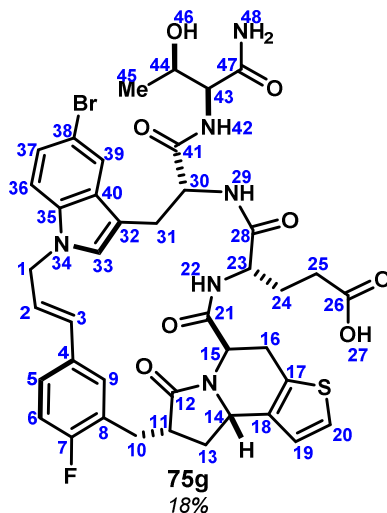


(500MHz, DMSO-*d*₆, 298K)

	¹³ C	¹ H	key correlation
1	29.7	3.50 (dd, <i>J</i> = 14.9, 7.9 Hz, 1H), 3.90 (dd, <i>J</i> = 14.9, 5.0 Hz, 1H)	HMBC 1→2,3,32,33
2	128.1	6.64 (ddd, <i>J</i> = 15.8., 7.9, 5.0 Hz, 1H)	COSY 2→1
3	128.9	6.57 (d, <i>J</i> = 15.8 Hz, 1H)	HMBC 3→1
4	133.0	-	
5	126.4	7.11-7.14 (m, 1H) overlap	HMBC 5→3,7
6	114.0	7.07 (dd, <i>J</i> _{HF} = 9.8 Hz, <i>J</i> _{HH} = 8.5 Hz, 1H)	HMBC 6→4,8
7	159.0 (d, <i>J</i> _{CF} ≈ 230 Hz)	-	
8	126.8	-	HMBC 9→7
9	124.7	7.88 (d, <i>J</i> = 7.2 Hz, 1H)	HMBC 10→8,9
10	25.6	2.73 (br d, <i>J</i> = 16.3 Hz, 1H), 2.81-2.88 (m, 1H) overlap	
11	39.6	3.26-3.34 (m, 1H) obscured	
12	174.9	-	HMBC 13→11
13	33.9	1.54 (ddd, <i>J</i> = 12.0, 11.1, 10.8 Hz, 1H), 2.80-2.85 (m, 1H) overlap	HMBC 14→13
14	51.5	4.35 (dd, <i>J</i> = 10.8, 4.5 Hz, 1H)	HMBC 15→14,17,21
15	48.8	4.83 (br d, <i>J</i> = 8.1 Hz, 1H)	HMBC 16→21
16	22.9	2.98 (dd, <i>J</i> = 16.6, 8.1 Hz, 1H), 3.21-3.28 (m, 1H) overlap	
17	131.3	-	
18	134.2	-	
19	123.4	6.88 (d, <i>J</i> = 5.2 Hz, 1H)	HMBC 19→17,18,20
20	123.9	7.37 (d, <i>J</i> = 5.2 Hz, 1H)	HMBC 20→17,18
21	168.2	-	
22	-	7.14-7.20 (m, 1H) overlap	
23	51.0	4.13-4.18 (m, 1H) overlap	HMB 23→28
24	26.8	0.82-0.89 (m, 1H), 1.59-1.68 (m, 1H)	
25	28.5	1.39-1.49 (m, 1H), 1.73-1.82 (m, 1H)	TOCSY 25→22,23,24,25'

26	173.2	-	
27	-	11.84 (br s, 1H)	
28	170.2	-	
29	-	8.32 (br d, $J = 8.7$ Hz, 1H)	HMBC 29→28
30	54.1	4.75-4.81 (m, 1H) overlap	
31	26.7	2.89 (dd, $J = 14.2, 10.6$ Hz, 1H), 3.22 (dd, $J = 14.2, 5.6$ Hz, 1H)	HMBC 31→32,41
32	105.7	-	
33	136.4	-	
34	-	11.03 (s, 1H)	HMBC 34→32,35,40
35	133.3	-	
36	113.9	7.06 (d, $J = 8.5$ Hz, 1H)	HMBC 36→40
37	122.3	7.01 (dd, $J = 8.5, 1.8$ Hz, 1H)	HMBC 37→39
38	110.9	-	
39	120.0	7.63 (d, $J = 1.8$ Hz, 1H)	HMBC 39→32,35,37,38
40	131.0	-	
41	170.6	-	
42	-	7.91 (br d, $J = 8.2$ Hz, 1H)	
43	57.8	4.11-4.16 (m, 1H) overlap	HMBC 43→47
44	66.0	3.97 (ddd, $J = 6.3, 5.5, 3.5$ Hz, 1H)	TOCSY 44→42,43,45
45	19.4	0.81 (d, $J = 6.3$ Hz, 3H)	HMBC 45→43,44
46	-	4.76 (d, $J = 5.5$ Hz, 1H)	HMBC 46→43,44,45
47	172	-	
48	-	7.12 (br s, 1H) overlap, 7.18 (br s, 1H)	TOCSY 48'→48

MS m/z 877.2/879.1 (calc'd: $C_{41}H_{43}BrFN_6O_8S$, $[M+H]^+$, 877.2/879.2).

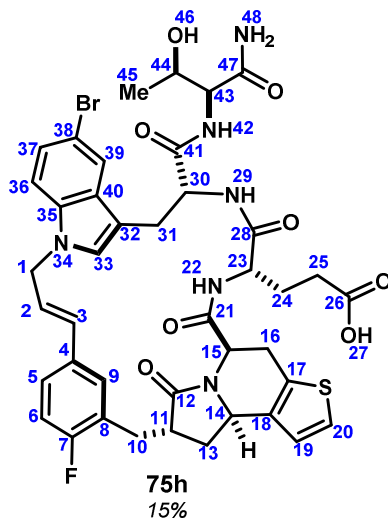


(500MHz, DMSO-*d*₆, 298K)

	¹³ C	¹ H	key correlation
1	46.9	4.90 (br d, <i>J</i> = 4.7 Hz, 2H)	NOESY 1→33,36 HMBC 1→2,33,35
2	125.5	6.54 (dt, <i>J</i> = 15.9, 4.7 Hz, 1H)	HMBC 2→4
3	129.0	6.21 (br d, <i>J</i> = 15.9 Hz, 1H)	
4	133.2	-	
5	125.7	7.40-7.46 (m, 1H) overlap	NOESY 5→2,3,6 HMBC 5→9
6	114.9	7.14 (dd, <i>J</i> _{HF} = 9.6 Hz, <i>J</i> _{HH} = 8.5 Hz, 1H)	
7	160.1 (d, <i>J</i> _{CF} ≈ 240 Hz)	-	
8	124.3	-	
9	130.0	7.27-7.30 (m, 1H)	HMBC 9→5
10	25.8	2.83-2.91 (m, 2H)	HMBC 10→7,8,12,13 COSY 10→11
11	40.2	2.53-2.59 (m, 1H)	HMBC 11→8,12
12	176.2	-	
13	27.7	1.77-1.84 (m, 1H), 2.16-2.22 (m, 1H)	HMBC 13→10,12
14	56.6	4.41 (br d, <i>J</i> = 7.9 Hz, 1H)	COSY 14→13,16
15	55.3	3.89 (dd, <i>J</i> = 8.7, 7.4 Hz, 1H)	COSY 15→16 HMBC 15→12,21
16	24.7	2.97-3.03 (m, 2H)	HMBC 16→17,18
17	133.4	-	
18	137.0	-	
19	124.2	6.95 (d, <i>J</i> = 5.2 Hz, 1H)	HMBC 19→14,17,18 NOESY 19→14
20	124.0	7.35 (d, <i>J</i> = 5.2 Hz, 1H)	HMBC 20→17,18,19
21	167.8	-	
22	-	7.41-7.44 (m, 1H) overlap	HMBC 22→21
23	52.2	4.23-4.27 (m, 1H)	HMBC 23→28

24	26.7	1.43-1.53 (m, 1H), 1.85-1.93 (m, 1H)	
25	30.0	2.05-2.17 (m, 2H)	HMBC 25→26
26	174.2	-	
27	-	12.03 (br s, 1H)	
28	170.4	-	
29	-	7.89 (d, $J = 8.6$ Hz, 1H)	TOCSY 29→30,31
30	53.8	4.70 - 4.76 (m, 1H)	
31	27.7	2.90-2.96 (m, 1H), 3.17-3.23 (m, 1H)	HMBC 31→32 COSY 31→30
32	109.7	-	
33	128.9	7.29 (s, 1H)	HMBC 33→32,40
34	-	-	
35	134.1	-	
36	111.6	7.32 (d, $J = 8.7$ Hz, 1H)	HMBC 36→35,38,40
37	123.2	7.14 (dd, $J = 8.7, 1.8$ Hz, 1H)	HMBC 37→35
38	111.1	-	
39	121.0	7.77 (d, $J = 1.8$ Hz, 1H)	TOCSY 39→36,37 HMBC 39→35
40	129.5	-	
41	171.1	-	
42	-	8.02 (d, $J = 8.9$ Hz, 1H)	TOCSY 42→43,44,45,46 HMBC 42→41
43	57.9	4.19 (dd, $J = 8.7, 3.6$ Hz, 1H)	
44	66.2	4.05-4.11 (m, 1H)	COSY 44→43,46
45	20.0	1.10 (d, $J = 6.4$ Hz, 3H)	COSY 45→44
46	-	4.88-4.90 (m, 1H) overlap	
47	171.9	-	
48	-	7.11 (brs, 1H), 7.21 (brs, 1H)	HMBC 48→47 TOCSY 48→48'

MS m/z 877.2/879.1 (calc'd: $C_{41}H_{43}BrFN_6O_8S$, $[M+H]^+$, 877.2/879.2)

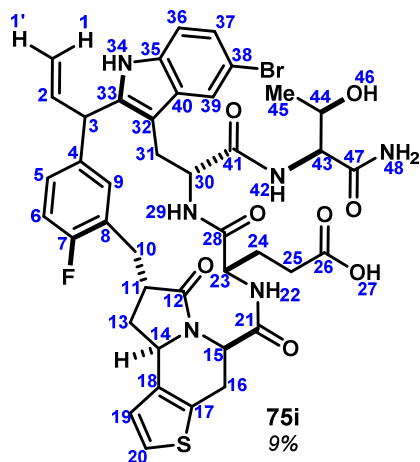


(500MHz, DMSO-*d*₆, 298K)

	¹³ C	¹ H	key correlation
1	46.9	4.90 (br d, <i>J</i> = 4.7 Hz, 2H)	NOESY 1→33,36 HMBC 1→2,33,35
2	125.5	6.54 (dt, <i>J</i> = 15.9, 4.7 Hz, 1H)	HMBC 2→4
3	129.0	6.21 (br d, <i>J</i> = 15.9 Hz, 1H)	
4	133.2	-	
5	125.7	7.40-7.46 (m, 1H) overlap	NOESY 5→2,3,6 HMBC 5→9
6	114.9	7.14 (dd, <i>J</i> _{HF} = 9.6 Hz, <i>J</i> _{HH} = 8.5 Hz, 1H)	
7	160.1 (d, <i>J</i> _{CF} ≈ 240 Hz)	-	
8	124.3	-	
9	130.0	7.27-7.30 (m, 1H)	HMBC 9→5
10	25.8	2.83-2.91 (m, 2H)	HMBC 10→7,8,12,13 COSY 10→11
11	40.2	2.53-2.59 (m, 1H)	HMBC 11→8,12
12	176.2	-	
13	27.7	1.77-1.84 (m, 1H), 2.16-2.22 (m, 1H)	HMBC 13→10,12
14	56.6	4.41 (br d, <i>J</i> = 7.9 Hz, 1H)	COSY 14→13,16
15	55.3	3.89 (dd, <i>J</i> = 8.7, 7.4 Hz, 1H)	COSY 15→16 HMBC 15→12,21
16	24.7	2.97-3.03 (m, 2H)	HMBC 16→17,18
17	133.4	-	
18	137.0	-	
19	124.2	6.95 (d, <i>J</i> = 5.2 Hz, 1H)	HMBC 19→14,17,18 NOESY 19→14
20	124.0	7.35 (d, <i>J</i> = 5.2 Hz, 1H)	HMBC 20→17,18,19
21	167.8	-	
22	-	7.41-7.44 (m, 1H) overlap	HMBC 22→21
23	52.2	4.23-4.27 (m, 1H)	HMBC 23→28

24	26.7	1.43-1.53 (m, 1H), 1.85-1.93 (m, 1H)	
25	30.0	2.05-2.17 (m, 2H)	HMBC 25→26
26	174.2	-	
27	-	12.03 (br s, 1H)	
28	170.4	-	
29	-	7.89 (d, $J = 8.6$ Hz, 1H)	TOCSY 29→30,31
30	53.8	4.70 - 4.76 (m, 1H)	
31	27.7	2.90-2.96 (m, 1H), 3.17-3.23 (m, 1H)	HMBC 31→32 COSY 31→30
32	109.7	-	
33	128.9	7.29 (s, 1H)	HMBC 33→32,40
34	-	-	
35	134.1	-	
36	111.6	7.32 (d, $J = 8.7$ Hz, 1H)	HMBC 36→35,38,40
37	123.2	7.14 (dd, $J = 8.7, 1.8$ Hz, 1H)	HMBC 37→35
38	111.1	-	
39	121.0	7.77 (d, $J = 1.8$ Hz, 1H)	TOCSY 39→36,37 HMBC 39→35
40	129.5	-	
41	171.1	-	
42	-	8.02 (d, $J = 8.9$ Hz, 1H)	TOCSY 42→43,44,45,46 HMBC 42→41
43	57.9	4.19 (dd, $J = 8.7, 3.6$ Hz, 1H)	
44	66.2	4.05-4.11 (m, 1H)	COSY 44→43,46
45	20.0	1.10 (d, $J = 6.4$ Hz, 3H)	COSY 45→44
46	-	4.88-4.90 (m, 1H) overlap	
47	171.9	-	
48	-	7.11 (brs, 1H), 7.21 (brs, 1H)	HMBC 48→47 TOCSY 48→48'

MS m/z 877.2/879.1 (calc'd: $C_{41}H_{43}BrFN_6O_8S$, $[M+H]^+$, 877.2/879.2).



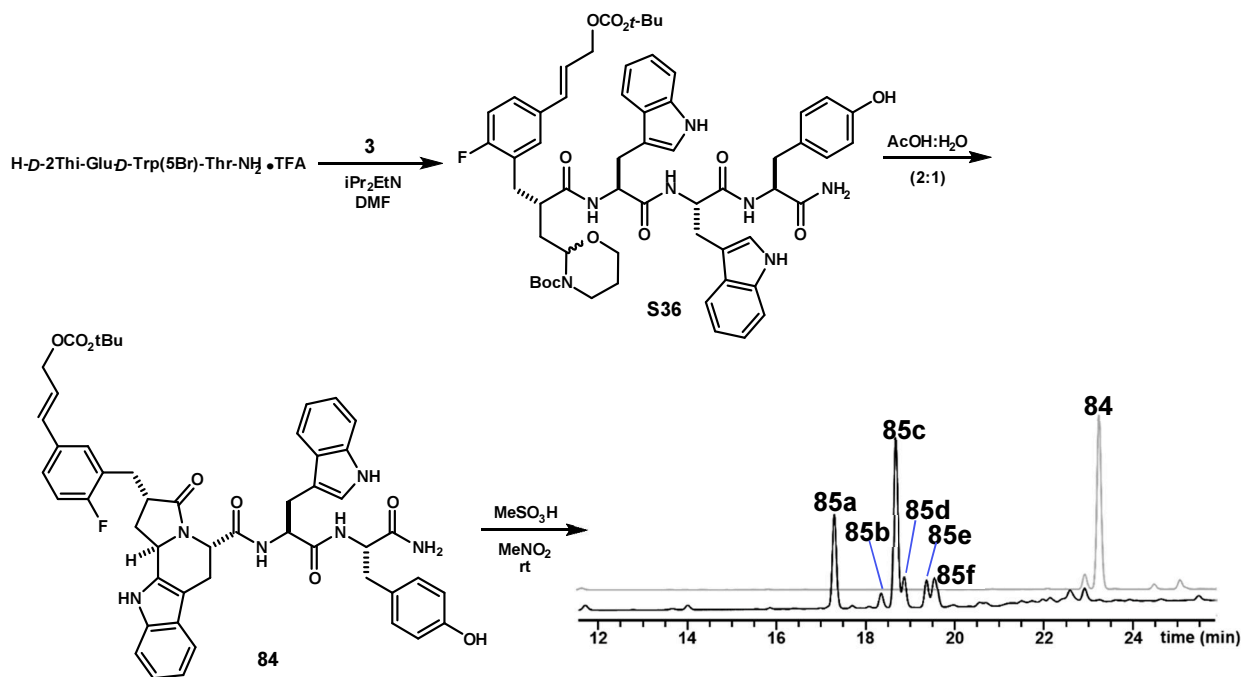
(500MHz, DMSO-*d*₆, 298K)

	¹³ C	¹ H	key correlation
1	117.0	5.05 (d, <i>J</i> = 17.1 Hz, 1H), 5.24 (d, <i>J</i> = 10.5 Hz, 1H)	
2	137.4	6.41 (ddd, <i>J</i> = 17.1, 10.5, 8.2 Hz, 1H)	
3	45.6	5.11 (d, <i>J</i> = 8.2 Hz, 1H)	HMBC 3→2,4,6,33
4	133.4	-	
5	115.3	6.94 (dd, <i>J</i> _{HF} = 10.0, <i>J</i> _{HH} = 8.5 Hz, 1H)	HMBC 5→7 COSY 5→6 TOCSY 5→6,9
6	126.8	6.79-6.93 (m, 1H)	
7	158.9 (d, <i>J</i> _{CF} ≈ 250 Hz)	-	
8	not observed	-	
9	not observed	7.41-7.45 (m, 1H)	NOESY 9→3
10	31.5	2.70-2.76 (m, 1H), 3.01-3.06 (m, 1H)	NOESY 10→9 HMBC 10→12
11	39.9	2.37-2.42 (m, 1H)	
12	177.7	-	
13	32.1	2.26-2.32 (m, 1H), 2.55-2.62 (m, 1H)	HMBC 13'→12
14	56.8	4.84-4.88 (m, 1H)	COSY 14→13 NOESY 14→15,19
15	54.6	4.33-4.36 (m, 1H) overlap	HMBC 15→12,21 NOESY 15→22
16	24.9	2.90-3.01 (m, 2H)	
17	134.1	-	
18	136.2	-	
19	124.2	7.06-7.09 (m, 1H)	NOESY 19→14 HMBC 19→17,18,20
20	124.2	7.41 (d, <i>J</i> = 5.2 Hz, 1H)	HMBC 20→17,18
21	168.3	-	
22	-	8.52 (d, <i>J</i> = 6.8 Hz, 1H)	TOCSY 22→23,24,25 NOESY 22→29

23	52.7	4.17-4.23 (m, 1H)	
24	25.3	1.79-1.89 (m, 1H), 2.11-2.20 (m, 1H)	
25	30.1	2.35-2.42 (m, 2H)	
26	174.3	-	
27	-	12.13 (br s, 1H)	
28	171.6	-	
29	-	8.22 (d, $J = 5.3$ Hz, 1H)	HMBC 29→28 NOESY 29→42
30	54.6	4.31-4.34 (m, 1H) overlap	
31	24.0	2.49-2.56 (m, 1H) overlap, 3.21-3.29 (m, 1H)	
32	104.8	-	
33	140.0	-	
34	-	10.97 (s, 1H)	HMBC 34→32,33,35,40
35	133.7	-	
36	112.6	7.25 (d, $J = 8.5$ Hz, 1H)	HMBC 36→38,40
37	122.3	7.06-7.09 (m, 1H) overlap	
38	111.0	-	
39	120.2	7.58 (d, $J = 1.8$ Hz, 1H)	TOCSY 39→36,37 HMBC 39→38
40	130.3	-	
41	not observed	-	
42	-	7.59-7.64 (m, 1H)	HMBC 42→41
43	58.1	3.80 (dd, $J = 8.7, 2.4$ Hz, 1H)	HMBC 43→47
44	64.8	3.94-4.01 (m, 1H)	
45	18.8	0.21 (br d, $J = 5.5$ Hz, 3H)	TOCSY 45→42,43,44,46
46	-	4.30-4.34 (m, 1H) overlap	
47	172.1	-	
48	-	7.00 (br s, 1H), 7.09 (br s, 1H)	TOCSY 48→48'

MS m/z 877.2/879.1 (calc'd: $C_{41}H_{43}BrFN_6O_8S$, $[M+H]^+$, 877.2/879.2).

Macrocycles 85a–f:



Acyclic cinnamyl carbonate S36. Compound **84** was prepared analogously to compound **70** with the following exceptions. The reaction was worked up by partitioning between sat. NaHCO_3 and EtOAc , and the organic phase was washed with sat. NaHCO_3 , 1N HCl , H_2O , brine, dried over Na_2SO_4 and concentrated. Purification was accomplished by column chromatography on SiO_2 eluted with 0→10% MeOH in CHCl_3 afforded **84** as a colorless film. A yield was not recorded. $^1\text{H NMR}$ (CD_3OD , 500 MHz, ~1:1 mixture of diastereomers): δ 1.28 (s, 9H), 1.37 (s, 9H), 1.44 (s, 9H), 1.45 (s, 9H), 1.53–1.69 (m, 2H), 1.92–2.00 (m, 1H), 2.06 (ddd, $J = 14.0, 8.1, 5.8$ Hz, 1H), 2.33–2.45 (m, 2H), 2.46–2.54 (m, 1H), 2.53–2.62 (m, 2H), 2.62–2.74 (m, 3H), 2.74–3.12 (m, 16H), 3.37–3.49 (m, 2H), 3.54–3.66 (m, 2H), 3.73–3.84 (m, 2H), 4.40 (dd, $J = 7.8, 6.2$ Hz, 1H), 4.44–4.52 (m, 3H), 4.52–4.58 (m, 2H), 4.55 (br d, $J = 6.3$ Hz, 2H), 4.60 (br d, $J = 6.3$ Hz, 2H), 5.30–5.39 (m, 1H), 5.45 (dd, $J = 8.1, 6.4$ Hz, 1H), 6.13 (dt, $J = 15.9, 6.2$ Hz, 1H), 6.17 (dt, $J = 15.9, 6.2$ Hz, 1H), 6.44 (br d, $J = 15.9$ Hz, 1H), 6.50 (br d, $J = 15.9$ Hz, 1H), 6.65 (d, $J = 8.5$ Hz, 2H), 6.70 (d, $J = 8.4$ Hz, 2H), 6.74–6.77 (m, 2H), 6.83 (s, 1H), 6.86–6.93 (m, 4H), 6.93–7.03 (m, 7H), 7.04–7.15 (m, 6H), 7.15–7.22 (m, 2H), 7.29 (apt t, $J = 7.7$ Hz, 1H), 7.32 (apt t, $J = 7.8$ Hz, 1H), 7.40–7.46 (m, 3H), 7.48 (d, $J = 7.9$ Hz, 1H). $^{13}\text{C NMR}$ (CD_3OD , 126 MHz, ~1:1 mixture of diastereomers): δ 177.0, 176.9, 176.5, 176.4, 176.0, 175.9, 174.38, 174.36, 174.05, 174.03, 173.4, 173.3, 163.1, 161.2, 157.2, 155.5, 154.93, 154.92, 137.92, 137.91, 137.89, 137.84, 134.03, 134.00, 133.90, 133.87, 133.75, 133.71, 131.34, 131.26, 130.8, 130.73, 130.69, 129.1, 129.0, 128.7, 128.6, 128.5, 128.0, 127.9, 127.84, 127.78, 127.3, 127.2, 124.5, 124.3, 124.1, 122.6, 122.54, 122.52, 120.0, 119.93, 119.90, 119.44, 119.38, 119.31, 119.28, 116.6, 116.5, 116.4, 116.3, 116.2, 112.4, 112.3, 110.7, 110.64, 110.57, 110.51, 83.0, 82.9, 81.7, 81.6, 68.29, 68.27, 61.0, 60.6, 56.2, 56.1, 56.0, 55.9, 55.3, 55.2, 46.0, 44.4, 44.3, 38.6, 38.4, 37.6, 32.8, 32.6, 32.1, 31.8, 30.7, 28.7, 28.61, 28.55, 28.4, 28.3, 28.2, 28.0, 26.2, 26.0. MS m/z 958.3 (calc'd: $\text{C}_{53}\text{H}_{61}\text{FN}_7\text{O}_9$, $[\text{M-Boc}+2\text{H}]^+$, 958.8); 940.5 (calc'd: $\text{C}_{53}\text{H}_{59}\text{FN}_7\text{O}_8$, $[\text{M-OCO}_2\text{tBu}+2\text{H}]^+$, 940.4).

Pyrrolo tetrahydro- β -carboline (84). Intermediate **S36** (147 mg, 138 μmol) was dissolved in $\text{AcOH:H}_2\text{O}$ (2:1, 15.7 mL) and stirred at rt for 4 hr. The mixture was concentrated to give **84** (106 mg, 88%) as a colorless film. An analytical sample was obtained by preparative HPLC purification. $^1\text{H NMR}$ ($\text{DMSO-}d_6$, 500 MHz): δ 1.43 (s, 9H), 1.90–2.00 (m, 2H), 2.56–2.64 (m, 2H), 2.69 (dd, $J = 13.9, 7.9$ Hz, 1H), 2.79–2.88 (m, 2H), 2.99 (dd, $J = 14.6, 9.5$ Hz, 1H), 3.05–3.13 (m, 2H), 3.20 (d, $J = 15.6$ Hz, 1H), 6.37 (dt, $J = 15.9, 6.2$ Hz, 1H), 6.65 (d, $J = 8.5$ Hz, 2H), 6.67 (br d, $J = 16.0$ Hz, 1H), 6.92–6.98 (m, 1H), 6.98 (d, $J = 8.5$ Hz, 2H), 6.99–7.03 (m, 1H), 7.03–7.06 (m, 2H), 7.12 (d, $J = 2.0$ Hz, 1H), 7.16 (dd, $J_{\text{HF}} = 9.7, J_{\text{HH}} = 8.3$ Hz, 1H), 7.21 (br d, $J = 8.1$ Hz, 1H), 7.29 (br s, 1H), 7.33 (d, $J = 8.1$ Hz, 1H), 7.36 (br d, $J = 7.8$ Hz, 1H), 7.40 (ddd, $J_{\text{HH}} = 8.3, 2.0$ Hz, $J_{\text{HF}} = 5.0$ Hz, 1H), 7.47 (dd, $J_{\text{HF}} = 7.3$ Hz, $J_{\text{HH}} = 2.0$ Hz, 1H), 7.59 (d, $J = 7.9$ Hz, 1H), 7.92 (d, J

= 8.0 Hz, 1H), 8.15 (d, $J = 7.8$ Hz, 1H), 9.19 (br s, 1H), 10.78 (s, 1H), 10.81 (d, $J = 1.6$ Hz, 1H). MS m/z 765.3 (calc'd: $C_{45}H_{42}FN_6O_5$, $[M-Boc+2H]^+$, 765.3).

Macrocycles 85a–f. Compound **84** (78 mg, 90 μ mol) was suspended in $MeNO_2$ (18 mL) and treated with $MeSO_3H$ (88 μ L, 1.4 mmol). The mixture was stirred for 2 hr at rt, then quenched with iPr_2EtN , concentrated, reconstituted in DMSO and purified by semi-preparative HPLC method A. Fraction B was re-purified by the same method, and fraction E was re-purified by semi-preparative HPLC method B. Yields were not determined.

Analytical HPLC method:

Column: Waters XBridge™ C18, 4.6x250mm, 5 μ m.

Solvent A: $H_2O + 0.1\%v$ TFA

Solvent B: ACN + 0.1%v TFA

Flow rate: 1.00 ml/min

Time	%B
0	42
2	42
25	60
26	42
31	42

Semi-preparative HPLC method A:

Column: Waters XBridge™ C18, 10x250mm, 5 μ m.

Solvent A: $H_2O + 0.1\%v$ TFA

Solvent B: ACN + 0.1%v TFA

Flow rate: 7.00 ml/min

Time	%B
0	42
2	42
16	50
16.2	100
19	100
19.5	42

Semi-preparative HPLC method B:

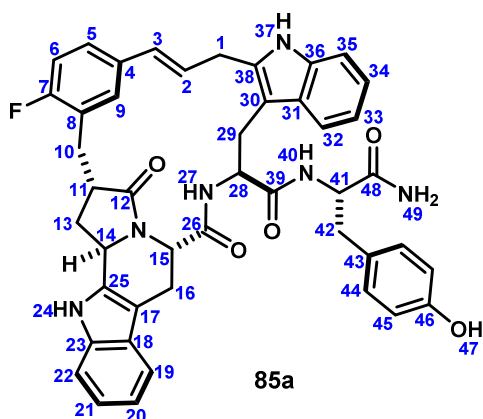
Column: Waters XSelect™ C18, 10x250mm, 5 μ m.

Solvent A: $H_2O + 0.1\%v$ TFA

Solvent B: ACN + 0.1%v TFA

Flow rate: 6.00 ml/min

Time	%B
0	43
1	43
31	54



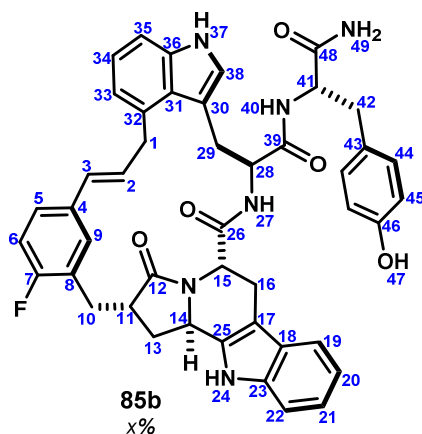
(500MHz, $DMSO-d_6$, 298K)

	^{13}C	1H	key correlation
1	291.0	3.57 (dd, $J = 16.8, 5.6$ Hz, 1H), 3.67 (dd, $J = 16.8, 5.1$ Hz, 1H)	HMBC 1→2,3,30,38

2	126.7	6.24 (ddd, $J = 15.8, 5.6, 5.1$ Hz, 1H)	TOCSY 2→1,3 HMBC 2→4
3	128.9	5.87 (d, $J = 15.8$ Hz, 1H)	
4	133.3	-	
5	124.6	7.34-7.37 (m, 1H) overlap	HMBC 5→7 TOCSY 5→7,9
6	114.6	7.09 (dd, $J_{HF} = 9.9$ Hz, $J_{HH} = 1.8$ Hz, 1H)	HMBC 6→4,7
7	159.4 (d, $J \approx 240$ Hz)	-	
8	123.4	-	
9	129.9	6.69 (dd, $J_{HF} = 7.4$ Hz, $J_{HH} = 1.8$ Hz, 1H)	HMBC 9→5,7
10	27.6	2.76-2.82 (m, 1H) overlap, 3.00 (dd, $J = 13.5, 5.2$ Hz, 1H)	HMBC 10→8,11,12
11	42.2	2.78-2.84 (m, 1H) overlap	
12	173.3	-	
13	29.2	1.95 (ddd, $J = 12.7, 9.5, 9.5$ Hz, 1H), 2.26 (dd, $J = 12.7, 8.0$ Hz, 1H)	HMBC 13→10,11,12 COSY 13→14
14	51.2	4.32 (dd, $J = 9.5, 8.0$ Hz, 1H)	HMBC 14→25
15	47.3	4.97 (d, $J = 8.3$ Hz, 1H)	HMBC 15→14,16,26 COSY 15→16
16	23.6	2.78-2.84 (m, 1H) overlap, 2.94 (d, $J = 16.8$ Hz, 1H) overlap	HMBC 16→15,17,25,26
17	102.9	-	
18	126.2	-	
19	117.8	7.33-7.36 (m, 1H) overlap	
20	118.2	6.88-6.92 (m, 1H) overlap	HMBC 20→18
21	120.2	6.95 (ddd, $J = 7.9, 7.1, 1.0$ Hz, 1H)	HMBC 21→19
22	110.4	7.17 (br d, $J = 7.9$ Hz, 1H)	HMBC 22→18
23	135.6	-	
24	-	10.81 (s, 1H)	HMBC 24→17,18,23,25
25	133.7	-	
26	169.9	-	
27	-	8.33 (d, $J = 7.8$ Hz, 1H)	
28	54.7	4.19 (ddd, $J = 7.8, 7.8, 7.8$ Hz, 1H)	HMBC 28→29,39 COSY 28→27
29	25.6	2.93-2.97 (m, 2H) overlap	HMBC 29→28,30,31,38
30	106.4	-	
31	128.8	-	
32	117.9	7.51 (d, $J = 7.9$ Hz, 1H)	HMBC 32→36
33	120.2	6.99 (ddd, $J = 7.9, 7.0, 0.9$ Hz, 1H)	
34	117.9	7.03 (ddd, $J = 8.0, 7.0, 1.1$ Hz, 1H)	HMBC 34→36
35	110.2	7.27 (d, $J = 8.0$ Hz, 1H)	
36	134.8	-	
37	-	10.89 (s, 1H)	HMBC 37→30
38	133.4	-	

39	171.3	-	
40	-	7.33-7.36 (m, 1H) overlap	HMBC 40→39
41	52.7	4.23 (ddd, $J = 7.7, 6.2, 6.2$ Hz, 1H)	HMBC 41→43 COSY 41→40
42	36.9	2.69 (dd, $J = 13.4, 6.2$ Hz, 1H), 2.77-2.81 (m, 1H) overlap	HMBC 42→43
43	126.7	-	
44	130.2	6.90 (d, $J = 8.3$ Hz, 2H)	
45	114.5	6.61 (d, $J = 8.3$ Hz, 2H)	HMBC 45→43,46
46	155.7	-	
47	-	9.14 (br s, 1H)	
48	171.8	-	
49	-	6.89 (br s, 1H) overlap, 7.29 (br s, 1H)	HMBC 49→48 TOCSY 49'→49

MS m/z 765.3 (calc'd: $C_{45}H_{42}FN_6O_5$, $[M+H]^+$, 765.3).



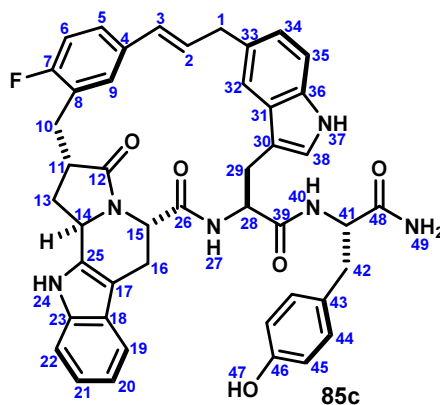
(500MHz, DMSO- d_6 , 298K)

	^{13}C	1H	key correlation
1	37.0	3.59-3.68 (m, 1H), 3.85-3.95 (m, 1H)	
2	130.5	6.30 (ddd, $J = 15.8, 6.2, 4.9$ Hz, 1H)	COSY 2→1,1' HMBC 2→4
3	128.5	5.98 (br d, $J = 15.8$ Hz, 1H)	
4	133.3	-	
5	125.4	7.13-7.18 (m, 1H)	HMBC 5→9
6	114.7	7.02-7.07 (m, 1H)	HMBC 6→4
7	159.7 (d, $J \approx 250$ Hz)	-	
8	124.1	-	
9	129.5	6.99-7.03 (m, 1H)	HMBC 10→8,9,12
10	28.3	2.86-2.92 (m, 1H) overlap, 3.01-3.08 (m, 1H)	HMBC 11→12
11	42.2	2.87-2.94 (m, 1H) overlap	
12	173.2	-	

13	29.3	2.00 (ddd, $J = 11.6, 10.1, 9.9$ Hz, 1H), 2.32-2.40 (m, 1H)	COSY 13→11 TOCSY 13→10,10',11,13' HMBC 13→12
14	51.2	4.57 (apt t, $J = 8.3$ Hz, 1H)	HMBC 14→17 COSY 14→13
15	48.1	5.22 (d, $J = 7.9$ Hz, 1H)	HMBC 15→12,17,26
16	24.7	2.80-2.86 (m, 1H) overlap, 2.94 (br dd, $J = 16.2, 8.1$ Hz, 1H)	
17	103.1	-	
18	126.3	-	
19	110.9	7.21 (d, $J = 8.1$ Hz, 1H)	HMBC 19→18
20	120.7	-	
21	118.2	6.97-7.01 (m, 1H)	TOCSY 21→19,20,22
22	117.7	7.34 (d, $J = 7.8$ Hz, 1H)	HMBC 22→17,18,20 COSY 22→21
23	135.6	-	
24	-	10.89 (s, 1H)	HMBC 24→17,18,23,25
25	134.2	-	
26	170.1	-	
27	-	8.56 (br d, $J = 5.0$ Hz, 1H)	
28	52.7	4.31-4.37 (m, 1H)	HMBC 28→39 TOCSY 28→27,29
29	28.9	3.14 (dd, $J = 15.5, 2.4$ Hz, 1H), 3.32 (dd, $J = 15.5, 10.3$ Hz, 1H)	
30	111.1	-	
31	125.8	-	
32	131.2	-	
33	120.5	6.77 (d, $J = 7.1$ Hz, 1H)	HMBC 33→1 COSY 33→34
34	121.0	6.93-6.97 (m,1H) overlap	HMBC 34→32,36
35	110.0	7.19 (d, $J = 8.2$ Hz, 1H)	COSY 35→34
36	136.6	-	
37	-	10.81 (br d, $J = 1.8$ Hz, 1H)	HMBC 37→30,31,36,38
38	122.0	7.00-7.21 (m, 1H)	HMBC 38→30,36
39	170.3	-	
40	-	8.35 (br s, 1H)	
41	53.1	4.42 (ddd, $J = 8.7, 7.9, 4.7$ Hz, 1H)	HMBC 41→39,43,48
42	36.1	2.74 (dd, $J = 14.4, 8.7$ Hz, 1H), 2.84 (dd, $J = 14.4, 4.7$ Hz, 1H)	TOCSY 42→40,41 HMBC 42→39,43,48
43	127.8	-	
44	129.8	7.01 (d, $J = 8.3$ Hz, 2H)	HMBC 44→46
45	115.0	6.73 (d, $J = 8.3$ Hz, 2H)	HMBC 45→43,46
46	155.8	-	
47	-	9.28 (br s, 1H)	HMBC 47→46
48	172.8	-	

49	-	6.88 (br s, 1H), 7.31 (br s, 1H)	HMBC 49→48
-----------	---	----------------------------------	------------

MS *m/z* 765.3 (calc'd: C₄₅H₄₂FN₆O₅, [M+H]⁺, 765.3).

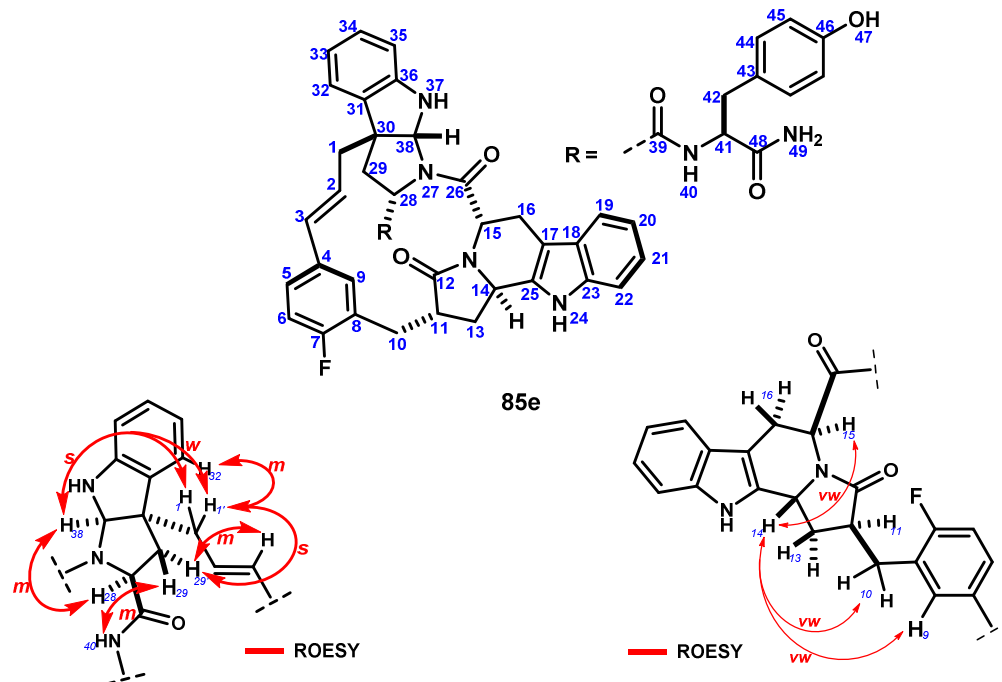


(500MHz, DMSO-*d*₆, 298K)

	¹³ C	¹ H	key correlation
1	37.5	3.54 (br dd, <i>J</i> = 16.6, 6.7 Hz, 1H), 3.60 (br dd, <i>J</i> = 16.6, 5.4 Hz, 1H)	HMBC 1→2,3,33,34
2	129.6	6.36 (ddd, <i>J</i> = 15.8, 6.7, 5.4 Hz, 1H)	HMBC 2→4,33 TOCSY 2→1,3
3	129.3	6.11 (br d, <i>J</i> = 15.8 Hz, 1H)	
4	133.6	-	
5	125.5	7.30 (ddd, <i>J</i> _{HH} = 8.4, 2.0 Hz, <i>J</i> _{HF} = 5.1 Hz, 1H)	TOCSY 5→6,9 HMBC 5→9
6	114.6	7.12 (dd, <i>J</i> _{HF} = 10.0, <i>J</i> _{HH} = 8.4 Hz, 1H)	HMBC 6→4,8
7	159.9 (d, <i>J</i> ≈240 Hz)	-	
8	124.5	-	
9	128.8	7.00-7.03 (m, 1H) overlap	HMBC 9→3,5
10	28.4	2.92-3.00 (m, 1H) overlap	HMBC 10→8,11,12,13
11	41.3	2.81-2.87 (m, 1H)	COSY 11→13,13'
12	173.7	-	
13	29.7	2.06 (ddd, <i>J</i> = 12.5, 9.0, 9.0 Hz, 1H), 2.29 (ddd, <i>J</i> = 12.5, 7.5, 2.6 Hz, 1H)	
14	50.7	4.97 (dd, <i>J</i> = 9.0, 7.5 Hz, 1H)	HMBC 14→25
15	48.2	5.00 (d, <i>J</i> = 8.2 Hz, 1H)	HMBC 15→12,14,26
16	24.2	2.93-2.98 (m, 1H) overlap, 3.05 (br d, <i>J</i> = 14.8 Hz, 1H)	HMBC 16→17,25
17	103.1	-	
18	126.2	-	
19	117.4	7.34 (d, <i>J</i> = 7.7 Hz, 1H)	HMBC 19→23
20	118.2	6.91-6.95 (m, 1H) overlap	
21	120.4	6.97-7.00 (m, 1H) overlap	HMBC 21→23 COSY 21→22
22	110.6	7.22 (d, <i>J</i> = 8.0 Hz, 1H)	HMBC 22→20

23	135.8	-	
24	-	10.93 (s, 1H)	HMBC 24→17,18,23,25
25	133.5	-	
26	170.5	-	
27	-	8.28 (d, $J = 8.1$ Hz, 1H)	HMBC 27→26
28	52.3	4.62 (ddd, $J = 8.1, 7.1, 7.1$ Hz, 1H)	HMBC 28→26,29,39
29	27.9	2.88 (dd, $J = 14.6, 6.8$ Hz, 1H), 3.08 (dd, $J = 14.6, 7.3$ Hz, 1H)	HMBC 29→30
30	109.0	-	
31	127.2	-	
32	117.4	7.37 (br s, 1H)	TOCSY 32→34,35 HMBC 32→34
33	128.9	-	
34	122.2	6.92-6.95 (m, 1H) overlap	HMBC 34→36
35	111.0	7.27 (d, $J = 8.2$ Hz, 1H)	HMBC 35→33
36	134.9	-	
37	-	10.74 (br d, $J = 1.6$ Hz, 1H)	HMBC 37→30,31,36,38
38	123.9	6.98-7.00 (m, 1H) overlap	HMBC 38→36
39	170.8	-	
40	-	7.50 (br d, $J = 7.6$ Hz, 1H)	HMBC 40→39
41	53.3	4.17 (ddd, $J = 7.6, 6.8, 6.8$ Hz, 1H)	COSY 41→42 HMBC 41→39,42,43,48
42	36.3	2.46-2.56 (m, 2H) overlap	HMBC 42→41,43,48
43	127.1	-	
44	129.8	6.77 (d, $J = 8.5$ Hz, 2H)	HMBC 44→46
45	114.5	6.56 (d, $J = 8.5$ Hz, 2H)	
46	155.6	-	
47	-	9.12 (br s, 1H)	
48	172.2	-	
49	-	6.83 (br s, 1H), 7.17 (br s, 1H)	HMBC 49→48 TOCSY 49→49'

MS m/z 765.3 (calc'd: $C_{45}H_{42}FN_6O_5$, $[M+H]^+$, 765.3).

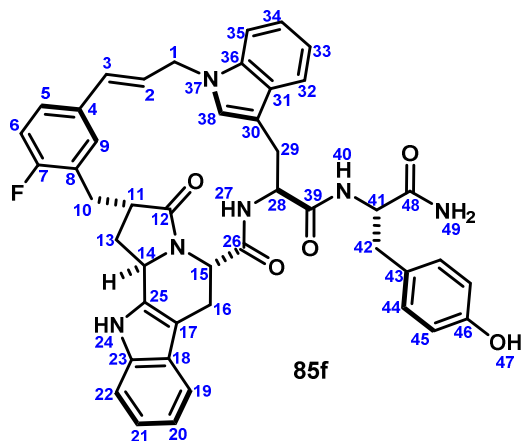


(500MHz, DMSO-*d*₆, 298K)

¹³ C	¹ H	key correlation
1	38.8	2.57-2.62 (m, 1H), 2.86 (dd, <i>J</i> = 12.5, 10.4 Hz, 1H)
2	126.9	6.08-6.16 (m, 1H) overlap
3	130.0	6.59 (d, <i>J</i> = 15.8 Hz, 1H)
4	133.6	-
5	126.6	7.06-7.10 (m, 1H) overlap
6	114.6	7.04-7.10 (m, 1H) overlap
7	159.7 (d, <i>J</i> ≈ 250 Hz)	-
8	130.0	-
9	128.0	7.45 (d, ⁴ <i>J</i> _{HF} = 7.2 Hz, 1H)
10	28.7	2.93-2.99 (m, 1H) overlap, 3.02-3.08 (m, 1H) overlap
11	43.2	3.00-3.06 (m, 1H) overlap
12	173.6	-
13	29.2	2.13-2.21 (m, 1H), 2.27-2.34 (m, 1H)
14	51.3	4.42 (dd, <i>J</i> = 8.0, 8.0 Hz, 1H)
15	45.0	5.66 (d, <i>J</i> = 7.4Hz, 1H)
16	23.6	2.93-3.05 (m, 2H) overlap
17	103.2	-
18	126.6	-
19	118.1	7.38 (d, <i>J</i> = 7.6 Hz, 1H)
		HMBC 1→30,38 ROESY 1'→29',32,38; 1→38
		HMBC 2→4,5,9
		TOCSY 3→1,2 HMBC 3→4 ROESY 3→29'
		HMBC 5→2
		HMBC 6→4,8
		HMBC 9→4,8
		HMBC 10→11,12 TOCSY 10→11,13,13',14
		HMBC 13'→12
		HMBC 14→13,17,25 ROESY 14→9,10
		HMBC 15→12,14,16,26
		HMBC 16→15,26 TOCSY 16→15,16'
		HMBC 19→23

20	118.5	6.95 (dd, $J = 7.6, 7.0$ Hz, 1H)	HMBC 20→18,22 COSY 20→19
21	120.6	6.99 (dd, $J = 7.7, 7.0$ Hz, 1H)	HMBC 21→19,23
22	110.7	7.22 (d, $J = 7.7$ Hz, 1H)	COSY 22→21 HMBC 22→17,18
23	135.7	-	
24	-	10.88 (s, 1H)	ROESY 24→22,14 HMBC 24→17,23,25
25	134.1	-	
26	169.0	-	
27	-	-	
28	61.8	4.10 (dd, $J = 10.0, 7.1$ Hz, 1H)	HMBC 28→30 TOCSY 28→29,29' ROESY 28→38
29	42	1.79 (dd, $J = 13.6, 7.2$ Hz, 1H), 2.45 (dd, $J = 13.6, 10.2$ Hz, 1H)	HMBC 29→30
30	57.3	-	
31	135.8	-	
32	122.1	7.14-7.19 (m, 1H) overlap	HMBC 32→34,36
33	119.2	6.83 (dd, $J = 7.4, 7.4$ Hz, 1H)	
34	128.1	7.14-7.19 (m, 1H) overlap	HMBC 34→32
35	110	6.78 (d, $J = 8.1$ Hz, 1H)	COSY 35→34 TOCSY 35→32,33,34
36	147.5	-	
37	-	7.33 (d, $J = 4.7$ Hz, 1H)	HMBC 37→31 ROESY 37→35
38	82.2	6.12 (d, $J = 4.7$ Hz, 1H)	
39	170.0	-	
40	-	7.43 (d, $J = 9.0$ Hz, 1H)	ROESY 40→29
41	52.1	4.10-4.16 (m, 1H)	HMBC 41→43, 48
42	38.4	2.23 (dd, $J = 13.4, 8.8$ Hz, 1H), 2.59 (dd, $J = 13.4, 4.7$ Hz, 1H) overlap	HMBC 42→43,48
43	126.9	-	
44	130.1	6.46 (d, $J = 8.3$ Hz, 2H)	HMBC 44→46
45	114.5	6.29 (d, $J = 8.3$ Hz, 2H)	HMBC 45→43,46
46	155.4	-	
47	-	9.01 (s, 1H)	HMBC 47→45,46
48	172.1	-	
49	-	6.68 (br s, 1H), 7.20 (br s, 1 H)	HMBC 49→48 TOCSY 49→49'

MS m/z 765.3 (calc'd: $C_{45}H_{42}FN_6O_5$, $[M+H]^+$, 765.3).



(500MHz, DMSO-*d*₆, 298K)

	¹³ C	¹ H	key correlation
1	46.1	4.72 (dd, <i>J</i> = 15.3, 8.0 Hz, 1H), 5.02 (dd, <i>J</i> = 15.3, 3.5 Hz, 1H)	HMBC 1'→38
2	124.9	6.08 (ddd, <i>J</i> = 15.6, 8.0, 3.5 Hz, 1H)	TOCSY 2→1,3 HMBC 2→4
3	130.8	6.40 (br d, <i>J</i> = 15.6 Hz, 1H)	HMBC 3→5,9
4	132.3	-	
5	127.0	7.25-7.29 (m, 1H) overlap	HMBC 5→9 TOCSY 5→6,9
6	120.9	7.13-7.19 (m, 1H) overlap	HMBC 6→7,8
7	160.0 (d, <i>J</i> ≈230 Hz)	-	
8	124.3	-	
9	127.8	7.10 (br d, <i>J</i> _{HF} = 6.8 Hz, 1H)	HMBC 9→10
10	26.4	2.89-2.95 (m, 1H) overlap, 2.97-3.02 (m, 1H) overlap	
11	41.4	2.76-2.81 (m, 1H) overlap	
12	174.5	-	
13	28.2	2.76-2.81 (m, 1H) overlap	HMBC 13→10,12,14 COSY 13'→11
14	50.7	4.96 (dd, <i>J</i> = 6.9, 6.9 Hz, 1H)	
15	48.6	5.13 (d, <i>J</i> = 7.7 Hz, 1H)	COSY 15→16 HMBC 15→14,26
16	24.5	2.94-3.06 (m, 2H) overlap	HMBC 16→17
17	103.0	-	
18	126.0	-	
19	117.5	7.36 (d, <i>J</i> = 7.7 Hz, 1H)	HMBC 19→23 COSY 19→20
20	118.3	6.93 (dd, <i>J</i> = 7.7, 7.0 Hz, 1H)	HMBC 20→22
21	120.4	6.99 (dd, <i>J</i> = 8.0, 7.0 Hz, 1H)	HMBC 21→23
22	110.5	7.22 (d, <i>J</i> = 8.0 Hz, 1H)	
23	135.5	-	
24	-	10.90 (s, 1H)	

25	133.4	-	
26	170.4	-	
27	-	8.53 (d, $J = 8.9$ Hz, 1H)	HMBC 27→26 COSY 27→28
28	52.3	4.48 (dd $J = 12.5, 8.9$ Hz, 1H)	COSY 28→29
29	27.5	2.85 (dd, $J = 14.9, 12.5$ Hz, 1H), 2.95-3.00 (m, 1H) overlap	HMBC 29→28,30,36,38
30	110.7	-	
31	127.3	-	
32	118.0	7.55 (d, $J = 7.7$ Hz, 1H)	HMBC 32→36 COSY 32→33
33	118.3	7.04-7.08 (m, 1H)	
34	120.9	7.13-7.19 (m, 1H) overlap	
35	109.5	7.50 (d, $J = 8.0$ Hz, 1H)	HMBC 35→31 COSY 35→34
36	135.8	-	
37	-	-	
38	124.5	7.13 (s, 1H)	HMBC 38→30,31
39	170.8	-	
40	-	7.59 (d, $J = 7.4$ Hz, 1H)	HMBC 40→39 COSY 40→41
41	53.0	4.29 (ddd, $J = 7.4, 6.9, 5.9$ Hz, 1H)	HMBC 41→48
42	36.6	2.67 (dd, $J = 13.6, 6.2$ Hz, 1H), 2.74-2.79 (m, 1H)	HMBC 42→43,44,48
43	126.6	-	
44	130.0	6.87 (d, $J = 8.1$ Hz, 2H)	HMBC 44→46
45	114.5	6.60 (d, $J = 8.1$ Hz, 2H)	
46	155.6	-	
47	-	9.14 (s, 1H)	HMBC 47→45,46
48	172.1	-	
49	-	7.07 (br s, 1H), 7.42 (br s, 1H)	TOCSY 49→49'

MS m/z 765.3 (calc'd: $C_{45}H_{42}FN_6O_5$, $[M+H]^+$, 765.3).

Chapter 6 Experimental Appendix

General remarks

See remarks Chapter 3 Experimental Appendix

NMR methods

Special NMR considerations are described in Chapter 3 Experimental Appendix.

Peptide synthesis

See methods Chapter 5 Experimental Appendix.

General procedures for template couplings and acid-promoted macrocyclization

General Procedure A - Acylation of peptides with template 3:

See methods Chapter 5 Experimental Appendix.

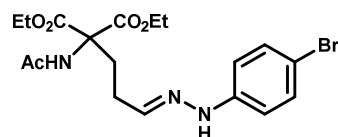
General Procedure C - Acid promoted macrocyclization / isomerization:

(Note: Commercial nitromethane should be aged over activated 3 Å molecular sieves for approximately one week. Alternatively, nitromethane may be treated with oven dried Brockmann type 1 neutral alumina overnight. These procedures appear to remove an as of yet unidentified contaminant, which without removal results in darkly colored reactions and diminished product purity. Acidolyses appeared to be insensitive to trace water content ~40-200ppm.) See methods Chapter 5 Experimental appendix. Acyclic precursors were purified by preparative HPLC (Waters Sunfire C18, 30x150mm, linear 40→100%ACN + 0.1%v TFA over 15 min, 30 mL min⁻¹)

Non-natural tryptophan and phenylalanine analogs

Fmoc 5-substituted D- and L-tryptophans. Synthetic 5-substituted tryptophans were prepared according to the procedures of Porter and co-workers with few alterations,¹ and transformed instead to N_α-Fmoc derivatives. The preparation of D- and L-5-bromotryptophan is exemplary.

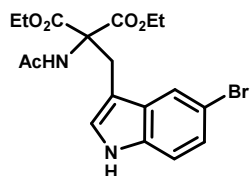
Diethyl 2-acetamido-2-(3-oxopropyl)malonate 4-bromophenylhydrazone (S1).



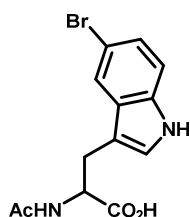
4-Bromophenylhydrazine hydrochloride was converted to its free base by partitioning between 10%wt NaOH and EtOAc. The organic extract was dried, a small amount of benzene was added, and the mixture was concentrated to dryness. To a flame dried 500 mL 3-neck round bottom flask fitted with a dropping funnel under argon was added diethyl acetamidomalonate (29.7 g, 137 mmol), benzene (60 mL) and freshly prepared NaOEt (3.4 mL, 1M in EtOH). The apparatus was fitted with an immersion thermometer, and acrolein (freshly distilled from CaSO₄ in vacuo, 10.0 mL, 150 mmol) was added dropwise at a rate such that the internal temperature remained below 30 °C. The mixture was stirred for an additional 2 hrs, then fitted with a Dean-Stark apparatus, treated with AcOH (3.9 mL) and 4-bromophenylhydrazine (28.1 g, 150 mmol), and heated to reflux for 2 hrs collecting 5.2 mL of H₂O. The mixture was cooled overnight and concentrated to give crude **S1** (70.9 g, > 100%) as a viscous oil, which was used without purification.

¹ Porter, J.; Dykert, J.; Rivier, J. *Int. J. Pept. Protein Res.* **1987**, *30*, 13.

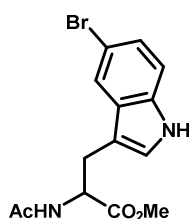
Diethyl 2-acetamido-2-((5-bromoindol-3-yl)methyl)malonate (S2). Crude hydrazone **S1** (70.9 g, 137 mmol) was treated with 5%aq H₂SO₄ (300 mL) and heated to reflux for 24 hrs, after which HPLC-UV analysis indicated complete consumption of starting **S1**. The mixture was cooled in an ice bath, the supernatant was discarded, and the resulting still wet viscous red oil was carried forward without purification.



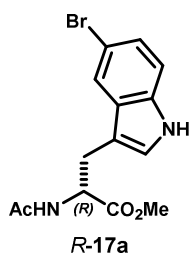
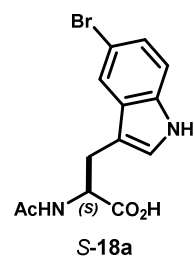
N-Acetyl-5-bromo-tryptophan (S3). Crude **S2** (137 mmol) was treated with NaOH (8.2 g, 206 mmol) in dioxane:H₂O (1:1, 280 mL) and heated to reflux for 12.5 hrs. HPLC-MS analysis indicated complete consumption of starting **S2**, but conversion to a ~4:1 mixture of the intermediate malonic acid which resisted decarboxylation. The mixture was cooled and the dioxane removed by rotary evaporation. The mixture was diluted with 1M NaOH (100 mL) and H₂O (200 mL), and washed with EtOAc (2x 150 mL). The aqueous phase was cooled in an ice bath and acidified to pH < 2 with 6N HCl and extracted into EtOAc (x3). The organic extract was washed with brine, dried over Na₂SO₄ and concentrated to give 35 g of a brown foam. This material was placed under an argon atmosphere, lowered into an oil bath pre-heated to 160 °C and let stand until gas evolution ceased (~20 min) and cooled to give crude **S3** (30g, 67%) as a brown foam, which was used without purification.



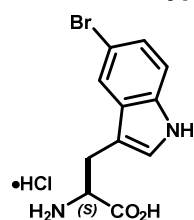
N-Acetyl-5-bromo-tryptophan methyl ester (17a). Crude **S3** (30 g, 92 mmol) was dissolved in MeOH (300 mL), cooled in an ice bath and SOCl₂ (10.7 mL, 148 mmol) was added dropwise (*Caution! gas evolution and spattering can occur if SOCl₂ is added too quickly*). The mixture was allowed to warm to rt, stirred overnight, and concentrated. The residual oil was partitioned between EtOAc and sat. NaHCO₃, and the organic phase was washed sequentially with 1M NaOH (x2), 1N HCl (x1), and brine, then dried over Na₂SO₄. The resulting reddish brown solution treated with a small amount of Norit, filtered through a pad of SiO₂ rinsing with EtOAc, and concentrated to give **17a** (16.8 g, 36% from diethyl acetamidomalonnate) as an orange foam. NMR matched *R*-**17a**.



N-Acetyl-5-bromo-L-tryptophan (S-18a) and N-Acetyl-5-bromo-D-tryptophan methyl ester (R-17a).

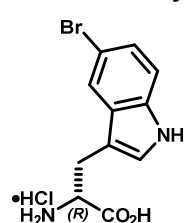


Racemic methyl ester **17a** (16.8 g, 49.6 mmol) was dissolved in ACN (125 mL), and then 80mM Tris-HCl buffer (375 mL, pH 7.8) was added slowly while stirring, resulting in a suspension of a small amount of oily material. CaCl₂ (3 g, 27 mmol) was added followed by bovine α-chymotrypsin (34 mg, ≥40 units/mg). The mixture was warmed to 40 °C (*Note: this may either be accomplished with a water bath, or by affixing the reaction to a rotary evaporator*) and periodically readjusted to pH 7.8 by addition of 1M NaOH, and stirred overnight at which point HPLC-UV analysis indicated unchanging product composition (*Note: while a 1:1 mixture of S-18a:R-17a is often observed, we have also observed what initially appears to be over-reaction, but in fact arises from uneven sampling of a heterogeneous reaction. Therefore, monitoring by pH change or until the product ratio is stable is most reliable*). The volatiles were removed by rotary evaporation, and the residual aqueous phase was extracted with EtOAc (x3). The organic phase was back-extracted with 5% K₂CO₃ (x2), and the combined aqueous phase was cooled and acidified to pH < 2 with conc. HCl and extracted with EtOAc (x3). The first extract was dried over Na₂SO₄ and concentrated to give *L*-acid **S-18a** (7.4 g, 46%) and *D*-ester **R-17a** (9.0 g, 54%). (**S-18a**): m.p. 58-60 °C, [α]_D²¹ = +11.4 ° (c = 1, MeOH). 1.78 (s, 3H), 2.95 (dd, J = 14.6, 8.6, 1H), 3.10 (dd, J = 14.6, 5.1 Hz, 1H), 4.41 (dd, J = 8.6, 7.9, 5.1 Hz, 1H), 7.14 (dd, J = 8.6, 2.0 Hz, 1H), 7.18 (d, J = 2.0 Hz, 1H), 7.28 (d, J = 8.6 Hz, 1H), 7.68 (d, J = 1.6 Hz, 1H), 7.9 Hz, 1H), 11.04 (d, J = 1.6 Hz, 1H), 12.49 (br s, 1H). (**R-17a**): m.p. ~140 °C softens, 155-158 °C melts, [α]_D²¹ = -29.8 ° (c = 1, MeOH). ¹H NMR (600 MHz, DMSO-*d*₆) δ 1.78 (s, 3H), 2.97 (dd, J = 14.6, 8.4 Hz, 1H), 3.07 (dd, J = 14.6, 5.7 Hz, 1H), 3.54 (s, 3H), 4.43 (ddd, J = 8.4, 7.6, 5.7 Hz, 1H), 7.14 (dd, J = 8.6, 1.9 Hz, 1H), 7.19 (dd, 2.0 Hz, 1H), 7.28 (d, J = 8.6 Hz, 1H), 7.63 (d, J = 1.8 Hz, 1H), 8.32 (d, J = 7.6 Hz, 1H), 11.1, (br s, 1H).

5-Bromo-L-tryptophan hydrochloride (S-S4).

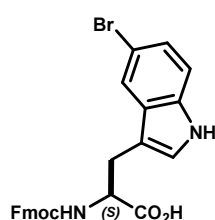
Method A – acid hydrolysis: Compound **S-18a** (9.4 g, 29 mmol) was treated with 2N HCl (145 mL) and warmed to reflux under an argon atmosphere. The mixture was stirred for 6 hrs after which HPLC-UC analysis indicated complete conversion. The mixture was concentrated to dryness to give a brown solid, which was recrystallized from H₂O to give the hydrochloride of **S-S4** (3.8 g, 41%) as a brown crystalline solid. $[\alpha]_D^{21} = +4.6^\circ$ ($c = 1$, 1M NaOH). *Method B – enzymatic deacetylation.* Compound **S-18a** (7.4 g crude) was dissolved in H₂O (250 mL) by the addition of NH₄OH and warming. Adjusted to 40 °C and to pH ~ 7.8 by addition of solid CO₂ and added CoCl₂ (4 mL of 50 mM soln) followed by Amano acylase I (350 mg,

Sigma, $\geq 30,000$ U/g). After stirring for 1.5 hrs, an off-white precipitate began to form, and after stirring overnight, HPLC-UV analysis indicated 98.2% conversion. Several drops of silicone oil were added, and the mixture was concentrated at 60 °C by rotary evaporation to give the free base of **S-S4** (6.1 g net wt., 43% from **17a**) as a beige solid. (Note: severe bumping results during concentration of this heterogeneous mixture, and is mitigated somewhat by the addition of polydimethylsiloxane). $[\alpha]_D^{21} = +4.60^\circ$ ($c = 1$, 1M NaOH). ¹H NMR (600 MHz, DMSO-*d*₆) δ 3.22 (br d, $J = 6.1$ Hz, 2H), 4.09 (apt br t, $J = 5.8$ Hz, 1H), 7.15 (dd, $J = 8.4, 1.7$ Hz, 1H), 7.27 (d, $J = 1.7$ Hz, 1H), 7.31 (d, $J = 8.4$ Hz, 1H), 7.74 (d, $J = 1.4$ Hz, 1H), 8.32 (br s, 3H), 11.29-11.32 (m, 1H), 13.76 (s, 1H).

5-Bromo-D-tryptophan hydrochloride (R-S4).

(90 mL) and heated to reflux for 3 hrs, after which HPLC-UV analysis showed >95% conversion. The dark brown solution was treated with Norit and stirred for several minutes, then filtered through a pad of Celite, rinsing with H₂O. The acidic, still brown filtrate was applied to a column of Dowex-50X8-400 cation exchange resin (~20x80cm). The flow-through was passed over the column a second time. HPLC-UV analysis of the dark brown second flow through showed no residual **R-18a**. The column was then washed with H₂O until the eluent pH was neutral (~200 mL), at which point the product was eluted with 1M NH₄OH to collect a light brown, foamy liquid. Several drops of silicone oil were added,

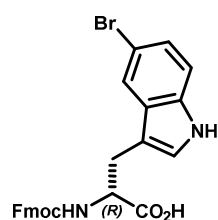
and the mixture in ~250 mL portions in a 2L flask was concentrated at 60 °C by rotary evaporation to give **R-S4** (6.1 g, 43% from **17a**) as a beige solid. (Note: severe bumping results during concentration of this heterogeneous mixture, and is mitigated somewhat by the addition of polydimethylsiloxane). $[\alpha]_D^{21} = -4.39^\circ$ ($c = 1$, 1M NaOH).

N α -Fmoc-5-bromo-L-tryptophan (S-19a).

Compound **S-S4** (6.1 g, 21.5 mmol) was dissolved in THF:sat. NaHCO₃ (1:1, 200 mL) and treated with Fmoc-ONSu (7.6 g, 22.6 mmol). The mixture was stirred at rt for 3 hrs, after which HPLC-UV analysis indicated complete conversion to product. The volatiles were removed by rotary evaporation, and the aqueous remainder was basified to pH ~10 by the addition of 1M NaOH, then washed with Et₂O (x2) (Note: the product forms an immiscible layer in between the aqueous and ethereal phases). The combined Et₂O phase was back extracted with 5%aq K₂CO₃ (x2), and the combined aqueous was cooled in an ice bath, EtOAc was added, and the mixture was acidified to pH < 2 with conc. HCl. The aqueous was extracted with EtOAc (x2),

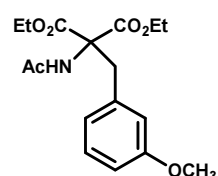
and washed with H₂O (x1), brine, dried over Na₂SO₄, treated with a small amount of Norit, and filtered through a pad of SiO₂ rinsing with EtOAc. The filtrate was concentrated to an oil, which was triturated with hexanes. The resulting solid was ground in a mortar and pestle under hexanes, and then filtered to collect **S-19a** (9.7 g, 89%) as a white solid. $[\alpha]_D^{21} = -12.3^\circ$ ($c = 1$, MeOH). ¹H NMR (500 MHz, DMSO-*d*₆) δ 2.99 (dd, $J = 14.6, 9.8$ Hz, 1H), 3.15 (dd, $J = 14.6, 4.5$ Hz, 1H), 4.13-4.24 (m, 4H), 7.16 (dd, $J = 8.6, 1.8$ Hz, 1H), 7.22-7.32 (m, 4H), 7.37 (br apt t, $J = 7.2$ Hz, 1H), 7.39 (br apt t, $J = 7.2$ Hz, 1H), 7.61 (d, $J = 7.6$ Hz, 1H), 7.64 (d, $J = 7.5$ Hz, 1H), 7.71 (d, $J = 8.3$ Hz, 1H), 7.75 (d, $J = 1.5$ Hz, 1H), 7.85 (d, $J = 7.6$ Hz, 2H), 11.07 (d, $J = 1.5$ Hz, 1H), 12.70 (br s, 1H). ¹³C NMR (126 MHz, DMSO-*d*₆) δ 174.0, 170.8, 156.5, 144.23, 144.20, 141.1, 135.2, 129.6, 128.1, 127.5, 125.9, 125.8, 125.7, 123.8, 121.0, 120.6, 113.9, 111.6, 110.7, 66.1, 60.2, 55.5, 47.0, 27.1, 21.2, 14.6.

***N*_α-Fmoc-5-bromo-*L*-tryptophan (*R*-19a).** Compound *R*-S4 (3.7 g, 11.6 mmol) was reacted with Fmoc-ONSu (4.1 g, 12.2 mmol) in the same manner as for enantiomer *S*-19a to give *R*-19a (5.65 g, 96%) as a white solid. $[\alpha]_D^{21} = +12.6^\circ$ (*c* = 1, MeOH). NMR matched enantiomer *S*-19a.

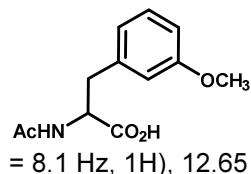


Ring-substituted *N*_α-Fmoc- *D*- & *L*-phenylalanines. Synthetic phenylalanine analogs and amino acids with heterocyclic or naphthyl side chains were prepared according to the procedures of Porter and co-workers with few alterations,² and transformed instead to *N*_α-Fmoc derivatives. The preparation of *D*- and *L*-3-methoxyphenylalanine is exemplary.

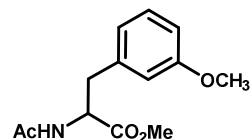
Diethyl 2-acetamido-2-(3-methoxybenzyl)malonate (S5**).** Ethanol (110 mL) was treated with Na⁰ (2.21 g, 96 mmol), and to the resulting mixture was added diethyl acetamidomalonate (20.8 g, 96 mmol), and after stirring 10 min, 3-methoxybenzyl chloride (15.2 g, 97 mmol) was added. The mixture was warmed to reflux overnight, then diluted with H₂O (110 mL) and cooled to rt (*Note: in some cases, the product crystallized from this mixture*). The oily residue was collected, and the aqueous was extracted with EtOAc (x3), dried over Na₂SO₄ and concentrated to give moderately pure **S5** (31.5 g, 97%) as a yellow oil which began to crystallize upon standing. ¹H NMR (500 MHz, CDCl₃) δ 1.26 (t, *J* = 7.1 Hz, 6H), 1.99 (s, 3H), 3.71 (s, 3H), 4.6 (dq, *J* = 7.1, 3.5 Hz, 2H), 4.25 (dq, *J* = 7.1, 3.6 Hz, 1H), 6.51-6.53 (m, 1H), 6.54-6.56 (m, 0.5H), 6.56-6.59 (m, 1H), 6.74 (dd, *J* = 8.3, 2.2 Hz, 1H), 7.13 (apt t, *J* = 7.9 Hz, 1H). ¹³C NMR (126 MHz, CDCl₃) δ 168.9, 167.4, 159.3, 136.6, 129.1, 122.0, 115.7, 112.3, 67.0, 62.5, 54.9, 37.7, 22.9, 13.9.



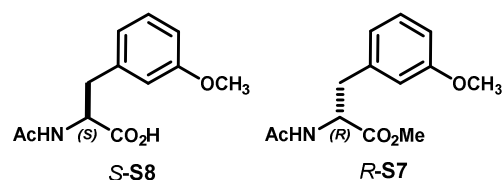
***N*-Acetyl-3-methoxyphenylalanine (**S6**).** Compound **S5** (31.5 g, 93.5 mmol) was treated with NaOH (4.5 g, 112 mmol) in dioxane:H₂O (180 mL), and the mixture was heated to reflux overnight. The mixture was cooled and worked up analogously to compound **S3** to give **S6** (21 g, 92%) as an off-white solid. ¹H NMR (500 MHz, CDCl₃) δ 1.75 (s, 3H), 2.77 (dd, *J* = 13.8, 9.6 Hz, 1H), 2.97 (dd, *J* = 13.8, 4.8 Hz, 1H), 3.69 (s, 3H), 4.36 (ddd, *J* = 9.6, 8.1, 4.8 Hz, 1H), 6.71-6.78 (m, 3H), 7.15 (t, *J* = 7.9 Hz, 1H), 8.14 (d, *J* = 8.1 Hz, 1H), 12.65 (br s, 1H).



***N*-Acetyl-3-methoxyphenylalanine methyl ester (**S7**).** Compound **S6** (21 g, ~89 mmol) was esterified analogously to compound **S7**.

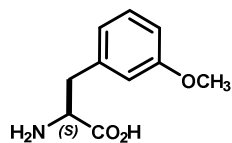


***N*-Acetyl-*L*-3-methoxyphenylalanine (*S*-S8) and *N*-Acetyl-*D*-3-methoxyphenylalanine methyl ester (*R*-S7).** Methyl ester **S7** (19.3 g, 77 mmol) was dissolved in MeOH (177 mL), 80 mM Tris-HCl buffer (702 mL, pH 7.8) was added, and readjusted to pH 7.8. Added CaCl₂ (20 mL of 2M soln) followed by bovine α-chymotrypsin (97 mg, ≥40 units/mg). The mixture was stirred at rt overnight and worked up analogously to compounds *S*-18a, *R*-17a to give *L*-acid **S8** (8.0 g, 44%) as a waxy crystalline solid and *D*-ester **R-S7** (8.3 g, 43%) as a waxy solid. **S-S8**: m.p. 139-143 °C, $[\alpha]_D^{21} = +34.9^\circ$ (*c* = 1, MeOH). **R-S7**: m.p. 92-94 °C, $[\alpha]_D^{21} = -41.5^\circ$ (*c* = 1, EtOAc).

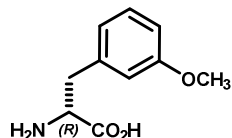


² Porter, J.; Dykert, J.; Rivier, J. *Int. J. Pept. Protein Res.* **1987**, *30*, 13.

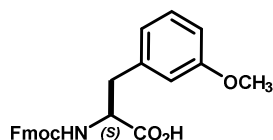
L-3-Methoxyphenylalanine (S-S9). Compound **S-S8** (8.0 g, 34 mmol) was hydrolyzed analogously to compound **S-S4**. The hydrochloride salt was suspended in EtOAc and treated with excess propylene oxide (*Caution! Carcinogen & exotherm*). The resulting solution was concentrated, triturated with cold Et₂O and filtered to give **S-S9** (6.5 g, 98%) as a white solid. m.p. 209-210 °C, $[\alpha]_D^{20} = -10.7^\circ$ (c = 1, H₂O). ¹H NMR (600 MHz, DMSO-*d*₆) δ 3.05 (dd, *J* = 14.0, 6.7 Hz, 1H), 3.15 (dd, *J* = 14.0, 5.3 Hz, 1H), 3.74 (s, 3H), 3.88 (br dd, *J* = 6.7, 5.3 Hz, 1H), 6.81 (dd, *J* = 8.2, 1.7 Hz, 1H), 6.86 (br d, *J* = 7.4 Hz, 1H), 6.91 (br s, 1H), 7.21 (apt t, *J* = 7.8 Hz, 1H), 8.14 (br s, 3H). ¹³C NMR (150 MHz, DMSO-*d*₆) δ 170.3, 159.3, 136.5, 129.6, 121.7, 115.3, 112.8, 55.0, 53.1, 35.6.



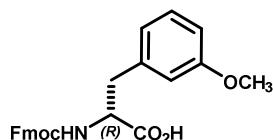
D-3-Methoxyphenylalanine (R-S9). Compound **R-S7** (8.3 g, 33 mmol) was hydrolyzed analogously to **S-S8** to give **R-S9** (7.0 g, quant.) as a white solid. m.p. 209-211 °C, $[\alpha]_D^{20} = +11.6^\circ$ (c = 1, H₂O). NMR matched enantiomer **S-S9**.



Fmoc-L-3-Methoxyphenylalanine (S-23a). Compound **S-S9** (6.53 g, 33.5 mmol) was reacted with Fmoc-ONSu (11.3 g, 33.5 mmol) in the same manner as for **S-19a** to give **S-23a** (11.6 g, 85%) as a white powder. $[\alpha]_D^{23} = -5.73^\circ$ (c = 1, MeOH). ¹H NMR (600 MHz, DMSO-*d*₆, major rotamer) δ 2.83 (dd, *J* = 13.7, 10.8 Hz, 1H), 3.05 (dd, *J* = 13.7, 4.2 Hz, 1H), 3.69 (s, 3H), 4.13-4.21 (m, 4H), 6.76 (dd, *J* = 8.1, 2.2 Hz, 1H), 6.83 (br d, *J* = 7.6 Hz, 1H), 6.86-6.88 (m, 1H), 7.17 (t, *J* = 7.9 Hz, 1H), 7.26 (td, *J* = 7.3, 0.4 Hz, 1H), 7.29 (td, *J* = 7.3, 0.4 Hz, 1H), 7.36-7.41 (m, 2H), 7.63 (apt t, *J* = 7.6 Hz, 2H), 7.75 (d, *J* = 8.5 Hz, 1H), 7.86 (d, *J* = 7.6 Hz, 2H), 12.75 (br s, 1H). ¹³C NMR (150 MHz, DMSO-*d*₆, mixture of rotamers) δ 173.8, 173.3, 159.6, 156.4, 144.22, 144.19, 141.15, 141.13, 140.0, 129.7, 129.6, 128.1, 127.5, 125.8, 125.7, 121.8, 120.6, 115.30, 115.28, 112.3, 66.1, 55.9, 55.35, 55.33, 47.0, 36.9, 25.7.



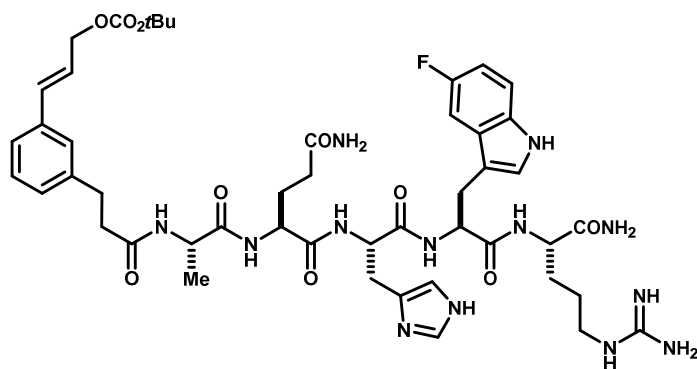
Fmoc-D-3-Methoxyphenylalanine (R-23a). Compound **R-S9** (7.0 g, 35.9 mmol) was reacted with Fmoc-ONSu (12.1 g, 35.9 mmol) in the same manner as for **S-23a** to give **R-23a** (11.7 g, 75%) as a white powder. $[\alpha]_D^{23} = +6.94^\circ$ (c = 1, MeOH). NMR matched enantiomer **S-23a**.



Macrocycles from divergent internal cinnamylations of 5-substituted tryptophans

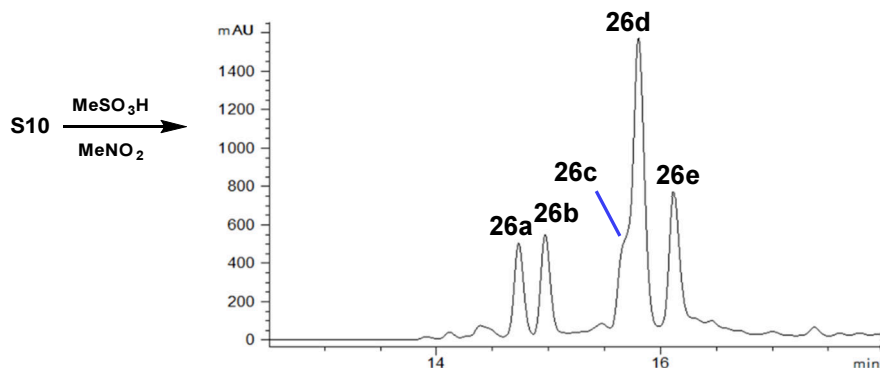
Ala-Gln-His-Trp(5F)-Arg (26a–26e):

Acyclic intermediate S10. Compound **S10** (122 mg) was prepared from peptide Ala-Gln-His-Trp(5F)-Arg-NH₂ template **5** according to General Procedure A. ¹H NMR (DMSO-*d*₆, 500 MHz): δ 10.98 (d, *J* = 2.3 Hz, 1H), 8.96 (d, *J* = 1.2 Hz, 1H), 8.24 (d, *J* = 7.9 Hz, 1H), 8.06-8.16 (m, 4H), 7.74 (t, *J* = 5.7 Hz, 1H), 7.39 (dd, *J* = 16.0, 2.5 Hz, 1H), 7.36 (br. s, 1H), 7.23-7.34 (m, 7H), 7.09-7.14 (m, 2H), 6.87-6.93 (m, 2H), 6.65 (d, *J* = 15.9 Hz, 1H), 6.35 (dt, *J* = 16.0, 6.2 Hz, 1H), 4.68 (dd, *J* = 6.5, 1.0 Hz, 2H), 4.52-4.60 (m, 2H), 4.18-4.28 (m, 2H), 4.16 (ddd, *J* = 7.9, 5.6 Hz, 1H), 3.03-3.17 (m, 4H), 2.94 (dd, *J* = 15.9, 15.9 Hz, 2H), 2.75-2.84 (m, 2H), 2.39-4.29 (m, 2H), 2.04-2.17



(m, 2H), 1.80-1.91 (m, 1H), 1.65-1.79 (m, 2H), 1.45-1.55 (m, 2H), 1.43 (s, 9H), 1.15 (d, $J = 7$ Hz, 3H). ^{13}C NMR (DMSO- d_6 , 126 MHz): δ 174.1, 173.1, 172.7, 171.6, 171.4, 171.3, 169.8, 157.6, 156.8, 155.8, 152.8, 141.7, 135.8, 133.7, 133.4, 132.7, 129.3, 129.1, 128.6, 128.0, 127.5, 127.4, 126.4, 125.9, 124.2, 123.3, 117.7, 116.8, 115.3, 115.2, 112.2, 112.1, 109.9, 109.9, 81.5, 66.9, 55.0, 53.4, 52.4, 52.2, 51.5, 48.3, 36.6, 31.3, 30.8, 29.1, 27.3, 25.0, 17.9. MS m/z 1002.7 (calc'd: $\text{C}_{48}\text{H}_{64}\text{N}_{13}\text{O}_{10}$, $[\text{M}+\text{H}]^+$, 1002.5).

Macrocycles 26a–26e:



Acyclic intermediate **S10** (122 mg, 121 μmol) was cyclized following General Procedure C and purified by the preparative HPLC method A. Compounds **26a**, **26c** and **26e** were re-purified by preparative HPLC method B to give **26a** (5.7 mg, 5%), **26b** (6.0 mg, 6%), **26c** (5.2 mg, 5%), **26d** (27 mg, 25%), and **26e** (10.4, 10%).

Preparative HPLC method A:

Column: Waters XBridge™ C₁₈, 19x250mm, 5 μm .

Solvent A: H₂O + 0.1%v TFA

Solvent B: ACN + 0.1%v TFA

Flow rate: 18.00 ml/min

Time	%B
0	30
2	30
30	100

Preparative HPLC method B:

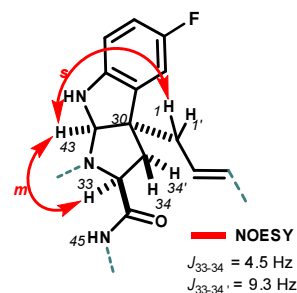
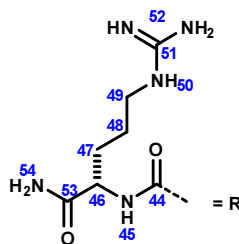
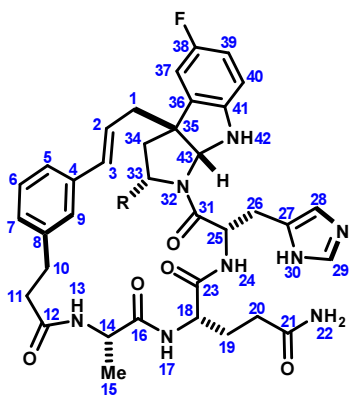
Column: Waters XBridge™ C₁₈, 19x250mm, 5 μm .

Solvent A: H₂O + 0.1%v TFA

Solvent B: ACN + 0.1%v TFA

Flow rate: 18.00 ml/min

Time	%B
0	30
2	30
30	55

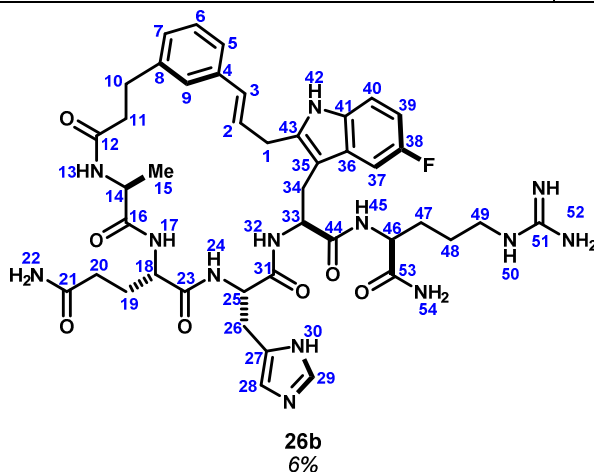


(600MHz & 500 MHz, DMSO- d_6 , 298K)

	^{13}C	^1H	key correlations
1	40.7	2.44 (dd, $J = 14.3, 8.8$ Hz, 1H), 2.68-2.73 (m, 1H)	HMBC 1→35,43
2	124.2	5.91 (ddd, $J = 15.7, 8.8, 6.5$ Hz, 1H)	COSY 2→1
3	134.2	6.55 (d, $J = 15.7$ Hz, 1H)	HMBC 3→1,4,5,9

4	136.7	-	
5	122.2	7.04-7.07 (m, 1H) overlap	
6	128.1	7.11-7.16 (m, 1H) overlap	HMBC 6→4,8
7	127.1	7.03-7.07 (m, 1H) overlap	
8	141.3	-	
9	126.2	7.13 (br s, 1H) overlap	HMBC 9→5,7
10	28.7	2.71-2.79 (m, 1H), 2.95-3.01 (m, 1H)	HMBC 10→8,12
11	34.3	2.51-2.57 (m, 1H), 2.59-2.66 (m, 1H)	HMBC 11→8,12
12	171.3	-	
13	-	8.09 (d, $J = 8.1$ Hz, 1H)	
14	48.3	4.13-4.19 (m, 1H) overlap	HMBC 14→16
15	17.6	1.20 (d, $J = 7.3$ Hz, 3H)	HMBC 15→14,16 COSY 15→14 TOCSY 15→14,13
16	171.8	-	
17	-	7.00-7.03 (m, 1H) overlap	HMBC 17→16
18	50.6	4.19 (ddd, $J = 8.1, 7.8, 5.4$ Hz, 1H)	HMBC 18→19,20
19	28.4	1.59-1.70 (m, 1H), 1.70-1.80 (m, 1H)	
20	31.0	1.99 (ddd, $J = 15.5, 9.5, 5.8$ Hz, 1H), 2.08 (ddd, $J = 15.5, 9.9, 5.7$ Hz, 1H)	HMBC 20→21
21	173.5	-	
22	-	6.84 (br s, 1H), 7.31 (br s, 1H)	HMBC 22→21
23	171.0	-	
24	-	8.77 (d, $J = 8.1$ Hz, 1H)	TOCSY 24→25,26 HMBC 24→23
25	48.3	5.07 (ddd, $J = 9.7, 8.1, 5.2$ Hz, 1H)	HMBC 25→31
26	25.6	3.17 (dd, $J = 15.9, 5.1$ Hz, 1H), 3.00 (dd, $J = 15.9, 9.7$ Hz, 1H)	HMBC 26→27,28,31
27	128.3	-	
28	117.3	7.50 (s, 1H)	HMBC 28→27,29
29	133.5	8.99 (s, 1H)	HMBC 29→27,28 TOCSY 29→28
30	-	Not detected	
31	170.2	-	
32	-	-	
33	60.1	4.62 (dd, $J = 9.3, 4.5$ Hz, 1H)	TOCSY 33→34 HMBC 33→1,34,35,44
34	40.0	2.21 (dd, $J = 13.3, 4.5$ Hz, 1H), 2.46-2.52 (m, 1H) overlap	HMBC 34→35
35	57.8	-	
36	135.0	-	
37	109.8	7.10-7.14 (m, 1H)	HMBC 37→38,41
38	156.5 (d, $J \approx 230$ Hz)	-	
39	114.0	6.81-6.88 (m, 1H) overlap	HMBC 39→38,41
40	109.8	6.84 (dd, $J_{HH} = 9.1$ Hz, $J_{HF} = 2.6$ Hz, 1H)	HMBC 40→36,38 COSY 40→39

41	144.8	-	
42	-	Not detected	
43	80.3	6.19 (s, 1H)	
44	169.9	-	
45	-	7.56 (d, $J = 8.2$ Hz, 1H)	HMBC 45→44
46	50.6	4.04 (ddd, $J = 8.2, 8.0, 6.0$ Hz, 1H)	COSY 46→47 HMBC 46→44,54
47	29.9	0.97-1.06 (m, 1H) overlap, 1.33-1.42 (m, 1H) overlap	HMBC 47→49
48	24.4	1.00-1.11 (m, 1H) overlap, 1.36-1.46 (m, 1H) overlap	
49	39.8	2.89-2.97 (m, 1H) overlap, 3.03-3.11 (m, 1H)	HMBC 49→51
50	-	7.42 (apt t, $J = 5.6$ Hz, 1H)	
51	156.3	-	
52	-	14.11 (br s, 3H)	
53	172.4	-	
54	-	7.08 (br s, 1H), 7.40 (br s, 1H)	HMBC 55'→54 TOCSY 55'→55

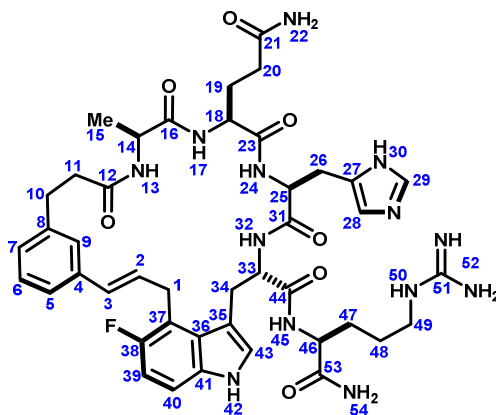


(600MHz, DMSO- d_6 , 298K)

	^{13}C	^1H	key correlations
1	32.4	3.52 (dd, $J = 15.3, 5.6$ Hz, 1H), 3.64 (dd, $J = 15.3, 6.3$ Hz, 1H)	HMBC 1→38,39,40
2	129.3	6.39 (ddd, $J = 15.8, 6.3, 5.6$ Hz, 1H)	TOCSY 2→1,2 HMBC 2→4
3	129.9	6.30 (br d, $J = 15.8$ Hz, 1H)	HMBC 3→4
4	137.0	-	
5	124.1	7.13-7.17 (m, 1H) overlap	HMBC 5→7,9
6	128.3	7.15-7.19 (m, 1H) overlap	HMBC 6→4,8
7	127.3	7.10 (br d, $J = 7.2$ Hz, 1H)	HMBC 7→9
8	141.1	-	
9	124.5	7.10 (br s, 1H) overlap	HMBC 9→7
10	30.2	2.69-2.76 (m, 1H), 2.77-2.82 (m, 1H) overlap	HMBC 10→7,8,9,12
11	35.4	2.31 (ddd, $J = 14.3, 6.5, 6.5$ Hz, 1H), 2.44-2.51 (m, 1H) overlap	HMBC 11→8,12
12	171.4	-	

13	-	8.07 (d, $J = 7.6$ Hz, 1H)	HMBC 13→12
14	47.7	4.12 (qd, $J = 7.6, 7.1$ Hz, 1H)	HMBC 14→15,16
15	17.6	0.85 (d, $J = 7.1$ Hz, 3H)	HMBC 15→15,16
16	172.3	-	
17	-	7.86 (d, $J = 7.7$ Hz, 1H)	HMBC 17→16
18	52.3	3.98 (ddd, $J = 8.0, 7.8, 5.4$ Hz, 1H)	TOCSY 18→17,18,20 HMBC 18→19,20,23
19	27.3	1.50-1.58 (m, 1H) overlap, 1.70-1.81 (m, 1H) overlap	HMBC 19→20,21
20	30.9	1.91-2.00 (m, 2H)	HMBC 20→21
21	173.9	-	
22	-	6.78 (br s, 1H), 7.22 (br s, 1H) overlap	TOCSY 22→22'
23	171.2	-	
24	-	7.56 (br d, $J = 6.8$ Hz, 1H)	HMBC 24→23
25	50.7	4.45 (ddd, $J = 7.2, 6.8, 5.8$ Hz, 1H)	COSY 25→24
26	27.6	2.93 (dd, $J = 15.3, 7.6$ Hz, 1H), 3.05-3.12 (m, 1H) overlap	HMBC 26→27
27	128.9	-	
28	116.8	7.28 (s, 1H)	HMBC 28→27,30
29	-	not observed	
30	134.0	8.95 (br s, 1H)	HMBC 30→27,28
31	170.0	-	
32	-	8.07 (d, $J = 7.4$ Hz, 1H)	HMBC 32→31
33	53.7	4.60 (ddd, $J = 10.9, 7.4, 3.3$ Hz, 1H)	TOCSY 33→32,34
34	27.7	2.85 (dd, $J = 14.4, 11.1$ Hz, 1H), 3.13-3.20 (m, 1H) overlap	HMBC 34→33,35
35	109.8	-	
36	133.0	-	
37	103.8	7.57 (d, $J_{HF} = 11.1$ Hz, 1H)	HMBC 37→35,41,38,39
38	155.3 (d, $J \approx 230$ Hz)	-	
39	120.1	-	
40	112.8	7.21 (d, $J_{HF} = 6.4$ Hz, 1H)	HMBC 40→38
41	133.0	-	
42	-	10.83 (d, $J = 1.3$ Hz, 1H)	HMBC 42→35,36,41
43	125.7	7.17-7.19 (m, 1H) overlap	
44	172.2	-	
45	-	8.70 (br d, $J = 7.8$ Hz, 1H)	HMBC 45→44
46	52.2	4.25 (ddd, $J = 7.8, 7.8, 6.1$ Hz, 1H)	TOCSY 46→45,47,48,49
47	28.9	1.55-1.63 (m, 1H) overlap, 1.71-1.78 (m, 1H) overlap	HMBC 47→46
48	25.1	1.47-1.57 (m, 2H) overlap	HMBC 48→49
49	40.3	3.09-3.16 (m, 2H) overlap	HMBC 49→47,48,51
50	-	14.17 (br s) overlap	
51	156.9	-	

52	-	14.17 (br s) overlap	
53	173.3	-	
54	-	7.14 (br s, 1H), 7.39 (br s, 1H)	TOCSY 54'→54

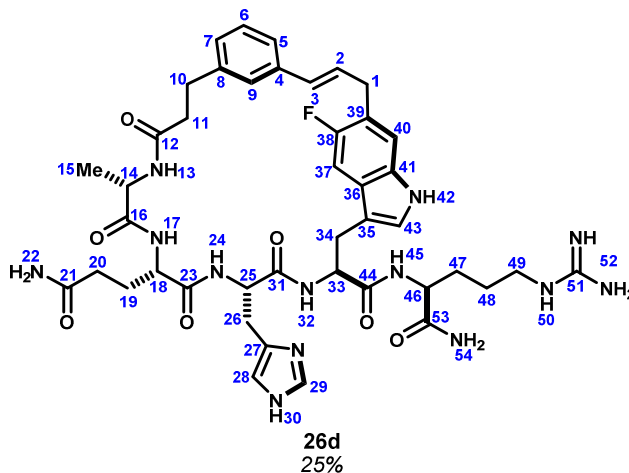


26c
5%

(600MHz, DMSO-*d*₆, 298K)

	¹³ C	¹ H	key correlations
1	27.3	3.80-3.91 (m, 2H)	HMBC 1→2,3,37
2	129.2	6.44 (dt, <i>J</i> = 15.8, 6.0 Hz, 1H)	HMBC 2→4,37
3	129.9	6.20 (br d, <i>J</i> = 15.8 Hz, 1H)	HMBC 3→5,9 TOCSY 3→2,1
4	136.9	-	
5	124.4	6.99-7.02 (m, 1H) overlap	
6	128.1	7.13 (dd <i>J</i> = 7.6, 7.6 Hz, 1H)	HMBC 6→4,8
7	127.5	6.99-7.02 (m, 1H) overlap	
8	141.4	-	
9	125.7	7.35 (br s, 1H)	HMBC 9→3,5,7
10	30.4	2.76-2.87 (m, 2H)	HMBC 10→8,12
11	35.9	2.44 (ddd, <i>J</i> = 14.6, 5.7, 5.7 Hz, 1H), 2.56 (ddd, <i>J</i> = 14.6, 9.3, 5.8 Hz, 1H)	HMBC 11→8,12
12	172.6	-	
13	-	8.11 (d, <i>J</i> = 6.0 Hz, 1H)	HMBC 13→12
14	49.3	3.97-4.03 (m, 1H)	HMBC 14→16
15	17.3	1.09 (d, <i>J</i> = 7.2 Hz, 3H)	HMBC 15→14 TOCSY 15→14,13
16	173.2	-	
17	-	8.01 (d, <i>J</i> = 7.5 Hz, 1H)	
18	53.0	4.00-4.06 (m, 1H) overlap	HMBC 18→23
19	26.8	1.62-1.70 (m, 1H) overlap, 1.73-1.82 (m, 1H) overlap	HMBC 19→21,23
20	30.9	1.95-2.03 (m, 1H), 2.04-2.11 (m, 1H)	HMBC 20→21
21	174.1	-	
22	-	6.87(br s, 1H), 7.30 (br s, 1H) overlap	

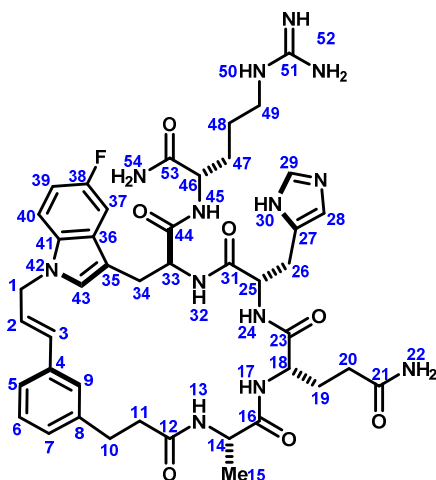
23	171.9	-	
24	-	8.27 (d, $J = 7.9$ Hz, 1H)	HMBC 24→23
25	51.5	4.60 (ddd, $J = 9.3, 7.9, 5.1$ Hz, 1H)	HMBC 25→31
26	26.2	3.03-3.09 (m, 1H) overlap, 3.22-3.27 (m, 1H)	HMBC 26→27,31
27	129.7	-	
28	116.3	7.30 (s, 1H) overlap	HMBC 28→29 TOCSY 28→29
29	134.1	8.97 (br s, 1H)	
30	-	Not observed	
31	169.7	-	
32	-	7.92 (d, $J = 7.9$ Hz, 1H)	HMBC 32→31
33	54.3	4.71 (ddd, $J = 8.7, 7.9, 5.6$ Hz, 1H)	HMBC 33→44
34	29.3	3.02-3.07 (m, 1H), 3.29 (dd, $J = 14.8, 5.3$ Hz, 1H)	HMBC 34→44
35	110.4	-	
36	125.7	-	
37	116.2	-	
38	154.9	-	
39	109.3	6.92 (dd, $J_{HF} = 9.7$ Hz, $J_{HH} = 8.9$ Hz, 1H)	HMBC 39→37,41
40	110.7	7.21 (dd, $J_{HH} = 8.9$ Hz, $J_{HF} = 4.4$ Hz, 1H)	HMBC 40→36
41	133.4	-	
42	-	10.95 (d, $J = 2.4$ Hz, 1H)	TOCSY 42→43 HMBC 42→41
43	125.9	7.13 (d, $J = 2.4$ Hz, 1H)	
44	170.7	-	
45	-	8.01 (d, $J = 7.5$ Hz, 1H)	TOCSY 45→46,47,48,49,50 HMBC 45→44
46	51.9	4.14 (ddd, $J = 8.1, 7.5, 6.0$ Hz, 1H)	HMBC 46→53
47	28.3	1.44-1.53 (m, 1H), 1.62-1.70 (m, 1H)	
48	24.4	1.36-1.45 (m, 2H)	
49	40.2	3.03-3.09 (m, 2H) overlap	HMBC 49→47,51
50	-	7.47 (t, $J = 5.5$ Hz, 1H)	
51	156.6	-	
52	-	13.95-14.37 (m, 3H)	
53	173.0	-	
54	-	6.92 (br s, 1H) overlap, 6.99 (br s, 1H) overlap	TOCSY 54'→54



(600MHz, DMSO-*d*₆, 298K)

	¹³ C	¹ H	key correlations
1	32.4	3.52 (dd, <i>J</i> = 15.3, 5.6 Hz, 1H), 3.64 (dd, <i>J</i> = 15.3, 6.3 Hz, 1H)	HMBC 1→38,39,40
2	129.3	6.39 (ddd, <i>J</i> = 15.8, 6.3, 5.6 Hz, 1H)	TOCSY 2→1,2 HMBC 2→4
3	129.9	6.30 (br d, <i>J</i> = 15.8 Hz, 1H)	HMBC 3→4
4	137.0	-	
5	124.1	7.13-7.17 (m, 1H) overlap	HMBC 5→7,9
6	128.3	7.15-7.19 (m, 1H) overlap	HMBC 6→4,8
7	127.3	7.10 (br d, <i>J</i> = 7.2 Hz, 1H)	HMBC 7→9
8	141.1	-	
9	124.5	7.10 (br s, 1H) overlap	HMBC 9→7
10	30.2	2.69-2.76 (m, 1H), 2.77-2.82 (m, 1H) overlap	HMBC 10→7,8,9,12
11	35.4	2.31 (ddd, <i>J</i> = 14.3, 6.5, 6.5 Hz, 1H), 2.44-2.51 (m, 1H) overlap	HMBC 11→8,12
12	171.4	-	
13	-	8.07 (d, <i>J</i> = 7.6 Hz, 1H)	HMBC 13→12
14	47.7	4.12 (qd, <i>J</i> = 7.6, 7.1 Hz, 1H)	HMBC 14→15,16
15	17.6	0.85 (d, <i>J</i> = 7.1 Hz, 3H)	HMBC 15→15,16
16	172.3	-	
17	-	7.86 (d, <i>J</i> = 7.7 Hz, 1H)	HMBC 17→16
18	52.3	3.98 (ddd, <i>J</i> = 8.0, 7.8, 5.4 Hz, 1H)	TOCSY 18→17,18,20 HMBC 18→19,20,23
19	27.3	1.50-1.58 (m, 1H) overlap, 1.70-1.81 (m, 1H) overlap	HMBC 19→20,21
20	30.9	1.91-2.00 (m, 2H)	HMBC 20→21
21	173.9	-	
22	-	6.78 (br s, 1H), 7.22 (br s, 1H) overlap	TOCSY 22→22'
23	171.2	-	
24	-	7.56 (br d, <i>J</i> = 6.8 Hz, 1H)	HMBC 24→23
25	50.7	4.45 (ddd, <i>J</i> = 7.2, 6.8, 5.8 Hz, 1H)	COSY 25→24
26	27.6	2.93 (dd, <i>J</i> = 15.3, 7.6 Hz, 1H), 3.05-3.12 (m, 1H) overlap	HMBC 26→27

27	128.9	-	
28	116.8	7.28 (s, 1H)	HMBC 28→27,30
29	-	not observed	
30	134.0	8.95 (br s, 1H)	HMBC 30→27,28
31	170.0	-	
32	-	8.07 (d, $J = 7.4$ Hz, 1H)	HMBC 32→31
33	53.7	4.60 (ddd, $J = 10.9, 7.4, 3.3$ Hz, 1H)	TOCSY 33→32,34
34	27.7	2.85 (dd, $J = 14.4, 11.1$ Hz, 1H), 3.13-3.20 (m, 1H) overlap	HMBC 34→33,35
35	109.8	-	
36	133.0	-	
37	103.8	7.57 (d, $J_{HF} = 11.1$ Hz, 1H)	HMBC 37→35,41,38,39
38	155.3 (d, $J \approx 230$ Hz)	-	
39	120.1	-	
40	112.8	7.21 (d, $J_{HF} = 6.4$ Hz, 1H)	HMBC 40→38
41	133.0	-	
42	-	10.83 (d, $J = 1.3$ Hz, 1H)	HMBC 42→35,36,41
43	125.7	7.17-7.19 (m, 1H) overlap	
44	172.2	-	
45	-	8.70 (br d, $J = 7.8$ Hz, 1H)	HMBC 45→44
46	52.2	4.25 (ddd, $J = 7.8, 7.8, 6.1$ Hz, 1H)	TOCSY 46→45,47,48,49
47	28.9	1.55-1.63 (m, 1H) overlap, 1.71-1.78 (m, 1H) overlap	HMBC 47→46
48	25.1	1.47-1.57 (m, 2H) overlap	HMBC 48→49
49	40.3	3.09-3.16 (m, 2H) overlap	HMBC 49→47,48,51
50	-	14.17 (br s) overlap	
51	156.9	-	
52	-	14.17 (br s) overlap	
53	173.3	-	
54	-	7.14 (br s, 1H), 7.39 (br s, 1H)	TOCSY 54'→54



26e
10%

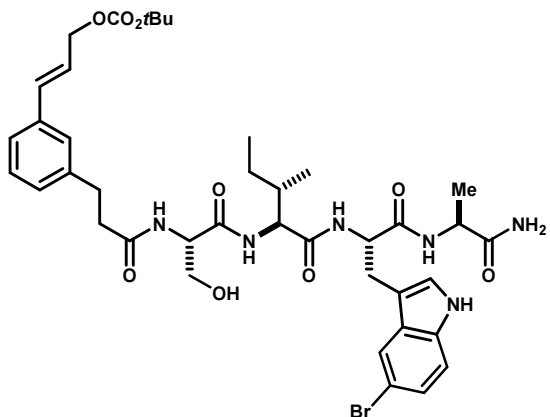
(600MHz, DMSO-*d*₆, 298K)

	¹³ C	¹ H	key correlations
1	47.1	4.83 (dd, <i>J</i> 15.5, 6.4 Hz, 1H), 4.99 (dd, <i>J</i> = 15.5, 5.7 Hz, 1H)	HMBC 1→41,43
2	125.4	6.37 (ddd, <i>J</i> = 15.7, 6.4, 5.7 Hz, 1H)	HMBC 2→4
3	131.9	6.65 (br d, <i>J</i> = 15.7 Hz, 1H)	TOCSY 3→2,1
4	135.9	-	
5	125.1	7.15-7.20 (m, 1H) overlap	
6	128.5	7.19-7.24 (m, 1H) overlap	HMBC 6→4,8
7	127.8	7.09 (br d, <i>J</i> = 7.1 Hz, 1H)	
8	141.6	-	
9	125.6	7.25 (br s, 1H) overlap	
10	30.7	2.73-2.86 (m, 2H)	HMBC 10→8,12
11	36.3	2.36-2.51 (m, 2H)	HMBC 11→8,12
12	172.6	-	
13	-	8.24 (d, <i>J</i> = 6.4 Hz, 1H)	HMBC 13→12
14	49.6	7.94-7.98 (m, 1H)	HMBC 14→16
15	17.3	1.14 (d, <i>J</i> = 7.2 Hz, 3H)	TOCSY 15→14,13
16	173.2	-	
17	-	7.81-7.88 (m, 1H)	HMBC 17→16
18	49.6	4.08-4.16 (m, 1H)	
19	27.4	1.65-1.74 (m, 1H), 179-1.87 (m, 1H)	HMBC 19→21
20	31.0	1.95-2.11 (m, 2H)	HMBC 20→21
21	174.1	-	
22	-	6.81 (br s, 1H), 7.30 (br s, 1H)	HMBC 22→21
23	171.9	-	
24	-	8.12 (d, <i>J</i> = 7.6 Hz, 1H)	HMBC 24→23
25	51.4	4.55-4.62 (m, 1H) overlap	HMBC 25→31
26	26.8	2.92-3.01 (m, 1H) overlap, 3.06-3.12 (m, 1H)	

27	129.6	-	
28	116.9	7.25 (s, 1H) overlap	HMBC 28→29
29	134.1	8.95 (br s, 1H)	HMBC 29→27,28
30	-	Not detected	
31	170.7	-	
32	-	8.02 (d, $J = 7.2$ Hz, 1H)	HMBC 32→31
33	53.3	4.52-4.59 (m, 1H)	HMBC 33→34
34	27.3	2.92-3.01 (m, 1H) overlap, 3.12-3.22 (m, 1H)	HMBC 34→33,35
35	109.9	-	
36	128.0	-	
37	103.9	7.45 (dd, $J_{HF} = 9.9$ Hz, $J_{HH} = 2.3$ Hz, 1H)	HMBC 37→41
38	157.1 (d, $J \approx 220$ Hz)	-	
39	109.4	6.98 (ddd, $J_{HF} = 9.1$ Hz, $J_{HH} = 9.1, 2.3$ Hz, 1H)	HMBC 39→41
40	111.1	7.48 (dd, $J_{HH} = 9.1$ Hz, $J_{HF} = 4.5$ Hz, 1H)	HMBC 40→36
41	132.8	-	
42	-	-	
43	128.5	7.28 (s, 1H)	HMBC 43→1
44	171.9	-	
45	-	8.22 (d, $J = 8.1$ Hz, 1H)	
46	52.2	4.19-4.28 (m, 1H)	HMBC 46→53
47	29.1	1.54-1.64 m, 1H), 1.69-1.79 (m, 1H)	
48	25.0	1.43-1.57 (m, 2H)	
49	40.5	3.08-3.15 (m, 2H) overlap	HMBC 49→51
50	-	7.61 (t, $J = 5.1$ Hz, 1H)	
51	156.9	-	
52	-	14.03-14.44 (m, 3H)	
53	173.4	-	
54	-	7.15 (br s, 1H), 7.31 (br s, 1H)	HMBC 54→53

Ser-Ile-Trp(5Br)-Ala (27a–27e):

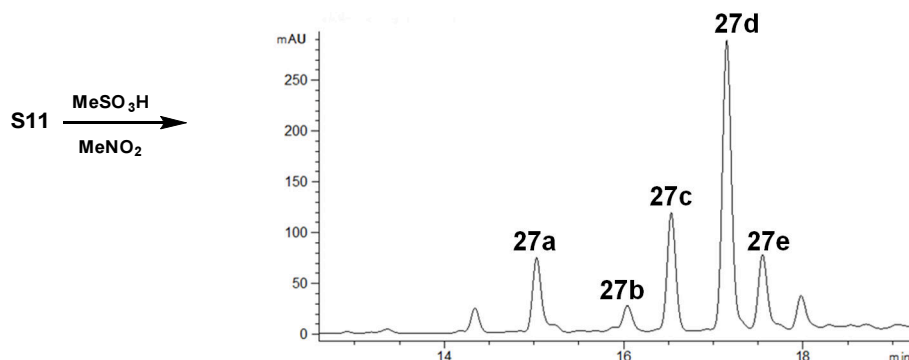
Acyclic intermediate S11. Compound S11 (82 mg) was prepared from peptide Ser-Ile-Trp(5Br)-Ala-NH₂ template **5** according to General Procedure A.



according to General Procedure A. ¹H NMR (DMSO-*d*₆, 500 MHz): δ 11.00 (d, *J* = 2.5 Hz, 1H), 7.96 (d, *J* = 7.8 Hz, 1H), 7.89 (d, *J* = 8.3 Hz, 1H), 7.84 (d, *J* = 7.5 Hz, 1H), 7.83 (d, *J* = 7.9 Hz, 1H), 7.74 (d, *J* = 1.8 Hz, 1H), 7.26- 7.30 (m, 1H), 7.26 (br. s, 1H), 7.23-7.24 (m, 1H), 7.21 (t, *J* = 7.6 Hz, 1H), 7.17 (d, *J* = 2.3 Hz, 1H), 7.14 (d, *J* = 2 Hz, 1H), 7.13 (d, *J* = 2 Hz, 1H), 7.1 (br. d, *J* = 7.5 Hz, 1H), 7.07 (br. s, 1H), 6.99 (br. s, 1H), 6.61 (d, *J* = 15.9 Hz, 1H), 6.32 (dt, *J* = 15.6, 6.2 Hz, 1H), 4.65 (dd, *J* = 6.3, 6.2 Hz, 2H), 4.5 (ddd, *J* = 9.2, 8.2, 5.0 Hz, 1H), 4.41 (apt q, *J* = 6.7 Hz, 1H), 4.15 (dddd, *J* = 7.2, 7.2, 7.2, 7.2 Hz, 1H), 4.07 (dd, *J* = 7.8, 6.2 Hz, 1H), 3.56 (dd, *J* = 10.4, 6.0 Hz, 1H), 3.51 (dd, *J* = 10.4, 6.3 Hz, 1H), 3.11 (dd, *J* = 14.9, 4.8 Hz, 1H), 2.85 (dd, *J* = 14.7, 9.4 Hz, 1H), 2.78 (app t, *J* = 7.9 Hz, 2H), 2.43-2.49 (m, 3H), 1.60-2.49 (m, 1H), 1.41

(s, 9H), 1.19 (d, *J* = 7 Hz, 3H), 1.08- 1.16 (m, 1H), 0.90-1.00 (m, 1H), 0.65 (d, *J* = 6.7 Hz, 3H). ¹³C NMR (DMSO-*d*₆, 126 MHz): δ 174.4, 172.1, 171.3, 171.3, 171.2, 153.3, 142.2, 136.3, 135.2, 133.9, 129.5, 129.1, 128.5, 126.9, 126.0, 124.7, 123.8, 121.2, 113.7, 111.5, 110.3, 82.0, 67.4, 62.2, 58.0, 55.0, 53.6, 48.7, 37.1, 36.7, 31.4, 27.85, 27.78, 27.6, 24.3, 18.6, 15.7, 11.7. MS *m/z* 841.4 (calc'd: C₄₀H₅₃BrN₆O₉, [M+H]⁺, 841.1).

Macrocycles 27a–27e:



Acyclic intermediate **5** (82 mg) was cyclized following General Procedure C and purified by the preparative HPLC method A (below) to give **27a** (7.9 mg, 11%), **27b** (2.2 mg, 3%), **27c** (8.1 mg, 11%), **27d** (19.2 mg, 27%), and **27e** (7.6 mg, 11%).

Preparative HPLC method A:

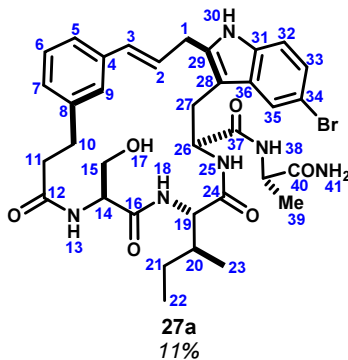
Column: Waters Sunfire™ C₁₈, 19x250mm, 5μm.

Solvent A: H₂O + 0.1%v TFA

Solvent B: ACN + 0.1%v TFA

Flow rate: 18.00 ml/min

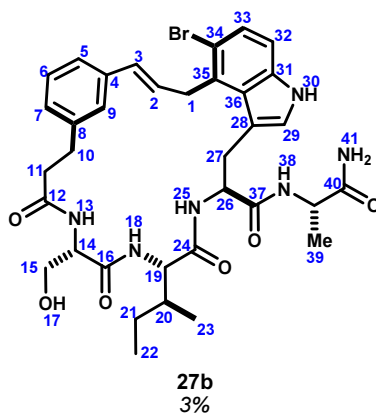
Time	%B
0	30
2	30
30	100



(500MHz, DMSO-*d*₆, 298K)

	¹³ C	¹ H	key correlations
1	29.6	3.62-3.68 (m, 1H), 3.70-3.76 (m, 1H)	HMBC 1→29, 28
2	126.7	6.53-6.60 (m, 1H) overlap	COSY 2→1
3	131.4	6.53-6.60 (m, 1H) overlap	
4	136.8	-	
5	123.6	7.16-7.20 (m, 1H) overlap	
6	127.9	7.17-7.21 (m, 1H) overlap	
7	127.4	7.02-7.06 (m, 1H)	HMBC 7→5
8	141.4	-	
9	125.3	7.31 (br s, 1H) overlap	HMBC 9→3,5
10	29.9	2.68-2.75 (m, 1H), 3.02-3.10 (m, 1H) overlap	HMBC 10→7,8,9
11	35.1	2.41 (ddd, <i>J</i> = 14.9, 9.2, 2.2 Hz, 1H), 2.58-2.65 (m, 1H)	
12	171.5	-	
13	-	8.11 (d, <i>J</i> = 8.4 Hz, 1H)	
14	55.3	4.25 (ddd, <i>J</i> = 8.4, 5.5, 5.5 Hz, 1H)	
15	61.4	3.46-3.54 (m, 2H)	
16	169.4	-	
17	-	not observed	
18	-	7.29-7.32 (m, 1H) overlap	HMBC 18→16
19	56.6	4.06 (dd, <i>J</i> = 8.0, 6.6 Hz, 1H)	
20	37.3	1.60-1.69 (m, 1H)	
21	23.4	0.88-0.98 (m, 1H), 1.22-1.33 (m, 1H)	
22	10.9	0.71 (t, <i>J</i> = 7.4 Hz, 3H)	
23	15.0	0.68 (d, <i>J</i> = 6.7 Hz, 3H)	
24	170.3	-	
25	-	8.25 (d, <i>J</i> = 8.8 Hz, 1H)	
26	53.6	4.60 (ddd, <i>J</i> = 9.0, 8.8, 5.9 Hz, 1H)	HMBC 26→28
27	26.1	2.91 (dd, <i>J</i> = 14.4, 9.4 Hz, 1H), 3.04-3.10 (m, 1H) overlap	HMBC 27→28,29,36
28	105.9	-	
29	136.6	-	
30	-	10.94 (s, 1H)	

31	133.6	-	
32	112.3	7.17 (d, $J = 8.6$ Hz, 1H)	HMBC 32→36
33	122.4	7.06 (dd, $J = 8.6, 1.9$ Hz, 1H)	HMBC 33→31,34, TOCSY 33→32,35
34	110.6	-	
35	120.1	7.70 (d, $J = 1.9$ Hz, 1H)	HMBC 35→28,31,33,34
36	130.1	-	
37	170.6	-	
38	-	7.84 (d, $J = 7.5$ Hz, 1H)	
39	18.3	1.20 (d, $J = 7.1$ Hz, 3H)	
40	47.9	4.17 (dq, $J = 7.1, 7.1$ Hz, 1H)	
41	173.5	-	
42	-	7.00 (br s, 1H), 7.20 (br s, 1H)	TOCSY 42→42', HMBC 42→41

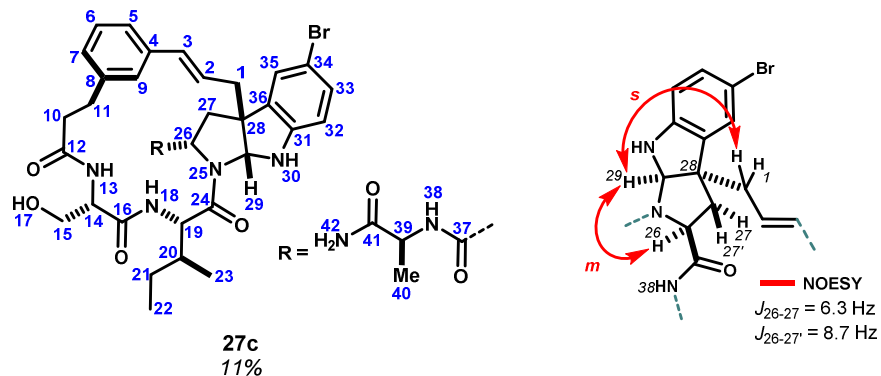


(500MHz, 600MHz, DMSO- d_6 , 298K)

*Note: This isolated compound was contaminated *O*-tert-butoxycarbonyl(cinnamyl alcohol 3-propionic acid)

	^{13}C	^1H	key correlations
1	34.9	3.93-3.99 (m, 1H), 4.23-4.28 (m, 1H) overlap	COSY 1→1', HMBC 1→34,35,36
2	128.4	6.45 (ddd, $J = 16.06, 6.0, 5.5$ Hz, 1H)	HMBC 2→4
3	129.8	6.20 (br d, $J = 16.0$ Hz, 1H)	HMBC 3→4
4	137.0	-	
5	122.9	7.00 (br d, $J = 7.5$ Hz, 1H)	HMBC 5→3
6	127.9	7.10 (dd, $J = 7.5, 7.5$ Hz, 1H)	HMBC 6→4,8, TOCSY 6→5,7,9
7	127.3	6.99 (br d, $J = 7.5$ Hz, 1H) overlap	
8	141.3	-	
9	124.6	7.22 (br s, 1H)	HMBC 9→3
10	28.9	2.68-2.74 (m, 1H) overlap, 3.01-3.05 (m, 1H) overlap	HMBC 10→7,8,9,12
11	34.3	2.48-2.53 (m, 1H) obscured, 2.66-2.72 (m, 1H) overlap	HMBC 11→9,12
12	171.5	-	
13	-	8.10 (d, $J = 8.3$ Hz, 1H)	HMBC 13→12, COSY 13→14

14	56.1	4.23-4.27 (m, 1H) overlap	HMBC 14→15,16
15	62.0	3.50-3.55 (m, 1H), 3.60 (ddd, $J = 11.0, 5.7, 5.7$ Hz, 1H)	HMBC 15→16
16	169.3	-	
17	-	4.90 (dd, $J = 5.7, 5.7$ Hz, 1H)	HMBC 17→14,15
18	-	7.34 (d, $J = 8.3$ Hz, 1H)	HMBC 18→16, COSY 18→19
19	56.3	4.30 (dd, $J = 8.3, 7.4$ Hz, 1H)	COSY 19→20, HMBC 19→24
20	37.1	1.65-1.72 (m, 1H)	COSY 20→21,23
21	23.9	0.98-1.06 (m, 1H), 1.39-1.48 (m, 1H)	
22	10.9	0.79 (t, $J = 7.3$ Hz, 3H)	COSY 22→21
23	14.8	0.80 (d, $J = 6.6$ Hz, 3H)	
24	170.2	-	
25	-	8.34 (d, $J = 7.3$ Hz, 1H)	HMBC 25→24, COSY 25→26
26	54.3	4.61 (ddd, $J = 7.8, 7.8, 7.3$ Hz, 1H)	HMBC 26→28, COSY 26→27
27	29.1	3.09-3.14 (m, 2H)	HMBC 27→28
28	109.6	-	
29	126.1	7.06 (d, $J = 2.5$ Hz, 1H)	HMBC 29→28,31,36
30	-	11.06 (d, $J = 2.5$ Hz, 1H)	
31	135.6	-	
32	111.8	7.18 (d, $J = 8.6$ Hz, 1H)	HMBC 32→31,34,36
33	124.6	7.26 (d, $J = 8.6$ Hz, 1H)	HMBC 33→31
34	114.9	-	
35	129.7	-	
36	126.6	-	
37	169.5	-	
38	-	7.78 (d, $J = 7.6$ Hz, 1H)	HMBC 38→37
39	18.1	4.16 (dq, $J = 7.6, 7.0$ Hz, 1H)	
40	47.8	1.14 (d, $J = 7.0$ Hz, 1H)	
41	173.3	-	
42	-	6.90 (br s, 1H), 6.91 (br s, 1H)	HMBC 42→41



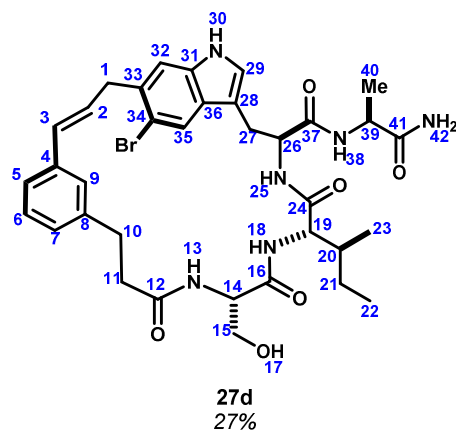
(500MHz, DMSO-*d*₆, 298K)

	¹³ C	¹ H	key correlations
1	39.5	2.51-2.55 (m, 2H)	HMBC 1→28,29 NOESY 1↔29
2	124.1	6.18 (ddd, <i>J</i> = 15.7, 8.2, 7.0 Hz, 1H)	COSY 2→1, HMBC 2→4
3	134.3	6.57 (d, <i>J</i> = 15.7 Hz, 1H)	
4	136.8	-	
5	124.4	7.03 (br d, <i>J</i> = 7.6 Hz, 1H)	HMBC 5→3, TOCSY 5→6,7,9
6	128.0	7.16 (dd, <i>J</i> = 7.6, 7.6 Hz, 1H)	HMBC 6→4,8
7	127.5	7.01 (br d, <i>J</i> = 7.6 Hz, 1H)	
8	141.4	-	
9	124.5	7.38 (br s, 1H)	HMBC 9→3
10	29.8	2.75 (apt dd, <i>J</i> = 14.0, 9.8 Hz, 1H), 3.02 (apt dd, <i>J</i> = 14.0, 10.7 Hz, 1H)	HMBC 10→7,9,12
11	35.8	2.31-2.36 (m, 1H) overlap, 2.47-2.54 (m, 1H) overlap	
12	171.3	-	
13	-	7.98 (d, <i>J</i> = 7.9 Hz, 1H)	HMBC 13→12
14	54.7	4.35 (ddd, <i>J</i> = 7.9, 7.0, 5.4 Hz, 1H)	COSY 14→13
15	61.5	3.54 (dd, <i>J</i> = 10.7, 7.0 Hz, 1H), 3.60 (dd, <i>J</i> = 10.7, 5.4 Hz, 1H)	COSY 15→14
16	170.2	-	
17	-	not observed	
18	-	8.03 (d, <i>J</i> = 6.1 Hz, 1H)	HMBC 18→16
19	55.6	4.23 (dd, <i>J</i> = 9.1, 6.1 Hz, 1H)	HMBC 19→24
20	36.4	1.71-1.77 (m, 1H) overlap	COSY 20→19
21	24.1	1.18-1.25 (m, 1H), 1.66-1.73 (m, 1H) overlap	
22	11.0	0.89 (t, <i>J</i> = 7.5 Hz, 3H)	COSY 22→21
23	14.8	0.99 (d, <i>J</i> = 6.8 Hz, 3H)	COSY 23→20
24	172.3	-	
25	-	-	
26	60.3	4.42 (dd, <i>J</i> = 8.7, 6.3 Hz, 1H)	COSY 26→27, HMBC 26→24 NOESY 26↔29
27	38.3	2.09 (dd, <i>J</i> = 13.0, 6.3 Hz, 1H), 2.32-2.37 (m, 1H) overlap	HMBC 27→26,28,29,37

28	56.8	-	
29	80.8	6.35 (s, 1H)	HMBC 29→1,24,27,31,36
30	-	not observed	
31	147.8	-	
32	111.1	6.50 (d, $J = 8.3$ Hz, 1H)	HMBC 32→34,36
33	130.6	7.14 (dd, $J = 8.3, 2.1$ Hz, 1H)	HMBC 33→31
34	108.8	-	
35	124.9	7.31 (d, $J = 2.1$ Hz, 1H)	HMBC 35→31
36	136.7	-	
37	169.4	-	
38	-	7.33 (d, $J = 7.1$ Hz, 1H)	
39	47.4	3.98 (dq, $J = 7.1, 6.8$ Hz, 1H)	HMBC 39→41
40	17.9	0.83 (d, $J = 6.8$ Hz, 3H)	COSY 40→39, HMBC 40→41
41	173.3	-	
42	-	6.90 (br s, 1H), 7.38 (br s, 1H)	HMBC 42→41, TOCSY 42→42'

Coupling constants from 1D-TOCSY

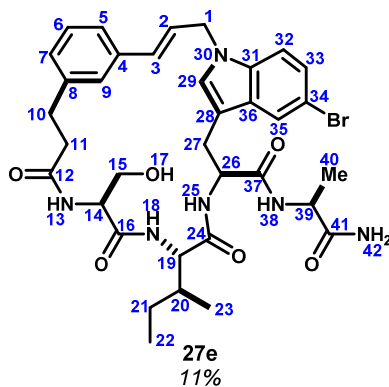
26	4.42 (dd, $J = 8.8, 6.3$ Hz, 1H)
27β	2.35 (dd, $J = 13.0, 8.7$ Hz, 1H)
27α	2.09 (dd, $J = 13.0, 6.3$ Hz, 1H)



(500MHz, DMSO- d_6 , 340K)

	¹³ C	¹ H	key correlations
1	38.0	3.68 (apt d, $J = 4.1$ Hz, 2H)	
2	129.0	6.38 (ddd, $J = 16.0, 5.9, 5.9$ Hz, 1H)	HMBC 2→4
3	129.4	6.16 (br d, $J = 16.0$ Hz, 1H)	HMBC 3→5,9
4	136.8	-	
5	123.1	7.18 (d, $J = 8.0$ Hz, 1H) overlap	
6	127.6	7.16 (dd, $J = 8.0, 8.0$ Hz, 1H) overlap	HMBC 6→4,9
7	126.8	6.97 (br d, $J = 8.0$ Hz, 1H)	
8	140.6	-	

9	124.4	7.03 (br s, 1H)	HMBC 9→3,5,7,10
10	29.3	2.78 (ddd, $J = 14.8, 7.8, 3.5$ Hz, 1H), 2.83-2.89 (m, 1H) overlap	
11	34.7	2.32 (ddd, $J = 14.9, 7.8, 3.5$ Hz, 1H), 2.50-2.56 (m, 1H)	HMBC 11→12
12	171.4	-	
13	-	7.46 (d, $J = 7.4$ Hz, 1H)	
14	53.9	4.12 (apt dd, $J = 11.9, 6.0$ Hz, 1H)	
15	61.6	3.03 (dd, $J = 10.8, 6.0$ Hz, 1H), 2.84-2.89 (m, 1H) overlap	
16	not observed	-	
17	-	not observed	
18	-	7.38-7.42 (m, 1H) overlap	
19	56.8	4.03 (dd, $J = 7.9, 6.4$ Hz, 1H)	HMBC 19→24
20	35.8	1.72-1.80 (m, 1H)	
21	23.4	0.99-1.08 (m, 1H), 1.30-1.38 (m, 1H)	
22	10.5	0.80 (t, $J = 7.4$ Hz, 3H)	
23	14.8	0.84 (d, $J = 6.8$ Hz, 3H)	
24	170.0	-	
25	-	7.38-7.42 (m, 1H) overlap	
26	52.9	4.62 (apt dd, $J = 14.4, 7.5$ Hz, 1H)	HMBC 26→37
27	26.5	3.08-3.12 (m, 1H) obscured	HMBC 27→28,37
28	108.8	-	
29	125.0	7.15 (br s, 1H) overlap	HMBC 29→28,31,36
30	-	10.69 (br s, 1H)	HMBC 30→31
31	135.4	-	
32	113.0	7.32 (s, 1H)	HMBC 32→1,36
33	130.0	-	
34	113.6	-	
35	121.7	7.83 (s, 1H)	HMBC 35→28,31,33,34
36	127.4	-	
37	170.3	-	
38	-	7.60 (br s, 1H)	
39	47.6	4.29 (qd, $J = 7.1, 7.0$ Hz, 1H)	HMBC 39→37,41
40	17.6	1.23 (d, $J = 7.1$ Hz, 3H)	HMBC 40→41
41	173.4	-	
42	-	6.82 (br s, 1H), 7.06 (br s, 1H)	



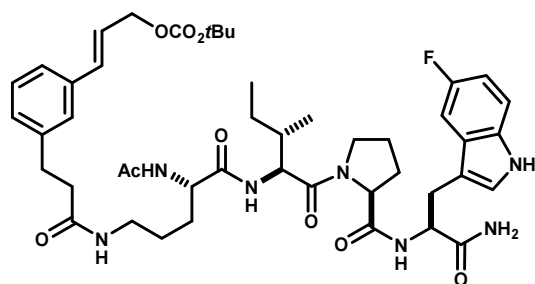
(500MHz, DMSO-*d*₆, 298K)

	¹³ C	¹ H	key correlations
1	47.5	4.83-4.90 (m, 2H)	HMBC 1→2,3,29,31
2	124.7	6.59-6.67 (m, 1H) overlap	HMBC 2→4
3	132.6	6.59-6.67 (m, 1H) overlap	
4	136.2	-	
5	124.5	7.16-7.20 (m, 1H) overlap	HMBC 5→3
6	127.9	7.20 (dd, <i>J</i> = 7.5, 7.3 Hz, 1H) overlap	HMBC 6→4,8
7	128.1	7.04 (ddd, <i>J</i> = 7.3, 1.5, 1.5 Hz, 1H)	
8	141.5	-	
9	124.7	7.41 (br s, 1H)	HMBC 9→3, TOCSY 9→5,6,7
10	29.6	2.70-2.76 (m, 1H), 2.94-3.00 (m, 1H) overlap	HMBC 10→7,8,9
11	34.7	2.42 (ddd, <i>J</i> = 14.5, 8.5, 2.7 Hz, 1H), 2.46-2.51 (m, 1H) obscured	HMBC 11→8
12	171.4	-	
13	-	7.87 (d, <i>J</i> = 7.4 Hz, 1H)	
14	54.5	4.22-4.27 (m, 1H) overlap	HMBC 14→16
15	61.4	3.34-3.40 (m, 2H) obscured	HMBC 15→16
16	170.0	-	
17	-	not observed	HMBC 18→16
18	-	7.70 (d, <i>J</i> = 8.0 Hz, 1H)	HMBC 19→24
19	57.1	4.01 (dd, <i>J</i> = 8.0, 7.1 Hz, 1H)	
20	35.9	1.60-1.68 (m, 1H)	
21	23.6	0.95-1.02 (m, 1H), 1.27-1.34 (m, 1H)	
22	10.7	0.73 (dd, <i>J</i> = 7.6, 7.6 Hz, 3H) overlap	
23	15.0	0.72 (d, <i>J</i> = 7.1 Hz, 3H) overlap	
24	171.2	-	
25	-	7.98 (d, <i>J</i> = 8.2 Hz, 1H)	HMBC 25→24,27
26	52.2	4.56 (ddd, <i>J</i> = 8.6, 8.2, 4.8 Hz, 1H)	HMBC 26→37, COSY 26→25,27
27	26.5	2.99-3.94 (m, 2H) overlap	
28	109.2	-	
29	128.6	7.35 (s, 1H)	HMBC 29→1,27,31,36

30	-	-	
31	134.5	-	
32	111.4	7.44 (d, $J = 8.7$ Hz, 1H)	HMBC 32→34,36
33	123.1	7.21 (dd, $J = 8.7, 1.9$ Hz, 1H)	HMBC 33→31,35
34	111.1	-	
35	120.9	7.78 (d, $J = 1.9$ Hz, 1H)	HMBC 35→31,33
36	129.3	-	
37	170.9	-	
38	-	7.94 (d, $J = 7.3$ Hz, 1H)	HMBC 38→37
39	47.8	4.21 (dq, $J = 7.3, 7.2$ Hz, 1H)	HMBC 39→41
40	18.1	1.17 (d, $J = 7.2$ Hz, 1H)	HMBC 40→39
41	173.8	-	
42	-	7.02 (br s, 1H), 7.32 (br s, 1H)	

Ac-Orn-Ile-Pro-Trp(5F) (28a–28b):

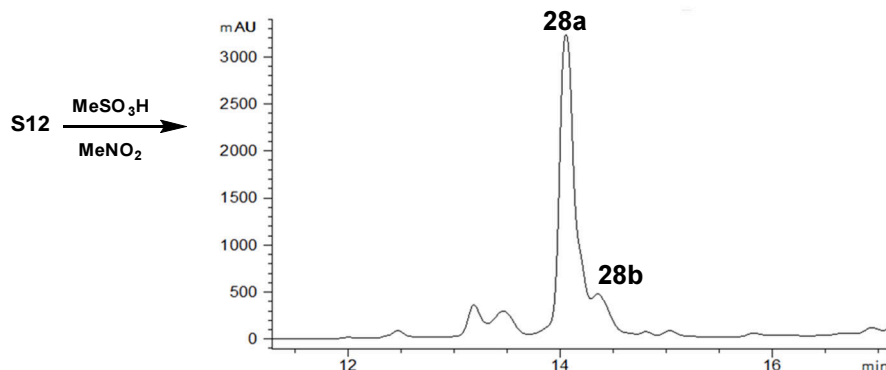
Acyclic intermediate S12. Compound **S12** (78.4mg) was prepared from peptide Ac-Orn(H)-Ile-Pro-Trp(5F)-NH₂ template **5** according to General Procedure A.



¹H NMR (DMSO-*d*₆, 500 MHz): δ 10.93 (d, $J = 2.5$ Hz, 1H), 7.97 (d, $J = 8.3$ Hz, 1H), 7.89 (d, $J = 8.4$ Hz, 1H), 7.83 (t, $J = 5.6$ Hz, 1H), 7.28-7.37 (m, 5H), 7.22-7.27 (m, 3H), 7.11 (br. d, $J = 7.3$ Hz, 1H), 7.04 (br. s, 1H), 6.89 (ddd, $J = 9.1, 9.1, 2.5$ Hz, 1H), 6.64 (d, $J = 16$ Hz, 1H), 6.34 (dt, $J = 16.0, 6.2$ Hz, 1H), 4.68 (dd, $J = 6.2, 1.1$ Hz, 2H), 4.38 (ddd, $J = 7.0, 7.0, 7.0$ Hz, 1H), 4.26-4.35 (m, 3H), 3.74 (ddd, $J = 9.6, 6.6, 6.6$ Hz, 1H), 3.53 (ddd, $J = 9.6, 5.7, 6.0$ Hz, 1H), 2.96-3.10 (m, 4H), 2.8 (app t, $J = 7.8$ Hz, 2H), 2.37 (app t, $J =$

7.8 Hz, 2H), 1.93-2.03 (m, 1H), 1.70-1.91 (m, 6H), 1.47-1.60 (m, 2H), 1.44 (s, 9H), 1.27-2.39 (m, 2H), 1.00-1.08 (m, 1H), 0.84 (d, $J = 6.8$ Hz, 3H), 0.81 (t, $J = 7.4$ Hz, 1H). ¹³C NMR (DMSO-*d*₆, 126 MHz): δ 173.0, 171.7, 171.2, 171.1, 170.2, 169.2, 155.7, 152.8, 141.8, 135.8, 133.4, 132.7, 128.6, 128.0, 127.7, 127.7, 126.4, 125.8, 124.2, 123.3, 112.1, 112.0, 110.32, 110.28, 108.9, 108.7, 103.3, 103.1, 81.5, 67.0, 66.9, 59.5, 54.5, 53.3, 51.9, 47.2, 38.1, 36.9, 36.1, 31.0, 29.6, 28.9, 27.3, 25.8, 24.4, 24.1, 22.5, 14.9, 10.8. MS *m/z* 876.5 (calc'd: C₄₆H₆₂N₇O₉, [M+H]⁺, 876.5).

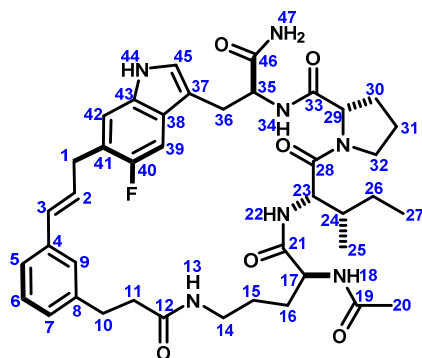
Macrocycles 28a–28b:



Acyclic intermediate **S12** (78.4 mg) was cyclized following General Procedure C and purified by the preparative HPLC method A (below) to give **28a** (23.2 mg, 34%) and **28b** (12.6 mg, 19%).

Preparative HPLC method A:
 Column: Waters XBridge™ C₁₈, 19x250mm, 5µm.
 Solvent A: H₂O + 0.1%v TFA
 Solvent B: ACN + 0.1%v TFA
 Flow rate: 18.00 ml/min

Time	%B
0	30
2	30
30	100

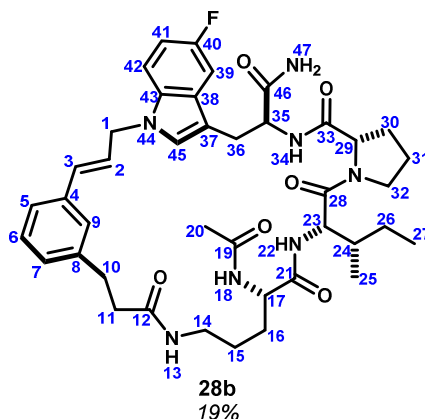


28a
34%

(500MHz, DMSO-*d*₆, 298K)

	¹³ C	¹ H	key correlations
1	47.1	4.83 (dd, <i>J</i> 15.5, 6.4 Hz, 1H), 4.99 (dd, <i>J</i> = 15.5, 5.7 Hz, 1H)	HMBC 1→41,43
2	125.4	6.37 (ddd, <i>J</i> = 15.7, 6.4, 5.7 Hz, 1H)	HMBC 2→4
3	131.9	6.65 (br d, <i>J</i> = 15.7 Hz, 1H)	TOCSY 3→2,1
4	135.9	-	
5	125.1	7.15-7.20 (m, 1H) overlap	
6	128.5	7.19-7.24 (m, 1H) overlap	HMBC 6→4,8
7	127.8	7.09 (br d, <i>J</i> = 7.1 Hz, 1H)	
8	141.6	-	
9	125.6	7.25 (br s, 1H) overlap	
10	30.7	2.73-2.86 (m, 2H)	HMBC 10→8,12
11	36.3	2.36-2.51 (m, 2H)	HMBC 11→8,12
12	172.6	-	
13	-	8.24 (d, <i>J</i> = 6.4 Hz, 1H)	HMBC 13→12
14	49.6	7.94-7.98 (m, 1H)	HMBC 14→16
15	17.3	1.14 (d, <i>J</i> = 7.2 Hz, 3H)	TOCSY 15→14,13
16	173.2	-	
17	-	7.81-7.88 (m, 1H)	HMBC 17→16
18	49.6	4.08-4.16 (m, 1H)	
19	27.4	1.65-1.74 (m, 1H), 1.79-1.87 (m, 1H)	HMBC 19→21
20	31.0	1.95-2.11 (m, 2H)	HMBC 20→21
21	174.1	-	

22	-	6.81 (br s, 1H), 7.30 (br s, 1H)	HMBC 22→21
23	171.9	-	
24	-	8.12 (d, $J = 7.6$ Hz, 1H)	HMBC 24→23
25	51.4	4.55-4.62 (m, 1H) overlap	HMBC 25→31
26	26.8	2.92-3.01 (m, 1H) overlap, 3.06-3.12 (m, 1H)	
27	129.6	-	
28	116.9	7.25 (s, 1H) overlap	HMBC 28→29
29	134.1	8.95 (br s, 1H)	HMBC 29→27,28
30	-	Not detected	
31	170.7	-	
32	-	8.02 (d, $J = 7.2$ Hz, 1H)	HMBC 32→31
33	53.3	4.52-4.59 (m, 1H)	HMBC 33→34
34	27.3	2.92-3.01 (m, 1H) overlap, 3.12-3.22 (m, 1H)	HMBC 34→33,35
35	109.9	-	
36	128.0	-	
37	103.9	7.45 (dd, $J_{HF} = 9.9$ Hz, $J_{HH} = 2.3$ Hz, 1H)	HMBC 37→41
38	157.1 (d, $J \approx 220$ Hz)	-	
39	109.4	6.98 (ddd, $J_{HF} = 9.1$ Hz, $J_{HH} = 9.1, 2.3$ Hz, 1H)	HMBC 39→41
40	111.1	7.48 (dd, $J_{HH} = 9.1$ Hz, $J_{HF} = 4.5$ Hz, 1H)	HMBC 40→36
41	132.8	-	
42	-	-	
43	128.5	7.28 (s, 1H)	HMBC 43→1
44	171.9	-	
45	-	8.22 (d, $J = 8.1$ Hz, 1H)	
46	52.2	4.19-4.28 (m, 1H)	HMBC 46→53
47	29.1	1.54-1.64 m, 1H), 1.69-1.79 (m, 1H)	
48	25.0	1.43-1.57 (m, 2H)	
49	40.5	3.08-3.15 (m, 2H) overlap	HMBC 49→51
50	-	7.61 (t, $J = 5.1$ Hz, 1H)	
51	156.9	-	
52	-	14.03-14.44 (m, 3H)	
53	173.4	-	
54	-	7.15 (br s, 1H), 7.31 (br s, 1H)	HMBC 54→53



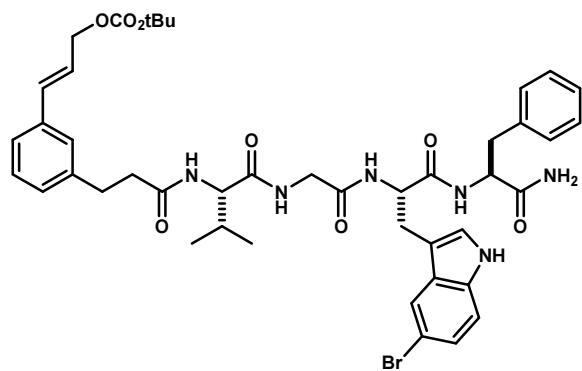
(500MHz, DMSO-*d*₆, 298K)

	¹³ C	¹ H	key correlations
1	47.0	4.49 (dd, <i>J</i> = 16.3, 5.6 Hz, 1H), 4.96 (dd, <i>J</i> = 16.6, 5.6, Hz, 1H)	HMBC 1→43,45
2	125.6	6.33 (ddd, <i>J</i> = 15.8, 5.6, 5.6 Hz, 1H)	TOCSY 2→3,1
3	131.4	6.48 (br d, <i>J</i> = 15.8 Hz, 1H)	HMBC 3→4
4	136.1	-	
5	124.3	7.16-7.19 (m, 1H) overlap	
6	128.3	7.14-7.19 (m, 1H) overlap	HMBC 6→4,8
7	127.6	7.03-7.07 (m, 1H)	
8	141.7	-	
9	125.8	7.15 (br s, 1H)	
10	30.6	2.72 (t, <i>J</i> = 7.5 Hz, 2H)	HMBC 10→8,12
11	36.7	2.23-2.32 (m, 2H)	HMBC 11→8,12
12	171.2	-	
13	-	7.69 (br t, <i>J</i> = 5.7 Hz, 1H)	HMBC 13→12 COSY 13→14
14	37.3	2.82-2.90 (m, 1H), 2.97-3.03 (m, 1H)	COSY 14→15
15	25.4	1.15-1.24 (m, 2H)	COSY 15→16,16' TOCSY 15→16,17
16	29.0	1.27-1.34 (m, 1H), 1.39-1.46 (m, 1H)	HMBC 16→17 COSY 16→17
17	51.6	4.22-4.28 (m, 1H)	HMBC 17→21
18	-	7.89 (d, <i>J</i> = 8.0 Hz, 1H)	
19	169.1	-	
20	22.0	1.79 (s, 3H)	
21	171.7	-	
22	-	7.99 (d, <i>J</i> = 8.6 Hz, 1H)	HMBC 22→21
23	54.4	4.25-4.30 (m, 1H)	
24	35.6	1.67-1.74 (m, 1H)	
25	15.1	0.81 (d, <i>J</i> = 6.7 Hz, 3H)	
26	23.5	0.95-1.03 (m, 1H), 1.43-1.51 (m, 1H)	
27	10.6	0.76 (t, <i>J</i> = 7.4 Hz, 3H)	

28	170.3	-	
29	59.7	4.16 (dd, $J = 8.2, 5.0$ Hz, 1H)	TOCSY 29→30,31,32 HMBC 29→33
30	28.7	1.57-1.65 (m, 1H), 1.84-1.89 (m, 1H)	
31	23.8	1.59-1.65 (m, 1H), 1.68-1.75 (m, 1H)	
32	46.8	3.45-3.51 (m, 1H), 3.55-3.61 (m, 1H)	
33	171.6	-	
34	-	7.79 (d, $J = 8.1$ Hz, 1H)	HMBC 34→33
35	52.6	4.36-4.42 (m, 1H)	COSY 35→36 HMBC 35→46
36	26.5	2.96-3.03 (m, 1H), 3.08-3.14 (m, 1H)	HMBC 36→35,37
37	110.4	-	
38	128.1	-	
39	103.4	7.37 (dd, $J_{HF} = 10.1, J_{HH} = 2.4$ Hz, 1H)	HMBC 39→40,43
40	156.9 (d, $J \approx 230$ Hz)	-	
41	108.9	6.93 (ddd, $J_{HF} = 9.4$ Hz, $J_{HH} = 8.9, 2.4$ Hz, 1H)	HMBC 41→43
42	110.6	7.44 (dd, $J_{HH} = 8.9$ Hz, $J_{HF} = 4.5$ Hz, 1H)	HMBC 42→38,40
43	132.5	-	
44	-	-	
45	128.7	7.35 (br s, 1H)	HMBC 45→37,38,43
46	173.3	-	
47	-	7.11 (br s, 1H), 7.27 (br s, 1H)	TOCSY 47→47'

Val-Gly-Trp(5Br)-Phe (29a–29f):

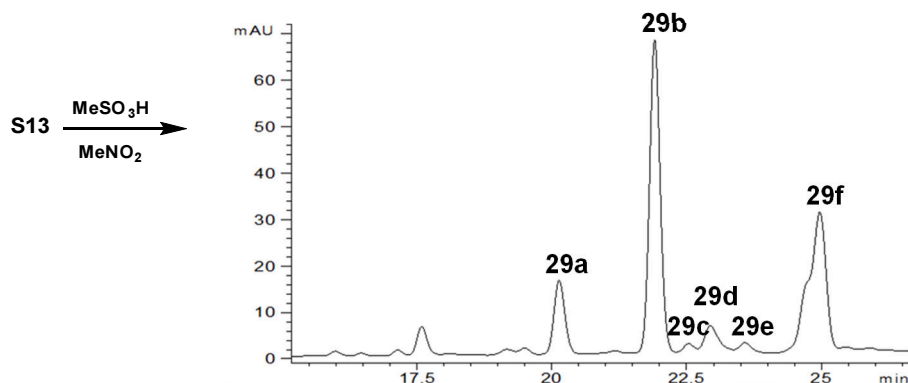
Acyclic intermediate S13. Compound **S13** (82 mg) was prepared from peptide Val-Gly-Trp(5Br)-Phe-NH₂



and template **5** according to General Procedure A. ¹H NMR (DMSO-*d*₆, 500 MHz): δ 0.77 (d, $J = 6.8$ Hz, 3H), 0.78 (d, $J = 6.8$ Hz, 3H), 1.43 (s, 9H), 1.86-1.96 (m, 1H), 2.41 (ddd, $J = 14.5, 8.7, 5.9$ Hz, 1H), 2.55 (dd, $J = 14.5, 8.3$ Hz, 1H), 2.72-2.88 (m, 4H), 3.03 (apt dt, $J = 14.1, 4.9$ Hz, 2H), 3.55 (dd, $J = 16.6, 5.4$ Hz, 1H), 3.74 (dd, $J = 16.6, 6.0$ Hz, 1H), 4.11 (dd, $J = 8.2, 6.9$ Hz, 1H), 4.42 (ddd, $J = 8.6, 8.6, 5.1$ Hz, 1H), 4.47 (ddd, $J = 9.0, 8.1, 4.8$ Hz, 1H), 4.66 (dd, $J = 6.2, 1.1$ Hz, 2H), 6.31 (dt, $J = 15.9, 6.2$ Hz, 1H), 6.61 (br d, $J = 15.9$ Hz, 1H), 7.05-7.11 (m, 2H), 7.13-7.30 (m, 12H), 7.74 (d, $J = 1.9$ Hz, 1H), 7.88 (d, $J = 8.3$ Hz, 1H), 8.02 (d, $J = 8.0$ Hz, 1H), 8.08 (d, $J = 8.3$ Hz, 1H), 8.16 (t, $J = 5.7$ Hz, 1H), 11.01

(d, $J = 1.9$ Hz, 1H). ¹³C NMR (DMSO-*d*₆, 126 MHz): δ 173.2, 172.2, 172.1, 171.5, 169.2, 153.3, 142.1, 138.4, 136.3, 135.2, 133.9, 129.7, 129.6, 129.0, 128.5 (2), 126.8, 126.7, 125.9, 124.7, 123.74, 123.70, 121.1, 113.8, 111.5, 110.4, 82.0, 67.4, 58.5, 54.5, 53.9, 42.4, 37.8, 36.9, 31.4, 30.6, 27.8, 19.6, 18.6.

Macrocycles 29a–29f:



Acyclic intermediate **S13** (82 mg, 97 μmol) was cyclized following General Procedure C and purified by the preparative HPLC method A. Compound **29f** was re-purified by the same method to give **29a** (6.7 mg, 6%), **29b** (22.1 mg, 20%), **29d** (9.1 mg, 8%) and **29f** (15.3 mg, 14%). Compounds **29c** and **29e** were not pursued.

Preparative HPLC method A:

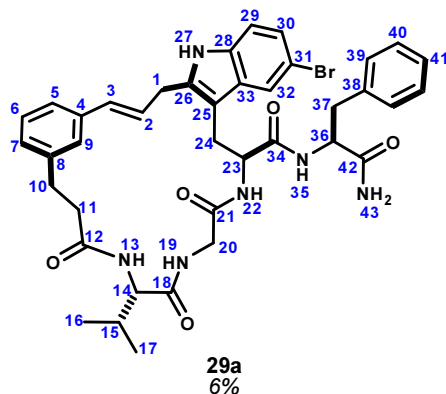
Column: Waters XBridge™ C₁₈, 19x250mm, 5 μm .

Solvent A: H₂O + 0.1%v TFA

Solvent B: ACN + 0.1%v TFA

Flow rate: 18.00 ml/min

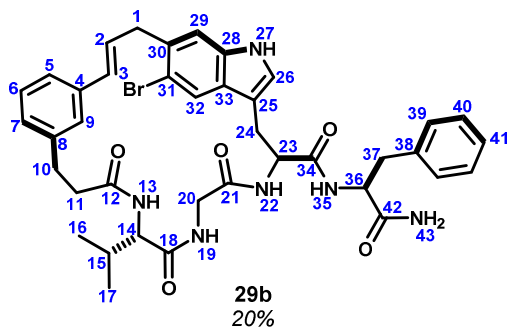
Time	%B
0	30
2	30
30	100



(500MHz, DMSO-*d*₆, 298K)

	¹³ C	¹ H	key correlations
1	28.3	3.53 (dd, <i>J</i> = 17.2, 5.9 Hz, 1H), 3.81 (dd, <i>J</i> = 17.2, 5.9 Hz, 1H)	HMBC 1→25,26
2	127.6	6.56 (ddd, <i>J</i> = 16.0, 5.9, 5.9 Hz, 1H)	HMBC 2→4, COSY 2→1
3	130.2	6.37 (br d, <i>J</i> = 16.0 Hz, 1H)	
4	136.9	-	
5	123.0	7.26 (d, <i>J</i> = 7.9 Hz, 1H) overlap	HMBC 5→9,3
6	127.97	7.18 (dd, <i>J</i> = 7.9, 7.9 Hz, 1H) overlap	HMBC 6→4,8
7	127.95	6.99 (d, <i>J</i> = 7.9 Hz, 1H) overlap	

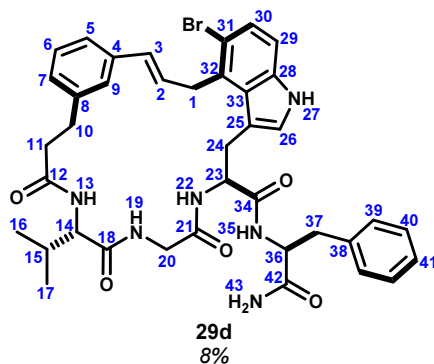
8	140.7	-	
9	124.9	7.20 (s, 1H) overlap	
10	29.8	2.73-2.78 (m, 1H) overlap, 2.89-2.96 (m, 1H) overlap	HMBC 10→9
11	34.0	2.34-2.40 (m, 1H), 2.72-2.79 (m, 1H) overlap	TOCSY 11→11',10
12	171.3	-	
13	-	7.78 (d, $J = 9.1$ Hz, 1H)	TOCSY 13→14,15,16,17, HMBC 13→12
14	58.0	3.92 (dd, $J = 9.1, 6.0$ Hz, 1H)	HMBC 14→18
15	29.1	1.92-1.98 (m, 1H)	
16	17.6	0.76 (d, $J = 3.7$ Hz, 3H)	
17	19.0	0.77 (d, $J = 3.7$ Hz, 3H)	
18	170.8	-	
19	-	6.97 (dd, $J = 8.0, 2.9$ Hz, 1H) overlap	
20	41.1	3.12 (dd, $J = 16.7, 2.9$ Hz, 1H), 3.76 (dd, $J = 16.7, 8.0$ Hz, 1H)	TOCSY 20→19, HMBC 20→18,21
21	167.6	-	
22	-	8.04-8.08 (m, 1H) overlap	HMBC 22→21
23	53.1	4.51-4.56 (m, 1H)	HMBC 23→34
24	26.7	2.72-2.79 (m, 1H) overlap, 2.96-3.00 (m, 1H) obscured	HMBC 24→25,26,33,34
25	106.6	-	
26	136.4	-	
27	-	11.00 (s, 1H)	
28	134.1	-	
29	112.3	7.21 (d, $J = 8.5$ Hz, 1H) overlap	HMBC 29→31
30	122.5	7.12 (dd, $J = 8.5, 1.6$ Hz, 1H)	HMBC 30→28,31
31	110.7	-	
32	120.0	7.73 (d, $J = 1.6$ Hz, 1H)	HMBC 32→25,28,30,31
33	129.8	-	
34	171.1	-	
35	-	8.04-8.08 (m, 1H) overlap	HMBC 35→34
36	53.5	4.49 (ddd, $J = 9.0, 8.0, 5.0$ Hz, 1H)	HMBC 36→34,38,42
37	37.3	2.86 (dd, $J = 13.7, 9.0$ Hz, 1H), 3.05 (dd, $J = 13.7, 5.0$ Hz, 1H)	HMBC 37→38,39
38	137.5	-	
39	129.0	7.22 (d, $J = 7.7$ Hz, 2H) overlap	
40	127.9	7.26 (dd, $J = 7.7, 7.7$ Hz, 2H) overlap	HMBC 40→38
41	126.0	7.15-7.18 (m, 1H) overlap	
42	172.4	-	
43	-	7.15 (br s, 1H), 7.46 (br s, 1H)	HMBC 43→42, TOCSY 43→43'



(600MHz, DMSO-*d*₆, 340K)

	¹³ C	¹ H	key correlations
1	38.3	3.61-3.67 (m, 1H) overlap, 3.69-3.75 (m, 1H) overlap	HMBC 1→3
2	129.0	6.40 (ddd, <i>J</i> = 16.0, 5.6, 5.6 Hz, 1H)	HMBC 2→4, COSY 2→1
3	129.1	6.08 (br d, <i>J</i> = 16.0 Hz, 1H)	HMBC 3→4,5,9
4	137.0	-	
5	122.6	7.21 (br d, <i>J</i> = 8.0 Hz, 1H)	HMBC 5→3,7,9
6	127.6	7.17 (dd, <i>J</i> = 8.0, 8.0 Hz, 1H) overlap	HMBC 6→8,4
7	126.7	6.99 (d, <i>J</i> = 8.0 Hz, 1H) overlap	
8	140.9	-	
9	124.5	6.99 (br s, 1H) overlap	HMBC 9→3,5,7
10	29.1	2.68-2.74 (m, 1H), 2.86-2.92 (m, 1H) overlap	HMBC 10→8
11	34.3	2.42-2.48 (m, 1H), 2.53-2.59 (m, 1H)	HMBC 11→8
12	170.9	-	
13	-	7.39 (d, <i>J</i> = 8.7 Hz, 1H)	HMBC 13→12
14	57.8	3.92 (dd, <i>J</i> = 8.7, 5.9 Hz, 1H)	COSY 14→13, HMBC 14→18
15	29.5	1.83-1.90 (m, 1H)	COSY 15→14
16	17.0	0.68 (d, <i>J</i> = 6.7 Hz, 3H) overlap	COSY 16→15
17	18.6	0.69 (d, <i>J</i> = 6.6 Hz, 3H) overlap	
18	170.3	-	
19	-	7.26-7.31 (m, 1H) overlap	
20	40.8	3.09-3.17 (m, 1H) overlap, 3.66-3.72 (m, 1H) overlap	HMBC 20→18,21
21	167.4	-	
22	-	7.75-7.86 (m, 1H) overlap	
23	54.8	4.50-4.56 (m, 1H) overlap	COSY 23→22
24	27.6	2.76-2.82 (m, 1H), 3.04-3.10 (m, 1H) overlap	
25	109.9	-	
26	124.4	7.13 (d, <i>J</i> = 2.1 Hz, 1H)	HMBC 26→25,28,33, COSY 26→27
27	-	10.71 (br s, 1H)	HMBC 27→25,26,28,33
28	135.1	-	
29	113.1	7.31 (s, 1H)	HMBC 29→1
30	129.6	-	

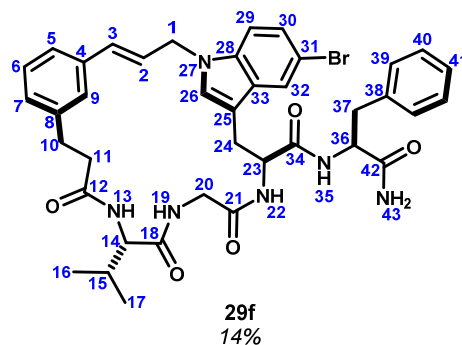
31	113.8	-	
32	121.9	8.00 (s, 1H)	HMBC 32→25,28,30,31
33	128.1	-	
34	170.5	-	
35	-	7.84 (d, $J = 8.1$ Hz, 1H) overlap	HMBC 35→34
36	53.1	4.56 (ddd, $J = 8.5, 8.1, 5.4$ Hz, 1H) overlap	HMBC 36→38,42
37	37.2	2.91 (dd, $J = 13.9, 8.5$ Hz, 1H) overlap, 3.10 (dd, $J = 13.9, 5.4$ Hz, 1H) overlap	HMBC 37→38,39
38	137.4	-	
39	128.6	7.25-7.28 (m, 2H) overlap	HMBC 39→41
40	127.5	7.25-7.28 (m, 2H) overlap	HMBC 40→38
41	125.5	7.16-7.20 (m, 1H) overlap	
42	172.1	-	
43	-	Not observed	



(500MHz, DMSO- d_6 , 298K)

	^{13}C	^1H	key correlations
1	34.9	3.93 (br dd, $J = 16.6, 4.1$ Hz, 1H), 4.03 (dd, $J = 16.6, 6.3$ Hz, 1H)	HMBC 1→31,33
2	128.2	6.42 (ddd, $J = 16.0, 6.3, 4.1$ Hz, 1H)	COSY 2→1, HMBC 2→4,5
3	129.8	6.13 (br d, $J = 16.0$ Hz, 1H)	
4	136.8	-	
5	123.1	6.99 (dd, $J = 7.9$ Hz, 1H) overlap	
6	127.90	7.14-7.19 (m, 1H) overlap	HMBC 6→8,4
7	127.30	7.09 (d, $J = 7.9$ Hz, 1H) overlap	HMBC 7→10
8	141.3	-	
9	124.62	7.28 (br s, 1H)	HMBC 9→10,5,7
10	29.3	2.68-2.75 (m, 1H) overlap, 2.96-3.03 (m, 1H) overlap	HMBC 10→7,8,9
11	34.3	2.40-2.47 (m, 1H), 2.69-2.77 (m, 1H) overlap	HMBC 11→8
12	171.7	-	
13	-	7.95 (d, $J = 8.6$ Hz, 1H)	TOCSY 13→14,15,16,17, HMBC 13→12
14	57.5	4.24 (dd, $J = 8.6, 5.6$ Hz, 1H)	HMBC 14→18

15	30.1	2.03-2.11 (m, 1H)	HMBC 15→18
16	17.3	0.78 (d, $J = 6.9$ Hz, 3H)	
17	19.1	0.82 (d, $J = 6.9$ Hz, 3H)	
18	171.0	-	
19	-	7.82-7.86 (m, 1H) overlap	HMBC 19→18
20	42.3	3.58 (dd, $J = 16.4, 4.8$ Hz, 1H), 3.78 (dd, $J = 16.4, 6.1$ Hz, 1H)	COSY 20→19, HMBC 20→18
21	168.2	-	
22	-	8.11 (d, $J = 8.1$ Hz, 1H)	HMBC 22→21
23	54.0	4.59 (ddd, $J = 8.4, 8.1, 5.9$ Hz, 1H)	HMBC 23→24
24	29.3	2.96-3.03 (m, 1H) overlap, 3.15 (dd, $J = 14.7, 8.4$ Hz, 1H)	HMBC 24→25,34
25	110.1	-	
26	125.5	6.90 (d, $J = 2.2$ Hz, 1H)	HMBC 26→25,33
27	-	11.05 (d, $J = 2.2$ Hz, 1H)	HMBC 27→25,26,28,33
28	135.6	-	
29	111.6	7.17 (d, $J = 8.5$ Hz, 1H) overlap	HMBC 29→31
30	124.55	7.25 (d, $J = 8.5$ Hz, 1H) overlap	
31	114.7	-	
32	129.5	-	
33	126.3	-	
34	170.0	-	
35	-	7.85 (d, $J = 8.3$ Hz, 1H)	HMBC 35→34
36	53.6	4.39 (ddd, $J = 8.5, 8.3, 5.3$ Hz, 1H)	HMBC 36→34,42
37	37.2	2.74-2.81 (m, 1H) overlap, 2.96-3.02 (m, 1H) overlap	HMBC 37→38,39,42
38	137.4	-	
39	128.9	7.18 (d, $J = 7.7$ Hz, 2H) overlap	HMBC 39→37
40	127.8	7.20-7.25 (m, 2H) overlap	
41	126.0	7.14-7.19 (m, 1H) overlap	
42	172	-	
43	-	6.99 (br s, 1H) overlap, 7.10 (br s, 1H) overlap	TOCSY 43→43', HMBC 43→42



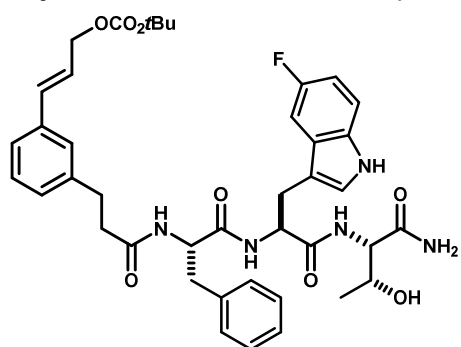
(500MHz, DMSO- d_6 , 298K)

	¹³ C	¹ H	key correlations
1	46.8	4.85 (dd, <i>J</i> = 16.7, 6.1 Hz, 1H), 4.91 (dd, <i>J</i> = 16.7, 5.2 Hz, 1H)	HMBC 1→2,3,28.
2	125.6	6.51 (ddd, <i>J</i> = 15.9, 6.1, 5.2 Hz, 1H)	COSY 2→3,1 HMBC 2→4
3	131.5	6.34 (d, <i>J</i> = 15.9 Hz, 1H)	
4	135.8	-	
5	123.5	7.20-7.23 (m, 1H)	HMBC 5→3
6	127.70	7.16-7.20 (m, 1H)	HMBC 6→4,8
7	128.10	7.03 (br d, <i>J</i> = 7.3 Hz, 1H)	
8	140.6	-	
9	125.80	7.24 (br s, 1H)	HMBC 9→5,7
10	30.1	2.72-2.79 (m, 1H), 2.85-2.93 (m, 1H)	
11	34.7	2.37 (ddd, <i>J</i> = 14.4, 7.8, 3.7 Hz, 1H), 2.65-2.72 (m, 1H)	HMBC 11→8,12 TOCSY 11→11',10,1'
12	171.3	-	
13	-	7.77 (d, <i>J</i> = 8.6 Hz, 1H)	HMBC 13→12 TOCSY 13→14,15,16,17
14	57.9	3.89 (dd, <i>J</i> = 8.6, 6.2 Hz, 1H)	HMBC 14→18
15	29.1	1.90-1.99 (m, 1H)	
16	17.7	0.77 (d, <i>J</i> = 6.9 Hz, 3H)	
17	18.7	0.78 (d, <i>J</i> = 6.8 Hz, 3H)	
18	170.6	-	
19	-	7.20-7.23 (m, 1H)	HMBC 19→18
20	40.9	3.14 (dd, <i>J</i> = 16.8, 4.4 Hz, 1H), 3.63 (dd, <i>J</i> = 16.8, 7.0 Hz, 1H)	HMBC 20→18,21 TOCSY 20→19
21	167.6	-	
22	-	8.00 (d, <i>J</i> = 9.1 Hz, 1H)	HMBC 22→21 TOCSY 22→23,24
23	51.9	4.56 (ddd, <i>J</i> = 11.4, 9.1, 3.1 Hz, 1H)	HMBC 23→25
24	27.2	2.66-2.73 (m, 1H), 3.04-3.10 (m, 1H)	HMBC 24→25,26,33
25	109.8	-	
26	128.0	7.23 (br s, 1H)	HMBC 26→25
27	-	-	
28	134.3	-	
29	111.7	7.42 (d, <i>J</i> = 8.8 Hz, 1H)	HMBC 29→31,33
30	123.10	7.19-7.24 (m, 1H)	HMBC 30→31
31	110.8	-	
32	121.1	7.84 (d, <i>J</i> = 1.9 Hz, 1H)	HMBC 32→28,31
33	129.1	-	
34	170.9	-	
35	-	8.21 (d, <i>J</i> = 8.1 Hz, 1H)	HMBC 35→34 TOCSY 35→36,37
36	53.4	4.49 (ddd, <i>J</i> = 8.9, 8.1, 4.9 Hz, 1H)	HMBC 36→38,42
37	37.1	2.85 (dd, <i>J</i> = 13.8, 8.9 Hz, 1H), 3.04 (dd, <i>J</i> = 13.8, 4.9 Hz, 1H)	HMBC 37→38

38	137.5	-	
39	128.9	7.22-7.25 (m, 2H)	TOCSY 39→41
40	127.5	7.24-7.28 (m, 2H)	HMBC 40→38
41	126.0	7.15-7.19 (m, 1H)	HMBC 41→39
42	172.4	-	
43	-	7.11 (br s, 1H), 7.43 (br s, 1H)	TOCSY 43→43' HMBC 43→42

Phe-Trp(5F)-Thr (30a–30l):

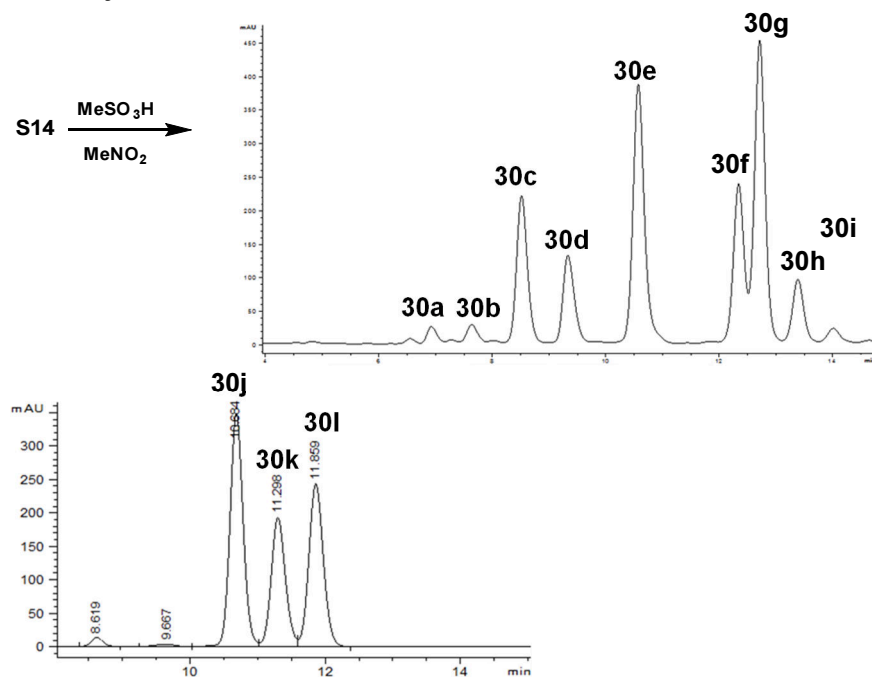
Acyclic intermediate S14. Compound **S14** was prepared from peptide Phe-Trp(5F)-Thr-NH₂ template **5**



according to General Procedure A. ¹H NMR (DMSO-*d*₆, 500 MHz): δ 10.97 (d, *J* = 2.2 Hz, 1H), 8.29 (d, *J* = 7.8 Hz, 1H), 8.08 (d, *J* = 8.1 Hz, 1H), 7.8 (d, *J* = 8.6 Hz, 1H), 7.41 (dd, *J* = 10.2, 2.4 Hz, 1H), 7.32 (dd, *J* = 8.8, 4.5 Hz, 1H), 7.29 (d, *J* = 2.2 Hz, 1H), 7.26 (br. d, *J* = 7.8 Hz, 1H), 7.23 (br. s, 1H), 7.21 (br. s, 1H), 7.2 (br. s, 1H), 7.14-7.18 (m, 4H), 7.09 (br. s, 1H), 7.01 (d, *J* = 8.1 Hz, 1H), 6.9 (ddd, *J* = 9.0, 9.0, 2.3 Hz, 1H), 6.63 (d, *J* = 15.7 Hz, 1H), 6.33 (dt, *J* = 15.9, 6.2 Hz, 1H), 4.67 (dd, *J* = 6.3, 1.1 Hz, 2H), 4.63 (ddd, *J* = 8.6, 8.0, 4.9 Hz, 1H), 4.54 (ddd, *J* = 9.9, 8.4, 4.0 Hz, 1H), 4.16 (dd, *J* = 8.7, 3.2 Hz, 1H), 4.08 (dddd, *J* = 6.2, 6.2, 6.2, 3.4 Hz, 1H), 3.17 (dd, *J* = 15.0, 4.6 Hz, 1H), 3.02 (dd, *J* = 15.3, 9.3 Hz, 1H), 2.97 (dd, *J* = 13.7, 4.0 Hz, 1H), 2.71 (dd, *J* = 13.9, 16.0 Hz, 1H),

2.65 (app t, *J* = 7.9 Hz, 2H), 2.23-2.38 (m, 2H), 1.4 (s, 9H), 1.02 (d, *J* = 6.4 Hz, 3H). ¹³C NMR (DMSO-*d*₆, 125 MHz): δ 172.0, 171.5, 171.4, 171.3, 157.6, 155.8, 152.8, 141.7, 137.9, 135.8, 133.4, 132.7, 129.1, 128.6, 127.9, 127.6, 127.5, 126.4, 126.1, 125.9, 124.1, 123.2, 112.14, 112.06, 110.2, 110.2, 109.0, 108.8, 103.3, 103.1, 81.5, 66.9, 66.3, 58.0, 53.7, 53.5, 37.4, 36.7, 30.9, 27.3, 19.9. MS *m/z* 758.8 (calc'd: C₄₁H₄₈FN₅O₈, [M+H]⁺, 758.4).

Macrocycles 30a–30l:



Acyclic intermediate **S14** was cyclized following General Procedure C and purified by the preparative HPLC method A. Compound **30g** was re-purified by preparative HPLC method B. Yields were not recorded.

Preparative HPLC method A:

Column: Waters XBridge™ C₁₈, 19x250mm, 5μm.

Solvent A: H₂O + 0.1%v TFA

Solvent B: ACN + 0.1%v TFA

Flow rate: 18.00 ml/min

Time	%B
0	40
2	40
30	60

Preparative HPLC method B:

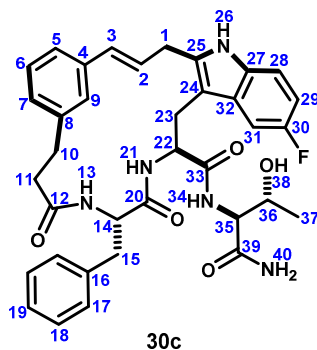
Column: Waters Sunfire™ C₁₈, 19x250mm, 5μm.

Solvent A: H₂O + 0.1%v TFA

Solvent B: ACN + 0.1%v TFA

Flow rate: 18.00 ml/min

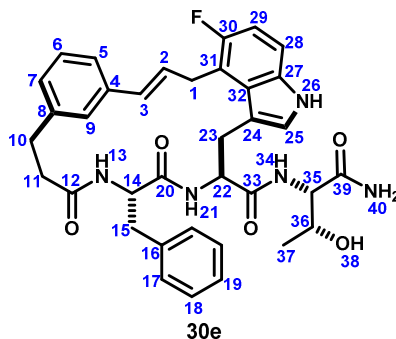
Time	%B
0	45
2	45
30	55



(500MHz, DMSO-*d*₆, 298K)

¹³ C	¹ H	key correlations
1	30.0 3.57 (dd, <i>J</i> = 15.3, 7.2 Hz, 1H), 3.80 (dd, <i>J</i> = 15.3, 6.3 Hz, 1H)	TOCSY 1→2,3 HMBC 1→2,3,24,25
2	127.6 6.07 (dt, <i>J</i> = 15.6, 6.9 Hz, 1H)	HMBC 2→1,4
3	131.0 6.43 (d, <i>J</i> = 15.9 Hz, 1H)	HMBC 3→1,4,5,9
4	136.8 -	
5	123.6 7.10 (m, 1H) overlap	HMBC 5→9
6	127.9 7.13 (m, 1H) overlap	HMBC 6→4
7	124.0 7.10 (m, 1H) overlap	HMBC 7→5,9
8	141.2 -	
9	125.0 6.98 (br. s, 1)	HMBC 10→8,9 TOCSY 10→11
10	30.4 2.62 (m, 1H) overlap, 2.88 (ddd, <i>J</i> = 13.7, 11.0, 5.6 Hz, 1H)	HMBC 11→8,12
11	35.8 1.98 (ddd, <i>J</i> = 14.0, 7.6, 3.1 Hz, 1H), 2.40 (ddd, <i>J</i> = 13.6, 11.0, 2.6 Hz, 1H)	
12	171.2 -	
13	- 8.07 (d, <i>J</i> = 8.9 Hz, 1H)	COSY 13→14 TOCSY 13→14,15,15' HMBC 13→12
14	52.7 4.75 (ddd, <i>J</i> = 9.3, 9.5, 3.8 Hz, 1H)	HMBC 14→15
15	38.0 2.98 (m, 1H) overlap, 2.65 (m, 1H) overlap	HMBC 15→14,16,17
16	138.1 -	
17	129.5 7.16 (m, 1H) overlap	HMBC 17→18
18	127.7 7.17 (m, 1H) overlap	HMBC 18→16,17

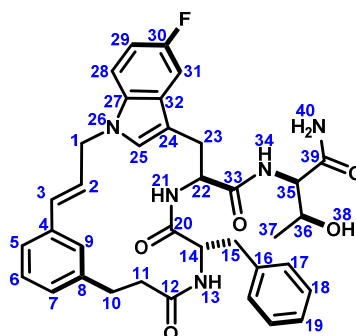
19	128.0	7.14 (m, 1H) overlap	
20	172.1	-	
21	-	8.59 (d, $J = 7.8$ Hz, 1H)	COSY 21→22 TOCSY 21→22,23 HMBC 21→20
22	54.1	4.66 (ddd, $J = 10.2, 7.6, 5.1$ Hz, 1H)	HMBC 22→23
23	26.2	3.07 (dd, $J = 15.1, 5.2$ Hz, 1H), 2.97 (m, 1H) overlap	HMBC 23→22,24,32
24	106.4	-	
25	136.4	-	
26	-	10.91 (s, 1H)	HMBC 26→24,25,27,32
27	131.8	-	
28	111.2	7.18 (m, 1H) overlap	HMBC 28→30 TOCSY 28→29
29	108.4	6.81 (ddd, $J = 9.3, 9.3, 2.5$ Hz, 1H)	TOCSY 29→28,31 HMBC 29→27,30
30	156.6	-	
31	103.4	7.24 (dd, $J = 10.3, 2.7$ Hz, 1H)	HMBC 31→27,30
32	129.0	-	
33	172.1	-	
34	-	7.73 (d, $J = 8.7$ Hz, 1H)	HMBC 34→33 TOCSY 34→35,36,37
35	57.8	4.13 (dd, $J = 8.7, 2.9$ Hz, 1H)	HMBC 35→36,39
36	66.2	4.07 (m, 1H)	
37	19.5	1.05 (d, $J = 6.4$ Hz, 3H)	
38	-	4.96 (d, $J = 4.9$ Hz, 1H)	
39	172.0	-	
40	-	6.93 (m, 1H) overlap	HMBC 40→39
41	30.0	3.57 (dd, $J = 15.3, 7.2$ Hz, 1H), 3.80 (dd, $J = 15.3, 6.3$ Hz, 1H)	TOCSY 1→2,3 HMBC 1→2,3,24,25
42	127.6	6.07 (dt, $J = 15.6, 6.9$ Hz, 1H)	HMBC 2→1,4



(500MHz, DMSO- d_6 , 298K)

	^{13}C	^1H	key correlations
1	27.8	3.76 (dd, $J = 16.6, 5.9$ Hz, 1H), 3.90 (br. d, $J = 16.0$ Hz, 1H)	TOCSY1→2,3 HMBC 1→2,3,31
2	130.0	6.07 (d, $J = 15.8$ Hz, 1H)	HMBC 2→1,31
3	128.8	6.35 (dt, $J = 16.0, 5.5$ Hz, 1H)	HMBC 3→1,5,9,30,32

4	136.5	-	
5	122.9	7.00 (m, 1H) overlap	HMBC 5→9
6	127.8	7.06 (m, 1H) overlap	HMBC 6→4,8
7	127.1	7.06 (m, 1H) overlap	HMBC 7→9
8	141.3	-	
9	125.8	6.99 (br. s, 1H)	HMBC 9→5,7
10	29.6	2.91 (m, 1H) overlap, 2.52 (m, 1H) overlap	HMBC 10→7,8,9,11,12
11	35.7	2.32 (app t, 13.5 Hz, 1H), 2.08 (m, 1H) overlap	HMBC 11→8,12
12	170.7	-	
13	-	8.10 (d, $J = 8.9$ Hz, 1H)	HMBC 13→12 TOCSY 13→14,15,15'
14	52.6	4.82 (ddd, $J = 9.7, 9.7, 4.1$ Hz, 1H)	HMBC 14→15
15	38.0	2.89 (m, 1H) overlap, 2.64 (dd, $J = 13.3, 10.5$ Hz, 1H)	HMBC 15→14,16,17
16	137.7	-	
17	128.8	7.21 (m, 1H) overlap	
18	127.6	7.21 (m, 1H) overlap	
19	127.6	7.15 (m, 1H) overlap	HMBC 19→17
20	171.1	-	
21	-	8.62 (d, $J = 6.6$ Hz, 1H)	HMBC 21→20 TOCSY 21→22,23
22	53.2	4.66 (m, 1H)	
23	29.1	3.30 (m, 1H) overlap, 3.06 (br. d, $J = 13.4$ Hz, 1H)	HMBC 23→22,24
24	110.6	-	HMBC 25→27
25	125.8	7.13 (m, 1H) overlap	HMBC 26→24,25,27
26	-	10.96 (br. s, 1H)	
27	133	-	
28	110.0	7.18 (m, 1H) overlap	
29	108.8	6.89 (m, 1H) overlap	HMBC 29→27,30,31
30	154.5	-	
31	115.6	-	
32	125.8	-	
33	170.7	-	
34	-	7.74 (d, $J = 8.3$ Hz, 1H)	HMBC 34→33 TOCSY 34→35,36,37
35	57.8	4.08 (dd, $J = 8.7, 3.0$ Hz, 1H)	
36	65.8	4.02 (m, 1H)	
37	19.8	0.99 (d, $J = 6.4$ Hz, 3H)	HMBC 37→35,36
38	-	4.9 (d, $J = 5.1$ Hz, 1H)	HMBC 38→35,36,37
39	171.7	-	
40	-	7.03 (m, 1H) overlap	HMBC 40→39
41	27.8	3.76 (dd, $J = 16.6, 5.9$ Hz, 1H), 3.90 (br. d, $J = 16.0$ Hz, 1H)	TOCSY1→2,3 HMBC 1→2,3,31
42	130.0	6.07 (d, $J = 15.8$ Hz, 1H)	HMBC 2→1,31

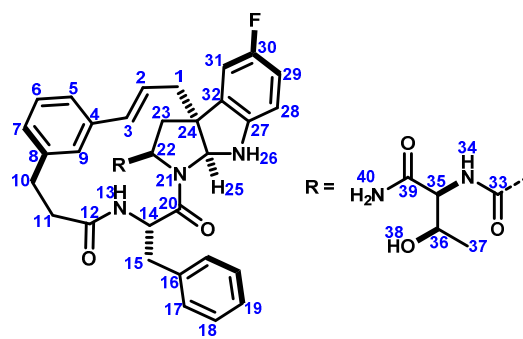


30k

(500MHz, DMSO-*d*₆, 298K)

	¹³ C	¹ H	key correlations
1	46.6	4.95 (ddd, <i>J</i> = 16.4, 4.7, 1.6 Hz, 1H), 4.83 (dd, <i>J</i> = 16.4, 6.9 Hz, 1H)	TOCSY1→2,3 HMBC 1→2,3,25
2	125.5	6.07 (ddd, <i>J</i> = 15.8, 7.1, 4.5 Hz, 1H)	HMBC 2→1,3,4
3	131.0	6.22 (br d, <i>J</i> = 15.9 Hz, 1H)	
4	135.7	-	
5	124.7	7.11 (m, 1H) overlap	HMBC 5→9,7
6	127.8	7.15 (m, 1H) overlap	HMBC 6→4,8
7	128.2	6.96 (m, 1H) overlap	
8	142.0	-	
9	124.5	6.92 (m, 1H) overlap	HMBC 9→7
10	29.1	2.46 (m, 1H) overlap, 2.95 (m, 1H) overlap	HMBC 10→7,8,9,11,12
11	35.5	2.08 (ddd, <i>J</i> = 15.1, 7.2, 2.4 Hz, 1H), 2.40 (ddd, <i>J</i> = 15.2, 11.6, 2.3 Hz, 1H)	TOCSY 11→10
12	170.6	-	
13	-	7.68 (d, <i>J</i> = 8.5 Hz, 1H)	HMBC 13→12 TOCSY 13→14,15
14	52.6	4.71 (m, 1H) overlap	
15	38.9	2.70 (dd, <i>J</i> = 13.6, 8.0 Hz, 1H), 3.02 (dd, <i>J</i> = 13.6, 4.1 Hz, 1H)	HMBC 15→14,16,17,20
16	137.6	-	
17	129.4	7.08 (m, 1H) overlap	HMBC 17→15
18	127.8	7.15 (m, 1H) overlap	HMBC 18→16
19	126.4	7.11 (m, 1H) overlap	HMBC 19→17
20	170.6	-	
21	-	8.60 (d, <i>J</i> = 8.7 Hz, 1H)	TOCSY 21→22,23 HMBC 21→20
22	52.6	4.74 (m, 1H) overlap	HMBC 22→23
23	27.2	3.10 (br. d, <i>J</i> = 14.8 Hz, 1H), 2.90 (m, 1H) overlap	HMBC 23→22,24,25
24	110.8	-	
25	128.1	7.28 (s, 1H)	HMBC 25→1,32,38
26	-	-	
27	132.6	-	

28	110.9	7.45 (dd, $J = 7.8, 4.5$ Hz, 1H)	HMBC 28→32 TOCSY 28→29,31
29	109.2	6.94 (m, 1H) overlap	HMBC 29→27,30
30	157.0	-	
31	103.8	7.51 (dd $J = 9.9, 2.4$ Hz, 1H)	HMBC 31→27,30
32	127.8	-	
33	171.9	-	
34	-	7.96 (d, $J = 8.8$ Hz, 1H)	TOCSY 34→35,36 HMBC 34→33
35	58.0	4.21 (dd, $J = 8.8, 3.1$ Hz, 1H)	HMBC 35→36
36	66.4	4.10 (m, 1H)	
37	20.0	1.07 (d, $J = 6.4$ Hz, 3H)	HMBC 37→35,36
38	-	not observed	
39	172.2	-	
40	-	7.2 (br. s, 2H)	HMBC 40→39
41	46.6	4.95 (ddd, $J = 16.4, 4.7, 1.6$ Hz, 1H), 4.83 (dd, $J = 16.4, 6.9$ Hz, 1H)	TOCSY1→2,3 HMBC 1→2,3,25
42	125.5	6.07 (ddd, $J = 15.8, 7.1, 4.5$ Hz, 1H)	HMBC 2→1,3,4



301

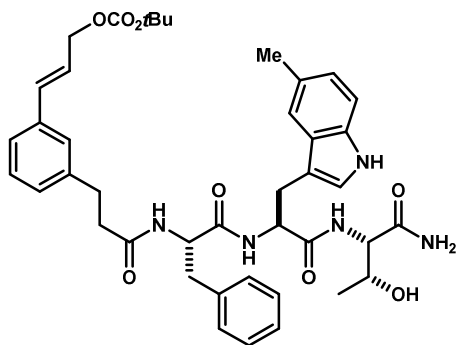
(600 MHz & 500MHz, DMSO- d_6 , 298K)

	^{13}C	^1H	key correlations
1	39.0	2.51-2.57 (m, 1H), 2.79-2.85 (m, 1H)	HMBC 1→24
2	125.0	6.09 (ddd, $J = 15.8, 9.7, 6.2$ Hz, 1H)	TOCSY 2→3,1
3	132.6	6.62 (d, $J = 15.8$ Hz, 1H)	HMBC 3→4
4	136.9	-	
5	124.2	7.05 (br d, $J = 8.5$ Hz, 1H)	HMBC 5→9,7
6	127.9	7.15 (dd, $J = 8.5, 7.4$ Hz, 1H)	HMBC 6→4,8
7	127.0	6.99 (br d, $J = 7.4$ Hz, 1H)	
8	140.5	-	
9	124.9	7.18 (br s, 1H)	HMBC 9→3
10	30.9	2.62-2.67 (m, 1H), 2.85-2.90 (m, 1H)	
11	37.4	2.05 (ddd, $J = 13.5, 6.9, 3.8$ Hz, 1H), 2.35 (ddd, $J = 13.5, 10.8, 3.1$ Hz, 1H)	
12	171.4	-	

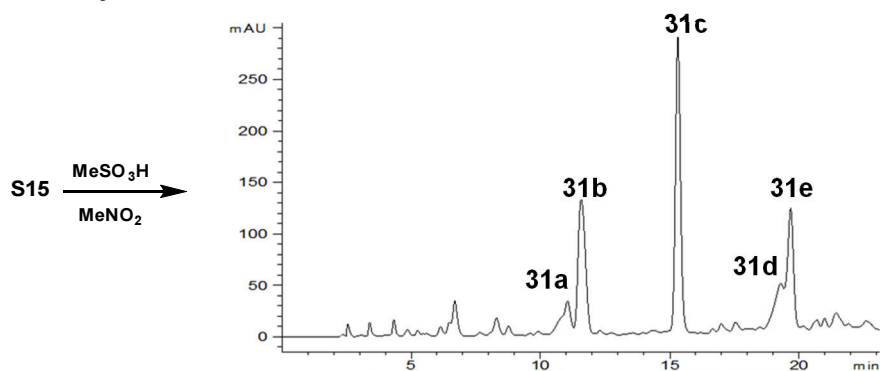
13	-	7.96 (d, $J = 8.8$ Hz, 1H)	HMBC 13→12
14	50.1	5.33 (ddd, $J = 8.9, 8.8, 4.8$ Hz, 1H)	HMBC 14→20
15	38.6	2.82-2.87 (m, 1H), 3.08 (dd, $J = 14.0, 4.8$ Hz, 1H)	HMBC 15→16,17 TOCSY 15→14,13
16	136.7	-	
17	129.9	7.38 (d, $J = 7.4$ Hz, 2H)	HMBC 17→19
18	127.8	7.27 (dd, $J = 7.4, 7.4$ Hz, 2H)	HMBC 18→16
19	126.1	7.20-7.23 (m, 1H)	HMBC 18→17
20	171.2	-	
21	-	-	
22	61.5	4.48 (dd, $J = 10.3, 5.5$ Hz, 1H)	HMBC 22→24 COSY 22→23
23	40.0	2.10 (dd, $J = 13.6, 5.5$ Hz, 1H), 2.51-2.55 (m, 1H)	HMBC 23→24
24	57.6	-	
25	81.6	6.16 (br s, 1H)	COSY 25→26 HMBC 25→27
26	-	6.32 (br s, 1H)	
27	143.8	-	
28	110.5	6.51 (dd, $J_{HH} = 8.6$ Hz, $J_{HF} = 4.6$ Hz, 1H)	HMBC 28→30,32
29	113.7	6.84 (ddd, $J_{HF} = 9.0$ Hz, $J_{HH} = 8.6, 2.7$ Hz, 1H)	HMBC 29→27,30
30	156.8 (d, $J \approx 240$ Hz)	-	
31	109.3	7.02 (dd, $J_{HF} = 8.4$ Hz, $J_{HH} = 2.7$ Hz, 1H)	HMBC 31→27,30
32	136.9	-	
33	170.4	-	
34	-	7.49 (d, $J = 8.0$ Hz, 1H)	HMBC 34→33
35	57.5	3.86 (ddd, $J = 8.0, 2.6$ Hz, 1H)	HMBC 35→39
36	65.6	3.90-3.96 (m, 1H)	
37	19.4	0.77 (d, $J = 6.6$ Hz, 3H)	COSY 37→36 TOCSY 37→36,35,34
38	-	not detected	
39	171.5	-	
40	-	6.73 (br s, 1H), 7.19 (br s, 1H)	TOCSY 40→40'
41	39.0	2.51-2.57 (m, 1H), 2.79-2.85 (m, 1H)	HMBC 1→24
42	125.0	6.09 (ddd, $J = 15.8, 9.7, 6.2$ Hz, 1H)	TOCSY 2→3,1

Phe-Trp(5Me)-Thr (31a–31e):

Acyclic intermediate S15. Compound **S15** (40mg) was prepared from peptide Phe-Trp(5Me)-Thr-NH₂ and template **5** according to General Procedure A.



Macrocycles 31a–31e:



Acyclic intermediate **S15** (40 mg, 53 μmol) was cyclized following General Procedure C and purified by the preparative HPLC method A. Compound **31e** was re-purified by the same method to give **31b** (7.2 mg, 21%), **31c** (11.9 mg, 35%), and **31e** (4.7 mg, 14%). Compounds **31a** and **31d** were not pursued.

Preparative HPLC method A:

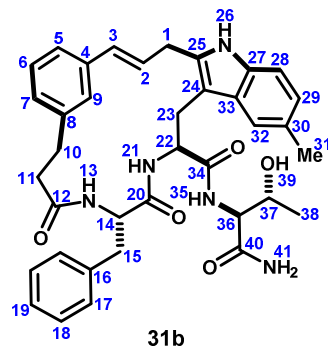
Column: Waters Sunfire™ C₁₈, 19x250mm, 5 μm .

Solvent A: H₂O + 0.1%v TFA

Solvent B: ACN + 0.1%v TFA

Flow rate: 18.00 ml/min

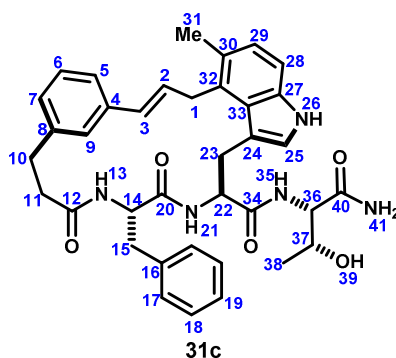
Time	%B
0	40
2	40
30	60



(600MHz, DMSO-*d*₆, 298K)

	¹³ C	¹ H	key correlations
1	29.8	3.56 (dd, <i>J</i> = 15.6, 6.9 Hz, 1H), 3.78 (dd, <i>J</i> = 15.6, 5.9 Hz, 1H)	HMBC 1→24,25
2	127.8	6.08 (apt dt, <i>J</i> = 15.7, 6.8 Hz, 1H)	COSY 2→1, HMBC 2→4
3	130.3	6.40 (d, <i>J</i> = 15.7 Hz, 1H)	
4	136.6	-	
5	123.9	7.09-7.12 (m, 1H) overlap	
6	127.8	7.14 (dd, <i>J</i> = 7.4, 7.4 Hz, 1H) overlap	
7	127.1	6.95 (br d, <i>J</i> = 7.4 Hz, 1H)	HMBC 7→5
8	141.0	-	
9	124.4	6.98-7.00 (m, 1H) overlap	
10	30.0	2.59-2.65 (m, 1H) overlap, 2.06-2.92 (m, 1H)	HMBC 10→8
11	35.8	2.00 (ddd, <i>J</i> = 14.0, 7.7, 3.1 Hz, 1H), 2.37-2.42 (m, 1H) overlap	
12	171.0	-	
13	-	8.08 (d, <i>J</i> = 8.8 Hz, 1H)	TOCSY 13→14,15, HMBC 13→12
14	52.5	4.79 (ddd, <i>J</i> = 9.4, 9.4, 3.8 Hz, 1H)	
15	38.2	2.61-2.66 (m, 1H) overlap, 2.97-3.02 (m, 1H) overlap	HMBC 15→16
16	137.6	-	
17	129.1	7.17-7.19 (m, 2H) overlap	HMBC 17→19
18	127.4	7.17-7.20 (m, 2H) overlap	HMBC 18→16
19	125.7	7.12-7.15 (m, 1H) overlap	HMBC 19→17
20	172.0	-	
21	-	8.62 (d, <i>J</i> = 7.6 Hz, 1H)	TOCSY 21→22,23, HMBC 21→20
22	54.2	4.67 (ddd, <i>J</i> = 10.6, 7.6, 4.6 Hz, 1H)	
23	26.0	3.02 (dd, <i>J</i> = 14.9, 10.6 Hz, 1H), 3.10 (dd, <i>J</i> = 14.9, 4.6 Hz, 1H) overlap	HMBC 23→24,25
24	105.3	-	
25	133.9	-	
26	-	10.64 (s, 1H)	HMBC 26→24,25,33
27	133.3	-	
28	109.9	7.11 (d, <i>J</i> = 8.3 Hz, 1H) overlap	HMBC 28→30,33

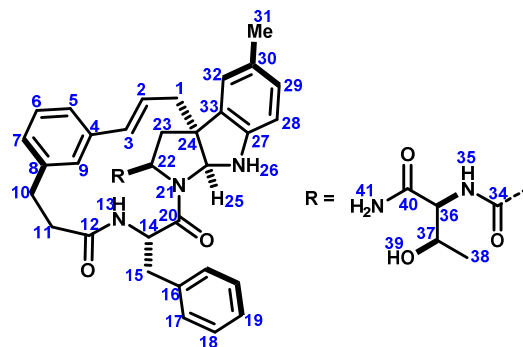
29	121.6	6.83 (dd, $J = 8.3, 1.3$ Hz, 1H)	HMBC 29→32,31
30	126.3	-	
31	21.1	2.39 (s, 3H)	HMBC 31→29,30,32
32	117.6	7.30 (br s, 1H)	HMBC 32→29,31
33	129.0	-	
34	171.9	-	
35	-	7.66 (d, $J = 8.5$ Hz, 1H)	HMBC 35→34
36	57.5	4.16 (dd, $J = 8.5, 3.1$ Hz, 1H)	HMBC 36→40
37	66.0	4.08-4.13 (m, 1H) overlap	
38	19.7	1.08 (d, $J = 6.4$ Hz, 3H)	HMBC 38→36,37
39	-	not observed	
40	171.8	-	
41	-	6.98-7.00 (m, 1H) overlap, 7.10-7.12 (m, 1H) overlap	HMBC 41→40, TOCSY 41→41'



(500MHz, DMSO- d_6 , 320K)

	^{13}C	^1H	key correlations
1	32.0	3.82-3.91 (m, 2H)	
2	128.9	6.37 (dt, $J = 16.0, 5.4$ Hz, 1H)	HMBC 2→4,32, COSY 2→1
3	129.6	6.07 (d, $J = 16.0$ Hz, 1H)	HMBC 3→5,9
4	136.7	-	
5	123.0	7.02 (d, $J = 8.0$ Hz, 1H)	
6	127.7	7.09 (dd, $J = 8.0, 8.0$ Hz, 1H) overlap	HMBC 6→4,8
7	126.8	6.94 (d, $J = 8.0$ Hz, 1H) overlap	
8	141.1	-	
9	125.3	7.07 (br s, 1H) overlap	
10	29.7	2.54-2.59 (m, 1H) obscured, 2.91-2.97 (m, 1H) overlap	HMBC 10→7,9,12
11	35.9	2.09-2.15 (m, 1H), 2.33-2.39 (m, 1H) overlap	HMBC 11→8,12
12	170.6	-	
13	-	7.94 (d, $J = 9.1$ Hz, 1H)	HMBC 13→12
14	52.5	4.80-4.88 (m, 1H)	
15	37.9	2.66-2.72 (m, 1H), 2.92-2.97 (m, 1H) overlap	HMBC 15→16,17
16	137.7	-	

17	128.8	7.23-7.24 (m, 2H) overlap	HMBC 17→15
18	127.5	7.23-7.25 (m, 2H) overlap	
19	125.6	7.14-7.19 (m, 1H)	
20	171.0	-	
21	-	8.44-8.48 (m, 1H)	HMBC 21→20
22	53.4	4.63-4.70 (m, 1H)	
23	29.5	3.14-3.19 (m, 1H), 3.39 (dd, $J = 13.9, 9.9$ Hz, 1H)	HMBC 23→24
24	109.5	-	
25	123.3	7.06-7.08 (m, 1H) overlap	HMBC 25→24,27,33
26	-	10.66 (br s, 1H)	COSY 26→25, HMBC 26→24,25,27,33
27	135.4	-	
28	109.2	7.12 (d, $J = 8.3$ Hz, 1H) overlap	HMBC 28→30,33
29	123.6	6.91 (d, $J = 8.3$ Hz, 1H)	HMBC 29→27,31,32
30	125.2	-	
31	18.4	2.34 (s, 3H)	HMBC 31→29,30,32
32	128.4	-	
33	126.0	-	
34	170.7	-	
35	-	7.59 (d, $J = 8.4$ Hz, 1H)	
36	57.6	4.13 (dd, $J = 8.4, 3.0$ Hz, 1H)	HMBC 36→40
37	65.8	4.04-4.09 (m, 1H)	
38	19.6	1.05 (d, $J = 6.2$ Hz, 1H)	COSY 38→37, HMBC 38→36,37
39	-	not observed	
40	171.6	-	
41	-	6.87 (br s, 1H), 6.95 (br s, 1H) overlap	



31e

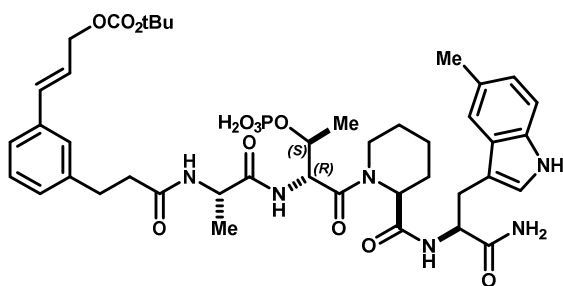
(500MHz, DMSO-*d*₆, 298K)

	¹³ C	¹ H	key correlations
1	39.3	2.51-2.57 (m, 1H), 2.80 (dd, <i>J</i> = 13.7, 10.0 Hz, 1H)	HMBC 1→24,25
2	126.3	6.05-6.14 (m, 1H)	
3	132.1	6.63 (d, <i>J</i> = 15.8 Hz, 1H)	TOCSY 3→2,1 HMBC 3→4
4	136.9	-	
5	124.3	7.04 (br d, <i>J</i> = 7.6 Hz, 1H)	HMBC 5→3,7
6	128.2	7.15 (dd, <i>J</i> = 7.6, 7.6 Hz, 1H)	HMBC 6→4,8
7	126.8	6.99 (br d, <i>J</i> = 7.6 Hz, 1H)	HMBC 7→5
8	140.5	-	
9	125.0	7.18 (br s, 1H)	
10	30.6	2.62-2.69 (m, 1H), 2.82-2.90 (m, 1H)	
11	37.1	2.01-2.08 (m, 1H), 2.32-3.39 (m, 1H)	HMBC 11→8 TOCSY 11→10,10',11'
12	171.1	-	
13	-	7.96 (d, <i>J</i> = 8.8 Hz, 1H)	HMBC 13→12
14	49.8	5.34 (ddd, <i>J</i> = 8.8, 8.8, 4.8 Hz, 1H)	HMBC 14→20
15	38.3	2.89 (dd, <i>J</i> = 13.9, 8.8 Hz, 1H), 3.09 (dd, <i>J</i> = 13.9, 4.8 Hz, 1H)	HMBC 15→16,17 TOCSY 14→15,13
16	136.5	-	
17	129.8	7.39 (d, <i>J</i> = 7.4 Hz, 2H)	TOCSY 17→18,19
18	127.8	7.28 (dd, <i>J</i> = 7.4, 7.4 Hz, 2H)	HMBC 18→16
19	126.0	7.20-7.24 (m, 1H)	HMBC 19→17
20	171.3	-	
21	-	-	
22	61.6	4.43 (dd, <i>J</i> = 10.4, 5.7 Hz, 1H)	HMBC 22→23,24
23	40.2	2.00-2.07 (m, 1H), 2.50-2.57 (m, 1H)	
24	57.3	-	
25	81.4	6.11 (s, 1H)	HMBC 25→22,24
26	-	not detected	
27	144.9	-	
28	109.9	6.45 (d, <i>J</i> = 7.8 Hz, 1H)	HMBC 28→33
29	128.0	6.84 (dd, <i>J</i> = 7.8, 0.9 Hz, 1H)	HMBC 29→32

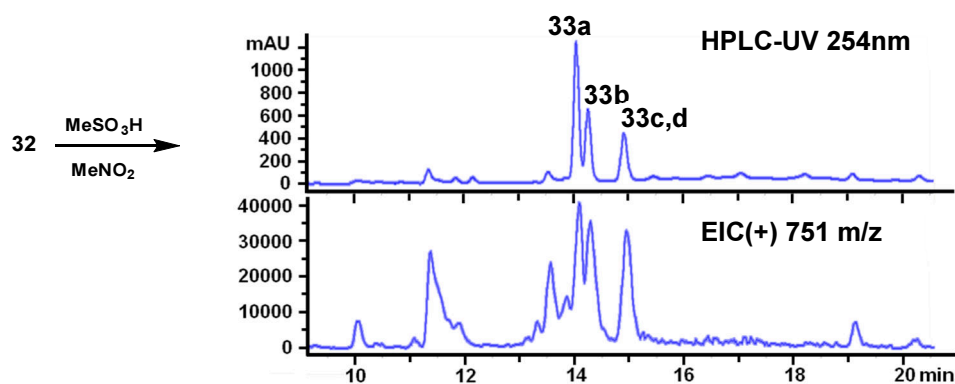
30	127.3	-	
31	20.4	2.21 (s, 1H)	HMBC 31→28,30,32
32	122.0	6.91-6.93 (m, 1H)	HMBC 32→27,29
33	135.5	-	
34	170.4	-	
35	-	7.51 (d, $J = 7.8$ Hz, 1H)	
36	57.2	3.84 (dd, $J = 7.8, 2.5$ Hz, 1H)	HMBC 36→40
37	65.2	3.91-3.97 (m, 1H)	HMBC 37→40
38	19.3	0.78 (d, $J = 6.6$ Hz, 3H)	COSY 38→37 TOCSY 38→35,36,37
39	-	not detected	
40	171.5	-	
41	-	6.68 (br s, 1H), 7.20 (br s, 1H)	HMBC 41→40 TOCSY 41→41'

Ala-D-pThr-Pip-Trp(5Me) (33a–33d):

Acyclic intermediate 32. Compound **32** (111 mg, 45%) was prepared from peptide H-Ala-*D*-pThr-Pip-Trp(5Me)-NH₂ (199 mg, 290 μmol) and template **5** (115 mg, 290 μmol) according to General Procedure A. MS m/z ESI(+) 869.0 (calc'd: C₄₂H₅₈N₆O₁₂P, [M+H]⁺, 869.4); ESI(-) 866.8 (calc'd: C₄₂H₅₆N₆O₁₂P, [M+H]⁺, 867.4).



Macrocycles 33a-d:



Acyclic intermediate **32** (106 mg, 53 μmol) was cyclized following General Procedure C and purified by semi-preparative HPLC method A. All compounds were subsequently re-purified and **33c/33d** resolved using preparative HPLC method B to give **33a** (17.3 mg, 19%), **33b** (8.2 mg, 9%), **33c** (7 mg, 7%) and **33d** (10 mg, 9%).

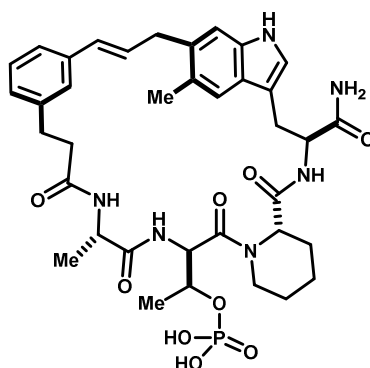
Semi-preparative HPLC method A:
 Column: Waters XSelect™ C₁₈, 10x250mm, 5μm.
 Solvent A: H₂O + 0.1%v TFA
 Solvent B: ACN + 0.1%v TFA
 Flow rate: 7.00 ml/min

Time	%B
0	35
2	35
12.4	38

Preparative HPLC method B:
 Column: Waters XBridge™ PFP, 19x250mm, 5μm.
 Solvent A: H₂O + 0.1%v TFA
 Solvent B: ACN + 0.1%v TFA
 Flow rate: 18.00 ml/min

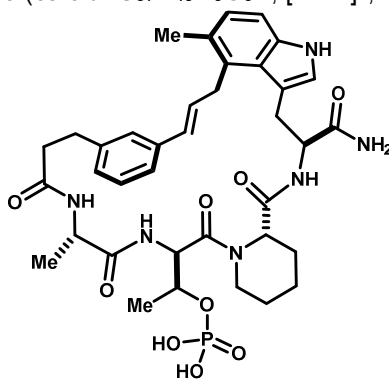
Time	%B
0	30
2	30
20	52.5

*Note: The macrocyclic linkages in the following products were assigned based on 2D NMR correlations of the cinnamyl moiety, as in other examples, but complete resonance assignment was not yet completed at the time of writing.



33a
19%

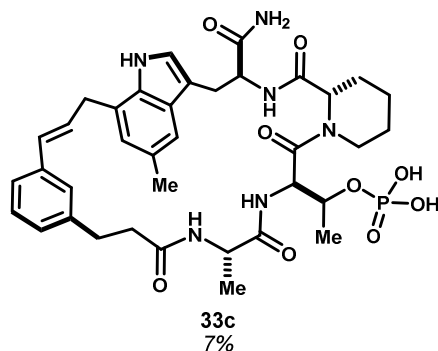
¹H NMR (DMSO-*d*₆, 500 MHz): δ 10.57 (d, *J* = 1.7 Hz, 1H), 8.19 (d, *J* = 7.9 Hz, 1H), 7.66 (d, *J* = 7.7 Hz, 1H), 7.52 (s, 1H), 7.37 (d, *J* = 7.9 Hz, 1H), 7.12-7.17 (m, 4H), 7.1 (s, 1H), 6.94-7.00 (m, 2H), 6.31 (dt, *J* = 15.9, 6.1 Hz, 1H), 6.21 (d, *J* = 15.9 Hz, 1H), 4.81-4.88 (m, 2H), 4.27-4.37 (m, 2H), 4.25 (dq, *J* = 7.3, 7.3 Hz, 1H), 3.82 (br. d, *J* = 12.1 Hz, 1H), 3.6 (dd, *J* = 16.0, 5.8 Hz, 1H), 3.45 (dd, *J* = 15.6, 5.7 Hz, 1H), 3.34 (ddd, *J* = 12.6, 12.6, 2.6 Hz, 1H), 3 (dd, *J* = 14.3, 2.0 Hz, 1H), 2.89 (apt t, *J* = 13 Hz, 1H), 2.55-2.71 (m, 2H), 3.24 (s, 3H), 2.20-2.33 (m, 3H), 1.38-1.54 (m, 4H), 1.20-1.31 (m, 1H), 1.02 (d, *J* = 6 Hz, 3H), 1.01 (d, *J* = 7.2 Hz, 3H). MS *m/z* ESI(+) 751.0 (calc'd: C₃₇H₄₈N₆O₉P, [M+H]⁺, 751.3)



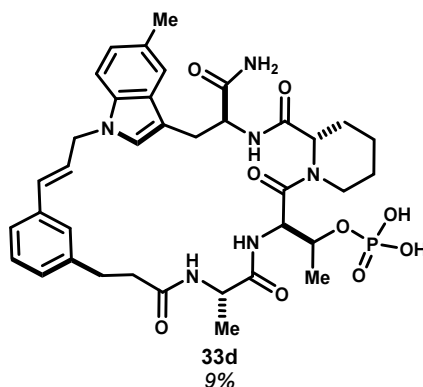
33b
9%

¹H NMR (DMSO-*d*₆, 500 MHz): δ 10.78 (d, *J* = 2 Hz, 1H), 8.3 (d, *J* = 4.6 Hz, 1H), 7.98 (d, *J* = 9.1 Hz, 1H), 7.8 (d, *J* = 7.3 Hz, 1H), 7.53 (s, 1H), 7.28 (s, 1H), 7.2 (s, 1H), 7.14-7.11 (m, 3H), 6.98 (d, *J* = 7.7 Hz, 1H), 6.9 (d, *J* = 7.6 Hz, 1H), 6.83 (d, *J* = 8.3 Hz, 1H), 6.43 (dt, *J* = 15.3, 6.8 Hz, 1H), 6.32 (d, *J* = 15.8 Hz, 1H), 5.09 (d, *J* = 2.4 Hz, 1H), 4.94 (ddd, *J* = 9.1, 9.1, 5.0 Hz, 1H), 4.69 (t, *J* = 6.2 Hz, 1H), 4.39 (dddd, *J* = 19.0, 6.3, 6.3, 6.3 Hz, 1H), 4.12 (dq, *J* = 7 Hz, 1H), 3.97-4.04 (m, 2H), 3.75-3.87 (m, 3H), 3.68 (dd, *J* = 14.9, 9.5 Hz, 1H), 3.08 (t, *J* = 12.1 Hz, 1H), 2.9 (dd, *J* = 15.1, 4.3 Hz, 1H), 2.69-2.78 (m, 3H), 2.31 (s, 3H), 2.19-2.26

(m, 2H), 1.53-1.60 (m, 1H), 1.28-1.44 (m, 3H), 1.15 (d, $J = 6.2$ Hz, 3H), 0.71 (d, $J = 6.8$ Hz, 3H). MS m/z ESI(+) 751.0 (calc'd: $C_{37}H_{48}N_6O_9P$, $[M+H]^+$, 751.3)



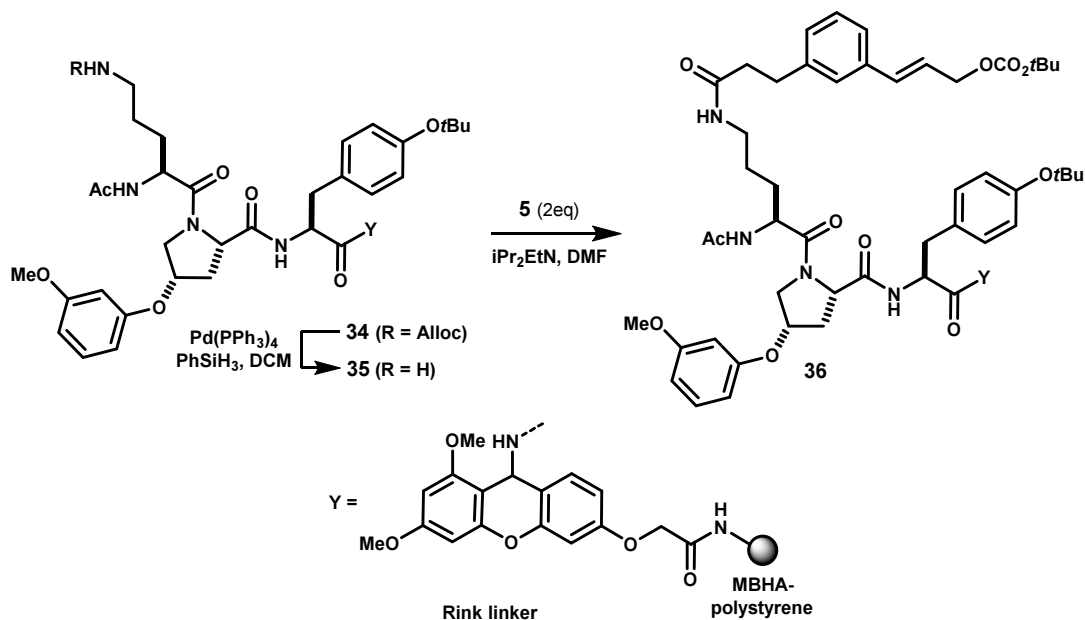
1H NMR (DMSO- d_6 , 500 MHz): δ 10.51 (d, $J = 1.8$ Hz, 1H), 8.42 (d, $J = 8.5$ Hz, 1H), 7.7 (d, $J = 7.2$ Hz, 1H), 7.53 (s, 1H), 7.44 (s, 1H), 7.23 (d, $J = 2.3$ Hz, 1H), 7.15-7.20 (m, 2H), 7.11 (d, $J = 7.7$ Hz, 1H), 6.97 (br. s, 1H), 6.77 (s, 1H), 6.55 (d, $J = 15.7$ Hz, 1H), 6.51 (br. s, 1H), 6.2 (dt, $J = 15.7, 6.6$ Hz, 1H), 6.82-6.88 (m, 2H), 4.65-4.43 (m, 1H), 4.21-4.29 (m, 2H), 3.84 (d, $J = 12.2$ Hz, 1H), 3.8 (dd, $J = 15.0, 7.1$ Hz, 1H), 3.55 (dd, $J = 15.1, 5.2$ Hz, 1H), 3 (br. d, $J = 12.1$ Hz, 1H), 2.87 (t, $J = 13.4$ Hz, 1H), 2.64-2.72 (m, 2H), 2.36 (s, 3H), 2.19-2.34 (m, 3H), 1.41-1.53 (m, 3H), 1.17-1.27 (m, 1H), 1.09 (d, $J = 7.2$ Hz, 3H), 0.98 (d, $J = 6.4$ Hz, 3H). MS m/z ESI(+) 751.0 (calc'd: $C_{37}H_{48}N_6O_9P$, $[M+H]^+$, 751.3)



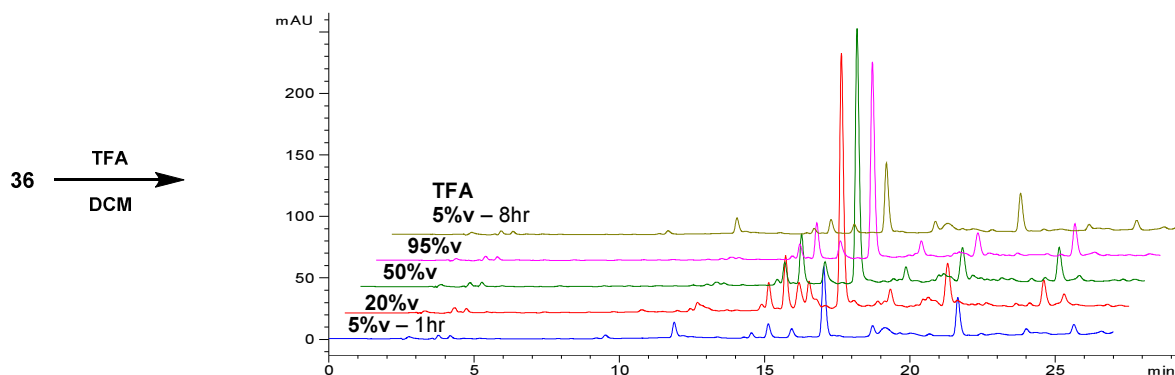
1H NMR (DMSO- d_6 , 500 MHz): δ 8.38 (d, $J = 8.3$ Hz, 1H), 7.76 (d, $J = 7.6$ Hz, 1H), 7.55-7.61 (m, 2H), 7.28 (d, $J = 7$ Hz, 1H), 7.20-7.25 (m, 4H), 7.05-7.11 (m, 2H), 7.01 (s, 1H), 8.88 (d, $J = 8.9$ Hz, 1H), 6.5 (d, $J = 16$ Hz, 1H), 6.16 (dt, $J = 16.0, 5.7$ Hz, 1H), 4.90-5.01 (m, 1H), 4.89-4.92 (m, 2H), 4.84 (dd, $J = 7.2, 4.0$ Hz, 1H), 4.37-4.44 (m, 1H), 4.34 (ddd, $J = 11.9, 7.6, 3.0$ Hz, 1H), 4.23 (dq, $J = 7.6, 7.6$ Hz, 1H), 3.88 (d, $J = 12.5$ Hz, 1H), 3.15-3.25 (m, 1H), 3.03 (dd, $J = 14.4, 2.6$ Hz, 1H), 2.9 (dd, $J = 14.2, 12.5$ Hz, 1H), 2.68-2.81 (m, 3H), 2.36 (s, 3H), 2.26 (ddd, $J = 12.9, 11.8, 6.4$ Hz, 1H), 2.17 (ddd, $J = 13.0, 11.5, 4.7$ Hz, 1H), 1.40-1.58 (m, 4H), 1.18-1.30 (m, 1H), 1.09 (d, $J = 7.4$ Hz, 3H), 0.99 (d, $J = 6.4$ Hz, 3H). MS m/z ESI(+) 751.0 (calc'd: $C_{37}H_{48}N_6O_9P$, $[M+H]^+$, 751.3).

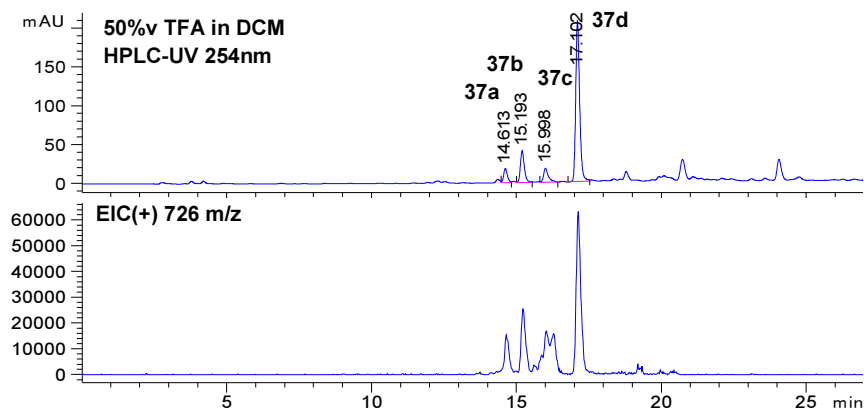
Solid-phase synthesis of template-based composite macrocycles

On-resin acidolysis using the Rink amide linker



Acyclic intermediate 36: Resin-bound peptide **34** was assembled on Rink amide MBHA resin (0.7 mmol/g) using standard Fmoc synthesis methods (see section **Peptide synthesis**). The N-terminal acetamide was installed using AcOH/HBTU. In a peptide synthesis vessel, resin-bound **34** (~0.1 mmol) was swollen in DCM, degassed by sparging with argon for 15 min, then treated with PhSiH_3 (300 μL , 2.4 mmol) and $\text{Pd}(\text{PPh}_3)_4$ (12 mg, 0.01 mmol). The mixture was mixed by sparging with argon for 30 min, then drained and this process repeated once. The solvent was exchanged for N,N -DMF, template **5** (120 mg, 0.3 mmol) and $i\text{Pr}_2\text{EtN}$ (53 μL , 0.3 mmol) was added, and the mixture was agitated overnight, then rinsed sequentially with DMF, DCM, MeOH and dried to give resin-bound **36** (214 mg, ~80%).





On-resin acidolysis of 36: Portions of **36** (10-12 mg, 3.7-4.5 μmol) were treated with 5, 20, 50, or 95%v TFA in DCM (1 mL) and agitated on a wrist-action shaker. After 1 hr, an aliquot (500 μL) was removed from each reaction and filtered, concentrated in vacuo, reconstituted in MeOH (500 μL) and analyzed by HPLC-UV/MS using HPLC method A (below).

Analytical HPLC method A:

Column: Waters Sunfire™ C₁₈, 4.6x150mm, 5 μm .

Solvent A: H₂O + 0.1%v HCO₂H

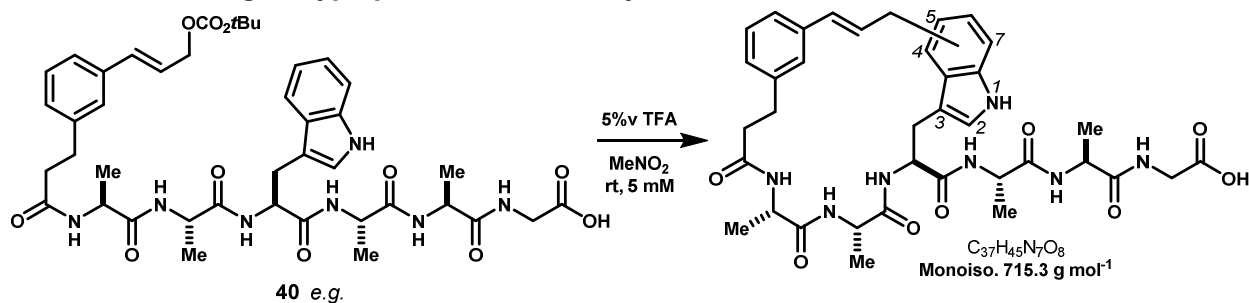
Solvent B: ACN + 0.1%v HCO₂H

Flow rate: 1.00 ml/min

Time	%B
0	30
2	30
25	65
29	30
30	30

Solid-phase synthesis using the 2-chlorotrityl linker

Positional scanning of tryptophan-based macrocyclizations:



2-Chlorotrityl chloride resin pre-loaded with glycine (20 μmol , 0.64 mmol/g, see **5-S25**) was dispensed by pipet as an isopycnic suspension in *N,N*-DMF into a 24-well MiniBlock™ XT fitted with fritted polypropylene tubes. Peptide coupling reactions were carried out using Fmoc-AA-OH (4 eq, 0.45M in NMP), *i*Pr₂EtN (8 eq, 1.0M in NMP) and HBTU (0.4 eq, 0.45M in NMP) for 10 min. Deprotection steps were carried out using 20%v piperidine in *N,N*-DMF (1 mL) for 1 min, drained, and repeated for 10min. All reactions were vigorously mixed using an orbital platform at >250rpm. The *N*-termini were acylated by treatment with **5** (3 eq, 0.45 M in NMP) and *i*Pr₂EtN (6eq, 1.0 M in NMP) for >40 min. The resins were then individually suspended in *N,N*-DMF by aspirating several times with a pipettor, and one half was transferred to an empty 24-well MiniBlock™. The resin was thoroughly washed with *N,N*-DMF, then DCM, and one half was cleaved

by the action of TFE:AcOH:DCM (1:1:8, 2 mL) for 1 hr to give template-containing acyclic precursors. The remaining resin-bound intermediates were used in on-resin acidolysis experiments.

A1	Tyr	Ala	Ala	Ala	Ala	Gly
A2	Ala	Tyr	Ala	Ala	Ala	Gly
A3	Ala	Ala	Tyr	Ala	Ala	Gly
A4	Ala	Ala	Ala	Tyr	Ala	Gly
A5	Ala	Ala	Ala	Ala	Tyr	Gly
38	B1	Trp	Ala	Ala	Ala	Gly
39	B2	Ala	Trp	Ala	Ala	Gly
40	B3	Ala	Ala	Trp	Ala	Gly
41	B4	Ala	Ala	Ala	Trp	Gly
42	B5	Ala	Ala	Ala	Ala	Trp
C1	Phe(3OMe)	Ala	Ala	Ala	Ala	Gly
C2	Ala	Phe(3OMe)	Ala	Ala	Ala	Gly
C3	Ala	Ala	Phe(3OMe)	Ala	Ala	Gly
C4	Ala	Ala	Ala	Phe(3OMe)	Ala	Gly
C5	Ala	Ala	Ala	Ala	Phe(3OMe)	Gly
D1	Thi	Ala	Ala	Ala	Ala	Gly
D2	Ala	Thi	Ala	Ala	Ala	Gly
D3	Ala	Ala	Thi	Ala	Ala	Gly
D4	Ala	Ala	Ala	Thi	Ala	Gly
D5	Ala	Ala	Ala	Ala	Thi	Gly

Solution-phase acidolysis of acyclic intermediates 38–42.

Acyclic intermediates **38–42** were dissolved in MeOH and dispensed in 2 μ mol portions into 0.5dram vials and taken to dryness. To the dry residues was added MeNO₂ (380 μ L, aged over 4Å MS) followed by TFA (20 μ L), and the mixtures were mixed on an orbital shaker for 1 hr, then concentrated in vacuo and reconstituted in DMSO (300 μ L) for HPLC-UV/MS analysis by the following method. Chromatograms are shown and annotated in the text (see Chapter 6.4).

Analytical HPLC method A:

Column: Agilent XBD C₁₈, 4.6x150mm, 5 μ m.

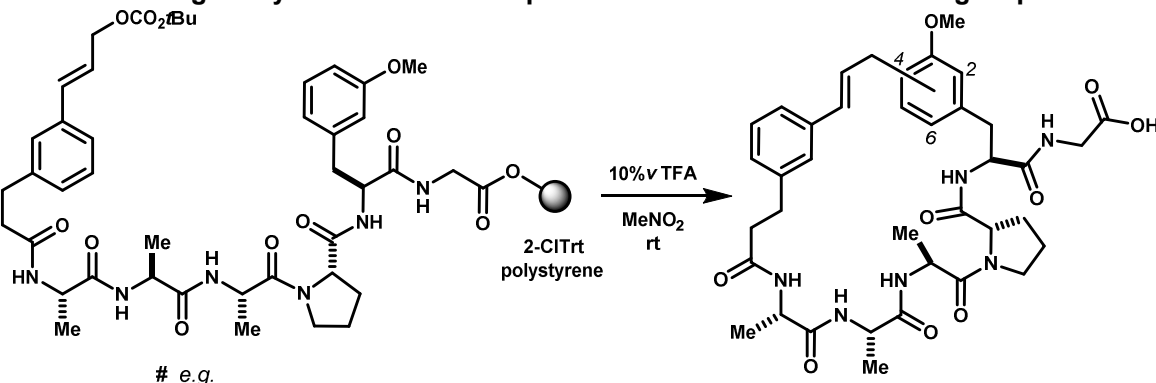
Solvent A: H₂O + 0.1%v TFA

Solvent B: ACN + 0.1%v TFA

Flow rate: 1.00 ml/min

Time	%B
0	15
0.5	15
18	100
20	100
22	15
23	15

Positional scanning of aryl side chain nucleophiles in Pro- & Glu-Pro-containing sequences



Parallel solid-phase synthesis was carried out on 10 μ mol scale and split in half in the same manner as for tryptophan sequences (see above). One half was cleaved and a subset of these materials were analyzed to check the purity of acyclic intermediates, which were all >95% area purity by HPLC-UV at 254nm and 280nm.

On-resin acidolysis:

Resin-bound acyclic intermediates were treated with 10% v/v TFA in MeNO₂ (1 mL) and mixed on an orbital shaker for 3 hr, which caused the resin to turn deep purple with solutions ranging from colorless to pink, turquoise or brown – the color typically faded over the course of the reaction. The solutions were then drained from the MiniBlock™ into vials, the resin was rinsed with 10% v/v TFA in MeNO₂ (500 μ L), and the holdup was gently forced through by applying a positive pressure of air to the reaction tubes. The filtrate solutions were either evaporated immediately (frequently returned incomplete reactions – see text) or allowed to stand up to 12 hrs (no degradation of product purity was observed – see text). The solutions were concentrated by rotary evaporation, dried briefly in vacuo, and reconstituted in DMSO (250 μ L) for HPLC-UV/MS analysis. Representative chromatograms (highlighted) are shown and annotated in the text (see Chapter 6.4), and all chromatograms are listed in the Supplementary Data Appendix for this chapter.

Set 1:

A1	Ala	Tyr	Ala	Pro	Ala	Gly
A2	Ala	Ala	Tyr	Pro	Ala	Gly
A3	Ala	Ala	Ala	Pro	Tyr	Gly
A4	Ala	Phe(3OMe)	Ala	Pro	Ala	Gly
A5	Ala	Ala	Phe(3OMe)	Pro	Ala	Gly
43	A6	Ala	Ala	Pro	Phe(3OMe)	Gly
44	B1	Ala	2Thi	Pro	Ala	Gly
B2	Ala	Ala	2Thi	Pro	Ala	Gly
B3	Ala	Ala	Ala	Pro	2Thi	Gly
B4	Ala	Bthi	Ala	Pro	Ala	Gly
B5	Ala	Ala	Bthi	Pro	Ala	Gly
B6	Ala	Ala	Ala	Pro	Bthi	Gly
C1	Ala	Tyr	Pro	Ala	Ala	Gly
C2	Ala	Ala	Pro	Tyr	Ala	Gly
C3	Ala	Ala	Pro	Ala	Tyr	Gly
C4	Ala	Phe(3OMe)	Pro	Ala	Ala	Gly
C5	Ala	Ala	Pro	Phe(3OMe)	Ala	Gly
C6	Ala	Ala	Pro	Ala	Phe(3OMe)	Gly
D1	Ala	2Thi	Pro	Ala	Ala	Gly
D2	Ala	Ala	Pro	2Thi	Ala	Gly
D3	Ala	Ala	Pro	Ala	2Thi	Gly

	<i>D4</i>	Ala	Bthi	Pro	Ala	Ala	Gly
45	<i>D5</i>	Ala	Ala	Pro	Bthi	Ala	Gly
	<i>D6</i>	Ala	Ala	Pro	Ala	Bthi	Gly

Set 2:

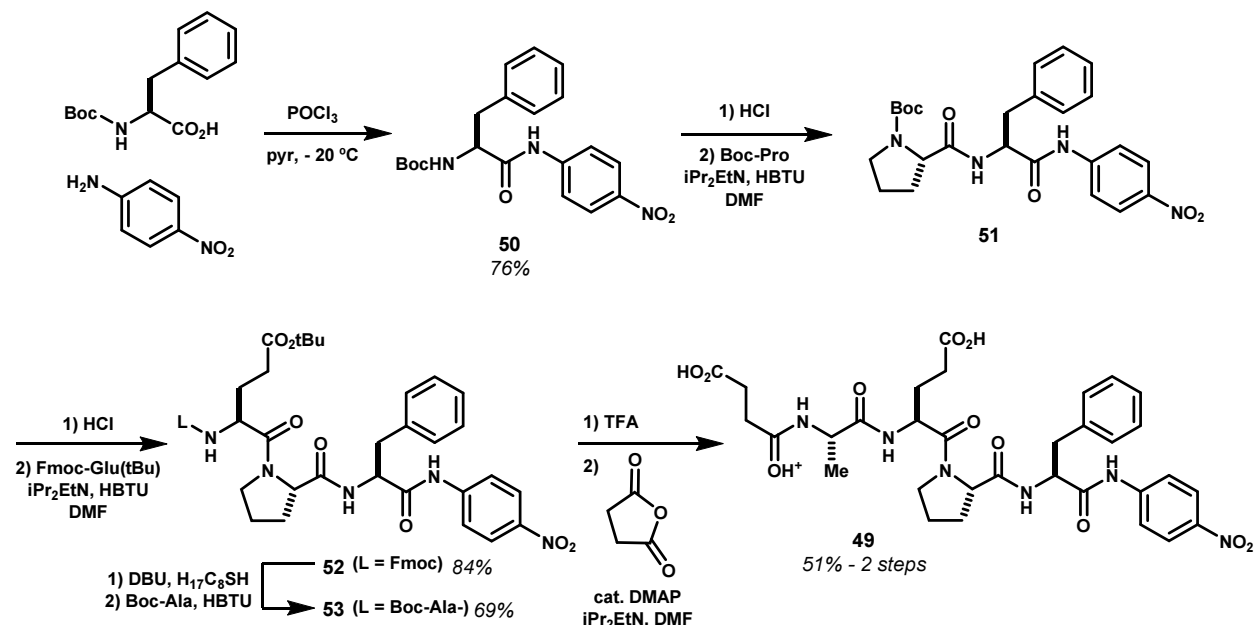
	<i>A1</i>	Ala	Tyr	Glu	Pro	Ala	Gly
46	<i>A2</i>	Ala	Ala	Glu	Pro	Tyr	Gly
	<i>A3</i>	Ala	Trp	Glu	Pro	Ala	Gly
	<i>A4</i>	Ala	Ala	Glu	Pro	Trp	Gly
	<i>A5</i>	Ala	Nal2	Glu	Pro	Ala	Gly
47	<i>A6</i>	Ala	Ala	Glu	Pro	Nal2	Gly
	<i>B1</i>	Ala	2Thi	Glu	Pro	Ala	Gly
	<i>B2</i>	Ala	Ala	Glu	Pro	2Thi	Gly
	<i>B3</i>	Ala	Glu	Pro	Tyr	Ala	Gly
	<i>B4</i>	Ala	Glu	Pro	Ala	Tyr	Gly
	<i>B5</i>	Ala	Glu	Pro	Trp	Ala	Gly
48	<i>B6</i>	Ala	Glu	Pro	Ala	Trp	Gly
	<i>C1</i>	Ala	Glu	Pro	Nal2	Ala	Gly
	<i>C2</i>	Ala	Glu	Pro	Ala	Nal2	Gly
	<i>C3</i>	Ala	Glu	Pro	2Thi	Ala	Gly
	<i>C4</i>	Ala	Glu	Pro	Ala	2Thi	Gly
	<i>C5</i>	Glu	Pro	Tyr	Ala	Ala	Gly
	<i>C6</i>	Glu	Pro	Ala	Tyr	Ala	Gly
	<i>D1</i>	Glu	Pro	Trp	Ala	Ala	Gly
	<i>D2</i>	Glu	Pro	Ala	Trp	Ala	Gly
	<i>D3</i>	Glu	Pro	Nal2	Ala	Ala	Gly
	<i>D4</i>	Glu	Pro	Ala	Nal2	Ala	Gly
	<i>D5</i>	Glu	Pro	2Thi	Ala	Ala	Gly
	<i>D6</i>	Glu	Pro	Ala	2Thi	Ala	Gly

Pin1 α -chymotrypsin-linked kinetic assay:

hPin1 Subcloning, expression and purification

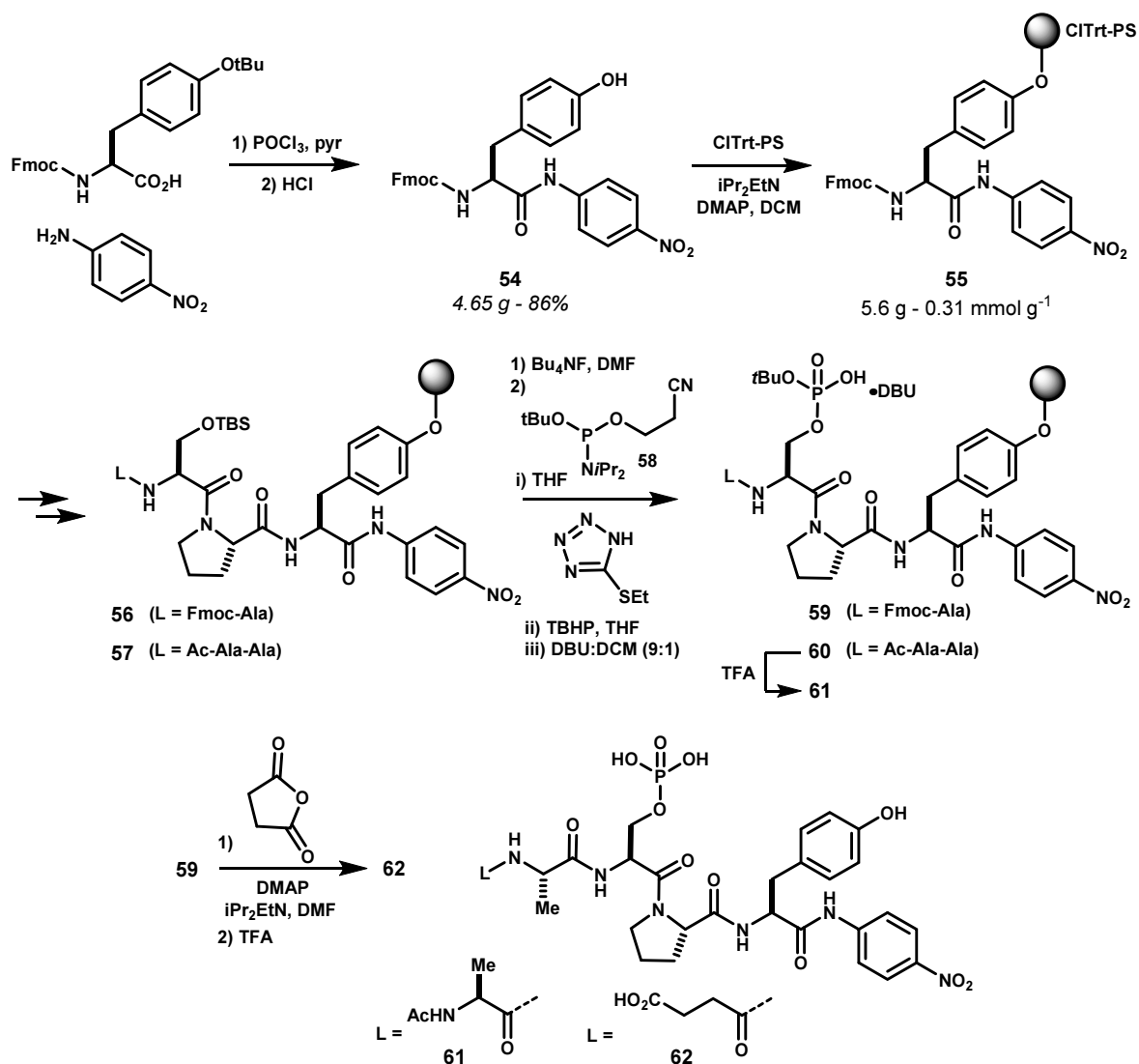
Gateway Entry clone 100005608 (accession DQ892978) bearing wt hPin1 in vector pENTR221 (OpenBiosystems) was cultured overnight at 37 °C in 5 mL LB broth containing 50 μ g/mL Kanamycin. Cells were pelleted and the plasmid was isolated by Miniprep according to the manufacturer's protocol. This plasmid was used in the LR reaction with a bacterial pGEX-6-P1 (N-GST-S-tag) destination vector. The crude LR reaction was transformed into chemically competent DH5 α by incubation for 30 min at 4 °C, heat shock at 42 °C for 45 sec, and recovery at 4 °C for 10 min. The transformation mixture (~50 μ L) was diluted in fresh LB (700 μ L) and incubated 90 min at 37 °C. Cells were pelleted (3500g, 3 min) and the supernatant was discarded. The pellet was resuspended in the residual media, and plated on LB+ampicillin (75 μ g/mL) and incubated at 37 °C overnight. Two colonies were picked and each incubated in sterile LB+ampicillin (50 μ g/mL, 5 mL) alongside two sterile controls. A portion of the overnight cultures was diluted 1x with glycerol:H₂O (1:1, v:v) and store at -80 °C. Additional portions (3 mL) were pelleted, resuspended in H₂O and the plasmids were isolated by Miniprep column eluting with PCR H₂O (35 μ L). Sequencing of both colonies indicated 100% similarity with the hPin1 ORF.

Synthesis of Pin1 chromogenic substrates



Substrate Suc-Ala-Glu-Pro-Phe-*p*-nitroanilide (49). Boc-L-Phenylalanine (2.65 g, 10 mmol) and *p*-nitroaniline (1.38 g, 10 mmol) were suspended in pyridine (30 mL), cooled in a salt/ice bath, and POCl₃ (1.02 mL, 11 mmol) was added dropwise.³ The mixture was stirred for 45 min, then carefully quenched with H₂O (*Caution! Delayed, vigorous exotherm.*) and extracted with EtOAc (x3). The organic phase was washed with sat. NaHCO₃ (x3), NH₄Cl (x1), brine, dried over MgSO₄ and concentrated to an oily residue. Recrystallization from *i*PrOH:H₂O several times gave **50** (2.91 g, 76%) as faintly yellow needles. A portion of this material (2.19 g, 5.7 mmol) was treated with 4N HCl in dioxane, allowed to stand until gas evolution ceased, and concentrated. The crude residue was dissolved in DMF (25 mL) and treated with *i*Pr₂EtN (2.0 mL, 5.7 mmol) to pH >10 followed by Boc-Pro-OH (1.23 g, 5.7 mmol) and HBTU (2.16 g, 5.7 mmol). The mixture was stirred for 2 hrs, then partitioned between EtOAc and sat. NaHCO₃, and the organic phase was washed successively with sat. NaHCO₃ (x2), sat. NH₄Cl (x3), brine, dried over MgSO₄ and concentrated to give **51** as a yellow solid, which was treated with 4N HCl as before. The resulting residue was coupled to Fmoc-Glu(tBu)-OH (1.45 g, 3.4 mmol) in the same manner as for proline, and purified by column chromatograph on SiO₂ eluted with 100% EtOAc to give **52** (3.8 g, 84%) as a yellow foam. This material was dissolved in THF (25 mL) and treated with octyl mercaptan (8 mL) and DBU (750 μL) for 30 min. The THF was removed by rotary evaporation, and the residue was triturated several times with Et₂O. A portion of this material (~1.9 mmol, by vol.) was dissolved in DMF (20 mL) and coupled to Boc-Ala in the same manner as for proline. Purification by column chromatograph on SiO₂ eluted with 100% EtOAc to give **53** (970 mg, 69%) as a yellow foam. This material was treated with TFA until gas evolution ceased, then concentrated to dryness, co-evaporated from toluene, dissolved in DMF (7 mL), and treated with *i*Pr₂EtN (230 μL, 1.3 mmol) to pH >10 followed by succinic anhydride (262 mg, 2.6 mmol) and a small amount of DMAP. The mixture was stirred at rt overnight, then diluted with EtOAc and washed with 1N HCl (x3), brine, dried over Na₂SO₄, concentrated and purified by HPLC (Sunfire C18 30x150mm 20→80% ACN+0.1% TFA over 15min) to give **49** (459 mg, 51%) as a pale yellow solid. Stock solutions (100 mM – 6.4 mM) were prepared by dissolving in anhydrous TFE (distilled from LiCl and stored over 3Å MS) containing 0.5 M LiCl. **49**: MS *m/z* ESI(+) 683.1 (calc'd: C₃₂H₃₉N₆O₁₁, [M+H]⁺, 683.3).

³ Rijkers, D. T. S.; Adams, H. P. H. M.; Hemker, H. C.; Tesser, G. I. *Tetrahedron* **1995**, *51*, 11235.



Phosphorylated substrate Ac-AApSPY-pNA (61), Suc-ApSPY-pNA (62). Fmoc-Tyr(tBu)-OH (1.38 g, 3 mmol) and *p*-nitroaniline (0.414 g, 3 mmol) were reacted in the same manner as for **50**, except that the product was recrystallized from *i*PrOH alone. This material was treated with 4N HCl in dioxane to give **54** (4.65 g, 86% 2 steps) as a white solid. Compound **54** (1.57 g, 3 mmol) was dissolved in DMF (2 mL) and added to 2-chlorotrylchloride polystyrene resin (3.6 g, 0.84 mmol/g, 3 mmol) which had been pre-swollen in dry DCM under argon. Then added *i*Pr₂EtN (2.6 mL, 15 mmol) and agitated on wrist action shaker for 1 hr. Additional DMF (2 mL) was added, and shaking continued for 3 hrs. MeOH was added, and shaking continued for 30 min. The resin was then collected by filtration and washed thoroughly with DMF then DCM, and dried in vacuo to give **55** (5.6 g, 0.31 mmol/g, 58%), the loading of which was determined by spectrophotometric quantification of the dibenzofulvene released upon treatment with DBU. Resin-bound **55** was elongated to intermediates **56** and **57** by standard Fmoc solid-phase synthesis methods. These intermediates (~100 μmol) were treated with Bu₄NF in DMF for 1 hr, then filtered, and washed thoroughly with DMF. The fritted reaction vessel was then fitted with a septum and flushed with argon, and the resin was thoroughly washed with anhydrous THF. THF (1 mL) was added, followed by *O*-β-cyanoethyl-*O*'-tert-butyl *N,N*-diisopropyl phosphoramidite⁴ (319 mg, 1 mmol) and 2-ethylthio-1*H*-tetrazole (130 mg, 1 mmol). The mixture was then agitated periodically for 1 hr, filtered, and washed thoroughly with THF. Fresh THF (1 mL) was added, followed by T-Hydro (70%aq 137 μL, 1 mmol), and the mixture was agitated periodically

⁴ Kupihár, Z.; Váradi, G.; Monostori, É.; Tóth, G. K. *Tetrahedron Lett.* **2000**, *41*, 4457.

for 30 min, then filtered and washed with DCM. The resin was treated with 20% *v* DBU in DCM (1 mL) and mixed for 1 min, then filtered and this process was repeated for 1 hr to give **59** and **60**. Resin-bound **59** was treated with succinic anhydride (50 mg, 0.5 mmol) and DMAP (122 mg, 1 mmol) in DMF (1 mL) until the Kaiser test was negative. Treatment of **59** and **60** with TFA gave **62** and **61**, respectively, which were purified by preparative HPLC, lyophilized, and dissolved in anhydrous TFE (distilled from LiCl and stored over 3 Å MS) containing 0.5 M LiCl. Dilutions were made to attain stock solutions at 40 mM and 10 mM. **54**: ¹H NMR (400 MHz, DMSO-*d*₆) δ 2.80 (dd, *J* = 13.6, 9.9 Hz, 1H), 2.95 (dd, *J* = 13.6, 4.9 Hz, 1H), 4.13-4.26 (m, 3H), 4.37 (ddd, *J* = 9.9, 9.1, 4.9 Hz, 1H), 6.67 (d, *J* = 8.4 Hz, 2H), 7.14 (d, *J* = 8.4 Hz, 2H), 7.28 (br d, *J* = 7.4 Hz, 1H), 7.32 (br d, *J* = 7.3 Hz, 1H), 7.40 (apt t, *J* = 7.5 Hz, 2H), 7.67 (apt t, *J* = 7.5 Hz, 2H), 7.79-7.94 (m, 5H), 8.23 (d, *J* = 9.1 Hz, 1H), 9.20 (br s, 1H), 10.71 (s, 1H). **61**: MS *m/z* ESI(+) 749.9 (calc'd: C₃₁H₄₁N₇O₁₃P, [M+H]⁺, 750.3). **62**: MS *m/z* ESI(+) 736.9 (calc'd: C₃₀H₃₈N₆O₁₄P, [M+H]⁺, 737.2).

Determination of hPin1 kinetic constants

General: The Pin1 α-chymotrypsin-linked continuous spectrophotometric assay was carried out according to literature protocols with few changes.^{5,6,7,8} Reactions were monitored using a Hewlett-Packard HP8453 diode-array UV/Visible spectrophotometer equipped with a Peltier temperature control. Experimental extinction coefficients for *p*-nitroaniline in 35 mM HEPES pH 7.4 were found to be: ε₃₉₀ = 13109 M⁻¹ cm⁻¹; ε₄₀₀ = 11835 M⁻¹ cm⁻¹; ε₄₁₀ = 9662 M⁻¹ cm⁻¹; ε₄₂₀ = 7091 M⁻¹ cm⁻¹; ε₄₃₀ = 4746 M⁻¹ cm⁻¹; ε₄₄₀ = 2895 M⁻¹ cm⁻¹. Background was corrected based on a 510nm reference. All reactions were run at 10 °C.

Substrate %*cis* determination: The following stock solutions were prepared: *assay buffer*: 35 mM HEPES pH 7.4; *bovine α-chymotrypsin*: (Type II, ≥40 U/mg, Sigma) 60 mg/mL in 1 mM HCl; *GST-Pin1*: 7 μM in assay buffer; *substrate*: varying concentrations ≤ 100 mM in anhydrous TFE containing 0.5 M LiCl (*vide supra*). All solutions were stored in ice before use, with the exception of substrate solutions, which were kept in septum-capped vials under argon. Aliquots of the substrate solutions were transferred to oven dried, capped vials by syringe immediately before use and subsequently dispensed into the reaction using a pipettor. A masked semi-micro cuvette was charged with assay buffer (880 μL) and v and incubated at 10 °C for 2 min. Data acquisition (simultaneous 390, 400, 410, 420, 430, 440nm at 0.1 s intervals) was started, and substrate (10 μL of 100 mM or 6.4 mM) was added and the solution mixed by carefully aspirating with a 100 μL pipettor so as to not introduce air bubbles. The spontaneous reaction was observed for several seconds, then Pin1 (10 μL) was added and mixed by aspiration in the same manner, and the reaction progress was followed to completion (120 s). For high substrate concentrations, calculations were based on longer wavelengths such that *A*_{max} < 1.5. The isomer composition was calculated as follows:

$$\%cis = \frac{A_{max} - A_{trans}}{A_{max} - A_0}$$

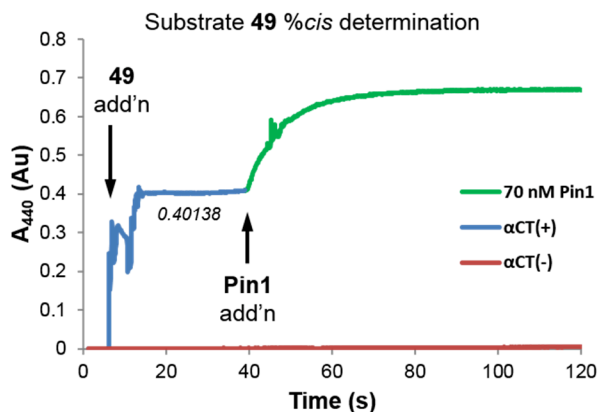
Progress curve for substrate Suc-AEPFpNA (**49**) (100 mM stock solution) alongside control reaction lacking α-chymotrypsin:

⁵ Wang, X. J.; Xu, B.; Mullins, A. B.; Neiler, F. K.; Etkorn, F. a. *J. Am. Chem. Soc.* **2004**, *126*, 15533.

⁶ Yaffe, M. B.; Schutkowski, M.; Shen, M.; Zhou, X. Z.; Stukenberg, P. T.; Rahfeld, J. U.; Xu, J.; Kuang, J.; Kirschner, M. W.; Fischer, G.; Cantley, L. C.; Lu, K. P. *Science* **1997**, *278*, 1957.

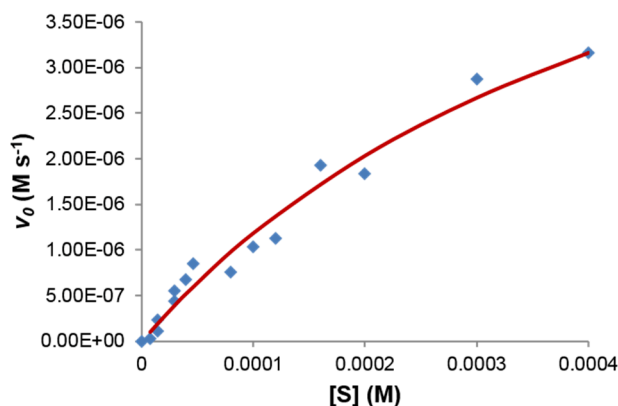
⁷ Ranganathan, R.; Lu, K. P.; Hunter, T.; Noel, J. P. *Cell* **1997**, *89*, 875.

⁸ Kofron, J. L.; Kuzmic, P.; Kishore, V.; Colón-Bonilla, E.; Rich, D. H. *Biochemistry* **1991**, *30*, 6127.



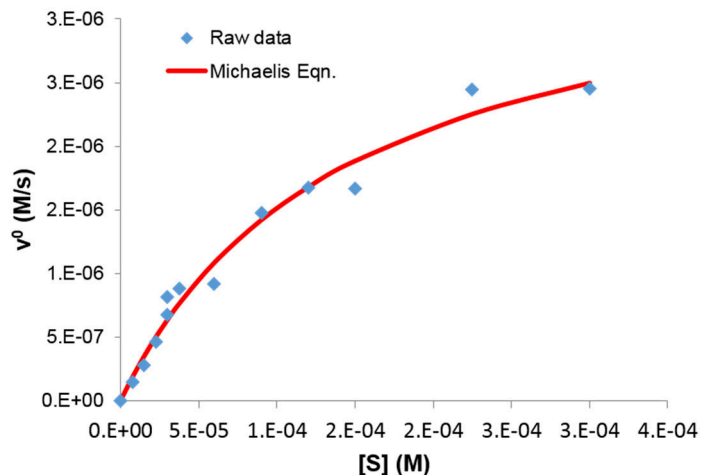
$$\%cis = \frac{0.6685 - 0.4014}{0.6685 - 0} = 40\%$$

Determination of the kinetic constants K_{cat} and K_m : Assay conditions were identical to those for %*cis* determination, except that cuvette was initially charged with assay buffer (880 μ L), Pin1 (10 μ L) and equilibrated for 2 min at 10 $^{\circ}$ C prior to the introduction of TFE + 0.5 M LiCl (X μ L), α -chymotrypsin (100 μ L), substrate (Y μ L, X + Y = 10 μ L). Enzyme concentration was estimated based on initial Bradford assay (6 mg/mL) and a calculated MW = 43 kDa, and used in the assay at 70 nM final. Substrate concentrations were based on weights used in volumetric preparation, and were corrected for the %*cis* isomer. Initial rate data were collected over a range of substrate concentrations, and fitted to the Michaelis-Menten equation by non-linear least squares analysis using the Solver add-on in Microsoft Excel. Suc-AEPFpNA (**49**) (6.4mM = 46% *cis*; 100mM = 40% *cis*):



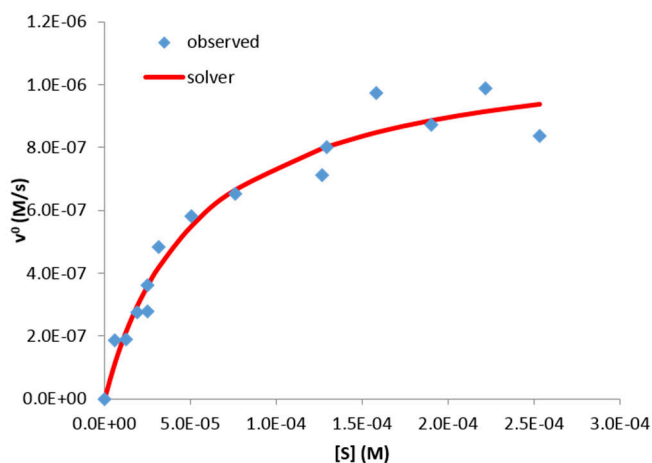
$$\begin{aligned}
 [E] \text{ (M)} &= 6.98\text{E-}08 \\
 V_{\max} \text{ (M/s)} &= 7.07\text{E-}06 \\
 K_m \text{ (M)} &= 4.95\text{E-}04 \\
 K_{\text{cat}} \text{ (s}^{-1}\text{)} &= 1.01\text{E+}02 \\
 K_{\text{cat}}/K_m \text{ (M}^{-1}\text{s}^{-1}\text{)} &= 2.05\text{E+}05
 \end{aligned}$$

Ac-AApSPY-pNA (**61**) (10 mM = 37% *cis*):



$[E]$ (M) = 2.33E-08
 V_{\max} (M/s) = 3.67E-06
 K_m (M) = 1.14E-04
 K_{cat} (s^{-1}) = 1.58E+02
 K_{cat}/K_m ($\text{M}^{-1}\cdot\text{s}^{-1}$) = 1.39E+06

Suc-ApSPY-pNA (**62**) (10 mM = 32% *cis*):



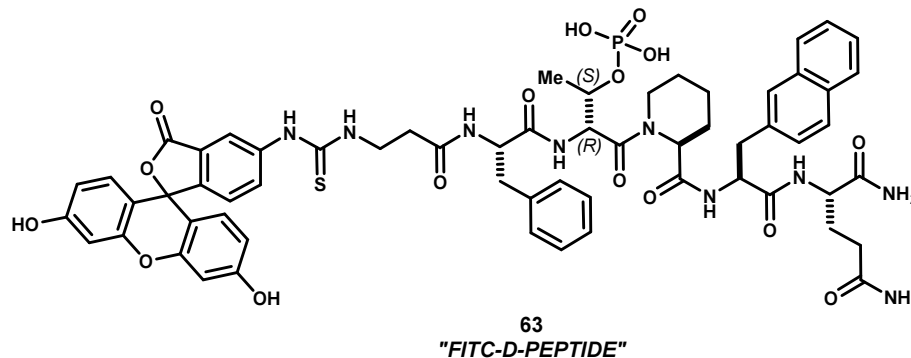
$[E]$ (M) = 7.75E-09
 V_{\max} (M/s) = 1.14E-06
 K_m (M) = 5.42E-05
 K_{cat} (s^{-1}) = 1.47E+02
 K_{cat}/K_m ($\text{M}^{-1}\cdot\text{s}^{-1}$) = 2.71E+06

Competitive inhibition assay: Competitive inhibition assays were run in the same manner as for the determination of kinetic constants, except that Pin1 was pre-incubated with the inhibitor (1% v DMSO final) for 2 min prior to initiating the reaction by the addition of substrate and α -chymotrypsin. In the case of compound **33b**, IC_{50} was approximated by non-linear least squares curve fitting of initial rate to the equation.

In this case, (Suc-AEPF-pNA, $K_m = 500 \mu\text{M}$) $[S]$ was $200 \mu\text{M}$ and K_i was accordingly estimated by the Cheng-Prusoff equation assuming competitive inhibition.

$$v = \frac{v_{max}}{1 + [I]/IC_{50}} \quad \text{and} \quad K_i = \frac{IC_{50}}{1 + [S]/K_m}$$

Development of a Pin1 fluorescence polarization assay



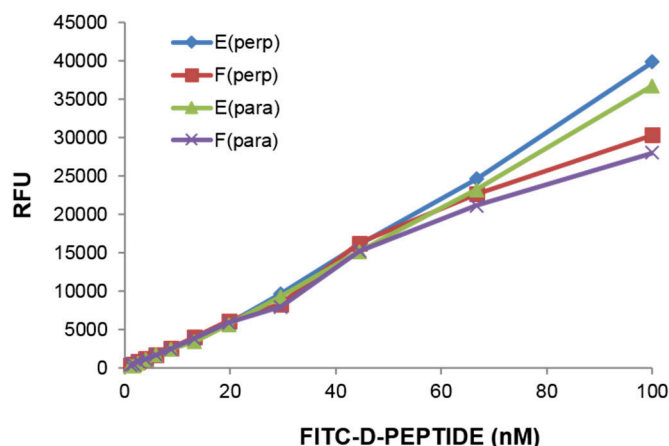
Synthesis of FITC-D-PEPTIDE (L63*): Boc- β -Ala-Phe-*D*-Thr(OH)-Pip-2Nal-Gln⁹ was assembled on Tentagel Rink amide resin using PyBOP for coupling reactions subsequent to pipecolic acid in order to introduce the free *D*-threonine side chain. On resin phosphorylation was carried out using *O*- β -cyanoethyl-*O*'-tert-butyl *N,N*-diisopropyl phosphoramidite in the same manner as for substrates **61** and **62**. The resulting phosphopeptide was cleaved from the resin by the action of TFA:H₂O (95:5), precipitated, and then reacted with fluorescein 5-isothiocyanate (FITC Isomer 1), purified by preparative HPLC and lyophilized. Stock solutions (10 mM, 10 μM) were prepared in DMSO and stored at -20 °C shielded from light when not in use. **L63***: MS *m/z* ESI(+) 1241.8 (calc'd: C₆₁H₆₅N₉O₁₆PS, [M+H]⁺, 1242.4).

Control experiments assessing the performance of L63*: The performance of fluorescent ligand **L63*** was assessed following reported experimental recommendations.¹⁰ Fluorescence and fluorescence polarization (FP) measurements were conducted using a Tecan Infinite® M1000 Pro in 96-well flat bottom black polystyrene plates (Greiner). The GST-S-tag-Pin1 construct was neither fluorescent, nor did it quench the fluorescence of probe **L63***. Assay buffer was 35 mM HEPES pH 7.4.

Ligand L63* fluorescence is linearly concentration-dependent: In duplicate, blank assay buffer + 2% *v/v* DMSO (100 μL) was loaded into wells 2→12 of a 96-well black plate. Assay buffer (294 μL), **L63*** (3 μL of 10 μM stock), and DMSO (3 μL) was added to wells 1, and serially 1.5x by transferring 200 μL sequentially into wells 2→12. The plate was read for fluorescence polarization ($\lambda_{exc} = 470 \text{ nm}$, 5 nm bandwidth; $\lambda_{em} = 520 \text{ nm}$, 10 nm bandwidth). The absolute intensity of the resulting parallel and perpendicular polarized emission is shown below:

⁹ Wildemann, D.; Erdmann, F.; Alvarez, B. H.; Stoller, G.; Zhou, X. Z.; Fanghänel, J.; Schutkowski, M.; Lu, K. P.; Fischer, G. *J. Med. Chem.* **2006**, *49*, 2147.

¹⁰ Rossi, A. M.; Taylor, C. W. *Nat. Protoc.* **2011**, *6*, 365.



Determination of dissociation constant of L63* by FP equilibrium saturation binding. In duplicate, a microplate was loaded with: well 1 – assay buffer (189 μ L), Pin1 (7.14 μ L, 6.0 mg/mL stock) and L63* (4 μ L, 250 nM stock); wells 2-12 – 100 μ L of assay buffer + L63* (2.5 nM final) containing 2%v DMSO final. Serial 2x dilution was achieved by sequential transfer of 100 μ L from row 1 to rows 2→12 to give $[E] = 5.0 \mu\text{M} \rightarrow 0.20 \text{ nM}$. Fluorescence polarization data ($\lambda_{\text{exc}} = 470 \text{ nm}$, 5 nm bandwidth; $\lambda_{\text{em}} = 520 \text{ nm}$, 10 nm bandwidth) were acquired in the same manner as before. The dissociation constant ($K_d = 18.2 \pm 6.3 \text{ nM}$) and Hill coefficient ($h = 1.3$) were determined by non-linear least squares curve fitting to the following equation using the Solver add-on in Microsoft Excel. Reported values represent the average of three trials on separate days.

$$\alpha = \frac{[E \cdot L^*]}{[E_{\text{Tot}}]} = \frac{([E]/k_d)^h}{1 + ([E]/k_d)^h}$$

Determination of dissociation constants for non-labeled ligands by competition binding with L63*. Competition binding was performed in duplicate using 100 nM Pin1, 0.5 nM L63* and a final concentration of 2%v DMSO. Inhibitors were titrated in duplicate using a 16-point serial 2x dilution or 11-point serial 3x dilution. FP data collection was the same as for saturation binding experiments. Dissociation constants were determined by non-linear least squares curve fitting to the following equation using the Solver add-on in Microsoft Excel.

$$K_d^I = \frac{[L^*R]_{50} IC_{50} K_d^{L^*}}{L_{\text{tot}}^* R_{\text{tot}} + [L^*R]_{50} (R_{\text{tot}} - L_{\text{tot}}^* + [L^*R]_{50} - K_d^{L^*})}$$

Synthesis of a Pin1-targeted library using synchronous resin release and template-induced macrocyclization

Sequence design. Pin1-targeted peptides sequences were designed within the positional variants Glu-Pro-X-X-X-Gly, X-Glu-Pro-X-X-Gly, X-X-Glu-Pro-X-Gly, where X was randomly filled. Histidine, arginine and cysteine were not included in this pilot library. X positions were filled using a random number generator in Microsoft Excel. Sequences were filtered to display at least one nucleophilic aryl side chain, and redundant sequences were eliminated.

Synthesis of Pilot Library A. Parallel solid-supported synthesis was carried out using 48-well MiniBlock™ (Bohdan/Mettler) reactors equipped with fritted polypropylene reaction tubes. 2-Chlorotrityl polystyrene was pre-loaded with Fmoc-glycine (0.64 mmol/g) and deprotected. This resin (5 μ mol or 10 μ mol) was dispensed into individual wells as an isopycnic suspension in DMF. This was achieved by preparing a volumetric suspension of the resin in DMF (10-20 mg/mL). The even suspension was maintained by bubbling with argon introduced via a needle, which was briefly removed before pipetting each aliquot (500 μ L). The liquid

was drained, and the resin washed with DMF. Peptide synthesis was as follows. Where possible, liquid handling was accomplished using 8-channel pipettors.

Amino acid array: Amino acid solutions were pre-dispensed into transparent, V-bottom 96-well 200 μ L polypropylene storage plates (ABGene AB-1058) using templates generated in Microsoft Excel, which were printed and placed beneath the plate to allow visual coordination with the amino acid being dispensed.

Amide coupling: Concentrations were such that minimal adjustment of the pipettors was necessary. To each well was added NMP (44 μ L) to saturate the frit, followed by *i*Pr₂EtN (8 eq, 1.0 M in NMP), Fmoc-AA-OH (4 eq, 0.45 M in NMP), and HBTU (4 eq, 0.45M), and the mixture was agitated on an orbital shaker (> 250rpm) for 30min, then drained under vacuum and washed sequentially with DMF, DCM and DMF.

Fmoc-deprotection: 20%v Piperidine in DMF (200 μ L) was added to each well. After 1 min., the liquid was drained under vacuum. Fresh solution was added, and the mixture was agitated on an orbital shaker (> 250rpm) for 15 min, then again drained, washed sequentially with DMF, DCM and DMF, and the hold-up forced through by applying gentle positive pressure of air.

Acylation by Template 5: To each well was added NMP (44 μ L) to saturate the frit, followed by *i*Pr₂EtN (4 eq, 1.0 M in NMP) and Template 5 (3 eq, 0.3 M in NMP). The mixture was agitated on an orbital shaker (> 250rpm) for 2-3 hrs, then drained and washed sequentially with DMF (x2), DCM (x2). The hold-up was forced through and the resin freed of solvent by applying vacuum and gentle positive pressure of air.

Synchronous resin release & template-induced macrocyclization: To each well was added 5%v TFA in MeNO₂ (1 mL), and the resulting mixture was agitated on an orbital shaker (> 250rpm) for 1 hr. The solutions were then drained into a 96-well 2.2 mL polypropylene storage plates (Greiner). The resin was then rinsed with the fresh solution (500 μ L) and the hold-up was forced through by applying a gentle positive pressure of air. The receiver plate was capped, and allowed to stand at rt overnight. The mixtures were then concentrated using a Thermo Savant Speed-vac equipped with a Teflon-lined pump, and further dried under high vacuum.

Preparation & storage of 10 mM stock solutions: Crude dried residues from the acidolysis step were dissolved in DMSO (500 μ L or 1000 μ L) to give 10 mM solutions, assuming 100% recovery based on the initial loading of Fmoc-glycine immobilized on 2-chlorotriyl polystyrene resin. Solutions were capped and stored at -20 °C when not in use.

Pilot Library A sequences

Mol. ID.	Plate	Well	Sequence	NB/P	MW	Analyzed?
A0001	A1	A1	Tyr-Ala-Ala-Ala-Ala-Gly	TR5-75	692.4	Y
A0002	A1	A2	Ala-Tyr-Ala-Ala-Ala-Gly	TR5-68	692.4	Y
A0003	A1	A3	Ala-Ala-Tyr-Ala-Ala-Gly	TR5-68	692.4	Y
A0004	A1	A4	Ala-Ala-Ala-Tyr-Ala-Gly	TR5-68	692.4	Y
A0005	A1	A5	Ala-Ala-Ala-Ala-Tyr-Gly	TR5-68	692.4	Y
A0006	A1	A6	Trp-Ala-Ala-Ala-Ala-Gly	TR5-73	715.4	Y
A0007	A1	A7	Ala-Trp-Ala-Ala-Ala-Gly	TR5-73	715.4	Y
A0008	A1	A8	Ala-Ala-Trp-Ala-Ala-Gly	TR5-73	715.4	Y
A0009	A1	A9	Ala-Ala-Ala-Trp-Ala-Gly	TR5-73	715.4	Y
A0010	A1	A10	Ala-Ala-Ala-Ala-Trp-Gly	TR5-73	715.4	Y
A0011	A1	A11	Phe(3OMe)-Ala-Ala-Ala-Ala-Gly	TR5-75	706.4	Y
A0012	A1	A12	Ala-Phe(3OMe)-Ala-Ala-Ala-Gly	TR5-68	706.4	Y
A0013	A1	B1	Ala-Ala-Phe(3OMe)-Ala-Ala-Gly	TR5-68	706.4	Y
A0014	A1	B2	Ala-Ala-Ala-Phe(3OMe)-Ala-Gly	TR5-68	706.4	Y
A0015	A1	B3	Ala-Ala-Ala-Ala-Phe(3OMe)-Gly	TR5-68	706.4	Y
A0016	A1	B4	Thi-Ala-Ala-Ala-Ala-Gly	TR5-75	682.3	Y
A0017	A1	B5	Ala-Thi-Ala-Ala-Ala-Gly	TR5-68	682.3	Y
A0018	A1	B6	Ala-Ala-Thi-Ala-Ala-Gly	TR5-68	682.3	Y
A0019	A1	B7	Ala-Ala-Ala-Thi-Ala-Gly	TR5-68	682.3	Y

A0020	A1	B8	Ala-Ala-Ala-Ala-Thi-Gly	TR5-68	682.3	Y
A0021	A1	B9	Nal2-Ala-Ala-Ala-Ala-Gly	TR5-71	727.8	Y
A0022	A1	B10	Ala-Nal2-Ala-Ala-Ala-Gly	TR5-71	727.8	Y
A0023	A1	B11	Ala-Ala-Nal2-Ala-Ala-Gly	TR5-71	727.8	Y
A0024	A1	B12	Ala-Ala-Ala-Nal2-Ala-Gly	TR5-71	727.8	Y
A0025	A1	C1	Ala-Ala-Ala-Ala-Nal2-Gly	TR5-71	727.8	Y
A0026	A1	C2	BThi-Ala-Ala-Ala-Ala-Gly	TR5-71	733.9	Y
A0027	A1	C3	Ala-BThi-Ala-Ala-Ala-Gly	TR5-71	733.9	Y
A0028	A1	C4	Ala-Ala-BThi-Ala-Ala-Gly	TR5-71	733.9	Y
A0029	A1	C5	Ala-Ala-Ala-BThi-Ala-Gly	TR5-71	733.9	Y
A0030	A1	C6	Ala-Ala-Ala-Ala-BThi-Gly	TR5-71	733.9	Y
A0031	A1	C7	Trp(5Me)-Ala-Ala-Ala-Ala-Gly	TR5-71	730.8	Y
A0032	A1	C8	Ala-Trp(5Me)-Ala-Ala-Ala-Gly	TR5-71	730.8	Y
A0033	A1	C9	Ala-Ala-Trp(5Me)-Ala-Ala-Gly	TR5-71	730.8	Y
A0034	A1	C10	Ala-Ala-Ala-Trp(5Me)-Ala-Gly	TR5-71	730.8	Y
A0035	A1	C11	Ala-Ala-Ala-Ala-Trp(5Me)-Gly	TR5-71	730.8	Y
A0036	A1	C12	Trp(5F)-Ala-Ala-Ala-Ala-Gly	TR5-71	734.8	Y
A0037	A1	D1	Ala-Trp(5F)-Ala-Ala-Ala-Gly	TR5-71	734.8	Y
A0038	A1	D2	Ala-Ala-Trp(5F)-Ala-Ala-Gly	TR5-71	734.8	Y
A0039	A1	D3	Ala-Ala-Ala-Trp(5F)-Ala-Gly	TR5-71	734.8	Y
A0040	A1	D4	Ala-Ala-Ala-Ala-Trp(5F)-Gly	TR5-71	734.8	Y
A0041	A1	D5	Ala-Tyr-Ala-Pro-Ala-Gly	TR5-76	719.8	Y
A0042	A1	D6	Ala-Ala-Tyr-Pro-Ala-Gly	TR5-76	719.8	Y
A0043	A1	D7	Ala-Ala-Ala-Pro-Tyr-Gly	TR5-76	719.8	Y
A0044	A1	D8	Ala-Phe(3OMe)-Ala-Pro-Ala-Gly	TR5-76	733.8	Y
A0045	A1	D9	Ala-Ala-Phe(3OMe)-Pro-Ala-Gly	TR5-76	733.8	Y
A0046	A1	D10	Ala-Ala-Ala-Pro-Phe(3OMe)-Gly	TR5-76	733.8	Y
A0047	A1	D11	Ala-Thi-Ala-Pro-Ala-Gly	TR5-76	709.8	Y
A0048	A1	D12	Ala-Ala-Thi-Pro-Ala-Gly	TR5-76	709.8	Y
A0049	A1	E1	Ala-Ala-Ala-Pro-Thi-Gly	TR5-76	709.8	Y
A0050	A1	E2	Ala-BThi-Ala-Pro-Ala-Gly	TR5-76	759.9	Y
A0051	A1	E3	Ala-Ala-BThi-Pro-Ala-Gly	TR5-76	759.9	Y
A0052	A1	E4	Ala-Ala-Ala-Pro-BThi-Gly	TR5-76	759.9	Y
A0053	A1	E5	Ala-Tyr-Pro-Ala-Ala-Gly	TR5-76	719.8	Y
A0054	A1	E6	Ala-Ala-Pro-Tyr-Ala-Gly	TR5-76	719.8	Y
A0055	A1	E7	Ala-Ala-Pro-Ala-Tyr-Gly	TR5-76	719.8	Y
A0056	A1	E8	Ala-Phe(3OMe)-Pro-Ala-Ala-Gly	TR5-76	733.8	Y
A0057	A1	E9	Ala-Ala-Pro-Phe(3OMe)-Ala-Gly	TR5-76	733.8	Y
A0058	A1	E10	Ala-Ala-Pro-Ala-Phe(3OMe)-Gly	TR5-76	733.8	Y
A0059	A1	E11	Ala-Thi-Pro-Ala-Ala-Gly	TR5-76	709.8	Y
A0060	A1	E12	Ala-Ala-Pro-Thi-Ala-Gly	TR5-76	709.8	Y
A0061	A1	F1	Ala-Ala-Pro-Ala-Thi-Gly	TR5-76	709.8	Y
A0062	A1	F2	Ala-BThi-Pro-Ala-Ala-Gly	TR5-76	759.9	Y
A0063	A1	F3	Ala-Ala-Pro-BThi-Ala-Gly	TR5-76	759.9	Y
A0064	A1	F4	Ala-Ala-Pro-Ala-BThi-Gly	TR5-76	759.9	Y
A0065	A1	F5	Ala-Tyr-Glu-Pro-Ala-Gly	TR5-79	777.9	Y
A0066	A1	F6	Ala-Ala-Glu-Pro-Tyr-Gly	TR5-79	777.9	Y
A0067	A1	F7	Ala-Trp-Glu-Pro-Ala-Gly	TR5-79	800.9	Y
A0068	A1	F8	Ala-Ala-Glu-Pro-Trp-Gly	TR5-79	800.9	Y
A0069	A1	F9	Ala-Nal2-Glu-Pro-Ala-Gly	TR5-79	811.9	Y
A0070	A1	F10	Ala-Ala-Glu-Pro-Nal2-Gly	TR5-79	811.9	Y
A0071	A1	F11	Ala-Thi-Glu-Pro-Ala-Gly	TR5-79	767.9	Y
A0072	A1	F12	Ala-Ala-Glu-Pro-Thi-Gly	TR5-79	767.9	Y
A0073	A1	G1	Ala-Glu-Pro-Tyr-Ala-Gly	TR5-79	777.9	Y
A0074	A1	G2	Ala-Glu-Pro-Ala-Tyr-Gly	TR5-79	777.9	Y
A0075	A1	G3	Ala-Glu-Pro-Trp-Ala-Gly	TR5-79	800.9	Y
A0076	A1	G4	Ala-Glu-Pro-Ala-Trp-Gly	TR5-79	800.9	Y
A0077	A1	G5	Ala-Glu-Pro-Nal2-Ala-Gly	TR5-79	811.9	Y
A0078	A1	G6	Ala-Glu-Pro-Ala-Nal2-Gly	TR5-79	811.9	Y
A0079	A1	G7	Ala-Glu-Pro-Thi-Ala-Gly	TR5-79	767.9	Y
A0080	A1	G8	Ala-Glu-Pro-Ala-Thi-Gly	TR5-79	767.9	Y

A0081	A1	G9	Glu-Pro-Tyr-Ala-Ala-Gly	TR5-79	777.9	Y
A0082	A1	G10	Glu-Pro-Ala-Tyr-Ala-Gly	TR5-79	777.9	Y
A0083	A1	G11	Glu-Pro-Trp-Ala-Ala-Gly	TR5-79	800.9	Y
A0084	A1	G12	Glu-Pro-Ala-Trp-Ala-Gly	TR5-79	800.9	Y
A0085	A1	H1	Glu-Pro-Nal2-Ala-Ala-Gly	TR5-79	811.9	Y
A0086	A1	H2	Glu-Pro-Ala-Nal2-Ala-Gly	TR5-79	811.9	Y
A0087	A1	H3	Glu-Pro-Thi-Ala-Ala-Gly	TR5-79	767.9	Y
A0088	A1	H4	Glu-Pro-Ala-Thi-Ala-Gly	TR5-79	767.9	Y
A0089	A1	H5	Asn-Leu-Tyr-Pro-Phe-Gly	HY1-38	880.0	Y
A0090	A1	H6	Ile-Glu-Pro-Trp-Asn-Gly	HY1-38	885.0	Y
A0091	A1	H7	Phe-Glu-Pro-Lys-Trp-Gly	HY1-38	933.1	Y
A0092	A1	H8	Gln-Glu-Pro-Gly-Tyr-Gly	HY1-38	819.9	Y
A0093	A1	H9	Lys-Glu-Pro-Gly-Tyr-Gly	HY1-38	819.9	Y
A0094	A1	H10	Phe-Glu-Pro-Tyr-Tyr-Gly	HY1-38	944.5	Y
A0095	A1	H11	empty			
A0096	A1	H12	empty			
A0097	A2	A1	Gln-pSer-Pro-Gly-Tyr-Gly	HY1-39_4	857.8	Y
A0098	A2	A2	Lys-pSer-Pro-Gly-Tyr-Gly	HY1-39_5	857.9	Y
A0099	A2	A3	Phe-Ile-Glu-Pro-Tyr-Gly	TR5-116	895.0	Y
A0100	A2	A4	Gln-Nal2-Glu-Pro-Ser-Gly	TR5-116	883.4	Y
A0101	A2	A5	Glu-Lys-Glu-Pro-Tyr-Gly	TR5-116	891.4	Y
A0102	A2	A6	Ile-Tyr-Glu-Pro-Phe-Gly	TR5-116	894.4	Y
A0103	A2	A7	Ser-Nal2-Glu-Pro-Gln-Gly	TR5-116	883.4	Y
A0104	A2	A8	Trp-Orn-Glu-Pro-Trp-Gly	TR5-116	957.5	Y
A0105	A2	A9	Phe-Phe-Glu-Pro-Tyr-Gly	TR5-116	928.4	Y
A0106	A2	A10	Met-Met-Glu-Pro-Orn-Gly	TR5-116	847.4	Y
A0107	A2	A11	Met-Leu-Glu-Pro-Trp-Gly	TR5-116	901.4	Y
A0108	A2	A12	Trp-Asp-Glu-Pro-Ala-Gly	TR5-116	843.4	Y
A0109	A2	B1	Gly-Trp-Glu-Pro-Lys-Gly	TR5-116	842.4	Y
A0110	A2	B2	Val-Gly-Glu-Pro-Nal2-Gly	TR5-116	790.4	Y
A0111	A2	B3	Glu-Glu-Pro-Tyr-Thr-Gly	TR5-116	864.4	Y
A0112	A2	B4	Nal1-Glu-Pro-Tyr-Glu-Gly	TR5-116	960.4	Y
A0113	A2	B5	Ala-Glu-Pro-Ser-Tyr-Gly	TR5-116	792.3	Y
A0114	A2	B6	Tyr-Glu-Pro-Ala-Ala-Gly		776.4	Y
A0115	A2	B7	Trp-Glu-Pro-Ala-Ala-Gly		800.9	Y
A0116	A2	B8	Nal1-Glu-Pro-Tyr-Thr-Gly	TR5-114	933.0	Y
A0117	A2	B9	Glu-Glu-Pro-Tyr-Val-Gly	TR5-114	862.9	Y
A0118	A2	B10	Glu-Glu-Pro-Gly-Tyr-Gly	TR5-114	820.9	Y
A0119	A2	B11	Gly-Glu-Pro-Thr-Nal1-Gly	TR5-114	826.9	Y
A0120	A2	B12	Ser-Glu-Pro-Tyr-Lys-Gly	TR5-114	851	Y
A0121	A2	C1	Trp-Glu-Pro-Trp-Thr-Gly	TR5-114	945.1	Y
A0122	A2	C2	Ile-Glu-Pro-Ser-Tyr-Gly	TR5-114	834.9	Y
A0123	A2	C3	Phe-Glu-Pro-Asp-Trp-Gly	TR5-114	920	Y
A0124	A2	C4	Tyr-Glu-Pro-Trp-Ala-Gly	TR5-114	892	Y
A0125	A2	C5	The remainder of plate A2 was left unfilled to accommodate expansion of the 'non-targeted' set.			
A0192	A2	H12				
A0193	A3	A1	Phe4OMe-Trp-Glu-Pro-Tyr-Gly	TR5-133		
A0194	A3	A2	Thi2-Glu-Pro-Ala-Nal1-Gly	TR5-133		
A0195	A3	A3	Phe3OMe-Val-Glu-Pro-Asp-Gly	TR5-133		
A0196	A3	A4	Tyr-Glu-Pro-Met-Nal2-Gly	TR5-133		
A0197	A3	A5	Glu-Tyr-Glu-Pro-Gly-Gly	TR5-133		
A0198	A3	A6	Trp5Me-Glu-Pro-Phe4OMe-Glu-Gly			
A0199	A3	A7	Asp-Tyr-Glu-Pro-Lys-Gly	TR5-133		
A0200	A3	A8	Bthi-Glu-Pro-Val-Glu-Gly	TR5-133		
A0201	A3	A9	Lys-Gly-Glu-Pro-Tyr-Gly	TR5-133		
A0202	A3	A10	Ile-Glu-Pro-Ile-Tyr-Gly	TR5-133		
A0203	A3	A11	Trp5F-Ala-Glu-Pro-Glu-Gly	TR5-133		
A0204	A3	A12	Phe4OMe-Glu-Pro-Ala-Pro-Gly	TR5-133		
A0205	A3	B1	Tyr-Glu-Pro-Gly-Trp5Me-Gly	TR5-133		
A0206	A3	B2	Trp5Me-Bthi-Glu-Pro-Nal2-Gly	TR5-133		
A0207	A3	B3	Nal1-Glu-Pro-Trp5Me-Trp5Br-Gly	TR5-133		

A0208	A3	B4	Tyr3OMe-Met-Glu-Pro-Ala-Gly	TR5-133		
A0209	A3	B5	Trp5Br-Glu-Pro-Nal1-Pro-Gly	TR5-133		
A0210	A3	B6	Asp-Tyr-Glu-Pro-Lys-Gly	TR5-133		
A0211	A3	B7	Tyr3OMe-Glu-Pro-Ala-Phe-Gly	TR5-133		
A0212	A3	B8	Trp-Tyr-Glu-Pro-Phe3OMe-Gly	TR5-133		
A0213	A3	B9	Gln-Glu-Pro-Ala-Bthi-Gly	TR5-133		
A0214	A3	B10	Nal2-Phe-Glu-Pro-Bthi-Gly	TR5-133	1018.4	y
A0215	A3	B11	Gln-Glu-Pro-Bthi-Trp-Gly	TR5-133		
A0216	A3	B12	Nal1-Trp5Me-Glu-Pro-Asn-Gly	TR5-133		
A0217	A3	C1	Trp-Ala-Glu-Pro-Gln-Gly	TR5-133		
A0218	A3	C2	Thi2-Glu-Pro-Thi2-Met-Gly	TR5-133		
A0219	A3	C3	Trp-BAla-Glu-Pro-Trp5Br-Gly	TR5-133		
A0220	A3	C4	Phe4OMe-Glu-Pro-Glu-Ile-Gly	TR5-133		
A0221	A3	C5	Tyr3OMe-Ile-Glu-Pro-Trp5Me-Gly			
A0222	A3	C6	Trp-Glu-Pro-Trp5Me-Trp-Gly	TR5-133		
A0223	A3	C7	Tyr-Trp-Glu-Pro-Ala-Gly	TR5-133		
A0224	A3	C8	Tyr-Glu-Pro-Nal1-Met-Gly	TR5-133		
A0225	A3	C9	Orn-Leu-Glu-Pro-Met-Gly	TR5-133		
A0226	A3	C10	Ala-Glu-Pro-Trp5Me-Glu-Gly	TR5-133		
A0227	A3	C11	Val-Phe-Glu-Pro-Phe3OMe-Gly	TR5-133		
A0228	A3	C12	Ala-Glu-Pro-Bthi-Nal1-Gly	TR5-133		
A0229	A3	D1	Trp5Me-Glu-Pro-Nal2-Asp-Gly	TR5-133		
A0230	A3	D2	Bthi-Met-Glu-Pro-Bthi-Gly	TR5-133		
A0231	A3	D3	Glu-Glu-Pro-Gly-Nal2-Gly	TR5-133		
A0232	A3	D4	Phe4OMe-Trp5Me-Glu-Pro-Met-Gly			
A0233	A3	D5	Tyr-Glu-Pro-Pro-Val-Gly	TR5-133		
A0234	A3	D6	Tyr-Pro-Glu-Pro-Trp-Gly	TR5-133		
A0235	A3	D7	Phe-Glu-Pro-Ile-Nal1-Gly	TR5-133		
A0236	A3	D8	Asp-BAla-Glu-Pro-Thi2-Gly	TR5-133		
A0237	A3	D9	Nal1-Glu-Pro-Tyr-Glu-Gly	TR5-133	960.4	y
A0238	A3	D10	Tyr-Ile-Glu-Pro-Pro-Gly	TR5-133		
A0239	A3	D11	Phe-Glu-Pro-Thr-Thi2-Gly	TR5-133		
A0240	A3	D12	Orn-Thr-Glu-Pro-Phe4OMe-Gly	TR5-133		
A0241	A3	E1	Tyr3OMe-Trp5Br-Glu-Pro-Thr-Gly			
A0242	A3	E2	Trp5F-Glu-Pro-Tyr3OMe-Ala-Gly	TR5-133		
A0243	A3	E3	Gln-Trp5Me-Glu-Pro-Pro-Gly	TR5-133		
A0244	A3	E4	Trp5Me-Glu-Pro-Pro-Pro-Gly	TR5-133		
A0245	A3	E5	Nal2-Ile-Glu-Pro-Thr-Gly	TR5-133		
A0246	A3	E6	Met-Glu-Pro-Asn-Trp5Br-Gly	TR5-133		
A0247	A3	E7	Met-Phe-Glu-Pro-Tyr-Gly	TR5-133		
A0248	A3	E8	Orn-Glu-Pro-Tyr3OMe-Asn-Gly	TR5-133		
A0249	A3	E9	Leu-Tyr-Glu-Pro-Thr-Gly	TR5-133		
A0250	A3	E10	Nal1-Glu-Pro-Orn-Trp5Me-Gly	TR5-133		
A0251	A3	E11	Trp5F-Nal1-Glu-Pro-Trp5F-Gly	TR5-133		
A0252	A3	E12	Tyr3OMe-Glu-Pro-Ala-Val-Gly	TR5-133		
A0253	A3	F1	Thi2-Glu-Pro-Gly-Nal1-Gly	TR5-133		
A0254	A3	F2	Trp-Nal1-Glu-Pro-Lys-Gly	TR5-133		
A0255	A3	F3	Trp-Glu-Pro-Ser-Met-Gly	TR5-133		
A0256	A3	F4	Tyr-Ala-Glu-Pro-Tyr-Gly	TR5-133		
A0257	A3	F5	Ser-Glu-Pro-Trp5F-Asn-Gly	TR5-133		
A0258	A3	F6	Phe4OMe-Tyr-Glu-Pro-Asp-Gly	TR5-133		
A0259	A3	F7	Nal1-Glu-Pro-Thr-Val-Gly	TR5-133		
A0260	A3	F8	Trp5Me-Asp-Glu-Pro-Asp-Gly	TR5-133		
A0261	A3	F9	Gly-Glu-Pro-Nal1-Nal1-Gly	TR5-133		
A0262	A3	F10	Glu-Leu-Glu-Pro-Trp-Gly	TR5-133		
A0263	A3	F11	Bthi-Glu-Pro-Phe4OMe-Ile-Gly	TR5-133		
A0264	A3	F12	Trp-Trp5Me-Glu-Pro-Tyr-Gly	TR5-133		
A0265	A3	G1	Ile-Phe3OMe-Glu-Pro-Leu-Gly	TR5-133		
A0266	A3	G2	Orn-Glu-Pro-Tyr3OMe-Tyr-Gly	TR5-133		
A0267	A3	G3	Glu-Trp5Me-Glu-Pro-Trp-Gly	TR5-133		
A0268	A3	G4	Pro-Glu-Pro-Tyr-Phe4OMe-Gly	TR5-133		

A0269	A3	G5	Tyr3OMe-Ala-Glu-Pro-Leu-Gly	TR5-133		
A0270	A3	G6	Tyr-Glu-Pro-Nal1-Ala-Gly	TR5-133		
A0271	A3	G7	Trp5F-Asp-Glu-Pro-Gly-Gly	TR5-133		
A0272	A3	G8	Ala-Glu-Pro-Thr-Bthi-Gly	TR5-133		
A0273	A3	G9	Pro-Trp5F-Glu-Pro-BAla-Gly	TR5-133		
A0274	A3	G10	Nal2-Glu-Pro-Asp-Thr-Gly	TR5-133		
A0275	A3	G11	Trp-Thr-Glu-Pro-Lys-Gly	TR5-133		
A0276	A3	G12	Nal1-Glu-Pro-Tyr3OMe-Phe3OMe-Gly			
A0277	A3	H1	Nal2-Glu-Pro-Leu-Tyr3OMe-Gly	TR5-133		
A0278	A3	H2	Leu-Trp5Br-Glu-Pro-Trp5F-Gly	TR5-133		
A0279	A3	H3	Pro-Glu-Pro-Trp-Nal2-Gly	TR5-133		
A0280	A3	H4	Tyr-Met-Glu-Pro-Ala-Gly	TR5-133		
A0281	A3	H5	Ser-Glu-Pro-Trp5F-Trp5Br-Gly	TR5-133		
A0282	A3	H6	Trp5F-Tyr3OMe-Glu-Pro-Trp5Me-Gly			
A0283	A3	H7	Trp5Br-Glu-Pro-Nal2-Glu-Gly	TR5-133		
A0284	A3	H8	Trp-Orn-Glu-Pro-Phe3OMe-Gly	TR5-133		
A0285	A3	H9	Bthi-Glu-Pro-Trp5Br-Thr-Gly	TR5-133		
A0286	A3	H10	BAla-BAla-Glu-Pro-Thi2-Gly	TR5-133		
A0287	A3	H11	Trp5Br-Glu-Pro-Nal1-Met-Gly	TR5-133		
A0288	A3	H12	Lys-Orn-Glu-Pro-Trp5Me-Gly	TR5-133		
A0289	A4	A1	Thi2-Glu-Pro-Thr-Leu-Gly	TR5-133		
A0290	A4	A2	Ala-Trp5Me-Glu-Pro-Nal2-Gly	TR5-133		
A0291	A4	A3	Trp5F-Glu-Pro-Met-Phe4OMe-Gly			
A0292	A4	A4	Nal1-Lys-Glu-Pro-Tyr-Gly	TR5-133		
A0293	A4	A5	Tyr3OMe-Glu-Pro-Lys-Ser-Gly	TR5-133		
A0294	A4	A6	Tyr-Nal2-Glu-Pro-Trp5Me-Gly	TR5-133		
A0295	A4	A7	Asp-Glu-Pro-Asp-Trp-Gly	TR5-133		
A0296	A4	A8	Nal1-Phe3OMe-Glu-Pro-Thr-Gly	TR5-133		
A0297	A4	A9	Gln-Glu-Pro-Nal1-Gly-Gly	TR5-133		
A0298	A4	A10	Tyr-Asp-Glu-Pro-Glu-Gly	TR5-133		
A0299	A4	A11	Thr-Glu-Pro-Trp-Trp5F-Gly	TR5-133		
A0300	A4	A12	Phe4OMe-Nal1-Glu-Pro-Ile-Gly	TR5-133		
A0301	A4	B1	Glu-Trp-Glu-Pro-Tyr3OMe-Gly	TR5-133		
A0302	A4	B2	Orn-Glu-Pro-Met-Phe3OMe-Gly	TR5-133		
A0303	A4	B3	Phe4OMe-Asp-Glu-Pro-Thr-Gly	TR5-133		
A0304	A4	B4	Ala-Glu-Pro-Tyr-Phe3OMe-Gly	TR5-133		
A0305	A4	B5	Asn-Tyr3OMe-Glu-Pro-Bthi-Gly	TR5-133		
A0306	A4	B6	Asp-Glu-Pro-Asp-Trp-Gly	TR5-133		
A0307	A4	B7	Leu-Bthi-Glu-Pro-Lys-Gly	TR5-133		
A0308	A4	B8	Thi2-Glu-Pro-Met-Trp-Gly	TR5-133		
A0309	A4	B9	Thi2-Orn-Glu-Pro-Nal1-Gly	TR5-133		
A0310	A4	B10	Bthi-Glu-Pro-Ala-Tyr3OMe-Gly	TR5-133		
A0311	A4	B11	Ser-Phe3OMe-Glu-Pro-Bthi-Gly	TR5-133		
A0312	A4	B12	Ser-Glu-Pro-Lys-Thi2-Gly	TR5-133		
A0313	A4	C1	Ile-Glu-Pro-Lys-Tyr3OMe-Gly	TR5-133		
A0314	A4	C2	Ala-Nal1-Glu-Pro-Trp5Br-Gly	TR5-133		
A0315	A4	C3	Gln-Glu-Pro-Ala-Tyr3OMe-Gly	TR5-133		
A0316	A4	C4	Trp5Br-Tyr3OMe-Glu-Pro-BAla-Gly			
A0317	A4	C5	Leu-Glu-Pro-Leu-Trp5Me-Gly	TR5-133		
A0318	A4	C6	Phe-Orn-Glu-Pro-Trp5F-Gly	TR5-133		
A0319	A4	C7	Tyr-Glu-Pro-Ile-Tyr-Gly	TR5-133		
A0320	A4	C8	Trp5F-Asp-Glu-Pro-Pro-Gly	TR5-133		
A0321	A4	C9	Val-Glu-Pro-Orn-Phe4OMe-Gly	TR5-133		
A0322	A4	C10	BAla-Trp5Me-Glu-Pro-Trp5Me-Gly			
A0323	A4	C11	Ile-Glu-Pro-Bthi-Phe3OMe-Gly	TR5-133		
A0324	A4	C12	Ile-Met-Glu-Pro-Lys-Gly	TR5-133		
A0325	A4	D1	Ala-Nal2-Glu-Pro-Trp5F-Gly	TR5-133		
A0326	A4	D2	Nal2-Glu-Pro-Phe3OMe-Ala-Gly	TR5-133		
A0327	A4	D3	Tyr-Thi2-Glu-Pro-Bthi-Gly	TR5-133		
A0328	A4	D4	Gln-Glu-Pro-Nal1-Lys-Gly	TR5-133		
A0329	A4	D5	Orn-Thi2-Glu-Pro-Trp5Me-Gly	TR5-133		

A0330	A4	D6	Asn-Glu-Pro-Bthi-Asn-Gly	TR5-133		
A0331	A4	D7	Tyr-Met-Glu-Pro-Ser-Gly	TR5-133		
A0332	A4	D8	Leu-Glu-Pro-Orn-Bthi-Gly	TR5-133		
A0333	A4	D9	Pro-Tyr-Glu-Pro-Phe-Gly	TR5-133		
A0334	A4	D10	Ile-Glu-Pro-Pro-Thi2-Gly	TR5-133		
A0335	A4	D11	Ala-Lys-Glu-Pro-Trp5Br-Gly	TR5-133		
A0336	A4	D12	Gly-Glu-Pro-Gly-Trp5Br-Gly	TR5-133		
A0337	A4	E1	Trp5F-Glu-Pro-Ile-Glu-Gly	TR5-133		
A0338	A4	E2	Leu-Bthi-Glu-Pro-Ala-Gly	TR5-133		
A0339	A4	E3	Nal2-Glu-Pro-Glu-Nal2-Gly	TR5-133		
A0340	A4	E4	Thi2-Ile-Glu-Pro-Gln-Gly	TR5-133		
A0341	A4	E5	Gln-Glu-Pro-Trp5F-Ser-Gly	TR5-133		
A0342	A4	E6	BAla-Trp5F-Glu-Pro-Ile-Gly	TR5-133		
A0343	A4	E7	Nal1-Glu-Pro-Nal1-Thr-Gly	TR5-133		
A0344	A4	E8	Thr-Trp-Glu-Pro-Thi2-Gly	TR5-133		
A0345	A4	E9	Lys-Glu-Pro-Phe-Trp5Br-Gly	TR5-133		
A0346	A4	E10	Phe4OMe-BAla-Glu-Pro-Gly-Gly	TR5-133		
A0347	A4	E11	Trp5F-Glu-Pro-Gly-Ala-Gly	TR5-133		
A0348	A4	E12	Pro-Trp5Br-Glu-Pro-Nal2-Gly	TR5-133		
A0349	A4	F1	Phe3OMe-Gly-Glu-Pro-Tyr3OMe-Gly			
A0350	A4	F2	Tyr3OMe-Glu-Pro-Tyr-Glu-Gly	TR5-133		
A0351	A4	F3	Lys-Asn-Glu-Pro-Bthi-Gly	TR5-133		
A0352	A4	F4	Phe3OMe-Glu-Pro-Thr-Asp-Gly	TR5-133		
A0353	A4	F5	Orn-Glu-Glu-Pro-Thi2-Gly	TR5-133		
A0354	A4	F6	Trp-Glu-Pro-Tyr-Bthi-Gly	TR5-133		
A0355	A4	F7	Thi2-Met-Glu-Pro-Ala-Gly	TR5-133		
A0356	A4	F8	Bthi-Glu-Pro-Leu-Trp5Br-Gly	TR5-133		
A0357	A4	F9	Nal2-Thi2-Glu-Pro-Val-Gly	TR5-133		
A0358	A4	F10	Bthi-Glu-Pro-Gly-Thr-Gly	TR5-133		
A0359	A4	F11	Bthi-Ile-Glu-Pro-Nal1-Gly	TR5-133	984.4	y
A0360	A4	F12	Orn-Glu-Pro-Gly-Trp5Br-Gly	TR5-133		
A0361	A4	G1	Phe3OMe-Glu-Pro-Nal1-Glu-Gly	TR5-133		
A0362	A4	G2	Orn-Tyr3OMe-Glu-Pro-Orn-Gly	TR5-133		
A0363	A4	G3	Thi2-Glu-Pro-Gly-Bthi-Gly	TR5-133		
A0364	A4	G4	Trp5Br-Trp5Me-Glu-Pro-Leu-Gly	TR5-133		
A0365	A4	G5	Ser-Glu-Pro-Thi2-Bthi-Gly	TR5-133		
A0366	A4	G6	Leu-Met-Glu-Pro-Trp5Br-Gly	TR5-133		
A0367	A4	G7	Phe4OMe-Glu-Pro-Asn-Ala-Gly	TR5-133		
A0368	A4	G8	Ser-Pro-Glu-Pro-Trp5Me-Gly	TR5-133		
A0369	A4	G9	Nal1-Glu-Pro-Nal2-Orn-Gly	TR5-133		
A0370	A4	G10	Gly-Tyr3OMe-Glu-Pro-Thi2-Gly	TR5-133		
A0371	A4	G11	Phe4OMe-Glu-Pro-Thr-Trp5F-Gly			
A0372	A4	G12	Nal1-Nal2-Glu-Pro-Glu-Gly	TR5-133		
A0373	A4	H1	Asn-Glu-Glu-Pro-Trp5Me-Gly	TR5-133		
A0374	A4	H2	Thi2-Glu-Pro-Thr-Ala-Gly	TR5-133		
A0375	A4	H3	Val-Trp-Glu-Pro-Pro-Gly	TR5-133		
A0376	A4	H4	Ala-Glu-Pro-Leu-Trp5F-Gly	TR5-133		
A0377	A4	H5	Orn-Thi2-Glu-Pro-Phe4OMe-Gly	TR5-133		
A0378	A4	H6	Trp-Glu-Pro-Nal2-Phe-Gly	TR5-133		
A0379	A4	H7	Asn-Asp-Glu-Pro-Trp5F-Gly	TR5-133		
A0380	A4	H8	Tyr-Glu-Pro-Thr-Ile-Gly	TR5-133		
A0381	A4	H9	Nal2-Trp5Br-Glu-Pro-Ser-Gly	TR5-133		
A0382	A4	H10	Trp5Me-Glu-Pro-Lys-Gly-Gly	TR5-133		
A0383	A4	H11	Nal2-Ser-Glu-Pro-Glu-Gly	TR5-133		
A0384	A4	H12	Bthi-Glu-Pro-Trp-Nal2-Gly	TR5-133		
A0385	A5	A1	Nal2-Glu-Pro-Nal1-Met-Gly	TR5-135		
A0386	A5	A2	Glu-Pro-Trp5Br-Thr-Met-Gly	TR5-135		
A0387	A5	A3	Gln-Glu-Pro-Bthi-Met-Gly	TR5-135		
A0388	A5	A4	Glu-Pro-Gly-Tyr3OMe-Phe-Gly	TR5-135		
A0389	A5	A5	Asp-Glu-Pro-Tyr-Val-Gly	TR5-135	849.4	y
A0390	A5	A6	Glu-Pro-Ala-Tyr3OMe-Nal2-Gly	TR5-135		

A0391	A5	A7	Val-Glu-Pro-Nal2-Leu-Gly	TR5-135		
A0392	A5	A8	Glu-Pro-Ser-Ile-Thi2-Gly	TR5-135		
A0393	A5	A9	Trp-Glu-Pro-Tyr-Ser-Gly	TR5-135		
A0394	A5	A10	Glu-Pro-Gln-Met-Phe-Gly	TR5-135		
A0395	A5	A11	Trp5Me-Glu-Pro-Tyr3OMe-Val-Gly			
A0396	A5	A12	Glu-Pro-Leu-Bthi-Phe3OMe-Gly	TR5-135		
A0397	A5	B1	Glu-Pro-Tyr-Thr-Asp-Gly	TR5-135		
A0398	A5	B2	Tyr-Glu-Pro-Thi2-Trp5Me-Gly	TR5-135		
A0399	A5	B3	Glu-Pro-Trp-Ala-Trp-Gly	TR5-135		
A0400	A5	B4	Nal1-Glu-Pro-Phe3OMe-Tyr3OMe-Gly		1038.4	y
A0401	A5	B5	Glu-Pro-Tyr-Phe3OMe-Lys-Gly	TR5-135		
A0402	A5	B6	Val-Glu-Pro-Nal2-Leu-Gly	TR5-135		
A0403	A5	B7	Glu-Pro-Tyr-Lys-Pro-Gly	TR5-135	859.4	y
A0404	A5	B8	Trp5Br-Glu-Pro-Bthi-Asp-Gly	TR5-135	1053.3	y
A0405	A5	B9	Glu-Pro-Nal1-Glu-Nal2-Gly	TR5-135	994.4	y
A0406	A5	B10	Trp5F-Glu-Pro-Asn-Ile-Gly	TR5-135		
A0407	A5	B11	Glu-Pro-Ile-Thi2-Val-Gly	TR5-135		
A0408	A5	B12	Val-Glu-Pro-Asn-Trp-Gly	TR5-135	870.4	y
A0409	A5	C1	Phe4OMe-Glu-Pro-Thi2-Tyr-Gly	TR5-135	965.1	y
A0410	A5	C2	Glu-Pro-Thr-Bthi-Phe4OMe-Gly	TR5-135	952.4	y
A0411	A5	C3	Trp-Glu-Pro-Gly-Thr-Gly	TR5-135		
A0412	A5	C4	Glu-Pro-Phe3OMe-Pro-Gly-Gly	TR5-135		
A0413	A5	C5	Trp5Br-Glu-Pro-Thi2-Nal2-Gly	TR5-135		
A0414	A5	C6	Glu-Pro-Ile-Trp5Me-Trp5Br-Gly	TR5-135		
A0415	A5	C7	Val-Glu-Pro-Asn-Thi2-Gly	TR5-135		
A0416	A5	C8	Glu-Pro-Met-Ala-Nal1-Gly	TR5-135		
A0417	A5	C9	Asp-Glu-Pro-Nal2-Met-Gly	TR5-135		
A0418	A5	C10	Glu-Pro-Phe-Trp-Tyr3OMe-Gly	TR5-135		
A0419	A5	C11	Asn-Glu-Pro-Orn-Trp5Me-Gly	TR5-135		
A0420	A5	C12	Glu-Pro-Tyr3OMe-Thr-Phe3OMe-Gly			
A0421	A5	D1	Glu-Pro-Pro-Nal1-Phe3OMe-Gly	TR5-135		
A0422	A5	D2	Tyr-Glu-Pro-Pro-Trp5F-Gly	TR5-135	935.4	y
A0423	A5	D3	Glu-Pro-Phe4OMe-Trp-Phe-Gly	TR5-135		
A0424	A5	D4	Thi2-Glu-Pro-Nal1-Bthi-Gly	TR5-135	1024.4	y
A0425	A5	D5	Glu-Pro-Tyr3OMe-Thr-Nal2-Gly	TR5-135		
A0426	A5	D6	Trp5Br-Glu-Pro-Pro-Ala-Gly	TR5-135		
A0427	A5	D7	Glu-Pro-Lys-Gly-Tyr3OMe-Gly	TR5-135		
A0428	A5	D8	Phe-Glu-Pro-Bthi-Lys-Gly	TR5-135		
A0429	A5	D9	Glu-Pro-Nal2-Orn-Trp5Br-Gly	TR5-135	1046.4	y
A0430	A5	D10	BAla-Glu-Pro-Met-Bthi-Gly	TR5-135		
A0431	A5	D11	Glu-Pro-Gly-Val-Trp5Br-Gly	TR5-135		
A0432	A5	D12	Lys-Glu-Pro-Thi2-Nal1-Gly	TR5-135		
A0433	A5	E1	Trp5Br-Glu-Pro-Trp5Me-Gly-Gly	TR5-135		
A0434	A5	E2	Glu-Pro-BAla-Trp5F-Ala-Gly	TR5-135		
A0435	A5	E3	Nal2-Glu-Pro-Phe-Thi2-Gly	TR5-135	968.4	y
A0436	A5	E4	Glu-Pro-Trp5Br-Trp5Me-Asp-Gly	TR5-135		
A0437	A5	E5	Ile-Glu-Pro-Pro-Tyr-Gly	TR5-135		
A0438	A5	E6	Glu-Pro-Ser-Phe4OMe-Leu-Gly	TR5-135		
A0439	A5	E7	Trp5F-Glu-Pro-Thi2-Phe3OMe-Gly			
A0440	A5	E8	Glu-Pro-Phe3OMe-Phe3OMe-Thi2-Gly			
A0441	A5	E9	Bthi-Glu-Pro-Trp-BAla-Gly	TR5-135		
A0442	A5	E10	Glu-Pro-Ile-Trp5Br-Thi2-Gly	TR5-135		
A0443	A5	E11	Phe4OMe-Glu-Pro-Trp5F-Ile-Gly	TR5-135	965.4	y
A0444	A5	E12	Glu-Pro-Trp5F-Orn-Trp5Br-Gly	TR5-135		
A0445	A5	F1	Glu-Pro-Trp5Me-BAla-Phe3OMe-Gly			
A0446	A5	F2	Phe-Glu-Pro-Met-Lys-Gly	TR5-135		
A0447	A5	F3	Glu-Pro-Val-Nal2-Ala-Gly	TR5-135		
A0448	A5	F4	Thi2-Glu-Pro-Thr-Met-Gly	TR5-135		
A0449	A5	F5	Glu-Pro-Met-Phe4OMe-Trp5F-Gly			
A0450	A5	F6	Trp5F-Glu-Pro-Ala-Glu-Gly	TR5-135		
A0451	A5	F7	Glu-Pro-Asn-Phe-Nal2-Gly	TR5-135		

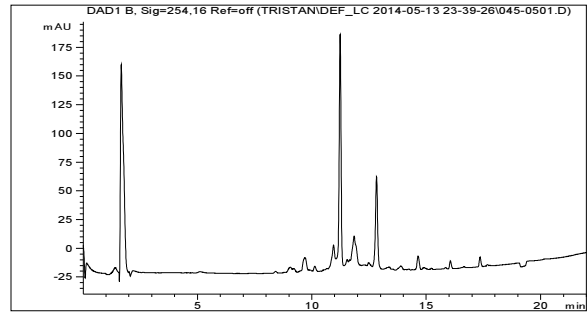
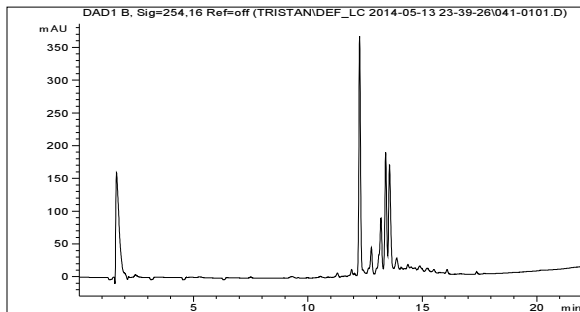
A0452	A5	F8	Trp5F-Glu-Pro-Phe-Thi2-Gly	TR5-135	975.4	y
A0453	A5	F9	Glu-Pro-Phe-Trp5Br-Phe3OMe-Gly			
A0454	A5	F10	Phe4OMe-Glu-Pro-Asn-Trp5Me-Gly			
A0455	A5	F11	Glu-Pro-Phe4OMe-Lys-Phe3OMe-Gly			
A0456	A5	F12	Pro-Glu-Pro-Bthi-Ala-Gly	TR5-135		
A0457	A5	G1	Glu-Glu-Pro-Gly-Thi2-Gly	TR5-135	810.3	y
A0458	A5	G2	Glu-Pro-Ala-Ala-Tyr3OMe-Gly	TR5-135		
A0459	A5	G3	Phe4OMe-Glu-Pro-Trp5F-Tyr3OMe-Gly			
A0460	A5	G4	Glu-Pro-Glu-Tyr3OMe-Glu-Gly	TR5-135		
A0461	A5	G5	Tyr-Glu-Pro-Trp-Ile-Gly	TR5-135		
A0462	A5	G6	Glu-Pro-Bthi-Tyr3OMe-Thi2-Gly	TR5-135		
A0463	A5	G7	Ser-Glu-Pro-Ile-Trp5F-Gly	TR5-135		
A0464	A5	G8	Glu-Pro-Trp5F-Gly-Glu-Gly	TR5-135	861.9	y
A0465	A5	G9	Tyr3OMe-Glu-Pro-Nal1-Trp-Gly	TR5-135		
A0466	A5	G10	Glu-Pro-Thi2-Tyr3OMe-Ala-Gly	TR5-135		
A0467	A5	G11	Phe-Glu-Pro-Phe4OMe-Gly-Gly	TR5-135		
A0468	A5	G12	Glu-Pro-Pro-Leu-Phe4OMe-Gly	TR5-135		
A0469	A5	H1	Glu-Pro-Nal2-Ser-Gly-Gly	TR5-135		
A0470	A5	H2	Trp5F-Glu-Pro-BAla-Val-Gly	TR5-135		
A0471	A5	H3	Glu-Pro-Pro-Trp-Bthi-Gly	TR5-135		
A0472	A5	H4	Phe-Glu-Pro-Thi2-Gln-Gly	TR5-135		
A0473	A5	H5	Glu-Pro-Asn-Trp5F-Gly-Gly	TR5-135		
A0474	A5	H6	Nal1-Glu-Pro-Trp5F-Trp-Gly	TR5-135	1059.2	y
A0475	A5	H7	Glu-Pro-Thr-Bthi-Gln-Gly	TR5-135	903.4	y
A0476	A5	H8	Tyr3OMe-Glu-Pro-Val-Ile-Gly	TR5-135		
A0477	A5	H9	Glu-Pro-Trp5F-Trp5Br-Ser-Gly	TR5-135		
A0478	A5	H10	Phe3OMe-Glu-Pro-Phe3OMe-Lys-Gly			
A0479	A5	H11	Glu-Pro-Ala-Thi2-Ala-Gly	TR5-135		
A0480	A5	H12	Glu-Glu-Pro-Ala-Thi2-Gly	TR5-135		
A0481	A6	A1	Glu-Pro-Trp-Nal1-Asp-Gly	TR5-135		
A0482	A6	A2	Met-Glu-Pro-Trp5F-Trp5Br-Gly	TR5-135		
A0483	A6	A3	Glu-Pro-Nal2-Glu-Phe4OMe-Gly	TR5-135		
A0484	A6	A4	Phe4OMe-Glu-Pro-Phe3OMe-Thi2-Gly			
A0485	A6	A5	Glu-Pro-Nal2-Trp5Me-Leu-Gly	TR5-135		
A0486	A6	A6	Gln-Glu-Pro-Tyr-Ser-Gly	TR5-135		
A0487	A6	A7	Glu-Pro-Phe-Phe3OMe-Orn-Gly	TR5-135		
A0488	A6	A8	Thr-Glu-Pro-Ile-Trp5Me-Gly	TR5-135		
A0489	A6	A9	Glu-Pro-Ser-Val-Trp5Me-Gly	TR5-135		
A0490	A6	A10	Phe-Glu-Pro-Ile-Trp-Gly	TR5-135		
A0491	A6	A11	Glu-Pro-Nal2-Met-Leu-Gly	TR5-135		
A0492	A6	A12	BAla-Glu-Pro-Lys-Bthi-Gly	TR5-135	884.4	y
A0493	A6	B1	Val-Glu-Pro-Bthi-Thr-Gly	TR5-135		
A0494	A6	B2	Glu-Pro-Glu-Orn-Phe4OMe-Gly	TR5-135		
A0495	A6	B3	Val-Glu-Pro-Trp5F-Bthi-Gly	TR5-135		
A0496	A6	B4	Glu-Pro-Pro-Tyr-Thi2-Gly	TR5-135		
A0497	A6	B5	Trp-Glu-Pro-Trp-Glu-Gly	TR5-135	972.4	y
A0498	A6	B6	Glu-Pro-Phe-Phe3OMe-Orn-Gly	TR5-135		
A0499	A6	B7	Trp-Glu-Pro-Val-Gly-Gly	TR5-135		
A0500	A6	B8	Glu-Pro-Thi2-Tyr3OMe-Trp5Br-Gly			
A0501	A6	B9	BAla-Glu-Pro-Trp-Trp5F-Gly	TR5-135		
A0502	A6	B10	Glu-Pro-Glu-Gly-Trp5Me-Gly	TR5-135		
A0503	A6	B11	Thi2-Glu-Pro-Nal1-Ile-Gly	TR5-135		
A0504	A6	B12	Glu-Pro-Asp-Asn-Tyr3OMe-Gly	TR5-135		
A0505	A6	C1	Glu-Pro-Phe3OMe-Tyr-Glu-Gly	TR5-135		
A0506	A6	C2	Phe-Glu-Pro-Trp-Trp5Br-Gly	TR5-135	1068.4	y
A0507	A6	C3	Glu-Pro-Asn-BAla-Trp5F-Gly	TR5-135		
A0508	A6	C4	Nal2-Glu-Pro-Nal2-Asn-Gly	TR5-135	979.4	y
A0509	A6	C5	Glu-Pro-Ser-Asn-Tyr3OMe-Gly	TR5-135		
A0510	A6	C6	Leu-Glu-Pro-Trp5F-Asp-Gly	TR5-135		
A0511	A6	C7	Glu-Pro-Trp-Nal1-Bthi-Gly	TR5-135		
A0512	A6	C8	Gly-Glu-Pro-Tyr-Leu-Gly	TR5-135		

A0513	A6	C9	Glu-Pro-Trp-Met-Ile-Gly	TR5-135		
A0514	A6	C10	Bthi-Glu-Pro-Trp-Ala-Gly	TR5-135		
A0515	A6	C11	Glu-Pro-Tyr3OMe-Nal2-Tyr3OMe-Gly			
A0516	A6	C12	Val-Glu-Pro-Phe4OMe-Trp5Me-Gly			
A0517	A6	D1	Leu-Glu-Pro-Tyr3OMe-Tyr3OMe-Gly			
A0518	A6	D2	Glu-Pro-Leu-Gly-Tyr3OMe-Gly	TR5-135		
A0519	A6	D3	Trp5Br-Glu-Pro-Thi2-Ser-Gly	TR5-135		
A0520	A6	D4	Glu-Pro-Val-Tyr-Val-Gly	TR5-135		
A0521	A6	D5	Bthi-Glu-Pro-Gln-Leu-Gly	TR5-135		
A0522	A6	D6	Glu-Pro-Bthi-Nal2-Asp-Gly	TR5-135	987.1	y
A0523	A6	D7	Gln-Glu-Pro-Phe3OMe-Orn-Gly	TR5-135		
A0524	A6	D8	Glu-Pro-Tyr3OMe-Trp-Ala-Gly	TR5-135	921.4	y
A0525	A6	D9	Asn-Glu-Pro-Ala-Trp5Br-Gly	TR5-135		
A0526	A6	D10	Glu-Pro-Leu-Ser-Nal2-Gly	TR5-135		
A0527	A6	D11	Asp-Glu-Pro-Trp5Me-BAla-Gly	TR5-135		
A0528	A6	D12	Glu-Pro-Nal1-Trp5Me-Phe3OMe-Gly			
A0529	A6	E1	Glu-Pro-Tyr-Pro-Asn-Gly	TR5-135	865.4	y
A0530	A6	E2	Nal1-Glu-Pro-Met-Trp5Br-Gly	TR5-135		
A0531	A6	E3	Glu-Pro-Bthi-Ile-Met-Gly	TR5-135		
A0532	A6	E4	Trp-Glu-Pro-Val-Lys-Gly	TR5-135		
A0533	A6	E5	Glu-Pro-Nal1-Asn-Bthi-Gly	TR5-135		
A0534	A6	E6	Gly-Glu-Pro-Phe4OMe-Glu-Gly	TR5-135		
A0535	A6	E7	Glu-Pro-Phe3OMe-Thi2-Pro-Gly	TR5-135		
A0536	A6	E8	Ser-Glu-Pro-Bthi-Orn-Gly	TR5-135		
A0537	A6	E9	Glu-Pro-Tyr3OMe-Bthi-Phe-Gly	TR5-135		
A0538	A6	E10	Ser-Glu-Pro-Phe4OMe-Gly-Gly	TR5-135		
A0539	A6	E11	Glu-Pro-Gln-Trp5Br-Ile-Gly	TR5-135		
A0540	A6	E12	Trp-Glu-Pro-Thi2-Lys-Gly	TR5-135		
A0541	A6	F1	Trp-Glu-Pro-Gly-Asn-Gly	TR5-135		
A0542	A6	F2	Glu-Pro-Thi2-Phe4OMe-Phe4OMe-Gly			
A0543	A6	F3	Trp5F-Glu-Pro-Tyr3OMe-Asn-Gly			
A0544	A6	F4	Glu-Pro-Trp5Me-Nal1-Phe3OMe-Gly			
A0545	A6	F5	Val-Glu-Pro-Met-Trp5Me-Gly	TR5-135	902.1	y
A0546	A6	F6	Glu-Pro-Phe-Ala-Nal2-Gly	TR5-135		
A0547	A6	F7	Trp-Glu-Pro-Nal1-Trp5F-Gly	TR5-135		
A0548	A6	F8	Glu-Pro-Gly-Phe4OMe-Thr-Gly	TR5-135		
A0549	A6	F9	Tyr3OMe-Glu-Pro-Leu-Asp-Gly	TR5-135	892.4	y
A0550	A6	F10	Glu-Pro-Pro-Trp-Tyr3OMe-Gly	TR5-135	947.4	y
A0551	A6	F11	Met-Glu-Pro-Ala-Met-Gly	TR5-135		
A0552	A6	F12	Glu-Pro-Met-Nal2-Orn-Gly	TR5-135		
A0553	A6	G1	Glu-Pro-Phe-Tyr3OMe-Nal1-Gly	TR5-135		
A0554	A6	G2	Asn-Glu-Pro-Tyr-Glu-Gly	TR5-135	877.9	y
A0555	A6	G3	Glu-Pro-Leu-Phe4OMe-Asp-Gly	TR5-135		
A0556	A6	G4	Asp-Glu-Pro-Phe3OMe-Gly-Gly	TR5-135		
A0557	A6	G5	Glu-Pro-Trp5F-Pro-Pro-Gly	TR5-135		
A0558	A6	G6	Gln-Glu-Pro-Gln-Bthi-Gly	TR5-135		
A0559	A6	G7	Glu-Pro-Orn-Tyr-Asn-Gly	TR5-135		
A0560	A6	G8	Tyr3OMe-Glu-Pro-Phe-Pro-Gly	TR5-135		
A0561	A6	G9	Glu-Pro-Met-Ser-Pro-Gly	TR5-135		
A0562	A6	G10	Phe3OMe-Glu-Pro-Val-Thr-Gly	TR5-135		
A0563	A6	G11	Glu-Pro-Ser-Trp5Me-Leu-Gly	TR5-135	871.4	y
A0564	A6	G12	Bthi-Glu-Pro-Ser-Trp5Br-Gly	TR5-135	1027	y
A0565	A6	H1	Thi2-Glu-Pro-Trp5Me-Glu-Gly	TR5-135	954.1	y
A0566	A6	H2	Glu-Pro-Phe4OMe-Nal1-Ser-Gly	TR5-135		
A0567	A6	H3	Leu-Glu-Pro-Trp5Br-Ser-Gly	TR5-135		
A0568	A6	H4	Glu-Pro-Pro-Trp5Me-Phe3OMe-Gly			
A0569	A6	H5	Gly-Glu-Pro-Orn-Phe4OMe-Gly	TR5-135		
A0570	A6	H6	Glu-Pro-Thr-Pro-Tyr-Gly	TR5-135		
A0571	A6	H7	Gln-Glu-Pro-Tyr3OMe-Orn-Gly	TR5-135		
A0572	A6	H8	Glu-Pro-Phe4OMe-Tyr3OMe-Ile-Gly		954.4	y
A0573	A6	H9	Phe-Glu-Pro-Asn-Thi2-Gly	TR5-135		

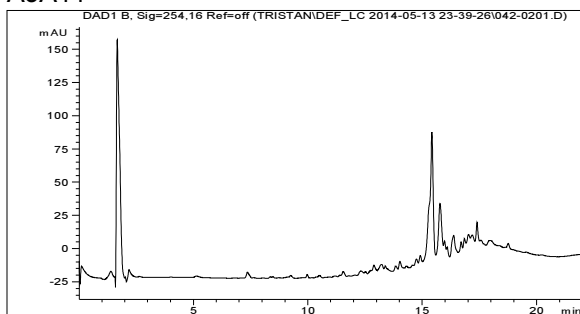
A0574	A6	H10	Glu-Pro-Phe4OMe-Tyr-Lys-Gly	TR5-135		
A0575	A6	H11	Leu-Glu-Pro-Bthi-Trp5F-Gly	TR5-135		
A0576	A6	H12	Glu-Pro-Phe-Met-Pro-Gly	TR5-135		

Quality Control HPLC-UV/MS analysis of random sequences

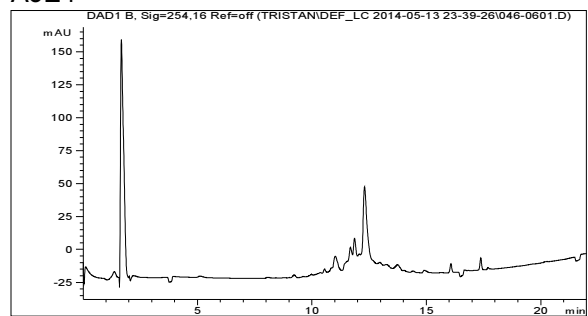
A3A1



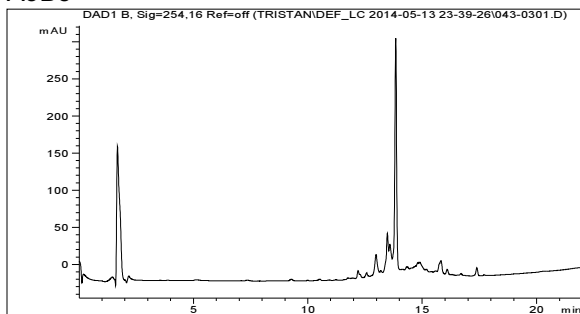
A3A11



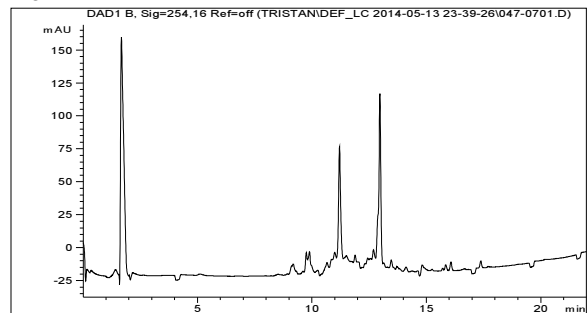
A3E4



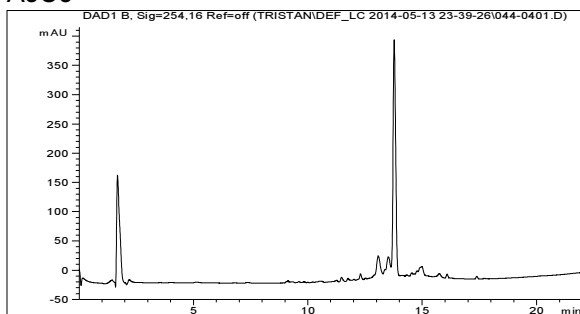
A3B8



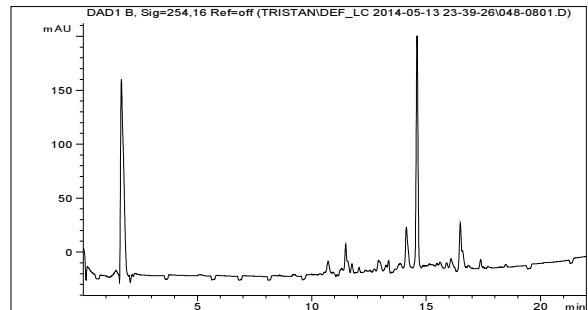
A3E12



A3C3

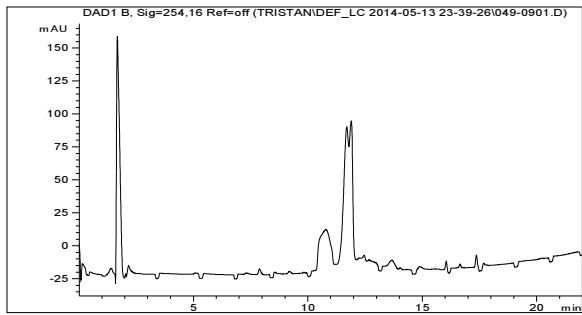


A3F7

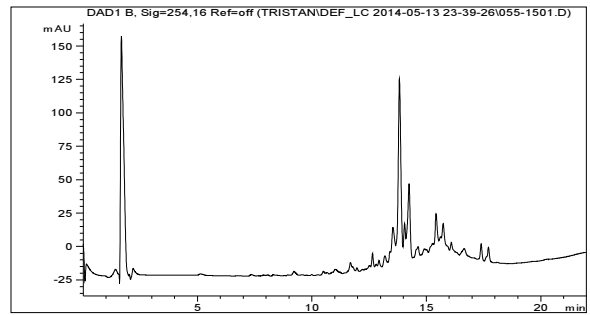


A3D5

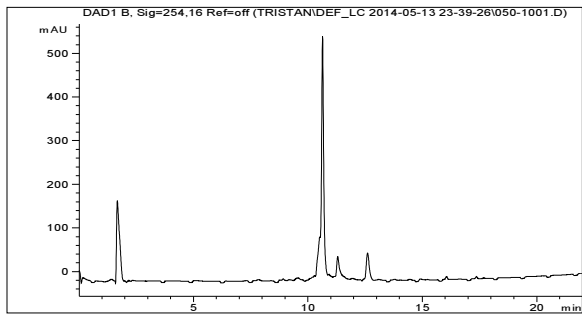
A3G9



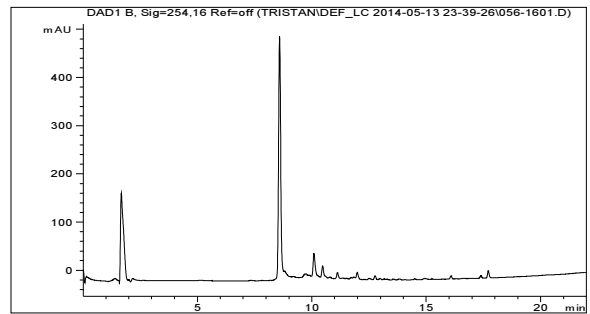
A3H10



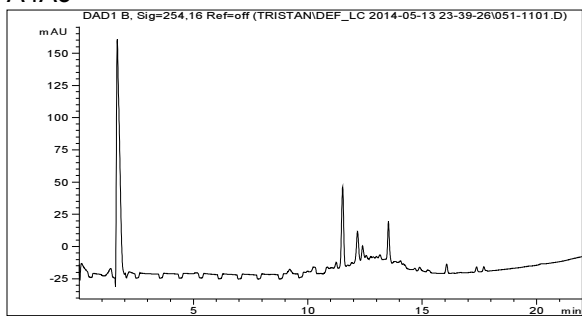
A4D7



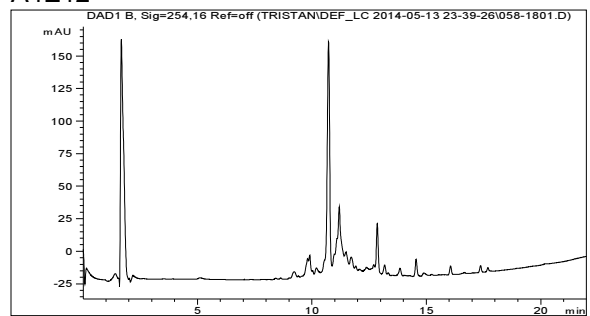
A4A3



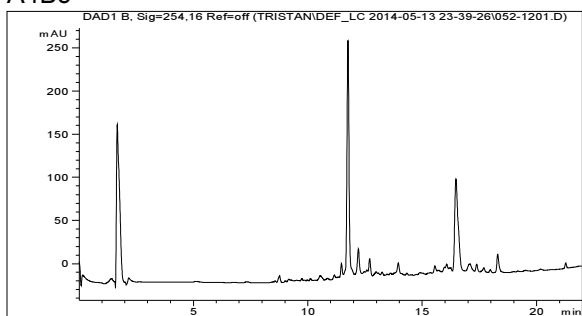
A4E12



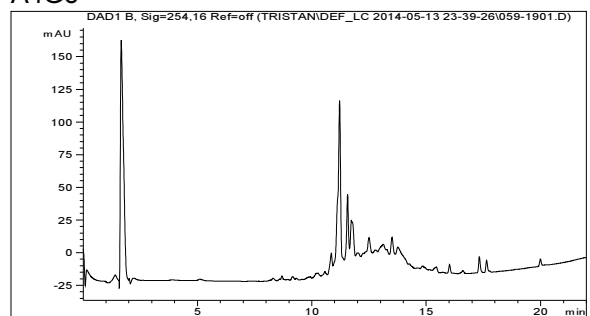
A4B5



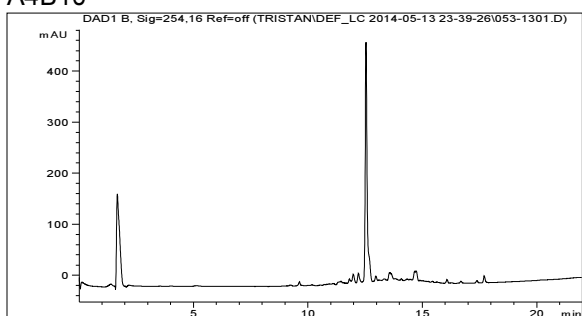
A4G8



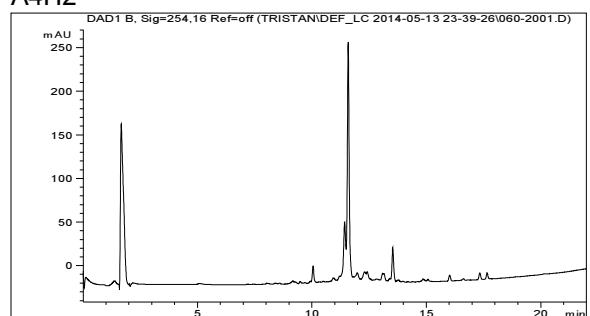
A4B10



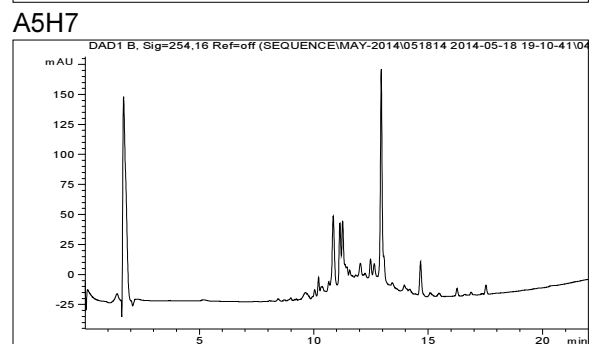
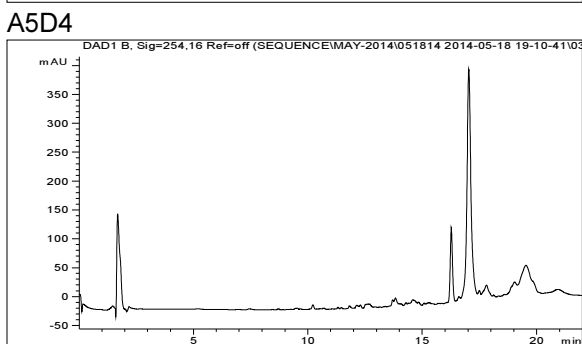
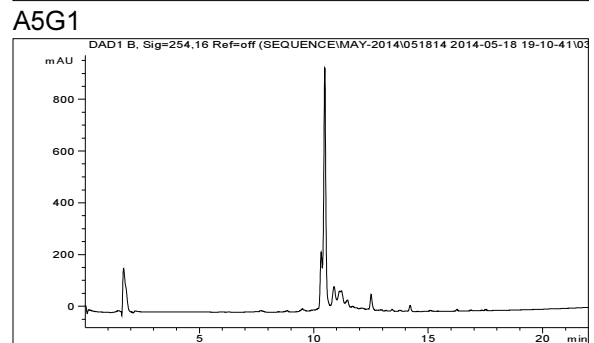
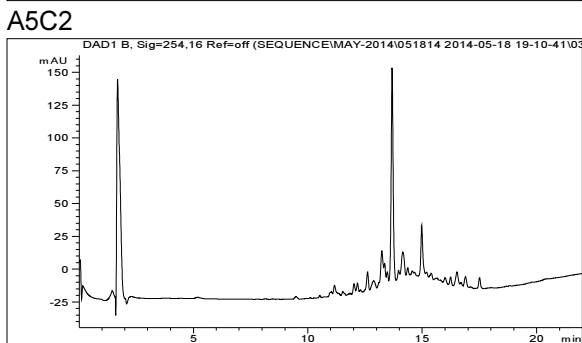
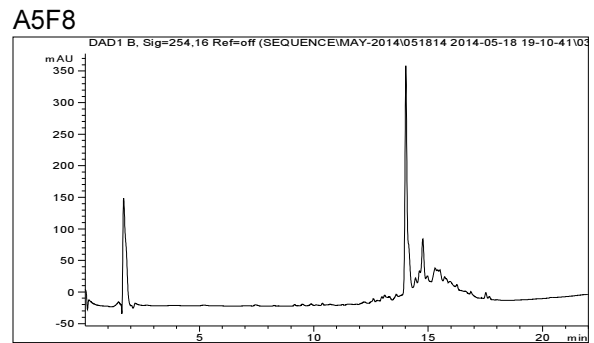
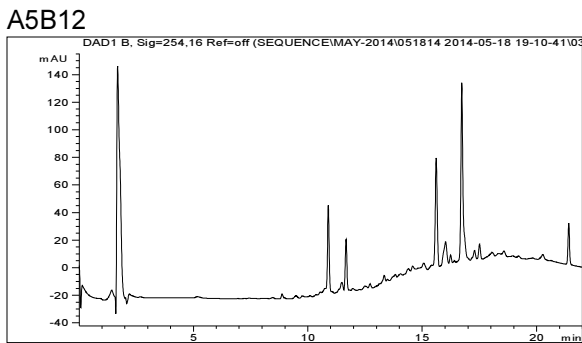
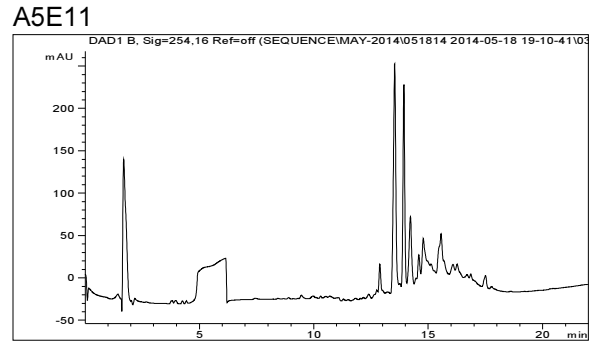
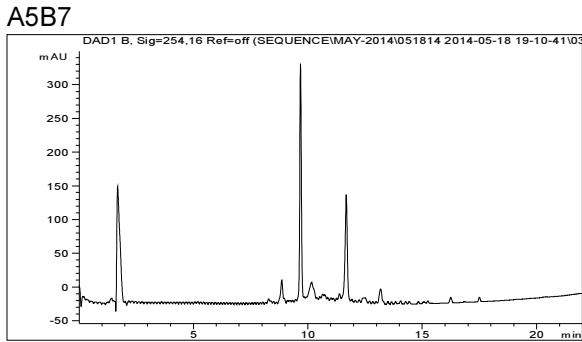
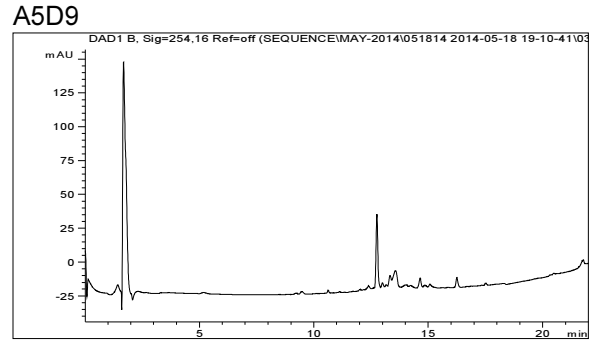
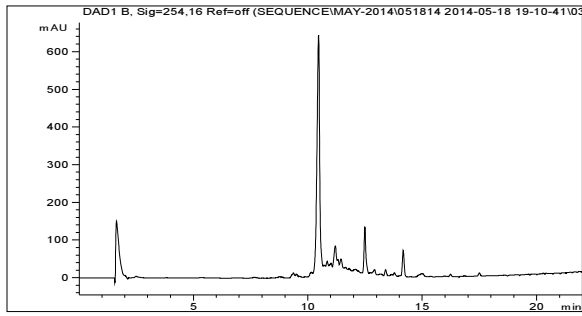
A4H2



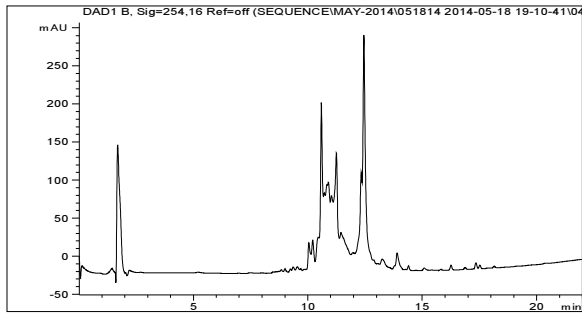
A4D1



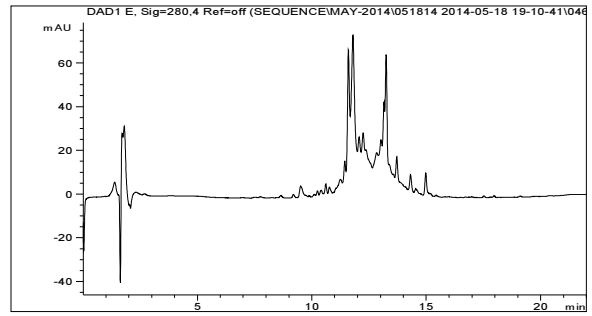
A5A5



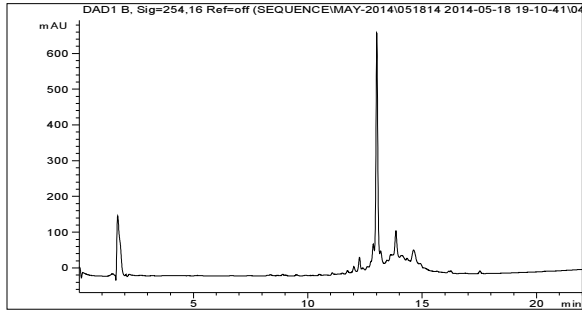
A6A12



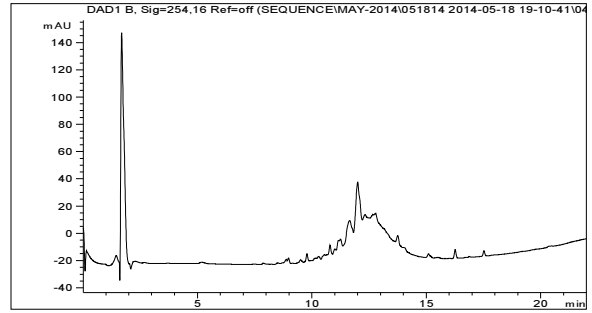
A6F9



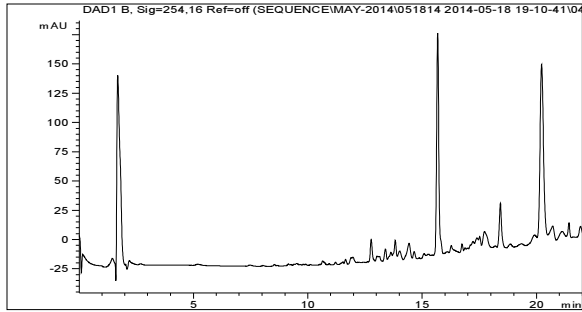
A6B5



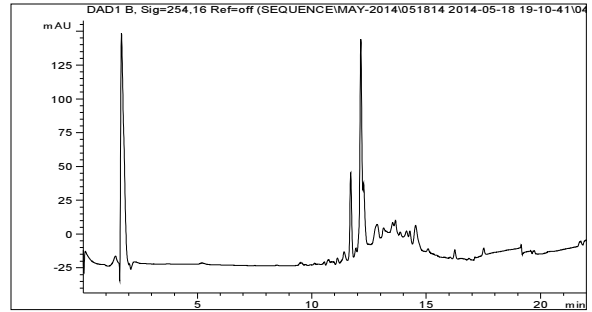
A6F10



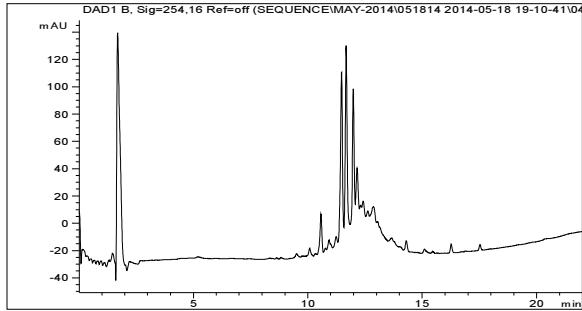
A6C4



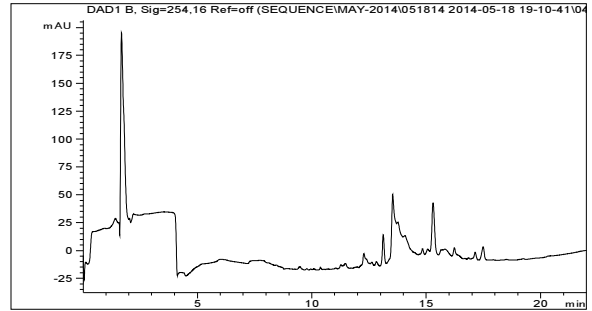
A6G11



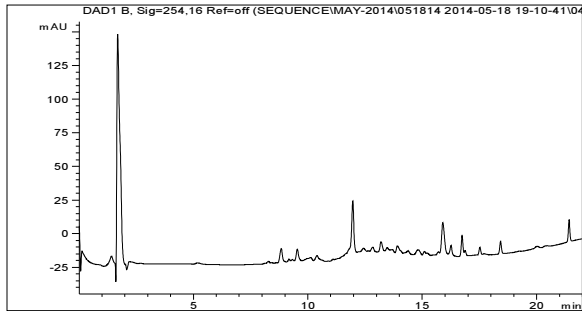
A6D8



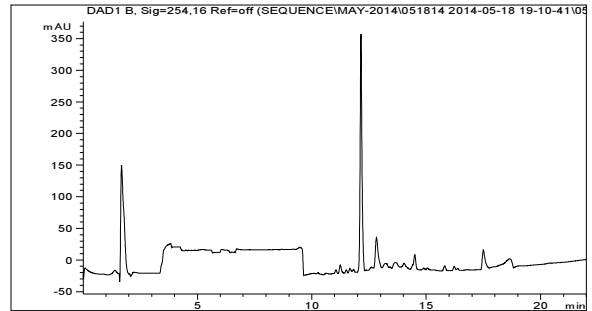
A6H2



A6E1



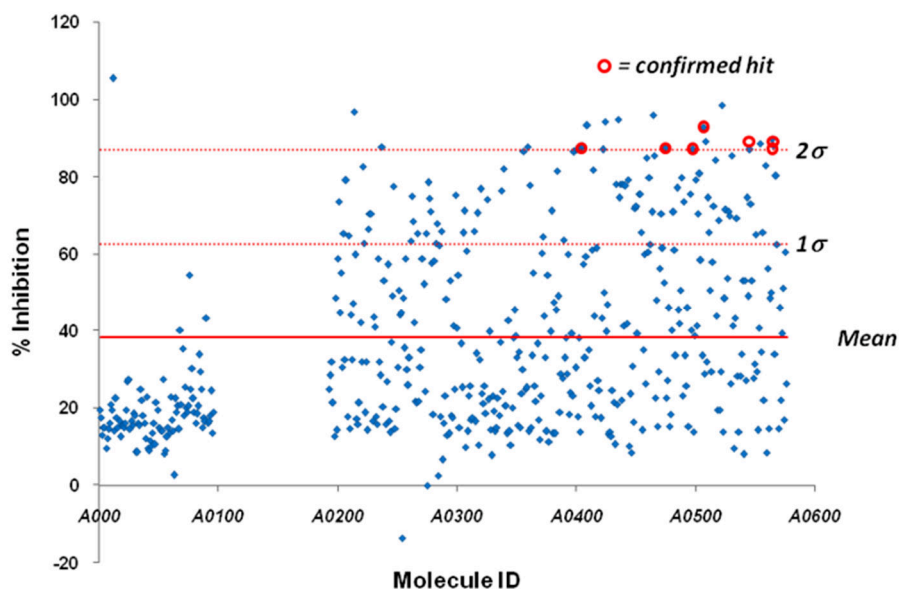
A6H8



Singlicate screening of Pilot Library A

Screening of Pilot Library A was carried out by competition binding against **L63*** (0.5 nM) and Pin1 (100 nM) in the same manner as for the determination of dissociation constants for non-labeled ligands. Data were normalized to 100% inhibition achieved by saturating concentrations (10 μ M) of *D*-PEPTIDE (**3**), and uninhibited negative controls were defined as 20 mP. Hits were defined as +2 σ above the mean over all data (mean = 38%, σ = 24%). Percent inhibition was defined as:

$$\%inh = \left[1 - \frac{P_{exp} - P_{(+)}}{P_{(-)} - P_{(+)}} \right] \times 100\%$$



Mol. ID.	Plate	Well	Hit?	%Inh. @ 10uM
A0001	A1	A1	n	19
A0002	A1	A2	n	17
A0003	A1	A3	n	13
A0004	A1	A4	n	15
A0005	A1	A5	n	15
A0006	A1	A6	n	10
A0007	A1	A7	n	12
A0008	A1	A8	n	14
A0009	A1	A9	n	16
A0010	A1	A10	n	21
A0011	A1	A11	n	19
A0012	A1	A12	y	105
A0013	A1	B1	n	14
A0014	A1	B2	n	22
A0015	A1	B3	n	17
A0016	A1	B4	n	15
A0017	A1	B5	n	16
A0018	A1	B6	n	13
A0019	A1	B7	n	15
A0020	A1	B8	n	15
A0021	A1	B9	n	15
A0022	A1	B10	n	16

A0023	A1	B11	n	19
A0024	A1	B12	n	27
A0025	A1	C1	n	27
A0026	A1	C2	n	14
A0027	A1	C3	n	16
A0028	A1	C4	n	15
A0029	A1	C5	n	18
A0030	A1	C6	n	18
A0031	A1	C7	n	9
A0032	A1	C8	n	9
A0033	A1	C9	n	16
A0034	A1	C10	n	15
A0035	A1	C11	n	25
A0036	A1	C12	n	22
A0037	A1	D1	n	18
A0038	A1	D2	n	16
A0039	A1	D3	n	12
A0040	A1	D4	n	23
A0041	A1	D5	n	10
A0042	A1	D6	n	9
A0043	A1	D7	n	12
A0044	A1	D8	n	10
A0045	A1	D9	n	14
A0046	A1	D10	n	16
A0047	A1	D11	n	11

A0048	A1	D12	n	21
A0049	A1	E1	n	19
A0050	A1	E2	n	15
A0051	A1	E3	n	14
A0052	A1	E4	n	14
A0053	A1	E5	n	14
A0054	A1	E6	n	27
A0055	A1	E7	n	8
A0056	A1	E8	n	9
A0057	A1	E9	n	13
A0058	A1	E10	n	15
A0059	A1	E11	n	14
A0060	A1	E12	n	23
A0061	A1	F1	n	17
A0062	A1	F2	n	14
A0063	A1	F3	n	3
A0064	A1	F4	n	22
A0065	A1	F5	n	19
A0066	A1	F6	n	20
A0067	A1	F7	n	14
A0068	A1	F8	n	40
A0069	A1	F9	n	21
A0070	A1	F10	n	35
A0071	A1	F11	n	18
A0072	A1	F12	n	25
A0073	A1	G1	n	20
A0074	A1	G2	n	19
A0075	A1	G3	n	20
A0076	A1	G4	n	55
A0077	A1	G5	n	25
A0078	A1	G6	n	30
A0079	A1	G7	n	22
A0080	A1	G8	n	19
A0081	A1	G9	n	16
A0082	A1	G10	n	18
A0083	A1	G11	n	20
A0084	A1	G12	n	34
A0085	A1	H1	n	29
A0086	A1	H2	n	25
A0087	A1	H3	n	15
A0088	A1	H4	n	17
A0089	A1	H5	n	16
A0090	A1	H6	n	43
A0091	A1	H7	n	16
A0092	A1	H8	n	16
A0093	A1	H9	n	18
A0094	A1	H10	n	24
A0095	A1	H11	n	14
A0096	A1	H12	n	19
A0097	*Note: Plate A2 unfilled to accommodate expansion of non-targeted library.			
A0192				
A0193	A3	A1	n	25
A0194	A3	A2	n	28
A0195	A3	A3	n	32
A0196	A3	A4	n	21
A0197	A3	A5	n	13
A0198	A3	A6	n	49
A0199	A3	A7	n	14
A0200	A3	A8	n	59
A0201	A3	A9	n	73
A0202	A3	A10	n	45

A0203	A3	A11	n	55
A0204	A3	A12	n	30
A0205	A3	B1	n	65
A0206	A3	B2	n	32
A0207	A3	B3	n	79
A0208	A3	B4	n	18
A0209	A3	B5	n	65
A0210	A3	B6	n	15
A0211	A3	B7	n	44
A0212	A3	B8	n	32
A0213	A3	B9	n	47
A0214	A3	B10	y	97
A0215	A3	B11	n	60
A0216	A3	B12	n	17
A0217	A3	C1	n	16
A0218	A3	C2	n	21
A0219	A3	C3	n	42
A0220	A3	C4	n	32
A0221	A3	C5	n	83
A0222	A3	C6	n	63
A0223	A3	C7	n	19
A0224	A3	C8	n	32
A0225	A3	C9	n	14
A0226	A3	C10	n	66
A0227	A3	C11	n	70
A0228	A3	C12	n	70
A0229	A3	D1	n	17
A0230	A3	D2	n	44
A0231	A3	D3	n	41
A0232	A3	D4	n	18
A0233	A3	D5	n	16
A0234	A3	D6	n	59
A0235	A3	D7	n	32
A0236	A3	D8	n	28
A0237	A3	D9	y	88
A0238	A3	D10	n	20
A0239	A3	D11	n	53
A0240	A3	D12	n	16
A0241	A3	E1	n	27
A0242	A3	E2	n	57
A0243	A3	E3	n	17
A0244	A3	E4	n	14
A0245	A3	E5	n	37
A0246	A3	E6	n	49
A0247	A3	E7	n	78
A0248	A3	E8	n	15
A0249	A3	E9	n	20
A0250	A3	E10	n	30
A0251	A3	E11	n	51
A0252	A3	E12	n	44
A0253	A3	F1	n	45
A0254	A3	F2	n	-14
A0255	A3	F3	n	49
A0256	A3	F4	n	35
A0257	A3	F5	n	59
A0258	A3	F6	n	30
A0259	A3	F7	n	26
A0260	A3	F8	n	33
A0261	A3	F9	n	63
A0262	A3	F10	n	75
A0263	A3	F11	n	68
A0264	A3	F12	n	42
A0265	A3	G1	n	22

A0266	A3	G2	n	21
A0267	A3	G3	n	65
A0268	A3	G4	n	22
A0269	A3	G5	n	30
A0270	A3	G6	n	35
A0271	A3	G7	n	59
A0272	A3	G8	n	52
A0273	A3	G9	n	24
A0274	A3	G10	n	65
A0275	A3	G11	n	0
A0276	A3	G12	n	79
A0277	A3	H1	n	74
A0278	A3	H2	n	71
A0279	A3	H3	n	58
A0280	A3	H4	n	18
A0281	A3	H5	n	58
A0282	A3	H6	n	63
A0283	A3	H7	n	68
A0284	A3	H8	n	3
A0285	A3	H9	n	62
A0286	A3	H10	n	18
A0287	A3	H11	n	66
A0288	A3	H12	n	7
A0289	A4	A1	n	16
A0290	A4	A2	n	23
A0291	A4	A3	n	48
A0292	A4	A4	n	13
A0293	A4	A5	n	13
A0294	A4	A6	n	53
A0295	A4	A7	n	18
A0296	A4	A8	n	18
A0297	A4	A9	n	41
A0298	A4	A10	n	25
A0299	A4	A11	n	75
A0300	A4	A12	n	41
A0301	A4	B1	n	55
A0302	A4	B2	n	15
A0303	A4	B3	n	37
A0304	A4	B4	n	25
A0305	A4	B5	n	65
A0306	A4	B6	n	71
A0307	A4	B7	n	10
A0308	A4	B8	n	61
A0309	A4	B9	n	14
A0310	A4	B10	n	23
A0311	A4	B11	n	26
A0312	A4	B12	n	17
A0313	A4	C1	n	18
A0314	A4	C2	n	66
A0315	A4	C3	n	16
A0316	A4	C4	n	34
A0317	A4	C5	n	71
A0318	A4	C6	n	10
A0319	A4	C7	n	32
A0320	A4	C8	n	77
A0321	A4	C9	n	24
A0322	A4	C10	n	21
A0323	A4	C11	n	26
A0324	A4	C12	n	19
A0325	A4	D1	n	74
A0326	A4	D2	n	22
A0327	A4	D3	n	40
A0328	A4	D4	n	14

A0329	A4	D5	n	8
A0330	A4	D6	n	23
A0331	A4	D7	n	19
A0332	A4	D8	n	14
A0333	A4	D9	n	15
A0334	A4	D10	n	23
A0335	A4	D11	n	18
A0336	A4	D12	n	37
A0337	A4	E1	n	76
A0338	A4	E2	n	24
A0339	A4	E3	n	82
A0340	A4	E4	n	21
A0341	A4	E5	n	21
A0342	A4	E6	n	13
A0343	A4	E7	n	43
A0344	A4	E8	n	14
A0345	A4	E9	n	10
A0346	A4	E10	n	20
A0347	A4	E11	n	38
A0348	A4	E12	n	45
A0349	A4	F1	n	39
A0350	A4	F2	n	33
A0351	A4	F3	n	15
A0352	A4	F4	n	35
A0353	A4	F5	n	15
A0354	A4	F6	n	24
A0355	A4	F7	n	30
A0356	A4	F8	n	87
A0357	A4	F9	n	25
A0358	A4	F10	n	25
A0359	A4	F11	y	88
A0360	A4	F12	n	14
A0361	A4	G1	n	78
A0362	A4	G2	n	15
A0363	A4	G3	n	34
A0364	A4	G4	n	55
A0365	A4	G5	n	26
A0366	A4	G6	n	22
A0367	A4	G7	n	37
A0368	A4	G8	n	17
A0369	A4	G9	n	12
A0370	A4	G10	n	23
A0371	A4	G11	n	60
A0372	A4	G12	n	64
A0373	A4	H1	n	44
A0374	A4	H2	n	33
A0375	A4	H3	n	14
A0376	A4	H4	n	55
A0377	A4	H5	n	11
A0378	A4	H6	n	40
A0379	A4	H7	n	71
A0380	A4	H8	n	13
A0381	A4	H9	n	47
A0382	A4	H10	n	13
A0383	A4	H11	n	45
A0384	A4	H12	n	81
A0385	A5	A1	n	49
A0386	A5	A2	n	19
A0387	A5	A3	n	29
A0388	A5	A4	n	28
A0389	A5	A5	n	64
A0390	A5	A6	n	33
A0391	A5	A7	n	38

A0392	A5	A8	n	29
A0393	A5	A9	n	60
A0394	A5	A10	n	18
A0395	A5	A11	n	24
A0396	A5	A12	n	39
A0397	A5	B1	n	23
A0398	A5	B2	n	86
A0399	A5	B3	n	30
A0400	A5	B4	y	87
A0401	A5	B5	n	18
A0402	A5	B6	n	38
A0403	A5	B7	n	14
A0404	A5	B8	y	88
A0405	A5	B9	y	88
A0406	A5	B10	n	57
A0407	A5	B11	n	33
A0408	A5	B12	n	59
A0409	A5	C1	y	93
A0410	A5	C2	n	35
A0411	A5	C3	n	26
A0412	A5	C4	n	20
A0413	A5	C5	n	61
A0414	A5	C6	n	82
A0415	A5	C7	n	44
A0416	A5	C8	n	18
A0417	A5	C9	n	62
A0418	A5	C10	n	27
A0419	A5	C11	n	25
A0420	A5	C12	n	17
A0421	A5	D1	n	43
A0422	A5	D2	y	87
A0423	A5	D3	n	50
A0424	A5	D4	y	94
A0425	A5	D5	n	40
A0426	A5	D6	n	47
A0427	A5	D7	n	13
A0428	A5	D8	n	14
A0429	A5	D9	n	13
A0430	A5	D10	n	25
A0431	A5	D11	n	21
A0432	A5	D12	n	11
A0433	A5	E1	n	78
A0434	A5	E2	n	21
A0435	A5	E3	y	95
A0436	A5	E4	n	75
A0437	A5	E5	n	78
A0438	A5	E6	n	22
A0439	A5	E7	n	78
A0440	A5	E8	n	41
A0441	A5	E9	n	78
A0442	A5	E10	n	42
A0443	A5	E11	n	79
A0444	A5	E12	n	10
A0445	A5	F1	n	24
A0446	A5	F2	n	8
A0447	A5	F3	n	31
A0448	A5	F4	n	16
A0449	A5	F5	n	72
A0450	A5	F6	n	72
A0451	A5	F7	n	39
A0452	A5	F8	n	76
A0453	A5	F9	n	76
A0454	A5	F10	n	66

A0455	A5	F11	n	14
A0456	A5	F12	n	35
A0457	A5	G1	n	60
A0458	A5	G2	n	26
A0459	A5	G3	n	85
A0460	A5	G4	n	60
A0461	A5	G5	n	80
A0462	A5	G6	n	63
A0463	A5	G7	n	71
A0464	A5	G8	y	96
A0465	A5	G9	n	85
A0466	A5	G10	n	23
A0467	A5	G11	n	48
A0468	A5	G12	n	15
A0469	A5	H1	n	29
A0470	A5	H2	n	56
A0471	A5	H3	n	70
A0472	A5	H4	n	62
A0473	A5	H5	n	53
A0474	A5	H6	y	88
A0475	A5	H7	n	23
A0476	A5	H8	n	27
A0477	A5	H9	n	46
A0478	A5	H10	n	15
A0479	A5	H11	n	18
A0480	A5	H12	n	40
A0481	A6	A1	n	71
A0482	A6	A2	n	61
A0483	A6	A3	n	33
A0484	A6	A4	n	77
A0485	A6	A5	n	45
A0486	A6	A6	n	42
A0487	A6	A7	n	51
A0488	A6	A8	n	80
A0489	A6	A9	n	23
A0490	A6	A10	n	73
A0491	A6	A11	n	33
A0492	A6	A12	n	26
A0493	A6	B1	n	46
A0494	A6	B2	n	15
A0495	A6	B3	n	76
A0496	A6	B4	n	40
A0497	A6	B5	y	87
A0498	A6	B6	n	14
A0499	A6	B7	n	39
A0500	A6	B8	n	79
A0501	A6	B9	n	41
A0502	A6	B10	n	70
A0503	A6	B11	n	81
A0504	A6	B12	n	58
A0505	A6	C1	n	33
A0506	A6	C2	y	93
A0507	A6	C3	n	29
A0508	A6	C4	y	89
A0509	A6	C5	n	32
A0510	A6	C6	n	75
A0511	A6	C7	n	66
A0512	A6	C8	n	51
A0513	A6	C9	n	29
A0514	A6	C10	n	58
A0515	A6	C11	n	72
A0516	A6	C12	n	84
A0517	A6	D1	n	44

A0518	A6	D2	n	19
A0519	A6	D3	n	69
A0520	A6	D4	n	19
A0521	A6	D5	n	29
A0522	A6	D6	y	98
A0523	A6	D7	n	14
A0524	A6	D8	n	49
A0525	A6	D9	n	71
A0526	A6	D10	n	54
A0527	A6	D11	n	71
A0528	A6	D12	n	70
A0529	A6	E1	n	26
A0530	A6	E2	n	85
A0531	A6	E3	n	41
A0532	A6	E4	n	10
A0533	A6	E5	n	43
A0534	A6	E6	n	69
A0535	A6	E7	n	28
A0536	A6	E8	n	14
A0537	A6	E9	n	28
A0538	A6	E10	n	34
A0539	A6	E11	n	53
A0540	A6	E12	n	8
A0541	A6	F1	n	53
A0542	A6	F2	n	27
A0543	A6	F3	n	75
A0544	A6	F4	n	49
A0545	A6	F5	y	87
A0546	A6	F6	n	73
A0547	A6	F7	n	53

A0548	A6	F8	n	28
A0549	A6	F9	n	31
A0550	A6	F10	n	65
A0551	A6	F11	n	29
A0552	A6	F12	n	14
A0553	A6	G1	n	41
A0554	A6	G2	y	89
A0555	A6	G3	n	34
A0556	A6	G4	n	66
A0557	A6	G5	n	22
A0558	A6	G6	n	83
A0559	A6	G7	n	8
A0560	A6	G8	n	56
A0561	A6	G9	n	15
A0562	A6	G10	n	49
A0563	A6	G11	n	50
A0564	A6	G12	y	90
A0565	A6	H1	y	88
A0566	A6	H2	n	34
A0567	A6	H3	n	80
A0568	A6	H4	n	63
A0569	A6	H5	n	15
A0570	A6	H6	n	46
A0571	A6	H7	n	22
A0572	A6	H8	n	39
A0573	A6	H9	n	51
A0574	A6	H10	n	17
A0575	A6	H11	n	60
A0576	A6	H12	n	26

HPLC Analysis of hits & re-screening at 1 μM

All hits were analyzed by HPLC-UV/MS using the following method. Intractable mixtures comprising non-isomeric or non-cyclic material were not pursued.

Analytical HPLC method A:

Column: Agilent XBD C₁₈, 4.6x150mm, 5 μm .

Solvent A: H₂O + 0.1%v TFA

Solvent B: ACN + 0.1%v TFA

Flow rate: 1.00 ml/min

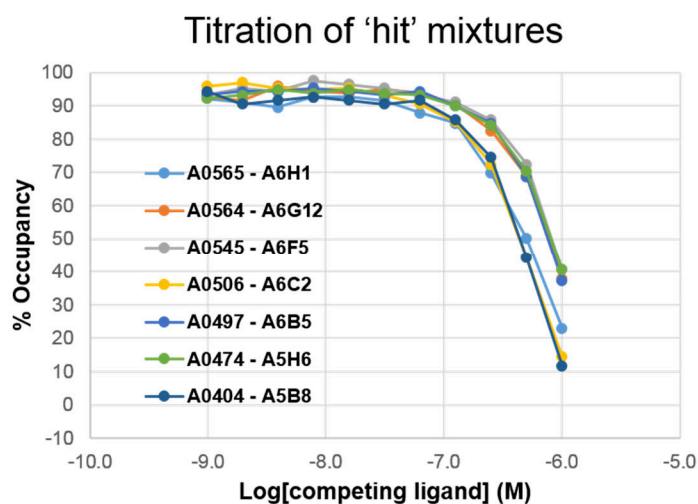
Time	%B
0	15
0.5	15
18	100
20	100
22	15
23	15

Hits (see below) were cherry picked and re-screened in the same manner as for the primary screen, but at 1 μM . Those which retained activity were titrated by a 2x serial dilution from 1 μM . IC₅₀ was determined as follows based on estimated aggregate mixture concentration.

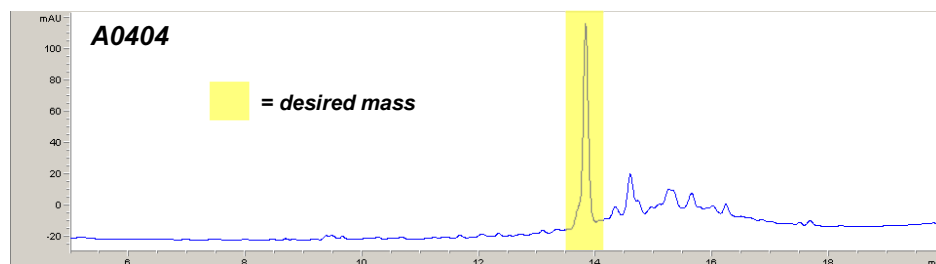
$$\%occupancy = \frac{100\%}{1 + [I]/I_{50}} \quad \text{and} \quad IC_{50} = I_{50} - [E]/2$$

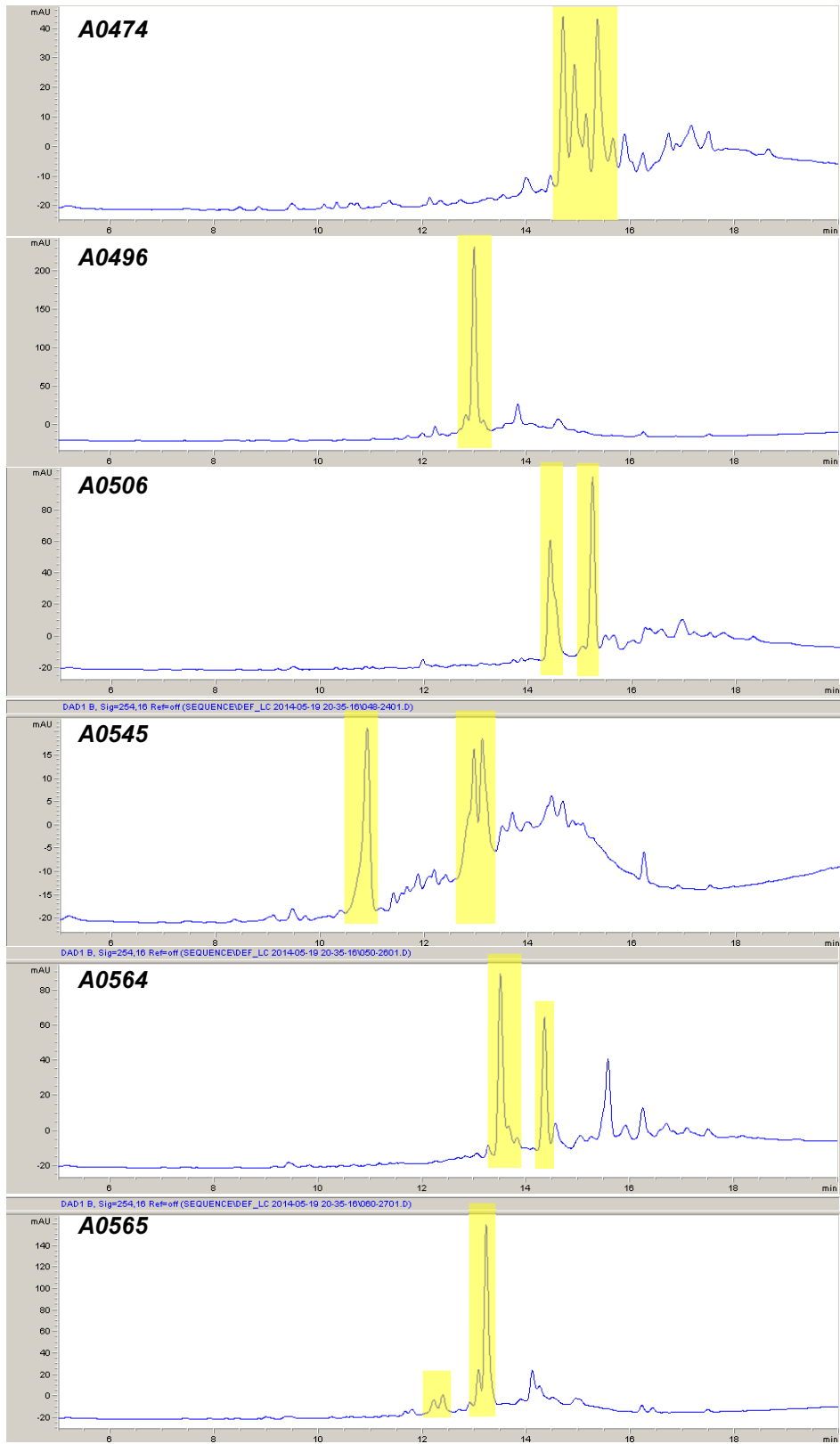
Mol. ID.	Plate	Well	Hit?	%Inh. 10 μM	%Inh. 1 μM	Sequence
A0012	A1	A12	y	105	5	Ala-Phe(3OMe)-Ala-Ala-Ala-Gly
A0214	A3	B10	y	97	19	Nal2-Phe-Glu-Pro-Bthi-Gly

A0237	A3	D9	y	88	26	Nal1-Glu-Pro-Tyr-Glu-Gly
A0359	A4	F11	y	88	22	Bthi-Ile-Glu-Pro-Nal1-Gly
A0400	A5	B4	y	87	30	Nal1-Glu-Pro-Phe3OMe-Tyr3OMe-Gly
A0404	A5	B8	y	88	92	Trp5Br-Glu-Pro-Bthi-Asp-Gly
A0405	A5	B9	y	88	17	Glu-Pro-Nal1-Glu-Nal2-Gly
A0409	A5	C1	y	93	37	Phe4OMe-Glu-Pro-Thi2-Tyr-Gly
A0422	A5	D2	y	87	34	Tyr-Glu-Pro-Pro-Trp5F-Gly
A0424	A5	D4	y	94	37	Thi2-Glu-Pro-Nal1-Bthi-Gly
A0435	A5	E3	y	95	31	Nal2-Glu-Pro-Phe-Thi2-Gly
A0464	A5	G8	y	96	10	Glu-Pro-Trp5F-Gly-Glu-Gly
A0474	A5	H6	y	88	88	Nal1-Glu-Pro-Trp5F-Trp-Gly
A0497	A6	B5	y	87	75	Trp-Glu-Pro-Trp-Glu-Gly
A0506	A6	C2	y	93	94	Phe-Glu-Pro-Trp-Trp5Br-Gly
A0508	A6	C4	y	89	85	Nal2-Glu-Pro-Nal2-Asn-Gly
A0522	A6	D6	y	98	41	Glu-Pro-Bthi-Nal2-Asp-Gly
A0545	A6	F5	y	87	70	Val-Glu-Pro-Met-Trp5Me-Gly
A0554	A6	G2	y	89	74	Asn-Glu-Pro-Tyr-Glu-Gly
A0564	A6	G12	y	90	69	Bthi-Glu-Pro-Ser-Trp5Br-Gly
A0565	A6	H1	y	88	66	Thi2-Glu-Pro-Trp5Me-Glu-Gly



<i>IC₅₀</i> (nM)	Sequence
A0404 – 420	Trp5Br-Glu-Pro-Bthi-Asp-Gly
A0474 – 940	Nal1-Glu-Pro-Trp5F-Trp-Gly
A0496 – 880	Trp-Glu-Pro-Trp-Glu-Gly
A0506 – 430	Phe-Glu-Pro-Trp-Trp5Br-Gly
A0545 – 990	Val-Glu-Pro-Met-Trp5Me-Gly
A0564 – 870	Bthi-Glu-Pro-Ser-Trp5Br-Gly
A0565 – 470	Thi2-Glu-Pro-Trp5Me-Glu-Gly





Re-synthesis & assay of hits, des-glycine congeners & acyclic congeners

Hit sequences (25 μmol) were assembled on 2-chlorotrityl polystyrene resin pre-loaded with glycine (0.64 mmol/g) in the same manner as for the library synthesis, except that couplings were 60 minutes and deprotections were 1 min then 30 min and template **5** was reacted overnight. Side chain protected acyclic intermediates were released from the resin by treatment with 1:1:8 AcOH:TFE:DCM for 1 hr, concentrated, and purified by column chromatography on SiO_2 eluted with 4 \rightarrow 8% MeOH in DCM + 2%v AcOH to give protected linear intermediates: **lin-A0404** (11.5 mg); **lin-A0474** (11.6 mg); **lin-A0496** (12.4 mg); **lin-A0506** (12.2 mg); **lin-A0545** (8.6 mg); **lin-A0564** (11.4 mg); **lin-A0565** (10.3 mg) These materials were individually reacted with 5%v TFA in MeNO_2 for 4.5 hr, then concentrated, dissolved in DMSO and fractionated by preparative HPLC method B.

The des-glycine, C-terminal carboxamide analogs of the same seven hit sequences lacking Gly6 (25 μmol) were assembled on Rink amide MBHA resin, released from the resin by treatment with 95:5 TFA:H₂O and a small amount of iPr_3SiH for 4 hrs, or TFA:PhSMe:H₂O: iPr_3SiH (90:5:2.5:2.5) for 1 hr in the case of A0565. Crude peptides were recovered by precipitation from cold Et₂O and centrifugation, dried, and subsequently reacted with template **5** (1 eq) and iPr_2EtN (5 eq) in DMF (500 μL) for 3 hrs. The resulting mixtures were purified directly by preparative HPLC method A. The intermediates of sequences A0474 and A0506 were re-purified by column chromatography on SiO_2 eluted with 0 \rightarrow 8% MeOH in DCM + 2%v AcOH to give des-glycine linear intermediates: **lin-A0404 Δ Gly** (17.3 mg); **lin-A0474 Δ Gly** (8.2 mg); **lin-A0496 Δ Gly** (9.3 mg); **lin-A0506 Δ Gly** (11.6 mg); **lin-A0545 Δ Gly** (6.7 mg); **lin-A0564 Δ Gly** (13.4 mg); **lin-A0565 Δ Gly** (13.5 mg, 59%). These materials were individually reacted with 5%v TFA in MeNO_2 for 4.5 hr, then concentrated, dissolved in DMSO and fractionated by preparative HPLC method B.

Preparative HPLC method A:

Column: Waters Sunfire C₁₈, 19x150mm, 5 μm .

Solvent A: H₂O + 0.1%v TFA

Solvent B: ACN + 0.1%v TFA

Flow rate: 20.00 ml/min

Time	%B
0	20
1	20
4	58
19	75

Preparative HPLC method B:

Column: Waters Sunfire C₁₈, 19x250mm, 5 μm .

Solvent A: H₂O + 0.1%v TFA

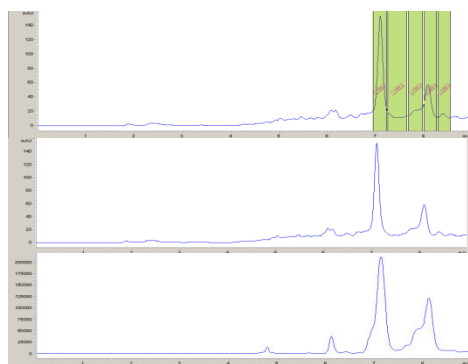
Solvent B: ACN + 0.1%v TFA

Flow rate: 18.00 ml/min

Time	%B
0	30
1	30
3	55
18	80

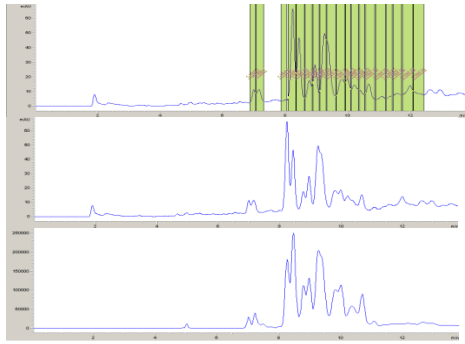
Acidolysis of re-synthesized hits (+Gly):

A0404



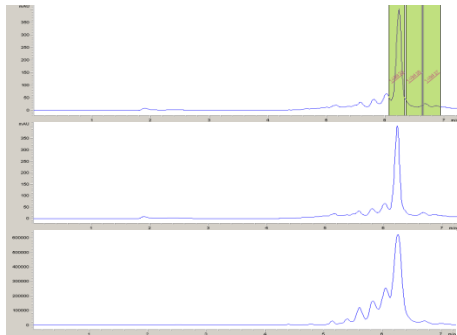
	fxn#	tare (g)	gross (g)	net (mg)	MW	vol. to 10mM (μL)
TR5-153A	1	2.60637	2.60832	1.95	1055.0	185
TR5-153B	3	2.61111	2.61183	0.72		68
TR5-153C	4	2.6127	2.61372	1.02		97

A0474



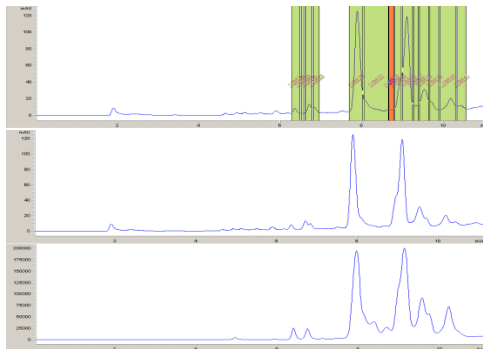
	fxn#	tare (g)	gross (g)	net (mg)	MW	vol. to 10mM (μ L)
TR5-154A	6,7	2.60586	2.60651	0.65	1059.2	61
TR5-154B	9	2.61337	2.61425	0.88		83
TR5-154C	18	2.61312	2.61402	0.90		85
TR5-154D	17	2.61931	2.61973	0.42		40
TR5-154E	16	2.61003	2.61052	0.49		46
TR5-154F	15	2.61463	2.61523	0.60		57
TR5-154G	14	2.61659	2.61733	0.74		70
TR5-154H	13	2.61316	2.61366	0.50		47
TR5-154I	12	2.62501	2.62542	0.41		39
TR5-154J	11,10	2.61984	2.62058	0.74		70
TR5-154K	19	2.61309	2.61351	0.42		40

A0496



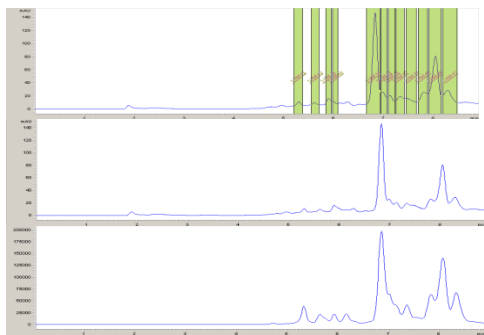
	fxn#	tare (g)	gross (g)	net (mg)	MW	vol. to 10mM (μ L)
TR5-155A	25	2.61602	2.62054	4.52	973.1	464

A0506



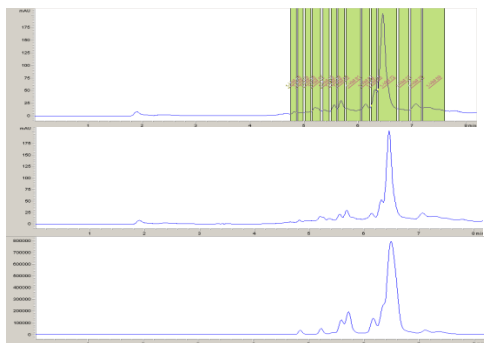
	fxn#	tare (g)	gross (g)	net (mg)	MW	vol. to 10mM (μ L)
TR5-156A	32	2.61934	2.62093	1.59	1070.0	149
TR5-156B	31	2.62739	2.62819	0.80		75
TR5-156C	29	2.59694	2.59735	0.41		38
TR5-156D	28	2.6231	2.62463	1.53		143
TR5-156E	38	2.61036	2.61109	0.73		68
TR5-156F	39	2.62107	2.62154	0.47		44
TR5-156G	40	2.61146	2.61200	0.54		50

A0545



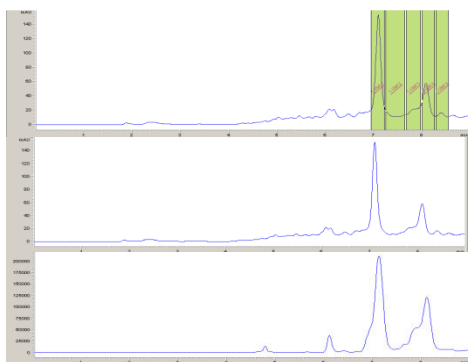
	fxn#	tare (g)	gross (g)	net (mg)	MW	vol. to 10mM (μL)
	TR5-158A	54	2.60808	2.60941	1.33	1027.0
	TR5-158B	53	2.61446	2.61485	0.39	38
	TR5-158C	52	2.62081	2.62115	0.34	33
	TR5-158D	51	2.62562	2.62597	0.35	34
	TR5-158E	50	2.61016	2.61053	0.37	36
	TR5-158F	49	2.60383	2.60420	0.37	36
	TR5-158G	58	2.61065	2.61167	1.02	99
	TR5-158H	47	2.61191	2.61263	0.72	70

A0564



	fxn#	tare (g)	gross (g)	net (mg)	MW	vol. to 10mM (μL)
	TR5-159A	59	2.62310	2.62340	0.30	954.1
	TR5-159B	60	2.61635	2.61677	0.42	44
	TR5-159C	62	2.60892	2.60926	0.34	36
	TR5-159D	63	2.60134	2.60170	0.36	38
	TR5-159E	72	2.61715	2.62112	3.97	416
	blank		2.61293	2.61292	-0.01	

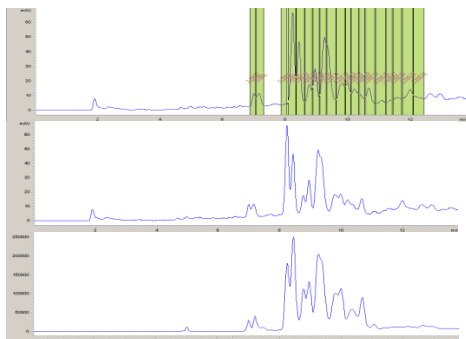
A0565



	fxn#	tare (g)	gross (g)	net (mg)	MW	vol. to 10mM (μL)
	TR5-153A	1	2.60637	2.60832	1.95	1055.0
	TR5-153B	3	2.61111	2.61183	0.72	68
	TR5-153C	4	2.6127	2.61372	1.02	97

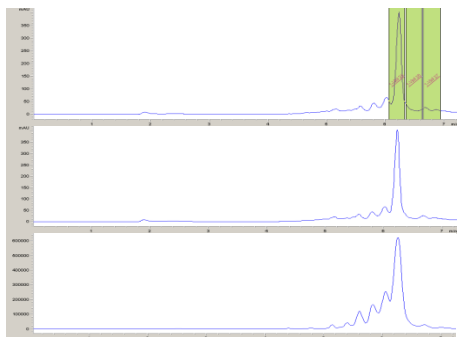
Acidolysis of re-synthesized hits (-Gly):

A0474ΔG



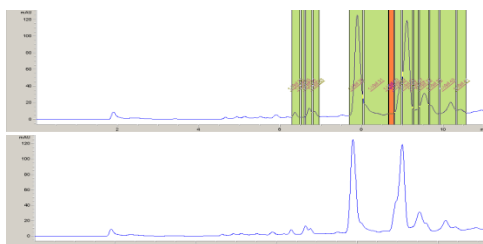
	fxn#	tare (g)	gross (g)	net (mg)	MW	vol. to 10mM (μL)
TR5-154A	6,7	2.60586	2.60651	0.65	1059.2	61
TR5-154B	9	2.61337	2.61425	0.88		83
TR5-154C	18	2.61312	2.61402	0.90		85
TR5-154D	17	2.61931	2.61973	0.42		40
TR5-154E	16	2.61003	2.61052	0.49		46
TR5-154F	15	2.61463	2.61523	0.60		57
TR5-154G	14	2.61659	2.61733	0.74		70
TR5-154H	13	2.61316	2.61366	0.50		47
TR5-154I	12	2.62501	2.62542	0.41		39
TR5-154J	11,10	2.61984	2.62058	0.74		70
TR5-154K	19	2.61309	2.61351	0.42		40

A0496ΔG



	fxn#	tare (g)	gross (g)	net (mg)	MW	vol. to 10mM (μL)
TR5-155A	25	2.61602	2.62054	4.52	973.1	464

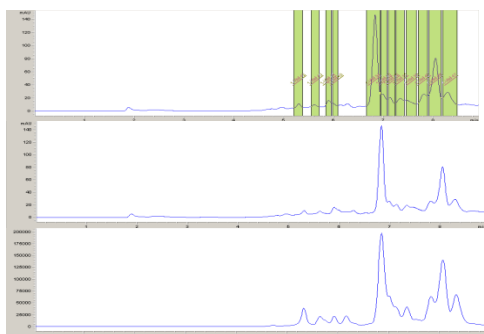
A0506ΔG





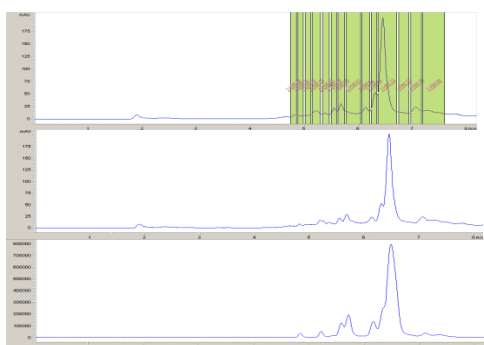
	fxn#	tare (g)	gross (g)	net (mg)	MW	vol. to 10mM (μL)	
	TR5-156A	32	2.61934	2.62093	1.59	1070.0	149
	TR5-156B	31	2.62739	2.62819	0.80		75
	TR5-156C	29	2.59694	2.59735	0.41		38
	TR5-156D	28	2.6231	2.62463	1.53		143
	TR5-156E	38	2.61036	2.61109	0.73		68
	TR5-156F	39	2.62107	2.62154	0.47		44
	TR5-156G	40	2.61146	2.61200	0.54		50

A0564ΔG



	fxn#	tare (g)	gross (g)	net (mg)	MW	vol. to 10mM (μL)	
	TR5-158A	54	2.60808	2.60941	1.33	1027.0	130
	TR5-158B	53	2.61446	2.61485	0.39		38
	TR5-158C	52	2.62081	2.62115	0.34		33
	TR5-158D	51	2.62562	2.62597	0.35		34
	TR5-158E	50	2.61016	2.61053	0.37		36
	TR5-158F	49	2.60383	2.60420	0.37		36
	TR5-158G	58	2.61065	2.61167	1.02		99
	TR5-158H	47	2.61191	2.61263	0.72		70

A0565ΔG



	fxn#	tare (g)	gross (g)	net (mg)	MW	vol. to 10mM (μL)	
	TR5-159A	59	2.62310	2.62340	0.30	954.1	31
	TR5-159B	60	2.61635	2.61677	0.42		44
	TR5-159C	62	2.60892	2.60926	0.34		36
	TR5-159D	63	2.60134	2.60170	0.36		38
	TR5-159E	72	2.61715	2.62112	3.97		416
	blank		2.61293	2.61292	-0.01		

Screening of re-synthesized mixtures & des-glycine analogs

Mixtures:

Sequence	Re-synthesized		Cyclo (Δ Gly)		Acyclic (seco- Δ Gly)	
	Cmpd	IC ₅₀ (μ M)	Cmpd	IC ₅₀ (μ M)	Cmpd	IC ₅₀ (μ M)
Trp(5Br)-Glu-Pro-Bthi-Asp-[Gly]	TR5-153 (A0434)	0.2	TR5-145 (A0434 Δ Gly)	0.7	TR5-143A (seco-A0434 Δ Gly)	9.6
1Nal-Glu-Pro-Trp(5F)-Trp-[Gly]	TR5-154 (A0474)	1.7	TR5-146 (A0474 Δ Gly)	4.0	TR5-143B (seco-A0474 Δ Gly)	7.0
Trp-Glu-Pro-Trp-Glu-[Gly]	TR5-155 (A0497)	2.1	TR5-147 (A0497 Δ Gly)	8.0	TR5-143C (seco-A0497 Δ Gly)	19
Phe-Glu-Pro-Trp-Trp(5Br)-[Gly]	TR5-156 (A0506)	2.1	TR5-148 (A0506 Δ Gly)	5.3	TR5-143D (seco-A0506 Δ Gly)	8.8
Val-Glu-Pro-Met-Trp(5Me)-[Gly]	TR5-157 (A0545)	13	TR5-149 (A0545 Δ Gly)	76	TR5-143E (seco-A0545 Δ Gly)	18
Bthi-Glu-Pro-Ser-Trp(5Br)-[Gly]	TR5-158 (A0564)	2.7	TR5-150 (A0564 Δ Gly)	15	TR5-143F (seco-A0564 Δ Gly)	23
2Thi-Glu-Pro-Tr(5Me)-Glu-[Gly]	TR5-159 (A0565)	1.1	TR5-152 (A0565 Δ Gly)	9.4	TR5-144 (seco-A0565 Δ Gly)	16

Purified components:

Sequence	Re-synthesized hits Purified constituents	
	Cmpd.	IC ₅₀ (μ M)
Trp(5Br)-Glu-Pro-Bthi-Asp-Gly	TR5-153A	1.6
	TR5-153B	0.55
	TR5-153C	1.1
1Nal-Glu-Pro-Trp(5F)-Trp-Gly	TR5-154A	18
	TR5-154B	7.1
	TR5-154C	11
	TR5-154D	23
	TR5-154E	22
	TR5-154F	21
	TR5-154G	12
	TR5-154H	9.4
	TR5-154I	16
	TR5-154J	15
	TR5-154K	18
Trp-Glu-Pro-Trp-Glu-Gly	TR5-155A	15
Phe-Glu-Pro-Trp-Trp(5Br)-Gly	TR5-156A	14
	TR5-156B	15
	TR5-156C	21
	TR5-156D	23
	TR5-156E	14
	TR5-156F	16
	TR5-156G	23
Val-Glu-Pro-Met-Trp(5Me)-Gly	TR5-157	13
Bthi-Glu-Pro-Ser-Trp(5Br)-Gly	TR5-158A	150
	TR5-158B	24
	TR5-158C	21
	TR5-158D	11
	TR5-158E	7.7
	TR5-158F	6.4
	TR5-158G	10
2Thi-Glu-Pro-Tr(5Me)-Glu-Gly	TR5-158H	8.6
	TR5-159A	7.1
	TR5-159B	6.6
	TR5-159C	4.0
	TR5-159D	5.9
TR5-159E	8.7	

Sequence	Purified constituents (Δ Gly)	
	Cmpd.	IC ₅₀ (μ M)
Trp(5Br)-Glu-Pro-Bthi-Asp	crude mixt.	0.97
	TR5-145A	5.0
	TR5-145B	3.2
	TR5-145C	2.8
1Nal-Glu-Pro-Trp(5F)-Trp	crude mixt.	4
	TR5-146A	2.8

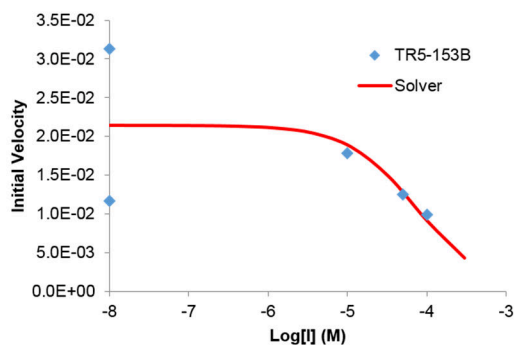
	TR5-146B	33
	TR5-146C	30
	TR5-146D	36
	TR5-146E	28
	TR5-146F	18
	TR5-146G	20
	TR5-146H	23
Trp-Glu-Pro-Trp-Glu	crude mixt.	8
	TR5-147A	12
	TR5-147B	51
Phe-Glu-Pro-Trp-Trp(5Br)	crude mixt.	5.3
	TR5-148A	0.68
	TR5-148B	65
	TR5-148C	87
	TR5-148D	17
	TR5-148E	21
Val-Glu-Pro-Met-Trp(5Me)*	crude mixt.	76
Bthi-Glu-Pro-Ser-Trp(5Br)	crude mixt.	15
	TR5-150A	26
	TR5-150B	>100
	TR5-150C	>100
	TR5-150D	82
	TR5-150E	26
2Thi-Glu-Pro-Tr(5Me)-Glu	crude mixt.	9.4
	TR5-152A	35
	TR5-152B	26
	TR5-152C	47

*This mixture was not pursued (apparent Met S-alkylation)

Assay of isolated components A0404-B and A0506 Δ Gly-A in kinetic chymotrypsin-linked assay

Measurements were carried out by measuring initial rate at different concentrations of inhibitor by the same method as outlined above using substrate Suc-AEPF-pNA.

A0404-B



$$v = v_{max} / (1 + [I]/IC_{50})$$

$$IC_{50} = 7.4E-05$$

Cheng-Prusoff:

$$K_i = IC_{50} / (1 + [S]/K_m)$$

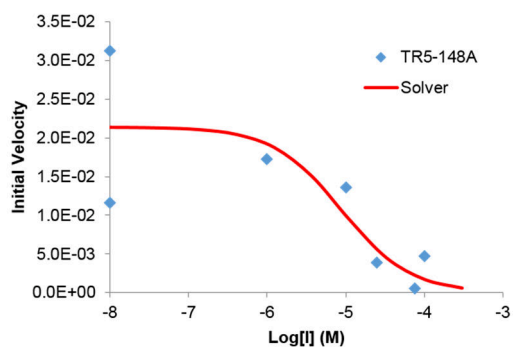
$$[S] (M) = 7.00E-05$$

$$K_m (M) = 4.95E-04$$

$$K_i = 6.5E-05$$

(35% cis)

A0506ΔGly-A



$$v = v_{max} / (1 + [I]/IC_{50})$$

$$IC_{50} = 8.8E-06$$

Cheng-Prusoff:

$$K_i = IC_{50} / (1 + [S]/K_m)$$

$$K_i = 7.7E-06$$

$$[S] (M) \quad 7.00E-05$$

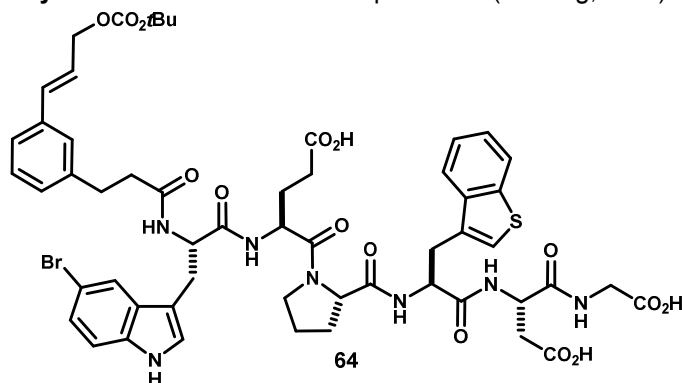
(35% cis)

$$K_m (M) \quad 4.95E-04$$

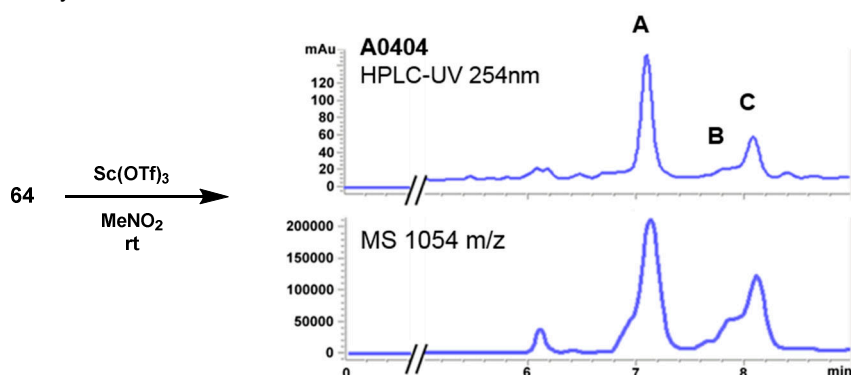
Scale up, isolation & structure determination of Pin1-active macrocycles

Macrocycles 65a-c:

Acyclic intermediate 64. Compound **64** (153 mg, 57%) was prepared from peptide H-Trp(5Br)-Glu-Pro-Bthi-Asp-Gly-OH and template **5** according to General Procedure A. MS *m/z* 1053.4/1055.4 (calc'd: C₅₀H₅₃BrN₇O₁₂S, [M-OCO₂tBu]⁺, 1054.3).



Macrocycles 65a-c:



Acyclic intermediate **64** (122 mg, 104 μ mol) was suspended in MeNO₂ (21 mL) and treated with Sc(OTf)₃ (51 mg, 104 μ mol). The mixture was stirred for 1.5 hr, quenched with iPr₂EtN (87 μ L), concentrated and purified by preparative HPLC method A to give fractions **A** (24.8 mg), **B** (5.1 mg) and **C** (18.4 mg) (combined 44% of theory). Fractions **B** and **C** were re-purified by preparative HPLC method B to give **B1** (0.5mg), **B2** (0.5 mg), **B3** (1.8 mg, 1.6%), **B4** (0.6 mg), **C1** (4.1 mg, 3.7%), **C2** (4.0 mg, 3.6%), and **C3** (2.2 mg, 2.0%).

Preparative HPLC method A:

Column: Waters Sunfire™ C₁₈, 19x250mm, 5 μ m.

Solvent A: H₂O + 0.1%v TFA

Solvent B: ACN + 0.1%v TFA

Flow rate: 18.00 ml/min

Time	%B
0	50
2	50
20	80

Preparative HPLC method B:

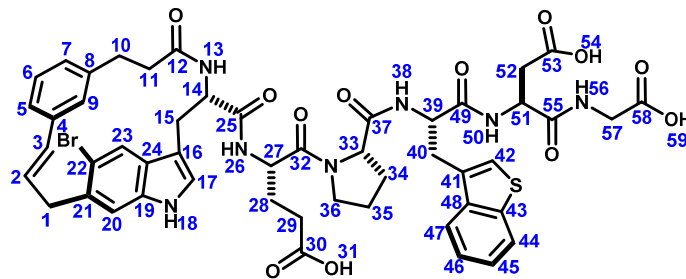
Column: Waters Xbridge™ PFP, 19x250mm, 5 μ m.

Solvent A: H₂O + 0.1%v TFA

Solvent B: ACN + 0.1%v TFA

Flow rate: 18.00 ml/min

Time	%B
0	35
2	35
3	40
20	60

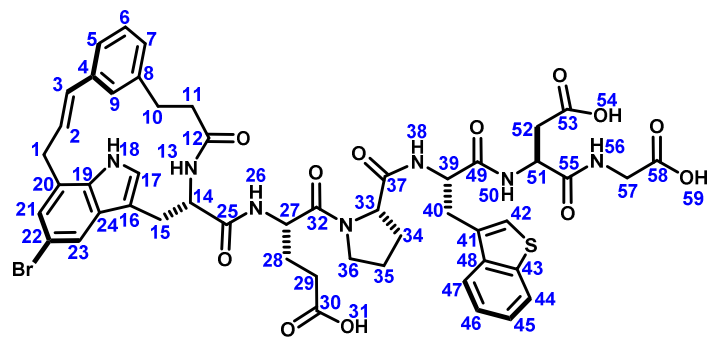


65a

(600MHz, DMSO-*d*₆, 298K)

	¹³ C	¹ H	key correlations
1	38.0	3.41 (br d, <i>J</i> = 16.1 Hz, 1H, 3.77-3.82 (m, 1H) overlap	HMBC 1→21,20,22
2	128.4	6.30 (ddd, <i>J</i> = 16.2, 3.9, 3.9 Hz, 1H)	
3	132.9	3.69 (br d, <i>J</i> = 16.2 Hz, 1H) overlap	HMBC 3→1
4	136.0	-	
5	119.5	7.17 (br d, <i>J</i> = 7.7 Hz, 1H)	HMBC 5→3,9 NOESY 5→2
6	127.9	7.05 (dd, <i>J</i> = 7.7, 7.5 Hz, 1H)	HMBC 6→4,7
7	127.0	6.83 (br d, <i>J</i> = 7.5 Hz, 1H)	HMBC 7→9 NOESY 7→10
8	141.3	-	
9	128.4	5.51 (s, 1H)	HMBC 9→3
10	26.0	2.45 (dd, <i>J</i> = 17.3, 5.8 Hz, 1H), 3.02 (dd, <i>J</i> = 17.3, 12.8 Hz, 1H)	
11	31.3	2.15 (dd, <i>J</i> = 15.7, 12.8 Hz, 1H), 2.22-2.29 (m, 1H)	
12	171.7	-	
13	-	7.40-7.43 (m, 1H) overlap	HMBC 13→12
14	52.7	4.68-4.73 (m, 1H)	HMBC 14→25
15	28.0	2.77 (dd, <i>J</i> = 14.3, 13.1 Hz, 1H), 3.25 (dd, <i>J</i> = 14.3, 4.0 Hz, 1H)	HMBC 15→16 TOCSY 15→13,14
16	109.2	-	
17	126.7	7.23 (d, <i>J</i> = 1.7 Hz, 1H)	HMBC 17→16
18	-	10.92-10.94 (m, 1H)	COSY 18→17 HMBC 18→16 NOESY 18→17,20
19	136.8	-	
20	115.8	7.23 (s, 1H)	HMBC 20→21
21	131.9	-	
22	116.5	-	
23	122.8	8.17 (s, 1H)	HMBC 23→16,21
24	126.8	-	
25	172.7	-	
26	-	8.49 (br d, <i>J</i> = 7.9 Hz, 1H)	HMBC 26→25,27 TOCSY 26→27,28,29
27	49.8	4.58-4.62 (m, 1H) overlap	
28	26.8	1.71-1.78 (m, 1H), 1.90-1.98 (m, 1H)	HMBC 28→29,32
29	36.1	2.30-2.42 (m, 2H)	HMBC 29→28

30	174.4	-	
31	-	12.17 (br s, 1H)	
32	170.4	-	
33	59.5	4.38 (dd, $J = 8.3, 4.1$ Hz, 1H)	COSY 33→34 TOCSY 33→34,35,36
34	29.0	1.77-1.84 (m, 1H), 1.99-2.06 (m, 1H)	HMBC 34→37
35	24.5	1.79-1.90 (m, 2H)	
36	46.9	3.57-3.68 (m, 2H)	
37	171.8	-	
38	-	8.21 (br d, $J = 7.7$ Hz, 1H)	HMBC 38→37
39	52.3	4.64-4.69 (m, 1H) overlap	
40	30.2	3.11 (dd, $J = 15.2, 8.6$ Hz, 1H), 3.31 (dd, $J = 15.2, 5.0$ Hz, 1H)	HMBC 40→39,48 NOESY 40→42,47
41	132.0	-	
42	123.7	7.50 (s, 1H)	HMBC 42→41,43,48
43	139.6	-	
44	122.8	7.93 (d, $J = 7.2$ Hz, 1H)	HMBC 44→48
45	124.0	7.35 (ddd, $J = 7.9, 7.2, 0.5$ Hz, 1H)	
46	123.9	7.40-7.43 (m, 1H) overlap	
47	121.9	7.89 (d, $J = 8.1$ Hz, 1H)	COSY 47→46 HMBC 47→41,43
48	139.0	-	
49	171.0	-	
50	-	8.26 (br d, $J = 7.8$ Hz, 1H)	HMBC 50→49 TOCSY 50→51,52
51	49.3	4.59-4.64 (m, 1H)	
52	36.1	2.50-2.55 (m, 1H), 2.69 (dd, $J = 16.6, 5.7$ Hz, 1H)	HMBC 52→51,53,55
53	171.9	-	
54	-	12.17 (br s, 1H)	
55	170.8	-	
56	-	7.89-7.94 (m, 1H) overlap	
57	40.8	3.72 (dd, $J = 17.6, 5.2$ Hz, 1H), 3.78 (dd, $J = 17.6, 5.8$ Hz, 1H)	HMBC 57→58,55
58	171.1	-	
59	-	12.17 (br s, 1H)	

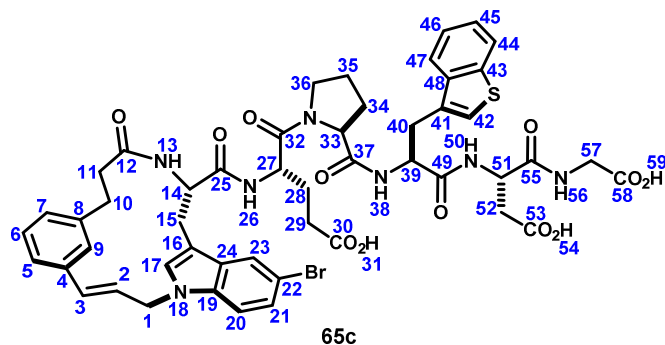


65b

(500MHz, DMSO-*d*₆, 298K)

	¹³ C	¹ H	key correlations
1	33.3	3.50 (br d, <i>J</i> = 16.7 Hz, 1H), 3.89 (dd, <i>J</i> = 16.7, 5.5 Hz, 1H)	HMBC 1→2,3,19,20,21
2	126.5	6.13 (ddd, <i>J</i> = 16.3, 5.5, 2.9 Hz, 1H)	TOCSY 2→1,3
3	131.9	4.59-4.65 (m, 1H) overlap	HMBC 3→2,4
4	137.1	-	
5	120.2	7.20 (d, <i>J</i> = 7.7 Hz, 1H)	TOCSY 5→6,7,9 HMBC 53
6	127.9	7.08 (dd, <i>J</i> = 7.7, 7.6 Hz, 1H)	HMBC 6→4,8
7	126.5	6.85 (d, <i>J</i> = 7.6 Hz, 1H)	
8	142.3	-	
9	123.7	5.67 (br s, 1H)	
10	26.9	2.31-2.38 (m, 1H) overlap, 3.14-3.23 (m, 1H) overlap	HMBC 10→8,12
11	34.5	2.12 (dd, <i>J</i> = 15.1, 12.1 Hz, 1H), 2.35-2.44 (m, 1H) overlap	HMBC 11→8,12
12	171.8	-	
13	-	8.06 (d, <i>J</i> = 8.3 Hz, 1H)	HMBC 13→12
14	53.1	4.43 (ddd, <i>J</i> = 12.5, 8.3, 3.1 Hz, 1H)	
15	27.0	2.74 (dd, <i>J</i> = 14.0, 12.5, Hz, 1H), 3.17 (dd, <i>J</i> = 14.0, 3.1 Hz, 1H)	HMBC 15→16
16	109.5	-	
17	126.4	7.25 (d, <i>J</i> = 2.2 Hz, 1H)	HMBC 17→16,19,24
18	-	10.58 (br d, <i>J</i> = 2.2 Hz, 1H)	HMBC 18→16,17 COSY 18→17
19	134.5	-	
20	125.8	-	
21	123.6	7.10 (d, <i>J</i> = 1.8 Hz, 1H)	HMBC 21→1,23
22	111.0	-	
23	119.3	7.92-7.94 (m, 1H) overlap	HMBC 23→16,19,21,22
24	127.6	-	
25	172.0	-	
26	-	8.42 (d, <i>J</i> = 7.7 Hz, 1H)	HMBC 26→25
27	49.5	4.57-4.63 (m, 1H) overlap	
28	26.2	1.72-1.81 (m, 1H) overlap, 1.92-2.01 (m, 1H) overlap	HMBC 28→27,29,30,32

29	29.2	2.32-2.39 (m, 2H) overlap	HMBC 29→27,28,30
30	174.0	-	
31	-	12.15 (br s, 1H) overlap	
32	169.7	-	
33	59.1	4.38 (dd, $J = 8.2, 4.2$ Hz, 1H)	HMBC 33→34,35 TOCSY 33→34,35,36
34	28.6	1.76-1.85 (m, 1H) overlap, 1.98-2.06 (m, 1H) overlap	
35	24.3	1.80-1.92 (m, 2H) overlap	
36	46.6	3.56-3.72 (m, 2H)	
37	171.5	-	
38	-	8.25 (d, $J = 7.7$ Hz, 1H)	TOCSY 38→39,40
39	52.0	4.66 (ddd, $J = 8.9, 7.7, 5.5$ Hz, 1H)	
40	30.0	3.11 (dd, $J = 15.4, 8.9$ Hz, 1H), 3.26-3.34 (m, 1H)	HMBC 40→41
41	131.6	-	
42	123.6	7.93 (s, 1H) overlap	HMBC 42→41
43	139.2	-	
44	122.5	7.92-7.96 (m, 1H) overlap	
45	123.9	7.36 (ddd, $J = 8.0, 7.1, 0.7$ Hz, 1H)	COSY 45→44
46	123.7	7.42 (ddd, $J = 8.0, 7.0, 1.0$ Hz, 1H)	COSY 46→45 HMBC 46→44
47	121.6	7.90 (br d, $J = 8.0$ Hz, 1H)	COSY 47→46 HMBC 47→43
48	138.6	-	
49	170.7	-	
50	-	8.29 (d, $J = 8.0$ Hz, 1H)	HMBC 50→49
51	49.1	4.58-4.64 (m, 1H) overlap	
52	35.6	2.53 (dd, $J = 16.5, 7.3$ Hz, 1H), 2.68 (dd, $J = 16.5, 5.7$ Hz, 1H)	HMBC 52→53,55
53	171.5	-	
54	-	12.15 (br s, 1H) overlap	
55	170.5	-	
56	-	7.92-7.97 (m, 1H)	HMBC 56→55
57	40.5	3.68-3.81 (m, 2H)	HMBC 57→58
58	170.6	-	
59	-	12.15 (br s, 1H) overlap	

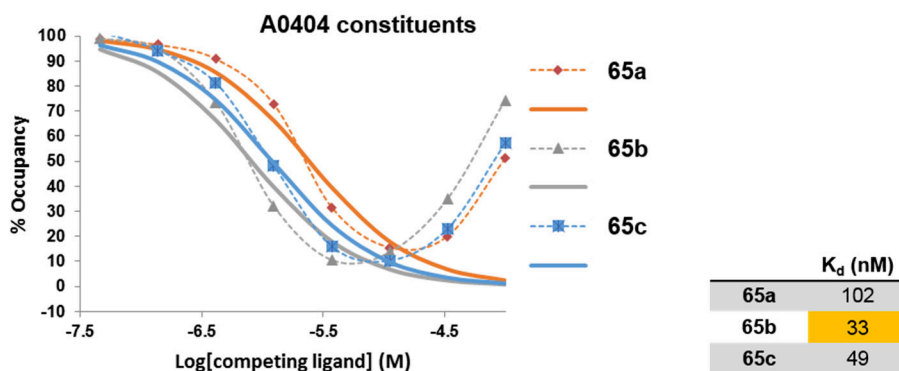


(500MHz, DMSO-*d*₆, 298K)

	¹³ C	¹ H	key correlations
1	46.1	4.79 (d, <i>J</i> = 7.0 Hz, 2H)	HMBC 1→2,3,17,19
2	127.7	5.98 (dt, <i>J</i> = 15.5, 7.0 Hz, 1H)	HMBC 2→4,5 COSY 2→1
3	132.0	6.47 (d, <i>J</i> = 15.5 Hz, 1H)	HMBC 3→4
4	137.4	-	
5	123.6	6.98 (br d, <i>J</i> = 7.6 Hz, 1H) overlap	HMBC 5→3
6	127.7	7.13 (dd, <i>J</i> = 7.6, 7.6 Hz, 1H)	HMBC 6→4,8
7	127.4	6.99 (br d, <i>J</i> = 7.6 Hz, 1H)	HMBC 7→10
8	141.2	-	
9	125.0	6.68 (br s, 1H)	HMBC 9→3,5,7,10
10	26.7	2.60-2.67 (m, 1H) overlap, 3.05-3.15 (m, 1H) overlap	HMBC 10→8
11	32.4	2.35-2.41 (m, 1H) overlap, 2.60-2.69 (m, 1H) overlap	HMBC 11→8,12
12	172.1	-	
13	-	8.27-8.32 (m, 1H) overlap	
14	53.2	4.48 (ddd, <i>J</i> = 12.1, 7.9, 2.4 Hz, 1H)	HMBC 14→16,25 TOCSY 14→13,15,15'
15	26.5	2.85 (dd, <i>J</i> = 14.2, 13.2 Hz, 1H), 3.04 (br d, <i>J</i> = 14.2 Hz, 1H)	HMBC 15→16,25
16	111.9	-	
17	129.3	7.35 (s, 1H) overlap	HMBC 17→16,19,24
18	-	-	
19	136.1	-	
20	112.4	7.57 (d, <i>J</i> = 8.8 Hz, 1H)	HMBC 20→24
21	123.6	7.25 (dd, <i>J</i> = 8.8, 1.9 Hz, 1H)	
22	111.6	-	
23	121.0	7.86 (d, <i>J</i> = 1.9 Hz, 1H)	HMBC 23→19
24	130.0	-	
25	171.9	-	
26	-	8.27-8.32 (m, 1H) overlap	TOCSY 26→27,28,29
27	49.4	4.55-4.62 (m, 1H) overlap	
28	26.3	1.70-1.80 (m, 1H) overlap, 1.91-1.99 (m, 1H) overlap	HMBC 28→27,30,32
29	29.2	2.35 (dd, <i>J</i> = 7.4, 7.4 Hz, 2H) overlap	HMBC 29→27,30
30	174.0	-	

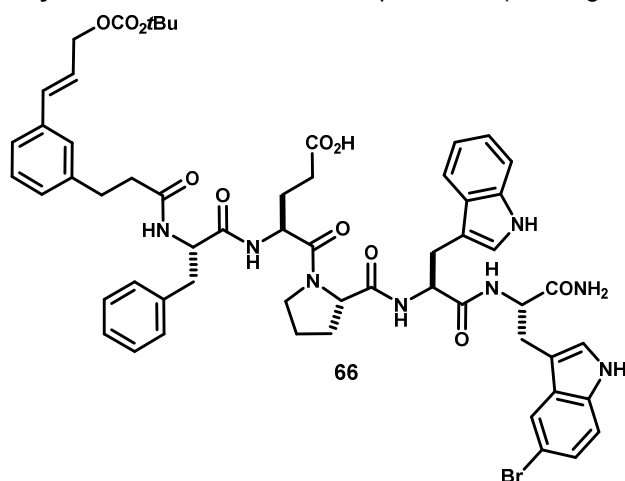
31	-	12.25 (br s, 1H) overlap	
32	169.6	-	
33	59.1	4.37 (dd, $J = 8.1, 4.2$ Hz, 1H)	HMBC 33→34,35,37 TOCSY 33→34,35,36
34	28.6	1.77-1.85 (m, 1H) overlap, 1.98-2.07 (m, 1H)	HMBC 34→36,37
35	24.3	1.80-1.91 (m, 2H) overlap	HMBC 35→36
36	46.5	3.56-3.70 (m, 2H)	
37	171.4	-	
38	-	8.24 (br d, $J = 7.8$ Hz, 1H)	
39	52.0	4.65 (ddd, $J = 8.1, 7.8, 5.3$ Hz, 1H)	
40	30.0	3.07-3.15 (m, 1H) overlap, 3.26-3.34 (m, 1H)	HMBC 40→39,41,48,49
41	131.6	-	
42	123.4	7.50 (s, 1H)	HMBC 42→41,43,48
43	139.2	-	-
44	122.5	7.92 (br d, $J = 8.2$ Hz, 1H)	HMBC 44→48
45	123.9	7.33-7.37 (m, 1H) overlap	HMBC 45→43,47
46	123.9	7.41 (ddd, $J = 8.0, 7.1, 0.9$ Hz, 1H)	HMBC 46→44,48 COSY 46→47
47	121.6	7.89 (br d, $J = 8.0$ Hz, 1H)	HMBC 47→43
48	138.6	-	
49	170.6	-	
50	-	8.27-8.32 (m, 1H) overlap	
51	49.1	4.58-4.64 (m, 1H) overlap	HMBC 51→52
52	35.7	2.34-2.40 (m, 1H) overlap, 2.60-2.69 (m, 1H) overlap	HMBC 52→51,53
53	171.5	-	
54	-	12.25 (br s, 1H) overlap	
55	170.5	-	
56	-	7.95 (dd, $J = 5.9, 5.7$ Hz, 1H)	HMBC 56→55
57	40.6	3.71 (dd, $J = 17.5, 5.7$ Hz, 1H), 3.78 (dd, $J = 17.5, 5.9$ Hz, 1H)	HMBC 57→58
58	170.6	-	
59	-	12.25 (br s, 1H) overlap	

FP Assay results for 65a-c:

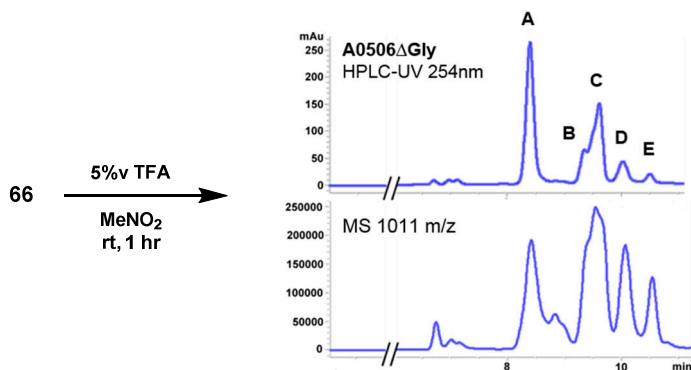


Macrocycles 67a-67:

Acyclic intermediate 64. Compound **64** (137 mg, 51%) was prepared from peptide H-Phe-Glu-Pro-Trp-Trp(5Me)-NH₂ and template **5** according to General Procedure A. MS *m/z* 1128.4/1130.6 (calc'd: C₅₈H₆₆BrN₈O₁₁, [M+H]⁺, 1129.4).



Macrocycles 67a-67:



Acyclic intermediate **66** (109 mg, 96.5 μ mol) was treated with 5%v TFA in MeNO₂ (19.3 mL). The mixture was stirred for 1.5, then concentrated and purified by preparative HPLC method A to give fractions A (26.2 mg), B (4.2 mg), C (15.0 mg), D (7.3 mg) and E (3.2 mg). Fraction A was re-purified by HPLC method B to give **67a1** (3.4 mg), A2 (mixed, 1.5 mg), A3 (19.2 mg). Fraction A3 was again re-purified by semi-preparative HPLC method C to give **67a3** (7.9 mg) and A3B (3.6 mg). Fraction B was re-purified by semi-preparative HPLC method D to give **67b1** (4.5 mg) and C (1.2 mg). Fraction C was re-purified by semi-preparative

HPLC method D to give **67c1** (14.2 mg), C2 (mixed, 3.0 mg) and **67c3** (6.5 mg). Fraction E was re-purified by semi-preparative HPLC method E to give **67e1** (1.3 mg).

Preparative HPLC method A:

Column: Waters Sunfire™ C₁₈, 19x250mm, 5µm.

Solvent A: H₂O + 0.1%v TFA

Solvent B: ACN + 0.1%v TFA

Flow rate: 18.00 ml/min

Time	%B
0	30
1	30
3	55
20	75

Preparative HPLC method B:

Column: Waters X-Select™ PFP, 19x250mm, 5µm.

Solvent A: H₂O + 0.1%v TFA

Solvent B: ACN + 0.1%v TFA

Flow rate: 18.00 ml/min

Time	%B
0	25
1	25
3	45
20	65

Semi-preparative HPLC method C:

Column: Waters X-Bridge™ Phenyl, 10x250mm, 5µm.

Solvent A: H₂O + 0.1%v TFA

Solvent B: ACN + 0.1%v TFA

Flow rate: 6.00 ml/min

Time	%B
0	30
1	30

4	43
22	46
25	30
27	30

Semi-preparative HPLC method D:

Column: Waters X-Bridge™ Phenyl, 10x250mm, 5µm.

Solvent A: H₂O + 0.1%v TFA

Solvent B: ACN + 0.1%v TFA

Flow rate: 6.00 ml/min

Time	%B
0	35
1	35
4	48
20	58
22	35
25	35

Semi-preparative HPLC method E:

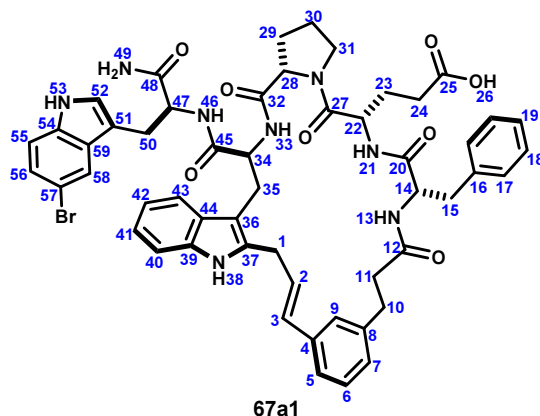
Column: Waters X-Bridge™ Phenyl, 10x250mm, 5µm.

Solvent A: H₂O + 0.1%v TFA

Solvent B: ACN + 0.1%v TFA

Flow rate: 6.00 ml/min

Time	%B
0	30
1	30
4	45
22	55
25	30
27	30

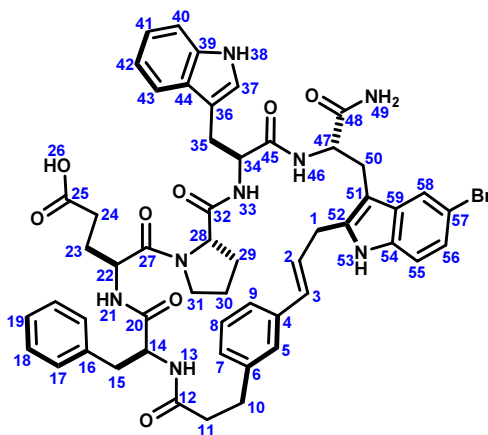


(500MHz, 600 MHz, DMSO-*d*₆, 298K)

	¹³ C	¹ H	key correlations
1	29.2	3.94 (dd, <i>J</i> = 15.2, 5.0 Hz, 1H), 3.49 (dd, <i>J</i> = 15.2, 8.9 Hz, 1H)	HMBC 1→50,53
2	127.5	6.29 (ddd, <i>J</i> = 15.7, 8.9, 5.0 Hz, 1H)	COSY 2→1 HMBC 2→4
3	130.4	6.65 (d, <i>J</i> = 15.7 Hz, 1H)	COSY 3→2 HMBC 3→4,5,9
4	136.7	-	
5	125.0	7.12-7.16 (m, 1H) overlap	HMBC 5→3
6	128.0	7.19-7.24 (m, 1H) overlap	HMBC 6→4,8
7	126.5	7.03 (br d, <i>J</i> = 7.6 Hz, 1H)	
8	141.1	-	
9	124.0	7.34 (br s, 1H)	HMBC 9→3
10	31.3	2.60-2.66 (m, 1H), 2.66-2.72 (m, 1H)	HMBC 10→8,12
11	36.8	2.24-2.36 (m, 2H)	HMBC 11→8,12
12	171.7	-	
13	-	8.18 (d, <i>J</i> = 8.9 Hz, 1H)	
14	55.4	4.30 (ddd, <i>J</i> = 10.4, 8.9, 4.4 Hz, 1H)	COSY 14→13,15 HMBC 14→12,20
15	36.7	2.74 (dd, <i>J</i> = 13.8, 10.4 Hz, 1H), 2.92-2.98 (m, 1H) overlap	HMBC 15→16,17,20
16	137.6	-	
17	128.7	7.13-7.18 (m, 2H) overlap	HMBC 17→17
18	127.9	7.20-7.25 (m, 2H) overlap	HMBC 18→16,18
19	126.2	7.15-7.19 (m, 1H) overlap	
20	170.6	-	
21	-	7.42 (d, <i>J</i> = 7.3 Hz, 1H)	
22	49.0	4.55 (ddd, <i>J</i> = 7.3, 7.0, 4.4 Hz, 1H)	HMBC 22→27
23	26.7	1.56-1.64 (m, 1H), 1.92-1.99 (m, 1H)	HMBC 23'→27
24	28.5	2.08-2.15 (m, 1H) overlap, 2.16-2.24 (m, 1H)	
25	173.9	-	
26	-	12.01 (br s, 1H)	
27	168.4	-	

28	58.7	4.40-4.48 (m, 1H) overlap	HMBC 28→32 TOCSY 28→29,30,31 COSY 28→29
29	28.9	2.07-2.16 (m, 1H) overlap, 1.80-1.89 (m, 1H)	HMBC 29→32
30	24.0	1.73-1.80 (m, 2H)	
31	46.3	3.56 (ddd, $J = 9.8, 6.8, 6.8$ Hz, 1H), 3.46-3.52 (m, 1H) overlap	
32	171.7	-	
33	-	8.15 (d, $J = 8.5$ Hz, 1H)	
34	54.9	4.40-4.43 (m, 1H) overlap	COSY 34→33,35 HMBC 34→36
35	26.6	2.93-2.98 (m, 2H)	HMBC 35→36
36	106.3	-	
37	127.5	-	
38	-	10.66 (s, 1H)	
39	135.5	-	
40	110.3	7.23 (d, $J = 8.0$ Hz, 1H) overlap	TOCSY 40→41,42,43
41	120.3	7.00 (ddd, $J = 8.0, 7.0, 1.1$ Hz, 1H)	
42	118.0	6.94 (ddd, $J = 7.8, 7.0, 0.8$ Hz, 1H)	HMBC 42→44
43	117.9	7.53 (d, $J = 7.8$ Hz, 1H)	HMBC 43→39
44	127.6	-	
45	171.6	-	
46	-	7.66 (d, $J = 7.7$ Hz, 1H)	HMBC 46→45
47	52.7	4.52 (ddd, $J = 7.7, 7.2, 5.9$ Hz, 1H)	HMBC 47→51
48	172.6	-	
49	-	7.45 (br s, 1H), 7.12 (br s, 1H)	HMBC 49→48 TOCSY 49→49'
50	27.6	3.13 (dd, $J = 14.7, 5.7$ Hz, 1H), 2.97 (dd, $J = 14.7, 7.2$ Hz, 1H) overlap	HMBC 50→51,52
51	109.4	-	
52	125.0	7.12-7.16 (m, 1H) overlap	HMBC 52→51
53	-	11.03 (d, $J = 1.7$ Hz, 1H)	HMBC 53→52,54 TOCSY 53→52
54	134.4	-	
55	113.0	7.29 (d, $J = 8.5$ Hz, 1H)	HMBC 55→57,59
56	123.0	7.11-7.17 (m, 1H) overlap	HMBC 56→54,57
57	110.7	-	
58	120.7	7.79 (d, $J = 1.7$ Hz, 1H)	HMBC 58→54,57
59	129.3	-	

MS m/z 1011.2/1011.3 (calc'd: $C_{53}H_{56}BrN_8O_8$, $[M+H]^+$, 1011.3).



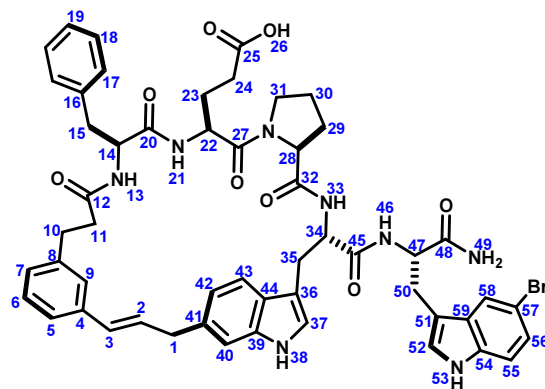
67a3

(600 MHz, DMSO-*d*₆, 298K)

	¹³ C	¹ H	key correlations
1	29.1	3.59 (dd, <i>J</i> = 16.2, 5.0 Hz, 1H), 3.69 (dd, <i>J</i> = 16.2, 5.6 Hz, 1H)	HMBC 1→51,52
2	130.7	6.35 (ddd, <i>J</i> = 15.9, 5.6, 5.0 Hz, 1H)	COSY 2→1 HMBC 2→4
3	126.5	6.39 (d, <i>J</i> = 15.9 Hz, 1H)	HMBC 3→5,9
4	136.6	-	
5	123.6	7.11-7.14 (m, 1H) overlap	
6	128.2	7.14-7.18 (m, 1H) overlap	HMBC 6→4,8
7	126.9	7.01-7.04 (m, 1H) overlap	
8	141.2	-	
9	125.7	7.20-7.22 (m, 1H) overlap	
10	30.2	2.66-2.72 (m, 1H), 2.81-2.88 (m, 1H)	HMBC 10→8,12
11	35.7	2.31-2.37 (m, 1H), 2.42-2.48 (m, 1H)	HMBC 11→8,12
12	171.3	-	
13	-	8.20 (d, <i>J</i> = 8.7 Hz, 1H) overlap	HMBC 13→12,14
14	53.9	4.43-4.48 (m, 1H) overlap	HMBC 14→16
15	36.6	2.74 (dd, <i>J</i> = 13.8, 8.9 Hz, 1H), 2.94-2.99 (m, 1H) overlap	HMBC 15→14,16,17
16	137.5	-	
17	128.8	7.13-7.15 (m, 2H) overlap	HMBC 17→17,19
18	127.9	7.20-7.24 (m, 2H) overlap	HMBC 18→16,18
19	126.1	7.14-7.18 (m, 1H) overlap	
20	170.6	-	
21	-	7.61 (br d, <i>J</i> = 7.4 Hz, 1H) overlap	
22	49.7	4.40-4.45 (m, 1H) overlap	
23	26.3	1.34-1.41 (m, 1H), 1.66-1.73 (m, 1H)	HMBC 23→25,27
24	29.1	2.03 (apt dd, <i>J</i> = 7.4, 7.4 Hz, 1H)	HMBC 24→25
25	173.9	-	
26	-	12.05 (br s, 1H)	
27	170.2	-	

28	60.2	4.16 (dd, $J = 8.3, 4.3$ Hz, 1H)	COSY 28→29
29	27.8	1.61-1.67 (m, 1H) overlap, 1.80-1.87 (m, 1H)	
30	24.1	1.55-1.61 (m, 1H), 1.61-1.67 (m, 1H) overlap	
31	46.4	3.21-3.31 (m, 2H) overlap	
32	170.8	-	
33	-	7.61 (br d, $J = 7.4$ Hz, 1H) overlap	TOCSY 33→34,35 HMBC 33→32
34	53.4	4.43-4.48 (m, 1H) overlap	HMBC 34→36
35	26.5	3.05 (dd, $J = 14.9, 8.9$ Hz, 1H), 3.22-3.26 (m, 1H) overlap	HMBC 35→36,45
36	109.8	-	
37	123.0	7.01-7.03 (m, 1H) overlap	
38	-	10.76 (d, $J = 1.3$ Hz, 1H)	HMBC 38→39,44
39	135.9	-	
40	111.1	7.30 (d, $J = 8.1$ Hz, 1H)	HMBC 40→42,44
41	120.7	7.01-7.05 (m, 1H) overlap	HMBC 41→39
42	118.1	6.94 (dd, $J = 7.8, 7.0$ Hz, 1H)	HMBC 42→44
43	118.0	7.49 (d, $J = 7.8$ Hz, 1H)	HMBC 43→39,41 COSY 43→42
44	127.3	-	
45	170.5	-	
46	-	7.86 (d, $J = 8.1$ Hz, 1H)	TOCSY 46→47,50 COSY 43→42
47	53.6	4.40-4.45 (m, 1H) overlap	HMBC 47→48
48	172.6	-	
49	-	7.03 (br s, 1H) overlap, 7.15 (br s, 1H) overlap	HMBC 49→48
50	26.5	2.93-2.98 (m, 1H) overlap, 3.16 (dd, $J = 14.4, 7.7$ Hz, 1H)	
51	106.3	-	
52	136.6	-	
53	-	11.0 (s, 1H)	HMBC 53→59
54	133.9	-	
55	112.3	7.20-7.23 (m, 1H)	HMBC 55→59
56	122.3	7.10 (dd, $J = 8.5, 1.9$ Hz, 1H)	
57	110.7	-	
58	120.2	7.69 (d, $J = 1.5$ Hz, 1H)	HMBC 58→56,54
59	130.3	-	

MS m/z 1011.3/1011.3 (calc'd: $C_{53}H_{56}BrN_8O_8$, $[M+H]^+$, 1011.3).

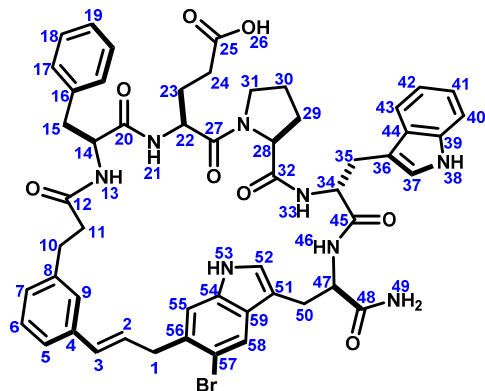


67b1

(600 MHz, DMSO-*d*₆, 298K)

	¹³ C	¹ H	key correlations
1	38.8	3.54 (dd, <i>J</i> = 14.9, 5.8 Hz, 1H), 3.59 (dd, <i>J</i> = 14.9, 6.7 Hz, 1H)	HMBC 1→40,41,42
2	131.0	6.46 (ddd, <i>J</i> = 15.7, 6.7, 5.8 Hz, 1H)	HMBC 2→4,41 COSY 2→1
3	129.0	6.39 (d, <i>J</i> = 15.7 Hz, 1H)	HMBC 3→4,5,9
4	137.1	-	
5	124.6	7.11-7.14 (m, 1H) overlap	HMBC 5→7
6	128.0	7.15-7.19 (m, 1H) overlap	HMBC 6→4
7	127.0	6.97 (br d, <i>J</i> = 7.6 Hz, 1H)	HMBC 7→5
8	141.3	-	
9	124.1	7.17 (br s, 1H) overlap	HMBC 9→5,7
10	30.0	2.51-2.58 (m, 1H), 2.65-2.72 (m, 1H)	HMBC 10→8,12
11	36.3	2.27-2.32 (m, 2H)	HMBC 11→8,12
12	171.0	-	
13	-	8.08 (d, <i>J</i> = 8.9 Hz, 1H)	HMBC 13→12
14	54.0	4.34-4.40 (m, 1H) overlap	HMBC 14→20
15	37.2	2.73 (dd, <i>J</i> = 13.6, 9.6 Hz, 1H), 2.95 (dd, <i>J</i> = 13.6, 4.8 Hz, 1H)	HMBC 15→14,16,17,20
16	137.5	-	
17	128.8	7.13-7.17 (m, 2H) overlap	HMBC 17→17,19
18	127.8	7.20-7.25 (m, 2H) overlap	HMBC 18→16,18
19	126.1	7.14-7.19 (m, 1H) overlap	HMBC 19→17
20	170.2	-	
21	-	7.53 (br d, <i>J</i> = 7.8 Hz, 1H)	HMBC 21→20 COSY 21→22
22	48.9	4.27-4.34 (m, 1H)	
23	26.4	1.45-1.56 (m, 1H), 1.58-1.67 (m, 1H)	
24	28.5	2.00-2.09 (m, 1H), 2.10-2.18 (m, 1H)	HMBC 24→25
25	174.1	-	
26	-	11.97 (br s, 1H)	
27	not observed	-	

28	59.0	4.18 (dd, $J = 8.3, 4.5$ Hz, 1H)	COSY 28→29 HMBC 28→32
29	28.3	1.78-1.86 (m, 1H), 1.91-2.01 (m, 1H)	HMBC 29→31,32
30	24.2	1.67-1.75 (m, 2H)	
31	46.3	3.28-3.37 (m, 1H)	
32	171.1	-	
33	-	7.60 (br d, $J = 6.7$ Hz, 1H)	HMBC 33→32 TOCSY 33→34,35
34	54.6	4.34-4.40 (m, 1H) overlap	HMBC 34→36
35	27.0	2.88 (dd, $J = 14.7, 10.1$ Hz, 1H), 3.04 (dd, $J = 14.7, 2.7$ Hz, 1H)	HMBC 35→36
36	109.2	-	
37	123.8	7.04 (br s, 1H)	HMBC 37→36,39,44
38	-	10.74 (d, $J = 1.2$ Hz, 1H)	HMBC 38→36,37,39
39	136.4	-	
40	111.2	7.11-7.19 (m, 1H) overlap	HMBC 40→42
41	132.5	-	
42	119.7	6.90 (dd, $J = 8.1, 0.8$ Hz, 1H)	HMBC 42→40,44
43	118.2	7.57 (d, $J = 8.1$ Hz, 1H)	HMBC 43→36,39,41,44 COSY 43→42
44	125.8	-	
45	171.4	-	
46	-	7.77-7.81 (m, 1H) overlap	
47	52.9	4.49 (ddd, $J = 8.0, 7.5, 5.6$ Hz, 1H)	HMBC 47→50
48	172.8	-	
49	-	7.14 (br s, 1H) overlap, 7.44 (br s, 1H)	TOCSY 49→49' HMBC 49→48
50	27.3	2.98 (dd, $J = 14.7, 7.5$ Hz, 1H), 3.16 (dd, $J = 14.7, 5.6$ Hz, 1H)	HMBC 50→51
51	109.6	-	
52	125.2	7.21-7.22 (m, 1H) overlap	
53	-	11.00 (d, $J = 1.2$ Hz, 1H)	HMBC 53→51,52,54 TOCSY 53→52
54	134.4	-	
55	113.1	7.31 (d, $J = 8.7$ Hz, 1H)	HMBC 55→59
56	123.0	7.14-7.18 (m, 1H) overlap	HMBC 56→54
57	110.9	-	
58	120.6	7.79-7.81 (m, 1H) overlap	HMBC 58→51,56
59	129.1	-	

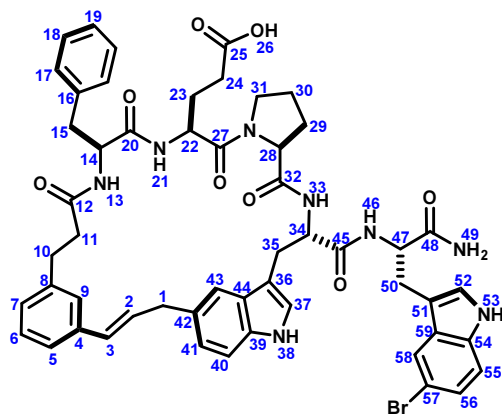


67c1

(600 MHz, DMSO-*d*₆, 298K)

	¹³ C	¹ H	key correlations
1	38.8	3.60-3.66 (m, 1H) , 3.75-3.80 (m, 1H)	HMBC 1→2,3,56
2	129.7	6.34-6.38 (m, 1H) overlap	HMBC 2→4 COSY 2→1
3	128.9	6.34-6.38 (m, 1H) overlap	HMBC 3→4,5,9
4	137.0	-	
5	124.1	7.16-7.18 (m, 1H) overlap	HMBC 5→3
6	128.0	7.13-7.15 (m, 1H) overlap	HMBC 6→4,8
7	126.9	6.95-6.97 (m, 1H) overlap	
8	141.2	-	
9	124.6	7.14-7.17 (m, 1H) overlap	
10	30.7	2.50-2.61 (m, 1H)	HMBC 10→8,12
11	36.9	2.22-2.31 (m, 1H)	HMBC 11→8,12
12	171.1	-	
13	-	8.10 (d, <i>J</i> = 8.9 Hz, 1H)	HMBC 13→12
14	54.6	4.31-4.36 (m, 1H) overlap	
15	37.5	2.75 (dd, <i>J</i> = 13.8, 9.9 Hz, 1H), 2.95 (dd, <i>J</i> = 13.8, 4.4 Hz, 1H)	HMBC 15→14,15,17
16	137.6	-	
17	128.9	7.12-7.15 (m, 2H) overlap	HMBC 17→17,19
18	127.9	7.23 (dd, <i>J</i> = 7.4, 7.4 Hz, 2H)	HMBC 18→16,18
19	126.1	7.15-7.19 (m, 1H) overlap	
20	170.5	-	
21	-	7.48 (d, <i>J</i> = 7.9 Hz, 1H)	TOCSY 21→22,23,24
22	48.9	4.45 (ddd, <i>J</i> = 9.1, 8.2, 3.9 Hz, 1H)	
23	26.5	1.35-1.43 (m, 1H), 1.54-1.62 (m, 1H) overlap	HMBC 23→25
24	28.8	2.09 (dd, <i>J</i> = 6.8, 6.8 Hz, 2H)	HMBC 24→25
25	173.8	-	
26	-	12.01 (br s, 1H)	
27	not detected	-	

28	59.7	4.12 (dd, $J = 8.6, 3.3$ Hz, 1H)	COSY 28→29 HMBC 28→32
29	26.4	1.47-1.53 (m, 1H) overlap, 1.63-1.71 (m, 1H)	
30	23.5	1.27-1.34 (m, 1H), 1.50-1.58 (m, 1H) overlap	
31	46.1	3.19-3.23 (m, 1H), 3.35-3.31 (m, 1H) overlap	HMBC 31→30
32	169.9	-	
33	-	6.94-6.97 (m, 1H) overlap	HMBC 33→32 TOCSY 33→34,35
34	52.3	4.53 (ddd, $J = 7.4, 7.1, 5.2$ Hz, 1H)	HMBC 34→32,36,45
35	27.5	3.00 (dd, $J = 14.8, 7.1$ Hz, 1H), 3.27 (dd, $J = 14.8, 5.2$ Hz, 1H)	HMBC 35→36,37,44
36	109.0	-	
37	123.6	7.09 (d, $J = 2.0$ Hz, 1H)	HMBC 37→44
38	-	10.77 (d, $J = 2.0$ Hz, 1H)	HMBC 38→37,44
39	135.7	-	
40	110.9	7.29 (d, $J = 8.1$ Hz, 1H)	HMBC 40→44
41	120.5	7.03 (dd, $J = 8.1, 7.0, 0.8$ Hz, 1H)	HMBC 41→39
42	117.9	6.95 (ddd, $J = 7.9, 7.0, 0.8$ Hz, 1H) overlap	HMBC 42→44
43	118.0	7.51 (d, $J = 7.9$ Hz, 1H)	
44	127.6	-	
45	170.6	-	
46	-	8.16 (d, $J = 8.2$ Hz, 1H)	TOCSY 46→47,50
47	53.1	4.32-4.37 (m, 1H) overlap	
48	173.6	-	
49	-	7.15 (br s, 1H) overlap, 7.60 (br s, 1H) overlap	HMBC 49→48
50	27.3	2.92 (dd, $J = 14.4, 11.1$ Hz, 1H), 3.09 (dd, $J = 14.4, 2.7$ Hz, 1H)	HMBC 50→47,51
51	109.5	-	
52	125.6	7.20 (d, $J = 2.0$ Hz, 1H)	
53	-	10.91 (d, $J = 2.0$ Hz, 1H)	HMBC 53→51,52,54,59
54	135.6	-	
55	113.4	7.34 (s, 1H)	HMBC 55→57,59
56	130.4	-	
57	113.9	-	
58	121.7	8.01 (s, 1H)	HMBC 58→54,56,57
59	127.4	-	

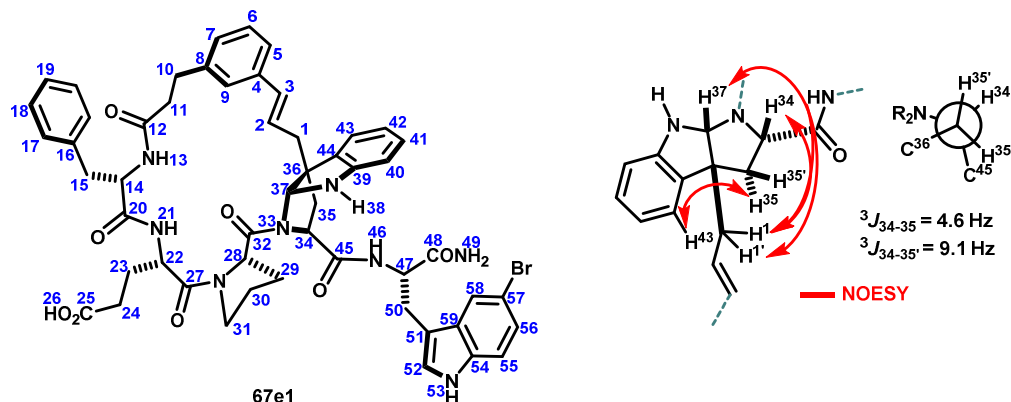


67c3

(600 MHz, DMSO-*d*₆, 298K)

	¹³ C	¹ H	key correlations
1	38.5	3.56 (dd, <i>J</i> = 15.6, 6.3 Hz, 1H), 3.61 (dd, <i>J</i> = 15.6, 6.0 Hz, 1H)	HMBC 1→41,42,43
2	130.2	6.52 (ddd, <i>J</i> = 15.7, 6.3, 6.0 Hz, 1H)	HMBC 2→4,9 COSY 2→1
3	129.5	6.46 (d, <i>J</i> = 15.7 Hz, 1H)	HMBC 3→4
4	137.1	-	
5	124.1	7.12-7.17 (m, 1H) overlap	
6	128.0	7.15-7.19 (m, 1H) overlap	HMBC 6→4,8
7	126.9	7.01 (br d, <i>J</i> = 7.5 Hz, 1H)	HMBC 7→9,5
8	141.2	-	
9	124.3	7.28 (br s, 1H)	HMBC 9→7
10	30.2	2.63-2.72 (m, 1H) overlap, 2.74-2.81 (m, 1H)	HMBC 10→8,12
11	35.9	2.32-2.44 (m, 2H)	
12	171.3	-	
13	-	8.20 (d, <i>J</i> = 8.5 Hz, 1H)	HMBC 13→12,14
14	54.4	7.35-7.42 (m, 1H) overlap	
15	30.1	2.63-2.72 (m, 1H) overlap, 2.88-2.96 (m, 1H)	HMBC 15→16,17
16	137.6	-	
17	128.7	7.15-7.22 (m, 2H) overlap	
18	127.9	7.17-7.22 (m, 2H) overlap	HMBC 18→16
19	126.0	7.12-7.17 (m, 1H) overlap	
20	170.4	-	
21	-	7.64-7.72 (m, 1H)	
22	49.8	7.35-7.42 (m, 1H) overlap	HMBC 22→27
23	26.0	1.54-1.63 (m, 1H) overlap, 1.70-1.79 (m, 1H)	HMBC 23→22,27
24	28.7	2.08-2.23 (m, 1H)	HMBC 24→22
25	173.9	-	
26	-	12.07 (br s, 1H)	
27	168.8	-	
28	59.4	4.25 (dd, <i>J</i> = 7.9, 5.7 Hz, 1H)	HMBC 28→32

29	28.3	1.55-1.64 (m, 1H) overlap, 1.86-1.95 (m, 1H)	HMBC 29→32
30	24.3	1.64-1.72 (m, 2H) overlap	
31	46.4	3.40-3.51 (m, 2H) obscured	COSY 31→30 TOCSY 31→28,29,30
32	170.9	-	
33	-	7.88 (br d, $J = 7.2$ Hz, 1H)	
34	53.1	4.57 (ddd, $J = 7.2, 7.1, 6.9$ Hz, 1H)	HMBC 34→36
35	27.2	2.89-2.98 (m, 1H) overlap, 3.05-3.12 (m, 1H) overlap	
36	109.6	-	
37	128.2	7.02 (d, $J = 1.7$ Hz, 1H)	HMBC 37→44
38	-	10.77 (d, $J = 1.7$ Hz, 1H)	TOCSY 38→37,39,44 HMBC 38→39
39	134.5	-	
40	110.9	7.23 (d, $J = 8.3$ Hz, 1H)	HMBC 40→42,44
41	122.0	6.94 (dd, $J = 8.3, 0.9$ Hz, 1H)	HMBC 41→43 COSY 41→43
42	129.6	-	
43	116.8	7.42 (br s, 1H)	HMBC 43→41,44
44	127.6	-	
45	170.7	-	
46	-	7.91 (d, $J = 7.9$ Hz, 1H)	HMBC 46→45
47	52.9	4.47 (ddd, $J = 7.9, 7.9, 5.9$ Hz, 1H)	HMBC 47→48,51
48	172.8	-	
49	-	7.07 (br s, 1H), 7.34 (br s, 1H)	HMBC 49→48
50	27.3	2.92-3.00 (m, 1H) overlap, 3.07-3.14 (m, 1H) overlap	
51	109.7	-	
52	125.2	7.17-7.19 (m, 1H)	
53	-	11.03 (d, $J = 1.5$ Hz, 1H)	TOCSY 53→52,58 HMBC 53→52,59
54	134.5	-	
55	113.0	7.30 (d, $J = 8.7$ Hz, 1H)	HMBC 55→59
56	123.0	7.16 (dd, $J = 8.7, 1.8$ Hz, 1H)	HMBC 56→58
57	110.8	-	
58	120.5	7.79 (d, $J = 1.8$ Hz, 1H)	COSY 58→56 HMBC 58→54,56
59	128.9	-	



(600 MHz, DMSO-*d*₆, 298K)

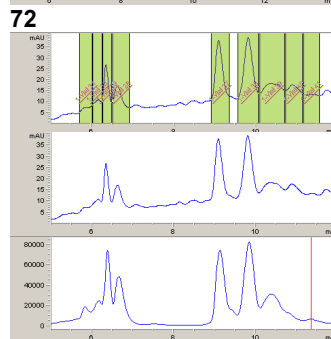
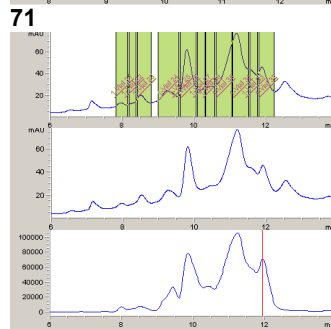
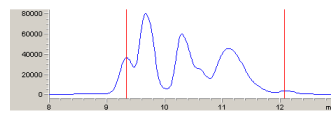
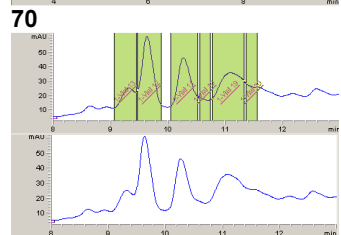
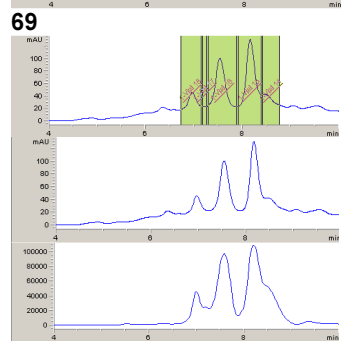
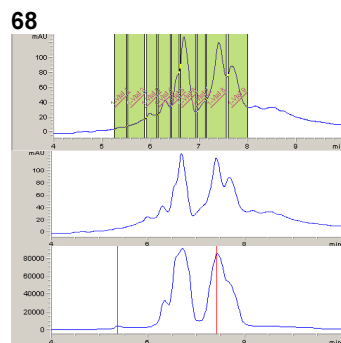
	¹³ C	¹ H	key correlations
1	39.8	2.49-2.56 (m, 1H) obscured, 2.57-2.63 (m, 1H)	HMBC 1→36,37
2	124.6	6.13 (ddd, <i>J</i> = 15.5, 9.2, 5.7 Hz, 1H)	HMBC 2→4
3	133.7	6.58 (d, <i>J</i> = 15.5 Hz, 1H)	HMBC 3→4,5,9
4	136.6	-	
5	123.5	7.02-7.06 (m, 1H) overlap	HMBC 5→7
6	128.3	7.13-7.06 (m, 1H)	HMBC 6→4,8
7	127.1	7.01-7.05 (m, 1H) overlap	HMBC 7→5
8	141.2	-	
9	124.8	7.22 (br s, 1H)	HMBC 9→5,7
10	29.6	2.68-2.74 (m, 1H) overlap	HMBC 10→8,12
11	35.1	2.34-2.42 (m, 1H) overlap, 2.49-2.57 (m, 1H)	HMBC 11→8,12
12	171.4	-	
13	-	8.14 (d, <i>J</i> = 9.3 Hz, 1H)	TOCSY 13→14,15 HMBC 13→12
14	54.4	4.41 (ddd, <i>J</i> = 10.2, 9.3, 4.0 Hz, 1H)	HMBC 14→12,16,20
15	37.3	2.81 (dd, <i>J</i> = 13.9, 10.2 Hz, 1H), 3.08 (dd, <i>J</i> = 13.9, 4.0 Hz, 1H)	HMBC 15→16,17,20
16	137.4	-	
17	128.8	7.17-7.20 (m, 2H) overlap	HMBC 17→17,19
18	128.0	7.28 (apt t, <i>J</i> = 7.2 Hz, 2H)	HMBC 18→16,18
19	126.2	7.18-7.22 (m, 1H) overlap	
20	170.3	-	
21	-	7.32 (d, <i>J</i> = 7.7 Hz, 1H)	HMBC 21→20
22	48.9	4.70 (ddd, <i>J</i> = 7.7, 7.3, 4.9 Hz, 1H)	COSY 22→21,23 TOCSY 22→21,23,24 HMBC 22→27
23	26.8	1.64-1.72 (m, 1H), 1.89-1.98 (m, 1H) overlap	HMBC 23→25
24	28.8	2.22-2.37 (m, 2H) overlap	HMBC 24→25
25	173.9	-	
26	-	12.12 (br s, 1H)	
27	168.7	-	
28	57.3	4.83 (dd, <i>J</i> = 7.5, 5.7 Hz, 1H)	COSY 28→29

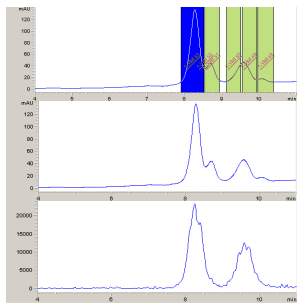
29	29.0	1.78-1.86 (m, 1H) overlap, 2.33-2.40 (m, 1H)	HMBC 29→32
30	24.7	1.82-1.90 (m, 1H) overlap, 1.95-2.03 (m, 1H) overlap	
31	47.1	3.56-3.63 (m, 1H), 3.75-3.82 (m, 1H)	
32	171.7	-	
33	-	-	
34	60.3	4.51 (dd, $J = 9.1, 4.8$ Hz, 1H)	
35	38.5	2.16 (dd, $J = 13.1, 4.8$ Hz, 1H), 2.38-2.46 (m, 1H) overlap	HMBC 35→45
36	57.5	-	
37	79.6	6.06 (d, $J = 4.4$ Hz, 1H)	NOESY 37→1,28,38 HMBC 37→34,36
38	-	6.83 (d, $J = 4.4$ Hz, 1H)	HMBC 38→36
39	148.4	-	
40	110.1	6.68 (d, $J = 7.7$ Hz, 1H)	HMBC 40→41,42,44
41	123.5	7.02-7.06 (m, 1H) overlap	HMBC 41→39
42	119.0	6.72 (dd, $J = 7.5, 7.5$ Hz, 1H)	HMBC 42→43,44
43	128.0	7.19-7.23 (m, 1H) overlap	HMBC 43→36,39,41
44	133.6	-	
45	169.5	-	
46	-	7.22-7.26 (m, 1H) overlap	
47	51.9	4.17 (ddd, $J = 7.7, 7.7, 6.3$ Hz, 1H)	COSY 47→46,50 HMBC 47→45,48,50
48	172.3	-	
49	-	6.98 (br s, 1H), 7.13 (br s, 1H) overlap	HMBC 49→48 TOCSY 49→49'
50	27.6	2.29-2.35 (m, 1H), 2.43-2.50 (m, 1H)	HMBC 50→48
51	109.2	-	
52	124.8	6.81 (d, $J = 1.8$ Hz, 1H)	HMBC 52→59,51
53	-	12.91 (br s, 1H)	TOCSY 53→52,58 NOESY 53→55
54	134.4	-	
55	112.9	7.23-7.27 (m, 1H) overlap	HMBC 55→59,57
56	123.0	7.11-7.15 (m, 1H) overlap	
57	110.7	-	
58	120.5	7.64 (d, $J = 1.7$ Hz, 1H)	COSY 58→56 TOCSY 58→56,55 HMBC 58→51,56,57
59	129.0	-	

Focused Library A

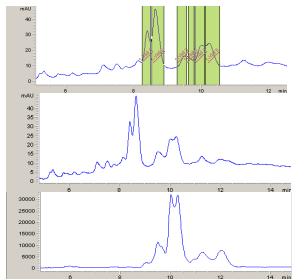
Macrocycle

A0404	Trp5Br	Glu	Pro	Bthi	Asp	Gly	monoiso. mass	MS obs. [M+H] ⁺
68	Trp5Br	Glu	Pro	Trp	Asp	Gly	1036.3	1037.3
69	Trp5Br	Glu	Pro	Thi	Asp	Gly	1003.2	1004.2
70	Trp5Br	Asp	Pro	BThi	Asp	Gly	1039.2	1040.2
71	Trp5Br	D-Glu	Pro	BThi	Asp	Gly	1053.3	1054.2
72	Trp5Br	Ser	Pro	BThi	Asp	Gly	1011.3	1012.1
73	Trp5Br	pSer	Pro	BThi	Asp	Gly	1091.2	1090.2 (-)
74	Trp5Br	Glu	Pip	Bthi	Asp	Gly	1067.3	1067.9
75	Trp5Br	Glu	Mor	Bthi	Asp	Gly	1069.3	1070.2
76	Ala	Glu	Pro	Bthi	Asp	Gly	860.3	861.2
77	Tyr	Glu	Pro	Bthi	Asp	Gly	952.3	953.1
78	Trp5F	Glu	Pro	Bthi	Asp	Gly	993.3	994.2
79	Trp5Me	Glu	Pro	Bthi	Asp	Gly	989.4	990.3
80	Trp5Br	Glu	Pro	Bthi	Glu	Gly	1067.3	1068.2
81	Trp5Br	Glu	Pro	Bthi	Ala	Gly	1009.3	1010.2

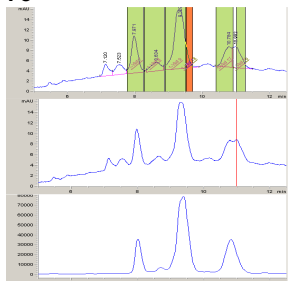




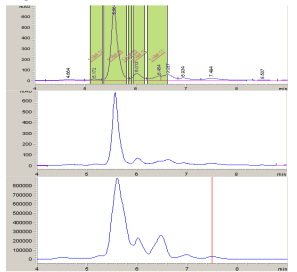
74



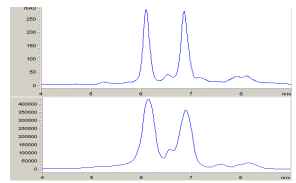
75



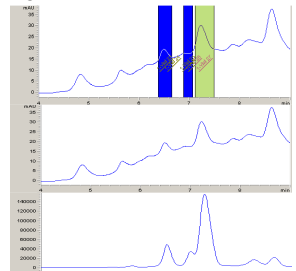
76



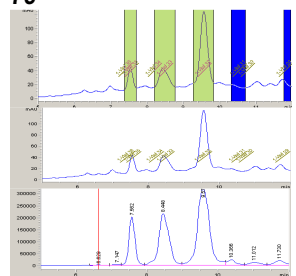
77



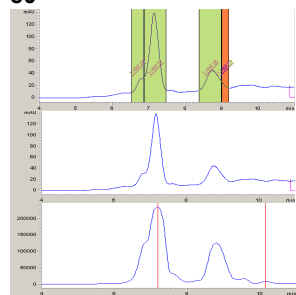
78



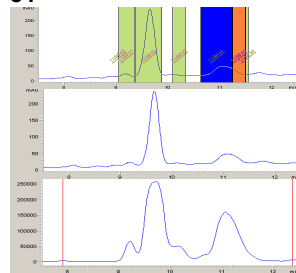
79



80



81

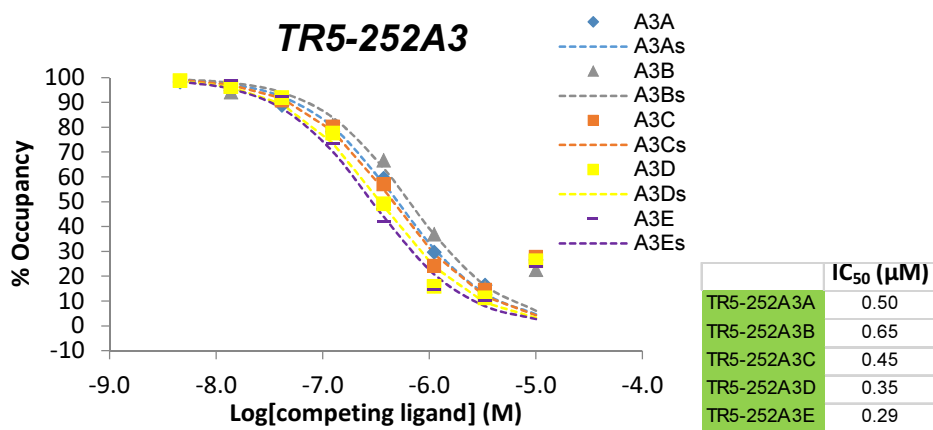


Screening of Library A at 1.1 μM :

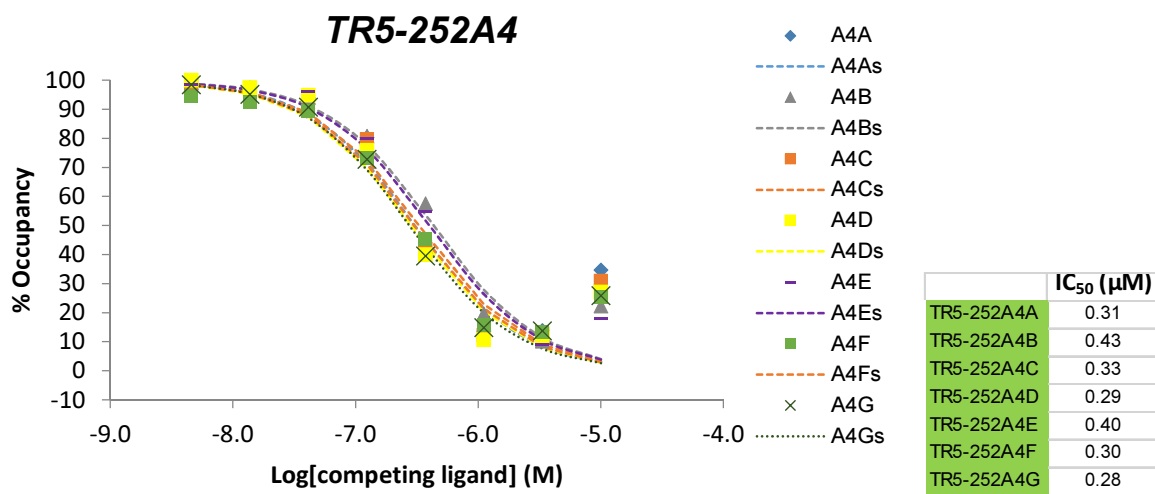
NB/P	stock well	raw data 1.1 μM	% Inh. 1.1 μM	IC ₅₀ (μM)
TR5-252A1A	1A	104	56	
	1B	100	58	
	1C	99	59	
	1D	76	71	
	1E	86	66	
	1F	66	76	
TR5-252A2A	1G	72	73	
	1H	80	69	
	2A	75	71	
	2B	80	69	
TR5-252A3A	2C	55	82	0.50
TR5-252A3B	2D	88	64	0.65
TR5-252A3C	2E	46	87	0.45
TR5-252A3D	2F	37	91	0.35
TR5-252A3E	2G	45	87	0.29
TR5-252A4A	2H	52	83	0.31
TR5-252A4B	3A	41	89	0.43
TR5-252A4C	3B	40	90	0.33
TR5-252A4D	3C	37	91	0.29
TR5-252A4E	3D	33	93	0.40
TR5-252A4F	3E	33	93	0.30
TR5-252A4G	3F	30	95	0.28
TR5-252A5A	3G	140	37	
	3H	148	33	
	4A	144	36	
	4B	95	61	
	4C	93	62	
	4D	73	72	
TR5-252A6A	4E	66	76	
	4F	41	89	1.1
	4G	55	82	1.6
	4H	47	86	1.3
	5A	52	83	0.77
	5B	49	85	0.73
TR5-252B1B	5C	59	80	0.78
TR5-252B1C	5D	41	89	0.64
TR5-252B2A	5E	202	5	
	5F	175	19	
	5G	155	30	
TR5-252B3A	5H	166	24	
	6A	139	38	
	6B	163	26	
TR5-252B4A	6C	45	87	0.52
TR5-252B4B	6D	52	83	0.58
TR5-252B4C	6E	44	88	0.48
TR5-252B5A	6F	109	54	
	6G	110	53	
	6H	105	56	
TR5-252B6A	7A	102	57	
	7B	125	45	
	7C	58	80	
	7D	54	82	
TR5-252C1A	7E	94	61	
	7F	149	33	
	7G	93	62	
	7H	90	63	
	8A	92	62	

TR5-256A	8B	83	67
TR5-256B	8C	79	69
TR5-256C	8D	54	82
TR5-256D	8E	57	81

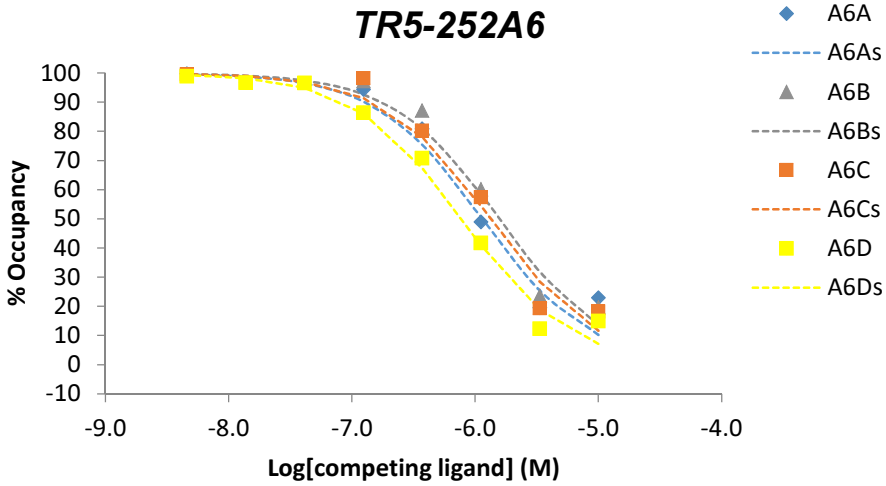
Titration of hit sequences from Focused Library A:



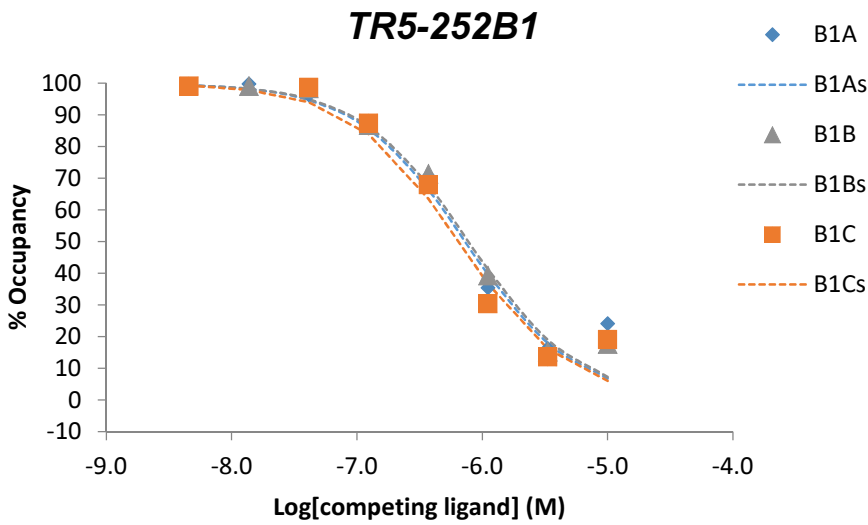
Trp5Br-Asp-Pro-BThi-Asp-Gly



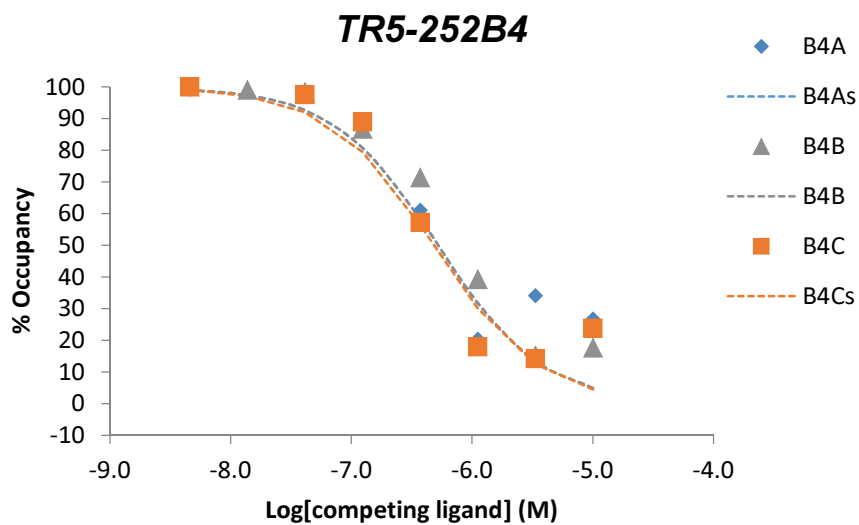
Trp5Br-D-Glu-Pro-Bthi-Asp-Gly



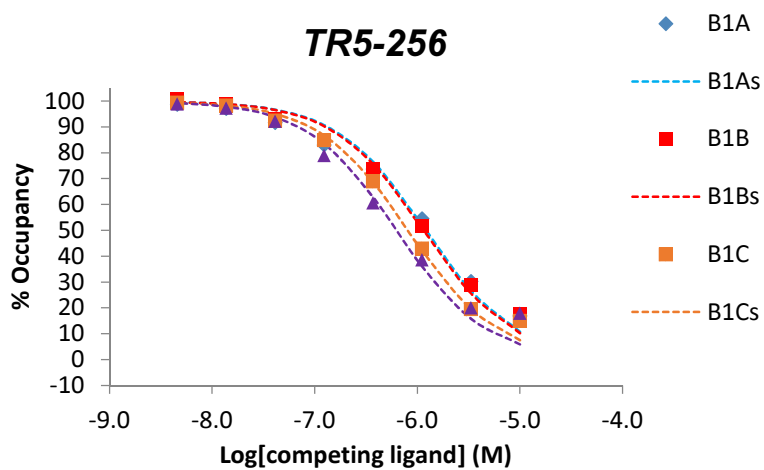
Trp5Br-Glu-Pip-Bthi-Asp-Gly



Trp5Br-Glu-Mor-Bthi-Asp-Gly



Trp5F-Glu-Pro-Bthi-Asp-Gly



Trp5Br-pSer-Pro-Bthi-Asp-Gly

Focused Library B

Parent A05060	Phe	Glu	Pro	Trp	Trp(5Br)	acidolysis prod (EM)	MS obs. [M+H] ⁺
82	Ala	Glu	Pro	Trp	Trp(5Br)	934.3	935.2
83	Tyr	Glu	Pro	Trp	Trp(5Br)	1026.3	1027.2
84	Nal1	Glu	Pro	Trp	Trp(5Br)	1060.4	1061.3
85	Nal2	Glu	Pro	Trp	Trp(5Br)	1060.4	1061.2
86	Phe	Ala	Pro	Trp	Trp(5Br)	952.3	953.3
87	Phe	D-Glu	Pro	Trp	Trp(5Br)	1010.3	1011.2
88	Phe	Ser	Pro	Trp	Trp(5Br)	968.3	969.3
89	Phe	D-Ser	Pro	Trp	Trp(5Br)	968.3	969.3
90	Phe	Glu	Pip	Trp	Trp(5Br)	1024.4	1025.3
91	Phe	Glu	Mor	Trp	Trp(5Br)	1026.3	1027.2
92	Phe	Glu	Pro	Ala	Trp(5Br)	895.3	896.2
93	Phe	Glu	Pro	Phe	Trp(5Br)	971.3	972.2
94	Phe	Glu	Pro	Nal1	Trp(5Br)	1021.3	1022.3
95	Phe	Glu	Pro	Nal2	Trp(5Br)	1021.3	1022.3
96	Phe	Glu	Pro	Trp	Trp(5F)	950.4	951.3
97	Phe	Glu	Pro	Trp	Trp(5Me)	946.4	947.4
98	Phe	Glu	Pro	Trp	Phe(3OMe)	923.4	924.3